郭永怀文集

GUO YONGHUAI WENJI

郭永怀 著

科学出版社
www.sciencep.com

(O—3497.0101)

ISBN 978-7-03-024260-0

定 价：128.00 元

郭永怀文集

郭永怀　著

科学出版社
北京

内 容 简 介

郭永怀是著名的力学家、应用数学家，我国近代力学事业奠基人之一。为纪念郭永怀诞辰一百周年，我们再次编辑出版《郭永怀文集》。

本文集共收录了作者 24 篇期刊论文和研究报告。其中，1943~1955 年期间发表的 14 篇论文内容涉及直管中的可压缩流动、有限振幅柱面和球面波的传播、可压缩流体二维无旋亚声速、超声速混合型流动和上临界马赫数、光滑跨声速绕流及其稳定性、斜激波从平板边界层的反射、中等雷诺数下绕平板的流动等。这些论文反映了作者在跨声速流动和奇异摄动理论两个领域中为国际公认的学术成就，后者被命名为 PLK 方法。1956~1957 年期间发表的 5 篇论文：绕平板和楔的高超声速流动、普朗特数和解离对高超声速流动的影响以及增补的 5 篇文章是作者在高超声速流动领域的研究成果以及他在回国后的学术报告和发表的文章，涉及现代空气动力学的发展方向、发射卫星和返地回收的科学和技术问题，体现了他在参与“两弹一星”技术领导工作中的学术思想。

本书可供流体力学、空气动力学、应用数学专业、航空航天工程科技人员以及高等院校有关专业教师、研究生和高年级学生参考。

图书在版编目(CIP)数据

郭永怀文集/郭永怀著. —北京：科学出版社，2009
ISBN 978-7-03-024260-0

I. 郭… II. 郭… III. 力学-文集 IV. 03-53

中国版本图书馆 CIP 数据核字(2009) 第 036892 号

责任编辑：鄢德平 孟积兴/责任印制：钱玉芬 / 封面设计：陈 敬

科学出版社 出版
北京东黄城根北街 16 号
邮政编码：100717
http://www.sciencep.com

中国科学院印刷厂印刷
科学出版社发行 各地新华书店经销
*
2009 年 3 月第 一 版 开本：787×1092 1/16
2009 年 3 月第一次印刷 印张：41 1/2 插页：8
印数：1—800 字数：975 000

定价：128.00 元

(如有印装质量问题，我社负责调换（科印）)

为什么回到祖国？——我作为一个中国人，有责任回到祖国，和人民一道，共同建设我们的美丽的山河。

对于所有的问题，我们都是空怀若谷，不经过讨论，就没有定论。对每一方面，我们需要权威，但是权威绝不能专有真理。

郭永怀

代　序*

现在已是八十年代的第一春．还要倒数到第十一个冬天，郭永怀同志因公乘飞机，在着陆事故中牺牲了．是的，就那么十秒钟吧，一个有生命、有智慧的人，一位全世界知名的优秀应用力学家就离开了人世；生和死，就那么十秒钟!

十秒钟是短暂的．但回顾往事，郭永怀同志和我相知却跨越了近三十个年头，而这是世界风云多变的三十个年头呵．我第一次与他相识是在 1941 年底，在美国加州理工学院．当时在航空系的有林家翘先生、有钱伟长同志，还有郭永怀同志和我．在地球物理系的有傅承义同志．林先生是一位应用数学家．傅承义同志专的是另外一行．钱伟长同志是个多才多艺的人．所以，虽然我们经常在一起讨论问题，但和我最相知的只有郭永怀一人．他具备应用力学工作所要求的严谨与胆识．当时航空技术的大问题是突破“声障”进入超声速飞行，所以研究跨声速流场是个重要课题，但描述运动的偏微分方程是非线性的，数学问题难度很大．永怀同志因问题对技术发展有重大意义，故知难而进，下决心攻关，终于发现对某一给定外形，在均匀的可压缩理想气体来流中，当来流马赫数达到一定值，物体附近的最大流速达到局部声速，即来流马赫数为下临界马赫数；来流马赫数再高，物体附近出现超声速流场，但数学解仍然存在；来流马赫数再增加，数学解会突然不可能，即没有连续解，这就是上临界马赫数．所以真正有实际意义的是上临界马赫数而不是以前大家所注意的下临界马赫数，这是一个重大发现．

1946 年秋，郭永怀同志任教于由 W. R. Sears 主持的美国康奈尔大学航空学院，我也去美国麻省理工学院，两校都在美国东部，而加州理工学院在西部，相隔近三千公里，他和我就驾车旅行．有这样知己的同游，是难得的，所以当他到了康奈尔而留下来，而我还要一个人驾车继续东行到麻省理工学院时，我感到有点孤单．

1949 年我再次搬家，又到美国加州理工学院任教，所以再一次开车西去，中途到康奈尔．这次我们都结了婚，是家人相聚了，蒋英也再次见到我常称道的郭永怀和李佩同志．这次聚会还有 Sears 夫妇，都是我们在加州理工学院的熟朋友．我们都是我们的老师 Theodore von Kármán 的学生，学术见解很一致，谈起来逸趣横生．这时郭永怀同志已对跨声速气动力学提出了一个新课题：既然超出上临界马赫数不可能有连续解，在流场的超声速区就要出现激波，而激波的位置和形状是受附面层影响的，因此必须研究激波与附面层的相互作用．这个问题比上临界马赫数问题更难，连数学方法都得另辟新途径．这就是 PLK 方法中 Kuo（郭）的来源，现在我们称奇异摄动法．这项工作是郭永怀同志的又一重大贡献．

郭永怀同志之所以能取得这两项重大成果，是因为他治学严谨而遇事看得准，有见识；而一旦看准，有胆量去攻关．当然这是我们从旁见到的，我们也许见不到的是他刻苦的功夫，呕心沥血的劳动．

我以后再见到永怀同志是 1953 年冬，他和李佩同志到加州理工学院．他讲学；我也有机会向他学习奇异摄动法．我当时的心情是很坏的，美国政府因不许我归回祖国而限制我的人身自由，我满腔怒火，向我多年的知己倾诉．他的心情其实也是一样的，但他

---

* 摘自《郭永怀文集》，北京：科学出版社，1982．原题为“写在《郭永怀文集》的后面”．

克制地劝我说，不能性急，也许要到 1960 年美国总统选举后，形势才能转化，我们才能回国．所幸的是：在中国共产党领导下，新中国有亿万人民的团结，迅速强大起来了，我们都比这个日程早得多回到祖国，我在 1955 年，他在 1956 年．

郭永怀同志归国后，奋力工作，是中国科学院力学研究所的主要学术领导人；他做的比我要多得多．但这还不是他的全部工作，1957 年初，有关方面问我谁是承担核武器爆炸力学工作最合适的人，我毫无迟疑地推荐了郭永怀同志．郭永怀同志对发展我国核武器是有很大的贡献的．

所以我认为郭永怀同志是一位优秀的应用力学家，他把力学理论和火热的改造客观世界的革命运动结合起来了．其实这也不只是应用力学的特点，也是一切技术科学所共有的，一方面是精深的理论，一方面是火样的斗争，是冷与热的结合，是理论与实践的结合．这里没有胆小鬼的藏身处，也没有私心重的活动地；这里需要的是真才实学和献身精神．郭永怀同志的崇高品德就在这里!

由于郭永怀同志的这些贡献，我想人民是感谢他的．周恩来总理代表党和全国人民对郭永怀同志无微不至的关怀就是证据．大家辛勤工作，为翻译、编辑和出版这本文集付出了劳动，也是个证据．是的，人民感谢郭永怀同志！作为我们国家的一个科学技术工作者，作为一个共产党员，活着的目的就是为人民服务，而人民的感谢就是一生最好的评价!

我们忘不了郭永怀同志，这本文集是一件很好的纪念品，一本很好的学习材料．

钱学森

1980 年 1 月 16 日

再版前言

在郭永怀先生诞辰一百周年之际，我们再次编辑出版了《郭永怀文集》（简称《文集》）。与 30 年前的中译本不同，郭永怀先生在国外发表的 19 篇期刊论文和研究报告全部以原文刊出。同时，文集中还增加了他回国初期的 5 篇重要文章。这对于了解他的科学成就，领悟他的学术思想，保存他的历史文献具有重要意义。

他在国外期间发表的学术论文，集中展现了他在空气动力学和应用数学领域为世界公认的科学成就：

在跨声速流动领域的 8 篇文章中，他和钱学森一起提出了“上临界马赫数”的概念，研究了激波与边界层的相互作用，发现光滑的跨声速混合流动可以维持到上下临界马赫数间的来流速度，激波的出现将导致波后压力陡增，产生漩涡，乃至发生分离，并可通过黏性层影响上游。从而回答了当时航空工程界聚焦的问题：当飞行速度接近声速时，在绕翼型和飞行器的流场中什么时候会实际出现激波？激波的出现对其气动性能可能产生什么样的影响以及如何减轻和避免气动失速影响的措施。这是 20 世纪 40 年代人类为突破“声障”最有影响的研究成果，并为跨声速飞机设计奠定理论基础。

与奇异摄动理论领域相关的 3 篇论文，研究了中等雷诺数和高速边界层问题。由于黏性扩散或压缩性效应使边界层厚度增加，流动偏折明显，需要计算高阶近似。这时由于没有现成的数学方法可以依循，郭永怀提出了边界层问题中消除高阶奇性并使解一致有效的方法。他不仅给出平板边界层二阶阻力系数和激波边界层黏性干扰的结果，同时也发展了 H. Poincaré 的参数摄动法和 J. Lighthill 的坐标摄动法。1956 年，钱学森在《应用力学评论》（*Applied Mechanics Reviews*）撰文，将该方法命名为“PLK 方法”。

20 世纪 50 年代中，郭永怀在解决了航空领域的难题后，敏锐地意识到人类即将进入空间时代，在 1956~1957 发表的 5 篇文章中，开始关注高超声速流动问题，并深入分析了 Prandtl 数和气体解离对流动，摩阻和传热的可能影响。1963 年，他还指导研究人员完成了高速湍流边界层传热的分析。

郭永怀先生在 1957 年中国力学学术大会和 60 年代星际航行座谈会上的报告，精辟地指明了现代空气动力学的发展方向，深刻分析我国发射卫星和返地回收需要解决的若干科学和技术问题。在我们已经实现了载人航天的今天，重新阅读这些文献，就会更加赞叹郭永怀先生的远见卓识。

郭永怀先生在国外学习和研究的 16 年都是在做准备，都是为了“和人民一道共同建设美丽的山河！”。在他回国后有限的时间里，精力全部集中在领导我国力学学科规划工作，倡导高超声速空气动力学、磁流体力学和爆炸力学等新兴学科，支持研制系列激波管和激波风洞，规划我国的空气动力学试验基地等方面。他高瞻远瞩确定的方向，迄今仍是航空、航天和能源等工程中富有生命力和挑战性的课题。这一时期郭永怀先生的科学成就主要体现在他为我国近代力学事业奠基和“两弹一星”的科学实践活动中。

在我国科学技术界，郭永怀先生是将国家需求和学科前沿结合的楷模，是研究工作

和技术工作衔接的典范，是理论和实验研究并重的表率，郭永怀先生的学术思想是留给我们的宝贵财富。我们一定要继承和发扬郭永怀先生的科学精神和高尚品格，为把我国建设成创新型的现代化国家而不懈努力！

在编辑《文集》的过程中，力学所图书信息中心的朱涛、张凌晨同志做了细致工作，也得到了科学出版社的全力支持，谨此致谢！

中国科学院力学研究所

中国力学学会

2009 年 3 月

目　　录

1　On the force and moment acting on a body in shear flow
（物体在剪切流中所受的力和力矩 1943 年）..... 1

2　The flow of a compressible viscous fluid through a straight pipe
（可压缩黏性流体在直管中的流动 1943 年）..... 4

3　Two-dimensional irrotational mixed subsonic and supersonic flow of a compressible fluid and the upper critical Mach number
（可压缩流体二维无旋亚声速和超声速混合型流动及上临界马赫数 1946 年）..... 22

4　On the stability of transonic flows
（论跨声速流的稳定性 1947 年）.....159

5　The propagation of a spherical or a cylindrical wave of finite amplitude and the production of shock waves
（有限振幅球面波或柱面波的传播及激波的产生 1947 年）.....161

6　Two-dimensional irrotational transonic flows of a compressible fluid
（可压缩流体二维无旋跨声速流动 1948 年）.....173

7　On the hodograph method
（关于速度图方法 1949 年）.....264

8　Two-dimensional transonic flow past airfoils
（绕翼型的二维跨声速流 1951 年）.....265

9　On the stability of two-dimensional smooth transonic flows
（论二元光滑跨声速流的稳定性 1951 年）.....313

10　On the flow of an incompressible viscous fluid past a flat plate at moderate Reynolds numbers
（中等雷诺数下不可压缩黏性流体绕平板的流动 1953 年）.....320

11　Reflection of a weak shock wave from a boundary layer along a flat plate.
I: Interaction of weak shock waves with laminar and turbulent boundary layers analyzed by momentum-integral method
（弱激波从沿平板的边界层的反射 I：用动量积分方法分析弱激波与层流和湍流边界层的相互作用 1953 年）.....339

12　Reflection of weak shock wave from a boundary layer along a flat plate.
II: Interaction of oblique shock wave with a laminar boundary layer analyzed by differential-equation method
（弱激波从沿平板的边界层的反射 II：用微分方程方法分析斜激波与层流边界层的相互作用 1953 年）……405

13　Plane subsonic and transonic potential flows
（平面亚、跨音速势流 1954 年）……465

14　A similarity rule for the interaction between a conical field and a plane shock
（锥型流和激波相互作用的相似律 1955 年）……559

15　Viscous flow along a flat plate moving at high supersonic speeds
（沿高超声速运动平板的黏性流动[I] 1956 年）……561

16　Viscous flow along a flat plate moving at high supersonic speeds
（沿高超声速运动平板的黏性流动[II] 1956 年）……573

17　The effects of Prandtl number on high-speed viscous flows over a flat plate
（Prandtl 数对绕平板高速黏性流的影响 1956 年）……575

18　Compressible viscous flow past a wedge moving at hypersonic speeds
（楔的高超声速可压缩黏性绕流 1956 年）……577

19　Dissociation effects in hypersonic viscous flows
（高超声速黏性流动中的离解效应 1957 年）……592

20　现代空气动力学的问题 （1957 年）……598

21　在关于苏联发射成功第一颗人造卫星座谈会上的发言记录 （1957 年）……605

22　高超速钝体湍流传热问题 （1963 年）……607

23　宇宙飞船的回地问题 （1965 年）……624

24　激波的介绍……631

郭永怀生平……637

郭永怀传……638

ON THE FORCE AND MOMENT ACTING ON A BODY IN SHEAR FLOW* [1)]

By YUNG-HUAI KUO (*California Institute of Technology*)

Recently, H. S. Tsien solved the problem[1] of a Joukowsky airfoil in a steady, two-dimensional flow of constant vorticity distribution. It is interesting to note that the hydrodynamical forces can be expressed in a form similar to the well known Blasius' theorem, involving contour integration of the complex potential function. The following derivation of the formulae is believed to be simpler than that of Tsien.

1. **Equations of motion.** Let u and v be the velocity components parallel to the x- and y-axis, respectively. In the case of two-dimensional steady motion, the Eulerian dynamical equations are:

$$u\frac{\partial u}{\partial x}+v\frac{\partial v}{\partial x}-v\left(\frac{\partial v}{\partial x}-\frac{\partial u}{\partial y}\right)=-\frac{1}{\rho}\frac{\partial p}{\partial x}, \tag{1.1}$$

$$u\frac{\partial u}{\partial y}+v\frac{\partial v}{\partial y}+u\left(\frac{\partial v}{\partial x}-\frac{\partial u}{\partial y}\right)=-\frac{1}{\rho}\frac{\partial p}{\partial y}, \tag{1.2}$$

where p is the pressure and ρ, the density of the fluid. The equation of continuity is

$$\frac{\partial u}{\partial x}+\frac{\partial v}{\partial y}=0. \tag{1.3}$$

For the type of shear flow considered by Tsien,[1] the vorticity is constant everywhere in the field and equal to $-k$. Thus

$$\frac{\partial v}{\partial x}-\frac{\partial u}{\partial y}=-k, \qquad k>0. \tag{1.4}$$

At the first sight, it seems that the problem might not be definite as one has four equations for three variables. By eliminating p between Eqs. (1.1) and (1.2), however, the result can be reduced to Eq. (1.3) by means of Eq. (1.4). This shows that any solution which satisfies Eqs. (1.3) and (1.4) is consistent with Eqs. (1.1) and (1.2).

To simplify the problem, the solution is written in the following form:

$$u=ky+u', \tag{1.5}$$

$$v=v'. \tag{1.6}$$

Then Eqs. (1.3) and (1.4) reduce to

$$\frac{\partial u'}{\partial x}+\frac{\partial v'}{\partial y}=0, \tag{1.7}$$

$$\frac{\partial v'}{\partial x}-\frac{\partial u'}{\partial y}=0. \tag{1.8}$$

* Received June 21, 1943.

[1] H. S. Tsien, *Symmetrical Joukowski airfoils in shear flow*, Quarterly Appl. Math., **1**, 129 (1943).

1) Published in *Quarterly of Applied Mathematics*, 1943, 1(1): 273~275

These equations are satisfied by

$$u' = \frac{\partial \psi}{\partial y}, \qquad v' = -\frac{\partial \psi}{\partial x}; \tag{1.9}$$

or

$$u' = \frac{\partial \varphi}{\partial x}, \qquad v' = \frac{\partial \varphi}{\partial y}; \tag{1.10}$$

where ψ and φ are the imaginary and real parts of the complex potential $F(z)$; namely,

$$\varphi + i\psi = F(z), \qquad z = x + iy; \tag{1.11}$$

and

$$u' - iv' = w'(z). \tag{1.12}$$

For a given problem the function $F(z)$ is so determined that the velocity component normal to the contour of the body is zero.

By virtue of Eqs. (1.4), (1.5), and (1.6), Eqs. (1.1) and (1.2) give

$$p = -\frac{\rho}{2} q'^2 - \rho k u' y + \rho k \psi, \tag{1.13}$$

where $q'^2 = u'^2 + v'^2$, and the constant of integration is absorbed in ψ.

2. Force and moment. If the motion is two-dimensional and steady, the components of the hydrodynamical force and moment[2] acting on the body are given by

$$X = -\oint p dy - \rho \oint u(udy - vdx), \tag{2.1}$$

$$Y = \oint p dx + \rho \oint v(vdx - udy), \tag{2.2}$$

$$M = \oint p(xdx + ydy) - \rho \oint (-v^2 xdx - u^2 ydy + uvydx + uvxdy), \tag{2.3}$$

where the contour integrals are taken along a closed curve containing the body. Using Eqs. (1.5), (1.6) and (1.13), the above equations can be written as:

$$X = -\frac{\rho}{2} \oint [(u'^2 - v'^2)dy - 2u'v'dx] - \rho k \oint [(\psi + u'y)dy - v'ydx], \tag{2.4}$$

$$Y = -\frac{\rho}{2} \oint [(u'^2 - v'^2)dx + 2u'v'dy] + \rho k \oint [(\psi - u'y)dx - v'ydy], \tag{2.5}$$

$$M = -\mathrm{Re}\left[\frac{\rho}{2} \oint zw'^2 dz\right] + \rho k \oint [(\psi - u'y)(xdx + ydy) - (v'yx - 2u'y^2)dy + v'y^2 dx]. \tag{2.6}$$

---

[2] W. F. Durand, *Aerodynamic theory*, vol. 2, Springer, Berlin, 1935, pp. 31–33.

If only bodies with closed boundary are considered, no sources can exist within the field of flow. Then the stream function ψ is single-valued, and

$$\oint \psi dx = \oint x(v'dx - u'dy),$$

$$\oint \psi dy = \oint y(v'dx - u'dy).$$

From these relations, it is not difficult to deduce

$$X = -\frac{\rho}{2}\oint [(u'^2 - v'^2)dy - 2u'v'dx], \tag{2.7}$$

$$Y = -\frac{\rho}{2}\oint [(u'^2 - v'^2)dx + 2u'v'dy]$$

$$+ \rho k \oint [v'(xdx - ydy) - u'(ydx + xdy)], \tag{2.8}$$

$$M = -\operatorname{Re}\left[\frac{\rho}{2}\oint zw'^2dz\right]$$

$$+\frac{\rho k}{2}\oint [-u'\{(x^2 - y^2)dy + 2xydx\} + v'\{(x^2 - y^2)dx - 2xydy\}]. \tag{2.9}$$

These at once suggest the following alternative expressions:

$$X - iY = \frac{i\rho}{2}\oint w'^2dz + i \operatorname{Im}\left[\rho k \oint w'zdz\right], \tag{2.10}$$

and

$$M = -\operatorname{Re}\left[\frac{\rho}{2}\oint z\left(w' - \frac{ikz}{2}\right)^2 dz\right]. \tag{2.11}$$

Eqs. (2.10) and (2.11) may be regarded as an extension of Blasius' theorem. They can be easily identified with the expressions given by Tsien.[1] The calculation of force and moment, however, can be simplified to a certain extent by using these new expressions.

The writer wishes to thank Dr. H. S. Tsien for the use of his paper before publication and for his helpful discussions.

THE FLOW OF A COMPRESSIBLE VISCOUS FLUID THROUGH A STRAIGHT PIPE [1)]

By Y. H. Kuo

Introduction

The problem of determining a steady flow of incompressible viscous fluid through a straight pipe of any section is easily reduced to a problem of Dirichlet. This is the familiar Hagen-Poiseuille[1] flow, and a pipe of circular section is particularly well known. If, however, the fluid is compressible, the problem of steady flow becomes much more difficult. Although the problem has been treated experimentally[2] and by the rather crude method of hydraulics,[3] there does not appear to have been any previous mathematical treatment.

The method of the present paper is that of development in series in powers of the Mach number, which is supposed to be small. The operation with series is formal, no attempt being made to discuss the convergence.

The boundary condition of zero velocity on the wall of the tube, together with the information regarding the pressure drop, is not sufficient to make the mathematical problem definite. It is, in fact, a question of finding *a* solution rather than *the* solution; the simplest solution is taken, as in the classical case of the incompressible fluid, where the same partial indeterminacy also occurs.

Part I deals with a pipe of general section. The equations of motion expressed in terms of momentum vector and specific volume are given and the process of power series development is explained. This may, for small values of Mach number, be regarded as a process of successive approximations.

The zero approximation is the Hagen-Poiseuille flow.

In the first approximation the flow remains parallel to the walls of the pipe, and the determination of the velocity again reduces to a Dirichlet problem (5.3).

In the second approximation the velocity is no longer parallel to the walls. The component of momentum parallel to the walls is a linear function of the distance along the pipe (6.3), the determination of the coefficient of this function again depending on Dirichlet problems (6.8), (6.9). The transverse momentum component is proportional to $f_\alpha^{(2)}$ in (6.13), and this is independent of distance along the pipe; its determination is reduced to a Dirichlet problem (6.14) and a biharmonic problem (6.15).

In the zero approximation the pressure is a linear function of distance along the pipe (4.7), in the first approximation a quadratic function (5.8), and in the second approximation a cubic function (6.27).

The drag and flux are considered in §7.

In Part II the pipe is of circular section and explicit solutions are given.

[1] Hagen, Pogg. Ann., **46**, 423 (1839).
[2] Poiseuille, Comp. Rend. **11** and **12**, (1840–1).
[3] Reynolds, Phil. Trans. Roy. Soc. London, **174**, 935 (1883).

1) Published in *Journal of Mathematics and Physics*, 1943, 22: 13~30

Part I. Pipe of a general section

1. The equations of motion

We shall consider a compressible viscous fluid flowing steadily through a pipe of any constant section, under the influence of the difference between the pressures applied at the ends of the pipe. It is assumed that the pipe has a well-rounded mouth-piece so that it introduces no initial disturbances. The domain of the mathematical theory is the interior of the pipe between two normal sections at a distance l' apart (the "length" of the pipe); these sections are called the "entrance" and "outlet".

Let x_i' be Cartesian coordinates with the origin at the mean centre of the entrance, the axis of x_0' lying along the axis of the pipe; let u_i' be the components of the velocity. Then in the pipe itself the motion satisfies the general equations[4,5] of steady motion in the absence of body force

$$\rho' u_j' u_{i,j}' = -p_{,i}' + \mu \Delta' u_i' + \frac{\mu}{3}\theta_{,i}', \tag{1.1}$$

where $\theta' = \partial u_i'/\partial x_i'$, $\Delta'(= \partial^2/\partial x_i' \partial x_i')$ is the Laplacian operator, ρ' the density, p' the pressure and μ the viscosity, which is a function of temperature, but within wide limits, independent of pressure. With these is associated the equation of continuity

$$(\rho' u_i')_{,i} = 0. \tag{1.2}$$

Here the equations are expressed in accordance with the indicial notation; the Latin suffixes have the range 0, 1, 2, the comma indicates partial differentiation and summation is understood for repeated suffixes. We shall assume the motion to be either isothermal or adiabatic, so that a definite pressure density relation exists. We shall in both cases treat μ as a constant, its variations under change of pressure being neglected in both cases and its variation under change of temperature being neglected in the adiabatic case.

We now find it convenient to define a few constants which are useful in the later calculation. Let $\bar{p}'$ be the mean pressure over the cross-section at the outlet, defined as

$$\bar{p}' = \frac{1}{A}\int\int p'\, dx_1'\, dx_2' \qquad \text{for} \quad x_0' = l', \tag{1.3}$$

where A is the area of the cross-section. Let $\bar{\rho}'$ be the density corresponding to $\bar{p}'$ according to the pressure-density relation of the fluid. Finally, let $\bar{u}'$ be the mean velocity over a cross-section, weighted by the density so that it is independent of the particular section chosen, namely,

$$\bar{u}' = \frac{1}{\bar{\rho}' A}\int\int \rho' u_0'\, dx_1'\, dx_2' \qquad \text{for any} \quad x_0'. \tag{1.4}$$

[4] W. Müller, Einführung in die Theorie der zähen Flüssigkeiten, (Leipzig, 1932) p. 13.
[5] H. Lamb, Hydrodynamics, (Cambridge, 1932) p. 577.

We shall now be able to express the equations in dimensionless form by the following transformation:

$$(1.5)\qquad x_i = \frac{x_i'}{2m}, \qquad u_i = \frac{u_i'}{\bar{u}'}, \qquad p = \frac{p' - \bar{p}'}{\bar{\rho}'\bar{u}'^2}, \qquad \rho = \frac{\rho'}{\bar{\rho}'},$$

where m is the hydraulic mean radius of the section, i.e. $m = A/P$ where P is the perimeter of the bounding curve C. Substituting (1.5) in (1.1) and (1.2), we have

$$(1.6)\qquad \rho u_\beta u_{\alpha,\beta} + \rho u_0 u_{\alpha,0} = -p_{,\alpha} + \frac{2}{R}\Delta u_\alpha + \frac{2}{3R}\theta_{,\alpha},$$

$$(1.7)\qquad \rho u_\beta u_{0,\beta} + \rho u_0 u_{0,0} = -p_{,0} + \frac{2}{R}\Delta u_0 + \frac{2}{3R}\theta_{,0},$$

$$(1.8)\qquad (\rho u_\beta)_{,\beta} + (\rho u_0)_{,0} = 0,$$

the Greek suffixes having the range 1, 2; here $\theta = \partial u_j/\partial x_j$, R is the Reynolds' number, i.e., $R = 4m\bar{u}'/\nu$ where $\nu\left(=\frac{\mu}{\bar{\rho}'}\right)$ is the mean kinematic viscosity.

The boundary conditions to be satisfied by u_i are

$$(1.9)\qquad u_i = 0 \quad \text{on} \quad C.$$

These seem to be the only essential boundary conditions. As we shall see later that, they are generally not sufficient to ensure a definite solution. We shall make use of this partial indeterminacy to obtain analytically simple solutions, hoping that the physical validity of such solutions may be justified in the same way that the solutions of Saint Venant in elasticity are justified.

It is convenient to have the constancy of the flux of mass across any section expressed in integral form; in dimensionless variables, it reads

$$(1.10)\qquad \int\int \rho u_0\, dx_1\, dx_2 = \frac{P^2}{4A}.$$

Once the velocity u_i is known we can solve for p from (1.6) and (1.7). As the differential equations involving p are of the first order there will be one arbitrary constant at our disposal, which will be determined by the condition at the outlet. This is

$$(1.11)\qquad \int\int p\, dx_1\, dx_2 = 0 \qquad \text{for} \quad x_0 = l = \frac{l'}{2m}.$$

2. The pressure-density relation

The equations (1.6), (1.7) and (1.8) which involve five unknowns cannot be solved without using a relation connecting p and ρ. As remarked above, we shall suppose the change of state to be either isothermal or adiabatic. It would appear necessary to treat the case of a gas and that of a liquid separately. However, as we shall see below, it is possible to justify a common treatment as approximately valid from a physical point of view.

Let M denote the Mach number; it is defined as the ratio of the mean velocity $\bar{u}'$ of the fluid to that of sound in the fluid, namely,

$$M = \frac{\bar{u}'}{c_0}, \tag{2.1}$$

where c_0 is the velocity of sound in the fluid at the pressure $\bar{p}'$, i.e. $c_0^2 = (dp'/d\rho')_{\rho=\bar{\rho}'}$.

Suppose we are dealing with the perfect gas under the isothermal condition, the pressure-density relationship is Boyle's law

$$\rho' = kp',$$

where k is a constant. With this law the value of $\bar{\rho}'$ corresponding to $\bar{p}'$ is

$$\bar{\rho}' = k\bar{p}'.$$

Taking the difference of these two equations and converting to dimensionless variables, we have

$$\rho = 1 + M^2 p. \tag{2.2}$$

Similarly, under the adiabatic condition the pressure-density relationship takes the form

$$\rho^\gamma = 1 + \gamma M^2 p, \tag{2.3}$$

where γ is the ratio of the specific heats.

For mathematical reasons, we consider only those cases in which the viscosity μ may be regarded as a constant. This is certainly the case for the isothermal motion of a gas. It will not be accurate when the change is adiabatic, for the temperature no longer remains constant. However in gases, air for instance, the viscosity depends only slightly on temperature; for an increase of temperature from 0° to 20°C, the increase[6] in μ is about 6 percent, so we can take it as constant for small change in temperature.

In the case of a liquid, the general thermodynamic properties are rather vague and no definite laws have ever been established. However, it is an experimental fact that when[7] water flows through a pipe, the temperature everywhere is sensibly the same so long as the flow is laminar; and that[8] under a constant temperature, the pressure density-relation is approximately linear for a moderate range of pressures. Consequently, the isothermal law (2.2) will be assumed to be valid also for liquid.

As a mathematical convenience, we may regard the equation (2.2) as a special case of the equation (2.3), although they represent entirely different physical processes. Hence we shall use (2.3), reducing to (2.2) when required by putting $\gamma = 1$.

[6] H. Lamb, Loc. cit.[5] p. 576.
[7] Barnes and Coker, Proc. Roy. Soc. A 74, 341 (1904).
[8] P. W. Bridgman, Proc. Roy. Soc. A 48, 309 (1912); A 49, 1 (1913); A 66, 185 (1931).

3. Method of approximation

We have now in (1.6), (1.7), (1.8) and (2.3) a complete system of non-linear partial differential equations of the second order for the variables u_i, p, and ρ. We shall proceed towards their solution by a method of successive approximations in which the equations are linearized by suitable assumptions.

When we eliminate p between (1.6) and (1.7) and introduce the momentum vector V_i

$$u_i = \sigma V_i , \tag{3.1}$$

where $\sigma = \frac{1}{\rho}$, we obtain two equations

$$\begin{aligned} &\{V_\beta(\sigma V_\alpha)_{,\beta} + V_0(\sigma V_\alpha)_{,0}\}_{,0} - \{V_\beta(\sigma V_0)_{,\beta} + V_0(\sigma V_0)_{,0}\}_{,\alpha} \\ &\qquad = \frac{2}{R}\Delta\{(\sigma V_\alpha)_{,0} - (\sigma V_0)_{,\alpha}\} ; \end{aligned} \tag{3.2}$$

and the equation of continuity becomes

$$V_{\beta,\beta} + V_{0,0} = 0. \tag{3.3}$$

We suppose that the dependent variables can be developed in series of ascending power of M^2:

$$V_i = V_i^{(0)} + M^2 V_i^{(1)} + M^4 V_i^{(2)} + \cdots , \tag{3.4}$$

$$\sigma = 1 + M^2\sigma^{(1)} + M^4\sigma^{(2)} + \cdots , \tag{3.5}$$

$$p = p^{(0)} + M^2 p^{(1)} + M^4 p^{(2)} + \cdots . \tag{3.6}$$

By virtue of (2.3) which can be written as

$$\sigma = (1 + \gamma M^2 p)^{-\frac{1}{\gamma}}, \tag{3.7}$$

(3.5) and (3.6) give the following relations by binomial expansion:

$$\begin{aligned} &\sigma^{(1)} = -p^{(0)}, \qquad \sigma^{(2)} = -p^{(1)} + \frac{\gamma+1}{2}(p^{(0)})^2, \\ &\sigma^{(3)} = -p^{(2)} + (\gamma+1)p^{(1)}p^{(0)} - \frac{(\gamma+1)(2\gamma+1)}{6}(p^{(0)})^3, \cdots . \end{aligned} \tag{3.8}$$

Substituting the expressions (3.4) and (3.5) in (3.2) and (3.3) and collecting terms of equal powers of M, we obtain sets of equations from the vanishing of the coefficients of all powers of M. These equations are complicated, but it is necessary to set them down in order to make the later developments intelligible. The equations corresponding to M^0 M^2, M^4 are as follows

$$\begin{aligned} &\{V_\beta^{(0)} V_{\alpha,\beta}^{(0)} + V_0^{(0)} V_{\alpha,0}^{(0)}\}_{,0} - \{V_\beta^{(0)} V_{0,\beta}^{(0)} + V_0^{(0)} V_{0,0}^{(0)}\}_{,\alpha} \\ &\qquad = \frac{2}{R}\Delta\{V_{\alpha,0}^{(0)} - V_{0,\alpha}^{(0)}\}, \end{aligned} \tag{3.9}$$

$$V^{(0)}_{\beta,\beta} + V^{(0)}_{0,0} = 0; \tag{3.10}$$

$$\{V^{(0)}_{\beta} u^{(1)}_{\alpha,\beta} + V^{(1)}_{\beta} V^{(0)}_{\alpha,\beta} + V^{(0)}_{0} u^{(1)}_{\alpha,0} + V^{(1)}_{0} V^{(0)}_{\alpha,0}\}_{,0}$$

$$- \{V^{(0)}_{\beta} u^{(1)}_{0,\beta} + V^{(1)}_{\beta} V^{(0)}_{0,\beta} + V^{(0)}_{0} u^{(1)}_{0,0} + V^{(1)}_{0} V^{(0)}_{0,0}\}_{,\alpha} = \frac{2}{R}\Delta\{u^{(1)}_{\alpha,0} - u^{(1)}_{0,\alpha}\}, \tag{3.11}$$

$$V^{(1)}_{\beta,\beta} + V^{(1)}_{0,0} = 0; \tag{3.12}$$

$$\{V^{(0)}_{\beta} u^{(2)}_{\alpha,\beta} + V^{(1)}_{\beta} u^{(1)}_{\alpha,\beta} + V^{(2)}_{\beta} V^{(0)}_{\alpha,\beta} + V^{(0)}_{0} u^{(2)}_{\alpha,0} + V^{(1)}_{0} u^{(1)}_{\alpha,0} + V^{(2)}_{0} V^{(0)}_{\alpha,0}\}_{,0}$$

$$-\{V^{(0)}_{\beta} u^{(2)}_{0,\beta} + V^{(1)}_{\beta} u^{(1)}_{0,\beta} + V^{(2)}_{\beta} V^{(0)}_{0,\beta} + V^{(0)}_{0} u^{(2)}_{0,0} + V^{(1)}_{0} u^{(1)}_{0,0} + V^{(2)}_{0} V^{(0)}_{0,0}\}_{,\alpha} \tag{3.13}$$

$$= \frac{2}{R}\Delta\{u^{(2)}_{\alpha,0} - u^{(2)}_{0,\alpha}\},$$

$$V^{(2)}_{\beta,\beta} + V^{(2)}_{0,0} = 0; \tag{3.14}$$

where

$$u^{(m)}_{i} = \sum_{n=0}^{n=m} \sigma^{(n)} V^{(m-n)}_{i}.$$

To solve for the pressure, we shall also require equations deduced by substituting from (3.4), (3.5), (3.6) in the equations of motion (1.6), (1.7), (1.8). These equations corresponding to M^0, M^2, M^4 are as follows:

$$V^{(0)}_{j} V^{(0)}_{i,j} = -p^{(0)}_{,i} + \frac{2}{R}\Delta V^{(0)}_{i}, \tag{3.15}$$

$$V^{(0)}_{j} u^{(1)}_{i,j} + V^{(1)}_{j} V^{(0)}_{i,j} = -p^{(1)}_{,i} + \frac{2}{R}\Delta u^{(1)}_{i} + \frac{2}{3R}\theta^{(1)}_{,i}, \tag{3.16}$$

$$V^{(0)}_{j} u^{(2)}_{i,j} + V^{(1)}_{j} u^{(1)}_{i,j} + V^{(2)}_{j} V^{(0)}_{i,j} = -p^{(2)}_{,i} + \frac{2}{R}\Delta u^{(2)}_{i} + \frac{2}{3R}\theta^{(2)}_{,i}, \tag{3.17}$$

where $\theta^{(m)} = u^{(m)}_{j,j}$.

We shall start to solve these sets of equations from zero approximation, for which a simple assumption will be made so that the equations are linearized. After the velocity for the zero approximation has been found, we can put it in the equations (3.17) and (3.18) and thereby the pressure $p^{(0)}$ can be calculated. This gives $\sigma^{(1)}$ through the first of (3.8). Then substituting $V^{(0)}_{i}$ and $\sigma^{(1)}$ in the equations (3.11) we can calculate the corresponding quantities for the next approximation; and so on. In this manner, we can proceed to any order of approximation as it is required.

The boundary conditions on C for the momentum components of all approximations are

$$V^{(n)}_{0} = V^{(n)}_{\alpha} = 0. \qquad (n = 0, 1, 2, \cdots) \tag{3.18}$$

These, as we said before, are generally insufficient to determine all the arbitrary functions arising from the integration of the equations. We shall introduce further the "normalization conditions" which follow from (1.10), namely,

3.19) $$\iint V_0^{(0)}\, dx_1\, dx_2 = \frac{P^2}{4A},$$

3.20) $$\iint V_0^{(n)}\, dx_1\, dx_2 = 0 \qquad (n = 1, 2, 3, \cdots)$$

for any x_0.

For the pressure, we have only the end conditions which require the constants in any case to be in conformity with (1.11) such that

(3.21) $$\iint p^{(n)}\, dx_1\, dx_2 = 0 \qquad (n = 0, 1, 2, \cdots)$$

for $x_0 = l$.

4 Zero approximation

To solve the equations for the zero approximation, we assume $V_\alpha^{(0)} = 0$; then the equations (3.9) and (3.10) are reduced to

(4.1) $$\Delta V_{0,\alpha}^{(0)} = 0,$$

(4.2) $$V_{0,0}^{(0)} = 0.$$

These equations are satisfied by taking for $V_0^{(0)}$ any function of x_1, x_2, which satisfies

(4.3) $$\underset{2}{\Delta} V_0^{(0)} = -\Pi;$$

where $\underset{2}{\Delta}$ is the two-dimensional Laplacian operator and Π is a constant. The solution is to satisfy the conditions

(4.4) $$V_0^{(0)} = 0 \quad \text{on} \quad C,$$

(4.5) $$\iint V_0^{(0)}\, dx_1\, dx_2 = \frac{P^2}{4A}.$$

On account of (4.5) from which the constant Π is determined, the solution is unique.

If we put $V_0^{(0)}$ back into (3.15), we get

(4.6) $$\Pi = -\frac{R}{2} p_{,0}^{(0)}.$$

On integration of this equation, we obtain by (3.21)

(4.7) $$p^{(0)} = \frac{2\Pi}{R}(l - x_0).$$

The zero approximation is the well-known Poiseuille motion.

Knowing $p^{(0)}$, we have, by the first of (3.8)

(4.8) $$\sigma^{(1)} = -\frac{2\Pi}{R}(l - x_0).$$

5. First approximation

For the first approximation, we again assume that the components of the velocity, except that along x_0 , vanish. Thus on putting $V_\alpha^{(0)} = 0$ the equations (3.11) and (3.12) are simplified to

$$\{V_0^{(0)}(V_0^{(1)} + \sigma^{(1)} V_0^{(0)})_{,0}\}_{,\alpha} = \frac{2}{R} \Delta V_{0,\alpha}^{(1)} , \tag{5.1}$$

$$V_{0,0}^{(1)} = 0. \tag{5.2}$$

These equations are satisfied by taking for $V_0^{(1)}$ any function of x_1 , x_2 which satisfies

$$\underset{2}{\Delta} V_0^{(1)} = \Pi\{V_0^{(0)}\}^2 + C_0^{(1)} , \tag{5.3}$$

where $C_0^{(1)}$ is an arbitrary constant. The boundary condition

$$V_0^{(1)} = 0 \quad \text{on} \quad C, \tag{5.4}$$

together with the further condition

$$\iint V_0^{(1)} \, dx_1 \, dx_2 = 0 \quad \text{for any} \quad x_0 , \tag{5.5}$$

is sufficient for a unique solution.

With $V_0^{(1)}$ so calculated, we can proceed to solve for $p^{(1)}$ from the equations (3.16), namely,

$$0 = -p_{,\alpha}^{(1)} + \frac{2}{3R} (\sigma_{,0}^{(1)} V_0^{(0)})_{,\alpha} , \tag{5.6}$$

$$0 = -p_{,0}^{(1)} + \frac{2C_0^{(1)}}{R} + \frac{4\Pi^2}{R^2} (l - x_0). \tag{5.7}$$

Integrating we have

$$p^{(1)} = -\frac{2\Pi^2}{R^2} (l - x_0)^2 - \frac{2C_0^{(1)}}{R} (l - x_0) + \frac{4\Pi}{3R^2} (V_0^{(0)} - 1), \tag{5.8}$$

where the constants of integration are determined in accordance with (1.11). From the second of (3.8), we have

$$\sigma^{(2)} = \frac{2\Pi^2(\gamma + 2)}{R^2} (l - x_0)^2 + \frac{2C_0^{(1)}}{R} (l - x_0) - \frac{4\Pi}{3R^2} (V_0^{(0)} - 1), \tag{5.9}$$

6. Second approximation

Making use of the results obtained above, we reduce the equations (3.13) to

$$\begin{aligned} V_0^{(0)} V_{\alpha,00}^{(2)} - (V_\beta^{(2)} V_{0,\beta}^{(0)} + V_0^{(0)} V_{0,0}^{(2)})_{,\alpha} = \frac{2}{R} \Delta(V_{\alpha,0}^{(2)} - V_{0,\alpha}^{(2)}) \\ + \frac{4(\gamma + 1)\Pi^2}{R^2} x_0\{V_0^{(0)}\}^2 + F_{,\alpha} , \end{aligned} \tag{6.1}$$

where

$$F = \frac{4\Pi}{R} V_0^{(1)} V_0^{(0)} - \frac{2}{R}\left(C_0^{(1)} + \frac{2(\gamma+1)\Pi^2}{R} l\right)\{V_0^{(0)}\}^2 - \frac{2}{R}\left\{\frac{4(3\gamma+8)\Pi^2}{3R^2} V_0^{(0)} - \frac{8\pi}{3R^2} V_{0,\beta}^{(0)} V_{0,\beta}^{(0)}\right\},$$

while the equation of continuity remains

$$V_{\beta,\beta}^{(2)} + V_{0,0}^{(2)} = 0. \tag{6.2}$$

We shall seek a particular solution of the form

$$V_0^{(2)} = f_0^{(2)} + x_0 g_0^{(2)}, \tag{6.3}$$

$$V_\alpha^{(2)} = f_\alpha^{(2)}, \tag{6.4}$$

where $f_0^{(2)}$, $g_0^{(2)}$, and $f_\alpha^{(2)}$ are functions of x_1 and x_2. Substituting these in (6.1) and equating the coefficients of equal powers of x_0, we obtain the following set of equations:

$$\frac{2}{R}\underset{2}{\Delta} f_{0,\alpha}^{(2)} - (f_\beta^{(2)} V_{0,\beta}^{(0)} + V_0^{(0)} g_0^{(2)})_{,\alpha} = F_{,\alpha}, \tag{6.5}$$

$$0 = -\frac{2}{R}\underset{2}{\Delta} g_{0,\alpha}^{(2)} + \frac{4(\gamma+1)\Pi^2}{R^2}\{V_0^{(0)}\}_{,\alpha}^2. \tag{6.6}$$

Similarly, the equation of continuity (6.2) yields

$$f_{\beta,\beta}^{(2)} + g_0^{(2)} = 0. \tag{6.7}$$

The integration of equations (6.5) and (6.6) gives at once two equations:

$$\underset{2}{\Delta} g_0^{(2)} = \frac{2(\gamma+1)\Pi^2}{R}(V_0^{(0)})^2 + C_0^{(2)}, \tag{6.8}$$

$$\underset{2}{\Delta} f_0^{(2)} = \frac{R}{2}(F + f_\beta^{(2)} V_{0,\beta}^{(0)} + V_0^{(0)} g_0^{(2)}) + D_0^{(2)}, \tag{6.9}$$

where $C_0^{(2)}$ and $D_0^{(2)}$ are arbitrary constants. The equation (6.8) now involves only one unknown $g_0^{(2)}$ and is to be solved subject to the boundary condition

$$g_0^{(2)} = 0 \quad \text{on} \quad C, \tag{6.10}$$

and the further condition

$$\int\int g_0^{(2)}\, dx_1\, dx_2 = 0. \tag{6.11}$$

We have now in (6.7) and (6.9) two equations for three unknowns. This problem is, at the first sight, indeterminate. However, by eliminating $p^{(2)}$ between the equations (3.17) we obtain another independent equation:

$$\underset{2}{\Delta}(V_{\alpha,\beta}^{(2)} - V_{\beta,\alpha}^{(2)}) = 0. \tag{6.12}$$

To solve this system of equations, we write, without loss of generality, for the vector $f_\alpha^{(2)}$:

$$f_\alpha^{(2)} = \varphi_{,\alpha}^{(2)} + \epsilon_{\alpha\beta}\psi_{,\beta}^{(2)}, \tag{6.13}$$

where $\varphi^{(2)}$ and $\psi^{(2)}$ are functions of x_1, x_2, and $\epsilon_{\alpha\beta}$ the permutation symbol ($\epsilon_{11} = \epsilon_{22} = 0$; $\epsilon_{12} = -\epsilon_{21} = 1$). Substituting (6.13) in (6.7) and (6.12) we have

$$\underset{2}{\Delta}\varphi^{(2)} + g_0^{(2)} = 0, \tag{6.14}$$

$$\underset{2}{\Delta}\underset{2}{\Delta}\psi^{(2)} = 0. \tag{6.15}$$

The boundary conditions for $\varphi^{(2)}$ and $\psi^{(2)}$ on C, according to (3.18), are

$$\frac{\partial\varphi^{(2)}}{\partial s} + \frac{\partial\psi^{(2)}}{\partial n} = 0, \tag{6.16}$$

$$\frac{\partial\varphi^{(2)}}{\partial n} - \frac{\partial\psi^{(2)}}{\partial s} = 0, \tag{6.17}$$

where n refers to the outer normal. Furthermore, we have from (6.11) on eliminating $g_0^{(2)}$ from (6.14)

$$\int_C \frac{\partial\varphi^{(2)}}{\partial n}\,ds = 0,$$

by Green's theorem. We shall satisfy this condition by the special assumption

$$\frac{\partial\varphi^{(2)}}{\partial n} = 0, \tag{6.18}$$

on C. On account of this, (6.17) and (6.16) now become

$$\psi^{(2)} = \text{const.} = 0, \tag{6.19}$$

$$\frac{\partial\psi^{(2)}}{\partial n} = -\frac{\partial\varphi^{(2)}}{\partial s}. \tag{6.20}$$

A substitution of $g_0^{(2)}$ and $f_\alpha^{(2)}$ in (6.9) will enable us to solve for $f_0^{(2)}$. Thus

$$\underset{2}{\Delta} f_0^{(2)} = \frac{R}{2}\left(F + f_\beta^{(2)} V_{0,\beta}^{(0)} + V_0^{(0)} g_0^{(2)}\right) + D_0^{(2)} \tag{6.21}$$

with the boundary condition

$$f_0^{(2)} = 0 \quad \text{on} \quad C, \tag{6.22}$$

and a further condition

$$\iint f_0^{(2)}\,dx_1\,dx_2 = 0. \tag{6.23}$$

It is seen that the equations (6.8), (6.14), (6.21) and (6.15) together with the boundary conditions (6.10), (6.18), (6.22) and (6.19) (6.20) constitute the complete mathematical problem. When these equations are solved, (6.3), (6.4) and (6.13) will give the momentum components.

The equations for $p^{(2)}$ now take the following forms:

$$0 = -p^{(2)}_{,\alpha} + \frac{2}{R}\Delta_2 f^{(2)}_\alpha + \frac{2}{3R}(\sigma^{(1)}_{,0} V^{(1)}_0 + \sigma^{(2)}_{,0} V^{(0)}_0)_{,\alpha}, \tag{6.24}$$

$$V^{(0)}_{0,\beta} V^{(2)}_\beta + V^{(0)}_0 g^{(2)}_0 + 2\sigma^{(1)}_{,0} V^{(1)}_0 V^{(0)}_0 + \sigma^{(2)}_{,0}(V^{(0)}_0)^2$$

$$= -p^{(2)}_{,0} + \frac{2}{R}\Delta(V^{(2)}_0 + \sigma^{(1)} V^{(1)}_0 + \sigma^{(2)} V^{(0)}_0) + \frac{2}{3R}\sigma^{(2)}_{,00} V^{(0)}_0. \tag{6.25}$$

A lengthy reduction gives

$$p^{(2)}_{,\alpha} = \frac{2}{R}\Delta_2 f^{(2)}_\alpha + \chi_{,\alpha} + P_0(l - x_0)V^{(0)}_{0,\alpha}, \tag{6.26}$$

$$p^{(2)}_{,0} = -P_0 V^{(0)}_0 - P_1 - 2P_2(l - x_0) - 3P_3(l - x_0)^2, \tag{6.27}$$

where

$$\chi = \frac{2}{3R}\left(\sigma^{(1)}_{,0} V^{(1)}_0 - \frac{2C^{(1)}_0}{R} V^{(0)}_0\right), \qquad P_0 = -\frac{8\Pi^2(\gamma + 2)}{3R^3}$$

$$P_1 = -\frac{2}{R}(D^{(2)}_0 + lC^{(2)}_0), \qquad P_2 = \frac{1}{R}\left(C^{(2)}_0 + \frac{4\Pi}{R} C^{(1)}_0\right), \qquad P_3 = \frac{4(\gamma + 2)\Pi^3}{3R^3}.$$

Integreting we have

$$p^{(2)} = P_0(l - x_0)V^{(0)}_0 + P_1(l - x_0) + P_2(l - x_0)^2$$

$$+ P_3(l - x_0)^3 + \chi + \frac{4C^{(1)}_0}{3R^2}. \tag{6.27}$$

From the third of (3.8), we have

$$\sigma^{(2)} = -\frac{4\Pi^3(2\gamma + 3)(\gamma + 2)}{3R^3}(l - x_0)^3$$

$$-\left\{\frac{4\Pi C^{(1)}_0(\gamma + 2)}{R^2} + \frac{C^{(2)}_0}{R}\right\}(l - x_0)^2 + \frac{8\Pi^2(\gamma + 2)}{3R^3}(l - x_0) \tag{6.28}$$

$$+ \frac{8\Pi^2}{3R^3}(V^{(0)}_0 + \gamma + 1) - \chi - \frac{4C^{(1)}_0}{3R^2}.$$

7. Drag and flux

In steady flow along the pipe, the skin friction is given by

$$\tau = -\mu\left(\frac{\partial u'_0}{\partial n'}\right)_{n'=0},$$

where n' refers to outer normal to the boundary C. The total resistance or drag is, therefore,

$$D = -2m\mu\bar{u}' \iint \left(\frac{\partial u_0}{\partial n}\right)_{n=0} dS,$$

where the integral is extended over the whole inner surface of the pipe. Introducing the drag coefficient $C_D = D/\frac{1}{2}\bar{\rho}'\bar{u}'^2S'$, and expressing in terms of V_0, we find

$$C_D = -\frac{4}{RS}\int\int \left\{\frac{\partial}{\partial n}(\sigma V_0)\right\}_{n=0} dS. \tag{7.1}$$

Now both V_0 and σ have already been expanded in powers of M. Substituting V_0 and σ respectively from (3.4) and (3.5) in (7.1), we get a new series

$$C_D = C_D^{(0)} + M^2C_D^{(1)} + M^4C_D^{(2)} + \cdots \tag{7.2}$$

of which the general term is

$$C_D^{(r)} = -\frac{4}{RS}\int\int \left\{\sum_{s=0}^{s=r}\frac{\partial}{\partial n}(\sigma^{(s)}V_0^{(r-s)})\right\}_{n=0} dS. \tag{7.3}$$

Another important quantity in the problem of pipe-flow is the flux across any section of the pipe which is given by

$$Q = \int\int \rho' u_0' dx_1' dx_2' .$$

From (3.19) and (3.20) it follows that

$$Q = \bar{\rho}'\,\bar{u}'\,A. \tag{7.4}$$

Let H denote the pressure-head. It is easy to show that

$$H = \frac{4m^2\bar{\rho}'\bar{u}'^2}{A}\int\int (p)_{x_0=0}\, dx_1\, dx_2 . \tag{7.5}$$

This quantity, aside from the dimensions of the pipe, is the only parameter on which the nature of the flow depends. Consequently, it is convenient to define a flux coefficient C_Q such that

$$\frac{Q}{H\cdot\dfrac{AV}{\nu}} = \frac{1}{C_Q}, \tag{7.6}$$

where

$$C_Q = \frac{4m^2lR}{A}\int\int (p)_{x_0=0}\, dx_1\, dx_2 .$$

Substituting p from (3.6), we will have also a series

$$C_Q = C_Q^{(0)} + M^2C_Q^{(1)} + M^4C_Q^{(2)} + \cdots , \tag{7.7}$$

where the rth term is

$$C_Q^{(r)} = \frac{4m^2lR}{A}\int\int (p^{(r)})_{x_0=0}\, dx_1\, x_2 . \tag{7.8}$$

If $p^{(r)}$ is known, $C_Q^{(r)}$ can be calculated; and, when put back in (7.7), we will have C_Q

The way in which the flux coefficient is defined here is not conventional. It is simply a mathematical convenience. For actual calculation its reciprocal should be considered.

Part II. Flow through a circular pipe

8. Poiseuille motion

In this section, we shall choose, as an example to illustrate our method, a pipe with circular section of radius a. We shall use cylindrical coordinates, and assume that the motion possesses axial symmetry. Taking the origin at the centre of the section, the relations between the two systems of coordinates are:

$$x_0 = x_0\,,$$

$$x_1 = r\cos\theta,$$

$$x_2 = r\sin\theta,$$

where r and θ are the polar coordinates in the x_1 and x_2 plane and r is dimensionless, defined according to (1.5) with $m = a/2$.

As each dependent variable is now independent of θ, the Laplacian operator may be written

$$\underset{2}{\Delta} = \frac{1}{r}\frac{d}{dr}\left(r\frac{d}{dr}\right). \tag{8.1}$$

Consequently, equation (4.3) becomes

$$\frac{1}{r}\frac{d}{dr}\left(r\frac{dV_0^{(0)}}{dr}\right) = -\Pi. \tag{8.2}$$

With boundary condition (4.4), this gives

$$V_0^{(0)} = \frac{\Pi}{4}\,(1 - r^2). \tag{8.3}$$

The constant Π is to be determined in accordance with the condition (4.5); this yields

$$\Pi = 8. \tag{8.4}$$

Thus the velocity distribution for Poiseuille motion assumes the usual form:

$$V_0^{(0)} = 2\,(1 - r^2), \qquad V_\alpha^{(0)} = 0. \tag{8.5}$$

The corresponding pressure is

$$p^{(0)} = \frac{16}{R}\,(l - x_0), \tag{8.6}$$

where the Reynolds number now is $R = 2a\bar{u}'/\nu$. Similarly, we have

$$\sigma^{(1)} = -\frac{16}{R}(l - x_0). \tag{8.7}$$

9. First approximation

For the first approximation, we have made the assumption that the component of momentum in the x_1, x_2 plane is zero. The component along x_0 is given by equation (5.3), namely

$$\frac{1}{r}\frac{d}{dr}\left(r\frac{dV_0^{(1)}}{dr}\right) = 32(1 - r^2)^2 + C_0^{(1)}. \tag{9.1}$$

Integrating we have

$$V_0^{(1)} = 32\left(\frac{r^2}{4} - \frac{r^4}{8} + \frac{r^6}{36}\right) + \frac{C_0^{(1)}}{4}r^2 + C_1^{(1)}. \tag{9.2}$$

The values of $C_0^{(1)}$, $C_1^{(1)}$ are found by substitution in (5.4), (5.5) and we obtain

$$C_0^{(1)} = -16, \tag{9.3}$$

$$C_1^{(1)} = -\frac{8}{9}, \tag{9.4}$$

and so

$$V_0^{(1)} = -\frac{4}{9}(-2r^6 + 9r^4 - 9r^2 + 2). \tag{9.5}$$

The pressure $p^{(1)}$ is then given by

$$p^{(1)} = -\frac{128}{R}(l - x_0)^2 + \frac{32}{R}(l - x_0) + \frac{32}{3R^2}(1 - 2r^2). \tag{9.6}$$

Consequently, the specific volume $\sigma^{(2)}$ is

$$\sigma^{(2)} = \frac{128(\gamma + 2)}{R}(l - x_0)^2 - \frac{32}{R}(l - x_0) - \frac{32}{3R^2}(1 - 2r^2). \tag{9.7}$$

10. Second approximation

To simplify the equations (6.1), we have made the assumption that the momentum component $V_0^{(2)}$ for the second approximation possesses the following form:

$$V_0^{(2)} = f_0^{(2)} + x_0 g_0^{(2)},$$

where $f_0^{(2)}$ and $g_0^{(2)}$ are both functions of r alone due to the symmetry. Now $g_0^{(2)}$ is found to satisfy

$$\frac{1}{r}\frac{d}{dr}\left(r\frac{dg_0^{(2)}}{dr}\right) = \frac{572(\gamma + 1)}{R}(1 - r^2)^2 + C_0^{(2)}; \tag{10.1}$$

which has the solution

$$g_0^{(2)} = \frac{512(\gamma+1)}{R}\left(\frac{r^2}{4} - \frac{r^4}{8} + \frac{r^6}{36}\right) + \frac{C_0^{(2)}}{4} r^2 + C_1^{(2)}. \tag{10.2}$$

The constants of integration, determined to satisfy the conditions (6.10), (6.11) are

$$C_0^{(2)} = -\frac{256(\gamma+1)}{R}, \tag{10.3}$$

$$C_1^{(2)} = -\frac{128(\gamma+1)}{9R}. \tag{10.4}$$

Substituting back in (10.2), we have

$$g_0^{(2)} = \frac{64(\gamma+1)}{R}(2r^6 - 9r^4 + 9r^2 - 2). \tag{10.5}$$

As the equation (6.21) for $f_0^{(2)}$ involves the momentum components in the r, θ plane, it cannot be solved so long as the latter quantities remain unknown. They were connected by $\varphi^{(2)}$ and $\psi^{(2)}$ in (6.13) which can be solved from (6.14) and (6.15), namely:

$$\frac{1}{r}\frac{d}{dr}\left(r\frac{d\varphi^{(2)}}{dr}\right) + g_0^{(2)} = 0, \tag{10.6}$$

$$\left\{\frac{1}{r}\frac{d}{dr}\left(r\frac{d}{dr}\right)\right\}\left\{\frac{1}{r}\frac{d}{dr}\left(r\frac{d\psi^{(2)}}{dr}\right)\right\} = 0, \tag{10.7}$$

with the following boundary conditions for $r = 1$:

$$\frac{d\varphi^{(2)}}{dr} = 0, \tag{10.8}$$

$$\psi^{(2)} = 0, \tag{10.9}$$

$$\frac{d\psi^{(2)}}{dr} = 0. \tag{10.10}$$

Substituting $g_0^{(2)}$ from (10.5) in (10.6), we find

$$\frac{1}{r}\frac{d}{dr}\left(r\frac{d\varphi^{(2)}}{dr}\right) = -\frac{64(\gamma+1)}{9R}(2r^6 - 9r^4 + 9r^2 - 2). \tag{10.11}$$

The solution satisfying the boundary condition (10.8), is

$$\varphi^{(2)} = -\frac{2(\gamma+1)}{9R} r^8 - 8r^6 + 18r^4 - 16r^2) + \varphi_0, \tag{10.12}$$

where the constant of integration φ_0 may be arbitrary.

The solution of (10.7), with the boundary conditions (10.9), (10.10) is easily shown to be

$$\psi^{(2)} = \frac{k}{4}(2r^2 \log r - r^2 + 1), \tag{10.13}$$

the constant k being arbitrary. But the vorticity must be finite at the centre; this gives $k = 0$ and hence

$$\psi^{(2)} = 0. \tag{10.14}$$

Thus we arrive at the following results for the momentum components in the r, θ plane:

$$f_r^{(2)} = \frac{16(\gamma+1)}{9R}(-r^7 + 6r^5 - 9r^3 + 4r), \tag{10.15}$$

$$f_\theta^{(2)} = 0. \tag{10.16}$$

This shows that in addition to the main flow along the axis of the pipe there is a radial component which diverges from the centre outward and is symmetrical with respect to the axis of the pipe.

Substituting $g_0^{(2)}$ and $f_r^{(2)}$ respectively from (10.5) and (10.15) in (6.21), a simple reduction gives

$$\begin{aligned}\frac{1}{r}\frac{d}{dr}\left(r\frac{df_0^{(2)}}{dr}\right) = {} & \frac{\Pi^4}{288}(-2r^8 + 11r^6 - 18r^4 + 11r^2 - 2) \\ & - \frac{\Pi}{2}\left[\frac{2(\gamma+1)}{R} - \frac{1}{4}\right](1-r^2)^2 \\ & - \frac{\Pi^3}{3R^2}[(3\gamma+8) - 3(\gamma+2)r^2] \\ & + \frac{(\gamma+1)\Pi^4}{1152}(-3r^8 + 16r^6 - 27r^4 + 18r^2 - 4) + D_0^{(2)}.\end{aligned} \tag{10.17}$$

Integrating we obtain

$$\begin{aligned}f_0^{(2)} = {} & \frac{\Pi^4}{288}\left(-\frac{r^{10}}{50} + \frac{11r^8}{64} - \frac{18r^6}{36} + \frac{11r^4}{16} - \frac{r^2}{2}\right) \\ & - \frac{\Pi^3}{3R^2}\left[\frac{(3\gamma+8)}{4}r^2 - \frac{3(\gamma+2)}{16}r^4\right] \\ & + \frac{(\gamma+1)\Pi^4}{1152}\left[-\frac{3r^{10}}{100} + \frac{r^8}{4} - \frac{3r^6}{4} + \frac{9r^4}{8} - r^2\right] \\ & + \left[\frac{8(\gamma+1)}{R} - 1\right]\left[\frac{r^2}{4} - \frac{r^4}{8} + \frac{r^6}{36}\right] + \frac{D_0^{(2)}}{4}r^2 + D_1^{(2)},\end{aligned} \tag{10.18}$$

where the constants of integration are chosen to satisfy (6.22) and (6.23). Hence two algebraic equations result, which have the solution:

$$D_0^{(2)} = \frac{11\Pi^4}{30\times 288} - \frac{7(\gamma+1)\Pi^4}{5\times 1152} + \left[\frac{4(\gamma+1)l}{R} - \frac{1}{2}\right] + \frac{2(\gamma+3)\Pi^3}{3R^2}. \tag{10.19}$$

$$D_1^{(2)} = \frac{331\Pi^4}{480\times 288} + \frac{151(\gamma+1)\Pi^4}{200\times 1152} + \frac{1}{9}\left[\frac{2(\gamma+1)l}{R} - \frac{1}{4}\right] + \frac{(\gamma+2)\Pi^3}{48R^2}. \tag{10.20}$$

With the constants so determined we have for $f_0^{(2)}$:

$$\begin{aligned} f_0^{(2)} = {} & \frac{8}{2700}[-96r^{10}+825r^8-2400r^6+3300r^4-19600r^2+331] \\ & +\frac{4(\gamma+1)}{45}[-12r^{10}+100r^8-300r^6+450r^4-540r^2+302] \\ & +\left[\frac{(\gamma+1)l}{9R}-\frac{1}{72}\right][-2r^6+9r^4-9r^2+2] \\ & +\frac{32(\gamma+2)}{3R^2}[3r^4-4r^2+1], \end{aligned} \tag{10.21}$$

which, together with $g_0^{(2)}$, will give $V_0^{(2)}$ by (6.3).

The corresponding pressure $p^{(2)}$ is given by

$$\begin{aligned} p^{(2)} = {} & 2P_0(l-x_0)(1-r^2)+P_1(l-x_0) \\ & +P_2(l-x_0)^2+P_3(l-x_0)^3+\frac{128}{27R^2}[2r^6-9r^4+\tfrac{5}{2}], \end{aligned} \tag{10.22}$$

where

$$P_0=-\frac{512(\gamma+2)}{3R^3}, \qquad P_1=\frac{2}{9}\left[\frac{344\gamma+71}{270}+\frac{252(\gamma+1)l}{R}+\frac{1024(\gamma+3)}{R^2}\right]$$

$$P_2=-\frac{256(\gamma+3)}{R^2}, \qquad P_3=\frac{2048(\gamma+2)}{3R^3}.$$

11. Drag and flux

As the velocity and pressure have already been found approximately, we can now calculate the corresponding drag and flux. This calculation is reduced to the calculation of their respective coefficients (7.3), (7.8). For the rth term of the drag coefficient, we find

$$C_D^{(r)} = -\frac{4}{RS}\int_0^l \left\{\sum_{s=0}^{s=R}\frac{d}{dr}(\sigma^{(s)}V^{(r-s)})\right\}_{r=1} dx_0 . \tag{11.1}$$

Substituting $\sigma^{(s)}$ and $V_0^{(r)}$, given in the previous sections, in the above equation, we obtain the following:

$$C_D^{(0)} = \frac{16}{R}, \tag{11.2}$$

$$C_D^{(1)} = -\frac{128l}{R^2}+\frac{32}{R}, \tag{11.3}$$

$$\begin{aligned} C_D^{(2)} = {} & \frac{169200\gamma+675774}{1215R}-\frac{24(\gamma+1)l}{9R}+\frac{2048(\gamma+2)l^2}{R^2} \\ & +\frac{256(9\gamma+5)l}{3R^2}-\frac{512(\gamma+1)}{3R^3} \end{aligned} \tag{11.4}$$

The complete expression for C_D will be of the form:

$$C_D = \frac{16}{R} - \left(\frac{128l}{R^2} - \frac{32}{R}\right)M^2 + \left[\frac{169200\gamma + 675774}{1215R} - \frac{24(\gamma+1)l}{9R} + \frac{2048(\gamma+2)l^2}{R^2} + \frac{256(9\gamma+5)l}{3R^2} - \frac{512(\gamma+1)}{3R^3}\right]M^4 + \cdots. \tag{11.5}$$

The first term gives the usual frictional drag for an incompressible fluid, while the other terms represent the contribution of compressibility. That this effect is positive or negative depends on the relative magnitude of l and R.

For the flux coefficients (7.8), we have

$$C_Q^{(r)} = 2lR\int_0^1 (p^{(r)})_{x_0=0}\, r\, dr, \tag{11.6}$$

for the general term of the C_Q series; the first three terms have the following values:

$$C_Q^{(0)} = 16l^2, \tag{11.7}$$

$$C_Q^{(1)} = -128l^3 + 32l^2, \tag{11.8}$$

$$C_Q^{(2)} = \frac{1344\gamma + 71}{135}l^2 + \frac{248\gamma - 264}{R}l^3 + \frac{5632\gamma + 17408}{3R^2}l^2 + \frac{2048(\gamma+2)}{3R^2}l^4. \tag{11.9}$$

The complete expression for C_Q is

$$C_Q = 16l^2 - (128l^3 - 32l^2)M^2 + \left[\frac{1344\gamma + 71}{135}l^2 + \frac{248\gamma - 264}{R}l^3 + \frac{5632\gamma + 17408}{3R^2}l^2 + \frac{2048(\gamma+2)}{3R^2}l^4\right]M^4 + \cdots. \tag{11.10}$$

The flux coefficient is reduced by compressibility. That is, for a given pressure head, the flux is increased by compressibility.

12. Summary

The problem of the subsonic flow through a pipe of a general section has been treated by the method of series development in ascending even powers of Mach number. Zero approximation is Hagen-Poiseuille motion. The solutions of the equations for the first and second approximations are all reduced to the problem of Dirichlet and the biharmonic problem with specified boundary conditions. The method has been applied to the case of a pipe of circular section for which explicit solutions have been obtained.

The paper was written while the author held a Sino-British Indemnity Fund Scholarship in the Department of Applied Mathematics at the University of Toronto. He wishes to take this opportunity to express his gratitude to Prof. J. L. Synge for suggesting the problem and for his constant guidance in the course of the work.

NATIONAL ADVISORY COMMITTEE FOR AERONAUTICS

TECHNICAL NOTE No. 995

TWO-DIMENSIONAL IRROTATIONAL MIXED SUBSONIC AND SUPERSONIC FLOW OF A COMPRESSIBLE FLUID AND THE UPPER CRITICAL MACH NUMBER [1)]

By Hsue-Shen Tsien and Yung-Huai Kuo

SUMMARY

The problem of flow of a compressible fluid past a body with subsonic flow at infinity is formulated by the hodograph method. The solution in the hodograph plane is first constructed about the origin by superposition of the particular integrals of the transformed equations of motion with a set of constants which would determine, in the limiting case, a known incompressible flow. This solution is then extended outside the circle of convergence by analytic continuation.

The previous difficulty of the Chaplygin method of slow convergence of the series has been overcome by using the asymptotic properties of the hypergeometric functions so that numerical solutions can be obtained without difficulty. It is emphasized that, for a solution covering the whole domain of the field of flow, both fundamental solutions of the hypergeometrical differential equation are required.

Explicit formulas for numerical calculations are given for the flow about a body, such as an elliptic cylinder, and for the periodic flow such as would exist over a wavy surface.

Numerical examples based on the incompressible flow solution of an elliptic cylinder of thickness ratio of 0.6 are computed for free-stream Mach numbers of 0.6 and 0.7.

The results of this investigation indicate an appreciable distortion in the shape of the bodies in compressible flow from that of incompressible flow, which necessitates a series of computations with various values of the geometric parameter in order that the desired body shapes can be selected for a given Mach number. It also is shown that the breakdown of irrotational flow depends solely upon the occurrence of limiting

---

1) *NACA Technical Note*, 1946, No. 995

lines, which, in turn, are dependent on the boundary conditions.

The numerical calculations show that at a free-stream Mach number of 0.6, irrotational supersonic flow exists up to a local Mach number of 1.25; whereas breakdown occurs at 1.22 for a Mach number of 0.7.

INTRODUCTION

When a flow of nonviscous incompressible fluid is irrotational, it is well known that the problem can be reduced to either the problem of Dirichlet or that of Neumann, and that there exists a unique solution for any given boundary conditions. When the fluid is nonviscous but compressible, the variation of density makes the mathematical problem very difficult and complex. In this case, a pure potential flow throughout the region is not always possible for a given body; this depends very much upon the condition at infinity. If a certain speed of the flow at infinity is reached, regions within the field of flow will be created in which the irrotational flow does not exist owing to the appearance of "limiting lines." Such regions were picturesquely designated as "forbidden regions" by Th. von Kármán (reference 1), and they appear when the local speed of the flow considerably exceeds the local speed of sound. It has been shown that the occurrence of limiting lines is directly connected with the breakdown of irrotational flow and with the resultant increase in drag of the body due to shock waves. In other words, if there is a limiting line in the field of flow, the isentrcpic irrotational flow must break down. However, the irrotational flow may break down before the appearance of limiting line due to the instability of the velocity field. On the other hand, shock waves can occur only in supersonic flow. Therefore, there is no danger of breakdown of isentropic flow if the whole field of flow is subsonic. Consequently, the Mach number corresponding to the first appearance of local speed equal to that of sound can be designated as the "lower critical Mach number"; and the Mach number corresponding to the first appearance of limiting lines can be designatcd as the "upper critical Mach number." The actual critical Mach number for a given body will be influenced by the boundary layer and hence the Reynolds number. However, it must lie between these two limiting critical values. (See reference 2.) Thus, knowledge of these critical speeds of the flow are essential for the design of efficient aerodynamic bodies.

To determine the critical Mach numbers, the general problem of flow of a compressible fluid about a given body must be solved. The often-used methods treating such a problem are Janzen-Rayleigh's method of successive approximations and Glauert-Prandtl's method of small perturbation. The latter method has been extended recently by both Hantzsche and Wendt (reference 3) and C. Kaplan (reference 4). Indeed, both methods yield valuable information regarding the effects of compressibility and are useful for many practical design problems, particularly the determination of the lower critical Mach number of a given body. But, so far as the general problem of limiting line and upper critical number is concerned, none seems to be adequate, owing to the doubtful convergence of such successive approximations at the required high Mach numbers.

An entirely different approach first was made by Molenbroek (reference 5) and Chaplygin (reference 6) by introducing the velocity components instead of the usual space coordinates as independent variables. The advantage of the method is that, instead of a nonlinear differential equation as is the case in the physical plane, it leads to a linear one in the velocity or hodograph plane. The particular solutions of this linear equation are found to be products of trigonometric functions of the angle of inclination of velocity vector and hypergeometric functions of the magnitude of the velocity vector. It is then possible to construct a general solution from the particular solutions of the differential equation. The difficulty, however, is that the character of the field in the physical plane to which the solution in the hodograph plane corresponds cannot be determined beforehand. This difficulty prevents the exact formulation of the boundary value problem in the hodograph plane. Chaplygin has overcome this handicap by first choosing a "suitable solution" in the hodograph plane and then proceeding to find the corresponding flow in the physical plane. The suitable solution is one which, in the limiting case of zero Mach number at infinity, becomes identical with the incompressible flow over a body similar to the body concerned. This will ensure the satisfaction of the proper boundary conditions in the physical plane. Furthermore, such a solution would be exact both for the subsonic and for the supersonic regions, as no approximation is introduced. Therefore, it is particularly suitable for the problem of determining the upper critical Mach number for a given body, as limiting lines occur only in mixed subsonic and supersonic flows. This method is followed in the present report, except for the introduction of the transformed potential function χ, for easy calculation of the space coordinates.

For the flow around a body, Chaplygin's procedure will lead to a solution in the form of an infinite series, each term of which is a product of a trigonometric function and a hypergeometric function. To put the method on a firm foundation, it is necessary to establish the convergence of the infinite series. Chaplygin himself has done this for the subsonic region. Thus, only the extension to include the supersonic region remains to be completed. In part I of this report, the general properties of hypergeometric functions of large order are investigated in preparation for the proof of the convergence given in part II. The essential point in these parts is to establish the upper and lower bounds for the hypergeometric functions so that the sum of the infinite series can be discussed. It is appropriate to mention here that for the proper representation of the general solution in the hodograph plane, both fundamental solutions of the hypergeometric differential equation are required. This fact has not been considered by many of the previous investigators in this field. In other cases (reference 7) the investigator has chosen to work with only the first solution.

The general solution constructed by the Chaplygin method is really an existence theorem. [a]The extremely slow convergence of the series makes numerical calculation very difficult, if not impossible. This, in fact, constitutes the main difficulty of the method. In part III of the present report, this difficulty is overcome by using the asymptotic properties of the hypergeometric functions. The result is the separation of the solution in the hodograph plane into two parts. One part is of closed form and is the product of a universal function of the velocity and the same solution as for incompressible flow but with a velocity distortion; or velocity correction. For instance, the first part of the stream function for the compressible flow is equal to the product of the universal function of velocity and the stream function for the incompressible flow with the magnitude of velocity modified by a given rule. The other part is an infinite series which converges rapidly everywhere except in a small region on both sides of a critical circle with a radius equal to $q = c$ in the hodograph plane. In practice, by using only a few terms of the infinite series, this zone of slow convergence can be limited to such a small interval that it is of no consequence. Thus the Chaplygin procedure is improved to a point where actual numerical calculations can be made without difficulty.

As a result of this part of the study it becomes clear

that by the mere substitution of a different speed scale, or velocity distortion, in the solution for an incompressible fluid, an accurate enough solution for the compressible flow cannot be obtained. For if this were the case, then not only the second part of the solution (the rapidly convergent series given by the present method) would be negligible, but also the value of the multiplying universal function of velocity in the first part of the solution would be unity. However, the value of the second part of the solution is not small compared with that of the first part for a speed near that of sound, and the value of the multiplying function of velocity is far from unity. In other words, the usual so-called hodograph method (reference 8) cannot, in general, yield satisfactory results, for mixed subsonic and supersonic flow. On the other hand, the present method does show that the second part of the solution is zero and the multiplying function in the first part takes the constant value of unity, if the isentropic exponent is equal to -1. This means that for this particular case, a simple speed distortion is sufficient. This is, of course, in accordance with the previous investigation of von Kármán (reference 1) and Tsien (reference 9) and L. Bers (reference 10).

Furthermore, the present method also shows that the rules of speed distortion for the first part of the solution can be used only for subsonic flow and that there is a singularity at the local sonic speed. For regions of supersonic flow, the first part of the solution involves both the incompressible stream function and the incompressible potential function. Thus even without considering the second part of the solution, there is no possibility of making the compressible stream lines coincide with those for incompressible flow in the hodograph plane by a simple stretching of the speed scale. The mathematical basis of this fact is the change in character of the differential equation from elliptic to hyperbolic in the transition from subsonic to supersonic flow. For the supersonic regions, it is not possible to use a real transformation of the velocity variable to convert the differential equation of flow to the Laplace equation, and thus make a simple connection between the compressible and the incompressible flows. This is one of the difficulties of the previously proposed hodograph method. In fact, writers using this method must generally limit their calculation to subsonic speeds. (See references 9, 10.) Now this limit is removed, and the whole field of mixed subsonic and supersonic flows can be treated at once with ease.

For the purely subsonic flow, the second part of the

solution is small compared with the first part and may be neglected. Furthermore, if only the zero streamline representing the body is considered, the universal multiplying function of velocity is of no importance. In other words, for this case, a simple speed distortion from the solution of incompressible flcw is sufficient to give accurate enough results. Hcwever, the subject of the "best" velocity distortion rule in subsonic regions has been the subject of many discussions. (See references 1 and 6.) The present analysis is considered tc settle this question. This is due to the fact that the present velocity distortion rule is obtained from the asymptotic properties of the hypergeometric functions, and that such properties are definite and unique. Therefore, the resultant velocity distortion rule is not the result of uncertain speculation. Furthermore, it is also the best rule, because the analysis implies that this rule will make the second part of the solution, or the correction terms, the smallest. This distortion rule is found to coincide with that of Temple and Yarwood. (See reference 11.)

For the purely supersonic flow, the second part of the solution is again small compared with the first part and may be neglected. In fact, the solution then can be reduced to that of the simple wave equation with the inclination of the velocity vector and the distorted velocity as independent variables. This is, of course, the counterpart of the fact that by a simple distortion in velocity, the differential equation for subsonic flows can be reduced to the Laplace equation. The usefulness of this new result for purely supersonic flow has yet to be exploited.

Once the general problem of mixed subsonic and supersonic flow around a body is solved, the determination of the upper critical Mach number or the Mach number for the first appearance of the limiting lines is a simple matter. This problem is discussed in part IV of the report. A simple method is developed, based on the properties of the limiting line as given by von Kármán (reference 1), Ringleb (reference 12), Tollmien (reference 13), and Tsien (reference 2).

To test the practicability of the method developed, two numerical examples are worked out in detail. However, in order to reduce the amcunt of computaticnal work and in view of the limited time available, a slightly different procedure actually is used. This procedure is only approximate but is

believed to be sufficiently accurate in the supersonic region to give a satisfactory description of the most interesting features of such flows. The examples chosen are derived from the incompressible solution of an elliptic cylinder of thickness ratio 0.6. The free-stream Mach numbers of the compressible flow are 0.6 and 0.7 for these two examples. The first case gives a smooth flow over an "elliptic" cylinder of thickness ratio 0.42. The maximum local Mach number is approximately 1.25. Thus a considerable supersonic region exists. The second case gives a flow with limiting line.

Finally, it must be said that owing to the limitation of time, only the case of flow without circulation is investigated in detail. The explicit formulas for numerical calculation are given for two cases: (a) Flow around a body such as an ellipse, (b) periodic flow pattern such as that over a wavy surface. However, it is believed that more general cases can be studied by a slight extension of the present results and use of the same method of approach.

This investigation, conducted at the Guggenheim Aeronautics Laboratory, California Institute of Technology, was sponsored by and conducted with the financial assistance of the National Advisory Committee for Aeronautics.

NOTATIONS

The symbols used in this report are classified according to the following groups:

A. Physical Quantities

x, y Cartesian coordinates

u, v the velocity components

q the absolute value of the velocity vector

ϑ the inclination of the velocity vector with x-axis

ρ density of the fluid

ρ_o density of the fluid at $q = 0$

p pressure within the fluid corresponding to ρ

p_o pressure at $q = 0$

γ ratio of the specific heats

c the local speed of sound

c_o the speed of sound at $q = 0$

U the value of q at infinity, assuming parallel to the x-axis. With subscript, however, it may be a function of τ.

B. Hydrodynamic Functions in the Physical Plane

$z = x + iy$

$W_o(z) = \varphi_o(x,y) + i\psi_o(x,y)$ complex potential for incompressible flow in z

φ_o velocity potential for incompressible flow

ψ_o stream function for incompressible flow

φ velocity potential for compressible flow

ψ stream function for compressible flow

C. Hydrodynamic Functions in the Hodograph Plane

$w = u - iv$

$W_o(w) = \varphi_o(u,v) + i\psi_o(u,v)$ complex potential for incompressible flow in w

$\varphi_o(u,v)$ velocity potential for incompressible flow

$\psi_o(u,v)$ stream function for incompressible flow

$\Lambda_o(w) = zw - W_o(w) = \chi_o(u,v) - i\sigma_o(u,v)$ transformed complex potential function

$\chi_o(u,v) = ux + vy - \varphi_o(x,y)$; $x = \frac{\partial \chi_o}{\partial u}$,

$y = \frac{\partial \chi_o}{\partial v}$ transformed potential function

$W(w;\tau)$ the complex potential function for compressible flow

$\psi(u,v) = \mathrm{Im}\left\{W(w;\tau)\right\}$ stream function for compressible flow

$\Lambda(w;\tau)$ transformed complex potential function for compressible flow

$\chi(u,v) = ux + vy - \varphi(x,y) = R\imath\left\{\Lambda(w;\tau)\right\}$ transformed potential function for compressible flow

$$\Theta_o(u,v) = \frac{\partial \chi_o}{\partial \vartheta}$$

$$\Omega_o(u,v) = \frac{\partial \sigma_o}{\partial \vartheta}$$

$\psi(q,\vartheta) = \psi_1(q,\vartheta) + \psi_2^{(\imath)}(q,\vartheta)$; $\psi_1(q,\vartheta)$ represents the contribution by the velocity distorsion; $\psi_2^{(\imath)}(q,\vartheta)$ stands for the transformed infinite series, where the superscript $\imath$ may either mean i the inner, or o the outer solution. In the case of coordinates, the notation is exactly the same.

$$G_\upsilon^{(\alpha)}(\tau) = \underline{F}_\upsilon(\tau)\Delta B_n^{(\alpha)} + \frac{B_n \Delta \underline{F}_\upsilon(\tau)}{f(\tau_1)T^\upsilon(\tau_1)}$$

$$\tilde{G}_\upsilon^{(\alpha)}(\tau) = \underline{\tilde{F}}_\upsilon(\tau)\Delta \tilde{B}_n^{(\alpha)} + \frac{B_n \Delta \underline{F}_\upsilon(\tau)}{f(\tau_1)T^\upsilon(\tau_1)}$$

$$\tilde{G}_{\upsilon,1}^{(\alpha)}(\tau) = \frac{\upsilon - 1}{\upsilon + 1}\underline{\tilde{F}}_{\upsilon,1}(\tau)\Delta \tilde{B}_n^{(\alpha)} + \frac{\tilde{B}_n \Delta \underline{\tilde{F}}_{\upsilon,1}(\tau)}{f(\tau_1)T^\upsilon(\tau_1)}$$

D. Parameters and Variables

ν positive rational numbers

m,n positive integers

α denotes 1 or 2 when used as superscript with a bracket

or $\alpha = \sqrt{\frac{\gamma + 1}{\gamma - 1}}$

β denotes the dependence on β when used as subscript

or $\beta = \frac{1}{\gamma - 1}$

$\lambda = \frac{2(2\beta)^{\alpha/2}}{(1 + \alpha)^{\alpha}} \frac{1}{\sqrt{2\beta\tau_1}} \frac{1}{T(\tau_1)}$ the ratio of the distorted speed to that at infinity

$\tau = \frac{1}{2\beta} \frac{q^2}{c_o^2}$

$\mu = \cos^{-1}\sqrt{\frac{\alpha^2\tau - 1}{2\beta\tau}}$

ξ,η With superscript or subscript they denote some functions of τ or stand for the two families of the characteristic parameters $\vartheta + \omega(\tau)$, $\vartheta - \omega(\tau)$ of the partial differential equations for $\psi(q,\vartheta)$ or $\chi(q,\vartheta)$.

ζ complex variable or $\zeta(\tau)$ a function of τ

$M_1 = \frac{U}{c_1}$ the Mach number at infinity

$\tau_1 = \frac{1}{2\beta} \frac{U^2}{c_o^2}$

ϵ geometrical parameter of the body

Δ Laplacian or difference between exact and approximate values of a function or a constant

E. Hypergeometric Functions

a,b,c parameters of the hypergeometric functions. In particular, a_ν, b_ν, c_ν are defined by (29).

$\underline{F}_\nu(\tau) = F(a_\nu, b_\nu; c_\nu; \tau)$ first integral of the hypergeometric equation associated with the stream function

$$\underline{F}_{-\nu}(\tau) = F(1 + a_\nu - c_\nu, 1 + b_\nu - c_\nu; 2 - c_\nu; \tau)$$

$$F_\nu(\tau) = \frac{\pi\ \tau^{-\nu}}{(2\beta c_o^2)^\nu\, \Gamma(c_\nu-1)\Gamma(c_\nu)} \left[\frac{\Gamma(a_\nu)\Gamma(b_\nu)}{\Gamma(1+a_\nu-c_\nu)\Gamma(1+b_\nu-c_\nu)}\ \tau^\nu\ \underline{F}_\nu(\tau)\right.$$

$$\left. - \frac{\Gamma(c_\nu)}{\Gamma(2-c_\nu)}\ \underline{F}_{-\nu}(\tau)\right] \quad \text{second integral of the same equation}$$

$$\underline{G}_\nu(\tau) = q^{2\nu}\ F_\nu(\tau)$$

$$\underline{F}_{\nu,1}(\tau) = F(1+a_\nu, 1+b_\nu; 1+c_\nu; \tau)$$

$$\underline{F}_\nu^{(r)}(\tau) = \underline{F}_\nu(\tau)/\underline{F}_\nu(\tau_1)$$

$$\underline{F}_{\nu,1}^{(r)}(\tau) = \underline{F}_{\nu,1}(\tau)/\underline{F}_\nu(\tau_1)$$

$$\underline{F}^*_\nu(\tau) = \underline{F}_\nu(\tau) + i\, F_\nu(\tau)$$

$$R_\nu(\tau) = \left|\underline{F}^*_\nu(\tau)\right|$$

$$\Phi_\nu(\tau) = \arg \underline{F}^*_\nu(\tau)$$

If any function or a constant is associated with $\chi(q, \vartheta)$, it will be marked on top by a symbol ~, such as $\underline{F}_\nu(\tau)$.

PART I

DIFFERENTIAL EQUATIONS OF COMPRESSIBLE FLOW AND PROPERTIES OF THEIR PARTICULAR SOLUTIONS

1. Equations of Motion

It is proposed to study the irrotational steady motion of an inviscid nonconducting compressible fluid in an infinitely extended domain containing a cylindrical body with its axis perpendicular to the constant velocity at infinity. The flow is then two-dimensional. Let x and y be the Cartesian coordinates and u and v the velocity components parallel to the x- and the y-axis. The dynamical equations governing such a motion, in the absence of body force, are

$$\rho u \frac{\partial u}{\partial x} + \rho v \frac{\partial u}{\partial y} = - \frac{\partial p}{\partial x} \tag{1}$$

$$\rho u \frac{\partial v}{\partial x} + \rho v \frac{\partial v}{\partial y} = - \frac{\partial p}{\partial y} \tag{2}$$

Here p is the pressure and ρ the density of the fluid, both being continuous functions of x and y. In addition, the following equation of continuity must be satisfied:

$$\frac{\partial}{\partial x} (\rho u) + \frac{\partial}{\partial y} (\rho v) = 0 \tag{3}$$

Furthermore, since the velocity is constant at infinity, the flow is irrotational there. Then, according to Thomson's theorem, if the pressure is a function of the density alone, the flow will remain irrotational; that is,

$$\frac{\partial v}{\partial x} - \frac{\partial u}{\partial y} = 0 \tag{4}$$

In the case of flow of an inviscid nonconducting gas, the thermodynamic change of state of the gas is adiabatic. If

the flow is assumed to be continuous, exeluding shock waves, then the relation between p and ρ must be that of an isentropic process:

$$p = \text{constant}\ \rho^{\gamma} \tag{5}$$

where γ is the ratio of the specific heats.

As in the case of incompressible flow, there are more equations than the number of the variables. However, by virtue of equations (4) and (5), the dynamical equations (1) and (2) reduce to a single differential equation and can be integrated easily to give a relation between the pressure and the magnitude q of the velocity: namely,

$$p = p_o \left\{1 - \frac{\gamma - 1}{2} \frac{q^2}{c_o^2}\right\}^{\frac{\gamma}{\gamma-1}}, \quad \text{with} \quad q^2 = u^2 + v^2 \tag{6}$$

Here p_o and c_o are respectively the pressure and the speed of sound at the stagnation point $q = 0$ and $c = \sqrt{\frac{dp}{d\rho}}$. It is possible to obtain a similar relation between ρ and q by means of equation (5):

$$\rho = \rho_o \left\{1 - \frac{\gamma - 1}{2} \frac{q^2}{c_o^2}\right\}^{\frac{1}{\gamma-1}} \tag{7}$$

where ρ_o denotes the value of ρ at $q = 0$.

After integrating the dynamical equations, the velocities u and v can be determined from the kinematic conditions specified by equations (3) and (4). By eliminating ρ from equation (3), the result is

$$\left(1 - \frac{u^2}{c^2}\right)\frac{\partial u}{\partial x} - \frac{2uv}{c^2}\frac{\partial u}{\partial y} + \left(1 - \frac{v^2}{c^2}\right)\frac{\partial v}{\partial y} = 0 \tag{8}$$

where $c^2 = \gamma p/\rho$ and thus can be calculated in terms of the speed by equations (6) and (7). It is of interest to note that the equation of continuity (8) now, unlike the case of incompressible flow, becomes dependent on the dynamical equations and, consequently, is nonlinear. This change in the

character of the fundamental equation makes the direct solution of the problem in space coordinates very difficult.

2. Transformation of the Differential Equations

The assumption of irrotationality implies the existence of a velocity-potential for such a flow. If this function is introduced to eliminate u and v, equations (4) and (8) would give rise to a nonlinear partial differential equation of the second order. The problem is further complicated by the possible appearance of supersonic regions, or regions where the speed of flow is larger than the local sonic speed. This means that for some part of the domain, the equation is of the elliptic type; while in the other part, it is of the hyperbolic type. Thus the equation not only is nonlinoar but also is of mixed type, and there is as yet no successful method to deal with it directly in the physical plane. Molenbroek (reference 5) and Chaplygin (reference 6) made some progress in solving the problem by transforming the equations from the physical to the hodograph plane in which u and v are taken as the independent variables. If this is done, the differential equations become linear and thus can be solved by well-known methods.

Let the transformation be defined by

$$u = u(x,y) \tag{9}$$

$$v = v(x,y) \tag{10}$$

If u and v are continuous functions of x and y with continuous partial derivatives, and if the Jacobian $\left(\frac{\partial(x,y)}{\partial(u,v)}\right)$ is finite and nonvanishing, a unique inverse transformation exists. Under these conditions, equations (8) and (4) are easily transformed into

$$\left(1 - \frac{u^2}{c^2}\right)\frac{\partial y}{\partial v} + \frac{2uv}{c^2}\frac{\partial x}{\partial v} + \left(1 - \frac{v^2}{c^2}\right)\frac{\partial x}{\partial u} = 0 \tag{11}$$

$$\frac{\partial x}{\partial v} - \frac{\partial y}{\partial u} = 0 \tag{12}$$

Corresponding to $\varphi(x,y)$ in the physical plane, there is introduced here a function $\chi(u,v)$ defined by

$$\chi = xu + yv - \varphi; \quad x = \frac{\partial \chi}{\partial u}, \quad y = \frac{\partial \chi}{\partial v} \tag{13}$$

While equation (12) is satisfied identically, equation (11) becomes

$$\left(1 - \frac{u^2}{c^2}\right)\frac{\partial^2 \chi}{\partial v^2} + \frac{2vu}{c^2}\frac{\partial^2 \chi}{\partial v \partial u} + \left(1 - \frac{v^2}{c^2}\right)\frac{\partial^2 \chi}{\partial u^2} = 0 \tag{14}$$

As c is a function of q alone, the equation for $\chi(u,v)$ is then linear. From equation (13) it is recognized that if $\chi(u,v)$ is known, a one-to-one correspondence between the space coordinates and the velocity components can be easily established.

However, it is also clear that this function is inconvenient for obtaining the streamlines and the flow in the physical plane. To solve this part of the problem, a plan may be adopted similar to Chaplygin's by introducing both the potential function $\varphi(x,y)$ and the stream function $\psi(x,y)$ defined by:

$$u = \frac{\partial \varphi}{\partial x}, \quad v = \frac{\partial \varphi}{\partial y} \tag{15}$$

$$\rho u = \rho_o \frac{\partial \psi}{\partial y}, \quad \rho v = -\rho_o \frac{\partial \psi}{\partial x} \tag{16}$$

From these definitions are obtained immediately the following equivalent relations:

$$d\varphi = udx + vdy \tag{17}$$

$$\rho_o d\psi = -\rho v dx + \rho u dy \tag{18}$$

For the subsequent calculations, it was found convenient to introduce the polar coordinates in the hodograph plane defined by:

$$u = q \cos \theta, \quad v = q \sin \theta \tag{19}$$

where θ is the inclination of the velocity vector to the x-axis. Functions dx and dy can be solved for from equations (17) and (18). As dx and dy are exact differentials, the conditions of integrability then give:

$$\frac{\partial \varphi}{\partial q} = - \frac{\rho_o}{\rho} \left(1 - \frac{q^2}{c^2}\right) \frac{1}{q} \frac{\partial \psi}{\partial \theta} \tag{20}$$

$$\frac{1}{q} \frac{\partial \varphi}{\partial \theta} = \frac{\rho_o}{\rho} \frac{\partial \psi}{\partial q} \tag{21}$$

By eliminating φ between equations (20) and (21), an equation for ψ is obtained:

$$q^2 \frac{\partial^2 \psi}{\partial q^2} + \left(1 + \frac{q^2}{c^2}\right) q \frac{\partial \psi}{\partial q} + \left(1 - \frac{q^2}{c^2}\right) \frac{\partial^2 \psi}{\partial \theta^2} = 0 \tag{22}$$

Equation (14) can also be transformed in polar coordinates. The procedure is straightforward and yields

$$q^2 \frac{\partial^2 \chi}{\partial q^2} + \left(1 - \frac{q^2}{c^2}\right) q \frac{\partial \chi}{\partial q} + \left(1 - \frac{q^2}{c^2}\right) \frac{\partial^2 \chi}{\partial \theta^2} = 0 \tag{23}$$

There is an additional relation between χ and φ derived from equation (13):

$$\varphi = q\chi_q - \chi \tag{24}$$

Since φ is connected with ψ, this relation ensures that ψ and χ are properly connected and represent the same flow pattern in the physical plane. It can be thus considered as the equation of compatibility. Equations (22), (23), and (24) are the three fundamental equations in the present problem dealing with the two-dimensional flow of a compressible fluid.

3. The Particular Solutions of the Differential Equations

As the differential equations for $\psi(q,\theta)$ and $\chi(q,\theta)$ are linear, a general solution can certainly be built by superimposing the particular integrals of the equations. To obtain the particular integrals, let $\psi(q,\theta)$ and $\chi(q,\theta)$ be of the following forms:

$$\psi(q,\theta) = q^{\nu}\,\psi_{\nu}(q)\,e^{i\nu\theta}$$

$$\chi(q,\theta) = q^{\nu}\,\chi_{\nu}(q)\,e^{i\nu\theta}$$

where ν is any real number. By substituting in equations (22) and (23), the equations satisfied by $\psi_{\nu}(q)$ and $\chi_{\nu}(q)$ are:

$$q^2\frac{d^2\psi_{\nu}}{dq^2} + \left(2\nu + 1 + \frac{q^2}{c^2}\right) q\frac{d\psi_{\nu}}{dq} + \nu(\nu+1)\frac{q^2}{c^2}\psi_{\nu} = 0 \quad (25)$$

$$q^2\frac{d^2\chi_{\nu}}{dq^2} + \left(2\nu + 1 - \frac{q^2}{c^2}\right) q\frac{d\chi_{\nu}}{dq} + \nu(\nu-1)\frac{q^2}{c^2}\chi_{\nu} = 0 \quad (26)$$

Now each of these equations can be further reduced by changing the independent variable. The appropriate transformation is found to be

$$\tau = \frac{1}{2\beta}\frac{q^2}{c_o^2}, \qquad \text{with} \quad \beta = \frac{1}{\gamma - 1}$$

By expanding the gas to zero pressure, or vacuum, the maximum velocity is obtained. Equation (6) shows that the maximum speed is $q_{max} = \sqrt{\frac{2}{\gamma-1}}\,c_o$. Therefore, the maximum value of τ is unity. Similarly, it is found that for the speed of the flow equal to the local sonic speed, $\tau = \frac{1}{2\beta+1}$, equations (25) and (26) then become

$$\tau(1-\tau)\psi_{\nu}''(\tau) + \left[c_{\nu} - (a_{\nu} + b_{\nu} + 1)\tau\right]\psi_{\nu}'(\tau) - a_{\nu}b_{\nu}\psi_{\nu}(\tau) = 0 \quad (27)$$

$$\tau(1-\tau)\chi_\nu''(\tau) + \left[c_\nu - (a_\nu + \beta + b_\nu + \beta + 1)\tau\right]\chi_\nu'(\tau) - (a_\nu + \beta)(b_\nu + \beta)\chi_\nu(\tau) = 0 \quad (28)$$

where

$$a_\nu + b_\nu = \nu - \beta, \quad a_\nu b_\nu = -\frac{1}{2}\beta\nu(\nu+1), \quad \text{and} \quad c_\nu = \nu + 1 \quad (29)$$

These are the hypergeometric equations, of which equation (27) was first obtained by Chaplygin in 1904. (See reference 6.) The differential equation of this type has three regular singularities at 0, 1, and $+\infty$. If the differences of the two exponents at the respective singularities: namely, $c - 1$, $a - b$, $a + b - c$, are not integers or zero, the two fundamental independent solutions are $F(a,b;\ c;\ \tau)$ and $\tau^{1-c}\ F(1 + a - c,\ 1 + b - c;\ 2 - c;\ \tau)$. They are single-valued and regular in the whole plane with a cut from +1 to $+\infty$. The function $F(a,b;\ c;\ \tau)$ known as the hypergeometric function of general parameters a, b, and c, is defined by the hypergeometric series which is absolutely and uniformly convergent when $|\tau| < 1$, provided $Re(c - a - b) > 0$. For $|\tau| > 1$, analytic continuation has to be used. Furthermore, it is normalized so that at $\tau = 0$

$$F(a,b;\ c;\ 0) = 1 \quad (30)$$

Hence, the particular solutions of equation (27) are

$$F(a_\nu, b_\nu; c_\nu; \tau), \quad \tau^{1-c_\nu}\ F(1 + a_\nu - c_\nu,\ 1 + b_\nu - c_\nu;\ 2 - c_\nu; \tau) \quad (31)$$

The particular solutions of equations (28) are

$$F(a_\nu + \beta;\ b_\nu + \beta;\ c_\nu;\ \tau), \quad \tau^{1-c_\nu}\ F(1 + a_\nu + \beta - c_\nu,\ 1 + b_\nu + \beta - c_\nu;\ 2 - c_\nu;\ \tau) \quad (32)$$

Here a_ν, b_ν, and c_ν are parameters defined by equation (29).

When ν is a positive integer while a_ν and b_ν remain as they are, the second integral will reduce to a constant multiple of the first one. This case was first studied by Gauss (reference 14), who found a second integral involving a logarithmic term by considering the limiting value of the integrals given as ν tends to an integral value. The method has been further developed by Tannery (reference 15) and Goursat (reference 16). However, the form regarded as conventional nowadays was that obtained by Frobenius' general method. According to this method, the pair of fundamental solutions of a hypergeometric equation are

$$F(a,b;\ n+1;\ \tau),\quad K_n\,\tau^{-n}\left\{\tau^n F(a,b;\ n+1;\ \tau)\log\tau + \tau^n\, Q_n^{(1)}(a,b;\ \tau) + P_{n-1}^{(1)}(\tau)\right\} \tag{33}$$

when $c_n = n + 1$, n being a positive integer; and

$$Q_n^{(1)}(a,b;\tau) = \frac{\Gamma(n+1)}{\Gamma(a)\Gamma(b)}\sum_0^\infty \frac{\Gamma(a+m)\Gamma(b+m)}{\Gamma(m+1)\Gamma(n+1+m)}\psi(a,b;\ m)\,\tau^m$$

$$P_{n-1}^{(1)}(\tau) = (-1)^{n+1}\frac{\Gamma(n+1)}{\Gamma(a)\Gamma(b)}\sum_0^{n-1}(-1)^m\frac{\Gamma(a-n+m)\Gamma(b-n+m)\Gamma(n-m)}{\Gamma(m+1)}\tau^m \tag{34}$$

$$\psi(a,b;\ m) = \sum_{r=0}^{m-1}\left[\frac{1}{a+r}+\frac{1}{b+r}-\frac{1}{n+1+r}\right]-\sum_{r=1}^{m}\frac{1}{r}$$

Here a, b may be either a_n, b_n or $a_n + \beta$, $b_n + \beta$ defined in equation (29) according to whether the system (33) is referred to as solutions of equation (27) or (28). And K_n can be determined so that the product of the second integral and q^{2n} satisfies the condition (30).

In view of the fact that the second integral in (33) does not constitute a family of solutions with the second integral given in (31) or (32), it is very desirable to define a new function as second integral which will be continuous in ν as well as in τ. Let $\underline{F}_\nu(\tau)$ denote the first integral

$F(a,b;\ c_\nu;\ \tau)$. As a second integral, take the linear combination of the solutions:

$$F_\nu(\tau) = K_\nu \left\{\Gamma(1 - c_\nu)\Gamma(a)\Gamma(b)\underline{F}_\nu(\tau) + \Gamma(1 - c_\nu)\Gamma(1 + a - c_\nu)\Gamma(1 + b - c_\nu)\tau^{1-c_\nu}\ \underline{F}_{-\nu}(\tau)\right\} \quad (35)$$

where

$$\underline{F}_{-\nu}(\tau) = F(1 + a - c_\nu,\ 1 + b - c_\nu;\ 2 - c_\nu;\ \tau)$$

This is evidently a solution and valid for all values of ν. The constant K_ν is determined subject to the following condition:

$$q^{2\nu}\ F_\nu(\tau) = 1 \quad \text{for} \quad \tau = 0 \quad (36)$$

The value of K_ν then is found to be

$$K^{-1} = (2\beta c_o)^\nu\ \Gamma(c_\nu - 1)\Gamma(1 + a - c_\nu)\Gamma(1 + b - c_\nu)$$

Using the relation

$$\Gamma(c_\nu)\Gamma(1 - c_\nu) = \pi\ \csc\ c_\nu\pi$$

equation (35), when multiplied by $q^{2\nu}$, will define a new function $\underline{G}_\nu(\tau)$: $a,\ b \neq -n$

$$\underline{G}_\nu(\tau) = \frac{\pi}{\sin\ c_\nu\pi}\left[\frac{\Gamma(a)\Gamma(b)\ \tau^\nu\ \underline{F}_\nu(\tau)}{\Gamma(c_\nu)\Gamma(c_\nu - 1)\Gamma(1 + a - c_\nu)\Gamma(1 + b - c_\nu)} - \frac{\underline{F}_{-\nu}(\tau)}{\Gamma(c_\nu - 1)\Gamma(2 - c_\nu)}\right] \quad (37)$$

When ν takes integral values, the expression in the bracket vanishes; however, the limit of the ratio exists:

$$\underline{G}_n(\tau) = \lim_{\nu \to n} \underline{G}_\nu(\tau) \quad (38)$$

The usual definition of the limit of a quotient gives

$$(\tau) = (-1)^{n+1}\left[\frac{\partial}{\partial\nu}\frac{\Gamma(a)\Gamma(b)\ \tau^{\nu}\ \underline{F}_{\nu}(\tau)}{\Gamma(\nu+1)\Gamma(a-\nu)\Gamma(b-\nu)} - \frac{\partial}{\partial\nu}\frac{\underline{F}_{-\nu}(\tau)}{\Gamma(\nu)\Gamma(1-\nu)}\right]_{\nu=n}$$

By considering separately the first n terms in $\underline{F}_{-\nu}(\tau)$, as $\Gamma(1-\nu)$ has poles at $\nu = n$, a straightforward reduction yields:

$$\underline{G}_n(\tau) = \underline{C}_n\ \tau^n \log\tau\ \underline{F}_n(\tau) + \tau^n Q_n^{(2)}(\tau) + P_{n-1}^{(2)}(\tau) \quad (39)$$

where

$$Q_n^{(2)}(\tau) = \frac{(-1)^{n+1}}{\Gamma(n)\Gamma(-n+a)\Gamma(-n+b)}\sum_{m=0}^{\infty}\left[\psi(a+m)+\psi(b+m)-\psi(c_n+m)-\psi(m+1)\right]\frac{\Gamma(a+m)\Gamma(b+m)}{\Gamma(c_n+m)\Gamma(m+1)}\tau^m$$

$$P_{n-1}^{(2)}(\tau) = \frac{1}{\Gamma(n)\Gamma(a-n)\Gamma(b-n)}\sum_{m=0}^{n-1}(-1)^m\frac{\Gamma(a-n+m)\Gamma(b-n+m)\Gamma(n-m)}{\Gamma(m+1)}\tau^m$$

$$\underline{C}_n = \frac{(-1)^{n+1}\Gamma(a)\Gamma(b)}{\Gamma(n)\Gamma(n+1)\Gamma(a-n)\Gamma(b-n)}$$

and $\psi(\xi)$ denotes the derivative of $\log\Gamma(\xi)$. It can be seen that the difference between (33) and (39) lies only in a constant multiple of the first integral which has been absorbed in $Q_n^{(2)}(\tau)$.

In the following discussions, the two fundamental solutions of the hypergeometric differential equation will be taken as $\underline{F}_{\nu}(\tau)$ and $q^{-2\nu}\underline{G}_{\nu}(\tau)$. The normalization conditions given by (30) and (36) are chosen for the continuous passage of a compressible to an incompressible flow. Ultimately, these functions are again defined in terms of power series which are absolutely and uniformly convergent within the domain $|\tau| < 1$. However, since the maximum value of τ attainable by the fluid is unity, the continuation of the solutions beyond the unit circle will not be discussed here.

Thus $\underline{F}_\nu(\tau)$ and $q^{-2\nu}\underline{G}_\nu(\tau)$ denote the two independent integrals of equation (27) where ν is any positive number. The particular solutions of equation (22) are then:

$$q^\nu \underline{F}_\nu(\tau)\left[A_\nu^{(1)} \cos \nu\vartheta + A_\nu^{(2)} \sin \nu\vartheta\right], \quad q^{-\nu}\underline{G}_\nu(\tau)\left[B_\nu^{(1)} \cos \nu\vartheta + B_\nu^{(2)} \sin \nu\vartheta\right] \tag{40}$$

where $A_\nu^{(1)}$, $A_\nu^{(2)}$, $B_\nu^{(1)}$, and $B_\nu^{(2)}$ are constants. Similarly, those of equation (23) are

$$q^\nu \underline{\tilde{F}}_\nu(\tau)\left[\tilde{A}_\nu^{(1)} \cos \nu\vartheta + \tilde{A}_\nu^{(2)} \sin \nu\vartheta\right], \quad q^{-\nu}\underline{\tilde{G}}_\nu(\tau)\left[\tilde{B}_\nu^{(1)} \cos \nu\vartheta + \tilde{B}_\nu^{(2)} \sin \nu\vartheta\right] \tag{41}$$

where $\underline{\tilde{F}}_\nu(\tau)$ and $q^{-2\nu}\underline{\tilde{G}}_\nu(\tau)$ are the two independent integrals of equation (28) and $\tilde{A}_\nu^{(1)}$, $\tilde{A}_\nu^{(2)}$, $\tilde{B}_\nu^{(1)}$, and $\tilde{B}_\nu^{(2)}$ are constants.

In addition to these solutions, there are two other integrals each of which is a function of one variable only. Assuming $\psi = \psi(q)$ or $\psi(\vartheta)$, then equations (22) and (23) yield respectively:

$$c_1 \vartheta \quad \text{and} \quad c_2 \int (1 - \tau)^\beta \frac{d\tau}{\tau} \tag{42}$$

$$\tilde{c}_1 \vartheta \quad \text{and} \quad \tilde{c}_2 \int (1 - \tau)^{-\beta} \frac{d\tau}{\tau} \tag{43}$$

which correspond to the fundamental solution of the Laplace equation.

As c_o approaches infinity, all these particular solutions reduce to the familiar harmonic functions: namely,

$$q^\nu\left[A_\nu^{(1)} \cos \nu\vartheta + A_\nu^{(2)} \sin \nu\vartheta\right], \quad q^{-\nu}\left[B_\nu^{(1)} \cos \nu\vartheta + B_\nu^{(2)} \sin \nu\vartheta\right] \tag{44}$$

and

$$c_1 \vartheta, \qquad c_2 \log q \tag{45}$$

This property which is the consequence of (30) and (36) is essential in the method presented in this report for connecting a compressible flow with the incompressible flow of similar configuration.

In the subsequent calculations, another integral will be encountered for the function $\chi(q, \vartheta)$ which corresponds to the imaginary part of $w \log w e^{i\pi}$ or $q \log q \sin \vartheta - q(\pi - \vartheta) \cos \vartheta$ of the incompressible flow. Suppose the solution possesses the form:

$$\chi(q, \vartheta) = \chi_1(q) \sin \vartheta - \chi_2(q)(\pi - \vartheta) \cos \vartheta \tag{46}$$

By substituting the expression in equation (23), χ_1 and χ_2 are found to satisfy simultaneously the following differential equations:

$$q^2 \chi_1''(q) + \left(1 - \frac{q^2}{c^2}\right)\left(q\chi_1' - \chi_1\right) = 2\left(1 - \frac{q^2}{c^2}\right)\chi_2 \tag{47}$$

$$q^2 \chi_2'' + \left(1 - \frac{q^2}{c^2}\right)\left(q\chi_2' - \chi_2\right) = 0 \tag{48}$$

Equation (48) can be easily integrated by putting $\chi_2 = qk_2(q)$. The condition that $\chi_2 \to q$ as $c_0 \to \infty$ requires $k_2(q)$ to be a constant. The second integral of equation (48) is just the second of (43) which, in the limit, tends to $\log q$. Thus $\chi_2 = q$ is the appropriate solution. With this solution, it is possible to proceed to solve equation (47) by assuming $\chi_1 = q\,k_1(q)$. The equation for $k_1(q)$ is again integrable by quadrature, and the result is

$$k_1(q) = \frac{1}{2(\beta + 1)}\left[(2\beta + 1)\log \tau - \frac{1}{\tau} + K_1 \int^{\tau} (1 - \tau)^{-\beta} \frac{d\tau}{\tau^2}\right] + K_2 \tag{49}$$

where K_1 and K_2 are the constants of integration. Hence, the desired particular integral is

$$\chi(q,\vartheta) = qk_1(\tau) \sin \vartheta - q(\pi - \vartheta) \cos \vartheta \qquad (50)$$

The correspondence between solutions for compressible flow and for incompressible flow is summarized in table 1.

4. The Properties of the Hypergeometric Functions of Large Order

The behavior of $F(a_\nu, b_\nu; c_\nu; \tau)$ for large positive values of ν has been discussed by Chaplygin in connection with the question of convergence of his series solution for the flow of a gas jet. However, his discussions are limited to the subsonic flow and, for this reason, the value of τ is restricted to the interval $0 \leq \tau \leq \frac{1}{2\beta + 1}$. In the more general problem where both subsonic and supersonic flow may exist, the whole interval $0 < \tau < 1$ has to be considered. Furthermore, both integrals of the hypergeometric equation are involved, as will be shown in part II. As a preparation for the proof of the convergence of the solutions, the properties of the hypergeometric functions of large order in the extended interval will be discussed presently.

Chaplygin (reference 6) introduced a new function $\frac{\nu}{2\tau} \xi_\nu(\tau)$ defined as the logarithmic derivative of $\tau^{\frac{\nu}{2}} \underline{F}_\nu(\tau)$: namely,

$$\nu\xi_\nu(\tau) = 2\tau \frac{d}{d\tau} \log \tau^{\frac{\nu}{2}} \underline{F}_\nu(\tau), \quad \nu \neq 0 \qquad (51)$$

where $\underline{F}_\nu(\tau)$ denotes the first integral of the hypergeometric equation (27) or (28) and ν can be either an integer or not an integer. Then in the place of equation (27) or (28), the corresponding differential equation for ξ_ν is a Riccati equation:

$$X(\xi_\nu) \equiv \xi_\nu' \pm \frac{\beta}{1 - \tau}\xi_\nu + \frac{\nu}{2\tau}\left[\xi_\nu^2 - \frac{1 - (2\beta + 1)}{1 - \tau}\right] = 0 \qquad (52)$$

where the lower sign corresponds to equation (28). As shown by Chaplygin, $\underline{F}_\nu(\tau)$, although an oscillatory function,

can have no root in $0 \leq \tau \leq \frac{1}{2\beta + 1}$ and, consequently, $\xi_\nu(\tau)$ is finite and continuous in the same interval. Moreover, it can be deduced also that $\xi_\nu(0) = 1$ and $\xi_\nu'(0) = -\beta$. Since $\xi_\nu'(\tau)$ does not change sign in $0 \leq \tau \leq \frac{1}{2\beta + 1}$; $\xi_\nu(\tau)$ is monotonic decreasing and eventually vanishes at $\tau_o \leq \tau^*$, τ^* being the first root of the hypergeometric function for $\nu > 0$. Since τ^* is a decreasing function of ν, when ν becomes large, τ^* and consequently τ_o will differ from $\frac{1}{2\beta + 1}$ by a small quantity.

Chaplygin's theorem.- In $0 \leq \tau \leq \frac{1}{2\beta + 1}$, if a monotonic continuous function $\eta_\nu(\tau)$ satisfies (i) $\eta_\nu(0) = 1$ and (ii) $X(\eta_\nu) \gtrless 0$, then

$$\eta_\nu(\tau) \gtrless \xi_\nu(\tau), \quad \nu > 1 \tag{53}$$

The proof is given in Chaplygin's paper (reference 6.) In the case of the second integral $F_\nu(\tau)$, the theorem is still true with the signs of inequalities reversed because it can be verified that $X(\xi_{-\nu}) = 0$, where $\xi_{-\nu}(\tau)$ corresponds to the case of $F_\nu(\tau)$ instead of $\underline{F}_\nu(\tau)$ in (51), and $\xi_{-\nu}(0) = -1$; therefore $\xi_{-\nu}(\tau)$ is negative in $0 \leq \tau \leq \frac{1}{2\beta + 1}$.

Corollary (51).- In $0 \leq \tau \leq \frac{1}{2\beta + 1}$, the functions $\underline{F}_\nu(\tau)$ and $\underline{G}_\nu(\tau)$ fall respectively between the limits:

(i) $$T_1^{\nu}(\tau) < \underline{F}_\nu(\tau) < T_2^{\nu}(\tau) \tag{54}$$

(ii) $$T_1^{-\nu}(\tau) > \underline{G}_\nu(\tau) > T_2^{-\nu}(\tau), \quad \nu > 1 \tag{55}$$

where

$$T_1(\tau) = \exp\left\{-\int_0^\tau \left[1 - \sqrt{\frac{1 - (2\beta + 1)\tau}{1 - \tau}}\right] \frac{d\tau}{2\tau}\right\} \tag{56}$$

$$T_2(\tau) = \exp\left\{-\int_0^\tau \left[1 - (1 - \tau)^\beta\right] \frac{d\tau}{2\tau}\right\} \tag{57}$$

This can be verified easily by choosing η_ν to be $\sqrt{\frac{1 - (2\beta + 1)\tau}{1 - \tau}}$ or $(1 - \tau)^\beta$. As, evidently, in $0 \leq \tau \leq \frac{1}{2\beta+1}$ when

$$\nu > 1, \quad \sqrt{\frac{1 - (2\beta + 1)\tau}{1 - \tau}} < \xi_\nu < (1 - \tau)^\beta \tag{58}$$

and

$$-\left(1+O\left(\frac{1}{\nu}\right)\right)\sqrt{\frac{1 - (2\beta + 1)\tau}{1 - \tau}} > \xi_{-\nu} > -(1 - \tau)^\beta \tag{59}$$

and furthermore, $X(\eta_\nu) \gtrless 0$ are satisfied, consequently, it follows the results.

Corollary (52).- In $0 \leq \tau \leq \frac{1}{2\beta + 1}$, the absolute value of the logarithmic derivative of $F(a_\nu, b_\nu; c_\nu; \tau)$ divided by ν, is bounded both above and below - that is,

$$M_1(\tau) \leq \frac{F(a_\nu + 1, b_\nu + 1; c_\nu + 1; \tau)}{F(a_\nu, b_\nu; c_\nu; \tau)} \leq M_2(\tau) \tag{60}$$

where $M_1(\tau)$ and $M_2(\tau)$ are independent of ν. This really is a consequence of (58) and (59).

It shall be noted that the results established in the foregoing are applicable to $\underline{F}_\nu(\tau) = F(a_\nu + \beta, b_\nu + \beta; c_\nu; \tau)$, provided ν is large, because then the two equations (27) and (28) tend to be the same.

Obviously, Chaplygin's theorem ceases to be true when $\tau > \frac{1}{2\beta + 1}$. For in the interval $\frac{1}{2\beta + 1} < \tau < 1$, the solutions of the hypergeometric equation are oscillatory and, hence, within any closed interval in $\frac{1}{2\beta + 1} < \tau < 1$ the number of roots of $\underline{F}_\nu(\tau)$ will be proportional to ν. (See reference 17.) When ν is large, there will be a large number of roots in the interval. As a consequence, the function

$\xi_\upsilon(\tau)$ will have there an ever increasing number of simple poles, and a finite interval in which $\xi_\upsilon(\tau)$ remains finite for all υ does not exist.

To carry the investigation over into $\frac{1}{2\beta + 1} < \tau < 1$, the method is modified. Let $\underline{F}_\upsilon(\tau)$ and $F_\upsilon(\tau)$ be two independent solutions of equation (27) or (28); and let the linear combination be denoted by

$$F_\upsilon^*(\tau) = \underline{F}_\upsilon(\tau) + i\, F_\upsilon(\tau) \tag{61}$$

The complex function is, of course, a solution of the same differential equation. In terms of its modulus $R_\upsilon(\tau)$ and argument $\Phi_\upsilon(\tau)$, the function may also be expressed as

$$F_\upsilon^*(\tau) = R_\upsilon(\tau)\, e^{i\Phi_\upsilon(\tau)} \tag{62}$$

where both $R_\upsilon(\tau)$ and $\Phi_\upsilon(\tau)$ are continuous functions with continuous derivatives. By comparing with (61), it is necessary to have

$$\underline{F}_\upsilon(\tau) = R_\upsilon(\tau) \cos \Phi_\upsilon(\tau) \tag{63}$$

$$F_\upsilon(\tau) = R_\upsilon(\tau) \sin \Phi_\upsilon(\tau) \tag{64}$$

According to the Sturm separation theorem, $\underline{F}_\upsilon(\tau)$ and $F_\upsilon(\tau)$ never vanish simultaneously in any closed interval and $R_\upsilon(\tau)$ never vanishes in $\frac{1}{2\beta + 1} < \tau < 1$ and remains positive in the whole interval. Then corresponding to (51), a complex function $\xi_\upsilon^*(\tau)$ can be defined as follows:

$$\upsilon\, \xi_\upsilon^*(\tau) = 2\tau \frac{d}{d\tau} \log \tau^{\frac{\upsilon}{2}} F_\upsilon^*(\tau) \tag{65}$$

which satisfies the same equation (52). On separating into real and imaginary parts, the Riccati equation for $\xi_\upsilon^*(\tau)$ becomes

$$X_1\left(\xi_\nu^{(1)}, \xi_\nu^{(2)}\right) \equiv \xi_\nu'^{(1)} + \frac{\beta}{1-\tau}\,\xi_\nu^{(1)} + \frac{\nu}{2\tau}\left[\xi_\nu^{2(1)} - \xi_\nu^{2(2)} + \frac{(2\beta+1)\tau - 1}{1-\tau}\right] = 0 \quad (66)$$

$$X_2\left(\xi_\nu^{(2)}, \xi_\nu^{(1)}\right) \equiv \xi_\nu'^{(2)} + \frac{\beta}{1-\tau}\,\xi_\nu^{(2)} + \frac{\nu}{\tau}\,\xi_\nu^{(2)}\xi_\nu^{(1)} = 0 \quad (67)$$

where $\xi_\nu^{(1)}$ and $\xi_\nu^{(2)}$ are real continuous functions of τ defined as

$$\xi_\nu^{*}(\tau) = \xi_\nu^{(1)}(\tau) + i\,\xi_\nu^{(2)}(\tau) \quad (68)$$

Their connection with $R_\nu(\tau)$ and $\Phi_\nu(\tau)$ separately are given by means of (65): namely,

$$\nu\,\xi_\nu^{(1)}(\tau) = 2\tau\frac{d}{d\tau}\log \tau^{\frac{\nu}{2}} R_\nu(\tau) \quad (69)$$

$$\nu\,\xi_\nu^{(2)}(\tau) = 2\tau\frac{d}{d\tau}\,\Phi_\nu(\tau) \quad (70)$$

Now equation (67) can be integrated in terms of $\xi_\nu^{(1)}(\tau)$ and whence $\xi_\nu^{(2)}(\tau)$ can be eliminated from equation (66). Then the equations for $\xi_\nu^{(1)}$ and $\xi_\nu^{(2)}$ are

$$X_1\left(\xi_\nu^{(1)}\right) \equiv \xi_\nu'^{(1)} + \frac{\beta}{1-\tau}\,\xi_\nu^{(1)} + \frac{\nu}{2\tau}\left[\xi_\nu^{2(1)} - \xi_0^{\,2}(1-\tau)^{2\beta} e^{-2\nu\int_{\tau_0}^{\tau}\xi_\nu^{(1)}\frac{d\tau}{\tau}} + \frac{(2\beta+1)\tau - 1}{1-\tau}\right] = 0 \quad (71)$$

$$\xi_\nu^{(2)}(\tau) = -\xi_0(1-\tau)^{\beta}\, e^{-\nu\int_{\tau_0}^{\tau}\xi_\nu^{(1)}\frac{d\tau}{\tau}}, \quad \xi_0 = \frac{2}{\left(\tau_0^{\frac{1}{2}} R_\nu(\tau_0)\right)^2} \quad (72)$$

Equation (71) together with the condition $\xi_\nu^{(1)}(0) = -1$ determines uniquely the solution $\xi_\nu^{(1)}(\tau)$. The actual value of $\xi_\nu^{(1)}(\tau)$ can be expressed, of course, in terms of the known hypergeometric functions. But the problem on hand is to determine the properties of $\xi_\nu^{(1)}(\tau)$ for large ν which are given by the following theorem.

Theorem (52).- If $\eta_\nu^{(1)}(\tau)$ is continuous and monotonic in $\tau_o < \tau < 1$ and satisfies $X_1(\eta_\nu^{(1)}) \gtrless 0$, then for all $\nu > N$

$$\eta_\nu^{(1)}(\tau) \gtrless \xi_\nu^{(1)}(\tau) \tag{73}$$

The proof is given in appendix A.

Corollary (53).- In $\tau_o < \tau < 1$, the following inequality holds for the modulus of $\underline{F}_\nu^*(\tau)$:

$$R_\nu(\tau)/R_\nu(\tau_o) < \left(\frac{\tau_o}{\tau}\right)^{\nu/a}, \quad \nu > N \tag{74}$$

where

$$(2\beta + 1)\tau_o - 1 \geq 0$$

For in $\tau_o < \tau < 1$, $\xi_\nu^{(1)} < 0$; and hence $\eta_\nu^{(1)}(\tau) = 0$. satisfies the condition $0 > \xi_\nu^{(1)}(\tau)$, which gives (74) by integration.

Now, since $\xi_\nu^{(1)}(\tau)$ is bounded by zero for all $\nu \neq 0$ in $\tau_o < \tau < 1$, it is implied also that

$$R_\nu(\tau) < T_3{}^\nu(\tau) \tag{75}$$

where $T_3(\tau) = \frac{t_o}{\tau^{1/a}}$. Here the constant t_o can be determined by joining T_3 at $\tau = \tau_o$ with T_1 or T_2 defined by equations (56) and (57). Then from equations (63) and (64) it follows that for $\nu > N$

$$\left|\underline{F}_\nu(\tau)\right| < T_3{}^\nu(\tau) \tag{76}$$

$$\left|\underline{G}_\nu(\tau)\right| < T_3{}^{-\nu}(\tau), \quad \tau_o < \tau < 1 \tag{77}$$

PART II

CONSTRUCTION OF THE SOLUTIONS FOR COMPRESSIBLE FLOW AROUND A BODY

5. Chaplygin's Procedure

In the previous sections, the particular solutions of the differential equations in the hodograph plane are obtained. Since the differential equations in the hodograph plane are linear, superposition of solutions is allowed. In other words, if these particular solutions are multiplied by different constants and then added together, the sum is again a solution of the differential equations. By this procedure, general solutions can be constructed from the particular solutions.

However, there is a difficulty in such a method of constructing the general solution — the difficulty of making a proper choice of the multiplying constants for the particular solutions so that the resultant solution will give a flow satisfying the boundary conditions specified in the physical plane. This can be seen from the fact that the space coordinates x and y are obtained from χ which is not explicitly connected with ψ, the stream function. In fact, to obtain the coordinate x and y directly from ψ would involve an integration in the hodograph plane. Thus the linearization of differential equations in the hodograph plane is obtained at the expense of the simplicity in boundary value problem. To guarantee that ψ and χ do actually belong to the same flow in the physical plane, an additional condition besides the differential equations for ψ and χ has to be satisfied. This condition will be discussed in section 11.

Chaplygin (reference 6) suggested an ingenious method of solving this difficulty by using the well-known solutions of the incompressible flow. The first step in this method is to find the incompressible flow around a body "similar" to the body concerned. (The meaning of the word "similar" will be made clear in the following paragraph.)

The stream function ψ_o, for instance, is then expressed in terms of the speed q and the inclination θ. The function

ψ_o (q, θ) can be expanded into an infinite series each term of which is of the form $q^n \cos n\vartheta$ or $q^n \sin n\vartheta$. For the flow around a body with constant velocity U at infinity, the function $\psi_o(q, \vartheta)$ has a singularity at the point $q = U$, $\theta = 0$ in the hodograph plane, since there all the stream-lines, or lines of constant ψ_o originate. Thus, there are two forms of the series expansion of ψ_o: One is convergent within the circle $q = U$; while the other is convergent outside of the circle $q = U$. The first, or "inside," series must be regular at the origin of the hodograph plane. Therefore, only positive values of the integers n can occur. The second, or "outside," series can have both positive and negative ν. Chaplygin's method is to use the inside series for ψ_o as the starting point for obtaining the desired solution ψ for the compressible fluid. He suggested choosing the multiplying coefficient of the particular solutions for the compressible flow by the condition that for the limiting case of infinite sonic speed, or incompressible fluid, the series will degenerate to the inside series of the incompressible flow already obtained. The series for the compressible stream function ψ so constructed can be called as the inside series of ψ. The outside series for ψ then can be obtained by the method of analytical continuation with the aid of the "outside series" of the incompressible flow.

These solutions so constructed for the compressible flow contain the Mach number of the undisturbed flow as a parameter. They constitute a family of singly infinite solutions. Included in this family of solutions is the limiting case of zero Mach number of the free stream. This limiting case will give the incompressible flow around a body used as the starting point of this method. For other values of the free-stream Mach number, the body contour is generally different from that corresponding to zero Mach number. Thus, if the compressible flow around a given body is desired, the body shape for the initial incompressible flow must be slightly different from the given body shape. However, if a geometric parameter is included in the solution, such an adjustment is not difficult to make.

It may be stated here that owing to the regularity of the solution at the origin of the hodograph plane, only the first solution of the hypergeometric differential equation appears in the inside series. For the outside series, both the first and the second solution of the hypergeometric differential equation are necessary. This is in direct analogy with the appearance of both positive and negative exponents of q in

the incompressible outside series. This fact is particularly important, since preyious investigators seem to be unaware of it. Chaplygin himself did not use the second solution of the hypergeometric differential equation, but that is simply because, for his problem, there is no singularity in the hodograph plane and hence only the inside series is needed.

6. The Functions for Incompressible Flow

Following the procedure outlined in the previous section, the analysis starts with the functions required in defining an irrotational incompressible flow. For this case, the sonic speed c_o tends to infinity, and the equations for the velocity potential $\varphi_o(x,y)$ and the stream function $\psi_o(x,y)$ all became harmonic:

$$\Delta\varphi_o = 0 \tag{78}$$

$$\Delta\psi_o = 0 \tag{79}$$

where Δ stands for the Laplacian operator. If $W_o(z)$ is the complex potential, it can be shown that

$$W_o(z) = \varphi_o + i\,\psi_o \tag{80}$$

where

$$z = x + i\,y$$

If w denotes the complex velocity $u-i\,v$, it is connected with $W_o(z)$ by

$$w = \frac{dW_o}{dz} \equiv w(z) \tag{81}$$

If $w'(z)\neq 0$, it always is possible to solve for z in terms of w; namely,

$$z = z_o(w) \tag{82}$$

In general, this solution is not single-valued and will be discussed later. By introducing this relation into equation (80), the complex potential function in the hodograph plane can be obtained

$$W_o(w) = \varphi_o(u,v) + i\,\psi_o(u,v) \tag{83}$$

In case equation (82) is many-valued, this would correspond to one branch of the function.

It is clear that in this case $\chi_o(u,v)$ is also a harmonic function. Let $\sigma_o(u,v)$ be the conjugate function defined by

$$\frac{\partial \chi_o}{\partial u} = -\frac{\partial \sigma_o}{\partial v} \tag{84}$$

$$\frac{\partial \chi_o}{\partial v} = \frac{\partial \sigma_o}{\partial u} \tag{85}$$

Hence

$$\Lambda_o(w) = \chi_o - i\,\sigma_o \tag{86}$$

where

$$w = u - i\,v$$

Thus $\Lambda_o(w)$ is an analytic function of w. From equation (13) the derivative of $\Lambda_o(w)$ with respect to w must be z. That is,

$$\frac{d\Lambda_o}{dw} = z_o(w)$$

But $z_o(w)$ already has been found from equation (82). Therefore,

$$\Lambda_o(w) = \int z_o(w)dw + \text{constant} \tag{87}$$

The real part of $\Lambda_0(w)$ gives $\chi_0(u,v)$ as required, according to (86).

7. Conformal Mapping of Incompressible Flow on the Hodograph Plane

Before the construction of solutions for the compressible flow, the general character of the solutions in the hodograph plane should be examined. This can be done easily by investigating the behavior of the transition function $z_0(w)$ for an incompressible fluid. To start with the simplest case first, consider a steady irrotational flow in an infinite, simply connected domain D bounded by a curve C in the z-plane, with a parallel flow at infinity (fig. 1). At every point z of D there is one, and only one, velocity vector $\vec{q}$. If the curve C is mapped into $\underline{C}$ and infinity corresponds to a point $\underline{P}$ on the axis of reals of w within $\underline{C}$, then the domain D is mapped into $\underline{D}$ by a mapping function

$$w = w(z)$$

defined in (81), where $w(z)$ is an analytic function of z. The inverse function

$$z = z_0(w)$$

will set up a continuous one-to-one correspondence between w- and z-plane, provided the mapping is conformal. This requires that $w(z)$ is analytic, simple within D, and $w'(z) \neq 0$.

However, for most problems these conditions cannot be satisfied throughout the field of flow. In the first place, the function $w(z)$ is generally nonsimple, for example, in the case of a uniform flow, $w(z) = \text{constant}$, thus $w'(z) \equiv 0$ and the whole z-plane corresponds only to a point in the w-plane. Furthermore, the complex velocity for a two-dimensional boundary-value problem generally can be put in the following form:

$$w = w_\infty + w^*(z)$$

where w_∞ is a constant. The boundary condition requires that $w^*(z) = 0$ and, as a consequence, $w'^*(z) = 0$ as z becomes infinite. Therefore, in all cases, the point $\underline{P}$ in the w-plane, is a singular point. It is a branch point at w_∞ if $z_o(w)$ is many-valued; or a pole, if otherwise. In practice, there are two kinds of singularities that play a dominant role in the problem of two-dimensional flow. These singularities will be investigated presently.

Branch point of order 1.[1]- It may be recalled that, when a closed body is present in a uniform flow, there always exist two stagnation points both of which correspond to the origin of the w-plane. If a streamline PS is followed, for instance,(see fig. 2) from $+\infty$ to S, the portion SMS' and then to $-\infty$, a curve $\underline{PS}$ in w-plane would be described twice. This indicates that the function $z_o(w)$ possesses two branches of Riemann surfaces joining together about the branch point $\underline{P}$. In order to make the domain $\underline{D}$ single-valued, a cut is put along the axis of reals from the branch point to $+\infty$. Then one portion of the z-plane is mapped into a definite branch of the Riemann surfaces in the w-plane, and this will be defined as the domain D. If the body is symmetrical with respect to the coordinate axes with parallel flow at infinity, then the domain $D: R\,z \leq 0$ will be mapped conformally into $\underline{D}$ on one branch of the Riemann surfaces and $D': R\,z > 0$ on the other, where the region within C is excluded.

Logarithmic singularity.- The flow over a wavy surface, for instance, placed parallel to a uniform stream has a periodic nature. For such flows there are infinitely many points in the physical plane that have the same velocity. Hence, there are an infinite number of branches in the w-plane, each of which corresponds to a definite portion of the z-plane. The function $z_o(w)$ must have a term $\log\left(1 - \frac{w}{U}\right)$ and the point $\underline{P}$ now is a logarithmic singularity. If, however, a cut is introduced from the branch point to $+\infty$ and $-\pi < \arg\left(1 - \frac{w}{U}\right) < \pi$, then the domain $\underline{D}$ is again made single-valued.

---

[1]The function $z_o(w)$ is said to have a branch point of order k at $w = w_\infty$ if its inverse $w(z)$ contains the part w^* which has a zero of order $k + 1$ at $z = \infty$.

8. Construction of a Solution about the Origin

Stream function.— From the considerations of the last section, the domain within a circle with radius $|w| = \underline{PS} = U$, where U is the absolute value of w at infinity in z—plane, is in all cases single—valued. If a function $W_o(w)$ is associated with a definite flow in z—plane, from section 6 it is an analytic function of w and regular within the circle $|w| = U$. Consequently, the following Taylor expansion exists:

$$W_o(w) = \sum_{n=o}^{\infty} A_n w^n, \quad |w| < U \tag{88}$$

where A_n's are, in general, complex. Since $w = qe^{-i\vartheta}$ and by (80) the imaginary part of $W_o(w)$ is equal to incompressible stream function ψ_o, it can be written as

$$\psi_o(q,\vartheta) = \mathrm{Im}\left\{W_o(w)\right\} = \sum_{n=o}^{\infty} q^n \left\{A_n^{(1)} \cos n\vartheta + A_n^{(2)} \sin n\vartheta\right\} \tag{89}$$

According to Chaplygin's procedure, the corresponding compressible solution can be obtained by simply replacing the function q^n in equation (89) by the corresponding $q^n \underline{F}_n^{(r)}(\tau)$ as shown by (40). The second integral is excluded by the regularity requirement at $q = 0$. However, in order to preserve the proper singularity at the point (U,O) in the hodograph plane, the compressible stream function ψ is written as

$$\psi(q,\vartheta) = \sum_{n=o}^{\infty} q^n \underline{F}_n^{(r)}(\tau) \left\{A_n^{(1)} \cos n\vartheta + A_n^{(2)} \sin n\vartheta\right\} \tag{90}$$

where

$$\underline{F}_n^{(r)}(\tau) = \frac{\underline{F}_n(\tau)}{\underline{F}_n(\tau_1)} = \frac{F(a_n, b_n; c_n; \tau)}{F(a_n, b_n; c_n; \tau_1)}, \quad q < U \tag{91}$$

and $\tau_1 = \frac{1}{2\beta}\frac{U^2}{c_o^2}$, the value of τ_1 corresponding to the free-stream velocity U. It is seen that if $c_o \to \infty$, then $\tau = \tau_1 \to 0$, and $\underline{F}_n^{(r)}(\tau) \to 1$ due to the normalizing condition (30). Thus the solution is reduced to the incompressible form. Furthermore, if $q \to U$ the character of the solution is exactly like that of the incompressible solution. Hence, all the specified conditions are satisfied. Of course, for the mixed subsonic and supersonic flow, the free-stream Mach number is always less than unity. Thus $\tau_1 < 1/2\beta+1$.

For later analysis as given in part III, it is convenient to write ψ in a different form. Since $\underline{F}_n^{(r)}(\tau)$ is a purely real quantity, a complex function $W(w;\tau)$ can be constructed as

$$W(w;\tau) = \sum_{n=0}^{\infty} A_n \underline{F}_n^{(r)}(\tau)\, w^n, \qquad |w| < U \tag{92}$$

Then, similar to the relation between equations (88) and (89), $\psi(q,\theta)$ can be taken as the imaginary part of the new function $W(w;\tau)$. Thus,

$$\psi(q,\theta) = \mathrm{Im}\left\{W(w;\tau)\right\} \tag{93}$$

<u>Transformed potential function</u>.— Similarly, it is possible to construct another function $\Lambda(w;\tau)$ defined by

$$\Lambda(w;\tau) = \sum_{n=0}^{\infty} \tilde{A}_n \tilde{\underline{F}}_n^{(r)}(\tau)\, W^n, \qquad q < U \tag{94}$$

In this expression, the coefficients $\tilde{A}_n$ are obtained from the expansion of $\Lambda_o(w)$ for the incompressible flow (87):

$$\Lambda_o(w) = \sum_{n=0}^{\infty} \tilde{A}_n w^n, \qquad |w| < U \tag{95}$$

and

$$\mathfrak{F}_n^{(r)}(\tau) = \frac{\tilde{F}_n(\tau)}{F_n(\tau_1)} \qquad (96)$$

Equation (96) is the result of equation (91) and the equation of compatibility given by equation (24). Then the function $\chi(q,\vartheta)$ for the compressible flow is given by

$$\chi(q,\vartheta) = Rl\left\{\Lambda(w;\tau)\right\} \qquad (97)$$

The functions $W(w;\tau)$ and $\Lambda(w;\tau)$ are actually regular at the origin and satisfy the imposed conditions. However, the following question may be raised: Do the series (92) and (94) converge and represent the functions $\psi(q,\vartheta)$ and $\chi(q,\vartheta)$ in the domain of validity? To settle this question, it is necessary to prove the following theorem:

Theorem (88). If the constants A_n and $\tilde{A}_n$ are given in equations (88) and (95), while $F_n^{(r)}(\tau)$ and $\tilde{F}_n^{(r)}(\tau)$ are defined respectively by equations (91) and (96), the series (92) and (94) are uniformly and absolutely convergent in the same domain as those of (88) and (95). The proof is given in appendix B.

9. Analytic Continuation of the Solution

Branch Point of Order 1

Stream function.— As proved in the appendix B, the series (92) is absolutely and uniformly convergent and does represent a regular function $W(w;\tau)$ for every τ in $0 \leq \tau \leq \tau_1$ and on the circle of convergence it agrees with $W_o(Ue^{-i\theta})$, of which the Fourier expansion exists:

$$W_o(Ue^{-i\theta}) = \sum_{n=o}^{\infty} A_n U^n e^{-in\theta} \qquad (98)$$

In the present section, it is proposed to continue the solution (92) analytically outside the domain $|w| \leq U$ with the initial value given by equation (98). The domain outside $|w| \leq U$ is generally many-valued. To fix ideas, discuss first the case of a branch point of order 1. Generally, the function $W_o(w)$ has other singularities besides the one at $w = U$.[1] However, such singularities lie outside the region of interest and thus need not be investigated. Let the nearest singularity be given by $|w| = V > U$. Then, the domain to be considered outside $|w| = U$ is an annulus with a cut joining the two singularities. The proper representation of $W_o(w)$ in such a region which has a branch point of order 1 at $w = U$, is

$$W_o(w) = iw^{-\frac{1}{2}} W_o^*(w) \tag{99}$$

where $W_o^*(w)$ is single-valued and regular within the open annulus $U < |w| < V$. Hence, in any closed domain

$$U + \delta \leq |w| \leq V - \delta, \ \delta$$

being a small number, there exists a uniformly and absolutely convergent series:

$$W_o^*(w) = \sum_{n=o}^{\infty} \left[B_n w^n + C_n w^{-n} \right] \tag{100}$$

which, on substituting in (99), will give the continuation of the Taylor series (88).

---

[1]For instance, in the problem of the flow around an elliptic cylinder treated in part V, there are two singularities of the W_o function given by equation (280): namely, $w = 1$ and $w = 1/\epsilon^2$. The first singularity corresponds to the flow at infinity and is the singularity under discussion. The second singularity corresponds to a point inside the circle of the ζ-plane, the plane of the circular section. Since only the flow outside the circle of the ζ-plane is of interest here, the singularity $w = 1/\epsilon^2$ need not be investigated. In other words, it is necessary only to expand the W_o function in the annular region $1 < \left|\frac{w}{U}\right| < \frac{1}{\epsilon^2}$.

The solution for a compressible fluid, which has the same character of singularities as $W_o(w)$ and is valid in the annulus $U < |w| < V$, can be obtained from (100) by introducing the proper hypergeometric functions corresponding to each exponent of w. That is:

$$W^{(o)}(w;\tau) = i \sum_{n=o}^{\infty} \left[B_n^* \underline{F}_\nu(\tau) w^\nu + C_n^* \underline{G}_\nu(\tau) w^{-\nu} \right] \quad (101)$$

which is the continuation of $W^{(i)}(w;\tau)$. Here $\nu = n + \frac{1}{2}$, n being a positive integer; $\underline{F}_\nu(\tau)$ and $q^{-2\nu} \underline{G}_\nu(\tau)$ are the first and second integrals of the hypergeometric equation; and B_n^* and C_n^* are constants. It should be noticed that the coefficients B_n^* and C_n^* in the outside series for the compressible flow are not equal to B_n and C_n in equation (100) for the outside series of the incompressible flow. The outside series of the incompressible flow is used only to give the proper form of $W^{(o)}(w;\tau)$ for the desired branch point characteristics; while the exact determination of $W^{(o)}(w;\tau)$ has to be made by the conditions of continuity, which will be discussed presently.

Since the partial differential equation considered here is of the second order, to ensure that $W^{(o)}(w;\tau)$ is the analytic continuation of $W^{(i)}(w;\tau)$, two conditions have to be imposed at the boundary of the respective regions of convergence; that is, the circle $q = U$. These two conditions are the following:

$$W^{(i)}(Ue^{-i\theta}; \tau_1) = W^{(o)}(Ue^{-i\theta}; \tau_1) \quad (102)$$

$$\left[\frac{\partial}{\partial q} W^{(i)}(w;\tau)\right]_{\tau=\tau_1} = \left[\frac{\partial}{\partial q} W^{(o)}(w;\tau)\right]_{\tau=\tau_1} \quad (103)$$

On account of equations (102) and (103), there are two relations which have the imaginary parts:

$$\sum_{n=0}^{\infty}\left[B_n^*\ \underline{F}_\nu(\tau_1)\ U^\nu + C_n^*\ \underline{G}_\nu(\tau_1)\ U^{-\nu}\right]\cos\nu\vartheta = -\sum_{n=0}^{\infty} A_n\ U^n\ \sin n\vartheta$$

$$0 \le \vartheta < 2\pi$$

$$\sum_{n=0}^{\infty}\left[B_n^*\ U^\nu\ (\nu\underline{F}_\nu(\tau) + 2\tau_1\underline{F}_\nu'(\tau_1)) + C_n^*\ U^{-\nu}(-\nu\underline{G}_\nu(\tau_1) + 2\tau_1\ \underline{G}_\nu'(\tau_1))\right]\cos\nu\vartheta$$

$$= -\sum_{n=0}^{\infty} A_n\ U^n\left(n + 2\tau_1\frac{\underline{F}_n'(\tau_1)}{\underline{F}_n(\tau_1)}\right)\sin n\vartheta$$

Here the prime denotes differentiation with respect to τ. Evidently, the coefficients on the left-hand side can be solved for in terms of the known constants A_n. They are:

$$B_n^*\ \underline{F}_\nu(\tau_1)\ U^\nu + C_n^*\ \underline{G}_\nu(\tau_1)\ U^{-\nu} = -\frac{1}{\pi}\sum_{m=0}^{\infty} A_m\ U^m\left(\frac{1}{m+\nu} + \frac{1}{m-\nu}\right) \quad (104)$$

$$B_n^*\ U^\nu\ (\nu\underline{F}_\nu(\tau_1) + 2\tau_1\underline{F}_\nu'(\tau_1)) + C_n^*\ U^{-\nu}\ (-\nu\underline{G}_\nu(\tau_1) + 2\tau_1\underline{G}_\nu'(\tau_1))$$

$$= -\frac{1}{\pi}\sum_{m=0}^{\infty} m\ A_m\ U^m\xi_m(\tau_1)\left(\frac{1}{m+\nu} + \frac{1}{m-\nu}\right) \quad (105)$$

From these two equations, the constants B_n^* and C_n^* can be uniquely determined, provided the determinant $\Delta(\underline{F}_\nu, F_\nu)$ does not vanish. These results are:

$$B_n^* U^{\nu} = - \frac{\underline{G}_{\nu}(\tau_1)}{2\nu\pi(1-\tau_1)^{\beta}} \sum_{m=0}^{\infty} A_m U^m \left(\frac{1}{m+\nu} + \frac{1}{m-\nu}\right)\left(m\xi_m(\tau_1) - \nu\xi_{-\nu}(\tau_1)\right) \quad (106)$$

$$C_n^* U^{-\nu} = + \frac{\underline{F}_{\nu}(\tau_1)}{2\nu\pi(1-\tau_1)^{\beta}} \sum_{m=0}^{\infty} A_m U^m \left(\frac{1}{m+\nu} + \frac{1}{m-\nu}\right)\left(m\xi_m(\tau_1) - \nu\xi_{\nu}(\tau_1)\right) \quad (107)$$

as the Wronskian $\Delta(\underline{F}_{\nu}, F_{\nu}) = - \frac{\nu}{\tau} q^{-2\nu} (1-\tau)^{\beta} \neq 0$ and $\xi_{\nu}(\tau)$ is defined in (51).

The solution is again formal. To prove that the function $W(w;\tau)$ is a regular function in the annulus region, the truth of the following theorem must be first demonstrated. (See appendix O.)

Theorem (98). If the constants B_n^* and C_n^* are determined according to (102) and (103) and if the series (100) converges uniformly and absolutely in a closed domain $U + \delta \leq |w| \leq V - \delta$, then the series (101) will converge uniformly and absolutely in the domain $U + \delta \leq |w| \leq V - \delta$, $\delta > 0$.

Transformed potential function.- By a similar procedure, the continuation of (94) is

$$\Lambda^{(o)}(w;\tau) = 1 \sum_{n=0}^{\infty} \left[\tilde{B}_n^* \underline{\tilde{F}}_{\nu}(\tau) w^{\nu} + \tilde{C}_n^* \underline{\tilde{G}}_{\nu}(\tau) w^{-\nu}\right] \quad (108)$$

where $\underline{\tilde{F}}_{\nu}(\tau)$ and $\underline{\tilde{G}}_{\nu}(\tau)$ are the first and second integrals of equation (28) and the constants $\tilde{B}_n^*$ and $\tilde{C}_n^*$ can be similarly determined; namely,

$$\tilde{B}_n^* U^{\nu} = \frac{\tilde{G}_{\nu}(\tau_1)}{2\pi\nu(1-\tau_1)^{-\beta}} \sum_{n=0}^{\infty} \tilde{A}_m U^m \left(\frac{1}{m+\nu} - \frac{1}{m-\nu}\right)\left(m\tilde{\xi}_m(\tau_1) - \nu\tilde{\xi}_{-\nu}(\tau_1)\right) \underline{\tilde{F}}_m^{(r)}(\tau_1) \quad (109)$$

$$\tilde{C}_n^* U^{-\nu} = \frac{\tilde{\underline{F}}_\nu(\tau_1)}{2\pi\nu(1-\tau_1)^{-\beta}} \sum_{n=0}^{\infty} A_m U^m \left(\frac{1}{m+\nu} - \frac{1}{m-\nu}\right)\left(m\tilde{\xi}_m(\tau_1) - \nu\tilde{\xi}_\nu(\tau_1)\right)\tilde{\underline{F}}_m^{(r)}(\tau_1) \tag{110}$$

The solution determined so far is understood to be the principal branch of the function $W(w;\tau)$. It was assumed that the flow at infinity is parallel to the x-axis. If, in addition, the body is symmetrical with respect to the coordinate axes, the expression for the seccnd branch of $W^{(o)}(w;\tau)$ will be identical. However, in a more general case where asymmetry exists, the two branches will require separate consideration.

10. Continuation — Logarithmic Singularity

Stream function.— Consider now the second important type of singularity: it is assumed here that the only singularity possessed by the function $W_o(w)$ in the finite part of the w-plane is a logarithmic branch point at $w = U$ about which infinitely many Riemann surfaces are joined. By analogy with (99), $W_o(w)$ now can be conveniently written as

$$W_o(w) = W_o^*(w) + \tilde{W}_o(w) \tag{111}$$

where $W_o^*(w)$ is a regular function in the entire domain with possibly an essential singularity at infinity, and hence generally is given by a Taylor series or a polynomial in w, and $\tilde{W}_o(w) = \tilde{\varphi}_o(q,\vartheta) + i\tilde{\psi}_o(q,\vartheta)$ is an analytic function which characterizes the singularity of $W_o(w)$. Thus, aside from a constant factor,

$$\tilde{W}_o(w) = \frac{1}{i}\log\left(1 - \frac{w}{U}\right) \tag{112}$$

If a cut is laid from $+U$ to $+\infty$ and the argument of $\left(1 - \frac{w}{U}\right)$ is restricted in $-\pi < \arg\left(1 - \frac{w}{U}\right) < \pi$, then the function $\tilde{W}_o(w)$ will be single-valued in the whole cut plane.

The question of constructing a solution for the compressible fluid consists, therefore, of two parts: $W_o^*(w)$ and $\tilde{W}_o(w)$. However, the construction for $W_o^*(w)$ is, in principle, exactly the same as that of (92) and hence only $\tilde{W}_o(w)$ will be considered. First, let $\tilde{W}_o(w)$ be developed into power series in the respective domains of validity. The imaginary parts are:

$$\tilde{\psi}_o^{(i)}(q,\vartheta) = \sum_{n=1}^{\infty} \frac{1}{n}\left(\frac{q}{U}\right)^n \cos n\vartheta, \quad q < U \tag{113}$$

$$\tilde{\psi}_o^{(o)}(q,\vartheta) = -\log\frac{q}{U} + \sum_{n=1}^{\infty} \frac{1}{n}\left(\frac{q}{U}\right)^{-n} \cos n\vartheta, \quad q > U \tag{114}$$

The corresponding expression for $\tilde{\psi}(q,\vartheta)$, accordingly, will be:

$$\tilde{\psi}^{(i)}(q,\vartheta) = \sum_{n=1}^{\infty} A_n \underline{F}_n(\tau)\left(\frac{q}{U}\right)^n \cos n\vartheta, \quad q < U \tag{115}$$

$$\tilde{\psi}^{(o)}(q,\vartheta) = -B\int_{\tau_1}^{\tau}(1-\tau)^{\beta}\frac{d\tau}{\tau} + \sum_{n=1}^{\infty} C_n \underline{G}_n(\tau)\left(\frac{q}{U}\right)^{-n}\cos n\vartheta, \quad q > U \tag{116}$$

where $\underline{F}_n(\tau)$ stands for $F(a_n, b_n; c_n; \tau)$ and $\underline{G}_n(\tau)$ is defined by (39).

The function $\tilde{W}_o(w)$ may be regarded as the complex potential of a complex source situated at $w = U$. It is known that in this case the normal derivative of $\tilde{\psi}_o(q,\vartheta)$

on $|w| = U$ is a constant, except at $w = U$, where it becomes infinite. This boundary value can be expanded uniquely:

$$-\sum_{n=1}^{\infty} \cos n\vartheta = \frac{1}{2}, \quad \vartheta \neq 0 \tag{117}$$

The corresponding problem in the case of compressible flow can be put in an analogous manner: to find a function $\psi(q,\vartheta)$ which is continuous together with continuous partial derivatives and the normal derivative of which on $|w| = U$ is constant. Thus, the conditions (102) and (103) in conjuction with equation (117) demand:

$$\underline{F}_n(\tau_1) A_n - \underline{G}_n(\tau_1) C_n = 0 \tag{118}$$

$$\left[n \underline{F}_n(\tau_1) + 2\tau_1 \underline{F}_n'(\tau_1)\right] A_n + \left[n \underline{G}_n(\tau_1) - 2\tau_1 \underline{G}_n'(\tau_1)\right] C_n = 4B(1-\tau_1)^{\beta} \tag{119}$$

where the constant B can be determined when the normal derivative $\psi_q(q,\theta)$ on $|w| = U$ is assigned. By solving equations (118) and (119) and using the relation of the Wronskian of the two independent integrals of equation (27), there is obtained

$$A_n = \frac{2}{n} B \underline{G}_n(\tau_1) \tag{120}$$

$$C_n = \frac{2}{n} B \underline{F}_n(\tau_1) \tag{121}$$

Thus the function $\tilde{\psi}(q,\theta)$ is completely determined.

Transformed potential function.— The associated function $\chi(q,\theta)$ can be similarly constructed. As $\Lambda_o(w)$ is derived

from (87) by integration of the inverse mapping function, it must involve a term $\left(1 - \frac{w}{U}\right) \log \left(1 - \frac{w}{U}\right)$ which represents the singularity of the function $\Lambda_o(w)$. As in equation (111), $\Lambda_o(w)$ is split again into two parts:

$$\Lambda_o(w) = \Lambda_o^*(w) + \tilde{\Lambda}_o(w) \tag{122}$$

where $\Lambda_o^*(w)$ is an entire function and $\tilde{\Lambda}_o(w)$ is

$$\tilde{\Lambda}_o(w) = \frac{1}{i}\left(1 - \frac{w}{U}\right) \log \left(1 - \frac{w}{U}\right) \tag{123}$$

Now the solution corresponding to $\log \left(1 - \frac{w}{U}\right)$ can be determined in exactly the same manner except that the hypergeometric functions involved are $\underline{\tilde{F}}_n(\tau)$ and $\underline{\tilde{G}}_n(\tau)$ instead of $\underline{F}_n(\tau)$ and $\underline{G}_n(\tau)$. The part that will require special consideration is the term $\frac{w}{U} \log \left(1 - \frac{w}{U}\right)$. Let it be denoted by $\tilde{\lambda}_o(w) = \tilde{\chi}_o - i\tilde{\sigma}_o$:

$$\tilde{\lambda}_o(w) = -\frac{1}{i}\frac{w}{U} \log \left(1 - \frac{w}{U}\right) \tag{124}$$

This function is also multiple-valued. Let the argument of $\left(1 - \frac{w}{U}\right)$ again be restricted in $-\pi < \arg \left(1 - \frac{w}{U}\right) < \pi$; then in the cut plane the result will be

$$\tilde{\lambda}_o^{(i)} = \frac{1}{i} \sum_{n=1}^{\infty} \frac{1}{n} \left(\frac{w}{U}\right)^{n+1}, \quad |w| < U \tag{125}$$

$$\tilde{\lambda}_o^{(o)} = \frac{1}{i} \left[-\frac{w}{U} \log \frac{w}{U} e^{i\pi} + \sum_{n=1}^{\infty} \frac{1}{n} \left(\frac{w}{U}\right)^{-n+1} \right], |w| > U \tag{126}$$

According to equation (86), the function $\tilde{\chi}_o(q,\vartheta)$ is defined as the real part of $\Lambda_o(w)$. That part represented by equations (125) and (126) is then

$$\tilde{\chi}_o^{(i)}(q,\vartheta) = -\sum_{n=2}^{\infty} \frac{1}{n-1}\left(\frac{q}{U}\right)^n \sin n\vartheta \qquad (127)$$

$$\tilde{\chi}_o^{(o)}(q,\vartheta) = \frac{q}{U}\log\frac{q}{U}\sin\vartheta - \frac{q}{U}(\pi-\vartheta)\cos\vartheta + \sum_{n=1}^{\infty} \frac{1}{n+1}\left(\frac{q}{U}\right)^{-n} \sin n\vartheta \qquad (128)$$

The particular solution corresponding to

$$\frac{q}{U}\log\frac{q}{U}\sin\vartheta - \frac{q}{U}(\pi-\vartheta)\cos\vartheta$$

already has been given in equation (50). Hence the solution for the compressible flow is

$$\tilde{\chi}^{(i)}(q,\vartheta) = -\sum_{n=2}^{\infty} \tilde{A}_n \tilde{F}_n(\tau)\left(\frac{q}{U}\right)^n \sin n\vartheta \qquad (129)$$

$$\tilde{\chi}^{(o)}(q,\vartheta) = \frac{q}{U}k(\tau)\sin\vartheta - \frac{q}{U}(\pi-\vartheta)\cos\vartheta + \sum_{n=1}^{\infty} \tilde{C}_n \tilde{G}_n(\tau)\left(\frac{q}{U}\right)^{-n} \sin n\vartheta \qquad (130)$$

where

$$k(\tau) = \frac{1}{2(\beta+1)}\left[(2\beta+1)\log\frac{\tau}{\tau_1} - \left(\frac{1}{\tau}-\frac{1}{\tau_1}\right) + K_1\int_{\tau_1}^{\tau}(1-\tau)^{-\beta}\frac{d\tau}{\tau^2}\right] \qquad (131)$$

The conditions (102) and (103) together with an expansion

$$\frac{1}{2}\sin\vartheta + \sum_{n=2}^{\infty}\left(\frac{1}{n+1}+\frac{1}{n-1}\right)\sin n\vartheta = (\pi-\vartheta)\cos\vartheta,\quad 0<\vartheta<2\pi$$

require that:

$$\underline{\tilde{F}}_n(\tau_1)\,\tilde{A}_n + \underline{G}_n(\tau_1)\,\tilde{C}_n = \frac{1}{n+1}+\frac{1}{n-1} \tag{132}$$

$$\left[n\,\underline{\tilde{F}}_n(\tau_1) + 2\tau_1\,\underline{\tilde{F}}'_n(\tau_1)\right]\tilde{A}_n$$

$$+\left[-n\,\underline{\tilde{G}}_n(\tau_1)+2\tau_1\,\underline{\tilde{G}}'_n(\tau_1)\right]\tilde{C}_n = \frac{1}{n+1}+\frac{1}{n-1};\ n\neq 1 \tag{133}$$

and

$$\underline{\tilde{G}}_1(\tau_1)\,\tilde{C}_1 = \frac{1}{2} \tag{134}$$

$$\left[-\underline{\tilde{G}}_1(\tau_1)+2\tau_1\,\underline{\tilde{G}}'_1(\tau_1)\right]\tilde{C}_1 + 2\tau_1\,k'(\tau_1) = \frac{1}{2},\ n=1 \tag{135}$$

By solving (132) and (133) for $\tilde{A}_n$ and $\tilde{C}_n$, there is obtained:

$$\tilde{A}_n = \frac{(1-\tau_1)^{\beta}}{n^2-1}\left(1-n\tilde{\xi}_{-n}(\tau_1)\right)\underline{\tilde{G}}_n(\tau_1) \tag{136}$$

$$\tilde{C}_n = -\frac{(1-\tau_1)^{\beta}}{n^2-1}\left(1-n\tilde{\xi}_n(\tau_1)\right)\underline{\tilde{F}}_n(\tau_1),\ n\neq 1 \tag{137}$$

by using the Wronskian of the independent integrals of equation (28). With C_1 given by (134), the constant K_1 can be solved for from (135); it is

$$K_1 = -(1-\tau_1)^{\beta}\left[1 + \beta\tau_1 + (\beta+1)\tau_1^2\frac{\tilde{G}_1'(\tau_1)}{\tilde{G}_1(\tau_1)}\right] \quad (138)$$

The solutions $\psi(q,\vartheta)$ and $\chi(q,\vartheta)$ in the whole domain under consideration are uniquely determined. Since the dominant properties of the hypergeometric functions discussed in section 4 hold, in general, the equation of convergence can be similarly settled.

11. Transition to Physical Plane

In the previous sections, it has been proved that, for a given incompressible flow for which two associated functions $\psi_0(q,\vartheta)$ and $\chi(q,\vartheta)$ are defined, there exist two associated functions $\psi(q,\vartheta)$ and $\chi(q,\vartheta)$ for the corresponding compressible flow, depending upon two parameters γ and τ_1. The question is whether the associated functions $\psi(q,\vartheta)$ and $\chi(q,\vartheta)$ belong to the same flow pattern in the physical plane. To answer this question it is necessary to fall back once more on the equation of compatibility (24); since when $\psi(q,\vartheta)$ is given, $\varphi(q,\vartheta)$ is known by solving equations (20) and (21). Hence, if $\chi(q,\vartheta)$, satisfying equation (23) and approaching χ_0 as $C_0 \longrightarrow \infty$ is to be associated with $\psi(q,\vartheta)$ for the same flow, then it is necessary that the equation of compatibility be satisfied. Except in the case of logarithmic singularity in section 10 where the complete $\psi(q,\vartheta)$ function was not discussed, this condition has been properly considered.

Once the relationship between $\psi(q,\vartheta)$ and $\chi(q,\vartheta)$ is established, the next object is to calculate the flow pattern $\psi(x,y)$ = constant in the physical plane corresponding to $\psi(q,\vartheta)$ and $\chi(q,\vartheta)$. In the first place, the fact that the transformation defined by equations (9) and (10) is generally one-to-one must be recalled. Suppose that in the hodograph plane there is a line defined by

$$\psi(q,\vartheta) = \text{constant} = K \quad (139)$$

which will correspond to a definite streamline in the physical plane or a definite part of it. The streamline can be obtained by eliminating one of the two variables in $x(q,\theta)$ and $y(q,\theta)$.

To do this, first the equation (139) is solved for ϑ; namely,

$$\vartheta = \vartheta(q,K) \tag{140}$$

provided $\psi_{\vartheta}(q,\vartheta) \neq 0$. Introducing this relation into equation (13) which, when transformed into polar coordinates, are

$$x = \cos\vartheta \frac{\partial\chi}{\partial q} - \frac{\sin\vartheta}{q} \frac{\partial\chi}{\partial\vartheta} \tag{141}$$

$$y = \sin\vartheta \frac{\partial\chi}{\partial q} + \frac{\cos\vartheta}{q} \frac{\partial\chi}{\partial\vartheta} \tag{142}$$

gives a parametric representation of this particular streamline corresponding to $\psi(q,\theta) = K$ in the hodograph plane.

PART III

IMPROVEMENT OF THE CONVERGENCE OF SOLUTION BY THE ASYMPTOTIC PROPERTIES OF HYPERGEOMETRIC FUNCTIONS

12. General Concepts

The significance of the general solutions constructed in part II of the present report when viewed from the practical point, rests in the fact that they constitute an existence theorem. It shows that an irrotational isentropic flow about a body can be obtained from the corresponding problem of an incompressible fluid, if the free-stream Mach number is not too high. However, the solution in the form of a slowly convergent infinite series cannot be conveniently used to obtain numerical values, as the labor of computation would be prohibitive.

By examining the infinite series obtained in part II, the essential difference between the compressible flow solution and the incompressible flow solution is seen to be associated with the fact that, while in incompressible flow solution the individual terms of the series are of the forms

$$q^{\nu} \begin{matrix} \cos \nu\vartheta \\ \sin \nu\vartheta \end{matrix} \qquad q^{-\nu} \begin{matrix} \cos \nu\vartheta \\ \sin \nu\vartheta \end{matrix}$$

in compressible flow solution the individual terms of the series are of the forms

$$q^{\nu}\, \underline{F}_{\nu}(\tau) \begin{matrix} \cos \nu\vartheta \\ \sin \nu\vartheta \end{matrix} \qquad q^{-\nu}\, \underline{G}_{\nu}(\tau) \begin{matrix} \cos \nu\vartheta \\ \sin \nu\vartheta \end{matrix}$$

If it were possible to write

$$q^{\nu}\, \underline{F}_{\nu}(\tau) = \left[Q(q)\right]^{\nu}, \quad q^{-\nu}\, \underline{G}_{\nu}(\tau) = \left[Q(q)\right]^{-\nu}$$

there would be no difference between the incompressible flow

solution and the compressible flow solution except the "distortion of the speed" q by the new scale Q. In fact, this possibility is realized under the special condition of $\gamma = -1$ as shown by von Kármán (reference 1) and Tsien (reference 9).

For the case of isentropic flow with the general exponent γ there is no such scale factor Q. However, if ν is assumed to be very large, then there is such a function Q, at least to a first approximation. In other words, the leading term in the asymptotic representations of $\underline{F}_\nu(\tau)$ and $\underline{G}_\nu(\tau)$ does give the desired form. On the other hand, the use of asymptotic representation necessarily implies an approximation. But this defect is not difficult to remedy as the difference between an exact hypergeometric function and its asymptotic form can be added to the approximate solution as a correction term. Since there are an infinite number of terms in the series form of the solution and each gives a correction term, the correction terms also constitute an infinite series. Therefore, the original infinite series is now transformed into a closed function plus another infinite series of correction terms. At first sight, such a transformation seems unable to give a result that will avoid the difficulty of prohibitive computational work. But actually, owing to the good approximation given by the asymptotic representation even for moderate values of ν, the correction series converges very rapidly. A few terms seem to be all that are necessary. Thus, for all practical purposes, the original infinite series is now converted into a closed function with "speed distortion" plus a few correction terms. The fundamentally interesting point is that for the case of a general exponent γ, the simple method of speed distortion will not give an accurate enough solution. (Cf. reference 8.)

The change in type of the differential equation at the sonic speed also introduces a singularity in the speed distortion function Q. However, by using the correction terms, the effect of the singularity can be limited to a very narrow range in the neighborhood of sonic speed, and no practical difficulty is experienced. This will be made clear by the numerical example given in part V of this report.

13. Asymptotic Solutions of the Hypergeometric Equations

Let $U_\nu(\tau)$ and $V_\nu(\tau)$ be two new dependent variables defined by

$$\psi_\upsilon(\tau) = \tau^{-\frac{\upsilon+1}{2}} (1 - \tau)^{\frac{\beta}{2}} U_\upsilon(\tau) \qquad (143)$$

$$\chi_\upsilon(\tau) = \tau^{-\frac{\upsilon+1}{2}} (1 - \tau)^{-\frac{\beta}{2}} V_\upsilon(\tau) \qquad (144)$$

The differential equations (27) and (28) reduce respectively to

$$U_\upsilon''(\tau) - \left[\upsilon^2 \varphi(\tau) + \rho_\beta(\tau)\right] U_\upsilon(\tau) = 0 \qquad (145)$$

$$V_\upsilon''(\tau) - \left[\upsilon^2 \varphi(\tau) + \rho_{-\beta}(\tau)\right] V_\upsilon(\tau) = 0 \qquad (146)$$

where

$$\varphi(\tau) = \frac{1 - (2\beta + 1)\tau}{4\tau^2(1 - \tau)}$$

$$\rho_{\pm\beta}(\tau) = \frac{\beta\tau(\beta\tau \pm 2) - (1 - \tau)^2}{4\tau^2(1 - \tau)^2}$$

Both equations (145) and (146) involve a constant parameter υ which is real and positive but otherwise arbitrary for any fixed constant β. In the interval $0 < \tau < 1$ in which the flow takes place, the functions $\varphi(\tau)$ and $\rho_{\pm\beta}(\tau)$ are finite and continuous except at the extremities $\tau = 0$ and $\tau = 1$. To avoid the repetition, let equations (145) and (146) be replaced by

$$U''_{\alpha,\upsilon}(\tau) - \left[\upsilon^2 \varphi(\tau) + \rho_\alpha(\tau)\right] U_{\alpha,\upsilon}(\tau) = 0 \qquad (147)$$

where $U_{\beta,\upsilon}(\tau) = U_\upsilon(\tau)$ when $\alpha = \beta$; and $U_{-\beta,\upsilon}(\tau) = V_\upsilon(\tau)$ when $\alpha = -\beta$. In the interval $\delta \le \tau \le \frac{1}{2\beta+1} - \delta$, $\delta > 0$, $\varphi(\tau)$ is bounded from zero and is positive. F. Horn

(reference 18) showed that when ν is a large positive number, a pair of solutions of the following forms exist in the interval concerned:

$$U^{(1)}_{\alpha,\nu}(\tau) \sim e^{\nu X}\left[\varphi^{-\frac{1}{4}} + \frac{f_{11}(\tau)}{\nu} + \frac{f_{12}(\tau)}{\nu^2} + \ldots + \frac{f_{1s}(\tau)}{\nu^s}\right] \quad (148)$$

$$U^{(2)}_{\alpha,\nu}(\tau) \sim e^{-\nu K}\left[\varphi^{-\frac{1}{4}} + \frac{f_{21}(\tau)}{\nu} + \frac{f_{22}(\tau)}{\nu^2} + \ldots + \frac{f_{2s}(\tau)}{\nu^s}\right] \quad (149)$$

where

$$K(\tau) = \int^{\tau} \varphi^{\frac{1}{2}}(\tau)\, d\tau, \qquad 0 < \tau < \frac{1}{2\beta + 1} \quad (150)$$

A constant in equation (150) was left out, as it can be absorbed in the constant factor in equations (148) and (149). This representation can be shown to be unique as long as ν remains greater than a large positive number N. By substituting $U^{(1)}_{\alpha,\nu}(\tau)$ and $U^{(2)}_{\alpha,\nu}(\tau)$ in equation (147) and choosing the coefficients $f_{r,s}(\tau)$ ($r = 1$ and 2; and $s = 1, 2, 3, \ldots$) to make the individual terms vanish, equation (147) reduces to

$$2K' f'_{1,s+1} + K'' f_{1,s+1} = \rho_\alpha f_{1,s} - f''_{1,s} \quad (151)$$

$$2K' f'_{2,s+1} + K'' f_{2,s+1} = -\rho_\alpha f_{2,s} + f''_{2,s}, \quad s = 0,1,2,\ldots \quad (152)$$

where $f_{1,0}(\tau) = f_{2,0}(\tau) = \varphi^{-\frac{1}{4}}$. The coefficients $f_{r,s}(\tau)$ then are given successively by a first order ordinary differential equation and their determination does not involve any difficulty. The problem is thus formally solved.

Obviously, the solution is of the exponential type when $\varphi(\tau)$ is positive in the range concerned and of an oscillatory type when $\varphi(\tau)$ is negative. Now in the interval $\delta \leq \tau \leq 1 - \delta$, $\delta > 0$ where $\varphi(\tau) \gtrless 0$ when $\tau \lessgtr \frac{1}{2\beta + 1}$, both types of solution exist. It is evident that in the neighborhood of $\tau = \frac{1}{2\beta + 1}$ a change of character of the solutions

must take place, but the manner in which the transition occurs cannot be deduced from equations (148) and (149) because of the failure of the representation of the solutions in the neighborhood $\tau = \frac{1}{2\beta + 1}$. This is closely related to the Stokes phenomenon.

The method was extended by Jeffreys (reference 19) to include the case where $\varphi(\tau)$ has a simple root in an interval under consideration and can be applied suitably to the first order of approximation. The general problem has been treated by Langer (reference 20) in a series of papers, considering both the case where ν and τ are real and that where ν and τ are complex. Attention was given especially to the Stokes phenomenon, and a law of connection of the solution valid on each side of the critical point was explicitly stated. In the present case, however, only the first approximation is used and Jeffreys' method is adopted for convenience.

It is seen from equations (148) and (149) that the first approximation depends only on $\varphi(\tau)$, and the effect of $\rho_\alpha(\tau)$ is felt only by the higher order terms. Hence, for the first approximation only, equation (147) can be written as

$$U_\nu''(\tau) - \nu^2 \varphi(\tau) U_\nu(\tau) = 0 \tag{153}$$

where $U_{\beta,\nu} = U_{-\beta,\nu} = U_\nu$. Thus, when $\nu > N$, the dominant terms of the asymptotic solutions are

$$U_\nu^{(1)}(\tau) \sim \varphi^{-\frac{1}{4}} e^{\nu K} \left[1 + O\left(\frac{1}{\nu}\right)\right] \tag{154}$$

$$U_\nu^{(2)}(\tau) \sim \varphi^{-\frac{1}{4}} e^{-\nu K} \left[1 + O\left(\frac{1}{\nu}\right)\right] \qquad 0 < \tau < \frac{1}{2\beta+1} \tag{155}$$

Here $O\left(\frac{1}{\nu}\right)$, in each case, denotes the fact that the term is uniformly of the order ν^{-1} when ν is sufficiently large in an interval $\delta \le \tau \le \frac{1}{2\beta + 1} - \delta$, $\delta > 0$ and is a function of ν^{-1}.

where $\varphi(\tau) < 0$ and K is a pure imaginary quantity $i\omega$ where ω is real, the dominant terms of the asymptotic solutions must be a linear combination of equations (148) and (149) and must be of the forms:

$$U_\upsilon^{(1)}(\tau) \sim \frac{c_1}{\varphi^{\frac{1}{4}}} \cos(\upsilon\omega + \epsilon_\upsilon) \tag{156}$$

$$U_\upsilon^{(2)}(\tau) \sim \frac{c_2}{\varphi^{\frac{1}{4}}} \sin(\upsilon\omega + \epsilon_\upsilon); \quad \frac{1}{2\beta+1} < \tau < 1 \tag{157}$$

where c_1, c_2, and ϵ_υ are constants to be determined.

The question of determination of these constants is actually the same as that of determining the mode of continuation of the asymptotic representation of the solutions in the range $\frac{1}{2\beta+1} + \delta \leq \tau \leq 1 - \delta$. This can be done, according to Jeffreys, by considering the solutions valid in the neighborhood of $\tau = \frac{1}{2\beta+1}$. Let $\xi = \tau - \frac{1}{2\beta+1}$. When ξ is sufficiently small and υ is large, equation (153) can be written approximately as

$$U_\upsilon''(\xi) + \upsilon^2 \varphi'(0)\, \xi\, U_\upsilon(\xi) = 0 \tag{158}$$

provided $\frac{\varphi^{(n)}(0)}{n!\,\varphi'(0)} \sim 1$. This is known as Stokes equation.

The independent integrals are

$$\xi^{\frac{1}{2}} H_{\frac{1}{3}}^{(1)}(\zeta), \quad \xi^{\frac{1}{2}} H_{\frac{1}{3}}^{(2)}(\zeta); \quad \text{with} \quad \zeta = \frac{2}{3}\upsilon\varphi'^{\frac{1}{2}}(0)\,\xi^{\frac{3}{2}} \tag{159}$$

where $H_{\frac{1}{3}}^{(1)}(\zeta)$ and $H_{\frac{1}{3}}^{(2)}(\zeta)$ are the Hankel functions of order $\frac{1}{3}$. Consider as two independent solutions the following linear combinations:

$$U_\upsilon^{(1)}(\xi) = \xi^{\frac{1}{2}} H_{\frac{1}{3}}^{(1)}(\zeta) + \xi^{\frac{1}{2}} H_{\frac{1}{3}}^{(2)}(\zeta) \tag{160}$$

$$U_{\nu}^{(2)}(\xi) = \xi^{\frac{1}{2}} H_{\frac{1}{3}}^{(1)}(\zeta) - \xi^{\frac{1}{2}} H_{\frac{1}{3}}^{(2)}(\zeta) \qquad (161)$$

As $H_{\frac{1}{3}}^{(1)}(\zeta)$ and $H_{\frac{1}{3}}^{(2)}(\zeta)$ are analytic functions in the whole ζ-plane, this immediately provides a means of identifying the asymptotic forms that represent the same function.

Suppose first that for $\arg \xi = 0$, the solutions are given in equations (160) and (161). The same solutions for which $\arg \xi = \pi$ and $\arg \zeta = \frac{3}{2}\pi$ are

$$U_{\nu}^{(1)}(\xi) = \xi^{\frac{1}{2}} e^{\frac{\pi i}{2}} H_{\frac{1}{3}}^{(1)}\left(\zeta e^{\frac{3\pi i}{2}}\right) + \xi^{\frac{1}{2}} e^{\frac{\pi i}{2}} H_{\frac{1}{3}}^{(2)}\left(\zeta e^{\frac{3\pi i}{2}}\right) \qquad (162)$$

$$U_{\nu}^{(2)}(\xi) = \xi^{\frac{1}{2}} e^{\frac{\pi i}{2}} H_{\frac{1}{3}}^{(1)}\left(\zeta e^{\frac{3\pi i}{2}}\right) - \xi^{\frac{1}{2}} e^{\frac{\pi i}{2}} H_{\frac{1}{3}}^{(2)}\left(\zeta e^{\frac{3\pi i}{2}}\right) \qquad (163)$$

Now

$$H_{\frac{1}{3}}^{(1)}\left(\zeta e^{\frac{\pi i}{2}} e^{\pi i}\right) = -e^{-\frac{\pi i}{2}} H_{\frac{1}{3}}^{(2)}\left(\zeta e^{\frac{\pi i}{2}}\right)$$

$$H_{\frac{1}{3}}^{(2)}\left(\zeta e^{\frac{\pi i}{2}} e^{\pi i}\right) = 2\cos\frac{\pi}{3} H_{\frac{1}{3}}^{(2)}\left(\zeta e^{\frac{\pi i}{2}}\right) + e^{\frac{\pi i}{3}} H_{\frac{1}{3}}^{(1)}\left(\zeta e^{\frac{\pi i}{2}}\right)$$

and when ζ is large and $-\pi < \arg \zeta e^{\frac{\pi i}{2}} < \pi$, the dominant terms of the asymptotic expansions of $H_{\frac{1}{3}}^{(1)}\left(\zeta e^{\frac{\pi i}{2}}\right)$ and $H_{\frac{1}{3}}^{(2)}\left(\zeta e^{\frac{\pi i}{2}}\right)$ are

$$H_{\frac{1}{3}}^{(1)}\left(\zeta e^{\frac{\pi i}{2}}\right) \sim \sqrt{\frac{2}{\pi\zeta}}\, e^{i\left(\zeta e^{\frac{\pi i}{2}} - \frac{\pi}{6} - \frac{\pi}{2}\right)} \left\{1 + O\left(\frac{1}{\zeta}\right)\right\}$$

$$H_{\frac{1}{3}}^{(2)}\left(\zeta e^{\frac{\pi i}{2}}\right) \sim \sqrt{\frac{2}{\pi\zeta}}\, e^{-i\left(\zeta e^{\frac{\pi i}{2}} - \frac{\pi}{6}\right)} \left\{1 + O\left(\frac{1}{\zeta}\right)\right\}$$

By substituting in equations (162) and (163) and neglecting the term of lower order in ζ, there is obtained by expanding at the same time equations (160) and (161):

$$2\xi^{-\frac{1}{4}} \cos\left(\zeta - \frac{\pi}{4}\right) \longrightarrow \xi^{-\frac{1}{4}} e^{-\zeta} \tag{164}$$

$$\xi^{-\frac{1}{4}} \sin\left(\zeta - \frac{\pi}{4}\right) \longrightarrow \xi^{-\frac{1}{4}} e^{\zeta} \tag{165}$$

Here the arrow is used to indicate the transition of the asymptotic representation of the same function from the left-hand to the right-hand member. For small ξ, $\xi^{-\frac{1}{4}} \sim \varphi^{-\frac{1}{4}}$, and $\zeta \sim -\nu w$; (156) and (157) finally become

$$U_\nu^{(1)}(\tau) \sim \frac{2}{\varphi^{\frac{1}{4}}} \cos\left(\nu w - \frac{\pi}{4}\right)\left\{1 + O\left(\frac{1}{\nu}\right)\right\} \tag{166}$$

$$U_\nu^{(2)}(\tau) \sim \frac{1}{\varphi^{\frac{1}{4}}} \cos\left(\nu w + \frac{\pi}{4}\right)\left\{1 + O\left(\frac{1}{\nu}\right)\right\} \quad \frac{1}{2\beta+1} < \tau < 1 \tag{167}$$

with $c_1 = 2$, $c_2 = -1$, and $\epsilon_\nu = -\frac{\pi}{4}$. Under the hypothesis just made, the pair of expressions (154), (166) and (155), (167) actually represent respectively the dominant terms of the two asymptotic expansions of the solutions $U_\nu^{(1)}(\tau)$ and $U_\nu^{(2)}(\tau)$ for a ν which may be any positive but large number.

14. The Asymptotic Representation of $F(a_\nu, b_\nu; c_\nu; \tau)$ and $F(a_\nu + \beta, b_\nu + \beta; c_\nu; \tau)$

The dominant terms of the asymptotic expansion of $U_\nu^{(1)}(\tau)$ and $U_\nu^{(2)}(\tau)$ are given respectively by (154), (166) and (155), (167). By evaluating the simple integrals in (154) and (166), the explicit expressions for the first approximation of $U_\nu^{(1)}(\tau)$ and $U_\nu^{(2)}(\tau)$ are

$$U_\nu^{(1)}(\tau) \sim (2\beta)^{\frac{-\nu(\alpha-1)}{2}} \left\{\frac{4(1-\tau)}{1-\alpha^2\tau}\right\}^{\frac{1}{4}} \tau^{\frac{\nu+1}{2}} \quad T^{\nu}*(\tau) \qquad (168)$$

$$U_\nu^{(2)}(\tau) \sim (2\beta)^{\frac{\nu(\alpha-1)}{2}} \left\{\frac{4(1-\tau)}{1-\alpha^2\tau}\right\}^{\frac{1}{4}} \tau^{-\frac{\nu+1}{2}} \quad T^{-\nu}*(\tau) \qquad 0<\tau<\frac{1}{2\beta+1} \qquad (169)$$

$$U_\nu^{(1)}(\tau) \sim 2\left\{\frac{4(1-\tau)}{\alpha^2\tau-1}\right\}^{\frac{1}{4}} \tau^{\frac{1}{2}} \cos\left(\nu w - \frac{\pi}{4}\right) \qquad (170)$$

$$U_\nu^{(2)}(\tau) \sim \left\{\frac{4(1-\tau)}{\alpha^2\tau-1}\right\}^{\frac{1}{4}} \tau^{\frac{1}{2}} \cos\left(\nu w + \frac{\pi}{4}\right) \qquad \frac{1}{2\beta+1}<\tau<1 \qquad (171)$$

where

$$T^*(\tau) = \frac{\left[\alpha(1-\tau)^{\frac{1}{2}} + (1-\alpha^2\tau)^{\frac{1}{2}}\right]^{\alpha}}{(1-\tau)^{\frac{1}{2}} + (1-\alpha^3\tau)^{\frac{1}{2}}}, \qquad \alpha = \left[\frac{\gamma+1}{\gamma-1}\right]^{\frac{1}{2}} \qquad (172)$$

$$\omega(\tau) = \alpha \tan^{-1}\sqrt{\frac{\alpha^2\tau-1}{\alpha^2(1-\tau)}} - \tan^{-1}\sqrt{\frac{\alpha^2\tau-1}{1-\tau}}$$

The values of the function $\omega(\tau)$ are given in figure 3 together with the function $\mu(\tau)$, defined by $\cos\mu = 1/M$. In the respective ranges of validity, each pair of expressions differs from the exact solution only by a constant factor which can be determined to satisfy the normalization conditions (30) and (36). By substituting equation (168) into equation (143), these were found to be

$$c_{\mp\nu} = \frac{1}{\sqrt{2}}(2\beta)^{\mp\frac{\alpha-1}{2}\nu}\left\{\frac{2}{(1+\alpha)^2}\right\}^{\pm\nu}$$

Thus, the expressions for the desired asymptotic forms, when $\nu > N$, are, for the interval $0 \le \tau < \frac{1}{2\beta+1}$,

$$\underline{F}_{\nu}(\tau) \sim f(\tau)\, T^{\nu}(\tau) \tag{173}$$

$$\underline{G}_{\nu}(\tau) \sim f(\tau)\, T^{-\nu}(\tau) \tag{174}$$

where

$$f(\tau) = \frac{(1-\tau)^{\frac{\beta}{2}+\frac{1}{4}}}{(1-\alpha^2\tau)^{\frac{1}{4}}}, \quad T(\tau) = \frac{2}{(1+\alpha)^{\alpha}} \frac{\left[\alpha(1-\tau)^{\frac{1}{2}} + (1-\alpha^2\tau)^{\frac{1}{2}}\right]^{\alpha}}{(1-\tau)^{\frac{1}{2}} + (1-\alpha^2\tau)^{\frac{1}{2}}} \tag{175}$$

For the interval $\frac{1}{2\beta+1} < \tau < 1$, they are

$$\underline{F}_{\nu}(\tau) \sim f(\tau)\, T^{\nu}(\tau) \cos\left(\nu\omega - \frac{\pi}{4}\right) \tag{176}$$

$$\underline{G}_{\nu}(\tau) \sim \frac{1}{2} f(\tau)\, T^{-\nu}(\tau) \cos\left(\nu\omega + \frac{\pi}{4}\right) \tag{177}$$

where

$$f(\tau) = 2\,\frac{(1-\tau)^{\frac{\beta}{2}+\frac{1}{4}}}{(\alpha^2\tau-1)^{\frac{1}{4}}}, \quad T(\tau) = 2\,\frac{(2\beta)^{\frac{\alpha}{2}}}{(1+\alpha)^{\alpha}}\,\frac{1}{\sqrt{2\beta\tau}} \tag{178}$$

The values of $T(\tau)$ are given (fig. 4) as a function of τ together with the local Mach number M.

Similarly, as from (153) $U_{\nu}(\tau) \sim V_{\nu}(\tau)$, corresponding expressions for $F(a_{\nu} + \beta,\ b_{\nu} + \beta;\ c_{\nu};\ \tau)$ are:

$$\underline{\tilde{F}}_{\nu}(\tau) \sim g(\tau)\, T^{\nu}(\tau) \tag{179}$$

$$\underline{\tilde{G}}_{\nu}(\tau) \sim g(\tau)\, T^{-\nu}(\tau) \qquad 0 \le \tau < \frac{1}{2\beta+1} \tag{180}$$

where

$$g(\tau) = \frac{(1-\tau)^{-\frac{\beta}{2}+\frac{1}{4}}}{(1-\alpha^2\tau)^{\frac{1}{4}}} \tag{181}$$

and

$$\underset{\sim}{F}_{\nu}(\tau) \sim g(\tau)\, T^{\nu}(\tau) \cos\left(\nu w - \frac{\pi}{4}\right) \qquad (182)$$

$$\frac{1}{2\beta+1} < \tau < 1$$

$$\underset{\sim}{G}_{\nu}(\tau) \sim \frac{1}{2}\, g(\tau)\, T^{-\nu}(\tau) \cos\left(\nu w + \frac{\pi}{4}\right) \qquad (183)$$

where

$$g(\tau) = 2\,\frac{(1-\tau)^{-\frac{\beta}{2}+\frac{1}{4}}}{(\alpha^2\tau - 1)^{\frac{1}{4}}} \qquad (184)$$

Here $\underset{\sim}{F}_{\nu}(\tau)$ denotes invariably tho first integral $F(a_\nu, b_\nu; c_\nu; \tau)$ while $\underset{\sim}{G}_{\nu}(\tau)$, wben multiplied by $q^{-2\nu}$, denotes the second integral $F_\nu(\tau)$, defined by equation (37) when ν is not an integer or by equation (39) when ν is an integer, since the asymptotic expansions are valid for both integral and nonintegral values of ν, provided $\nu > N$.

In the domains of validity, the asymptotic expansicns may be differentiated with respect to τ with the same order of approximation. Hence, for $\nu > N$, it can be shown that

for $0 \le \tau < \frac{1}{2\beta+1}$

$$\underset{\sim}{F}_{\nu,1}(\tau) \sim h(\tau)\, T^{\nu}(\tau) \left\{1 + O\left(\frac{1}{\nu}\right)\right\} \qquad (185)$$

$$\underset{\sim}{G}_{\nu,1}(\tau) \sim h(\tau)\, T^{-\nu}(\tau) \left\{1 + O\left(\frac{1}{\nu}\right)\right\} \qquad (186)$$

where

$$h(\tau) = 2\,(1-\tau)^{-\frac{\alpha^2}{4}}\,(1-\alpha^2\tau)^{-\frac{1}{4}}\left[(1-\tau)^{\frac{1}{2}} + (1-\alpha^2\tau)^{\frac{1}{2}}\right]^{-1} \qquad (187)$$

and for $\frac{1}{2\beta+1} < \tau < 1$

$$\underset{\sim}{F}_{\nu,1}(\tau) \sim h(\tau)\, T^{2}(\tau) \cos\left(\nu w - \mu - \frac{\pi}{4}\right)\left\{1 + O\left(\frac{1}{\nu}\right)\right\} \qquad (188)$$

$$\underset{\nu,1}{\tilde{G}}(\tau) \sim \frac{1}{2} h(\tau)\, T^{-\nu}(\tau) \cos\left(\nu w + \mu + \frac{\pi}{4}\right)\left\{1 + 0\left(\frac{1}{\nu}\right)\right\} \quad (189)$$

where

$$h(\tau) = 4(1-\tau)^{-\frac{\alpha^2}{4}} (\alpha^2\tau - 1)^{-\frac{1}{4}} (2\beta\tau)^{-\frac{1}{2}}, \quad \mu(\tau) = \cos^{-1}\sqrt{\frac{1-\tau}{2\beta\tau}} \quad (190)$$

The values of the functions $g(\tau)$ and $h(\tau)$ are given in figure 5.

It is interesting to note that when $\gamma = -1$ the constant α vanishes and only the exponential type of solutions exist. In the case of $\psi_\nu(\tau)$ the solution is exact, namely, for $\beta = -\frac{1}{2}$

$$\underset{\nu}{F}(\tau) = \left[\frac{2}{1 + \sqrt{1 + \frac{q^2}{c_o^2}}}\right]^{\nu} \quad (191)$$

$$\underset{-\nu}{F}(\tau) = \left[\frac{2}{1 + \sqrt{1 + \frac{q^2}{c_o^2}}}\right]^{-\nu} \quad (192)$$

of which the first is in agreement with the result obtained by Tsien (reference 9), while for $\chi_\nu(\tau)$ the solutions which are not exact reduce to

$$\underset{\nu}{\tilde{F}}(\tau) \sim \left[1 + \frac{q^2}{c_c^2}\right]^{\frac{1}{2}} \left[\frac{2}{1 + \left(1 + \frac{q^2}{c_o^2}\right)^{\frac{1}{2}}}\right]^{\nu} \left\{1 + 0\left(\frac{1}{\nu}\right)\right\} \quad (193)$$

$$\nu \geq N$$

$$\underset{\nu}{\tilde{G}}(\tau) \sim \left[1 + \frac{q^2}{c_o^2}\right]^{\frac{1}{2}} \left[\frac{2}{1 + \left(1 + \frac{q^2}{c_o^2}\right)^{\frac{1}{2}}}\right]^{-\nu} \left\{1 + 0\left(\frac{1}{\nu}\right)\right\} \quad (194)$$

This may be the cause that destroys the analogy between the coordinates of the corresponding compressible flows and the incompressible flows.

For $\gamma = 1.405$ and $\nu = n + \frac{1}{2}$, n being a positive integer, the three groups of functions $\underline{F}_{\nu}(\tau)$, $\underline{F}_{-\nu}(\tau)$; $\tilde{\underline{F}}_{\nu}(\tau)$, $\tilde{\underline{F}}_{-\nu}(\tau)$; and $\tilde{\underline{F}}_{\nu,1}(\tau)$, $\tilde{\underline{F}}_{-\nu,1}(\tau)$, together with their asymptotic expressions were calculated for τ varying from 0 to 0.5 and n from 0 to 10. The results are presented in tables 2 to 13. The behavior of the approximation is illustrated in figures 6 to 11. It can be observed that the degree of approximation of the functions increases, on the one hand, with ν for any fixed τ. On the other hand, for any fixed n, the approximation becomes worse as τ approaches the critical point $\tau = \frac{1}{2\beta + 1}$, corresponding to the local sonic speed. On the whole, if the critical point $\tau = \frac{1}{2\beta + 1}$ is not reached, the agreement can generally be regarded as excellent, especially for larger values of n.

15. Transformation of the Function $W(w;\tau)$

Branch Point of Order 1

The function $W(w;\tau)$ for a flow that possesses a branch point of order 1 was given in sections 8 and 9. The forms of representation, as can be seen, are not, in general, suitable for practical calculation. The difficulty is twofold: First, the series involves infinitely many hypergeometric functions which themselves are, in turn, defined as infinite series. The convergence of hypergeometric series generally decreases with an increase of the parameter ν. This means that it is very difficult to compute the value of the later terms of the series for $W(w;\tau)$. Secondly, the convergenoe of the power series defining the function $W(w;\tau)$ itself is, as expected, very slow in the neighborhood of the singularity. To increase the convergence, the following method is used:

Observe that the corresponding function for the incompressible flow that has the same character of singularity is

$$W_o^{(i)}(w) = \sum_{n=0}^{\infty} A_n w^n, \qquad |w| < U$$

which is absolutely and uniformly convergent in any closed domain in $|w| < U$. Now, if in (92) $\tilde{F}_n^{(r)}(\tau)$ is replaced by

$$F_n^{(r)}(\tau) \cong \frac{f(\tau)}{f(\tau_1)} t^n(\tau), \qquad 0 \leq \tau < \frac{1}{2\beta+1} \tag{195}$$

where $t(\tau) = \frac{T(\tau)}{T(\tau_1)}$, as by hypothesis, $0 < \tau_1 << \frac{1}{2\beta+1}$; then it is clear that

$$W^{(i)}(w;\tau) \cong \frac{f(\tau)}{f(\tau_1)} \sum_{n=0}^{\infty} A_n (tw)^n, \qquad |tw| < U \tag{196}$$

which is also absolutely and uniformly convergent in the same domain as $W_o(w)$ and, consequently, (196) will be denoted by $\frac{f(\tau)}{f(\tau_1)} W_o(tw)$. In doing this, however, the restriction that (195) holds only when n is greater than a large number N is violated. The error can be removed by adding to and subtracting from (91) the quantity given in (196); then it follows immediately that

$$W^{(i)}(w;\tau) = W_1(w;\tau) + W_a^{(i)}(w;\tau) \tag{197}$$

where

$$W_1(w;\tau) = \frac{f(\tau)}{f(\tau_1)} W_o(tw) \tag{198}$$

$$W_a^{(i)}(w;\tau) = \sum_{n=0}^{\infty} A_n G_n(\tau) w^n, \qquad |w| < U \tag{199}$$

with

$$G_n(\tau) = \underline{F}_n^{(r)}(\tau) - \frac{f(\tau)}{f(\tau_1)}\, t^n(\tau)$$

Here n is a positive integer. The function $W(w;\tau)$ then is represented by the sum of two functions $W_1(w;\tau)$, which is of closed form, and $W_2^{(i)}(w;\tau)$, which is the difference of two convergent power series and hence is also convergent. But, according to the theory of asymptotic expansion, $G_n(\tau)$ tends to zero as n approaches infinity. In fact, $G_n(\tau)$ is of order n^{-1}; therefore, the convergence of $W(w;\tau)$ is increased by the order of n^{-1}. This actually is the gist of the whole problem.

As the form of the representation of the hypergeometric function given in equation (195) is valid for all τ in $0 \leq \tau < \frac{1}{2\beta+1}$, $W_1(w;\tau)$ given by equation (198) holds automatically even outside the circle $|w| = U$. For this reason, $W_1(w;\tau)$ should be identical in form with that derived from equation (101). That this is the case can be seen from the following consideration. For, in addition to equation (195), if it is assumed that

$$\underline{G}_\nu(\tau) \cong f(\tau)\, T^{-\nu}(\tau) \tag{200}$$

it follows that

$$\xi_\nu(\tau_1) = -\xi_{-\nu}(\tau_1) = \sqrt{\frac{1-\alpha^2\tau_1}{1-\tau_1}} \tag{201}$$

then equations (106) and (107) yield, by equations (108) and (109),

$$B_n^* \cong \frac{B_n}{f(\tau_1)}\, T^{-\nu}(\tau_1), \qquad C_n^* \cong \frac{C_n}{f(\tau_1)}\, T^{\nu}(\tau_1) \tag{202}$$

By using these sets of approximate coefficients and replacing $\underline{F}_\nu(\tau)$ and $\underline{G}_\nu(\tau)$ by their respective asymptotic expression, the following relation is obtained with the aid of equation (100)

$$W^{(o)}(w;\tau) = W_1(w;\tau) + W_2^{(o)}(w;\tau) \tag{203}$$

where

$$W_2^{(o)}(w;\tau) = i \sum_{n=0}^{\infty} \left\{ G_\nu^{(1)}(\tau)\, w^\nu + G_\nu^{(2)}(\tau)\, w^{-\nu} \right\} \tag{204}$$

In this case the coefficients B_n^* and C_n^*, as well as the functions $\underline{F}_\nu(\tau)$ and $\underline{G}_\nu(\tau)$ used in deriving $W_1(w;\tau)$, are approximate. Hence, if both are corrected, $G_\nu^{(1)}(\tau)$ and $G_\nu^{(2)}(\tau)$ should be of the forms

$$\left.\begin{aligned} G_\nu^{(1)}(\tau) &= \Delta B_n^*\, \underline{F}_\nu(\tau) + \frac{B_n}{f(\tau_1)}\, T^{-\nu}(\tau_1)\, \Delta \underline{F}_\nu(\tau) \\ G_\nu^{(2)}(\tau) &= \Delta C_n^*\, \underline{G}_\nu(\tau) + \frac{C_n}{f(\tau_1)}\, T^{\nu}(\tau_1)\, \Delta \underline{G}_\nu(\tau) \end{aligned}\right\} \tag{205}$$

where

$$\left.\begin{aligned} \Delta B_n^* &= B_n^* - \frac{B_n}{f(\tau_1)}\, T^{-\nu}(\tau_1), \quad \Delta \underline{F}_\nu(\tau) = \underline{F}_\nu(\tau) - f(\tau)\, T^{\nu}(\tau) \\ \Delta C_n^* &= C_n^* - \frac{C_n}{f(\tau_1)}\, T^{\nu}(\tau_1), \quad \Delta \underline{G}_\nu(\tau) = \underline{G}_\nu(\tau) - f(\tau)\, T^{-\nu}(\tau) \end{aligned}\right\} \tag{206}$$

Here the differences ΔB_n^* and ΔC_n^* depend upon the condition at infinity for any sets of constants B_n and C_n, while those of $\Delta \underline{F}_\nu(\tau)$ and $\Delta \underline{G}_\nu(\tau)$ are functions of τ only and, for this reason, can be tabulated once for all. It also can be shown that the order of ΔB_n^* is at least of n^{-1} and therefore the convergence of (204) is again increased by n^{-1}.

Consequently, if $\psi(q,\theta) = \psi_1(q,\theta) + \psi_2^{(l)}(q,\theta)$ where the superscript (l) denotes either (i) or (o), and if the coefficients are real, the stream function for the subsonic flow is according to (93) given by

$$\Psi_1(q,\theta) = \frac{f(\tau)}{f(\tau_1)}\,\Psi_0(tq,\theta), \qquad 0 \le \tau \le \frac{1}{2\beta+1} \tag{207}$$

$$\Psi_2^{(i)}(q,\theta) = -\sum_{n=0}^{\infty} A_n G_n(\tau)\, q^n \sin n\theta, \qquad q < U \tag{208}$$

and in $U < q < V$

$$\Psi_2^{(o)}(q,\theta) = \sum_{n=0}^{\infty}\left[G_\nu^{(1)}(\tau)\; q^\nu + G_\nu^{(2)}(\tau)\; q^{-\nu}\right]\cos \nu\theta \tag{209}$$

with θ restricted by $0 \le \theta < 2\pi$. This result is striking in that for $\tau = \tau_1$, $\Psi(U,\theta) \equiv \Psi_1(U,\theta)$ as $G_\nu(\tau_1) = 0$; that is, the function $\Psi_1(q,\theta)$ represents the correct singularity of the exact function. Far away from the singularity the term $\Psi_2^{(l)}(q,\theta)$ ($l = i$ or o) gradually comes into prominence, especially near $\tau = \frac{1}{2\beta+1}$; but the convergence there is already so rapid that a small number of terms is enough to secure a high accuracy in $\Psi(q,\theta)$.

It is interesting to estimate the magnitude of the second part of the stream function. By noting the fact that $G_n(\tau_1) = 0$, $G_\nu(\tau_1) = 0$, the expansions of the $G_n(\tau)$ and $G_\nu(\tau)$ are

$$G_n(\tau) = G_n'(\tau_1)\,(\tau - \tau_1) + \ldots, \qquad 0 < \tau < \tau_1$$

$$G_\nu(\tau) = G_\nu(\tau_1)\,(\tau - \tau_1) + \ldots, \qquad \tau_1 < \tau < \frac{1}{2\beta+1}$$

Then from corollary (52), it is shown that for $\vartheta \neq 0$

$$\Psi_2^{(l)}(q,\theta) \sim \left(\frac{\partial \varphi_o}{\partial \theta}\right)_{q=U}(\tau - \tau_1) + \ldots$$

In other words, the second part of the solution is of the order of magnitude of $(\tau - \tau_1)$. However, the magnitude of

$(\tau - \tau_1)$ depends essentially upon τ_1 for a given incompressible flow. If τ_1 is not small, then when $\tau = 0$, $|\tau - \tau_1|$ will be large. Thus for large free-stream Mach numbers, the second part of the solution ψ_2 cannot be neglected. This means that for high free-stream Mach numbers the correct solution for compressible flow is considerably more complicated than the usually assumed simple speed distortion rule would lead one to believe. Thus, any theory based upon such a simple rule cannot be accurate enough for transonic flows.

On the other hand, if τ_1 is small, or $\tau_1 << \frac{1}{2\beta + 1}$, then the value of $|\tau - \tau_1|$ for $\tau = 0$ is small. Furthermore, if the maximum velocity of the flow is well below the sonic velocity, then the maximum value of τ also is small, thus $|\tau - \tau_1|$ for the whole flow is small. Tnen the second part of the solution ψ_2 is negligible. However, even then the solution for the compressible flow cannot be expressed as the solution of the incompressible solution by a simple distortion of the velocity scale, as is generally assumed in the so-called hodograph method. For this would be the case only if the multiplying factor $f(\tau)/f(\tau_1)$ is identically equal to 1. Since the multiplying factor is a function of the magnitude of velocity, the streamlines of the compressible flow and the streamlines of the incompressible flow cannot be made to correspond to each other. On the other hand, equation (207) shows that if ψ_o is zero, then ψ_1 is also zero. Thus there is this <u>one</u> streamline, the zero streamline, in both flows satisfying the requirement of direct mapping. Since the zero streamline generally is chosen to represent the contour of the body, on the surface of the body in purely subsonic flows, the velocity of the compressible flow can be calculated from the incompressible flow by a simple "correction formula." This formula is given by equating the velocity q of the incompressible fluid to the velocity function tq of the compressible flow. Thus

$$\left(\frac{q}{U}\right)_o = \sqrt{\frac{\tau}{\tau_1}}\, t = \sqrt{\frac{\tau}{\tau_1}}\, \frac{T(\tau)}{T(\tau_1)}$$

where the subscript o denotes the quantity for incompressible flow and $T(\tau)$ is given by equation (175). This formula is the same as that suggested by G. Temple and J. Yarwood (reference 11). This coincidence of Temple's theory with the

present investigation can be considered as a further substantiation of the method.

For the supersonic regions, $\underline{F}_\nu(\tau)$ and $\underline{G}_\nu(\tau)$ in (101) should be replaced by

$$\left.\begin{aligned} \underline{F}_\nu(\tau) &\cong f(\tau)\, T^\nu(\tau) \cos\left(\nu w - \frac{\pi}{4}\right) \qquad (210)\\ \underline{G}_\nu(\tau) &\cong \frac{1}{2} f(\tau)\, T^{-\nu}(\tau) \cos\left(\nu w + \frac{\pi}{4}\right) \qquad (211) \end{aligned}\right\} \quad \frac{1}{2\beta+1} < \tau < 1$$

where $f(\tau)$, $T(\tau)$ and $\omega(\tau)$ are given in (178) and (172); then by writing

$$\underline{F}_\nu(\tau) \cong \frac{1}{2} f(\tau) \left\{ e^{i\left(\nu w - \frac{\pi}{4}\right)} + e^{-i\left(\nu w - \frac{\pi}{4}\right)} \right\}$$

and substituting as before in equation (101), it leads again to the sum of $W_1(w;\tau)$ and $W_2^{(o)}(w;\tau)$, where

$$W_1(w;\tau) = \frac{f(\tau)}{4f(\tau_1)} \left[e^{-\frac{\pi i}{4}} i \sum_{n=o}^{\infty} \left\{ B_n \left(twe^{i\omega}\right)^\nu + C_n \left(twe^{i\omega}\right)^{-\nu} \right\} \right.$$

$$\left. + e^{\frac{\pi i}{4}} i \sum_{n=o}^{\infty} \left\{ B_n \left(twe^{-i\omega}\right)^\nu + C_n \left(twe^{-i\omega}\right)^{-\nu} \right\} \right]$$

and

$$W_2(w;\tau) = i \sum_{n=o}^{\infty} \left\{ G_\nu^{(1)}(\tau)\, w^\nu + G_\nu^{(2)}(\tau)\, w^{-\nu} \right\}, \qquad \frac{1}{2\beta+1} < \tau < 1$$

According to equation (100), $W_1(w;\tau)$ also can be summed:

$$W_1(w;\tau) = \frac{1}{4} \frac{f(\tau)}{f(\tau_1)} \left[e^{-\frac{\pi i}{4}} W_o\left(twe^{\omega i}\right) + e^{\frac{\pi i}{4}} W_o\left(twe^{-\omega i}\right) \right] \qquad (212)$$

Furthermore, from (178) it can be seen that $|tw| = \lambda U$, λ being a constant given by

$$\lambda = \frac{2(2\beta)^{\frac{\alpha}{2}}}{(1+\alpha)^{\alpha}\,(2\beta\tau_1)^{\frac{1}{2}}}\,\frac{1}{T(\tau_1)} > 1 \qquad (213)$$

which is a function of the Mach number and the characteristic constant β of the gas but independent of the shape of the boundary. The value of this function λ is given in table 14 and figure 12 for $\gamma = 1.405$. As a consequence, the functions constituting the stream function for the supersonic flow are

$$\psi_1(q,\vartheta) = 2^{-\frac{5}{2}}\,\frac{f(\tau)}{f(\tau_1)}\left[\psi_0(\vartheta+\omega)+\psi_0(\vartheta-\omega)+\Phi_0(\vartheta+\omega)-\Phi_0(\vartheta-\omega)\right] \qquad (214)$$

$$\vartheta - \omega \geq 0$$

$$\psi_2(q,\vartheta) = \sum_{n=0}^{\infty}\left\{G_\nu^{(1)}(\tau)\,q^{\nu}+G_\nu^{(2)}(\tau)\,q^{-\nu}\right\}\cos\nu\vartheta,\quad U < q < V \qquad (215)$$

Here the functions Ψ_0 and Φ_0 are defined, on account of (213), by

$$\Psi_0(\vartheta\pm\omega)\equiv\psi_0(\lambda U,\vartheta\pm\omega),\qquad \Phi_0(\vartheta\pm\omega)\equiv\varphi_0(\lambda U,\vartheta\pm\omega) \qquad (216)$$

where φ_0 and ψ_0 are the velocity potential and the stream function, respectively, of the corresponding incompressible flow. The functions $G_\nu^{(1)}(\tau)$ and $G_\nu^{(2)}(\tau)$ are the same as defined in (205) except that $\Delta\underline{F}_\nu(\tau)$ and $\Delta\underline{G}_\nu(\tau)$ now are given by

$$\left.\begin{aligned} \Delta \underset{\sim}{F}_{\nu}(\tau) &= \underset{\sim}{F}_{\nu}(\tau) - \frac{f(\tau)}{2}\, T^{\nu} \cos\left(\nu\omega - \frac{\pi}{4}\right) \\ \Delta \underset{\sim}{G}_{\nu}(\tau) &= \underset{\sim}{G}_{\nu}(\tau) - \frac{f(\tau)}{2}\, T^{-\nu} \cos\left(\nu\omega + \frac{\pi}{4}\right) \end{aligned}\right\} \quad (217)$$

Unlike the previous calculations, $G_{\nu}^{(1)}(\tau)$ in (211) is not of the order of ν^{-1} due to the presence of 1/2 in front of $f(\tau)\, T^{\nu} \cos\left(\nu\omega - \frac{\pi}{4}\right)$. This, however, does not offer a serious objection, as the series in which it appears already converges with $(tq)^{\nu}$, t being less than unity.

It is worth noting, moreover, that in the hyperbolic domain the function $\psi_1(q, \vartheta)$ depends, aside from a factor $f(\tau)$, only on the two independent families of characteristics defined by

$$\xi = \vartheta + \omega, \quad \eta = \vartheta - \omega \quad (218)$$

This result is most striking, as it shows that the main part of the solution satisfies the simple wave equation and thus clearly demonstrates its hyperbolic character. With both the incompressible stream function ψ_0 and the incompressible potential function φ_0 appearing in the solution, it is impossible to establish a simple relation between the incompressible streamlines and the compressible streamlines. Since such a simple relation is the foundation of the so-called speed correction formula for a quick estimation of velocity distribution in compressible flow from that of incompressible flow over the same body, this idea cannot be extended to supersonic regions. On the other hand, this also indicates that although the differential equation for $\psi(q, \vartheta)$ is hyperbolic in the supersonic range, it cannot be reduced to the simple wave equation by a mere distortion of the speed scale as given by the function $\omega(\tau)$. For if this were the case, then $\psi_1(q, \vartheta)$ would constitute an exact solution without the additional $\psi_2^{(o)}(q, \vartheta)$. This fact is all the more important as the additional $\psi_2^{(o)}(q, \vartheta)$ is not small in comparison with $\psi_1(q, \vartheta)$ for the mixed subsonic and supersonic flows, especially for the transitional region near sonic velocity. However, in the case of pure supersonic flow, $\psi_2^{(o)}(q, \vartheta)$ might be small; then $\psi_1(q, \vartheta)$ alone may

be used as a satisfactory approximation. Of course, when $\gamma = -1$, then, as in the corresponding case in subsonic flow, the exact differential equation for the stream function can be reduced to the simple wave equation. In this case, the appropriate form for the speed function ω is

$$\omega(q) = - \tan^{-1} \sqrt{\frac{1}{\frac{q^2}{q_1^2 - c_1^2} - 1}} \qquad (219)$$

where the subscript 1 denotes the conditions at the point of tangency of the true isentropic curve and the approximating tangent. This agrees with the result obtained by N. Coburn. (See reference 21.)

16. Continuation: Logarithmic Singularity

In the case of the logarithmic singularity the function $W(w;\tau)$ was broken up into two parts of which only the one that characterizes the singularity was given in equations (115) and (116). As an example, it is proposed to show that this problem can be treated by the same method. If the same approximation is introduced as in equations (195) and (201), then the coefficients defined in equations (121) and (122) become approximately:

$$A_n \cong \frac{1}{n} \frac{T^{-n}(\tau_1)}{f(\tau_1)}, \qquad C_n \cong \frac{1}{n} \frac{T^{n}(\tau_1)}{f(\tau_1)} \qquad (220)$$

with $B\, f^2(\tau_1) = \frac{1}{2}$, so chosen that the form of equation (207) is again preserved. With these coefficients and if there is written for the function inside the circle $q = U$:

$$\tilde{\Psi}^{(i)}(q,\vartheta) = \tilde{\Psi}_1(q,\vartheta) + \tilde{\Psi}_2^{(i)}(q,\vartheta)$$

Equation (115) reduces to the sum of

$$\tilde{\Psi}_1(q,\vartheta) = \frac{f(\tau)}{f(\tau_1)} \tilde{\Psi}_0(tq,\vartheta), \qquad 0 \le \tau < \frac{1}{2\beta + 1} \qquad (221)$$

$$\tilde{\psi}_2^{(i)}(q,\vartheta) = \sum_{n=1}^{\infty} \frac{1}{n} \tilde{G}_n(\tau) \left(\frac{q}{U}\right)^n \cos n\vartheta, \qquad q < U \tag{222}$$

where

$$\tilde{G}_n(\tau) = \underline{F}_n(\tau)\, \Delta\underline{G}_n(\tau_1) + \frac{\Delta\underline{F}_n(\tau)}{f(\tau_1)\, T^n(\tau_1)} \tag{223}$$

with

$$\left.\begin{aligned} \Delta\underline{F}_n(\tau) &= \underline{F}_n(\tau) - f(\tau)\, T^n(\tau) \\ \Delta\underline{G}_n(\tau_1) &= \frac{\underline{G}_n(\tau_1)}{f^2(\tau_1)} - f^{-1}(\tau_1)\, T^{-n}(\tau_1) \end{aligned}\right\} \tag{224}$$

Similarly, in the case of equation (116) it reduces to

$$\tilde{\psi}^{(o)}(q,\vartheta) = \tilde{\psi}_1(q,\vartheta) + \tilde{\psi}_2^{(o)}(q,\vartheta)$$

Here $\tilde{\psi}_1(q,\vartheta)$ is again the same as (221); while $\tilde{\psi}_2^{(o)}(q,\vartheta)$ is

$$\tilde{\psi}_2^{(o)}(q,\vartheta) = -\frac{1}{2f^2(\tau_1)} \int_{\tau_1}^{\tau} (1-\tau)^{\beta} \frac{d\tau}{\tau} + \frac{f(\tau)}{f(\tau_1)} \log \frac{tq}{U}$$

$$+ \sum_{n=1}^{\infty} \frac{1}{n} \tilde{G}_n^{(o)} \left(\frac{q}{U}\right)^{-n} \cos n\vartheta \tag{225}$$

where

$$\tilde{G}_n^{(o)}(\tau) = \underline{G}_n(\tau)\, \Delta\underline{F}_n(\tau_1) + f^{-1}(\tau_1)\, T^n(\tau_1)\, \Delta\underline{G}_n(\tau) \tag{226}$$

with

$$\Delta\underline{F}_n(\tau_1) = \frac{\underline{F}_n(\tau_1)}{f^2(\tau_1)} - \frac{T^n(\tau_1)}{f(\tau_1)}, \quad \Delta\underline{G}_n(\tau) = \underline{G}_n(\tau) - f(\tau)\, T^{-n}(\tau) \tag{227}$$

Unlike the previous case, $\tilde{\Psi}(q,\vartheta) = \tilde{\Psi}_0(q,\vartheta)$ when, and only when, c_0 tends to infinity. Because of (221), however, the singularity of $\tilde{\Psi}(q,\vartheta)$ remains unchanged.

Again, if in (116)

$$\underline{G}_n(\tau) \cong \frac{1}{2} f(\tau)\, T^{-n}(\tau) \cos\left(n\omega + \frac{\pi}{4}\right)$$

is substituted for $\underline{G}_n(\tau)$, it can similarly be shown that

$$\tilde{\Psi}_1(q,\vartheta) = 2^{-\frac{5}{2}} \frac{f(\tau)}{f(\tau_1)} \left[\tilde{\Psi}_0(\vartheta+\omega) + \tilde{\Psi}_0(\vartheta-\omega) - \tilde{\Phi}_0(\vartheta+\omega) + \tilde{\Phi}_0(\vartheta-\omega)\right] \quad (228)$$

$$\vartheta - \omega \geq 0$$

$$\tilde{\Psi}_2^{(o)}(q,\vartheta) = -\frac{1}{2f^2(\tau_1)} \int_{\tau_1}^{\tau} (1-\tau)^{\beta} \frac{d\tau}{\tau} + 2^{-\frac{3}{2}} \frac{f(\tau)}{f(\tau_1)} (\log \lambda - \omega)$$

$$+ \sum_{n\pm 1}^{\infty} \frac{\tilde{G}_n^{(o)}}{n} \left(\frac{q}{U}\right)^{-n} \cos n\vartheta \quad (229)$$

where $\tilde{\Psi}_0(\vartheta \pm \omega)$ and $\tilde{\Phi}_0(\vartheta \pm \omega)$ are defined analogously to (216), and $\Delta\underline{G}_n(\tau)$ in $\tilde{G}_n^{(o)}(\tau)$ is now given by

$$\Delta\underline{G}_n(\tau) = \underline{G}_n(\tau) - \frac{1}{2} f(\tau)\, T^{-n}(\tau) \cos\left(n\omega + \frac{\pi}{4}\right) \quad (230)$$

This seems to indicate that the results obtained so far for $\psi_1(q,\vartheta)$ are quite general: It may differ for different cases, at most, by a constant factor. The general property, however, is not shared by $\psi_2(q,\vartheta)$, the character of which changes radically with the nature of the singularity and the shape of the boundary. Hence, its importance in the present problem is evident.

17. The Coordinate Functions $x(q,\vartheta)$ and $y(q,\vartheta)$

Whenever the function $\chi(q,\vartheta)$ for a boundary problem is determined, the coordinate functions $x(q,\vartheta)$ and $y(q,\vartheta)$ can be calculated according to equations (141) and (142). Suppose, for instance, a boundary is assigned with the property that the function $\Lambda(w;\tau)$ is truly described by (94) and (110), of which the real part $\chi(q,\vartheta)$, defined within the circle $|w| = U$, is

$$\chi(q,\vartheta) = \sum_{n=0}^{\infty} \tilde{A}_n \, \tilde{\underline{F}}_n^{(r)}(\tau) \, q^n \cos n\vartheta, \qquad q < U \tag{231}$$

where the constants $\tilde{A}_n$ in (94) are again real and are regarded as known, and $\tilde{\underline{F}}_n^{(r)}(\tau) = \tilde{\underline{F}}_n(\tau)/\underline{F}_n(\tau_1)$.

As the series is absolutely and uniformly convergent in $q < U$, it can be differentiated partially term by term with respect to q and ϑ. When the differential coefficients $\chi_q(q,\vartheta)$ and $\chi_\vartheta(q,\vartheta)$ are calculated and are substituted in equations (141) and (142), there results:

$$x(q,\vartheta) = \sum_{n=1}^{\infty} n \, \tilde{A}_n \, \tilde{\underline{F}}_n^{(r)} \, q^{n-1} \cos (n-1)\vartheta$$

$$-\beta\tau \sum_{n=1}^{\infty} n \, \tilde{A}_n \, \frac{n-1}{n+1} \, \tilde{\underline{F}}_{n,1}^{(r)}(\tau) \, q^{n-1} \cos n\vartheta \cos \vartheta \tag{232}$$

$$y(q,\vartheta) = -\sum_{n=1}^{\infty} n \, \tilde{A}_n \, \tilde{\underline{F}}_n^{(r)} \, q^{n-1} \sin (n-1)\vartheta$$

$$-\beta\tau \sum_{n=1}^{\infty} n \, \tilde{A}_n \, \frac{n-1}{n+1} \, \underline{F}_{n,1}^{(r)}(\tau) \, q^{n-1} \cos n\vartheta \sin \vartheta \tag{233}$$

where

$$\underline{F}_{n,1}^{(r)}(\tau) = \frac{F(a_n + \beta + 1, \; b_n + \beta + 1; \; c_n + 1; \; \tau)}{F(a_n, \; b_n; \; c_n; \; \tau_1)} \tag{234}$$

Now, since

$$x_o(q,\vartheta) = \sum_{n=1}^{\infty} n\,\tilde{A}_n\, q^{n-1} \cos(n-1)\vartheta$$

and

$$y_o(q,\vartheta) = -\sum_{n=1}^{\infty} n\,\tilde{A}_n\, q^{n-1} \sin(n-1)\vartheta$$

$$\sigma_o(q,\vartheta) = \sum_{n=1}^{\infty} \tilde{A}_n\, q^{n} \sin n\vartheta$$

by introducing the approximaticn given by equations (179) and (185), that is

$$\underset{\sim}{\tilde{F}}_n^{(r)}(\tau) \cong \frac{g(\tau)}{f(\tau_1)}\, t^n(\tau)$$

$$0 \le \tau < \frac{1}{2\beta+1}$$

$$\underset{\sim}{\tilde{F}}_{n,1}^{(r)}(\tau) \cong \frac{h(\tau)}{f(\tau_1)}\, t^n(\tau)$$

by defining

$$x(q,\vartheta) = x_1(q,\vartheta) + x_2^{(l)}(q,\vartheta) \qquad (235)$$

$$y(q,\vartheta) = y_1(q,\vartheta) + y_2^{(l)}(q,\vartheta) \qquad (236)$$

it can be shown by the same manner that

$$x_1(q,\vartheta) = \frac{g(\tau)}{f(\tau_1)}\, t(\tau)\, x_o(tq,\vartheta) - \frac{\beta\tau}{q}\,\frac{h(\tau)}{f(\tau_1)}\,\Omega_o(tq,\vartheta)\cos\vartheta \qquad (237)$$

$$0 \le \tau < \frac{1}{2\beta+1}$$

$$y_1(q,\vartheta) = \frac{g(\tau)}{f(\tau_1)}\, t(\tau)\, y_o(tq,\vartheta) - \frac{\beta\tau}{q}\,\frac{h(\tau)}{f(\tau_1)}\,\Omega_o(tq,\vartheta)\sin\vartheta \qquad (238)$$

and

$$x_2^{(i)}(q,\vartheta) = \sum_{n=1}^{\infty} n\,\tilde{A}_n\,\tilde{G}_n(\tau)\,q^{n-1}\cos(n-1)\vartheta$$

$$-\beta\tau\sum_{n=1}^{\infty} n\,\tilde{A}_n\,\tilde{G}_{n,1}(\tau)\,q^{n-1}\cos n\vartheta\cos\vartheta \qquad (239)$$

$$q < U$$

$$y_2^{(i)}(q,\vartheta) = -\sum_{n=1}^{\infty} n\,\tilde{A}_n\,\tilde{G}_n(\tau)\,q^{n-1}\sin(n-1)\vartheta$$

$$-\beta\tau\sum_{n=1}^{\infty} n\,\tilde{A}_n\,\tilde{G}_{n,1}(\tau)\,q^{n-1}\cos n\vartheta\sin\vartheta \qquad (240)$$

where

$$\tilde{G}_n(\tau) = \frac{F(a_n+\beta,\ b_n+\beta;\ c_n;\ \tau)}{F(a_n,\ b_n;\ c_n;\ \tau_1)} - \frac{g(\tau)}{f(\tau_1)}\,t^n(\tau) \qquad (241)$$

$$\tilde{G}_{n,1}(\tau) = \frac{n-1}{n+1}\,\frac{F(a_n+\beta+1,\ b_n+\beta+1;\ c_n+1;\tau)}{F(a_n,\ b_n;\ c_n;\ \tau_1)} - \frac{h(\tau)}{f(\tau_1)}\,t^n(\tau) \qquad (242)$$

$$\Omega_o(q,\vartheta) = \frac{\partial\sigma_o}{\partial\vartheta} \qquad (243)$$

On the other hand, the expression for $\chi(q,\vartheta)$ valid outside the circle of convergence is

$$\chi(q,\vartheta) = \sum_{n=o}^{\infty}\left[\tilde{B}_n^*\,\underline{\tilde{F}}_\nu(\tau)\,q^\nu - \tilde{C}_n^*\,\underline{\tilde{G}}_\nu(\tau)\,q^{-\nu}\right]\sin\nu\vartheta \qquad (244)$$

provided the coefficients $\tilde{B}_n^*$ and $\tilde{C}_n^*$ in (110) are real. The functions $x(q,\vartheta)$ and $y(q,\vartheta)$ corresponding to (244) can be found similarly. These are:

$$x(q,\vartheta) = \sum_{n=0}^{\infty} \left\{ \nu \tilde{B}_n^* \underline{\tilde{F}}_\nu (\tau)\ q^{\nu-1} \sin(\nu-1)\vartheta + \nu \tilde{C}_n^* \underline{\tilde{G}}_\nu(\tau)\ \bar{q}^{\nu-1} \sin(\nu+1)\vartheta \right\}$$

$$- \beta\tau \sum_{n=0}^{\infty} \left\{ \nu \tilde{B}_n^* \frac{\nu-1}{\nu+1} \underline{\tilde{F}}_{\nu,1}(\tau)\ q^{\nu-1} + \nu \tilde{C}_n^* \frac{\nu+1}{\nu-1} \underline{\tilde{G}}_{\nu,1}(\tau)\ q^{-\nu-1} \right\} \sin \nu\vartheta \cos\vartheta \qquad (245)$$

$$U < q < V$$

$$y(q,\vartheta) = \sum_{n=0}^{\infty} \left\{ \nu \tilde{B}_n^* \underline{\tilde{F}}_\nu(\tau)\ q^{\nu-1} \cos(\nu-1)\vartheta - \nu \tilde{C}_n^* \underline{\tilde{G}}_\nu(\tau)\ \bar{q}^{\nu-1} \cos(\nu+1)\vartheta \right\}$$

$$- \beta\tau \sum_{n=0}^{\infty} \left\{ \nu \tilde{B}_n^* \frac{\nu-1}{\nu+1} \underline{\tilde{F}}_{\nu,1}(\tau)\ q^{\nu-1} + \nu \tilde{C}_n^* \frac{\nu+1}{\nu-1} \underline{\tilde{G}}_{\nu,1}(\tau)\ q^{-\nu-1} \right\} \sin \nu\vartheta \sin\vartheta \qquad (246)$$

Here the constants $\tilde{B}_n^*$ and $\tilde{C}_n^*$ satisfy the relations (109) and (110) and can be reduced to

$$\tilde{B}_n^* \cong \frac{\tilde{B}_n}{f(\tau_1)}\ T^{-\nu}(\tau_1), \qquad \tilde{C}_n^* \cong \frac{\tilde{C}_n}{f(\tau_1)}\ T^{\nu}(\tau_1) \qquad (247)$$

provided the same approximation is made as in (202). Furthermore,

$$x_o(q,\vartheta) = \sum_{n=0}^{\infty} \left\{ \nu \tilde{B}_n\ q^{\nu-1} \sin(\nu-1)\vartheta + \nu \tilde{C}_n\ q^{-\nu-1} \sin(\nu+1)\vartheta \right\}$$

$$y_0(q,\vartheta) = \sum_{n=0}^{\infty} \left\{ \upsilon \tilde{B}_n \, q^{\upsilon-1} \cos(\upsilon-1)\vartheta - \upsilon \hat{C}_n \, q^{-\upsilon-1} \cos(\upsilon+1)\vartheta \right\}$$

and if $\underline{\tilde{F}}_\upsilon(\tau)$ and $\underline{\tilde{F}}_{\upsilon,1}(\tau)$ for the high-order terms are substituted by the asymptotic forms: namely,

$$\underline{\tilde{F}}_\upsilon(\tau) \cong g(\tau)\, T^{\upsilon}(\tau), \quad \underline{\tilde{F}}_{\upsilon,1}(\tau) \cong h(\tau)\, T^{-\upsilon}(\tau); \quad 0 \le \tau < \frac{1}{2\beta+1}$$

then in like manner (245) and (246) can be transformed and can each be represented by the sum of two functions $x_1(q,\vartheta)$, $y_1(q,\vartheta)$, and $x_2(q,\vartheta)$, $y_2(q,\vartheta)$, where x_1 and y_1 are the same as (237) and (238); while x_2 and y_2 are:

$$x_2^{(0)}(q,\vartheta) = \sum_{n=0}^{\infty} \upsilon \left\{ \hat{G}_\upsilon^{(1)}(\tau) q^{\upsilon-1} \sin(\upsilon-1)\vartheta + \tilde{G}_\upsilon^{(2)}(\tau) q^{-\upsilon-1} \sin(\upsilon+1)\vartheta \right\}$$

$$- \beta\tau \sum_{n=0}^{\infty} \upsilon \left\{ \tilde{G}_{\upsilon,1}^{(1)}(\tau) q^{\upsilon-1} + \tilde{G}_{\upsilon,1}^{(2)}(\tau) q^{-\upsilon-1} \right\} \sin \upsilon\vartheta \cos\vartheta \quad (248)$$

$$\tau_1 \le \tau < \frac{1}{2\beta+1}$$

$$y_2^{(0)}(q,\vartheta) = \sum_{n=0}^{\infty} \upsilon \left\{ \hat{G}_\upsilon^{(1)}(\tau) q^{\upsilon-1} \cos(\upsilon-1)\vartheta - \tilde{G}_\upsilon^{(2)}(\tau) q^{-\upsilon-1} \cos(\upsilon+1)\vartheta \right\}$$

$$- \beta\tau \sum_{n=0}^{\infty} \upsilon \left\{ \tilde{G}_{\upsilon,1}^{(1)}(\tau) q^{\upsilon-1} + \hat{G}_{\upsilon,1}^{(2)}(\tau) q^{-\upsilon-1} \right\} \sin \upsilon\vartheta \sin\vartheta \quad (249)$$

where $\tilde{G}_\upsilon^{(\alpha)}$ and $\tilde{G}_{\upsilon,1}^{(\alpha)}$ are defined by:

$$\left.\begin{aligned} \tilde{G}_\upsilon^{(1)}(\tau) &= \Delta\tilde{B}_n^* \, \underline{\tilde{F}}_\upsilon(\tau) + \frac{\tilde{B}_n}{f(\tau_1)} T^{-\upsilon}(\tau_1) \, \Delta\underline{\tilde{F}}_\upsilon(\tau) \\ \tilde{G}_\upsilon^{(2)}(\tau) &= \Delta C_n^* \, \underline{\tilde{G}}_\upsilon(\tau) + \frac{\tilde{C}_n}{f(\tau_1)} T^{\upsilon}(\tau_1) \, \Delta\underline{\tilde{G}}_\upsilon \end{aligned}\right\} \quad (250)$$

$$\left.\begin{aligned}\tilde{G}^{(1)}_{\nu,1}(\tau) &= \Delta\tilde{B}^{*}_{n}\,\frac{\nu-1}{\nu+1}\,\underline{\tilde{F}}_{\nu,1}(\tau) + \frac{\tilde{B}_n}{f(\tau_1)}\,T^{-\nu}(\tau_1)\,\Delta\underline{\tilde{F}}_{\nu,1}(\tau)\\ \tilde{G}^{(2)}_{\nu,1}(\tau) &= \Delta\tilde{C}^{*}_{n}\,\frac{\nu-1}{\nu+1}\,\underline{\tilde{G}}_{\nu,1} + \frac{\tilde{C}_n}{f(\tau_1)}\,T^{\nu}(\tau_1)\,\Delta\underline{\tilde{G}}_{\nu,1}\end{aligned}\right\} \quad (251)$$

with

$$\left.\begin{aligned}\Delta\underline{\tilde{F}}_{\nu,1}(\tau) &= \frac{\nu-1}{\nu+1}\,\underline{\tilde{F}}_{\nu,1}(\tau) - h(\tau)\,T^{\nu}(\tau)\\ \Delta\underline{\tilde{G}}_{\nu,1}(\tau) &= \frac{\nu+1}{\nu-1}\,\underline{\tilde{G}}_{\nu,1}(\tau) - h(\tau)\,T^{-\nu}(\tau)\end{aligned}\right\} \quad (252)$$

while $\Delta\tilde{B}^{*}_{n}$ and $\Delta\underline{\tilde{F}}_{\nu}(\tau)$ are defined just the same as those given in equation (206).

Similarly, if the hypergeometric functions involved in the high-order terms are substituted by

$$\underline{\tilde{F}}_{\nu}(\tau) \cong g(\tau)\,T^{\nu}\cos\left(\nu\omega-\frac{\pi}{4}\right),\quad \underline{\tilde{F}}_{\nu,1}(\tau) \cong h(\tau)\,T^{\nu}\cos\left(\nu\omega-\mu-\frac{\pi}{4}\right)$$

$$\underline{\tilde{G}}_{\nu}(\tau) \cong \frac{1}{2}\,g(\tau)\,T^{-\nu}\cos\left(\nu\omega+\frac{\pi}{4}\right),\quad \underline{\tilde{G}}_{\nu,1}(\tau) \cong \frac{1}{2}\,h(\tau)\,T^{-\nu}\cos\left(\nu\omega+\mu+\frac{\pi}{4}\right)$$

and by resolving the products of the trigonometric functions into sums: for instance,

$$\begin{aligned}2\sin(\nu-1)\vartheta\cos\left(\nu\omega-\frac{\pi}{4}\right) &= \sin\left[(\nu-1)(\vartheta+\omega)+\left(\omega-\frac{\pi}{4}\right)\right]\\ &\quad+\sin\left[(\nu-1)(\vartheta-\omega)-\left(\omega-\frac{\pi}{4}\right)\right]\\ 2\sin(\nu+1)\vartheta\cos\left(\nu\omega+\frac{\pi}{4}\right) &= \sin\left[(\nu+1)(\vartheta+\omega)-\left(\omega-\frac{\pi}{4}\right)\right]\\ &\quad+\sin\left[(\nu+1)(\vartheta-\omega)+\left(\omega-\frac{\pi}{4}\right)\right]\end{aligned}$$

a brief reduction gives when $\frac{1}{2\beta + 1} < \tau < 1$,

$$x_1(q,\vartheta) = \frac{t(\tau)}{4}\frac{g(\tau)}{f(\tau_1)}\left\{\left[X_0(\vartheta + \omega) + X_0(\vartheta - \omega)\right]\cos\left(\frac{\pi}{4} - \omega\right)\right.$$

$$\left. - \left[Y_0(\vartheta + \omega) - Y_0(\vartheta - \omega)\right]\sin\left(\frac{\pi}{4} - \omega\right)\right\}$$

$$- \frac{\beta\tau}{4q}\frac{h(\tau)}{f(\tau_1)}\left\{\left[\Omega_0(\vartheta + \omega) + \Omega_0(\vartheta - \omega)\right]\cos\left(\mu + \frac{\pi}{4}\right)\right.$$

$$\left. - \left[\Theta_0(\vartheta + \omega) - \Theta_0(\vartheta - \omega)\right]\sin\left(\frac{\pi}{4} + \mu\right)\right\}\cos\vartheta \qquad (253)$$

$$y_1(q,\vartheta) = \frac{t(\tau)}{4}\frac{g(\tau)}{f(\tau_1)}\left\{\left[Y_0(\vartheta + \omega) + Y_0(\vartheta - \omega)\right]\cos\left(\frac{\pi}{4} - \omega\right)\right.$$

$$\left. + \left[X_0(\vartheta + \omega) - X_0(\vartheta - \omega)\right]\sin\left(\frac{\pi}{4} - \omega\right)\right\}$$

$$- \frac{\beta\tau}{4q}\frac{h(\tau)}{f(\tau_1)}\left\{\left[\Omega_0(\vartheta + \omega) + \Omega_0(\vartheta - \omega)\right]\cos\left(\mu + \frac{\pi}{4}\right)\right.$$

$$\left. - \left[\Theta_0(\vartheta + \omega) - \Theta_0(\vartheta - \omega)\right]\sin\left(\frac{\pi}{4} - \omega\right)\right\}\sin\vartheta \qquad (254)$$

by the fact that $qt = \lambda U$ in the interval under consideration.

Here

$$X_0(\vartheta \pm \omega) = x_0(\lambda U, \vartheta \pm \omega), \quad Y_0(\vartheta \pm \omega) = y_0(\lambda U, \vartheta \pm \omega)$$

$$\Theta_c(\vartheta \pm \omega) \equiv \Theta_0(\lambda U, \vartheta \pm \omega), \quad \Omega_0(\vartheta \pm \omega) \equiv \Omega_0(\lambda U, \vartheta \pm \omega)$$

where

$$\Theta_o(q,\vartheta) = \frac{\partial \chi_o}{\partial \vartheta}$$

and

$$x_2^{(o)}(q,\vartheta)$$

$$= \sum_{n=o}^{\infty} \upsilon \left\{ \tilde{G}_\upsilon^{(1)}(\tau) q^{\upsilon-1} \sin (\upsilon-1)\vartheta + \tilde{G}_\upsilon^{(2)}(\tau) q^{-\upsilon-1} \sin (\upsilon+1)\vartheta \right\}$$

$$-\beta\tau \sum_{n=o}^{\infty} \upsilon \left\{ \tilde{G}_{\upsilon,1}^{(1)}(\tau) q^{\upsilon-1} + \tilde{G}_{\upsilon,1}^{(2)}(\tau) q^{-\upsilon-1} \right\} \sin \upsilon\vartheta \cos \vartheta \qquad (255)$$

$$\frac{1}{2\beta+1} < \tau < 1$$

$$y_2^{(o)}(q,\vartheta)$$

$$= \sum_{n=o}^{\infty} \upsilon \left\{ \tilde{G}_\upsilon^{(1)}(\tau) q^{\upsilon-1} \cos (\upsilon-1) - \tilde{G}_\upsilon^{(2)}(\tau) q^{-\upsilon-1} \cos (\upsilon+1)\vartheta \right\}$$

$$-\beta\tau \sum_{n=o}^{\infty} \upsilon \left\{ \tilde{G}_{\upsilon,1}^{(1)}(\tau) q^{\upsilon-1} + \tilde{G}_{\upsilon,1}^{(2)}(\tau) q^{-\upsilon-1} \right\} \sin \upsilon\vartheta \sin \vartheta \qquad (256)$$

where $\tilde{G}_\upsilon^{(\alpha)}(\tau)$ and $\tilde{G}_{\upsilon,1}^{(\alpha)}(\tau)$ retain the definitions given in (250) and (251) except that $\Delta\underline{\tilde{F}}_\upsilon(\tau)$, $\Delta\underline{\tilde{F}}_{\upsilon,1}(\tau)$, $\Delta\underline{\tilde{G}}_\upsilon(\tau)$, and $\Delta\underline{\tilde{G}}_{\upsilon,1}(\tau)$ are replaced by

$$\left.\begin{aligned}
\Delta\underline{\tilde{F}}_\upsilon(\tau) &= \underline{\tilde{F}}_\upsilon(\tau) - \frac{1}{2} g(\tau)\, T^\upsilon \cos\left(\upsilon w - \frac{\pi}{4}\right) \\
\Delta\underline{\tilde{F}}_{\upsilon,1}(\tau) &= \frac{\upsilon-1}{\upsilon+1} \underline{\tilde{F}}_{\upsilon,1} - \frac{h(\tau)}{2} T^\upsilon \cos\left(\upsilon w - \mu - \frac{\pi}{4}\right) \\
\Delta\underline{\tilde{G}}_\upsilon(\tau) &= \underline{\tilde{G}}_\upsilon(\tau) - \frac{g(\tau)}{2} T^{-\upsilon} \cos\left(\upsilon w + \frac{\pi}{4}\right) \\
\Delta\underline{\tilde{G}}_{\upsilon,1}(\tau) &= \frac{\upsilon+1}{\upsilon-1} \underline{\tilde{G}}_{\upsilon,1} - \frac{h(\tau)}{2} T^{-\upsilon} \cos\left(\upsilon w + \mu + \frac{\pi}{4}\right)
\end{aligned}\right\} \qquad (257)$$

respectively. It must be noted again that the orders of $\tilde{G}_{\nu}^{(1)}(\tau)$ and $\tilde{G}_{\nu,1}^{(1)}(\tau)$ are the same as those of $\Delta\underline{\tilde{F}}_{\nu}(\tau)$ and $\Delta\underline{\tilde{F}}_{\nu,1}(\tau)$, respectively, because of the way they are defined in (257). For the same reason as stated in section 15, this again cannot jeopardize the basic assumption of convergence of the series.

PART IV

CRITERIA FOR THE UPPER CRITICAL MACH NUMBER

18. Limiting Line and the Breakdown of Isentropic Flow

The solutions constructed in the previous sections are known to be regular in the hodograph plane except at a few singular points. It is also known that for the limiting case of infinite sonic speed, or $c_0 \rightarrow \infty$, the solution will give the desired flow pattern in the physical plane. When the sonic speed is finite or when the Mach number of the free stream is different from zero, there is no guarantee as to the behavior of the solution in the physical plane except the probable continuity of the flow pattern with respect to the free-stream Mach number. It is found that such continuity in the flow pattern actually exists up to a certain Mach number. In other words, the pattern of the compressible flow is only slightly different from that of the incompressible flow up to a certain Mach number at which the so-called limiting lines appear. At the limiting line, the acceleration of the flow is infinite and the flow is reversed. It was shown by Tollmein (reference 13) and Tsien (reference 2) that, without considering viscosity, the flow cannot be continued across the limiting lines, and a forbidden region is created in the space where no fluid can enter. In other words, continuity of flow pattern exists up to a critical Mach number beyond which no isentropic flow is possible with the imposed physical boundary conditions.

The breakdown of isentropic flow, or the compressibility burble, can be effected in two ways. First of all, the acceleration in the neighborhood of the limiting line is very large. Thus each one of the following factors gives appreciable alterations in the dynamic relations:

(a) Viscous stress due to ordinary viscosity of the fluid (reference 22)

(b) Stress due to expansion or compression of the fluid, or viscous stress due to the second viscosity coefficient (reference 23, pp. 351 and 358)

(c) Small but appreciable relaxation time required for the vibrational modes of the molecules to reach equilibrium state (reference 24)

(d) Heat conduction from fluid element to fluid element

Secondly, the isentropic flow also can break down through the appearance of shock waves. The breakdown of isentropic flow is associated with the introduction of vorticity to the flow. Thus the flow becomes rotational with part of the mechanical energy of the fluid converted into heat energy. All these factors tend to increase the entropy of the fluid and finally to increase the drag of the body. Thus the critical Mach number so defined is of great physical importance to the aerodynamic characteristics of the body concerned.

Of course, the isentropic flow might break down due to the instability of flow fluid with the final appearance of shock waves. Furthermore, the action of boundary layer and possible condensation of one component of the fluid[1] on the flow might lead also to the premature destruction of the isentropic flow. On the other hand, shock waves can appear only in supersonic flow; thus, if the speed of the fluid is everywhere subsonic, there is no danger of the compressibility burble. Hence, the free-stream Mach number for the first appearance of sonic speed in the field is called the "lower critical Mach number"; while the free-stream Mach number for the first appearance of limiting lines is called the "upper critical Mach number." (See reference 2.) The latter is always higher than the former, due to the fact that limiting lines appear only in supersonic flow. The actual critical Mach number for the compressibility burble must lie between these two limits and depends, among other parameters, upon the Reynolds number of the flow.

19. The Condition for the Limiting Line

At the limiting hodograph, or the hodograph of the limiting line, it was shown (references 1, 2, 12, and 13) that

$$\frac{\partial(x,y)}{\partial(u,v)} \equiv -\left(\frac{\rho_0}{\rho q}\right)^2 \left[\psi_q^2 - \left(\frac{1}{c^2} - \frac{1}{q^2}\right)\psi_\vartheta^2\right] = 0 \qquad (258)$$

[1]The phenomenon of condensation shocks due to water vapor in the air flow around an airfoil was first brought to the attention of the authors by Kate Liepmann, who observed them in wind-tunnel experiments.

Since the factor before the term ψ_{ϑ}^{2} is positive for supersonic regions only, $c < q$, where $\rho \neq 0$, the limiting line can appear only when the local speed exceeds that of sound. It should be noted that the vanishing of the Jacobian is the condition for the failure of the hodograph method, as the transformation (9) and (10) would no longer be one-to-one and continuous. Thus, the appearance of the limiting lines is then the physical counterpart of the singularity of the transformation.

As $\psi(\tau,\vartheta)$ is known, equation (258) defines two lines in the hodograph plane:

$$2\tau\left[\frac{1-\tau}{\alpha^{2}\tau-1}\right]^{\frac{1}{2}}\psi_{\tau}-\psi_{\vartheta}=0 \qquad (259)$$

$$2\tau\left[\frac{1-\tau}{\alpha^{2}\tau-1}\right]^{\frac{1}{2}}\psi_{\tau}+\psi_{\vartheta}=0,\quad \tau\geq\frac{1}{2\beta+1} \qquad (260)$$

Geometrically, this expresses the fact that the streamline $\psi(q,\vartheta)$ = constant and a characteristic curve belonging to either family has a common tangent (reference 1). The problem can then be formulated based on this property: the necessary and sufficient condition for the existence of a limiting line is that there exists a solution between the two simultaneous equations

$$2\tau\left[\frac{1-\tau}{\alpha^{2}\tau-1}\right]^{\frac{1}{2}}\psi_{\tau}-\psi_{\vartheta}=0 \qquad (261)$$

$$\psi=0 \qquad (262)$$

or

$$2\tau\left[\frac{1-\tau}{\alpha^{2}\tau-1}\right]^{\frac{1}{2}}\psi_{\tau}+\psi_{\vartheta}=0 \qquad (263)$$

$$\psi=0 \qquad (264)$$

where $\psi(\tau,\vartheta)$ is a definite branch associated with the largest possible τ for a given boundary and a free-stream

Mach number. The zero streamline is chosen, as it generally gives the highest velocity and is the place for the earliest appearance of the limiting line.

Generally, these equations may not possess a solution for a known function $\psi(\tau,\vartheta)$ when the parameter M_1 is assigned. This means that there will be a system of boundaries corresponding to a sequence of values of M_1, for which the limiting line does not occur. The first Mach number for which equations (261) and (262) have a solution will be defined as the upper critical Mach number and the corresponding boundary as the critical boundary.

The actual solution of the equation is, in general, difficult owing to the fact that $\psi(\tau,\vartheta)$ is, in most cases, represented by an infinite series. However, if the streamlines are determined in the hodograph plane for the calculation of the shape of the body, a simple graphical test of whether there is a point of tangency between the zero streamline and the characteristic can be easily made. On the other hand, if the form (214) and (215), for instance, is used, an approximate analytic solution can be obtained without involving much labor.

20. The Approximate Determination of the Upper Critical Mach Number

As can be seen from section 15, the importance of $\psi_2^{(o)}(\tau,\vartheta)$ relative to $\psi_1(\tau,\vartheta)$ will decrease as τ recedes from the critical circle $\tau = \frac{1}{2\beta+1}$ toward the supersonic region. For the first appearance of the limiting line, τ is almost always high, especially when the boundary is a slender closed body. Let this be the case; then $\psi_2^{(o)}(\tau,\vartheta)$ can be neglected in comparison with $\psi_1(\tau,\vartheta)$ and a great simplification is possible. The zero streamline then can be represented approximately by

$$\psi(\tau,\vartheta) \equiv \psi_1(\tau,\vartheta) = 0$$

Furthermore, a simple reduction shows that the two pairs of equations, (261), (262) and (263), (264) reduce respec tively to

$$\Phi_o'(\eta) + \Psi_o'(\eta) = 0 \tag{265}$$

$$\Phi_o(\xi) + \Psi_o(\xi) = \Phi_o(\eta) - \Psi_o(\eta) \tag{266}$$

or

$$\Phi_o'(\xi) + \Psi_o'(\xi) = 0 \tag{267}$$

$$\Phi_o(\eta) - \Psi_o(\eta) = \Phi_o(\xi) + \Psi_o(\xi) \tag{268}$$

where ξ and η are the characteristic parameters defined in equation (218). This reduction is made possible by the fact that $f(\tau)$ never vanishes in the interval $\frac{1}{2\beta+1} < \tau < 1$.

Whenever the stream function Ψ_o and the potential function φ_o of the incompressible flow are given, the functions Ψ_o and Φ_o can be easily obtained by substituting λU for q according to equation (216). Then, since λ decreases with an increase in the free-stream Mach number M, as shown in table 14 and figure 12, the upper critical Mach number will be given by the largest value of λ that gives a solution either of equations (265) and (266) or equations (267) and (268). An analytical solution can be made, as the functions Ψ_o and Φ_o are quite simple.

There is, however, an interesting direct geometrical interpretation of these sets of equations in the physical plane of the incompressible flow as shown by figure 13. According to equations (216), the functions Ψ_o and Φ_o are the stream function ψ_o and the potential function φ_o at the constant value of the speed λU. Since $\lambda > 1$, for the body shown in figure 13, the constant speed λU curve C_λ forms a loop symmetrical with respect to the y-axis.

The variables are really the angle of inclination of the incompressible velocity vector. Along the constant speed curve C_λ from the point S_2 to P, the angle of inclination of the velocity vector is monotonically decreasing. Therefore, the parameter of the angle of inclination can be replaced by the distances along the curve C_λ. Let equation (267) be satisfied at the point $S = S_2$; then

$$\Phi_o'(S_2) = -\Psi_o'(S_2) \tag{269}$$

This means that, at the point $S = S_2$, the rate of change of the potential function φ_o along C_λ is equal to the negative of the rate of change of the stream function ψ_o. Since potential lines and streamlines in incompressible flow form an infinitesimal square mesh, this condition requires that the angle between the tangent to the curve C_λ at $S = S_2$ be 45°, as shown in figure 13. This is easily seen by remembering that from S_2 to P, the value of the stream function increases while the value of the potential function decreases, because of the indicated flow direction. Thus the point S_2 can be easily determined by this graphical condition. Equation (268) can then be written as

$$\Phi_o(s) - \Psi_o(S) = \Phi_o(S_2) + \Psi_o(S_2) \tag{270}$$

If this condition is satisfied at a point S_1, then the condition for a limiting line is completely satisfied. A similar graphical interpretation for the equations (265) and (266) can be worked out for the side of the constant speed curve lying to the right of the y-axis. From these considerations, it is clear that the upper critical Mach number is the lowest free-stream Mach number which gives a constant speed C_λ containing two points, S_1 and S_2, defined by equations (269) and (270).

PART V

APPLICATION — ELLIPTIC CYLINDERS

21. Preliminary Discussions

This part of the report is devoted to the application of the general method, developed in part III, to the study of the flow of a compressible fluid around an elliptic cylinder. According to sections 8 and 9, if a solution were constructed about the stagnation point, the continuation of this solution would require that conditions (102) and (103) and, hence, (106) and (107) be satisfied. These equations involve two sets of hypergeometric functions with parameters m and $m + 1/2$, as well as their derivatives. To shorten the lengthy calculations, in view of the limited amount of time available, the following approximate procedure was adopted.

Given the domain $\underline{D}$, the solution valid in the annulus region, rather than that about the stagnation point, was first constructed. The constants which determine the Laurent expansion of the solution, B_n^* and C_n^*, for example, are now assigned and, consequently, the set of hypergeometric functions with integral parameters is not immediately required. The difficulty, however, is the question of whether it is possible to continue the solution within the circle of convergence. This continuation may not be possible owing to the stringent continuity conditions given by equations (102) and (103), and to the requirement that the function must be regular within the circle $q = U$.

This, however, does not offer a serious objection from the practical point of view. In the first place, the summed function ($\psi_1(q,\vartheta)$, for instance) actually holds even within the circle of convergence $q < U$, and the correction function $\psi_2(q,\vartheta)$, is generally small compared with $\psi_1(q,\vartheta)$ due to the close asymptotic approximation of the hypergeometric functions in the elliptic domain. In other words, although the solution within the circle of convergence strictly represents a different flow, numerically it approximates very closely that defined in the annulus region. In the second place, since this region $q < U$ is relatively unimportant in the case of mixed flow, where τ_1 is very much less than $\frac{1}{2\beta+1}$ — that is, for free-stream Mach number considerably less

than unity - the inaccuracy of the solution is limited to a small region in the hodograph plane. Furthermore, the most interesting phenomena of such a flow, such as the appearance of limiting lines, always take place in the annulus region. Therefore, this modified procedure, although unsatisfactory from the general view point, is an expedient capable of yielding an interesting result and furnishing a test of the practicability of the proposed solution.

The situation also may be considered from another angle. The procedure used in this section can be derived by replacing the functions $\xi_{\nu}(\tau)$ and $\xi_{-\nu}(\tau)$ with the approximate values given in equation (201) in the expressions for the coefficients involved in the solution within the annulus region, that is, (106) and (107). Thus the procedure may be regarded as an appropriate method of approximation. The error introduced is generally negligible if $\tau_1 << \frac{1}{2\beta+1}$. This is indicated by the fact that the correction function $\psi_2(q,\tau)$, for instance, is very small in comparison with $\psi_1(q,\vartheta)$ when $q \leq U$.

Another simplification is made by using the elementary integral $q^{-2\nu} \underline{F}_{-\nu}(\tau)$ instead of $q^{-2\nu} \underline{G}_{\nu}(\tau)$ in the continued solution, as, in this case, $\underline{F}_{-\nu}(\tau)$ is a well-defined function. In doing so, the asymptotic behavior of the second solution remains unchanged because the first term in $\underline{G}_{\nu}(\tau)$ is always small in comparison with the second.

If, however, all the required hypergeometric functions are computed, there is no difficulty in carrying out the exact method developed in part III of the report for any accurate study of two-dimensional flow. For this reason, the expressions for the hydrodynamic functions derived for both the exact and approximate procedures for the problem at hand are given.

In the numerical example, detailed calculations are made for the flow of air about a cylindrical body derived from the incompressible flow about an elliptic section with a ratio of the minor and major axes equal to 0.6. The calculations were carried out for two different free-stream Mach numbers, 0.6 and 0.7.

22. The Functions $z_o(w)$, $W_o(w)$ and $\Lambda_o(w)$

The irrotational flow of an incompressible fluid about

an elliptic cylinder with the velocity at infinity parallel to the major axis is represented by the complex potential $W_o(z_o)$:

$$W_o(z_o) = \zeta + \frac{1}{\zeta} \tag{271}$$

with

$$z_o = \zeta + \frac{\epsilon^2}{\zeta} \tag{272}$$

For convenience in practical calculation, all the physical quantities z_o, q, and ρ, will be normalized consistently thrcughout the present part. The major and minor axes of the section are respectively $1 + \epsilon^2$ and $1 - \epsilon^2$, where $\epsilon < 1$; $q = 1$ at infinity and $\rho = 1$ when $q = 0$. This will automatically render the hydrodynamic functions dimensionless and the constants U and ρ_o will be eliminated from the formulas in the succeeding sections.

By differontiating (271) with respect to z_o, the dimensionless complex velocity of the flow is

$$w = \frac{\zeta^2 - 1}{\zeta^2 - \epsilon^2}$$

Thus

$$\zeta = - \left[\frac{1 - \epsilon^2 w}{1 - w}\right]^{1/2}, \qquad |1 - \epsilon^2 w| \neq 0 \tag{273}$$

This function is two-valued with two branch points at $w = 1$ and $w = \epsilon^{-2}$. In order to make $z_o(w)$ a single-valued function of w, the expression (273) is supposed to be the principal value so that $|\arg(1-w)| < \pi$ and $1 < |w| < \epsilon^{-2}$. The condition $|\epsilon^2 w| < 1$ must be satisfied, for $w = \epsilon^{-2}$ corresponds to $\zeta = 0$, which is another singularity. With the principal value so defined, if the negative sign in (273) is taken, then the domain D corresponds to the half plane $R\ell\ \zeta \leq 0$ and $|\zeta| \geq 1$. On the other hand, since the trans-

formation (272) is one-to-one when $|\zeta| \geq 1$, then the domain D, which is R$\{z_o \leq 0$ with the region inside the section excluded, corresponds uniquely to $\underline{D}$.

Consequently, the inverse mapping function $z_o(w)$ is

$$z_o(w) = -\left\{\left[\frac{1-\epsilon^2 w}{1-w}\right]^{1/2} + \epsilon^2\left[\frac{1-w}{1-\epsilon^2 w}\right]^{1/2}\right\} \qquad (274)$$

which will be single-valued, provided a cut is introduced to join the branch points in such a way that the argument of $(1-w)$ is restricted to $-\pi < \arg(1-w) < \pi$ and $|\epsilon^2 w| < 1$. On separating into real and imaginary parts, it is found that as $0 \leq \vartheta < 2\pi$

$$x_o(q,\vartheta) = -\frac{1}{2^{\frac{1}{2}}}\left[\left\{I(q,\vartheta) + J(q,\vartheta)\right\}^{1/2} + \epsilon^2\left\{I_\epsilon(q,\vartheta) + J^{-1}(q,\vartheta)\right\}^{1/2}\right] \qquad (275)$$

$$y_o(q,\vartheta) = \frac{1}{2^{\frac{1}{2}}}\left[\left\{-I(q,\vartheta) + J(q,\vartheta)\right\}^{1/2} - \epsilon^2\left\{-I_\epsilon(q,\vartheta) + J^{-1}(q,\vartheta)\right\}^{1/2}\right] \qquad (276)$$

with $w = q\,e^{-i\vartheta}$, where the functions $I(q,\vartheta)$, $I_\epsilon(q,\vartheta)$, and $J(q,\vartheta)$ stand for:

$$I(q,\vartheta) = \frac{1-(1+\epsilon^2)q\cos\vartheta + \epsilon^2 q^2}{1 - 2q\cos\vartheta + q^2} \qquad (277)$$

$$I_\epsilon(q,\vartheta) = \frac{1-(1+\epsilon^2)q\cos\vartheta + \epsilon^2 q^2}{1 - 2\epsilon^2 q\cos\vartheta + \epsilon^4 q^2} \qquad (278)$$

$$J(q,\vartheta) = \left[\frac{1-2\epsilon^2 q\cos\vartheta + \epsilon^4 q^2}{1-2q\cos\vartheta + q^2}\right]^{1/2} \qquad (279)$$

On the other hand, substituting equation (273) in equation (271), the function $W_o(z_o)$ is carried over into D; namely,

$$W_o(w) = -\left\{\left[\frac{1-\epsilon^2 w}{1-w}\right]^{\frac{1}{2}} + \left[\frac{1-w}{1-\epsilon^2 w}\right]^{\frac{1}{2}}\right\} \qquad (280)$$

Now $W_o(w) = \varphi_o(q,\vartheta) + i\psi_o(q,\vartheta)$, and similarly

$$\varphi_o(q,\vartheta) = \frac{1}{2^{\frac{1}{2}}}\left[\left\{I(q,\vartheta) + J(q,\vartheta)\right\}^{\frac{1}{2}} + \left\{I_\epsilon(q,\vartheta) + J^{-1}(q,\vartheta)\right\}^{\frac{1}{2}}\right] \qquad (281)$$

$$\psi_o(q,\vartheta) = \frac{1}{2^{\frac{1}{2}}}\left[\left\{-I(q,\vartheta) + J(q,\vartheta)\right\}^{\frac{1}{2}} - \left\{-I_\epsilon(q,\vartheta) + J^{-1}(q,\vartheta)\right\}^{\frac{1}{2}}\right] \qquad (282)$$

By integrating $z_o(w)$, according to (87), the transformed prtential function $\Lambda_o(w)$, aside from a constant, takes the form:

$$\Lambda_o(w) = 2(1-w)^{\frac{1}{2}}(1-\epsilon^2 w)^{\frac{1}{2}} \qquad (283)$$

The principal value of this function is again defined by restricting the argument of $(1-w)$ to $-\pi < \arg(1\ w) < \pi$ and $|w| < \epsilon^{-2}$. Within this domain D, the real and imaginary parts are:

$$\varkappa_o(q,\vartheta) = 2^{\frac{1}{2}}[K(q,\vartheta) + L(q,\vartheta)]^{\frac{1}{2}} \qquad (284)$$

$$0 \le \vartheta < 2\pi$$

$$\sigma_o(q,\vartheta) = -2^{\frac{1}{2}}[-K(q,\vartheta) + L(q,\vartheta)]^{\frac{1}{2}} \qquad (285)$$

as $\Lambda_o(w) = \varkappa_o(q,\vartheta) - i\sigma_o(q,\vartheta)$, where the functions $K(q,\vartheta)$ and $L(q,\vartheta)$ are defined by:

$$K(q,\vartheta) = 1 - (1+\epsilon^2)q\cos\vartheta + \epsilon^2 q^2 \cos 2\vartheta \quad (286)$$

$$L(q,\vartheta) = [1-2q\cos\vartheta + q^2]^{\frac{1}{2}}\,[1-2\epsilon^2 q\cos\vartheta + \epsilon^4 q^2]^{\frac{1}{2}} \quad (287)$$

23. Expansions of $W_o(w)$ and $\Lambda_o(w)$

The function $W_o(w)$ defined in (280) is single-valued and regular everywhere in $|w| < 1$ and, hence, possesses the following expansion:

$$W_o(w) = -\sum_{n=o}^{\infty} A_n w^n, \quad |w| < 1 \quad (288)$$

where the coefficients A_n are real and given by

$$A_n = 2S_n^{(i)} - (1+\epsilon^2)\,S_{n-1}^{(i)} \quad n \geq 1 \quad (289)$$

$$A_o = 2S_o^{(i)} = 2$$

with

$$S_n^{(i)}(\epsilon^2) = \frac{1}{\pi}\sum_{m=o}^{n} \frac{\Gamma(n-m+\frac{1}{2})\Gamma(m+\frac{1}{2})}{\Gamma(n-m+1)\Gamma(m+1)}\,\epsilon^{2m}$$

However, in the region outside $|w| < 1$ the function $W_o(w)$ is doubled-valued; and when a cut is put between the branch points $w = 1$ and $w = \epsilon^{-2}$, the principal value is discontinuous along the positive axis of reals within the annulus region. To obtain the desired expansion, the function is written in the following form

$$W_o(w) = \frac{1}{w^{\frac{1}{2}}}\,\frac{2-(1+\epsilon^2)w}{(1-w^{-1})^{\frac{1}{2}}\,(1-\epsilon^2 w)^{\frac{1}{2}}} \quad (290)$$

Now $(1-w^{-1})^{-\frac{1}{2}}\ (1-\epsilon^2 w)^{\frac{1}{2}}$ is single-valued and continuous within the annulus region; its Laurent expansion is

$$(1-w^{-1})^{-\frac{1}{2}}\ (1-\epsilon^2 w)^{-\frac{1}{2}} = S_o^{(o)} + \sum_{n=1}^{\infty} S_n^{(o)} \left[\epsilon^{2n}\ w^n + w^{-n}\right], \qquad 1 < |w| < \epsilon^{-2} \tag{291}$$

where

$$S_n^{(o)}(\epsilon^2) = \frac{1}{\pi} \sum_{m=o}^{\infty} \frac{\Gamma(n+m+\frac{1}{2})\Gamma(m+\frac{1}{2})}{\Gamma(n+m+1)\Gamma(m+1)}\ \epsilon^{2m} \tag{292}$$

Substituting $(1-w)^{-\frac{1}{2}}\ (1-\epsilon^2 w)^{-\frac{1}{2}}$ from (291) in (290), the expansion for $W_o(w)$ in the annulus region is

$$W_o(w) = i \sum_{n=o}^{\infty} \left[B_n\ \epsilon^{2n}\ w^{\nu} + C_n\ w^{-\nu}\right], \qquad 1 < |w| < \epsilon^{-2} \tag{293}$$

when the constants B_n, C_n and the exponent ν are defined by:

$$\left.\begin{aligned} B_n &= 2\ \epsilon^2\ S_{n+1}^{(o)} - (1+\epsilon^2)\ S_n^{(o)} \\ C_n &= 2\ S_n^{(o)} - (1+\epsilon^2)\ S_{n+1}^{(o)} \\ \nu &= n + \tfrac{1}{2} \end{aligned}\right\} \tag{294}$$

Similarly, the transformed potential function $\Lambda_o(w)$ can be expanded and is:

$$\Lambda_o(w) = 2 \sum_{n=o}^{\infty} \tilde{A}_n\ w^n, \qquad |w| < 1 \tag{295}$$

when the constants $\tilde{A}_n$ are

$$\left.\begin{aligned} \tilde{A}_n &= S_n^{(i)} - (1+\epsilon^2)\ S_{n-1}^{(i)} + \epsilon^2\ S_{n-2}^{(i)} \\ \tilde{A}_1 &= -\frac{1}{2}(1+\epsilon^2), \quad \tilde{A}_o = 1 \end{aligned}\right\} \tag{296}$$

and $S_n^{(i)}$ is given in (289).

On the other hand, in the annulus region the expansion is

$$\Lambda_o(w) = -\,2i \sum_{n=o}^{\infty} \left[\tilde{B}_n\ \epsilon^{2n}\ w^n + \tilde{C}_n\ w^{-n} \right], \quad 1 < |w| < \epsilon^{-2} \tag{297}$$

with the constants $\tilde{B}_n$ and $\tilde{C}_n$ defined as

$$\left.\begin{aligned} \tilde{B}_n &= S^{(o)}_{n-1} - (1+\epsilon^2)\ S^{(o)}_n + \epsilon^2\ S^{(o)}_{n+1}, \quad n \geq 1 \\ \tilde{B}_o &= 2\ \epsilon^2\ S^{(o)}_1 - (1+\epsilon^2)\ S^{(o)}_o \\ \tilde{C}_n &= S^{(o)}_n - (1+\epsilon^2)\ S^{(o)}_{n+1} + \epsilon^2\ S^{(o)}_{n+2} \end{aligned}\right\} \tag{298}$$

where $S^{(o)}_n\ (\epsilon^2)$ is defined in (292).

24. The Stream Function $\psi(q, \vartheta)$

The relationship between the domain $\underline{D}$ and D is thus fully established and the functions corresponding to such domains are also given. From the general scheme developed in sections 8 and 9 the solutions for the similar motion of a compressible fluid can be constructed. First of all, the stream function $\psi(q,\vartheta)$ governing the subsonic flow is the sum of $\psi_1(q,\vartheta)$ and $\psi_2(q,\vartheta)$. According to (207), (208), and (209), for $0 \leq \tau < \frac{1}{2\beta+1}$

$$\psi_1(q,\vartheta) = \frac{1}{2^{\frac{1}{2}}} \frac{f(\tau)}{f(\tau_1)} \left\{ \left[-I(tq,\vartheta) + J(tq,\vartheta) \right]^{\frac{1}{2}} - \left[-I_\epsilon(tq,\vartheta) + J^{-1}(tq,\vartheta) \right]^{-\frac{1}{2}} \right\} \tag{299}$$

where the functions $I(tq,\vartheta)$, $I_\epsilon(tq,\vartheta)$, and $J(tq,\vartheta)$ are obtained from I, I_ϵ, and J in (272) to (279) by replacing q by tq, t being defined in (195). For $q < 1$, the function $\psi_2(q,\vartheta)$ is

$$\psi_2^{(1)}(q,\vartheta) = \sum_{n=0}^{\infty} A_n G_n(\tau)\, q^n \sin n\vartheta \tag{300}$$

where A_n is definod in (289) and $G_n(\tau)$ in (199). For $q > 1$ and in subsonic region the function $\psi_2^{(0)}(q,\vartheta)$:

$$\psi_2^{(0)}(q,\vartheta) = \sum_{n=0}^{\infty}\left[G_\nu^{(1)}(\tau)\,\epsilon^{2n}\, q^{\nu} + G_\nu^{(2)}(\tau)\, q^{-\nu}\right]\cos\nu\vartheta, \quad 0 \le \vartheta < 2\pi \tag{301}$$

where $G_\nu^{(1)}(\tau)$ and $G_\nu^{(2)}(\tau)$ are defined by (205) with the constants B_n and C_n defined in (294).

When the motion becomes supersonic, the continuation of $\psi_1(q,\vartheta)$ defined in (299) gives

$$\begin{aligned}\psi_1(q,\vartheta) = \frac{1}{8}\frac{f(\tau)}{f(\tau_1)}\Big\{&\left[-I(\lambda,\xi)+J(\lambda,\xi)\right]^{\frac{1}{2}} - \left[-I_\epsilon(\lambda,\xi)+J^{-1}(\lambda,\xi)\right]^{\frac{1}{2}} \\ &+ \left[-I(\lambda,\eta)+J(\lambda,\eta)\right]^{\frac{1}{2}} - \left[-I_\epsilon(\lambda,\eta)+J^{-1}(\lambda,\eta)\right]^{\frac{1}{2}} \\ &- \left[+I(\lambda,\xi)+J(\lambda,\xi)\right]^{\frac{1}{2}} - \left[-I_\epsilon(\lambda,\xi)+J^{-1}(\lambda,\xi)\right]^{\frac{1}{2}} \qquad \frac{1}{2\beta+1} < \tau < 1 \\ &\pm \left[I(\lambda,\eta)+J(\lambda,\eta)\right]^{\frac{1}{2}} \pm \left[I_\epsilon(\lambda,\eta)+J^{-1}(\lambda,\eta)\right]^{\frac{1}{2}}\Big\}\end{aligned} \tag{302}$$

according to (214). Here ξ and η are the characteristic parameters defined in (218). The upper sign in the last two terms corresponds to $\eta > 0$ while the lower one, to $\eta < 0$.

The accompanying function $\psi_2^{(o)}(q,\vartheta)$ is

$$\psi_2^{(o)}(q,\vartheta) = \sum_{n=0}^{\infty} \left[G_\nu^{(1)}(\tau)\, \epsilon^{2n}\, q^{\nu} + G_\nu^{(2)}(\tau)\, q^{-\nu} \right] \cos \nu\vartheta, \quad \frac{1}{2\beta+1} < \tau < 1 \tag{303}$$

Here the functions $G_\nu^{(1)}(\tau)$ and $G_\nu^{(2)}(\tau)$ are defined by (205) in conjunction with (217) in such a way that (303) will be the continuation of (301). It also should be noticed that the variable is restricted to $\frac{1}{2\beta+1} < \tau < 1$ instead of $\frac{1}{2\beta+1} < \tau < \tau_1\epsilon^{-4}$, as $\tau_1\epsilon^{-4}$ is generally greater than unity, which is impossible for the actual gas.

It should be remembered that $\psi_2^{(i)}(q,\vartheta)$ is always negligible compared with $\psi_1(q,\vartheta)$ within and on the unit circle $q = 1$ when τ_1 is small in comparison with $\frac{1}{2\beta+1}$; $\psi(q,\vartheta)$ can be approximately represented by $\psi_1(q,\vartheta)$ alone throughout the interior of the unit circle. As a consequence, the calculation can be simplified considerably by constructing first a solution for the annulus region by using $\underline{F}_{-\nu}(\tau)$ instead of $\underline{G}_\nu(\tau)$ and making an approximate connection across the unit circle. In that event, the stream function will be reduced to

$$\psi(q,\vartheta) \cong \psi_1(q,\vartheta) \tag{304}$$

when $0 \le q \le 1$; here $\psi_1(q,\vartheta)$ is again defined in (299). On the other hand, when $\tau_1 < \tau < \frac{1}{2\beta+1}$,

$$\psi(q,\vartheta) = \psi_1(q,\vartheta) + \psi_2^{(o)}(q,\vartheta) \tag{305}$$

where the function $\psi_2^{(o)}(q,\vartheta)$ which is small on $q = 1$ is given by

$$\psi_2^{(o)}(q,\vartheta) = \sum_{n=o}^{\infty} \left[B_n G_\nu(\tau)\ \epsilon^{2n}\ q^\nu + C_n G_{-\nu}(\tau) q^{-\nu} \right] \cos \nu\vartheta \quad (306)$$

Here the functions $G_\nu(\tau)$ and $G_{-\nu}(\tau)$ can be shown to be

$$G_\nu(\tau) = \underline{F}_\nu^{(r)}(\tau) - \frac{f(\tau)}{f(\tau_1)}\ t^\nu, \quad G_{-\nu}(\tau) = \underline{F}_{-\nu}^{(r)}(\tau) - \frac{f(\tau)}{f(\tau_1)}\ t^{-\nu} \quad (307)$$

and the coefficients B_n and C_n are defined in (294).

The continuation of $\psi_1(q,\vartheta)$ is naturally the expression given in (302) while that of (306) differs only in the definition of $G_\nu(\tau)$ and $G_{-\nu}(\tau)$ which are

$$G_\nu(\tau) = \underline{F}_\nu^{(r)}(\tau) - \frac{1}{2}\ \frac{f(\tau)}{f(\tau_1)}\ t^\nu \cos\left(\nu\omega - \frac{\pi}{4}\right)$$

$$G_{-\nu}(\tau) = \underline{F}_{-\nu}^{(r)}(\tau) - \frac{1}{2}\ \frac{f(\tau)}{f(\tau_1)}\ t^{-\nu} \cos\left(\nu\omega + \frac{\pi}{4}\right) \qquad \frac{1}{2\beta+1} < \tau < 1 \quad (308)$$

25. The Coordinate Functions $x(q,\vartheta)$ and $y(q,\vartheta)$

With the functions $z_o(w)$ and $\Lambda_o(w)$ defined in sections 22 and 23, the corresponding functions $\Lambda(w;\tau)$ and consequently $z(w;\tau)$ for the motion of a compressible fluid can be constructed. The coordinate functions derived from $\Lambda(w;\tau)$ are given respectively by the sum of two functions $x_1(q,\vartheta)$ and $y_1(q,\vartheta)$ which, according to equations (237) to (238), are

$$x_1(q,\vartheta) = -\frac{t(\tau)}{2^{\frac{1}{2}}}\frac{g(\tau)}{f(\tau_1)}\left\{\left[I(tq,\vartheta)+J(tq,\vartheta)\right]^{\frac{1}{2}}\right.$$

$$\left.+\epsilon^2\left[I_\epsilon(tq,\vartheta)+J^{-1}(tq,\vartheta)\right]^{\frac{1}{2}}\right\}$$

$$-\frac{\beta\tau}{2}\frac{h(\tau)}{f(\tau_1)}\frac{t\sin 2\vartheta}{\sigma_o(tq,\vartheta)}\left\{-1+4\epsilon^2 tq\cos\vartheta-\epsilon^2\right.$$

$$\left.+J(tq,\vartheta)+\epsilon^2 J^{-1}(tq,\vartheta)\right\} \qquad (309)$$

$$y_1(q,\vartheta) = \frac{t(\tau)}{2^{\frac{1}{2}}}\frac{g(\tau)}{f(\tau_1)}\left\{\left[-I(tq,\vartheta)+J(tq,\vartheta)\right]^{\frac{1}{2}}\right.$$

$$\left.-\epsilon^2\left[-I_\epsilon(tq,\vartheta)+J^{-1}(tq,\vartheta)\right]^{\frac{1}{2}}\right\}$$

$$-\beta\tau\frac{h(\tau)}{f(\tau_1)}\frac{t\sin^2\vartheta}{\sigma_o(tq,\vartheta)}\left\{-1+4\epsilon^2 tq\cos\vartheta-\epsilon^2\right.$$

$$\left.+J(tq,\vartheta)+\epsilon^2 J^{-1}(tq,\vartheta)\right\} \qquad (310)$$

where $\sigma_o(tq,\vartheta)$ is obtained from $\sigma_o(q,\vartheta)$ in (285) by replacing q by tq. The functions $x_2^{(i)}(q,\vartheta)$ and $y_2^{(i)}(q,\vartheta)$, according to equations (239) and (240), are

$$x_2^{(i)}(q,\vartheta) = 2\sum_{n=1}^{\infty} n\,\tilde{A}_n\,\tilde{G}_n(\tau)\,q^{n-1}\cos(n-1)\vartheta$$

$$-2\beta\tau\sum_{n=1}^{\infty} n\,\tilde{A}_n\,\tilde{G}_{n,1}(\tau)\,q^{n-1}\cos n\vartheta\cos\vartheta \qquad (311)$$

$$q < 1$$

$$y_2^{(1)}(q,\vartheta) = -2\sum_{n=1}^{\infty} n\,\tilde{A}_n\,\tilde{G}_n(\tau)\,q^{n-1}\sin(n-1)\vartheta$$

$$-2\beta\tau\sum_{n=1}^{\infty} n\,\tilde{A}_n\,\tilde{G}_{n,1}(\tau)\,q^{n-1}\cos n\vartheta\sin\vartheta \quad (312)$$

Here the functions $\tilde{G}_n(\tau)$ and $\tilde{G}_{n,1}(\tau)$ are defined by equations (241) and (242) and the constants $\tilde{A}_n$ by (296).

The same functions valid in the annulus region are again represented by the sums $x_1(q,\vartheta) + x_2^{(o)}(q,\vartheta)$ and $y_1(q,\vartheta) + y_2^{(o)}(q,\vartheta)$, where $x_1(q,\vartheta)$ and $y_1(q,\vartheta)$ are defined by equations (309) and (310), respectively. When $\tau_1 \le \tau < \frac{1}{2\beta+1}$, $x_2^{(o)}(q,\vartheta)$, and $y_2^{(o)}(q,\vartheta)$ are

$$x_2^{(o)}(q,\vartheta) = -2\sum_{n=0}^{\infty}\nu\left[\tilde{G}_\nu^{(1)}(\tau)\,\epsilon^{2n}\,q^{\nu-1}\sin(\nu-1)\vartheta\right.$$

$$\left.+\,\tilde{G}_\nu^{(2)}(\tau)q^{-\nu-1}\sin(\nu+1)\vartheta\right]+2\beta\tau\sum_{n=0}^{\infty}\nu\left[\tilde{G}_{\nu,1}^{(1)}(\tau)\epsilon^{2n}q^{\nu-1}\right.$$

$$\left.+\,\tilde{G}_{\nu,1}^{(2)}(\tau)\,q^{-\nu-1}\right]\sin\nu\vartheta\cos\vartheta \quad (313)$$

$$y_2^{(o)}(q,\vartheta) = -2\sum_{n=0}^{\infty}\nu\left[\tilde{G}_\nu^{(1)}(\tau)\epsilon^{2n}q^{\nu-1}\cos(\nu-1)\vartheta\right.$$

$$\left.+\,\tilde{G}_\nu^{(2)}(\tau)\,q^{-\nu-1}\cos(\nu+1)\vartheta\right]$$

$$+\,2\beta\tau\sum_{n=0}^{\infty}\nu\left[\tilde{G}_{\nu,1}^{(1)}(\tau)\epsilon^{2n}q^{\nu-1}+\tilde{G}_{\nu,1}^{(2)}(\tau)q^{-\nu-1}\right]\sin\nu\vartheta\sin\vartheta \quad (314)$$

The functions $\tilde{G}_\nu^{(\alpha)}(\tau)$, $\tilde{G}_{\nu,1}^{(\alpha)}(\tau)$ are defined in equations (250) and (251) together with equations (252) with the constants $\tilde{B}_n$ and $\tilde{C}_n$ defined in equations (298).

On the other hand, when $\frac{1}{2\beta+1} < \tau < 1$, the continued expressions of $x_1(q,\vartheta)$, $y_1(q,\vartheta)$ across the critical circle $\tau = \frac{1}{2\beta+1}$ are, according to equations (253) and (254),

$$x_1(q,\vartheta) = -\frac{t(\tau)}{2^{5/2}}\frac{g(\tau)}{f(\tau_1)}\left\{\left[I(\lambda,\xi)+J(\lambda,\xi)\right]^{\frac{1}{2}}\right.$$

$$+\epsilon^2\left[I_\epsilon(\lambda,\xi)+J^{-1}(\lambda,\xi)\right]^{\frac{1}{2}}+\left[I(\lambda,\eta)+J(\lambda,\eta)\right]^{\frac{1}{2}}$$

$$\left.+\epsilon^2\left[I_\epsilon(\lambda,\eta)+J^{-1}(\lambda,\eta)\right]^{\frac{1}{2}}\right\}\cos\left(\frac{\pi}{4}-\omega\right)$$

$$-\frac{t(\tau)}{2^{5/2}}\frac{g(\tau)}{f(\tau_1)}\left\{\left[-I(\lambda,\xi)+J(\lambda,\xi)\right]^{\frac{1}{2}}-\epsilon^2\left[-I_\epsilon(\lambda,\xi)\right.\right.$$

$$\left.+J^{-1}(\lambda,\xi)\right]^{\frac{1}{2}}-\left[-I(\lambda,\eta)+J(\lambda,\eta)\right]^{\frac{1}{2}}+\epsilon^2\left[-I_\epsilon(\lambda,\eta)\right.$$

$$\left.\left.+J^{-1}(\lambda,\eta)\right]^{\frac{1}{2}}\right\}\sin\left(\frac{\pi}{4}-\omega\right)-\frac{\beta\tau\,h(\tau)\cos\vartheta}{4\,q\,f(\tau_1)}\left\{\left[\frac{\lambda\sin\xi}{\sigma_o(\lambda,\xi)}\right.\right.$$

$$\times\left(-1+4\epsilon^2\lambda\cos\xi-\epsilon^2+J(\lambda,\xi)+\epsilon^2J^{-1}(\lambda,\xi)\right)$$

$$+\frac{\lambda\sin\eta}{\sigma_o(\lambda,\eta)}\left(-1+4\epsilon^2\lambda\cos\eta-\epsilon^2+J(\lambda,\eta)\right.$$

$$\left.\left.+\epsilon^2J^{-1}(\lambda,\eta)\right)\right]\cos\left(\mu+\frac{\pi}{4}\right)-\left[\frac{\lambda\sin\xi}{\chi_o(\lambda,\xi)}\right.$$

$$\times\left(1-4\epsilon^2\lambda\cos\xi+\epsilon^2+J(\lambda,\xi)+\epsilon^2J^{-1}(\lambda,\xi)\right)$$

$$-\frac{\lambda\sin\eta}{\chi_o(\lambda,\eta)}\left(1-4\epsilon^2\lambda\cos\eta+\epsilon^2+J(\lambda,\eta)\right.$$

$$\left.\left.\left.+\epsilon^2J^{-1}(\lambda,\eta)\right)\right]\sin\left(\mu+\frac{\pi}{4}\right)\right\} \qquad (315)$$

$$y_1(q,\vartheta) = \frac{t(\tau)}{2^{5/2}} \frac{g(\tau)}{f(\tau_1)} \left\{ \left[- I(\lambda,\xi) + J(\lambda,\xi) \right]^{\frac{1}{2}} - \epsilon^2 \left[- I_\epsilon(\lambda,\xi) \right.\right.$$

$$\left. + J^{-1}(\lambda,\xi) \right]^{\frac{1}{2}} + \left[- I(\lambda,\eta) + J(\lambda,\eta) \right]^{\frac{1}{2}} - \epsilon^2 \left[- I_\epsilon(\lambda,\eta) \right.$$

$$\left. \left. + J^{-1}(\lambda,\eta) \right]^{\frac{1}{2}} \right\} \cos\left(\frac{\pi}{4} - \omega\right) + \frac{t(\tau)}{2^{5/2}} \frac{g(\tau)}{f(\tau_1)} \left\{ - \left[I(\lambda,\xi) \right.\right.$$

$$\left. + J(\lambda,\xi) \right]^{\frac{1}{2}} - \epsilon^2 \left[I_\epsilon(\lambda,\xi) + J^{-1}(\lambda,\xi) \right]^{\frac{1}{2}}$$

$$+ \left[I(\lambda,\eta) + J(\lambda,\eta) \right]^{\frac{1}{2}} + \epsilon^2 \left[I_\epsilon(\lambda,\eta) + J^{-1}(\lambda,\eta) \right]^{\frac{1}{2}} \right\}$$

$$\times \sin\left(\frac{\pi}{4} - \omega\right) - \frac{\beta\tau\, h(\tau) \sin\vartheta}{4q\, f(\tau_1)} \left\{ \left[\frac{\lambda \sin\xi}{\sigma_o(\lambda,\xi)} \right.\right.$$

$$\times \left(- 1 + 4\epsilon^2 \lambda \cos\xi - \epsilon^2 + J(\lambda,\xi) + \epsilon^2 J^{-1}(\lambda,\xi) \right)$$

$$+ \frac{\lambda \sin\eta}{\sigma_o(\lambda,\eta)} \left(-1 + 4\epsilon^2 \lambda \cos\eta - \epsilon^2 + J(\lambda,\eta) \right)$$

$$\left. + \epsilon^2 J^{-1}(\lambda,\eta) \right) \left] \cos\left(\mu + \frac{\pi}{4}\right) - \left[\frac{\lambda \sin\xi}{\chi_o(\lambda,\xi)} \left(1 - 4\epsilon^2 \lambda \cos\xi \right.\right.$$

$$\left. + \epsilon^2 + J(\lambda,\xi) + \epsilon^2 J^{-1}(\lambda,\xi) \right) - \frac{\lambda \sin\eta}{\chi_o(\lambda,\eta)} \left(1 - 4\epsilon^2 \lambda \cos\eta \right.$$

$$\left. \left. \left. + \epsilon^2 + J(\lambda,\eta) + \epsilon^2 J^{-1}(\lambda,\eta) \right) \right] \sin\left(\mu + \frac{\pi}{4}\right) \right\} \qquad (316)$$

While $x_2(q,\vartheta)$ and $y_2(q,\vartheta)$ remain to be defined by equations (313) and (314) except the functions $\tilde{G}_{\upsilon}^{(\alpha)}(\tau)$ and $\tilde{G}_{\upsilon,1}^{(\alpha)}(\tau)$ are replaced by those given in equations (250), (251) together with equations (257).

By the same argument as that used for the stream function, the practical calculation of $x(q,\vartheta)$ and $y(q,\vartheta)$ can be simplified by neglecting $x_2^{(i)}(q,\vartheta)$ and $y_2^{(i)}(q,\vartheta)$ when $q < 1$; namely,

$$x(q,\vartheta) \cong x_1(q,\vartheta) \tag{317}$$

$$y(q,\vartheta) \cong y_1(q,\vartheta), \quad 0 \le q \le 1 \tag{318}$$

where $x_1(q,\vartheta)$ and $y_1(q,\vartheta)$ are defined in equations (309) and (310); and in the annulus region

$$x(q,\vartheta) = x_1(q,\vartheta) + x_2^{(o)}(q,\vartheta) \tag{319}$$

$$\tau_1 < \tau < 1$$

$$y(q,\vartheta) = y_1(q,\vartheta) + y_2^{(o)}(q,\vartheta) \tag{320}$$

Here $x_1(q,\vartheta)$ and $y_1(q,\vartheta)$ are either given by equations (309), (310) or (315), (316). The terms $x_2^{(o)}(q,\vartheta)$ and $y_2^{(o)}(q,\vartheta)$, on the other hand, become

$$x_2^{(o)}(q,\vartheta) = -2\sum_{n=0}^{\infty}\nu\left[\tilde{B}_n\tilde{G}_\nu(\tau)\epsilon^{2n}\ q^{\nu-1}\ \sin(\nu-1)\vartheta + \tilde{C}_n\tilde{G}_{-\nu}(\tau)q^{-\nu-1}\ \sin(\nu+1)\vartheta\right] + 2\beta\tau\sum_{n=0}^{\infty}\nu\left[\tilde{B}_n\tilde{G}_{\nu,1}(\tau)\epsilon^{2n} \times q^{\nu-1} + \tilde{C}_n\tilde{G}_{\nu,1}(\tau)\ q^{-\nu-1}\right]\sin\nu\vartheta\cos\vartheta \qquad (321)$$

$$y_2^{(o)}(q,\vartheta) = -2\sum_{n=0}^{\infty}\nu\left[\tilde{B}_n\tilde{G}_\nu(\tau)\epsilon^{2n}\ q^{\nu-1}\ \cos(\nu-1)\vartheta - \tilde{C}_n\tilde{G}_{-\nu}(\tau)q^{-\nu-1}\ \cos(\nu+1)\vartheta\right] + 2\beta\tau\sum_{n=0}^{\infty}\nu\left[\tilde{B}_n\tilde{G}_{\nu,1}(\tau)\epsilon^{2n} \times q^{\nu-1} + \tilde{C}_n\tilde{G}_{-\nu,1}\ q^{-\nu-1}\right]\sin\nu\vartheta\sin\vartheta \qquad (322)$$

For $\tau_1 \le \tau < \dfrac{1}{2\beta+1}$, the functions $\tilde{G}_\nu(\tau)$, $\tilde{G}_{\nu,1}(\tau)$ are defined as

$$\tilde{G}_\nu(\tau) = \underset{\sim}{\tilde{F}}_\nu^{(r)}(\tau) - \frac{g(\tau)}{f(\tau_1)}\ t^\nu, \qquad \tilde{G}_\nu'(\tau) = \underset{\sim}{\tilde{F}}_{-\nu}^{(r)}(\tau) - \frac{g(\tau)}{f(\tau_1)}\ t^{-\nu} \qquad (323)$$

$$\left.\begin{aligned}\tilde{G}_{\nu,1}(\tau) &= \frac{\nu-1}{\nu+1}\ \underset{\sim}{\tilde{F}}_{\nu,1}^{(r)}(\tau) - \frac{h(\tau)}{f(\tau_1)}\ t^\nu\\ \tilde{G}_{-\nu,1}(\tau) &= \frac{\nu+1}{\nu-1}\ \underset{\sim}{\tilde{F}}_{-\nu,1}^{(r)}(\tau) - \frac{h(\tau)}{f(\tau_1)}\ t^{-\nu}\end{aligned}\right\} \qquad (324)$$

For $\dfrac{1}{2\beta+1} < \tau < 1$

$$\left.\begin{aligned}\tilde{G}_\nu(\tau) &= \underset{\sim}{\tilde{F}}_\nu^{(r)}(\tau) - \frac{1}{2}\frac{g(\tau)}{f(\tau_1)}\ t^\nu\ \cos\left(\nu\omega - \frac{\pi}{4}\right)\\ \tilde{G}_{-\nu}(\tau) &= \underset{\sim}{\tilde{F}}_{-\nu}^{(r)}(\tau) - \frac{1}{2}\frac{g(\tau)}{f(\tau_1)}\ t^{-\nu}\ \cos\left(\nu\omega + \frac{\pi}{4}\right)\end{aligned}\right\} \qquad (325)$$

$$\left.\begin{aligned}\tilde{G}_{\nu,1}(\tau) &= \frac{\nu-1}{\nu+1}\,\tilde{\underline{F}}^{(r)}_{\nu,1}(\tau) - \frac{1}{2}\,\frac{h(\tau)}{f(\tau_1)}\,t^{\nu}\cos\left(\nu\omega-\mu-\frac{\pi}{4}\right)\\ \tilde{G}_{-\nu,1}(\tau) &= \frac{\nu+1}{\nu-1}\,\tilde{\underline{F}}^{(r)}_{-\nu,1}(\tau) - \frac{h(\tau)}{2f(\tau_1)}\,t^{-\nu}\cos\left(\nu\omega+\mu+\frac{\pi}{4}\right)\end{aligned}\right\}\quad(326)$$

CONCLUSIONS

As an example, the motion of air past a cylindrical body was considered by taking $\epsilon = \frac{1}{2}$. The flow patterns in the τ,ϑ— plane for two free—stream Mach numbers $M_1 = 0.6$ and 0.7 have been calculated and were given in figures 14 and 15. It should be noticed that there is considerable distortion in the shape of the bodies in the compressible flow from that in the incompressible flow. If the compressible flow around a given body is desired, a series of computations should be made with various geometric parameters ϵ, so that the desired body shape at a definite Mach number M_1 could be picked out.

These computations definitely demonstrate the practicability of the proposed method. They also show that, in the case of two—dimensional motion of a compressible fluid, the mixed subsonic and supersonic flows exist within the field of an irrotational isentropic flow about a suitable body, and the transition from one to the other is continuous and reversible. Furthermore, the breakdown of the irrotational isentropic flow depends solely upon the occurrence of limiting lines which, in turn, is determined by the condition at infinity or the shape of the boundary, while the magnitude of the local speed attained is immaterial. In the case of $M_1 = 0.6$, the irrotational supersonic flow continues to exist up to the local Mach number $M = 1.25$; whereas for $M_1 = 0.7$ it breaks down as soon as $M = 1.22$ is reached. The singular behavior of the streamline is marked by the point of tangency of $\Psi = 0$ with a characteristic at $M = 1.22$.

The calculation of the flow pattern in the physical plane is yet to be completed. When this is done, the pressure distribution can be compared with that over the same body of the incompressible flow.

Guggenheim Aeronautical Laboratory,
California Instituto of Technology,
Pasadena, Calif., April 17, 1945.

REFERENCES

1. von Kármán, Th.: Compressibility Effects in Aerodynamics. Jour. Aero. Sci., vol. 8, no. 9, July 1941, pp. 337–356.

2. Tsien, Hsue-Shen: The "Limiting Line" in Mixed Subsonic and Supersonic Flow of Compressible Fluids. NACA TN No. 961, 1944.

3. Hantzsche, W., and Wendt, H.: Der Kompressibilitätseinfluss für dünne wenig gekrümmte Profile bei Unterschallgeschwindigkeit. Z.f.a.M.M., vol. 22, 1942, pp. 72–86.

4. Kaplan, Carl: The Flow of a Compressible Fluid past a Curved Surface. NACA ARR No. 3K02, 1943. The Flow of a Compressible Fluid past a Circular Profile. NACA ARR No. L4G15, 1944.

5 Molenbroek, P.: Über einige Bewegungen eines Gases mit Annahme eines Geschwindigkeitspotontials. Archiv der Math. und Phys. (Grunert-Hoppe), ser. 2, vol. 9, 1890, p. 157.

6. Chaplygin, S.: Gas Jets. NACA TM No. 1063, 1944.

7. Borgman, Stofan A.: On Two-Dimensional Flows of Compressible Fluids. NACA TN No. 972, 1945.

8. Garrick, I. E., and Kaplan, Carl: On the Flow of a Compressible Fluid by the Hodograph Method. I - Unification and Extension of Present-Day Results. NACA ACR No. L4C24, 1944. (Classification changed to "Restricted," Oct. 11, 1944)

9. Tsien, Hsue-Shen: Two-Dimensional Subsonic Flow of Compressible Fluids. Jour. Aero. Sci., vol. 6, no. 10, Aug. 1939, pp. 399–407.

10. Bers, Lipman: On a Method of Constructing Two-Dimensional Subsonic Compressible Flows around Closed Profiles. NACA TN No. 969, 1945.

11. Temple, G., and Yarwood, J.: The Approximate Solution of the Hodograph Equations for Compressible Flow. Rep. No. S.M.E. 3201, R.A.E., 1942.

12. Ringleb, Friedrich: Über die Differentialgleichungen einer adiabatischen Gasströmung und den Strömungsstoss. Deutsche Math., vol. 5, no. 5, 1940, pp. 337–384.

13. Tollmien, W.: Grenzlinien adiabatischer Potentialströmungen. Z.f.a.M.M., Bd. 21, 1941, pp. 140–152.

14. Gauss, C. F. Werke, vol. 3, pp. 207–229.

15. Tannery, J.: Propriétes des intégrales dcs équations différentielles linéaires. Ann. Sci. de e'Ecole Normale Superieure, ser. 2, vol. 4, 1875, pp. 113–182.

16. Goursat, E.: Sur l'équations différentielle linéaire qui admet pour intégrale hypergéométrique. Ann. Sci. de e'Ecole Hormale Superioure, ser. 2, vol. 10, 1881, pp. S3–S142.

17. Ince, E. L.: Ordinary Differential Equations. Longmans, Green and Co., 1927, p. 227.

18. Horn, F.: Über eine lineare Differentialgleichung zweiter Ordnung mit einem willkürlich en Parameter. Math. Ann., vol. 52, 1899, pp. 271–292.

19. Joffreys, H.: On Certain Approximate Solutions of Linear Differential Equations of the Second Order. Proc. London Math. Soc., ser. 2, vol. 23, pp. 428–436.

20. Langer, R. E.: On the Asymptotic Solutions of Ordinary Differential Equations. Trans. Am. Math. Soc., vol. 33, 1931, pp. 23–64; vol. 34, 1932, pp. 447–480.

21. Coburn, N.: The Kármán–Tsien Pressure – Volume Relation in the Two–Dimensional Supersonic Flow of Compressible Fluids. Quarterly of Appl. Math., 1945.

22. Kraft, Hans, and Dibble, Charles G.: Some Two Dimensional Adiabatic Compressible Flow Patterns. Jour. Aero. Sci., vol. 11, 1944, pp. 283–298.

23. Busemann, A.: Gasdynamik. Handbuch der Experimentalphysik, Akademische Verlags Leipzig, sec. 1, pt. IV, 1931, pp. 341 to 460.

24. Kantrowitz, A.: Effects of Heat–Capacity Lag in Gas Dynamics. NACA ARR No. 4A22, 1944.

APPENDIX A

PROOF OF THEOREM(52)

To facilitate the discussion, equation (71) is first written in the form:

$$X_1(\xi_\nu^{(1)}) \equiv \xi_\nu'^{(1)}(\tau) + \frac{\nu}{2\tau}\,\zeta_1\,\zeta_2 = 0$$

where

$$\zeta_1(\tau) = \xi_\nu^{(1)}(\tau) + \frac{\beta\tau}{\nu(1-\tau)} + \gamma_\nu(\tau)$$

$$\zeta_2(\tau) = \xi_\nu^{(1)}(\tau) + \frac{\beta\tau}{\nu(1-\tau)} - \gamma_\nu(\tau)$$

and

$$\gamma_\nu(\tau) = \left\{\frac{1-(2\beta+1)\tau}{1-\tau} + \frac{\beta^2\tau^2}{\nu^2(1-\tau)^2} + \frac{4(1-\tau)^2\beta}{\tau^\nu\, R_\nu^2(\tau)}\right\}^{\frac{1}{2}}$$

when ν is large, the character of the functions ζ_1 and ζ_2 can be easily studied in the $\tau, \xi_\nu^{(1)}$-plane (fig. 16) by neglecting the third term under the radical sign. This can be justified in the following manner: Consider the case when ν is positive and large but not an integer. In the interval $0 \le \tau \le \frac{1}{2\beta+1}$, $\underline{F}_\nu(\tau) \ll F_\nu$ because $F_\nu(\tau) \sim \tau^{-\nu}\underline{F}_{-\nu}(\tau)$ by equations (35) and (55). Then $\tau^{\frac{\nu}{2}} R_\nu(\tau) \sim \tau^{-\frac{\nu}{2}} T_1^{-\nu}$. Therefore, $\tau^{\frac{\nu}{2}} R_\nu(\tau) \gg 1$ when ν is large. But both $\underline{F}_\nu(\tau)$ and $F_\nu(\tau)$ are continuous with respect to ν; so the foregoing result applies equally to the case of integral ν. Hence, the third term in the radical for $\gamma_\nu(\tau)$ can be neglected for large ν.

Owing to the manner in which γ_ν is defined, corresponding to each ν there is a line $\tau = \tau_0 > \frac{1}{2\beta+1}$ such that

$\gamma_\nu^2(\tau) \gtrless 0$ when $\tau \lesseqgtr \tau_0$. As a consequence ζ_1 and ζ_2 are real or complex conjugate according as $\tau \lesseqgtr \tau_0$. In $0 \leq \tau \leq \tau_0$, $\zeta_1 = 0$ and $\zeta_2 = 0$ will give two 1-parameter families radiating from (0, -1) and (0,1), respectively, and joining together at a point where $\gamma_\nu^2 = 0$. If $0 \leq \tau \leq \tau_0$, the product $\zeta_1\zeta_2$ may be negative or positive according to whether the point lies to the left or the right of the curve $\zeta_1 = 0$ and $\zeta_2 = 0$. On the other hand, if $\tau > \tau_0$, $\zeta_1\zeta_2$ is always positive.

Now $\xi_\nu^{'(1)}(0) = \beta$, while the initial slope of $\zeta_1 = 0$ is $\beta\left(1 - \frac{1}{\nu}\right)$, the integral curve must lie above $\zeta_1 = 0$, and below $\zeta_2 = 0$. If it were not, the integral curve would cross the curve $\zeta_1 = 0$, $\zeta_2 = 0$, where $\xi_\nu^{'(1)}(\tau) = 0$, and $\xi_\nu^{'(1)}(\tau)$ would be negative somewhere in $0 \leq \tau \leq \frac{1}{2\beta + 1}$. This is not possible, for $\xi_\nu^{(1)} \sim \xi_{-\nu}$ by an argument similar to that used for determining the magnitude of $\tau\bar{2}\, R_\nu(\tau)$ and according to (55) $-\sqrt{\frac{1 - (2\beta + 1)\tau}{1 - \tau}} > \xi_{-\nu} > -(1 - \tau)^\beta$ in $0 \leq \tau \leq \frac{1}{2\beta + 1}$. Hence $\xi_\nu^{'(1)} > 0$ in $0 \leq \tau \leq \frac{1}{2\beta + 1}$ and $\xi_\nu^{(1)}$ continues to increase until it intersects with $\zeta_1 = 0$. After it crosses the curve $\zeta_1 = 0$, $\xi_\nu^{'(1)} < 0$ and never changes sign as $\zeta_1\zeta_2 > 0$ in $\tau_0 < \tau < 1$. Consequently, $\xi_\nu^{(1)}(\tau)$ is monotonic and decreasing in the interval $\tau_0 < \tau < 1$. When ν is sufficiently large, τ_0 will approach very rapidly to $\frac{1}{2\beta + 1}$ and $\tau_0 = \frac{1}{2\beta + 1}$ when ν becomes infinite.

Proof of theorem (52).- Form the following identity:

$$X_1(\eta_\nu^{(1)}) \equiv (\eta_\nu^{'(1)} - \xi_\nu^{'(1)}) + (\eta_\nu^{(1)} - \xi_\nu^{(1)})\left[\frac{\beta}{1 - \tau} + \frac{\nu}{2\tau}(\eta_\nu^{(1)} + \xi_\nu^{(1)})\right] + \frac{\nu}{\tau}\xi_0^2(1 - \tau)^{2\beta} e^{-\nu}\int_{\tau_0}^{\tau}(\eta_\nu^{(1)} + \xi_\nu^{(1)})\frac{d\tau}{\tau} \sinh \nu \int_{\tau_0}^{\tau}(\eta_\nu^{(1)} - \xi_\nu^{(1)})\frac{d\tau}{\tau} \gtrless 0 \quad (A1)$$

It can be shown that the differential expression possessew an integration factor

$$(\eta_\nu^{(1)} - \xi_\nu^{(1)})\tau^{2\nu}(1-\tau)^{-2\beta} R_\nu^2 S_\nu^2 \qquad (A2)$$

where

$$R_\nu = R_\nu(\tau_0)\exp\left\{\nu\int_{\tau_0}^{\tau}(\xi_\nu^{(1)} - 1)\frac{d\tau}{2\tau}\right\}$$

$$S_\nu = S_\nu(\tau_0)\exp\left\{\nu\int_{\tau_0}^{\tau}(\eta_\nu^{(1)} - 1)\frac{d\tau}{2\tau}\right\}$$

It will be noticed that the sign of (A2) is determined by the first factor $(\eta_\nu^{(1)} - \xi_\nu^{(1)})$ only. On multiplying (A1) by (A2) and integrating the resulting total differential from τ_0 to τ, with a suitably chosen initial value $\eta_\nu^{(1)}(\tau_0) = \xi_\nu^{(1)}(\tau_0)$ it is found that

$$\frac{1}{2}(\eta_\nu^{(1)} - \xi_\nu^{(1)})^2\tau^{2\nu}(1-\tau)^{-2\beta} R_\nu^2 S_\nu^2 + \xi_0^2 R_\nu^2(\tau_0)S_\nu^2(\tau_0)$$

$$\times\left[\cosh\ \nu\int_{\tau_0}^{\tau}(\eta_\nu^{(1)} - \xi_\nu^{(1)})\frac{d\tau}{\tau} - 1\right] > 0$$

which is positive if and only if $\eta_\nu^{(1)} - \xi_\nu^{(1)} \gtrless 0$ everywhere in $\tau_0 < \tau < 1$. Since both $\xi_\nu^{(1)}$ and $\eta_\nu^{(1)}$ are continuous and monotonic, the condition is both necessary and sufficient. Furthermore, it should be noticed that the condition $\eta_\nu^{(1)}(\tau_0) = \xi_\nu^{(1)}(\tau_0)$ is purely a convenience. If $\eta_\nu^{(1)}(\tau_0) \neq \xi_\nu^{(1)}(\tau_0)$, the validity of the theorem is not in the least impaired.

APPENDIX B

PROOF OF THEOREM (88)

Consider the first series: Multiplying throughout the inequality (58), namely,

$$\xi_n(\tau) > \sqrt{\frac{1-(2\beta+1)\tau}{1-\tau}}, \qquad 0 < \tau < \frac{1}{2\beta+1}$$

by $\frac{u}{2\tau}$ and integrating both sides from τ to τ_1 shows that

$$\underline{F}_n^{(r)}(\tau) < t_1^n(\tau)$$

where $t_1(\tau) = \frac{T_1(\tau)}{T_1(\tau_1)} \geq 1$. Then it follows that

$$\left| A_n \underline{F}_n^{(r)}(\tau)\, w^n \right| < \left| A_n (t_1 w)^n \right|$$

Now $\sum_{n=0}^{\infty} \left| A_n (t_1 w)^n \right|$ converges when $|t_1 w| < U$ due to equation (88). By Weirstrass's theorem, the series (92) is uniformly and absolutely convergent if $|t_1 w| = t_1 q < U$. Now $t_1(\tau_1) = 1$; thus $t_1 q$ is equal to U when $q = U$ and $= {}_1$. The term $t_1 q$ is zero if $q = 0$ and remains positive for $0 < q < U$. By the definition of $T_1(\tau)$ given by equation (56), it can be easily shown that

$$\frac{d}{dq} t_1 q > 0$$

for $0 < \tau < \tau_1$. Thus $t_1 q$ increases monotonically from zero to U in the interval $0 \leq \tau \leq \tau_1$. Therefore, the series (92) is uniformly and absolutely convergent in any closed domain in $|w| < U$.

Similarly, the convergence of the series (94) can be established.

APPENDIX C

PROOF OF THEOREM (98)

It is observed that the following identities exist among the constants involved in (98) and (99):

$$B_n U^{\nu} = -\frac{1}{2\nu\pi} \sum_{m=0}^{\infty} A_m U^m \left(\frac{1}{m+\nu} + \frac{1}{m-\nu}\right)(m+\nu)$$

$$C_n U^{-\nu} = \frac{1}{2\nu\pi} \sum_{m=0}^{\infty} A_m U^m \left(\frac{1}{m+\nu} + \frac{1}{m-\nu}\right)(m-\nu)$$

Now, by the inequalities (58) and (59), the functions $\xi_{\nu}(\tau_1)$, $\xi_{-\nu}(\tau_1)$ can be bounded both above and below for all $\nu \neq 0$, when $0 \leq \tau \leq \frac{1}{2\beta+1}$. And if a smaller value of $\Delta(\underline{F}_{\nu}, F_{\nu})$ is taken, it can be deduced that

$$\left| B_n^* \right| \leq M_1 \frac{|B_n|}{\underline{F}_{\nu}(\tau_1)}$$

$$\left| C_n^* \right| \leq M_2 \frac{|C_n|}{\underline{G}_{\nu}(\tau_1)}$$

where M_1 and M_2 are constants independent of n. On the other hand, from the inequality (58)

$$\xi_{\nu}(\tau) < (1-\tau)^{\beta}, \qquad 0 \leq \tau \leq \frac{1}{2\beta+1}$$

it follows that

$$\frac{\underline{F}_{\upsilon}(\tau)}{\underline{F}_{\upsilon}(\tau_1)} < t_2^{\upsilon}(\tau), \qquad \tau_1 \le \tau \le \frac{1}{2\beta+1}$$

Consequently, the first part of (101) can be dominated:

$$\left|B_n^{*}\ \underline{F}_{\upsilon}(\tau)\ w^{\upsilon}\right| < \left|B_n (t_2 w)^{\upsilon}\right|$$

where $t_2(\tau) = \frac{T_2(\tau)}{T_2(\tau_1)}$. The continuation of this inequality for $\tau > \frac{1}{2\beta+1}$ can be easily done by defining a new $t_2(\tau)$.

By hypothesis, $\sum_{n=0}^{\infty} \left| B_n (t_2 w)^{\upsilon} \right|$ converges if $|t_2 w| < V$.

Since $t_2(\tau) \le t_2(\tau_1)$ for $\tau_1 \le \tau < 1$, the inequality $|t_2 w| < V$ is uniformly bounded.

Similarly, it can be shown that

$$\left|C_n^{*}\ \underline{G}_{\upsilon}(\tau)\ w^{-\upsilon}\right| < \left|C_n (t_1 w)^{-\upsilon}\right|$$

But $\sum_{n=0}^{\infty} \left| C_n (t_1 w)^{-\upsilon} \right|$ converges if $|t_1 w| > U$. Since on $|w| = U$ $t_1(\tau_1) = 1$ and $\frac{d}{dq} \log |t_1 w| > 0$ when $0 < \tau < \frac{1}{2\beta+1}$ or $\frac{d}{dq} |t_1 w| = 0$ when $\frac{1}{2\beta+1} < \tau < 1$, the condition $|t_1 w| > U$ holds for all τ in $\tau_1 \le \tau < 1$. Hence, by Weierstrass's theorem the series (101) converges uniformly and absolutely in $U + \delta \le |w| \le V - \delta$.

TABLES OF THE HYPERGEOMETRIC FUNCTIONS

The values of the hypergeometric functions given in tables 1 to 5 are calculated from power series for $\gamma = 1.405$. The function $\underline{\tilde{F}}_{-\nu,1}(\tau)$ in table 6 is connected with $\underline{\tilde{F}}_{\nu}(\tau)$, $\underline{\tilde{F}}_{-\nu}(\tau)$, and $\underline{\tilde{F}}_{\nu,1}(\tau)$ through the following equation:

$$\frac{\beta(\nu+1)}{2(\nu-1)}\,\tau\,\underline{\tilde{F}}_{\nu}(\tau)\,\underline{\tilde{F}}_{-\nu,1}(\tau)$$

$$= \underline{\tilde{F}}_{\nu}(\tau)\,\underline{\tilde{F}}_{-\nu}(\tau) - \frac{\beta(\nu-1)}{2(\nu+1)}\,\tau\,\underline{\tilde{F}}_{\nu,1}(\tau)\,\underline{\tilde{F}}_{-\nu}(\tau) - (1-\tau)^{-\beta}$$

This is simply the Wronskian of the two independent integrals of the hypergeometric equation and it helds everywhere excopt at the singularities $\tau = 0$ and $\tau = 1$. Tables 7 to 12 contain the corresponding approximate functions as indicated.

The numbers in these tables are expressed in tcrms of appropriate powers of 10. However, a notation was devised in which only the powers are given while the base "10" is omitted. Thus, $5.14159 \times 10^{m} \equiv 3.14159,\ m$. Here m may be either a positive or negative integer, or zero. Unless indicated by the sign † on the heading, accidental errors were detected and eliminated by the difference method.

TABLE 1.- CORRESPONDING PARTICULAR INTEGRALS FOR THE SOLUTIONS OF COMPRESSIBLE FLOW AND INCOMPRESSIBLE FLOW

	Compressible	Incompressible
$\psi(q,\theta)$	$q^{\nu}\ \underline{F}_{\nu}(\tau)\ \begin{matrix}\cos\ \nu\theta\\ \sin\ \nu\theta\end{matrix}$ $q^{-\nu}\ \underline{G}_{\nu}(\tau)\ \begin{matrix}\cos\ \nu\theta\\ \sin\ \nu\theta\end{matrix}$ $\int_{\theta} (1-\tau)^{\beta}\ \frac{d\tau}{\tau}$	$q^{\nu}\ \begin{matrix}\cos\ \nu\theta\\ \sin\ \nu\theta\end{matrix}$ $q^{-\nu}\ \begin{matrix}\cos\ \nu\theta\\ \sin\ \nu\theta\end{matrix}$ $\log q$ θ
$\chi(q,\theta)$.	$q^{\nu}\ \underline{\tilde{F}}_{\nu}(\tau)\ \begin{matrix}\cos\ \nu\theta\\ \sin\ \nu\theta\end{matrix}$ $q^{-\nu}\ \underline{\tilde{G}}_{\nu}(\tau)\ \begin{matrix}\cos\ \nu\theta\\ \sin\ \nu\theta\end{matrix}$ $\int_{\theta} (1-\tau)^{-\beta}\ \frac{d\tau}{\tau}$	$q^{\nu}\ \begin{matrix}\cos\ \nu\theta\\ \sin\ \nu\theta\end{matrix}$ $q^{-\nu}\ \begin{matrix}\cos\ \nu\theta\\ \sin\ \nu\theta\end{matrix}$ $\log q$ θ

The functions $\underline{F}_{\nu}(\tau)$, $q^{-2\nu}\underline{G}_{\nu}(\tau)$ and $\underline{\tilde{F}}_{\nu}(\tau)$, $q^{-2\nu}\underline{\tilde{G}}_{\nu}(\tau)$ are respectively the two independent integrals of equations (27) and (28).

TABLE 14

τ	λ	M	τ	M	τ	M
0	∞	0	0.17	1.0057	0.28	1.3858
.02	2.2554	.10078	.18	1.0412	.29	1.4202
.04	1.6376	.20576	.19	1.0763	.30	1.4548
.06	1.3751	.31521	.20	1.1111	.32	1.5244
.08	1.2267	.42941	.21	1.1457	.34	1.5950
.10	1.1322	.54870	.22	1.1802	.36	1.6667
.12	1.0697	.67340	.23	1.2145	.38	1.7398
.14	1.0283	.80391	.24	1.2498	.40	1.8140
.15	1.0141		.25	1.2830	.42	1.8910
.16	1.0041	.94062	.26	1.3172	.44	1.9698
.165	1.0011		.27	1.3515	.46	2.0510

TABLE 2

τ	$F_{1/2}(\tau)$	$F_{3/2}(\tau)$	$F_{5/2}(\tau)$	$F_{7/2}(\tau)$	$F_{9/2}(\tau)$	$F_{11/2}(\tau)$	$F_{13/2}(\tau)$	$F_{15/2}(\tau)$	$F_{17/2}(\tau)$	$F_{19/2}(\tau)$	$F_{21/2}(\tau)$
0	1.00000, 0	1.00000, 0	1.00000, 0	1.00000, 0	1.00000, 0	1.00000, 0	1.00000, 0	1.00000, 0	1.00000, 0	1.00000, -0	1.00000, 0
.10	9.40692, -1	8.26748, -1	7.23508, -1	6.31726, -1	5.50840, -1	4.79886, -1	4.17817, -1	3.63614, -1	3.16339, -1	2.75137, -1	2.39525, -1
.12	9.29261, -1	7.94694, -1	6.75536, -1	5.72109, -1	4.83487, -1	4.08015, -1	3.43978, -1	2.89778, -1	2.43980, -1	2.05332, -1	1.72739, -1
.14	9.18112, -1	7.63945, -1	6.29860, -1	5.16693, -1	4.22513, -1	3.44761, -1	2.80876, -1	2.28661, -1	1.85821, -1	1.50967, -1	1.22575, -1
.15	9.12605, -1	7.48807, -1	6.07873, -1	4.90498, -1	3.94290, -1	3.16120, -1	2.52960, -1	2.02124, -1	1.61322, -1	1.28641, -1	1.02495, -1
.16	9.07143, -1	7.33892, -1	5.86410, -1	4.65282, -1	3.67496, -1	2.89341, -1	2.27271, -1	1.78196, -1	1.39516, -1	1.09110, -1	8.52437, -2
.165	9.04429, -1	7.26516, -1	5.75910, -1	4.53033, -1	3.54621, -1	2.76621, -1	2.16219, -1	1.67109, -1	1.29659, -1	1.00303, -1	7.75697, -2
.17	9.01726, -1	7.19196, -1	5.65503, -1	4.41018, -1	3.42087, -1	2.64333, -1	2.03672, -1	1.56581, -1	1.20163, -1	9.20855, -2	7.04764, -2
.175	8.99035, -1	7.11930, -1	5.55249, -1	4.29235, -1	3.29881, -1	2.52468, -1	1.92611, -1	1.46585, -1	1.13335, -1	8.44275, -2	6.39285, -2
.18	8.96355, -1	7.04719, -1	5.45130, -1	4.17682, -1	3.18004, -1	2.41012, -1	1.82027, -1	1.37102, -1	1.03035, -1	7.72969, -2	5.78904, -2
.185	8.93684, -1	6.97563, -1	5.35140, -1	4.06356, -1	3.06448, -1	2.29956, -1	1.71898, -1	1.28111, -1	9.52408, -2	7.06536 -2	5.23290, -2
.19	8.91217, -1	6.90461, -1	5.25281, -1	3.95253, -1	2.95208, -1	2.19288, -1	1.62213, -1	1.19592, -1	8.79255, -2	6.44991, -2	4.72128, -2
.195	8.88380, -1	6.83611, -1	5.15553, -1	3.84370, -1	2.84274, -1	2.09003, -1	1.52955, -1	1.11523, -1	8.10647, -2	5.96499, -2	4.25122, -2
.20	8.85743, -1	6.76417, -1	5.05952, -1	3.73707, -1	2.73642, -1	1.99083, -1	1.44109, -1	1.03890, -1	7.46365, -2	5.34693, -2	3.81990, -2
.21	8.80715, -1	6.62589, -1	4.87834, -1	3.53020, -1	2.53258, -1	1.80315, -1	1.27601, -1	8.98454, -2	6.29906, -2	4.40049, -2	3.06307, -2
.22	8.75312, -1	6.48974, -1	4.68817, -1	3.33172, -1	2.34026, -1	1.62911, -1	1.12582, -1	7.73225, -2	5.28229, -2	3.69219, -2	2.43131, -2
.23	8.70161, -1	6.35571, -1	4.50995, -1	3.14141, -1	2.15882, -1	1.46839, -1	1.08352, -1	6.61895, -2	4.39813, -2	2.90544, -2	1.90736, -2
.24	8.65054, -1	6.22379, -1	4.33662, -1	2.96901, -1	1.98792, -1	1.31893, -1	8.65939, -2	5.63245, -2	3.63254, -2	2.32524, -2	1.47590, -2
.25	8.59991, -1	6.09396, -1	4.16807, -1	2.78436, -1	1.82708, -1	1.18145, -1	7.64363, -2	4.76140, -2	2.97302, -2	1.83780, -2	1.12607, -2
.26	8.54973, -1	5.96618, -1	4.00425, -1	2.61721, -1	1.67591, -1	1.06480, -1	6.53835, -2	3.99519, -2	2.40758, -2	1.43192, -2	8.38040, -3
.27	8.49998, -1	5.84048, -1	3.84507, -1	2.45734, -1	1.53401, -1	9.38418, -2	5.63524, -2	3.32399, -2	1.92562, -2	1.09583, -2	6.09334, -3
.28.	8.45066, -1	5.71682, -1	3.69046, -1	2.30457, -1	1.40094, -1	8.31600, -2	4.82637, -2	2.73864, -2	1.51753, -2	8.20153, -3	4.28202, -3
.29	8.40177, -1	5.59519, -1	3.54034, -1	2.15869, -1	1.27636, -1	7.33811, -2	4.10444, -2	2.23067, -2	1.17406, -2	5.96281, -3	2.86731, -3
.30	8.35332, -1	5.47557, -1	3.39463, -1	2.01951, -1	1.15989, -1	6.44493, -2	3.46231, -2	1.79223, -2	8.87599, -3	4.16579, -3	1.78066, -3
.32	8.25771, -1	5.24232, -1	3.11619, -1	1.76035, -1	9.49754, -2	4.89140, -2	2.39154, -2	1.09549, -2	4.56947, -3	1.63491, -3	3.63965, -4
.34	8.16381, -1	5.01692, -1	2.85451, -1	1.52558, -1	7.67739, -2	3.61599, -2	1.56592, -2	5.97058, -3	1.75636, -3	1.61765, -4	-3.44649, -4
.36	8.07162, -1	4.79926, -1	2.60899, -1	1.31370, -1	6.11184, -2	2.58157, -2	9.43050, -3	2.53632, -3	3.65867, -5	-5.94075, -4	-6.15156, -4
.38	7.98111, -1	4.58923, -1	2.37908, -1	1.12320, -1	4.77556, -2	1.75508, -2	4.85885, -3	2.90912, -4	-9.06462, -4	-8.86334, -4	-6.35443, -4
.40	7.89228, -1	4.38670, -1	2.16418, -1	9.52680, -2	3.64602, -2	1.10641, -2	1.62280, -3	-1.06371, -3	-1.31917, -3	-8.99307, -4	-5.31185, -4
.42	7.80512, -1	4.19514, -1	1.96369, -1	8.00764, -2	2.70013, -2	6.06927, -3	-5.54379, -4	-1.77029, -3	-1.38933, -3	-7.62517, -4	-3.82053, -4
.44	7.71962, -1	4.00362, -1	1.77706, -1	6.66119, -2	1.91178, -2	2.36621, -3	-1.90872, -3	-2.02354, -3	-1.25658, -3	-6.63137, -4	-2.34660, -4
.46	7.63677, -1	3.82284, -1	1.60368, -1	5.47462, -2	1.27936, -2	1.50059, -4	-2.63949, -3	-1.77681, -3	-1.02127, -3	-5.56237, -4	-1.12718, -4
.48	7.55355, -1	3.64899, -1	1.44304, -1	4.43554, -2	7.67404, -3	-2.12546, -3	-2.90284, -3	-1.74815, -3	-7.52560, -4	-1.73337, -4	-2.48137, -5
.50	7.47296, -1	3.48202, -1	1.29454, -1	3.53204, -2	3.65270, -3	-4.82362, -3	-2.86466, -3	-1.42591, -3	-4.95152, -4	-2.923 ?, -5	+2.96827, -5

TABLE 3

τ	$\underline{F}_{-1/2}(\tau)$	$\underline{F}_{-3/2}(\tau)$	$\underline{F}_{-5/2}(\tau)$	$\underline{F}_{-7/2}(\tau)$	$\underline{F}_{-9/2}(\tau)$	$\underline{F}_{-11/2}(\tau)$	† $\underline{F}_{-13/2}(\tau)$	† $\underline{F}_{-15/2}(\tau)$	† $\underline{F}_{-17/2}(\tau)$	† $\underline{F}_{-19/2}(\tau)$	† $\underline{F}_{-21/2}(\tau)$
0	1.00000, 0	1.00000, 0	1.00000, 0	1.00000, 0	1.00000, 0	1.00000, 0	1.00000, 0	1.00000, 0	1.00000, 0	1.00000, 0	1.00000, 0
.10	1.05839, 0	1.12055, 0	1.41771, 0	1.72608, 0	2.05119, 0	2.40370, 0	2.79348, 0	3.23017, 0	3.72368, 0	4.28471, 0	4.92493, 0
.12	1.06928, 0	1.13121, 0	1.49211, 0	1.90884, 0	2.38596, 0	2.93835, 0	3.58302, 0	4.33940, 0	5.22992, 0	6.28099, 0	7.52351, 0
.14	1.07993, 0	1.13814, 0	1.55369, 0	2.07768, 0	2.72458, 0	3.52556, 0	4.51962, 0	5.75483, 0	7.28997, 0	9.19794, 0	1.15685, 1
.15	1.08516, 0	1.14030, 0	1.57887, 0	2.15267, 0	2.88480, 0	3.81970, 0	5.01470, 0	6.54253, 0	8.49524, 0	1.09896, 1	1.41736, 1
.16	1.09032, 0	1.14163, 0	1.59995, 0	2.21920, 0	3.03264, 0	4.10061, 0	5.50301, 0	7.34428, 0	9.76040, 0	1.29287, 1	1.70796, 1
.165	1.09289, 0	1.14201, 0	1.60889, 0	2.24883, 0	3.10039, 0	4.23237, 0	5.73721, 0	7.73704, 0	1.03932, 1	1.39181, 1	1.85944, 1
.17	1.09543, 0	1.14219, 0	1.61675, 0	2.27577, 0	3.16314, 0	4.35628, 0	5.96026, 0	8.11576, 0	1.10104, 1	1.48961, 1	2.01070, 1
.175	1.09796, 0	1.14218, 0	1.62348, 0	2.29984, 0	3.22029, 0	4.47061, 0	6.16844, 0	8.47296, 0	1.15990, 1	1.58367, 1	2.15772, 1
.18	1.10048, 0	1.14199, 0	1.62910, 0	2.32087, 0	3.27119, 0	4.57366, 0	6.35782, 0	8.80050, 0	1.21425, 1	1.67116, 1	2.29539, 1
.185	1.10298, 0	1.14162, 0	1.63355, 0	2.33875, 0	3.31524, 0	4.66369, 0	6.52426, 0	9.08955, 0	1.26235, 1	1.74878, 1	2.41773, 1
.19	1.10546, 0	1.14108, 0	1.63687, 0	2.35325, 0	3.35182, 0	4.73892, 0	6.66343, 0	9.33066, 0	1.30229, 1	1.81289, 1	2.51778, 1
.195	1.10793, 0	1.14036, 0	1.63903, 0	2.36430, 0	3.38032, 0	4.79756, 0	6.77089, 0	9.51383, 0	1.33197, 1	1.85906, 1	2.58766, 1
.20	1.11039, 0	1.13949, 0	1.64000, 0	2.37172, 0	3.40014, 0	4.83784, 0	6.84198, 0	9.62282, 0	1.34816, 1	1.88307, 1	2.61858, 1
.21	1.11525, 0	1.13724, 0	1.63842, 0	2.37525, 0	3.41159, 0	4.85625, 0	6.85711, 0	9.60926, 0	1.33653, 1	1.84450, 1	2.52419, 1
.22	1.12006, 0	1.13439, 0	1.63210, 0	2.36293, 0	3.38194, 0	4.78045, 0	6.67156, 0	9.15810, 0	1.24449, 1	1.65504, 1	2.14934, 1
.23	1.12481, 0	1.13095, 0	1.62106, 0	2.33411, 0	3.30746, 0	4.59764, 0	6.24957, 0	8.26238, 0	1.05258, 1	1.27029, 1	1.40274, 1
.24	1.12950, 0	1.12695, 0	1.60536, 0	2.28816, 0	3.18493, 0	4.29634, 0	5.55798, 0	6.76110, 0	7.40995, 0	6.46595, 0	1.90868, 0
.25	1.13414, 0	1.12244, 0	1.58503, 0	2.22477, 0	3.01181, 0	3.86685, 0	4.56782, 0	4.60497, 0	2.91933, 0	-2.55113, 0	-1.56729, 1
.26	1.13871, 0	1.11743, 0	1.56018, 0	2.14373, 0	2.78619, 0	3.30152, 0	3.25617, 0	1.73352, 0	-3.08469, 0	-1.46518, 1	-3.93195, 1
.27	1.14323, 0	1.11196, 0	1.53092, 0	2.04504, 0	2.50693, 0	2.59526, 0	1.60707, 0	-1.89268, 0	-1.06908, 1	-3.00024, 1	-6.93167, 1
.28	1.14770, 0	1.10605, 0	1.49738, 0	1.92884, 0	2.17366, 0	1.74570, 0	-3.86533, -1	-6.28854, 0	-1.99169, 1	-4.85917, 1	-1.05466, 2
.29	1.15211, 0	1.09973, 0	1.45973, 0	1.79545, 0	1.78683, 0	8.53485, -1	-3.82193, 0	-1.14393, 1	-3.06982, 1	-7.01848, 1	-1.47011, 2
.30	1.15646, 0	1.09304, 0	1.41812, 0	1.64535, 0	1.34769, 0	-3.77564, -1	-5.38566, 0	-1.72970, 1	-4.28751, 1	-9.42783, 1	-1.92579, 2
.32	1.16500, 0	1.07861, 0	1.32381, 0	1.29780, 0	3.21587, -1	-3.02435, 0	-1.15868, 1	-3.07613, 1	-7.02522, 1	-1.46595, 2	-2.86312, 2
.34	1.17333, 0	1.06296, 0	1.21609, 0	8.93074, -1	-8.78444, -1	-6.09800, 0	-1.86550, 1	-4.65705, 1	-9.86607, 1	-1.95922, 2	-3.63051, 2
.36	1.18145, 0	1.04630, 0	1.09682, 0	4.40208, -1	-2.21429, 0	-9.45145, 0	-2.60588, 1	-6.00562, 1	-1.23174, 2	-2.28798, 2	-3.82623, 2
.38	1.18935, 0	1.02881, 0	9.67976, -1	-5.00266, -2	-3.63755, 0	-1.29941, 1	-3.32151, 1	-7.21257, 1	-1.37846, 2	-2.29903, 2	-3.15371, 2
.40	1.19706, 0	1.01064, 0	8.31623, -1	-5.65487, -1	-5.09175, 0	-1.62038, 1	-3.91243, 1	-7.96883, 1	-1.36028, 2	-1.85609, 2	-1.32887, 2
.42	1.20456, 0	9.91968, -1	6.89872, -1	-1.09309, 0	-6.51410, 0	-1.91385, 1	-4.32731, 1	-7.99367, 1	-1.14410, 2	-8.63367, 1	1.70387, 2
.44	1.21187, 0	9.72948, -1	5.44847, -1	-1.61923, 0	-7.84357, 0	-2.14584, 1	-4.48151, 1	-7.17273, 1	-6.87397, 1	6.63477, 1	5.67107, 2
.46	1.21899, 0	9.53707, -1	3.98639, -1	-2.13027, 0	-9.01412, 0	-2.29447, 1	-4.31290, 1	-5.39505, 1	4.00007, -1	2.59577, 2	9.94177, 2
.48	1.22591, 0	9.34408, -1	2.53286, -1	-2.61293, 0	-9.96814, 0	-.234099, 1	-3.79201, 1	-2.67117, 1	8.74707, 1	4.67467, 2	1.35427, 3
.50	1.23266, 0	9.15143, -1	1.10727, -1	-3.05472, 0	-1.06545, 1	-2.27261, 1	-2.91157, 1	-8.7286 , 0	1.83516, 2	6.52937, 2	1.53557, 3

TABLE 4

τ	$\tilde{F}_{1/2}(\tau)$	$\tilde{F}_{3/2}(\tau)$	$\tilde{F}_{5/2}(\tau)$	$\tilde{F}_{7/2}(\tau)$	$\tilde{F}_{9/2}(\tau)$	$\tilde{F}_{11/2}(\tau)$	$\tilde{F}_{13/2}(\tau)$	$\tilde{F}_{15/2}(\tau)$	$\tilde{F}_{17/2}(\tau)$	$\tilde{F}_{19/2}(\tau)$	$\tilde{F}_{21/2}(\tau)$
0	1.00000, 0	1.00000, 0	1.00000, 0	1.00000, 0	1.00000, 0	1.00000, 0	1.00000, 0	1.00000, 0	1.00000, 0	1.00000, 0	1.00000, 0
.10	1.02253, 0	9.60632, -1	8.65636, -1	7.68544, -1	6.77456, -1	5.94730, -1	5.20766, -1	4.55215, -1	3.97426, -1	3.46662, -1	3.02175, -1
.12	1.02756, 0	9.62136, -1	8.38224, -1	7.24388, -1	6.20321, -1	5.28408, -1	4.48602, -1	3.79976, -1	3.21318, -1	2.71383, -1	2.28994, -1
.14	1.03281, 0	9.43406, -1	8.10616, -1	6.80974, -1	5.65617, -1	4.66675, -1	3.83376, -1	3.14003, -1	2.56617, -1	2.09374, -1	1.70610, -1
.15	1.03551, 0	9.38948, -1	7.96735, -1	6.59551, -1	5.39173, -1	4.37484, -1	3.53240, -1	2.84246, -1	2.28146, -1	1.82770, -1	1.46199, -1
.16	1.03827, 0	9.34427, -1	7.82803, -1	6.38317, -1	5.13332, -1	4.19773, -1	3.24641, -1	2.56517, -1	2.02045, -1	1.58815, -1	1.24604, -1
.165	1.03987, 0	9.32141, -1	7.75816, -1	6.27773, -1	5.00638, -1	3.95746, -1	3.10998, -1	2.43385, -1	1.89850, -1	1.47768, -1	1.14781, -1
.17	1.04109, 0	9.29839, -1	7.68817, -1	6.17278, -1	4.88093, -1	3.82370, -1	2.97682, -1	2.30725, -1	1.78196, -1	1.37309, -1	1.05568, -1
.175	1.04252, 0	9.27520, -1	7.61804, -1	6.06830, -1	4.75699, -1	3.69268, -1	2.84739, -1	2.18527, -1	1.67069, -1	1.27415, -1	9.69363, -2
.18	1.04397, 0	9.25183, -1	7.54777, -1	5.96432, -1	4.63455 -1	3.56574, -1	2.72164, -1	2.06781, -1	1.56450, -1	1.18063, -1	8.88560, -2
.185	1.04643, 0	9.22829, -1	7.47736, -1	5.86083, -1	4.51360, -1	3.43822, -1	2.59949, -1	1.95475, -1	1.46323, -1	1.09232, -1	8.13007, -2
.19	1.04691, 0	9.20457, -1	7.40681, -1	5.75784, -1	4.39415, -1	3.31491, -1	2.48089, -1	1.84598, -1	1.36673, -1	1.00900, -1	7.42442, -2
.195	1.04841, 0	9.18068, -1	7.33611, -1	5.65535, -1	4.27619, -1	3.19416, -1	2.36579, -1	1.74140, -1	1.27483, -1	9.30451, -2	6.76613, -2
.20	1.04992, 0	9.15659, -1	7.26528, -1	5.55335, -1	4.15972, -1	3.07595, -1	2.25412, -1	1.64091, -1	1.18737, -1	8.56588, -2	6.15277, -2
.21	1.05230, 0	9.10786, -1	7.12317, -1	5.35087, -1	3.93124, -1	2.84726, -1	2.04085, -1	1.45177, -1	1.02521, -1	7.21522, -2	5.05158, -2
.22	1.05614, 0	9.05835, -1	6.98047, -1	5.15041, -1	3.70870, -1	2.62803, -1	1.84065, -1	1.27778, -1	8.79050, -2	6.02599, -2	4.10322, -2
.23	1.05936, 0	9.00806, -1	6.83715, -1	4.95203, -1	3.49208, -1	2.41870, -1	1.65304, -1	1.11813, -1	7.47776, -2	4.98307, -2	3.29142, -2
.24	1.06266, 0	8.95694, -1	6.69322, -1	4.75571, -1	3.28136, -1	2.21889, -1	1.47759, -1	9.72075, -2	6.30301, -2	4.07323, -2	2.60114, -2
.25	1.06604, 0	8.90496, -1	6.54864, -1	4.56150, -1	3.07652, -1	2.02841, -1	1.31386, -1	8.38876, -2	5.25589, -2	3.28409, -2	2.01863, -2
.26	1.06950, 0	8.85210, -1	6.40342, -1	4.36942, -1	2.87755, -1	1.84708, -1	1.16140, -1	7.17813, -2	4.32651, -2	2.60403, -2	1.53124, -2
.27	1.07305, 0	8.79833, -1	6.25752, -1	4.17949, -1	2.68443, -1	1.67473, -1	1.01979, -1	6.08189, -2	3.50538, -2	2.02219, -2	1.12740, -2
.28	1.07669, 0	8.74362, -1	6.11079, -1	3.99174, -1	2.49714, -1	1.51115, -1	8.88898, -2	5.09333, -2	2.78547, -2	1.52852, -2	7.96572, -3
.29	1.08042, 0	8.68792, -1	5.96314, -1	3.80621, -1	2.31566, -1	1.35618, -1	7.67413, -2	4.20588, -2	2.15215, -2	1.11358, -2	5.29181, -3
.30	1.08425, 0	8.63120, -1	5.81562, -1	3.62289, -1	2.13997, -1	1.20963, -1	6.55817, -2	3.41321, -2	1.60320, -2	7.68658, -3	3.16544, -3
.32	1.09221, 0	8.51457, -1	5.51734, -1	3.26310, -1	1.80588, -1	9.41032, -2	4.59760, -2	2.08796, -2	7.21412, -3	2.57258, -3	2.49754, -4
.34	1.10063, 0	8.39338, -1	5.21591, -1	2.91262, -1	1.49470, -1	7.03861, -2	2.97227, -2	1.07105, -2	7.98990, -4	-6.29683, -4	-1.31670, -3
.36	1.10954, 0	8.26726, -1	4.91116, -1	2.87170, -1	1.20628, -1	4.96611, -2	1.66104, -2	3.19266, -3	-3.73923, -3	-2.40270, -3	-1.95931, -3
.38	1.11898, 0	8.13792, -1	4.60288, -1	2.24064, -1	9.40421, -2	3.17771, -2	6.03759, -3	-2.07404, -3	-6.87387, -3	-3.14716, -3	-2.00887, -3
.40	1.12902, 0	7.99860, -1	4.29084, -1	1.91964, -1	6.96946, -2	1.65772, -2	-1.98761, -3	-5.45776, -3	-9.02991, -3	-3.19032, -3	-1.71558, -3
.42	1.13972, 0	7.85822, -1	3.97480, -1	1.60933, -1	4.75656, -2	3.90922, -3	-7.84725, -3	-7.29513, -3	-1.05881, -2	-2.79384, -3	-1.26203, -3
.44	1.15114, 0	7.70425, -1	3.65460, -1	1.30976, -1	2.76346, -2	-6.38482, -3	-1.18131, -2	-7.89179, -3	-1.18892, -2	-2.16146, -3	-7.74904, -4
.46	1.16338, 0	7.54598, -1	3.32955, -1	1.02145, -1	9.87962, -3	-1.44637, -2	-1.41465, -2	-7.52273, -3	-1.32383, -2	-1.44623, -3	-3.35647, -4
.48	1.17663, 0	7.37924, -1	2.99968, -1	7.44810, -2	-5.72230, -3	-2.36344, -2	-1.60977, -2	-6.43288, -3	-1.49087, -2	-7.57447, -4	+1.00377, -5
.50	1.19071, 0	7.20312, -1	2.66446, -1	4.80325, -2	-1.91957, -2	-2.46214, -2	-1.49059, -2	-4.83756, -3	-1.71471, -2	-1.67292, -4	2.43597, -4

TABLE 5

τ	$\tilde{F}_{-1/2}(\tau)$	$\tilde{F}_{-3/2}(\tau)$	$\tilde{F}_{-5/2}(\tau)$	$\tilde{F}_{-7/2}(\tau)$	$\tilde{F}_{-9/2}(\tau)$	$\tilde{F}_{-11/2}(\tau)$	$\tilde{F}_{-13/2}(\tau)$	$\tilde{F}_{-15/2}(\tau)$	$\tilde{F}_{-17/2}(\tau)$	$\tilde{F}_{-19/2}(\tau)$	$\tilde{F}_{-21/2}(\tau)$
0	1.00000, 0	1.00000, 0	1.00000, 0	1.00000, 0	1.00000, 0	1.00000, 0	1.00000, 0	1.00000, 0	1.00000, 0	1.00000, 0	1.00000, 0
.10	8.00892, -1	1.67185, 0	2.11594, 0	2.51348, 0	2.92685, 0	3.37677, 0	3.87757, 0	4.44205, 0	5.08274, 0	5.81360, 0	6.64972, 0
.12	7.67300, -1	1.74279, 0	2.34632, 0	2.95210, 0	3.62862, 0	4.40740, 0	5.31493, 0	6.37910, 0	7.63149, 0	9.10873, 0	1.08544, 1
.14	7.12257, -1	1.79153, 0	2.54879, 0	3.38068, 0	4.37911, 0	5.60413, 0	7.11764, 0	8.99243, 0	1.13169, 1	1.41997, 1	1.77743, 1
.15	6.89160, -1	1.80740, 0	2.63522, 0	3.60150, 0	4.74977, 0	6.22964, 0	8.11157, 0	1.05092, 1	1.35651, 1	1.74591, 1	2.24192, 1
.16	6.65663, -1	1.81752, 0	2.70976, 0	3.76074, 0	5.10184, 0	6.84454, 0	9.11876, 0	1.20984, 1	1.59928, 1	2.11094, 1	2.67521, 1
.165	6.53760, -1	1.82041, 0	2.74209, 0	3.84332, 0	5.26676, 0	7.72687, 0	9.61556, 0	1.28942, 1	1.72361, 1	2.29849, 1	3.05882, 1
.17	6.41751, -1	1.82182, 0	2.77090, 0	3.91953, 0	5.42181, 0	7.42084, 0	1.00938, 1	1.36735, 1	1.84660, 1	2.48835, 1	3.34724, 1
.175	6.29636, -1	1.82177, 0	2.79600, 0	3.98868, 0	5.56512, 0	7.68438, 0	1.05469, 1	1.44183, 1	1.96554, 1	2.67380, 1	3.63128, 1
.18	6.17410, -1	1.82024, 0	2.81720, 0	4.05005, 0	5.69471, 0	7.92551, 0	1.09652, 1	1.51121, 1	2.07705, 1	2.84888, 1	3.90136, 1
.185	6.050740 -1	1.81720, 0	2.83434, 0	4.10291, 0	5.80852, 0	8.13935, 0	1.13384, 1	1.57337, 1	2.17724, 1	3.00655, 1	4.14478, 1
.19	5.92625, -1	1.81267, 0	2.84724, 0	4.14655, 0	5.90445, 0	8.32074, 0	1.16552, 1	1.62601, 1	2.26169, 1	3.13854, 1	4.34694, 1
.195	5.80060, -1	1.80662, 0	2.85574, 0	4.18023, 0	5.98032, 0	8.46431, 0	1.19036, 1	1.66660, 1	2.32540, 1	3.23540, 1	4.49029, 1
.20	5.67378, -1	1.79904, 0	2.85965, 0	4.20322, 0	6.03394, 0	8.56441, 0	1.20706, 1	1.69241, 1	2.36284, 1	3.28638, 1	4.55460, 1
.21	5.41653, -1	1.77928, 0	2.85309, 0	4.21425, 0	6.06534, 0	8.61069, 0	1.21056, 1	1.68774, 1	2.33425, 1	3.20172, 1	4.36196, 1
.22	5.15436, -1	1.75330, 0	2.82624, 0	4.17383, 0	5.98052, 0	8.41095, 0	1.16441, 1	1.58626, 1	2.12176, 1	2.77520, 1	3.52512, 1
.23	4.88698, -1	1.72100, 0	2.77789, 0	4.07623, 0	5.76031, 0	7.91461, 0	1.05625, 1	1.35985, 1	1.66490, 1	1.96177, 1	1.82495, 1
.24	4.61429, -1	1.68229, 0	2.70681, 0	3.91586, 0	5.38685, 0	7.07039, 0	8.73318, 0	9.79024, 1	8.99249, 0	5.87423, 0	-1.02029, 1
.25	4.33605, -1	1.63707, 0	2.61182, 0	3.68733, 0	4.84183, 0	5.82752, 0	6.02826, 0	4.14123, 0	-2.40221, 0	-1.84421, 1	-5.28308, 1
.26	4.05202, -1	1.58625, 0	2.49182, 0	3.38643, 0	4.10792, 0	4.13714, 0	2.32552, 0	-3.63181, 0	-1.81466, 1	-4.93864, 1	-1.12090, 2
.27	3.76200, -1	1.52671, 0	2.34574, 0	3.00528, 0	3.16880, 0	1.95394, 0	-2.48709, 0	-1.37802, 1	-3.87654, 1	-8.99703, 1	-1.89792, 2
.28	3.46571, -1	1.46134, 0	2.17255, 0	2.54232, 0	2.00960, 0	-7.62341, -1	-8.60472, 0	-2.65047, 1	-6.56340, 1	-1.40799, 2	-2.87666, 2
.29	3.16291, -1	1.38903, 0	1.97129, 0	1.99236, 0	6.17218, -1	-4.04521, 0	-1.66005, 1	-4.29331, 1	-9.59151, 1	-2.01987, 2	-4.02893, 2
.30	2.85332, -1	1.30964, 0	1.74105, 0	1.35168, 0	-1.01931, 0	-7.91965, 0	-2.44135, 1	-6.00989, 1	-1.32492, 2	-2.72472, 2	-5.32652, 2
.32	2.21258, -1	1.12915, 0	1.19021, 0	-2.14314, -1	-5.05571, 0	-1.74900, 1	-4.55801, 1	-1.04167, 2	-2.19261, 2	-4.34121, 2	-9.16299, 2
.34	1.54090, -1	9.18760, -1	5.13902, -1	-2.17479, 0	-1.01305, 1	-2.94368, 1	-7.14952, 1	-1.56252, 2	-3.16041, 2	-5.97782, 2	-1.05987, 3
.36	8.36415, -2	6.77247, -1	-2.93008, -1	-4.53849, 0	-1.62171, 1	-4.34790, 1	-1.00772, 2	-2.11116, 2	-4.16818, 2	-7.14923, 2	-1.13299, 3
.38	9.26131, -3	4.03256, -1	-1.23454, 0	-7.30206, 0	-2.32205, 1	-5.94545, 1	-1.31003, 2	-2.60430, 2	-4.63663, 2	-7.18256, 2	-8.75530, 2
.40	-6.90636, -2	9.52728, -2	-2.31348, 0	-1.04483, 1	-3.09675, 1	-7.53560, 1	-1.59694, 2	-2.93013, 2	-4.57159, 2	-6.50341, 2	-1.23827, 2
.42	-1.51922, -1	-2.48382, -1	-3.53126, 0	-1.39444, 1	-3.91985, 1	-9.08302, 1	-1.79335, 2	-2.94789, 2	-3.53561, 2	-7.8174 ?, 1	1.23162, 3
.44	-2.39785, -1	-6.29646, -1	-4.88782, 0	-1.77401, 1	-4.75605, 1	-1.04238, 2	-1.87549, 2	-2.51383, 2	-1.19812, 2	+6.79217, 2	3.16928, 3
.46	-3.33223, -1	-1.06064, 0	-6.38142, 0	-2.17661, 1	-5.56041, 1	-1.13586, 2	-1.77439, 2	-1.49208, 2	+2.63399, 2	1.72653, 3	5.42030, 3
.48	-4.32896, -1	-1.51424, 0	-8.00840, 0	-2.59318, 1	-6.31298, 1	-1.16751, 2	-1.43178, 2	+2.21192, 1	7.93197, 2	2.95775, 3	7.50837, 3
.50	-5.39575, -1	-2.02198, 0	-9.76294, 0	-3.01237, 1	-6.84633, 1	-1.11466, 2	-7.96315, 1	2.65768, 2	2.43521, 3	4.16443, 3	8.65307, 3

TABLE 6

τ	$\tilde{F}_{1/2,1}(\tau)$	$\hat{F}_{3/2,1}(\tau)$	$\tilde{F}_{5/2,1}(\tau)$	$\tilde{F}_{7/2,1}(\tau)$	$\tilde{F}_{9/2,1}(\tau)$	$\tilde{F}_{11/2,1}(\tau)$	$\tilde{F}_{13/2,1}(\tau)$	$\tilde{F}_{15/2,1}(\tau)$	$\tilde{F}_{17/2,1}(\tau)$	$\tilde{F}_{19/2,1}(\tau)$	$\tilde{F}_{21/2,1}(\tau)$
0	1.00000, 0	1.00000, 0	1.00000, 0	1.00000, 0	1.00000, 0	1.00000, 0	1.00000, 0	1.00000, 0	1.00000, 0	1.00000, 0	1.00000, 0
.10	1.20003, 0	1.13160, 0	1.03256, 0	9.27334, -1	8.25307, -1	7.30312, -1	6.43752, -1	5.65890, -1	4.96434, -1	4.34827, -1	3.80406, -1
.12	1.24830, 0	1.16243, 0	1.03984, 0	9.12019, -1	7.90837, -1	6.80772, -1	5.83106, -1	4.97660, -1	4.23597, -1	3.59813, -1	3.05138, -1
.14	1.29993, 0	1.19507, 0	1.04741, 0	8.96412, -1	7.56534, -1	6.32718, -1	5.25848, -1	4.35030, -1	3.58652, -1	2.94889, -1	2.41942, -1
.15	1.32712, 0	1.21211, 0	1.05151, 0	8.88495, -1	7.39446, -1	6.09252, -1	4.98469, -1	4.05736, -1	3.28963, -1	2.65901, -1	2.14400, -1
.16	1.35528, 0	1.22967, 0	1.05530, 0	8.80499, -1	7.22402, -1	5.86159, -1	4.71913, -1	3.77747, -1	3.01038, -1	2.39071, -1	1.89326, -1
.166	1.36973, 0	1.23865, 0	1.05733, 0	8.76471, -1	7.13896, -1	5.74754, -1	4.58940, -1	3.64223, -1	2.89715, -1	2.29429, -1	1.77663, -1
.17	1.38445, 0	1.24777, 0	1.05937, 0	8.72422, -1	7.05402, -1	5.63443, -1	4.40171, -1	3.51033, -1	2.74809, -1	2.14286, -1	1.66555, -1
.175	1.39944, 0	1.25702, 0	1.06144, 0	8.68353, -1	6.96919, -1	5.52226, -1	4.33602, -1	3.38145, -1	2.62310, -1	2.02625, -1	1.55983, -1
.18	1.41470, 0	1.26642, 0	1.06363, 0	8.64262, -1	6.88447, -1	5.41104, -1	4.21235, -1	3.25563, -1	2.50211, -1	1.91436, -1	1.46927, -1
.185	1.43024, 0	1.27597, 0	1.06565, 0	8.60150, -1	6.79987, -1	5.30077, -1	4.09066, -1	3.13285, -1	2.38503, -1	1.80703, -1	1.36370, -1
.19	1.44607, 0	1.28567, 0	1.06778, 0	8.56017, -1	6.71538, -1	5.19144, -1	3.97096, -1	3.01305, -1	2.27179, -1	1.70414, -1	1.27292, -1
.195	1.46220, 0	1.29552, 0	1.06994, 0	8.51861, -1	6.63101, -1	5.08306, -1	3.85323, -1	2.89622, -1	2.16230, -1	1.60557, -1	1.18677, -1
.20	1.47863, 0	1.30553, 0	1.07213, 0	8.47684, -1	6.54675, -1	4.97563, -1	3.73747, -1	2.78230, -1	2.05650, -1	1.51118, -1	1.10507, -1
.21	1.51243, 0	1.32603, 0	1.07658, 0	8.39260, -1	6.37859, -1	4.76363, -1	3.51178, -1	2.56305, -1	1.84102, -1	1.33460, -1	9.54330, -2
.22	1.54755, 0	1.34720, 0	1.08112, 0	8.30744, -1	6.21092, -1	4.55546, -1	3.29381, -1	2.35502, -1	1.66850, -1	1.17311, -1	8.19421, -2
.23	1.58405, 0	1.36909, 0	1.08578, 0	8.22132, -1	6.04373, -1	4.35112, -1	3.08346, -1	2.15789, -1	1.49459, -1	1.02612, -1	6.99108, -2
.24	1.62200, 0	1.39171, 0	1.09055, 0	8.13421, -1	5.87704, -1	4.15063, -1	2.88067, -1	1.97136, -1	1.33329, -1	8.92618, -2	5.92227, -2
.25	1.66150, 0	1.41512, 0	1.09543, 0	8.04609, -1	5.71085, -1	3.95401, -1	2.68532, -1	1.79514, -1	1.18402, -1	7.71756, -2	4.97677, -2
.26	1.70262, 0	1.43935, 0	1.10044, 0	7.95692, -1	5.54518, -1	3.76126, -1	2.49734, -1	1.62893, -1	1.04622, -1	6.62707, -2	4.14415, -2
.27	1.74546, 0	1.46443, 0	1.10557, 0	7.86666, -1	5.38004, -1	3.57241, -1	2.31663, -1	1.47242, -1	9.19344, -2	5.64681, -2	3.41430, -2
.28	1.79011, 0	1.49043, 0	1.11084, 0	7.77529, -1	5.21543, -1	3.38747, -1	2.14310, -1	1.32533, -1	8.02849, -2	4.76917, -2	2.77898, -2
.29	1.83670, 0	1.51738, 0	1.11624, 0	7.68276, -1	5.05136, -1	3.20645, -1	1.97666, -1	1.18737, -1	6.96212, -2	3.98686, -2	2.22850, -2
.30	1.88532, 0	1.54534, 0	1.12179, 0	7.58904, -1	4.88785, -1	3.02938, -1	1.81721, -1	1.05823, -1	5.98920, -2	3.29290, -2	1.75505, -2
.32	1.98918, 0	1.60462, 0	1.13334, 0	7.39786, -1	4.56255, -1	2.68712, -1	1.51891, -1	8.26283, -2	4.30385, -2	2.14362, -2	1.00926, -2
.34	2.10282, 0	1.66845, 0	1.14556, 0	7.20138, -1	4.23961, -1	2.36082, -1	1.24744, -1	6.24199, -2	2.93387, -2	1.27144, -2	4.86532, -3
.36	2.22752, 0	1.73771, 0	1.15850, 0	6.99920, -1	3.91914, -1	2.05064, -1	1.00200, -1	4.52705, -2	1.84272, -2	6.31080, -3	1.39198, -3
.38	2.36481, 0	1.81298, 0	1.17226, 0	6.79089, -1	3.60125, -1	1.75673, -1	7.81776, -2	3.08561, -2	9.95791, -3	1.81685, -3	-7.35494, -4
.40	2.51646, 0	1.89502, 0	1.18691, 0	6.57594, -1	3.28608, -1	1.47924, -1	5.85941, -2	1.89558, -2	3.60510, -3	-1.13327, -3	-1.86216, -3
.42	2.68460, 0	1.98476, 0	1.20255, 0	6.35378, -1	2.97374, -1	1.21836, -1	4.13637, -2	9.35188, -3	-9.37188, -4	-2.86447, -3	-2.27552, -3
.44	2.87173, 0	2.08328, 0	1.21931, 0	6.12378, -1	2.66441, -1	9.74275, -2	2.63983, -2	1.82997, -3	-3.95479, -3	-3.66243, -3	-2.21080, -3
.46	3.08088, 0	2.19185, 0	1.23732, 0	5.88518, -1	2.35825, -1	7.47181, -2	1.36070, -2	-3.82048, -3	-5.71341, -3	-3.77545, -3	-1.85620, -3
.48	3.31571, 0	2.31202, 0	1.25675, 0	5.63715, -1	2.05544, -1	5.37297, -2	2.89593, -3	-7.80648, -3	-6.45857, -3	-3.41626, -3	-1.35790, -3
.50	3.58063, 0	2.44563, 0	1.27779, 0	5.37870, -1	1.75621, -1	3.44858, -2	-5.83218, -3	-1.03310, -2	-6.41547, -3	-2.76389, -3	-8.25006, -4

TABLE 7

τ	$\tilde{F}_{-1/2,1}(\tau)$		$\tilde{F}_{-3/2,1}(\tau)$		$\tilde{F}_{-5/2,1}(\tau)$		$\tilde{F}_{-7/2,1}(\tau)$		$\tilde{F}_{-9/2,1}(\tau)$		$\tilde{F}_{-11/2,1}(\tau)$		$\tilde{F}_{-13/2,1}(\tau)$		$\tilde{F}_{-15/2,1}(\tau)$		$\tilde{F}_{-17/2,1}(\tau)$		$\tilde{F}_{-19/2,1}(\tau)$		$\tilde{F}_{-21/2,1}(\tau)$	
0	1.00000,	0	1.00000,	0	1.00000,	0	1.00000,	0	1.00000,	0	1.00000,	0	1.00000,	0	1.00000,	0	1.00000,	0	1.00000,	0	1.00000,	0
.10	1.15823,	0	4.42163,	-1	1.67670,	0	2.77963,	0	3.77324,	0	4.71787,	0	5.65971,	0	6.63494,	0	7.69322,	0	8.80658,	0	7.87890,	0
.12	1.19615,	0	3.23581,	-1	1.52093,	0	2.82519,	0	4.21870,	0	5.74867,	0	7.46418,	0	9.41564,	0	1.17533,	1	1.42513,	1	1.31198,	1
.14	1.23663,	0	2.02270,	-1	1.27591,	0	2.64275,	0	4.30263,	0	6.34974,	0	8.88812,	0	1.20520,	1	1.63376,	1	2.09370,	1	2.09748,	1
.15	1.25790,	0	1.40531,	-1	1.12111,	0	2.45530,	0	4.16386,	0	6.36661,	0	9.22060,	0	1.27240,	1	1.82964,	1	2.39492,	1	2.56353,	1
.16	1.27991,	0	7.96450,	-2	9.46386,	-1	2.19925,	0	3.87620,	0	6.12456,	0	9.14621,	0	1.32059,	1	1.95739,	1	2.59376,	1	3.03061,	1
.165	1.29120,	0	4.64967,	-2	8.49844,	-1	2.04465,	0	3.67204,	0	5.88994,	0	8.91703,	0	1.30447,	1	1.98170,	1	2.62834,	1	3.24462,	1
.17	1.30269,	0	1.47556,	-2	7.49260,	-1	1.87203,	0	3.42510,	0	5.57106,	0	8.53824,	0	1.26352,	1	1.96691,	1	2.60292,	1	3.43095,	1
.175	1.31439,	0	-1.71897,	-2	6.43698,	-1	1.68112,	0	3.13363,	0	5.16166,	0	7.99346,	0	1.19407,	1	1.95642,	1	2.50334,	1	3.57645,	1
.18	1.32628,	0	-4.93430,	-2	5.33227,	-1	1.47177,	0	2.79597,	0	4.65577,	0	7.26647,	0	1.09237,	1	1.81867,	1	2.31429,	1	3.66546,	1
.185	1.33840,	0	-8.17085,	-2	4.17912,	-1	1.24383,	0	2.41065,	0	4.04765,	0	6.34140,	0	9.54661,	0	1.66176,	1	2.01975,	1	3.68030,	1
.19	1.35073,	0	-1.14294,	-1	2.97819,	-1	9.97206,	-1	1.97632,	0	3.33198,	0	5.20279,	0	7.77185,	0	1.44118,	1	1.60286,	1	3.60106,	1
.195	1.36328,	0	-1.47092,	-1	1.73016,	-1	7.31847,	-1	1.49182,	0	2.50383,	0	3.83603,	0	5.66283,	0	1.14947,	1	9.38276,	0	3.40587,	1
.20	1.37606,	0	-1.80120,	-1	4.35729,	-2	4.47734,	-1	9.56101,	-1	1.55872,	0	2.22731,	0	2.88430,	0	7.79362,	0	3.33507,	0	3.07104,	1
.21	1.40234,	0	-2.46867,	-1	-2.28949,	-1	-1.76609,	-1	-2.71791,	-1	-6.97655,	-1	-1.76506,	0	-4.01080,	0	-2.23285,	0	-1.62844,	1	1.87986,	1
.22	1.42961,	0	-3.14570,	-1	-5.19178,	-1	-8.75136,	-1	-1.71154,	0	-3.46162,	0	-6.85760,	0	-1.31405,	1	-1.61473,	1	-4.40372,	1	-1.88591,	0
.23	1.45793,	0	-3.83268,	-1	-8.26516,	-1	-1.64650,	0	-3.36398,	0	-6.74685,	0	-1.31049,	1	-2.46641,	1	-3.52810,	1	-8.08264,	1	-3.34772,	1
.24	1.48734,	0	-4.53005,	-1	-1.15035,	0	-2.48872,	0	-5.23640,	0	-1.05548,	1	-2.05260,	1	-3.86501,	1	-6.67502,	1	-1.27063,	2	-7.80258,	1
.25	1.51792,	0	-5.23825,	-1	-1.49003,	0	-3.39913,	0	-7.29248,	0	-1.48729,	1	-2.90976,	1	-5.50523,	1	-8.32837,	1	-1.83472,	2	-1.37066,	2
.26	1.54972,	0	-5.95776,	-1	-1.84493,	0	-4.37443,	0	-9.55201,	0	-1.96738,	1	-3.87493,	1	-7.36874,	1	-1.13664,	2	-2.45881,	2	-2.11339,	2
.27	1.58281,	0	-6.68908,	-1	-2.21434,	0	-5.41065,	0	-1.19908,	1	-2.49138,	1	-5.03564,	1	-9.42190,	1	-1.46656,	2	-3.15074,	2	-3.00505,	2
.28	1.61728,	0	-7.43277,	-1	-2.59756,	0	-6.50314,	0	-1.45905,	1	-3.05329,	1	-6.07380,	1	-1.16138,	2	-1.80965,	2	-3.86620,	2	-4.02693,	2
.29	1.65320,	0	-8.18940,	-1	-2.99385,	0	-7.64661,	0	-1.73286,	1	-3.64528,	1	-7.26525,	1	-1.38754,	2	-2.14706,	2	-4.55810,	2	-5.14194,	2
.30	1.69065,	0	-8.95959,	-1	-3.40246,	0	-8.83508,	0	-2.01788,	1	-4.25781,	1	-8.47973,	1	-1.61190,	2	-2.45493,	2	-5.16624,	2	-6.29134,	2
.32	1.77054,	0	-1.05433,	0	-4.25339,	0	-1.13198,	1	-2.60870,	1	-5.49728,	1	-1.08259,	2	-2.01111,	2	-2.86267,	2	-6.83220,	2	-8.34089,	2
.34	1.85778,	0	-1.21899,	0	-5.14357,	0	-1.38959,	1	-3.20182,	1	-6.63000,	1	-1.27520,	2	-2.25468,	2	-2.75516,	2	-5.18408,	2	-9.23627,	2
.36	1.95335,	0	-1.39057,	0	-6.06562,	0	-1.64912,	1	-3.76112,	1	-7.60901,	1	-1.38194,	2	-2.21906,	2	-1.81791,	2	-2.50924,	2	-7.73739,	2
.38	2.06837,	0	-1.56990,	0	-7.01143,	0	-1.90222,	1	-4.24450,	1	-8.18655,	1	-1.35408,	2	-1.77535,	2	+2.46746,	1	2.73928,	2	-2.52934,	2
.40	2.17418,	0	-1.75784,	0	-7.97208,	0	-2.13945,	1	-4.60461,	1	-8.22140,	1	-1.14230,	2	-8.08123,	1	3.62999,	2	1.07353,	3	+7.37065,	2
.42	2.30237,	0	-1.95646,	0	-8.93768,	0	-2.35018,	1	-4.78983,	1	-7.53855,	1	-7.02419,	1	+7.53641,	1	8.40863,	2	2.07530,	3	2.21336,	3
.44	2.44482,	0	-2.16400,	0	-9.89719,	0	-2.52266,	1	-4.74556,	1	-5.97172,	1	+2.23207,	-1	2.91840,	2	1.43076,	3	3.14185,	3	4.04131,	3
.46	2.60378,	0	-2.38491,	0	-1.08382,	1	-2.64393,	1	-4.41575,	1	-3.37787,	1	9.70506,	1	5.59780,	2	2.07404,	3	4.02083,	3	5.83612,	3
.48	2.78201,	0	-2.61992,	0	-1.17468,	1	-2.69982,	1	-3.84513,	1	+3.44903,	0	2.20014,	2	8.57613,	2	2.67861,	3	4.36293,	3	7.23171,	3
.50	2.98280,	0	-2.87114,	0	-1.26069,	1	-2.67489,	1	-2.68133,	1	5.23818,	1	3.63460,	2	1.15005,	3	3.12506,	3	3.77955,	3	7.32971,	3

TABLE 8.- $\underline{F}_{\nu}^{(o)}(\tau) = f(\tau)\ T^{\nu}(\tau) \longrightarrow f(\tau)\ T^{\nu}(\tau)\ \cos\left(\nu\omega - \frac{\pi}{4}\right)$

τ	$\underline{F}_{1/2}^{(o)}(\tau)$	$\underline{F}_{3/2}^{(o)}(\tau)$	$\underline{F}_{5/2}^{(o)}(\tau)$	$\underline{F}_{7/2}^{(o)}(\tau)$	$\underline{F}_{9/2}^{(o)}(\tau)$	$\underline{F}_{11/2}^{(o)}(\tau)$	$\underline{F}_{13/2}^{(o)}(\tau)$	$\underline{F}_{15/2}^{(o)}(\tau)$	$\underline{F}_{17/2}^{(o)}(\tau)$	$\underline{F}_{19/2}^{(o)}(\tau)$	$\underline{F}_{21/2}^{(o)}(\tau)$
.02	9.89043, -1	9.64366, -1	9.40305, -1	9.16845, -1	8.93970, -1	8.71665, -1	8.49917, -1	8.28712, -1	8.08036, -1	7.87875, -1	7.68217, -1
.04	9.81477, -1	9.31947, -1	8.84917, -1	8.40259, -1	7.97856, -1	7.57592, -1	7.19360, -1	6.83058, -1	6.48587, -1	6.15856, -1	5.84777, -1
.06	9.78634, -1	9.03632, -1	8.34378, -1	7.70431, -1	7.11385, -1	6.56865, -1	6.06623, -1	5.60039, -1	5.17116, -1	4.77486, -1	4.40891, -1
.08	9.82797, -1	8.80976, -1	7.89704, -1	7.07869, -1	6.34549, -1	5.68808, -1	5.09878, -1	4.57063, -1	4.09701, -1	3.67255, -1	3.29206, -1
.10	9.98316, -1	8.67001, -1	7.52959, -1	6.53918, -1	5.67904, -1	4.93204, -1	4.28330, -1	3.71989, -1	3.23069, -1	2.80565, -1	2.43661, -1
.12	1.03492, 0	8.68573, -1	7.28964, -1	6.11796, -1	5.13460, -1	4.30930, -1	3.61665, -1	3.03634, -1	2.54746, -1	2.13800, -1	1.79435, -1
.14	1.12150, 0	9.06499, -1	7.32713, -1	5.92244, -1	4.78704, -1	3.86931, -1	3.12752, -1	2.52794, -1	2.04331, -1	1.65158, -1	1.33496, -1
.15	1.21594, 0	9.62870, -1	7.62405, -1	6.03626, -1	4.77954, -1	3.78447, -1	2.99656, -1	2.37269, -1	1.87871, -1	1.48757, -1	1.17787, -1
.16	1.43733, 0	1.11286, 0	8.61644, -1	6.67136, -1	5.16536, -1	3.99013, -1	3.09651, -1	2.39750, -1	1.86629, -1	1.43725, -1	1.11180, -1
.165	1.77527, 0	1.35777, 0	1.03845, 0	7.94235, -1	6.07450, -1	4.64892, -1	3.55331, -1	2.71766, -1	2.07853, -1	1.58971, -1	1.21565, -1
.17	2.98346, 0	2.26111, 0	1.69854, 0	1.28160, 0	9.67006, -1	7.29635, -1	5.50531, -1	4.15392, -1	3.13426, -1	2.36483, -1	1.78438, -1
.175	2.06247, 0	1.53761, 0	1.14614, 0	8.54387, -1	6.36892, -1	4.74754, -1	3.53887, -1	2.61916, -1	1.96626, -1	1.46561, -1	1.09242, -1
.18	1.76592, 0	1.30266, 0	9.60844, -1	7.08667, -1	5.22637, -1	3.85409, -1	2.84192, -1	2.09641, -1	1.54488, -1	1.13891, -1	8.39555, -2
.185	1.59244, 0	1.16351, 0	8.49924, -1	6.20721, -1	4.53232, -1	3.30868, -1	2.41491, -1	1.76223, -1	1.28569, -1	9.37840, -2	6.83972, -2
.19	1.47126, 0	1.06572, 0	7.71681, -1	5.58486, -1	4.04013, -1	2.92140, -1	2.11158, -1	1.52562, -1	1.10182, -1	7.96442, -2	5.74038, -2
.195	1.37864, 0	9.90878, -1	7.11764, -1	5.10589, -1	3.66084, -1	2.62272, -1	1.87771, -1	1.34334, -1	9.60388, -2	6.86150, -2	4.89904, -2
.20	1.30390, 0	9.30366, -1	6.62938, -1	4.71769, -1	3.35310, -1	2.38040, -1	1.68795, -1	1.19662, -1	8.45994, -2	5.98000, -2	4.22285, -2
.21	1.18753, 0	8.36116, -1	5.87026, -1	4.11061, -1	2.87115, -1	2.00077, -1	1.39114, -1	9.65216, -2	6.68336, -2	4.61870, -2	3.18587, -2
.22	1.09862, 0	7.64385, -1	5.29204, -1	3.64720, -1	2.50305, -1	1.71109, -1	1.16639, -1	7.90955, -2	5.35033, -2	3.60757, -2	2.42494, -2
.23	1.02675, 0	7.06681, -1	4.82631, -1	3.27378, -1	2.20673, -1	1.47763, -1	9.84394, -2	6.62368, -2	4.30163, -2	2.82268, -2	1.84094, -2
.24	9.66405, -1	6.58445, -1	4.43616, -1	2.95965, -1	1.95625, -1	1.28253, -1	8.34320, -2	5.38736, -2	3.45389, -2	2.19882, -2	1.39007, -2
.25	9.14389, -1	6.17021, -1	4.10028, -1	2.68844, -1	1.74159, -1	1.11574, -1	7.07345, -2	4.43935, -2	2.75871, -2	1.69730, -2	1.03385, -2
.26	8.68646, -1	5.80716, -1	3.80511, -1	2.45035, -1	1.55356, -1	9.70698, -2	5.98502, -2	3.64024, -2	2.18440, -2	1.29264, -2	7.63683, -3
.27	8.27790, -1	5.48363, -1	3.54141, -1	2.23772, -1	1.38667, -1	8.43758, -2	5.04444, -2	2.96305, -2	1.70884, -2	9.66225, -3	5.34348, -3
.28	7.90840, -1	5.19156, -1	3.30282, -1	2.04584, -1	1.23714, -1	7.31373, -2	4.22786, -2	2.38802, -2	1.31538, -2	7.04083, -3	3.84046, -3
.29	7.57068, -1	4.92479, -1	3.08461, -1	1.87110, -1	1.10237, -1	6.31635, -2	3.51791, -2	1.90062, -2	9.91462, -3	4.95455, -3	2.33674, -3
.30	7.25975, -1	4.67960, -1	2.88376, -1	1.71084, -1	9.80291, -2	5.42846, -2	2.90000, -2	1.48748, -2	7.25698, -3	3.30619, -3	1.35146, -3
.32	6.70151, -1	4.23917, -1	2.52364, -1	1.42689, -1	7.68466, -2	3.93380, -2	1.89878, -2	8.48627, -3	3.36774, -3	1.04900, -3	1.08178, -3
.34	6.20992, -1	3.85159, -1	2.20817, -1	1.18310, -1	5.92761, -2	2.75161, -2	1.15689, -2	4.07367, -3	9.25234, -4	-2.06100, -4	-4.75533, -4
.36	5.76927, -1	3.50441, -1	1.92835, -1	9.72485, -2	4.47172, -2	1.82667, -2	6.10691, -3	1.15648, -3	-4.92892, -4	-7.99940, -4	-6.61575, -4
.38	5.36904, -1	3.18976, -1	1.67829, -1	7.90176, -2	3.27109, -2	1.11127, -2	2.28204, -3	-6.50167, -4	-1.20150, -3	-9.81436, -4	-8.31046, -4
.40	5.00158, -1	2.90193, -1	1.45533, -1	6.32597, -2	2.29020, -2	5.72187, -3	-2.85008, -4	-1.64655, -3	-1.44186, -3	-9.25138, -4	-8.00405, -4
.42	4.66139, -1	2.63699, -1	1.25202, -1	4.96853, -2	1.49833, -2	1.77123, -3	-1.88852, -3	-2.48134, -3	-1.39353, -3	-7.51445, -4	-5.41763, -4
.44	4.34424, -1	2.39199, -1	1.07048, -1	3.80619, -2	8.69761, -3	-1.00215, -3	-2.67053, -3	-2.11722, -3	-1.18595, -3	-5.38797, -4	-2.00086, -4
.46	4.04696, -1	2.16473, -1	9.07389, -2	2.81867, -2	3.81561, -3	-2.82746, -3	-3.09894, -3	-1.92264, -3	-9.10079, -4	-3.34957, -4	-8.07136, -5
.48	3.76233, -1	1.95351, -1	6.74098, -2	1.98803, -2	1.32100, -4	-3.90216, -3	-3.33262, -3	-1.59826, -3	-6.26381, -4	-1.65424, -4	-2.52259, -6
.50	3.50230, -1	1.75684, -1	5.43218, -2	1.29782, -2	-2.53621, -3	-4.39783, -3	-2.78413, -3	-1.22235, -3	-3.71628, -4	-4.02791, -5	-4.18885, -6

TABLE 9.- $\underset{-\nu}{F}^{(o)}(\tau) = f(\tau)\ T^{-\nu}(\tau) \longrightarrow \frac{1}{2} f(\tau)\ T^{-\nu}(\tau)\ \cos\left(\nu\omega + \frac{\pi}{4}\right)$

τ	$\underset{-1/2}{F}^{(o)}(\tau)$	$\underset{-3/2}{F}^{(o)}(\tau)$	$\underset{-5/2}{F}^{(o)}(\tau)$	$\underset{-7/2}{F}^{(o)}(\tau)$	$\underset{-9/2}{F}^{(o)}(\tau)$	$\underset{-11/2}{F}^{(o)}(\tau)$	$\underset{-13/2}{F}^{(o)}(\tau)$	$\underset{-15/2}{F}^{(o)}(\tau)$	$\underset{-17/2}{F}^{(o)}(\tau)$	$\underset{-19/2}{F}^{(o)}(\tau)$	$\underset{-21/2}{F}^{(o)}(\tau)$
0.02	1.01435, 0	1.04031, 0	1.06693, 0	1.09423, 0	1.12223, 0	1.15094, 0	1.18039, 0	1.21060, 0	1.24157, 0	1.27334, 0	1.30593, 0
0.04	1.03364, 0	1.08857, 0	1.14643, 0	1.20736, 0	1.27153, 0	1.33910, 0	1.41027, 0	1.48523, 0	1.56416, 0	1.64729, 0	1.73484, 0
0.06	1.05986, 0	1.14783, 0	1.24310, 0	1.34628, 0	1.45802, 0	1.57904, 0	1.71010, 0	1.85205, 0	2.00577, 0	2.17225, 0	2.35255, 0
0.08	1.09639, 0	1.22310, 0	1.36443, 0	1.52217, 0	1.69809, 0	1.89436, 0	2.11330, 0	2.35755, 0	2.63003, 0	2.93400, 0	3.27310, 0
0.10	1.14952, 0	1.32362, 0	1.52410, 0	1.75493, 0	2.02073, 0	2.32679, 0	2.67920, 0	3.08499, 0	3.55224, 0	4.09025, 0	4.70975, 0
0.12	1.23322, 0	1.46926, 0	1.75068, 0	2.08596, 0	2.48545, 0	2.96146, 0	3.52862, 0	4.20441, 0	5.00962, 0	5.96905, 0	7.11221, 0
0.14	1.38750, 0	1.71659, 0	2.12373, 0	2.62744, 0	3.25062, 0	4.02161, 0	4.97546, 0	6.15555, 0	7.61553, 0	9.42179, 0	1.16565, 1
0.15	1.53566, 0	1.93944, 0	2.44939, 0	3.09343, 0	3.90680, 0	4.93446, 0	6.23139, 0	7.86986, 0	9.93913, 0	1.25525, 1	1.58530, 1
0.16	1.85639, 0	2.39764, 0	3.09669, 0	3.99955, 0	5.16565, 0	6.67173, 0	8.61692, 0	1.11293, 1	1.43741, 1	1.85648, 1	2.39777, 1
0.165	2.32115, 0	3.03488, 0	3.96807, 0	5.18822, 0	6.78355, 0	8.86942, 0	1.15967, 1	1.51626, 1	1.98249, 1	2.59209, 1	3.38913, 1
0.17	1.97704, 0	2.62022, 0	3.47696, 0	4.60237, 0	6.09965, 0	8.08400, 0	1.07140, 1	1.41995, 1	1.88189, 1	2.49412, 1	3.30551, 1
0.175	1.38331, 0	1.85558, 0	2.48904, 0	3.33870, 0	4.47831, 0	6.00685, 0	8.05695, 0	1.08066, 1	1.44944, 1	1.94403, 1	2.60757, 1
0.18	1.19687, 0	1.62226, 0	2.19864, 0	2.97957, 0	4.03752, 0	5.47065, 0	7.41185, 0	1.00410, 1	1.36014, 1	1.84229, 1	2.49508, 1
0.185	1.08951, 0	1.49049, 0	2.03856, 0	2.78751, 0	3.81068, 0	5.20810, 0	7.11615, 0	9.72065, 0	1.32748, 1	1.81236, 1	2.47362, 1
0.19	1.01502, 0	1.39982, 0	1.92951, 0	2.65822, 0	3.66014, 0	5.03680, 0	6.92715, 0	9.52115, 0	1.30782, 1	1.79521, 1	2.46253, 1
0.195	9.58226, -1	1.33082, 0	1.84651, 0	2.55947, 0	3.54396, 0	4.90170, 0	6.77165, 0	9.34345, 0	1.28752, 1	1.77174, 1	2.43445, 1
0.20	9.12386, -1	1.27494, 0	1.77869, 0	2.47727, 0	3.44396, 0	4.77857, 0	6.61655, 0	9.14090, 0	1.25975, 1	1.73152, 1	2.37306, 1
0.21	8.40756, -1	1.18656, 0	1.66788, 0	2.33714, 0	3.26928, 0	4.50231, 0	6.24245, 0	8.66135, 0	1.16569, 1	1.57371, 1	2.10311, 1
0.22	7.87016, -1	1.11560, 0	1.57419, 0	2.20397, 0	3.05775, 0	4.19690, 0	5.68605, 0	7.58025, 0	9.90410, 0	1.25725, 1	1.53538, 1
0.23	7.29396, -1	1.06431, 0	1.48579, 0	2.06489, 0	2.81952, 0	3.76601, 0	4.88319, 0	6.06990, 0	7.05475, 0	7.30395, 0	7.10740, 0
0.24	7.00090, -1	9.98920, -1	1.39893, 0	1.91322, 0	2.53530, 0	3.21218, 0	3.79353, 0	3.93931, 0	2.95415, 0	-4.99969, -1	-2.81451, 0
0.25	6.65402, -1	9.47280, -1	1.31099, 0	1.74612, 0	2.19831, 0	2.52035, 0	2.38206, 0	1.10702, 0	-2.61475, 0	-1.12276, 1	-2.91660, 1
0.26	6.34158, -1	8.98063, -1	1.22048, 0	1.56128, 0	1.80448, 0	1.68068, 0	6.23765, 0	-2.48611, 0	-9.77445, 0	-2.51542, 1	-5.56570, 1
0.27	6.05584, -1	8.50527, -1	1.12675, 0	1.35793, 0	1.35267, 0	6.89815, -1	-1.49096, 0	-6.86430, 0	-1.85750, 1	-4.23645, 1	-8.84745, 1
0.28	5.79147, -1	8.05993, -1	1.02938, 0	1.13598, 0	8.42660, -1	-4.52903, -1	-3.96352, 0	-1.20262, 1	-2.89943, 1	-6.27515, 1	-1.27225, 2
0.29	5.54476, -1	7.58697, -1	9.28625, -1	8.96665, -1	2.78121, -1	-1.73890, 0	-6.77225, 0	-1.79149, 1	-4.08778, 1	-8.58920, 1	-1.70775, 2
0.30	5.31244, -1	7.13734, -1	8.23800, -1	6.38875, -1	-3.42830, -1	-3.16872, 0	-9.90920, 0	-2.44750, 1	-5.40535, 1	-1.11252, 2	-2.17516, 2
0.32	4.88404, -1	6.26910, -1	6.04795, -1	7.79700, -2	-1.72409, 0	-6.37915, 0	-1.69445, 1	-3.90549, 1	-8.26015, 1	-1.64058, 2	-3.09189, 2
0.34	4.49410, -1	5.38827, -1	3.74912, -1	-6.34045, -1	-3.25521, 0	-9.93145, 0	-2.34783, 1	-5.43695, 1	-1.10463, 2	-2.09452, 2	-3.73929, 2
0.36	4.13515, -1	4.54018, -1	1.38204, -1	-1.17927, 0	-4.87107, 0	-1.36061, 1	-3.21358, 1	-6.80790, 1	-1.31899, 2	-2.53893, 2	-3.73154, 2
0.38	3.80199, -1	3.71185, -1	-1.01642, -1	-1.83946, 0	-6.49930, 0	-1.71478, 1	-3.87758, 1	-7.80525, 1	-1.40383, 2	-2.19833, 2	-2.72873, 2
0.40	3.49107, -1	2.90807, -1	-3.40012, -1	-2.49311, 0	-8.05630, 0	-2.02670, 1	-4.36049, 1	-8.16840, 1	-1.29698, 2	-1.54454, 2	-4.98521, 1
0.42	3.19980, -1	2.13267, -1	-5.72770, -1	-3.11942, 0	-9.45830, 0	-2.26740, 1	-4.57567, 1	-8.46765, 1	-9.52630, 1	-3.14725, 1	2.93140, 2
0.44	2.92630, -1	1.39091, -1	-7.95420, -1	-3.69668, 0	-1.06211, 1	-2.40959, 1	-4.45007, 1	-6.18020, 1	-3.56233, 0	-1.43921, 2	7.16435, 2
0.46	2.66912, -1	6.87472, -2	-1.00382, 0	-4.20472, 0	-1.14689, 1	-2.43071, 1	-3.93544, 1	-3.64254, 1	4.64526, 1	3.52680, 2	1.14148, 3
0.48	2.42713, -1	2.69075, -3	-1.53858, 0	-4.62520, 0	-1.19375, 1	-2.31634, 1	-2.08625, 1	-1.65651, 0	1.43391, 2	5.61960, 2	1.45880, 3
0.50	2.19955, -1	-5.86493, -2	-1.67610, 0	-4.94366, 0	-1.19840, 1	-2.05734, 1	-1.72385, 1	-4.00740, 1	2.43137, 2	7.29125, 2	1.67858, 3

TABLE 10.- $\tilde{\underline{F}}_{p}^{(o)}(\tau) = g(\tau)\, T^{p}(\tau) \longrightarrow g(\tau)\, T^{p}(\tau) \cos\left(p\omega - \frac{\pi}{4}\right)$

τ	$\tilde{\underline{F}}_{1/2}^{(o)}(\tau)$	$\tilde{\underline{F}}_{3/2}^{(o)}(\tau)$	$\tilde{\underline{F}}_{5/2}^{(o)}(\tau)$	$\tilde{\underline{F}}_{7/2}^{(o)}(\tau)$	$\tilde{\underline{F}}_{9/2}^{(o)}(\tau)$	$\tilde{\underline{F}}_{11/2}^{(o)}(\tau)$	$\tilde{\underline{F}}_{13/2}^{(o)}(\tau)$	$\tilde{\underline{F}}_{15/2}^{(o)}(\tau)$	$\tilde{\underline{F}}_{17/2}^{(o)}(\tau)$	$\tilde{\underline{F}}_{19/2}^{(o)}(\tau)$	$\tilde{\underline{F}}_{21/2}^{(o)}(\tau)$
.02	1.03963, 0	1.01369, 0	9.88402, -1	9.63742, -1	9.39697, -1	9.16251, -1	8.93390, -1	8.71101, -1	8.49366, -1	8.28176, -1	8.07511, -1
.04	1.08656, 0	1.03078, 0	9.78762, -1	9.29366, -1	8.82469, -1	8.37935, -1	7.95648, -1	7.55496, -1	7.17370, -1	6.81168, -1	6.46793, -1
.06	1.14018, 0	1.06279, 0	9.72109, -1	8.97606, -1	8.28813, -1	7.65294, -1	7.06642, -1	6.52485, -1	6.02479, -1	5.56305, -1	5.13669, -1
.08	1.20746, 0	1.08237, 0	9.70230, -1	8.96712, -1	7.79607, -1	6.98838, -1	6.26436, -1	5.61535, -1	5.03359, -1	4.51209, -1	4.04462, -1
.10	1.29495, 0	1.12461, 0	9.76686, -1	8.48217, -1	7.36645, -1	6.39750, -1	5.55600, -1	4.82518, -1	4.19060, -1	3.63929, -1	3.16060, -1
.12	1.41902, 0	1.19094, 0	9.99512, -1	8.38858, -1	7.04026, -1	5.90865, -1	4.95893, -1	4.16188, -1	3.49292, -1	2.93150, -1	2.46031, -1
.14	1.62754, 0	1.31553, 0	1.06333, 0	8.59476, -1	6.94705, -1	5.61522, -1	4.53872, -1	3.66860, -1	2.96529, -1	2.39681, -1	1.93732, -1
.15	1.81630, 0	1.43828, 0	1.13883, 0	9.01660, -1	7.13939, -1	5.65301, -1	4.47608, -1	3.54418, -1	2.80630, -1	2.22204, -1	1.75943, -1
.16	2.21066, 0	1.71161, 0	1.32540, 0	1.02608, 0	7.94448, -1	6.13694, -1	4.76253, -1	3.68743, -1	2.85503, -1	2.21053, -1	1.70995, -1
.165	2.77097, 0	2.11930, 0	1.62089, 0	1.23970, 0	9.48150, -1	7.25168, -1	5.54625, -1	4.24191, -1	3.24432, -1	2.48133, -1	1.89778, -1
.17	4.72637, 0	3.55034, 0	2.69081, 0	2.03030, 0	1.53193, -0	1.15587, 0	8.72144, -1	6.58217, -1	4.96533, -1	3.74629, -1	2.82683, -1
.175	3.31647, 0	2.47233, 0	1.84300, 0	1.37386, 0	1.02413, -0	7.63403, -1	5.69069, -1	4.05090, -1	3.16183, -1	2.35670, -1	1.75659, -1
.18	2.86255, 0	2.12636, 0	1.56840, 0	1.15677, 0	8.53116, -1	6.29112, -1	4.63889, -1	3.42036, -1	2.52177, -1	1.86905, -1	1.37041, -1
.185	2.63893, 0	1.92812, 0	1.40845, 0	1.02863, 0	7.51075, -1	5.48305, -1	4.00188, -1	2.92025, -1	2.13061, -1	1.55415, -1	1.13345, -1
.19	2.47544, 0	1.79311, 0	1.29837, 0	9.39669, -1	6.79759, -1	4.91534, -1	3.55283, -1	2.56687, -1	1.85381, -1	1.33835, -1	9.65840, -2
.195	2.35534, 0	1.69287, 0	1.21601, 0	8.72316, -1	6.25436, -1	4.48075, -1	3.20796, -1	2.29496, -1	1.64078, -1	1.17225, -1	8.36970, -2
.20	2.26219, 0	1.61413, 0	1.15030, 0	8.18491, -1	5.81743, -1	4.12985, -1	2.92841, -1	2.07429, -1	1.46774, -1	1.03749, -1	7.32630, -2
.21	2.12529, 0	1.49637, 0	1.05058, 0	7.35646, -1	5.13841, -1	3.58072, -1	2.48968, -1	1.72742, -1	1.19610, -1	8.26595, -2	5.70166, -2
.22	2.02900, 0	1.41171, 0	9.77366, -1	6.73587, -1	4.62278, -1	3.16014, -1	2.15231, -1	1.46078, -1	9.88131, -2	6.66268, -2	4.47852, -2
.23	1.95765, 0	1.34739, 0	9.20208, -1	6.24195, -1	4.20556, -1	2.81732, -1	1.87689, -1	1.24384, -1	8.20170, -2	5.38186, -2	3.51003, -2
.24	1.90304, 0	1.29661, 0	8.73569, -1	5.82184, -1	3.86225, -1	2.52556, -1	1.64294, -1	1.06085, -1	6.80140, -2	4.32992, -2	2.73733, -2
.25	1.86046, 0	1.25542, 0	8.34263, -1	5.47003, -1	3.54363, -1	2.27014, -1	1.43920, -1	9.03252, -2	5.61301, -2	3.46341, -2	2.10352, -2
.26	1.82695, 0	1.22137, 0	8.00298, -1	5.15363, -1	3.26748, -1	2.04201, -1	1.25878, -1	7.65623, -2	4.59427, -2	2.71871, -2	1.58516, -2
.27	1.80155, 0	1.19342, 0	7.70731, -1	4.87004, -1	3.01787, -1	1.83630, -1	1.09784, -1	6.44860, -2	3.71902, -2	2.10283, -2	1.16292, -2
.28	1.77972, 0	1.16832, 0	7.43273, -1	4.60400, -1	2.78408, -1	1.64690, -1	9.51444, -2	5.37404, -2	2.96016, -2	1.58448, -2	8.19256, -3
.29	1.70372, 0	1.10828, 0	6.94167, -1	4.21076, -1	2.48080, -1	1.42144, -1	7.91678, -2	4.27697, -2	2.23121, -2	1.11498, -2	5.25865, -3
.30	1.75144, 0	1.12896, 0	6.95719, -1	4.12747, -1	2.36499, -1	1.30964, -1	6.99637, -2	3.58860, -2	1.75078, -2	7.97632, -3	3.26045, -3
.32	1.73673, 0	1.09860, 0	6.54014, -1	3.69786, -1	1.99152, -1	1.01946, -1	4.92078, -2	2.19926, -2	8.72767, -3	2.71864, -3	2.80349, -3
.34	1.73244, 0	1.07452, 0	6.16035, -1	3.30061, -1	1.65368, -1	7.87616, -2	3.22470, -2	1.13647, -2	2.57564, -3	-5.74978, -3	-1.32608, -3
.36	1.73656, 0	1.06483, 0	5.80435, -1	2.92719, -1	1.34599, -1	5.49528, -2	1.83819, -2	3.48102, -3	-1.48361, -3	-2.40793, -3	-1.99135, -3
.38	1.74787, 0	1.03842, 0	5.46362, -1	2.57239, -1	1.06489, -1	3.61771, -2	7.42911, -3	-2.11660, -3	-3.91145, -3	-3.19504, -3	-2.05435, -3
.40	1.76556, 0	1.02438, 0	5.13202, -1	2.23307, -1	8.08441, -2	2.01980, -2	-1.00608, -3	-5.81232, -3	-5.08977, -3	-3.26574, -3	-1.76643, -3
.42	1.78914, 0	1.01213, 0	4.80553, -1	1.90703, -1	5.75092, -2	6.79837, -3	-7.24856, -3	-9.52393, -3	-5.34867, -3	-2.98421, -3	-1.31176, -3
.44	1.81833, 0	1.00119, 0	4.48061, -1	1.59312, -1	3.64048, -2	-4.19461, -3	-1.11778, -2	-8.86186, -3	-4.96392, -3	-2.25519, -3	-8.37482, -4
.46	1.85305, 0	9.91200, -1	4.15481, -1	1.29063, -1	1.74711, -2	-1.29465, -2	-1.41896, -2	-8.80350, -3	-4.16712, -3	-1.53372, -3	-3.59576, -4
.48	1.89097, 0	9.81846, -1	3.88606, -1	9.99196, -2	6.63943, -4	-1.96124, -2	-1.67499, -2	-8.03295, -3	-3.14823, -3	-8.31431, -4	-1.26787, -5
.50	1.93927, 0	9.72785, -1	3.00787, -1	7.18620, -2	-1.40378, -2	-2.43514, -2	-1.54161, -2	-6.76831, -3	-2.05775, -3	-2.23031, -4	-2.319421, -4

TABLE 11.- $\tilde{F}^{(0)}_{-\upsilon}(\tau) = g(\tau)\ T^{-\upsilon}(\tau) \longrightarrow \frac{1}{2}g(\tau)\ T^{-\upsilon}(\tau)\ \cos\left(\nu\omega + \frac{\pi}{4}\right)$

τ	$\tilde{F}^{(0)}_{-1/2}(\tau)$	$\tilde{F}^{(0)}_{-3/2}(\tau)$	$\tilde{F}^{(0)}_{-5/2}(\tau)$	$\tilde{F}^{(0)}_{-7/2}(\tau)$	$\tilde{F}^{(0)}_{-9/2}(\tau)$	$\tilde{F}^{(0)}_{-11/2}(\tau)$	$\tilde{F}^{(0)}_{-13/2}(\tau)$	$\tilde{F}^{(0)}_{-15/2}(\tau)$	$\tilde{F}^{(0)}_{-17/2}(\tau)$	$\tilde{F}^{(0)}_{-19/2}(\tau)$	$\tilde{F}^{(0)}_{-21/2}(\tau)$
.02	1.06623, 0	1.09352, 0	1.12150, 0	1.15020, 0	1.17963, 0	1.20981, 0	1.24077, 0	1.27252, 0	1.30508, 0	1.33847, 0	1.37273, 0
.04	1.14326, 0	1.20401, 0	1.26801, 0	1.33540, 0	1.40638, 0	1.48111, 0	1.55983, 0	1.64274, 0	1.73004, 0	1.82199, 0	1.91882, 0
.06	1.23481, 0	1.33730, 0	1.44830, 0	1.56851, 0	1.69870, 0	1.83969, 0	1.99239, 0	2.15777, 0	2.33686, 0	2.53082, 0	2.74089, 0
.08	1.34702, 0	1.50270, 0	1.67634, 0	1.87014, 0	2.08627, 0	2.32740, 0	2.59640, 0	2.89649, 0	3.23125, 0	3.60471, 0	4.02133, 0
.10	1.49108, 0	1.71691, 0	1.97696, 0	2.27637, 0	2.62115, 0	3.01815, 0	3.47527, 0	4.00163, 0	4.60772, 0	5.30559, 0	6.10916, 0
.12	1.69092, 0	2.01455, 0	2.40043, 0	2.86014, 0	3.40790, 0	4.06058, 0	4.83823, 0	5.76483, 0	6.86889, 0	8.18440, 0	9.75184, 0
.14	2.01367, 0	2.49115, 0	3.08200, 0	3.81289, 0	4.71736, 0	5.83624, 0	7.22049, 0	8.93306, 0	1.10512, 1	1.36731, 1	1.69161, 1
.15	2.29388, 0	2.89702, 0	3.65875, 0	4.62078, 0	5.83574, 0	7.37080, 0	9.30808, 0	1.17555, 1	1.48465, 1	1.87502, 1	2.36803, 1
.16	2.85518, 0	3.68764, 0	4.76280, 0	6.15143, 0	7.94492, 0	1.02613, 1	1.32531, 1	1.71172, 1	2.21078, 1	2.85532, 1	3.68784, 1
.165	3.52301, 0	4.73705, 0	6.19364, 0	8.09814, 0	1.06862, 1	1.38440, 1	1.81009, 1	2.36668, 1	3.09441, 1	4.04592, 1	5.28999, 1
.17	3.13201, 0	4.15093, 0	5.50817, 0	7.29103, 0	9.66300, 0	1.28066, 1	1.69729, 1	2.24946, 1	2.98127, 1	3.95116, 1	5.23776, 1
.175	2.22438, 0	2.98379, 0	4.00240, 0	5.36866, 0	7.20117, 0	9.65907, 0	1.29557, 1	1.73771, 1	2.33071, 1	3.12604, 1	4.19268, 1
.18	1.95367, 0	2.64805, 0	3.58888, 0	4.86361, 0	6.59052, 0	8.92985, 0	1.20985, 1	1.63901, 1	2.22018, 1	3.00721, 1	4.07277, 1
.185	1.80649, 0	2.46998, 0	3.37822, 0	4.61935, 0	6.31491, 0	8.63065, 0	1.17926, 1	1.61087, 1	2.19965, 1	3.00337, 1	4.09918, 1
.19	1.70780, 0	2.35524, 0	3.24646, 0	4.47253, 0	6.15830, 0	8.47457, 0	1.16551, 1	1.60196, 1	2.20045, 1	3.02049, 1	4.14328, 1
.195	1.63709, 0	2.27364, 0	3.15467, 0	4.37273, 0	6.05468, 0	8.37431, 0	1.15690, 1	1.59528, 1	2.19966, 1	3.02693, 1	4.15914, 1
.20	1.58294, 0	2.21194, 0	3.08592, 0	4.29791, 0	5.97606, 0	8.29053, 0	1.14793, 1	1.58589, 1	2.18561, 1	3.00408, 1	4.11712, 1
.21	1.50468, 0	2.12355, 0	2.98495, 0	4.18271, 0	5.83304, 0	8.05765, 0	1.11719, 1	1.53270, 1	2.08620, 1	2.81642, 1	3.76387, 1
.22	1.45352, 0	2.06036, 0	2.90731, 0	4.07042, 0	5.64724, 0	7.75109, 0	1.05013, 1	1.39997, 1	1.82915, 1	2.32196, 1	2.93563, 1
.23	1.40978, 0	2.01020, 0	2.83288, 0	3.93645, 0	5.37584, 0	7.18046, 0	9.31063, 0	1.15732, 1	1.34700, 1	1.39261, 1	1.35513, 1
.24	1.37862, 0	1.96707, 0	2.75477, 0	3.76751, 0	4.99251, 0	6.32542, 0	7.47022, 0	7.75729, 0	5.81731, 0	-9.84541, -1	-5.54233, 0
.25	1.35380, 0	1.92738, 0	2.66741, 0	3.55274, 0	4.47279, 0	5.12803, 0	4.64666, 0	2.25240, 0	-5.32010, 0	-2.28444, 1	-5.93406, 1
.26	1.33378, 0	1.88884, 0	2.56694, 0	3.28372, 0	3.79522, 0	3.53484, 0	1.31193, 0	-6.22884, 0	-2.05578, 1	-5.29048, 1	-1.17059, 2
.27	1.31797, 0	1.85100, 0	2.45219, 0	2.95532, 0	2.94386, 0	1.50128, 0	-3.24484, 0	-1.49390, +1	-4.04255, 1	-9.21996, 1	-1.92550, 2
.28	1.30333, 0	1.81384, 0	2.31654, 0	2.55643, 0	1.89634, 0	-1.01922, 0	-8.91958, 0	-2.70640, 1	-6.52494, 1	-1.41217, 2	-2.86310, 2
.29	1.29167, 0	1.76740, 0	2.16325, 0	2.08880, 0	6.47883, -1	-4.06081, 0	-1.57760, 1	-4.17329, 1	-9.52252, 1	-2.00086, 2	-3.97822, 2
.30	1.28157, 0	1.72193, 0	1.98745, 0	1.54132, 0	-8.27091, -1	-7.64462, 0	-2.39063, 1	-6.90469, 1	-1.30406, 2	-2.68352, 2	-5.24766, 2
.32	1.26572, 0	1.62467, 0	1.66737, 0	2.02063, -1	-4.46807, 0	-1.65319, 1	-4.39125, 1	-1.01213, 2	-2.14066, 2	-4.25165, 2	-8.01279, 2
.34	1.25376, 0	1.60323, 0	1.04593, 0	-1.48988, 0	-9.08138, 0	-2.77068, 1	-6.54998, 1	-1.51680, 2	-3.08170, 2	-5.84329, 2	-1.04319, 3
.36	1.24468, 0	1.36660, 0	4.15995, -1	-3.64961, 0	-1.46620, 1	-4.09545, 1	-9.67291, 1	-2.04918, 2	-3.97017, 2	-7.04020, 2	-1.12320, 3
.38	1.23773, 0	1.20838, 0	-3.30892, -1	-5.98831, 0	-2.11583, 1	-5.68241, 1	-1.26233, 2	-2.54098, 2	-4.57013, 2	-7.15660, 2	-8.88330, 2
.40	1.23235, 0	1.02655, 0	-1.20024, 0	-8.80068, 0	-2.84387, 1	-7.15425, 1	-1.53925, 2	-2.88345, 2	-4.57837, 2	-5.45223, 2	-1.75978, 2
.42	1.22815, 0	8.18666, -1	-2.19844, 0	-1.19730, 1	-3.63030, 1	-8.70278, 1	-1.75624, 2	-2.48243, 2	-3.65640, 2	-1.20798, 2	1.12514, 3
.44	1.22484, 0	5.82181, -1	-3.32932, 0	-1.64729, 1	-4.44558, 1	-1.00656, 2	-1.86263, 2	-2.58679, 2	-1.49106, 1	6.02397, 2	2.99872, 3
.46	1.22215, 0	3.14783, -1	-4.59635, 0	-1.92528, 1	-5.25145, 1	-1.11209, 2	-1.80198, 2	-1.66787, 2	2.12700, 2	1.61487, 3	5.22668, 3
.48	1.21989, 0	1.36241, -2	-7.73800, 0	-2.32465, 1	-5.99986, 1	-1.16370, 2	-1.04856, 2	-8.32572, 0	7.20692, 2	2.82444, 3	7.33202, 3
.50	1.21792, 0	-3.24763, -1	-9.27525, 0	-2.73737, 1	-6.63570, 1	-1.18918, 2	-9.54518, 1	-2.21895, 2	1.34629, 3	4.03726, 3	9.29452, 3

TABLE 12.- $\tilde{F}^{(o)}_{\nu,1}(\tau) = h(\tau)\ T^{\nu}(\tau) \longrightarrow h(\tau)\ T^{\nu}(\tau)\ \cos\left(\nu w - \mu - \frac{\pi}{4}\right)$

τ	$\tilde{F}^{(o)}_{1/2,1}(\tau)$	$\tilde{F}^{(o)}_{3/2,1}(\tau)$	$\tilde{F}^{(o)}_{5/2,1}(\tau)$	$\tilde{F}^{(o)}_{7/2,1}(\tau)$	$\tilde{F}^{(o)}_{9/2,1}(\tau)$	$\tilde{F}^{(o)}_{11/2,1}(\tau)$	$\tilde{F}^{(o)}_{13/2,1}(\tau)$	$\tilde{F}^{(o)}_{15/2,1}(\tau)$	$\tilde{F}^{(o)}_{17/2,1}(\tau)$	$\tilde{F}^{(o)}_{19/2,1}(\tau)$	$\tilde{F}^{(o)}_{21/2,1}(\tau)$
.02	1.0890, 0	1.0618, 0	1.0364, 0	1.0096, 0	9.8433, -1	9.5977, -1	9.3583, -1	9.1248, -1	8.8971, -1	8.6751, -1	8.4587, -1
.04	1.1958, 0	1.1355, 0	1.0782, 0	1.0238, 0	9.7212 -1	9.2306, -1	8.7648, -1	8.3224, -1	7.9024, -1	7.5036, -1	7.1250, -1
.06	1.3274, 0	1.2257, 0	1.1318, 0	1.0450, 0	9.6493, -1	8.9098, -1	8.2269, -1	7.5964, -1	7.0142, -1	6.4767, -1	5.9803, -1
.08	1.4954, 0	1.3404, 0	1.2016, 0	1.0771, 0	9.6549, -1	8.6493, -1	7.7580, -1	6.9542, -1	6.2338, -1	5.5879, -1	5.0090, -1
.10	1.7213, 0	1.4949, 0	1.2983, 0	1.1275, 0	9.7919, -1	8.5039, -1	7.3854, -1	6.4139, -1	5.5702, -1	4.8376, -1	4.2013, -1
.12	2.0522, 0	1.7224, 0	1.4455, 0	1.2132, 0	1.0182, 0	8.5453, -1	7.1718, -1	6.0190, -1	5.0516, -1	4.2396, -1	3.5582, -1
.14	2.6233, 0	2.1204, 0	1.7139, 0	1.3863, 0	1.1197, 0	9.0507, -1	7.3156, -1	5.9131, -1	4.7795, -1	3.8632, -1	3.1226, -1
.15	3.1458, 0	2.4911, 0	1.9725, 0	1.5617, 0	1.2365, 0	9.7910, -1	7.7525, -1	6.1385, -1	4.8605, -1	3.8485, -1	3.0473, -1
.16	4.2322, 0	3.2768, 0	2.5371, 0	1.9644, 0	1.5209, 0	1.1749, 0	9.1175, -1	7.0593, -1	5.4658, -1	4.2319, -1	3.2736, -1
.165	5.7440, 0	4.3932, 0	3.3600, 0	2.5698, 0	1.9655 0	1.5032, 0	1.1497, 0	8.7932, -1	6.7252, -1	5.1436, -1	3.9340, -1
.17	1.0065, 0	7.5871, 0	5.7252, 0	4.3203, 0	3.2600, 0	2.4600, 0	1.8562, 0	1.4007, 0	1.0559, 0	7.9755, -1	6.0182, -1
.175	6.0065, 0	4.4232, 0	3.3486, 0	2.4996, 0	1.8660 0	1.3912, 0	1.0399, 0	7.7630, -1	5.7964, -1	4.3255, -1	3.2287, -1
.18	4.6172, 0	3.4233, 0	2.5378, 0	1.8810, 0	1.3940, 0	1.0329, 0	7.5616, -1	5.6664, -1	4.1991, -1	3.1085, -1	2.3016, -1
.185	3.7891, 0	2.7991, 0	2.0656, 0	1.5250, 0	1.1247, 0	8.2918, -1	6.1087, -1	4.4990, -1	3.3120, -1	2.4371, -1	1.7925, -1
.19	3.2093, 0	2.3710, 0	1.7492, 0	1.2893, 0	9.4870, -1	6.9703, -1	5.1174, -1	3.7535, -1	2.7503, -1	2.0140, -1	1.4725, -1
.195	2.7704, 0	2.0545, 0	1.5586, 0	1.1202, 0	8.2404, -1	6.0484, -1	4.4298, -1	3.3031, -1	2.3634, -1	1.7218, -1	1.2525, -1
.20	2.4217, 0	1.8094, 0	1.3442, 0	9.9432, -1	7.3220, -1	5.3715, -1	4.0082, -1	2.9454, -1	2.0802, -1	1.5080, -1	1.0906, -1
.21	1.8962, 0	1.4542, 0	1.0994, 0	8.2062, -1	5.8496, -1	4.4502, -1	3.2403, -1	2.3453, -1	1.6889, -1	1.2096, -1	8.6292, -2
.22	1.5163, 0	1.2128, 0	9.3938, -1	7.1075, -1	5.2818, -1	3.8692, -1	2.8018, -1	2.0090, -1	1.4286, -1	1.0085, -1	7.0741, -2
.23	1.2280, 0	1.0419, 0	8.3174, -1	6.3850, -1	4.7587, -1	3.4743, -1	2.4948, -1	1.7727, -1	1.2368, -1	8.6207, -2	5.8114, -2
.24	1.0332, 0	9.4665, -1	7.5710, -1	5.8852, -1	4.4124, -1	3.2115, -1	2.2915, -1	1.5756, -1	1.0828, -1	7.2783, -2	4.9361, -2
.25	8.2084, -1	8.3498, -1	7.0474, -1	5.5284, -1	4.1170, -1	2.9800, -1	2.0937, -1	1.4159, -1	9.5259, -2	6.3131, -2	4.1300, -2
.26	6.7298, -1	7.5780, -1	6.6788, -1	5.3322, -1	3.9055, -1	2.7705, -1	1.9041, -1	1.2656, -1	8.3852, -2	5.3839, -2	3.4373, -2
.27	5.5067, -1	7.0728, -1	6.4203, -1	5.0845, -1	3.7332, -1	2.6084, -1	1.7413, -1	1.1417, -1	7.3274, -2	4.6939 -2	2.8321, -2
.28	4.4824, -1	6.7019, -1	6.2417, -1	4.9404, -1	3.5868, -1	2.4624, -1	1.6234, -1	1.0364, -1	6.4390, -2	3.9052, -2	2.3149, -2
.29	3.6158, -1	6.4314, -1	6.1199, -1	4.8259, -1	3.4558, -1	2.3066, -1	1.4977, -1	9.2624, -2	5.5976, -2	3.2742, -2	1.8587, -2
.30	2.8833, -1	6.2479, -1	6.0458, -1	4.7354, -1	3.3375, -1	2.1994, -1	1.3793, -1	8.3091, -2	4.8275, -2	2.7080, -2	1.4171, -2
.32	1.7133, -1	6.0590, -1	5.9844, -1	4.5910, -1	3.1176, -1	1.9681, -1	1.1589, -1	6.5189, -2	3.4925, -2	1.7776, -2	8.5209, -3
.34	8.4097, -2	6.0474, -1	6.0014, -1	4.4730, -1	2.9088, -1	1.7294, -1	9.5719, -2	4.9586, -2	2.3938, -2	1.0601, -2	4.1277, -3
.36	1.8133, -2	6.1568, -1	6.0628, -1	4.3634, -1	2.7023, -1	1.5098, -1	7.7256, -2	3.6119, -2	1.5094, -2	5.2777, -3	1.1831, -3
.38	-3.2075, -2	6.3622, -1	6.1547, -1	4.2180, -1	2.4961, -1	1.2994, -1	6.0060, -2	2.4705, -2	8.1629, -3	1.6089, -3	-6.3726, -4
.40	-7.0245, -2	6.6297, -1	6.2523, -1	4.1362, -1	2.2843, -1	1.0961, -1	4.5369, -2	1.5128, -2	2.9143, -3	-9.8337, -4	-1.6039, -3
.42	-9.9071, -2	6.9597, -1	6.3656, -1	4.0154, -1	2.0713, -1	9.0312, -2	3.1924, -2	7.3605, -3	-8.6088, -4	-2.4543, -3	-1.9661, -3
.44	-1.2043, -1	7.3411, -1	6.4808, -1	3.8739, -1	1.8557, -1	7.1974, -2	2.0151, -2	1.2420, -3	-3.3780, -3	-3.1335, -3	-1.9107, -3
.46	-1.3563, -1	7.7697, -1	6.5965, -1	3.7242, -1	1.6381, -1	5.4743, -2	1.0025, -2	-3.6531, -3	-4.8441, -3	-3.2263, -3	-1.6021, -3
.48	-1.4666, -1	8.2454, -1	7.3456, -1	3.5610, -1	1.4191, -1	3.8697, -2	-4.1007, -3	-6.6184, -3	-5.4660, -3	-2.9123, -3	-1.1672, -3
.50	-1.5119, -1	8.7676, -1	7.3424, -1	3.3825, -1	1.2008, -1	2.3874, -2	-5.4212, -3	-8.6539, -3	-5.0648, -3	-2.3428, -3	-7.0109, -4

TABLE 13.- $\tilde{F}^{(0)}_{-\nu,1}(\tau) = h(\tau)\ T^{-\nu}(\tau) \longrightarrow \frac{1}{2}h(\tau)\ T^{-\nu}(\tau)\ \cos\left(w + \mu + \frac{\pi}{4}\right)$

τ	$\tilde{F}^{(0)}_{-1/2,1}(\tau)$	$\tilde{F}^{(0)}_{-3/2,1}(\tau)$	$\tilde{F}^{(0)}_{-5/2,1}(\tau)$	$\tilde{F}^{(0)}_{-7/2,1}(\tau)$	$\tilde{F}^{(0)}_{-9/2,1}(\tau)$	$\tilde{F}^{(0)}_{-11/2,1}(\tau)$	$\tilde{F}^{(0)}_{-13/2,1}(\tau)$	$\tilde{F}^{(0)}_{-15/2,1}(\tau)$	$\tilde{F}^{(0)}_{-17/2,1}(\tau)$	$\tilde{F}^{(0)}_{-19/2,1}(\tau)$	$\tilde{F}^{(0)}_{-21/2,1}(\tau)$
.02	1.1169, 0	1.1455, 0	1.1748, 0	1.2048, 0	1.2357, 0	1.2673, 0	1.2997, 0	1.3330, 0	1.3671, 0	1.4021, 0	1.4379, 0
.04	1.2594, 0	1.3263, 0	1.3968, 0	1.4711, 0	1.5492, 0	1.6316, 0	1.7183, 0	1.8096, 0	1.9058, 0	2.0071, 0	2.1138, 0
.06	1.4376, 0	1.5569, 0	1.6862, 0	1.8261, 0	1.9777, 0	2.1418, 0	2.3196, 0	2.5121, 0	2.7207, 0	2.9465, 0	3.1910, 0
.08	1.6682, 0	1.8610, 0	2.0760, 0	2.3160, 0	2.5837, 0	2.8823, 0	3.2155, 0	3.5871, 0	4.0017, 0	4.4642, 0	4.9802, 0
.10	1.9820, 0	2.2822, 0	2.6279, 0	3.0259, 0	3.4842, 0	4.0119, 0	4.6195, 0	5.3192, 0	6.1246, 0	7.0625, 0	8.1206, 0
.12	2.4453, 0	2.9135, 0	3.4716, 0	4.1364, 0	4.9286, 0	5.8726, 0	6.9972, 0	8.3373, 0	9.9340, 0	1.1837, 1	1.4103, 1
.14	3.2455, 0	4.0153, 0	4.9676, 0	6.1458, 0	7.6035, 0	9.4070, 0	1.1638, 1	1.4398, 1	1.7813, 1	2.2039, 1	2.7266, 1
.15	3.9730, 0	5.0176, 0	6.3369, 0	8.0031, 0	1.0107, 1	1.2766, 1	1.6121, 1	2.0360, 1	2.5714, 1	3.2475, 1	4.1014, 1
.16	5.4661, 0	7.0597, 0	9.1181, 0	1.1776, 1	1.5210, 1	1.9645, 1	2.5372, 1	3.2770, 1	4.2324, 1	5.4663, 1	7.0601, 1
.165	7.5103, 0	9.8196, 0	1.2839, 1	1.6787, 1	2.1949, 1	2.8698, 1	3.7522, 1	4.9060, 1	6.4146, 1	8.3869, 1	1.0966, 2
.17	6.6624, 0	8.8295, 0	1.1701, 1	1.5506, 1	2.0548, 1	2.7232, 1	3.6089, 1	4.7825, 1	6.3382, 1	8.3994, 1	1.1131, 2
.175	4.0226, 0	5.3875, 0	7.2156, 0	9.6669, 0	1.2942, 1	1.7337, 1	2.3210, 1	3.1080, 1	4.1618, 1	5.5739, 1	7.4650, 1
.18	3.1143, 0	4.1990, 0	5.6581, 0	7.6259, 0	1.0276, 1	1.3844, 1	1.8648, 1	2.5112, 1	3.3812, 1	4.5536, 1	6.1258, 1
.185	2.5631, 0	3.4655, 0	4.6826, 0	6.3229, 0	8.5318, 0	1.1504, 1	1.5500, 1	2.0866, 1	2.8065, 1	3.7714, 1	5.0631, 1
.19	2.1699, 0	2.9279, 0	3.9419, 0	5.2981, 0	7.1102, 0	9.5237, 0	1.2718, 1	1.6926, 1	2.2471, 1	2.9736, 1	3.9229, 1
.195	1.8617, 0	2.5757, 0	3.3246, 0	4.4129, 0	5.8082, 0	7.6445, 0	1.0451, 1	1.2860, 1	1.6436, 1	2.0737, 1	2.5737, 1
.20	1.6103, 0	2.1257, 0	2.8996, 0	3.6006, 0	4.8483, 0	5.7800, 0	7.1060, 0	8.4735, 0	9.6697, 0	1.0277, 1	9.5511, 0
.21	1.2153, 0	1.5140, 0	1.8242, 0	2.0874, 0	2.1774, 0	1.8854, 0	8.2516, -1	-1.6642, 0	-6.6914, 0	-1.6069, 1	-3.2854, 1
.22	9.0427, -1	9.9909, -1	9.5263, -1	6.1244, -1	-3.6941, -1	-2.4701, 0	-6.5994, 0	-1.4259, 1	-2.7938, 1	-5.1716, 1	-9.2215, 1
.23	6.5050, -1	5.4114, -1	1.1911, -1	-9.2106, -1	-3.1171, 0	-7.3626, 0	-1.5359, 1	-2.9663, 1	-5.4744, 1	-9.7910, 1	-1.6603, 2
.24	4.3456, -1	1.2106, -1	-5.7453, -1	-2.4924, 0	-6.0921, 0	-1.2942, 1	-2.5514, 1	-4.6919, 1	-8.7346, 1	-1.5515, 2	-2.7029, 2
.25	2.9049, -1	-2.7419, -1	-1.5128, 0	-3.9343, 0	-9.3088, 0	-1.9105, 1	-3.7067, 1	-6.9218, 1	-1.2566, 2	-2.2314, 2	-3.8915, 2
.26	7.7457, -2	-6.5220, -1	-2.3325, 0	-5.8263, 0	-1.2766, 1	-2.5870, 1	-4.9951, 1	-8.8200, 1	-1.6914, 2	-3.0063, 2	-5.2420, 2
.27	-7.5337, -2	-1.0180, 0	-3.1616, 0	-7.6306, 0	-1.6450, 1	-3.3188, 1	-6.4007, 1	-1.1937, 2	-2.1675, 2	-3.8463, 2	-6.6906, 2
.28	-2.1586, -1	-1.3739, 0	-4.0026, 0	-9.2861, 0	-2.0306, 1	-4.0977, 1	-7.9008, 1	-1.4724, 2	-2.6674, 2	-4.7133, 2	-8.1388, 2
.29	-3.4674, -1	-1.7262, 0	-4.8560, 0	-1.1408, 1	-2.4401, 1	-4.9131, 1	-9.4521, 1	-1.7587, 2	-3.1691, 2	-5.5499, 2	-9.4525, 2
.30	-4.6578, -1	-2.0737, 0	-5.7237, 0	-1.3388, 1	-2.8610, 1	-5.7540, 1	-1.1516, 2	-2.0423, 2	-3.6441, 2	-6.2849, 2	-1.0469, 3
.32	-6.9816, -1	-2.7621, 0	-7.4987, 0	-1.7478, 1	-3.7254, 1	-7.4439, 1	-1.4104, 2	-2.5446, 2	-4.3684, 2	-7.0907, 2	-1.0725, 3
.34	-9.1032, -1	-3.4501, 0	-9.3159, 0	-2.1667, 1	-4.5850, 1	-9.0166, 1	-1.6591, 2	-2.8492, 2	-4.5038, 2	-4.7079, 2	-7.1038, 2
.36	-1.1144, 0	-4.1433, 0	-1.1167, 1	-2.5833, 1	-5.3870, 1	-1.0287, 2	-1.7953, 2	-2.8037, 2	-3.6759, 2	-3.1445, 2	2.0631, 2
.38	-1.3099, 0	-4.8496, 0	-1.3041, 1	-2.9857, 1	-6.0735, 1	-1.0927, 2	-1.7572, 2	-2.2484, 2	-1.5332, 2	3.0880, 2	1.7605, 3
.40	-1.5042, 0	-5.5636, 0	-1.4896, 1	-3.3528, 1	-6.5651, 1	-1.1062, 2	-1.4800, 2	-1.0453, 2	2.1517, 2	1.2490, 3	3.8505, 3
.42	-1.7007, 0	-6.2976, 0	-1.6731, 1	-3.6724, 1	-6.7977, 1	-1.0082, 2	-9.0994, 1	2.0764, 2	7.3761, 2	2.4363, 3	6.1266, 3
.44	-1.9017, 0	-7.0612, 0	-1.8511, 1	-3.9226, 1	-6.6891, 1	-7.9219, 1	-8.6908, -1	3.5704, 2	1.3793, 3	3.6887, 3	7.9344, 3
.46	-2.1096, 0	-7.8268, 0	-2.0201, 1	-4.0817, 1	-6.1600, 1	-4.3841, 1	1.2361, 2	6.8598, 2	2.0621, 3	4.7036, 3	8.3832, 3
.48	-2.3272, 0	-8.6267, 0	-2.1317, 1	-4.1264, 1	-5.1338, 1	6.4675, 0	3.5509, 2	1.0487, 3	2.6612, 3	5.0741, 3	6.3901, 3
.50	-2.5575, 0	-9.5268, 0	-2.2206, 1	-4.0322, 1	-3.5417, 1	7.2131, 1	4.6080, 2	1.4009, 3	3.0105, 3	4.3463, 3	1.1653, 3

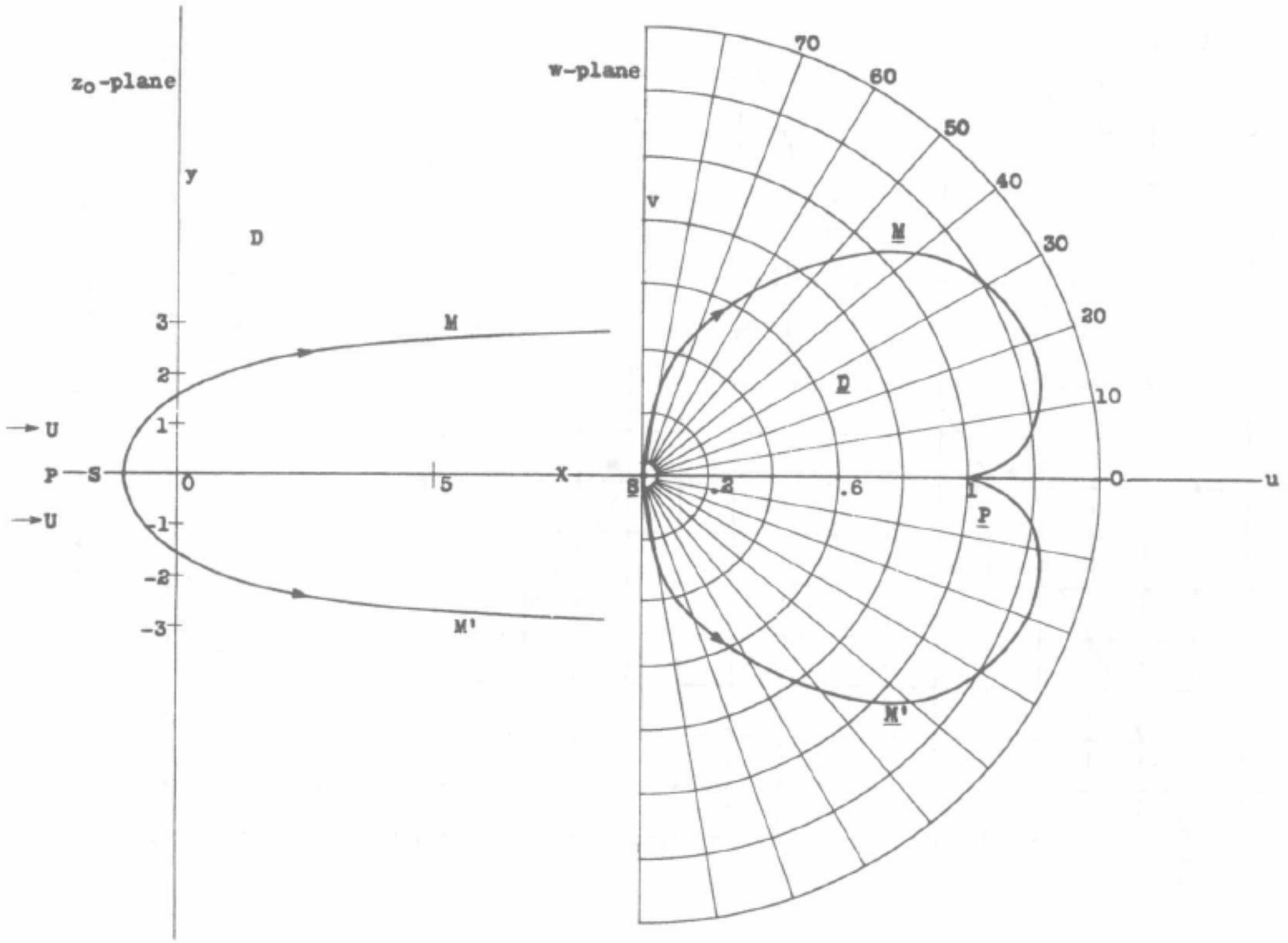

Figure 1.- The mapping of the whole plane D.

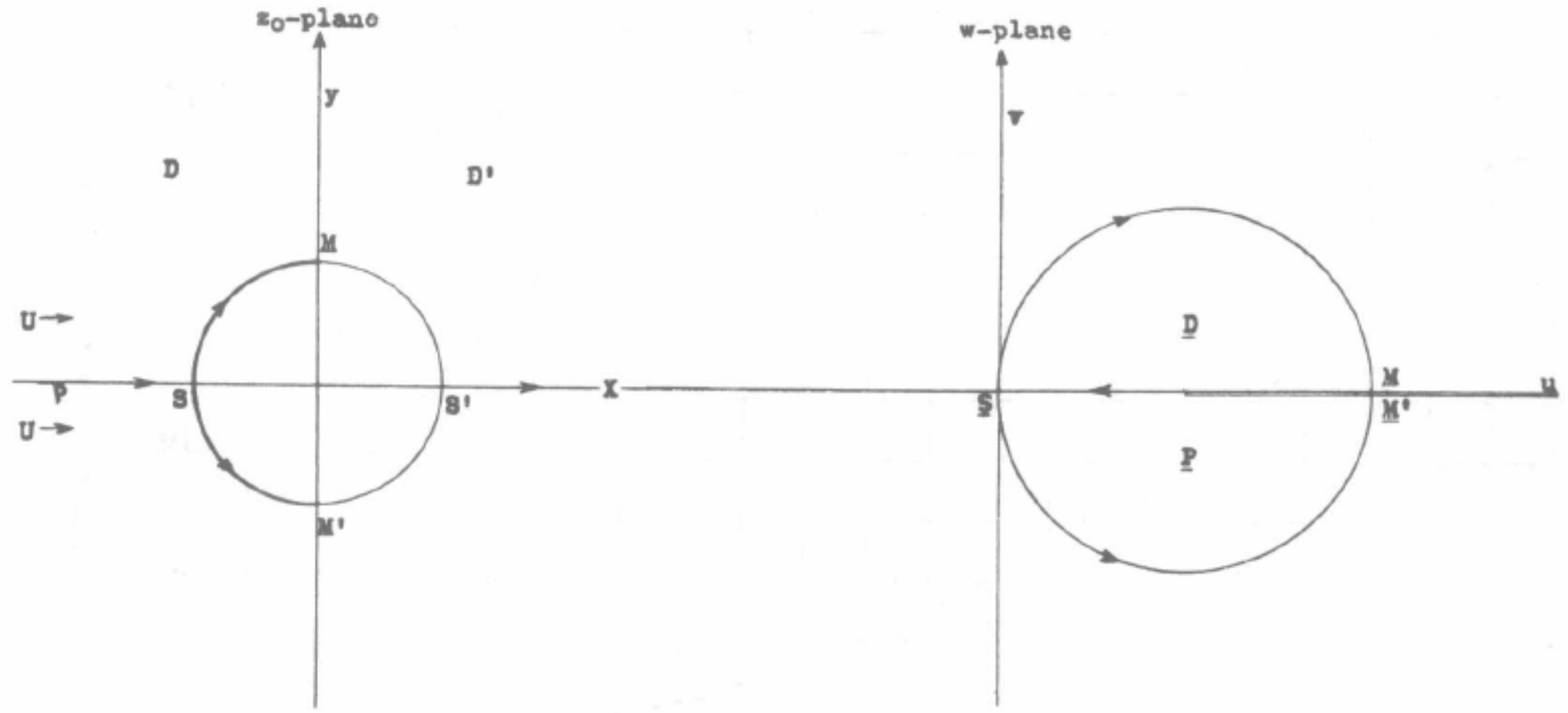

Figure 2.- The mapping of the half plane D.

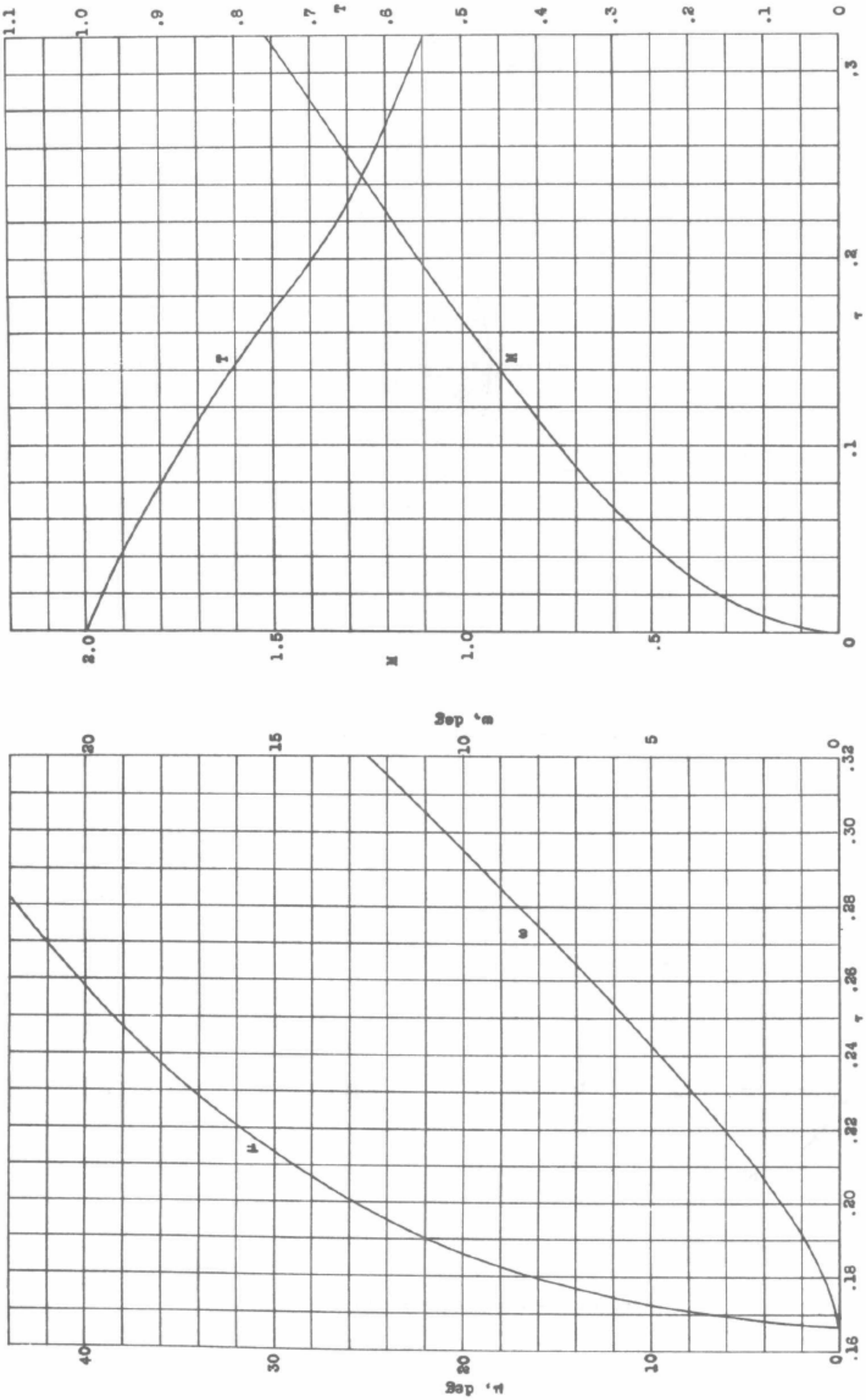

Figure 4.- T(τ); M(τ); γ = 1.405.

Figure 3.- w(τ); μ(τ); γ = 1.405.

NACA TN No. 995

Figs. 5,6

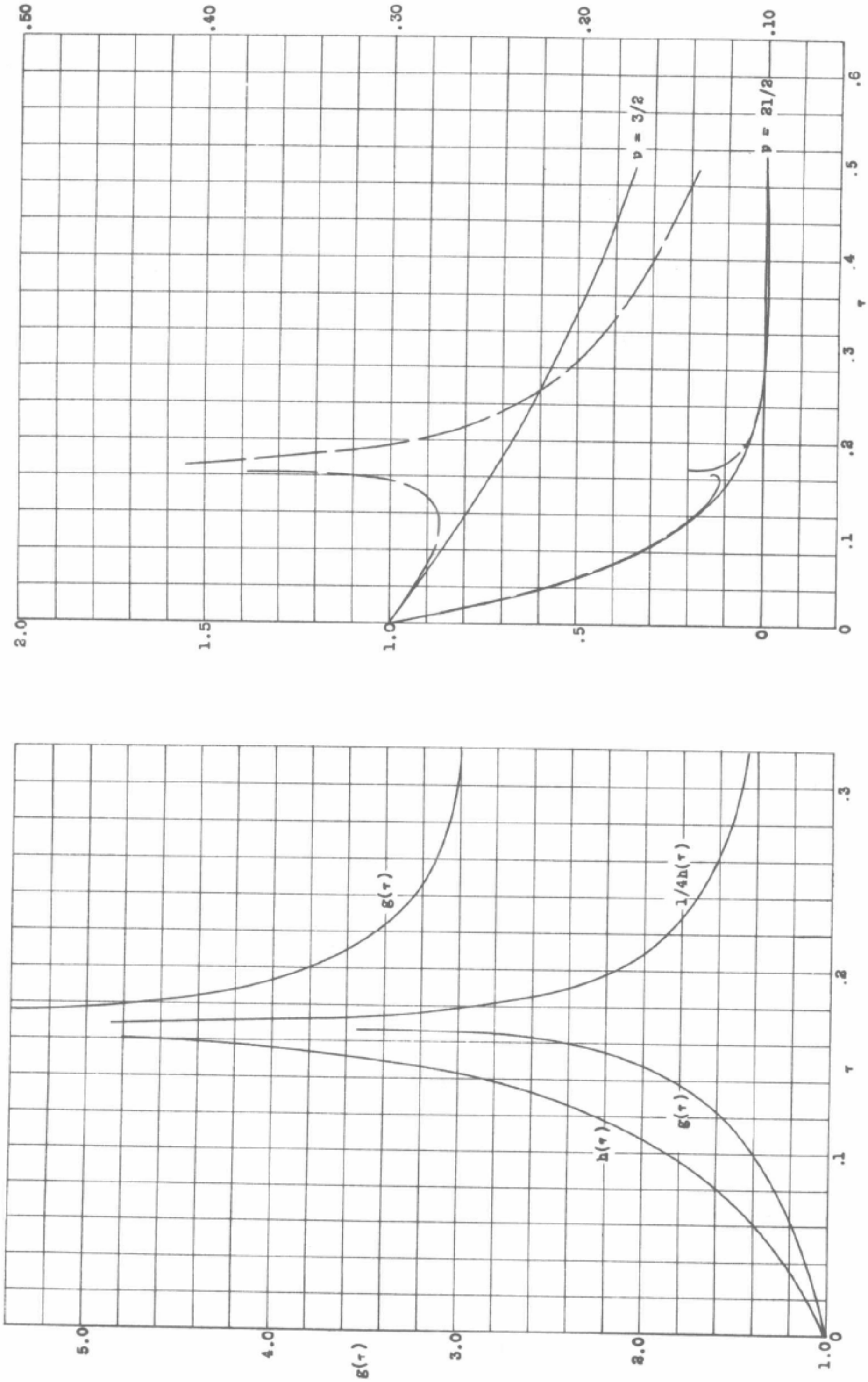

Figure 6.- $F_p(\tau)$; $\gamma = 1.405$. The dash line denotes the approximate values of $F_p(\tau)$.

Figure 5.- $g(\tau)$; $h(\tau)$; $\gamma = 1.405$.

NACA TN No. 995

Fige. 7,8

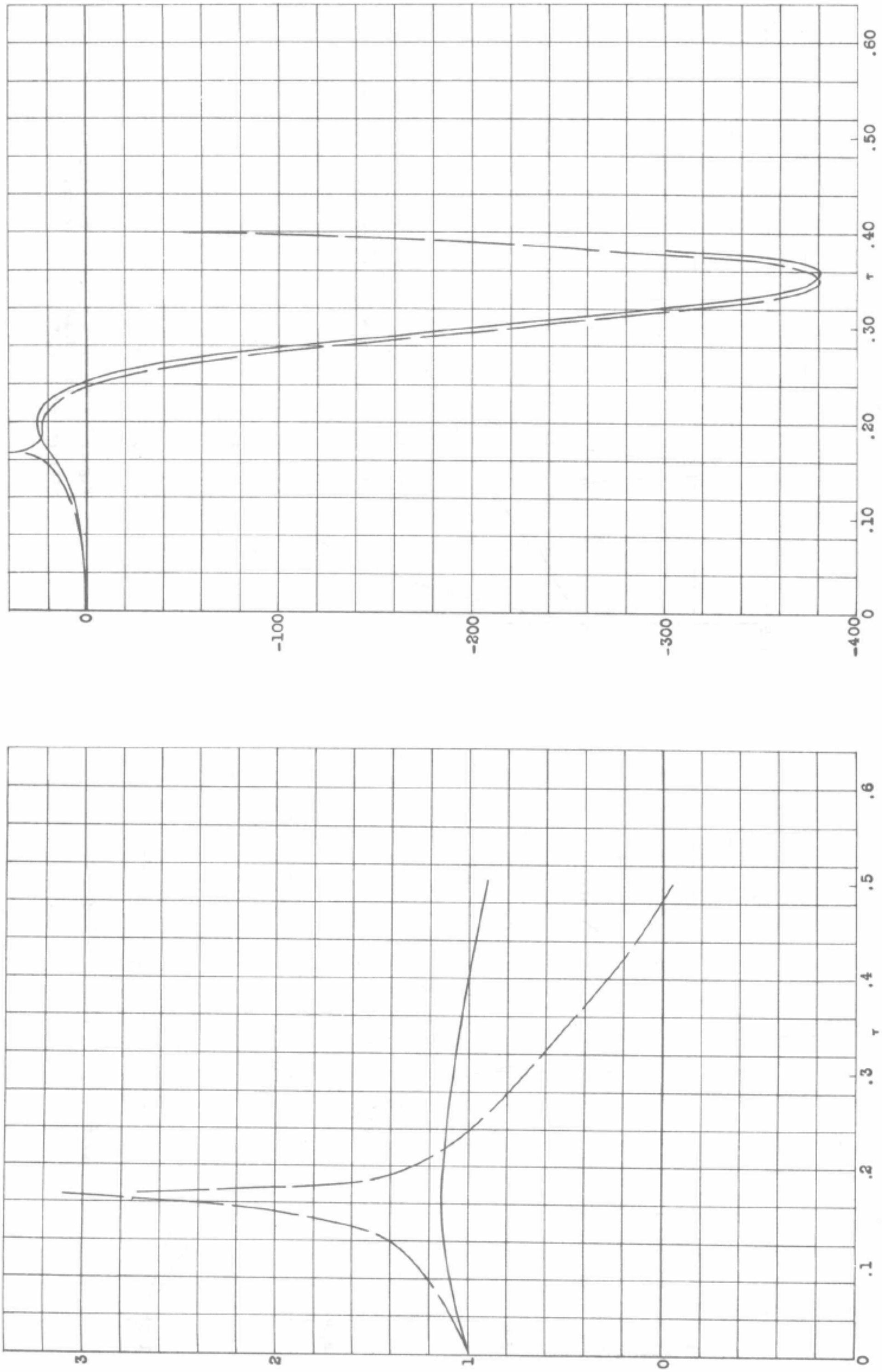

Figure 8.- $\underline{F}$ - 21/2(τ); γ = 1.405.

Figure 7.- $\underline{F}$ - 3/2(τ); γ = 1.405.

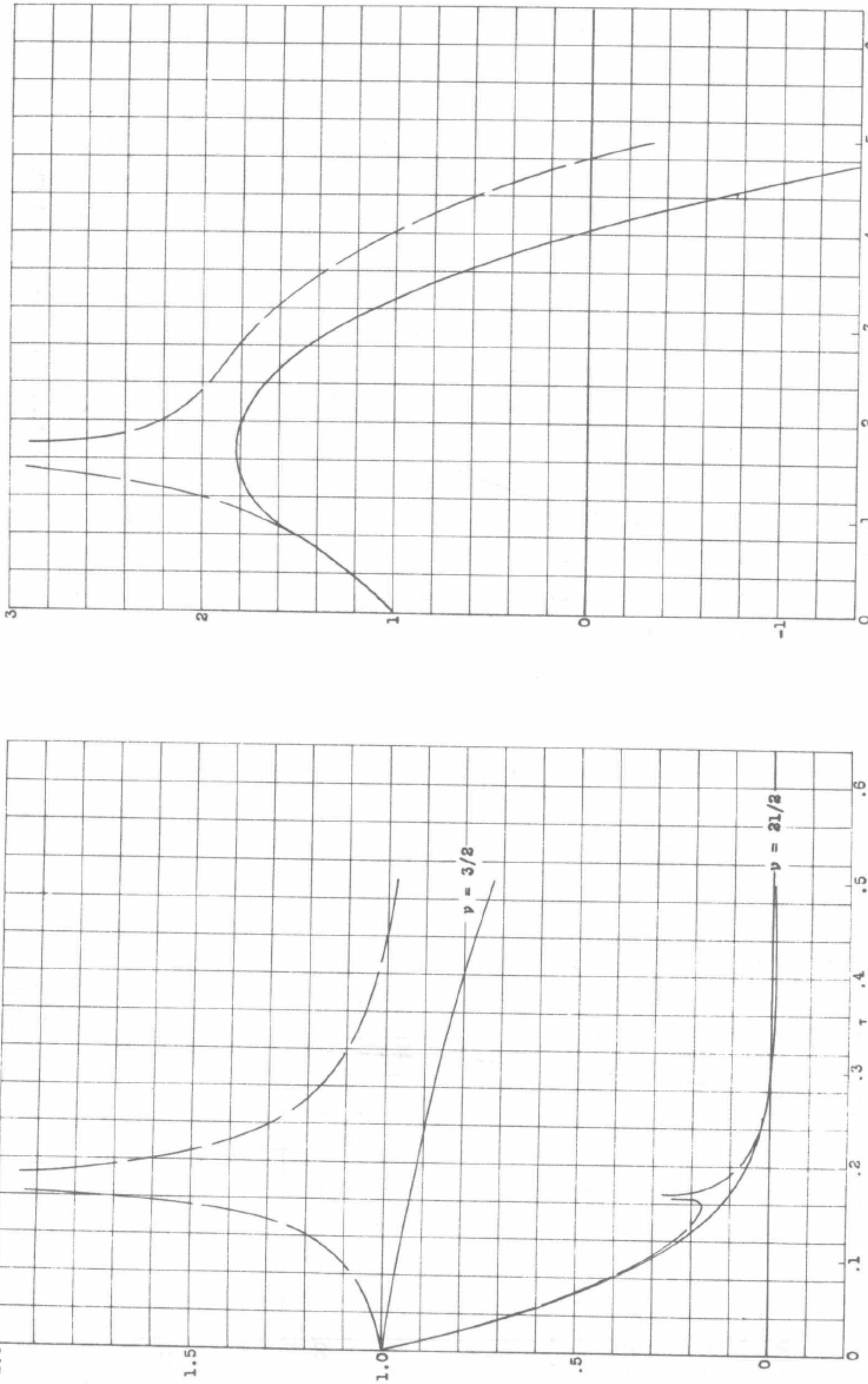

Figure 10.- $\bar{F} - 3/2(\tau)$; $\gamma = 1.405$.

Figure 9.- $\bar{F}_\nu(\tau)$; $\gamma = 1.405$.

NACA TN No. 995

Figs. 11,12

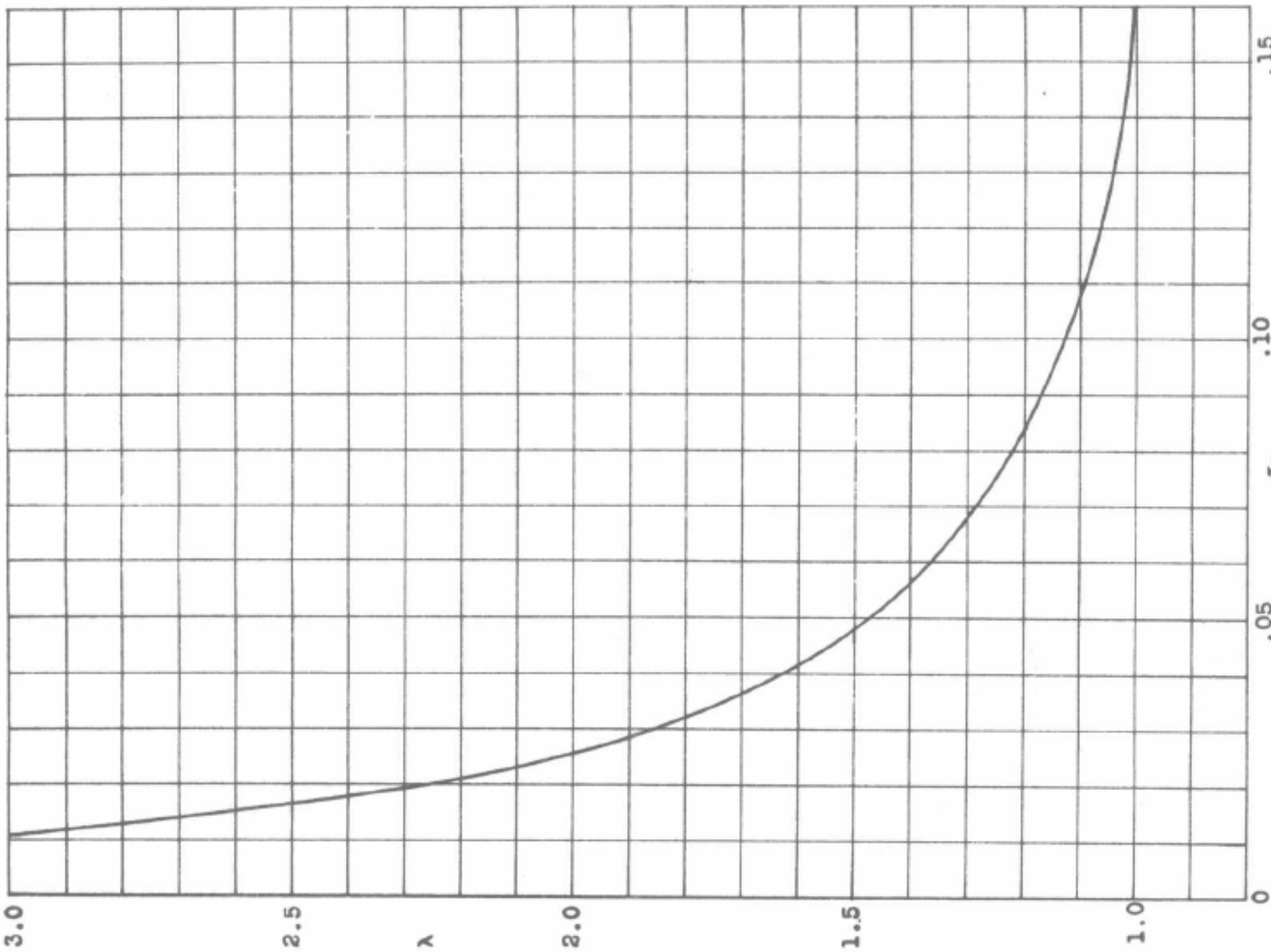

Figure 12.- $\lambda(\tau_1)$; $\gamma = 1.405$.

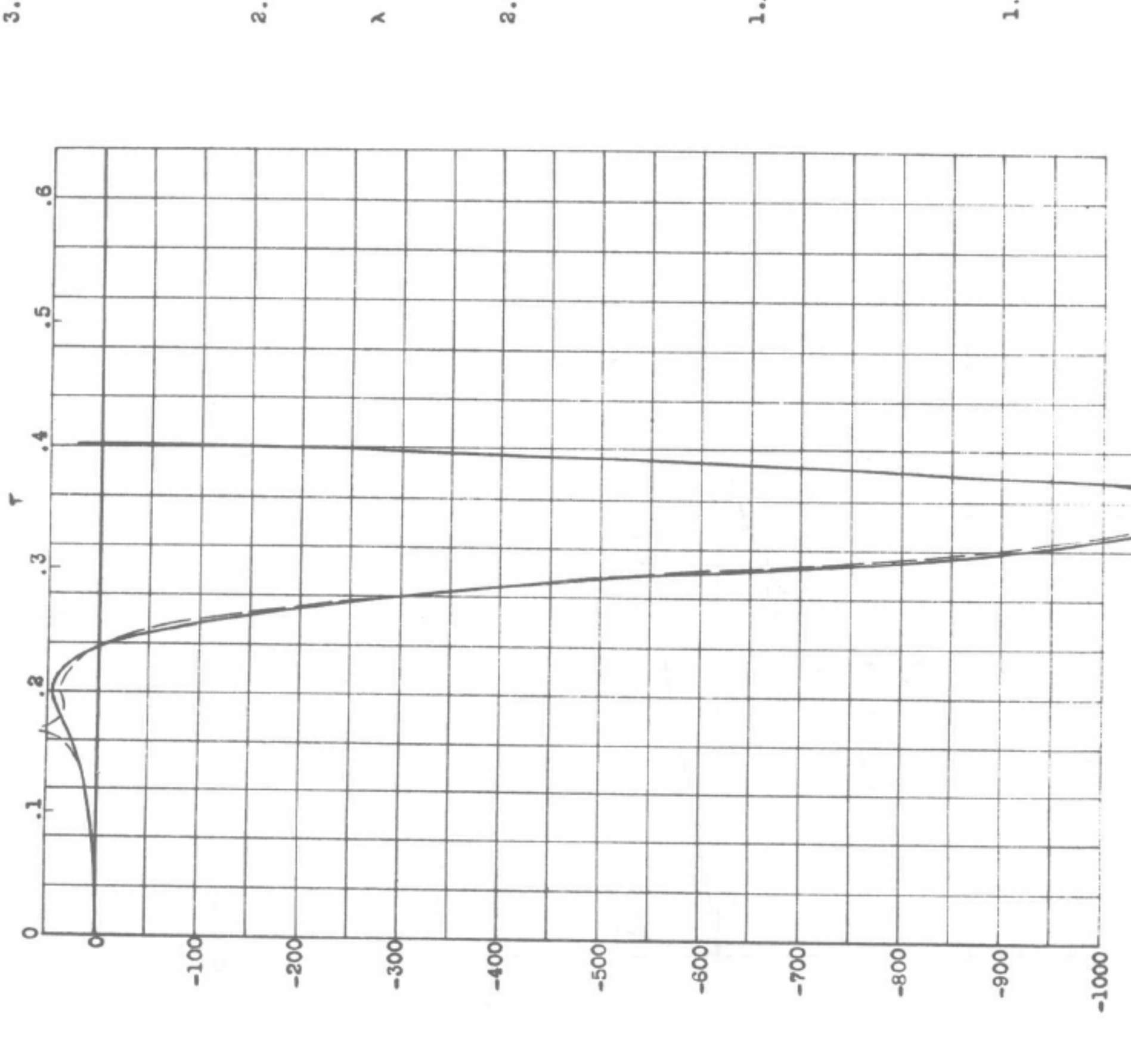

Figure 11.- $\overline{F} - 21/2(\tau)$; $\gamma = 1.405$.

NACA TN No. 995 Figs. 13,14

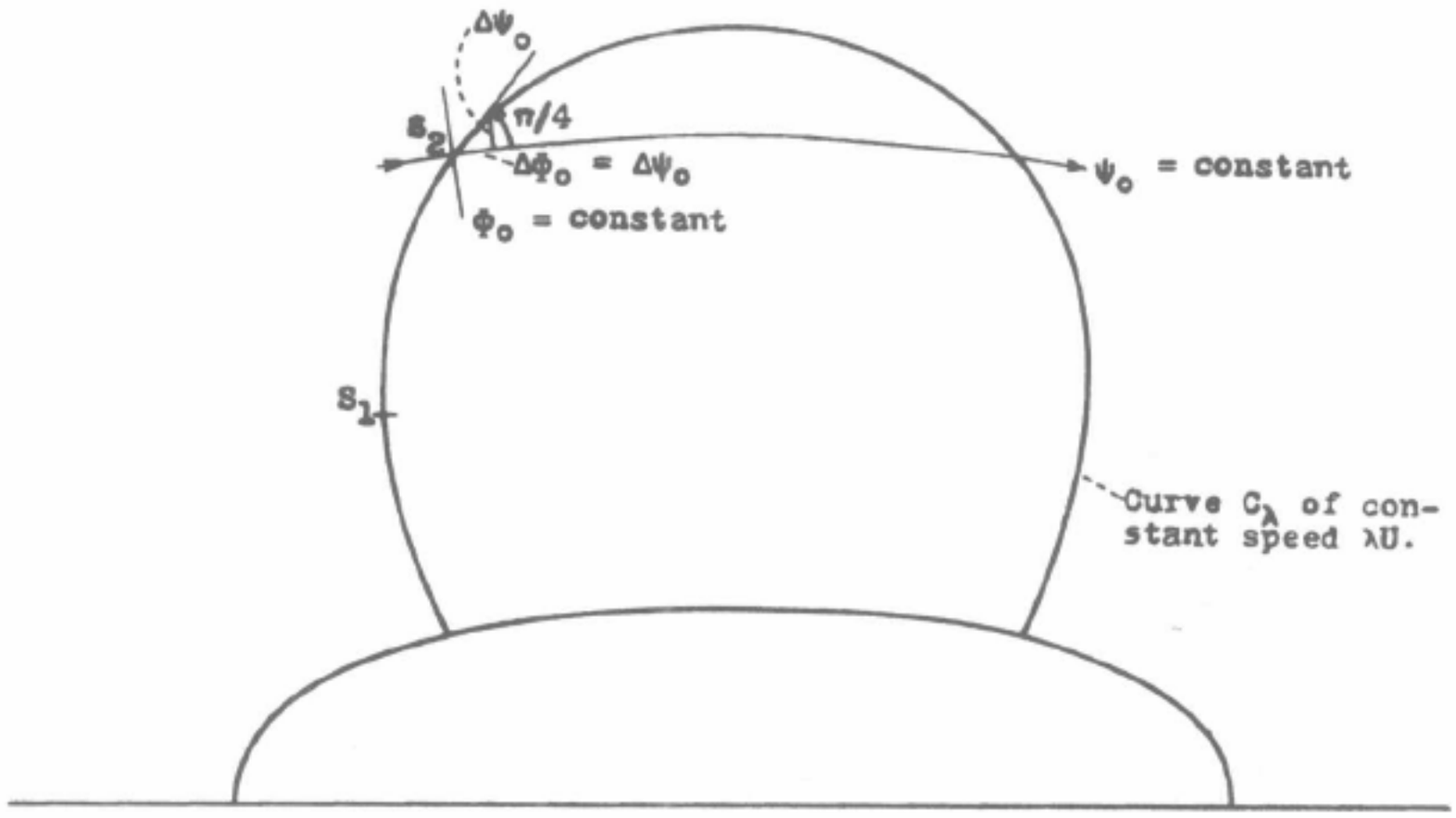

Figure 13.- Geometrical condition of eq. (20.5).

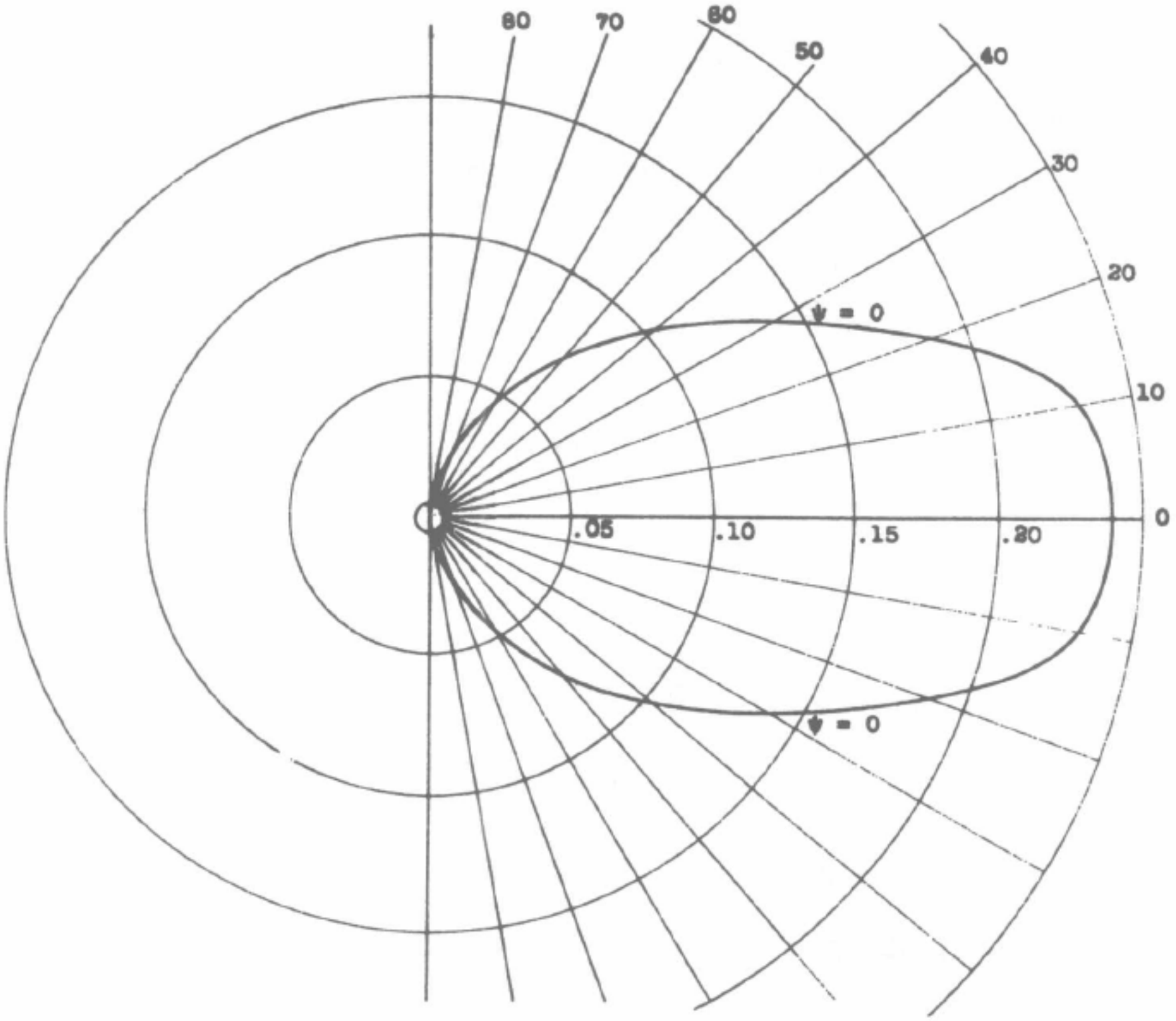

Figure 14.- The compressible flow in τ, θ-plane.
$\epsilon = 1/2$; $M_1 = 0.6$.

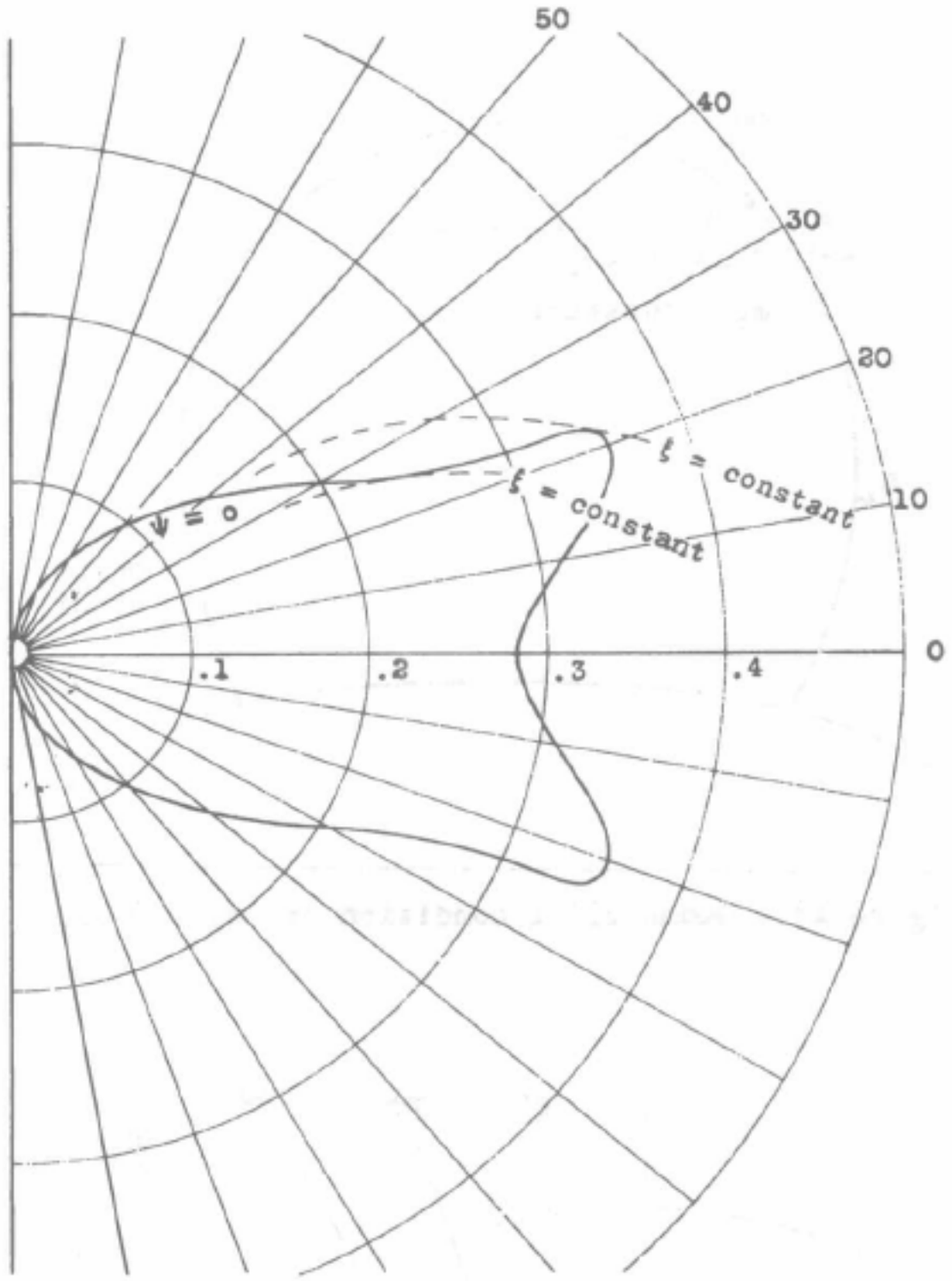

Figure 15.- The compressible flow in τ, θ-plane.
$\epsilon = 1/2$; $M = 0.7$.

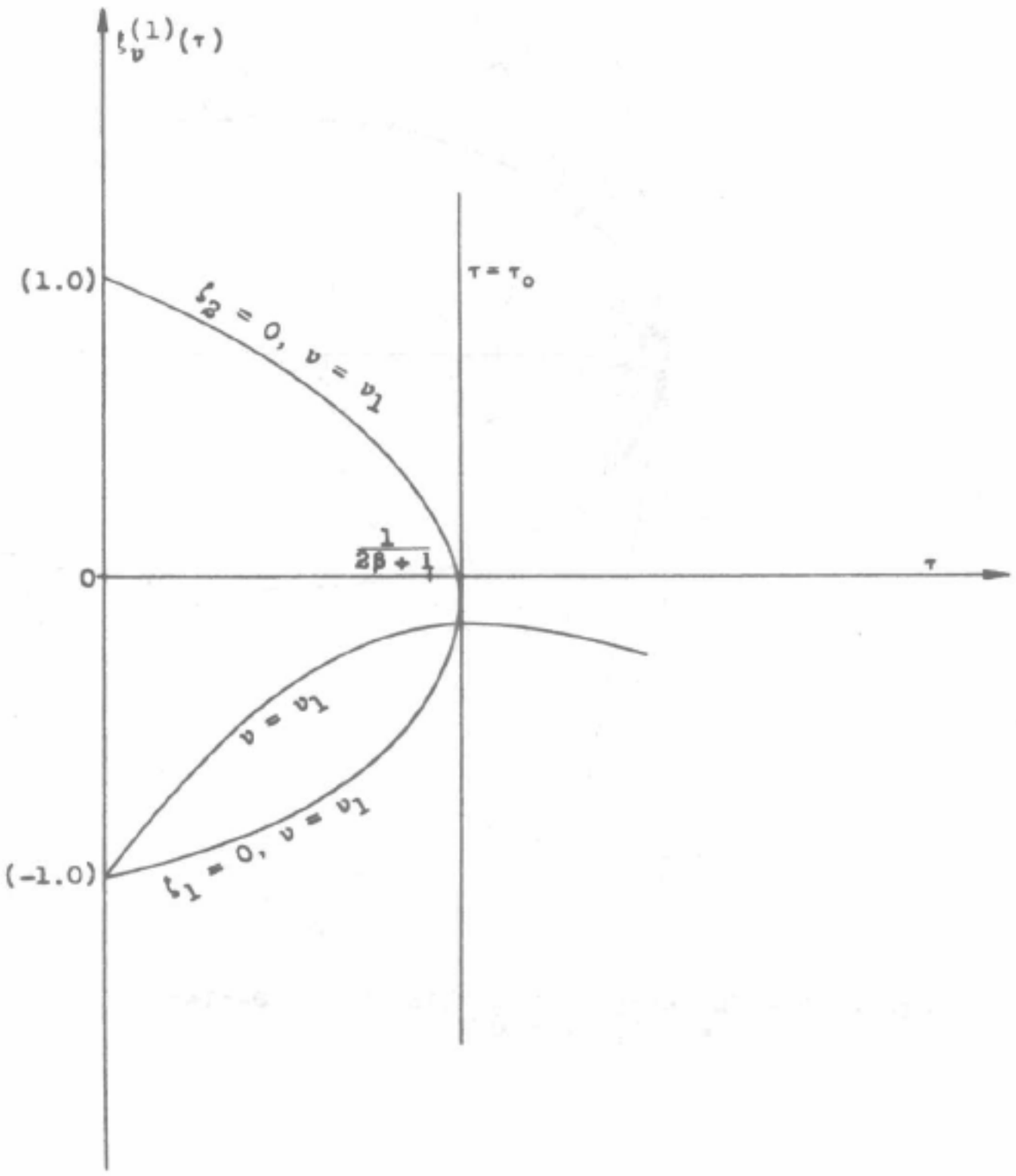

Figure 16.- The behavior of the integral-curve; $\zeta_v^{(1)}(\tau)$.

ON THE STABILITY OF TRANSONIC FLOWS [1]

BY

Y. H. KUO

It has been theoretically established that the potential flow of a compressible frictionless fluid can actually accelerate or decelerate smoothly through the sonic line in a transonic field as long as the limiting line is not present. The lack of experimental confirmation, however, leads some investigators to question the existence of such type of flows. A. Kantrowitz [3] and J. P. Brown [1] studied the one-dimensional channel flows. The most interesting result is that, when a disturbance characterized by a compression wave travels upstream in a decelerating field, it approaches a stationary state and the wave becomes a shock. The flow is then concluded to be unstable.

In the present paper, a two-dimensional motion is considered. For practical interest, the problem is restricted to a flow around a thin body and hence can be solved by iteration process. By expanding the potential function, taking the thickness ratio as a parameter, the successive approximations can be determined by solving a set of differential equations subject to the prescribed boundary conditions. The equation for the zero-order term is non-linear. Those for higher order terms are all linear but inhomogeneous.

As a disturbance, a special motion has been assumed. It can be shown that, in the case of a plane wave, if the characteristic curve on which both the disturbance potential and its partial derivatives vanish is chosen as a new variable, there exists a simple exact solution. This gives a velocity that at any moment is a linear function of the coordinate x, say. This solution can therefore be used to define a triangular velocity-wave form, which terminates in a discontinuity at a definite maximum velocity to be determined later. The advantage of such a wave is that it is, from the very beginning, discontinuous. Therefore, the singularity encountered by B. Riemann in his study of propagation of plane wave of finite amplitude can never appear. By tracing the history of the wave form during its propagation upstream, it has been found that the slope of the velocity at the tail of the wave decreases with time and approaches zero as time becomes infinite. The velocity of the wave-head also decreases with time but remains always finite. It is clear that once this wave is introduced, it will disappear from the field after a sufficient length of time.

As for the first approximation where the equation involves functions depending upon the shape of the boundary, the body has to be specified. For its simplicity, a slightly curved wavy surface is chosen. In this case when the free-stream Mach number is 0.9 with a thickness about four percent of the wave-length, supersonic regions are locally established at the crests of the surface, as was found by H. Görtler [2]. The mathematical problem is to solve an inhomogeneous partial differential equation subject to the given boundary conditions. By superposition, a solution can thus be constructed. When the velocity of the disturb-

1) Published in *Proceedings of Symposia in Applied Mathematics*, 1949, 1: 72~73

ance-flow is determined, the Rankine-Hugoniot relations can be applied at the wave-head to give a shock-velocity. Since the shock is curved, the strength is restricted to be very weak so that the change of entropy can be neglected. For physical interest, the history of this wave is again traced and the deformation of the triangular wave, due to the presence of the body, is also evaluated.

Bibliography

1. J. P. Brown, *The stability of compressible flows and transition through the speed of sound*, AAF Technical Report 5410.

2. H. Görtler, *Gasströmungen mit Übergang von Unterschall-zu Überschallgeschwindigkeiten*, Zeitschrift für Angewandte Mathematic und Mechanik vol. 20 (1940) pp. 254–262.

3. A. Kantrowitz, *The formation and stability of normal shock waves in channel flows*, NACA Technical Note 1225.

Cornell University,
Ithaca, N. Y.

THE PROPAGATION OF A SPHERICAL OR A CYLINDRICAL WAVE OF FINITE AMPLITUDE AND THE PRODUCTION OF SHOCK WAVES* [1)]

BY

YUNG-HUAI KUO

California Institute of Technology

1. Introduction. When a mass of gas is set into motion by a sudden rise of pressure which possesses either a cylindrical symmetry or a spherical symmetry in the case of an explosion, pressure or density will be propagated into space as a cylindrical or spherical wave of finite amplitude in a manner different from that of the propagation of sound. The most conspicuous phenomenon of such a non-linear wave motion is perhaps the appearance of a shock wave. In the case of plane waves of finite amplitude, the problem was studied independently by B. Riemann[1] and S. Earnshaw.[2] It was shown that when a compressed slab of gas is released, two progressive waves are produced travelling in opposite directions, with constant deformation in the waveform during the course of the propagation. Eventually both waves develop into shock waves.

With regard to the spherical or cylindrical compression waves, the situation is quite different because the amplitude of the wave falls off at a much greater rate than for plane waves, while the wave propagates from the center of disturbances. The question is whether this rapid diminution of amplitude would prevent the formation of a shock. J. J. Unwin[3] has calculated a specific example of motion produced by a sudden release of a compressed sphere of air, and concluded that there is no indication of the development of a shock wave. Inasmuch as he adopted a numerical method for one special case, the concludion reached cannot be regarded as general. In fact, W. Hantzsche and H. Wendt[4] considered a similar problem, where the sphere had a finite radius and expanded with the speed of sound into still air. The motion, in its early stage, is supposed to be continuous in pressure or density and velocity. But after a finite duration, the wave-front becomes a discontinuity surface characterized by an infinite velocity gradient in spite of the diminution of amplitude.

In view of these disagreeing results, it is felt that it is desirable to investigate this problem from a broad standpoint taking account of all initial boundary conditions. The problem of explosion such as the burst of a bomb is only one of many similar problems and, to be sure, the most interesting one. According to G. I. Taylor, the physical process taking place during an explosion can be treated, as a combination of two problems. The first problem is concerned with the effects produced in the atmos-

* Received May 15, 1946.

[1] Riemann, B., *Über die Fortpflanzung ebener Luftwellen von endlicher Schwingungsweite*, Abhandlungen d. Gesellschaft der Wissenschaften zu Göttingen, Math.-Phys. Klase **8,** 43 (1860).

[2] Earnshaw, S., *On the mathematical theory of sound*, Phil. Trans. Roy. Soc. London, **150,** 133 (1860).

[3] Unwin, J. J., *The production of waves by a sudden release of a spherical distribution of compressed air in the atmosphere*. Proc. Roy. Soc. (A) **178,** 153 (1941).

[4] Hantzche, W. and Wendt, H., *Zum Verdichtungsstoss bei Zylinder- und Kugelwellen*, Jahrbuch 1940 der deutschen Luftfahrtforschung I, 536.

1) Published in *Quarterly of Applied Mathematics*, 1947, 4(4): 349~360

phere by a rapidly expanding spherical or cylindrical solid shell which compresses the surrounding air. In this case the motion of air in contact with the shell is completely prescribed by the motion of shell itself. The second problem deals with the motion produced by a compressed sphere or cylinder of air which is suddenly released. Each one of these constitutes a separate mathematical problem. To enlarge the scope of this discussion, the very meaning of the term explosion will be understood here as any process that is capable to create a pressure disturbance with spherical or cylindrical symmetry, propagating as a wave of finite amplitude.

An explosion is assumed to take place, during a short interval of time, in an infinite space which is filled only with air not abstructed by any solid bodies. Since the coefficients of viscosity and heat conduction for gases are generally very small, so long as the motion is continuous, the air may be regarded as non-viscous and non-conducting. The thermodynamic change of state of a fluid-particle along the path is then adiabatic; and if, initially, the entropy of the air is uniform throughout the space, the motion is isentropic. For the first problem stated above this condition is satisfied. Namely, at the moment the shell starts to expand, the outside air may certainly be assumed to be at the standard conditions. After the shell has started to expand, it compresses the air and, thereby, sets it into motion; but, during this process, no heat has been imparted to the air, its thermodynamic state must remain on the same adiabatic curve. In the case of a compressed sphere or cylinder of air, it is reasonable to assume that the pressure or density was built under adiabatic compression at all points. Hence as long as the motion is continuous, it will be isentropic.

The present study reveals that such a continuous and isentropic motion generally does not exist in the whole field. This type of motion breaks down when a "limiting line" appears, which would make the solution multi-valued. This would be impossible unless the motion is discontinuous. Hence, the appearance of a "limiting line" serves to indicate the necessity of presence of a shock wave in the actual motion. After the shock is formed, the Rankine-Hugoniot theory asserts that the process through which a fluid-particle has undergone by crossing the shock-front is irreversible and, consequently, the entropy increases in a discontinuous manner. The jump in entropy is not constant, however. It varies as the shock wave propagates, because the conditions at the shock change with time. As a result the motion behind such a non-uniform shock cannot be isentropic. Therefore once the "limiting line" appears, isentropic flow cannot be maintained and the resultant flow cannot be analyzed by the present method.

The mathematical condition for the appearance of a "limiting line" in the case of a spherical or cylindrical isentropic motion is that one of the two families of characteristics admits an envelope, just as in the case of a plane wave. Along this envelope the accelerations of the fluid-particles are infinite. In fact, a closer examination indicates that the motion generally must break down even before the "limiting line" is reached. It then seems that any motion of a compressible fluid has a tendency to develop a shock wave and that the effect of the "spreading" in the case of a non-linear spherical or cylindrical wave plays but a minor role.

2. Differential equations of motion. The motion under consideration is supposed to be axially or spherically symmetric, i.e., at any instant the velocity u, pressure p and density ρ depend on the time and the radial distance x only. If the effects of viscosity and of body force are neglected, the equations governing the motion are

$$u_t + uu_x + \frac{p_x}{\rho} = 0, \tag{2.1}$$

$$\rho_t + u\rho_x + \rho\left(u_x + \frac{\alpha u}{x}\right) = 0. \tag{2.2}$$

Here the subscripts denote the partial derivatives with respect to the variable indicated by the subscript; $\alpha = 1$ for a cylindrical and $\alpha = 2$ for a spherical wave. In each case, the variable x will be interpreted differently. Furthermore, it is assumed that the motion is continuous and that the effects of viscosity and heat-transfer in the fluid can be ignored. If initially constant, throughout the fluid, the entropy then remains constant. In other words, for an ideal gas the relation between the pressure and density is

$$p = K\rho^\gamma, \tag{2.3}$$

where γ stands for the ratio of the specific heats and K is a constant. With a set of appropriate initial conditions the mathematical problem can then be solved, at least theoretically. However, we may understand the singular behavior of such a solution and the conditions for its existence without actually solving the differential equations.

By eliminating the pressure with the aid of Eq. (2.3) and by introducing the square of the sonic speed as a variable in the place of the density, we reduce Eqs. (2.1) and (2.2) to

$$u_t + uu_x + v_x = 0, \tag{2.4}$$

$$v_t + uv_x + \beta v\left(u_x + \frac{\alpha u}{x}\right) = 0, \tag{2.5}$$

where

$$\beta v = c^2, \qquad \beta = \gamma - 1,$$

and c is the speed of sound defined by $\sqrt{\gamma(p/\rho)}$. This system of differential equations is of the hyperbolic type, the two families of real characteristics C being determined by

$$(dx - udt)^2 - \beta v dt^2 = 0, \tag{2.6}$$

where v is positive.

As it stands, this system of equations can reveal but little information concerning the behavior of the solution. To expose such properties, one has to transform the differential equations to a new coordinate-system and then study the condition under which the transformation would be valid. In the case of a steady irrotational motion, this is well-known as the hodograph method which has been effectively and successfully applied by W. Tollmien[5] and H. S. Tsien[6] in investigating the two dimensional and three dimensional isentropic motion respectively. By a slight modification, it can also be applied to the present problem. To this end, the following one-one point-transformation is introduced

[5] Tollmien, W., *Grenzlinien adiabatischer Potentialströmungen*, Z. angew. Math. Mech. **21,** 140 (1941).

[6] Tsien, H. S., *The "limiting line" in mixed subsonic and supersonic flows of compressible fluids*, N.A.C.A. Tech. Note 961 (1945).

$$u = u(t, x), \qquad v = v(t, x). \tag{2.7}$$

We have

$$u_t = \frac{x_v}{J}, \qquad u_x = -\frac{t_v}{J},$$

$$v_t = -\frac{x_u}{J}, \qquad v_x = \frac{t_u}{J},$$

provided the Jacobian $J(u, v) \equiv t_u x_v - t_v x_u \neq 0$. Equations (2.4) and (2.5) will then be transformed into

$$x_v - u t_v + t_u = 0, \tag{2.8}$$

$$x_u - u t_u + \beta v t_v - \frac{\alpha\beta uv}{x}(t_u x_v - t_v x_u) = 0. \tag{2.9}$$

This system of equations can be simplified considerably by introducing a function $\chi(u, v)$ defined by

$$x - ut = \chi_u, \qquad t = -\chi_v, \tag{2.10}$$

so that Eq. (2.8) is satisfied identically while Eq. (2.9) reduces to

$$\chi_{uu} - \beta v \chi_{vv} - \frac{\alpha\beta uv}{x}(\chi_{uu}\chi_{vv} - \chi_{uv}^2 - \chi_v \chi_{vv}) = \chi_v. \tag{2.11}$$

The corresponding characteristics Γ in the u, v-plane are determined by

$$\left(1 - \frac{\alpha\beta uv}{x}\chi_{vv}\right) dv^2 - \frac{2\alpha\beta uv}{x}\chi_{uv} du dv - \alpha\beta uv\left(\frac{1}{\alpha u} + \frac{\chi_{uu} - \chi_v}{x}\right) du^2 = 0. \tag{2.12}$$

3. Limiting line. The relationship between the characteristics C and Γ associated respectively with the differential equation in the t, x- and u, v-planes has an important bearing on the singular character of the solution and its elucidation often contributes much toward the understanding of the nature of the physical problem. For this purpose, we first transform the differential equation (2.6) by means of the following pair of relations:

$$dx = (\chi_{uu} - \chi_v - u\chi_{uv})du + (\chi_{uv} - u\chi_{vv})dv,$$
$$dt = -\chi_{uv} du - \chi_{vv} dv.$$

Substituting in Eq. (2.6) together with Eq. (2.11), we bring the equation of the characteristics C into the form

$$J\left[\left(1 - \frac{\alpha\beta uv}{x}\chi_{vv}\right) dv^2 - \frac{2\alpha\beta uv}{x}\chi_{uv} du dv - \alpha\beta uv\left(\frac{1}{\alpha u} + \frac{\chi_{uu} - \chi_v}{x}\right) du^2\right] = 0. \tag{3.1}$$

This shows that if $J \neq 0$, the characteristics C in the t, x-plane correspond to the characteristics Γ in the u, v-plane. However, circumstances may arise such that

$$J(u, v) \equiv \chi_{uu}\chi_{vv} - \chi_{uv}^2 - \chi_v \chi_{vv} = 0, \tag{3.2}$$

while

$$\left(1 - \frac{\alpha\beta uv}{x}\chi_{vv}\right)dv^2 - \frac{2\alpha\beta uv}{x}\chi_{uv}dudv - \alpha\beta uv\left(\frac{1}{\alpha u} + \frac{\chi_{uu} - \chi_v}{x}\right)du^2 \neq 0$$

and the characteristic equation (2.6) is again satisfied. This means that if a point moves along a line λ defined by Eq. (3.2), the corresponding point will describe a line l in the t, x-plane, having the same tantents as the characteristics C. It does not coincide, however, with any one of the characteristics C. This may be proved as follows.

The differential equation for the path s of a fluid-particle in the t, x-plane is

$$\left(\frac{dx}{dt}\right)_s = u. \tag{3.3}$$

The corresponding path σ in the u, v-plane is given by

$$\left(\frac{dv}{du}\right)_\sigma = -\frac{\chi_{uu} - \chi_v}{\chi_{uv}}. \tag{3.4}$$

Now the differential equation for one family of characteristics, say Γ_+, is

$$\left(\frac{dv}{du}\right)_{\Gamma_+} = -\frac{\chi_{uu} - \chi_v + \sqrt{\beta v}\,\chi_{uv}}{\chi_{uv} + \sqrt{\beta v}\,\chi_{vv}}. \tag{3.5}$$

On the other hand, the vanishing of the Jacobian, when combined with Eq. (2.11), can be written as

$$(\chi_{uv} - \sqrt{\beta v}\,\chi_{vv})(\chi_{uv} + \sqrt{\beta v}\,\chi_{vv}) = 0. \tag{3.6}$$

It is easy to see that

$$\left(\frac{dv}{du}\right)_\sigma = \left(\frac{dv}{du}\right)_{\Gamma_+}, \quad \text{if} \quad \chi_{uv} = \sqrt{\beta v}\,\chi_{vv} \tag{3.7}$$

or

$$\left(\frac{dv}{du}\right)_\sigma = \left(\frac{dv}{du}\right)_{\Gamma_-}, \quad \text{if} \quad \chi_{uv} = -\sqrt{\beta v}\,\chi_{vv}. \tag{3.8}$$

The condition under which this result holds is both necessary and sufficient. This shows that the lines λ_+ and λ_- are respectively the locus of the points of tangency of the path σ with Γ_+ and σ with Γ_-. Furthermore, the paths σ do not have an envelope and that of Γ is

$$\beta v = 0$$

which corresponds to $\rho = 0$ and is, of course, uninteresting. Hence, it cannot belong to either family of the characteristics Γ. The only alternative is that it is an envelope of one family of the characteristics C in the t, x-plane. By analogy with the steady irrotational motion it is again called "limiting line," the justification will be found in the following section.

4. The properties of the "limiting line." Being the envelope of one family of real

characteristics in the t, x-plane, the "limiting line" will be entirely in the field of motion. It is, therefore, paramount to investigate the behavior of the solution along this line.

Consider first the line element of a path s of a fluid-particle at the "limiting line" l. Generally, for any line element one obtains from Eq. (2.10)

$$dx = (\chi_{uu} - u\chi_{uv} - \chi_v)du + (\chi_{uv} - u\chi_{vv})dv,$$
$$dt = -\chi_{uv}du - \chi_{vv}dv.$$

Along a path s given by $dx/dt = u$, we have

$$(\chi_{uu} - \chi_v)du + \chi_{uv}dv = 0.$$

Using this relation to eliminate dv from dx and dt and by regarding u as a parameter, we obtain the following parametric equations for the path s:

$$dx = u\,\frac{\chi_{uu}\chi_{vv} - \chi_{uv}^2 - \chi_v\chi_{vv}}{\chi_{uv}}\,du, \tag{4.1}$$

$$dt = \frac{\chi_{uu}\chi_{vv} - \chi_{uv}^2 - \chi_v\chi_{vv}}{\chi_{uv}}\,du. \tag{4.2}$$

According to our previous findings, $J=0$ yields two lines λ_+ and λ_-, each of which associates with only one group of characteristics Γ in the u, v-plane. This shows that on the "limiting line" dx and dt both become differentials of higher order and will change sign on crossing the line λ. This agrees, of course, with the cuspidal nature of the singularity.

Dividing both sides by dx and dt respectively, we obtain the following expressions for the derivatives u_x and u_t along s:

$$(u_x)_s = \frac{\chi_{uv}}{u(\chi_{uu}\chi_{vv} - \chi_{uv}^2 - \chi_v\chi_{vv})}, \tag{4.3}$$

$$(u_t)_s = \frac{\chi_{uv}}{\chi_{uu}\chi_{vv} - \chi_{uv}^2 - \chi_v\chi_{vv}}. \tag{4.4}$$

Thus on the "limiting line" the acceleration of a fluid-particle becomes infinite as χ_{uv} is finite there. This implies also an infinite pressure gradient [see Eq. (2.1)].

The physical state to which $J(u, v)=0$ corresponds can be readily deduced. It can be summarized in the statement that if the Jacobian vanishes, then the motion in the immediate neighborhood of the line $J=0$ is a compressive one. To prove this, let us consider the ratios v_t/u_x, u_t/v_x, u_t/u_x and v_t/v_x which, according to the relations obtined in Section 2, equal

$$\frac{v_t}{u_x} = -\beta v - u\frac{\chi_{uv}}{\chi_{vv}} - \frac{\alpha\beta uv}{x}\cdot\frac{J}{\chi_{vv}}, \qquad \frac{u_t}{u_x} = -u + \frac{\chi_{uv}}{\chi_{vv}},$$

$$\frac{u_t}{v_x} = u\,\frac{\chi_{vv}}{\chi_{uv}} - 1, \qquad \frac{v_t}{v_x} = -u + \beta v\,\frac{\chi_{vv}}{\chi_{uv}} + \frac{\alpha\beta uv}{x}\,\frac{J}{\chi_{uv}}.$$

In the u, v-plane, the expressions on the right-hand side are everywhere continuous. At the line λ_+ corresponding to $\chi_{uv} = \sqrt{\beta v}\chi_{vv}$, they become

$$\frac{v_t}{u_x} = -c^2\left(1-\frac{u}{c}\right) < 0, \qquad \frac{u_t}{u_x} = c\left(1-\frac{u}{c}\right) > 0,$$

$$\frac{u_t}{v_x} = -\left(1-\frac{u}{c}\right) < 0, \qquad \frac{v_t}{v_x} = c\left(1-\frac{u}{c}\right) > 0.$$

By continuity, the relative signs of the differential quotients hold in the neighborhood of the "limiting line." Thus, we conclude that either $v_t>0$, $v_x>0$ and $u_t<0$, $u_x<0$ or $v_t<0$, $v_x<0$ and $u_t>0$, $u_x>0$. The first case is exactly the condition for a compressive motion. Whereas the second case may either correspond to a rarefaction or to a change of sign of the Jacobian $J(u, v)$. As the rarefaction does not conform to the geometric properties of $J=0$, the second case corresponds to the second branch of the solution and hence can be disregarded.

5. Lost solution. In the previous sections, we assume that the Jacobian $J(u, v)$ does not vanish. Thus the one-to-one correspondence between the t, x- and u, v-planes is assured and the condition $J=0$ is restricted to the singular line l. In a special case the Jacobian may vanish identically, however. This vanishing of the Jacobian establishes a relation between v and u in the u, v-plane and, as a result, yields a class of solution not contained in the transformation (2.7). To study this form of solution, let us first set

$$v = v(u). \tag{5.1}$$

The differential equations (2.4) and (2.5) can then be rewritten as

$$u_t + \left(u + \frac{dv}{du}\right)u_x = 0, \tag{5.2}$$

$$u_t\frac{dv}{du} + \left(u\frac{dv}{du} + \beta v\right)u_x = -\frac{\alpha\beta uv}{x} \tag{5.3}$$

This type of solution has been discussed by K. Bechert[7] whose main result was as follows. By eliminating x and t the system of Eqs. (5.2) and (5.3) can be reduced to a second order non-linear total differential equation, based on the existence of a linear relation between t and x. By a slightly different procedure it can be shown that instead of a second order differential equation one can obtain a first order one of Abel's type being amenable to numerical integration. The main feature of the solution, however, can be discussed in the following manner.

Along $u=$const., i.e., along

$$du = u_x dx + u_t dt = 0,$$

the slope of the curve $u=$const. equals

$$\left(\frac{dx}{dt}\right)_u = -\frac{u_t}{u_x} = u + \frac{dv}{du}, \tag{5.4}$$

on account of Eq. (5.2). Since dv/du is a function of u alone, on $u=$const. $(dv/du)_u$ is

[7] Bechert, K., *Über die Ausbreitung von Zylinder- und Kugelwellen in reibungsfreien Gasen und Flüssigkeiten*, Ann. Phys. (5) **39**, 169 (1941).

constant. Therefore, the curve $u=$const. is a straight line in the t, x-plane. In conformity to the assumption (5.1), there exists a parameter ξ defined by

$$\xi = \frac{x}{c_0(t+t_0)}, \tag{5.5}$$

where c_0 is the speed of sound at $u=0$, and t_0 a suitable constant. It is clear that $\xi=$const. corresponds to $u=$const. In other words, both v and u may be regarded as functions of ξ.

If the determinant $v'^2-\beta v\neq 0$, u_x and u_t can be expressed in terms of u. We have

$$u_x = \frac{\alpha\beta uv}{x}\frac{1}{v'^2-\beta v}, \tag{5.6}$$

$$u_t = -\frac{\alpha\beta uv}{x}\frac{u+v'}{v'^2-\beta v}, \tag{5.7}$$

where the prime denotes the total differentiation with respect to u. Like in the general case, here again the solution possesses a singular line on which the partial derivatives generally become infinite. Its other properties will be studied presently. From Eq. (5.4) it is found that

$$\left(\frac{dx}{dt}\right)_u = u+v',$$

while the characteristics are

$$\left(\frac{dx}{dt}\right)_C = u\pm\sqrt{\beta v}.$$

On the other hand, where the singular line λ, i.e. the line

$$v'^2-\beta v=0, \tag{5.8}$$

intersects the integral-curve $v(u)$, we have

$$\left(\frac{dx}{dt}\right)_u = u\pm\sqrt{\beta v} = \left(\frac{dx}{dt}\right)_C. \tag{5.9}$$

This shows that at the singular point of the solution $v(u)$, the $u=$const. line becomes the envelope of one family of characteristics C. Hence the envelope is a straight line. Furthermore, according to Eqs. (4.1) and (4.2) the parametric equations of the path s are

$$dx = -\frac{x}{\alpha\beta vv'}(v'+\sqrt{\beta v})(v'-\sqrt{\beta v})du, \tag{5.10}$$

$$dt = -\frac{x}{\alpha\beta uvv'}(v'+\sqrt{\beta v})(v'-\sqrt{\beta v})du. \tag{5.11}$$

Since each factor on the right-hand side corresponds to a group of the characteristics C, on crossing the line λ, where this factor vanishes, the elements dx and dt change

their signs. This proves that the line l, the image of λ, possesses all the characteristics of a "limiting line."

It is interesting to note the difference between plane and spherical waves. In the former case, Eq. (5.8) would be satisfied identically. This lets the lines $u=$const. degenerate into the characteristics. Indeed, it is also possible for one family of the characteristics which are straight lines to have an envelope; the differential quotients u_x, u_t are finite, however. Consequently, we have no "limiting line," in the strict sense. This does not mean, of course, that the solution is regular. As a matter of fact, the solution already becomes many-valued before this line is reached.

6. Lost solution: a special problem. From the foregoing conclusions, a compressive spherical or cylindrical wave always becomes indeterminate when a singular line is reached. As an illustration the following special problem is considered.

Suppose there is a divergent spherical or cylindrical wave propagating with velocity c_0 into still air. On the wave-front, where the motion agrees with the outside conditions, the state-variables ρ, p become equal to those of the still air and the velocity is zero. The path of the wave-front is then described by

$$x = c_0(t + t_0). \tag{6.1}$$

The mathematical problem can thus be formulated in the following way:

$$\left.\begin{aligned} u &= 0, \quad \text{when} \quad x \geqq c_0(t + t_0), \\ u &\neq 0, \quad \text{when} \quad x < c_0(t + t_0). \end{aligned}\right\} \tag{6.2}$$

A particularly simple case will be the one where both the pressure and the velocity are propagated with constant speed. In other words, these quantities depend only on a common parameter.

To simplify the amount of mathematical work involved, the differential equations (2.4) and (2.5) will be put into the following equivalent form:

$$(c^2 - \phi_x^2)\phi_{xx} - 2\phi_x\phi_{xt} - \phi_{tt} + \frac{2c^2\phi_x}{x} = 0 \tag{6.3}$$

by introducing a potential-function $\phi(t, x)$:

$$u = \phi_x, \qquad c^2 - c_0^2 + \frac{\beta}{2}\phi_x^2 = -\beta\phi_t. \tag{6.4}$$

In the case of a lost solution, there exists a parameter ξ defined by (5.5) such that $\xi=1$ corresponds to the initial curve (6.1). Then,

$$\phi(t, x) = c_0^2(t + t_0)f(\xi) \tag{6.5}$$

and hence

$$u(t, x) = c_0 f'(\xi), \tag{6.6}$$

$$c^2 = c_0^2\left[1 - \frac{\beta}{2}f'^2 - \beta(f - \xi f')\right], \tag{6.7}$$

where the prime indicates the total differentiation with respect to ξ, and the function $f(\xi)$ satisfies

$$[c^2 - c_0^2(f' - \xi)^2]\xi f'' + 2c_0^2 f' = 0 \tag{6.8}$$

subject to the initial conditions

$$f(1) = 0, \qquad f'(1) = 0. \tag{6.9}$$

The first condition, namely $f(1)=0$, is necessary to make $c=c_0$ on $\xi=1$. When the conditions (6.9) are substituted in Eq. (6.8), it appears that $f''(1)$ is arbitrary. We need not be alarmed by this situation, but recall that in this particular type of initial value problem, the "support" is a characteristic. Physically, this means that the initial conditions prescribed in this manner do not "know" the internal structure of the motion, because they propagate ahead with larger speed. It is only natural, then, that such an arbitrariness should arise which enables us to fit properly the physical conditions specified. This arbitrariness is only a partial one, however, since for a compressive motion the sign of $f''(1)$ is necessarily negative; for on $\xi=1$

$$(\rho_t)_1 + \rho_0(u_x)_1 = 0,$$

according to Eq. (2.2). In a compressive motion $(\rho_t)_1>0$, it follows that

$$(u_x)_1 = \frac{c_0}{x} f''(1) < 0. \tag{6.10}$$

Thus, for any compressive motion the absolute value of $f''(1)$ is determined in consistence with the physical process.

The differential equation (6.8) which determines the interior motion of a mass of air, has two singular points in the ξ, f-plane given by the vanishing of the coefficient of $f''(\xi)$. The geometrical interpretation is evident, when (6.8) is written as

$$(c + u - c_0\xi)(c - u + c_0\xi) = -\left[\left(\frac{dx}{dt}\right)_{c_+} - \left(\frac{dx}{dt}\right)_{\xi}\right]\left[\left(\frac{dx}{dt}\right)_{c_-} - \left(\frac{dx}{dt}\right)_{\xi}\right] \tag{6.11}$$

that is, when one family of characteristics become tangent to a line $\xi=$const., an infinite curvature would occur if u is finite there. According to what has been said in the last section, this characterizes the "limiting line" of the solution.

Let us push the discussion a step further. For this purpose only the first order terms need be retained. Taking β as a small parameter, one has accordingly

$$f(\xi) = f_0(\xi) + \beta f_1(\xi) + \cdots . \tag{6.12}$$

Substituting in Eq. (6.8) we obtain

$$[1 - (f_0' - \xi)^2]\xi f_0'' + 2f_0' = 0. \tag{6.13}$$

This equation is free from f_0; letting $w=f'$ we find

$$\frac{dw}{d\xi} = \frac{w}{\xi}\,\frac{2}{(w-\xi)^2 - 1}, \qquad 0 \leqq \xi \leqq 1. \tag{6.14}$$

Aside from the two singular lines

$$w = \xi + 1, \tag{6.15}$$

$$w = \xi - 1, \tag{6.16}$$

where the slope of w is infinite, there are two additional singularities (1, 0) and (0, 0) where the slope is indeterminate. The point (1, 0) acts as a sort of nodal point which makes the initial condition insufficient. The point (0, 0) is a saddle point as locally the equation behaves like

$$\frac{dw}{d\xi} = -\frac{2w}{\xi}, \tag{6.17}$$

which form is obtained by neglecting $(w-\xi)^2$ as compared with 1.

The situation can now be summarized. The integral curve starting from (1, 0) rises as ξ decreases and eventually intersects with the line (6.15) where it will have a vertical tangent at $\xi<1$. After it crosses this line its slope changes sign. This causes the curve to bend backward again. Thus, ξ is seen to assume a minimum value. Owing to the fact that the origin is a saddle point, no integral curve could possibly cross the line $\xi=0$. This fact makes the continuation of the solution as far as $\xi=0$ impossible.

7. Continuation of the solution. The results obtained in the previous sections show that, in the case of the propagation of a spherical or cylindrical wave, a continuous solution does not exist throughout the domain considered and can be constructed, at most, as far as a singular line l in the t, x-plane from a suitably chosen initial data. The line l thus acts as a sort of "frontier" into which no solution can enter and at which the solution is turned back as a second branch. The domain then is doubly covered. Physically, this is impossible and hence must be rejected as a solution. The question is: is it possible to connect it with a different solution beyond this line?

First, consider the line λ as a "support" with a given set of initial data and then solve the initial value problem[8] for a Monge-Ampère equation. Regarding λ as a parameter, we have along the line λ

$$\frac{d}{d\lambda}\chi_u = \chi_{uu}\frac{du}{d\lambda} + \chi_{uv}\frac{dv}{d\lambda}, \tag{7.1}$$

$$\frac{d}{d\lambda}\chi_v = \chi_{uv}\frac{du}{d\lambda} + \chi_{vv}\frac{dv}{d\lambda}, \tag{7.2}$$

and hence

$$(\chi_{uu}\chi_{vv} - \chi_{uv}^2)\frac{du}{d\lambda} = \chi_{vv}\frac{d}{d\lambda}\chi_u - \chi_{uv}\frac{d}{d\lambda}\chi_v.$$

Substituting this into Eq. (2.11) we obtain a linear relation between the partial derivatives:

$$\chi_{uu} + \left[\frac{\alpha\beta uv}{x}\left\{\frac{d\chi_u/d\lambda}{du/d\lambda} - \chi_v\right\} - \beta v\right]\chi_{vv} - \frac{\alpha\beta uv}{x}\frac{d\chi_v/d\lambda}{du/d\lambda}\chi_{uv} = \chi_v. \tag{7.3}$$

Since λ is not a characteristic, Eqs. (7.1), (7.2) and (7.3) are sufficient for a unique determination of χ_{uu}, χ_{uv} and χ_{vv}; and consequently a unique integral surface. The uniqueness of the solution is sufficient to show that the solution, when transformed

[8] Courant, R. and Hilbert, D., *Methoden der math. Physik*, vol. 2, J. Springer, Berlin, 1937, p. 344.

back to the t, x-plane, will correspond to the very one that doubles back at the "limiting line." A continuous solution is thus out of the question.

The alternative procedure would be to continue it by joining it smoothly at the line λ to the lost solution. This is also impossible. Indeed, if this were possible, the line λ would have to coincide with the integral curve $v(u)$ in order to provide a continuous solution. This is contradictory, because it is easy to show that the line λ does not satisfy the differential equation for $v(u)$.

The other possibility which remains to be investigated is to identify the "limiting line" as a shock wave so as to construct a discontinuous solution. This would require the continued solution to satisfy the shock conditions. Since, in general, the "limiting line" l is curved, as a result there would be a non-uniform shock wave in the motion, for which both the speed and the strength are no longer constant and therefore the entropy would be constantly changing across the shock. This very fact makes the original assumption untenable. Hence to continue discontinuously a solution with entropy constant everywhere is also impossible.

The problem might be solved, however, if the original hypothesis of isentropic motion is abandoned. To include the possibility that a shock wave may exist within the motion, the continued solution must satisfy the following more general set of equations:

$$u_t + uu_x + \frac{p_x}{\rho} = 0, \tag{7.4}$$

$$\rho_t + u\rho_x + \rho\left(u_x + \frac{\alpha u}{x}\right) = 0, \tag{7.5}$$

$$(p\rho^{-\gamma})_t + u(p\rho^{-\gamma})_x = 0. \tag{7.6}$$

The task then is to construct a solution which should satisfy both the initial and the shock conditions in a region bounded by the initial curve, the shock line and a characteristic drawn to the initial curve through the point where the envelope first appears. The shock line, however, is not given, it should be chosen in such a way that it yields a solution fulfilling all the prescribed conditions. The mathematical problem thus turns out to be extremely difficult.

The author wishes to thank Dr. H. S. Tsien for his invaluable discussions and criticism.

NATIONAL ADVISORY COMMITTEE FOR AERONAUTICS

TECHNICAL NOTE NO. 1445

TWO-DIMENSIONAL IRROTATIONAL TRANSONIC FLOWS OF A COMPRESSIBLE FLUID [1]

By Yung-Huai Kuo

SUMMARY

The method developed in NACA TN No. 995 has been slightly modified and extended to include flows with circulation. The essential feature of the modified method is that in analytic continuation of the solution the alteration of the singularities of the incompressible solution due to the presence of the hypergeometric functions has been taken into account. It was found that for finite Mach number the only case in which the nature of the singularity of the incompressible solution can remain unchanged is for a ratio of specific heats equal to -1.

Two particular flows, one having a finite circulation and the other having zero circulation, have been studied. Both flows were derived from the incompressible flow about an elliptic cylinder of thickness ratio 0.60. The free-stream Mach number for both cases was taken to be 0.60 in order to avoid the appearance of limiting lines. The pressure distribution for the flow without circulation has been compared with that of incompressible flow over approximately the same body. The discrepancies between the exact results and those predicted by the approximate Von Kármán-Tsien and Glauert-Prandtl formulas are so wide as to show definitely that in this case the effect of geometry cannot be ignored, as is done in both approximate formulas. In general, it seems that the effect of geometry cannot be neglected and the conventional "pressure-correction" formulas are not valid, even in the subsonic region if the body is thick, especially if there is a supersonic region in the flow.

INTRODUCTION

This report is a continuation of the work reported in NACA TN No. 995. The method developed in that report has been slightly modified and extended in the present report to include flows with circulation. The general concept and method is outlined without the mathematical details in part I. The essential feature of the modified method is that in analytic continuation of the solution the alteration of the singularities of the incompressible solution due to the presence of the hypergeometric functions has been taken into account, as fully discussed

1) *NACA Technical Note*, 1948, No. 1445

in part II. It was found that for finite Mach number the only case in which the nature of the singularity of the incompressible solution can remain unchanged is for a ratio of specific heats equal to -1. Part III, which contains a discussion of the improvement of convergence of the power series, contains no essentially new material and is included primarily for the sake of completeness. Detailed proofs are given in appendixes A to F.

Part IV contains the study of two particular flows, one having a finite circulation and the other having zero circulation. Both are derived from the incompressible flow about an elliptic cylinder of thickness ratio 0.60. The free-stream Mach number for both cases is taken to be 0.60 in order to avoid the appearance of limiting lines. The pressure distribution for the flow without circulation has been compared with that of incompressible flow over approximately the same body. The discrepancies between the exact results and those predicted by the approximate Von Kármán-Tsien and Glauert-Prandtl formulas are so wide as to show definitely that in this case the effect of geometry cannot be ignored, as is done in both approximate formulas. In general, it seems that the effect of geometry cannot be neglected, and the conventional "pressure-correction" formulas are not valid, even in the subsonic region if the body is thick, especially if there is a supersonic region in the flow. The importance of this result cannot be overemphasized, as there is a widespread tendency in engineering practice to use simple pressure-correction formulas indiscriminately.

This work was conducted at the Guggenheim Aeronautical Laboratory of the California Institite of Technology under the sponsorship and with the financial assistance of the National Advisory Committee for Aeronautics.

I - CONCEPTS AND METHODS

General Consideration of Transonic Flows

The flow of a compressible ideal fluid about an infinite cylindrical body, unlike that of an incompressible fluid, depends on, among other conditions, the speed or Mach number at infinity. If the free-stream Mach number is below a certain value, the flow pattern will be very similar to that of an incompressible fluid even though part of the flow may be supersonic. However, as soon as the limiting Mach number is reached, the situation is entirely different. The phenomenon of major importance in this new situation is the appearance in the calculations of limiting lines in the supersonic region, characterized by the fact that the fluid particles there experience an infinite pressure gradient. It can be shown that if the assumptions of isotropy and of irrotationality of the flow are not rejected, it is impossible to continue the solution beyond these singular lines (reference 1). The failure of potential flow can be attributed to the effects of viscosity and conductivity of the fluid. Although the exact relation between the limiting line and shock

wave is still not established, there is reason to believe that in most cases the theoretical appearance of a limiting line necessarily implies the existence of a shock wave. Therefore, in practice the knowledge of the conditions under which the limiting lines appear for a given body is of paramount importance.

Chaplygin Hodograph Method

To solve the problem of a potential flow of compressible fluid, the use of the hodograph method was first suggested by P. Molenbroek (reference 2) and later by S. A. Chaplygin (reference 3). The advantage of this method is that in the case of two-dimensional potential flow it leads to a linear partial differential equation instead of a quasi-linear one, such as obtained in the physical plane. The particular solutions of this partial differential equation were found to be very similar to those for an incompressible fluid except that each consists of a hypergeometric function containing the Mach number as a parameter. Since the equation is linear, a general solution can be constructed for any assigned domain by the principle of superposition. The difficulty in connection with this method is that the solution so obtained in the hodograph plane may not transform to a "good" aerodynamic body. The problem of constructing a solution in the hodograph plane which corresponds to a desired body in the physical plane has proved to be extremely difficult.

The difficulty was partly solved by constructing a solution which, in the limit of zero Mach number, reduces to a known incompressible flow. Using this idea, Chaplygin studied the subsonic motion of a gas jet and F. Ringleb (reference 4) calculated the flow around a sharp edge. Following the same principle, Tsien (reference 5) for the first time solved the problem of a subsonic flow about a closed body, by simplifying the differential equation in such a manner that the difference between the compressible and incompressible solutions appears only in a modification of the speed scale. This method was later generalized by L. Bers (references 6 and 7) to include the flow with circulation. In the general case where the ratio of specific heats γ is not equal to -1, this simple form of speed distortion does not exist; therefore the method must be extended.

Critique of a Previous Method by Tsien and Kuo

In reference 8 the flow past a closed body as well as over a wavy surface of a gas with a characteristic constant γ greater than unity was considered. The method was based on the determination of two functions: the stream function and the transformed potential introduced through a Legendre transformation. When these two functions are properly chosen, the coordinate functions $x(q,\theta)$ and $y(q,\theta)$ are given by differentiation. Consequently, with the aid of the stream function, the flow pattern can be calculated.

The difficulty of the scheme is twofold. First, whenever a stream function and a transformed potential satisfying the conditions of continuity are constructed, they are required to satisfy the further condition of "compatibility" to ensure that they actually do belong to the same flow. In the case of circulation-free flow, this condition brings no difficulty. However, for a circulatory flow there seems to be an insufficient number of arbitrary constants to meet this stringent requirement. Second, the coexistence of two indirectly connected functions, such as the stream function and the transformed potential, automatically introduces two groups of hypergeometric functions and doubles the number of sets of unknown coefficients defining the power series. All these complications result in a large amount of labor.

In order to simplify the procedure, the velocity potential will be introduced instead of the transformed potential. Inasmuch as both the stream function and the velocity potential are directly connected by simple differential equations, the determination of one leads uniquely to that of the other. The difference between the particular integrals of these functions is simply as follows. For the stream function the particular integral contains, aside from the trigonometric function, the factor $q^{\nu}F\left(a_{\nu},b_{\nu};c_{\nu};\tau\right)$, where q is the speed of the flow and $F\left(a_{\nu},b_{\nu};c_{\nu};\tau\right)$ is the hypergeometric function. On the other hand, the particular integral of the velocity potential will have only an extra factor involving the logarithmic derivative of $F\left(a_{\nu},b_{\nu};c_{\nu};\tau\right)$. Furthermore, because of the two partial differential equations connecting them, both functions will have common coefficients. Thus, only one group of hypergeometric functions and one set of unknown constants are necessary for the complete determination of the two functions.

Construction of Solution in Hodograph Plane

Before outlining the procedure adopted here, it is perhaps proper to describe the mapping of an incompressible flow. In order to simplify the argument, the body has been assumed to be symmetrical with respect to the coordinate axes and the flow at infinity to be parallel to the major axis. Such a flow, when mapped onto the hodograph plane, will give rise to two branches of Riemann surfaces, each corresponding to one-half of the physical plane. Because of symmetry, the discussion may be restricted to, say, the left-half plane D (fig. 1). Because of the fact that the maximum and minimum velocities occur on the surface of the body, the whole field of flow is mapped into the interior of the hodograph D the boundary of which corresponds uniquely to the left-half portion of the body M'SM, and infinity corresponds to a point P on the positive axis of real values. Evidently, this point is singular.

With such a domain in the hodograph plane, it is possible to construct a compressible flow from a "similar" incompressible flow. By similar flow

is meant that at the limit of zero Mach number the compressible-flow solutions will reduce uniquely to the given incompressible flow. First, since the stagnation point, that is, the origin S, is a regular point, there exists a Taylor expansion in its neighborhood. As the singular point which corresponds to the infinity of the physical plane is an interior point, it must be on the circle of convergence C of the solution. Second, the solution represented by the Taylor expansion should be continued analytically for the whole domain. This can be done, of course, either formally by analytic continuation or by solving Cauchy's initial value problem. The former, however, is not practicable. As to the latter, use can be made of the known character of the singularity of the incompressible flow to determine the form of the expansion outside the circle of convergence C. If the Taylor expansion is regarded as given, the "outside" solution can be uniquely defined by the conditions of continuity across the circle of convergence C. This, of course, is based on the assumption that the character of the singularity is unchanged by compressibility.

It is found, however, that the assumption is not valid. Theoretically, it can be shown that, if a Taylor expansion corresponding to incompressible flow is given, then after each term of the expansion is multiplied by a proper hypergeometric function, the resulting solution will have a logarithmic singularity in addition to those it originally possessed. This means that the "distortion" due to compressibility becomes larger for larger speeds. It can also be shown that the character of the singularity is preserved for nonvanishing Mach number if and only if the ratio of the specific heats assumes the value of -1. In order to take this effect into account, the procedure is either to start with a special body to compensate it or to eliminate it by adding an extra term to the outside solution. The former procedure is difficult. By following the latter, the part of the outside solution which, in the limit, reduces to that of the incompressible flow is regarded as known. Then the Taylor expansion and the extra term added to the outside solution can be determined by the conditions of continuity. The extra term becomes zero for zero Mach number. Thus, it is seen that the Chaplygin condition is again satisfied but the procedure has been greatly extended.

The flow with a finite circulation has also been considered. In order to simplify the mathematical problem, the circulation has been assumed to be very small. Under this assumption the effect of circulation on the solution of the incompressible flow can be represented approximately by an arbitrary combination of vortices and doublets at the singularities of the hodograph. Therefore, to the original singularities there will be superposed a logarithmic one in order to define a circulation. Since the added part due to circulation is an even function, the resultant solution will be unsymmetric with respect to the major axis.

The solution for the similar compressible flow can be constructed in the same manner, with the exception that the conditions of continuity across the circle of convergence are insufficient to determine all the

arbitrary constants, in particular those characterizing the strengths of the vortices and the doublets. These are determined from the condition that at the stagnation point $dx = 0$ and $dy = 0$ and from the geometrical condition of symmetry. The former condition is satisfied in all cases irrespective of whether there is circulation, whereas the latter is required only when the circulation is finite.

Improvement of the Convergence of Power Series

The whole problem thus hinges on the method of carrying out the actual computation. It should be pointed out that inasmuch as the solutions, in the limit, reduce to harmonic functions, the convergence of the power series, especially in the neighborhood of the circle of convergence, is generally very slow. This is particularly true of the part $\sum_{0}^{\infty} q^{-\nu} F\left(a_\nu - \nu, b_\nu - \nu; 1 - \nu; \tau\right) \sin \nu\theta$ of the outside series, because it contains the hypergeometric functions which increase rapidly with ν. This situation can be eased somewhat by introducing the asymptotic expansions of the hypergeometric functions. For, after these are substituted in the solutions, the first- and sometimes even the second-order terms can be summed. As a result, the solution in each case can be broken up into two parts, one of which is of closed form and the other is a power series with improved convergence. Owing to the fact that the dominant terms give excellent approximation in the domain of validity, the value of the term given by the power series is usually of inferior order. For practical purposes when high accuracy is not desired, the amount of labor involved can be greatly reduced.

As was pointed out in reference 8, the summed part can be identified as the "speed distortion" in the subsonic region; in the supersonic region where the differential equation changes its type, it can be interpreted as a "standing wave," depending only on the two characteristic parameters. In this case both these simple solutions are known to be inaccurate, especially in the neighborhood of sonic speed. For full discussions, see reference 8.

It must be added that in the case of the derivatives of the hypergeometric functions the dominant terms cannot give as good an approximation, as can be seen by comparing $f^{(1)}(\tau)$ with $g^{(1)}(\tau)$ in table 1. For this reason, the coordinate functions which involve the hypergeometric functions as well as their derivatives have more important correction terms and hence require the use of many more terms for the actual computations.

II – CONSTRUCTION OF A SOLUTION IN HODOGRAPH PLANE

Transformed Differential Equations and Their Particular Solutions

Let u and v be the velocity components of a two-dimensional flow, parallel respectively to the x- and the y-axis of a Cartesian system. In the case of steady, irrotational, and isentropic motion of an inviscid, nonconducting, and compressible fluid, the Eulerian equations can be integrated to give the pressure p, the density ρ, or the sonic speed c in terms of the flow speed q:

$$p = p_o\left(1 - \frac{\gamma - 1}{2}\frac{q^2}{c_o^2}\right)^{\frac{\gamma}{\gamma-1}} \tag{1}$$

$$\rho = \rho_o\left(1 - \frac{\gamma - 1}{2}\frac{q^2}{c_o^2}\right)^{\frac{1}{\gamma-1}} \tag{2}$$

$$\left.\begin{aligned} c^2 &= c_o^2 - \frac{\gamma - 1}{2}q^2 \\ q^2 &= u^2 + v^2 \end{aligned}\right\} \tag{3}$$

where p_o, ρ_o, and c_o denote respectively the values of p, ρ, and c at the stagnation point, and γ is the ratio of the specific heats of the gas. Furthermore, because of the kinematic conditions, there exist a velocity potential φ and stream function ψ defined by

$$\left.\begin{aligned} u &= \varphi_x \\ v &= \varphi_y \end{aligned}\right\} \tag{4}$$

$$\left.\begin{aligned} \rho u &= -\rho_o \psi_y \\ \rho v &= \rho_o \psi_x \end{aligned}\right\} \tag{5}$$

where the subscripts indicate the partial derivatives.

By use of equations (4) and (5), the partial derivatives in the expressions for $d\varphi$ and $d\psi$ can be eliminated so that $d\varphi$ and $d\psi$ can be expressed linearly in terms of dx and dy or dx and dy can be expressed linearly in terms of $d\varphi$ and $d\psi$. Furthermore, if the Jacobian function $\frac{\partial(x,y)}{\partial(u,v)}$ is finite and nonvanishing, the correspondence between the physical xy- and the hodograph ub-plane is 1 to 1. Under this condition, by regarding u and v as independent variables, the relations connecting the differentials yield the following equalities:

$$x_\theta = \frac{1}{q}\left(\cos\theta\varphi_\theta - \frac{\rho_o}{\rho}\sin\theta\psi_\theta\right) \tag{6}$$

$$y_\theta = \frac{1}{q}\left(\sin\theta\varphi_\theta + \frac{\rho_o}{\rho}\cos\theta\psi_\theta\right) \tag{7}$$

and

$$x_q = \frac{1}{q}\left(\cos\theta\varphi_q - \frac{\rho_o}{\rho}\sin\theta\psi_q\right) \tag{8}$$

$$y_q = \frac{1}{q}\left(\sin\theta\varphi_q + \frac{\rho_o}{\rho}\cos\theta\psi_q\right) \tag{9}$$

where θ is the inclination of the velocity vector to the x-axis and accordingly

$$u = q\cos\theta$$

$$v = q\sin\theta$$

Finally, the condition of integrability demands that

$$q\varphi_q = -\frac{\rho_o}{\rho}\left(1 - M^2\right)\psi_\theta \tag{10}$$

$$\varphi_\theta = \frac{\rho_o}{\rho}q\psi_q \tag{11}$$

where $M = q/c$ is the local Mach number. These fundamental systems permit the complete determination of the functions φ and ψ. For by eliminating, say, $\varphi(q,\theta)$, the resultant equation for $\psi(q,\theta)$ is

$$\left(\frac{\rho_o}{\rho} q\psi_q\right)_q + \frac{\rho_o}{\rho q}(1 - M^2)\psi_{\theta\theta} = 0 \qquad (12)$$

If $\psi(q,\theta)$ is known, $\varphi(q,\theta)$ is determined uniquely, aside from a constant determined by equations (10) and (11).

The particular integrals of equation (12) are of the form:

$$\psi = \psi_\nu(q)e^{i\nu\theta}$$

where ν is a positive real number and the function $\psi_\nu(q)$ satisfies

$$\frac{d}{dq}\left(\frac{q}{\rho}\frac{d\psi_\nu}{dq}\right) - \frac{\nu^2}{\rho q}(1 - M^2)\psi_\nu = 0 \qquad (13)$$

If the substitutions, according to Chaplygin,

$$\psi_\nu(q) = q^\nu F_\nu(\tau)$$

and

$$\tau = \frac{1}{2\beta}\frac{q^2}{c_o^2} \quad \text{with} \quad \beta = \frac{1}{\gamma - 1} \qquad (14)$$

are made, equation (13) reduces to a familiar hypergeometric equation and $F_\nu(\tau)$ becomes one of the following integrals:

$$\left.\begin{aligned} &F(a_\nu, b_\nu; c_\nu; \tau) \\ &q^{-2\nu}F(1 + a_\nu - c_\nu,\ 1 + b_\nu - c_\nu;\ 2 - c_\nu;\ \tau) \end{aligned}\right\} \qquad (15)$$

when ν differs from an integer; or

$$\left.\begin{aligned} &F(a_n, b_n; c_n; \tau) \\ &q^{-2n}\left[C_n\tau^n F(a_n, b_n; c_n; \tau)\ \log_e \tau + C_n\tau^n Q_n + P_{n-1}\right] \end{aligned}\right\} \qquad (16)$$

when ν is a positive integer, where

$$Q_n = \frac{\Gamma(c_n)}{\Gamma(a_n)\Gamma(b_n)} \sum_0^\infty \Psi(a_n, b_n; m) \frac{\Gamma(a_n + m)\Gamma(b_n + m)}{\Gamma(c_n + m)\Gamma(m + 1)} \tau^m \qquad \tau < 1 \tag{17}$$

$$P_{n-1} = \frac{1}{\Gamma(n)\Gamma(a_n - n)\Gamma(b_n - n)} \sum_0^{n-1} (-1)^m \frac{\Gamma(a_n - n + m)\Gamma(b_n - n + m)\Gamma(n - m)}{\Gamma(m + 1)} \tau^m \tag{18}$$

$$\Psi(a_n, b_n; m) = \psi(a_n + m) + \psi(b_n + m) - \psi(c_n + m) - \psi(m + 1) - \psi(b_n) + \psi(c_n) \tag{19}$$

$$c_n = (-1)^{n+1} \frac{\Gamma(a_n)\Gamma(b_n)}{\Gamma(n)\Gamma(c_n)\Gamma(a_n - n)\Gamma(b_n - n)} \tag{20}$$

with

$$\left.\begin{aligned} a_\nu + b_\nu &= \nu - \beta \\ a_\nu b_\nu &= -\tfrac{1}{2}\beta\nu(\nu + 1) \\ c_\nu &= \nu + 1 \\ b_\nu &< 0 \end{aligned}\right\} \tag{21}$$

The hypergeometric equation thus possesses two distinct families of fundamental solutions according to whether ν differs from or is equal to an integer. The second

integral defined by expression (16) was found most appropriate for these particular parameters a_n and b_n. The reason for subtracting $C_n\left[\psi(b_n) - \psi(c_n)\right] F(a_n, b_n; c_n; \tau)$ from the second integral defined in reference 8 is to neutralize the contribution of the first integral and the discontinuities carried by $\psi(b_n)$, as b_n is negative.

In the following discussions, the two fundamental solutions of equation (13) will be denoted by $q^{\nu}F_{\nu}(\tau)$ and $q^{-\nu}F_{-\nu}(\tau)$ when ν is not an integer and by $q^{n}F_{n}(\tau)$ and $q^{-n}F_{-n}(\tau)$ when ν is an integer, where $F_{-n}(\tau)$ is defined by the expression within the bracket in expression (16). The normalization has been chosen for a continuous passage of a compressible to an incompressible flow. The most important property of $F_{-n}(\tau)$ from expression (16) is that when $n = 1$

$$F_{-1}(\tau) \equiv 1 \tag{22}$$

For this parameter the first integral reduces to

$$F_1(\tau) \equiv F(1, -\beta; 2; \tau) = \frac{1}{(\beta + 1)\tau}\left[1 - (1 - \tau)^{\beta+1}\right] \tag{23}$$

The particular integrals of equation (12) are then given by

$$\left.\begin{aligned} &q^{\nu}F_{\nu}(\tau)\begin{Bmatrix}\cos\\ \sin\end{Bmatrix}\nu\theta \\ &q^{-\nu}F_{-\nu}(\tau)\begin{Bmatrix}\cos\\ \sin\end{Bmatrix}\nu\theta \end{aligned}\right\} \tag{24}$$

when ν is not an integer and by

$$\left.\begin{aligned} &q^{n}F_{n}(\tau)\begin{Bmatrix}\cos\\ \sin\end{Bmatrix}n\theta \\ &q^{-n}F_{-n}(\tau)\begin{Bmatrix}\cos\\ \sin\end{Bmatrix}n\theta \end{aligned}\right\} \tag{25}$$

when ν is an integer n. In addition to these solutions, there are two other integrals, each of which is a function of only one variable. On assuming $\psi = \psi(q)$ or $\psi(\theta)$, equation (12) yields

$$\theta \quad \text{and} \quad \int (1 - \tau)^{\beta} \frac{d\tau}{\tau} \tag{26}$$

Since the particular integrals of $\psi(q,\theta)$ are known, those of $\varphi(q,\theta)$ are shown to be (see appendix A)

$$\left.\begin{aligned}(1-\tau)^{-\beta}q^{\nu}F_{\nu}(\tau)\xi_{\nu}(\tau)\begin{Bmatrix}\sin\\ \cos\end{Bmatrix}\nu\theta\\ (1-\tau)^{-\beta}q^{-\nu}F_{-\nu}(\tau)\xi_{\nu}(\tau)\begin{Bmatrix}\sin\\ \cos\end{Bmatrix}\nu\theta\end{aligned}\right\} \tag{27}$$

when ν is not an integer and

$$\left.\begin{aligned}(1-\tau)^{-\beta}q^{n}F_{n}(\tau)\xi_{n}(\tau)\begin{Bmatrix}\sin\\ \cos\end{Bmatrix}n\theta\\ (1-\tau)^{-\beta}q^{-n}F_{-n}(\tau)\xi_{-n}(\tau)\begin{Bmatrix}\sin\\ \cos\end{Bmatrix}n\theta\end{aligned}\right\} \tag{28}$$

when ν is an integer n. Here the functions $\xi_{\nu}(\tau)$ and $\xi_{-n}(\tau)$ for any positive value of ν are defined by

$$\left.\begin{aligned}\nu\xi_{\nu}(\tau) &= 2\tau\frac{d}{d\tau}\log_e \tau^{\nu/2}F_{\nu}(\tau)\\ \nu\xi_{-\nu}(\tau) &= 2\tau\frac{d}{d\tau}\log_e \tau^{-\nu/2}F_{-\nu}(\tau)\end{aligned}\right\} \tag{29}$$

The following expressions corresponding to expression (26) are similarly found:

$$(1-\tau)^{-\beta}-\frac{1}{2}\int(1-\tau)^{-\beta}\frac{d\tau}{\tau} \quad \text{and} \quad \theta \tag{30}$$

Hydrodynamic Functions of Incompressible Flows

By following the procedure adopted in reference 8, the analysis starts with the functions required in defining an irrotational incompressible flow. In the case of an incompressible fluid for which the sonic speed is infinite, the equations satisfied by the velocity potential φ and the stream function ψ become harmonic. If $W_o(z_o)$ is the complex potential, it can be shown that

$$W_o(z_o) = \varphi_o(x_o,y_o) + i\psi_o(x_o,y_o) \quad \text{with} \quad z_o = x_o + iy_o \tag{31}$$

In a simply connected domain, the functions φ_o and ψ_o are single-valued and continuous; φ_o can be many-valued only when the flow is now free from circulation Γ_o.

If w denotes the complex velocity $u - iv$, it connects with $W_o(z_o)$ by

$$w = \frac{dW_o(z_o)}{dz_o} \equiv w(z_o) \tag{32}$$

This establishes the relation between the physical and the hodograph plane. The inverse transformation

$$z_o = z_o(w) \tag{33}$$

exists, provided that $w'(z_o) \neq 0$. This function plays an important role in the present scheme of solution and will be known as the transition function. In general, as it is an inverse function, it is not single-valued, as discussed in reference 8. By introducing this relation into equation (31), the complex potential in the hodograph plane is

$$W_o(w) = \varphi_o(u,v) + i\psi_o(u,v) \tag{34}$$

In case the solution of equation (32) is many-valued, $W_o(w)$ will represent only one branch of its many solutions. When the flow is not free from circulation, the function $w(z_o)$ will contain Γ_o as a parameter. This extra term generally makes the transition function $z_o(w)$ more complex than it would be if Γ_o vanishes. In practice, the complication can be reduced to a certain extent by a linear superposition of the two effects such that the transition function becomes

$$z_o = z_o^{(o)}(w) + \frac{\Gamma_o}{4\pi} z_o^{(1)}(w) \tag{35}$$

This simplification can be justified as long as the circulation is weak so that terms of higher order may be neglected. With the transition function so defined, the complex potential may be, similarly,

$$W_o(w) = W_o^{(o)}(w) + \frac{\Gamma_o}{4\pi} W_o^{(1)}(w) \tag{36}$$

Here $z_o^{(o)}(w)$ and $W_o^{(o)}(w)$ are respectively the transition function and complex potential for zero circulation; $z_o^{(1)}(w)$ and $W_o^{(1)}(w)$, which represent the effect of circulation, are known when $W_o(w)$ is given. It can be shown that generally $W_o^{(1)}(w)$ can be represented by vortices and doublets at the singularities of $z_o(w)$. To this order of approximation, it is easy to see that the circulation Γ_o is correctly defined.

Conversely, when $W_o(w)$ is given, $z_o(w)$ can be obtained by integration:

$$z_o(w) = \int W_o'(w) \frac{dw}{w} + \text{Constant} \tag{37}$$

which, in fact, is equivalent to equation (32).

Construction of a Symmetric Solution about the Origin

From the considerations of reference 8, if the flow about a symmetric body placed at the origin of the xy-plane is mapped onto the hodograph plane, the whole left-half plane, exterior to the body, will correspond to a region in the hodograph plane, of which the point $w = U$, U being the modulus of w at infinity of the z_o-plane, is a singularity. Then the domain within the circle $|w| = U$ is single-valued and regular. If the complex potential $W_o(w)$ is associated with a definite flow in the z_o-plane, it must be analytic and regular within $|w| = U$. Consequently, it has the Taylor expansion:

$$W_o(w) = -\sum_0^\infty A_n w^n \qquad |w| < U \tag{38}$$

where the coefficients A_n are, in general, complex. If the body is symmetrical with respect to both coordinate axes, then the coefficient are real. Separating into real and imaginary parts yields, according to equation (34),

$$\psi_o(q,\theta) = \sum_2^\infty A_n q^n \sin n\theta \tag{39}$$

$$\varphi_o(q,\theta) = -\sum_0^\infty A_n q^n \cos n\theta \qquad q < 1 \tag{40}$$

where $w = qe^{-i\theta}$ and $A_1 = 0$ because $w'(z_o) \neq 0$ at $w = 0$. From now on, z_o, w, p, and ρ are normalized in terms of a, U, p_o, and ρ_o, respectively. Then $q = 1$ at infinity, and p and ρ will be unity at $w = 0$.

According to Chaplygin's procedure, the corresponding solutions for the compressible fluid can be obtained by simply replacing the function q^n in equations (39) and (40) by $q^n F_n(r)_{(\tau)}$ and $(1 - \tau)^{-\beta} q^n F_n(r)_{(\tau)} \xi_n(\tau)$, respectively, as shown by expressions (25) and (28). The second integrals are excluded by the condition of regularity at $q = 0$. Thus the following equations are obtained:

$$\psi(q,\theta) = \sum_{2}^{\infty} A_n q^n F_n(r)_{(\tau)} \sin n\theta \qquad (41)$$

$q < 1$

$$\varphi(q,\theta) = -(1 - \tau)^{-\beta} \sum_{2}^{\infty} A_n q^n F_n(r)_{(\tau)} \xi_n(\tau) \cos n\theta + \text{Constant} \qquad (42)$$

where

$$F_n(r)_{(\tau)} \equiv \frac{F_n(\tau)}{F_n(\tau_1)} = \frac{F(a_n,b_n;c_n;\tau)}{F(a_n,b_n;c_n;\tau_1)} \qquad (43)$$

and $\tau_1 = \frac{1}{2\beta} \frac{U^2}{c_o^2}$, that is, τ_1 corresponds to the free-stream velocity U.

It is seen that if $c_o \to \infty$, then both τ and τ_1 tend to zero and $F_n(r)_{(\tau)} \to 1$. Thus, the solutions are reduced to the incompressible form. Furthermore, if $q \to 1$, the character of the solution is exactly like that of the incompressible solution. Hence all the specified conditions are satisfied. It must be remembered that these conditions are valid only for subsonic flows, and for this reason τ_1 is restricted to the subsonic region.

The series (equation (41)) constructed in this manner is actually convergent and represents the function $\psi(q,\theta)$ within the circle of convergence $q = 1$ (reference 8).

Analytic Continuation of Solution (Branch Point of Order 1)

In this section, it is proposed to continue the solutions ψ and φ, represented respectively by equations (41) and (42), analytically outside

the domain $|w| \leq 1$. The domain outside $|w| \leq 1$ is generally many-valued. In order to be precise, let it be a branch point of order 1. Generally, the function $W_o(w)$ has other singularities in addition to the one at $w = 1$. However, such singularities lie outside the domain of interest and thus need not be investigated. Let the nearest singularity be given by $w = V > 1$. Then, the domain to be considered outside $|w| = 1$ is an annulus with a cut joining the two singularities. The proper representation of $W_o(w)$ in such a region which has a branch point of order 1 at $w = 1$ is

$$W_o(w) = iw^{-\frac{1}{2}} W_o^*(w) \tag{44}$$

where $W_o^*(w)$ is single-valued and regular within the open annulus $1 < |w| < V$. Hence, in any closed domain $1 + \delta \leq |w| \leq V - \delta$, δ being a positive value, there exists a uniformly and absolutely convergent series:

$$W_o^*(w) = \sum_0^\infty \left(B_n^* w^n + C_n^* w^{-n} \right) \tag{45}$$

which, on substituting in equation (44), will give the continuation of the Taylor series (equation (38)). This is

$$W_o(w) = i \sum_0^\infty \left(B_n w^\nu + C_n w^{-\nu} \right) \qquad 1 < |w| < V \tag{46}$$

where the constants B_n and C_n are real because of symmetry of the body and $\nu = n + \frac{1}{2}$, n being a positive integer.

In order to continue the solution of $\psi(q,\theta)$ outside the circle $q = 1$, two alternatives are encountered. Suppose, first, that the character of the singularities of $\psi_o(q,\theta)$ defined by equation (39) is unmodified by the hypergeometric functions. Then the solution for the compressible fluid, valid in the annulus $1 < |w| < V$, can be obtained by introducing the proper hypergeometric functions corresponding to the parameter ν. The continued solution would be

$$\psi(q,\theta) = \sum_0^\infty \left[\tilde{B}_n q^\nu F_\nu(r)_{(\tau)} + \tilde{C}_n q^{-\nu} F_{-\nu}(r)_{(\tau)} \right] \cos \nu\theta \qquad 1 < q < V \tag{47}$$

where

$$\left.\begin{aligned} F_\nu(r)_{(\tau)} &= \frac{F_\nu(\tau)}{F_\nu(\tau_1)} \\ F_{-\nu}(r)_{(\tau)} &= \frac{F_{-\nu}(\tau)}{F_{-\nu}(\tau_1)} \end{aligned}\right\} \qquad (48)$$

Here $F_\nu(\tau)$ and $q^{-2\nu}F_{-\nu}(\tau)$ are respectively the first and second integrals of the hypergeometric equation; $\tilde{B}_n$ and $\tilde{C}_n$ are constants. It may be added that the coefficients $\tilde{B}_n$ and $\tilde{C}_n$ are not the same as those in equation (46) for the incompressible flow but should be determined by the conditions of continuity.

Since the partial differential equation considered here is of the second order, in order to ensure that $\psi_{out}(q,\theta)$ is the analytic continuation of $\psi_{in}(q,\theta)$, two conditions must be satisfied at the boundary of the respective regions of convergence, that is, the circle $q = 1$. The two conditions are as follows:

$$\psi_{in}(q,\theta)\Big|_{q=1} = \psi_{out}(q,\theta)\Big|_{q=1} \qquad (49)$$

$$\frac{\partial}{\partial q}\psi_{in}(q,\theta)\Big|_{q=1} = \frac{\partial}{\partial q}\psi_{out}(q,\theta)\Big|_{q=1} \qquad (50)$$

It should be noted that the condition (equation (49)) in this particular case is identical with $\frac{\partial}{\partial\theta}\psi_{in}(q,\theta)\Big|_{q=1} = \frac{\partial}{\partial\theta}\psi_{out}(q,\theta)\Big|_{q=1}$ and that the values taken on the circle of convergence are the limiting values if such limit exists in each case. These conditions would be sufficient to determine both $\tilde{B}_n$ and $\tilde{C}_n$. However, the solution constructed by this method suffers serious distortion because, even though the values, say, ψ and ψ_o, agree on the circle $q = 1$, the tangent of ψ = Constant on $q = 1$ deviates from that of ψ_o = Constant. This, of course, will affect the character of the function $\psi_o(q,\theta)$. If $W_o(w)$ is defined by equation (38), the question arises as to the singularity after the coefficients are multiplied by the proper hypergeometric functions. The exact answer to this question has not been attempted, but a rough estimation given under theorem 1 seems sufficient for the present discussion.

Theorem 1.– A given Taylor expansion such as equation (38), which has a singularity at $w = 1$, is modified by multiplying its coefficients

with proper hypergeometric functions. If the hypergeometric functions can be represented in the neighborhood of $\tau = 0$ by

$$F_n(\tau) = f(\tau)T^n \left[1 + \frac{f^{(1)}(\tau)}{n} \right]$$

according to appendix C, then to its original singularities will be superposed a logarithmic one at either $w = 1$ or $w = 0$ (appendix B). This demonstrates that, in order to continue the Taylor series by the method just outlined, it is not possible to preserve the original singularity. In order to minimize this effect, the process is reversed. That is, start with a solution in $1 < q < V$ and continue the solution inwardly by satisfying the conditions of continuity on the circle $q = 1$. This is equivalent to assigning the thickness of the body first. Let the stream function $\Psi(q,\theta)$ in the annulus $1 < q < V$ be of the form:

$$\Psi(q,\theta) = \sum_0^\infty \left[B_n q^\nu F_\nu^{(r)}(\tau) + C_n q^{-\nu} F_{-\nu}^{(r)}(\tau) \right] \cos \nu\theta + \tilde{D}_o(\pi - \theta) + \sum_1^\infty \tilde{D}_n q^{-n} F_{-n}^{(r)}(\tau) \sin n\theta \quad (51)$$

where the coefficients B_n and C_n are given by equation (46) and the $\tilde{D}_n$'s are to be determined. The last two terms are introduced to counteract the distortion and are chosen so that the symmetry property of $\Psi(q,\theta)$ is preserved. If $\Psi(q,\theta)$ is defined by equation (41) with coefficients $\tilde{A}_n$ and equation (51) represents the solution, the constants $\tilde{A}_n$ and $\tilde{D}_n$ should satisfy, according to equations (49) and (50), on $q = 1$

$$\sum_1^\infty \left(\tilde{A}_m - \tilde{D}_m - \frac{2\tilde{D}_o}{m} \right) \sin m\theta = \sum_0^\infty (B_m + C_m) \cos \mu\theta$$

$$\sum_1^\infty m \left[\tilde{A}_m \xi_m(\tau_1) - \tilde{D}_m \xi_{-m}(\tau_1) \right] \sin m\theta = \sum_0^\infty \mu \left[B_m \xi_\mu(\tau_1) + C_m \xi_{-\mu}(\tau_1) \right] \cos \mu\theta$$

Here it has been tacitly assumed that the limits, as $q \to 1$, exist and $\tilde{A}_1 = 0$ in order to ensure the conditions $dx = dy = 0$ at $q = 0$, and in addition

$$\pi - \theta = 2 \sum_{1}^{\infty} \frac{\sin m\theta}{m} \qquad 0 < \theta < 2\pi$$

Multiplying both sides by $\sin n\theta$ and integrating term by term yields

$$\left.\begin{aligned} \tilde{A}_n - \tilde{D}_n - \frac{2\tilde{D}_0}{n} &= \frac{1}{\pi} \sum_{0}^{\infty} (B_m + C_m) I_{n\mu} \\ n\left[\tilde{A}_n \xi_n(\tau_1) - \tilde{D}_n \xi_{-n}(\tau_1)\right] &= \frac{1}{\pi} \sum_{0}^{\infty} \mu \left[B_m \xi_\mu(\tau_1) + C_m \xi_{-\mu}(\tau_1)\right] I_{n\mu} \end{aligned}\right\} \tag{52}$$

where

$$I_{n\mu} = \frac{1}{n + \mu} + \frac{1}{n - \mu}$$

$$\mu = m + \frac{1}{2}$$

If the right-hand members are regarded as definite quantities, the algebraic solution gives, for $n = 1$,

$$\left.\begin{aligned} \tilde{D}_0 &= -\frac{1}{2\pi} \sum_{0}^{\infty} \left\{ \left[\mu \xi_\mu(\tau_1) + 1\right] B_m + \left[\mu \xi_{-\mu}(\tau_1) + 1\right] C_m \right\} I_{1\mu} \\ \tilde{D}_1 &= \frac{1}{\pi} \sum_{0}^{\infty} \mu \left[B_m \xi_\mu(\tau_1) + C_m \xi_{-\mu}(\tau_1)\right] I_{1\mu} \end{aligned}\right\} \tag{53}$$

and, for $n > 1$,

$$n\tilde{A}_n = \frac{1}{\pi}\frac{1}{\xi_n(\tau_1) - \xi_{-n}(\tau_1)}\left(\sum_0^\infty \left\{\left[\mu\xi_\mu(\tau_1) - n\xi_{-n}(\tau_1)\right]B_m + \left[\mu\xi_{-\mu}(\tau_1) - n\xi_{-n}(\tau_1)\right]C_m\right\} - 2\pi\tilde{D}_0\xi_{-n}(\tau_1)\right) \tag{54}$$

$$n\tilde{D}_n = \frac{1}{\pi}\frac{1}{\xi_n(\tau_1) - \xi_{-n}(\tau_1)}\left(\sum_0^\infty \left\{\left[\mu\xi_\mu(\tau_1) - n\xi_n(\tau_1)\right]B_m + \left[\mu\xi_{-\mu} - n\xi_n(\tau_1)\right]C_m\right\} - 2\pi\tilde{D}_0\xi_n(\tau_1)\right) \tag{55}$$

where the determinant $n(\xi_n - \xi_{-n}) \neq 0$. It is observed that, as $\tau_1 \to 0$, $\tilde{D}_n \to 0$ and $\tilde{A}_n \to A_n$. Consequently, Chaplygin's condition is again satisfied. Furthermore, $\tilde{D}_n = 0$ also for $\gamma = -1$. In that event, the compressible and incompressible flows will have the same singularities.

The solution is formal. In order to prove that the function $\psi(q,\theta)$ represented by equations (41) and (51) is regular in the respective domains of validity, the truth of the following theorem must first be demonstrated.

Theorem 2.- If the constants $\tilde{A}_n$ and $\tilde{D}_n$ are defined by equations (54) and (55), respectively, and if the series (equations (38) and (46)) converge uniformly and absolutely in the domains specified, the series (equation (41)) with coefficients $\tilde{A}_n$ and equation (51) are uniformly and absolutely convergent in the corresponding domains (appendix E).

With $\psi(q,\theta)$ so determined, the velocity potential, as given in the section entitled "Transformed Differential Equations and Their Particular Solutions," is

$$\varphi(q,\theta) = -(1-\tau)^{-\beta}\sum_2^\infty \tilde{A}_n q^n F_n(r)(\tau)\cos n\theta + \text{Constant} \tag{56}$$

and

$$\varphi(q,\theta) = (1-\tau)^{-\beta} \sum_{0}^{\infty} \left[B_n q^{\nu} F_{\nu}^{(r)}(\tau) \xi_{\nu}(\tau) + C_n q^{-\nu} F_{-\nu}^{(r)}(\tau) \right] \sin \nu\theta$$

$$- (1-\tau)^{-\beta} \sum_{1}^{\infty} \tilde{D}_n q^{-n} F_{-n}^{(r)}(\tau) \xi_{-n}(\tau) \cos n\theta - \tilde{D}_o \left[(1-\tau)^{-\beta} - \frac{1}{2} \int_{\tau_1}^{\tau} (1-\tau)^{-\beta} \frac{d\tau}{\tau} \right] \quad (57)$$

Thus, the velocity potential is indeterminate only to the extent of a constant, which is not essential. It must be noted, however, that the conditions of continuity on $q = 1$ can be satisfied by making use of the conditions of equations (49) and (50) together with equation (13). This shows that when the stream function $\psi(q,\theta)$ is chosen for a domain in the hodograph plane, the associated velocity potential $\varphi(q,\theta)$ can be determined uniquely.

Construction of a Solution for Flow with Circulation

The presence of circulation creates asymmetry in the flow even when the body is symmetrical. In the case of incompressible flow and as long as the circulation is weak, the asymmetry of the stream function can be characterized, according to equation (36), by the linear combination of two terms:

$$\psi_o(q,\theta) = \psi_o^{(o)}(q,\theta) + \frac{\Gamma_o}{2\pi} \psi_o^{(1)}(q,\theta) \quad (58)$$

where $\psi_o^{(o)}(q,\theta)$ for a symmetrical body, as given by equation (39), is an odd function, whereas $\psi_o^{(1)}(q,\theta)$ is even. The complex potential $W_o^{(1)}(w)$ due to circulation must possess a logarithmic singularity in addition to poles at both $q = 1$ and $q = V$. The exact distribution of these vortices and doublets depends, of course, on the shape of the body. For convenience of discussion, it is assumed that $\psi_o^{(1)}(q,\theta)$ has the following simple representation: For $q < 1$,

$$\psi_o^{(1)}(q,\theta) = -\sum_0^\infty q^n \cos n\theta + \sum_1^\infty \frac{q^n}{n} \cos n\theta + \sum_0^\infty \left(\frac{q}{V}\right)^n \cos n\theta - \sum_1^\infty \frac{\left(\frac{q}{V}\right)^n}{n} \cos n\theta \tag{59}$$

and, for $1 < q < V$,

$$\psi_o^{(1)}(q,\theta) = \sum_1^\infty q^{-n} \cos n\theta + \sum_1^\infty \frac{q^{-n}}{n} \cos n\theta - \log_e q + \sum_0^\infty \left(\frac{q}{V}\right)^n \cos n\theta - \sum_1^\infty \frac{\left(\frac{q}{V}\right)^n}{n} \cos n\theta \tag{60}$$

Because of circulation, the function $\varphi_o^{(1)}(q,\theta)$ consists of: For $q < 1$,

$$\varphi_o^{(1)}(q,\theta) = -\sum_1^\infty q^n \sin n\theta + \sum_1^\infty \frac{q^n}{n} \sin n\theta + \sum_2^\infty \left(1 - \frac{1}{n}\right)\left(\frac{q}{V}\right)^n \sin n\theta + \tilde{A}_o^{(1)} \tag{61}$$

and, for $1 < q < V$,

$$\varphi_o^{(1)}(q,\theta) = -\sum_1^\infty q^{-n} \sin n\theta - \sum_1^\infty \frac{q^{-n}}{n} \sin n\theta - (\pi + \theta) + \sum_2^\infty \left(1 - \frac{1}{n}\right)\left(\frac{q}{V}\right)^n \sin n\theta \tag{62}$$

For a compressible flow it is assumed similarly that

$$\psi(q,\theta) = \psi^{(o)}(q,\theta) + \frac{\Gamma_o}{4\pi} \psi^{(1)}(q,\theta) \tag{63}$$

This assumption is justified only by the fact that Γ_o is small and the corresponding $\varphi^{(1)}(q,\theta)$ yields a correct circulation. In the case of a symmetrical body, $\psi^{(o)}(q,\theta)$ was

given in the two immediately preceding sections and $\psi^{(1)}(q,\theta)$ is to be determined by use of equations (59) and (60). However, in the case of the hodograph method, the solution actually is an inverse problem. A dissymmetry of the flow of a compressible fluid will contribute different distortions at the upper and lower surfaces of the body and eventually destroy its symmetry. Consequently, the contour may not even be closed. It is believed that this is the main difficulty previously experienced in connection with the hodograph method in which association of a compressible flow with incompressible flow is actually not allowed.

In the present discussion, the connection between the compressible and incompressible solutions has been abandoned and the form of the incompressible solution serves only as a guide for the construction of the compressible solution rather than as a restriction. This has been fully demonstrated in the preceding section. Accordingly, the function $\psi^{(1)}(q,\theta)$ may assume the following expression: For $q < 1$,

$$\psi^{(1)}(q,\theta) = -\sum_{0}^{\infty} A_n^{(1)} q^n F_n(\tau) \cos n\theta + \sum_{1}^{\infty} B_n^{(1)} q^n F_n(\tau) \cos n\theta$$

$$+ A_o^{(1)} \sum_{1}^{\infty} \left(1 - \frac{1}{n}\right)\left(\frac{q}{V}\right)^n F_n(r)(\tau) \cos n\theta + P(q,\theta) \tag{64}$$

and, for $1 < q < V$,

$$\psi^{(1)}(q,\theta) = \sum_{1}^{\infty} \left[C_n^{(1)} + D_n^{(1)}\right] q^{-n} F_{-n}(\tau) \cos n\theta - \frac{B_o^{(1)}}{2} \int_{\tau_1}^{\tau} (1 - \tau)^{\beta} \frac{d\tau}{\tau}$$

$$+ A_o^{(1)} \sum_{1}^{\infty} \left(1 - \frac{1}{n}\right)\left(\frac{q}{V}\right)^n F_n(\tau) \cos n\theta + P(q,\theta) \tag{65}$$

where

$$P(q,\theta) = C_o q^2 F_2(\tau) \sin 2\theta \tag{66}$$

Here the constants $A_n^{(1)}$, $B_n^{(1)}$, $C_n^{(1)}$, and $D_n^{(1)}$ characterize the strength of the vortices and doublets and are determined by the conditions of continuity at $q = 1$. Generally $P(q,\theta)$ is a polynomial and is introduced to add to $\psi^{(1)}(q,\theta)$ a mixed symmetry. The number of terms required is, from cause to effect, unknown and may be different for different bodies. In the present case, only one term is taken for simplicity. On assuming that every series converges uniformly and absolutely in the respective domain of validity and tends to a definite limit as $q \to 1$, the conditions of continuity at $q = 1$ are

$$\sum_1^\infty \left[A_n^{(1)} F_n(\tau_1) + C_n^{(1)} F_{-n}(\tau_1) \right] \cos n\theta = -A_o^{(1)} \qquad 0 < \theta < 2\pi$$

$$\sum_1^\infty n \left[A_n^{(1)} F_n(\tau_1) \xi_n(\tau_1) + C_n^{(1)} F_{-n}(\tau_1) \xi_{-n}(\tau_1) \right] \cos n\theta = 0$$

and

$$\sum_1^\infty \left[B_n^{(1)} F_n(\tau_1) - D_n^{(1)} F_{-n}(\tau_1) \right] \cos n\theta = 0 \qquad 0 < \theta < 2\pi$$

$$\sum_1^\infty n \left[B_n^{(1)} F_n(\tau_1) \xi_n(\tau_1) - D_n^{(1)} F_{-n}(\tau_1) \xi_{-n}(\tau_1) \right] \cos n\theta = -B_o^{(1)} (1 - \tau_1)^\beta$$

By the uniqueness theorem of expansion, since

$$\sum_1^\infty \cos n\theta = -\frac{1}{2} \qquad 0 < \theta < 2\pi$$

it follows that

$$A_n^{(1)} F_n(\tau_1) + C_n^{(1)} F_{-n}(\tau_1) = 2A_o^{(1)}$$

$$A_n^{(1)} F_n(\tau_1) \xi_n(\tau_1) + C_n^{(1)} F_{-n}(\tau_1) \xi_{-n}(\tau_1) = 0$$

and

$$B_n^{(1)} F_n(\tau_1) - D_n^{(1)} F_{-n}(\tau_1) = 0$$

$$B_n^{(1)} F_n(\tau_1)\xi_n(\tau_1) - D_n^{(1)} F_{-n}(\tau_1)\xi_{-n}(\tau_1) = \frac{2}{n}(1-\tau_1)^{\beta} B_o^{(1)}$$

The solutions are, respectively:

$$\left.\begin{aligned} A_n^{(1)} &= -A_o^{(1)}(1-\tau_1)^{-\beta} F_{-n}(\tau_1)\xi_{-n}(\tau_1) \\ C_n^{(1)} &= A_o^{(1)}(1-\tau_1)^{-\beta} F_n(\tau_1)\xi_n(\tau_1) \end{aligned}\right\} \tag{67}$$

$$\left.\begin{aligned} B_n^{(1)} &= B_o^{(1)} \frac{F_{-n}(\tau_1)}{n} \\ D_n^{(1)} &= B_o^{(1)} \frac{F_n(\tau_1)}{n} \end{aligned}\right\} \tag{68}$$

From theorem 2, it can easily be shown that $\psi^{(1)}(q,\theta)$ so defined is, as assumed, uniformly and absolutely convergent in any closed domain in $q < 1$ and $1 < q < V$ and that $\psi^{(1)}(q,\theta) = 0$ when $q = 0$. Furthermore, the arbitrary constants $A_o^{(1)}$, $B_o^{(2)}$, and $C_o^{(1)}$ are to be determined by the auxiliary conditions. In the first place, the condition that $dx = dy = 0$ at $q = 0$ demands that

$$-A_1^{(1)} + B_1^{(1)} = 0$$

which leads, because of expression (22), to

$$A_o^{(1)} = (1-\tau_1)^{\beta} B_o^{(1)} \tag{69}$$

In case there is no stagnation point, such as in the case of a body with a sharp trailing edge, this condition is again to be satisfied in order to avoid the multiplicities in x and y. The remaining two constants, namely, $B_o^{(1)}$ and $C_o^{(1)}$, will be determined by the condition of symmetry and will be discussed under Determination of Integration Constants.

Similarly, the function $\varphi(q,\theta)$ is

$$\varphi(q,\theta) = \varphi^{(o)}(q,\theta) + \frac{\Gamma_o}{4\pi}\varphi^{(1)}(q,\theta) \tag{70}$$

Here the function $\varphi^{(o)}(q,\theta)$ is given by equations (56) and (57), and $\varphi^{(1)}(q,\theta)$, for $q < 1$, is

$$\varphi^{(1)}(q,\theta) = (1-\tau)^{-\beta}\left[\sum_{2}^{\infty} \tilde{A}_n(1) q^n F_n(\tau)\xi_n(\tau) \sin n\theta + Q(q,\theta)\right] + \tilde{A}_o \tag{71}$$

and, for $1 < q < V$, is

$$\varphi^{(1)}(q,\theta) = (1-\tau)^{-\beta}\left\{B_o(1) \sum_{1}^{\infty}\left[\tilde{B}_n(1) q^n F_n(\tau)\xi_n(\tau) + \tilde{C}_n(1) q^{-n} F_{-n}(\tau)\xi_{-n}\right] \sin n\theta + Q\right\} - B_o(1)(\pi + \theta) \tag{72}$$

where

$$\left.\begin{aligned} Q &= -C_o(1) q^2 F_2(\tau)\xi_2(\tau) \cos 2\theta \\ \tilde{A}_n(1) &= B_o(1)\left[\xi_{-n}(\tau_1) + \frac{1}{n}\right] F_{-n}(\tau_1) + A_o(1)\left(1 - \frac{1}{n}\right)\frac{1}{F_n(\tau_1)V^n} \\ \tilde{B}_n(1) &= (1-\tau_1)^{\beta}\left(1 - \frac{1}{n}\right)\frac{1}{F_n(\tau_1)V^n} \\ \tilde{C}_n(1) &= \left[\xi_n(\tau_1) + \frac{1}{n}\right] F_n(\tau_1) \end{aligned}\right\} \tag{73}$$

The velocity potential thus gives, by definition, a circulation Γ:

$$\Gamma = \oint d\varphi = \Gamma_o B_o(1) \tag{74}$$

where the integral is taken, in clockwise direction, about the branch point in two complete circuits.

Transition Functions

When a pair of functions $\psi(q,\theta)$ and $\varphi(q,\theta)$ are constructed in the hodograph plane, the flow pattern to which they correspond in the physical plane cannot be given directly but further integration of two differential equations is required. This process, however, does not involve any difficulty owing to the fact that both dx and dy are total differentials and consequently reduces to partial integration. In order to carry out the integration, first suppose that the functions $\psi(q,\theta)$ and $\varphi(q,\theta)$ are defined respectively by equations (41) and (56); then equations (6) and (7) become

$$x_\theta = \frac{(1-\tau)^{-\beta}}{q}\left[\sum_2^\infty n\tilde{A}_n F_n(r)(\tau)\xi_n(\tau)\sin n\theta\cos\theta - \sum_2^\infty n\tilde{A}_n q^n F_n(r)\cos n\theta\sin\theta\right]$$

$$y_\theta = \frac{(1-\tau)^{-\beta}}{q}\left[\sum_2^\infty n\tilde{A}_n F_n(r)(\tau)\xi_n(\tau)\sin n\theta\sin\theta + \sum_2^\infty n\tilde{A}_n q^n F_n(r)\cos n\theta\cos\theta\right] \qquad q < 1$$

Partial integration gives, for $q < 1$,

$$x(q,\theta) = -\frac{(1-\tau)^{-\beta}}{2q}\left\{\sum_2^\infty n\tilde{A}_n q^n F_n(r)(\tau)\xi_n(\tau)\left[\frac{\cos(n-1)\theta}{n-1} + \frac{\cos(n+1)\theta}{n+1}\right]\right.$$
$$\left. + \sum_2^\infty n\tilde{A}_n q^n F_n(r)(\tau)\left[\frac{\cos(n-1)\theta}{n-1} - \frac{\cos(n+1)\theta}{n+1}\right]\right\} + x(q) \qquad (75)$$

$$y(q,\theta) = \frac{(1-\tau)^{-\beta}}{2q}\left\{\sum_2^\infty n\tilde{A}_n q^n F_n(r)(\tau)\xi_n(\tau)\left[\frac{\sin(n-1)\theta}{n-1} - \frac{\sin(n+1)\theta}{n+1}\right]\right.$$
$$\left. + \sum_2^\infty n\tilde{A}_n q^n F_n(r)(\tau)\left[\frac{\sin(n-1)\theta}{n-1} + \frac{\sin(n+1)\theta}{n+1}\right]\right\} + y(q) \qquad (76)$$

Differentiating equations (75) and (76) partially with respect to q and using equation (13) to eliminate the derivative higher than the first yields x_q and y_q. By comparing these two expressions with those obtained directly from equations (8) and (9) it can be concluded that

$$x'(q) = 0$$

$$y'(q) = 0$$

Therefore, both $x(q)$ and $y(q)$ are constants denoted by x_{in} and y_{in}, respectively.

On the other hand, the following expressions for $x(q,\theta)$ and $y(q,\theta)$, corresponding to $\psi(q,\theta)$ and $\varphi(q,\theta)$ defined respectively by equations (51) and (57), can be proved similarly for $1 < q < V$:

$$x(q,\theta) = \frac{(1-\tau)^{-\beta}}{2q}\left\{\sum_0^\infty \nu\left[B_n q^{\nu} F_\nu^{(\gamma)}(\tau)\xi_\nu(\tau) + C_n q^{-\nu} F_{-\nu}^{(\gamma)}(\tau)\xi_{-\nu}(\tau)\right]\left[\frac{\sin(\nu-1)\theta}{\nu-1} + \frac{\sin(\nu+1)\theta}{\nu+1}\right]\right.$$

$$+ \sum_0^\infty \nu\left[B_n q^{\nu} F_\nu^{(\gamma)}(\tau) + C_n q^{-\nu} F_{-\nu}^{(\gamma)}(\tau)\right]\left[\frac{\sin(\nu-1)\theta}{\nu-1} - \frac{\sin(\nu+1)\theta}{\nu+1}\right]$$

$$- \sum_1^\infty n\tilde{D}_n q^{-n} F_{-n}^{(\gamma)}(\tau)\xi_{-n}(\tau)\left[\frac{\cos(n-1)\theta}{n-1} + \frac{\cos(n+1)\theta}{n+1}\right]$$

$$\left.+ \sum_1^\infty n\tilde{D}_n q^{-n} F_{-n}^{(\gamma)}(\tau)\left[-\frac{\cos(n-1)\theta}{n-1} + \frac{\cos(n+1)\theta}{n+1}\right] - 2\tilde{D}_0\cos\theta\right\} + x_{out} \qquad (77)$$

$$y(q,\theta) = \frac{(1-\tau)^{-\beta}}{2q}\left\{\sum_0^\infty \nu\left[B_n q^{\nu} F_\nu^{(r)}(\tau)\xi_\nu(\tau) + C_n q^{-\nu} F_{-\nu}^{(r)}(\tau)\xi_{-\nu}(\tau)\right]\left[\frac{\cos(\nu-1)\theta}{\nu-1} - \frac{\cos(\nu+1)\theta}{\nu+1}\right]\right.$$

$$+ \sum_0^\infty \nu\left[B_n q^{\nu} F_\nu^{(r)}(\tau) + C_n q^{-\nu} F_{-\nu}^{(r)}(\tau)\right]\left[\frac{\cos(\nu-1)\theta}{\nu-1} + \frac{\cos(\nu+1)\theta}{\nu+1}\right]$$

$$+ \sum_1^\infty n\tilde{D}_n q^{-n} F_{-n}^{(r)}(\tau)\xi_{-n}(\tau)\left[\frac{\sin(n-1)\theta}{n-1} - \frac{\sin(n+1)\theta}{n+1}\right]$$

$$\left.+ \sum_1^\infty n\tilde{D}_n q^{-n} F_{-n}^{(r)}(\tau)\left[\frac{\sin(n-1)\theta}{n-1} + \frac{\sin(n+1)\theta}{n+1}\right] - 2\tilde{D}_o \sin\theta\right\} + y_{out} \qquad (78)$$

where x_{out} and y_{out} are constants. The terms for $n = 1$ in the third and fourth sums would have given rise to a multivalued function θ, but it is eliminated by the fact that $F_{-1}(\tau) \equiv 1$ (expression (22)). These relations establish the correspondence between the hodograph and physical planes. Inasmuch as the correspondence is 1 to 1, a line in the hodograph plane defined by

$$\psi(q,\theta) = \text{Constant} = \kappa \qquad (79)$$

will correspond uniquely to a definite portion of a streamline in the physical plane. That is, eliminating one of the two variables, say, θ, from equations (75) and (76) and equations (77) and (78) by first solving equation (79), which gives

$$\theta = \theta(q,\kappa) \qquad (80)$$

yields two parametric equations for the streamline $\psi = \kappa$.

In the case of circulatory flow corresponding to equations (63) and (70), the transition functions $x(q,\theta)$ and $y(q,\theta)$ can be written as

$$x(q,\theta) = x^{(o)}(q,\theta) + \frac{\Gamma_o}{4\pi} x^{(1)}(q,\theta) \tag{81}$$

$$y(q,\theta) = y^{(o)}(q,\theta) + \frac{\Gamma_o}{4\pi} y^{(1)}(q,\theta) \tag{82}$$

Here $x^{(o)}$ and $y^{(o)}$ are those quantities given from equations (75) to (78), whereas $x^{(1)}$ and $y^{(1)}$ can be obtained by the same manner from $\psi^{(1)}$ and $\varphi^{(1)}$ defined respectively by equations (64) and (71). They are, for $q < 1$,

$$x^{(1)}(q,\theta) = \frac{(1-\tau)^{-\beta}}{2q}\left\{\sum_{2}^{\infty} n\tilde{A}_n(1)q^n F_n(\tau)\xi_n(\tau)\left[\frac{\sin(n-1)\theta}{n-1} + \frac{\sin(n+1)\theta}{n+1}\right]\right.$$

$$\left. + \sum_{2}^{\infty} n\tilde{A}_n(1)q^n F_n(\tau)\left[\frac{\sin(n-1)\theta}{n-1} - \frac{\sin(n+1)\theta}{n+1}\right] + P_x\right\} \tag{83}$$

$$y^{(1)}(q,\theta) = \frac{(1-\tau)^{-\beta}}{2q}\left\{\sum_{2}^{\infty} n\tilde{A}_n(1)q^n F_n(\tau)\xi_n(\tau)\left[\frac{\cos(n-1)\theta}{n-1} - \frac{\cos(n+1)\theta}{n+1}\right]\right.$$

$$\left. + \sum_{2}^{\infty} n\tilde{A}_n(1)q^n F_n(\tau)\left[\frac{\cos(n-1)\theta}{n-1} + \frac{\cos(n+1)\theta}{n+1}\right] + P_y\right\} + y_{in}^{(1)} \tag{84}$$

where

$$P_x = -2C_o(1)q^2F_2(\tau)\left[\xi_2(\tau)\left(\frac{\cos 3\theta}{3} + \cos\theta\right) - \frac{\cos 3\theta}{3} + \cos\theta\right] \tag{85}$$

$$P_y = -2C_o(1)q^2F_2(\tau)\left[\xi_2(\tau)\left(\frac{\sin 3\theta}{3} - \sin\theta\right) - \frac{\sin 3\theta}{3} - \sin\theta\right] \tag{86}$$

On the other hand, in the domain $1 < q < V$, they are

$$x^{(1)}(q,\theta) = \frac{(1-\tau)^{-\beta}}{2q}\left\{B_o(1)\sum_1^\infty n\left[\tilde{B}_n(1)q^nF_n(\tau)\xi_n(\tau) + \tilde{C}_n(1)q^{-n}F_{-n}(\tau)\xi_{-n}(\tau)\right]\left[\frac{\sin(n-1)\theta}{n-1}\right.\right.$$
$$\left. + \frac{\sin(n+1)\theta}{n+1}\right] + B_o(1)\sum_1^\infty n\left[\tilde{B}_n(1)q^nF_n(\tau) + \tilde{C}_n(1)q^{-n}F_{-n}(\tau)\right]\left[\frac{\sin(n-1)\theta}{n-1}\right.$$
$$\left.\left. - \frac{\sin(n+1)\theta}{n+1}\right] + P_x\right\} - \frac{B_o(1)}{q}\sin\theta \tag{87}$$

$$y^{(1)}(q,\theta) = \frac{(1-\tau)^{-\beta}}{2q}\left\{B_o(1)\sum_1^\infty n\left[\tilde{B}_n(1)q^nF_n(\tau)\xi_n(\tau) + \tilde{C}_n(1)q^{-n}F_{-n}(\tau)\xi_{-n}(\tau)\right]\left[\frac{\cos(n-1)\theta}{n-1}\right.\right.$$
$$\left. - \frac{\cos(n+1)\theta}{n+1}\right] + B_o(1)\sum_1^\infty n\left[\tilde{B}_n(1)q^nF_n(\tau) + \tilde{C}_n(1)q^{-n}F_{-n}(\tau)\right]\left[\frac{\cos(n-1)\theta}{n-1}\right.$$
$$\left.\left. + \frac{\cos(n+1)\theta}{n+1}\right] + P_y\right\} + \frac{B_o(1)}{q}\cos\theta + y_{out}(1) \tag{88}$$

Here, since $\tilde{B}_1^{(1)} = 0$, the terms for $n = 1$ again contribute no difficulty. The constants of integration in equations (83) and (87) are left out because they can be incorporated in equations (75) and (77), respectively.

Determination of Integration Constants

Consider first the case when the flow is symmetrical. The transition functions $x(q,\theta)$ and $y(q,\theta)$ for such a flow are given respectively by equations (75) and (76) for $q < 1$ and by equations (77) and (78) for $1 < q < V$, involving four arbitrary constants. Of these four constants, x_{out} and y_{in} can be chosen arbitrarily by translating the coordinate axes. Indeed, because of symmetry, it is preferable to choose

$$x_{out}(q,\theta) = 0 \quad \text{for} \quad q = q_U \quad \text{and} \quad \theta = 0 \tag{89}$$

$$y_{in}(q,\theta) = 0 \quad \text{for} \quad q = 0 \tag{90}$$

whence

$$x_{out} = \frac{(1-\tau_U)^{-\beta}}{q_U}\left\{\sum_1^\infty \frac{n^2}{n^2-1}\left[\tilde{D}_n q_U^{-n} F_{-n}(r)(\tau_U)\xi_{-n}(\tau_U) + \frac{\tilde{D}_n}{n} q_U^{-n} F_{-n}(r)(\tau_U)\right] + \tilde{D}_o\right\} \tag{91}$$

$$y_{in} = 0 \tag{92}$$

where q_U denotes the flow speed on the upper surface at the midsection of the body. Then x_{out} depends on τ_1 and tends to zero with τ_1.

The other two constants can now be determined by the condition of continuity at $q = 1$, namely,

$$x_{in}(1,\theta) = x_{out}(1,\theta) \tag{93}$$

$$y_{in}(1,\theta) = y_{out}(1,\theta) \qquad 0 < \theta < 2\pi \tag{94}$$

Since both limits exist, the integration of the identities yields

$$x_{in} = \frac{(1-\tau_1)^{-\beta}}{2\pi}\left\{\sum_0^\infty \nu\left[B_n\xi_\nu(\tau_1) + C_n\xi_{-\nu}(\tau_1)\right]\left[\frac{1}{(\nu-1)^2}+\frac{1}{(\nu+1)^2}\right]\right.$$
$$\left. + \sum_0^\infty \nu(B_n + C_n)\left[\frac{1}{(\nu-1)^2}-\frac{1}{(\nu+1)^2}\right]\right\} + x_{out} \qquad (95)$$

$$y_{out} = 0 \qquad (96)$$

The fact that $y_{out} = 0$ is the consequence of $y(q,\theta) = -y(q,2\pi-\theta)$; $2x_{in}$ will be defined as the chord of the body.

For the flow with circulation, according to the preceding section, there are six constants instead of four. Let those four arising from integration be considered first. Corresponding to equations (89) and (90) the following equations may be chosen:

$$x_{out}(o) = \frac{(1-\tau_U)^{-\beta}}{q_U}\left\{\sum_1^\infty \frac{n}{n^2-1}\tilde{D}_n q_U^{-n} F_{-n}(\tau_U)\left[n\xi_{-n}(\tau_U)+1\right]\right.$$
$$\left. + \tilde{D}_o - \frac{\Gamma_o}{8\pi}P_x(q_U,0)\right\} \qquad (97)$$

$$y_{out}(1) = 0 \qquad (98)$$

Then the condition of continuity at $q = 1$ gives

$$x_{in}(o) = \frac{(1-\tau_1)^{-\beta}}{2\pi}\left\{\sum_0^\infty \nu\left[B_n\xi_\nu(\tau_1) + C_n\xi_{-\nu}(\tau_1)\right]\left[\frac{1}{(\nu-1)^2}+\frac{1}{(\nu+1)^2}\right]\right.$$
$$\left. + \sum_0^\infty \nu(B_n + C_n)\left[\frac{1}{(\nu-1)^2}-\frac{1}{(\nu+1)^2}\right]\right\} + x_{out}(o) \qquad (99)$$

$$y_{in}(1) = -B_o(1) + \frac{A_o(1)}{F_1(\tau_1)V} \qquad (100)$$

In order to derive the second term in equation (100), use has been made of the fact that $F_1(\tau) - \frac{\beta\tau}{2}F_{1,1}(\tau) = (1-\tau)^{\beta}$, which is just the Wronskian of the particular integrals of the hypergeometric equation for $n = 1$.

The arbitrary constants $B_o^{(1)}$ and $C_o^{(1)}$, on the other hand, are determined by an entirely different consideration. The fact that $B_o^{(1)}$ and $C_o^{(1)}$ are different from unity and zero, respectively, as they would be if τ_1 tends to zero is due to the fact that the distortion produced by compressibility is nonuniform at the surfaces of the body. In order to correct this defect completely, a more elaborate method would have been required. For the present simple investigation in which symmetry is not strictly satisfied even in the limiting case of zero Mach number, the condition of symmetry will be applied to only a few selected points. First, let it be required that

$$\left.\begin{aligned} x_{out}(q_U, 0) &= 0 \\ x_{out}(q_L, 2\pi) &= 0 \end{aligned}\right\} \tag{101}$$

where q_L stands for the flow speed on the lower surface at the midsection of the body. These two equations determine uniquely $C_o^{(1)}$, namely,

$$\frac{\Gamma_o}{6\pi}C_o(1) = -\frac{\delta(q_U) - \delta(q_L)}{e_2(q_U) - e_2(q_L)} \tag{102}$$

where

$$\delta(q) = \frac{(1-\tau)^{-\beta}}{q}\left[\sum_1^{\infty}\frac{n}{n^2-1}\tilde{D}_n q^{-n}F_{-n}(\tau)(n\xi_{-n}+1) + \tilde{D}_o\right] \tag{103}$$

$$e_2(q) = (1-\tau)^{-\beta}qF_2(\tau)\left[2\xi_2(\tau)+1\right] \tag{104}$$

The value of $C_o^{(1)}$ becomes zero with τ_1 for $\tilde{D}_n \to 0$ as $\tau_1 \to 0$, as defined in equation (55).

The maximum distortion with respect to the y-axis will occur at the midsection. If the required body is assumed to be symmetrical, that is,

$$y(q_U,0) = \left| y(q_L,2\pi) \right|$$

the circulation will be so adjusted that

$$\Gamma_o B_o^{(1)} = 4\pi \frac{y^{(o)}(q_L,0) - y^{(o)}(q_U,0)}{y^{(1)}(q_U) + y^{(1)}(q_L)} \tag{105}$$

where $y^{(o)}(q,0) > 0$ is defined by equation (78) for $\theta = 0$ and $y^{(1)}(q)$ is given by

$$y^{(1)}(q) = \frac{(1-\tau)^{-\beta}}{q} \left\{ \sum_1^\infty \frac{n}{n^2-1} \left[\tilde{B}_n^{(1)} q^n F_n(\tau) \xi_n(\tau) + \tilde{C}_n^{(1)} q^{-n} F_{-n}(\tau) \xi_{-n}(\tau) \right] \right.$$

$$\left. + \sum_1^\infty \frac{n^2}{n^2-1} \left[\tilde{B}_n^{(1)} q^n F_n(\tau) + \tilde{C}_n^{(1)} q^{-n} F_{-n}(\tau) \right] \right\} + \frac{1}{q} \tag{106}$$

Thus, the circulation in the case of compressible flow is generally connected directly with the shape of the body. If, however, the camber is not controlled, $A_o^{(1)}$ may be taken equal to unity, by analogy with the case of incompressible flow. Then the condition of conformality (equation (69)) becomes the only condition to define the circulation. The relative merit of these two procedures can be ascertained only by comparing the numerical results.

III - IMPROVEMENT OF CONVERGENCE OF SOLUTION BY ASYMPTOTIC PROPERTIES OF HYPERGEOMETRIC FUNCTIONS

Transformation of Stream Function $\psi(q,\theta)$

The stream function $\psi(q,\theta)$ for a flow which was derived from $\psi_o(q,\theta)$ with a branch point of order 1 has been given. The form of representation is not, in general, suitable for practical calculation. The difficulty is twofold: First, the series involves an infinite number of hypergeometric functions which are, in turn, defined as infinite series. The convergence of the hypergeometric series in this particular instance decreases with increase of the parameter ν. This means that the computation for the later terms of the series for $\psi(q,\theta)$ will be increasingly laborious. Second, the convergence of the power series defining the function $\psi(q,\theta)$ is, as expected, very slow in the neighborhood of the circle of convergence. In order to render the method of any practical value, the task of transforming the series into a more rapidly convergent one is encountered. For this purpose the following procedure is adopted.

The stream function $\psi_o(q,\theta)$ for the similar incompressible flow is (see section entitled "Construction of a Symmetric Solution about the Origin")

$$\psi_o(q,\theta) = \sum_{2}^{\infty} A_n q^n \sin n\theta \qquad q < 1$$

which is absolutely and uniformly convergent in any closed domain in $q < 1$. Then it can justly be thought of as representing not merely a regular but a closed function. In doing this, of course, a large class of problems is automatically eliminated and those cases are then considered in which simple representation of both $\varphi_o(q,\theta)$ and $\psi_o(q,\theta)$ exists. This is justified only by the mounting difficulties faced in carrying out such a detailed investigation.

It is thus observed that the difference between the stream functions $\psi(q,\theta)$ and $\psi_o(q,\theta)$ lies only in the appearance, in the former, of the hypergeometric functions. If, however, approximation is allowed, then, according to expression (223), first let $F_n(\tau)$ be substituted by its asymptotic expression, namely,

$$F_n^{(r)}(\tau) \sim \frac{f(\tau)}{f(\tau_1)} t^n(\tau) \left[1 + O\left(\frac{1}{n}\right)\right] \qquad n > N \qquad (107)$$

where $t(\tau) = \frac{T(\tau)}{T(\tau_1)}$. Here the term involving $f^{(1)}(\tau) << 1$ has been neglected. Furthermore, as will be shown in equation (159), to the same order of approximation the coefficient $\tilde{A}_n$ can be written as

$$\tilde{A}_n \sim A_n + O\left(\frac{1}{n}\right) \qquad n > N \qquad (108)$$

By substituting the approximate values in equation (41) it can be shown that

$$\psi(q,\theta) \sim \frac{f(\tau)}{f(\tau_1)} \psi_o(qt,\theta) \qquad (109)$$

That is, to this order of approximation the power series representing the stream function $\psi(q,\theta)$ can be summed and is given by expression (109)

As was shown in reference 8, the asymptotic representation is valid only when the parameter n is large. Namely, during the summation of expression (109) the value neglected becomes smaller as n increases and approaches zero as n tends to infinity. This concentration of errors in the lower-order terms makes it especially easy to apply the correction if high accuracy is required. In doing this, the quantity given by expression (109) can be added and, at the same time, subtracted from $\psi(q,\theta)$. Then a simple manipulation shows that

$$\psi(q,\theta) = \psi_1(q,\theta) + \psi_2(q,\theta) \qquad (110)$$

where

$$\psi_1(q,\theta) = \frac{f(\tau)}{f(\tau_1)} \psi_o(qt,\theta) \qquad (111)$$

$$\psi_2(q,\theta) = \sum_{2}^{\infty} G_n(\tau) q^n \sin n\theta \qquad q < 1 \qquad (112)$$

with

$$G_n(\tau) = F_n(\tau)\Delta\tilde{A}_n + \frac{A_n}{f(\tau_1)T^n(\tau_1)}\Delta F_n(\tau) \qquad (113)$$

$$\left.\begin{aligned} \Delta\tilde{A}_n &= \frac{\tilde{A}_n}{F_n(\tau_1)} - \frac{A_n}{f(\tau_1)T^n(\tau_1)} \\ \Delta F_n(\tau) &= F_n(\tau) - f(\tau)T^n(\tau) \end{aligned}\right\} \qquad (114)$$

Here n is a positive integer. The stream function $\psi(q,\theta)$ is then represented by the sum of two functions $\psi_1(q,\theta)$ and $\psi_2(q,\theta)$. Of these, $\psi_1(q,\theta)$ is of closed form, which differs from $\psi_o(q,\theta)$ only by a change of scale of q, and $\psi_2(q,\theta)$ is a difference of two absolutely and uniformly convergent series and hence is absolutely and uniformly convergent. In fact, according to expressions (107) and (108), $G_n(\tau)$ is of order $\frac{A_n}{n}t^n(\tau)$; the convergence of $\psi(q,\theta)$ is therefore increased by 1/n. This actually is the gist of the whole problem.

In the annulus region $1 < q < V$; on the other hand, the stream function $\psi_o(q,\theta)$ is represented by

$$\psi_o(q,\theta) = \sum_0^\infty \left(B_n q^\nu + C_n q^{-\nu} \right) \cos \nu\theta$$

and the stream function $\psi(q,\theta)$ of the compressible flow is

$$\psi(q,\theta) = \sum_0^\infty \left[B_n q^\nu F_\nu^{(r)}(\tau) + C_n q^{-\nu} F_{-\nu}^{(r)}(\tau) \right] \cos \nu\theta$$

$$+ \tilde{D}_o(\pi - \theta) + \sum_1^\infty \tilde{D}_n q^{-n} F_{-n}^{(r)}(\tau) \sin n\theta$$

where B_n and C_n are assumed to be given by $\psi_o(q,\theta)$, and $F_\nu^{(r)}(\tau)$ stands for the ratio of $F_\nu(\tau)$ to $F_\nu(\tau_1)$. In this region, the hypergeometric functions will be of mixed character. If the critical point $\tau_c = \frac{1}{2\beta + 1}$ is not reached, they are of exponential type; beyond this point they will change over into oscillatory type. If τ_c lies in the range $1 < q < V$, the singularity of the asymptotic expansions of the hypergeometric functions will certainly be found inside the domain in question. If this neighborhood is excluded and the hypergeometric functions are first substituted by their asymptotic forms given in expressions (223) and (224), it can similarly be shown that, for $\tau_1 < \tau < \frac{1}{2\beta + 1}$,

$$\psi(q,\theta) = \psi_1(q,\theta) + \psi_2(q,\theta) + \psi_3(q,\theta) \qquad (115)$$

where

$$\psi_1(q,\theta) = \frac{f(\tau)}{f(\tau_1)} \psi_o(q,\theta)$$

$$\psi_2(q,\theta) = \sum_0^\infty \left[B_n H_\nu(\tau) q^\nu + C_n H_{-\nu}(\tau) q^{-\nu} \right] \cos \nu\theta \qquad (116)$$

$$\Psi_3(q,\theta) = \tilde{D}_o(\pi - \theta) + \sum_1^\infty \tilde{D}_n q^{-n} F_{-n}^{(r)}(\tau) \sin n\theta \qquad (117)$$

and

$$\left.\begin{aligned} H_\nu(\tau) &= F_\nu(\tau)\Delta F_\nu^{-1}(\tau_1) + \frac{1}{f(\tau_1)T^\nu(\tau_1)}\Delta F_\nu(\tau) \\ H_{-\nu}(\tau) &= F_{-\nu}(\tau)\Delta F_{-\nu}^{-1}(\tau_1) + \frac{1}{f(\tau_1)T^{-\nu}(\tau_1)}\Delta F_{-\nu}(\tau) \end{aligned}\right\} \qquad (118)$$

with

$$\Delta F_\nu^{-1}(\tau_1) = \frac{1}{F_\nu(\tau_1)} - \frac{1}{f(\tau_1)T_\nu(\tau_1)}$$

$$\Delta F_\nu(\tau) = F_\nu(\tau) - f(\tau)T^\nu(\tau)$$

In equation (115) $\Psi_1(q,\theta)$ again represents a closed function $\Psi_o(qt,\theta)$, and $\Psi_2(q,\theta)$, an absolutely and uniformly convergent series with improved convergence. The fact that $\Psi_3(q,\theta)$ is not summed is due to the fact that $\tilde{D}_n$ is of inferior order as compared with $\tilde{A}_n$. Even though $\tilde{D}_n$ decreases as $1/n$, $\Psi_3(q,\theta)$ will require fewer terms than $\Psi_2(q,\theta)$ although its coefficients behave like $n^{-3/2}$ (provided that the flow $\Psi_o(x_o,y_o)$ is of the nature of a doublet). Here the functions $H_\nu(\tau)$ are so defined that the functions of τ_1 and those of τ are separated so as to make possible the tabulation of $\Delta F\nu(\tau)$ and $\Delta F_{-\nu}(\tau)$.

In the region $\frac{1}{2\beta + 1} < \tau < 1$, on the other hand, $F_\nu(\tau)$ and $F_{-\nu}(\tau)$ are replaced respectively by

$$\frac{1}{2} f(\tau)T^\nu(\tau) \cos\left(\nu\omega - \frac{\pi}{4}\right)$$

$$\frac{1}{2} f(\tau)T^{-\nu}(\tau) \cos\left(\nu\omega + \frac{\pi}{4}\right)$$

where $f(\tau)$, $T(\tau)$, and $\omega(\tau)$ are given in table 1. The factor $1/2$ is introduced before the first expression for symmetry. By writing

$$2\cos\nu\theta\cos\left(\nu\omega-\frac{\pi}{4}\right)=\frac{1}{\sqrt{2}}\left(\cos\nu\xi+\cos\nu\eta+\sin\nu\xi-\sin\nu\eta\right)$$

$$2\cos\nu\theta\cos\left(\nu\omega+\frac{\pi}{4}\right)=\frac{1}{\sqrt{2}}\left(\cos\nu\xi+\cos\nu\eta-\sin\nu\xi+\sin\nu\eta\right)$$

with

$$\left.\begin{aligned}\xi&=\theta+\omega\\ \eta&=\theta-\omega\end{aligned}\right\}\tag{119}$$

the following expression, corresponding to equation (111), is obtained

$$\psi(q,\theta)\sim\frac{f(\tau)}{2^{5/2}f(\tau_1)}\left[\psi_o(\lambda,\xi)+\psi_o(\lambda,\eta)+\varphi_o(\lambda,\xi)-\varphi_o(\lambda,\eta)\right]$$

where λ is a constant defined by

$$\lambda=\frac{2(2\beta)^{\alpha/2}}{(1+\alpha)^{\alpha}(2\beta\tau_1)^{1/2}}\frac{1}{T(\tau_1)}>1\tag{120}$$

as from equation (228) $qt=\lambda U$ if $\frac{1}{2\beta+1}<\tau<1$. The constant λ then is a function of the free-stream Mach number and the characteristic constant of the gas but independent of the shape of the body. By eliminating the error introduced during summation, the stream function $\psi(q,\theta)$ in the supersonic range $\frac{1}{2\beta+1}<\tau<1$ is

$$\psi(q,\theta)=\psi_1(q,\theta)+\psi_2(q,\theta)+\psi_3(q,\theta)$$

where

$$\psi_1(q,\theta)=2^{-5/2}\frac{f(\tau)}{f(\tau_1)}\left[\psi_o(\lambda,\xi)+\psi_o(\lambda,\eta)+\varphi_o(\lambda,\xi)-\varphi_o(\lambda,\eta)\right]\tag{121}$$

$$\psi_2(q,\theta)=\sum_0^{\infty}\left[B_nH_\nu(\tau)q^{\nu}+C_nH_{-\nu}(\tau)q^{-\nu}\right]\cos\nu\theta\tag{122}$$

Here $\psi_3(q,\theta)$ is given by equation (117) and $H_\nu(\tau)$ and $H_{-\nu}(\tau)$, by equation (118), except that $\Delta F_\nu(\tau)$ and $\Delta F_{-\nu}(\tau)$ are defined by

$$\Delta F_{\pm\nu}(\tau) = F_{\pm\nu}(\tau) - \frac{1}{2}f(\tau)T^{\pm\nu}\cos\left(\nu\omega \mp \frac{\pi}{4}\right) \qquad (123)$$

Unlike the previous calculations, $H_\nu(\tau)$ in equation (122) is not of the order of $1/\nu$, owing to the presence of $1/2$ in front of $f(\tau)T^\nu \cos\left(\nu\omega - \frac{\pi}{4}\right)$. This, however, does not introduce a serious objection, as the series in which it appears now behaves like $B_n\lambda^\nu$, which, according to equation (120) ($\lambda > 1$), converges more rapidly than B_nq^ν in $\psi_o(q,\theta)$.

In the hyperbolic domain, moreover, the function $\psi_1(q,\theta)$ depends, aside from a factor $f(\tau)$, only on the two independent families of the characteristic parameters ξ and η defined by equation (119). This result is most striking, as it shows that the main part of the solution satisfies the simple wave equation and thus clearly demonstrates its hyperbolic character. With both the incompressible stream function $\psi_o(q,\theta)$ and the incompressible velocity potential $\varphi_o(q,\theta)$ appearing in the solution, it is impossible to establish a simple relation between the incompressible streamlines and the compressible streamlines. Since such a simple relation is the foundation of the so-called speed correction formula for a quick estimation of velocity distribution in compressible flow from that of incompressible flow over the same body, this idea cannot be extended to supersonic regions. On the other hand, this also indicates that, although the differential equation for $\psi(q,\theta)$ is hyperbolic in the supersonic range, it cannot be reduced to the simple wave equation by a mere distortion of the speed scale as given by the function $\omega(\tau)$. For if this were the case, then $\psi_1(q,\theta)$ would constitute an exact solution without the additional $\psi_2(q,\theta)$. This fact is all the more important as the additional $\psi_2(q,\theta)$ is not small in comparison with $\psi_1(q,\theta)$ for the mixed subsonic and supersonic flows, especially for the transitional region near the sonic velocity. However, in the case of pure supersonic flow, $\psi_2(q,\theta)$ might be small; then $\psi_1(q,\theta)$ alone may be used as a satisfactory approximation.

Transformation of Coordinate Functions $x(q,\theta)$ and $y(q,\theta)$

From equations (75) and (76) it is seen that the coefficients of the series defining the coordinate functions $x(q,\theta)$ and $y(q,\theta)$ are of the same order of magnitude as those of the series for the stream function $\psi(q,\theta)$ (equation (41)). By analogy with the preceding section the first-order terms in both x and y can be similarly summed. First, let them be written, for $q < 1$, as

$$x(q,\theta) = -\frac{(1-\tau)^{-\beta}}{q}\left\{\sum_{2}^{\infty}\frac{n\tilde{A}_n}{n-1}q^n F_n^{(\gamma)}(\tau)\cos(n-1)\theta - \frac{\beta\tau}{2}\sum_{2}^{\infty} n\tilde{A}_n q^n F_{n,1}^{(\gamma)}(\tau)\left[\frac{\cos(n-1)\theta}{n-1} + \frac{\cos(n+1)\theta}{n+1}\right]\right\} + x_{in} \tag{124}$$

$$y(q,\theta) = \frac{(1-\tau)^{-\beta}}{q}\left\{\sum_{2}^{\infty}\frac{n\tilde{A}_n}{n-1}q^n F_n^{(\gamma)}(\tau)\sin(n-1)\theta - \frac{\beta\tau}{2}\sum_{2}^{\infty} n\tilde{A}_n q^n F_{n,1}^{(\gamma)}(\tau)\left[\frac{\sin(n-1)\theta}{n-1} - \frac{\sin(n+1)\theta}{n+1}\right]\right\} \tag{125}$$

Now for the similar incompressible flow with complex potential defined by equation (38) the coordinate functions can easily be deduced as

$$x_o(q,\theta) = -\sum_{2}^{\infty}\frac{nA_n}{n-1}q^{n-1}\cos(n-1)\theta + x_{1n}(o) \tag{126}$$

$$q < 1$$

$$y_o(q,\theta) = \sum_{2}^{\infty}\frac{nA_n}{n-1}q^{n-1}\sin(n-1)\theta \tag{127}$$

Furthermore,

$$\frac{\cos(n-1)\theta}{n-1} + \frac{\cos(n+1)\theta}{n+1} = \frac{2n}{n^2-1}\left(\cos n\theta\cos\theta + \frac{\sin n\theta\sin\theta}{n}\right) \tag{128}$$

$$\frac{\sin(n-1)\theta}{n-1} - \frac{\sin(n+1)\theta}{n+1} = -\frac{2n}{n^2-1}\left(\cos n\theta\sin\theta - \frac{\sin n\theta\cos\theta}{n}\right) \quad n > 1 \tag{129}$$

If the hypergeometric functions are substituted by the dominant term of their asymptotic expansions and the coefficients are approximated by A_n, then $x(q,\theta)$ and $y(q,\theta)$ reduce to

$$x(q,\theta) \sim \frac{-(1-\tau)^{-\beta}}{q}\left[\frac{f(\tau)}{f(\tau_1)}\sum_{2}^{\infty}\frac{nA_n}{n-1}(qt)^n\cos(n-1)\theta - \beta\tau\frac{g(\tau)}{f(\tau_1)}\sum_{2}^{\infty}A_n(qt)^n\left(\cos n\theta\cos\theta+\frac{\sin n\theta\sin\theta}{n}\right)\right]+x_{in}$$

$$y(q,\theta) \sim \frac{(1-\tau)^{-\beta}}{q}\left[\frac{f(\tau)}{f(\tau_1)}\sum_{2}^{\infty}\frac{nA_n}{n-1}(qt)^n\sin(n-1)\theta + \beta\tau\frac{g(\tau)}{f(\tau_1)}\sum_{2}^{\infty}A_n(qt)^n\left(\cos n\theta\sin\theta-\frac{\sin n\theta\cos\theta}{n}\right)\right]$$

According to the indentities (equations (126), (127), (40), and (251)), it is evident that

$$x(q,\theta) \sim (1-\tau)^{-\beta}\left(\frac{f(\tau)t(\tau)}{f(\tau_1)}\left[x_o(qt,\theta)-x_{in}^{(o)}\right] - \frac{\beta\tau}{q}\frac{g(\tau)}{f(\tau_1)}\left\{\left[\varphi_o(qt,\theta)+A_o\right]\cos\theta-\chi(qt,\theta)\sin\theta\right\}\right)+x_{in}$$

$$y(q,\theta) \sim (1-\tau)^{-\beta}\left(\frac{f(\tau)t(\tau)}{f(\tau_1)}\left[y_o(qt,\theta)\right]-\frac{\beta\tau}{q}\frac{g(\tau)}{f(\tau_1)}\left\{\left[\varphi_o(qt,\theta)+A_o\right]\sin\theta+\chi(qt,\theta)\cos\theta\right\}\right)$$

In order to eliminate the error introduced, equations (124) and (125) can similarly be written as

$$x(q,\theta) = x_1(q,\theta) + x_2(q,\theta) \tag{130}$$

$$y(q,\theta) = y_1(q,\theta) + y_2(q,\theta) \tag{131}$$

Here $x_1(q,\theta)$ and $y_1(q,\theta)$ represent

$$x_1(q,\theta) = (1-\tau)^{-\beta}\left\{\frac{f(\tau)t(\tau)}{f(\tau_1)}x_o(qt,\theta) - \frac{\beta\tau}{q}\frac{g(\tau)}{f(\tau_1)}\left[\varphi_o(qt,\theta)\cos\theta - \chi(qt,\theta)\sin\theta\right]\right\} \tag{132}$$

$$y_1(q,\theta) = (1-\tau)^{-\beta}\left\{\frac{f(\tau)t(\tau)}{f(\tau_1)}y_o(qt,\theta) - \frac{\beta\tau}{q}\frac{g(\tau)}{f(\tau_1)}\left[\varphi_o(qt,\theta)\sin\theta + \chi(qt,\theta)\cos\theta\right]\right\} \tag{133}$$

and $x_2(q,\theta)$ and $y_2(q,\theta)$ are series valid for $q < 1$:

$$x_2(q,\theta) = -\frac{(1-\tau)^{-\beta}}{q}\left[\sum_2^\infty \frac{n}{n-1}G_n(\tau)q^n\cos(n-1)\theta - \beta\tau\sum_2^\infty G_{n,1}(\tau)q^n\left(\cos n\theta\cos\theta + \frac{\sin n\theta\sin\theta}{n}\right) + A_o\beta\tau\frac{g(\tau)}{f(\tau_1)}\cos\theta\right] + \Delta x_{in} \tag{134}$$

$$y_2(q,\theta) = \frac{(1-\tau)^{-\beta}}{q}\left[\sum_2^\infty \frac{n}{n-1}G_n(\tau)q^n\sin(n-1)\theta + \beta\tau\sum_2^\infty G_{n,1}(\tau)q^n\left(\cos n\theta\sin\theta - \frac{\sin n\theta\cos\theta}{n}\right) - A_o\beta\tau\frac{g(\tau)}{f(\tau_1)}\sin\theta\right] \tag{135}$$

where $G_n(\tau)$ is defined by equation (113), and $G_{n,1}(\tau)$ is given by

$$G_{n,1}(\tau) = F_{n,1}(\tau)\,\Delta\frac{n^2\tilde{A}_n}{(n^2-1)F_n(\tau_1)} + \frac{A_n}{f(\tau_1)T^n(\tau_1)}\,\Delta F_{n,1}(\tau) \tag{136}$$

with

$$\left.\begin{aligned} \Delta F_{n,1}(\tau) &= F_{n,1}(\tau) - g(\tau)T^n(\tau) \\ \Delta\frac{n^2\tilde{A}_n}{(n^2-1)F_n(\tau_1)} &= \frac{n^2\tilde{A}_n}{(n^2-1)F_n(\tau_1)} - \frac{A_n}{f(\tau_1)T^n(\tau_1)} \\ \Delta x_{in} &= x_{in} - \frac{f(\tau)t(\tau)}{f(\tau_1)(1-\tau)^\beta}x_{in}(o) \end{aligned}\right\} \tag{137}$$

From expressions (230) and (108), $G_{n,1}(\tau)$ is also of the order $\frac{An}{n}t^n$. Thus, the speed of convergence of $x_1(q,\theta)$ and $y_2(q,\theta)$ is the same as that of $\psi_2(q,\theta)$. However, because of the character of $g^{(1)}(\tau)$ as given in table 1 the second series in $x_2(q,\theta)$ and $y_2(q,\theta)$, aside from the factor $\beta\tau$, is generally of superior order as compared with the first one. The smallness of $f^{(1)}(\tau)$ is the main reason, incidently, that the summation generally stops at the first-order terms.

The coordinate functions for the annulus region can similarly be put in the forms:

$$x(q,\theta) = \frac{(1-\tau)^{-\beta}}{q}\left\{\sum_0^\infty \left[\frac{\nu B_n}{\nu-1}q^\nu F_\nu^{(r)}(\tau)\sin(\nu-1)\theta - \frac{\nu C_n}{\nu+1}q^{-\nu}F_{-\nu}^{(r)}(\tau)\sin(\nu+1)\theta\right]\right.$$
$$\left. - \frac{\beta\tau}{2}\sum_0^\infty \nu\left[B_n q^\nu F_{\nu,1}^{(r)}(\tau) - C_n q^{-\nu}F_{-\nu,1}^{(r)}(\tau)\right]\left[\frac{\sin(\nu-1)\theta}{\nu-1} + \frac{\sin(\nu+1)\theta}{\nu+1}\right]\right\} + x_3 \tag{138}$$

$$y(q,\theta) = \frac{(1-\tau)^{-\beta}}{q}\left\{\sum_{0}^{\infty}\left[\frac{\nu B_n}{\nu-1}q^{\nu}F_{\nu}^{(r)}(\tau)\cos(\nu-1)\theta + \frac{\nu C_n}{\nu+1}q^{-\nu}F_{-\nu}^{(r)}(\tau)\cos(\nu+1)\theta\right]\right.$$

$$\left. - \frac{\beta\tau}{2}\sum_{0}^{\infty}\nu\left[B_n q^{\nu}F_{\nu,1}^{(r)}(\tau) - C_n q^{-\nu}F_{-\nu,1}^{(r)}(\tau)\right]\left[\frac{\cos(\nu-1)\theta}{\nu-1} - \frac{\cos(\nu+1)\theta}{\nu+1}\right]\right\} + y_3 \quad (139)$$

Here $x_3(q,\theta)$ and $y_3(q,\theta)$, corresponding to $\psi_3(q,\theta)$, represent

$$x_3(q,\theta) = -\frac{(1-\tau)^{-\beta}}{2q}\left\{\sum_{1}^{\infty}\tilde{nD}_n q^{-n}F_{-n}^{(r)}(\tau)\xi_{-n}(\tau)\left[\frac{\cos(n+1)\theta}{n+1} + \frac{\cos(n-1)\theta}{n-1}\right]\right.$$

$$\left. - \sum_{1}^{\infty}\tilde{nD}_n q^{-n}F_{-n}^{(r)}(\tau)\left[\frac{\cos(n+1)\theta}{n+1} - \frac{\cos(n-1)\theta}{n-1}\right] + 2\tilde{D}_o\cos\theta\right\} + x_{out} \quad (140)$$

$$y_3(q,\theta) = -\frac{(1-\tau)^{-\beta}}{2q}\left\{\sum_{1}^{\infty}\tilde{nD}_n q^{-n}F_{-n}^{(r)}(\tau)\xi_{-n}(\tau)\left[\frac{\sin(n+1)\theta}{n+1} - \frac{\sin(n-1)\theta}{n-1}\right]\right.$$

$$\left. - \sum_{1}^{\infty}\tilde{nD}_n q^{-n}F_{-n}^{(r)}(\tau)\left[\frac{\sin(n+1)\theta}{n+1} + \frac{\sin(n-1)\theta}{n-1}\right] + 2\tilde{D}_o\sin\theta\right\} \quad (141)$$

Like $\psi_3(q,\theta)$, $x_3(q,\theta)$ and $y_3(q,\theta)$ are also of inferior order and hence further transformation is not required. But, for the other part, as the point $\tau = \frac{1}{2\beta+1}$ lies in the region $1 < q < V$, it demands separate consideration. First, let it be assumed that the critical speed is less than V; then for the region $1 < q < V$ but $\tau_1 < \tau < \frac{1}{2\beta+1}$, the following equations are obtained by use of the corresponding functions $x_o(q,\theta)$, $y_o(q,\theta)$, and $\varphi_o(q,\theta)$ of the similar incompressible flow:

$$x(q,\theta) = x_1(q,\theta) + x_2(q,\theta) + x_3(q,\theta) \tag{142}$$

$$y(q,\theta) = y_1(q,\theta) + y_2(q,\theta) + y_3(q,\theta) \tag{143}$$

Here $x_1(q,\theta)$ and $y_1(q,\theta)$ are given respectively by equations (132) and (133), except that $X(q,\theta)$ is replaced by $x(q,\theta) + A_o(\pi - \theta)$, and $x_2(q,\theta)$ and $y_2(q,\theta)$ are given by

$$x_2(q,\theta) = \frac{(1-\tau)^{-\beta}}{q}\left\{\sum_0^\infty \left[\frac{\nu B_n}{\nu-1}H_\nu(\tau)q^\nu \sin(\nu-1)\theta - \frac{\nu C_n}{\nu+1}H_{-\nu}(\tau)q^{-\nu}\sin(\nu+1)\theta\right]\right.$$
$$\left. - \beta\tau \sum_0^\infty \left[B_n H_{\nu,1}(\tau)q^\nu - C_n H_{-\nu,1}(\tau)q^{-\nu}\right]\left(\sin\nu\theta\cos\theta - \frac{\cos\nu\theta\sin\theta}{\nu}\right)\right\} \tag{144}$$

$$y_2(q,\theta) = \frac{(1-\tau)^{-\beta}}{q}\left\{\sum_0^\infty \left[\frac{\nu B_n}{\nu-1}H_\nu(\tau)q^\nu \cos(\nu-1)\theta + \frac{\nu C_n}{\nu+1}H_{-\nu}(\tau)q^{-\nu}\cos(\nu+1)\theta\right]\right.$$
$$\left. - \beta\tau \sum_0^\infty \left[B_n H_{\nu,1}(\tau)q^\nu - C_n H_{-\nu,1}(\tau)q^{-\nu}\right]\left(\sin\nu\theta\sin\theta + \frac{\cos\nu\theta\cos\theta}{\nu}\right)\right\} \tag{145}$$

where $H_\nu(\tau)$ and $H_{-\nu}(\tau)$ are the same as those defined by equation (118), and $H_{\nu,1}(\tau)$ and $H_{-\nu,1}(\tau)$ denote

$$\left.\begin{aligned} H_{\nu,1}(\tau) &= F_{\nu,1}(\tau)\Delta\frac{\nu^2 F_\nu^{-1}(\tau_1)}{\nu^2-1} + \frac{\Delta F_{\nu,1}(\tau)}{f(\tau_1)T^\nu(\tau_1)} \\ H_{-\nu,1}(\tau) &= F_{-\nu,1}\Delta\frac{\nu^2 F_{-\nu}^{-1}(\tau_1)}{\nu^2-1} + \frac{\Delta F_{-\nu,1}(\tau)}{f(\tau_1)T^\nu(\tau_1)} \end{aligned}\right\} \tag{146}$$

On the other hand, for $1 < q < V$ but $\frac{1}{2\beta + 1} < \tau < \tau_1 V^2$, the dominant terms of the hypergeometric functions, by expressions (226), (227), (233), and (234), are

$$F_\nu(\tau) \sim f(\tau)T^\nu \cos\left(\nu\omega - \frac{\pi}{4}\right)$$

$$F_{-\nu}(\tau) \sim \frac{1}{2}f(\tau)T^{-\nu} \cos\left(\nu\omega + \frac{\pi}{4}\right)$$

$$F_{\nu,1}(\tau) \sim g(\tau)T^\nu \cos\left(\nu\omega - \mu^o - \frac{\pi}{4}\right)$$

$$F_{-\nu,1}(\tau) \sim \frac{1}{2}g(\tau)T^{-\nu} \cos\left(\nu\omega + \mu^o + \frac{\pi}{4}\right)$$

By substituting these expressions for the corresponding hypergeometric functions and resolving the products such as

$$2 \cos\left(\nu\omega - \frac{\pi}{4}\right) \sin(\nu - 1)\theta = \sin\left[(\nu - 1)\xi - \left(\frac{\pi}{4} - \omega\right)\right] + \sin\left[(\nu + 1)\eta + \left(\frac{\pi}{4} - \omega\right)\right]$$

$$2 \sin\nu\theta \cos\left(\nu\omega - \mu^o - \frac{\pi}{4}\right) = \sin\left(\nu\xi - \mu^o - \frac{\pi}{4}\right) + \sin\left(\nu\eta + \mu^o + \frac{\pi}{4}\right)$$

into sums, a lengthy but straightforward reduction by means of the known identities, for example:

$$x_o(q,\theta) = \sum_0^\infty \left[\frac{\nu B_n}{\nu - 1}q^{\nu-1} \sin(\nu - 1)\theta - \frac{\nu C_n}{\nu + 1}q^{-\nu-1} \sin(\nu + 1)\theta\right]$$

$$y_o(q,\theta) = \sum_0^\infty \left[\frac{\nu B_n}{\nu - 1}q^{\nu-1} \cos(\nu - 1)\theta + \frac{\nu C_n}{\nu + 1}q^{-\nu-1} \cos(\nu + 1)\theta\right]$$

gives

$$x(q,\theta) = x_1(q,\theta) + x_2(q,\theta) + x_3(q,\theta) \tag{147}$$

$$y(q,\theta) = y_1(q,\theta) + y_2(q,\theta) + y_3(q,\theta) \tag{148}$$

Here $x_3(q,\theta)$ and $y_3(q,\theta)$ retain their definitions, and

$$x_1(q,\theta) = \frac{(1-\tau)^{-\beta} f(\tau) t(\tau)}{4 f(\tau_1)} \left\{ \left[x_o(\lambda,\xi) + x_o(\lambda,\eta) \right] \cos\left(\frac{\pi}{4} - \omega\right) - \left[y_o(\lambda,\xi) - y_o(\lambda,\eta) \right] \sin\left(\frac{\pi}{4} - \omega\right) \right.$$

$$\left. - \frac{\beta\tau}{\lambda} \frac{g(\tau)}{f(\tau_1)} \left[\Phi(q,\theta) \cos\theta - \Psi(q,\theta) \sin\theta \right] \right\} \tag{149}$$

$$y_1(q,\theta) = \frac{(1-\tau)^{-\beta} f(\tau) t(\tau)}{4 f(\tau_1)} \left\{ \left[y_o(\lambda,\xi) + y_o(\lambda,\eta) \right] \cos\left(\frac{\pi}{4} - \omega\right) + \left[x_o(\lambda,\xi) - x_o(\lambda,\eta) \right] \sin\left(\frac{\pi}{4} - \omega\right) \right.$$

$$\left. - \frac{\beta\tau}{\lambda} \frac{g(\tau)}{f(\tau_1)} \left[\Phi(q,\theta) \sin\theta + \Psi(q,\theta) \cos\theta \right] \right\} \tag{150}$$

where

$$\Phi(q,\theta) = \left[\varphi_o(\lambda,\xi) + \varphi_o(\lambda,\eta) \right] \cos\left(\mu^o + \frac{\pi}{4}\right) - \left[\psi_o(\lambda,\xi) - \psi_o(\lambda,\eta) \right] \sin\left(\mu^o + \frac{\pi}{4}\right) \tag{151}$$

$$\Psi(q,\theta) = \left[\chi(\lambda,\xi) + \chi(\lambda,\eta) + 2A_o(\pi - \theta) \right] \cos\left(\mu^o + \frac{\pi}{4}\right) + \left[\sigma(\lambda,\xi) - \sigma(\lambda,\eta) \right] \sin\left(\mu^o + \frac{\pi}{4}\right) \tag{152}$$

Again $x_2(q,\theta)$ and $y_2(q,\theta)$ are defined by equations (144) and (145), but the differences of the hypergeometric functions involved in $H_{\pm\nu}(\tau)$ and $H_{\pm\nu,1}(\tau)$ are now

$$\Delta F_{\pm\nu}(\tau) = F_{\pm\nu}(\tau) - \frac{f(\tau)}{2} T^{\pm\nu} \cos\left(\nu\omega \mp \frac{\pi}{4}\right)$$

$$\frac{1}{2\beta + 1} < \tau < 1$$

$$\Delta F_{\pm\nu,1}(\tau) = F_{\pm\nu,1}(\tau) - \frac{g(\tau)}{2} T^{\pm\nu} \cos\left(\nu\omega \mp \mu\rho \mp \frac{\pi}{4}\right)$$

Improvement of Convergence of $\tilde{A}_n$, $\tilde{D}_n$, and x_{in}

As seen from part II, as soon as the function $\psi_o(q,\theta)$ is specified, the coefficients of the inside and outside series can be chosen so as to make the conditions of continuity sufficient for the sets of unknown constants, for example, $\tilde{A}_n$ and $\tilde{D}_n$, to be determined. Inasmuch as the conditions are applied at the circle of convergence, it is generally very tedious to evaluate $\tilde{A}_n$ and $\tilde{D}_n$ from the slowly convergent series (equations (54) and (55)) when B_n and C_n are given. In order to bring these expressions to manageable forms, the following procedure can be used.

By considering the function $\psi_o(q,\theta)$ the following identities (appendix F) for $n > 1$ can be deduced without difficulty

$$A_n = \frac{1}{\pi} \int_0^\infty (B_m + C_m) I_{n\mu} \tag{153}$$

$$nA_n = \frac{1}{\pi} \int_0^\infty \mu(B_m - C_m) I_{n\mu} \tag{154}$$

$$\frac{A_n}{n} = \frac{1}{\pi} \int_0^\infty \frac{1}{\mu}(B_m - C_m) I_{n\mu} + \frac{4}{n} \tag{155}$$

Furthermore, the sum on the right-hand side of the second expression of equation (52) can be written as

$$\frac{1}{\pi}\sum_{0}^{\infty}\mu\left[B_m\xi_\mu(\tau_1)+C_m\xi_{-\mu}(\tau_1)\right]I_{n\mu}=\frac{1}{\pi}\sum_{0}^{\infty}\mu\left[B_m\tilde{\xi}_\mu(\tau_1)+C_m\tilde{\xi}_{-\mu}(\tau_1)\right]I_{n\mu}$$

$$+\frac{1}{\pi}\sum_{0}^{\infty}\mu\left[B_m\,\Delta\xi_\mu(\tau_1)+C_m\,\Delta\xi_{-\mu}(\tau_1)\right]I_{n\mu}$$

where, according to expressions (243) and (244), $\tilde{\xi}_{\pm\mu}(\tau_1)=\pm\xi_0(\tau_1)+\frac{\xi^{(1)}(\tau)}{\mu}\pm\frac{\xi^{(2)}(\tau_1)}{\mu^2}$ and

$$\Delta\xi_{\pm\mu}(\tau_1)=\tilde{\xi}_{\pm\mu}(\tau_1)-\tilde{\xi}_{\pm\mu}(\tau_1) \tag{156}$$

Then from equations (153), (154), and (155) it follows that

$$\frac{1}{\pi}\sum_{0}^{\infty}\mu\left[B_m\xi_\mu(\tau_1)+C_m\xi_{-\mu}(\tau_1)\right]I_{n\mu}=nA_n\tilde{\xi}_n(\tau_1)-\frac{4\xi^{(2)}(\tau_1)}{n}+\sigma_n \tag{157}$$

where

$$\sigma_n=\frac{1}{\pi}\sum_{0}^{\infty}\mu\left[B_m\Delta\xi_\mu(\tau_1)+C_m\Delta\xi_{-\mu}(\tau_1)\right]I_{n\mu} \tag{158}$$

Now by expressions (243) and (244) $\Delta\xi_{\pm\mu}\sim\mu^{-3}$; σ_n converges like $\mu^{-7/2}$ if C_m is of the order $m^{-1/2}$. From equation (157), equations (54) and (55) become

$$\bar{A}_n=\frac{1}{\xi_n(\tau_1)-\xi_{-n}(\tau_1)}\left\{\left[\tilde{\xi}_n(\tau_1)-\xi_{-n}(\tau_1)\right]A_n-\frac{1}{n}\left[2\tilde{D}_0\xi_{-n}(\tau_1)-\sigma_n\right]-\frac{4\xi^{(2)}(\tau_1)}{n^2}\right\} \tag{159}$$

$$\tilde{D}_n = \frac{1}{\xi_n(\tau_1) - \xi_{-n}(\tau_1)} \left\{ \frac{1}{n}\left[2\tilde{D}_0 \xi_n(\tau_1) - \sigma_n\right] + \frac{4\xi^{(2)}(\tau_1)}{n^2} + A_n \Delta\xi_n(\tau_1) \right\} \tag{160}$$

Another important constant in connection with the present problem is the major axis x_{in}, or the half-chord of the body. As shown in equation (95) it was also given in terms of slowly convergent series. In order to transform the series, it should be recalled that for the similar imcompressible flow the half-chord is

$$x_{in}(o) = \frac{1}{2\pi} \left\{ \sum_0^\infty \nu(B_n - C_n) \left[\frac{1}{(\nu - 1)^2} + \frac{1}{(\nu + 1)^2} \right] + \sum_0^\infty \nu(B_n + C_n) \left[\frac{1}{(\nu - 1)^2} - \frac{1}{(\nu + 1)^2} \right] \right\} \tag{161}$$

Then, by replacing $\xi_{\pm\nu}(\tau_1)$ by $\pm 1 \mp \beta\tau \dfrac{F_{\pm\nu,1}(\tau_1)}{F_{\pm\nu}(\tau_1)}$, respectively, it follows in the first place that

$$x_{in} = (1 - \tau_1)^{-\beta} \left\{ x_{in}(o) - \frac{\beta\tau_1}{2\pi} \sum_0^\infty \nu \left[B_n F_{\nu,1}^{(r)}(\tau_1) - C_n F_{-\nu,1}^{(r)} \right] \left[\frac{1}{(\nu - 1)^2} + \frac{1}{(\nu + 1)^2} \right] \right\} + x_{out} \tag{162}$$

Furthermore, by writing

$$\sum_0^\infty \nu \left[B_n F_{\nu,1}^{(r)} - C_n F_{-\nu,1}^{(r)} \right] \left[\frac{1}{(\nu - 1)^2} + \frac{1}{(\nu + 1)^2} \right] = \frac{g(\tau_1)}{f(\tau_1)} \sum_0^\infty \nu(B_n - C_n) \left[\frac{1}{(\nu - 1)^2} + \frac{1}{(\nu + 1)^2} \right]$$
$$+ \sum_0^\infty \nu \left[B_n \Delta F_{\nu,1}^{(r)} - C_n \Delta F_{-\nu,1}^{(r)} \right] \left[\frac{1}{(\nu - 1)^2} + \frac{1}{(\nu + 1)^2} \right]$$

where

$$\Delta F_{\nu,1}{}^{(r)}(\tau_1) = \frac{F_{\nu,1}(\tau_1)}{F_\nu(\tau_1)} - \frac{g(\tau_1)}{f(\tau_1)}$$

$$\Delta F_{-\nu,1}{}^{(r)}(\tau_1) = \frac{F_{-\nu,1}(\tau_1)}{F_{-\nu}(\tau_1)} - \frac{g(\tau_1)}{f(\tau_1)}$$

with equation (161), the following equation is obtained:

$$x_{in} = (1 - \tau_1)^{-\beta}\left\{ x_{in}(o)\left[1 - \frac{\beta\tau_1 g(\tau_1)}{f(\tau_1)}\right] + \frac{\beta\tau_1}{2\pi}\,\frac{g(\tau_1)}{f(\tau_1)} \sum_0^\infty \nu(B_n + C_n)\left[\frac{1}{(\nu-1)^2} - \frac{1}{(\nu+1)^2}\right]\right.$$
$$\left. - \sum_0^\infty \nu\left[B_n \Delta F_{\nu,1}{}^{(r)} - C_n \Delta F_{-\nu,1}{}^{(r)}\right]\left[\frac{1}{(\nu-1)^2} + \frac{1}{(\nu+1)^2}\right]\right\} + x_{out} \qquad (163)$$

Since $\Delta F_{\pm\nu,1}{}^{(r)}(\tau_1) = O\left(\frac{1}{\nu}\right)$, it is easy to see that both series now converge as $\nu^{-5/2}$. Because of the fact that $\beta\tau_1 << 1$, however, the contribution due to both series is generally small.

IV - APPLICATION TO CASE OF ELLIPTIC CYLINDER

The Functions $z_o(w)$, $W_o(w)$, and $\Lambda(w)$

An irrotational flow of an incompressible fluid about an elliptic cylinder with a circulation Γ_o is represented by the complex potential $W_o(z_o)$.

$$W_o(z_o) = \zeta + \frac{1}{\zeta} + \frac{i\Gamma_o}{2\pi} \log_e \zeta \quad \text{with} \quad z_o = \zeta + \frac{\epsilon^2}{\zeta} \tag{164}$$

where the flow at infinity is assumed to be parallel to the major axis of the cylinder. Here all the quantities have been rendered dimensionless by normalizing ζ by a length a and $W_o(z_o)$, by Ua. Then the major and minor axes are, respectively, $1 + \epsilon^2$ and $1 - \epsilon^2$, where $\epsilon^2 < 1$.

By differentiating equation (164) with respect to z_o, the dimensionless complex velocity of the flow is obtained, namely,

$$w = \frac{\zeta^2 + \frac{i\Gamma_o}{2\pi}\zeta - 1}{\zeta^2 - \epsilon^2}$$

the inverse solution of which is

$$\zeta(w) = -\frac{\frac{i\Gamma_o}{2\pi} + \left[4(1-w)(1-\epsilon^2 w) - \frac{\Gamma_o^2}{4\pi^2}\right]^{1/2}}{2(1-w)} \tag{165}$$

This function is two-valued with two simple branch points at $w = 1 + O(\Gamma_o^2)$ and $w = \epsilon^{-2} + O(\Gamma_o^2)$, namely, $V = \epsilon^{-2} + O(\Gamma_o^2)$. (See section entitled "Analytic Continuation of Solution (Branch Point of Order 1).") The principal value may be defined by the convention that $-\pi < \arg(1-w) < \pi$ and $1 < |w| < \epsilon^{-2}$ with a cut joining the two branch points. With the principal value so chosen, the domain wherein the real part of z_o is less than or equal to 0, excluding the interior of the body, corresponds uniquely to the hodograph given by $W(z_o)$ or, conversely, on account of symmetry, the domain wherein the real part of z_o is greater than or equal to 0 will correspond to the second branch of the function $\zeta(w)$.

By substituting $\zeta(w)$ in equations (165) and (164), an expansion regarding $\frac{\Gamma_o}{4\pi}$ as a small parameter gives in accordance with equations (35) and (36), provided that $\frac{\Gamma_o}{4\pi} \ll 1$,

$$z_o^{(o)}(w) = -\left[\left(\frac{1-\epsilon^2 w}{1-w}\right)^{1/2} + \epsilon^2\left(\frac{1-w}{1-\epsilon^2 w}\right)^{1/2}\right] \tag{166}$$

$$W_o^{(o)}(w) = -\left[\left(\frac{1-\epsilon^2 w}{1-w}\right)^{1/2} + \left(\frac{1-w}{1-\epsilon^2 w}\right)^{1/2}\right] \tag{167}$$

$$z_o^{(1)}(w) = -i\left(\frac{1}{1-w} - \frac{\epsilon^2}{1-\epsilon^2 w}\right) \tag{168}$$

$$W_o^{(1)}(w) = -i\left[\frac{1}{1-w} + \log_e(1-w) - \frac{1}{1-\epsilon^2 w} - \log_e(1-\epsilon^2 w) - 2\pi i\right] \tag{169}$$

The functions $z_o^{(o)}(w)$ and $W_o^{(o)}(w)$ are the transition function and the complex potential, respectively, for zero circulation (compare reference 1); and $z_o^{(1)}(w)$ and $W_o^{(1)}(w)$ represent the first-order contributions, due to circulation, to $z_o(w)$ and $W_o(w)$, respectively. On separating into real and imaginary parts, it was found that from $z_o^{(o)}(w)$ and $W_o^{(o)}(w)$ there result

$$x_o^{(o)}(q,\theta) = -\frac{1}{\sqrt{2}}\left\{\left[I(q,\theta) + J(q,\theta)\right]^{1/2} + \epsilon^2\left[I_\epsilon + J^{-1}(q,\theta)\right]^{1/2}\right\} \tag{170}$$

$$y_o^{(o)}(q,\theta) = \frac{1}{\sqrt{2}}\left\{\left[-I(q,\theta) + J(q,\theta)\right]^{1/2} - \epsilon^2\left[-I_\epsilon + J^{-1}(q,\theta)\right]^{1/2}\right\} \tag{171}$$

and

$$\varphi_o^{(o)}(q,\theta) = -\frac{1}{\sqrt{2}}\left\{\left[I(q,\theta) + J(q,\theta)\right]^{1/2} + \left[I_\epsilon + J^{-1}(q,\theta)\right]^{1/2}\right\} \tag{172}$$

$$\psi_o^{(o)}(q,\theta) = \frac{1}{\sqrt{2}}\left\{\left[-I(q,\theta) + J(q,\theta)\right]^{1/2} - \left[-I_\epsilon(q,\theta) + J^{-1}(q,\theta)\right]^{1/2}\right\} \tag{173}$$

where

$$I(q,\theta) = \frac{1-(1+\epsilon^2)q\cos\theta + \epsilon^2 q^2}{1-2q\cos\theta + q^2} \tag{174}$$

$$I_\epsilon(q,\theta) = \frac{1 - (1+\epsilon^2)q\cos\theta + \epsilon^2 q^2}{1 - 2\epsilon^2 q\cos\theta + \epsilon^4 q^2} \tag{175}$$

$$J(q,\theta) = \left(\frac{1 - 2\epsilon^2 q\cos\theta + \epsilon^4 q^2}{1 - 2q\cos\theta + q^2}\right)^{1/2} \tag{176}$$

Similarly, from $z_o^{(1)}(w)$ and $W_o^{(1)}(w)$,

$$x_o^{(1)}(q,\theta) = -\frac{q\sin\theta}{1 - 2q\cos\theta + q^2} + \frac{\epsilon^4 q\sin\theta}{1 - 2\epsilon^2 q\cos\theta + \epsilon^4 q^2} \tag{177}$$

$$y_o^{(1)}(q,\theta) = -\frac{1 - q\cos\theta}{1 - 2q\cos\theta + q^2} + \frac{\epsilon^2(1 - \epsilon^2 q\cos\theta)}{1 - 2\epsilon^2 q\cos\theta + \epsilon^4 q^2} \tag{178}$$

and, if $q < 1$,

$$\left.\begin{aligned}\varphi_o^{(1)}(q,\theta) = &-\frac{q\sin\theta}{1 - 2q\cos\theta + q^2} + \frac{\epsilon^2 q\sin\theta}{1 - 2\epsilon^2 q\cos\theta + \epsilon^4 q^2} + \tan^{-1}\frac{q\sin\theta}{1 - q\cos\theta} \\ &- \tan^{-1}\frac{\epsilon^2 q\sin\theta}{1 - \epsilon^2 q\cos\theta} - 2\pi\end{aligned}\right\} \tag{179}$$

or, if $q > 1$,

$$\left.\begin{aligned}\varphi_o^{(1)}(q,\theta) = &-\frac{q\sin\theta}{1 - 2q\cos\theta + q^2} + \frac{\epsilon^2 q\sin\theta}{1 - 2\epsilon^2 q\cos\theta + \epsilon^4 q^2} + \tan^{-1}\frac{q^{-1}\sin\theta}{1 - q^{-1}\cos\theta} \\ &- \tan^{-1}\frac{\epsilon^2 q\sin\theta}{1 - \epsilon^2 q\cos\theta} - (\pi - \theta)\end{aligned}\right\}$$

$$\psi_o^{(1)}(q,\theta) = -\frac{1 - q\cos\theta}{1 - 2q\cos\theta + q^2} + \frac{1 - \epsilon^2 q\cos\theta}{1 - 2\epsilon^2 q\cos\theta + \epsilon^4 q^2} - \frac{1}{2}\log_e(1 - 2q\cos\theta + q^2)$$

$$+ \frac{1}{2}\log_e(1 - 2\epsilon^2 q\cos\theta + \epsilon^4 q^2) \qquad (180)$$

From appendix F, the function $\Lambda(w)$ is defined by

$$\Lambda(w) = \int_0^w \left[W_o^{(o)}(w) + A_o\right]\frac{dw}{w}$$

where the constant A_o is 2, from equation (172). By substituting the function $W_o^{(o)}(w)$ from equation (167), the integration yields

$$\Lambda(w) = -\frac{2(1+\epsilon^2)}{\epsilon}\log_e\frac{(1-\epsilon^2 w)^{1/2} + \epsilon(1-w)^{1/2}}{1+\epsilon} + 4\log_e\frac{(1-\epsilon^2 w)^{1/2} + (1-w)^{1/2}}{2} \qquad (181)$$

On separating again into real and imaginary parts, it was found that

$$\sigma(q,\theta) = -\frac{1+\epsilon^2}{\epsilon}\log_e\frac{1}{2(1+\epsilon)^2}\left[(K_\epsilon + \epsilon K)^2 + (\tilde{K}_\epsilon + \epsilon\tilde{K})^2\right]$$

$$+ 2\log_e\frac{1}{8}\left[(K_\epsilon + K)^2 + (\tilde{K}_\epsilon + \tilde{K})^2\right] \qquad (182)$$

$$\chi(q,\theta) = -\frac{2(1+\epsilon^2)}{\epsilon}\tan^{-1}\frac{\tilde{K}_\epsilon + \epsilon\tilde{K}}{K_\epsilon + \epsilon K} + 4\tan^{-1}\frac{\tilde{K}_\epsilon + \tilde{K}}{K_\epsilon + K} \qquad (183)$$

where

$$K(q,\theta) = \left[(1 - 2q\cos\theta + q^2)^{1/2} + 1 - q\cos\theta\right]^{1/2} \qquad (184)$$

$$K_\epsilon(q,\theta) = \left[(1 - 2\epsilon^2 q\cos\theta + \epsilon^4 q^2)^{1/2} + 1 - \epsilon^2 q\cos\theta\right]^{1/2} \qquad (185)$$

$$\mathfrak{K}(q,\theta) = \left[(1 - 2q\cos\theta + q^2)^{1/2} - 1 + q\cos\theta\right]^{1/2} \qquad (186)$$

$$\mathfrak{K}_\epsilon(q,\theta) = \left[(1 - 2\epsilon^2 q\cos\theta + \epsilon^4 q^2)^{1/2} - 1 + \epsilon^2 q\cos\theta\right]^{1/2} \qquad (187)$$

Expansions of $W_o(w)$ and $z_o(w)$

As the domain considered is complex and has two singularities at $w = 1$ and $w = \epsilon^{-2}$, the function $W_o^{(o)}(w)$ defined by equation (167) is single-valued and continuous in $|w| < 1$ but is discontinuous across the cut in $1 < |w| < \epsilon^{-2}$. The expansions, as shown in reference 8, are

$$W_o^{(o)}(w) = -\sum_0^\infty A_n w^n \qquad |w| < 1 \qquad (188)$$

and

$$W_o^{(o)}(w) = i\sum_0^\infty (B_n w^\nu + C_n w^{-\nu}) \qquad 1 < |w| < \epsilon^{-2} \qquad (189)$$

where the coefficients are all real and are defined by

$$A_n = 2S_n^{(i)} - (1 + \epsilon^2)S_{n-1}^{(i)} \qquad n > 1 \qquad (190)$$

$$A_o = 2S_o^{(i)} = 2$$

$$A_1 = 0$$

with

$$S_n^{(i)} = \frac{1}{\pi}\sum_0^n \frac{\Gamma\left(n - m + \frac{1}{2}\right)\Gamma\left(m + \frac{1}{2}\right)}{\Gamma(n - m + 1)\Gamma(m + 1)}\,\epsilon^{2m} \qquad (191)$$

and

$$B_n = \left[2\epsilon^2 S_{n+1}^{(o)} - (1 + \epsilon^2)S_n^{(o)}\right]\epsilon^{2n} \qquad (192)$$

$$C_n = 2S_n^{(o)} - (1 + \epsilon^2)S_{n+1}^{(o)} \tag{193}$$

with

$$S_n^{(o)} = \frac{1}{\pi}\sum_{0}^{\infty} \frac{\Gamma\left(n + m + \frac{1}{2}\right)\Gamma\left(m + \frac{1}{2}\right)}{\Gamma(n + m + 1)\Gamma(m + 1)} \epsilon^{2m} \tag{194}$$

Similarly, the function $W_o^{(1)}(w)$, as defined by equation (169), can be easily expanded. It is, for $|w| < 1$,

$$W_o^{(1)}(w) = i\left(-\sum_{0}^{\infty} w^n + \sum_{1}^{\infty} \frac{w^n}{n} + \sum_{0}^{\infty} \epsilon^{2n} w^n - \sum_{1}^{\infty} \frac{\epsilon^{2n} w^n}{n}\right) - 2\pi \tag{195}$$

and, for $1 < |w| < \epsilon^{-2}$,

$$W_o^{(1)}(w) = i\left[\sum_{1}^{\infty} w^{-n} + \sum_{1}^{\infty} \frac{w^{-n}}{n} + \sum_{0}^{\infty} \epsilon^{2n} w^n - \sum_{1}^{\infty} \frac{\epsilon^{2n} w^n}{n} - \log_e q + i(\pi + \theta)\right] \tag{196}$$

By separating into real and imaginary parts, the following equations are obtained from $W_o^{(o)}(w)$:

$$\varphi_o^{(o)}(q,\theta) = -\sum_{2}^{\infty} A_n q^n \cos n\theta - 2 \tag{197}$$

$q < 1$

$$\psi_o^{(o)}(q,\theta) = \sum_{2}^{\infty} A_n q^n \sin n\theta \tag{198}$$

and

$$\varphi_o^{(o)}(q,\theta) = \sum_{0}^{\infty} \left(B_n q^{\nu} - C_n q^{-\nu}\right) \sin \nu\theta \tag{199}$$

$$\psi_o^{(o)}(q,\theta) = \sum_{0}^{\infty} (B_n q^{\nu} + C_n q^{-\nu}) \cos \nu\theta \qquad 1 < q < \epsilon^{-2} \qquad (200)$$

Similarly, from $W_o^{(1)}(w)$, the result is

$$\varphi_o^{(1)}(q,\theta) = -\sum_{2}^{\infty} A_n^{(1)} q^n \sin n\theta - 2\pi \qquad (201)$$

$$q < 1$$

$$\psi_o^{(1)}(q,\theta) = -\sum_{2}^{\infty} A_n^{(1)} q^n \cos n\theta \qquad (202)$$

where the coefficient $A_n^{(1)}$ is given by

$$A_n^{(1)} = \left(1 - \frac{1}{n}\right)\left(1 - \epsilon^{2n}\right) \qquad (203)$$

and

$$\varphi_o^{(1)}(q,\theta) = \sum_{1}^{\infty} \left[B_n^{(1)} q^n - C_n^{(1)} q^{-n}\right] \sin n\theta - (\pi + \theta) \qquad (204)$$

$$\psi_o^{(1)}(q,\theta) = \sum_{1}^{\infty} \left[B_n^{(1)} q^n + C_n^{(1)} q^{-n}\right] \cos n\theta - \log_e q + 1 \qquad (205)$$

where

$$B_n^{(1)} = \left(1 - \frac{1}{n}\right)\epsilon^{2n} \qquad (206)$$

$$C_n^{(1)} = 1 + \frac{1}{n} \qquad (207)$$

The expansion of $z_o(w)$ can be carried out in like manner, but it was found simpler to deduce it directly from equation (37). Then, corresponding to $W_o^{(o)}(w)$ defined by equations (188) and (189), $z_o^{(o)}(w)$ is

$$z_o^{(o)}(w) = -\sum_{2}^{\infty} \frac{nA_n}{n-1} w^n - (1 + \epsilon^2) \qquad |w| < 1 \qquad (208)$$

and

$$z_o^{(o)}(w) = i \sum_{0}^{\infty} \left(\frac{\nu B_n}{\nu - 1} w^{\nu-1} + \frac{\nu C_n}{\nu + 1} w^{-\nu-1} \right) \qquad 1 < |w| < \epsilon^{-2} \qquad (209)$$

In determining the constants of integration, use has been made of the fact that $z_o^{(o)}(o) = -(1 + \epsilon^2)$ from equation (77) and that $x_o^{(o)}(q,\theta) = 0$ and $y_o^{(o)}(q,\theta) = -y_o^{(o)}(q,2\pi - \theta)$.

On the other hand, corresponding to $W_o^{(1)}(w)$, $z_o^{(1)}(w)$ is

$$z_o^{(1)}(w) = -i \sum_{2}^{\infty} \frac{nA_n^{(1)}}{n - 1} w^{n-1} - i(1 - \epsilon^2) \qquad |w| < 1 \qquad (210)$$

and

$$z_o^{(1)}(w) = i \sum_{1}^{\infty} \left[\frac{nB_n^{(1)}}{n - 1} w^{n-1} + \frac{nC_n^{(1)}}{n + 1} w^{-n-1} \right] + \frac{i}{w} \qquad 1 < |w| < \epsilon^{-2} \qquad (211)$$

Here again the constants are determined with the aid of equation (168). By separating into real and imaginary parts, the coordinate functions are, for $q < 1$,

$$x_o^{(1)}(q,\theta) = -\sum_{2}^{\infty} \frac{nA_n}{n - 1} q^{n-1} \cos (n - 1)\theta - (1 + \epsilon^2) \qquad (212)$$

$$y_o^{(1)}(q,\theta) = \sum_{2}^{\infty} \frac{nA_n}{n - 1} q^{n-1} \sin (n - 1)\theta \qquad (213)$$

and, for $1 < q < \epsilon^{-2}$,

$$x_o^{(o)}(q,\theta) = -\sum_{0}^{\infty} \left[\frac{\nu B_n}{\nu - 1} q^{\nu-1} \sin (\nu - 1)\theta - \frac{\nu C_n}{\nu + 1} q^{-\nu-1} \sin (\nu + 1)\theta \right] \qquad (214)$$

$$y_o^{(o)}(q,\theta) = \sum_{0}^{\infty} \left[\frac{\nu B_n}{\nu - 1} q^{\nu-1} \cos (\nu - 1)\theta + \frac{\nu C_n}{\nu + 1} q^{-\nu-1} \cos (\nu + 1)\theta \right] \tag{215}$$

Similarly, from equations (210) and (211), for $q < 1$,

$$x_o^{(1)}(q,\theta) = - \sum_{2}^{\infty} \frac{n}{n - 1} A_n^{(1)} q^{n-1} \sin (n - 1)\theta \tag{216}$$

$$y_o^{(1)}(q,\theta) = - \sum_{2}^{\infty} \frac{n}{n - 1} A_n^{(1)} q^{n-1} \cos (n - 1)\theta - (1 - \epsilon^2) \tag{217}$$

and, for $1 < q < \epsilon^{-2}$,

$$x_o^{(1)}(q,\theta) = \sum_{1}^{\infty} \left[\frac{nB_n^{(1)}}{n - 1} q^{n-1} \sin (n - 1)\theta - \frac{nC_n^{(1)}}{n + 1} q^{-n-1} \sin (n + 1)\theta \right] - \frac{\sin \theta}{q} \tag{218}$$

$$y_o^{(1)}(q,\theta) = \sum_{1}^{\infty} \left[\frac{nB_n^{(1)}}{n - 1} q^{n-1} \cos (n - 1)\theta + \frac{nC_n^{(1)}}{n + 1} q^{-n-1} \cos (n + 1)\theta \right] + \frac{\cos \theta}{q} \tag{219}$$

where the first term in equation (219) gives rise to a constant ϵ^2 due to the definition of $B_n^{(1)}$.

Numerical Results and Discussion

In order to conclude this report, two numerical examples are presented for the purpose of testing the effectiveness of the method, of giving a general idea of the result that might be expected from a given similar incompressible flow, and, as far as possible, of evaluating the compressibility effects.

By taking $\epsilon = \frac{1}{2}$ and $M_1 = 0.60$, M_1 being the free-stream Mach number, the compressible flow without circulation is shown in figures 2 and 3 in both the τ,θ- and the x,y-planes. The flow is everywhere continuous and the highest Mach number attained at the central section is 1.24. The profile calculated in this case is symmetrical but is far different from the ellipse from which it was derived. The thickness ratio is 1:2 as compared with 3:5 of the original elliptic section. The lateral distortion thus is much more pronounced than that suffered by the longitudinal dimension. The characteristic feature in the case of transonic flows is that the central portion of the derived body where the flow is supersonic is always flat in comparison with the original body.

In order to exhibit the compressiblity effect, the corresponding problem of the incompressible flow over the same body must be solved. Technically, this does not offer any difficulty. However, in order to simplify the numerical work, an incompressible flow resulting from a superposition of a parallel flow on a source-sink combination has been considered. It gives rise to a body which, by adjusting the strength of and the distance between the source and sink, approximates closely the given body with an error of about 2 or 3 percent. (Compare fig. 3.) The pressure distributions over the same body for both compressible and incompressible fluids are compared in figure 4. The results calculated according to the Von Kármán-Tsien and the Glauert-Prandtl formulas are also given.

The wide disagreement between the exact and approximate curves serves as a proof that in the case of transonic flows the thickness effect of the body is no longer secondary and cannot be ignored entirely, as is done in both approximate formulas. The immediate cause for these discrepancies seems to be the fact that the point of equal pressure on the surface of the body in the case of compressible and incompressible fluids does not correspond with that of the free-stream pressure. This deviation has, in fact, been observed even in the case of subsonic flow about a Joukowski airfoil of thickness ratio 0.15 (reference 9). The reason is that the flow of a compressible fluid over a body is partly compressive and partly expansive. By increasing the free-stream Mach number, the speed of the flow in the neighborhood of the stagnation point tends to decrease and the speed far away from the stagnation point, that is, in the supersonic region, to increase. The hodograph corresponding to the zero streamline then becomes longer and flatter as the free-stream Mach number increases. Consequently, the point of intersection of the compressible and incompressible hodographs will shift toward the small inclination of the velocity vector, that is, away from the stagnation point. This effect will be more pronounced for larger thickness ratio as well as Mach number.

The general applicability of the Von Kármán-Tsien formula has been questioned and examined by Tsien and A. Fejer (reference 10) from purely geometric considerations, and the limitations therein raised seem to be further substantiated by the present result. The question, however, remains to be answered as to whether critical conditions for

the validity of the Von Kármán–Tsien theory could be given in terms of the thickness ratio and Mach number. From the practical point of view establishment of such conditions would constitute a result of major importance.

For the case of circulatory flow, $\frac{\Gamma_0}{4\pi}$ is taken to be 0.05. Here, for simplicity's sake, $A_0^{(1)} = 1$ and $B_0^{(1)} = (1 - \tau_1)^{-\beta}$ by equation (69), so that the circulation of the compressible flow is $(1 - \tau_1)^{-\beta}\Gamma_0$, according to equation (74). The constant $C_0^{(1)}$ could have been determined by successive approximations, but in this particular case it is small enough to be neglected. The calculated flow pattern is shown in figures 5 and 6 for both planes. The body, as expected, is unsymmetrical with a negative camber of about 2 percent. The highest Mach number reached at the upper surface is 1.33 and that at the lower surface is 1.15.

The lift coefficient is 0.65 corresponding to an angle of attack at zero lift of about 2.2°. For comparsion with the case of incompressible flow, the problem is simplified by considering the incompressible flow over the body resulting from the superposition of a small negative camber on a geometrically similar ellipse of thickness ratio 1:2. The estimated lift coefficient of such a system is approximately 0.45. The ratio of the two coefficients thus is nearly 1.5, which is much higher than the value of 1.25 given by the Glauert–Prandtl formula for the present case. Actually, if the oval shape is considered, the incompressible value of the lift coefficient would have been lower than that obtained, owing to the fact that the central flat portion reduces the speed of the flow and hence leads to a higher pressure. Thus, the ratio of about 1.5 should be regarded as a lower limit.

Guggenheim Aeronautical Laboratory
California Institute of Technology
Pasadina, Calif., September 5, 1946

APPENDIX A

PARTICULAR INTEGRALS OF $\varphi(q,\theta)$

Consider the total differential $d\varphi$ which from equations (10) and (11) is

$$d\varphi = -\frac{\rho_o}{\rho}(1-M^2)\frac{1}{q}\psi_\theta\, dq + \frac{\rho_o}{\rho} q\psi_q\, d\theta$$

If the particular integrals of ψ are given by the first group of expression (24), then

$$d\varphi = -\nu\frac{\rho_o}{\rho}(1-M^2)\frac{\psi_\nu(q)}{q}\begin{Bmatrix}-\sin\nu\theta\\ \cos\nu\theta\end{Bmatrix} dq$$

$$+\frac{\rho_o}{\rho} q\frac{d}{dq}\left[q^\nu F_\nu(\tau)\right]\begin{Bmatrix}\cos\nu\theta\\ \sin\nu\theta\end{Bmatrix} d\theta$$

From equation (13) $\psi_\nu(q)$ can be eliminated as follows:

$$d\varphi = \frac{\partial}{\partial q}\left[\frac{\rho_o}{\rho}q^\nu F_\nu(\tau)\xi_\nu(\tau)\right]\begin{Bmatrix}\sin\nu\theta\\ -\cos\nu\theta\end{Bmatrix} dq$$

$$+\frac{\partial}{\partial\theta}\left[\frac{\rho_o}{\rho}q^\nu F_\nu(\tau)\xi_\nu(\tau)\right]\begin{Bmatrix}\sin\nu\theta\\ -\cos\nu\theta\end{Bmatrix} d\theta$$

The integration therefore gives

$$\varphi = \frac{\rho_o}{\rho}q^\nu F_\nu(\tau)\xi_\nu(\tau)\begin{Bmatrix}\sin\nu\theta\\ -\cos\nu\theta\end{Bmatrix} + \text{Constant} \qquad (220)$$

Similarly, the following equation corresponding to the second group of expression (24) is obtained:

$$\varphi = \frac{\rho_o}{\rho}q^{-\nu} F_{-\nu}(\tau)\xi_{-\nu}(\tau)\begin{Bmatrix}\sin\nu\theta\\ -\cos\nu\theta\end{Bmatrix} + \text{Constant} \qquad (221)$$

APPENDIX B

PROOF OF THEOREM 1

Consider a small neighborhood of $q = 0$ where the hypergeometric functions can be accurately represented by

$$F_n(\tau) = f(\tau)T^n(\tau)\left[1 + \frac{f^{(1)}(\tau)}{n}\right]$$

If the complex potential for the similar incompressible flow is

$$W_o(w) = -\sum_0^\infty A_n w^n \qquad |w| < 1$$

let $W(w,\tau)$ be a new complex potential such that the stream function for the compressible flow is given by

$$\psi(q,\theta) = I_m\left[W(w,\tau)\right]$$

Then $W(w,\tau)$ must be of the form

$$W(w,\tau) = -\frac{f(\tau)}{f(\tau_1)}\left\{\sum_0^\infty A_n(tw)^n + \left[f^{(1)}(\tau) - f^{(1)}(\tau_1)\right]\sum_2^\infty \frac{A_n}{n}(tw)^n\right\} \qquad |w| < 1$$

But it is easily seen that

$$-\sum_2^\infty \frac{A_n}{n}(tw)^n = \int_0^{tw}\left[W_o(w) + A_o\right]\frac{dw}{w}$$

Therefore, $W(w,\tau)$ can be represented by two closed functions

$$W(w,\tau) = \frac{f(\tau)}{f(\tau_1)}\left\{W_o(wt) + \left[f^{(1)}(\tau) - f^{(1)}(\tau_1)\right]\int_0^{tw}\left[W_o(w) + A_o\right]\frac{dw}{w}\right\} \qquad (222)$$

The function represented by the integral, when continued, will give rise to a term $\log_e tw$. No longer is $w = 0$ a regular point; the singularity must be either at $w = 1$ or at origin.

APPENDIX C

ASYMPTOTIC REPRESENTATION OF HYPERGEOMETRIC FUNCTIONS

The asymptotic integration of the hypergeometric equation for a large positive parameter ν has been discussed (reference 8). It was shown that its solutions under this condition are of the exponential type when the variable ν is in the interval $\delta \leq \tau \leq \frac{1}{2\beta + 1} - \delta$, where $\delta > 0$, and of the oscillatory type when τ is in the interval $\frac{1}{2\beta + 1} + \delta \leq \tau \leq 1 - \delta$. The point $\tau = \frac{1}{2\beta + 1}$ is a singularity. Thus, to the first approximation, the hypergeometric functions for the interval are

$$F_\nu(\tau) \sim f(\tau)T^\nu(\tau)\left[1 + O\left(\frac{1}{\nu}\right)\right] \tag{223}$$

$$F_{-\nu}(\tau) \sim f(\tau)T^{-\nu}(\tau)\left[1 + O\left(\frac{1}{\nu}\right)\right] \qquad \nu > N \tag{224}$$

where

$$\left.\begin{aligned} f(\tau) &= (1 - \tau)^{\alpha^2/4}(1 - \alpha^2\tau)^{-1/4} \\ T(\tau) &= \frac{2}{(1 + \alpha)^\alpha}\frac{\left[\alpha(1 - \tau)^{1/2} + (1 - \alpha^2\tau)^{1/2}\right]^\alpha}{(1 - \tau)^{1/2} + (1 - \alpha^2\tau)^{1/2}} \end{aligned}\right\} \tag{225}$$

Here $O\left(\frac{1}{\nu}\right)$ in each case denotes the fact that the term is uniformly of the order of $1/\nu$ when ν is sufficiently large and is a function of $1/\nu$. For the interval $\frac{1}{2\beta + 1} < \tau < 1$, the hypergeometric functions are

$$F_\nu(\tau) \sim f(\tau)T^\nu(\tau)\cos\left(\nu\omega - \frac{\pi}{4}\right)\left[1 + O\left(\frac{1}{\nu}\right)\right] \tag{226}$$

$$F_{-\nu}(\tau) \sim \frac{1}{2}f(\tau)T^{-\nu}(\tau)\cos\left(\nu\omega + \frac{\pi}{4}\right)\left[1 + O\left(\frac{1}{\nu}\right)\right] \tag{227}$$

where

$$\left.\begin{aligned} f(\tau) &= 2(1-\tau)^{\alpha^2/4}(\alpha^2\tau - 1)^{-1/4} \\ T(\tau) &= 2\frac{(2\beta)^{\alpha/2}}{(1+\alpha)^{\alpha}}\frac{1}{\sqrt{2\beta\tau}} \end{aligned}\right\} \tag{228}$$

$$\omega(\tau) = \alpha \tan^{-1}\frac{1}{\alpha}\sqrt{\frac{\alpha^2\tau - 1}{1-\tau}} - \tan^{-1}\sqrt{\frac{\alpha^2\tau - 1}{1-\tau}} \tag{229}$$

The values of $f(\tau)$, $T(\tau)$, and $\omega(\tau)$ are given in table 1. Here the parameter ν may be any positive large number. When it is a large positive integer, these formulas will automatically represent the hypergeometric functions defined by expression (16).

In the respective domains of validity, the asymptotic expansions may be differentiated with respect to τ. To the same order of approximation, it can be shown that for $\nu > N$ in the interval

$$F_{\nu,1}(\tau) \sim g(\tau)T^{\nu}(\tau)\left[1 + O\left(\frac{1}{\nu}\right)\right] \tag{230}$$

$$F_{-\nu,1}(\tau) \sim g(\tau)T^{-\nu}(\tau)\left[1 + O\left(\frac{1}{\nu}\right)\right] \tag{231}$$

where

$$\left.\begin{aligned} g(\tau) &= \frac{2f(\tau)}{(1-\tau)\left[1 + \xi_c(\tau)\right]} \\ \xi_o(\tau) &= \sqrt{\frac{1-\alpha^2\tau}{1-\tau}} \end{aligned}\right\} \tag{232}$$

and in the interval $\frac{1}{2\beta + 1} < \tau < 1$

$$F_{\nu,1}(\tau) \sim g(\tau)T^{\nu}(\tau)\cos\left(\nu\omega - \mu^{o} - \frac{\pi}{4}\right)\left[1 + O\left(\frac{1}{\nu}\right)\right] \tag{233}$$

$$F_{-\nu,1}(\tau) \sim \frac{1}{2}g(\tau)T^{-\nu}(\tau)\cos\left(\nu\omega + \mu^{o} + \frac{\pi}{4}\right)\left[1 + O\left(\frac{1}{\nu}\right)\right] \tag{234}$$

where

$$\left.\begin{aligned} q(\tau) &= \frac{2f(\tau)}{\sqrt{2\beta\tau(1-\tau)}} \\ \mu^{\circ}(\tau) &= \cos^{-1}\sqrt{\frac{1-\tau}{2\beta\tau}} \end{aligned}\right\} \tag{235}$$

Here $F_{\nu,1}(\tau)$ and $F_{-\nu,1}(\tau)$ represent respectively the functions $F(a_\nu + 1, b_\nu + 1; c_\nu + 1; \tau)$ and $F(1 + a_\nu - c_\nu + 1, 1 + b_\nu - c_\nu + 1; 2 - c_\nu + 1; \tau)$. When ν takes integral values n, expressions (231) and (234) will represent asymptotically $F_{-n,1}(\tau)$. The values of $g(\tau)$ and $\mu^{\circ}(\tau)$ are given in table 1.

In practice, a more accurate representation for the functions $F_\nu(\tau)$ and $F_{-\nu}(\tau)$ and their derivatives is often required, especially in the interval $0 \leq \tau < \frac{1}{2\beta + 1}$. The fact that this is the case is quite evident in part III. In order to carry the approximation to the second order, according to the method given in reference 8, a simple evaluation gives

$$F_\nu(\tau) \sim f(\tau)T^\nu(\tau)\left[1 + \frac{f^{(1)}(\tau)}{\nu} + O\left(\frac{1}{\nu^2}\right)\right] \tag{236}$$

$$F_{-\nu}(\tau) \sim f(\tau)T^{-\nu}(\tau)\left[1 - \frac{f^{(1)}(\tau)}{\nu} + O\left(\frac{1}{\nu^2}\right)\right] \qquad 0 \leq \tau < \frac{1}{2\beta + 1} \tag{237}$$

where

$$f^{(1)}(\tau) = \frac{1}{16}\left[\frac{\alpha^2(\alpha^2 + 2)}{\beta}(1 - \xi_o) - \frac{8\beta^2}{\alpha}\log_e\frac{(1-\tau)^{1/2}(\alpha - \xi_o)}{\alpha - 1}\right.$$
$$\left. + \frac{6\beta + 1}{3\beta}\left(\xi_o^{-1} - 1\right) + \frac{10}{3}\left(1 - \xi_o^{-3}\right)\right] \tag{238}$$

Similarly, by differentiation with respect to τ of expressions (236) and (237), the following expressions are obtained:

$$F_{\nu,1}(\tau) \sim g(\tau)T^{\nu}(\tau)\left[1 + \frac{g^{(1)}(\tau)}{\nu} + O\left(\frac{1}{\nu}\right)\right] \qquad (239)$$

$$0 \leq \tau < \frac{1}{2\beta + 1}$$

$$F_{-\nu,1}(\tau) \sim g(\tau)T^{-\nu}(\tau)\left[1 - \frac{g^{(1)}(\tau)}{\nu} + O\left(\frac{1}{\nu}\right)\right] \qquad (240)$$

where

$$g^{(1)}(\tau) = f^{(1)}(\tau) + \frac{\alpha^2}{4\beta}(1 + \xi_0)(1 - \xi_0^{-2}) \qquad (241)$$

By comparison of the values of $f^{(1)}(\tau)$ and $g^{(1)}(\tau)$, the first approximation of $F_{\nu}(\tau)$ and $F_{-\nu}(\tau)$ is seen to be superior to that of $F_{\nu,1}(\tau)$ and $F_{-\nu,1}(\tau)$. The values $f^{(1)}(\tau)$ and $g^{(1)}(\tau)$ are given in table 1.

For $\gamma = 1.405$ and $\nu = n + 1/2$ and $\nu = n$, n being a positive integer, the two groups of functions $F_{\nu}(\tau)$, $F_{-\nu}(\tau)$ and $F_{\nu,1}(\tau)$, $F_{-\nu,1}(\tau)$ with their asymptotic expressions were calculated for values of τ varying from 0 to 0.34 and for values of n from 1 to 10. The results are presented in table 2.

APPENDIX D

ASYMPTOTIC REPRESENTATION FOR $\xi_\nu(\tau)$ AND $\xi_{-\nu}(\tau)$

Next in importance are the functions $\xi_\nu(\tau)$ and $\xi_{-\nu}(\tau)$, defined by equation (29). They are associated with the particular solutions of $\varphi(q,\theta)$, and eventually, through the latter, will appear in the various functions in the problem of compressible flow. As was shown in part II, the whole scheme is based on the stream function $\psi(q,\theta)$, and its determination depends on the efficiency of the determination of the coefficients of the power series representing $\psi(q,\theta)$. In order to facilitate such evaluation, the asymptotic expressions are again powerful tools. In deriving these expansions, it is also convenient to start from the differential equation for $\xi_\nu(\tau)$ which, from equation (13), is as follows:

$$\xi_\nu'(\tau) + \frac{\beta}{1-\tau}\xi_\nu(\tau) + \frac{\nu}{2\tau}\left[\xi_\nu^2(\tau) - \xi_o^2\right] = 0 \tag{242}$$

This is the celebrated Riccati equation. This proves to be an adequate form for the asymptotic development of $\xi_\nu(\tau)$ in the interval $0 \le \tau < \frac{1}{2\beta + 1}$. Suppose the expansions are of the following forms:

$$\xi_\nu(\tau) \sim \xi_o + \frac{\xi^{(1)}}{\nu} + \frac{\xi^{(2)}}{\nu^2} + O\left(\frac{1}{\nu^3}\right) \tag{243}$$

$$\xi_{-\nu}(\tau) \sim -\xi_o + \frac{\xi^{(1)}}{\nu} - \frac{\xi^{(2)}}{\nu^2} + O\left(\frac{1}{\nu^3}\right) \tag{244}$$

where $\xi_o(\tau)$ is defined by equation (232). Substituting these expressions in equation (242) and equating the coefficients of various values of ν^{-s} to zero yields for the interval

$$\xi^{(1)}(\tau) = \frac{\alpha^2\tau}{2(1-\tau)}\left(\xi_o^{-2} - 1\right) \tag{245}$$

$$\xi^{(2)}(\tau) = \frac{\alpha^2\tau(\beta\tau + 2)}{4\xi_o(1-\tau)^2}\left(1 - \xi_o^{-4}\right) - \frac{\xi^{(1)}(\tau)}{2\alpha^2\xi_o} \tag{246}$$

The values of $\xi^{(1)}$ and $\xi^{(2)}$ are given in table 1.

APPENDIX E

PROOF OF THEOREM 2

The first part of the proof, namely, the series

$$\psi(q,\theta) = \sum_{2}^{\infty} \tilde{A}_n q^n F_n^{(r)}(\tau) \sin n\theta \qquad q < 1$$

which is absolutely and uniformly convergent in any closed domain in $q < 1$, can be similarly carried out (reference 1), since according to equation (159) it can be deduced that for large values of n

$$|\tilde{A}_n| < M|A_n|$$

where M is a constant independent of n. Therefore, it follows that for $\tau_1 << \frac{1}{2\beta + 1}$ and $n > N$

$$|\tilde{A}_n q^n F_n^{(r)}(\tau)| < M|A_n (tq)^n|$$

For the series (equation (51)) it is noted that for $\tau \lesssim \frac{1}{2\beta + 1}$ and $\nu > N$

$$|F_\nu^{(r)}(\tau)| < Mt^\nu$$

$$|F_{-\nu}^{(r)}(\tau)| < Mt^{-\nu}$$

where the region $\frac{1}{2\beta + 1} - \delta \leq \leq \frac{1}{2\beta + 1} + \delta$, where $\delta > 0$ is assumed to be excluded. Here all the M's are different but independent of n. Furthermore, from equation (160), $\tilde{D}_n$ is bounded by

$$|\tilde{D}_n| < \frac{M}{n}$$

Consequently, for $n > N$, the following inequalities are obtained:

$$\left|B_n q^{\nu} F_{\nu}^{(r)}(\tau)\right| < M\left|B_n (qt)^{\nu}\right| \qquad qt < V$$

$$\left|C_n q^{-\nu} F_{-\nu}^{(r)}(\tau)\right| < M\left|C_n (qt)^{-\nu}\right| \qquad qt > 1$$

$$\left|\tilde{D}_n q^{-n} F_{-n}^{(r)}(\tau)\right| < M\,\frac{(tq)^{-n}}{n}$$

This completes the proof.

APPENDIX F

DEDUCTION OF IDENTITIES (153), (154), AND (155)

Consider the stream function of the similar incompressible flow

$$\psi_o(q,\theta) = \sum_2^\infty A_n q^n \sin n\theta \qquad q < 1$$

$$\psi_o(q,\theta) = \sum_0^\infty \left(B_n q^\nu + C_n q^{-\nu}\right) \cos \nu\theta \qquad 1 < q < V$$

At the circle of convergence the conditions of continuity give

$$\sum_2^\infty A_n \sin n\theta = \sum_0^\infty (B_n + C_n) \cos \nu\theta$$

$$\sum_2^\infty nA_n \sin n\theta = \sum_0^\infty \nu(B_n - C_n) \cos \nu\theta$$

Since the limits exist by hypothesis, by multiplying both sides by $\sin n\theta$, term-by-term integration then yields

$$A_n = \frac{1}{\pi} \sum_0^\infty (B_m + C_m) I_{n\mu} \tag{247}$$

$$nA_n = \frac{1}{\pi} \sum_0^\infty \mu(B_m - C_m) I_{n\mu} \tag{248}$$

where

$$I_{n\mu} = \frac{1}{n + \mu} + \frac{1}{n - \mu}$$

$$\mu = m + \frac{1}{2}$$

By use of appendix B, from

$$-\sum_{2}^{\infty}\frac{A_n}{n}w^n = \int_0^w \left[W_o(w) + A_o\right]\frac{dw}{w}$$

the following relation by continuation can be deduced. Denote this function by $\Lambda(w)$. Then

$$\Lambda(w) = -\sum_{2}^{\infty}\frac{A_n}{n}w^n \qquad |w| < 1$$

$$\Lambda(w) = i\sum_{0}^{\infty}\frac{1}{\nu}\left(B_n w^{\nu} - C_n w^{-\nu}\right) - A_o \log_e w + \text{Constant} \qquad 1 < |w| < V$$

where the constant of integration can be determined if the form of $\Lambda(w)$ is known. At the circle of convergence it can similarly be shown, by considering the imaginary part of $\Lambda(w)$, that

$$\frac{A_n}{n} = \frac{1}{\pi}\sum_{0}^{\infty}\frac{1}{\mu}(B_m - C_m)I_{n\mu} + \frac{4}{n} \qquad (249)$$

where the constant term is eliminated by integration.

Moreover, if $\Lambda(w) = \sigma + iX$, it follows that

$$\sigma(q,\theta) = -\sum_{2}^{\infty}\frac{A_n}{n}q^n \cos n\theta \qquad (250)$$

$$q < 1$$

$$\chi(q,\theta) = \sum_{2}^{\infty}\frac{A_n}{n}q^n \sin n\theta \qquad (251)$$

$$\sigma(q,\theta) = \sum_{0}^{\infty}\frac{1}{\nu}\left(B_n q^{\nu} + C_n q^{-\nu}\right)\sin \nu\theta + 2\log_e q + \sigma_o \qquad (252)$$

$$1 < q < V$$

$$\chi(q,\theta) = \sum_{0}^{\infty}\frac{1}{\nu}\left(B_n q^{\nu} - C_n q^{-\nu}\right)\cos \nu\theta - A_o(\pi - \theta) \qquad (253)$$

REFERENCES

1. Tollmien, W.: Grenzlinien adiabatischer Potentialstromungen. Z.f.a.M.M., vol. 21, no. 3, June 1941, pp. 140–152.

2. Molenbroek, P.: Über einige Bewegungen eines Gases mit Annahme eines Geschwindigkeitspotentials. Arch. d. Math. u. Phys., Grunert Hoppe, vol. 2, no. 9, 1890, p. 157.

3. Chaplygin, S.: Gas Jets. NACA TM No. 1063, 1944.

4. Ringleb, Friedrich: Exakte Lösungen der Differentialgleichungen einer adiabatischen Gasströmung. Z.f.a.M.M., vol. 20, no. 4, Aug. 1940, pp. 185–198.

5. Tsien, Hsue-Shen: Two-Dimensional Subsonic Flow of Compressible Fluids. Jour. Aero. Sci., vol. 6, no. 10, Aug. 1939, pp. 399–407.

6. Bers, Lipman: On a Method of Constructing Two-Dimensional Subsonic Compressible Flows around Closed Profiles. NACA TN No. 969, 1945.

7. Bers, Lipman: On the Circulatory Subsonic Flow of a Compressible Fluid past a Circular Cylinder. NACA TN No. 970, 1945.

8. Tsien, Hsue-Shen, and Kuo, Yung-Huai: Two-Dimensional Irrotational Mixed Subsonic and Supersonic Flow of a Compressible Fluid and the Upper Critical Mach Number. NACA TN No. 995, 1946.

9. Kaplan, Carl: Compressible Flow about Symmetrical Joukowski Profiles. NACA Rep. No. 621, 1937.

10. Tsien, Hsue-Shen, and Fejer, Andrej: A Method for Predicting the Transonic Flow over Airfoils and Similar Bodies from Data Obtained at Small Mach Numbers. Army Air Forces, Dec. 31, 1944

TABLE 1

τ	f	g	T	$(1-\tau)^{-\beta}$	M	$-\int^{\tau}(1-\tau)^{\beta}\frac{d\tau}{\tau}$	$-f^{(1)}$	$-g^{(1)}$	ξ_0	$\xi^{(1)}$	$\xi^{(2)}$
0.01	1.00038	1.02341	0.987591	1.02513	0.22334	4.62978	0.0070935	0.069428	0.974740	0.001575	0.003390
.02	1.00162	1.04920	.975050	1.05115	.31746	3.961051	.0035781	.134863	.948272	.006791	.012038
.03	1.00384	1.07775	.962369	1.07811	.39081	3.57983	.0089751	.217119	.920473	.016553	.041943
.04	1.00722	1.10954	.94935	1.10605	.45361	3.31621	.0179196	.312501	.891201	.032050	.088904
.05	1.01199	1.14526	.936535	1.13502	.50981	3.11694	.0317171	.424516	.860285	.054595	.166883
.06	1.01844	1.18570	.923360	1.16507	.56144	2.95832	.0522626	.558038	.827521	.087236	.297127
.07	1.02678	1.23176	.909988	1.21197	.60967	2.82770	.0823873	.720024	.792655	.132211	.506825
.08	1.03804	1.28554	.896397	1.22861	.65530	2.71751	.1264739	.920767	.755371	.194307	.849851
.09	1.05245	1.34851	.882567	1.26221	.69886	2.62291	.1915979	1.175123	.715263	.280335	1.423202
.10	1.07125	1.42397	.868464	1.29712	.74074	2.54053	.2898039	1.511895	.671791	.401099	2.416900
.11	1.09610	1.51651	.854048	1.33341	.781252	2.46804	.4430778	1.972760	.624221	.574823	4.235747
.12	1.12968	1.63378	.839267	1.37113	.82061	2.40366	.6952314	2.643391	.571489	.834809	7.848095
.13	1.17684	1.78931	.824049	1.41038	.859012	2.34610	1.145421	3.704775	.511954	1.24908	11.823761
.14	1.24743	2.01063	.808289	1.45122	.89661	2.29428	2.064247	5.620614	.442827	1.981513	37.881541
.15	1.36648	2.36673	.791805	1.49374	.93352	2.24741	4.465971	10.003688	.358525	3.55231	125.02174
.16	1.63348	3.12791	.774259	1.53803	.96986	2.20482	16.03668	27.88238	.243674	8.95921	962.9315

τ	f	g	T	$(1-\tau)^{-\beta}$	M	$-\int^{\tau}(1-\tau)^{\beta}\frac{d\tau}{\tau}$	ω^{o}	μ^{o}
0.17	4.85733	11.63759	0.754293	1.58419	1.0057	2.16598	0.01806	6.10861
.18	2.90766	6.81071	.733041	1.63232	1.0412	2.13040	.36479	16.16389
.19	2.44420	5.60734	.713490	1.68253	1.0763	2.09780	.89674	21.69972
.20	2.18183	4.90915	.695424	1.73494	1.1111	2.06776	1.55446	25.84194
.21	1.99922	4.41764	.678664	1.78964	1.1457	2.04007	2.28050	29.21389
.22	1.85891	4.03871	.663061	1.84686	1.1802	2.01448	3.06999	32.07833
.23	1.74464	3.73114	.648486	1.90665	1.2145	1.99078	3.90948	34.57667
.24	1.64795	3.47275	.634832	1.96919	1.2498	1.96882	4.78568	36.79528
.25	1.56391	3.25054	.622006	2.03465	1.2830	1.94842	5.69266	38.79222
.26	1.48938	3.05592	.609927	2.10322	1.3172	1.92945	6.62614	40.60833
.27	1.42228	2.88326	.598526	2.17508	1.3515	1.91181	7.58100	42.27445
.28	1.36113	2.72830	.587740	2.25043	1.3858	1.89537	8.55467	43.81278
.29	1.30486	2.58811	.577518	2.32950	1.4202	1.88004	9.54119	45.24417
.30	1.25267	2.46020	.567811	2.41254	1.4548	1.86573	10.54604	46.57667
.32	1.15821	2.23459	.549781	2.59154	1.5244	1.83991	12.58533	49.00611
.34	1.07420	2.04082	.533366	2.78978	1.5950	1.81733	14.66453	51.17333
.36	.998334	1.87187	.518338	3.01001	1.6667	1.79760	16.77201	53.13000
.38	.929024	1.72360	.504513	3.25546	1.7398	1.78031	18.90685	54.91444
.40	.865127	1.58933	.491739	3.53000	1.8140	1.76517	21.06373	56.55500

TABLE 2.- NUMERICAL VALUES OF HYPERGEOMETRIC FUNCTIONS AND THEIR ASYMPTOTIC REPRESENTATION

$F_\nu(\tau)$

τ \ ν	0.5	1.5	2.5	3.5	4.5	5.5	6.5	7.5	8.5	9.5	10.5
0.04	9.7568 ,-1	9.2786 ,-1	8.8182 ,-1	8.3781 ,-1	7.9586 ,-1	7.5593 ,-1	7.1796 ,-1	6.8186 ,-1	6.4755 ,-1	6.1495 ,-1	5.8397 ,-1
.06	9.6380 ,-1	8.9322 ,-1	8.2658 ,-1	7.6437 ,-1	7.0654 ,-1	6.5292 ,-1	6.0312 ,-1	5.5732 ,-1	5.1482 ,-1	4.7553 ,-1	4.3922 ,-1
.08	9.5211 ,-1	8.5952 ,-1	7.7384 ,-1	6.9574 ,-1	6.2504 ,-1	5.6122 ,-1	5.0375 ,-1	4.5205 ,-1	4.0559 ,-1	3.6385 ,-1	3.2636 ,-1
.10	9.4059 ,-1	8.2675 ,-1	7.2351 ,-1	6.3173 ,-1	5.5084 ,-1	4.7989 ,-1	4.1782 ,-1	3.6361 ,-1	3.1634 ,-1	2.7514 ,-1	2.3925 ,-1
.12	9.2926 ,-1	7.9489 ,-1	6.7554 ,-1	5.7211 ,-1	4.8349 ,-1	4.0802 ,-1	3.4398 ,-1	2.8978 ,-1	2.4398 ,-1	2.0533 ,-1	1.7274 ,-1
.14	9.1811 ,-1	7.6395 ,-1	6.2986 ,-1	5.1669 ,-1	4.2251 ,-1	3.4476 ,-1	2.8088 ,-1	2.2856 ,-1	1.8582 ,-1	1.5097 ,-1	1.2258 ,-1
.16	9.0714 ,-1	7.3389 ,-1	5.8641 ,-1	4.6528 ,-1	3.6750 ,-1	2.8934 ,-1	2.2727 ,-1	1.7820 ,-1	1.3952 ,-1	1.0911 ,-1	8.5244 ,-2
.18	8.9636 ,-1	7.0472 ,-1	5.4513 ,-1	4.1768 ,-1	3.1800 ,-1	2.4101 ,-1	1.8203 ,-1	1.3710 ,-1	1.0304 ,-1	7.7297 ,-2	5.7890 ,-2
.20	8.8574 ,-1	6.7642 ,-1	5.0595 ,-1	3.7371 ,-1	2.7364 ,-1	1.9908 ,-1	1.4411 ,-1	1.0389 ,-1	7.4637 ,-2	5.3469 ,-2	3.8199 ,-2
.22	8.7531 ,-1	6.4897 ,-1	4.6882 ,-1	3.3317 ,-1	2.3403 ,-1	1.6291 ,-1	1.1258 ,-1	7.7322 ,-2	5.2823 ,-2	3.5922 ,-2	2.4313 ,-2
.24	8.6505 ,-1	6.2238 ,-1	4.3366 ,-1	2.9590 ,-1	1.9879 ,-1	1.3189 ,-1	8.6594 ,-2	5.6325 ,02	3.6325 ,-2	2.3252 ,-2	1.4759 ,-2
.26	8.5497 ,-1	5.9662 ,-1	4.0043 ,-1	2.6172 ,-1	1.6759 ,-1	1.0548 ,-1	6.5384 ,-2	3.9952 ,-2	2.4076 ,-2	1.4319 ,-2	8.3804 ,-2
.28	8.4507 ,-1	5.7168 ,-1	3.6905 ,-1	2.3046 ,-1	1.4009 ,-1	8.3160 ,-1	4.8264 ,-2	2.7386 ,-2	1.5175 ,-2	8.2015 ,-3	4.2820 ,-3
.30	8.3533 ,-1	5.4756 ,-1	3.3947 ,-1	2.0195 ,-1	1.1599 ,-1	6.4449 ,-2	3.4623 ,-2	1.7922 ,-2	8.8760 ,-3	4.1658 ,-3	1.7807 ,-3
.32	8.2577 ,-1	5.2423 ,-1	3.1162 ,-1	1.7604 ,-1	9.4975 ,-2	4.8914 ,-2	2.3915 ,-2	1.0955 ,-2	4.5695 ,-3	1.6349 ,-3	3.6396 ,-4
.34	8.1638 ,-1	5.0169 ,-1	2.8545 ,-1	1.5256 ,-1	7.6774 ,-2	3.6160 ,-2	1.5659 ,-2	5.9706 ,-3	1.7564 ,-3	1.6177 ,-4	-3.4465 ,-4

$F_{-\nu}(\tau)$

τ \ ν	0.5	1.5	2.5	3.5	4.5	5.5	6.5	7.5	8.5	9.5	10.5
0.04	1.0242 ,0	1.0630 ,0	1.1548 ,0	1.2209 ,0	1.2833 ,0	1.3485 ,0	1.4177 ,0	1.4921 ,0	1.5694 ,0	1.6519 ,0	1.7390 ,0
.06	1.0358 ,0	1.0868 ,0	1.2444 ,0	1.3712 ,0	1.4892 ,0	1.6098 ,0	1.7382 ,0	1.8775 ,0	2.0263 ,0	2.1929 ,0	2.3989 ,0
.08	1.0472 ,0	1.1059 ,0	1.3338 ,0	1.5428 ,0	1.7468 ,0	1.9578 ,0	2.1838 ,0	2.4308 ,0	2.7038 ,0	3.0071 ,0	3.3452 ,0
.10	1.0584 ,0	1.1206 ,0	1.4177 ,0	1.7261 ,0	2.0512 ,0	2.4037 ,0	2.7935 ,0	3.2302 ,0	3.7237 ,0	4.2847 ,0	4.9249 ,0
.12	1.0693 ,0	1.1312 ,0	1.4921 ,0	1.9088 ,0	2.3860 ,0	2.9384 ,0	3.5830 ,0	4.3394 ,0	5.2299 ,0	6.2810 ,0	7.5235 ,0
.14	1.0799 ,0	1.1381 ,0	1.5537 ,0	2.0777 ,0	2.7246 ,0	3.5256 ,0	4.5196 ,0	5.7548 ,0	7.2900 ,0	9.1979 ,0	1.1569 ,1
.16	1.0903 ,0	1.1416 ,0	1.6000 ,0	2.2192 ,0	3.0326 ,0	4.1006 ,0	5.5030 ,0	7.3443 ,0	9.7604 ,0	1.2929 ,1	1.7080 ,1
.18	1.1005 ,0	1.1420 ,0	1.6291 ,0	2.3209 ,0	3.2712 ,0	4.5737 ,0	6.3578 ,0	8.8005 ,0	1.2143 ,1	1.6712 ,1	2.2954 ,1
.20	1.1104 ,0	1.1395 ,0	1.6400 ,0	2.3717 ,0	3.4001 ,0	4.8378 ,0	6.8420 ,0	9.6228 ,0	1.3482 ,1	1.8831 ,1	2.6186 ,1
.22	1.1201 ,0	1.1344 ,0	1.6321 ,0	2.3629 ,0	3.3819 ,0	4.7805 ,0	6.6716 ,0	9.1581 ,0	1.2445 ,1	1.6550 ,1	2.1493 ,1
.24	1.1295 ,0	1.1270 ,0	1.6054 ,0	2.2882 ,0	3.1849 ,0	4.2963 ,0	5.5580 ,0	6.7611 ,0	7.4100 ,0	6.4660 ,0	1.9037 ,0
.26	1.1387 ,0	1.1174 ,0	1.5602 ,0	2.1437 ,0	2.7862 ,0	3.3015 ,0	3.2562 ,0	1.7335 ,0	-3.0847 ,0	-1.4652 ,1	-3.9320 ,1
.28	1.1477 ,0	1.1061 ,0	1.4974 ,0	1.9288 ,0	2.1737 ,0	1.7457 ,0	-3.8653 ,-1	-6.2885 ,0	-1.9917 ,1	-4.8592 ,1	-1.0547 ,2
.30	1.1565 ,0	1.0930 ,0	1.4181 ,0	1.6454 ,0	1.3477 ,0	-3.7756 ,-1	-5.3857 ,0	-1.7297 ,1	-4.2875 ,1	-9.4278 ,1	-1.9258 ,2
.32	1.1650 ,0	1.0786 ,0	1.3238 ,0	1.2978 ,0	3.2159 ,-1	-3.0244 ,0	-1.1587 ,1	-3.0762 ,1	-7.0252 ,1	-1.4660 ,2	-2.8631 ,2
.34	1.1733 ,0	1.0630 ,0	1.2161 ,0	8.9307 ,-1	-8.7844 ,-1	-6.0980 ,0	-1.8655 ,1	-4.6571 ,1	-9.8661 ,1	-1.9592 ,2	-3.6305 ,2

NACA

TABLE 2.- NUMERICAL VALUES OF HYPERGEOMETRIC FUNCTIONS AND THEIR ASYMPTOTIC REPRESENTATION - Continued

$F_{\nu,1}(\tau)$

τ \ ν	0.5	1.5	2.5	3.5	4.5	5.5	6.5	7.5	8.5	9.5	10.5
0.04	9.6983 ,-1	9.4805 ,-1	9.1526 ,-1	8.7850 ,-1	8.4053 ,-1	8.0264 ,-1	7.6547 ,-1	7.2938 ,-1	6.9454 ,-1	6.6106 ,-1	6.2895 ,-1
.05	9.5485 ,-1	9.2252 ,-1	8.7448 ,-1	8.2154 ,-1	7.6796 ,-1	7.1568 ,-1	6.6559 ,-1	6.1814 ,-1	5.7346 ,-1	5.3161 ,-1	4.9251 ,-1
.08	8.9730 ,-1	8.9730 ,-1	8.3474 ,-1	7.6703 ,-1	6.9739 ,-1	6.3166 ,-1	5.2090 ,-1	5.2090 ,-1	4.7024 ,-1	4.2404 ,-1	3.8203 ,-1
.10	9.2515 ,-1	8.7239 ,-1	7.9604 ,-1	7.1492 ,-1	6.3626 ,-1	5.6302 ,-1	4.9629 ,-1	4.3627 ,-1	3.8272 ,-1	3.3522 ,-1	2.9327 ,-1
.12	9.1041 ,-1	8.4779 ,-1	7.5838 ,-1	6.6516 ,-1	5.7678 ,-1	4.9650 ,-1	4.2527 ,-1	3.6296 ,-1	3.0984 ,-1	2.6242 ,-1	2.2254 ,-1
.14	8.9575 ,-1	8.2349 ,-1	7.2175 ,-1	6.1770 ,-1	5.2131 ,-1	4.3599 ,-1	3.6235 ,-1	2.9977 ,-1	2.4714 ,-1	2.0320 ,-1	1.6672 ,-1
.16	8.8118 ,-1	7.9951 ,-1	6.8614 ,-1	5.7249 ,-1	4.6969 ,-1	3.8111 ,-1	3.0683 ,-1	2.4561 ,-1	1.9573 ,-1	1.5544 ,-1	1.2310 ,-1
.18	8.6668 ,-1	7.7585 ,-1	6.5154 ,-1	5.2947 ,-1	4.2176 ,-1	3.3149 ,-1	2.5806 ,-1	1.9945 ,-1	1.5329 ,-1	1.1727 ,-1	8.9399 ,-2
.20	8.5227 ,-1	7.5249 ,-1	6.1796 ,-1	4.8860 ,-1	3.7735 ,-1	2.8679 ,-1	2.1542 ,-1	1.6037 ,-1	1.1853 ,-1	8.7097 ,-2	6.3695 ,-2
.22	8.3794 ,-1	7.2946 ,-1	5.8539 ,-1	4.4982 ,-1	3.3630 ,-1	2.4666 ,-1	1.7835 ,-1	1.2752 ,-1	9.0343 ,-2	6.3512 ,-2	4.4368 ,-2
.24	8.2369 ,-1	7.0675 ,-1	5.5380 ,-1	4.1307 ,-1	2.9845 ,-1	2.1078 ,-1	1.4629 ,-1	1.0011 ,-1	6.7708 ,-2	4.5320 ,-2	3.0075 ,-2
.26	8.0953 ,-1	6.8436 ,-1	5.2321 ,-1	3.7832 ,-1	2.6365 ,-1	1.7883 ,-1	1.1874 ,-1	7.7449 ,-2	4.9744 ,-2	3.1499 ,-2	1.9704 ,-2
.28	7.9545 ,-1	6.6229 ,-1	4.9361 ,-1	3.4550 ,-1	2.3175 ,-1	1.5053 ,-1	9.5231 ,-2	5.8893 ,-2	3.5675 ,-2	2.1181 ,-2	1.2349 ,-2
.30	7.8147 ,-1	6.4055 ,-1	4.6498 ,-1	3.1457 ,-1	2.0260 ,-1	1.2557 ,-1	7.5324 ,-2	4.3864 ,-2	2.4825 ,-2	1.3637 ,-2	7.2747 ,-3
.32	7.6757 ,-1	6.1914 ,-1	4.3732 ,-1	2.8546 ,-1	1.7606 ,-1	1.0369 ,-1	5.8610 ,-2	3.1845 ,-2	1.6607 ,-2	8.2582 ,-3	3.8945 ,-3
.34	7.5376 ,-1	5.9806 ,-1	4.1062 ,-1	2.5813 ,-1	1.5197 ,-1	8.4623 ,-1	4.4715 ,-2	2.2374 ,-2	1.0517 ,-2	4.5429 ,-3	1.7440 ,-3

$F_{-\nu,1}(\tau)$

τ \ ν	0.5	1.5	2.5	3.5	4.5	5.5	6.5	7.5	8.5	9.5	10.5
0.04	9.5633 ,-1	7.0820 ,-1	1.4234 ,0	1.5898 ,0	1.6278 ,0	1.6554 ,0	1.6968 ,0	1.7689 ,0	1.8234 ,0	1.9032	1.9911 ,0
.06	9.3487 ,-1	5.7770 ,-1	1.4649 ,0	1.8778 ,0	2.0849 ,0	2.2203 ,0	2.3355 ,0	2.4731 ,0	2.5910 ,0	2.7851	3.3138 ,0
.08	9.1375 ,-1	4.5436 ,-1	1.4160 ,0	2.0750 ,0	2.5526 ,0	2.9348 ,0	3.2537 ,0	3.5806 ,0	3.9223 ,0	4.2932 ,0	4.7036 ,0
.10	8.9296 ,-1	3.4085 ,-1	1.2926 ,0	2.1429 ,0	2.9088 ,0	3.6372 ,0	4.3633 ,0	5.1151 ,0	5.9166 ,0	6.7896 ,0	7.7547 ,0
.12	8.7237 ,-1	2.3599 ,-1	1.1092 ,-1	2.0605 ,0	3.0767 ,0	4.1927 ,0	5.4438 ,0	6.8671 ,0	8.5020 ,0	1.0394 ,1	1.2592 ,1
.14	8.5214 ,-1	1.3939 ,-1	8.7917 ,-1	1.8210 ,0	2.9660 ,0	4.3755 ,0	6.1244 ,0	8.3050 ,0	1.1027 ,1	1.4428 ,1	1.8672 ,1
.16	8.3215 ,-1	5.0743 ,-2	6.1465 ,-1	1.4299 ,0	2.5201 ,0	3.9821 ,0	5.9467 ,0	8.5864 ,0	1.2126 ,1	1.6866 ,1	2.3188 ,1
.18	8.1253 ,-1	3.0225 ,-2	3.2667 ,-1	9.0162 ,-1	1.7128 ,-	2.8523 ,0	4.4517 ,0	6.6921 ,0	9.8209 ,0	1.4183 ,1	2.0225 ,1
.20	7.9316 ,-1	-1.0381 ,-1	2.5108 ,-2	2.5808 ,-1	5.5107 ,-1	8.9845 ,-1	1.2834 ,0	1.6485 ,0	1.9131 ,0	1.9326 ,0	1.2782 ,0
.22	7.7409 ,-1	-1.7032 ,-1	-2.8113 ,-1	-4.7390 ,-1	-9.2694 ,-1	-1.8743 ,0	-3.7128 ,0	-7.1668 ,0	-1.3205 ,1	-2.3824 ,1	-4.2083 ,1
.24	7.5530 ,-1	-2.3004 ,-1	-5.8418 ,-1	-1.2638 ,0	-2.6540 ,0	-5.3605 ,0	-1.0424 ,1	-1.9627 ,1	-3.5985 ,1	-6.4489 ,1	-1.1358 ,2
.26	7.3683 ,-1	-2.8327 ,-1	-8.7723 ,-1	-2.0799 ,0	-4.5416 ,0	-9.3549 ,0	-1.8424 ,1	-3.5036 ,1	-6.4761 ,1	-1.1686 ,2	-2.0680 ,2
.28	7.1867 ,-1	-3.3027 ,-1	-1.1543 ,0	-2.8898 ,0	-6.4835 ,0	-1.3568 ,1	-2.6990 ,1	-5.1607 ,1	-9.5502 ,1	-1.7181 ,2	-3.0115 ,2
.30	7.0078 ,-1	-3.7136 ,-1	-1.4104 ,0	-3.6621 ,0	-8.3641 ,0	-1.7649 ,1	-3.5149 ,1	-6.6813 ,1	-1.2193 ,2	-2.1458 ,2	-3.6171 ,2
.32	6.8320 ,-1	-4.0682 ,-1	-1.6413 ,0	-4.3680 ,0	-1.0056 ,1	-2.1213 ,1	-4.1774 ,1	-7.7603 ,1	-1.3625 ,2	-2.2802 ,2	-3.4477 ,2
.34	6.6592 ,-1	-4.3695 ,-1	-1.8438 ,0	-4.9811 ,0	-1.1477 ,1	-2.3873 ,1	-4.5708 ,1	-7.9730 ,1	-1.3050 ,2	-2.4367 ,2	-2.2428 ,2

NACA

TABLE 2.- NUMERICAL VALUES OF HYPERGEOMETRIC FUNCTIONS AND THEIR ASYMPTOTIC REPRESENTATION - Continued

$F_n(\tau)$

τ \ n	1	2	3	4	5	6	7	8	9	10
0.02	9.7556 ,-1	9.5146 ,-1	9.2787 ,-1	9.0482 ,01	8.8232 ,-1	8.6035 ,-1	8.3893 ,-1	8.1803 ,-1	7.9764 ,-1	7.7776 ,-1
.04	9.5159 ,-1	9.0459 ,-1	8.5955 ,-1	8.1658 ,-1	7.7565 ,-1	7.3671 ,-1	6.9968 ,-1	6.6449 ,-1	6.3104 ,-1	5.9927 ,-1
.06	9.2808 ,-1	8.5936 ,-1	7.9492 ,-1	7.3491 ,-1	6.7922 ,-1	6.2761 ,-1	5.7984 ,-1	5.3565 ,-1	4.9479 ,-1	4.5702 ,-1
.08	9.0507 ,-1	8.1574 ,-1	7.3384 ,-1	6.5949 ,-1	5.9230 ,-1	5.3173 ,-1	4.7722 ,-1	4.2820 ,-1	3.8416 ,-1	3.4460 ,-1
.10	8.8252 ,-1	7.7370 ,-1	6.7620 ,-1	5.8998 ,-1	5.1419 ,-1	4.4781 ,-1	3.8979 ,-1	3.3917 ,-1	2.9503 ,-1	2.5658 ,-1
.12	8.6044 ,-1	7.3320 ,-1	6.2188 ,-1	5.2605 ,-1	4.4422 ,-1	3.7467 ,-1	3.1574 ,-1	2.6591 ,-1	2.2383 ,-1	1.8834 ,-1
.14	8.3881 ,-1	6.9423 ,-1	5.7075 ,-1	4.6739 ,-1	3.8176 ,-1	3.1124 ,-1	2.5340 ,-1	2.0611 ,-1	1.6750 ,-1	1.3604 ,-1
.16	8.1765 ,-1	6.5675 ,-1	5.2271 ,-1	4.1370 ,-1	3.2620 ,-1	2.5650 ,-1	2.0128 ,-1	1.7770 ,-1	1.2339 ,-1	9.6451 ,-2
.18	7.9694 ,-1	6.2073 ,-1	4.7762 ,-1	3.6469 ,-1	2.7698 ,-1	2.0952 ,-1	1.5802 ,-1	1.1889 ,-1	8.9260 ,-2	6.6904 ,-2
.20	7.7669 ,-1	5.8614 ,-1	4.3539 ,-1	3.2008 ,-1	2.3357 ,-1	1.6948 ,-1	1.2241 ,-1	8.8091 ,-2	6.3191 ,-2	4.5205 ,-2
.22	7.5699 ,-1	5.5296 ,-1	3.9589 ,-1	2.7959 ,-1	1.9545 ,-1	1.3554 ,-1	9.3367 ,-2	6.3949 ,-2	4.3581 ,-2	2.9565 ,-2
.24	7.3752 ,-1	5.2114 ,-1	3.5901 ,-1	2.4295 ,-1	1.6216 ,-1	1.0700 ,-1	6.9915 ,-2	4.5280 ,-2	2.9086 ,-2	1.8539 ,-2
.26	7.1860 ,-1	4.9067 ,-1	3.2465 ,-1	2.0992 ,-1	1.3323 ,-1	8.3200 ,-2	5.1199 ,-2	3.1068 ,-2	1.8593 ,-2	1.0971 ,-2
.28	7.0012 ,-1	4.6151 ,-1	2.9270 ,-1	1.8024 ,-1	1.0825 ,-1	6.3530 ,-2	3.6461 ,-2	2.0449 ,-2	1.1186 ,-2	5.9468 ,-3
.30	6.8206 ,-1	4.3363 ,-1	2.6305 ,-1	1.5369 ,-1	8.6817 ,-2	4.7444 ,-2	2.5035 ,-2	1.2691 ,-2	6.1204 ,-3	2.7549 ,-3
.32	6.6444 ,-1	4.0701 ,-1	2.3560 ,-1	1.3004 ,-1	6.8572 ,-2	3.4447 ,-2	1.6339 ,-2	7.1790 ,-3	2.7966 ,-3	8.4739 ,-4
.34	6.4724 ,-1	3.8161 ,-1	2.1025 ,-1	1.0906 ,-1	5.3167 ,-2	2.4090 ,-2	9.8700 ,-3	3.4023 ,-3	7.3840 ,-4	-1.8867 ,-4

$F_{-n}(\tau)$

τ \ n	2	3	4	5	6	7	8	9	10	
0.02	1.0566 ,0	1.0844 ,0	1.1106 ,0	1.1381 ,0	1.1668 ,0	1.1963 ,0	1.2268 ,0	1.2580 ,0	1.2901 ,0	
.04	1.1182 ,0	1.1900 ,0	1.2521 ,0	1.3154 ,0	1.3825 ,0	1.4540 ,0	1.5298 ,0	1.6101 ,0	1.6949 ,0	
.06	1.1784 ,0	1.3128 ,0	1.4310 ,0	1.5486 ,0	1.6726 ,0	1.8061 ,0	1.9511 ,0	2.1088 ,0	2.2803 ,0	
.08	1.2349 ,0	1.4460 ,0	1.6465 ,0	1.8506 ,0	2.0673 ,0	2.3039 ,0	2.5623 ,0	2.8501 ,0	3.1705 ,0	
.10	1.2853 ,0	1.5815 ,0	1.8900 ,0	2.2227 ,0	2.5896 ,0	2.9996 ,0	3.4623 ,0	3.9876 ,0	4.5864 ,0	
.12	1.3285 ,0	1.7113 ,0	2.1467 ,0	2.6504 ,0	3.2386 ,0	3.9293 ,0	4.7432 ,0	5.7043 ,0	6.8412 ,0	
.14	1.3637 ,0	1.8275 ,0	2.3967 ,0	3.1010 ,0	3.9759 ,0	5.0644 ,0	6.4190 ,0	8.1046 ,0	1.0201 ,1	
.16	1.3903 ,0	1.9233 ,0	2.6175 ,0	3.5260 ,0	4.6458 ,0	6.2817 ,0	8.3331 ,0	1.1023 ,0	1.4546 ,1	
.18	1.4082 ,0	1.9928 ,0	2.7856 ,0	3.8647 ,0	5.3356 ,0	7.3413 ,0	1.0075 ,1	1.3801 ,1	1.8874 ,1	
.20	1.4174 ,0	2.0312 ,0	2.8789 ,0	4.0498 ,0	5.6657 ,0	7.8909 ,0	1.0946 ,1	1.5128 ,1	2.0828 ,1	
.22	1.4181 ,0	2.0351 ,0	2.8775 ,0	4.0144 ,0	5.5270 ,0	7.4993 ,0	1.0002 ,1	1.3057 ,1	1.6570 ,1	
.24	1.4105 ,0	2.0023 ,0	2.7657 ,0	3.6994 ,0	4.7442 ,0	5.7174 ,0	6.1920 ,0	5.2877 ,0	1.2961 ,0	
.26	1.3950 ,0	1.9318 ,0	2.5330 ,0	3.0590 ,0	3.1742 ,0	2.1608 ,0	-1.4121 ,0	-1.0271 ,1	-2.9431 ,1	
.28	1.3722 ,0	1.8239 ,0	2.1743 ,0	2.0673 ,0	7.3136 ,-1	-3.4001 ,0	-1.3348 ,1	-3.4722 ,1	-7.7641 ,1	
.30	1.3426 ,0	1.6799 ,0	1.6908 ,0	7.2324 ,-1	-2.5905 ,0	-1.0956 ,1	-2.9465 ,1	-6.7343 ,1	-1.4056 ,2	
.32	1.3068 ,0	1.5021 ,0	1.0896 ,0	-9.5010 ,-1	-6.7052 ,0	-2.0193 ,1	-4.8731 ,1	-1.0493 ,2	-2.0930 ,2	
.34	1.2655 ,0	1.2938 ,0	3.8379 ,-1	-2.9017 ,0	-1.1424 ,1	-3.0471 ,1	-6.9105 ,1	-1.4153 ,2	-2.6686 ,2	

NACA

TABLE 2.- NUMERICAL VALUES OF HYPERGEOMETRIC FUNCTIONS AND THEIR ASYMPTOTIC REPRESENTATION - Continued

$F_{n,1}(\tau)$

τ \ n	1	2	3	4	5	6	7	8	9	10
0.02	9.8091 ,-1	9.6592 ,-1	9.4773 ,-1	9.2798 ,-1	9.0757 ,-1	8.8695 ,-1	8.6636 ,-1	8.4596 ,-1	8.2582 ,-1	8.0601 ,-1
.04	9.6121 ,-1	9.3243 ,-1	8.9716 ,-1	8.5957 ,-1	8.2153 ,-1	7.8394 ,-1	7.4728 ,-1	7.1180 ,-1	6.7763 ,-1	6.4483 ,-1
.06	9.4181 ,-1	8.9954 ,-1	8.4827 ,-1	7.9468 ,-1	7.4159 ,-1	6.9033 ,-1	6.4152 ,-1	5.9545 ,-1	5.5219 ,-1	5.1172 ,-1
.08	9.2275 ,-1	8.6725 ,-1	8.0105 ,-1	7.3320 ,-1	6.6746 ,-1	6.0549 ,-1	5.4794 ,-1	4.9500 ,-1	4.4660 ,-1	4.0253 ,-1
.10	9.0382 ,-1	8.3557 ,-1	7.5548 ,-1	6.7503 ,-1	5.9887 ,-1	5.2882 ,-1	4.6545 ,-1	4.0871 ,-1	3.5825 ,-1	3.1359 ,-1
.12	8.8500 ,-1	8.0448 ,-1	7.1152 ,-1	6.2008 ,-1	5.3553 ,-1	4.5975 ,-1	3.9303 ,-1	3.3496 ,-1	2.8480 ,-1	2.4171 ,-1
.14	8.6632 ,-1	7.7399 ,-1	6.6916 ,-1	5.6824 ,-1	4.7719 ,-1	3.9773 ,-1	3.2974 ,-1	2.7229 ,-1	2.2416 ,-1	1.8410 ,-1
.16	8.4780 ,-1	7.4410 ,-1	6.2838 ,-1	5.1941 ,-1	4.2357 ,-1	3.4224 ,-1	2.7469 ,-1	2.1936 ,-1	1.7449 ,-1	1.3837 ,-1
.18	8.2943 ,-1	7.1481 ,-1	5.8916 ,-1	4.7350 ,-1	3.7443 ,-1	2.9278 ,-1	2.2705 ,-1	1.7496 ,-1	1.3415 ,-1	1.0244 ,-1
.20	8.1122 ,-1	6.8612 ,-1	5.5147 ,-1	4.3040 ,-1	3.2942 ,-1	2.4887 ,-1	1.80605 ,-1	1.3798 ,-1	1.0168 ,-1	7.4527 ,-2
.22	7.9315 ,-1	6.5804 ,-1	5.1528 ,-1	3.9003 ,-1	2.8860 ,-1	2.1007 ,-1	1.5099 ,-1	1.0744 ,-1	7.5820 ,-2	5.3128 ,-2
.24	7.7524 ,-1	6.3055 ,-1	4.8059 ,-1	3.5227 ,-1	2.5143 ,-1	1.7594 ,-1	1.2121 ,-1	8.2442 ,-2	5.5466 ,-2	3.6962 ,-2
.26	7.5747 ,-1	6.0367 ,-1	4.4735 ,-1	3.1705 ,-1	2.1778 ,-1	1.4607 ,-1	9.6094 ,-1	6.2182 ,-2	3.9656 ,-2	2.4956 ,-2
.28	7.3987 ,-1	5.7740 ,-1	4.1556 ,-1	2.8425 ,-1	1.8745 ,-1	1.2009 ,-1	7.5091 ,-2	4.5941 ,-2	2.7563 ,-2	1.6216 ,-2
.30	7.2241 ,-1	5.5172 ,-1	3.8518 ,-1	2.5380 ,-1	1.6020 ,-1	9.7628 ,-2	5.7687 ,-2	3.3117 ,-2	1.8476 ,-2	1.0005 ,-2
.32	7.0512 ,-1	5.2665 ,-1	3.5620 ,-1	2.2559 ,-1	1.3584 ,-1	7.8345 ,-2	4.3418 ,-2	2.3120 ,-2	1.1793 ,-2	5.7209 ,-3
.34	6.8799 ,-1	5.0219 ,-1	3.2858 ,-1	1.9953 ,-1	1.1416 ,-1	6.1919 ,-2	3.1857 ,-2	1.5473 ,-2	7.0062 ,-3	2.8765 ,-3

$F_{-n,1}(\tau)$

τ \ n	2	3	4	5	6	7	8	9	10
0.02	1.2228 ,0	1.2860 ,0	1.2600 ,0	1.2557 ,0	1.2684 ,0	1.2895 ,0	1.3154 ,0	1.3441 ,0	1.3748 ,0
.04	1.2521 ,0	1.5553 ,0	1.6167 ,0	1.6402 ,0	1.6737 ,0	1.7234 ,0	1.7871 ,0	1.8621 ,0	1.9461 ,0
.06	1.1915 ,0	1.7454 ,0	2.0045 ,0	2.1561 ,0	2.2775 ,0	2.4008 ,0	2.5390 ,0	2.6970 ,0	2.8762 ,0
.08	1.0875 ,0	1.8324 ,0	2.3440 ,0	2.7386 ,0	3.07878 ,0	3.4123 ,0	3.7356 ,0	4.0916 ,0	4.4827 ,0
.10	9.5180 ,-1	1.8088 ,0	2.5622 ,0	3.2708 ,0	3.9725 ,0	4.6949 ,0	5.4608 ,0	6.2912 ,0	7.2064 ,0
.12	7.9556 ,-1	1.6771 ,0	2.6013 ,0	3.6124 ,0	4.7469 ,0	6.0399 ,0	7.5282 ,0	9.2527 ,0	1.1260 ,1
.14	6.2676 ,-1	1.4458 ,0	2.4227 ,0	3.6217 ,0	5.1131 ,0	6.9783 ,0	9.3151 ,0	1.2243 ,1	1.5909 ,1
.16	4.5133 ,-1	1.1276 ,0	2.0083 ,0	3.1811 ,0	4.4880 ,0	6.8757 ,0	9.7226 ,0	1.3540 ,1	1.8646 ,1
.18	2.7410 ,-1	7.3753 ,-1	1.3594 ,0	2.2136 ,0	3.3979 ,0	5.0425 ,0	7.3225 ,0	1.0477 ,1	1.4838 ,1
.20	9.8738 ,-2	2.9209 ,-1	4.9514 ,-1	6.9372 ,-1	8.5198 ,-1	8.0533 ,-1	6.8678 ,-1	-0.16318 ,-2	-1.6240 ,0
.22	-7.1765 ,-2	-1.9159 ,-1	-5.5019 ,-1	-1.3445 ,0	-2.9251 ,0	-5.8686 ,0	-1.1154 ,1	-2.0387 ,1	-3.6196 ,1
.24	-2.3499 ,-1	-6.9648 ,-1	-1.7304 ,0	-3.7538 ,0	-7.8062 ,0	-1.5130 ,1	-2.8227 ,1	-5.1163 ,1	-9.0659 ,1
.26	-3.8915 ,-1	-1.2061 ,0	-2.9907 ,0	-6.5887 ,0	-1.3487 ,1	-2.6255 ,1	-4.9252 ,1	-8.9759 ,1	-1.5976 ,2
.28	-5.3258 ,-1	-1.7049 ,0	-4.2709 ,0	-9.4747 ,0	-1.9501 ,1	-3.8183 ,1	-7.1481 ,1	-1.2981 ,2	-2.3608 ,2
.30	-6.6410 ,-1	-2.1786 ,0	-5.5087 ,0	-1.2273 ,1	-2.5253 ,1	-4.9039 ,1	-9.0852 ,1	-1.6139 ,2	-2.7520 ,2
.32	-7.8290 ,-1	-2.6144 ,0	-6.6434 ,0	-1.4767 ,1	-3.0078 ,1	-5.7165 ,1	-1.0277 ,2	-1.7125 ,2	-2.6946 ,2
.34	-8.8830 ,-1	-3.0013 ,0	-7.6179 ,0	-1.6744 ,1	-3.3302 ,1	-6.0763 ,1	-1.0136 ,2	-1.5084 ,2	-1.7797 ,2

NACA

TABLE 2 - NUMERICAL VALUES OF HYPERGEOMETRIC FUNCTIONS AND THEIR ASYMPTOTIC REPRESENTATION - Continued

$f(\tau)T^{\nu}(\tau) \longrightarrow f(\tau)T^{\nu}(\tau) \cos\left(\nu\omega - \frac{\pi}{4}\right)$

τ \ ν	0.5	1.5	2.5	3.5	4.5	5.5	6.5	7.5	8.5	9.5	10.5
0.02	9.8904 ,-1	9.6437 ,-1	9.4031 ,-1	9.1685 ,-1	8.9397 ,-1	8.7167 ,-1	8.4992 ,-1	8.2871 ,-1	8.0804 ,-1	7.8788 ,-1	7.6822 ,-1
.04	9.8148 ,-1	9.3195 ,-1	8.8492 ,-1	8.4026 ,-1	7.9786 ,-1	7.5759 ,-1	7.1936 ,-1	6.8306 ,-1	6.4859 ,-1	6.1586 ,-1	5.8478 ,-1
.06	9.7863 ,-1	9.0363 ,-1	8.3438 ,-1	7.7043 ,-1	7.1139 ,-1	6.5687 ,-1	6.0652 ,-1	5.6004 ,-1	5.1712 ,-1	4.7749 ,-1	4.4089 ,-1
.08	9.8280 ,-1	8.8098 ,-1	7.8970 ,-1	7.0789 ,-1	6.3455 ,-1	5.6881 ,-1	5.0988 ,-1	4.5705 ,-1	4.0970 ,-1	3.6726 ,-1	3.2921 ,-1
.10	9.9832 ,-1	8.6706 ,-1	7.5296 ,-1	6.5392 ,-1	5.6790 ,-1	4.9320 ,-1	4.2833 ,-1	3.7199 ,-1	3.2305 ,-1	2.8957 ,-1	2.4366 ,-1
.12	1.0349 ,0	8.6857 ,-1	7.2896 ,-1	6.1180 ,-1	5.1346 ,-1	4.3093 ,-1	3.6167 ,-1	3.0353 ,-1	2.5475 ,-1	2.1380 ,-1	1.7944 ,-1
.14	1.1215 ,0	9.0650 ,-1	7.3271 ,-1	5.9224 ,-1	4.7870 ,-1	3.8693 ,-1	3.1275 ,-1	2.5279 ,-1	2.0433 ,-1	1.6516 ,-1	1.3350 ,-1
.16	1.4373 ,0	1.1129 ,0	8.6164 ,-1	6.6714 ,-1	5.1654 ,-1	3.9901 ,-1	3.0965 ,-1	2.3957 ,-1	1.8563 ,-1	1.4373 ,-1	1.1118 ,-1
.18	1.7659 ,0	1.3027 ,0	9.6084 ,-1	7.0867 ,-1	5.2264 ,-1	3.8541 ,-1	2.8419 ,-1	2.0954 ,-1	1.5449 ,-1	1.1389 ,-1	8.3956 ,-2
.20	1.3039 ,0	9.3037 ,-1	6.6294 ,-1	4.7177 ,-1	3.3531 ,-1	2.3804 ,-1	1.6880 ,-1	1.1956 ,-1	8.4599 ,-2	5.9800 ,-2	4.2229 ,-2
.22	1.0986 ,0	7.6439 ,-1	5.2920 ,-1	3.6472 ,-1	2.5031 ,-1	1.7111 ,-1	1.1654 ,-1	7.9096 ,-2	5.3503 ,-2	3.6076 ,-2	2.4249 ,-2
.24	9.6641 ,-1	6.5845 ,-1	4.4362 ,-1	2.9597 ,-1	1.9563 ,-1	1.2825 ,-1	8.3432 ,-2	5.3874 ,-2	3.4539 ,-2	2.1988 ,-2	1.3901 ,-2
.26	8.6865 ,-1	5.8072 ,-1	3.8051 ,-1	2.4504 ,-1	1.5536 ,-1	9.7090 ,-2	5.9850 ,-2	3.6402 ,-2	2.1844 ,-2	1.2926 ,-2	7.5363 ,-3
.28	7.9084 ,-1	5.1916 ,-1	3.3028 ,-1	2.0458 ,-1	1.2371 ,01	7.3137 ,-2	4.2279 ,-2	2.3830 ,-2	1.3154 ,-2	7.0408 ,-3	3.6405 ,-3
.30	7.2598 ,-1	4.6795 ,-1	2.8838 ,-1	1.7108 ,-1	9.8029 ,-2	5.4285 ,-2	2.9000 ,-2	1.4875 ,-2	7.2570 ,-3	3.3062 ,-3	1.3515 ,-3
.32	6.7015 ,-1	4.2392 ,-1	2.5236 ,-1	1.4269 ,-1	7.6847 ,-1	3.9338 ,-2	1.8988 ,-2	8.4863 ,-3	3.3677 ,-3	1.0490 ,-3	1.0918 ,-3
.34	6.2099 ,-1	3.8516 ,-1	2.2087 ,-1	1.1831 ,-1	5.9276 ,-1	2.7515 ,-2	1.1559 ,-2	4.0737 ,-3	9.2323 ,-4	2.0610 ,-4	-4.7533 ,-4

$f(\tau)T^{-\nu}(\tau) \longrightarrow \frac{1}{2}f(\tau)T^{-\nu}(\tau) \cos\left(\nu\omega + \frac{\pi}{4}\right)$

τ \ ν	0.5	1.5	2.5	3.5	4.5	5.5	6.5	7.5	8.5	9.5	10.5
0.02	1.0144 ,0	1.0403 ,0	1.0669 ,0	1.0942 ,0	1.1222 ,0	1.1509 ,0	1.1804 ,0	1.2106 ,0	1.2416 ,0	1.2733 ,0	1.3059 ,0
.04	1.0336 ,0	1.0886 ,0	1.1464 ,0	1.2074 ,0	1.2715 ,0	1.3391 ,0	1.4103 ,0	1.4852 ,0	1.5642 ,0	1.6473 ,0	1.7348 ,0
.06	1.0599 ,0	1.1478 ,0	1.2431 ,0	1.3463 ,0	1.4580 ,0	1.5790 ,0	1.7101 ,0	1.8521 ,0	2.0058 ,0	2.1723 ,0	2.3526 ,0
.08	1.0964 ,0	1.2231 ,0	1.3644 ,0	1.5222 ,0	1.6981 ,0	1.8944 ,0	2.1133 ,0	2.3576 ,0	2.6300 ,0	2.9340 ,0	3.2731 ,0
.10	1.1495 ,0	1.3236 ,0	1.5241 ,0	1.7549 ,0	2.0207 ,0	2.3268 ,0	2.6792 ,0	3.0850 ,0	3.5522 ,0	4.0903 ,0	4.7098 ,0
.12	1.2332 ,0	1.4693 ,0	1.7507 ,0	2.0860 ,0	2.4855 ,0	2.9615 ,0	3.5286 ,0	4.2044 ,0	5.0096 ,0	5.9691 ,0	7.1122 ,0
.14	1.3875 ,0	1.7166 ,0	2.1237 ,0	2.6274 ,0	3.2506 ,0	4.0216 ,0	4.9755 ,0	6.1556 ,0	7.6155 ,0	9.4218 ,0	1.1657 ,1
.16	1.8564 ,0	2.3976 ,0	3.0967 ,0	3.9996 ,0	5.1657 ,0	6.6717 ,0	8.6169 ,0	1.1129 ,1	1.4374 ,1	1.8565 ,1	2.3978 ,1
.18	1.1969 ,0	1.6223 ,0	2.1986 ,0	2.9796 ,0	4.0375 ,0	5.4707 ,0	7.4119 ,0	1.0041 ,1	1.3601 ,1	1.8423 ,1	2.4951 ,1
.20	9.1239 ,-1	1.2749 ,0	1.7787 ,0	2.4773 ,0	3.4440 ,0	4.7786 ,0	6.6166 ,0	9.1409 ,0	1.2598 ,1	1.7315 ,1	2.3731 ,1
.22	7.8702 ,-1	1.1156 ,0	1.5742 ,0	2.2040 ,0	3.0578 ,0	4.1969 ,0	5.6861 ,0	7.5803 ,0	9.9041 ,0	1.2573 ,1	1.5354 ,1
.24	7.0009 ,-1	9.9892 ,-1	1.3989 ,0	1.9132 ,0	2.5353 ,0	3.2122 ,0	3.7935 ,0	3.9393 ,0	2.9542 ,0	-4.9997 ,-1	-2.8145 ,0
.26	6.3416 ,-1	8.9806 ,0	1.2205 ,0	1.5613 ,0	1.8045 ,0	1.6807 ,0	6.2377 ,-1	-2.4861 ,0	-9.7745 ,0	-2.5154 ,1	-5.5657 ,1
.28	5.7915 ,-1	8.0599 ,0	1.0294 ,0	1.1360 ,0	8.4266 ,-1	-4.5290 ,-1	-3.9635 ,0	-1.2026 ,1	-2.8994 ,1	-6.2752 ,1	-1.2723 ,2
.30	5.3124 ,-1	7.1373 ,0	8.2380 ,-1	6.3888 ,-1	-3.4283 ,-1	-3.1687 ,0	-9.9092 ,0	-2.4475 ,1	-5.4054 ,1	-1.1123 ,2	-2.1752 ,2
.32	4.8840 ,-1	6.2691 ,0	6.0480 ,-1	7.7970 ,-2	-1.7241 ,0	-6.3792 ,0	-1.6945 ,1	-3.9055 ,1	-8.2602 ,1	-1.6406 ,2	-3.0919 ,2
.34	4.4941 ,-1	5.3883 ,0	3.7491 ,-1	-5.3405 ,-1	-3.2552 ,0	-9.9315 ,0	-2.3478 ,1	-5.4370 ,1	-1.1046 ,2	-2.0945 ,2	-3.7393 ,2

TABLE 2.- NUMERICAL VALUES OF HYPERGEOMETRIC FUNCTIONS AND THEIR ASYMPTOTIC REPRESENTATION - Continued

$q(\tau)T^{\nu} \longrightarrow q(\tau)T^{\nu} \cos\left(\nu\omega - \mu^{\circ} - \frac{\pi}{4}\right)$

τ \ ν	0.5	1.5	2.5	3.5	4.5	5.5	6.5	7.5	8.5	9.5	10.5
0.02	1.0360 ,0	1.0102 ,0	9.8498 ,-1	9.6040 ,-1	9.3644 ,-1	9.1307 ,-1	8.9029 ,-1	8.6808 ,-1	8.4642 ,-1	8.2530 ,-1	8.0471 ,-1
.04	1.0812 ,0	1.0266 ,0	9.7481 ,-1	9.2562 ,-1	8.7891 ,-1	8.3455 ,-1	7.9244 ,-1	7.5245 ,-1	7.1447 ,-1	6.7842 ,-1	6.4418 ,-1
.06	1.1394 ,0	1.0520 ,0	9.7141 ,-1	8.9696 ,-1	8.2822 ,-1	7.6476 ,-1	7.0613 ,-1	6.5202 ,-1	6.0205 ,-1	5.5591 ,-1	5.1330 ,-1
.08	1.2171 ,0	1.0910 ,0	9.7800 ,-1	8.7667 ,-1	7.8585 ,-1	7.0443 ,-1	6.3145 ,-1	5.6603 ,-1	5.0739 ,-1	4.5482 ,-1	4.0770 ,-1
.10	1.3270 ,0	1.1525 ,0	1.0009 ,0	8.6922 ,-1	7.5489 ,-1	6.5559 ,-1	5.6936 ,-1	4.9447 ,-1	4.2943 ,-1	3.7294 ,-1	3.2389 ,-1
.12	1.4967 ,0	1.2562 ,0	1.0543 ,0	8.8480 ,-1	7.4258 ,-1	6.2322 ,-1	5.2305 ,-1	4.3898 ,-1	3.6842 ,-1	3.0920 ,-1	2.5950 ,-1
.14	1.8077 ,0	1.4611 ,0	1.1810 ,0	9.5459 ,-1	7.7158 ,-1	6.2366 ,-1	5.0410 ,-1	4.0746 ,-1	3.2934 ,-1	2.6621 ,-1	2.1517 ,-1
.16	2.7517 ,0	2.1305 ,0	1.6496 ,0	1.2772 ,0	9.8888 ,-1	7.6565 ,-1	5.9281 ,-1	4.5899 ,-1	3.5537 ,-1	2.7515 ,-1	2.1304 ,-1
.18	2.8287 ,0	2.0973 ,0	1.5547 ,0	1.1524 ,0	8.5398 ,-1	6.3277 ,-1	4.6878 ,-1	3.4724 ,-1	2.5717 ,-1	1.9044 ,-1	1.4100 ,-1
.20	1.3958 ,0	1.0429 ,0	7.7499 ,-1	5.7312 ,-1	4.2203 ,-1	3.0959 ,-1	2.2634 ,-1	1.6497 ,-1	1.1990 ,-1	8.6915 ,-2	6.2858 ,-2
.22	8.2101 ,-1	6.5668 ,-1	5.0863 ,-1	3.8484 ,-1	2.8598 ,-1	2.0951 ,-1	1.5171 ,-1	1.0878 ,-1	7.7352 ,-2	5.4606 ,-2	3.8302 ,-2
.24	5.0887 ,-1	4.6596 ,-1	3.8448 ,-1	2.9866 ,-1	2.2293 ,-1	1.6170 ,-1	1.1474 ,-1	8.0010 ,-2	5.4989 ,-2	3.7329 ,-2	2.5069 ,-2
.26	3.1996 ,-1	3.6030 ,-1	3.1755 ,-1	2.5074 ,-1	1.8569 ,-1	1.3173 ,-1	9.0534 ,-2	6.0697 ,-2	3.9867 ,-2	2.5727 ,-2	1.6343 ,-2
.28	1.9919 ,-1	2.9781 ,-1	2.7736 ,-1	2.1953 ,-1	1.5937 ,-1	1.0942 ,-1	7.2138 ,-2	4.6055 ,-2	2.8615 ,-2	1.7353 ,-2	1.0287 ,-2
.30	1.1952 ,-1	2.5898 ,-1	2.5060 ,-1	1.9628 ,-1	1.3834 ,-1	9.1165 ,-2	5.7179 ,-2	3.4444 ,-2	2.0020 ,-2	1.1246 ,-2	6.1005 ,-3
.32	6.6117 ,-2	2.3381 ,-1	2.3092 ,-1	1.7714 ,-1	1.2030 ,-1	7.5557 ,-2	4.4721 ,-2	2.5154 ,-2	1.3477 ,-2	6.8593 ,-3	3.2876 ,-3
.34	3.0144 ,-2	2.1676 ,-1	2.1512 ,-1	1.6033 ,-1	1.0427 ,-1	6.1989 ,-2	3.4310 ,-2	1.7773 ,-2	8.5807 ,-3	3.7992 ,-3	1.4796 ,-3

$q(\tau)T^{-\nu} \longrightarrow \frac{1}{2}qT^{-\nu} \cos\left(\nu\omega + \mu^{\circ} + \frac{\pi}{4}\right)$

τ \ ν	0.5	1.5	2.5	3.5	4.5	5.5	6.5	7.5	8.5	9.5	10.5
0.02	1.0625 ,0	1.0897 ,0	1.1176 ,0	1.1462 ,0	1.1755 ,0	1.7056 ,0	1.2365 ,0	1.2681 ,0	1.3006 ,0	1.3338 ,0	1.3680 ,0
.04	1.1386 ,0	1.1992 ,0	1.2629 ,0	1.3300 ,0	1.4007 ,0	1.4751 ,0	1.5535 ,0	1.6361 ,0	1.7231 ,0	1.8146 ,0	1.9111 ,0
.06	1.2339 ,0	1.3363 ,0	1.4473 ,0	1.5674 ,0	1.6975 ,0	1.8384 ,0	1.9910 ,0	2.1562 ,0	2.3352 ,0	2.5290 ,0	2.7389 ,0
.08	1.3578 ,0	1.5147 ,0	1.6898 ,0	1.8851 ,0	2.1030 ,0	2.3460 ,0	2.6172 ,0	2.9197 ,0	3.2571 ,0	3.6336 ,0	4.0535 ,0
.10	1.5280 ,0	1.7594 ,0	2.0259 ,0	2.3328 ,0	2.6861 ,0	3.0929 ,0	3.5614 ,0	4.1007 ,0	4.7218 ,0	5.4370 ,0	6.2605 ,0
.12	1.7834 ,0	2.1249 ,0	2.5319 ,0	3.0168 ,0	3.5945 ,0	4.2829 ,0	5.1032 ,0	6.0805 ,0	7.2450 ,0	8.6326 ,0	1.0286 ,1
.14	2.2364 ,0	2.7668 ,0	3.4231 ,0	4.2349 ,0	5.2394 ,0	6.4821 ,0	8.0195 ,0	9.9216 ,0	1.2275 ,1	1.5186 ,1	1.8788 ,1
.16	3.5540 ,0	4.5901 ,0	5.9284 ,0	7.6569 ,0	9.8893 ,0	1.2773 ,1	1.6497 ,1	2.1306 ,1	2.7518 ,1	3.5541 ,1	4.5904 ,1
.18	1.9072 ,0	2.5714 ,0	3.4663 ,0	4.6718 ,0	6.2953 ,0	8.4813 ,0	1.1424 ,1	1.5385 ,1	2.0715 ,1	2.7885 ,1	3.7529 ,1
.20	9.2815 ,-1	1.2252 ,0	1.6031 ,0	2.0754 ,0	2.6516 ,0	3.3316 ,0	4.0952 ,0	4.8841 ,0	5.574 ,0	5.9239 ,0	5.5058 ,0
.22	4.8961 ,-1	5.4098 ,-1	5.1581 ,-1	3.2310 ,-1	-2.0003 ,-1	-1.3374 ,0	-3.5733 ,0	-7.7206 ,0	-1.5127 ,1	-2.8001 ,1	-4.9932 ,1
.24	2.2068 ,-1	6.1493 ,-2	-3.5453 ,-1	-1.2656 ,0	-3.0937 ,0	-6.5720 ,0	-1.2956 ,1	-2.4368 ,1	-4.4354 ,1	-7.8783 ,1	-1.3778 ,2
.26	3.6819 ,-2	-3.1011 ,-1	-1.1091 ,0	-2.7788 ,0	-6.0697 ,0	-1.2301 ,1	-2.3749 ,1	-4.4290 ,1	-8.0421 ,1	-1.4289 ,2	-2.4924 ,2
.28	-9.5925 ,-2	-6.1109 ,-1	-1.7787 ,0	-4.2161 ,0	-9.0383 ,0	-1.8209 ,1	-3.5108 ,1	-6.5426 ,1	-1.1853 ,2	-2.0944 ,2	-3.6166 ,2
.30	-1.9469 ,-1	-8.5953 ,-1	-2.3725 ,0	-5.5496 ,0	-1.1858 ,1	-2.3850 ,1	-4.5809 ,1	-8.4651 ,1	-1.5105 ,2	-2.6049 ,2	-4.3352 ,2
.32	-2.6939 ,-1	-1.0658 ,0	-2.8929 ,0	-6.7446 ,0	-1.4375 ,1	-2.8724 ,1	-5.4422 ,1	-9.8189 ,1	-1.6856 ,2	-2.7361 ,2	-4.1374 ,2
.34	-3.2630 ,-1	-1.2367 ,0	-3.3392 ,0	-7.7663 ,0	-1.6435 ,1	-3.2320 ,1	-5.9472 ,1	-1.0213 ,2	-1.6144 ,2	-2.2663 ,2	-2.5464 ,2

NACA

TABLE 2.- NUMERICAL VALUES OF HYPERGEOMETRIC FUNCTIONS AND THEIR ASYMPTOTIC REPRESENTATION - Continued

$f(\tau)T^{n} \longrightarrow f(\tau)T^{n} \cos\left(n\omega - \frac{\pi}{4}\right)$

τ \ n	1	2	3	4	5	6	7	8	9	10
0.02	9.7663 ,-1	9.5226 ,-1	9.2850 ,-1	9.0534 ,-1	8.8275 ,-1	8.6073 ,-1	8.3925 ,-1	8.1831 ,-1	7.9789 ,-1	7.7799 ,-1
.04	9.5639 ,-1	9.0813 ,-1	8.6230 ,-1	8.1878 ,-1	7.7746 ,-1	7.3823 ,-1	7.0097 ,-1	6.6560 ,-1	6.3201 ,-1	6.0011 ,-1
.06	9.4039 ,-1	8.6932 ,-1	8.0177 ,-1	7.4032 ,-1	6.8358 ,-1	6.3119 ,-1	5.8282 ,-1	5.3815 ,-1	4.9691 ,-1	4.5882 ,-1
.08	9.3050 ,-1	8.3409 ,-1	7.4768 ,-1	6.7022 ,-1	6.0078 ,-1	5.3854 ,-1	4.8274 ,-1	4.3273 ,-1	3.8790 ,-1	3.4771 ,-1
.10	9.3034 ,-1	8.0797 ,-1	7.0169 ,-1	6.0939 ,-1	5.2924 ,-1	4.5962 ,-1	3.9917 ,-1	3.4666 ,-1	3.0106 ,-1	2.6146 ,-1
.12	9.4810 ,-1	7.9571 ,-1	6.6781 ,-1	5.6047 ,-1	4.7039 ,-1	3.9478 ,-1	3.3133 ,-1	2.7807 ,-1	2.3338 ,-1	1.9587 ,-1
.14	1.0083 ,0	8.1498 ,-1	6.5874 ,-1	5.3245 ,-1	4.3038 ,-1	3.4787 ,-1	2.8118 ,-1	2.2727 ,-1	1.8370 ,-1	1.4849 ,-1
.16	1.2647 ,0	9.7923 ,-1	7.5818 ,-1	5.8703 ,-1	4.5451 ,-1	3.5191 ,-1	2.7247 ,-1	2.1096 ,-1	1.6334 ,-1	1.2647 ,-1
.18	1.5167 ,0	1.1188 ,0	8.2518 ,-1	6.0859 ,-1	4.4881 ,-1	3.3095 ,-1	2.4403 ,-1	1.7992 ,-1	1.3265 ,-1	9.7784 ,-2
.20	1.1016 ,0	7.8549 ,-1	5.5933 ,-1	4.0799 ,-1	2.8256 ,-1	2.0048 ,-1	1.4208 ,-1	1.0060 ,-1	7.1143 ,-2	5.0258 ,-2
.22	9.1698 ,-1	6.3639 ,-1	4.3957 ,-1	3.0230 ,-1	2.0705 ,-1	1.4128 ,-1	9.6050 ,-2	6.5080 ,-2	4.3951 ,-2	2.7730 ,-2
.24	7.9889 ,-1	5.4117 ,-1	3.6374 ,-1	2.4086 ,-1	1.5856 ,-1	1.0354 ,-1	6.7104 ,-2	4.3173 ,-2	2.7582 ,-2	1.7498 ,-2
.26	7.1218 ,-1	4.7116 ,-1	3.0597 ,-1	1.9547 ,-1	1.2303 ,-1	7.6358 ,-2	4.6755 ,-2	2.8233 ,-2	1.6834 ,-2	9.8894 ,-3
.28	6.4353 ,-1	4.1557 ,-1	2.6076 ,-1	1.5955 ,-1	9.5388 ,-2	5.5765 ,-2	3.1870 ,-2	1.7782 ,-2	9.6610 ,-3	5.0874 ,-3
.30	5.8651 ,-1	3.6922 ,-1	2.2312 ,-1	1.3005 ,-1	7.3264 ,-2	3.9864 ,-2	2.0885 ,-2	1.0464 ,-2	4.9489 ,-3	2.1515 ,-3
.32	5.3755 ,-1	3.2932 ,-1	1.9093 ,-1	1.0536 ,-1	5.5351 ,-2	2.7554 ,-2	1.2839 ,-2	5.4499 ,-2	1.9678 ,-3	4.6440 ,-4
.34	4.9449 ,-1	2.9423 ,-1	1.6297 ,-1	8.4475 ,-2	4.0817 ,-2	1.8091 ,-2	7.0579 ,-3	2.1371 ,-2	1.9764 ,-4	-4.0399 ,-4

$f(\tau)T^{-n} \longrightarrow \frac{1}{2}f(\tau)T^{-n} \cos\left(n\omega + \frac{\pi}{4}\right)$

τ \ n	1	2	3	4	5	6	7	8	9	10
0.02	1.0273 ,0	1.0535 ,0	1.0805 ,0	1.1081 ,0	1.1365 ,0	1.1656 ,0	1.1954 ,0	1.2260 ,0	1.2574 ,0	1.2895 ,0
.04	1.0608 ,0	1.1171 ,0	1.1765 ,0	1.2390 ,0	1.3049 ,0	1.3742 ,0	1.4473 ,0	1.5242 ,0	1.6052 ,0	1.6905 ,0
.06	1.1030 ,0	1.1945 ,0	1.2937 ,0	1.4010 ,0	1.5173 ,0	1.6433 ,0	1.7797 ,0	1.9274 ,0	2.0874 ,0	2.2606 ,0
.08	1.1580 ,0	1.2919 ,0	1.4412 ,0	1.6077 ,0	1.7935 ,0	2.0008 ,0	2.2321 ,0	2.4901 ,0	2.7779 ,0	3.0989 ,0
.10	1.2335 ,0	1.4203 ,0	1.6354 ,0	1.8831 ,0	2.1684 ,0	2.4968 ,0	2.8749 ,0	3.3104 ,0	3.8118 ,0	4.3891 ,0
.12	1.3460 ,0	1.6038 ,0	1.9110 ,0	2.2770 ,0	2.7130 ,0	3.2326 ,0	3.8517 ,0	4.5894 ,0	5.4683 ,0	6.5156 ,0
.14	1.5433 ,0	1.9093 ,0	2.3622 ,0	2.9225 ,0	3.6156 ,0	4.4732 ,0	5.5341 ,0	6.8467 ,0	8.4706 ,0	1.0480 ,1
.16	2.1097 ,0	2.7248 ,0	3.5193 ,0	4.54537 ,0	5.8706 ,0	7.5822 ,0	9.7929 ,0	1.2648 ,1	1.6336 ,1	2.1099 ,1
.18	1.3934 ,0	1.8886 ,0	2.5595 ,0	3.4685 ,0	4.6998 ,0	6.3678 ,0	8.6269 ,0	1.1687 ,1	1.5830 ,1	2.1440 ,1
.20	1.0646 ,0	1.5062 ,0	2.0996 ,0	2.9216 ,0	4.0578 ,0	5.6245 ,0	7.7792 ,0	1.0725 ,1	1.4770 ,1	2.0278 ,1
.22	9.3669 ,-1	1.3264 ,0	1.8646 ,0	2.5992 ,0	3.5876 ,0	4.8939 ,0	6.5800 ,0	8.6878 ,0	1.1201 ,1	1.3976 ,1
.24	8.3802 ,-1	1.1852 ,0	1.6415 ,0	2.2126 ,0	2.8732 ,0	3.5301 ,0	3.9533 ,0	3.6520 ,0	1.6561 ,0	-3.8627 ,0
.26	7.5795 ,-1	1.0533 ,0	1.3934 ,0	1.7070 ,0	1.8146 ,0	1.3218 ,0	-5.7242 ,-1	-5.4175 ,0	-1.6108 ,1	-3.7901 ,1
.28	6.8787 ,-1	9.2160 ,-1	1.1166 ,0	1.0669 ,0	3.7702 ,-1	-1.8198 ,0	-7.2150 ,0	-1.9010 ,1	-4.3084 ,1	-8.9945 ,1
.30	6.2405 ,-1	7.8731 ,-1	7.8725 ,-1	2.9601 ,-1	-1.4243 ,0	-5.8608 ,0	-1.5868 ,1	-3.6768 ,1	-7.8105 ,1	-1.5642 ,2
.32	5.6463 ,-1	6.4990 ,-1	4.3589 ,-1	-5.9016 ,-1	-3.5490 ,0	-1.0648 ,1	-2.6062 ,1	-5.7304 ,1	-1.1736 ,2	-2.2662 ,2
.34	5.0860 ,-1	5.0997 ,-1	6.3203 ,-2	-1.5671 ,0	-5.9035 ,0	-1.5907 ,1	-3.6952 ,1	-7.8132 ,1	-1.5354 ,2	-2.8234 ,2

NACA

TABLE 2.- NUMERICAL VALUES OF HYPERGEOMETRIC FUNCTIONS AND THEIR ASYMPTOTIC REPRESENTATION - Concluded

$q(\tau)T^{n}(\tau) \longrightarrow q(\tau)T^{n}(\tau) \cos\left(n\omega - \mu^{\circ} - \frac{\pi}{4}\right)$

τ \ n	1	2	3	4	5	6	7	8	9	10
0.02	1.0230 ,0	9.9750 ,-1	9.7261 ,-1	9.4834 ,-1	9.2468 ,-1	9.0161 ,-1	8.7912 ,-1	8.5718 ,-1	8.3580 ,-1	8.1494 ,-1
.04	1.0535 ,0	1.0003 ,0	9.4986 ,-1	9.0193 ,-1	8.5641 ,-1	8.1319 ,-1	7.7215 ,-1	7.3319 ,-1	6.9619 ,-1	6.6105 ,-1
.06	1.0948 ,0	1.0109 ,0	9.3344 ,-1	8.6190 ,-1	7.9585 ,-1	7.3485 ,-1	6.7853 ,-1	6.2653 ,-1	5.7851 ,-1	5.3418 ,-1
.08	1.1523 ,0	1.0329 ,0	9.2592 ,-1	8.2999 ,-1	7.4400 ,-1	6.6692 ,-1	5.9783 ,-1	5.3589 ,-1	4.8037 ,-1	4.3060 ,-1
.10	1.2367 ,0	1.0740 ,0	9.3275 ,-1	8.1006 ,-1	7.0351 ,-1	6.1097 ,-1	5.3061 ,-1	4.6081 ,-1	4.0020 ,-1	3.4756 ,-1
.12	1.3712 ,0	1.1508 ,0	9.6583 ,-1	8.1059 ,-1	6.8030 ,-1	5.7095 ,-1	4.7918 ,-1	4.0216 ,-1	3.3752 ,-1	2.8327 ,-1
.14	1.6251 ,0	1.3136 ,0	1.0618 ,0	8.5821 ,-1	6.9368 ,-1	5.6069 ,-1	4.5320 ,-1	3.6632 ,-1	2.9609 ,-1	2.3933 ,-1
.16	2.4213 ,0	1.8747 ,0	1.4515 ,0	1.1238 ,0	8.7014 ,-1	6.7371 ,-1	5.2163 ,-1	4.0387 ,-1	3.1270 ,-1	2.4211 ,-1
.18	2.4357 ,0	1.8058 ,0	1.3385 ,0	9.9205 ,-1	7.3511 ,-1	5.4465 ,-1	4.0347 ,-1	2.9884 ,-1	2.2131 ,-1	1.6389 ,-1
.20	1.2075 ,0	8.9962 ,-1	6.6684 ,-1	4.9205 ,-1	3.6164 ,-1	2.6482 ,-1	1.9330 ,-1	1.4072 ,-1	1.0197 ,-1	7.3952 ,-2
.22	7.3776 ,-1	5.7990 ,-1	4.4355 ,-1	3.3241 ,-1	2.4517 ,-1	1.7852 ,-1	1.2838 ,-1	9.1820 ,-2	6.5046 ,-2	4.5767 ,-2
.24	4.9558 ,-1	4.2729 ,-1	3.4090 ,-1	2.5912 ,-1	1.9046 ,-1	1.3654 ,-1	9.6007 ,-2	6.6442 ,-2	4.5373 ,-2	3.0631 ,-2
.26	3.5621 ,-1	3.4457 ,-1	2.8501 ,-1	2.1716 ,-1	1.5711 ,-1	1.0958 ,-1	7.4512 ,-2	4.9307 ,-2	3.2056 ,-2	2.0543 ,-2
.28	2.7133 ,-1	2.9588 ,-1	2.5019 ,-1	1.8862 ,-1	1.3282 ,-1	8.9240 ,-2	5.7850 ,-2	3.6418 ,-2	2.2349 ,-2	1.3398 ,-2
.30	2.1779 ,-1	2.6497 ,-1	2.2561 ,-1	1.6645 ,-1	1.1309 ,-1	7.2595 ,-2	4.4586 ,-2	2.6373 ,-2	1.5068 ,-2	8.5508 ,-3
.32	1.8327 ,-1	2.4386 ,-1	2.0631 ,-1	1.4769 ,-1	9.6129 ,-2	5.8510 ,-2	3.3745 ,-2	1.8525 ,-2	9.6802 ,-3	4.7888 ,-3
.34	1.6073 ,-1	2.2830 ,-1	1.8988 ,-1	1.3100 ,-1	8.1177 ,-2	4.6506 ,-2	2.4900 ,-2	1.2466 ,-2	5.7815 ,-3	2.4201 ,-3

$q(\tau)T^{-n}(\tau) \longrightarrow \frac{1}{2}q(\tau)T^{-n}(\tau) \cos\left(n\omega + \mu^{\circ} + \frac{\pi}{4}\right)$

τ \ n	1	2	3	4	5	6	7	8	9	10
0.02	1.0760 ,0	1.1036 ,0	1.1318 ,0	1.1608 ,0	1.1905 ,0	1.2209 ,0	1.2522 ,0	1.2842 ,0	1.3171 ,0	1.3508 ,0
.04	1.1685 ,0	1.2306 ,0	1.2960 ,0	1.3648 ,0	1.4374 ,0	1.5138 ,0	1.5942 ,0	1.6790 ,0	1.7682 ,0	1.8622 ,0
.06	1.2841 ,0	1.3907 ,0	1.5061 ,0	1.6311 ,0	1.7665 ,0	1.9131 ,0	2.0719 ,0	2.2439 ,0	2.4302 ,0	2.6319 ,0
.08	1.4341 ,0	1.5998 ,0	1.7847 ,0	1.9910 ,0	2.2211 ,0	2.4778 ,0	2.7642 ,0	3.0837 ,0	3.4401 ,0	3.8377 ,0
.10	1.6397 ,0	1.8880 ,0	2.1740 ,0	2.5023 ,0	2.8824 ,0	3.3189 ,0	3.8216 ,0	4.4004 ,0	5.0669 ,0	5.8343 ,0
.12	1.9467 ,0	2.3195 ,0	2.7637 ,0	3.2930 ,0	3.9237 ,0	4.6752 ,0	5.5705 ,0	6.6374 ,0	7.9086 ,0	9.4232 ,0
.14	2.4875 ,0	3.0775 ,0	3.8074 ,0	4.7104 ,0	5.8276 ,0	7.2098 ,0	8.9199 ,0	1.1036 ,1	1.3653 ,1	1.6891 ,1
.16	4.0390 ,0	5.2165 ,0	6.7375 ,0	8.7018 ,0	1.1239 ,1	1.4516 ,1	1.8748 ,1	2.4214 ,1	3.1274 ,1	4.0392 ,1
.18	2.2855 ,0	2.9856 ,0	4.0243 ,0	5.4232 ,0	7.2911 ,0	9.8436 ,0	1.3258 ,1	1.7852 ,1	2.4035 ,1	3.2350 ,1
.20	1.0675 ,0	1.4032 ,0	1.8267 ,0	2.3016 ,0	2.9792 ,0	3.7055 ,0	4.4924 ,0	5.2591 ,0	5.8111 ,0	5.8602 ,0
.22	5.2108 ,-1	5.4240 ,-1	4.4843 ,-1	1.16998 ,-1	-6.6758 ,-1	-2.2768 ,0	-5.3394 ,0	-1.0903 ,1	-2.0696 ,1	-4.1599 ,1
.24	1.6313 ,-1	-1.0276 ,-1	-7.2736 ,-1	-2.0286 ,0	-4.5637 ,0	-9.2942 ,0	-1.7855 ,1	-3.2992 ,1	-5.9273 ,1	-1.0422 ,2
.26	-9.7673 ,-2	-6.3264 ,-1	-1.7981 ,0	-4.1561 ,0	-8.7037 ,0	-1.7178 ,1	-3.2505 ,1	-5.9859 ,1	-1.0746 ,2	-1.8912 ,2
.28	-2.9762 ,-1	-1.0833 ,0	-2.7838 ,0	-6.2201 ,0	-1.2910 ,1	-2.5404 ,1	-4.8110 ,1	-8.8350 ,1	-1.5803 ,2	-2.75996 ,2
.30	-4.5501 ,-1	-1.4704 ,0	-3.6807 ,0	-8.1849 ,0	-1.6926 ,1	-3.3226 ,1	-6.2554 ,1	-1.1356 ,2	-1.9958 ,2	-3.3761 ,2
.32	-5.8031 ,-1	-1.8021 ,0	-4.4782 ,0	-9.9375 ,0	-2.0758 ,1	-3.9786 ,1	-7.3545 ,1	-1.2680 ,2	-2.1641 ,2	-3.3994 ,2
.34	-6.8054 ,-1	-2.0831 ,0	-5.1630 ,0	-1.1412 ,1	-2.3244 ,1	-4.4205 ,1	-7.8654 ,1	-1.3009 ,2	-1.9487 ,2	-2.5018 ,2

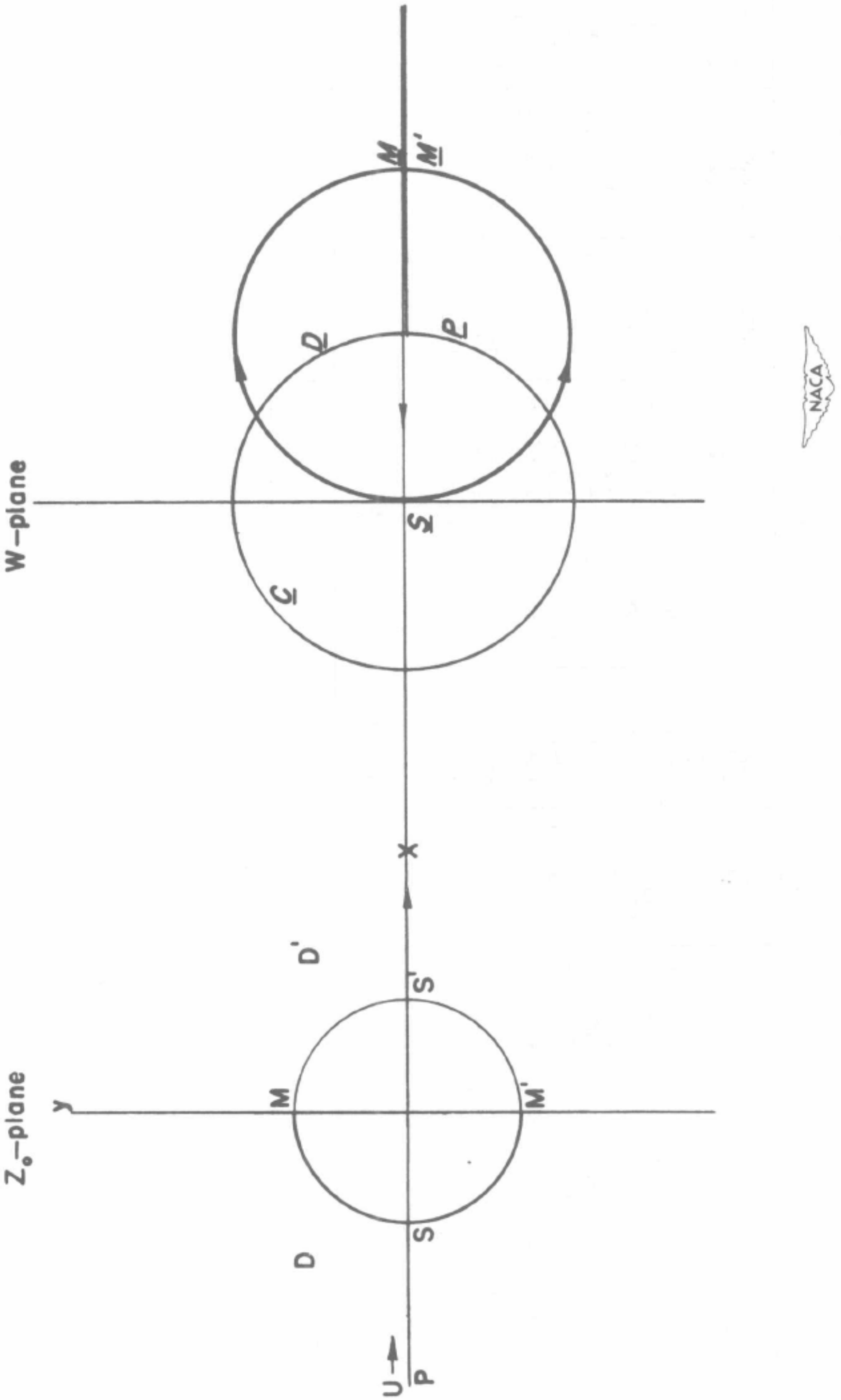

Figure 1.- Mapping of half plane D.

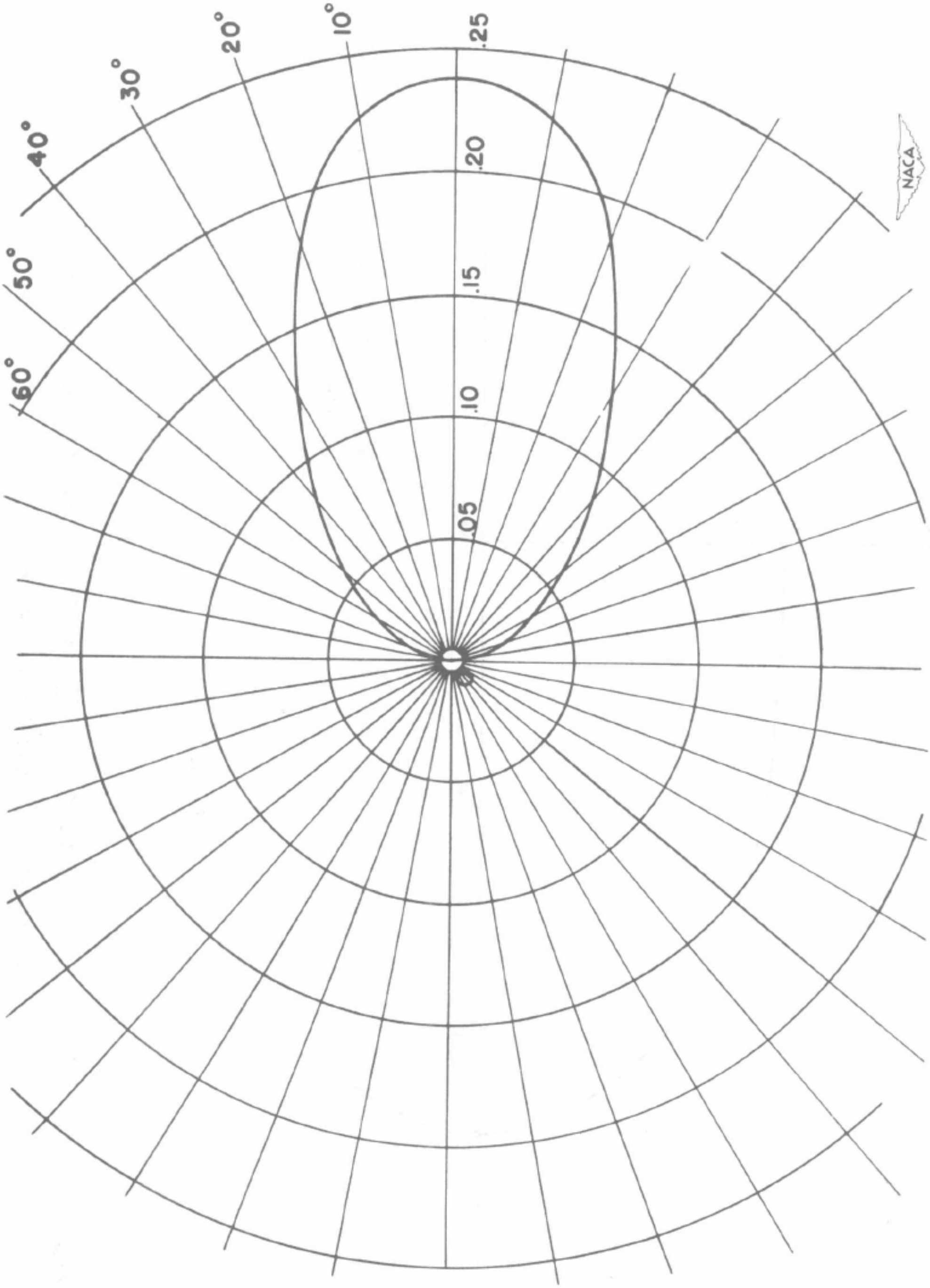

Figure 2.- Zero streamline of a compressible flow in hodograph plane. $\epsilon = \frac{1}{2}$; $M_1 = 0.60$; $r_o = 0$.

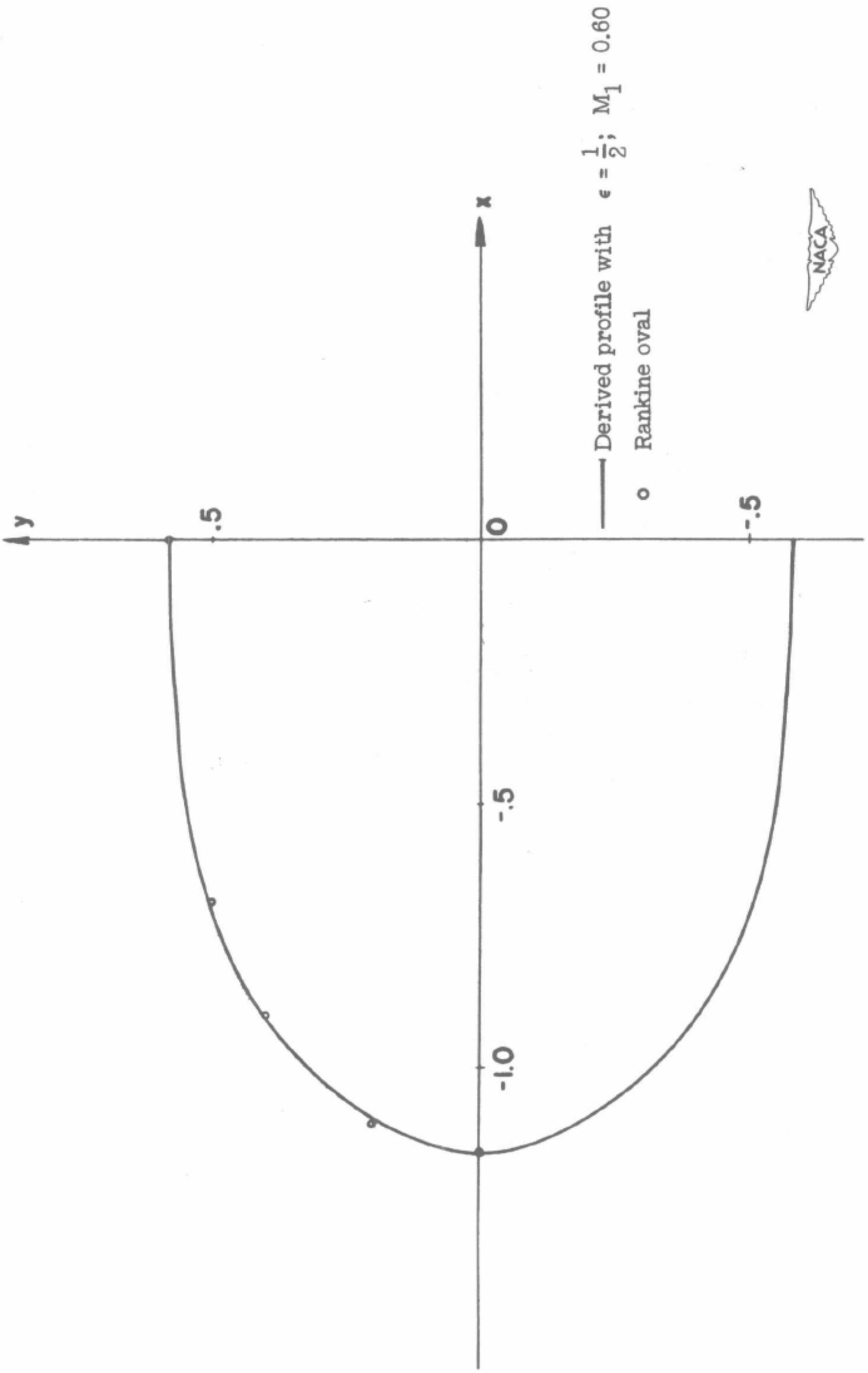

Figure 3.- Comparison of derived profile for $\epsilon = \frac{1}{2}$ and $M_1 = 0.60$ with profile given by source-sink combination for $M_1 = 0$.

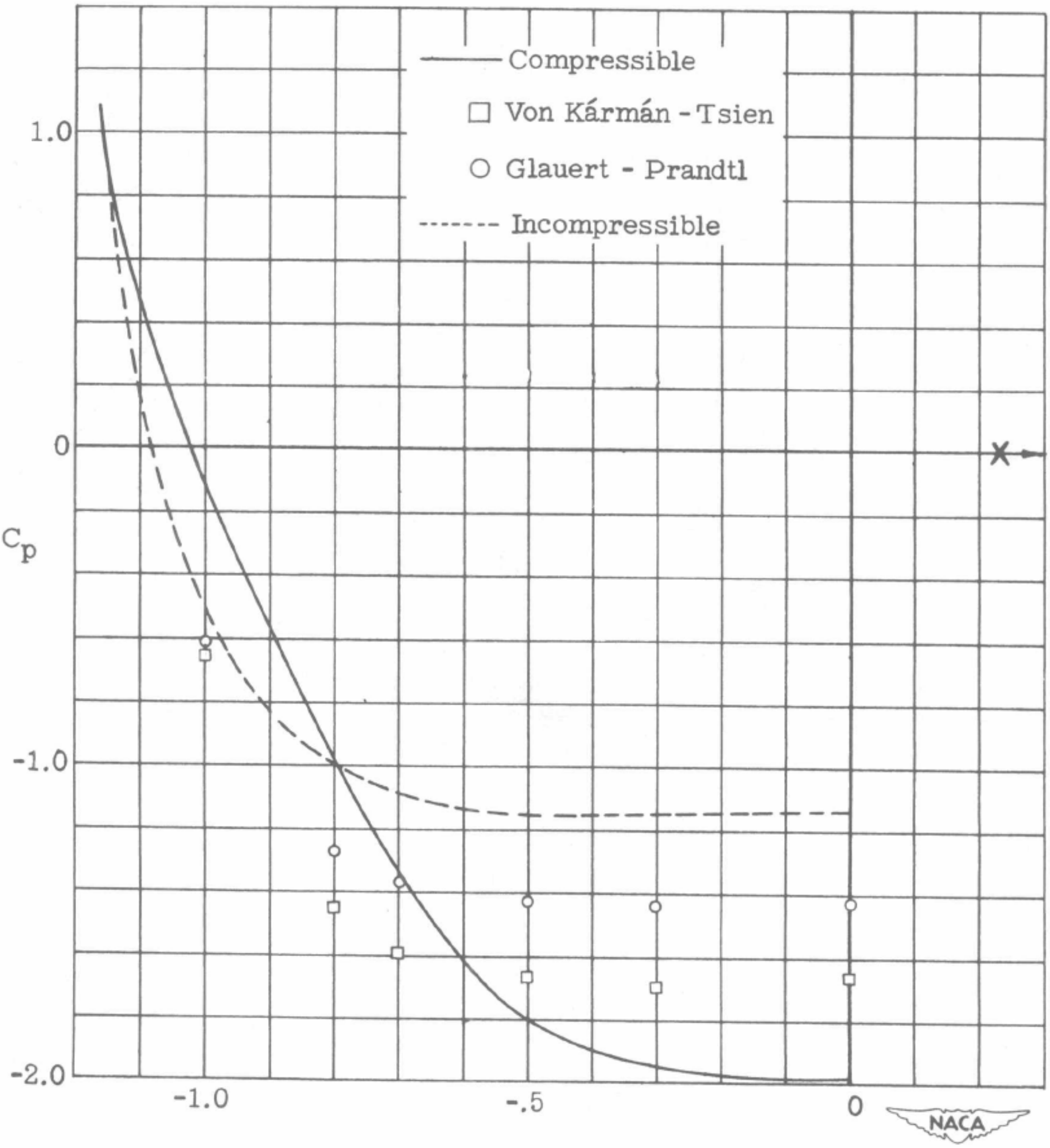

Figure 4.- Pressure distribution along major axis of ellipse.

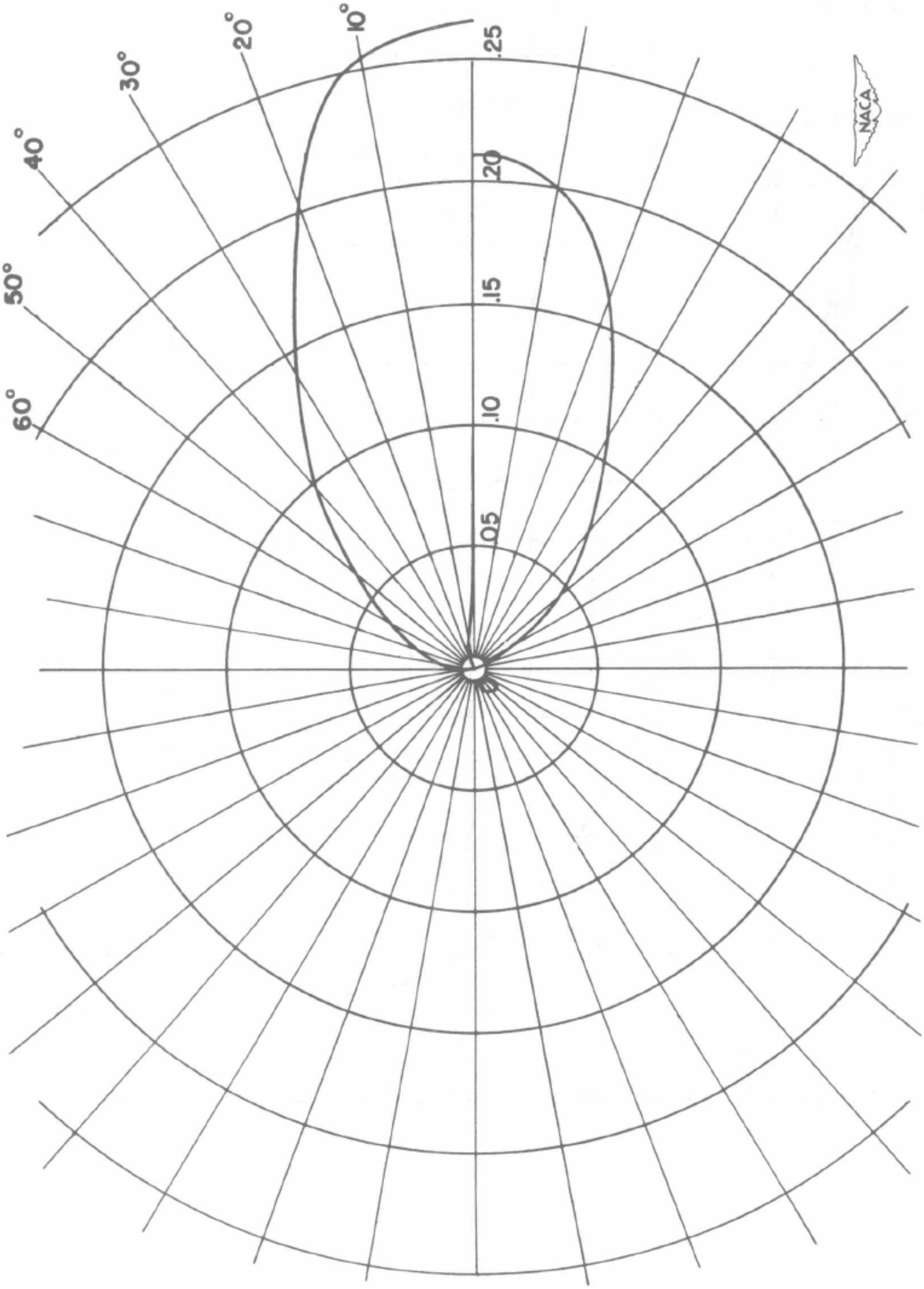

Figure 5.- Zero streamline of a compressible flow in hodograph plane. $\epsilon = \frac{1}{2}$; $M_1 = 0.60$; $\frac{\Gamma_o}{4\pi} = 0.05$.

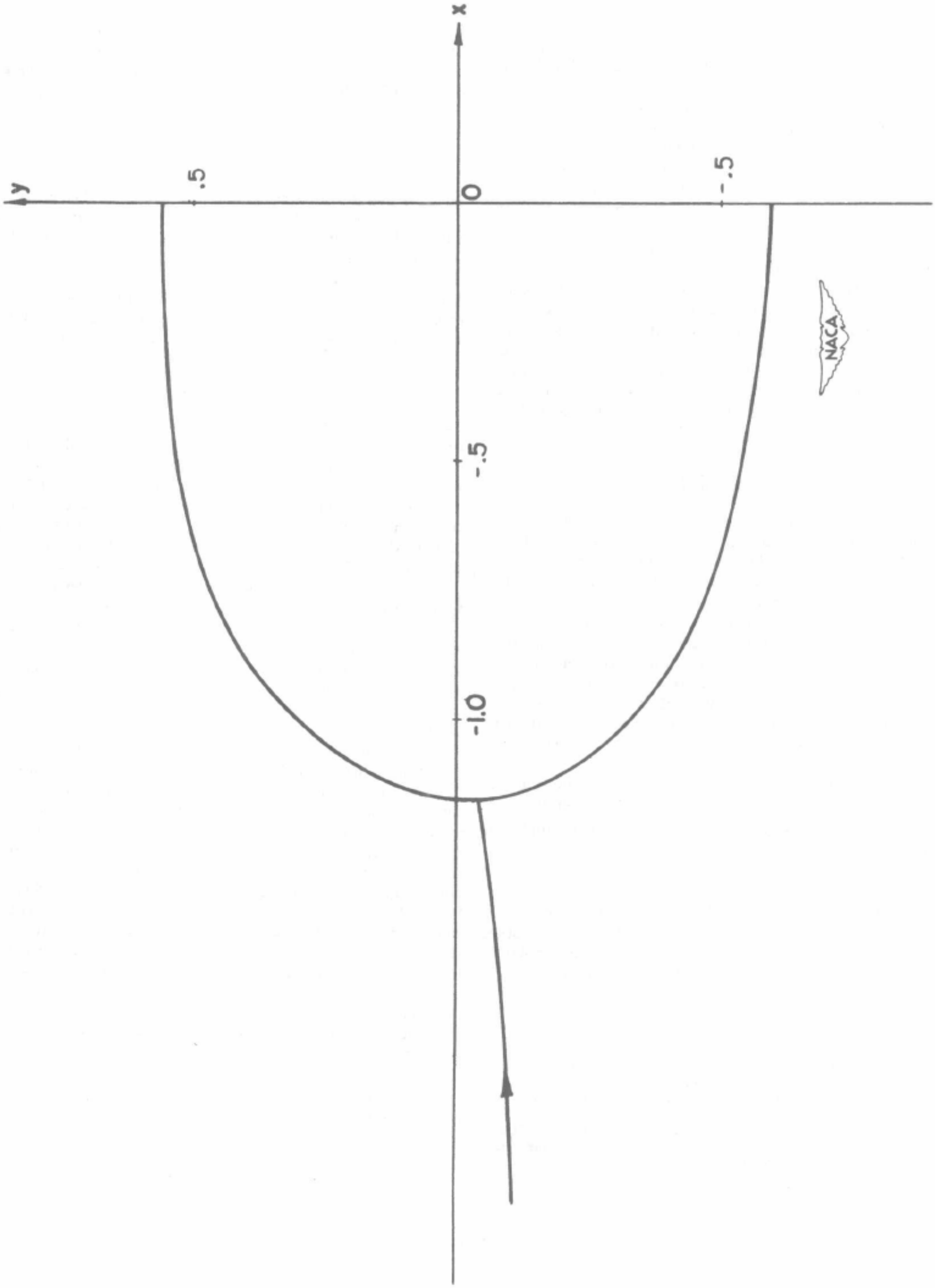

Figure 6.- Derived profile. $\epsilon = \frac{1}{2}$; $M_1 = 0.60$; $\frac{\Gamma_0}{4\pi} = 0.05$.

On the Hodograph Method [1)]

Y. H. Kuo
Assistant Professor of Aeronautical Engineering, Cornell University, Ithaca, N.Y.
December 20, 1948

THERE HAVE RECENTLY APPEARED two papers concerning the transonic flow of a compressible fluid about a closed cylinder, using the hodograph method, by M. J. Lighthill[1] and T. M. Cherry.[2] As is well known, such a flow is generally two-sheeted, with two branch points, in the hodograph plane. It is clear that a Taylor series is never sufficient to represent a complete solution in this situation. For this reason, the question of analytic continuation of a Taylor series always arises; it is in this connection that Lighthill and Cherry have made important contributions.

The Lighthill-Cherry method of continuation is essentially based on the property that the hypergeometric function $F_n(\tau)$ has simple poles at negative integers, so that it is accessible to a representation by a series of partial fractions. By means of this form of representation the authors are enabled to transform the original Taylor series into one with a larger radius of convergence. However, this requires the coefficients of the Taylor series to be $A_nT^{-n}(\tau_1)$ rather than $A_nF_n^{-1}(\tau_1)$, where A_n is the coefficient of the Taylor series of the corresponding incompressible flow, $T(\tau_1)$ a known function of

$$\tau\left(=\frac{\gamma-1}{2}\frac{q^2}{c_0^2}\right)$$

on the circle of convergence, which is always positive and nonvanishing in the subsonic range, and n an integer. Thus, the simplification in analytical continuation is brought about by the sacrifice of a closer resemblance to the incompressible flow on the circle of convergence.

In the appendixes of both papers, a previous paper by Tsien and Kuo[3] on the same subject is criticized and is, in fact, suspected of being incorrect, because the solution thereof does not agree with the new results. Both authors attempt to demonstrate the incorrectness by deriving a solution, for comparison, by their method. During the process, apparently, several basic facts have been overlooked, and, as a result, the criticism is not justified and should be clarified.

(a) To show that a solution, not satisfying his condition C (reference 2, page 76), continued by the Tsien-Kuo method from a Taylor series, diverges, Cherry considers as an example the function

$$W_0(w) = \sqrt{1-w} + w$$

where $w = qe^{-i\vartheta}$ is the complex velocity. This function consists of two component parts: one is an entire function and the other is singular at $w = 1$. Therefore, $W_0(w)$ has a branch point at $w = 1$. The proper expansion of this function is therefore

$$W_0(w) = \sum_0^\infty A_n w^n + w$$

for $|w| < 1$ and

$$W_0(w) = i\sum_0^\infty A_n w^{-[n-(1/2)]} + w$$

for $|w| > 1$. Both series are absolutely and uniformly convergent in their respective domains. Instead of taking the correct expansion shown above, Cherry, to demonstrate the supposed shortcomings of the Tsien-Kuo procedure, forces a second expansion of the form:

$$W_0(w) = i\sum_0^\infty [B_n w^{(1/2)-n} + C_n w^{n-(1/2)}]$$

and then computes the coefficients B_n and C_n by the rule of Tsien and Kuo. Clearly, by the lack of the proper singularity, this series has no choice but to diverge, and it must be noted that this divergence has nothing to do with the condition C. A difficulty like this can always be avoided by sound judgment.

(b) To show that the continued solution by Tsien and Kuo's method is incorrect, both authors deduce a solution by taking the same Taylor series as Tsien and Kuo—namely, for $q < 1$—

$$1^\psi(q, \vartheta) = \sum_1^\infty A_n q^n \frac{F_n(\tau)}{F_n(\tau_1)} \sin n\vartheta$$

but use their method of continuation. Indeed, the continued solution is different from Tsien and Kuo's result. The discrepancies, however, can be traced to an erroneous assumption, which seems to have been taken for granted by the authors. It must be remembered that the Lighthill-Cherry method of continuation depends on the expansibility of $F_n(\tau)T^{-1^n}(\tau_1)$ as a series of partial fractions. In the case of $F_n(\tau)/F_n(\tau_1)$, the method simply fails. As remarked by Cherry, the function $F_n(\tau)/F_n(\tau_1)$ is now regular at negative integers. Hence, the poles of the function are the zeros of $F_n(\tau_1)$. But for $\tau < (\gamma-1)/(\gamma+1)$ or in the subsonic range in which τ always lies, the hypergeometric function $F_n(\tau)$ is nonoscillatory and is positive for all real n. Therefore, $F_n(\tau_1)$ has no root in this interval.[4] Consequently, $F_n(\tau)/F_n(\tau_1)$ cannot be expanded as a series of partial fractions. In other words, Eqs. (53) and (54)[1] and (7.12) and ψ^{*2} are fictitious.

It is undeniable that the Tsien-Kuo method might run into a divergent series if not handled properly. This is not a characteristic feature, and it may be remarked, by way of analogy, that the lack of physical consideration will often lead to improper integrals and divergence in many problems, for example, in wing theory. The same, of course, can be true in the hodograph method. Fundamentally, Tsien and Kuo's method assumes nothing beyond the existence of a solution for a linear partial differential equation of two variables. If every requirement for a solution to exist is met, there should be no question as to whether the series or integral has a meaning. At this stage of the development of the hodograph method for transonic flows, an important criterion to judge any procedure is the amount of labor involved in carrying out the numerical calculation. It is this aspect of the Tsien-Kuo procedure which was thought unsatisfactory and was improved in a later report in 1946.[5]

---

[1] Lighthill, M. J., *The Hodograph Transformation in Transonic Flow. III*, Proc. Roy. Soc. A 191, pp. 352–369, 1947.

[2] Cherry, T. M., *Flow of a Compressible Fluid About a Cylinder*, Proc. Roy. Soc. A 192, pp. 45–79, 1947.

[3] Tsien, H. S., and Kuo, Y. H., *Two-Dimensional Irrotational Mixed Subsonic and Supersonic Flow of a Compressible Fluid and the Upper Critical Mach Number*, N.A.C.A. T.N. No. 995, 1946.

[4] Chaplygin, S., *Gas Jet*, N.A.C.A. T.N. No. 1063, 1944.

[5] Kuo, Y. H., *Two-Dimensional Irrotational Transonic Flows of a Compressible Fluid*, N.A.C.A. T.N. No. 1445, 1948.

1) Published in *Journal of the Aeronautical Sciences*, 1949, 16(3): 189

NATIONAL ADVISORY COMMITTEE FOR AERONAUTICS

TECHNICAL NOTE 2356

TWO-DIMENSIONAL TRANSONIC FLOW PAST AIRFOILS [1)]

By Yung-Huai Kuo

SUMMARY

This report concerns the problem of constructing solutions for transonic flows over symmetric airfoils. The aspect of the problem emphasized is, of necessity, not how to form a solution for compressible flow but how to simplify the initial phase of the problem, namely, the mapping of the incompressible flow. In the case of the symmetric Joukowski airfoil without circulation, the mapping is relatively simple, but the coefficients in the power series are difficult to evaluate. As a result, the problem requires simplification. Instead of the exact incompressible flow past the airfoil, an approximate flow is used, which is derived from a combination of source and sink. This flow differs only slightly from the exact one when the thickness is small. By the same method, the flow with circulation is also considered.

After the incompressible-flow functions are approximated in this fashion, the numerical calculation of the corresponding compressible flow, by the hodograph theory, does not present any essential difficulty.

INTRODUCTION

The problem of transonic potential flows has been considered in two previous reports (references 1 and 2). The object was, in the first place, to construct a solution for a closed body, and, secondly, to devise a method by which the flow can be easily calculated. The method of constructing a solution is essentially a method of analytic continuation. That is, a complex potential, which is known as a function of the complex velocity, is represented by a Taylor series about the origin of the hodograph plane and by another series in an annular region. Both series are convergent in their respective domains and agree on the common circle of convergence. In the interior region, a solution for compressible fluid can immediately be obtained by replacing the proper particular integrals in the Taylor series. The new solution does not affect the radius of convergence and, as Mach number tends to zero, reduces to that of the incompressible flow. The solution for the annular region cannot be formed by simply replacing the corresponding particular integrals in

1) *NACA Technical Note*, 1951, No. 2356

the outside series of the incompressible flow, because the solution so obtained does not agree with the inside series on the circle of convergence and, consequently, does not represent the same function.

The problem is then not so simple as it first appears to be. In order to make both series represent one solution, the idea of retaining the coefficients in both series of the incompressible flow must be abandoned. Instead, both the coefficients as well as the form of the solution are modified to satisfy the conditions on the circle of convergence (reference 2). A different approach to the same problem is that due to Lighthill and Cherry (references 3 and 4). Instead of choosing in advance the form of the outside series, they first transform the Taylor series into a double series, which, on interchanging the order of summation, can be summed to yield a single series. As a result, the series is valid anywhere except at the singularities in the domain considered, and analytic continuation is automatically accomplished. The continued outside series consists of two series; one is derived from the outside series of the incompressible flow and the other is a Taylor series.

The status of the hodograph method is then this: If a complex potential is given in series form, a corresponding solution for compressible fluid can be constructed, the body shape being unknown until the end of the calculation. It is apparent that the fundamental problem of determining the flow pattern about a given body remains unsolved. Moreover, even the transformation of the complex potential often poses many practical difficulties. Nevertheless, the hodograph method is still the only one available by which an exact solution may be sought. For this reason, there is still ground for further exploration along this line.

It is the object of this report to examine a case of more practical interest than that previously considered, in order to discover possible means of simplification. As a first attempt, a symmetric Joukowski airfoil is studied. In this case, if the rule of transforming incompressible to compressible flow is strictly followed, the calculation becomes extremely laborious. However, if a special case of small thickness - which is also of practical interest - is considered, the functions can be simplified to such an extent that numerical calculation is practical. The process is, in a sense, approximate. But as far as the compressible flow is concerned, the merit of a method lies only in whether it yields a good aerodynamic body or not. It has never been demonstrated that an exact incompressible potential function gives a better result. From this point of view, this is just another way of choosing a complex potential.

Finally, it must be emphasized that the present investigation is only the beginning, as far as practical calculations for useful airfoil profiles are concerned. Taking the approximate function as a guide, refinement is not difficult to make by introducing additional terms according to the character of the function. For instance, when circulation is present, the hydrodynamic functions for compressible flow transformed from those of incompressible flow for a symmetric body will give a negatively cambered airfoil. The necessity of applying correction terms is obvious.

This work was done at the Graduate School of Aeronautical Engineering of Cornell University under the sponsorship and with the financial assistance of the National Advisory Committee for Aeronautics.

FUNDAMENTAL EQUATIONS AND THEIR PARTICULAR SOLUTIONS

A steady, potential, and isotropic motion of a perfect gas in a plane satisfies a system of equations in the hodograph plane (references 1 and 2):

$$\left.\begin{aligned} q\frac{\partial\varphi}{\partial q} &= -\frac{\rho_o}{\rho}\left(1 - M^2\right)\frac{\partial\psi}{\partial\theta} \\ \frac{\partial\varphi}{\partial\theta} &= \frac{\rho_o}{\rho}\, q\frac{\partial\psi}{\partial q} \end{aligned}\right\} \qquad (1)$$

Here $\varphi(q,\theta)$ and $\psi(q,\theta)$ are, respectively, the velocity potential and stream function; q and θ, the magnitude and inclination of the velocity vector, respectively; ρ and M, the density of the fluid and the local Mach number, respectively; and ρ_o, the value of ρ at $q = 0$. (See appendix A for definitions of all symbols.)

This fundamental system, as shown previously (reference 2), can be solved and, in the case of $\psi(q,\theta)$, the particular integrals are

$$\left.\begin{aligned} &q^{\nu}F_{\nu}(\tau)\begin{Bmatrix}\cos\\ \sin\end{Bmatrix}\nu\theta \\ &q^{-\nu}F_{-\nu}(\tau)\begin{Bmatrix}\cos\\ \sin\end{Bmatrix}\nu\theta \end{aligned}\right\} \qquad (2)$$

$$\left.\begin{aligned} &\frac{\partial}{\partial\nu}\left[\tau^{\nu}F_{\nu}(\tau)\ \cos\ \nu\theta\right] \\ &\frac{\partial}{\partial\nu}\left[\tau^{\nu}F_{\nu}(\tau)\ \sin\ \nu\theta\right] \end{aligned}\right\} \tag{3}$$

and

$$\theta \quad \text{and} \quad \int^{\tau} (1-\tau)^{\beta}\,\frac{d\tau}{\tau} \tag{4}$$

and, in the case of $\varphi(q,\theta)$, are

$$\left.\begin{aligned} &(1-\tau)^{-\beta}q^{\nu}F_{\nu}(\tau)\xi_{\nu}(\tau)\begin{Bmatrix}\sin\\-\cos\end{Bmatrix}\nu\theta \\ &(1-\tau)^{-\beta}q^{-\nu}F_{-\nu}(\tau)\xi_{-\nu}(\tau)\begin{Bmatrix}\sin\\-\cos\end{Bmatrix}\nu\theta \end{aligned}\right\} \tag{5}$$

$$\left.\begin{aligned} &(1-\tau)^{-\beta}\,\frac{\partial}{\partial\nu}\left[\tau^{\nu}F_{\nu}(\tau)\xi_{\nu}\ \sin\ \nu\theta\right] \\ &(1-\tau)^{-\beta}\,\frac{\partial}{\partial\nu}\left[\tau^{\nu}F_{\nu}(\tau)\xi_{\nu}(\tau)\ \cos\ \nu\theta\right] \end{aligned}\right\} \tag{6}$$

$$(1-\tau)^{-\beta} - \frac{1}{2}\int^{\tau}(1-\tau)^{-\beta}\,\frac{d\tau}{\tau} \quad \text{and} \quad \theta \tag{7}$$

All these results are well-known except equations (3) and (6) which can be found in appendix B. Here $F_{\nu}(\tau)$ and $F_{-\nu}(\tau)$ stand, respectively, for the hypergeometric functions $F\left(a_{\nu},b_{\nu};\ \nu+1;\ \tau\right)$ and $F\left(a_{\nu}-\nu,b_{\nu}-\nu;\ 1-\nu;\ \tau\right)$ for nonintegral parameters ν. In case ν

is an integer n, the definition of the second integral is modified. The new function will include a logarithmic term (cf. reference 2) and is denoted by $F_{-n}(\tau)$. The functions $\xi_\nu(\tau)$ and $\xi_{-\nu}(\tau)$ are defined by

$$\left.\begin{aligned} \nu\xi_\nu(\tau) &= 2\tau \frac{d}{d\tau} \log_e \tau^{\nu/2} F_\nu(\tau) \\ \nu\xi_{-\nu}(\tau) &= 2\tau \frac{d}{d\tau} \log_e \tau^{-\nu/2} F_{-\nu}(\tau) \end{aligned}\right\} \tag{8}$$

and the constants a_ν and b_ν are defined by

$$\left.\begin{aligned} a_\nu + b_\nu &= \nu - \beta \qquad \beta = \frac{1}{\gamma - 1} \\ a_\nu b_\nu &= -\frac{1}{2}\beta\nu(\nu + 1) \end{aligned}\right\} \tag{9}$$

and the variable τ is

$$\tau = \frac{1}{2\beta} \frac{q^2}{c_o^2} \tag{10}$$

where γ is the ratio of specific heats of the gas and c_o, the speed of sound at $q = 0$.

Furthermore, $F_\nu(\tau)$ is an analytic function of both variables τ and ν. For fixed $\tau < \frac{\gamma - 1}{\gamma + 1}$, it has simple poles at $\nu = -n$ and, accordingly, possesses an expansion of the form (references 3 and 4):

$$F_\nu(\tau) = f(\tau)T^\nu - \sum_{m=1}^{\infty} \frac{c_m}{\nu + m} \tau^m T(\tau)^{m+\nu} F_m(\tau) \tag{11}$$

where

$$\left.\begin{aligned} f(\tau) &= \frac{(1-\tau)^{\gamma_1^2/4}}{\left(1-\gamma_1^2\tau\right)^{1/4}} \\ T(\tau) &= \frac{2}{\left(1-\gamma_1\right)^{\gamma_1}} \frac{\left[\gamma_1(1-\tau)^{1/2} + \left(1-\gamma_1^2\tau\right)^{1/2}\right]^{\gamma_1}}{(1-\tau)^{1/2} + \left(1-\gamma_1^2\tau\right)^{1/2}} \qquad \gamma_1 = \sqrt{\frac{\gamma+1}{\gamma-1}} \\ c_m &= \frac{\Gamma(a_m)\Gamma(m+1-b_m)}{\Gamma(a_m-m)\Gamma(1-b_m)m!(m-1)!} \end{aligned}\right\} \quad (12)$$

This expansion is valid for all values of ν except negative integers. When $\nu = -n$ the limiting process gives

$$F_{-n}(\tau) = f(\tau)T^{-n}(\tau) - \sum_{m=1}^{\infty}{}' \frac{c_m}{-n+m} \tau^m T^{m-n}(\tau) F_m(\tau) - c_n\left[\tau^n F_n(\tau)\log_e T + \frac{\partial}{\partial n}\left(\tau^n F_n\right)\right] \quad (13)$$

where the prime indicates that the term $m = n$ is to be excluded.

From these particular solutions one can construct a solution for any boundary in the hodograph plane. Once the functions $\varphi(q,\theta)$ and $\psi(q,\theta)$ are known, the flow pattern in the physical plane is given by integrating

$$\left.\begin{aligned} \frac{\partial x}{\partial\theta} &= \frac{1}{q}\left(\cos\theta\,\frac{\partial\varphi}{\partial\theta} - \frac{\rho_o}{\rho}\sin\theta\,\frac{\partial\psi}{\partial\theta}\right) \\ \frac{\partial y}{\partial\theta} &= \frac{1}{q}\left(\sin\theta\,\frac{\partial\varphi}{\partial\theta} + \frac{\rho_o}{\rho}\cos\theta\,\frac{\partial\psi}{\partial\theta}\right) \end{aligned}\right\} \quad (14)$$

and

$$\left.\begin{aligned}\frac{\partial x}{\partial q} &= \frac{1}{q}\left(\cos\theta\,\frac{\partial \varphi}{\partial q} - \frac{\rho_o}{\rho}\sin\theta\,\frac{\partial \psi}{\partial q}\right)\\ \frac{\partial y}{\partial q} &= \frac{1}{q}\left(\sin\theta\,\frac{\partial \varphi}{\partial q} + \frac{\rho_o}{\rho}\cos\theta\,\frac{\partial \psi}{\partial q}\right)\end{aligned}\right\} \tag{15}$$

where x and y are the coordinates of a point in the physical plane.

MAPPING OF AN INCOMPRESSIBLE FLOW

The potential flow of an incompressible fluid past a symmetric Joukowski airfoil without circulation is determined by a complex function ${}_oW(z)$:

$${}_oW(z) = \zeta + \epsilon + \frac{(1+\epsilon)^2}{\zeta + \epsilon} \qquad z = \zeta + \frac{1}{\zeta} \tag{16}$$

where

$$z = x + iy$$

$$\zeta = \xi + i\eta$$

Here all the physical quantities are made dimensionless by dividing, respectively, every length and velocity by the radius of the generating circle and the free-stream velocity. Then ϵ is a purely real number. The complex velocity w for such a flow is

$$w = \frac{\zeta^2(\zeta + 1 + 2\epsilon)}{(\zeta + 1)(\zeta + \epsilon)^2} \tag{17}$$

This equation expresses the relationship between w and ζ. It can also be interpreted as a transformation function from the ζ-plane to the w-plane. In other words, if a flow field in the physical plane is given, its image in the w-plane is immediately known by means of equation (17). Since the present problem is formulated in the w-plane instead of the z-plane, the flow field in the z-plane can be calculated from the inverse transformation $\zeta(w)$, which is given by solving

$$\zeta^3 + (1 + 2\epsilon)\zeta^2 - \frac{\epsilon(\epsilon + 2)w}{1 - w}\zeta - \frac{\epsilon^2 w}{1 - w} = 0 \tag{18}$$

The three solutions of this equation are:

$$\left.\begin{aligned}
\zeta_1(w) &= P(w) + Q(w) - \frac{1 + 2\epsilon}{3} \\
\zeta_2(w) &= -\frac{1}{2}\left[P(w) + Q(w)\right] - \frac{i\sqrt{3}}{2}\left[P(w) - Q(w)\right] - \frac{1 + 2\epsilon}{3} \\
\zeta_3(w) &= -\frac{1}{2}\left[P(w) + Q(w)\right] + \frac{i\sqrt{3}}{2}\left[P(w) - Q(w)\right] - \frac{1 + 2\epsilon}{3}
\end{aligned}\right\} \tag{19}$$

where

$$\left.\begin{aligned}
P(w) = -\frac{1}{3}\Bigg\{&(1 - \epsilon)^3 + \frac{9\epsilon(1 + \epsilon + \epsilon^2)}{1 - w} - \\
&\frac{i3^{3/2}\epsilon(1 + 2\epsilon)^{3/2}w^{1/2}}{(1 - w)^{3/2}}\left[1 - \frac{(1 - \epsilon)^3(1 + \epsilon)}{(1 + 2\epsilon)^3}w\right]\Bigg\} \\
Q(w) = -\frac{1}{3}\Bigg\{&(1 - \epsilon)^3 + \frac{9\epsilon\left(1 + \epsilon + \epsilon^2\right)}{1 - w} + \\
&\frac{i3^{3/2}\epsilon(1 + 2\epsilon)^{3/2}w^{1/2}}{(1 - w)^{3/2}}\left[1 - \frac{(1 - \epsilon)^3(1 + \epsilon)}{(1 + 2\epsilon)^3}w\right]\Bigg\}
\end{aligned}\right\} \tag{20}$$

This indicates that to a neighborhood in the w-plane there correspond, in general, three distinct neighborhoods in the ζ-plane or the z-plane (see fig. 1). The exceptional points where two of the three solutions become equal are given by $dw/d\zeta = 0$. This yields three points $\zeta = 0$, $\zeta = -\frac{1 + 2\epsilon}{2 + \epsilon}$, and $\zeta = \infty$ about which two of three

solutions join. Furthermore, it remains to investigate how the axis of reals, that is, $v = 0$, is mapped in the ζ-plane. By separating into real and imaginary parts, the velocity component v in terms of ξ and η is:

$$v = -\frac{2\epsilon\eta\left(\xi^2 + \epsilon\xi + \eta^2\right)\left[(2 + \epsilon)\xi + 1 + 2\epsilon\right]}{(\zeta\bar{\zeta} + 2\xi + 1)\left(\zeta\bar{\zeta} + 2\epsilon\xi + \epsilon^2\right)^2}$$

Then $v = 0$ corresponds to

$$\eta = 0$$

$$(2 + \epsilon)\xi + 1 + 2\epsilon = 0$$

$$\left(\xi + \frac{\epsilon}{2}\right)^2 + \eta^2 = \frac{\epsilon^2}{4}$$

In other words, the axis of reals of the w-plane corresponds to: (a) The axis of reals of the ζ-plane, (b) a straight line through one branch point parallel to the η-axis, and (c) a circle. Moreover, while u increases from zero to one along $v = 0$, $\zeta_1(w)$ decreases from the forward stagnation point to negative infinity, $\zeta_2(w)$ increases from zero to positive infinity, and $\zeta_3(w)$ decreases to a negative number. Evidently, branches I and II join smoothly at the line $\xi = -\frac{1 + 2\epsilon}{2 + \epsilon}$ and branches II and III meet along the circle $\left(\xi + \frac{\epsilon}{2}\right)^2 + \eta^2 = \frac{\epsilon^2}{4}$. Branch III then lies entirely inside the circle of radius $\epsilon/2$. Hence, the flow over a body with a sharp trailing edge, complicated as it is, remains essentially the same as that over the body which is symmetric about two axes with two stagnation points. Finally, by substituting equations (19) in equation (16), the corresponding branches of the complex potential are ${}_oW_1(w)$, ${}_oW_2(w)$, and ${}_oW_3(w)$.

When circulation is present, having the magnitude required by the condition of finite trailing-edge velocity at an angle of attack α, the complex potential is

$${}_oW(z) = (\zeta + \epsilon)e^{-i\alpha} + \frac{(1 + \epsilon)^2}{\zeta + \epsilon}e^{i\alpha} + 2i(1 + \epsilon)\sin\alpha\log_e(\zeta + \epsilon) \quad (21)$$

with $z = \zeta + \frac{1}{\zeta}$; and the complex velocity is

$$w = \frac{\zeta^2\left[(\zeta + \epsilon)e^{-i\alpha} + (1 + \epsilon)e^{i\alpha}\right]}{(\zeta + 1)(\zeta + \epsilon)^2} \tag{22}$$

The inverse transformation function $\zeta(w)$ in this case consists in the solution of

$$(e^{-i\alpha} - w)\zeta^3 + \left[\epsilon e^{-i\alpha} + (1 + \epsilon)e^{i\alpha} - (1 + 2\epsilon)w\right]\zeta^2 - \epsilon(2 + \epsilon)w\zeta - \epsilon^2 w = 0 \tag{23}$$

The solution of this equation can, of course, be given, but the expressions are so complex as to make any practical manipulation difficult. To bring out the complicated character of the Reimann surface it is sufficient to determine the branch points and branch lines. Now the branch points are $\zeta = 0$, $\zeta = \infty$ and

$$(1 + \epsilon)(1 - e^{2\alpha i})\zeta^2 + \epsilon\left[3 + \epsilon + (1 + \epsilon)e^{2\alpha i}\right]\zeta + 2\epsilon\left[\epsilon + (1 + \epsilon)e^{2\alpha i}\right] = 0$$

of which two are inside the body; and the wind axis in the hodograph plane, that is, the axis in the direction of the wind, corresponds, even for small values of α, to curves in the ζ-plane:

$$\alpha(1 + \epsilon)(\xi + 1 + 2\epsilon)\eta^4 + \epsilon\left[(2 + \epsilon)\xi + 1 + 2\epsilon\right]\eta^3 + \alpha(1 + \epsilon)\left[5\xi^3 + 6(1 + \epsilon)\xi^2 - (3 - 2\epsilon - \epsilon^2)\xi - (1 + \epsilon)^2\right]\eta^2 + \epsilon\xi(\xi + \epsilon)\left[(2 + \epsilon)\xi + 1 + 2\epsilon\right]\eta + \alpha(1 + \epsilon)\xi^2(\xi + 1)(\xi + \epsilon)^2 = 0$$

This equation is of degree four in η and five in ξ. It would be interesting to trace this equation for given values of ϵ and α. This was not done for the sole reason that the exact problem is too difficult, if not impossible, to handle. It should be remembered that the present procedure of constructing a solution of a compressible flow depends primarily on the knowledge of an incompressible-flow solution in the form of power series. Even in the case of zero circulation, as

can be seen from equations (20), the series expansion of the complex potential yields sets of coefficients which are, at least, double infinite series (cf. appendix C). One can easily see that the initial task alone is a formidable one, not to mention the later computation of the compressible-flow solution. This amount of labor is particularly unjustifiable in this problem because, even if one starts with an exact solution, he may still end up with a body very different from what he expected because of the distortion due to compressibility. For this reason deviation from the formal procedure is recommended wherever it is convenient. In this report, the case of small thickness and small angle of attack is studied first.

Before proceeding further, it is mentioned that the Joukowski airfoil is characterized by having a cusp at the trailing edge. Although the velocity is finite there, the acceleration is infinite and, consequently, the analyticity of the mapping function breaks down; namely, $d_oW/dw = 0$. In order to preserve this property in the case of compressible flow, the stream function $\psi(q,\theta)$ must satisfy

$$\left.\begin{aligned} \frac{\partial \psi}{\partial q} &= 0 \\ \frac{\partial \psi}{\partial \theta} &= 0 \end{aligned}\right\} \qquad (24)$$

In the case of symmetric flow, the first is satisfied identically. The second serves to determine the speed at the trailing edge.

APPLICATION TO THIN SYMMETRIC AIRFOILS

Consider the case of a thin symmetric airfoil present in a uniform flow without circulation, namely, $\alpha = 0$. Since the thickness ratio of a Joukowski airfoil is directly proportional to the parameter ϵ, for thin airfoils ϵ must be small. Suppose that the airfoil is so thin that terms higher than ϵ are negligible. Equation (18) is then simplified to

$$\zeta^2 + (1 + 2\epsilon)\zeta - \frac{2\epsilon w}{1 - w} = 0 \qquad (25)$$

of which the solutions are:

$$\left.\begin{aligned}\zeta_1(w) &= -\frac{1}{2}(1+2\epsilon)\left(1+\sqrt{\frac{1-\epsilon_1^2 w}{1-w}}\right)\\ \zeta_2(w) &= -\frac{1}{2}(1+2\epsilon)\left(1-\sqrt{\frac{1-\epsilon_1^2 w}{1-w}}\right)\end{aligned}\right\} \tag{26}$$

where $\epsilon_1 = \frac{1-2\epsilon}{1+2\epsilon}$, being of the order of magnitude unity.

By making such an approximation it is seen that the third solution disappears. This is explained by the fact that the third branch lies wholly inside a circle of area $\frac{1}{4}\pi\epsilon^2$ which, according to the present approximation, is zero; therefore $\zeta_3(w) = 0$. The branch points are now located at $\zeta = -\frac{1}{2}(1+2\epsilon)$ and $\zeta = \infty$, connected by the branch line (fig. 2) $2\xi + 1 + 2\epsilon = 0$.

The problem is indeed simple. The question, however, is: What flow is represented or, in other words, how is the complex potential modified? By using the simplified transformation function, a straightforward integration gives

$$_{o}W(z) = \zeta + \epsilon + \frac{1+2\epsilon}{2\epsilon}\log_e\left(1+\frac{2\epsilon}{\zeta}\right) \tag{27}$$

The flow in the ζ-plane is then that produced by the superposition of a sink and a source at, respectively, $\zeta = 0$ and $\zeta = -2\epsilon$ in a uniform flow. It is very easy to see that, if ϵ is small, the vanishing of the stream function corresponds closely to a circle with radius $1+\epsilon$ and center at $\zeta = -\epsilon$. Hence for small values of ϵ the curve in the z-plane will not differ much from a Joukowski airfoil. By substituting ζ_1 and ζ_2 from equations (26) in equation (27) the two branches of the complex potential are

$$
\left.
\begin{aligned}
{}_{o}W_1(w) &= -\frac{1}{2}\left[1 + (1 + 2\epsilon)\sqrt{\frac{1 - \epsilon_1{}^2 w}{1 - w}}\right] + \\
&\qquad \frac{1 + 2\epsilon}{2\epsilon} \log_e \left[1 - \frac{4\epsilon}{1 + 2\epsilon} \Big/ \left(\frac{1 - \epsilon_1{}^2 w}{1 - w}\right)^{1/2} + 1\right] \\
{}_{o}W_2(w) &= -\frac{1}{2}\left[1 - (1 + 2\epsilon)\sqrt{\frac{1 - \epsilon_1{}^2 w}{1 - w}}\right] + \\
&\qquad \frac{1 + 2\epsilon}{2\epsilon} \log_e \left[1 - \frac{4\epsilon}{1 + 2\epsilon} \Big/ -\left(\frac{1 - \epsilon_1{}^2 w}{1 - w}\right)^{1/2} + 1\right]
\end{aligned}
\right\} \tag{28}
$$

By taking $\epsilon = 0.08$, the hodograph $\psi_o(q,\theta) = 0$ from equations (28) and that of a symmetric Joukowski airfoil are compared in figure 3. It is seen that, except in the neighborhood of the singularity $w = 1$, the agreement is quite close even for a thickness ratio of about 10 percent.

For the case where a weak circulation is present, by the same method of approximation, equation (23) simplifies to

$$
\zeta^2 + \left(1 + 2\epsilon + \frac{2\alpha i}{1 - w}\right)\zeta - \frac{2\epsilon w}{1 - w} = 0 \tag{29}
$$

Here α is assumed to be the same order of magnitude as ϵ, and therefore the product of ϵ and α is also dropped. The solutions of this equation are

$$
\left.
\begin{aligned}
\zeta_1(w) &= -\frac{1+2\epsilon}{2}\left(1 + \sqrt{\frac{1 - \epsilon_1{}^2 w}{1 - w}}\right) + \alpha i \left[-\frac{1}{1 - w} - \frac{1}{(1 - w)^{1/2}\left(1 - \epsilon_1{}^2 w\right)^{1/2}}\right] \\
\zeta_2(w) &= -\frac{1+2\epsilon}{2}\left(1 - \sqrt{\frac{1 - \epsilon_1{}^2 w}{1 - w}}\right) + \alpha i \left[-\frac{1}{1 - w} + \frac{1}{(1 - w)^{1/2}\left(1 - \epsilon_1{}^2 w\right)^{1/2}}\right]
\end{aligned}
\right\} \tag{30}
$$

the corresponding complex potential is

$$ {}_{o}W(w) = (1 - \alpha i)\zeta + \epsilon + \frac{1 + 2\epsilon + \alpha i}{2\epsilon} \log_e \left(1 + \frac{2\epsilon}{\zeta}\right) + 2\alpha i \log_e (\zeta + 2\epsilon) \tag{31} $$

The body in the ζ-plane is again a circle, provided both ϵ and α are small. A substitution of ζ_1 and ζ_2 from equations (30) in equation (31) gives, respectively, ${}_{o}W_1(w)$ and ${}_{o}W_2(w)$.

It should be noted that, in the previous case when circulation was present, it altered radically the nature of the singularity of the flow. Now by comparing equations (30) with equations (26) one can see that circulation has introduced essentially no complication and hence the problem can be similarly handled as in the case where no circulation exists.

EXPANSIONS OF ${}_{o}W(w)$

When $\alpha = 0$.- For thin airfoils, as seen from the previous section, the domain of interest has two branch points $\zeta = -\frac{1}{2}(1 + 2\epsilon)$ and $\zeta = \infty$; the corresponding points in the w-plane are $w = 1$ and $w = \frac{1}{\epsilon_1{}^2}$, at each of which ${}_{o}W(w)$ becomes singular. As a result, two different expansions are required to represent each branch of ${}_{o}W(w)$. In the case of ${}_{o}W_1(w)$, the origin is a regular point; for ${}_{o}W_2(w)$ it is a logarithmic singularity.

Consider ${}_{o}W_1(w)$ for the case $\alpha = 0$ first: About the forward stagnation point $|\zeta| \neq 0$ and ${}_{o}W_1(w)$ can be simplified in the form:

$$ {}_{o}W_1(w) = \zeta_1 + \epsilon + \frac{1 + 2\epsilon}{\zeta_1} - \frac{\epsilon(1 + 2\epsilon)}{\zeta_1{}^2} + O(\epsilon^2) \tag{32} $$

By means of the relation:

$$ \zeta_1\zeta_2 = -\frac{2\epsilon w}{1 - w} $$

${}_0W_1(w)$ can be reduced to two elements $(1 - w)^{-1/2}\left(1 - \epsilon_1{}^2 w\right)^{-1/2}$ and $(1 - w)^{1/2}\left(1 - \epsilon_1{}^2 w\right)^{1/2}$ which possess the following expansions in the respective domains:

$$\left.\begin{aligned} (1 - w)^{-1/2}\left(1 - \epsilon_1{}^2 w\right)^{-1/2} &= \sum_0^\infty S_n{}^{(i)} w^n \\ (1 - w)^{1/2}\left(1 - \epsilon_1{}^2 w\right)^{1/2} &= \sum_0^\infty {}_1S_n{}^{(i)} w^n \end{aligned}\right\} \quad |w| < 1 \tag{33}$$

where

$$\left.\begin{aligned} S_n{}^{(i)} &= (-1)^n \sum_{m=0}^{n} \binom{-\frac{1}{2}}{m}\binom{-\frac{1}{2}}{n-m} \epsilon_1{}^{2(n-m)} \\ {}_1S_n{}^{(i)} &= (-1)^n \sum_{m=0}^{n} \binom{\frac{1}{2}}{m}\binom{\frac{1}{2}}{n-m} \epsilon_1{}^{2(n-m)} \end{aligned}\right\} \tag{34}$$

and

$$\left.\begin{aligned} (1 - w)^{-1/2}\left(1 - \epsilon_1{}^2 w\right)^{-1/2} &= \sum_0^\infty S_n{}^{(o)} \epsilon_1{}^{2n} w^n + \sum_1^\infty S_n{}^{(o)} w^{-n} \\ (1 - w)^{1/2}\left(1 - \epsilon_1{}^2 w\right)^{1/2} &= \sum_0^\infty {}_1S_n{}^{(o)} \epsilon_1{}^{2n} w^n + \sum_1^\infty {}_1S_n{}^{(o)} w^{-n} \end{aligned}\right\} \quad 1 < |w| < \frac{1}{\epsilon_1{}^2} \tag{35}$$

where

$$\left.\begin{aligned} S_n^{(o)} &= (-1)^n \sum_0^\infty \binom{-\frac{1}{2}}{m}\binom{-\frac{1}{2}}{m+n}\epsilon_1^{2m} \\ {}_1S_n^{(o)} &= (-1)^n \sum_0^\infty \binom{\frac{1}{2}}{m}\binom{\frac{1}{2}}{m+n}\epsilon_1^{2m} \end{aligned}\right\} \tag{36}$$

A simple reduction then yields

$${}_oW_1(w) = -A_o - \sum_2^\infty A_n w^n + O(\epsilon^2) \qquad |w| < 1 \tag{37}$$

where

$$A_n = \frac{1+2\epsilon}{2}\left(S_n^{(i)} - \epsilon_1^2 S_{n-1}^{(i)}\right) + \frac{(1+2\epsilon)^2}{4\epsilon}\left[S_{n+1}^{(i)} - \left(1+\epsilon_1^2\right)S_n^{(i)} + \epsilon_1^2 S_{n-1}^{(i)}\right] + \frac{(1+2\epsilon)^3}{8\epsilon}\left[-S_{n+2}^{(i)} + \left(2+\epsilon^2\right)S_{n+1}^{(i)} - 2\epsilon_1^2 S_n^{(i)} - S_n^{(i)} + \epsilon_1^2 S_{n-1}^{(i)}\right] \tag{38}$$

Here A_2 is zero, as is easily shown from equation (27); in the above expansion it would have been of the order of ϵ^2 and hence is included in the symbol $O(\epsilon^2)$. The velocity potential and stream function are, neglecting $O(\epsilon^2)$,

$$\left.\begin{aligned} {}_o\varphi_1 &= -A_o - \sum_2^\infty A_n q^n \cos n\theta \\ {}_o\psi_1 &= \sum_2^\infty A_n q^n \sin n\theta \end{aligned}\right\} \qquad q < 1 \tag{39}$$

If the expansions (35) are introduced, in the annulus region one will have

$$ {}_{o}W_1(w) = B_{-2}w^{-2} + B_{-1}w^{-1} + B_o + i\sum_{0}^{\infty}\left(B_\nu w^\nu + C_\nu w^{-\nu}\right) \qquad 1 < |w| < \frac{1}{\epsilon_1^2} \tag{40} $$

where

$$ \left.\begin{aligned}
B_o &= -\frac{(1+2\epsilon)(3+8\epsilon)}{8\epsilon} \\
B_{-1} &= \frac{(1+2\epsilon)^2}{2\epsilon} \\
B_{-2} &= -\frac{(1+2\epsilon)^3}{8\epsilon} \\
B_\nu &= \frac{1+2\epsilon}{2}\left(S_{n+1}(o) - S_n(o)\right) - \frac{(1+2\epsilon)^2}{4\epsilon}\,{}_1S_{n+1}(o) - \\
&\quad \frac{(1+2\epsilon)^3}{8\epsilon}\left({}_1S_{n+1}(o) - {}_1S_{n+2}(o)\right) \\
C_\nu &= \frac{1+2\epsilon}{2}\left(S_n(o) - \epsilon_1^2 S_{n+1}(o)\right) - \frac{(1+2\epsilon)^2}{4\epsilon}\,{}_1S_n(o) - \\
&\quad \frac{(1+2\epsilon)^3}{8\epsilon}\left({}_1S_n(o) - {}_1S_{n-1}(o)\right) \\
C_{1/2} &= \frac{1+2\epsilon}{2}\left(S_o(o) - \epsilon_1^2 S_1(o)\right) - \frac{(1+2\epsilon)^2}{4\epsilon}\,{}_1S_o(o) - \\
&\quad \frac{(1+2\epsilon)^3}{8\epsilon}\left({}_1S_o(o) - F_1^2\,{}_1S_1(o)\right)
\end{aligned}\right\} \tag{41} $$

$$ \nu = n + \frac{1}{2} $$

Separating into real and imaginary parts, ${}_o\varphi_1$ and ${}_o\psi_1$ are, approximately,

$$\left.\begin{aligned} {}_o\varphi_1 &= B_{-2}q^{-2}\cos 2\theta + B_{-1}q^{-1}\cos\theta + B_o + \sum_0^\infty \left(B_\nu q^\nu - C_\nu q^{-\nu}\right)\sin\nu\theta \\ {}_o\psi_1 &= B_{-2}q^{-2}\sin 2\theta + B_{-1}q^{-1}\sin\theta + \sum_0^\infty \left(B_\nu q^\nu + C_\nu q^{-\nu}\right)\cos\nu\theta \end{aligned}\right\} \quad (42)$$

for $1 < q < \frac{1}{\epsilon_1{}^2}$.

In the case of ${}_oW_2(w)$, as $w = 0$ is not a regular point, a Taylor expansion does not exist. It can be expanded, however, in the following form:

$${}_oW_2(w) = \sum_0^2 A_{-n}w^{-n} + \sum_2^\infty A_n w^n + O(\epsilon^2) \qquad |w| < 1 \qquad (43)$$

where A_n is defined in equation (38) while A_{-o}, A_{-1}, and A_{-2} are

$$\left.\begin{aligned} A_{-o} &= \frac{3(1+2\epsilon)}{4\epsilon} \\ A_{-1} &= \frac{(1+2\epsilon)^2}{\epsilon} \\ A_{-2} &= -\frac{(1+2\epsilon)^3}{4\epsilon} \end{aligned}\right\} \quad (44)$$

On the other hand, in the region $1 < |w| < \epsilon_1{}^{-2}$ the expansions are

$${}_oW_2(w) = \sum_0^2 B_{-n}w^{-n} - i\sum_0^\infty \left(B_\nu w^\nu + C_\nu w^{-\nu}\right) + O(\epsilon^2) \qquad (45)$$

Here the constants B_{-2}, B_{-1}, B_0, B_ν, and C_ν are defined in equations (41). It is clear that by circling once about $w = 1$ branch I goes smoothly over into branch II, as is easily seen from equations (40) and (45). Similarly, the velocity potential and stream function are, omitting $O(\epsilon^2)$,

$$\left.\begin{aligned} {}_o\Phi_2 &= \sum_{0}^{2} A_{-n} q^{-n} \cos n\theta + \sum_{2}^{\infty} A_n q^n \cos n\theta \\ {}_o\Psi_2 &= \sum_{1}^{2} A_{-n} q^{-n} \sin n\theta + \sum_{2}^{\infty} A_n q^n \sin n\theta \end{aligned}\right\} \quad 0 < q < 1 \qquad (46)$$

and for $1 < q < \epsilon^{-2}$

$$\left.\begin{aligned} {}_o\Phi_2 &= \sum_{0}^{2} B_{-n} q^{-n} \cos n\theta + \sum_{0}^{\infty} \left(B_\nu q^\nu - C_\nu q^{-\nu}\right) \sin \nu\theta \\ {}_o\Psi_2 &= \sum_{1}^{2} B_{-n} q^{-n} \sin n\theta - \sum_{0}^{\infty} \left(B_\nu q^\nu + C_\nu q^{-\nu}\right) \cos \nu\theta \end{aligned}\right\} \qquad (47)$$

When $\alpha \neq 0$.- When α is finite but small in the case of a thin airfoil, equations (30) show that

$$\left.\begin{aligned} \zeta_1 &= \zeta_1^{(o)} + \alpha\zeta_1^{(1)} \\ \zeta_2 &= \zeta_2^{(o)} + \alpha\zeta_2^{(1)} \end{aligned}\right\} \qquad (48)$$

where $\zeta_1^{(o)}$ and $\zeta_2^{(o)}$ are the transformation functions for $\alpha = 0$ and $\zeta_1^{(1)}$ and $\zeta_2^{(1)}$ are correction terms due to circulation. Therefore, they are defined as follows:

$$\left.\begin{aligned}
\zeta_1^{(o)} &= -\frac{1+2\epsilon}{2}\left(1+\sqrt{\frac{1-\epsilon_1^2 w}{1-w}}\right)\\
\zeta_2^{(o)} &= -\frac{1+2\epsilon}{2}\left(1-\sqrt{\frac{1-\epsilon^2 w}{1-w}}\right)\\
-i\zeta_1^{(1)} &= -\frac{1}{1-w}-\frac{1}{(1-w)^{1/2}\left(1-\epsilon_1^2 w\right)^{1/2}}\\
-i\zeta_2^{(1)} &= -\frac{1}{1-w}+\frac{1}{(1-w)^{1/2}\left(1-\epsilon_1^2 w\right)^{1/2}}
\end{aligned}\right\} \tag{49}$$

Similarly, the complex potential can be written as

$$\left.\begin{aligned}
{}_oW_1 &= {}_oW_1^{(o)} + \alpha\ {}_oW_1^{(1)}\\
{}_oW_2 &= {}_oW_2^{(o)} + \alpha\ {}_oW_2^{(1)}
\end{aligned}\right\} \tag{50}$$

where ${}_oW_1^{(o)}$ and ${}_oW_2^{(o)}$ are defined in equations (28) and ${}_oW_1^{(1)}$ and ${}_oW_2^{(1)}$ are found to be

$$\left.\begin{aligned}
-i\ {}_oW_1^{(1)} &= \zeta_1^{(1)} - \zeta_1^{(o)} + \frac{1+4\epsilon}{2\epsilon}\log_e\left(\zeta_1^{(o)}+2\epsilon\right) - \\
&\qquad \frac{1}{2\epsilon}\log_e\zeta_1^{(o)} - \frac{(1+2\epsilon)\zeta_1^{(1)}}{\zeta_1^{(o)}\left(\zeta_1^{(o)}+2\epsilon\right)}\\
-iW_2^{(1)} &= \zeta_2^{(1)} - \zeta_2^{(o)} + \frac{1+4\epsilon}{2\epsilon}\log_e\left(\zeta_1^{(o)}+2\epsilon\right) - \\
&\qquad \frac{1}{2\epsilon}\log_e\zeta_2^{(o)} - \frac{(1+2\epsilon)\zeta_2^{(1)}}{\zeta_2^{(o)}\left(\zeta_2^{(o)}+2\epsilon\right)}
\end{aligned}\right\} \tag{51}$$

which are valid if $\zeta^{(o)} \neq 0$.

To expand ${}_oW(w)^{(1)}$, besides the fundamental forms, expansions (33) and (35), it is required also to consider

$$\log_e \left[(1 - 2\epsilon)(1 - w)^{1/2} + (1 + 2\epsilon)\left(1 - \epsilon_1{}^2 w\right)^{1/2}\right]$$

and

$$\log_e \left[(1 - w)^{1/2} + \left(1 - \epsilon_1{}^2 w\right)^{1/2}\right]$$

For the first expression let

$$F(w) = \frac{d}{dw} \log_e \left[(1 - 2\epsilon)(1 - w)^{1/2} + (1 + 2\epsilon)\left(1 - \epsilon_1{}^2 w\right)^{1/2}\right]$$

By direct differentiation one obtains

$$F(w) = -\frac{\epsilon_1}{2} (1 - w)^{-1/2}\left(1 - \epsilon_1{}^2 w\right)^{-1/2}$$

By making use of equations (33) and (35), a term-by-term integration gives

$$\log_e \left[(1 - 2\epsilon)(1 - w)^{1/2} + (1 + 2\epsilon)\left(1 - \epsilon_1{}^2 w\right)^{1/2}\right] =$$

$$- \frac{\epsilon_1}{2} \sum_1^\infty \frac{S_{n-1}{}^{(i)}}{n} w^n + \log_e 2 \qquad |w| < 1 \quad (52a)$$

and, aside from a constant,

$$\log_e \left[(1 - 2\epsilon)(1 - w)^{1/2} + (1 + 2\epsilon)\left(1 - \epsilon_1{}^2 w\right)^{1/2}\right] =$$

$$\frac{i\epsilon_1}{2} \sum_0^\infty \frac{1}{\nu}\left(-S_{n+1}{}^{(o)} w^{-\nu} + S_n{}^{(o)} \epsilon_1{}^{2n} w^\nu\right) \qquad (52b)$$

A similar method yields

$$\log_e\left[(1-w)^{1/2}+\left(1-\epsilon_1{}^2w\right)^{1/2}\right]= -\frac{1}{2}\sum_1^\infty \frac{S_n{}^{(i)}}{n}w^n+\log_e 2 \qquad |w|<1 \qquad (53a)$$

and

$$\log_e\left[(1-w)^{1/2}+\left(1-\epsilon_1{}^2w\right)^{1/2}\right]= \frac{1}{2}\left[\log_e w+i\sum_0^\infty \frac{1}{\nu}\left(S_{n+1}{}^{(o)}\epsilon_1{}^{2n+2}w^\nu - S_n{}^{(o)}w^{-1}\right)\right] \quad 1<|w|<\epsilon_1{}^{-2} \qquad (53b)$$

Furthermore, $\dfrac{\zeta_1{}^{(1)}}{\zeta_1{}^{(o)}\left(\zeta_1{}^{(o)}+\epsilon\right)}$ can be written in an expansible form:

$$-\frac{1}{2\epsilon}\left(1+\epsilon_1\sqrt{\frac{1-w}{1-\epsilon_1{}^2w}}\right)$$

Collecting all the individual expansions, one finds

$$-i\ {}_oW_1{}^{(1)}=2\pi i+\sum_2^\infty A_n{}^{(1)}w^n+O\left(\epsilon^2\right) \qquad |w|<1 \qquad (54)$$

where

$$A_n{}^{(1)}=-\left(1+S_n{}^{(i)}\right)+\frac{1+2\epsilon}{2}\left(S_n{}^{(i)}-\epsilon_1{}^2S_{n-1}{}^{(i)}\right)+$$

$$\frac{1+4\epsilon}{4\epsilon}\frac{1}{n}\left(1-\epsilon_1{}^2S_{n-1}{}^{(i)}\right)-\frac{1}{4\epsilon}\frac{1}{n}\left(1-S_n{}^{(i)}\right)+$$

$$\frac{1-2\epsilon}{2\epsilon}\left(S_{n-1}{}^{(i)}-S_n{}^{(i)}\right) \qquad (55)$$

Here $A_1^{(1)}$ is of the order of ϵ^2 and therefore neglected. The real and imaginary parts of the correction term of ${}_oW(w)$ are, to the order of approximation considered,

$$\left.\begin{aligned} {}_o\Phi_1^{(1)} &= -2\pi + \sum_2^\infty A_n^{(1)} q^n \sin n\theta \\ {}_o\Psi_1^{(1)} &= \sum_2^\infty A_n^{(1)} q^n \cos n\theta \end{aligned}\right\} \qquad q < 1 \tag{56}$$

In the region $1 < |w| < \epsilon_1^{-2}$, with the exception of a constant

$$-i\ {}_oW_1^{(1)} = -\frac{1 + 4\epsilon}{4\epsilon} \log_e we^{\pi i} + \sum_1^\infty \left(1 + \frac{1}{n}\right) w^{-n} + \sum_0^\infty \left(B_\nu^{(1)} w^\nu + C_\nu^{(1)} w^{-\nu}\right) + o(\epsilon^2) \tag{57}$$

where

$$\left.\begin{aligned} B_\nu^{(1)} = \Bigg[& S_{n+1}^{(o)} \epsilon_1^2 - \frac{1 + 2\epsilon}{2}\left(S_{n+1}^{(o)} - S_n^{(o)}\right)\epsilon_1^2 + \frac{1 + 4\epsilon}{4\epsilon\nu} S_n^{(o)} - \\ & \frac{1}{4\epsilon\nu} S_{n+1}^{(o)} \epsilon_1^2 + \frac{1 + 2\epsilon}{2\epsilon}\left(S_{n+1}^{(o)} \epsilon_1^2 - S_n^{(o)}\right)\epsilon_1\Bigg] \epsilon_1^{2n} \\ C_\nu^{(1)} = S_n^{(o)} - & \frac{1 + 2\epsilon}{2}\left(S_n^{(o)} - \epsilon_1^2 S_{n+1}^{(o)}\right) - \frac{(1 + 4\epsilon)\epsilon_1}{4\epsilon\nu} S_{n+1}^{(o)} + \\ & \frac{1}{4\epsilon\nu} S_n^{(o)} + \frac{1 + 2\epsilon}{2\epsilon}\left(S_{n+1}^{(o)} - S_n^{(o)}\right)\epsilon_1 \end{aligned}\right\} \tag{58}$$

The corresponding functions ${}_o\varphi_1^{(1)}$ and ${}_o\psi_1^{(1)}$ are

$$\left.\begin{aligned}
{}_o\varphi_1^{(1)} &= \frac{1+4\epsilon}{4\epsilon}(\pi-\theta) - \sum_1^\infty \left(1+\frac{1}{n}\right)q^{-n}\sin n\theta + \\
&\quad \sum_0^\infty \left(B_\nu^{(1)}q^\nu - C_\nu^{(1)}q^{-\nu}\right)\sin\nu\theta + \text{Constant} \\
{}_o\psi_1^{(1)} &= -\frac{1+4\epsilon}{4\epsilon}\log_e q + \sum_1^\infty \left(1+\frac{1}{n}\right)q^{-n}\cos n\theta + \\
&\quad \sum_0^\infty \left(B_\nu^{(1)}q^\nu + C_\nu^{(1)}q^{-\nu}\right)\cos\nu\theta + \text{Constant}
\end{aligned}\right\} \tag{59}$$

Similarly, for the second branch the expansion is

$$-i\,{}_oW_2^{(1)} = C_o^{(1)} - \frac{1}{2\epsilon}\pi i - \frac{1}{2\epsilon}\log_e w + \sum_2^\infty C_n^{(1)}w^n + O(\epsilon^2) \qquad |w|<1 \tag{60}$$

where

$$\left.\begin{aligned}
C_o^{(1)} &= \frac{1+4\epsilon}{4\epsilon}\log_e\epsilon - \frac{1}{2\epsilon}\log_e\frac{1+2\epsilon}{2} + 2 \\
C_n^{(1)} &= -\left(1-S_n^{(i)}\right) - \frac{1+2\epsilon}{2}\left(S_n^{(i)} - \epsilon_1{}^2 S_{n-1}^{(i)}\right) + \\
&\quad \frac{1+4\epsilon}{4\epsilon n}\left(1+\epsilon_1 S_{n-1}^{(i)}\right) - \frac{1}{4\epsilon n}\left(1+S_n^{(i)}\right) + \\
&\quad \frac{1+2\epsilon}{2\epsilon}\left(S_n^{(i)} - S_{n-1}^{(i)}\right)\epsilon_1
\end{aligned}\right\} \tag{61}$$

For the region $1 < |w| < \epsilon_1^{-2}$, it is

$$-i\,{}_0W_2^{(1)} = -\frac{1}{2\epsilon}\log_e w - \log_e we^{\pi i} + \sum_1^\infty \left(1 + \frac{1}{n}\right)w^{-n} - \sum_0^\infty \left(B_\nu^{(1)}w^\nu + C_\nu w^{-\nu}\right) + o(\epsilon^2) \tag{62}$$

where a constant of order unity is again left out. The corresponding real and imaginary parts are:

$$\left.\begin{aligned} {}_0\varphi_2^{(1)} &= \frac{1}{2\epsilon}(\pi - \theta) + \sum_2^\infty C_n^{(1)}q^n \sin n\theta \\ {}_0\psi_2^{(1)} &= C_0^{(1)} - \frac{1}{2\epsilon}\log_e q + \sum_2^\infty C_n^{(1)}q^n \cos n\theta \end{aligned}\right\} \quad q < 1 \tag{63}$$

and, aside from a constant, in $1 < q < \epsilon_1^{-2}$,

$$\left.\begin{aligned} {}_0\varphi_2^{(1)} &= -\frac{1}{2\epsilon}\theta + (\pi - \theta) - \sum_1^\infty \left(1 + \frac{1}{n}\right)q^{-n}\sin n\theta - \sum_0^\infty \left(B_\nu^{(1)}q^\nu - C_\nu^{(1)}q^{-\nu}\right)\sin \nu\theta \\ {}_0\psi_2^{(1)} &= -\frac{1 + 4\epsilon}{4\epsilon}\log_e q + \sum_1^\infty \left(1 + \frac{1}{n}\right)q^{-n}\cos n\theta - \sum_0^\infty \left(B_\nu^{(1)}q^\nu + C_\nu^{(1)}q^{-\nu}\right)\cos \nu\theta \end{aligned}\right\} \tag{64}$$

CONSTRUCTION OF A SOLUTION FOR A SYMMETRIC AIRFOIL

The complex potential ${}_oW$ for a flow over a thin Joukowski airfoil has now been transformed and expanded in power series of w for both the case of zero circulation and of a weak circulation. Knowing the form of expansion of ${}_oW$, a solution relating to a flow of incompressible fluid about a certain body can be obtained immediately by replacing each term of the series by the proper particular integral as given in the section "Fundamental Equations and Their Particular Solutions." For instance, the complex potential in the case of zero circulation is

$$ {}_oW_1(w) = -\sum_0^\infty A_n w^n \qquad |w| < 1 $$

The complex potential $W_1(w,\tau)$ relating to a compressible flow is, accordingly,

$$ W_1(w,\tau) = -\sum_0^\infty A_n F_n{}^{(r)}(\tau) w^n + \sum_{m=2}^\infty h_m c_m \left(\sqrt{\tau}_1 T_1\right)^m \psi_m e^{im\theta} - $$

$$ A_2 c_2 \frac{\partial}{\partial n}\left[\left(\sqrt{\tau}_1 T_1\right)^n \psi_n e^{in\theta}\right]_{n=2} \qquad |w| < 1 \qquad (65) $$

of which the imaginary part gives the stream function, namely,

$$ \psi_1(q,\theta) = \mathrm{Im}\left[W_1(w,\tau)\right] \qquad (66) $$

Here the definition of $F_n{}^{(r)}(\tau)$ may be either $F_n(\tau)/F_n(\tau_1)$ (references 1 and 2) or $F_n(\tau)/T_1(\tau_1)$ (references 3 and 4), where $\tau = \tau_1$ when $q = 1$. It follows from equation (66) that the stream function is

$$ \psi_{1-}(q,\theta) = \sum_2^\infty A_n q^n F_n{}^{(r)}(\tau) \sin n\theta + \sum_2^\infty h_m c_m \left(\sqrt{\tau}_1 T_1\right)^m \psi_m \sin m\theta - $$

$$ A_2 c_2 \frac{\partial}{\partial n}\left[\left(\sqrt{\tau}_1 T_1\right)^n \psi_n \sin n\theta\right]_{n=2} \qquad q < 1 \qquad (67) $$

From equation (5) the velocity potential is

$$\varphi_{1-}(q,\theta) = A_o - (1 - \tau)^{-\beta} \sum_{2}^{\infty} A_n q^n F_n^{(r)}(\tau)\xi_n(\tau) \cos n\theta +$$

$$\sum_{2}^{\infty} h_m c_m \left(\sqrt{\tau}_1 T_1\right)^m \psi_m \xi_m \cos m\theta - A_2 c_2 \frac{\partial}{\partial n}\left[\left(\sqrt{\tau}_1 T_1\right)^n \psi_n \xi_n \cos n\theta\right]_{n=2}$$

$$q < 1 \quad (68)$$

Both series (equations (67) and (68)) converge only within the unit circle $q = 1$. In order to have a function to cover the whole field of flow, both series must be continued across the circle of convergence. There have been two alternative methods proposed to effect this continuation. The first method (references 1 and 2) is to have the solution corresponding to the flow in the upper z-plane arranged in one w-plane. After the series, for example, equations (39), (42), and (46), are modified, they are required to be continuous with continuous normal derivatives on the circle $q = 1$ (fig. 4). On account of compressibility, the modified solution will be discontinuous in normal derivative and hence W_{1-} and W_1 can no longer represent the same function. To correct this, one set of coefficients is left free and an extra series is added to W_1. These two sets of coefficients can then be determined by the condition at $q = 1$ (reference 2). The second procedure (references 3 and 4) is to proceed from a Taylor expansion, equation (67), say. Expressing the function $F_n(\tau)$ in the form of equation (11) gives rise to a convergent double series which, when the order of summation is changed, is transformed into a form being convergent even for values of q greater than unity. Analytical continuation is thus accomplished. In the following discussion, the latter procedure is adopted for simplicity.

At this point, the convention for numbering the branch of ${}_oW(w)$ is altered. Instead of dividing the z-plane fore and aft, it will be more convenient to divide the plane into upper and lower halves. Then ${}_oW_1(w)$ indicates the upper half and ${}_oW_2(w)$, the lower. The parts corresponding to the regions $q < 1$ fore, $1 < q < \epsilon_1^{-2}$, and $0 < q < 1$ aft are, respectively, ${}_oW_{1-}$, ${}_oW_1$, and ${}_oW_{1+}$.

By the second method, replacing $F_n(\tau)$ in equation (65) by equation (11) and, for evident reasons, adopting the definition $F_n^{(r)}(\tau) = F_n(\tau)\big/T_1(\tau_1)$, equation (65) can be written as

$$W_1(w,\tau) = -f(\tau) \sum_{0}^{\infty} A_n (tw)^n + \sum_{n=0}^{\infty} A_n (tw)^n \sum_{m=1}^{\infty} \frac{C_m}{n + m} \tau^m T^m F_m(\tau) +$$

$$\sum_{2}^{\infty} h_m c_m \left(\sqrt{\tau}_1 T_1\right)^m \psi_m e^{im\theta} - A_2 c_2 \frac{\partial}{\partial n}\left[\left(\sqrt{\tau}_1 T_1\right)^n \psi_n e^{in\theta}\right]_{n=2}$$

where $t = T/T_1$. The first series can be summed and, by changing the order of summation, the second series can be transformed into a single series. Thus

$$W_1(w,\tau) = f(\tau)\ {}_oW_1(\tilde{w}) - \sum_{m=1}^{\infty} C_m\left(\sqrt{\tau}_1 T_1\right)^m \psi_m(\tau) e^{im\theta} \int_0^{\tilde{w}} w^{m-1}\,{}_oW_1\ dw +$$

$$\sum_{2}^{\infty} h_m c_m \left(\sqrt{\tau}_1 T_1\right)^m \psi_m e^{im\theta} - A_2 c_2 \frac{\partial}{\partial n}\left[\left(\sqrt{\tau}_1 T_1\right)^n \psi_n e^{in\theta}\right]_{n=2} \qquad (69)$$

where $\tilde{w} = tw$ and $\psi_m(\tau) = \tau^{m/2} F_m(\tau)$. The first term corresponds to that resulting from the asymptotic summation (references 1 and 2) and, in the special case $\gamma = -1$, reduces to the Kármán-Tsien approximation. The integral in the second term is bounded and the series can be shown to be convergent for $q > 1$ (references 3 and 4).

By taking a path starting from the forward stagnation point to an arbitrary point in the annular region, namely,

$$\int_0^{\tilde{w}} w^{m-1}\,{}_oW_1(w)\ dw = \int_0^{\tilde{w}_1} w^{m-1}\,{}_oW_1(w)\ dw + \int_{\tilde{w}_1}^{\tilde{w}} w^{m-1}\,{}_oW_1(w)\ dw$$

where $\tilde{w}_1$ is a fixed point in the annular region, a simple transformation leads to

$$W_1 = \sum_{0}^{2}{}' B_{-n} F_{-n}{}^{(r)}{}_{(\tau)} w^{-n} + i \sum_{0}^{\infty} \left[B_\nu F_\nu{}^{(r)}{}_{(\tau)} w^\nu + C_\nu F_{-\nu}{}^{(r)}{}_{(\tau)} w^{-\nu}\right] +$$

$$\left(-A_2 c_2 + B_{-2} c_2\right) \frac{\partial}{\partial n}\left[\left(\sqrt{\tau}_1 T_1\right)^n \psi_n e^{in\theta}\right]_{n=2} \qquad (70)$$

by replacing ${}_oW_1$ by the proper expansion under the integral sign, where

$$h_m = \int_0^{\tilde{w}_1} w^{m-1}\,{}_oW_1\,dw - \sum_0^{2}{}' \frac{B_{-n}\tilde{w}_1{}^{-n}}{-n+m} - i\sum_0^{\infty}\left(\frac{B_\nu \tilde{w}_1{}^{\nu+w}}{\nu+m} + \frac{C_\nu \tilde{w}_1{}^{-\nu+w}}{-\nu+m}\right) - B_{-2}\log_e \tilde{w}_1 \tag{71}$$

The integral in equation (71) can be evaluated in the ζ-plane; namely,

$$\int_0^{\tilde{w}_1} w^{m-1}\,{}_oW_1\,dw = \int_{\zeta_o}^{\tilde{\zeta}_1} w^{m-1}\,{}_oW_1\,\frac{dw}{d\zeta}\,d\zeta$$

The fact that $\frac{\partial}{\partial n}\left[\left(\sqrt{\tau}_1 T_1\right)^n \psi_n e^{in\theta}\right]$ is a solution is shown in appendix B. Equation (70), evidently, is the continuation of equation (65). Proceeding further to a fixed point $\tilde{w}_2$ inside the unit circle but below the real axis, by describing a loop surrounding the point $w = 1$, the following proper transformation is arrived at:

$$W_1 = \sum_2^{\infty} h_m c_m \left(\sqrt{\tau}_1 T_1\right)^m \psi_m e^{im\theta} + \sum_1^{2} A_{-2}F_{-n}{}^{(r)}{}_{(\tau)}\,w^{-n} +$$

$$\sum_0^{\infty} A_n F_n{}^{(r)}{}_{(\tau)} w^n \tag{72}$$

where

$$h_m(\tilde{\zeta}_2) = \int_{\tilde{\zeta}_o}^{\tilde{\zeta}_2} w^{m-1}\,{}_oW_1\,\frac{dw}{d\zeta}\,d\zeta - \sum_1^{2}{}' \frac{A_n \tilde{w}_2{}^{-n+m}}{-n+m} - \sum_0^{\infty}\frac{A_n \tilde{w}_2{}^{n+m}}{n+m} - A_{-2}\log_e \tilde{w}_2$$

(73)

The path is quite arbitrary; in order to preserve the property of symmetry of the function it is so chosen that the h_m's are real. Equations (65), (70), and (72) together represent the first branch of the Riemann surface covering the entire upper z-plane. Separating into real and imaginary parts, the stream function is

$$\psi_1(q,\theta) = \sum_0^\infty \left[B_\nu q^\nu F_\nu^{(r)}(\tau) + C_\nu q^{-\nu} F_{-\nu}^{(r)}(\tau)\right] \cos \nu\theta + \sum_0^2 B_{-n} q^{-n} F_{-n}^{(r)}(\tau) \sin n\theta - \left(A_2 c_2 - B_{-2} c_2\right) \frac{\partial}{\partial n}\left[\left(\sqrt{\tau}_1 T_1\right)^n \psi_n \sin n\theta\right]_{n=2} \qquad 1 < q < \epsilon_1^{-2} \qquad (74)$$

and

$$\psi_{1+}(q,\theta) = \sum_2^\infty h_m\left(\tilde{\zeta}_2\right) c_m \left(\sqrt{\tau}_1 T_1\right)^m \psi_m(\tau) \sin m\theta - \sum_2^\infty A_n q^n F_n^{(r)}(\tau) \sin n\theta + \sum_1^2 A_{-n} q^{-n} F_{-n}^{(r)}(\tau) \sin n\theta \qquad q < 1 \qquad (75)$$

The velocity potential corresponding to equations (74) and (75) is

$$\varphi_1(q,\theta) = (1 - \tau)^{-\beta} \left\{ \sum_{0}^{2} B_{-n} q^{-n} F_{-n}^{(r)} \xi_{-n} \cos n\theta - \right.$$

$$\sum_{0}^{\infty} \left[B_\nu q^\nu F_\nu^{(r)}(\tau) \xi_\nu + C_\nu q^{-\nu} F_{-\nu}^{(r)}(\tau) \xi_{-\nu} \right] \sin \nu\theta +$$

$$\left. \left(A_2 c_2 - B_{-2} c_2 \right) \frac{\partial}{\partial n} \left[\left(\sqrt{\tau}_1 T_1 \right)^n \psi_n \xi_n \cos n\theta \right]_{n=2} \right\} \qquad 1 < q < \epsilon_1^{-2} \quad (76)$$

and

$$\varphi_{1+}(q,\theta) = (1 - \tau)^{-\beta} \left\{ - \sum_{2}^{\infty} h_m \left(\tilde{\zeta}_2 \right) c_m \left(\sqrt{\tau}_1 T_1 \right)^m \psi_m(\tau) \xi_m \cos m\theta - \right.$$

$$\sum_{1}^{2} A_{-n} q^{-n} F_{-n}^{(r)}(\tau) \xi_{-n} \cos n\theta +$$

$$\left. \sum_{2}^{\infty} A_n q^n F_n^{(r)}(\tau) \xi_n \cos n\theta \right\} \qquad 0 < q < 1 \quad (77)$$

By taking a path from the forward stagnation point but in the reverse direction, the second branch of $W(w,\tau)$ can be joined. Now the solution ${}_oW(w)$ to be considered in the integral appearing in equation (69) will be

$$\left.\begin{aligned} {}_oW_{2-} &= -\sum_0^\infty A_n w^n && |w| < 1 \\ {}_oW_2 &= \sum_0^2 B_{-n} w^{-n} - i \sum_0^\infty \left(B_\nu w^\nu + C_\nu w^{-\nu}\right) && 1 < |w| < \epsilon_1^{-2} \\ {}_oW_{2+} &= \sum_1^2 A_{-n} w^{-n} + \sum_0^\infty A_n w^{+n} && |w| < 1 \end{aligned}\right\} \quad (78)$$

Complete symmetry with respect to the u-axis makes it unnecessary to repeat the process.

In the case of the flow with circulation, the complex potential consists of two parts as shown in equations (50). The one which corresponds to zero circulation is given in equations (37), (40), and (43). The functions for the compressible flow are then given from equations (67) to (77). The part which takes into account the effect of a weak circulation is

$$\left.\begin{aligned} -i\ {}_oW_{1-}^{(1)} &= \sum_0^\infty A_n(1)_w{}^n && |w| < 1 \\ -i\ {}_oW_1^{(1)} &= B_o - \frac{1}{4\epsilon} we^{\pi i} + \sum_1^\infty \left(1 + \frac{1}{n}\right) w^{-n} + \sum_0^\infty \left(B_\nu(1)_w{}^\nu + C_\nu(1)_w{}^{-\nu}\right) - \log_e we^{\pi i} \\ -i\ {}_oW_{1+}^{(1)} &= -\frac{1}{2\epsilon} \log_e w + \sum_0^\infty C_n(1)_w{}^n && 0 < |w| < 1 \end{aligned}\right\} \quad (79)$$

By the convention adopted, ${}_oW_{1-}{}^{(1)}$, ${}_oW_1{}^{(1)}$, and ${}_oW_{1+}{}^{(1)}$ form the first branch of ${}_oW^{(1)}$ and correspond to the whole upper z-plane. The same method yields a solution for a compressible flow:

$$
\left.
\begin{aligned}
-iW_{1-}{}^{(1)} &= \sum_0^\infty A_n{}^{(1)}F_n{}^{(r)}{}_{(\tau)}w^n + \sum_2^\infty h_m{}^{(1)}c_m\left(\sqrt{\tau}_1T_1\right)^m\psi_m e^{im\theta} - \\
&\sum_2^\infty \left(1+\frac{1}{n}\right)c_n\frac{\partial}{\partial n}\left[\left(\sqrt{\tau}_1T_1\right)^n\psi_n e^{in\theta}\right] \\
-iW_1{}^{(1)} &= B_o - \frac{1}{4\epsilon}(\pi-\theta)i - \frac{1}{4\epsilon}\int_{\tau_1}^{\tau}(1-\tau)^\beta\frac{d\tau}{\tau} + \\
&\sum_1^\infty \left(1+\frac{1}{n}\right)F_{-n}{}^{(r)}{}_w{}^{-n} + \sum_0^\infty\left[B_\nu{}^{(1)}F_\nu{}^{(r)}{}_w{}^\nu + \right. \\
&\left. C_\nu{}^{(1)}F_{-\nu}{}^{(r)}{}_w{}^{-\nu}\right] - \left[(\pi-\theta)i + \int_{\tau_1}^{\tau}(1-\tau)^\beta\frac{d\tau}{\tau}\right] \\
-iW_{1+}{}^{(1)} &= \sum_2^\infty h_m{}^{(2)}c_m\left(\sqrt{\tau}_1T_1\right)^m\psi_m(\tau)e^{im\theta} - \\
&\sum_2^\infty \left(1+\frac{1}{n}\right)c_n\frac{\partial}{\partial n}\left[\left(\sqrt{\tau}_1T_1\right)^n\psi_n e^{in\theta}\right] - \\
&\frac{1}{2\epsilon}\left[-\theta i + \int_{\tau_1}^{\tau}(1-\tau)^\beta\frac{d\tau}{\tau}\right] + \sum_0^\infty C_n{}^{(1)}F_n{}^{(r)}{}_w{}^n
\end{aligned}
\right\} \quad (80)
$$

The real and imaginary parts are

$$\left.\begin{aligned}
\psi_{1-}^{(1)} &= \sum_{2}^{\infty} A_n^{(1)} q^n F_n^{(r)}(\tau) \cos n\theta + \\
&\sum_{2}^{\infty} h_m^{(1)} c_m \left(\sqrt{\tau}_1 T_1\right)^m \psi_m \cos m\theta - \\
&\sum_{2}^{n} \left(1 + \frac{1}{n}\right) c_n \frac{\partial}{\partial n}\left[\left(\sqrt{\tau}_1 T_1\right)^n \psi_n \cos n\theta\right] \qquad q < 1 \\
\psi_1^{(1)} &= -\frac{1 + 4\epsilon}{4\epsilon} \int_{\tau_1}^{\tau} (1 - \tau)^\beta \frac{d\tau}{\tau} - \sum_{1}^{\infty} \left(1 + \frac{1}{n}\right) q^{-n} F_{-n}^{(r)}(\tau) \cos n\theta + \\
&\sum_{0}^{\infty} \left[B_\nu^{(1)} q^\nu F_\nu^{(r)}(\tau) + C_\nu^{(1)} q^{-\nu} F_{-\nu}^{(r)}(\tau)\right] \cos \nu\theta + \\
&\text{Constant} \qquad 1 < q < \epsilon_1^{-2} \\
\psi_{1+}^{(1)} &= -\frac{1}{2\epsilon} \int_{\tau_1}^{\tau} (1 - \tau)^\beta \frac{d\tau}{\tau} + \sum_{2}^{\infty} h_m^{(2)} c_m \left(\sqrt{\tau}_1 T_1\right)^m \psi_m \cos m\theta - \\
&\sum_{2}^{\infty} \left(1 + \frac{1}{n}\right) c_n \frac{\partial}{\partial n}\left[\left(\sqrt{\tau}_1 T_1\right)^n \psi_n \cos n\theta\right] + \\
&\sum_{0}^{\infty} C_n^{(1)} q^n F_n^{(r)}(\tau) \cos n\theta \qquad 0 < q < 1
\end{aligned}\right\} \quad (81)$$

and

$$\varphi_{1-}^{(1)} = (1-\tau)^{-\beta}\left\{\sum_{2}^{\infty} A_n^{(1)} q^n F_n^{(r)}(\tau)\xi_n \sin n\theta + \right.$$

$$\sum_{2}^{\infty} h_m^{(1)} c_m \left(\sqrt{\tau}_1 T_1\right)^m \psi_m \xi_m \sin m\theta -$$

$$\left.\sum_{2}^{\infty} \left(1+\frac{1}{n}\right) c_n \frac{\partial}{\partial n}\left[\left(\sqrt{\tau}_1 T_1\right)^n \psi_n \xi_n \sin n\theta\right]\right\}$$

$$\varphi_1^{(1)} = (1-\tau)^{-\beta}\left\{\sum_{1}^{\infty}\left(1+\frac{1}{n}\right) q^{-n} F_{-n}^{(r)}(\tau)\xi_{-n} \sin n\theta + \right.$$

$$\left.\sum_{0}^{\infty}\left[B_n^{(1)} q^{\nu} F_{\nu}^{(r)}(\tau)\xi_{\nu} + C_{\nu}^{(1)} q^{-\nu} F_{-\nu}^{(r)}(\tau)\xi_{-\nu}\right]\sin \nu\theta\right\} + \quad (82)$$

$$\text{Constant} - \frac{1+4\epsilon}{4\epsilon}(\pi-\theta) \qquad 1 < q < \epsilon_1^{-2}$$

$$\varphi_{1+}^{(1)} = (1-\tau)^{-\beta}\left[-\sum_{2}^{\infty} h_m^{(2)} c_m \left(\sqrt{\tau}_1 T_1\right)^m \psi_m \sin m\theta - \right.$$

$$\sum_{2}^{\infty}\left(1+\frac{1}{n}\right) c_n \frac{\partial}{\partial n}\left[\left(\sqrt{\tau}_1 T_1\right)^n \psi_n \xi_n \sin n\theta\right] +$$

$$\left.\sum_{0}^{\infty} C_n^{(1)} q^n F_n^{(r)}(\tau)\xi_n \sin n\theta - \frac{1}{2\epsilon}(\pi-\theta)\right] \qquad q < 1$$

In a similar fashion, the second branch can also be connected by taking a path in the reverse direction and introducing successively the functions:

$$
\left.
\begin{aligned}
-i\ {}_oW_{2-}{}^{(1)} &= \sum_0^\infty A_n{}^{(1)}w^n && |w| < 1 \\
-i\ {}_oW_2{}^{(1)} &= -\frac{1+4\epsilon}{4\epsilon}\log_e we^{\pi i} + \sum_1^\infty \left(1+\frac{1}{n}\right)w^{-n} - \\
&\qquad \sum_0^\infty \left(B_\nu{}^{(1)}w^\nu + C_\nu{}^{(1)}w^{-\nu}\right) + \text{Constant} && 1 < |w| < \epsilon^{-2} \\
-i\ {}_oW_{2+}{}^{(1)} &= -\frac{1}{2\epsilon}\log_e w + \sum_0^\infty C_n{}^{(1)}w^n && |w| < 1
\end{aligned}
\right\} \quad (83)
$$

However, it should be added that, since the functions $W_1{}^{(1)}$ and $W_2{}^{(1)}$ do not merely differ by a sign, the $h_m{}^{(1)}$'s in $W_{2+}{}^{(1)}$ and $W_{1+}{}^{(1)}$ will not generally be equal. As a result, the two branches may not be joined with each other across the branch line $y = 0$, $x_2 < x < \infty$. In order to avoid this difficulty, the lower limit in the integral, for instance, equation (73), should be adjusted to make them equal.

Having the stream function and the velocity potential so chosen, the flow pattern in the physical plane can be calculated by integrating equations (14) and (15) to give the coordinate functions $x(q,\theta)$ and $y(q,\theta)$. When the flow is free of circulation, the stream function is antisymmetrical about the x-axis. By taking $x = x_1$, $y = 0$ as the stagnation point and $x = x_2$, $y = 0$ as the trailing edge, the constants of integration can be determined on the unit circle for $\theta > 0$. By symmetry, the reversal of the sign of θ gives the lower half of the flow.

When circulation is present, the symmetry property is destroyed and hence both branches have to be calculated separately. Since

both $W^{(o)}$ and $W^{(1)}$ are properly joined functions, the determination of integration constants on the unit circle for both branches would be sure to give a pair of continuous coordinate functions.

Cornell University
Ithaca, N. Y., August 10, 1948

APPENDIX A

SYMBOLS

q	magnitude of velocity vector
θ	inclination of velocity vector
ρ_o	value of ρ at $q = 0$
ρ	density of fluid
M	local Mach number
Ψ	stream function
φ	velocity potential
$F_\nu(\tau), F_{-\nu}(\tau)$	hypergeometric functions
ν	nonintegral parameter
m,n	integers
$\tau = \frac{1}{2\beta}\frac{q^2}{c_o^2}$	
a_ν, b_ν	parameters of hypergeometric functions
$\beta = \frac{1}{\gamma - 1}$	
$\xi_\nu(\tau), \xi_{-\nu}(\tau)$	functions defined by equations (8)
γ	ratio of specific heats of gas
c_o	speed of sound at $q = 0$
$T(\tau)$	defined by equations (12)
c_m	defined by equations (12)
$f(\tau)$	defined by equations (12)

$\gamma_1 = \sqrt{\frac{\gamma + 1}{\gamma - 1}}$

x,y	coordinates of point in physical plane
${}_oW(z)$	complex potential
$z = x + iy$	
ϵ	geometric parameter of body
w	complex velocity defined by equation (17)
P(w),Q(w)	defined by equations (20)
u,v	velocity components
$\zeta(w)$	transformation function defined by equation (18)
$\zeta_1(w),\zeta_2(w),\zeta_3(w)$	solutions of equation (18) given by equations (19)
${}_oW_1(w),{}_oW_2(w),{}_oW_3(w)$	branches of complex potential
α	angle of attack
$\epsilon_1 = \frac{1 - 2\epsilon}{1 + 2\epsilon}$	
${}_oW(w)$	complex potential for incompressible flow in w
Ψ_o	stream function for incompressible flow
Φ_o	velocity potential for incompressible flow
$S_n(i),{}_1S_n(i)$	defined by equations (34)
$S_n(o),{}_1S_n(o)$	defined by equations (36)
A_n	coefficient defined by equation (38)
${}_o\Phi_1,{}_o\Psi_1$	defined by equations (39)

$B_{-2}, B_{-1}, B_\nu, C_\nu$	defined by equations (41)
${}_o\Phi_2, {}_o\Psi_2$	defined by equations (46) and (47)
$\zeta_1^{(o)}, \zeta_2^{(o)}$	transformation functions
$\zeta_1^{(1)}, \zeta_2^{(1)}$	correction terms due to circulation
${}_oW_1^{(o)}, {}_oW_2^{(o)}$	defined by equations (28)
${}_oW_1^{(1)}, {}_oW_2^{(1)}$	defined by equations (51)
$B_\nu^{(1)}, C_\nu^{(1)}$	defined by equations (58)
${}_o\Phi_1^{(1)}, {}_o\Psi_1^{(1)}$	defined by equations (59)
$C_o^{(1)}, C_n^{(1)}$	defined by equations (61)
${}_o\Phi_2^{(1)}, {}_o\Psi_2^{(1)}$	defined by equations (63) and (64)
$W_1(w,\tau)$	defined by equation (65)
$F_n^{(r)}(\tau) = F_n(\tau)/T_1(\tau_1)$	
τ_1	value of τ at $q = 1$
T_1	value of T at $q = 1$
$\Psi_{1-}, \Psi_1, \Psi_{1+}$	branches of stream function
$\Phi_{1-}, \Phi_1, \Phi_{1+}$	branches of velocity potential
$t = T/T_1$	

${}_oW_1(\tilde{w})$	defined by equation (69)
$\tilde{w} = tw$	
$\Psi_m(\tau) = \tau^{m/2}F_m(\tau)$	
h_m	defined by equation (71)
${}_oW_{1-}^{(1)}, {}_oW_1^{(1)}, {}_oW_{1+}^{(1)}$	correction terms due to circulation
$\Psi_{1-}^{(1)}, \Psi_1^{(1)}, \Psi_{1+}^{(1)}$	defined by equations (81)
$\Phi_{1-}^{(1)}, \Phi_1^{(1)}, \Phi_{1+}^{(1)}$	defined by equations (82)
${}_oW_{2-}^{(1)}, {}_oW_2^{(1)}, {}_oW_{2+}^{(1)}$	defined by equations (83)

APPENDIX B

PARTICULAR SOLUTIONS OF FUNDAMENTAL EQUATIONS OF MOTION

If $\psi_m e^{in\theta}$ is a particular integral of differential equations (1), $\frac{\partial}{\partial n}\left(\psi_n e^{in\theta}\right)$ is also a solution. For the differential equation then becomes

$$\frac{d}{dq}\left(\frac{\rho_o}{\rho}\, q\, \frac{d\psi_n}{dq}\right) - n^2\, \frac{\rho_o}{\rho}\left(1 - M^2\right)\psi_n = 0$$

$$\frac{d}{dq}\left[\frac{\rho_o}{\rho}\, q\, \frac{d}{dq}\left(\frac{\partial \psi_n}{\partial n}\right)\right] - n^2\, \frac{\rho_o}{\rho q}\left(1 - M^2\right)\frac{\partial \psi_n}{\partial n} = 2n\, \frac{\rho_o}{\rho}\left(1 - M^2\right)\psi_n$$

As $\psi_n(q)$ satisfies the first equation, the second equation determines $\partial\psi_n/\partial n$. Now

$$d\varphi = -\frac{\rho_o}{\rho}\left(1 - M^2\right)\frac{\partial \psi}{\partial \theta}\, dq + \frac{\rho_o}{\rho}\, q\, \frac{\partial \psi}{\partial q}\, d\theta$$

By substituting $\frac{\partial}{\partial n}\left[\psi_n(q) e^{in\theta}\right]$ for ψ, it is easy to show

$$d\varphi = \frac{1}{n}\frac{\partial}{\partial q}\left(-i\, \frac{\rho_o q}{\rho}\, \frac{\partial^2 \psi_n}{\partial n \partial q} + \theta\, \frac{\rho_o q}{\rho}\, \frac{\partial \psi_n}{\partial q} + \frac{i}{n}\, \frac{\rho_o q}{\rho}\, \frac{\partial \psi_n}{\partial q}\right) e^{in\theta}\, dq +$$

$$\frac{1}{n}\frac{\partial}{\partial \theta}\left(-i\, \frac{\rho_o q}{\rho}\, \frac{\partial^2 \psi_n}{\partial n \partial q} + \theta\, \frac{\rho_o q}{\rho}\, \frac{\partial \psi_n}{\partial q} + \frac{i}{n}\, \frac{\rho_o q}{\rho}\, \frac{\partial \psi_n}{\partial q}\right) e^{in\theta}\, d\theta$$

Therefore

$$\varphi = -i\, \frac{\rho_o q}{\rho}\, \frac{\partial}{\partial n}\left(\frac{1}{n}\, \frac{\partial \psi_n}{\partial q}\, e^{in\theta}\right)$$

APPENDIX C

SERIES EXPANSION OF COMPLEX POTENTIAL

The Taylor expansion of the complex potential of a flow over a symmetric Joukowski airfoil is, for $0 < |w| < 1$,

$$ {}_oW_1 = \sum_0^\infty A_n w^n $$

$$ {}_oW_2 = -\frac{1}{2}\sum_0^\infty A_n w^n - \frac{\sqrt{3}}{2}\sum_0^\infty B_\nu w^\nu $$

$$ {}_oW_3 = -\frac{1}{2}\sum_0^\infty A_n w^n + \frac{\sqrt{3}}{2}\sum_0^\infty B_\nu w^\nu $$

where

$$ A_n = C_n + (1+\epsilon)^2 D_n $$

$$ B_\nu = C_\nu + (1+\epsilon)^2 D_\nu $$

$$ C_n = -\frac{2(1+2\epsilon)}{3}\sum_{j=0}^{\infty}\sum_{k=0}^{j/2}\sum_{l=0}^{k}\binom{\frac{1}{3}}{j}\binom{j}{2k}\binom{k}{l}\binom{-j-k}{n+k-j-l}(-1)^{n-j}3^{2j-k}\frac{\epsilon^j\left(1+\epsilon+\epsilon^2\right)^{j-2k}(1-\epsilon)^{3l}(1+\epsilon)^l}{(1+2\epsilon)^{3(j-k+l)}} $$

$$ C_\nu = -\frac{2(1+2\epsilon)}{3}\sum_{j=0}^{\infty}\sum_{k=0}^{j/2}\sum_{l=0}^{\infty}\binom{\frac{1}{3}}{j}\binom{j}{2k+1}\binom{k+\frac{1}{2}}{l}\binom{-j-k-\frac{1}{2}}{n+k-j-l+1}(-1)^{n-j}3^{2j-k-\frac{1}{2}}\frac{\epsilon^j\left(1+\epsilon+\epsilon^2\right)^{j-2k+1}(1-\epsilon)^{3l}(1+\epsilon)^l}{(1+2\epsilon)^{3\left(j-k+l-\frac{1}{2}\right)}} $$

$$ D_n = -\frac{2(1+2\epsilon)}{3}\sum_{j=0}^{\infty}\sum_{k=0}^{j/2}\sum_{l=0}^{k}\binom{\frac{1}{3}}{j}\binom{j}{2k}\binom{k}{l}\binom{j-k}{n-k-l}(-1)^{j+n}3^{2j-k}\frac{(1+\epsilon)^{j+l}(1-\epsilon)^{3l}(1+2\epsilon)^{3(k-l)}}{(2+\epsilon)^{3j}}\left(1+\epsilon+\epsilon^2\right)^{j-2k} $$

$$ D_\nu = -\frac{2(1+2\epsilon)}{3}\sum_{j=0}^{\infty}\sum_{k=0}^{j/2}\sum_{l=0}^{\infty}\binom{\frac{1}{3}}{j}\binom{j}{2k+1}\binom{k+\frac{1}{2}}{l}\binom{j-k-\frac{1}{2}}{n+k-l+1}(-1)^{n+j}3^{2j-k-\frac{1}{2}}\frac{(1+\epsilon)^{j+l}(1-\epsilon)^{3l}(1+2\epsilon)^{3\left(k-l+\frac{1}{2}\right)}\left(1+\epsilon+\epsilon^2\right)^{j-2k-1}}{(2+\epsilon)^{3j}} $$

$$ \nu = n + \frac{1}{2} $$

REFERENCES

1. Tsien, Hsue-Shen, and Kuo, Yung-Huai: Two-Dimensional Irrotational Mixed Subsonic and Supersonic Flow of a Compressible Fluid and the Upper Critical Mach Number. NACA TN 995, 1946.

2. Kuo, Yung-Huai: Two-Dimensional Irrotational Transonic Flows of a Compressible Fluid. NACA TN 1445, 1948.

3. Lighthill, M. J.: The Hodograph Transformation in Trans-Sonic Flow. Proc. Roy. Soc. (London), ser. A, vol. 191, no. 026, Nov. 18, 1947, pp. 323-369.

4. Cherry, T. M.: Flow of a Compressible Fluid about a Cylinder. Proc. Roy. Soc. (London), ser. A, vol. 192, no. 1028, Dec. 23, 1947, pp. 45-79.

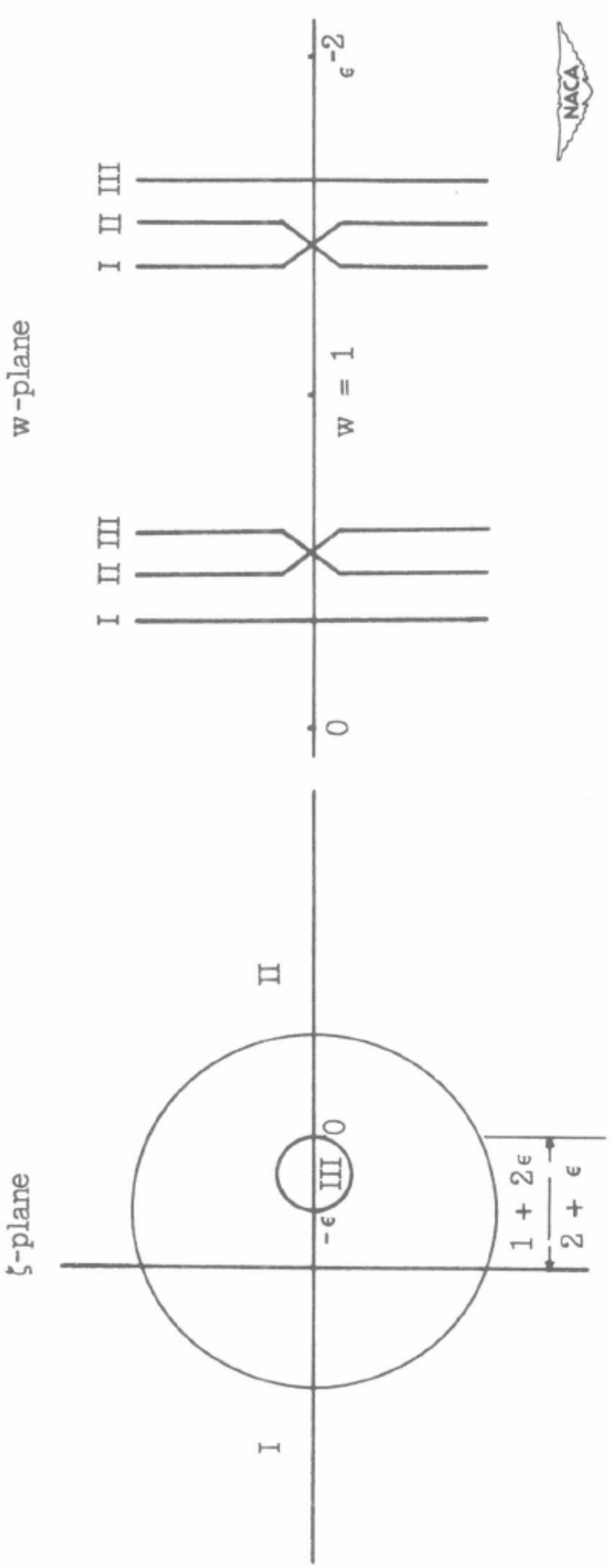

Figure 1.- Conformal representation of incompressible flow about symmetric Joukowski airfoil without circulation.

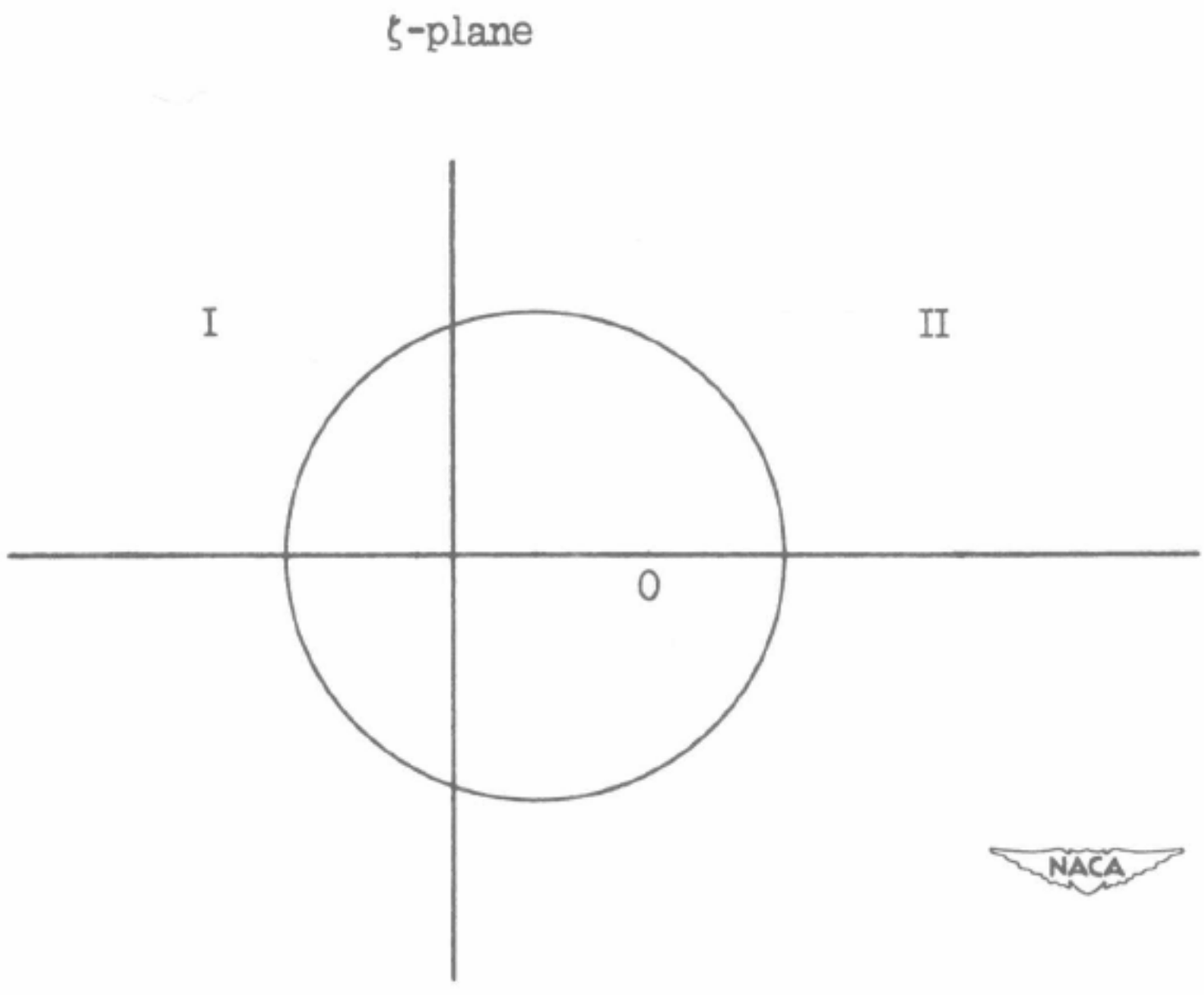

Figure 2.- Simplified ζ-plane for small values of ϵ.

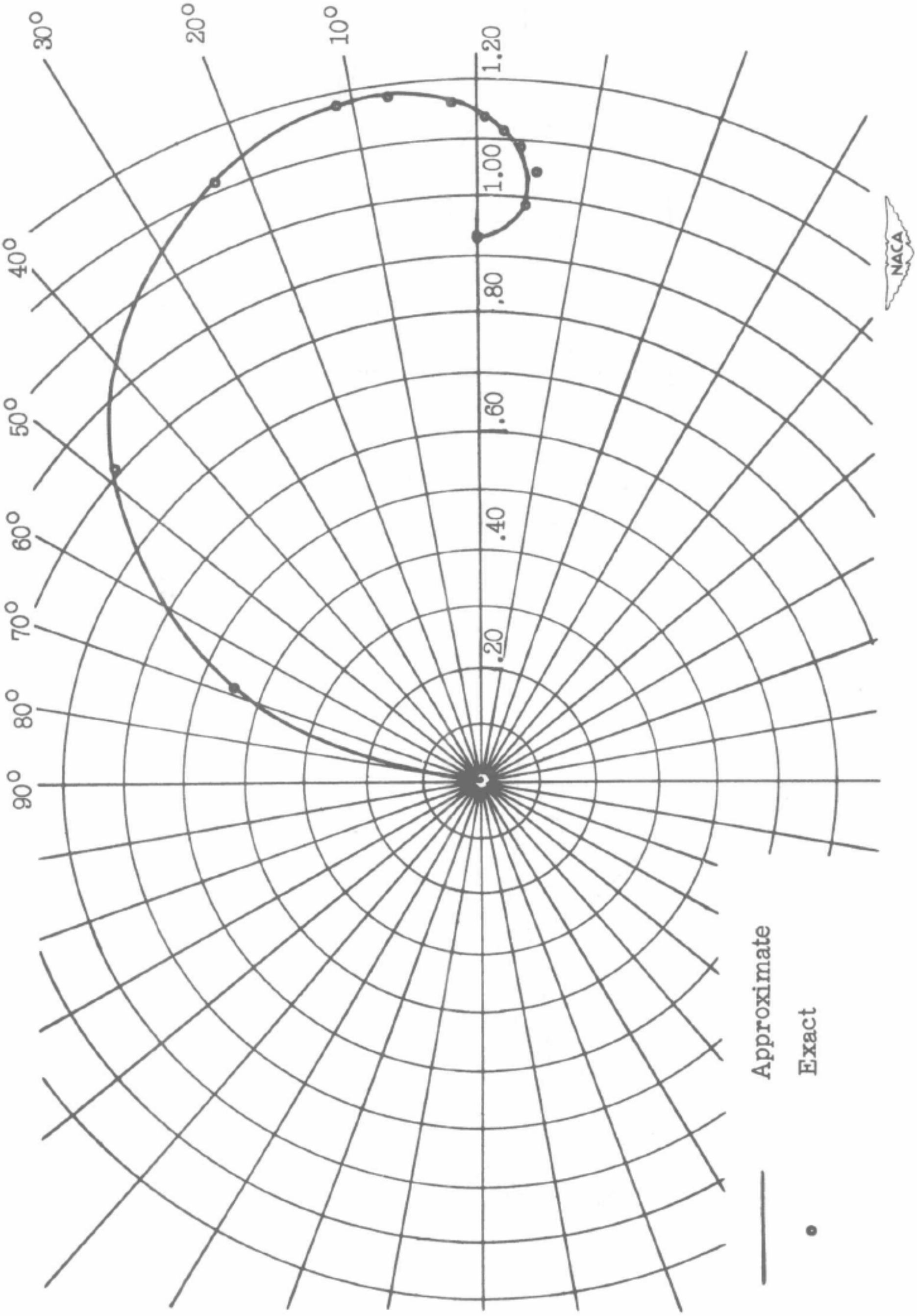

Figure 3.- Zero streamline of incompressible flow around symmetric airfcil in hodograph plane. $\epsilon = 0.08$.

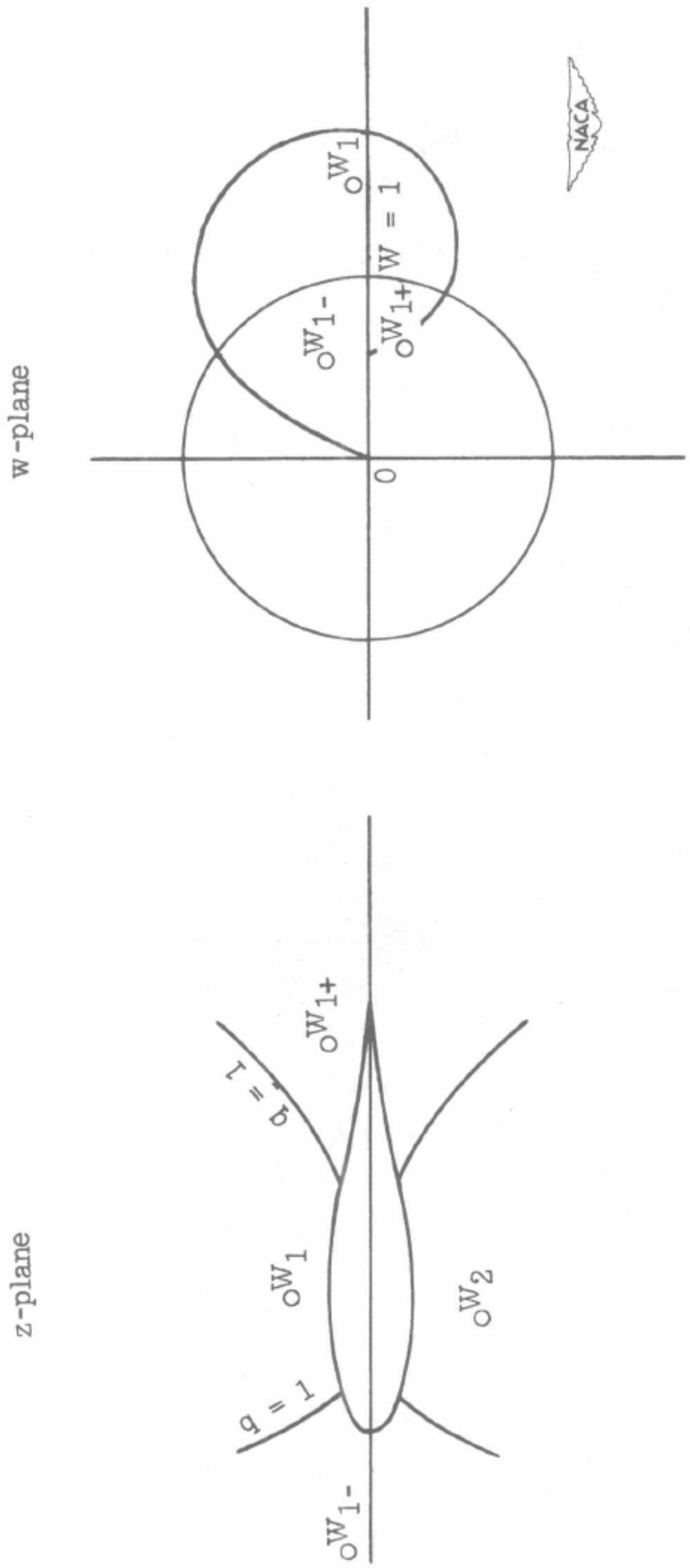

Figure 4.- Diagram showing correspondence between domains of z-plane and w-plane.

JOURNAL OF THE AERONAUTICAL SCIENCES

VOLUME 18 JANUARY, 1951 NUMBER 1

On the Stability of Two-Dimensional Smooth Transonic Flows* [1)]

YUNG-HUAI KUO

Cornell University

SUMMARY

Steady two-dimensional potential flows involving imbedded supercritical regions adjacent to a body have been calculated, but their existence has not yet been established experimentally. To further experimentation, the question of stability of such flows is examined.

Following the standard procedure, a theoretically possible flow is disturbed at a certain instant, and the behavior of the subsequent disturbance motion is investigated. By means of the transonic approximations, a simple solution valid in the neighborhood of the sonic line has been obtained. This study leads to the conclusion that (1) smooth decelcrating transonic flows over bodies at negative curvature are unstable to compression pulses; (2) smooth accelerating transonic flows over any surface are stable; and (3) smooth transonic flows with local supersonic region are unstable.

(1) INTRODUCTION

IT HAS BEEN SHOWN THEORETICALLY[1-8] that steady two-dimensional potential flows of gas past bodies may become locally supersonic at sufficiently high free-stream Mach Numbers. The supersonic regions are always located at the surface of a body, and their extent increases as the Mach Number is raised. It is found, moreover, that the transition from subsonic to supersonic flow and vice versa takes place continually, and it appears that such smooth flows occur over a range of Mach Numbers which is terminated by the appearance of limiting lines. On the other hand, wind-tunnel observations show that such smooth transonic flows are generally replaced by flows involving shock waves. The understanding and interpretation of this discrepancy between theory and experiment seems highly desirable and might lead to some device whereby the drag divergence and other undesirable phenomena associated with shock waves might be prevented or, at least, delayed to higher Mach Numbers. Hence, the establishment of criteria under which such flows are physically possible is not merely of academic interest but also of practical importance.

Since, theoretically, the smooth transonic flow could exist for a much wider range of Mach Numbers than it actually does, the question of its stability arises. To answer this question, one must introduce disturbances at a certain moment and follow their future course. If the original steady motion is unstable, the disturbances will grow and eventually become shock waves, resulting in increase of drag. On the other hand, if it is stable, the disturbances will die out and finally become Mach waves. There may also be cases where a disturbance approaches a steady state, resulting in what is known as neutral stability. It is difficult to make these general statements more precise at this point; nevertheless, they can be accepted as qualitative definitions of stability and instability.

In the present investigation, the type of disturbances considered will be a finite linear pulse, moving upstream, with a weak discontinuity at its head. By linear pulse is meant that at any instant the velocity-wave form is a linear function of space coordinates. This simplification may appear as artificial; however, observations in connection with ballistic waves show that the final state of any continuous pulse, traveling in still air, tends to become linear and is independent of the source of production. A continuous pulse propagating in a nonuniform steady flow may well develop into a complex shape, but a linear function could still be a good approximation to local conditions.

If linear pulses are assumed, there will occur only two types: (1) a disturbance, propagating against a steady stream, whose ancestor was a continuous ex-

Presented at the Aerodynamics Session, Eighteenth Annual Meeting, I A.S., New York, January 23–26, 1950. Revised and received September 15, 1950.

* This study was initiated by the work of A. Kantrowitz,[10] who considered the stability of one-dimensional channel flow, and is being carried out with the financial assistance of the National Advisory Committee for Aeronautics. The Committee has generously approved the publication of this preliminary report.

1) Published in *Journal of the Aeronautical Sciences*, 1951, 18(1): 1~6, 54

pansion pulse, will have a discontinuity at its head; (2) that disturbance whose ancestor was a continuous expansion pulse will have a discontinuity at its tail. These will be called compression and expansion pulses. respectively. Since an expansion pulse cannot penetrate into the supercritical region but is dissipated at the sonic line, only the compression type of pulse will be considered.

The problem of tracing the history of even a linear pulse is a formidable one. To reduce the amount of work involved, it is further assumed that all the disturbances were locally produced, by unsteadiness of the boundary layer, say, and are limited in extent laterally. Thus, the triangular pulses encountered near the sonic line may be thought of as having originated in that neighborhood. Consequently, the motion of the pulse can be studied by solutions valid "in the small" instead of "in the large." This brings about a great simplification because, by restricting the solutions to the neighborhood of the sonic line, one can introduce transonic approximations and obtain a simple solution.

Finally, it must also be said that, according to experimental observations in the case of airfoils, the pressure distribution over the surface does not exhibit the effects of separation or violent thickening of boundary layer until long after shock waves have been formed. This indicates that viscosity of the fluid has little influence on the character of the transonic flow outside the boundary layer, and therefore it can be neglected in the present study. Moreover, since the shock front is generally curved, the flow behind it cannot actually remain irrotational and isentropic. However, by dealing with the initial stage of the motion, when the shock strength is weak and the vorticity generated is small, the flow can be considered as isentropic. If a disturbance increases in strength and tends to become a shock, the approximation will become worse and eventually break down. The future event inferred therefrom is tantamount to extrapolation. The validity of the conclusions drawn, of course, must be established by experiment.

(2) Differential Equation of the Disturbances

Let $\varphi'(X, Y, t)$ be the velocity potential of a two-dimensional motion, defined by

$$\left.\begin{aligned} u &= \varphi_X', \quad v = \varphi_Y' \\ \frac{1}{2}(u^2 + v^2) &+ \frac{a^2 - a_0^2}{\gamma - 1} = -\varphi_t' \end{aligned}\right\} \tag{1}$$

Here, u and v are the velocity components, γ is the ratio of specific heats, a is the local speed of sound, and a_0 is the value of a at stagnation conditions; the subscripts denote partial differentiation with respect to the coordinates X and Y and the time t. The differential equation satisfied by $\varphi'(X, Y, t)$ is

$$(a^2 - u^2)\varphi'_{XX} + (a^2 - v^2)\varphi'_{YY} - \varphi'_{tt} - 2uv\varphi'_{XY} - 2v\varphi'_{Yt} - 2u\varphi'_{Xt} = 0 \tag{2}$$

If the motion is regarded as a superposition of a disturbance on a steady motion whose velocity potential is $\Phi(X, Y)$, the disturbance velocity potential ϕ can be defined as

$$\varphi' = \Phi + \phi \tag{3}$$

For the present problem, Φ is assumed known and satisfies

$$(c^2 - \Phi_X^2)\Phi_{XX} + (c^2 - \Phi_Y^2)\Phi_{YY} - 2\Phi_X\Phi_Y\Phi_{XY} = 0 \tag{4}$$

with

$$c^2 = a_0^2 - [(\gamma - 1)/2](\Phi_X^2 + \Phi_Y^2)$$

By substitution of Eq. (3) in Eq. (2) and making use of Eq. (4), the differential equation governing the disturbance motion is found to be

$$\begin{aligned}[c^2 - \Phi_X^2 - (\gamma - 1)\phi_t - (\gamma + 1)(\Phi_X\phi_X + {}^1/_2\phi_X^2) - (\gamma - 1)(\Phi_Y\phi_Y + {}^1/_2\phi_Y^2)]\phi_{XX} + [c^2 - \Phi_Y^2 - \\ (\gamma - 1)\phi_t - (\gamma - 1)(\Phi_X\phi_X + {}^1/_2\phi_X^2) - (\gamma + 1)(\Phi_Y\phi_Y + {}^1/_2\phi_Y^2)]\phi_{YY} - \phi_{tt} - 2[\Phi_X\Phi_Y + \Phi_X\phi_Y + \\ \Phi_Y\phi_X + \phi_X\phi_Y]\phi_{XY} - 2(\Phi_Y + \phi_Y)\phi_{Yt} - 2(\Phi_X + \phi_X)\phi_{Xt} = [(\gamma - 1)\phi_t + (\gamma + 1)(\Phi_X\phi_X + {}^1/_2\phi_X^2) + \\ (\gamma - 1)(\Phi_Y\phi_Y + {}^1/_2\phi_Y^2)]\Phi_{XX} + [(\gamma - 1)\phi_t + (\gamma - 1)(\Phi_X\phi_X + {}^1/_2\phi_X^2) + (\gamma + 1) \times \\ (\Phi_Y\phi_Y + {}^1/_2\phi_Y^2)]\Phi_{YY} + 2[\Phi_X\phi_Y + \Phi_Y\phi_X + \phi_X\phi_Y]\Phi_{XY}\end{aligned} \tag{5}$$

For a given steady flow $\Phi(X, Y)$, the problem would seem to be to solve this equation subject to a set of initial and boundary conditions. For an equation of such complexity, however, to seek an exact solution is not attractive; nor is it necessary because only certain features of the behavior of the disturbances are required. For this reason, the problem will be solved by introducing appropriate approximations.

It is assumed first that the disturbances are initially small and are produced in the neighborhood of the sonic line, so that the early stage of the pulse's life is spent entirely in the transonic region. As a result, the transonic characteristics of the steady flow will not be destroyed so long as the pulse is weak. Let ϵ be the thickness parameter of the body. If the disturbances are small and their transonic character is preserved, then, according to transonic approximation,[9] $\partial/\partial X \simeq 0(1)$ and $\partial/\partial Y \simeq 0(\epsilon^{1/4})$. By the time the state of the pulse under consideration is reached, the wave front is practically straight, and its direction of motion is nearly

parallel to the undisturbed flow. The time derivative must be the same order as the speed of propagation of plane waves. If the disturbances propagate against the steady flow, the time derivative must be of the order $|\Phi_x - c|$. Now $\Phi_x^2 - c^2 \simeq 0(\epsilon^{2/3})$, therefore, $\partial/\partial t \simeq 0(\epsilon^{2/3})$. For the disturbances traveling downstream, the same argument shows that the time derivative must be of the order unity.

As the pulse is predominantly plane, it might be represented in the form $\varphi(x, y, \tau) = \varphi^{(0)}(x, \tau) + \epsilon^{2/3}\varphi^{(1)} \times (x, y, \tau)$, where the orders of magnitude of $\varphi^{(0)}$ and $\varphi^{(1)}$ must be alike in order to satisfy the boundary condition of Eq. (9), below. This order of magnitude is arbitrary, depending on the strength of the disturbance considered. Since the motion must reduce to the propagation of a finite plane disturbance for vanishing ϵ, it will be assumed that $\varphi^{(0)}$ and $\varphi^{(1)}$ are $0(\epsilon^{2/3})$. In the following work, the two terms making up $\varphi(x, y, \tau)$ will be handled together; nevertheless, the argument above serves to indicate the relative magnitudes of derivatives of φ. To the order of ϵ^2, the upstream moving disturbance satisfies

$$(\gamma + 1)(\tilde{\Phi}_x + \varphi_x)\varphi_{xx} + 2\varphi_{x\tau} + (\gamma + 1)\tilde{\Phi}_{xx}\varphi_x = \varphi_{yy} - (\gamma - 1)\tilde{\Phi}_{xx}\varphi_\tau - \varphi_{\tau\tau} \quad (6)$$

Similar consideration gives an equation

$$\varphi_{\tau\tau} + 2\varphi_{\tau x} = 0 \quad (7)$$

for the downstream moving pulses. Here, $\tilde{\Phi}$ and φ are defined as follows:

$$\Phi = c^* l(x + \tilde{\Phi})$$
$$\phi = c^* l\varphi$$

and

$$x = X/l, \quad y = Y/l, \quad \tau = c^* t/l \quad (8)$$

where c^* is the critical sound speed associated with the enthalpy of the steady flow and l is a characteristic dimension of the body.

Eq. (7) shows that the downstream moving disturbances propagate without change of strength. If they are initially weak, they will stay weak. For this reason, only upstream moving disturbances require consideration. The equation governing the upstream moving disturbances is a partial differential equation in three variables; aside from initial conditions to be specified later, the solution is required to satisfy the boundary condition: for $y = 0$ and $\tau > 0$,

$$\varphi_y = \varphi_x g(x) \quad (9)$$

where $g(x)$ is the slope of the body. It is assumed that the solution is regular on the axis and that on the body y is everywhere small.

(3) Wave Form of a Pulse

Since, strictly speaking, Eq (6) is valid only in the transonic zone, a local solution should be sufficient for the present purpose. As the waves formed in the neighborhood of the sonic line must have lived long after the Riemann steepening has happened, the velocity wave form there can be approximated reasonably well by a discontinuous linear function in x and y at any time τ. If the origin of the axes coincides with the intersection of the sonic line with the body, the special wave form can be represented by

$$\varphi = f_1(\tau)x + f_2(\tau)y + \frac{1}{2}[f_3(\tau)x^2 + 2f_4(\tau)xy + f_4(\tau)y^2] \quad (10)$$

for values of x, y lying within the pulse area. Moreover, Φ_x, too, is to be approximated by a linear function of x and y—namely,

$$\tilde{\Phi}_x = \alpha x + \beta y \quad (11)$$

Of course, the sonic line, in general, is not a straight line; but, if the solution is restricted to a narrow region (a stream tube, say), Eq. (11) can certainly provide as accurate an approximation as desired by properly choosing the width of the stream tube. To be consistent with Eq. (11), the boundary condition (9) can be written as

$$\varphi_y = \varphi_x(m + kx), \quad y = 0, \tau > 0 \quad (12)$$

where m and k are, respectively, the slope and curvature of the body at the sonic line.

Upon substitution of Eq. (10), together with Eq. (11), in Eq. (6), there result

$$\left.\begin{aligned}
&(\gamma + 1)f_1 f_3 + 2f_1' + (\gamma + 1)\alpha f_1 = f_5 \\
&(\gamma + 1)(\alpha + f_3)f_3 + 2f_3' + (\gamma + 1)\alpha f_3 = -(\gamma - 1)\alpha f_1' - f_1'' \\
&(\gamma + 1)(\beta + f_4)f_3 + 2f_4' + (\gamma + 1)\alpha f_4 = -(\gamma - 1)\alpha m f_1' - m f_1''
\end{aligned}\right\} \quad (13)$$

The same substitution in Eq. (12) gives

$$\left.\begin{aligned}
f_2 &= m f_1 \\
f_4 &= k f_1 + m f_3
\end{aligned}\right\} \quad (14)$$

after the neglecting of terms of the order of x^2 and m^2. It is noticed that the order of the terms on the right-hand side of the second and third of Eqs. (13) is one order higher than that of the left-hand side. So, as a first approximation by neglecting high-order terms in f_3 and f_4, the system possesses the following solutions:

$$\left.\begin{aligned}
f_1 &= (Ae^{\nu\tau} - 1)^{-1}\left[\frac{2m}{k}\left(\frac{\beta}{m} - \alpha\right) + \frac{B}{k}e^{\nu\tau/2}\right] \\
f_2 &= m f_1 \\
f_3 &= 2\alpha(Ae^{\nu\tau} - 1)^{-1} \\
f_4 &= (Ae^{\nu\tau} - 1)^{-1}[2\beta + Be^{\nu\tau/2}] \\
f_5 &= (2m\nu/k)[\alpha - (\beta/m)](Ae^{\nu\tau} - 1)^{-1}
\end{aligned}\right\} \quad (15)$$

where ν stands for $(\gamma + 1)\alpha$ and A and B are constants of integration to be determined from initial condition. It is to be noted that, in the case of one-dimensional motion, the solution does not reduce exactly to

that of Kantrowitz,[10] inasmuch as $f_1(\tau) \neq 0$ here in contrast to the case considered by him.

Having the velocity wave form chosen to be linear in x and y, it is natural to assume initially a pulse that is bounded at the front side by a discontinuity, in which the velocity decreases linearly from a given value to zero. Since the partial derivatives of x and y bear a definite ratio, the rate of change in one direction fixes that in the other. As a result, the shape of the pulse can be determined by specifying the pressure discontinuity on the shock front or, alternatively, the normal velocity to the shock. Therefore, in addition to Eq. (12), the solution has to satisfy, at $\tau = 0$,

$$\varphi_x \sin \sigma - \varphi_y \cos \sigma = a + bx \tag{16}$$

on the shock, where σ is the shock angle and a, b are constants defining pressure ratio and its distribution. After approximating the shock front within a stream tube by a straight line perpendicular to the body,

$$y - y_0 = -(1/m_0)(x - x_0) \tag{17}$$

where m_0 is the slope of the body at x_0, a substitution of Eq. (10) in Eq. (16), making use of Eq. (17), yields two equations that possess a solution

$$\left.\begin{aligned} A &= 1 + \frac{2}{m_0 k \Delta}\left\{(m - m^2 m_0 - m_0)\alpha + \frac{m^2}{k}\left(\alpha - \frac{\beta}{m}\right)\nu + \frac{k(x_0 + my_0)}{1 + m^2}\left[-\alpha + \frac{m^2}{k}\left(\alpha - \frac{\beta}{m}\right)\nu\right]\right\} \\ B &= \frac{2a}{m_0 k (1 + m^2)^{1/2}\Delta}\left\{-m_0 k\alpha + \beta k(1 - mm_0) + m^2\left(\alpha - \frac{\beta}{m}\right)\nu - \right. \\ &\qquad \left. \frac{b}{a}\left[m_0 m (1 + m^2)\left(\alpha - \frac{\beta}{m}\right) - k\beta(x_0 + my_0) - m^2(x_0 + my_0)\left(\alpha - \frac{\beta}{m}\right)\nu\right]\right\} \end{aligned}\right\} \tag{18}$$

where

$$\Delta = -\frac{(1 - mm_0)a}{m_0(1 + m^2)^{1/2}} - \left[\frac{(1 + m^2)^{1/2}}{k} + \frac{x_0 + my_0}{m_0(1 + m^2)^{1/2}}\right]b$$

Thus, for a given flow, the constants A and B may be regarded as functions of a and b. By arbitrary choice of a and b, the motion within the pulse is defined. Being discontinuous in pressure, density, etc., the pulse cannot stay stationary but must propagate according to the Rankine-Hugoniot shock-wave relations. These provide an additional equation to trace the successive locations of the pulse. It must be pointed out that, although the Rankine-Hugoniot relations are employed, the pulse is still regarded as isentropic. The discrepancies in pressure, density, etc., are permissible as long as the pulse is weak.

Perhaps a word is also necessary concerning the process of continuation of solution to the next stream tube. This is done in exactly the same manner except that the boundary condition at a stream line, say, is replaced by continuity in velocity. The continued solution, which possesses no special interesting feature, will be omitted here.

(4) Propagation of a Triangular Pulse in Transonic Region

The solution can now be discussed without resort to detailed numerical calculation. Suppose the curvature k of the body is negative; the behavior of the pulse can be understood by examining the velocity components.

$$\varphi_x = (Ae^{\nu\tau} - 1)^{-1}\left[\frac{2m}{k}\left(\frac{\beta}{m} - \alpha\right) + \frac{B}{k}e^{\nu\tau/2} + 2\alpha x + (2\beta + Be^{\nu\tau/2})y\right]$$

$$\varphi_y = (Ae^{\nu\tau} - 1)^{-1}\left[\frac{2m^2}{k}\left(\frac{\beta}{m} - \alpha\right) + \frac{mB}{k}e^{\nu\tau/2} + (2\beta + Be^{\nu\tau/2})x + \frac{2m\nu}{k}\left(\alpha - \frac{\beta}{m}\right)y\right]$$

First, let $\Phi(x, y)$ represent a *decelerating* flow so that the velocity gradients α and β are both negative. Two cases are to be discussed: a compression and an expansion pulse. For a compression pulse, the velocity slope—namely, $[2\alpha + m(2\beta + Be^{\nu\tau/2})]/(Ae^{\nu\tau} - 1)$—is positive and the velocity is negative—i.e., $\varphi_x < 0$ and $\varphi_y > 0$. Since x, y, and m were assumed small, the character of the pulse depends upon the term $\{(2m/k)[(\beta/m) - \alpha] + (B/k)e^{\nu\tau/2}\} \times (Ae^{\nu\tau} - 1)^{-1}$ and the slope $2\alpha/(Ae^{\nu\tau} - 1)$. It follows that $Ae^{\nu\tau} - 1$ must be negative and that $(2m/k)[(\beta/m) - \alpha] + (B/k)e^{\nu\tau/2}$ must be positive. Because of the fact that ν is negative and $2m/k[(\beta/m) - \alpha]$ is positive, $|Ae^{\nu\tau} - 1|$ decreases with time, while $(2m/k)[(\beta/m) - \alpha] + (B/k)e^{\nu\tau/2}$ decreases or increases with time depending on whether B is positive or negative. In any case, since the rate of change of $e^{\nu\tau/2}$ is twice as slow as that of $e^{\nu\tau}$, the absolute value of the velocity is always increasing with time. Consequently, the momentum of the pulse continues to increase as the pulse propagates against the stream.

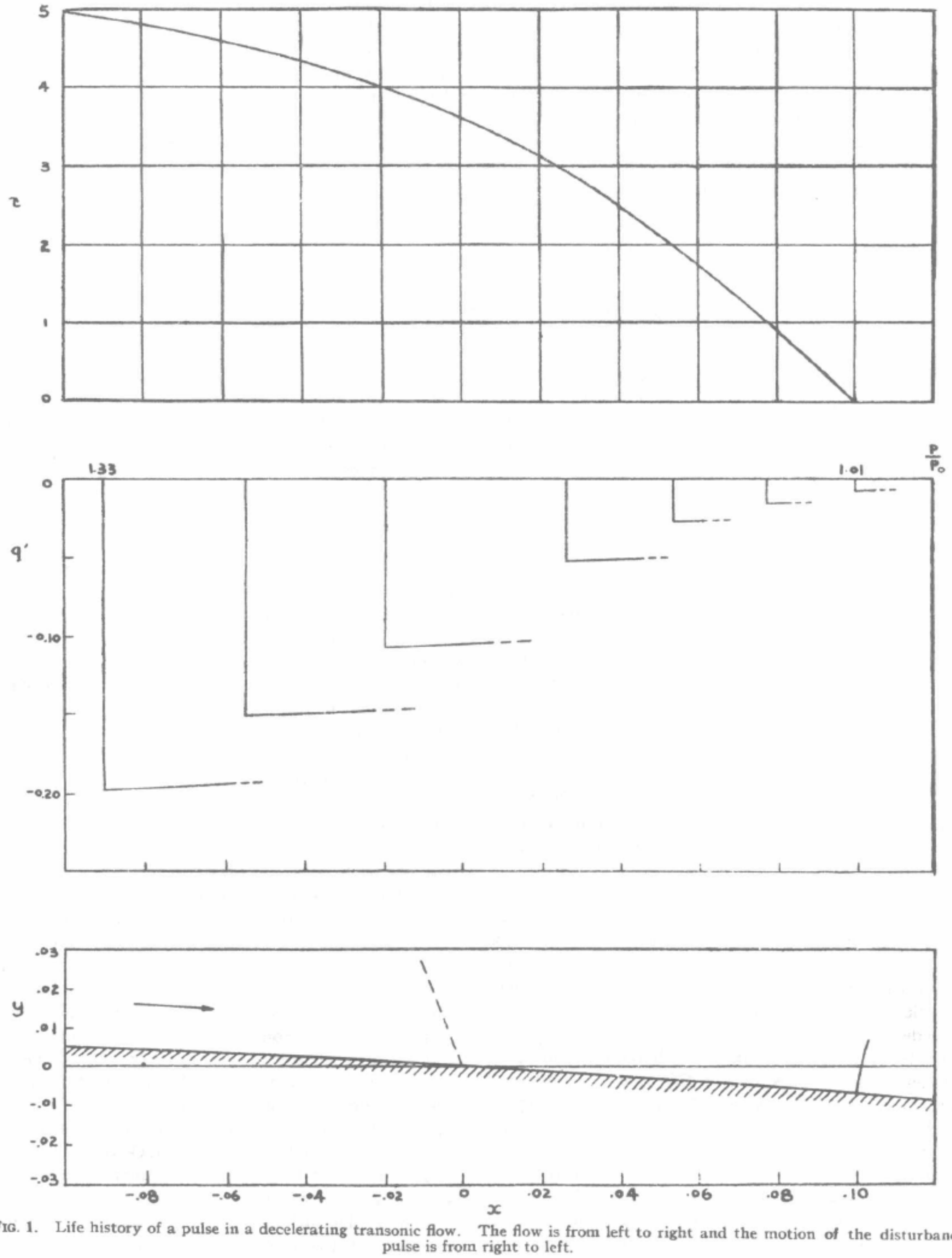

FIG. 1. Life history of a pulse in a decelerating transonic flow. The flow is from left to right and the motion of the disturbance pulse is from right to left.

It might be noted that the constant $(2m/k)\,[(\beta/m) - \alpha]$, being of the order $\epsilon^{1/3}$, is positive when m is negative. It might change sign if m were positive. This is not possible because the normal derivative of Φ_x, which is approximately equal to $\beta - \alpha m$ at the sonic line, is always negative in the case of a convex surface.

Next, consider an expansion pulse. In this case, the "head" of the pulse is continuous in both pressure and velocity, but there is a discontinuity at its "tail." Here again, the slope of the pulse is positive, but the velocity reverses its sign—that is, $\varphi_x > 0$ and $\varphi_y < 0$. This demands that $(2m/k)\,[(\beta/m) - \alpha] + (B/k)e^{\nu\tau/2}$ be negative. As a result, B must be larger than $2(\alpha m - \beta)$. This makes the absolute value of $(2m/k)\,[(\beta/m) - \alpha] + (B/k)e^{\nu\tau/2}$ decrease with time and vanish when τ is large. In other words, the slope of an expansion pulse while it propagates increases continuously to a steady value less than -2α, but its pressure discontinuity drops gradually to zero. Therefore, an expansion pulse, in the end, becomes a sound wave.

Consider now the case of an *accelerating* transonic flow for which α is positive. The velocity components can then be written as

$$\phi_x = e^{-\nu\tau}\,(A - e^{-\nu\tau})^{-1}\left[\frac{2m}{k}\left(\frac{\beta}{m} - \alpha\right) + \frac{B}{k}\,e^{\nu\tau/2} + 2\alpha x + (2\beta + Be^{\nu\tau/2})y\right]$$

$$\varphi_y = e^{-\nu\tau}\,(A - e^{-\nu\tau})^{-1}\left[\frac{2m^2}{k}\left(\frac{\beta}{m} - \alpha\right) + \frac{mB}{k}\,e^{\nu\tau/2} + (2\beta + Be^{\nu\tau/2})x + \frac{2m\nu}{k}\left(\alpha - \frac{\beta}{m}\right)y\right]$$

Since ν is positive, the expressions in the brackets will increase as $e^{\nu\tau/2}$, and, as a consequence, the velocity will decrease as $e^{-\nu\tau/2}$. Furthermore, $A - e^{-\nu\tau}$ tends to A instead of -1, this being an essential difference from the previous case. Since A is a large number, it further reduces the final strength of the pulse and thus accelerates the rate of its destruction. In short, any pulse, regardless of whether it is compression or expansion, cannot be sustained long in an accelerating transonic flow once it is accidentally produced.

(5) Conclusions and Discussion

From the foregoing sections, certain conclusions can be drawn concerning the stability of mixed potential flows over convex surfaces. It is clear that the upper surface of a body is convex if $k < 0$. To be specific, the flow over the upper surface will be considered here. According to the results presented above, any disturbance, of the type considered here, produced in accelerating transonic flow over such a surface vanishes almost instantly, and the unsteady flow therefore approaches the assumed steady flow as a final state. Thus, an accelerating flow of this type must be termed stable.

On the other hand, a disturbance propagating against a decelerating flow grows continuously by consuming the kinetic energy of the steady flow. This process of converting kinetic energy into pressure will continue to prevail until the pulse is so strong that it changes drastically the character of the whole flow pattern. The development of such a pulse is illustrated in Fig. 1. The decelerating transonic flow, therefore, is unstable to compression pulses. From this, one concludes that smooth transonic flows with local supersonic regions involving both accelerating and decelerating flows are unstable.

It is interesting to see that the curvature of the body plays no decisive role in the question of stability of two-dimensional smooth mixed flows. The major effect is evidently that of the velocity gradient Φ_{xx}, as in one-dimensional flow. One may suspect that the constant $(2m/k)[(\beta/m) - \alpha]$ might have an important influence. In the neighborhood of the sonic line, it can be shown that it represents the ratio of the normal derivative of Φ_x to the curvature $\dot{\kappa}$. As long as the slope of the surface there is small, the normal derivative of Φ_x is approximately the same as that of the speed. By the irrotationality condition, it follows that this constant is practically independent of the curvature k. Therefore, if the curvature is varied keeping other conditions unchanged, the constant will remain the same, and, as a result, the pulse will not differ.

As stated above, the major effect that decides the question of stability or instability is the velocity gradient. The conclusion drawn, therefore, is valid only if Φ_{xx} is finite and nonvanishing. Presumably, this covers the most important cases in practice. But the question arises: Is it possible that Φ_{xx} does vanish and that Φ_x has a point of inflection there—namely, $\Phi_x = \alpha x^3 + \ldots$? If it does happen, the question of stability is still open, and the problem has to be re-examined.

A word is also necessary regarding the thickness effect of the body. For convenience, the approximation is based on a small thickness parameter. Since the approximation is applied only locally, the solution will be valid as long as the slope of the surface in the region considered is small, regardless of whether the body is thick or thin. In the case of a thick body, the only restriction would be for low free-stream Mach Number, so that the local supersonic region occupies the flat portion of the surface. Therefore, basically, in consideration of the problem of stability, the thickness effect, too, does not enter.

(*Continued on page 54*)

54 JOURNAL OF THE AERONAUTICAL SCIENCES—JANUARY 1951

On the Stability of Two-Dimensional Smooth Transonic Flows

(*Continued from page 6*)

References

[1] Taylor, G. I., *The Flow of Air at High Speeds Past Curved Surfaces*, R. & M. British A.R.C., No. 1381, 1930.

[2] Görtler, H., *Gasströmungen mit Übergang von Unterschall- zu Überschallgeschwindigkeiten*, Z.a.M.M., Vol. 20, pp. 254–262, 1940.

[3] Ringleb, F., *Exakte Lösungen der Differential gleichungen einer adiabatischen Gasströmung*, Z.a.M.M., Vol. 20, pp. 185–198, 1940.

[4] Kaplan, C., *The Flow of a Compressible Fluid Past a Curved Surface*, N.A.C.A. A.R.R. No. 3K02, 1943.

[5] Tsien, H. S., and Kuo, Y. H., *Two-Dimensional Irrotational Mixed Subsonic and Supersonic Flow of a Compressible Fluid and the Upper Critical Mach Number*, N.A.C.A. T.N. No. 995, 1946.

[6] Kuo, Y. H., *Two-Dimensional Irrotational Transonic Flows of a Compressible Fluid*, N.A.C.A. T.N. No. 1445, 1948.

[7] Emmons, H. W., *The Theoretical Flow of a Frictionless, Adiabatic, Perfect Gas Inside of a Two-Dimensional Hyperbolic Nozzle*, N.A.C.A. T.N. No. 1003, 1946.

[8] Emmons, H. W., *Flow of a Compressible Fluid Past a Symmetrical Airfoil in a Wind Tunnel and in Free Air*, N.A.C.A. T.N. No. 1746, 1948.

[9] von Kármán, Th., *The Similarity Law of Transonic Flow*, Journ. Math. and Phys., Vol. 26, pp. 182–190, 1947.

[10] Kantrowitz, A., *The Formation and Stability of Normal Shock Waves in Channel Flows*, N.A.C.A. T.N. No. 1225, 1948.

ON THE FLOW OF AN INCOMPRESSIBLE VISCOUS FLUID PAST A FLAT PLATE AT MODERATE REYNOLDS NUMBERS* [1]

Y. H. Kuo

1. Introduction. The problem of two-dimensional steady flow of an incompressible viscous fluid past an obstacle is today dealt with mostly by two approximate methods. For extremely small Reynolds number, it was shown by Oseen (1) that the problem can be tackled by linearization. For extremely large Reynolds number, it can be solved by simplifying the Navier-Stokes equations by the concept of the boundary layer, first conceived by Prandtl (2). Oseen's method of solution, though linear, is usually difficult in evaluation of all the arbitrary constants involved. Moreover, owing to the fact that the form of solution, even the first approximation, is more often than not complex, successive approximations are usually not possible.

On the other hand, the boundary-layer solution is simple in form and, most important, sufficiently accurate, as was well established by experiments. It might be considered advantageous to develop the process of iteration by taking boundary layer solution as the first approximation. However, as was shown by H. L. Alden (3) in the case of semi-infinite plate, if the boundary layer solution is taken as the first approximation, then all the higher approximations become progressively more singular and, therefore, the resistance of the plate cannot be defined. For this reason, this procedure, too, fails.

The difficulties of the method adopted by Alden originates from the facts that the flow field surrounding the plate can actually be subdivided into several domains, not all of which meet the conditions required by the boundary-layer theory (cf. for instance, Carrier and Lin's discussion (4)). As the boundary-layer solution is supposed to be valid near the solid surface, in the neighborhood of the leading edge where the viscous region extends equally in the forward direction about the edge, the boundary layer approximations—namely, that the rates of change of the flow properties along and perpendicular to the plate differ by one order of magnitude—clearly break down. Poor approximation there inescapably causes a singularity to appear. If this solution is chosen as the first approximation to the dynamical equations, the higher approximations which satisfy differential equations containing highly singular terms which were absent in the first approximation, must be necessarily more singular. Thus, as the order of approximation increases, higher-order singularities unavoidably appear and, consequently, the drag integral must diverge.

This difficulty in the theory of perturbation is, of course, not new and frequently occurs in a variety of physical problems. The problem of rendering the approximate solutions uniformly valid has led M. J. Lighthill (5) to the dis-

* This study was carried out as part of a research program at the Graduate School of Aeronautical Engineering and was sponsored by the Office of Naval Research.

1) Published in *Journal of Mathematics and Physics*, 1953, 32: 83~101

covery of a method which has become an effective tool in solving non-linear problems. Basically, the idea seems to be that if the solution of an approximated equation to a non-linear total or partial differential equation does not represent uniformly a physical quantity over a domain, it can be improved in the neighborhood of the singularity by merely straining slightly the arguments of the solution. When this idea is formulated mathematically, the condition of uniformity in the analytic behavior of all approximations actually provides a unique way of straining the coordinates. The mathematical structure of the method is, therefore, by itself complete. In the example treated below, the differential equation of the first approximation is non-linear but its solution is singular at the leading edge of the plate. For this case, though not included in Lighthill's treatment, it can be shown that, without modification, Lighthill's technique can still be successfully applied. From this point of view, perhaps it is not without interest.

The first part of this paper (Part I) is devoted to the problem of flow past a finite flat plate. From the character of the external potential flow an expansion parameter is deduced, which turns out to be proportional to the maximum thickness ratio of the boundary layer. If this expansion parameter is adopted, then it can be shown that, to the second approximation, the problem of solving a viscous flow remains of the boundary-layer type. Namely, from the first-order pressure calculated from the maximum displacement of the stream-lines by viscosity, along the plate and in the wake, the second-order viscous flow in the boundary layer can be determined.

The first-order potential flow outside the boundary layer is shown to be very similar, especially near the leading edge, to that given by the linearized theory of flow over a thin airfoil with round leading edge in an inviscid fluid. At the trailing edge where the flow suffers a sudden change of direction, it produces a strong expansion by the appearance of a logarithmic singularity.

The complete solution of the second-order viscous flow leads to a law of resistance which coincides with the Blasius law for Reynolds number over 10^4. In the range of Reynolds numbers from 15 to 10^4, it agrees perfectly with the measurements of Z. Janour (6).

In Part II of the present work, the main problem is the uniformization of the analytic behavior of the successive approximations, taking the boundary layer solution as the basic approximation. It is found that in the case of a flat plate, if Lighthill's conditions are imposed to the third approximation (as the second approximation needs no modification), there results a second-order shift of one coordinate x, say, measured along the plate. According to this transformation, the original constant-velocity lines, being a family of parabolas with vertices at the leading edge, become a different family of parabolas whose vertices are now all separated and located ahead of the leading edge. Furthermore, the singular line which was formerly normal to the plate, passing through the leading edge, has now been completely eliminated. The interesting fact that, except at the leading edge, the improved Blasius solution will be nowhere singular, was expected to bring out the effect of the leading edge. This was investigated and, in-

deed, was the case. The flow in the immediate neighborhood of the leading edge is found to satisfy Stokes equation of slow viscous motion, as it should.

In the light of this discussion, two features of the boundary layer approximations deserve to be mentioned. First the dimension of the viscous region around the leading edge in which the boundary layer hypotheses are violated is actually of the order of ν/U_∞ where ν is the kinematic viscosity and U_∞ the forward speed and hence is extremely small, compared with the length of the plate when the Reynolds number is large. If the detailed information, such as velocity distribution, is not required, the significance of that region, for all practical purposes, could be ignored. Secondly, as the effect of straining the coordinates vanishes on the plate, the very existence of a finite viscous region about the plate does not affect the law of resistance deduced by boundary-layer theory, even to the second order approximation as calculated in Part I. This explains why, with the effect of leading edge poorly represented, the said improved boundary layer solution still yields a correct law of resistance for Reynolds number greater than 15.

2. Navier-Stokes equations and method of expansion. The problem of steady two-dimensional flow of an incompressible viscous fluid past a fixed infinite flat plate of chord length L will be treated here by expanding the velocity field in power series of a parameter ϵ. Let the rectangular Cartesian coordinate system $(\bar{x}, \bar{y})$ be adopted and assume that the plate is defined by $0 \leqq \bar{x} \leqq L$ and $\bar{y} = 0$. Referring to this system, the $\bar{x}$- and $\bar{y}$-components of the velocity will be denoted by $\bar{u}$ and $\bar{v}$ respectively and the pressure by $\bar{p}$. If the density ρ and the kinematic viscosity ν of the fluid are constant and if the non-dimensional variables are introduced:

$$\begin{aligned} u &= \bar{u}/U_\infty, \qquad v = Re^{\frac{1}{2}}\bar{v}/U_\infty = Re^{\frac{1}{2}}V, \qquad p = (\bar{p} - \bar{p}_\infty)/\rho U_\infty^2 \\ x &= \bar{x}/L, \qquad y = Re^{\frac{1}{2}}\bar{y}/U_\infty = Re^{\frac{1}{2}}Y, \qquad Re = U_\infty L/\nu \end{aligned} \tag{2.1}$$

where U_∞ and $\bar{p}_\infty$ are, respectively, the velocity and pressure at infinity, and Re, the Reynolds number; then the velocity and pressure are determined by the system:

$$\begin{aligned} \psi_y\psi_{xy} - \psi_x\psi_{yy} - \psi_{yyy} &= -p_x + Re^{-1}\psi_{yxx} \\ p_y + Re^{-1}(\psi_x\psi_{xy} - \psi_y\psi_{xx} + \psi_{xyy}) &= -Re^{-2}\psi_{xxx} \end{aligned} \tag{2.2}$$

and

$$u = \psi_y, \qquad v = -\psi_x$$

where ψ is the non-dimensional stream function and the subscripts denote partial differentiation with respect to the variable indicated.

To solve this problem from the standpoint of perturbation, it is assumed that the stream function ψ and the pressure p can be expanded in the forms:

$$\begin{aligned} \psi &= \psi^{(0)} + \epsilon\psi^{(1)} + \epsilon^2\psi^{(2)} + \cdots \\ p &= p^{(0)} + \epsilon p^{(1)} + \epsilon^2 p^{(2)} + \cdots \end{aligned} \tag{2.3}$$

If the boundary-layer flow is taken as the first approximation to the flow in question, $\psi^{(0)}$ then satisfies

$$\psi_y^{(0)}\psi_{xy}^{(0)} - \psi_x^{(0)}\psi_{yy}^{(0)} = \psi_{yyy}^{(0)} \tag{2.4}$$

as the pressure $p^{(0)} = 0$ in the case of flat plate. As will subsequently be developed, to the second approximation, the fundamental boundary-layer hypothesis still holds; namely that the viscous effects take place inside a narrow region along the solid surface, so that the flow outside this layer is essentially frictionless and irrotational. If the two flow fields join smoothly, the vertical velocity in the potential field, which is, by (2.3), $O(\epsilon)$ must equal to that of the viscous layer which is $O(Re^{-\frac{1}{2}})$ by boundary-layer theory. Therefore, ϵ must be $O(Re^{-\frac{1}{2}})$ and, for definiteness, can be taken as $Re^{-\frac{1}{2}}$. The parameter ϵ as defined in this manner does have the significance of a thickness ratio, as will be clear later.

By using this definition of ϵ, the eqs. (2.2), after the substitution of ψ and p from (2.3), can be expanded in power series of ϵ. On equating the coefficients of ϵ^n of both series to zero, there result two equations for $\psi^{(n)}$ and $p^{(n)}$, $n = 1, 2, 3, \cdots$. It is the purpose of Part I to deal with the second approximation oniy, the equations for n greater than or equal to 2 will not be given. For $n = 1$, these equations read:

$$\begin{aligned} \psi_y^{(0)}\psi_{xy}^{(1)} + \psi_{xy}^{(0)}\psi_y^{(1)} - \psi_x^{(0)}\psi_{yy}^{(1)} - \psi_{yy}^{(0)}\psi_x^{(1)} &= -p_x^{(1)} + \psi_{yyy}^{(1)} \\ 0 &= -p_y^{(1)} \end{aligned} \tag{2.5}$$

From the second of Eq. (2.5), it follows immediately that $p^{(1)}$ is a function of x and hence is constant inside the boundary layer at any fixed point x and joins the external pressure at the edge of the boundary layer. In other words, to the second approximation the problem of viscous flow past a flat plate remains within the framework of boundary-layer theory.

If $U_1(x)$ denotes the first-order velocity of the potential field on the edge of boundary layer, then from Bernoulli's equation, the first-order pressure is

$$p^{(1)} = -U_1(x) \tag{2.6}$$

Thus, the elimination of $p^{(1)}$ from Eq. (2.5) yields for $\psi^{(1)}$ an equation:

$$\psi_y^{(0)}\psi_{xy}^{(1)} + \psi_{xy}^{(0)}\psi_y^{(1)} - \psi_x^{(0)}\psi_{yy}^{(1)} - \psi_{yy}^{(0)}\psi_x^{(1)} = U_1'(x) + \psi_{yyy}^{(1)} \tag{2.7}$$

where the prime indicates total differentiation. This equation can now be integrated if the outside flow field is determined. The boundary conditions for any order of approximation can be expressed as:

$$\begin{aligned} \psi^{(n)} = \psi_y^{(n)} &= 0, \qquad \text{when} \quad y = 0 \\ \psi_y^{(n)} &= U_n(x), \qquad \text{when} \quad y = \infty \end{aligned} \tag{2.8}$$

3. First-order potential solution. In the preceding section, it has been shown that to the second approximation the flow field can still be subdivided into a viscous layer and a potential region. By choosing the boundary-layer solution as the first approximation, the first-order potential flow can now be determined.

As was shown by Blasius' solution (7), at the edge of the boundary layer the velocity u approaches the value one but $\bar{v}/U_\infty$ tends asymptotically to $(\frac{1}{2})\beta\,\epsilon\,x^{-\frac{1}{2}}$, β being a pure number (1.73 approximately). The fact that the velocity on the edge of the viscous layer is variable shows that the flow outside it must be deflected and therefore cannot be uniform. This will be the basic principle upon which the first-order potential solution shall be constructed.

The problem can thus be formulated by the potential theory in terms of the boundary value of the vertical velocity on the x-axis. First of all, it is zero for $x < 0$. In the interval $0 \leqq x \leqq 1$, $V = (\frac{1}{2})\beta\,\epsilon\,x^{-\frac{1}{2}}$, according to boundary-layer theory. On account of the wake behind the plate, however, there is no fore-and-aft symmetry and its effect should be separately considered.

According to Goldstein's theoretical study and Fage's experiments on the wake behind a flat plate (8), the boundary of the wake begins with the boundary layer at the trailing edge of the plate and grows rather slowly downstream as long as it remains laminar. The vertical velocity at the boundary of the wake varies as $-(x-1)^{1/3}$(9) in the neighborhood of the plate and asymptotically as $-(x-0.48)^{-3/2}$(10) at large distances downstream. Thus, it is seen that the limiting streamlines change suddenly from positive to negative inclinations with a discontinutiy at the trailing edge of the plate. From this incomplete information about the wake, the boundary value on the rest of the x-axis can only be approximately described. This has been carried out. However, owing to the fact that V varies slowly for x close to one and the coefficient of $(x-0.48)^{-3/2}$ is small, the final result is very little affected if the wake is replaced by a discontinuity in the inclination of the stream-lines at the trailing edge and remains parallel from there on. Namely, on the x-axis:

$$V = \begin{cases} 0 & \text{for} \quad x < 0 \\ (\frac{1}{2})\beta\,\epsilon\,x^{-\frac{1}{2}} & \text{for} \quad 0 \leqq x \leqq 1 \\ 0 & \text{for} \quad 1 < x \leqq \infty \end{cases} \tag{3.1}$$

If the velocity field in the potential region can be expanded in terms of a thickness parameter ϵ like the function ψ, then

$$\begin{aligned} u &= 1 + \epsilon U^{(1)}(\bar{x}/L, \bar{y}/L) + \cdots \\ V &= \epsilon V^{(1)}(\bar{x}/L, \bar{y}/L) + \cdots . \end{aligned} \tag{3.2}$$

From the potential theory, the first-order velocities $U^{(1)}$ and $V^{(1)}$, which vanish at infinity, are given, on account of (3.1), by the following:

$$\begin{aligned} U^{(1)} - iV^{(1)} &= \frac{\beta}{2\pi}\int_0^1 \frac{dt}{t^{\frac{1}{2}}(z-t)}, \\ &= -\frac{i\beta}{2\sqrt{z}} + \frac{\beta}{2\pi\sqrt{z}}\ln\frac{1+\sqrt{z}}{1-\sqrt{z}} \end{aligned} \tag{3.3}$$

where the complex variable z denotes $(x + iY)$.

From (3.3), the velocity $U^{(1)}$ reduces, on the plate $0 \leqq x \leqq 1$, to

$$U^{(1)}(x, 0) \equiv U_1(x) = \frac{\beta}{2\pi} \frac{1}{\sqrt{x}} \ln \frac{1 + \sqrt{x}}{1 - \sqrt{x}}, \qquad = \frac{\beta}{\pi}\left[1 + \frac{x}{3} + \frac{x^2}{5} + \cdots\right]. \tag{3.4}$$

The first-order pressure $p^{(1)}$ on the plate, following Eq. (2.6), reads:

$$p^{(1)} \equiv p_1(x) = -(\beta/\pi)[1 + x/3 + x^2/5 + \cdots .] \tag{3.5}$$

It is noted that due to the displacement of the stream-lines from the plate by the viscous effect, the resulting potential flow along the plate is accelerating. Consequently, the viscous layer, in turn, is subject to a favorable pressure gradient in the downstream direction.* Moreover, in spite of the fact that the vertical velocity $V^{(1)}$ is singular at the leading edge, the horizontal velocity $U^{(1)}$ and, hence the pressure, are regular there. On the other hand, $V^{(1)}$ is discontinuous but finite at the trailing edge, where $U^{(1)}$ has a logarithmic singularity. The consequence of these is that all the derivatives of the velocities, such as vorticity, in the viscous layer will be even more singular at both ends of the plate. This seems to be in agreement with the solutions obtained by Oseen's approximation. (11).

4. Solution of $\psi^{(1)}(x, y)$. After the velocity at the edge of the boundary layer has been determined, the equation (2.7) can be written as

$$\psi_y^{(0)}\psi_{xy}^{(1)} + \psi_{xy}^{(0)}\psi_y^{(1)} - \psi_x^{(0)}\psi_{yy}^{(1)} - \psi_{yy}^{(0)}\psi_x^{(1)} - \psi_{yyy}^{(1)} = (\beta/\pi)[\tfrac{1}{3} + \tfrac{2}{5}x + \cdots + [(n-1)/(2n-1)]x^{n-2} + \cdots] \tag{4.1}$$

By hypothesis, $\psi^{(0)}$ satisfies Eq. (2.6) and, according to Blasius, $\psi^{(0)} = x^{\frac{1}{2}} f_0(\eta)$ and $\eta = y/\sqrt{x}$, where the function f_0 can be obtained by integratng the equation

$$2f_0''' + f_0 f_0'' = 0 \tag{4.2}$$

These special forms of $\psi^{(0)}$ and $U_1(x)$ demand as solutions:

$$\psi^{(1)} = \frac{\beta}{\pi}\left[x^{\frac{1}{2}} f_1(\eta) + \tfrac{1}{3}x^{3/2} f_2(\eta) + \cdots + \frac{x^{n+\frac{1}{2}}}{2n-1} f_n(\eta) + \cdots\right] \tag{4.3}$$

* Note that this pressure gradient vanishes in the limit of an infinite plate. This is because the displacement thickness contour is then a parabola, and it is well known that in the flow past a parabola, the pressure on the surface becomes constant and equal to the mainstream pressure at distances from the leading edge compared with the focal length. (Also the pressure continued onto the axis is exactly constant to the right of the focus.) In the assumed flow (resulting from the finite length of the plate), however, the parabola is broken off at the trailing edge and becomes a line parallel to the stream. This breaking off is effectively like a sink distribution in the wake, and results in the accelerated flow along the plate which was calculated above.

whence

$$\psi_v^{(1)} = \frac{\beta}{\pi}\left[f_1' + \cdots + \frac{x^{n-1}}{2n-1} f_n' + \cdots\right]$$
$$\psi_x^{(1)} = \frac{\beta}{\pi}\left[\tfrac{1}{2}x^{-\frac{1}{2}}(f_1 - \eta f_1') + \cdots + \frac{x^{n-3/2}}{2(2n-1)}\{(2n-1)f_n - \eta f_n'\} + \cdots\right] \tag{4.4}$$

where $f_n(\eta)$'s are functions of η.

The substitution of $\psi^{(1)}$ from (4.3) in (4.1), after a simple reduction, gives:

$$2f_n''' + f_0 f_n'' - 2(n-1)f_0' f_n' + (2n-1)f_0'' f_n = -2(n-1) \tag{4.5}$$

where $n = 1, 2, 3, \cdots$. From the boundary conditions (2.8) and on account of (3.4), the functions f_n satisfy, for all n and $x > 0$:

$$f_n(0) = f_n'(0) = 0, \qquad f_n'(\infty) = 1 \tag{4.6}$$

As the coefficients of this equation cannot be expressed analytically by simple functions for the whole range of η, an analytical solution valid for all η and n is generally not possible. The problem, on the whole, is a numerical one. It is noticed, however, that for $n = 1$, the Eq. (4.5) assumes a particularly simple form:

$$2f_1''' + f_0 f_1'' + f_0'' f_1 = 0 \tag{4.7}$$

For this equation, it can be verified that the following combination of f_0 and f_0', which evidently satisfies (4.6), is a solution:

$$f_1 = \tfrac{1}{2}(f_0 + \eta f_0') \tag{4.8}$$

The cases $n = 2$ and $n = 3, 5, 9$ have been integrated numerically by Howarth (12) and Tani (13) respectively. It will be shown presently that for n greater than 10, say, simple approximate solutions can be found.

First of all, it is noticed that f_0' is a special solution of the equation:

$$2f_n''' + f_0 f_n'' - 2(n-1)f_0' f_n' + (2n-1)f_0'' f_n = 0$$

Therefore, the order of the Eq. (4.5) can be reduced by one if the substitution:

$$f_n = f_0' F_n(\eta) \tag{4.9}$$

is made. Elimination of f_n from Eq. (4.5) by virtue of (4.9) leads to:

$$2f_0' F_n''' + (6f_0'' + f_0 f_0')F_n'' - (f_0 f_0'' + 2(n-1)f_0'^2)F_n' = -2(n-1) \tag{4.10}$$

This equation can then be considered as second order in F_n'. If the coefficients of this equation are to be approximated by taking $f_0 = (\frac{1}{2})\alpha\eta^2$ in a range of $\eta \leqq \eta_1$, where α is 0.332 and η_1 is a fixed number to be specified later; then in the range $0 \leqq \eta \leqq \eta_1$, Eq. (4.10) will be replaced by

$$\eta^2 F_n''' + 3\eta F_n'' - (n - \tfrac{3}{4})\alpha\eta^3 F_n' = -\frac{n-1}{\alpha}\eta \tag{4.11}$$

The errors involved in the first and third coefficients are of the order η^3 and that of the second is of the order η^6. Therefore, if η_1 is not too large, this approximation is expected to be sufficiently accurate for the answers required.

It is observed, in the first place, that $(n-1)/\alpha^2(n-\frac{3}{4})\eta^2$ is a particular solution. Furthermore, the fundamental integrals of the homogeneous equation resulting from the cancellation of the term on the right-hand side of Eq. (4.11), are $n^{-1}I_{2/3}(\zeta)$ and $\eta^{-1}K_{2/3}(\zeta)$. The general solution then can be written as

$$F_n' = A\eta^{-1}I_{2/3}(\zeta) + C_1\eta^{-1}K_{2/3}(\zeta) + \frac{n-1}{\alpha^2(n-\frac{3}{4})}\frac{1}{\eta^2} \tag{4.12}$$

where $$\zeta = \tfrac{2}{3}(n-\tfrac{3}{4})^{\frac{1}{2}}\alpha^{\frac{1}{2}}\eta^{3/2}$$

Here $I_{2/3}$ and $K_{2/3}$ denote the Bessel functions of the first and second kinds of imaginary argument. In order that the condition at $\eta = 0$ be satisfied, the constant C_1 should be determined to cancel the singularity of $K_{2/3}$ which is η^{-1}. This condition requires that

$$C_1 = -\frac{n-1}{\alpha^2(n-\frac{3}{4})}\cdot\frac{\Gamma(\frac{1}{3})(n-\frac{3}{4})^{1/3}\alpha^{1/3}}{\pi 3^{1/6}}$$

Thus, the solution, with the conditions at $\eta = 0$ satisfied, is finally of the form:

$$f_n = f_0'\left\{A\int_0^\eta I_{2/3}(\zeta)\frac{d\eta}{\eta} - \frac{n-1}{\alpha^2(n-\frac{3}{4})}\int_0^\eta\left[\lambda_n K_{2/3}(\zeta) - \frac{1}{\eta}\right]\frac{d\eta}{\eta}\right\} \tag{4.13}$$

by putting $\lambda_n = \Gamma(\frac{1}{3})(n-\frac{3}{4})^{1/3}\alpha^{1/3}/\pi 3^{1/6}$, where the constant A remains to be determined.

On the other hand, when η is large, f_0 is approximately $\eta - \beta$. If this approximation is introduced in Eq. (4.10), it is transformed into

$$2F_n''' + (\eta-\beta)F_n'' - 2(n-1)F_n' = -2(n-1) \tag{4.14}$$

Moreover, it can be shown that by the substitutions:

$$F_n' = (\eta-\beta)e^{-(\eta-\beta)^2/4}G_n(\sigma) + 1 \tag{4.15}$$

and

$$\sigma = \tfrac{1}{4}(\eta-\beta)^2$$

Eq. (4.14) becomes a confluent hypergeometric equation for $G_n(\sigma)$:

$$\sigma G_n'' + (\tfrac{1}{2} + 1 - \sigma)G_n' - nG_n = 0 \tag{4.16}$$

whose two fundamental solutions are:

$${}_1F_1(n, \tfrac{3}{2}; \sigma) \qquad \text{and} \qquad \sigma^{-\frac{1}{2}}{}_1F_1(n-\tfrac{1}{2}, \tfrac{1}{2}; \sigma)$$

Therefore, the general solution for large η, by (4.15), can be expressed as

$$f_n' \equiv F_n' = (\eta-\beta)e^{-\sigma}[C_2{}_1F_1(n, \tfrac{3}{2}; \sigma) + C\sigma^{-\frac{1}{2}}{}_1F_1(n-\tfrac{1}{2}, \tfrac{1}{2}; \sigma)] + 1 \tag{4.17}$$

where C_2 and C are constants.

By virtue of the asymptotic behavior of the confluent hypergeometric function, namely as $\sigma \to \infty$

$$ {}_1F_1(a, b; \sigma) \approx [\Gamma(b)/\Gamma(a)]e^{\sigma}\sigma^{a-b}\,{}_2F_0(b - a, 1 - a; \sigma^{-1}) $$

the condition at infinity, i.e., $f_n'(\infty) = 1$, is satisfied if

$$ C_2 = -2[\Gamma(n)/\Gamma(n - \tfrac{1}{2})]C $$

By eliminating C_2 in terms of C, the solution for large η then assumes the final form:

$$ f_n = \eta + B + C\int_{\eta}^{\infty} e^{-\sigma}[{}_1F_1(n - \tfrac{1}{2}, \tfrac{1}{2}; \sigma) - 2[\Gamma(n)/\Gamma(n - \tfrac{1}{2})]\sigma^{\frac{1}{2}}\,{}_1F_1(n, \tfrac{3}{2}; \sigma)]\,d\eta \tag{4.18} $$

where B and C are constants.

If the two solutions (4.13) and (4.18) for small and large η, respectively, represent, in fact, the same function $f_n(\eta)$, then f_n, f_n' and f_n'' must be joned in a region where both solutions are valid. These three conditions are clearly both necessary and sufficient for the determination of the constants A, B and C.

5. Law of resistance. It can be shown that, up to the second approximation, the local shear remains $\rho\nu(\partial\bar{u}/\partial\bar{y})$. Thus, from Eq. (2.3) and (4.4) the shear stress τ on the plate is given by

$$ \tau = \rho U_\infty^2\,\epsilon\left[x^{-\frac{1}{2}}f_0''(0) + \frac{\beta\epsilon}{\pi}\sum_1^{\infty}\frac{x^{n-1-\frac{1}{2}}}{2n-1}f_n''(0) + \cdots\right] \tag{5.1} $$

If the total force experienced by one side of the plate per unit width is considered, the skin-friction coefficient C_f can be defined as

$$ C_f = \frac{1}{\frac{1}{2}\rho U_\infty^2 L}\int_0^L \tau\,d\bar{x} \tag{5.2} $$

From (5.1), the integration yeilds

$$ C_f = (4\alpha/\sqrt{Re}) + (\alpha_1/Re) + \cdots \tag{5.3} $$

where

$$ \alpha_1 = \frac{4\beta}{\pi}\sum_1^{\infty}\frac{f_n''(0)}{(2n-1)^2} \tag{5.4} $$

The skin-friction coefficient, to the second order, consists of two terms: the first is recognized as the Blasius law and the second, which varies inversely as the Reynolds number, constitutes the correction. This shows that, as the second term is inversely proportional to the Reynolds number, it becomes extremely small by comparison when the Reynolds number is large and, consequently, the resistance follows Blasius' law. However, as the Reynolds number decreases, the correction will gradually become significant. The point at which the re-

sistance deviates distinctly from the Blasius' law, depends, of course, on the value of α_1 .

To evaluate this sum, as is seen from (5.4), it requires only the initial curvature of the functions f_n . Because of the fact that the functions f_1 to f_9 are known exactly, the first nine terms can be accurately calculated. From the ninth term on, however, as the degree of accuracy in $f_n''(0)$ will be less important, the approximate values will be substituted.

Before the actual calculation of α_1 is carried out, the constant A appearing in the solution f_n should be first determined by joining the two solutions (4.13) and (4.18). It is noted that if η_1 is taken to be 3 (justified by the fact that linear approximation to f_0' differs from the exact value by only about 16 per cent) then $\zeta_1 \approx (9/2)(n - 3/4)^{\frac{1}{2}}$. Thus, only for moderate values of η will the argument of the Bessel functions in Ref. (13) be large. By means of the asymptotic form of the Bessel function, e.g. $I_{2/3}(\zeta) \approx (e^{\zeta}/\sqrt{2\pi\zeta})(1 + O(\zeta^{-1}))$ and $K_{2/3}(\zeta) \approx \sqrt{\pi}\, e^{-\zeta}/\sqrt{2\pi}(1 + O(\zeta^{-1}))$, the integrals in (4.13) can be asymptotically integrated. Furthermore, by the same asymptotic integration, namely both n and σ large, the integrand of (4.18) is equivalent asymptotically to $\exp(-\sigma/2 - \sqrt{n\sigma})$ $(1 + O(1/\sqrt{n}))$.

After these simplifications, two algebraic equations between A and C give a solution for A which can be readily shown to be of the order $n^{1/4}e^{-\zeta_1}$. For $n = 4$, say, $\zeta_1 = 9$ and A will be of the order 10^{-4}. Since the first term of $f_n''(0)$ is $2\alpha A[\eta^{-1}I_{2/3}(\zeta)]_0$, which is $O(n^{7/12}e^{-\zeta_1})$, it can be neglected by comparison with the second term. Hence, for large n, $f_n''(0)$ can be approximately given by

$$f_n''(0) \sim \frac{\Gamma(1/3)}{\Gamma(2/3)} \cdot \frac{n - 1}{(3\alpha)^{1/3}(n - 3/4)^{1/3}} \tag{5.5}$$

From Howarth's and Tani's solutions, $f_2''(0)$ and $f_3''(0)$, $f_5''(0)$, $f_9''(0)$* are 2.041 and 3.177, 5.010, 7.936 respectively. The approximate formula above gives the corresponding values to be respectively 1.838 and 3.022, 4.892, 7.844. From Dr. Tani's results, $f_4''(0)$, $f_6''(0)$, $f_7''(0)$ and $f_8''(0)$ were obtained graphically with the values, 4.083. 5.800, 6.570 and 7.290 respectively.

Of course, when n increases, the accuracy will certainly be improved. This seems to be sufficient to establish the reliability of this approximation. This result, incidentally, also establishes the convergence of the sum α_1 , because, for large n, $f_n''(0)$ is $O(n^{2/3})$. The sum then will converge like a Zeta function, $\zeta(1/3)$.

The actual summation of the series was performed, hence, in three separate steps: (a) the first nine terms were calculated by means of Howarth's and Tani's solutions. (b) the subsequent five terms were summed by substituting $f_n''(0)$ from (5.5) and finally (c) from the fourteenth term on, the infinite sum was converted into a definite integral by the Euler-MacLaurin formula with the integrand $(n - 1)^{2/3}/(2n - 1)^2$. Of these three steps, (b) and (c) unavoidably involve error. However, a conservative estimate places the fourth significant figure at most in doubt. The final answer is, accordingly, $\alpha_1 = 4.12$.

* Private communication.

By adopting this value in (5.3), the skin-friction coefficient C_f can be plotted as a function of Re as shown in Fig. 1. It is seen that, for Re greater than 10^4, C_f practically coincides with the Blasius' law. But in the range $10 < Re < 10^4$, they differ considerably; for instance, at $Re = 100$, the difference amounts to nearly 24 percent of the total value. In this range of moderate Reynolds numbers, the resistance of a plate has been measured by Janour (6), and, by comparison, the theoretical and experimental values agree surprisingly well provided the Reynolds number is not close to 10. Near $Re = 10$, the calculated values

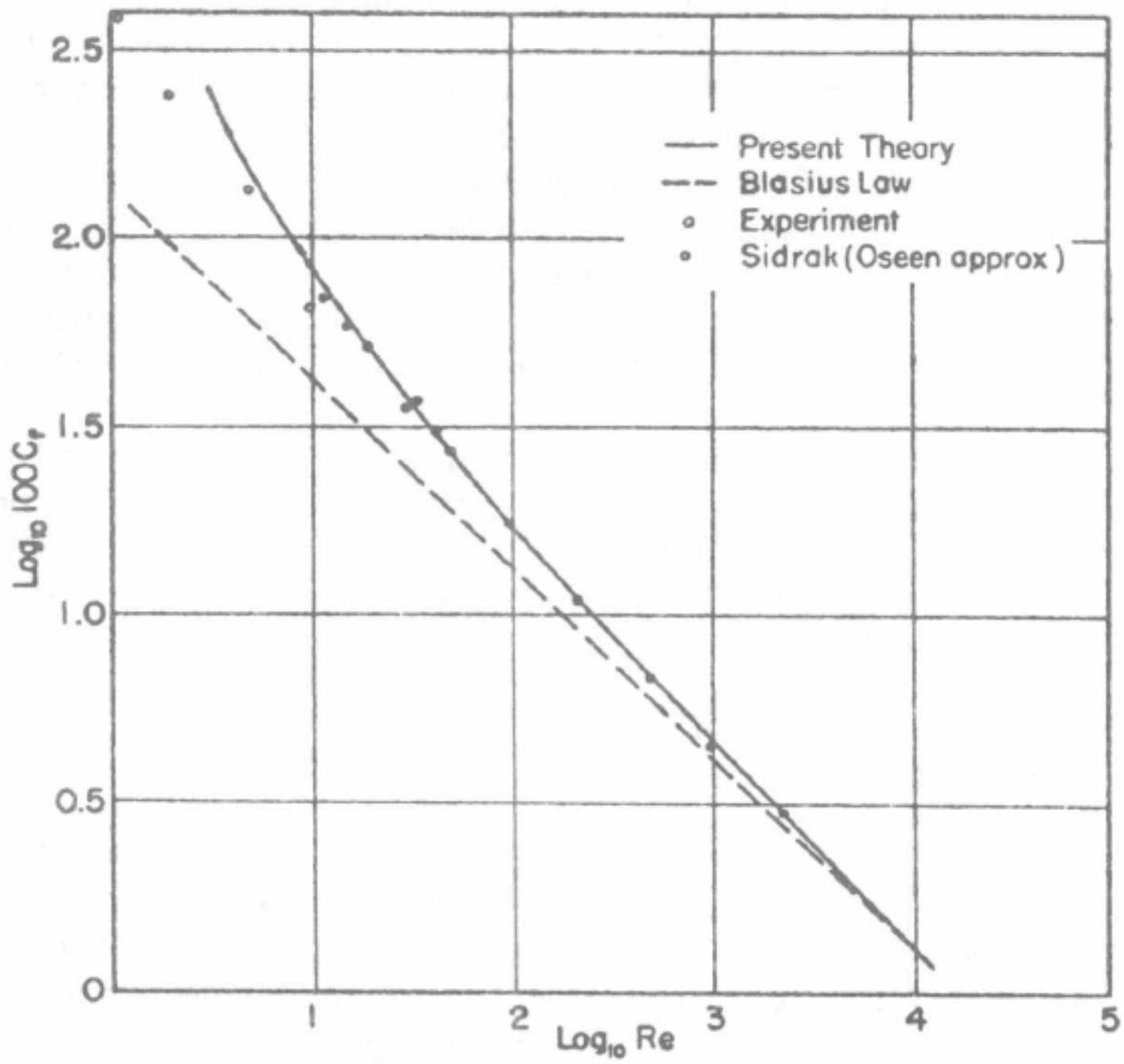

Fig 1 Resistance coefficient of a flat plate in parallel flow.

from (5.3) are higher than the measured ones. There seems to be better agreement between the results calculated by S. Sidrak (14) by Oseen's method of approximation and the experimental values (Ref. 6) at $Re = 10$, hence it is reasonable to presume that the second-order theory cannot be accurately applied for Reynolds number below 15, say.

One might postulate that if the approximation is pursued one stage further, the range of applicability of the resistance formula (5.3) could possibly be extended into the low Reynolds number regime and might even overlap with the solution approached from the other end of the Reynolds number, such as Sidrak's solution. If this were the case, there is, at least, one example where solution can be found for all Reynolds numbers. This general question of higher approximation will be discussed in what follows.

If the approximations were carried one step further, one would notice that the known function on the right-hand side of the non-homogeneous equation for $\psi^{(2)}(x, y)$ consists of two groups of terms, having as coefficients x^{-1} and x^{-2} respectively. In view of the fact that the form of the solution has been fixed by the choice of $\psi^{(0)} = \sqrt{x}\, f_0(\eta)$, $\psi^{(2)}$ will automatically take on a term like $x^{-\frac{1}{2}}f(\eta)$ in order to cancel the second term on the right-hand side of the equation for $\psi^{(2)}$. Consequently, the order of singularity at the leading edge must become progressively stronger as the order of approximation increases. This shows that the high approximation such as $\psi^{(2)}$, as obtained by the method outlined above, would not improve the accuracy of the first and second approximations but, on the contrary, would tend to worsen it as the leading edge is approached. Furthermore, if such high-order approximations are included in the integral for resistance (5.2), this integral obviously diverges. For this reason, this approach to the problem must be rejected.

6. Lighthill's method of improving bundary-layer solution near the leading edge. The source of the difficulty encountered by the method of perturbation adopted in section 2 is the fact that the solution of the first approximation, i.e., the boundary-layer theory, is singular in the whole line $x = 0$. It seems generally true as propounded by Lighthill (5), that whenever the solution of the first approximation to a non-linear differential equation is singular either along curves or at isolated points, these singularities, whichever they may be, will be passed on, in an accentuated form, to the rest of the successive approximations. To overcome such difficulties, as shown by Lighthill, the expansions (2.3) should be modified such that:

$$\begin{aligned} \psi &= \psi^{(0)}(\tilde{x}, \tilde{y}) + \epsilon\psi^{(1)}(\tilde{x}, \tilde{y}) + \epsilon^2\psi^{(2)}(\tilde{x}, \tilde{y}) + \cdots \\ p &= \epsilon p^{(1)}(\tilde{x}, \tilde{y}) + \epsilon^2 p^{(2)}(\tilde{x}, \tilde{y}) + \cdots \end{aligned} \tag{6.1}$$

where the variables $\tilde{x}$ and $\tilde{y}$ are related to x and y by the transformation, yet to be determined,

$$\begin{aligned} x &= \tilde{x} + \epsilon x^{(1)}(\tilde{x}, \tilde{y}) + \epsilon^2 x^{(2)}(\tilde{x}, \tilde{y}) + \cdots \\ y &= \tilde{y} \end{aligned} \tag{6.2}$$

The object of the transformation (6.2) is to bring into the problem extra degrees of freedom by means of which the "parental" singularties, such as $\sqrt{x}$, can be frozen during the course of the successive approximations. This will be demonstrated in the determination of $\psi^{(2)}$ as follows:

As the solution of $\psi^{(1)}$ given in section 4 has an identical singularity to that of $\psi^{(0)}$, no further change for Eq. (2.7) is necessary. The first-order function $x^{(1)}$ of the transformation (6.2) can, therefore, be taken as zero. The transformation then becomes

$$\begin{aligned} x &= \tilde{x} + \epsilon^2 x^{(2)}(\tilde{x}, \tilde{y}) + \cdots \\ y &= \tilde{y} \end{aligned} \tag{6.3}$$

According to this transformation, the derivatives $\partial/\partial x$ and $\partial/\partial y$ will be transformed, respectively, into $\partial/\partial\tilde{x} - \epsilon^2 x_{\tilde{x}}^{(2)}\,\partial/\partial\tilde{x}$ and $\partial/\partial\tilde{y} - \epsilon^2 x_{\tilde{y}}^{(2)}\,\partial/\partial\tilde{x}$. Thus, the largest terms produced by the transformation of derivatives can only be of the second order. As a consequence of this the equations for $\psi^{(0)}$ and $\psi^{(1)}$ in terms of the variables $\tilde{x}$ and $\tilde{y}$ will be the same as Eqs. (2.4) and (2.7). The equations for $\psi^{(2)}$ and $p^{(2)}$, however, are changed; viz.,

$$\begin{aligned}\psi_{\tilde{y}}^{(0)}\psi_{\tilde{x}\tilde{y}}^{(2)} + \psi_{\tilde{x}\tilde{y}}^{(0)}\psi_{\tilde{y}}^{(2)} - \psi_{\tilde{x}}^{(0)}\psi_{\tilde{y}\tilde{y}}^{(2)} - \psi_{\tilde{y}\tilde{y}}^{(0)}\psi_{\tilde{x}}^{(2)} - \psi_{\tilde{y}\tilde{y}\tilde{y}}^{(2)} \\ = [\psi_{\tilde{x}}^{(1)}\psi_{\tilde{y}\tilde{y}}^{(1)} - \psi_{\tilde{y}}^{(1)}\psi_{\tilde{y}\tilde{x}}^{(1)}] + [-p_{\tilde{x}}^{(2)} + \psi_{\tilde{y}\tilde{x}\tilde{x}}^{(0)} + \psi_{\tilde{y}\tilde{y}\tilde{y}}^{(0)}x_{\tilde{x}}^{(2)} \\ + (p_{\tilde{y}}^{(2)} - 2\psi_{\tilde{x}\tilde{y}\tilde{y}}^{(0)})x_{\tilde{y}}^{(2)} + \psi_{\tilde{y}}^{(0)}\psi_{\tilde{x}}^{(0)}x_{\tilde{x}\tilde{y}}^{(2)} - (\psi_{\tilde{x}}^{(0)2} + 3\psi_{\tilde{x}\tilde{y}}^{(0)})x_{\tilde{y}\tilde{y}}^{(2)} - \psi_{\tilde{x}}^{(0)}x_{\tilde{y}\tilde{y}\tilde{y}}^{(2)}]\end{aligned} \tag{6.4}$$

and

$$p_{\tilde{y}}^{(2)} + \psi_{\tilde{x}}^{(0)}\psi_{\tilde{x}\tilde{y}}^{(0)} - \psi_{\tilde{y}}^{(0)}\psi_{\tilde{x}\tilde{x}}^{(0)} + \psi_{\tilde{x}\tilde{y}\tilde{y}}^{(0)} = 0$$

As in Section 4, let the similarity variable $\tilde{\eta} = \tilde{y}/\sqrt{\tilde{x}}$ be introduced. Then it can readily be shown that the singularity of the first group of terms is $\tilde{x}^{-1}$ while that of the second group, due to terms like $p_{\tilde{x}}^{(2)}$ and $\psi_{\tilde{y}\tilde{x}\tilde{x}}^{(0)}$, is $\tilde{x}^{-3}$. If the singularity of $\psi^{(2)}$ were the same as $\psi^{(0)}$, the singularity of the left-hand side of the first of Eqs. (6.4) would be $\tilde{x}^{-1}$, which could balance only the first group on the right-hand side. If the second group is also to be cancelled, the singularity of $\psi^{(2)}$ should have been $\tilde{x}^{-\frac{1}{2}}$, which would make the resistance integral diverge. The role of the function $x^{(2)}(\tilde{x}, \tilde{y})$ is just to provide an extra condition to have this group of terms removed. Now, if $p^{(2)} = p_2(\tilde{x}) + P^{(2)}(\tilde{x}, \tilde{y})$ where $P^{(2)}(\tilde{x}, \tilde{y})$, from the second eq. (6.4), by partial integration

$$P^{(2)}(\tilde{x}, \tilde{y}) = \int (\psi_{\tilde{y}}^{(0)}\psi_{\tilde{x}\tilde{x}}^{(0)} - \psi_{\tilde{x}}^{(0)}\psi_{\tilde{x}\tilde{y}}^{(0)} - \psi_{\tilde{x}\tilde{y}\tilde{y}}^{(0)})\,d\tilde{y} \tag{6.5}$$

and $p_2(\tilde{x})$ should be determined by the consideration of the second-order potential flow, in analogy with $p_1(\tilde{x})$; then $x^{(2)}$ can be chosen:

$$\begin{aligned}\psi_{\tilde{y}\tilde{y}\tilde{y}}^{(0)}x_{\tilde{x}}^{(2)} + (P_{\tilde{y}}^{(2)} - 2\psi_{\tilde{x}\tilde{y}\tilde{y}}^{(0)})x_{\tilde{y}}^{(2)} + \psi_{\tilde{y}}^{(0)}\psi_{\tilde{x}}^{(0)}x_{\tilde{x}\tilde{y}}^{(2)} \\ - (\psi_{\tilde{x}}^{(0)2} + 3\psi_{\tilde{x}\tilde{y}}^{(0)})x_{\tilde{y}\tilde{y}}^{(2)} - \psi_{\tilde{x}}^{(0)}x_{\tilde{y}\tilde{y}\tilde{y}}^{(2)} = P_{\tilde{x}}^{(2)} - \psi_{\tilde{x}\tilde{x}\tilde{y}}^{(0)}\end{aligned} \tag{6.6}$$

It is noted that as $x^{(2)}$ is required to be regular at $\tilde{y} = 0$, both sides of eq. (6.6) vanish with $\tilde{y}$. For this reason, the constant of integration will be absorbed in the yet undetermined function $p_2(\tilde{x})$ which is also required to be regular.

7. Determination of the transformation function $x^{(2)}$. By the assumption $\psi^{(0)} = \sqrt{\tilde{x}}\,f_0(\tilde{\eta})$, together with Eq. (6.5), a straightforward reduction leads to an equation:

$$\begin{aligned}2(f_0 - \tilde{\eta}f_0')g_2''' + (f_0'^2 - \tilde{\eta}f_0f_0' - 6\tilde{\eta}f_0'')g_2'' + [2f_0'(f_0 - \tilde{\eta}f_0') - 6(f_0'' + \tfrac{1}{3}\tilde{\eta}f_0''')]g_2' \\ = 6\tilde{\eta}f_0'' + \tilde{\eta}^2f_0''' + \tfrac{1}{2}\tilde{\eta}f_0f_0' - f_0'^2 + \tfrac{1}{2}\tilde{\eta}^2f_0''^2\end{aligned} \tag{7.1}$$

where g_2 is a function of $\tilde{\eta}$ and is defined by

$$x^{(2)} = g_2(\tilde{\eta}) \tag{7.2}$$

It is noted that this equation has an integrating factor $f_0(\tilde{\eta})$ and, on multiplying both sides by $f_0(\tilde{\eta})$, an integration yields

$$2f_0(f_0 - \tilde{\eta}f_0')g_2'' - [2f_0'(f_0 - \tilde{\eta}f_0') + 4\tilde{\eta}f_0f_0'' - f_0^3 + \tilde{\eta}f_0^2f_0']g_2' = G(\tilde{\eta}) + \text{const.} \tag{7.3}$$

where

$$G(\tilde{\eta}) = \int_0^{\tilde{\eta}^2} f_0[6\tilde{\eta}f_0'' + \tilde{\eta}^2f_0''' + \tfrac{1}{2}\tilde{\eta}f_0f_0' - f_0^2 + \tfrac{1}{2}\tilde{\eta}^2f_0'^2]\, d\tilde{\eta}$$

If $g_2(\tilde{\eta})$ is regular at the origin and $g_2(0) = 0$ (i.e., $\tilde{y} = 0$ corresponsd to $x = \tilde{x}$ and therefore the plate remains fixed), then a unique solution is found by quadrature to be of the form:

$$g_2 = -\tfrac{1}{2}\int_0^{\tilde{\eta}}\left\{\frac{f_0}{(f_0 - \tilde{\eta}f_0')^2}\exp\left[-\tfrac{1}{2}\int_0^{\tilde{\eta}} f_0\, d\tilde{\eta}^2\right]\int_0^{\tilde{\eta}}\frac{(\tilde{\eta}f_0' - f_0)}{f_0^2}\cdot\exp\left[\tfrac{1}{2}\int_0^{\tilde{\eta}} f_0\, d\tilde{\eta}\right]G(\tilde{\eta})\, d\eta\right\}d\tilde{\eta} \tag{7.4}$$

As $G(\tilde{\eta})$ is $O(\tilde{\eta}^4)$ in the neighborhood of $\tilde{\eta} = 0$, it follows from Eq. (7.4) that $-g_2(\tilde{\eta})$ is $O(\tilde{\eta}^2)$. Therefore, the imposed conditions are satisfied.

The form of the solution given by (7.4), though closed, is not, however, convenient for numerical purposes. For this reason, a power-series solution will be given below by assuming f_0 to be

$$f_0 = \tfrac{1}{2}\alpha\tilde{\eta}^2 - \frac{\alpha^2}{2\cdot 5!}\tilde{\eta}^5 + \frac{11\alpha^3}{4\cdot 8!}\tilde{\eta}^8 - \frac{375\alpha^4}{8\cdot 11!}\tilde{\eta}^{11} + \cdots$$

First, the substitution of this expression under the integral sign gives the function $G(\tilde{\eta})$:

$$G = \frac{3\alpha^2}{4}\tilde{\eta}^4 - \frac{3\alpha^3}{140}\tilde{\eta}^7 + \frac{999\alpha^4}{20\cdot 8!}\tilde{\eta}^{10} - \cdots$$

Then by assuming a proper power series for g_2, and re-arranging terms on the left-hand side of Eq. (7.3), the identification of coefficients, suppressing the arbitrary constant, yields a solution

$$g_2 = -\left[\frac{1}{2\cdot 2!}\tilde{\eta}^2 - \frac{\alpha}{14\cdot 5!}\tilde{\eta}^5 + \frac{7\alpha^2}{30\cdot 8!}\tilde{\eta}^8 - \cdots\right] \tag{7.5}$$

valid for $\tilde{\eta} \leqq \tilde{\eta}_1$, $\tilde{\eta}_1$, being a fixed number.

On the other hand, for large $\tilde{\eta}$, f_0 is again approximated by $\tilde{\eta} - \beta$. The eq. (7.1) then reduces to

$$g_2''' + \tfrac{1}{2}(\tilde{\eta} - \beta)g_2'' + g_2' = -\tfrac{1}{2}(\tfrac{3}{2}\tilde{\eta} - \beta) \tag{7.6}$$

By the substitutions:

$$g_2' = -\tfrac{1}{2}(\tilde{\eta} - \tfrac{1}{2}\beta) + g'(t) \qquad \text{and} \qquad t = (1/\sqrt{2})(\tilde{\eta} - \beta) \tag{7.7}$$

Eq. (7.6) can be transformed into

$$g''' + tg'' + 2g' = 0$$

This equation can be twice integrated with the result

$$g' + tg = C_1 t + C_2$$

Further integration together with (7.7) yields the solution:

$$g_2 = -\tfrac{1}{4}(\bar{\eta} - \tfrac{1}{2}\beta)^2 + C_1 + C_2 e^{-\frac{1}{4}(\bar{\eta}-\beta)^2} + C_3 e^{-(\bar{\eta}-\beta)^2/4} \int_{\bar{\eta}_1}^{(\bar{\eta}-\beta)/\sqrt{2}} e^{t^2/4}\, dt \quad (7.8)$$

If the solutions (7.5) and (7.8) are joined at $\bar{\eta} = \bar{\eta}_1 = 3$, an approximate determination gives C_1, C_2 and C_3 the values -1.901, 1.264 and 0.431 respectively. Furthermore, it is noted that

$$e^{-t^2} \int_{t_1}^{t} e^{t^2}\, dt$$

approaches zero as t becomes infinite, the function g_2 tends to negative infinity as $-\frac{1}{4}(\bar{\eta} - \beta/2)^2$. g_2 so calculated is shown in Fig. 2.

Finally, it must be remarked once more that, by introducing the transformation function $x^{(2)}$ as given above, the singularity of $\psi^{(2)}$, if the solution of the equation for $\psi^{(2)}$ were to be found, could be maintained at $\sqrt{\bar{x}}$ and consequently the third-order correction to the resistance could be calculated. From a general standpoint, the problem can thus be considered as successfully solved.

8. Properties of the transformation. As was determined in the previous sections, the transformation (6.3) can now be discussed. It will be recalled first of all that the flow field of the Blasius solution is confined to the first quadrant with the plate coinciding with the positive $\bar{x}$-axis., both variables $\bar{x}$ and $\bar{y}$ being positive. From the definition of $\bar{\eta}$, if $\bar{x} \neq 0$, $\bar{y} = 0$ corresponds to $\bar{\eta} = 0$ and it follows that $x = \bar{x}$ as $g_2(0) = 0$. That is, the positive $\bar{x}$-axis is transformed into itself. On the other hand, if $\bar{x} = 0$ but $\bar{y} > 0$, $x = -\infty$ by eq. (7.4), but when $\bar{x}$ and $\bar{y}$ vanish simultaneously, $\bar{\eta}$ becomes arbitrary. If $\bar{\eta}$ varies from zero to infinity, the whole negative x-axis will be swept by the equation $x = \epsilon^2 g_2(\bar{\eta})$. Thus, the origin in the $\bar{x}$, $\bar{y}$-plane is turned into the whole negative x-axis. For values of $\bar{x}$ different from zero, it can readily be shown that every $\bar{x}$-const. line is mapped into a curve in the x, y-plane, which begins at a point on the positive x-axis and tends to negative infinity when $\bar{y}$ increases indefinitely. Consequently, the Blasius domain is transformed into the whole upper-half x, y-plane.

According to the Blasius solution, the first order velocity is a function of $\bar{\eta}$ and, following the definition of $\bar{\eta}$, its constant values lie on a family of parabolas with vertices at the origin. Since one of these parabolas defines the boundary layer, it would be of interest to determine this curve in the x, y-plane. By eliminating $\bar{x}$ from $\bar{y} = \bar{\eta}\sqrt{\bar{x}}$ by means of (6.3), $\bar{\eta}$ = const. then corresponds to

$$y = \bar{\eta}\sqrt{x - \epsilon^2 g_2(\bar{\eta})} \quad (8.1)$$

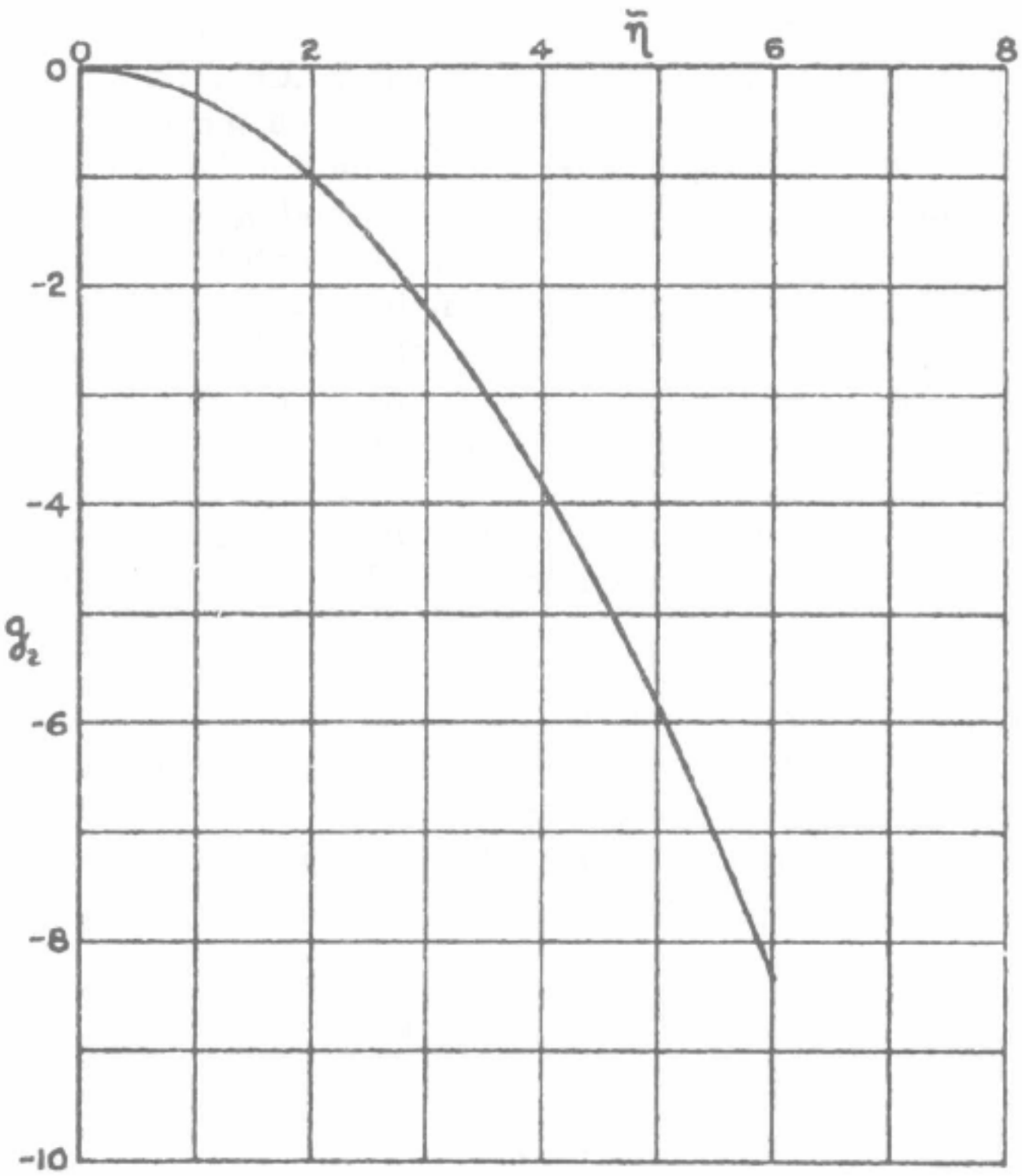

FIG. 2 THE FUNCTION $g_2(\bar{\eta})$

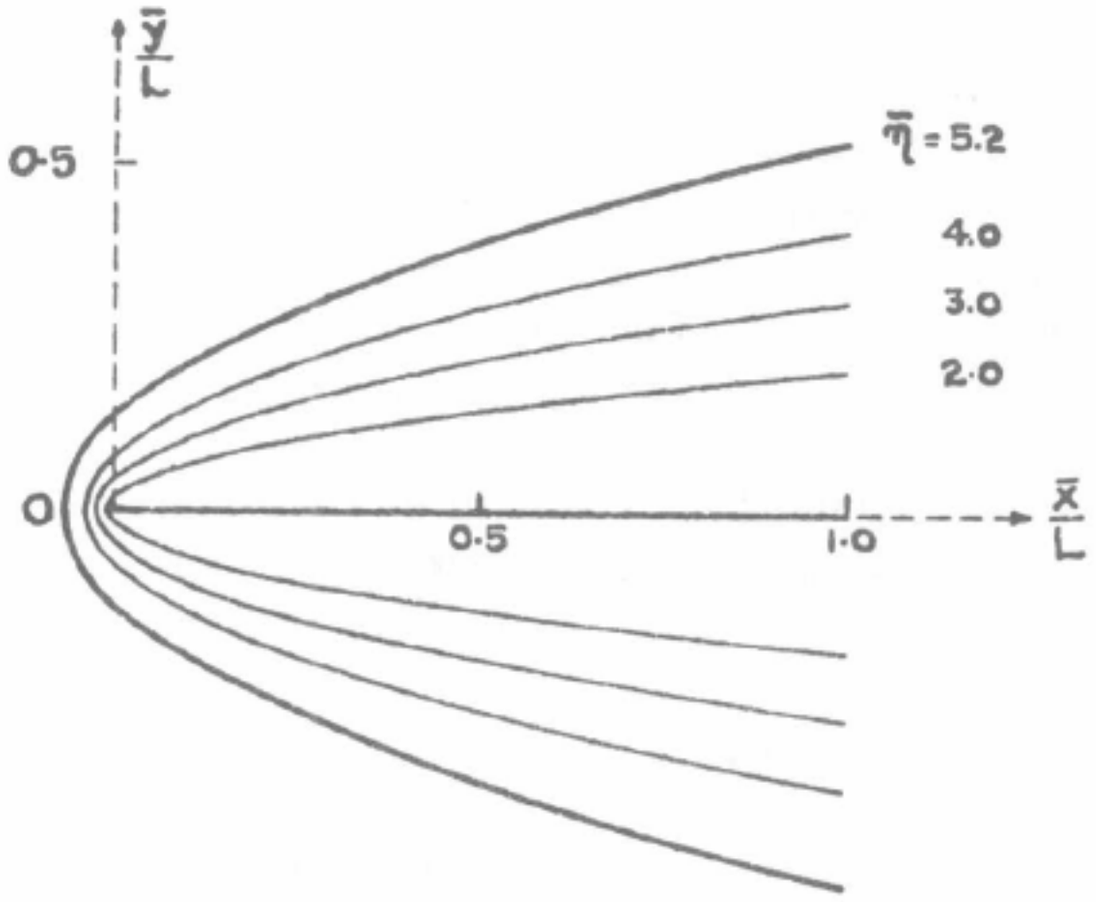

FIG. 3 BOUNDARY LAYER ON A FLAT PLATE AT R_e = 100

in the x, y-planes. This shows that the family of parabolas in the $\tilde{x}$, $\tilde{y}$-plane remains a family of parabolas after transformation. The difference lies in the fact that before the transformation to x, y-plane the vertices of the parabolas were all located at the origin; after transformation they are separated and given by $x_0 = \epsilon^2 g_2(\tilde{\eta})$ for each $\tilde{\eta}$. Since $g_2(0) = 0$ and $g_2(\infty) = -\infty$, this family of parabolas will cover the whole x, y-plane. The particular parabola which characterizes the boundary layer is conventionally taken to be $\tilde{\eta} = 5.2$. For this value of $\tilde{\eta}$, $g_2(\tilde{\eta}) = -6.30$. In the case of Reynolds number of 100, the graph is shown in Fig. 3. It is interesting to note that the region in the neighborhood of the leading edge, which was neglected in the Blasius solution, is an area of the order of ϵ^4 (linear dimension of the order of ν/U_∞). This result shows that the influence of the plate does spread ahead of the leading edge by diffusion at all Reynolds numbers and, therefore, is closer to physical reality that than predicated by the boundary-layer theory.

9. Deduced uniformly valid velocity field. A clear idea of the effects rendered to the solution by the transformation (6.3) can best be demonstrated through the examination of the velocity components in the x, y-plane. For this purpose, only the first order Blasius solution will be considered. By assuming $\psi = \psi^{(0)}$ and by making use of (6.3), the velocity components in the x, y-plane are as follows:

$$u = f_0'(\tilde{\eta}) + \frac{\epsilon^2 g_2'}{2\tilde{x} - \epsilon^2 \tilde{\eta} g_2'} (\tilde{\eta} f_0' - f_0) \tag{9.1}$$

$$V = \frac{\epsilon \sqrt{\tilde{x}}}{2\tilde{x} - \epsilon^2 \tilde{\eta}^2 g_2'} (\tilde{\eta} f_0' - f_0)$$

Since the denominator $2\tilde{x} - \epsilon^2 \tilde{\eta} g_2'$ in the expressions for u and V vanishes only at the leading edge, the solutions might still be singular there. However, the infinity in V on the $\tilde{y}$-axis is clearly removed. Indeed, V is now finite everywhere and on the negative x-axis it is zero. The effect on u is represented by an extra term which in most of the boundary layer is of the second order. The essential change lies in the fact that, whereas previously u was unity on the negative x-axis (or on the $\tilde{y}$-axis), it now varies with $\tilde{\eta}$ according to (9.1) for $\tilde{x} = 0$.

In order to bring out the exact nature of singularity at the leading edge, the function g_2 for small $\tilde{\eta}$ will be explicitly approximated by the leading term, namely by $-\tilde{\eta}^2/4$ according to (7.5). With this form of g_2, Eq. (6.3) yields a solution

$$2\tilde{x} = r + x, \qquad r^2 = x^2 + Y^2 \tag{9.2}$$

on elimination of $\tilde{\eta}$ by $y = \tilde{\eta}\sqrt{\tilde{x}}$. On account of (9.2) the same equation gives also

$$\epsilon^2 \tilde{\eta}^2 = 2(r - x) \tag{9.3}$$

If the Blasius solution is approximated also by the leading term, then from (9.2) and (9.3) the velocity components valid in the neighborhood of the plate are:

$$u = \frac{\sqrt{2\alpha}}{\epsilon}\sqrt{r-x} - \frac{\alpha}{2^{3/2}\epsilon}\frac{(r-x)^{3/2}}{r} \tag{9.4}$$

$$V = \frac{\alpha}{2^{3/2}\epsilon}\sqrt{r-x}\,\frac{Y}{r}$$

From this result, it can be deduced that the stream function is proportional to the real part of $z^{3/2} - \bar{z}^{\frac{1}{2}}z$ and, therefore, is biharmonic. This shows that in the neighborhood of the leading edge, the improved solution satisfies the Stokes equation and has a singularity similar to that predicated by Lin and Carrier (4). It is noted further that the velocities u and V, which were of different order of magnitude in boundary-layer theory, are now of the same order. This is another feature of the improved Blasius solution.

By the same method, the behavior of the solution at the edge of boundary layer can be investigated. For large $\bar{\eta}$, according to (7.8), $g_2(\bar{\eta})$ can be taken to be $-\bar{\eta}^2/4$. Then it can be shown similarly that for large $\bar{\eta}$

$$u = f_0' - \frac{\epsilon\beta}{2^{3/2}}\frac{\sqrt{r-x}}{r} \tag{9.5}$$

$$V = +\frac{\epsilon\beta}{2^{3/2}}\frac{\sqrt{r+x}}{r}$$

At the edge of the boundary layer, $Y = 0(\epsilon)$. In conformity to the convention adopted in Section 3, the edge of the boundary layer will be defined by $\bar{\eta} = \infty$ or $Y = 0$. Consequently, on the boundary $Y = 0$, the velocity components will take, as boundary values, 1 and $\epsilon\beta/2\sqrt{x}$, respectively, which agree with the Blasius solution. It should be pointed out that as the edge of the boundary layer is approached, the additional term in u and V become harmonic functions, and can be represented by $-i\epsilon\beta z^{-\frac{1}{2}}$. The fact that the boundary layer solution actually tends to the character of potential flow is, indeed, remarkable. It might be added that the same conclusions apply also to the next approximations.

10. Discussion. As the results given in the preceding sections all point in the right direction, there seems no doubt that the proposed scheme is a way of solving this type of problem. The only question that one may raise is whether or not the solution so obtained is unique? For the function $g_2(\bar{\eta})$ may involve an arbitrary constant. In section 7, it was chosen to be zero by the condition that the plate remains untransformed. If the constant were not zero, the parabolas would either cut the plate or have vertices ahead of the plate (according as whether it is positive or negative). Neither case would conform to the physical picture. Therefore, the condition $g_2(0) = 0$ must be the unique choice.

In section 9, there was a result that the velocity components in the neighborhood of the plate become the same order of magnitude. From this, one might expect an increase of wall shear stress because both $\partial u/\partial y$ and $\partial v/\partial x$ have to be

considered. However, it is easy to verify that all the extra terms give no contribution at the wall. As a result the wall shear agrees with that calculated by the boundary-layer theory. This is contrary to the belief that the flow near the leading edge is of the character of slow motion, and consequently, should have higher shear stress than that calculated in the boundary-layer theory. In the light of the new results, it can be concluded that the first order solution, even after the improvement by Lighthill's method, does not give additional shear stress. The second order contribution comes solely from the fact that the plate has a finite length in the flow direction. This seems to be consistent with the consideration by momentum theorem applied to a section of the wake behind the plate.

Finally, as pointed out in Section 9, the value of the second approximation to V at the edge of the boundary layer can be defined. With this as boundary value, the second-order pressure $p^{(2)}$ can similarly be determined and the problem of solving $\psi^{(2)}$ can be, at least in principle, carried out.

REFERENCES

1. Oseen, C. W., Über die Stokessche Formel und über eine verwandte Aufgabe in der Hydrodynamik, Arch. f. mate. astro. och fysik, 6, (1910).
2. Prandtl, L., Über Flüssigkeitsbewegung bei sehr kleiner Reibung, Proc. Third Inter. Cong. for Math. (1904) pp. 484–491.
3. Alden, Henry Leonard, Second approximation to the laminar boundary layer over a flat plate, Jour. Math. and Phys. **27**, 91–104, (1948).
4. Carrier, G. F. and Lin, C. C., On the nature of the boundary layer near the leading edge of a flat plate, Quart. Appl. Math. **6**, 63–68, (1948).
5. Lighthill, M. J., A technique for rendering approximate solutions to physical problems uniformly valid, Phil. Mag. **40**, 1179–1201, (1949).
6. Janour, Zbynek, Resistance of a plate in parallel flow at low Reynolds numbers, TM 1316 (1951).
7. Goldstein, S., Modern Developments in Fluid Dynamics, Oxford (1938) pp. 135–136.
8. Goldstein, S. (with an Appendix by A. Fage), On the two-dimensional steady flow of a viscous fluid behind a solid body. I. Proc. Roy. Soc. **A142**, 545–562, (1933).
9. Goldstein, S., Concerning some solutions of the boundary layer equations in hydrodynamics, Proc. Camb. Phil. Soc. **26**, 1–30, (1930).
10. Goldstein, S., On the two-dimensional steady flow of a viscous fluid behind a solid body. **II**. Proc. Roy. Soc. **A142**, 563–573, (1933).
11. Piercy, N. A. V. and Winny, H. F., The skin friction of a flat plate to Oseen's approximation, Proc. Roy. Soc. **A140**, 543–561, (1933).
12. Howarth, L., On the solution of the laminar boundary layer equations, Proc. Roy. Soc. **A164**, 547–579, (1938).
13. Tani, Itiro, On the solution of the laminar boundary layer equations, Jour. Phys. Soc. Japan **4**, 149–154, (1949).
14. Sidrak, Sobphly, The flow of a viscous liquid past an elliptic cylinder, Proc. Roy. Irish Acad. **A53**, 65–81, (1950).

Graduate School of Aeronautical Engineering
Cornell University, Ithaca, N. Y.

(Received May 4, 1953)

NATIONAL ADVISORY COMMITTEE FOR AERONAUTICS

TECHNICAL NOTE 2868

REFLECTION OF A WEAK SHOCK WAVE FROM A BOUNDARY LAYER ALONG A FLAT PLATE

I - INTERACTION OF WEAK SHOCK WAVES WITH LAMINAR AND TURBULENT BOUNDARY LAYERS ANALYZED BY MOMENTUM-INTEGRAL METHOD [1)]

By Alfred Ritter and Yung-Huai Kuo

SUMMARY

The present paper is concerned with the phenomena encountered when a plane oblique shock wave is incident upon the boundary layer of a flat plate. In an effort to simplify the problem, the flow field was divided into a viscous layer near the wall and a supersonic potential outer flow. The pressure disturbances due to the incident wave would be propagated upstream and downstream in the subsonic portion of the boundary layer, thus giving rise to perturbations of the boundary layer. By restricting the study to infinitesimal incident compression waves, only small perturbations were encountered and hence the ordinary linearized theory could be applied to the outer flow. In the laminar case, the boundary-layer treatment was based upon a momentum-integral equation previously derived by Howarth. The two flows must be compatible; hence, the deflection of the streamlines near the boundary layer was expressed in terms of the vertical velocity component along the edge of the boundary layer and this relation was used as a boundary condition for the outer flow. The boundary condition determined the form of solution upstream and downstream of the point of incidence. Determination of the constants of integration was accomplished by a consideration of conditions at infinity and a matching of the two flows at the point of incidence. With the outer flow thus determined, boundary-layer growth and pressure distribution were computed and results for the laminar case were obtained as follows:

(a) The pressure disturbance along the wall decreased exponentially from a definite value at the point of incidence to zero far upstream of the point of incidence. Downstream of the point of incidence, the pressure rose to a maximum value and then dropped off to the value corresponding to regular reflection.

---

1) *NACA Technical Note*, 1953, No. 2868

(b) The disturbances produced by the interaction decayed exponentially upstream; for a free-stream Mach number of approximately 2 and a Reynolds number of approximately 1500 in the undisturbed boundary-layer displacement thickness the upstream influence was of the order of 30 boundary-layer displacement thicknesses.

(c) The "self-induced" pressure gradient along the wall was such that the boundary layer might separate ahead of the point of incidence. If separation occurred, the separation point moved upstream as the shock strength was increased. With increasing Reynolds number, the separation point also moved upstream, whereas for increasing Mach number, the separation point moved downstream.

In the turbulent case the upstream influence was quite small and the incident wave must be reflected as a shock wave.

INTRODUCTION

It has been found that if the free-stream subsonic Mach number becomes high enough so that local supersonic zones are formed on an airfoil, sharp changes in the airfoil characteristics occur which cannot be explained by classical aerodynamics. The resulting loss of lift is accompanied by a large increase of drag in consequence of the appearance of shock waves on the surface of the airfoil. However, close study reveals that the drag increase is too large to be accounted for by the shock loss and change in skin friction. It must be caused by the sudden change of the flow pattern. This seems to indicate that the shock wave, when formed over the airfoil surface, modifies the character of the boundary layer in such a way as to create a wider wake.

At Guidonia, Ferri, by examining the measured pressure distributions over airfoils at supersonic speeds, found that for the forward portions of the airfoil the experimental pressure distribution agrees quite well with that calculated from potential-flow theory (reference 1). As the trailing edge is approached, however, the experimental pressures along the upper surface, for positive angles of attack, become considerably higher than the calculated ones. (At negative angles of attack, this behavior occurs along the lower surface.) This discrepancy is understandable in the light of the fact that the boundary layer on the rear portion of the airfoil is extremely sensitive to pressure disturbances. Since the flow far away from the airfoil has to return to its original pressure and direction, a shock wave must emanate at or near the trailing edge. There is a sharp pressure rise across the shock and pressure disturbances are transmitted upstream in the subsonic portion of the boundary layer causing a thickening of the layer near the trailing edge. This thickening, in turn, generates compression waves which travel downstream

and interact with the shock wave. The net result is that there is, starting from some point forward of the trailing edge, a gradual compression to the main-stream pressure. The pressure distribution is hence altered in such a manner as to give values of lift and pressure drag smaller than those calculated from theory. The measured moment coefficient will also differ from the theoretical values.

The preceding discussion shows that, in the transonic and supersonic regimes, the Mach number alone is insufficient to determine the flow characteristics; the Reynolds number can also be important. This was first demonstrated by Ackeret, Feldmann, and Rott in experiments which established the close relationship between the shock-wave pattern and the Reynolds number (reference 2). These prove beyond doubt that the flow far away from the wall depends intimately upon the character of the boundary layer, that is, the Reynolds number. Thus, under such circumstances, the concept of the boundary layer requires modification.

As a first step, a simplified problem of a plane shock wave incident upon the laminar boundary layer over a flat surface will be dealt with. For a number of years, Dr. H. W. Liepmann and his associates at the California Institute of Technology have been conducting experimental studies of shock-wave boundary-layer interaction. Recently they investigated the problem of the reflection of shock waves from boundary layers (reference 3). Based on the qualitative experimental data, some important conclusions were drawn regarding the reflection of an incident shock wave from a boundary layer:

(a) The type of boundary layer, whether laminar or turbulent, markedly affects the interaction. With a turbulent boundary layer, the reflection is practically the same as that for a regular reflection in nonviscous flow theory. For a laminar boundary layer, however, there is a large interaction zone near the point of incidence that is quite different from the regular inviscid reflection. The incident wave is apparently reflected as from a constant-pressure surface in the form of a Prandtl-Meyer fan. In returning to its final direction parallel to the wall, the deflected flow, behind the expansion, recompresses to the pressure appropriate to that behind a regular reflection.

(b) For $M = 1.4$ and $Re_x = \frac{Ux}{\nu_\infty} = 0.9 \times 10^6$, the influence of the incident wave extends upstream in a laminar layer a distance of the order of 50 boundary-layer displacement thicknesses. On the other hand, the upstream influence is practically negligible for the turbulent boundary layer.

(c) It appears that, except for very weak incident waves, the laminar layer almost always separates somewhere in front of the point of incidence, whereas no separation was found for the turbulent layer.

Quite recently, Barry, Shapiro, and Neumann (reference 4) made a similar study and their results are in substantial agreement with the GALCIT results. An advantage of their experiments, however, is that, although the tests were carried out at constant Mach number, the Reynolds number and shock strength were varied so that more qualitative as well as quantitative data are available to serve as a guide to future theoretical work.

Theoretical solutions of this problem have been almost as meager as the experimental results. A first attempt was made by Howarth (reference 5), who considered the case of a wave incident upon the interface bounding two semi-infinite uniform streams, one supersonic and one subsonic. Viscosity and heat conduction were neglected and the equations were linearized. He then demonstrated the upstream propagation of disturbances in the subsonic portion of the flow field and showed that an incident compression wave is reflected as compression upstream of the point of incidence while being reflected as expansion downstream of the point of incidence. However, these results can only be regarded as qualitative because of the obvious shortcomings of the model. In an effort to make the Howarth model more realistic, Tsien and Finston simulated the boundary layer with a uniform subsonic stream bounded by a wall on one side and a semi-infinite, uniform, supersonic stream on the other (reference 6). As before, viscosity and heat conduction were neglected and only small disturbances were considered. For the case of a compression wave incident upon the interface separating the two streams, it was shown that except for the local interaction, the incident compression wave is regularly reflected. Locally, however, the pressure along the interface exhibits compression ahead of the point of incidence and expansion immediately behind it. This local condition is qualitatively the same as that observed in experiments with shock reflection from laminar boundary layers; consequently there arose the speculation that perhaps the effects of viscosity and heat conduction were actually not too important in comparison with the effect of coexistence of supersonic and subsonic streams. If this were the case, it should follow that an improvement in the Tsien-Finston model could give rise to more quantitative results. Now an obvious discrepancy between the Tsien-Finston model and the physical situation is that the uniform subsonic stream, in attempting to simulate the boundary layer, is incapable of satisfying the "no-slip" condition at the wall. Thus, the next logical step in the development of the theory would appear to be that of considering a main-stream velocity that varies from zero at the wall to a given uniform supersonic velocity a short distance from the wall, and, in fact, this has been considered by Robinson (reference 7) and Lighthill (reference 8). Robinson assumed that the main-stream velocity varies continuously from zero at the wall to supersonic velocity some distance from the wall, whereas Lighthill assumed that the Mach number varies from zero at the wall to some supersonic value a short distance from the wall. A weak wave is incident upon the boundary layer and the reflected waves and upstream

influence were evaluated. Now with the improved model, however, both investigators found, contrary to experimental evidence, that the upstream influence is negligible. Although Robinson was chiefly concerned with the determination of the upstream influence, Lighthill considered, in some detail, the local reflection of the shock wave. He concluded that a shock is reflected locally as a "pressure ridge," that is, a rapid compression followed immediately by a rapid expansion. Now a note was added in the proof of reference 8 to the effect that experimental results of Mair and Bardsley (reference 9), obtained at the Fluid Motion Laboratory, Manchester, establish that the conclusions of negligible upstream influence and the shock being locally reflected as a pressure ridge are correct for the reflection of a weak shock from a turbulent boundary layer. (These results, however, had been previously observed by Ackeret and Liepmann.) As Lighthill pointed out, the conjecture that the theory is correct for velocity profiles typical of turbulent boundary layers but incorrect for profiles typical of laminar boundary layers may be valid. But until such time as the theory is modified to account for viscosity, as suggested by Lighthill, the present theory is incapable of predicting the effects of the interaction between a shock wave and a laminar boundary layer.

The preceding theories have neglected viscosity and heat conduction while considering infinitesimal waves and small disturbances. It would appear that the assumption of infinitesimal waves and small disturbances is valid since the linear theory, to be a good approximation, requires that the slopes of the streamlines be small. For weak incident shock waves, the slope of the displacement thickness would probably be small, except perhaps in the immediate vicinity of the wave. The neglection of viscosity, on the other hand, seems to be more serious. If the effects of viscosity were not too important, one would expect that, for fixed Mach number and shock strength, the effect of Reynolds number should be rather small. Actually, this is not the case since the results of Barry, Neumann, and Shapiro clearly show that changes in Reynolds number have a marked effect upon the shock-wave - laminar-boundary-layer interaction (reference 4). Hence it appears that a theory capable of predicting the effects of this complicated phenomenon must include the effects of viscosity.

At present, as far as the authors are aware, the only solution that includes viscous effects was given by Lees (reference 10). The Lees theory is based on an approximate relationship between the slope of the displacement thickness and the external pressure gradient derived from Prandtl-Meyer flow. By combining this relation with the momentum-integral equation and neglecting terms of the order of Re^{-1} Lees arrived at a third-order, linear, differential equation for the pressure. On the assumption that this equation is valid all along the boundary layer, he was able to determine the boundary-layer growth and pressure distribution. He found the upstream influence comparable with that which is observed

experimentally and showed, also, that the boundary layer always separates except in those cases where the incident wave is quite weak. However, his theoretical pressure distributions fail to exhibit the characteristic downstream behavior. This point will be discussed later.

Following the approach of Oswatitch and Wieghardt in their study of the growth of disturbances in a supersonic stream outside laminar or turbulent boundary layers (reference 11), the problem is treated as an outer flow, with a shock, in equilibrium with a boundary-layer flow. Instead of expressing the deflection of the streamline in terms of pressure rise, as in Lees' problem, a procedure after Oswatitch and Wieghardt is taken by connecting the vertical velocity of the outer flow with the streamline deflection, as given by the momentum integral of the boundary-layer flow. This reduces the problem to an inviscid one which can be solved systematically to any order of approximation.

This study was conducted at the Graduate School of Aeronautical Engineering of Cornell University under the sponsorship and with the financial assistance of the National Advisory Committee for Aeronautics.

SYMBOLS

a	speed of sound
A,B,C,D,E	constants
$b = \delta_1^*/\delta_o^*$	
c_p, c_v	specific heats at constant pressure and constant volume, respectively
f,g	functions of $\xi - m_\infty\eta$ and $\xi + m_\infty\eta$, respectively
$F = 2\eta - 2\eta^3 + \eta^4$	
g_1,g_2,g_3,g_4	defined by equations (8)
$G = \frac{1}{6}\eta(1 - \eta)^3$	
h	function of $\xi - m_\infty\eta$
$H \equiv \delta^*/\theta$	

k	coefficient of thermal conductivity
K	Kármán momentum equation for compressible viscous fluids
$m = \sqrt{M^2 - 1}$	
M	Mach number (U/a)
$M_o = U/a_o$	
$M_\infty = U/a_\infty$	
p	pressure
p'	perturbed pressure
Pr	Prandtl number ($\mu c_p/k$)
R	universal gas constant
Re	Reynolds number $(U\delta_o^*/\nu_o)$
$Re_x = U_x/\nu_o$	
T	temperature
u,v	velocity components parallel and normal to flow direction, respectively
u',v'	velocity perturbations nondimensionalized with U
U	free-stream velocity
x,y	coordinates parallel and normal to flow direction, respectively
x',y'	values of x and y in transformed plane $\left(x' = x;\ y' = \left(\frac{p}{p_o}\right)^{1/2} \int_0^y \frac{T_o}{T}\, dy\right)$
α	constant
$\beta \equiv \sigma^{\frac{3-2\gamma}{\gamma-1}} \Big/ \left(\frac{37}{315} - \frac{263}{630\sigma}\right)^2$	

γ ratio of specific heats (c_p/c_v)

δ boundary-layer thickness

δ^* boundary-layer displacement thickness

δ_o^* undisturbed boundary-layer displacement thickness

δ' boundary-layer thickness in transformed plane

δ'^* boundary-layer displacement thickness in transformed plane

Δ disturbed boundary-layer displacement thickness nondimensionalized with δ_o^*

ϵ flow-deflection angle

$\eta = y/\delta'$ or y/δ_o^*

θ boundary-layer momentum thickness $\left(\int_0^\delta \left(1 - \frac{u}{u_e}\right)\frac{\rho u}{\rho_e u_e}\,dy\right)$

θ' boundary-layer momentum thickness in transformed plane

$\lambda_1, \lambda_2, \lambda_3$ roots of equation (16)

$$\Lambda = \frac{(\delta')^2}{\nu_o}\left(1 + \frac{\gamma - 1}{2} M_e^2\right)\frac{du_e}{dx}$$

μ coefficient of viscosity

ν kinematic coefficient of viscosity

$\xi = x/\delta_o^*$

ρ density

$$\sigma = 1 - \frac{\gamma - 1}{2} M_o^2 = \left(1 + \frac{\gamma - 1}{2} M_\infty^2\right)^{-1}$$

τ shear stress

ϕ perturbation velocity potential, nondimensionalized with $U\delta_o^*$

Φ	total potential
χ	function of x' and y'
ψ	stream function

Subscripts

d	evaluated at distance of upstream influence
e	evaluated along edge of boundary layer
i	1, 2, or 3
l	laminar case
o	standard condition, such as stagnation point or undisturbed state
s	separation point
t	turbulent case
w	evaluated at wall
1,2,3	evaluated in regions 1, 2, or 3, respectively (see fig. 1)
∞	evaluated in undisturbed free stream

OUTLINE OF PRESENT INVESTIGATION

In the present study the effect of an infinitesimal compression wave incident upon the laminar boundary layer along a flat plate in supersonic flow will be considered. The pressure gradient in the flow direction is determined to the order of approximation of the ordinary boundary-layer theory solely by the shape of the boundary. The potential flow thus completely determines the boundary-layer growth. In the problem of interaction between a shock wave and a boundary layer, however, the phenomena are quite different. In that case the pressure disturbances that are propagated upstream in the subsonic portion of the boundary layer will affect the boundary-layer growth. It becomes clear that the outer flow influences the boundary-layer growth and that the boundary-layer growth, in turn, influences the outer flow, so that a solution that is simultaneously compatible with the two flows must be sought.

Another significant difference between the interaction and noninteraction problems occurs in the separation phenomenon. For the usual case of boundary-layer flow against a pressure gradient, it is known that the flow separates from the wall at the point where $\left(\frac{\partial u}{\partial y}\right)_w = 0$. Downstream of the separation point the original flow is deflected away from the wall by the backflow, a vortex layer separating the two flows. The interaction of a shock wave with a laminar boundary layer, however, produces a different form of separation. Experimental evidence indicates that along the wall there exists a short thin region, extending slightly upstream from the foot of the shock wave, in which the flow has practically zero velocity; the boundary between this separated flow and the main boundary-layer flow is a vortex sheet. A plausible explanation of this phenomenon is proposed by Lighthill, who suggests that the pressure discontinuity occurring when a shock interacts with a laminar boundary layer causes the flow to separate into some form of "bubble" at the base of the shock wave. Once such a bubble is produced, the boundary layer upstream of the separated region will be deflected so as to increase the external pressure gradient. This results in further separation of the boundary layer and hence further upstream deflection. This process of repeated separation causes the edge of the bubble to move upstream until such time as the induced pressure gradient is no longer able to cause separation of the boundary layer. The net result is the one indicated in experiments. Immediately behind the point of interaction, the deflected flow, in returning to its original direction parallel to the wall, undergoes a very rapid compression, thereby causing an extremely large pressure gradient. It is known from experimental results that the boundary layer downstream is turbulent, but whether the extreme pressure gradient causes separation and hence causes the boundary layer to become turbulent or whether the flow at that point is already turbulent and thus can sustain large pressure gradients must remain at this time a matter of conjecture. Whatever the case may be, in the problem for weak shock the flow will be assumed to remain laminar downstream of the point of incidence (cf. reference 12). Positive infinity in relation to the problem will be taken to mean a distance downstream of the order of 100 boundary-layer thicknesses. In addition, any mention of boundary-layer separation will refer to the "dead air bubble" phenomenon.

In the present theory it is assumed that the boundary-layer equations are applicable over the whole plane. Strictly speaking, the validity of the usual boundary-layer assumptions near the base of the shock wave is doubted, since separation occurs. However, it is believed that for weak incident waves, a theory based on the above assumptions will still enable one to determine some of the important characteristics of the flow. In particular it is desired to determine the extent of the separated region, since this investigation is merely the first step of a proposed theory which will endeavor to take separation into account.

The more refined theory is then expected to furnish, in the separation zone, slight corrections to the simplified theory.

The flow field is assumed to be divided into two distinct regions as follows:

(a) A thin layer adjacent to the plate wherein there is laminar-type boundary-layer flow

(b) An outer supersonic potential flow field

Since an infinitesimal compression wave is assumed, the upstream pressure propagation is expected to perturb the boundary layer just slightly, thus imposing small disturbances upon the outer flow. This justifies the linearization of the supersonic outer flow. (Results of this theory will of course be applicable only for fairly weak shock waves.) The flow field has been assumed to be separated into two distinct regions. In reality a continuous variation in velocity from zero at the boundary to some main-stream value a short distance from the wall is known to exist. The actual distance at which the velocity reaches its main-stream value is rather indefinite; hence the so-called boundary-layer displacement thickness $\delta^*(x)$ is defined. Physically it represents how much the potential flow streamlines are deflected because of the reduction in mass flow caused by the retarded velocities near the wall. The viscous effects are thus characterized by a layer whose thickness is $\delta^*(x)$, and the link connecting the outer flow to the boundary-layer flow is the condition that the line $y = \delta^*(x)$ is a streamline of the outer flow. The treatment of the boundary layer in the present study is based upon a momentum-integral equation previously derived by Howarth (reference 13). The deflection of the boundary layer is expressed in terms of the vertical velocity component along the edge of the layer and this relation is used as a boundary condition for the outer flow. Hence the over-all problem is then reduced to the solution of a purely supersonic potential-flow problem.

LAMINAR-BOUNDARY-LAYER EQUATIONS

The Prandtl boundary-layer equations for the two-dimensional steady flow of a viscous compressible fluid are:

$$u \frac{\partial u}{\partial x} + v \frac{\partial u}{\partial y} = - \frac{1}{\rho} \frac{\partial p}{\partial x} + \frac{1}{\rho} \frac{\partial}{\partial y} \left(\mu \frac{\partial u}{\partial y} \right)$$

$$0 = -\frac{1}{\rho}\frac{\partial p}{\partial y}$$

$$\frac{\partial}{\partial x}(\rho u) + \frac{\partial}{\partial y}(\rho v) = 0$$

$$\rho c_p\left(u\frac{\partial T}{\partial x} + v\frac{\partial T}{\partial y}\right) = u\frac{\partial p}{\partial x} + \mu\left(\frac{\partial u}{\partial y}\right)^2 + \frac{\partial}{\partial y}\left(k\frac{\partial T}{\partial y}\right)$$

$$p = R\rho T$$

Here u and v denote, respectively, the x and y components of the velocity and p, ρ, and T, the pressure, density, and temperature of the fluid. In order to simplify the problem, Howarth (reference 13) assumes that the coefficient of viscosity μ is proportional to the temperature and the Prandtl number is unity. These assumptions, of course, introduce some approximation, but according to the results of Emmons and Brainerd (references 14 and 15), the boundary-layer characteristics depend very insensitively on the form of $\mu(T)$ and the change of Prandtl number for moderate Mach numbers. Therefore, the simplifications brought about by this assumption justify the slight loss in accuracy.

By introduction of the stream function ψ

$$\rho u = \rho_o\frac{\partial \psi}{\partial y}$$

$$\rho v = -\rho_o\frac{\partial \psi}{\partial x}$$

and by introduction of the transformation

$$x' = x$$

$$y' = \left(\frac{p}{p_o}\right)^{1/2}\int_0^y \frac{T_o}{T}\,dy$$

$$\psi = \left(\frac{p}{p_o}\right)^{1/2}\chi(x',y')$$

the momentum equation is transformed into

$$\frac{\partial^2 \chi}{\partial x' \, \partial y'} \frac{\partial \chi}{\partial y'} - \frac{\partial^2 \chi}{(\partial y')^2} \frac{\partial \chi}{\partial x'} = u_e \frac{du_e}{dx'} \left[\frac{T}{T_e} - \frac{\gamma}{2a_e^2} \chi \frac{\partial^2 \chi}{(\partial y')^2} \right] + \nu_o \frac{\partial^3 \chi}{(\partial y')^3}$$

where ρ_o, T_o, and ν_o stand for the density, temperature, and kinematic viscosity of a standard condition, the stagnation point, say, and are constants, and the subscript e indicates the condition at the edge of the boundary layer. In the case of a thermally insulated plate $\left(\frac{\partial T}{\partial y}\right)_w = 0$, the condition of unity Prandtl number admits a special solution on the plate (reference 16)

$$c_p T + \frac{1}{2} u^2 = c_p T_e + \frac{1}{2} u_e^2$$

Upon elimination of T, there results the equation:

$$\frac{\partial^2 \chi}{\partial x' \, \partial y'} \frac{\partial \chi}{\partial y'} - \frac{\partial^2 \chi}{(\partial y')^2} \frac{\partial \chi}{\partial x'} = \nu_o \frac{\partial^3 \chi}{(\partial y')^3} + u_e \frac{du_e}{dx'} \left\{ 1 + \frac{\gamma - 1}{2a_e^2} \left[u_e^2 - \left(\frac{\partial \chi}{\partial y'} \right)^2 \right] - \frac{\gamma}{2a_e^2} \chi \frac{\partial^2 \chi}{(\partial y')^2} \right\} \quad (1)$$

Thus, it is seen that when $\frac{du_e}{dx} = 0$, that is, at constant pressure, this equation is identical to the equation for the incompressible fluid.

Let δ' be the boundary-layer thickness in the transformed plane, and define the corresponding displacement and momentum thicknesses by

$$\delta'^* = \int_0^{\delta'} \left(1 - \frac{u}{u_e} \right) dy'$$

$$\theta' = \int_0^{\delta'} \left(1 - \frac{u}{u_e} \right) \frac{u}{u_e} \, dy'$$

Then, by integrating equation (1) across the boundary layer, the equation relating the boundary-layer thicknesses with the velocity is

$$\frac{d\theta'}{dx'} + \left[\left(2 - \frac{u_e^2}{2a_e^2}\right)\theta' + \left(1 + \frac{\gamma - 1}{2}\frac{u_e^2}{a_e^2}\right)\delta'^*\right]\frac{1}{u_e}\frac{du_e}{dx'} = \frac{\nu_o}{u_e^2}\left(\frac{\partial u}{\partial y'}\right)_w \qquad (2)$$

The similarity of this equation to that of the incompressible flow suggests the applicability of the Kármán-Pohlhausen procedure.

If the velocity profile is given by (reference 13)

$$\frac{u}{u_e} = F(\eta) + \Lambda G(\eta)$$

where

$$F = 2\eta - 2\eta^3 + \eta^4$$

$$G = \frac{1}{6}\eta(1 - \eta)^3$$

$$\Lambda = \frac{(\delta')^2}{\nu_o}\left(1 + \frac{\gamma - 1}{2}M_e^2\right)\frac{du_e}{dx}$$

with

$$\eta = \frac{y'}{\delta'}$$

$$M_e = \frac{u_e}{a_e}$$

it follows that

$$\left.\begin{aligned} \theta' &= \frac{\delta'}{315}\left(37 - \frac{\Lambda}{3} - \frac{5\Lambda^2}{144}\right) \\ \delta'^* &= \frac{\delta'}{120}(36 - \Lambda) \\ \left(\frac{\partial u}{\partial y'}\right)_w &= \frac{u_e}{\delta'}\left(2 + \frac{\Lambda}{6}\right) \end{aligned}\right\} \qquad (3)$$

Substitution of the quantities of equations (3) into equation (2) gives rise to a relation between the boundary-layer thickness δ' and the velocity $u_e(x)$, with a parameter Λ. Now, in the present problem, as the flow in the boundary layer must be compatible with the potential field, the flow deflection $d\delta^*/dx$ of the boundary layer determines the flow in the outer field. Therefore, δ' should be eliminated. For this purpose, let the displacement thickness be introduced:

$$\delta^* = \int_0^{\delta} \left(1 - \frac{\rho u}{\rho_e u_e}\right) dy$$

But in the transformed plane there is

$$\delta'^* = \int_0^{\delta'} \left(1 - \frac{u}{u_e}\right) dy'$$

$$= \left(\frac{p}{p_o}\right)^{1/2} \int_0^{\delta} \frac{T_o}{T}\left(1 - \frac{u}{u_e}\right) dy$$

$$= \left(\frac{p}{p_o}\right)^{1/2} \frac{T_o}{T_e} \int_0^{\delta} \left[\left(\frac{T_e}{T} - 1\right) + \left(1 - \frac{\rho u}{\rho_e u_e}\right)\right] dy$$

By means of the temperature-velocity relation and Pohlhausen's profile this will yield

$$\delta'^* = \left(\frac{p}{p_o}\right)^{1/2} \frac{T_o}{T_e} \delta^* + \frac{\gamma - 1}{2} M_e^2 \left(-1 + \frac{367}{630} + \frac{1}{3} \frac{71}{2520} \Lambda + \frac{1}{252} \frac{\Lambda^2}{36}\right)\delta'$$

Now, from the second of equations (3), δ'^* is already expressed in terms of δ' and Λ. The elimination of δ'^* then gives

$$\frac{\gamma - 1}{72} \frac{M_e^2}{252}\left[\frac{1}{\nu_o} \frac{du_e}{dx}\left(1 + \frac{\gamma - 1}{2} M_e^2\right)\right]^2 (\delta')^5 +$$

$$\frac{1}{\nu_o} \frac{du_e}{dx}\left(1 + \frac{\gamma - 1}{2} M_e^2\right)\left(\frac{\gamma - 1}{6} \frac{71 M_e^2}{2520} + \frac{1}{120}\right)(\delta')^3 +$$

$$\left(\frac{\gamma - 1}{2} \frac{367 M_e^2}{630} - \frac{\gamma - 1}{2} M_e^2 - \frac{3}{10}\right)\delta' = -\left(\frac{p}{p_o}\right)^{1/2} \frac{T_o}{T_e} \delta^* \qquad (4)$$

Theoretically, this equation defines δ' as a function of δ^*. Only in the case of small pressure gradient, namely,

$$u_e = U(1 + u' + \ldots)$$

$$u' \ll 1$$

however, is a simple analytical solution possible. For by retaining only linear terms in u' and its derivatives there is obtained (reference 17)

$$\frac{U}{\nu_o}\left(\frac{1}{3}\frac{71}{2520}\sigma^{-2} - \frac{\sigma^{-1}}{945}\right)\frac{du'}{dx}(\delta')^3 + \left[\frac{37}{315} - \frac{263}{630\sigma} - \frac{263}{630}\frac{(\gamma - 1)M_o^2}{\sigma^2}u'\right]\delta' =$$

$$\left[\frac{2-\gamma}{\sigma^{2(\gamma-1)}} - \frac{2 - \gamma}{2}M_o^2\sigma^{\frac{4-3\gamma}{2(\gamma-1)}}u'\right]\delta^* \qquad (5)$$

where $M_o = \frac{U}{a_o}$ and $\sigma = 1 - \frac{\gamma - 1}{2}M_o^2$. Moreover, since u' is assumed to be small, that is, for weak interaction, the boundary-layer thickness δ' must also differ from the unperturbed value by a small amount. Therefore, to the first-order approximation there results the solution:

$$\delta' = \sigma^{\frac{2-\gamma}{2(\gamma-1)}}\left(-\frac{37}{315} + \frac{263}{630\sigma}\right)^{-1}\delta^* -$$

$$\left[\frac{263}{630}\frac{(\gamma - 1)M_o^2}{\sigma^{\frac{6-5\gamma}{2(\gamma-1)}}}\left(\frac{263}{630\sigma} - \frac{37}{315}\right)^{-2} + \frac{2 - \gamma}{2}M_o^2\sigma^{\frac{4-3\gamma}{2(\gamma-1)}}\left(\frac{263}{630\sigma} - \frac{37}{315}\right)^{-1}\right]u'\delta^* +$$

$$\frac{U}{\nu_o}\left(\frac{1}{3}\frac{71\sigma^{-2}}{2520} - \frac{\sigma^{-1}}{945}\right)\left(\frac{263}{630\sigma} - \frac{37}{315}\right)^{-4}\sigma^{\frac{3(2-\gamma)}{2(\gamma-1)}}\frac{du'}{dx}(\delta^*)^3 \qquad (6)$$

Let δ_o^* be the unperturbed displacement thickness and write

$$\delta^* = \delta_o^*(1 + \Delta)$$

Substituting equation (6) in the momentum equation (2), replacing x' by x, and keeping only first-order terms, one obtains, by taking into account $\delta_o^* \frac{d\delta_o^*}{dx} = \text{Constant}$, the following linear equation (reference 17):

$$g_1 \Delta + \frac{d\Delta}{d\xi} = g_2 u' + g_3 \frac{du'}{d\xi} + g_4 \frac{d^2u'}{d\xi^2} - \frac{1}{g_1} \frac{d\Delta}{d\xi}\left(g_2 u' + 3g_3 \frac{du'}{d\xi} + 5g_4 \frac{d^2u'}{d\xi^2}\right) \tag{7}$$

where

$$\xi = \frac{x}{\delta_o^*}$$

$$\left.\begin{aligned}
g_1 &= \frac{1}{R_e} \frac{(263)^2}{(37)(630)} \sigma^{-\frac{\gamma}{\gamma-1}} \left(1 - \frac{74}{263}\sigma\right)^2 \\
g_2 &= -g_1 \left[1 - \frac{2(\gamma - 1)M_o^2}{\sigma}\left(\frac{1}{1 - \frac{74}{263}\sigma} + \frac{2 - \gamma}{2(\gamma - 1)}\right)\right] \\
g_3 &= \frac{(3 - \gamma)M_o^2}{2\sigma} - 2 - \frac{\frac{15934}{9731} + \frac{74588}{360047}\frac{1}{\sigma}}{1 - \frac{74}{263}\sigma} \\
g_4 &= -R_e \sigma^{\frac{1}{\gamma-1}} \frac{5}{888}\left(\frac{630}{263}\right)^3 \left(1 - \frac{74}{263}\sigma\right)^{-3}
\end{aligned}\right\} \tag{8}$$

with

$$Re = \frac{U\delta_o^*}{\nu_o}$$

The momentum integral thus relates the displacement-thickness perturbation Δ to the velocity perturbation and its derivatives along the edge of the boundary layer.

SOLUTION OF BOUNDARY-VALUE PROBLEM OF OUTER FLOW

Until now the study has been directed at obtaining an explicit relationship for the boundary-layer displacement thickness as given in equation (7). Now the extent of the interaction zone is only a fraction of the distance from the leading edge of the plate, hence $\delta_o^*(x)$ can be assumed to be constant over this range. Equation (7) then becomes a linear equation with constant coefficients.

The problem is now one of determining the supersonic potential flow past a thin body whose thickness at any point corresponds to the perturbed boundary-layer thickness at that point. Consider the problem in the coordinates shown in figure 2.

The undisturbed thickness is seen to correspond to $y = 0$. Strictly speaking, the undisturbed thickness should be at $y = \delta_o^*$ in the physical plane. But since the outer flow does not depend upon the location of the origin of coordinates, the boundary conditions can be simplified slightly by choosing the axes as indicated in figure 2. Then, consistent with linear theory, the boundary conditions are satisfied at the undisturbed surface, namely, $y = 0$.

The linearized differential equation for the perturbation velocity potential of the supersonic stream is

$$m_\infty^2 \frac{\partial^2 \phi}{\partial \xi^2} - \frac{\partial^2 \phi}{\partial \eta^2} = 0 \tag{9}$$

where $\xi = \frac{x}{\delta_o^*}$ and $\eta = \frac{y}{\delta_o^*}$, and the general solution is given by

$$\phi = f(\xi - m_\infty \eta) + g(\xi + m_\infty \eta) \tag{10}$$

The incident waves will be taken as

$$\left.\begin{aligned} g(\xi + m_\infty\eta) &= 0 && \text{when} \quad \xi + m_\infty\eta < 0 \\ g(\xi + m_\infty\eta) &= -\frac{\epsilon}{m_\infty}(\xi + m_\infty\eta) && \text{when} \quad \xi + m_\infty\eta > 0 \end{aligned}\right\} \tag{11}$$

This corresponds to a simple compression wave, of deflection angle ϵ, incident upon the origin. (According to the above definition, the absolute value of ϵ will be used in any computations.)

Upstream Solution

The incident wave causes the boundary layer to be perturbed upstream and downstream of the point of incidence. Since no disturbances can be propagated upstream into the supersonic flow, the physically possible solutions in region 1 will be waves of the form $\phi_1 = f(\xi - m_\infty\eta)$. The normal velocity component at the boundary must be zero, hence the condition that the slope of the streamline is equal to the slope of the displacement boundary-layer thickness δ^* is imposed. The velocity vector of the supersonic flow has components $\left[U(1 + u'),Uv'\right]$, where $u' = \partial\phi/\partial\xi$ and $v' = \partial\phi/\partial\eta$, so that the linearized boundary condition becomes

$$\frac{d\,\Delta}{d\xi} = \frac{\partial\phi}{\partial\eta} \qquad \text{at} \quad \eta = 0$$

or

$$\frac{d\,\Delta}{d\xi} = -m_\infty f'(\xi) \qquad \text{at} \quad \eta = 0 \tag{12}$$

Now since the boundary condition is on $d\,\Delta/d\xi$ rather than Δ, equation (7) is differentiated with respect to ξ, considering δ_o^* to be constant:

$$g_1 \frac{d\Delta}{d\xi} + \frac{d^2\Delta}{d\xi^2} = g_2 \frac{du'}{d\xi} + g_3 \frac{d^2u'}{d\xi^2} + g_4 \frac{d^3u'}{d\xi^4} -$$

$$\frac{1}{g_1} \frac{d^2\Delta}{d\xi^2}\left(g_2u' + 3g_3 \frac{du'}{d\xi} + 5g_4 \frac{d^2u'}{d\xi^2}\right) -$$

$$\frac{1}{g_1} \frac{d\Delta}{d\xi}\left(g_2 \frac{du'}{d\xi} + 3g_3 \frac{d^2u'}{d\xi^2} + 5g_4 \frac{d^3u'}{d\xi^3}\right) \qquad (13)$$

If the boundary condition (12) is substituted into equation (13), and it is noted that at $\eta = 0$, $\frac{du'}{d\xi} = f''(\xi)$, and so forth, an ordinary nonlinear differential equation for $f(\xi)$ will be obtained. By linearizing this equation:

$$g_4 f^{iv}(\xi) + g_3 f'''(\xi) + \left(g_2 + m_\infty\right) f''(\xi) + g_1 m_\infty f'(\xi) = 0 \qquad (14)$$

The coefficients in equation (14) are constant for a specific case of Mach number and Reynolds number, hence the solution can be immediately written as

$$f(\xi) = A_o + Ae^{\lambda_2 \xi} + B_o e^{\lambda_1 \xi} + C_o e^{\lambda_3 \xi} \qquad (15)$$

where the λ_n's are roots of the equation

$$g_4\lambda^3 + g_3\lambda^2 + \left(g_2 + m_\infty\right)\lambda + g_1 m_\infty = 0 \qquad (16)$$

For the cases under consideration equation (16) has three real roots, one positive and two negative. Let $\lambda_2 > 0$, $\lambda_1 < 0$, and $\lambda_3 < 0$. In order to have all disturbances vanish as $\xi \longrightarrow -\infty$ it is seen from equation (15) that

$$B_o = C_o = A_o = 0$$

The upstream solution is then

$$f(\xi - m_\infty \eta) = Ae^{\lambda_2(\xi - m_\infty \eta)} \tag{17}$$

or in the physical plane

$$\left.\begin{aligned} \phi_1 &= Ae^{\frac{\lambda_2}{\delta_o^*}(x - m_\infty y)} \\ x - m_\infty y &< 0 \end{aligned}\right\} \tag{18}$$

The solution in region 2 follows immediately. The equation for the outer flow is linear, hence, by adding solutions,

$$\left.\begin{aligned} \phi_2 &= Ae^{\frac{\lambda_2}{\delta_o^*}(x - m_\infty y)} - \frac{\epsilon}{m_\infty}\frac{1}{\delta_o^*}(x + m_\infty y) \\ x - m_\infty y &< 0 \\ x + m_\infty y &> 0 \end{aligned}\right\} \tag{19}$$

Downstream Solution

In region 3 the solution to the linearized supersonic flow equation is

$$\phi_3 = g(\xi + m_\infty \eta) + h(\xi - m_\infty \eta)$$

But $g(\xi + M_\infty \eta)$ is known since it is the incident wave, hence use of the boundary condition at the interface will result in an ordinary differential equation for $h(\xi)$. The nondimensionalized boundary condition takes the form

$$\frac{d\,\Delta}{d\xi} = -m_\infty h'(\xi) - \epsilon \qquad \text{at} \quad \eta = 0 \tag{20}$$

since $$\frac{\partial \phi}{\partial \eta} = -\epsilon - m_\infty h'(\xi)$$

Substituting equation (20) into equation (13),

$$g_4 h^{iv} + g_3 h''' + (g_2 + m_\infty) h'' + g_1 m_\infty h' = -g_1 \epsilon \tag{21}$$

It can be seen that the complementary solution will be identical to equation (15). Hence the complete solution is

$$h(\xi) = D_o + Ee^{\lambda_2 \xi} + Be^{\lambda_1 \xi} + Ce^{\lambda_3 \xi} - \frac{\epsilon}{m_\infty} \xi \tag{22}$$

where again $\lambda_2 > 0$, $\lambda_1 < 0$, and $\lambda_3 < 0$. Choose $D_o = 0$ without affecting any of the physical quantities such as velocity or pressure since $h(\xi)$ merely represents a velocity potential. To eliminate the possibility of any velocity becoming infinite as $\xi \longrightarrow \infty$ put $E = 0$. Then the solution becomes

$$\left.\begin{aligned} h(\xi) &= Be^{\lambda_1 \xi} + Ce^{\lambda_3 \xi} - \frac{\epsilon}{m_\infty} \xi \\ h(\xi - m_\infty \eta) &= Be^{\lambda_1 (\xi - m_\infty \eta)} + Ce^{\lambda_3 (\xi - m_\infty \eta)} - \frac{\epsilon}{m_\infty} (\xi - m_\infty \eta) \end{aligned}\right\} \tag{23}$$

Then the perturbed velocity potential in region 3 is

$$\left.\begin{aligned} \phi_3 &= Be^{\frac{\lambda_1}{\delta_o^*}(x - m_\infty y)} + Ce^{\frac{\lambda_3}{\delta_o^*}(x - m_\infty y)} - \frac{2\epsilon}{m_\infty} \frac{x}{\delta_o^*} \\ & x - m_\infty y > 0 \end{aligned}\right\} \tag{24}$$

Determination of Constants

The problem now involves four constants A, B, C, and D[1] with three parameters M_∞, ϵ, and Re. Additional conditions must therefore be imposed in order to determine the constants as functions of the

---

[1]The constant D is a measure of the downstream boundary-layer thickness as shown in the following discussion.

parameters. It is noted that the outer flow field was divided into distinct regions by the lines OS and OM (figure 2), so that the boundary layers in regions 1 and 3 were treated independently of each other. These boundary layers are therefore related at the point of incidence by the following conditions:

(a) The boundary-layer displacement thickness must be continuous at $x = 0$

(b) The wall pressure must be continuous at $x = 0$

(c) Discontinuities, if any, must satisfy $\lim_{x_o \longrightarrow 0} \int_{-x_o}^{x_o} K \, dx = 0$

where $K = 0$ denotes the Kármán momentum equation for compressible viscous fluids

Condition (a).- Compute the boundary layers for regions 1 and 3 and then match the displacement thicknesses at the origin. One has as a boundary condition

$$\frac{d \Delta_i}{d\xi} = \frac{\partial \phi_i}{\partial \eta} \qquad \text{at} \quad \eta = 0, \quad i = 1 \text{ or } 3$$

where $\Delta_i = \frac{\delta_i^*}{\delta_o^*} - 1$ and δ_i^* is the total boundary-layer displacement thickness in regions 1 or 3.

From equation (18) one obtains for region 1

$$\frac{d \Delta_1}{d\xi} = -m_\infty \lambda_2 A e^{\lambda_2 \xi}$$

$$\Delta_1 = -m_\infty A e^{\lambda_2 \xi} + \text{Constant}$$

All disturbances vanish far upstream so that $\Delta_1(-\infty) = 0$. But since $\lambda_2 > 0$, the exponential term vanishes as $\xi \longrightarrow -\infty$, hence the constant equals zero. Therefore

$$\Delta_1 = -m_\infty A e^{\lambda_2 \xi}$$

or

$$\delta_1^* = \delta_o^* \left(1 - m_\infty A e^{\lambda_2 \frac{x}{\delta_o^*}} \right)$$

For region 3 one obtains, according to equations (24),

$$\frac{d\,\Delta_3}{d\xi} = -m_\infty B\lambda_1 e^{\lambda_1 \xi} - m_\infty C\lambda_3 e^{\lambda_3 \xi}$$

$$\Delta_3 = -m_\infty B e^{\lambda_1 \xi} - m_\infty C e^{\lambda_3 \xi} + \text{Constant}$$

Let $\Delta_{3(\infty)} = D$ and since the exponentials vanish at positive infinity, the constant equals D.
Therefore

$$\Delta_3 = -m_\infty B e^{\lambda_1 \xi} - m_\infty C e^{\lambda_3 \xi} + D$$

$$\delta_3^* = \delta_o^* \left(1 - m_\infty B e^{\lambda_1 \frac{x}{\delta_o^*}} - m_\infty C e^{\lambda_3 \frac{x}{\delta_o^*}} + D \right)$$

Thus it is seen that for the total downstream thickness

$$\lim_{\xi \longrightarrow \infty} \delta_3^* = \delta_o^*(1 + D)$$

By putting $\delta_1^* = \delta_3^*$ at $x = 0$,

$$A = B + C - \frac{D}{m_\infty} \tag{25}$$

Condition (b).- Since the validity of the usual boundary-layer assumptions in the interaction zone has been assumed in the case of weak shock interaction, the pressure at the wall, as a first approximation, equals the pressure at the interface. The pressure at the wall as well as at the interface is therefore required to be continuous. As a consequence, the pressure jump due to the incident wave must necessarily be neutralized by a reflected expansion wave. This deduction is actually confirmed by experiments.

The pressure in each region consists of an undisturbed pressure p_o plus a perturbed pressure p' due to the incident wave; $p = p_o + p'$. Since the undisturbed pressure is the same throughout the flow field, only the perturbed pressures, which, by small perturbation theory,

are $p' = -\rho_\infty U u'$, will be considered. The velocity potentials ϕ_1, ϕ_2, and ϕ_3 have previously been found, and, accordingly, the pressures are given by

$$p_1' = -\gamma M_\infty^2 p_o A \lambda_2 e^{\frac{\lambda_2}{\delta_o^*}(x - m_\infty y)} \tag{26}$$

$$p_3' = -\gamma M_\infty^2 p_o \left[B\lambda_1 e^{\frac{\lambda_1}{\delta_o^*}(x - m_\infty y)} + C\lambda_3 e^{\frac{\lambda_3}{\delta_o^*}(x - m_\infty y)} - \frac{2\epsilon}{m_\infty} \right] \tag{27}$$

The condition for continuous pressure at the origin is

$$p_1' = p_3'$$

hence

$$A\lambda_2 = B\lambda_1 + C\lambda_3 - \frac{2\epsilon}{m_\infty} \tag{28}$$

This condition shows that the discontinuity between regions 2 and 3 corresponds, in linear theory, to an expansion of the flow from regions 2 to 3 by a wave of the same magnitude as the incident wave. Now since λ_1 and λ_3 are negative, the downstream pressure along the interface $y = 0$ is

$$p_3' \longrightarrow \frac{\gamma M_\infty^2}{m_\infty} p_o(2\epsilon) \tag{29}$$

as $\xi \longrightarrow \infty$. This asymptotic value of the pressure is exactly twice the incident pressure rise; therefore, as anticipated, the incident wave is reflected as a regular reflection from a solid boundary.

Condition (c).- The Kármán momentum-integral equation for compressible fluids is

$$\frac{d}{dx}\int_0^\delta \rho u^2 \, dy - u_e \frac{d}{dx}\int_0^\delta \rho u \, dy = -\frac{dp}{dx}\delta - \tau_w$$

where τ_w indicates the wall shear stress. With the ordinary definitions of the displacement and momentum thicknesses, the equation becomes

$$\frac{d}{dx}\left(\rho_e u_e^2 \theta\right) + \rho_e u_e \delta^* \frac{du_e}{dx} = \tau_w$$

From the outer flow

$$\rho_e u_e \frac{du_e}{dx} = -\frac{dp}{dx}$$

$$\frac{d}{dx}\left(\rho_e u_e^2 \theta\right) - \delta^* \frac{dp}{dx} - \tau_w = 0$$

From the previous notation it is seen that

$$K \equiv \frac{d}{dx}\left(\rho_e u_e^2 \theta - \delta^* p\right) + p \frac{d\delta^*}{dx} - \tau_w$$

As the boundary-layer regions 1 and 3 are independently considered, the pressure gradient and velocity therein might be discontinuous at the origin. In order that the discontinuities be consistent with the dynamical equations, it is necessa that:

$$\lim_{x_o \longrightarrow 0} \int_{-x_o}^{x_o} \left[\frac{d}{dx}\left(\rho_e u_e^2 \theta - \delta^* p\right) + p \frac{d\delta^*}{dx} - \tau_w\right] dx = 0$$

or

$$\lim_{x_o \longrightarrow 0} \left[\left(\rho_e u_e^2 \theta - \delta^* p\right)_{-x_o}^{x_o} + \int_{-x_o}^{x_o} p \frac{d\delta^*}{dx} dx - \int_{-x_o}^{x_o} \tau_w \, dx\right] = 0$$

Now δ^* is required to be continuous at the origin, $p \frac{d\delta^*}{dx}$, discontimuous but finite, and the shear stress τ_w, finite; then, in the limit, the

two integrals vanish and

$$\lim_{x_o \longrightarrow 0} \left(\rho_e u_e{}^2 \theta - \delta^* p \right)_{-x_o}^{x_o} = 0$$

remains. Therefore, in the limit,

$$\rho_3 u_3{}^2 \theta_3 - \rho_1 u_1{}^2 \theta_1 - \delta^*(0)\left(p_3 - p_1\right) = 0 \tag{30}$$

The condition that $p_1 = p_3$ at $x = y = 0$ has already been imposed and hence equation (30) reduces to

$$\rho_1 u_1{}^2 \theta_1 = \rho_3 u_3{}^2 \theta_3 \qquad \text{at} \quad x = y = 0 \tag{31}$$

This equation, linearized in u' and its derivatives, becomes

$$\alpha_1 \delta_o^* \left(\frac{du_3'}{dx} - \frac{du_1'}{dx} \right) = \alpha_2 \left(u_3' - u_1' \right) \tag{32}$$

where

$$\alpha_1 \equiv - \frac{\mathrm{Re}}{\left(\frac{37}{315} - \frac{263}{630\sigma} \right)^3} \sigma^{\frac{3(2-\gamma)}{2(\gamma-1)}} \left\{ \frac{1}{111\sigma} + \frac{\left[\frac{1}{3}\left(\frac{71}{2520} \right)\sigma^{-2} - \frac{\sigma^{-1}}{945} \right]}{\left(\frac{37}{315} - \frac{263}{630\sigma} \right)} \right\}$$

$$\alpha_2 \equiv -\sigma^{\frac{2-\gamma}{2(\gamma-1)}} \left(\frac{37}{315} - \frac{263}{630\sigma} \right)^{-1} \left[2 + M_\infty{}^2 \left(\frac{263}{630} \frac{\gamma - 1}{\sigma} - 1 \right) \right]$$

The pressures were equal at the origin, so that, in linear theory, the streamwise perturbation velocities are also equal. Therefore $u_1' = u_3'$ at $x = y = 0$.

Now since $\alpha_1 \neq 0$ and $\alpha_2 \neq 0$, for the range of M_∞ and R_e studied

$$\frac{du_1'}{dx} = \frac{du_3'}{dx} \qquad \text{at} \quad x = y = 0 \tag{33}$$

It is therefore seen that, in the linear theory, continuous pressure also implies continuous pressure gradient. Since

$$\frac{du_1'}{dx} = \frac{A\lambda_2^2}{\delta_o^*} \qquad \text{at} \quad x = y = 0$$

$$\frac{du_3'}{dx} = \frac{1}{\delta_o^*}\left(B\lambda_1^2 + C\lambda_3^2\right) \qquad \text{at} \quad x = y = 0$$

there is obtained from equation (33)

$$A\lambda_2^2 = B\lambda_1^2 + C\lambda_3^2 \tag{34}$$

Conditions (a), (b), and (c) lead to equations (25), (28), and (34) for four constants A, B, C, and D. But previously it has been shown that

$$\lim_{\xi \longrightarrow \infty} \delta_3^* = \delta_o^*(1 + D)$$

Thus it is seen that D merely determines the downstream boundary-layer thickness, whereas A, B, and C determine the local character of the perturbation. Therefore, if the downstream thickness can be estimated, there will be a determinate problem. Assume for the present at least, that D is determined. The constants A, B, and C can then be solved for from the following equations:

$$A\lambda_2 = B\lambda_1 + C\lambda_3 - \frac{2\epsilon}{m_\infty}$$

$$A = B + C - \frac{D}{m_\infty}$$

$$A\lambda_2^2 = B\lambda_1^2 + C\lambda_3^2$$

The solution is

$$\left.\begin{aligned} A &= \frac{-(\lambda_3 + \lambda_1)}{(\lambda_2 - \lambda_3)(\lambda_2 - \lambda_1)}\left(-\frac{2\epsilon}{m_\infty}\right) + \frac{\lambda_1\lambda_3}{(\lambda_2 - \lambda_3)(\lambda_2 - \lambda_1)}\left(-\frac{D}{m_\infty}\right) \\ B &= \frac{(\lambda_3 + \lambda_2)}{(\lambda_3 - \lambda_1)(\lambda_2 - \lambda_1)}\left(-\frac{2\epsilon}{m_\infty}\right) - \frac{\lambda_2\lambda_3}{(\lambda_3 - \lambda_1)(\lambda_2 - \lambda_1)}\left(-\frac{D}{m_\infty}\right) \\ C &= \frac{-(\lambda_2 + \lambda_1)}{(\lambda_3 - \lambda_1)(\lambda_2 - \lambda_3)}\left(-\frac{2\epsilon}{m_\infty}\right) + \frac{\lambda_1\lambda_2}{(\lambda_3 - \lambda_1)(\lambda_2 - \lambda_3)}\left(-\frac{D}{m_\infty}\right) \end{aligned}\right\} \quad (35)$$

Evaluation of D.- It is seen from equations (35) that the local perturbations are determined once the constant D is specified. As it has been shown that D characterizes the thickening of the boundary layer through a shock, it can be determined approximately by the following consideration.

When a weak shock is incident upon the boundary layer, it is assumed that the Kármán momentum-integral equation

$$\frac{d\theta}{dx} + \theta\left[\frac{1}{\rho_e}\frac{d\rho_e}{dx} + \left(2 + \frac{\delta^*}{\theta}\right)\frac{1}{u_e}\frac{du_e}{dx}\right] = \frac{\tau_w}{\rho_e u_e{}^2}$$

is valid throughout the disturbed boundary-layer flow. For a given pressure distribution, the growth of the boundary layer is governed by this equation. When a shock is incident upon the boundary layer, it has been theoretically predicted and experimentally verified that the flow upstream of the point of incidence is separated over a considerable portion of the disturbed flow; hence the shear stress becomes relatively unimportant. Downstream of the point of incidence, since the flow is dominated by pressure forces, whether the flow is laminar or turbulent the shear is known, from experimental results, to be very small (reference 18). Hence for the present approximation, the shear stress can be neglected.

Furthermore, if the ratio $\delta^*/\theta \equiv H$ is regarded as a parameter, the momentum equation gives the momentum thickness as a function of $u_e(x)$. Now, it is known that H is substantially increased by the shock, and to a lesser extent by the compressibility. In going through a shock, H first increases because of the shock and then decreases because of the drop in Mach number. Hence, as a first approximation, H can be taken to be some constant average value over the interaction range. (This is

similar to the procedure mentioned by Nitzberg and Crandall (reference 19).) In particular, H will be taken as the value ahead of the interaction.

The momentum-integral equation now becomes:

$$\frac{1}{\theta}\frac{d\theta}{dx} + \frac{1}{\rho_e}\frac{d\rho_e}{dx} + (2 + H)\frac{1}{u_e}\frac{du_e}{dx} = 0$$

or

$$\frac{d}{dx}\left(\log_e \theta\rho_e u_e^{2+H}\right) = 0$$

Integrating between regions 1 and 3, stations far upstream and downstream of the point of incidence,

$$\theta_1\rho_1 u_1^{2+H} = \theta_3\rho_3 u_3^{2+H}$$

or

$$\frac{\delta_3^*}{\delta_1^*} = \frac{\rho_1}{\rho_3}\left(\frac{u_1}{u_3}\right)^{2+H} \tag{36}$$

For laminar flow over a flat plate where $\mu \propto T$, $P_r = 1$, and $(\partial T/\partial y)_w = 0$, the formula given by Lees (reference 20, p. 119) for H can be taken:

$$H = 2.50 + 3.50\left(\frac{\gamma - 1}{2}\right)M_\infty^2$$

The thickening predicted by equation (36) is shown in figure 3. Values of the density and velocity ratios were computed exactly and to first order in the deflection angle. For small deflection angles, the agreement between the "exact" thickness ratio and that obtained from linear theory is quite good. The crosses on figure 3 are the experimental values for various Reynolds numbers obtained by Barry, Shapiro, and Neumann (reference 4), and there is fair agreement between theory and experiment. Actually, the experimental data are visual estimates of the ratio of boundary-layer thicknesses, so that for a comparison between

theory and experiment, the ratio of boundary-layer thickness to displacement thickness would have to be assumed to be the same upstream as well as downstream of the point of incidence. In view of the assumption and the allowable experimental error in the visualization of schlieren photographs, the experimental values must be regarded as qualitative. The theoretical values of the thickness ratio are near the lower limit of the experimental values. This is probably due to the fact that the value of H was underestimated, since an average H through the interaction range would be larger than the initial value.

Evaluating D according to the linear theory,

$$\frac{\delta_3^*}{\delta_1^*} = \frac{\rho_1}{\rho_3}\left(\frac{u_1}{u_3}\right)^{2+H}$$

and

$$\frac{\rho_1}{\rho_3} = 1 - \frac{2M_\infty^2}{m_\infty}\epsilon$$

$$\frac{u_1}{u_3} = 1 + \frac{2\epsilon}{m_\infty}$$

hence

$$\frac{\rho_1}{\rho_3}\left(\frac{u_1}{u_3}\right)^{2+H} = 1 + \left(2 + H - M_\infty^2\right)\frac{2\epsilon}{m_\infty}$$

But

$$\frac{\delta_3^*}{\delta_1^*} = 1 + D$$

Therefore

$$D = \frac{2\epsilon}{m_\infty}\left(2 + H - M_\infty^2\right)$$

Now since

$$H = 2.50 + 3.50\left(\frac{\gamma - 1}{2}\right)M_\infty{}^2$$

$$D = \frac{2\epsilon}{m_\infty}\left(4.50 - 0.3M_\infty{}^2\right) \tag{37}$$

Effects of Downstream Thickening

Consider the constant A governing the upstream flow:

$$A = \frac{-\left(\lambda_3 + \lambda_1\right)}{\left(\lambda_2 - \lambda_3\right)\left(\lambda_2 - \lambda_1\right)}\left(-\frac{2\epsilon}{m_\infty}\right) + \frac{\lambda_1\lambda_3}{\left(\lambda_2 - \lambda_3\right)\left(\lambda_2 - \lambda_1\right)}\left(-\frac{D}{m_\infty}\right)$$

or

$$A = -\frac{2\epsilon}{m_\infty}\left[\frac{-\left(\lambda_3 + \lambda_1\right)}{\left(\lambda_2 - \lambda_3\right)\left(\lambda_2 - \lambda_1\right)} + \frac{\lambda_1\lambda_3}{\left(\lambda_2 - \lambda_3\right)\left(\lambda_2 - \lambda_1\right)}\left(\frac{4.50 - 0.3M_\infty{}^2}{m_\infty}\right)\right]$$

The coefficients are given in table I; hence it is seen that for all cases in the present range of Mach numbers and Reynolds numbers the contribution of D toward A amounts to less than 10 percent. Thus it is seen that, in the present range, a precise knowledge of the downstream thickness is not essential to the determination of the upstream flow.

The effect on the downstream flow is not quite so straightforward, since two constants B and C are involved. As an indication of the downstream flow, consider the pressure distribution along the wall. It has been seen that, far downstream, the pressure attains a constant value, namely the pressure that would have been anticipated had there been a regular reflection. Immediately behind the point of incidence the pressure is much lower than this end pressure since the flow has just undergone an expansion to the pressure that existed before the point of incidence. The manner in which the pressure proceeds from its value at the origin to its final downstream value is then of some importance. Does the pressure increase monotonically to its final value, or does the pressure at any point rise higher than the final value? Liepmann (reference 3) has found experimentally that for the reflection of a shock wave from a laminar boundary layer there indeed exists a definite downstream overcompression. The pressure rises sharply to some value higher than

the end pressure and then tapers off. The experimental findings of Barry, Shapiro, and Neumann (reference 4) also confirm this observation, although their results show the overcompression to be slightly less pronounced.

Consider the behavior of the theoretical downstream pressure distribution. Along the interface the total pressure is given as

$$p_3 = p_o - \gamma M_\infty{}^2 p_o \left(B\lambda_1 e^{\lambda_1 \frac{x}{\delta_o{}^*}} + C\lambda_3 e^{\lambda_3 \frac{x}{\delta_o{}^*}} - \frac{2\epsilon}{m_\infty} \right) \tag{38}$$

and

$$p_3 \longrightarrow p_o \left(1 + \frac{2\gamma M_\infty{}^2}{m_\infty} \epsilon \right) \tag{39}$$

as $\dfrac{x}{\delta_o{}^*} = \xi \longrightarrow \infty$

so that far downstream, consistent with linear theory, the correct pressure behind the regular reflection is obtained. Then

$$B = \frac{(\lambda_3 + \lambda_2)}{(\lambda_3 - \lambda_1)(\lambda_2 - \lambda_1)} \left(-\frac{2\epsilon}{m_\infty} \right) + \frac{\lambda_2 \lambda_3}{(\lambda_3 - \lambda_1)(\lambda_2 - \lambda_1)} \left(\frac{D}{m_\infty} \right)$$

wherein $\epsilon > 0$ and $D > 0$. Now $\lambda_2 > 0$, $\lambda_1 < 0$, and and λ_1 are of the same order of magnitude, while λ_3 times as small. Hence $B < 0$.

Consider

$$C = \frac{-(\lambda_2 + \lambda_1)}{(\lambda_3 - \lambda_1)(\lambda_2 - \lambda_3)} \left(-\frac{2\epsilon}{m_\infty} \right) + \frac{\lambda_1 \lambda_2}{(\lambda_3 - \lambda_1)(\lambda_2 - \lambda_3)} \left(-\frac{D}{m_\infty} \right)$$

$$C = \frac{2\epsilon}{m_\infty} \left[\frac{(\lambda_2 + \lambda_1)}{(\lambda_3 - \lambda_1)(\lambda_2 - \lambda_3)} - \frac{\lambda_1 \lambda_2}{(\lambda_3 - \lambda_1)(\lambda_2 - \lambda_3)} \left(\frac{4.50 - 0.3 M_\infty{}^2}{m_\infty} \right) \right]$$

Now the second term is always negative in the Mach number range considered, whereas the first term may be either positive or negative depending upon the sign of $\lambda_2 + \lambda_1$. It turns out that for $M_\infty > 2.4$ (approx.) the first term is positive, hence $C > 0$. For $M_\infty < 2.4$ (approx.) the first term is negative, but

$$\left|\frac{(\lambda_2 + \lambda_1)}{(\lambda_3 - \lambda_1)(\lambda_2 - \lambda_3)}\right| < \left|\frac{\lambda_1\lambda_2}{(\lambda_3 - \lambda_1)(\lambda_2 - \lambda_3)}\left(\frac{4.50 - 0.3M_\infty^2}{m_\infty}\right)\right|$$

hence C is positive. Thus for the whole range of Mach numbers and Reynolds numbers, $C > 0$.

The qualitative behavior of the downstream pressure distribution will now be established. The downstream pressure along the interface is

$$p_3 = p_o + \gamma M_\infty^2 p_o \frac{2\epsilon}{m_\infty} + \gamma M_\infty^2 p_o\left(-B\lambda_1 e^{\lambda_1\frac{x}{\delta_o^*}} - C\lambda_3 e^{\lambda_3\frac{x}{\delta_o^*}}\right)$$

The first two terms represent the constant end pressure while the third actually describes the variation of the pressure. Consider the curve

$$y = -B\lambda_1 e^{\lambda_1\frac{x}{\delta_o^*}} - C\lambda_3 e^{\lambda_3\frac{x}{\delta_o^*}}$$

It is known that $B < 0$, $C > 0$, $\lambda_1 < 0$, and $\lambda_3 < 0$; hence $-B\lambda_1 < 0$ and $-C\lambda_3 > 0$. The constants B and C are of the same order of magnitude, but λ_1 is about ten times as large as λ_3; hence

$$\left|B\lambda_1\right| > \left|C\lambda_3\right|$$

Therefore, when $x = 0$, y is negative and, when x becomes large, y is positive but small. The point at which the maximum occurs is given by

$$\left(\frac{x}{\delta_o^*}\right)_{y_{max}} = \frac{1}{\lambda_3 - \lambda_1}\log_e\left(-\frac{B\lambda_1^2}{C\lambda_3^2}\right)$$

If

$$y = -B\lambda_1 e^{\lambda_1 \frac{x}{\delta_o^*}} - C\lambda_3 e^{\lambda_3 \frac{x}{\delta_o^*}}$$

is now interpreted as the pressure variation, it is immediately seen that the theoretical pressure distribution exhibits the overcompression that is observed experimentally.

RESULTS AND DISCUSSION

It has been seen that if the downstream thickening is estimated, the constants A, B, and C are completely determined as functions of the flow parameters. With the outer flow thus determined, the boundary-layer growth and pressure distributions can now be computed, and hence the effects of Mach number, Reynolds number, and shock strength upon the upstream influence and the location of the separation point can be studied. (Of course, when the results are compared with experiment, the Reynolds numbers must be low enough so that the boundary layer will remain laminar, prior to the interaction, in the corresponding experimental case.)

Upstream Influence

In order to estimate the upstream influence of the interaction, define a length in which the pressure on the boundary-layer displacement thickness decays to a specified fraction of its amplitude at the origin. This length would then be determined solely by the exponent λ_2. For example, consider the upstream boundary-layer disturbance:

$$\delta_1^* = -m_\infty A \delta_o^* e^{\lambda_2 \frac{x}{\delta_o^*}}$$

At the origin

$$\delta_1^*(0) = -m_\infty A \delta_o^*$$

If x_d/δ_o^* is defined as the distance required in order that $\delta_1^* = \alpha(-m_\infty A\delta_o^*)$ at x_d/δ_o^* where $\alpha < 1$,

$$\alpha\left(-m_\infty A\delta_o^*\right) = -m_\infty A\delta_o^* e^{\lambda_2 \frac{x}{2\delta_o^*}}$$

Therefore

$$\frac{x_d}{\delta_o^*} = -\frac{1}{\lambda_2}\log_e\left(\frac{1}{\alpha}\right)$$

Since α is a constant it is seen that the upstream influence is then inversely proportional to λ_2. Values of λ_2 have been plotted in figure 4. (Values of λ_1 and λ_3 are plotted in figures 5 and 6, respectively.) For fixed Mach number, x_d/δ_o^* increases with increasing Reynolds number. For large Reynolds number, this dependence can be deduced from the equation:

$$\lambda^3 + \frac{g_3}{g_4}\lambda^2 + \left(\frac{g_2}{g_4} + \frac{m_\infty}{g_4}\right)\lambda + \frac{m_\infty g_1}{g_4} = 0$$

The coefficients are functions of Mach number and for the range of Mach numbers considered, the roots are real. When the Reynolds number is large, it can be shown that

$$\lambda_2 \approx \frac{\sqrt{m_\infty}}{\sqrt{-g_4}}$$

where $g_4(\mathrm{Re}, M_\infty) < 0$ and $g_4 \propto \mathrm{Re}$. This is in agreement with Lees' result. Consequently, for large Reynolds numbers, $x_d/\delta_o^* \propto \mathrm{Re}^{1/2}$. For fixed Reynolds numbers, the upstream influence decreases with increasing Mach number as indicated in figure 4(b). If the disturbance is considered to decay to, say, 5 percent of its amplitude at the origin, it is found that, at the high Reynolds numbers, and Mach numbers about 2 or less, the upstream influence is of the order of 30 boundary-layer displacement thicknesses.

The result that the upstream influence increases with Reynolds number may appear to be disconcerting since the viscous effects are expected to be more prevalent at the lower Reynolds numbers and hence to produce a greater influence upon the upstream flow. This apparent paradox arises because the upstream influence has been measured in multiples of a length which is also dependent upon Reynolds number. If the absolute values of upstream influence are considered,

$$\frac{x_d}{\delta_o^*} \propto Re^{1/2}$$

But

$$\delta_o^* \propto \frac{1}{Re_x^{1/2}} \propto \frac{1}{Re}$$

hence

$$x_d \propto \delta_o^* \, Re^{1/2}$$

or

$$x_d \propto Re^{-1/2}$$

Thus, measured on an absolute scale, the upstream influence increases with decreasing Reynolds number.

As defined above, the distance of the upstream influence is dependent solely upon Mach number and Reynolds number. It can be redefined so that it will also depend upon the shock strength. This is accomplished by defining the upstream influence to be that distance at which the disturbance decays to a given fraction of the undistrubed value. The perturbed boundary-layer displacement thickness ahead of the point of incidence is given by:

$$\delta_1^* = -m_\infty A \delta_o^* e^{\lambda \frac{x}{2\delta_o^*}}$$

where δ_o^* is the undisturbed displacement thickness. The upstream

influence is then the distance x_d/δ_o^* to the point where $\delta_1^* = b\delta_o^*$ and $b < 1$:

$$b\delta_o^* = -m_\infty A\delta_o^* e^{\lambda_2 \frac{x_d}{\delta_o^*}}$$

$$\lambda_2 \frac{x_d}{\delta_o^*} = \log_e \left(-\frac{b}{m_\infty A}\right)$$

$$\frac{x_d}{\delta_o^*} = -\frac{1}{\lambda_2} \log_e \left(-\frac{m_\infty A}{b}\right)$$

Now A is negative and decreases with increase of the deflection angle, so that for fixed Mach number and Reynolds number, the upstream influence decreases with shock strength. If the upstream influence is measured to the point at which the disturbance decays to 5 percent of its undisturbed value, $b = 0.05$. In figure 7, x_d/δ_o^* is plotted against deflection angle. For $\epsilon \leq 2^o$, the results seem to agree fairly well with the experimental values presented in figure 10, reference 2. For larger deflection angles, however, the theoretical values are too low in comparison with the experimental values. This might be due to the fact that the linear theory becomes less accurate as the deflection angle increases.

Boundary-Layer Separation

Since the outer potential flow is known, the point of separation can be computed on the basis that separation occurs when $(\partial u/\partial y)_w = 0$. Now $\partial u/\partial y$ is proportional to $\partial u/y'$ so that one can just as well use $(\partial u/\partial y')_w = 0$ as a criterion for separation. In view of the assumption of a Pohlhausen velocity profile, in the transformed plane

$$\left(\frac{\partial u}{\partial y'}\right)_w = \frac{u_e}{\delta'}\left(2 + \frac{\Lambda}{6}\right)$$

hence, as in the incompressible case, separation occurs at $\Lambda = -12$. Now it is known from experience in the incompressible case that, in regions of retarded flow, the Kármán-Pohlhausen method gives values of the skin friction that are too high and consequently predicts separation too late or not at all. This feature of the method is also to be

expected in the compressible case, since it was shown by Howarth that the effect of compressibility is equivalent to exaggerating the pressure gradient in the incompressible case (reference 13). In particular, Stewartson has used the Kármán-Pohlhausen method to treat the case of flow against a linear pressure gradient and has shown that the predicted distance from the leading edge to the separation point is an overestimate of the actual value (reference 21).

In the present problem, where the flow upstream of the point of incidence is subject to a positive pressure gradient, the same overestimation of the separation point will, of course, be expected. But the effects of Mach number, Reynolds number, and shock strength upon the separation point are of primary interest, so that inaccuracy in the absolute values is unimportant.

It is known from the boundary-layer theory that the parameter that defines the separation point is

$$\Lambda = \frac{(\delta')^2}{\nu_o} \frac{du_e}{dx}\left(1 + \frac{\gamma - 1}{2} M_e^2\right)$$

By neglecting products of u' and its derivatives,

$$\Lambda = \left[(\delta')^2/\nu_o\right](U/\sigma)(du'/dx)$$

Now, from equation (6), to the order of approximation,

$$\Lambda = \frac{\text{Re } \delta_o^*}{\left(\frac{37}{315} - \frac{263}{630\sigma}\right)^2} \sigma^{\frac{3-2\gamma}{\gamma-1}} \frac{du'}{dx}$$

Along the edge of the boundary layer, from the upstream solution (see equation (18))

$$\frac{du'}{dx} = A \frac{\lambda_2^2}{\delta_o^*} e^{\lambda_2 \frac{x}{\delta_o^*}}$$

so that

$$\Lambda = \frac{A\ Re\ \lambda_2{}^2}{\left(\frac{37}{315} - \frac{263}{630\sigma}\right)^2}\ \sigma^{\frac{3-2\gamma}{\gamma-1}}\ e^{\lambda_2 \frac{x}{\delta_o^*}}$$

For separation

$$-12 = \frac{A\ Re\ \lambda_2{}^2}{\left(\frac{37}{315} - \frac{263}{630\sigma}\right)^2}\ \sigma^{\frac{3-2\gamma}{\gamma-1}}\ e^{\lambda_2 \frac{x_s}{\delta_o^*}}$$

$$\frac{x_s}{\delta_o^*} = -\frac{1}{\lambda_2} \log_e \left(\frac{A\ Re\ \lambda_2{}^2}{-12}\ \beta\right) \tag{40}$$

where

$$\beta \equiv \frac{\sigma^{\frac{3-2\gamma}{\gamma-1}}}{\left(\frac{37}{315} - \frac{263}{630\sigma}\right)^2}$$

and λ_2 is positive, hence separation ahead of the point of incidence will be predicted only when $-\frac{1}{12} A\ Re\ \lambda_2{}^2 \beta > 1$.

Contrary to the separation phenomenon in ordinary boundary-layer flow, the location of the separation point is influenced by the Reynolds number. This is easily understood when one considers the fact that separation of the flow is controlled by the pressure gradient of the outer flow; according to boundary-layer theory, the outer flow depends solely upon the geometry of the body. Consequently, the location of the separation point is independent of Reynolds number. In the present problem, however, an outer flow that is compatible with the boundary-layer flow has to be found. This relationship is expressed by the condition which requires that the direction of the potential flow be the same as the slope of the displacement thickness. Since the boundary-layer growth depends upon the Reynolds number, the outer flow, and eventually the separation point, must also vary with Reynolds number.

In order to determine the effect of shock strength upcn the position of the separation point, the constant A must be examined:

$$A = -\frac{2\epsilon}{m_\infty}\left[\frac{-(\lambda_3 + \lambda_1)}{(\lambda_2 - \lambda_3)(\lambda_2 - \lambda_1)} + \frac{\lambda_1\lambda_3}{(\lambda_2 - \lambda_3)(\lambda_2 - \lambda_1)}\left(\frac{4.50 - 0.3M_\infty^2}{m_\infty}\right)\right]$$

For the range of Mach numbers and Reynolds numbers considered, the terms in the bracket are positive, since $\lambda_2 > 0$, $\lambda_1 < 0$, and $\lambda_3 < 0$. Therefore as ϵ is increased A becomes more negative; consequently $-\frac{1}{12} A \operatorname{Re} \lambda_2^2 \beta$ becomes more positive and hence the separation point moves upstream. Thus an increase of shock strength increases the distance between the separation point and the point of incidence.

To express x_s/δ_o^* explicitly in terms of Mach number and Reynolds number would be difficult; hence this relationship will be presented numerically by varying, separately, the Mach number and Reynolds number. In figure 8, lines of constant Reynolds number are plotted in the $x_s/\delta_o^*, \epsilon$ plane, and the separation point, measured in multiples of δ_o^*, moves upstream with increasing Reynolds number. This is not too surprising since the same behavior occurs with the upstream influence. As the upstream influence increases, the "self-induced" pressure gradient will begin farther upstream and hence separation will occur farther upstream. For fixed Reynolds number, the upstream influence increased with decreasing Mach number, and accordingly (see fig. 9) the separation point, measured in multiples of δ_o^*, moves upstream with decreasing Mach number.

Before closing the discussion on separation, the importance of D in the determination of the separation point should be discussed. The coefficients in the expression for A are such that, for fixed Reynolds number, Mach number, and deflection angle, the magnitude of A increases as D increases. The separation point has been seen to move upstream as A is increased in magnitude, hence an overestimation of the downstream thickening would result in a slight overestimation of the upstream distance to the separation point. In figure 9 the variation of separation point for different Mach numbers has been plotted for fixed Reynolds number. The location of the separation point for the case $D = 0$ has also been plotted in this figure. These curves thus give the greatest lower bound of the separation distance since it is known that actually $D > 0$. A comparison of results reveals that D has a very small effect upon the location of the separation point. For the higher Mach numbers in the range investigated, the percentage difference between the two cases may be fairly large, but the fact that the separation distance is measured in multiples of a boundary-layer displacement thickness must be

considered. In an actual experimental measurement of the absolute distance to the separation point, this difference will be extremely small. Hence, for practical purposes, one can consider $D = 0$ when estimating the separation point. The results obtained under such conditions will then yield a slight underestimation of the separation point.

Pressure Distribution

The pressure disturbance along the wall (fig. 10) decays exponentially from a definite value at the point of incidence to zero far upstream of that point. Downstream of the point of incidence the pressure rises to a maximum value before dropping to the value corresponding to regular reflection. This downstream overcompression has been observed experimentally, and it appears to be a characteristic feature of shock-wave interaction with a laminar boundary layer. The Lees' theory, as mentioned previously, failed to predict this downstream behavior. This is due to the fact that an incomplete solution for the pressure was used in the determination of the pressure distribution. The boundary layer was divided, longitudinally, into four regions, and it was assumed that the solutions to a third-order differential equation were valid in each region. In the two regions that extended to positive and negative infinity, certain solutions could be rejected since they became infinite at the ends of their respective regions. In the finite regions, however, the complete solutions must be retained. The incompleteness of the Lees' theory, then, arises from the fact that only one term of the general solution was used in each of the finite regions.

The linear theory yields pressure distributions that are similar irrespective of the size of the deflection angle. Now for very small angles, the experimental results exhibit the general behavior predicted by theory. In figure 10 the experimental values of the pressure distribution have been plotted for $\epsilon = 1^{\circ}$ and $M_{\infty} = 2.05$. (In this case, separation has probably not occurred since the wave is quite weak.) The values of the pressure ratio were taken from figure 13 of reference 4 and converted to the scale indicated. The upstream portion of this curve can be well represented by an exponential curve, thus verifying, at least for this case, the predicted exponential pressure rise. For larger deflection angles, the experimental pressure distributions are characterized by the familiar pressure "bump" ahead of the point of incidence, thus indicating that separation has occurred. The linear theory is inadequate, as regards predicting this upstream behavior; hence for large deflection angles the theory must be modified, possibly by taking account of the second-order effects upstream of the point of incidence.

SHOCK-WAVE INTERACTION WITH A TURBULENT BOUNDARY LAYER

Method of Approximations

When the flow in the boundary layer is turbulent, the Kármán momentum-integral equation will take on the same form as for the laminar boundary layer except that the quantities involved are not the exact, but average, values. However, since general relationships between the shear stress and the mean velocity in turbulent layers have not yet been established, rigorous treatment of the problem at this time is, of course, not possible. Here, for the purpose of exhibiting the characteristic difference between the laminar and turbulent cases, certain approximations are proposed.

The momentum-integral equation expresses the shear stress at the wall in terms of the growth of the boundary-layer momentum thickness and the velocity gradient. Using experimental results as a guide, the relative importance of these terms can be estimated. Experimental results of Fage and Sargent (reference 18) show that the shear stress in front of the shock is practically constant; behind the shock, it is very small. Therefore, unlike the laminar case, the shear stress to the first appproximation, both in front of and behind the shock, can be regarded as constant and hence has no effect on the perturbed flow. It follows then that, in the case of a turbulent boundary layer, the growth of the momentum thickness is influenced primarily by pressure changes due to the presence of the shock.

To simplify the problem further, it is noted, for practical purposes, that the shape parameter $H \equiv \delta^*/\theta$ is relatively insensitive to change even though there may be a considerable adverse pressure gradient. In the transonic case, where there is a normal shock in the local supersonic region and a large change in H is anticipated, H at its maximum is only increased by a factor of about 1.2 (see reference 2). The reason for this is possibly the fact that the increase by the shock may be counterbalanced by a decrease due to compressibility effect. Moreover, in the momentum-integral equation, the coefficient of the velocity gradient is positive and usually greater than unity within the Mach number range; hence one can ignore the slight variation in H and consider it a constant. By the same token, the Mach number in this coefficient can also be considered to be constant. (The Mach number enters when the density is eliminated in terms of the velocity.) Consequently, the momentum-integral equation reduces to:

$$\frac{d\,\Delta}{dx} + \alpha_3 \frac{du'}{dx} = 0$$

where

$$\alpha_3 \equiv 2 + H - M_\infty^2$$

Solution for Outer Flow

Similar to the previous case, for the upstream region $\phi_1 = f(\xi - m_\infty \eta)$. By applying the original condition $d\Delta/d\xi = \partial\phi/\partial\eta$ at $\eta = 0$, there is obtained from the linear theory

$$f = f_0 e^{m_\infty/\alpha_3(\xi - m_\infty\eta)} + \text{Constant}$$

Since $m_\infty/\alpha_3 > 0$, the disturbances vanish far upstream. When α_3 is evaluated the exponent m_∞/α_3 is found to be about one order larger than λ_2 of the laminar case. This is the well-known experimental result that there is very little upstream influence in the turbulent case. This, therefore, confirms the hypotheses made in the previous section.

For the downstream solution

$$\phi_3 = g(\xi - m_\infty\eta) - \frac{\epsilon}{m_\infty}(\xi + m_\infty\eta)$$

The original differential equation remains the same; hence the downstream solution would be

$$\phi_3 = g_0 e^{m_\infty/\alpha_3(\xi - m_\infty\eta)} - \frac{2\epsilon}{m_\infty}\xi + \text{Constant}$$

It shows that if the solution ϕ_1 is continued to the downstream side the velocities would become infinite at positive infinity and must be rejected. There is therefore a principal difference between the laminar and turbulent cases. In the laminar case several solutions for the outer flow were obtained and the solution appropriate for either upstream or downstream could be chosen. In the turbulent case there is no choice since there is only one solution for the outer flow, which, if continued, fails at positive infinity. This indicates that linearization of the flow is incapable of accounting for the flow near the point of incidence where the nonlinear effects become important. Since large changes in flow velocities can be brought about only through a shock, in the present problem a reflected shock must be considered.

From general considerations it can be argued that if one puts a shock wave between regions 2 and 3 and considers perturbations of a regular reflection it may be possible to obtain a solution which will satisfy the conditions at infinity. By perturbing the regular reflection, there would be, in each region, undisturbed quantities plus their perturbations. Consider the total potential in region 3:

$$\Phi_3 = \xi + f(\xi - m_3 y) + g(\xi + m_3 y)$$

At infinity $f' = g' = 0$; along the reflected wave $\xi - m_3\eta = 0$, to first order, the velocities are constant; hence

$$f' \pm g' = \text{Constant}$$

But to first order, along the wave, $f'(0) = \text{Constant}$; hence $g'(\xi) = \text{Constant}$. Therefore, $g'(\xi)$ is constant throughout region 3. But $g' = 0$ at infinity; hence $g' = 0$ in region 3.

Then at the boundary layer $d\Delta/d\xi = -m_3 f'(\xi)$ where f is nondimensional, and the substitution into the momentum-integral equation yields

$$-m_3 f' + \alpha_3 f'' = 0$$

$$f = \text{Constant} + f_o e^{m_3/\alpha_3 \xi}$$

$$f' = f_o \frac{m_3}{\alpha_3} e^{m_3/\alpha_3 \xi}$$

Now $f' = 0$ at infinity; hence one must choose $f_o = 0$, and thus

$$f = \text{Constant}$$

This means that behind the reflected shock, the flow, to the first order, is uniform. Since the flow behind the incident shock has undergone compression up to the reflected wave, it can be seen that, to satisfy the condition at infinity, the reflected shock must be followed by a very rapid expansion. Otherwise, the pressure after the second shock would have been higher than that after the regular reflection. It is therefore concluded that in the case of a turbulent boundary layer the incident shock is reflected as a shock and behind the reflected shock there

must be an abrupt expansion so as to cancel the overcompression brought about by the train of upstream compression waves. The existence of the sharp expansion behind the reflected shock was also confirmed by experiments (reference 9). The pressure distribution and boundary-layer growth, to the first order, appear to be discontinuous as shown in figure 12.

Downstream Thickening for Turbulent Boundary Layers

The downstream thickening can be estimated by use of the formula

$$\frac{\delta_3^*}{\delta_1^*} = \frac{\rho_1}{\rho_3}\left(\frac{u_1}{u_3}\right)^{2+H}$$

Now the difference between the laminar and turbulent cases is that H differs for the two cases. Since, in general, $H_t < H_l$, the downstream thickening in the turbulent case is less than the thickening in the corresponding laminar case. Empirical relations must be relied on to estimate H because of the lack of knowledge of the compressible turbulent boundary layer. According to Nitzberg and Crandall (reference 19), for local Mach numbers greater than the free-stream Mach number, but less than 1.4, the compressibility effect is well approximated by

$$H = H_{M=0}\left(1 + \frac{2}{5} M^2\right)$$

Use this relationship to estimate the downstream thickening and then compare the results with the existing experimental data. By assuming a 1/7-power law for the incompressible profile,

$$H = 1.29\left(1 + 0.4M_\infty^2\right)$$

The predicted thickening is shown in figure 13. It shows that the downstream thickening increases as the Mach number is decreased. This behavior is also present in the laminar case.

Using this value of H, it was found that the predicted thickening for $M_\infty = 1.44$ and $\epsilon = 4.5^\circ$ is larger than the visually estimated thickening in the experimental case. On the other hand, the predicted thickening for $M_\infty = 2$ and $\epsilon = 6^\circ$ is slightly less than the visually estimated thickening in the experimental case. It should be noted, however, that, for $M > 1.4$, a relationship has been used that is supposedly

valid for $M < 1.4$. Moreover, this relationship merely accounts for the effects of compressibility. It would appear that some effect of the shock must also be included in the determination of H. However, at this time, owing to the lack of exact information, it must be neglected. Consequently, it appears that if the relation $H = 1.29\left(1 + 0.4M_\infty^2\right)$ is used for Mach numbers not too much larger than 1.4, one can expect to have a minimum estimate of the downstream thickening.

SUMMARY OF RESULTS

An investigation of the reflection of a weak shock wave from a boundary layer along a flat plate yielded the following results.

Laminar Case

1. In all cases investigated, the pressure along the wall overcompresses downstream of the point of incidence. The pressure disturbance decays exponentially from a definite value at the point of incidence to zero far upstream of the point of incidence. Downstream, the pressure rises to a maximum value and then falls, gradually, to the constant value corresponding to regular reflection.

The exponential pressure rise appears to be verified in the case of a shock deflection angle of 1°, since separation has probably not occurred. For larger deflection angles (the next larger angle for which there are experimental pressure distributions is 3°), the experimental pressure distributions exhibit the familiar pressure bump between the separation point and the origin. For these angles, a true comparison between experimental results and theoretical results cannot be made since the present theory does not account for the effects of separation.

2. If the upstream influence is considered to be the distance to the point at which the disturbance has decayed to a specified fraction of its amplitude at the origin, the upstream influence, when measured in multiples of the boundary-layer displacement thickness δ_o^*, is found to increase with increasing Reynolds number: $x/\delta_o^* \propto \left(Re/m_\infty\right)^{1/2}$ where x is the coordinate parallel to the flow direction, Re is the Reynolds number, $m_\infty = \sqrt{M_\infty^2 - 1}$, and M_∞ is the free-stream Mach number. For decreasing Mach number, the upstream influence also increases. If the disturbance is considered to decay to, say, 5 percent of its amplitude at the origin, the upstream influence for $M_\infty \approx 2$ and $Re \approx 1500$ is of the order of 30 boundary-layer displacement thicknesses.

3. The pressure gradient is such that the boundary layer may separate ahead of the point of incidence. In the event of separation, an increase of shock strength, for fixed Mach numbers and Reynolds number, increases the distance between the separation point and the point of incidence. For fixed Mach number and shock-deflection angle, the separation point measured in multiples of δ_0^* moves upstream with increasing Reynolds number. For the case of $M_\infty = 1.44$ and $Re = 2000$, the boundary layer separates for all flow-deflection angles $\epsilon > 1.03^\circ$.

For fixed Reynolds number and shock-deflection angle, the separation point, measured in multiples of δ_0^*, moves upstream with decreasing Mach number.

For a complete determination of the constants of integration, an estimate of the downstream boundary-layer thickness was required. For the cases investigated, the effect of the downstream thickening on the outer flow is rather small. In fact, for practical purposes, this effect of downstream thickening can be neglected in the determination of the separation point. The distance between the origin and the separation point will then be slightly underestimated.

4. The present theory is applicable only in the case when a weak shock is incident upon a laminar boundary layer. In addition to the outer flow field, the boundary-layer displacement thickness has also been linearized. The latter linearization enables a linear differential equation with constant coefficients to be obtained for the perturbation velocity potential. This equation immediately yields the general solution of the outer flow. Upon investigating the size of the perturbations, the maximum velocity perturbations are found to be about 10 percent or less. The thickness perturbations, on the other hand, are much larger, being about 30 percent near the origin; thus the linearization of the displacement thickness becomes questionable as the point of incidence is approached. Had the displacement thickness not been linearized, a rather complicated nonlinear differential equation would have been obtained from the boundary condition for the perturbation velocity potential. A solution of this equation would be expected to yield more accurate results. However, it is problematical as to whether the equation could be solved without the imposition of additional assumptions which, in themselves, might nullify any accuracy that the nonlinear boundary condition may provide.

Turbulent Case

In the case of shock-wave interaction with a turbulent boundary layer the upstream influence is found to be considerably less than in the laminar case. In addition, to first order, the incident wave must

be reflected as a compression wave followed immediately by an expansion wave, so that the end pressure condition is satisfied.

Cornell University
Ithaca, N. Y., January 11, 1952

REFERENCES

1. Ferri, Antonio: Experimental Results with Airfoils Tested in the High-Speed Tunnel at Guidonia. NACA TM 946, 1940.

2. Ackeret, J., Feldmann, F., and Rott, N.: Investigations of Compression Shocks and Boundary Layers in Gases Moving at High Speed. NACA TM 1113, 1947.

3. Liepmann, H. W., Roshko, A., and Dhawan, S.: On the Reflection of Shock Waves From Boundary Layers. NACA TN 2334, 1951.

4. Barry, F. W., Shapiro, A. H., and Neumann, E. P.: The Interaction of Shock Waves with Boundary Layers on a Flat Surface. Jour. Aero. Sci., vol. 18, no. 4, April 1951, pp. 229-239.

5. Howarth, L.: The Propagation of Steady Disturbances in a Supersonic Stream Bounded on One Side by a Parallel Subsonic Stream. Proc. Cambridge Phil. Soc., vol. 44, pt. 3, July 1947, pp. 380-390.

6. Tsien, Hsue-Shen, and Finston, Morton: Interaction Between Parallel Streams of Subsonic and Supersonic Velocities. Jour. Aero. Sci., vol. 16, no. 9, Sept. 1949, pp. 515-528.

7. Robinson, A.: Wave Reflection near a Wall. Rep. No. 37, The College of Aero., Cranfield, May 1950.

8. Lighthill, M. J.: Reflection at a Laminar Boundary Layer of a Weak Steady Disturbance to a Supersonic Stream, Neglecting Viscosity and Heat Conduction. Quart. Jour. Mech. and Appl. Math., vol. III, pt. 3, Sept. 1950, pp. 303-325.

9. Bardsley, O., and Mair, W. A.: The Interaction between an Oblique Shock-Wave and a Turbulent Boundary-Layer. Phil. Mag., ser. 7, vol. XLII, no. 42, Jan. 1951, pp. 29-36.

10. Lees, Lester: Interaction between the Laminar Boundary Layer over a Plane Surface and an Incident Oblique Shock Wave. Rep. No. 143, Contract N6ori-270, Task Order No. 6, Office of Naval Research, Contract NOrd-7920, Task No. PRN-2-E, Bur. Ord., U. S. Navy, and Aero. Eng. Lab., Princeton Univ., Jan. 24, 1949.

11. Oswatitsch, K., and Wieghardt, K.: Theoretical Analysis of Stationary Potential Flows and Boundary Layers at High Speed. NACA TM 1189, 1948.

12. Kuo, Yung-Huai: Reflection of a Weak Shock Wave from a Boundary Layer along a Flat Plate. II - Interaction of Oblique Shock Wave with a Laminar Boundary Layer Analyzed by Differential-Equation Method. NACA TN 2869, 1953.

13. Howarth, Leslie: Concerning the Effect of Compressibility on Laminar Boundary Layers and Their Separation. Proc. Roy. Soc., (London), ser. A, vol. 194, no. 1036, July 1948, pp. 16-42.

14. Emmons, Howard W., and Brainerd, John Grist: Temperature Fffects in a Laminar Compressible-Fluid Boundary Layer along a Flat Plate. Jour. Appl. Mech., vol. 8, no. 3, Sept. 1941, pp. A-105 - A-110.

15. Brainerd, J. G., and Emmons, H. W.: Effect of a Variable Viscosity on Boundary Layers, with a Discussion of Drag Measurements. Jour. Appl. Mech. vol. 9, no. 1, March 1942, pp. A-1 - A-6.

16. Crocco, Luigi: Lo strato limite laminare nei gas. Monografie Scientifiche di Aeronautica. No. 3, Ministero della Difesa-Aeronautica, Roma, Dec. 1946.

17. Ritter, A.: On the Reflection of a Weak Shock Wave from a Boundary Layer along a Flat Plate. Thesis, Cornell Univ., 1951.

18. Fage, A., and Sargent, R. F.: Shock Wave and Boundary Layer Phenomena near a Flat Surface. Proc. Roy. Soc. (London), ser. A, vol. 190, no. 1020, June 17, 1947, pp. 1-20.

19. Nitzberg, Gerald E., and Crandall, Stewart: Some Fundamental Similarities between Boundary-Layer Flow at Transonic and Low Speeds. NACA TN 1623, 1948.

20. Lees, Lester: The Stability of the Laminar Boundary Layer in a Compressible Fluid. NACA Rep. 876, 1947.

21. Stewartson, K.: Correlated Incompressible and Compressible Boundary Layers. Proc. Roy. Soc. (London), ser. A, vol. 200, no. 1060, Dec. 22, 1949, pp. 84-100.

TABLE I

COEFFICIENTS USED IN DETERMINING CONSTANTS OF INTEGRATION

M_∞	$Re = \frac{U\delta_o^*}{\nu_o}$	$\frac{-(\lambda_3 + \lambda_1)}{(\lambda_2 - \lambda_3)(\lambda_2 - \lambda_1)}$	$\frac{\lambda_1\lambda_3}{(\lambda_2 - \lambda_3)(\lambda_2 - \lambda_1)}$	$\frac{(\lambda_3 + \lambda_2)}{(\lambda_3 - \lambda_1)(\lambda_2 - \lambda_1)}$	$\frac{-\lambda_2\lambda_3}{(\lambda_3 - \lambda_1)(\lambda_2 - \lambda_1)}$	$\frac{-(\lambda_2 + \lambda_1)}{(\lambda_3 - \lambda_1)(\lambda_2 - \lambda_3)}$	$\frac{\lambda_1\lambda_2}{(\lambda_3 - \lambda_1)(\lambda_2 - \lambda_3)}$
1.44	250	2.970	0.0642	0.965	0.0250	2.020	-0.961
	500	3.810	.0435	1.771	.0225	2.370	-.980
	1000	4.880	.0282	2.822	.0179	2.050	-.989
	2000	6.600	.0192	4.360	.0136	2.230	-.977
2	250	1.103	0.0546	0.747	0.0453	0.357	-0.992
	500	1.575	.0439	1.168	.0385	.408	-.994
	1000	2.182	.0330	1.815	.0311	.369	-.998
	2000	3.070	.0235	2.675	.0224	.396	-.999
2.5	250	0.402	0.0366	0.698	0.0785	-0.295	-1.043
	500	.651	.0363	1.038	.0706	-.386	-1.034
	1000	1.018	.0326	1.472	.0558	-.455	-1.022
	2000	1.540	.0287	2.025	.0434	-.488	-1.015

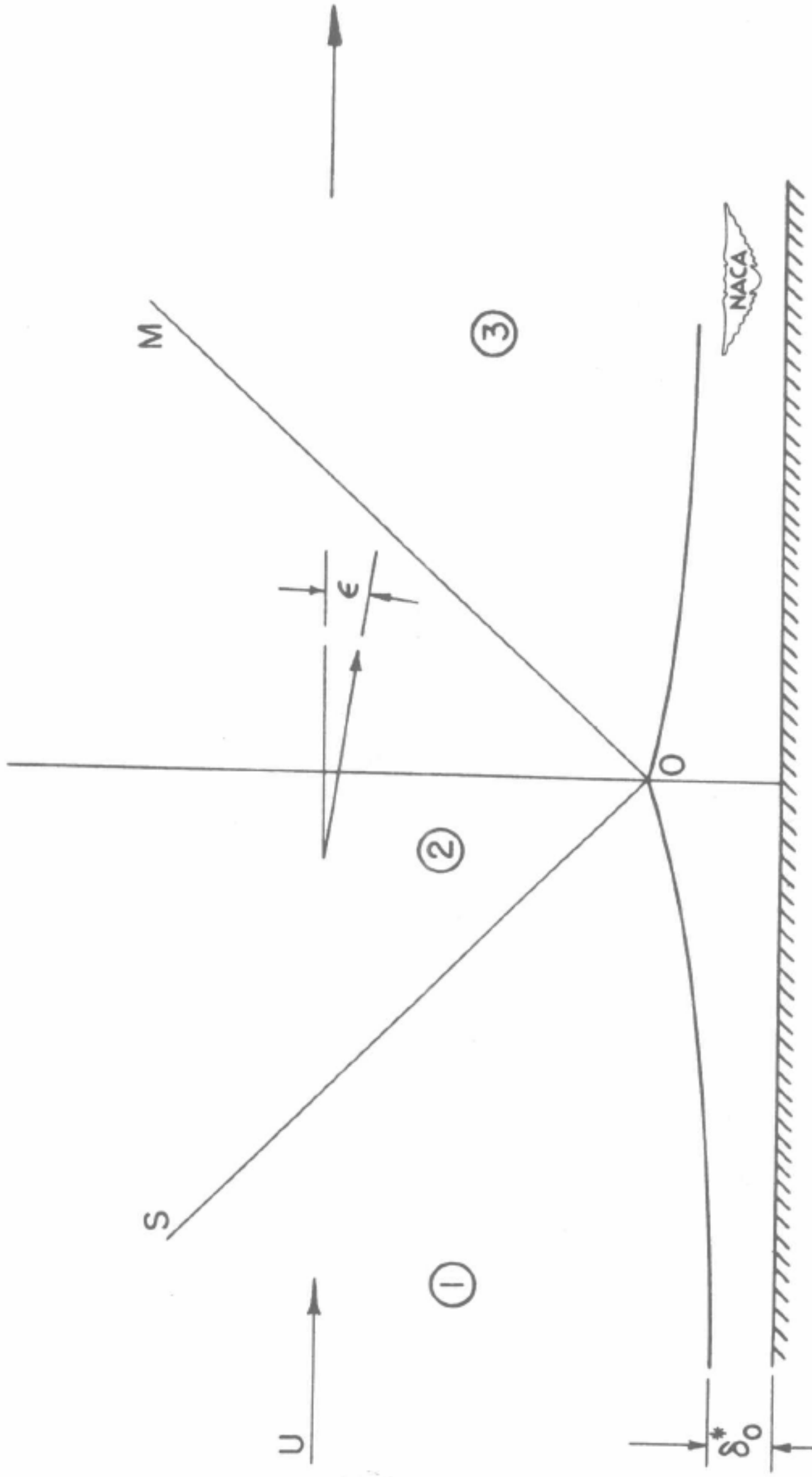

Figure 1.- Simplified model of shock-wave boundary-layer interaction.

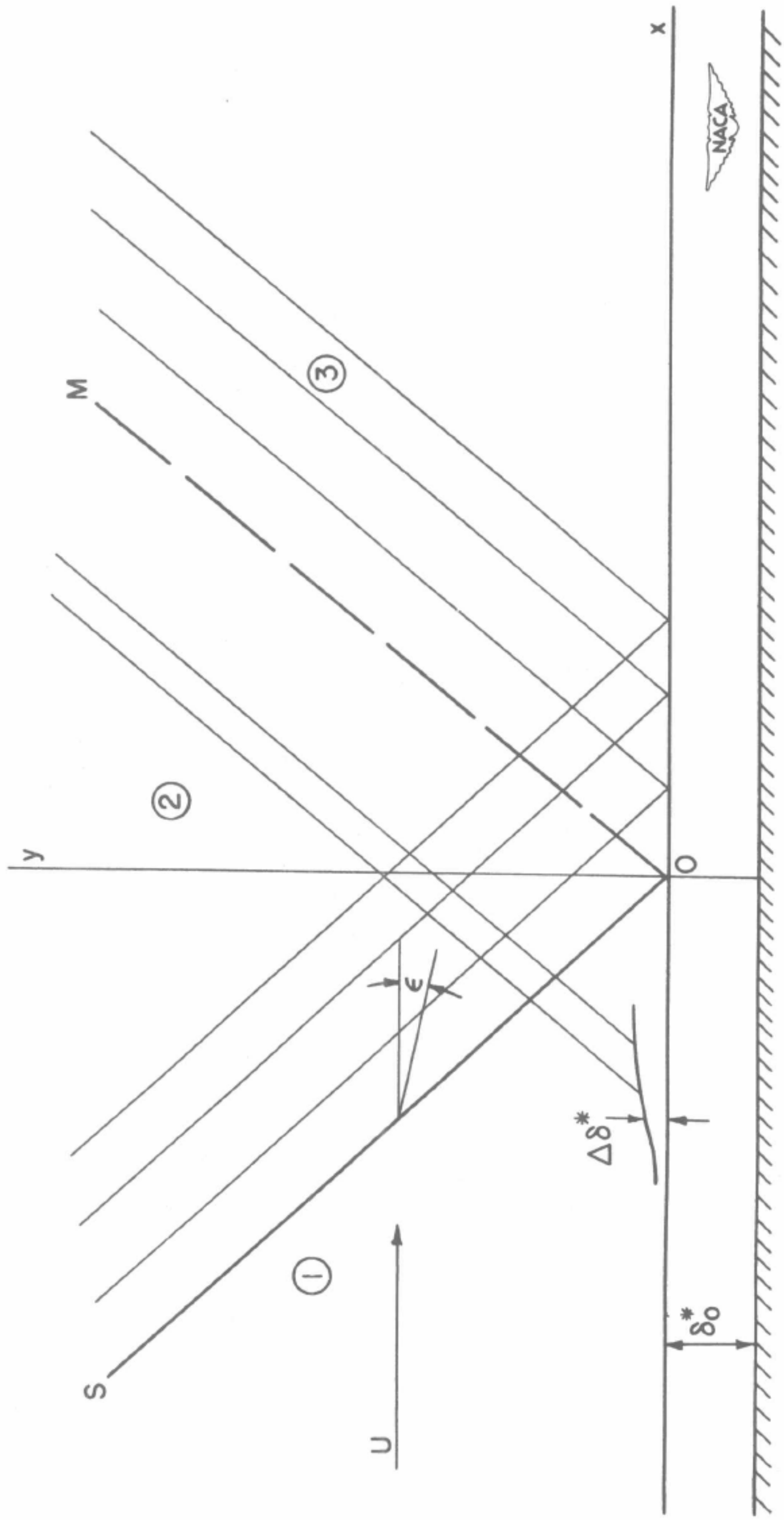

Figure 2.- Shock-wave boundary-layer interaction showing choice of axes.

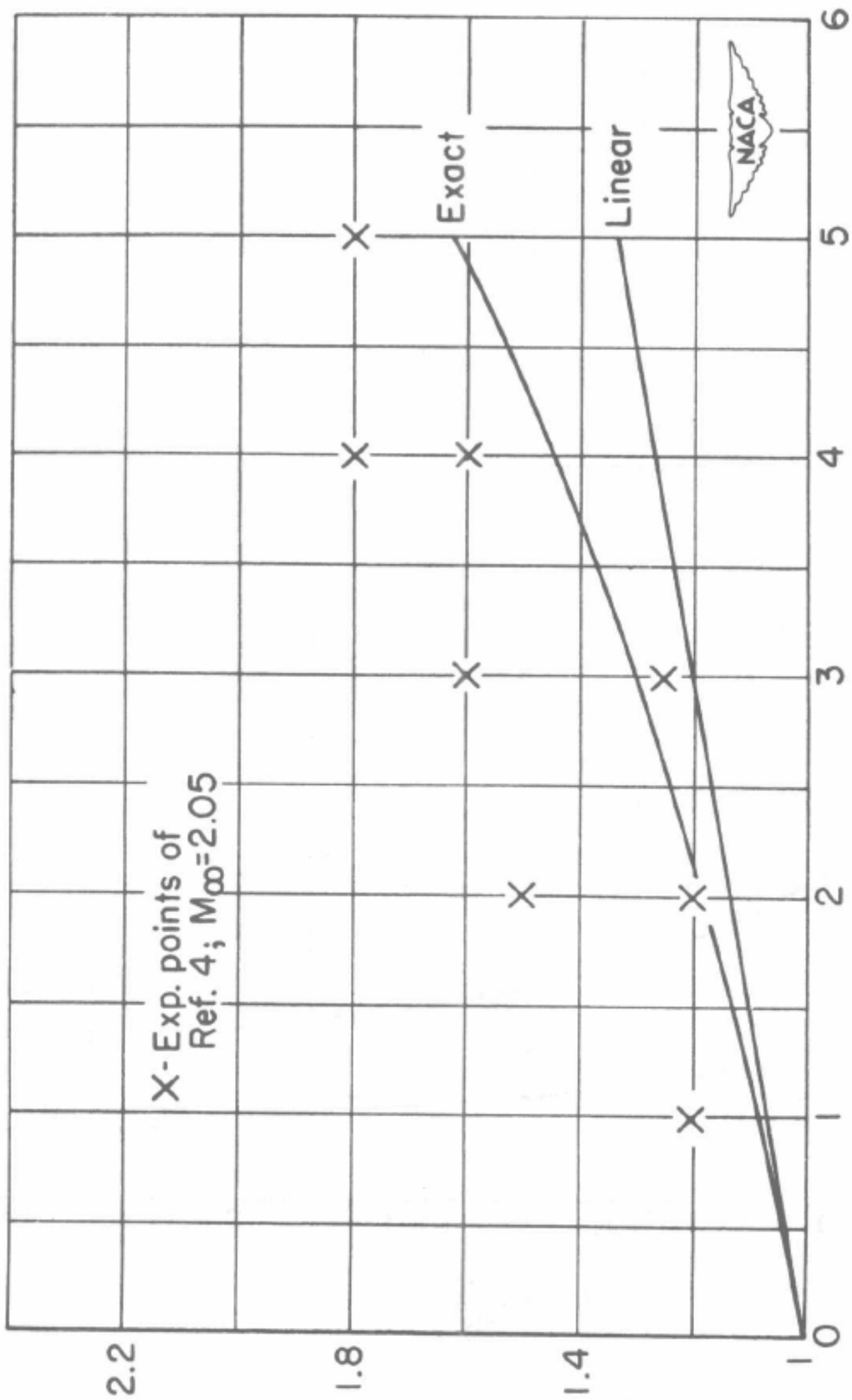

Figure 3.- Displacement-thickness ratio. Laminar case; $M_\infty = 2$;

$$\frac{\delta_3^*}{\delta_1^*} = \frac{\rho_1}{\rho_3}\left(\frac{u_1}{u_3}\right)^{2+H} \quad ; \text{ and } \quad H = 2.50 + 3.50\left(\frac{\gamma - 1}{2}\right)M_\infty^2 .$$

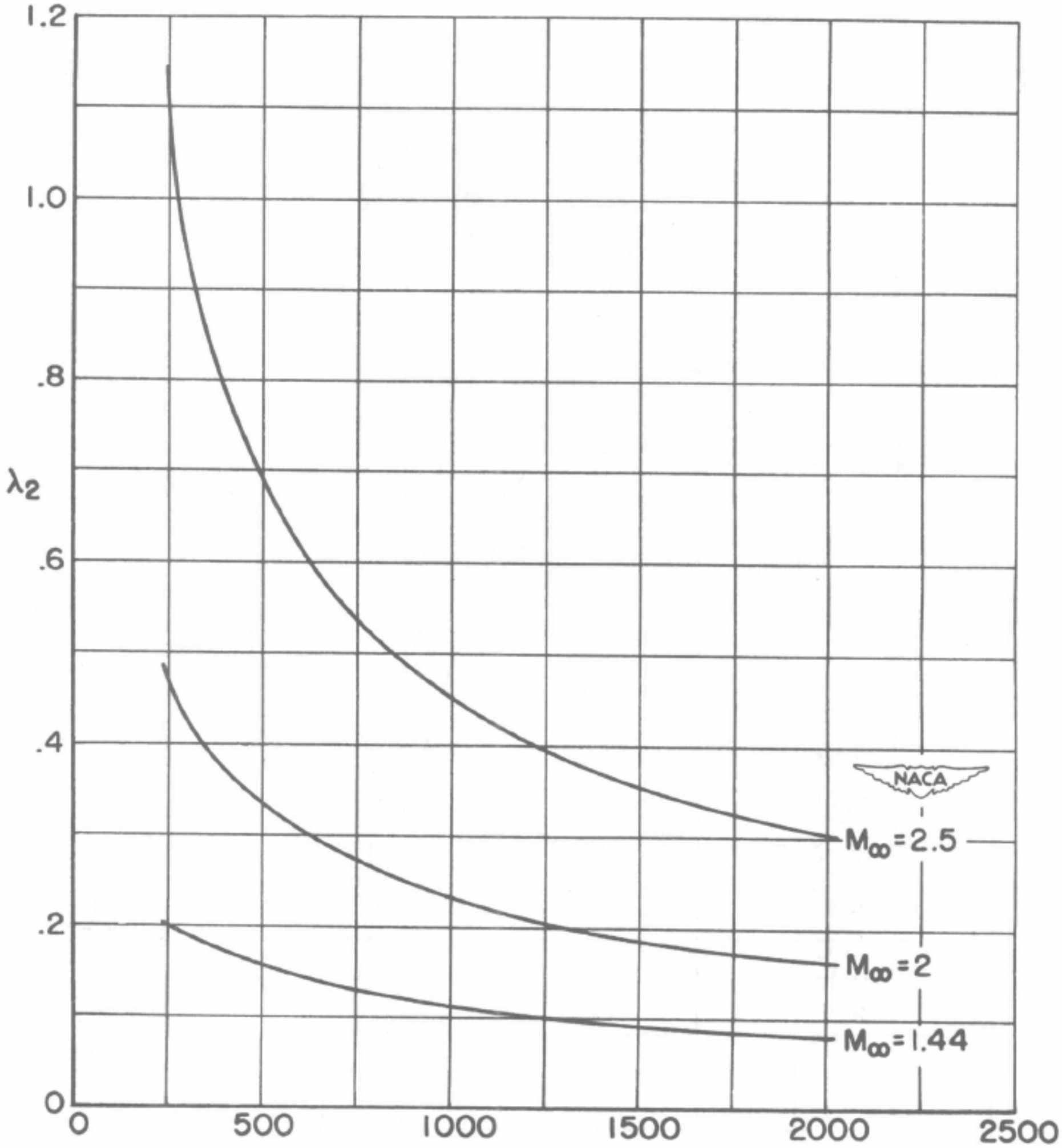

$$Re = \frac{U\delta_o}{\nu_o}$$

(a) Various values of M_∞.

Figure 4.- Measure of upstream influence. $x_d/\delta_o^* = -\frac{1}{\lambda_2}\log_e(1/\alpha)$; disturbance at x_d/δ_o^* is α percent of disturbance at origin.

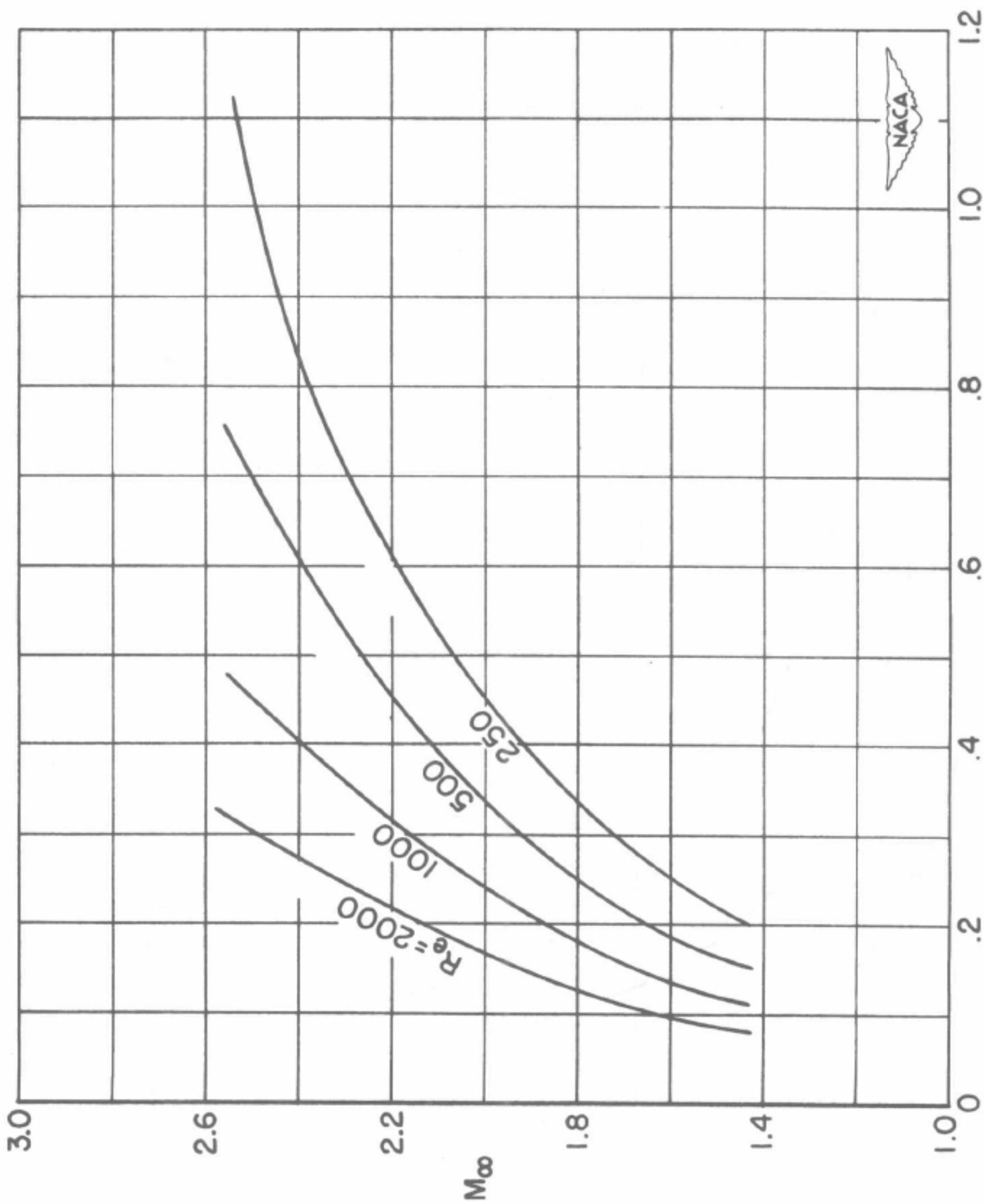

(b) Various values of R_e.

Figure 4.- Concluded.

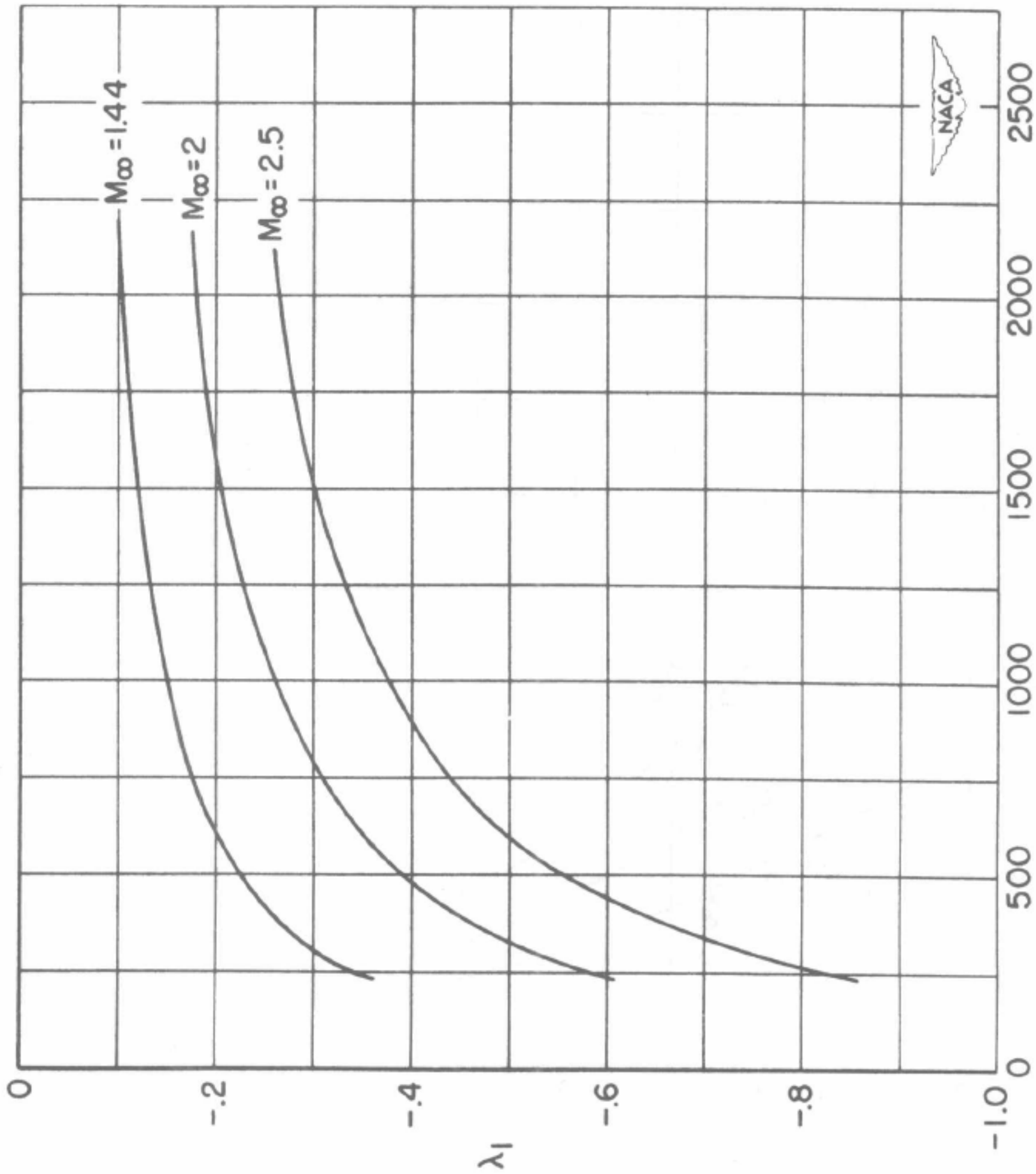

Figure 5.- Reynolds number against λ_1. $Re = U\delta_0^*/\nu_0$.

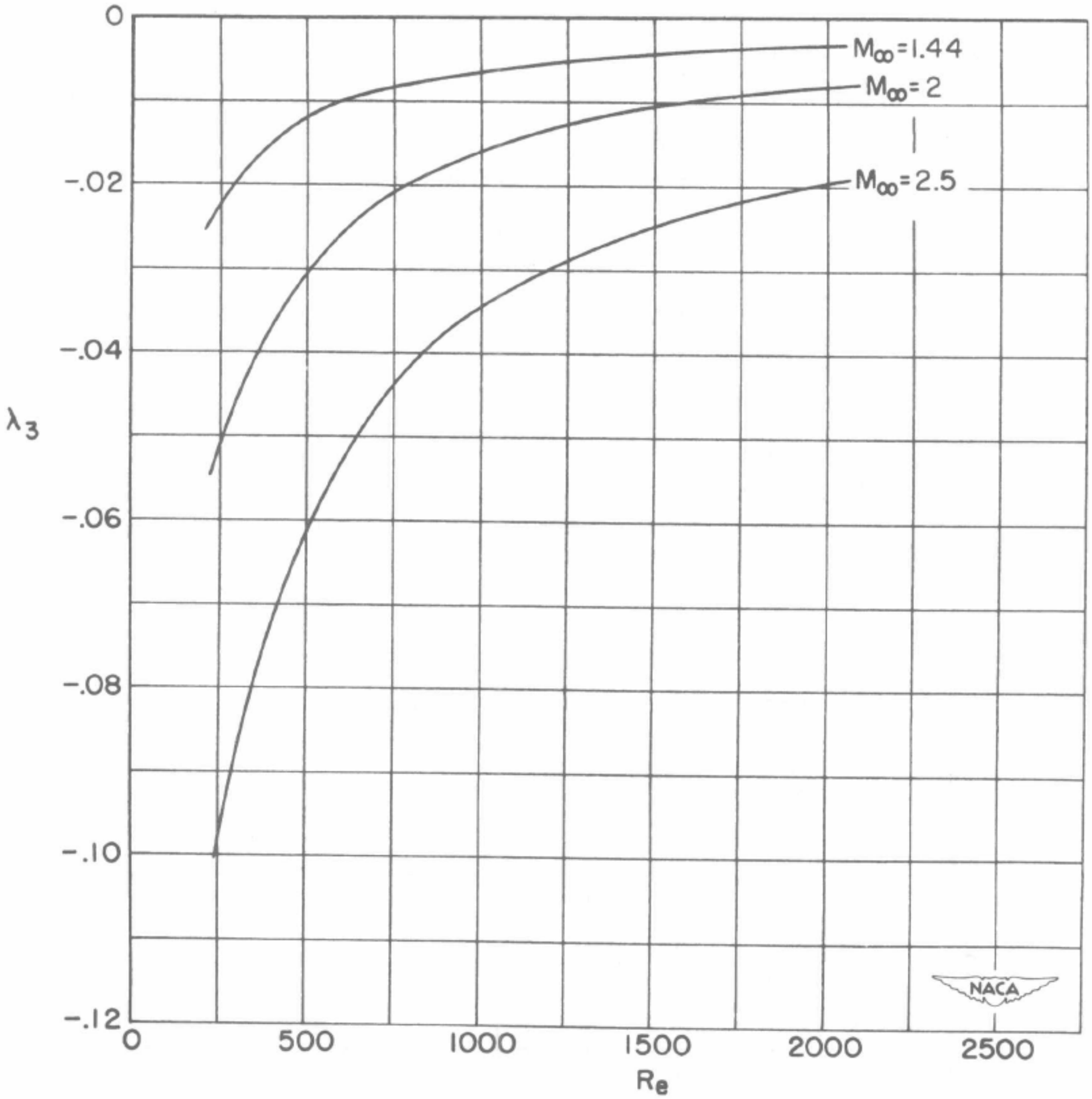

Figure 6.- Reynolds number against λ_3. $Re = U\delta_0^*/\nu_0$.

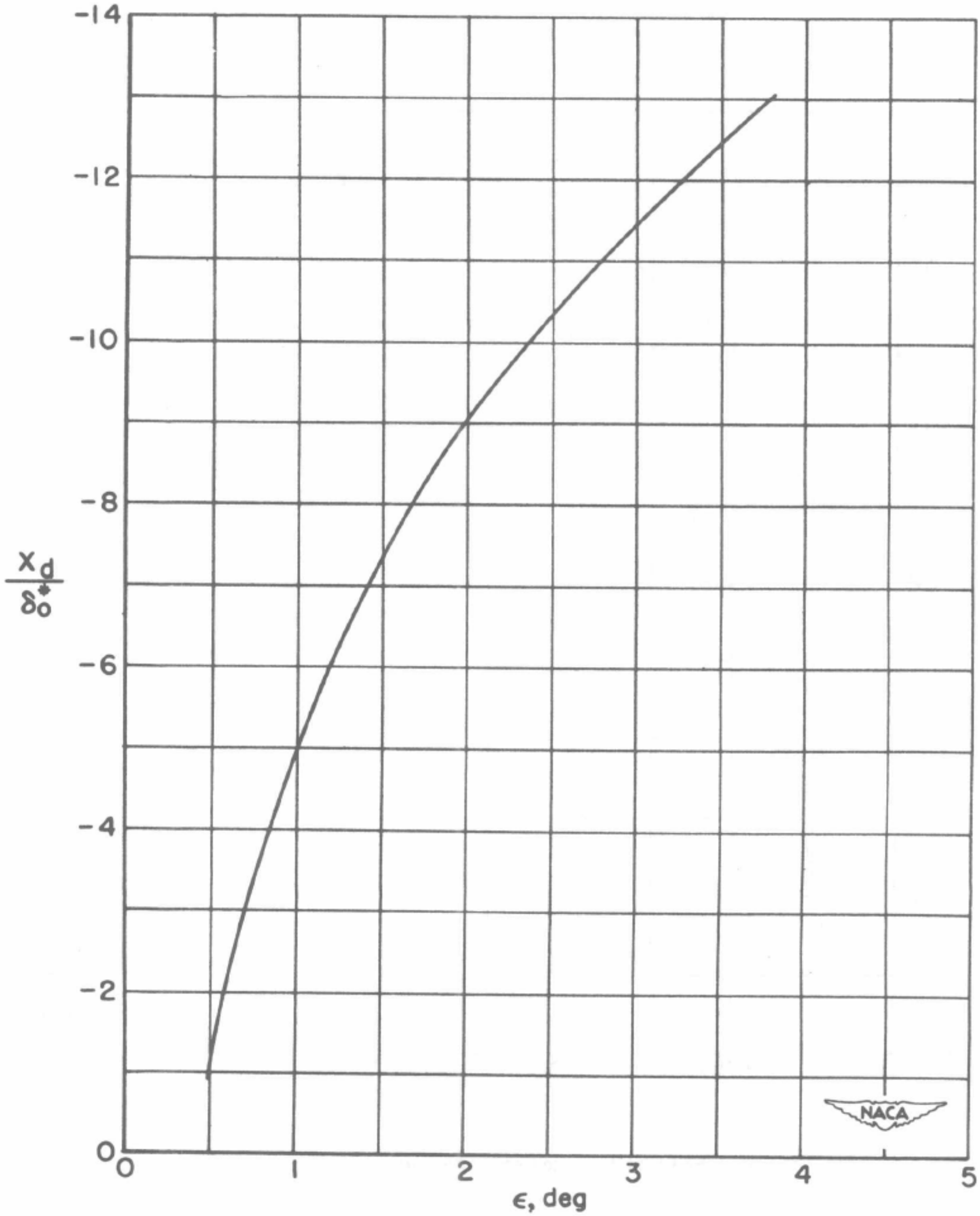

Figure 7.- Upstream influence against deflection angle. $M_\infty = 2$; $Re = U\delta_o^*/\nu_o = 2000$; and $Re_x = Ux/\nu_\infty \approx 51{,}600$.

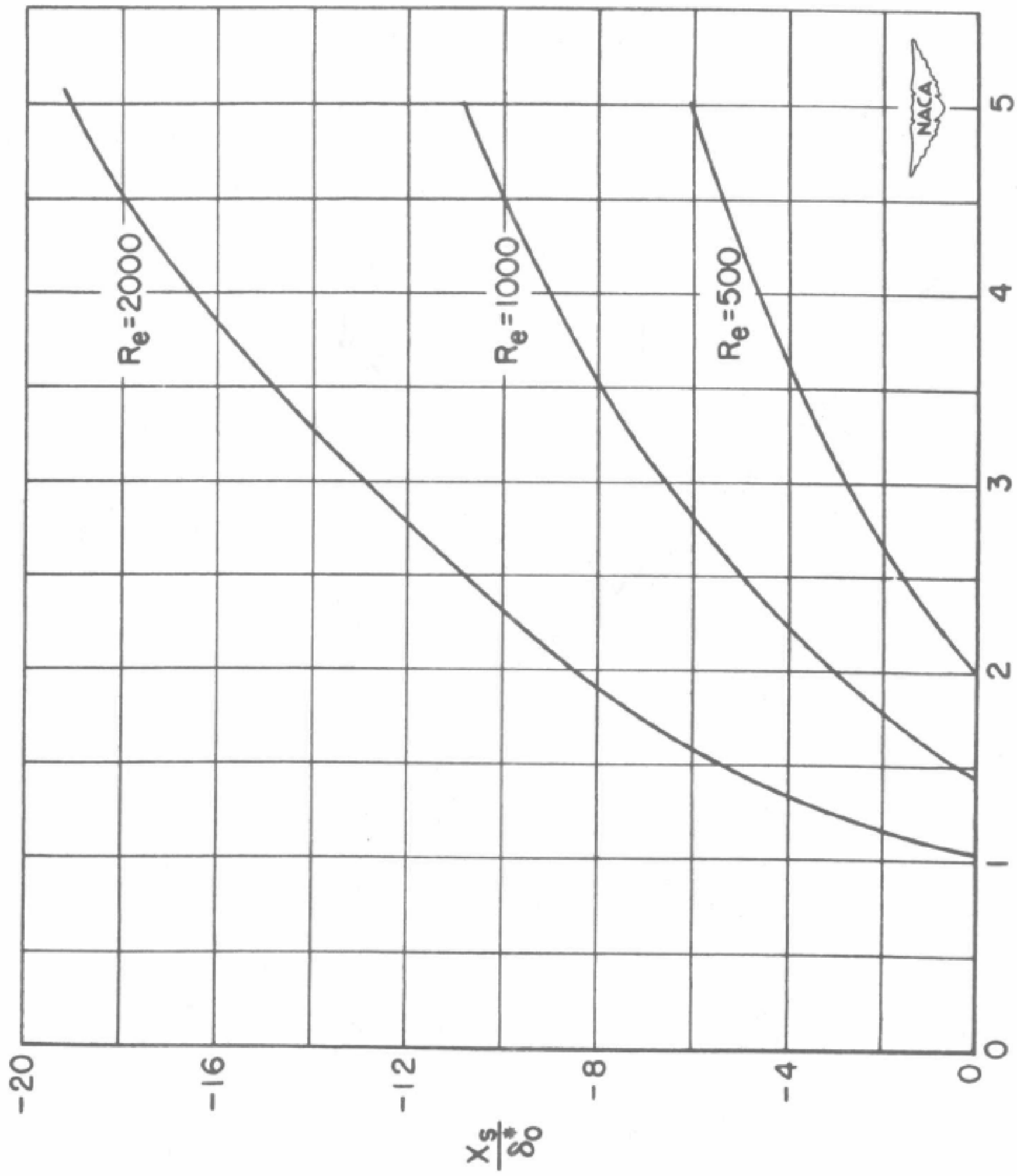

Figure 8.- Separation point against deflection angle. $M_\infty = 1.44$; $Re = U\delta_0^*/\nu_0$.

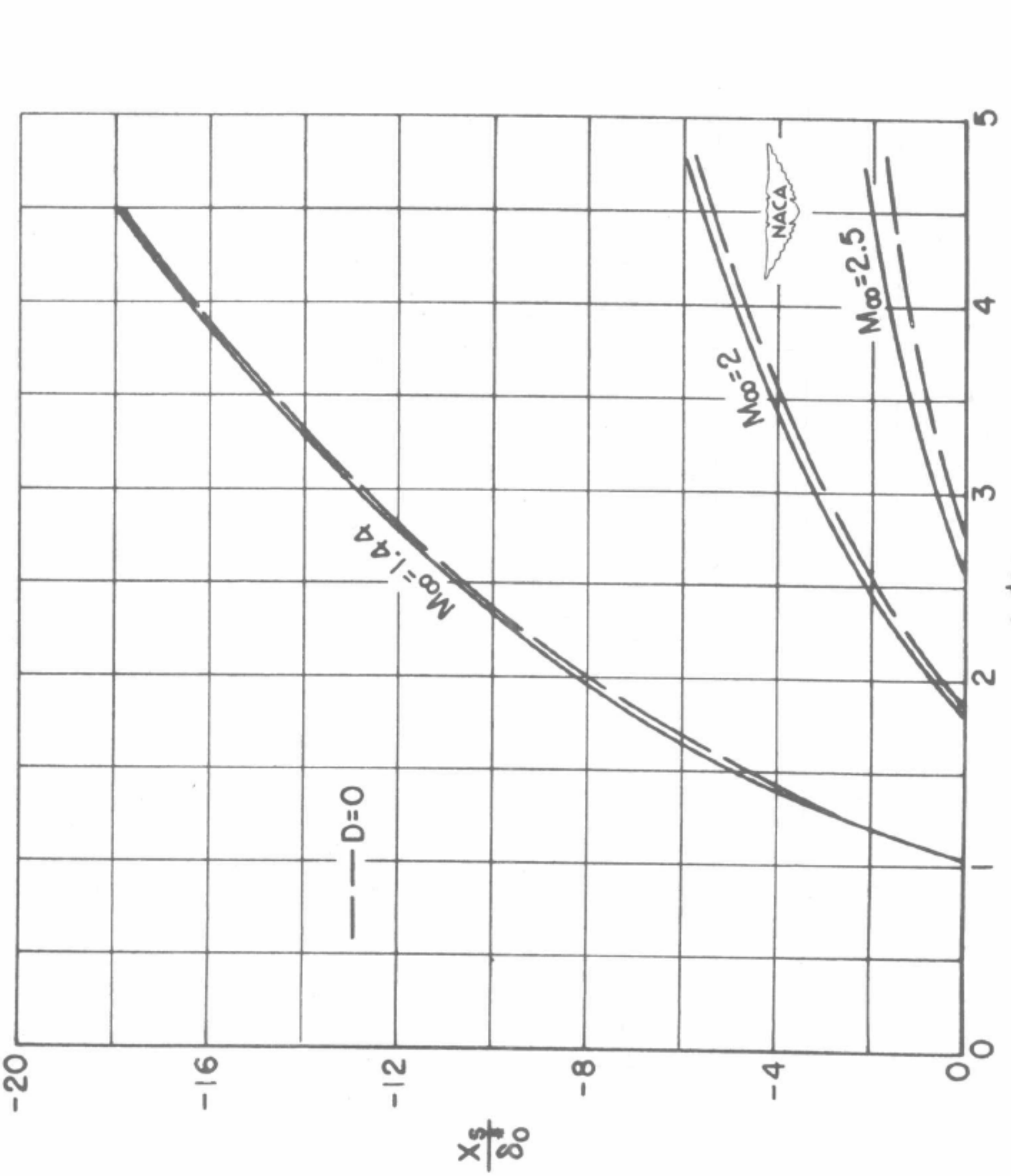

Figure 9.- Separation point against deflection angle. $Re = U\delta_0^*/\nu_0 = 2000$.

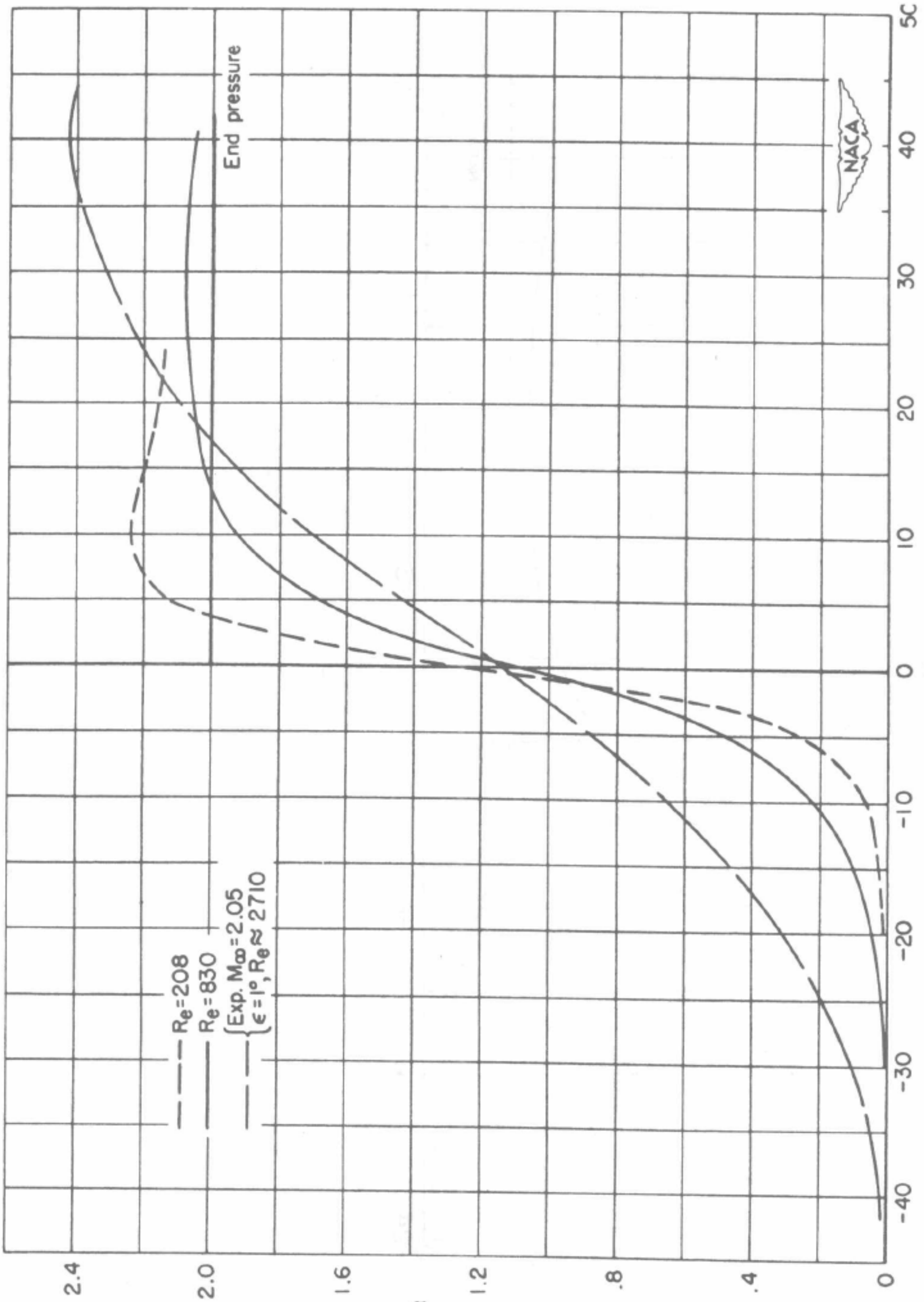

Figure 10.- Wall pressure distribution. $M_\infty = 2$; $Re = U\delta_0^*/\nu_\infty$.

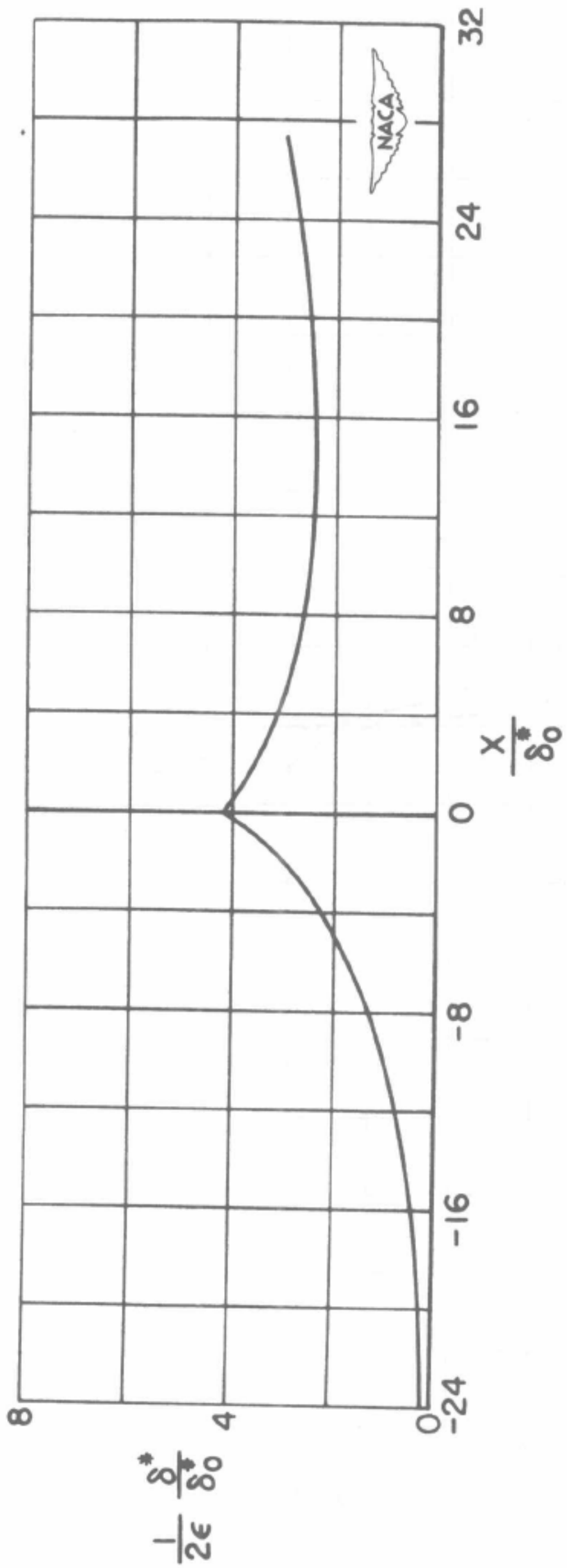

Figure 11.- Perturbed boundary-layer displacement thickness. $M_\infty = 1.44$; $Re = U\delta_0^*/\nu_0 = 500$.

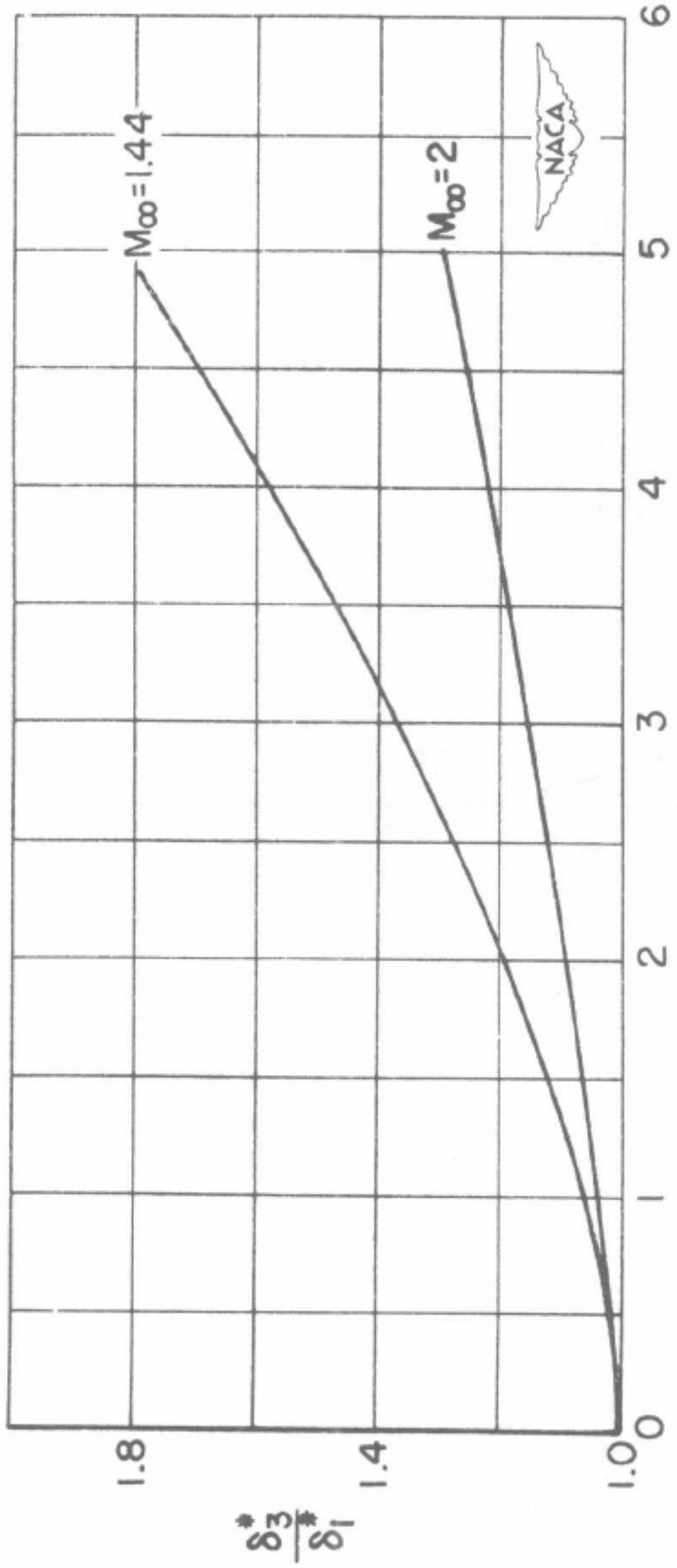

Figure 12.- Downstream thickening turbulent boundary layer

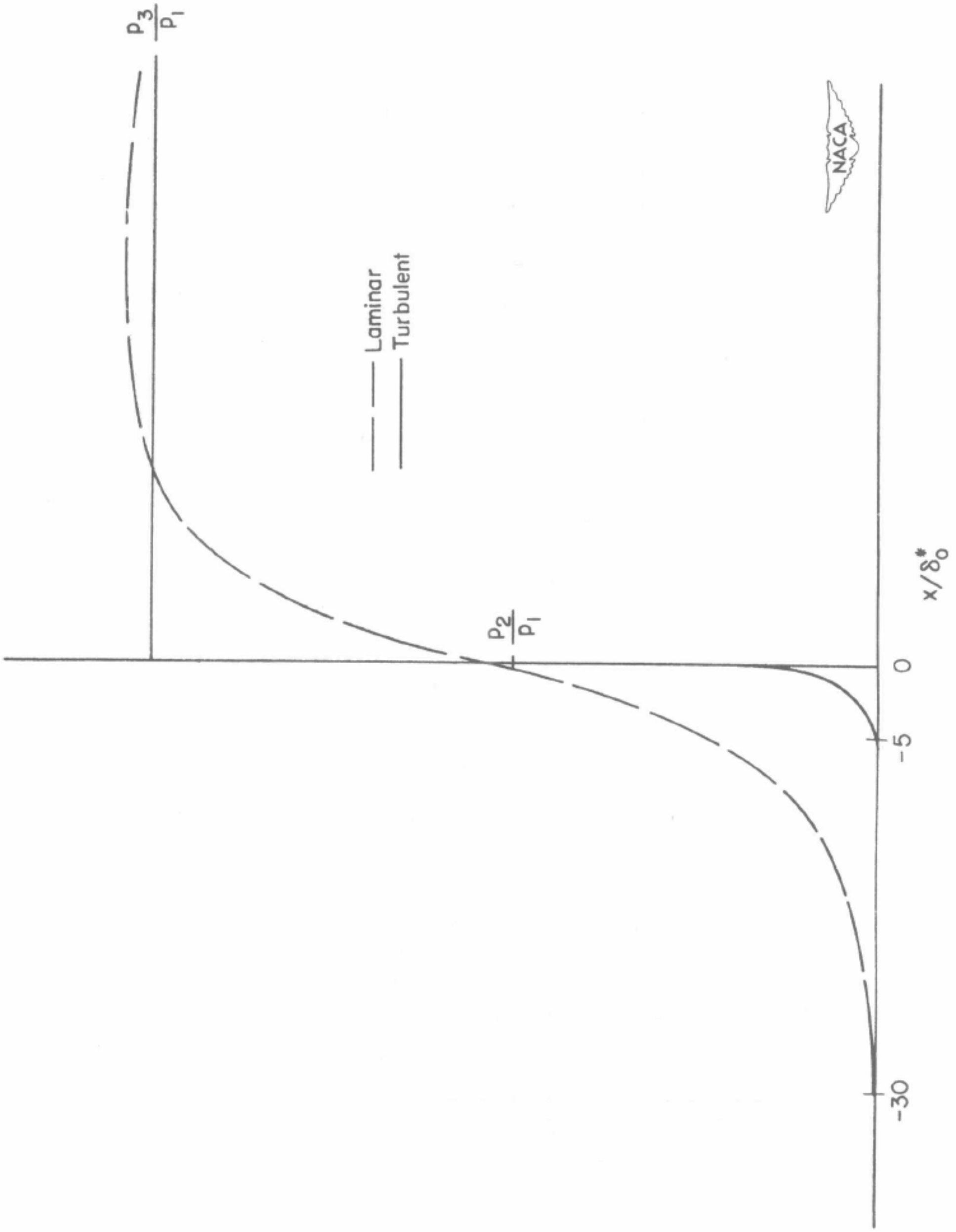

Figure 13.- Wall pressure distribution.

22921

NATIONAL ADVISORY COMMITTEE FOR AERONAUTICS

TECHNICAL NOTE 2869

REFLECTION OF WEAK SHOCK WAVE FROM A BOUNDARY LAYER ALONG A FLAT PLATE. II - INTERACTION OF OBLIQUE SHOCK WAVE WITH A LAMINAR BOUNDARY LAYER ANALYZED BY DIFFERENTIAL-EQUATION METHOD [1)]

By Yung-Huai Kuo

SUMMARY

By analogy with the boundary-layer concept, the flow produced by the interaction between a shock wave and a laminar boundary layer is subdivided into a viscous layer and a potential field. The assumptions that the compressibility effect in the inner layer is negligible and that the original flow in the outer layer is uniform lead to simple analytic solutions for the perturbed flow. The joining conditions at the interface between the layers determine an eigenvalue which gives the rate of decay and the character of the disturbances both upstream and downstream of the point of incidence. The final conclusions are in agreement with experiments.

INTRODUCTION

The present investigation is an independent study of the interaction of an oblique shock with a laminar boundary layer in a compressible supersonic stream. In reference 1, where interaction of weak shock waves with both laminar and turbulent boundary layers was treated, the integrated momentum across the boundary layer was considered, rather than the balance among various dynamic effects at each point. This momentum-integral method is simple and, in certain respects, powerful and capable of yielding useful qualitative information such as the upstream pressure influence, pressure distribution, and the growth of boundary-layer thickness due to the presence of a shock, but it fails in regard to what actually happens inside the boundary layer. In the present report a different approach has been adopted, with the intention of filling the gap left by the previous investigation. The purpose will, on the whole, be complementary, so as to provide a physical picture for the understanding of this complex phenomenon.

---

1) *NACA Technical Note*, 1953, No. 2869

Contrary to reference 1, the differential-equation method is employed here. According to available experimental observation, when an oblique shock is incident upon a laminar boundary layer the resultant flow bears no resemblance to the flow predicted by potential theory. For if the viscous flow is absent the flow ahead of the shock will not be affected. Because of the presence of the boundary layer in which there is a subsonic layer, however, a sudden decrease of pressure at a point will immediately be transmitted forward by the inability of the subsonic layer to support an excess pressure rise. When the pressure is transmitted, the flow in the boundary layer will be retarded and the streamlines distorted. Since the outer field is supersonic, this change occurring in the viscous layer will affect the whole potential field. This is actually observed. For stronger shocks, the flow in the boundary layer generally will separate and will have backflow under the influence of an adverse pressure gradient. An adequate theory that is able to account for the observed effects cannot be formulated unless the boundary-layer hypothesis is abandoned entirely. One therefore is faced by a much more difficult mathematical problem.

To restrict the scope and complexity of this study, let it be assumed first of all that the boundary is an insulated flat plate, and, secondly, that the incident shock is weak and its angle of incidence is such that regular reflection would be possible, were the flow frictionless, and, lastly, that the free-stream Mach number is not large. Under these assumptions, the angle of deflection of the flow in passing through the shock wave will be small, and the temperature variation between the free-stream condition and that of the plate will not be large. In fact, the study of a laminar boundary layer indicates that, for moderate Mach number, the temperature as well as the compressibility effects are unimportant (reference 2). This must remain true even if the flow is not boundary-layer flow. Therefore, without loss of generality, it will be assumed that the viscosity and thermal conductivity of the gas will be taken as constant and the Prandtl number is unity.

In order to bring the interaction problem within the scope of practical mathematical analysis, these simplifying hypotheses have to be made in the absence of a proper method of approximation, such as the boundary-layer theory. Broadly speaking, examination of schlieren photographs of the flow produced by the interaction between a shock and a laminar boundary layer will reveal that two characteristically different outer and inner regions exist for sufficiently high Reynolds number. The outer field is characterized by its strong potential character, whereas the region close to the wall is predominantly viscous, which is quite reminiscent of the boundary-layer flow. It appears natural, therefore, to assume a priori that the viscous effect is confined to a thin layer in the vicinity of the boundary and the outer main flow is potential. These two different flows are then in dynamical equilibrium. If one is disturbed, the other will be affected. Since

the outer field is supersonic, any local change will be felt in a much larger region than that in a subsonic field.

After the flow field is separated into two regions, specific assumptions regarding the structure of the viscous layer can be made. It is important to note that in the case of a compression incident wave, the overwhelming effect taking place in the viscous layer is the sudden decrease of the velocity or even reversal of flow (backflow). If backflow sets in, the flow speed in the subsonic region will be very much reduced. As a result of this, the streamlines will be pushed outward and the flow compressed. On account of the displacement of streamlines, the subsonic region will become thicker, and the thickening of the subsonic region is a decisive factor that distinguishes the strong from weak interactions. The importance of this dimension (the thickness of the subsonic layer) has already been established by Tsien and Finston (reference 3) in the case of inviscid theory.

The viscous layer, thus, must have two distinct sublayers, each displaying a different character. In the supersonic layer, the flow is characterized by large velocities and is not unlike that of an unseparated boundary layer. Therefore, for this layer both viscous and inertia forces are important. On the other hand, in the subsonic layer, especially with backflow, the average speed will be very small. In this case, because of slow motion and moderate temperature change, the change of density is always a lower-order effect. In fact, the contribution due to compressibility is proportional to the square of Mach number, and, if the average Mach number in the subsonic region is small, the compressibility effect is, indeed, negligible. Because of this physical fact, the subsonic layer will be taken as incompressible.

With these assumptions, the problem is finally solved by perturbation of weak incident waves. As a test of these assumptions, a simple flow with broken-line velocity profile is taken as the basic flow: In the incompressible layer, the velocity is a linear function of the distance from the plate; in the compressible layer, it is constant. The density in the basic flow is constant in each layer but takes different values. Thus, at the interface where the two flows join, the velocity is continuous but density is discontinuous. For this case, a first-order solution consistent with these assumptions is completely determined.

In the case of weak shock, excellent agreement with experiments has been achieved for the pressure distribution on the plate. It confirms the conjecture that separation of the flow as well as backflow always occur. Because of the occurrence of backflow, transition downstream of the point of incidence is unavoidable in the viscous layer. There are strong experimental evidences but detailed investigations are yet to be conducted. In the outer field, on the other hand, it is predicted that in the place of the regularly reflected shock there is a strong

expansion, and farther downstream a train of strong compression waves must exist, eventually forming an envelope. Therefore, downstream of the point of incidence a second shock must occur. This deduction is also confirmed by experiments.

Lastly, the importance of nonlinear effect is discussed.

This study was conducted at the Graduate School of Aeronautical Engineering, Cornell University, under the sponsorship and with the financial assistance of the National Advisory Committee for Aeronautics. The author wishes to acknowledge the efficient assistance of Mr. Nelson H. Kemp.

SYMBOLS

A	constant
a'	speed of sound
$C_1, C_2, C_3, C_4, C_5, C_6$	constants
D	constant
d	constant
d/dt	convective derivative
F,G	scalar functions
f_1, g_1	defined by equations (43) and (41), respectively
H	nondimensional enthalpy
$I_{1/3}\left(\frac{2}{3}\eta^{3/2}\right)$	Bessel function of first kind with imaginary argument
$J_{1/3}$	Bessel function of first kind with real argument
K_1, K_2, K_3, K_4	constants

$K_{1/3}\left(\frac{2}{3}\eta^{3/2}\right)$ Bessel function of second kind with imaginary argument

$$k = (\gamma - 1)M^2/R^2\left[1 + \left(\frac{4\gamma}{3} - 1\right)\frac{\lambda M^2}{R}\right]$$

$$\tilde{k} = \left[1 + \frac{4}{3}(\gamma - 1)\frac{M^2\lambda}{R}\right]\Bigg/\left(1 + \frac{4}{3}\frac{\gamma M^2\lambda}{R}\right)$$

L	length of plate from leading edge to point of incidence
M	Mach number
n	dilatation
P	pressure
P_1, P_2, P_3	constants
p	nondimensional pressure $\left(p'/\rho_\infty U_\infty^2\right)$
p'	pressure
R	Reynolds number $\left(U_\infty L/\nu_\infty\right)^{1/2}$
$r = \Gamma(1/3)/3^{2/3}$	
T	nondimensional temperature
T'	temperature
s,t	defined by equations (B4)
U	velocity
u,v	nondimensional velocity components
u',v'	velocity components
$U^{(1)}$, $V^{(1)}$	constants

$X = -d/\lambda_2$

x,y	nondimensional Cartesian coordinates
x',y'	coordinates
$Z(\tilde{\eta})$	defined by equation (C4)
z	defined by equation (30)
$\alpha = 0.332$	
$\tilde{\alpha} = \rho_o(0)_{\alpha R}$	
$\beta = \sqrt{M^2 - 1}$	
β_1	defined by equation (43)
β_2	defined by equation (C15)
Γ (z)	gamma function
γ	ratio of specific heats
Δ	Laplacian operator
$\delta\vartheta$	deflection of flow (equation (B6))
ϵ	flow-deflection angle
η	defined by equation (31)
$\tilde{\eta}$	defined by equation (C6)
$\Lambda(\eta)$	defined by equation (C5)
λ	eigenvalue
ν_∞	free-stream kinematic viscosity
ρ	nondimensional density
ρ'	density

ρ_o density at $y = 0$

$\sigma = \lambda R - \lambda^2$

$\tau = \lambda(\lambda\tilde{\alpha})^{-1/3}$

$\tilde{\tau}$ defined by equation (C7)

φ nondimensional velocity potential

ψ stream function

ω angle between velocity and shock

Subscripts:

C complementary

c solution in compressible layer

i solution in incompressible layer

o value on plate

p particular

s due to step wave

sep at separation point

t due to transmitted wave

x partial derivative with respect to x

y partial derivative with respect to y

1 in region 1, before shock (see fig. 1)

2 in region 2, behind shock (see fig. 1)

3 in region 3 (see fig. 1)

∞ free stream

$\parallel$ parallel to oblique shock wave

$\perp$ perpendicular to oblique shock wave

Superscripts:

(0) zeroth order

(1) first order

(2) second order

(3) third order

STATEMENT OF PROBLEM AND BASIC ASSUMPTIONS

Let there be a laminar boundary layer in a compressible viscous fluid along an insulated flat plate immersed in a steady uniform supersonic stream, and let an oblique shock be incident upon the plate. When the steady condition is established, the flow in the neighborhood exhibits a character which is entirely different from the original flow.

From all indications, this flow does not obey the boundary-layer approximation; nevertheless, for simplicity for future analysis, the concept of boundary layer, or viscous layer, will be retained. Namely, the whole flow field is visualized as consisting of inviscid and viscous flow in equilibrium with each other. The possibility of existence of such a demarcation line will be assumed at this moment. The solutions obtained are consistent with the assumption, as will be seen later, so that the theory is self-consistent at least. Naturally, its further justification rests upon experimental evidence.

The main feature in the viscous layer is that, in the case of a compression wave in the inviscid outer flow, backflow generally exists. For this reason, terms in the equations of motion which are unimportant according to boundary-layer approximation become decisive as the supposed large-order terms vanish. Therefore, the pressure gradients along both directions have to be considered. To simplify the mathematical process, some minor effects, such as the variation of the viscosity coefficient and thermal conductivity with temperature, will be neglected and the Prandtl number will be taken equal to 1. For moderate Mach numbers, less than 3, say, this neglect, according to boundary-layer investigations, will have little effect on the major characteristics of the flow.

The inviscid flow generally is rotational, as it involves shocks. This is particularly true in the case of a local supersonic zone over

a curved surface. For a purely supersonic flow, if the shock is slightly curved, the vorticity generated behind the shock is of high order and can be neglected. The perturbed flow in the outer region can then be regarded as irrotational.

As the region which is influenced by the presence of the shock, according to experimental observations, is confined to an area about the point of incidence, with a dimension only a fraction of the length of the plate, a point which lies at a distance about the length of the plate from the point of incidence will be considered as at infinity. Consequently, the boundary-layer flow will be replaced by a "shear flow" extending to both positive and negative infinities. This approximation is justified if the derivative along the flow is much larger in the perturbed flow than that in the original flow. For large Reynolds number, this condition can always be satisfied.

METHOD OF SOLUTION

The flow is supposed to be two dimensional and steady and the fluid is compressible. If the flow field can be subdivided into viscous and nonviscous regions, the flow in the viscous layer satisfies in dimensionless variables the system:

$$\rho \frac{du}{dt} = -p_x + \frac{1}{R}\left(\Delta u + \frac{1}{3} n_x\right) \tag{1}$$

$$\rho \frac{dv}{dt} = -p_y + \frac{1}{R}\left(\Delta v + \frac{1}{3} n_y\right) \tag{2}$$

$$(\rho u)_x + (\rho v)_y = 0 \tag{3}$$

$$\rho \frac{dH}{dt} = \frac{1}{R} \Delta H + \frac{(\gamma - 1)M^2}{R}\left[\left(\frac{du}{dt}\right)_x + \left(\frac{dv}{dt}\right)_y - \frac{2}{3}(un)_x - \frac{2}{3}(vn)_y\right] \tag{4}$$

and in the case of perfect gas

$$p = \left(\gamma M^2\right)^{-1} \rho T \tag{5}$$

Here the subscripts denote partial differentiations with respect to the Cartesian coordinate x or y indicated; the Laplacian operator Δ, the convective derivative d/dt, the nondimensional enthalpy H, and the dilatation n are defined by

$$\left.\begin{aligned} \Delta &= \frac{\partial^2}{\partial x^2} + \frac{\partial^2}{\partial y^2} \\ \frac{d}{dt} &= u\frac{\partial}{\partial x} + v\frac{\partial}{\partial y} \\ H &= T + \frac{\gamma - 1}{2} M^2\left(u^2 + v^2\right) \\ n &= u_x + v_y \end{aligned}\right\} \tag{6}$$

Furthermore, the velocity components u' and v', the pressure p', the density ρ', the temperature T', and the coordinates x' and y' are nondimensionalized as follows:

$$\left.\begin{aligned} u &= \frac{u'}{U_\infty} \\ v &= \frac{v'}{U_\infty} \\ p &= \frac{p'}{\rho_\infty U_\infty^2} \\ \rho &= \frac{\rho'}{\rho_\infty} \\ x &= \frac{x'}{\sqrt{\frac{\nu_\infty L}{U_\infty}}} \\ y &= \frac{y'}{\sqrt{\frac{\nu_\infty L}{U_\infty}}} \end{aligned}\right\} \tag{7}$$

where U_∞, ρ_∞, and ν_∞ are free-stream velocity, density, and kinematic viscosity, and L is the length of the plate from the leading edge to the point of incidence. Finally, the parameters γ, M, and $R = \left(\frac{U_\infty L}{\nu_\infty}\right)^{1/2}$ stand for, respectively, the ratio of specific heats, the free-stream Mach number, and the Reynolds number.

On the other hand, the inviscid flow in the outer region is assumed to be irrotational and, consequently, is determined by a nondimensional velocity potential $\varphi(x,y)$ satisfying the equation

$$\left[(a')^2 - (u')^2\right]\varphi_{xx} - 2u'v'\varphi_{xy} + \left[(a')^2 - (v')^2\right]\varphi_{yy} = 0 \qquad (8)$$

where the sound speed a' is given in terms of the velocity components u' and v' by the relation

$$(a')^2 = (a_\infty')^2 - \frac{\gamma - 1}{2}\left[(u')^2 + (v')^2 - U_\infty^2\right] \qquad (9)$$

By the assumption that these two different flows are in equilibrium with each other, the flow determined from equation (9) must join smoothly with that given by the system of equations (1) to (5) subject to the boundary conditions

$$u = v = 0$$

when $y = 0$ and

$$u = \varphi_x$$

$$v = \varphi_y$$

when $y = \infty$.

As the disturbances are initiated by the incident shock, it is expected that they are small if the incident wave is weak. From experience, this is at least the case in the field upstream of the point of incidence. If the shock strength is characterized by the flow-deflection angle ϵ, then for small values of ϵ the solutions are expanded in powers of ϵ:

$$\left.\begin{aligned} u &= u^{(0)} + \epsilon u^{(1)} + \epsilon^2 u^{(2)} + \cdots \\ v &= v^{(0)} + \epsilon v^{(1)} + \epsilon^2 v^{(2)} + \cdots \\ p &= p^{(0)} + \epsilon p^{(1)} + \epsilon^2 p^{(2)} + \cdots \\ \rho &= \rho^{(0)} + \epsilon \rho^{(1)} + \epsilon^2 \rho^{(2)} + \cdots \\ T &= T^{(0)} + \epsilon T^{(1)} + \epsilon^2 T^{(2)} + \cdots \end{aligned}\right\} \tag{10}$$

By substituting the quantities defined in equations (10) into the system of equations (1) to (5), there results the following system of equations, according to the powers of ϵ; namely, for the zero order,

$$\left.\begin{aligned} \rho^{(0)} \frac{d^{(0)}u^{(0)}}{dt} &= -p_x^{(0)} + \frac{1}{R}\left[\Delta u^{(0)} + \frac{1}{3} n_x^{(0)}\right] \\ \rho^{(0)} \frac{d^{(0)}v^{(0)}}{dt} &= -p_y^{(0)} + \frac{1}{R}\left[\Delta v^{(0)} + \frac{1}{3} n_y^{(0)}\right] \\ \left(\rho^{(0)}u^{(0)}\right)_x + \left(\rho^{(0)}v^{(0)}\right)_y &= 0 \\ \rho^{(0)} \frac{d^{(0)}H^{(0)}}{dt} &= \frac{1}{R}\Delta H^{(0)} + \frac{(\gamma - 1)M^2}{R}\left[\left(\frac{d^{(0)}u^{(0)}}{dt}\right)_x + \left(\frac{d^{(0)}v^{(0)}}{dt}\right)_y - \right. \\ &\qquad \left. \frac{2}{3}\left(u^{(0)}n^{(0)}\right)_x - \frac{2}{3}\left(v^{(0)}n^{(0)}\right)_y\right] \\ p^{(0)} &= (\gamma M^2)^{-1}\rho^{(0)}T^{(0)} \end{aligned}\right\} \tag{11}$$

where

$$\left.\begin{aligned} \frac{d^{(0)}}{dt} &= u^{(0)}\frac{\partial}{\partial x} + v^{(0)}\frac{\partial}{\partial y} \\ H^{(0)} &= T^{(0)} + \frac{\gamma - 1}{2}M^2\left(u^{(0)^2} + v^{(0)^2}\right) \\ n^{(0)} &= u_x^{(0)} + v_y^{(0)} \end{aligned}\right\} \tag{12}$$

for the first order,

$$\left.\begin{aligned} &\rho^{(0)}\left(\frac{d^{(0)}u^{(1)}}{dt} + \frac{d^{(1)}u^{(0)}}{dt}\right) + \rho^{(1)}\frac{d^{(0)}u^{(0)}}{dt} = -p_x^{(1)} + \\ &\frac{1}{R}\left(\Delta u^{(1)} + \frac{1}{3}n_x^{(1)}\right) \\ &\rho^{(0)}\left(\frac{d^{(0)}v^{(1)}}{dt} + \frac{d^{(1)}v^{(0)}}{dt}\right) + \rho^{(1)}\frac{d^{(0)}v^{(0)}}{dt} = -p_y^{(1)} + \\ &\frac{1}{R}\left(\Delta v^{(1)} + \frac{1}{3}n_y^{(1)}\right) \\ &\left(\rho^{(0)}u^{(1)} + \rho^{(1)}u^{(0)}\right)_x + \left(\rho^{(0)}v^{(1)} + \rho^{(1)}v^{(0)}\right)_y = 0 \\ &\rho^{(0)}\frac{d^{(0)}H^{(1)}}{dt} + \left(\rho^{(1)}\frac{d^{(0)}}{dt} + \rho^{(0)}\frac{d^{(1)}}{dt}\right)H^{(0)} = \frac{1}{R}\Delta H^{(1)} + \\ &\frac{(\gamma - 1)M^2}{R}\left[\left(\frac{d^{(0)}u^{(1)}}{dt} + \frac{d^{(1)}u^{(0)}}{dt}\right)_x + \left(\frac{d^{(0)}v^{(1)}}{dt} + \frac{d^{(1)}v^{(0)}}{dt}\right)_y - \right. \\ &\left.\frac{2}{3}\left(u^{(0)}n^{(1)} + u^{(1)}n^{(0)}\right)_x - \frac{2}{3}\left(v^{(0)}n^{(1)} + v^{(1)}n^{(0)}\right)_y\right] \\ &p^{(1)} = (\gamma M^2)^{-1}\left(\rho^{(0)}T^{(1)} + \rho^{(1)}T^{(0)}\right) \end{aligned}\right\} \tag{13}$$

where

$$\left.\begin{aligned} \frac{d^{(1)}}{dt} &= u^{(1)}\frac{\partial}{\partial x} + v^{(1)}\frac{\partial}{\partial y} \\ H^{(1)} &= T^{(1)} + (\gamma - 1)\,u^{(0)}u^{(1)} + v^{(0)}v^{(1)} \\ n^{(1)} &= u_x^{(1)} + v_y^{(1)} \end{aligned}\right\} \tag{14}$$

and for the second order,

$$\left.\begin{aligned} &\rho^{(0)}\left(\frac{d^{(0)}u^{(2)}}{dt} + \frac{d^{(1)}u^{(1)}}{dt} + \frac{d^{(2)}u^{(1)}}{dt}\right) + \rho^{(1)}\left(\frac{d^{(0)}u^{(1)}}{dt} + \frac{d^{(1)}u^{(0)}}{dt}\right) + \rho^{(2)}\frac{d^{(0)}u^{(0)}}{dt} = \\ &-p_x^{(2)} + \frac{1}{R}\left(\Delta u^{(2)} + \frac{1}{3}n_x^{(2)}\right) \\ &\rho^{(0)}\left(\frac{d^{(0)}v^{(2)}}{dt} + \frac{d^{(1)}v^{(1)}}{dt} + \frac{d^{(2)}v^{(1)}}{dt}\right) + \rho^{(1)}\left(\frac{d^{(0)}v^{(1)}}{dt} + \frac{d^{(1)}v^{(0)}}{dt}\right) + \rho^{(2)}\frac{d^{(0)}v^{(0)}}{dt} = \\ &-p_y^{(2)} + \frac{1}{R}\left(\Delta v^{(2)} + \frac{1}{3}n_y^{(2)}\right) \\ &\left(\rho^{(0)}u^{(2)} + \rho^{(1)}u^{(1)} + \rho^{(2)}u^{(0)}\right)_x + \left(\rho^{(0)}v^{(2)} + \rho^{(1)}v^{(1)} + \rho^{(2)}v^{(0)}\right)_y = 0 \\ &\rho^{(0)}\frac{d^{(0)}H^{(2)}}{dt} + \left(\rho^{(0)}\frac{d^{(1)}}{dt} + \rho^{(1)}\frac{d^{(0)}}{dt}\right)H^{(1)} + \left(\rho^{(0)}\frac{d^{(2)}}{dt} + \rho^{(1)}\frac{d^{(1)}}{dt} + \rho^{(2)}\frac{d^{(0)}}{dt}\right)H^{(0)} = \\ &\frac{1}{R}\Delta H^{(2)} + \frac{(\gamma - 1)M^2}{R}\left[\left(\frac{d^{(0)}u^{(2)}}{dt} + \frac{d^{(1)}u^{(1)}}{dt} + \frac{d^{(2)}u^{(0)}}{dt}\right)_x + \right. \\ &\left.\left(\frac{d^{(0)}v^{(2)}}{dt} + \frac{d^{(1)}v^{(1)}}{dt} + \frac{d^{(2)}v^{(0)}}{dt}\right)_y - \frac{2}{3}\left(u^{(0)}n^{(2)} + u^{(1)}n^{(1)} + u^{(2)}n\right)_x - \right. \\ &\left.\frac{2}{3}\left(v^{(0)}n^{(2)} + v^{(1)}n^{(1)} + v^{(2)}n^{(0)}\right)_y\right] \\ &p^{(2)} = \left(\gamma M^2\right)^{-1}\left(\rho^{(0)}T^{(2)} + \rho^{(1)}T^{(1)} + \rho^{(2)}T^{(0)}\right) \end{aligned}\right\} \tag{15}$$

where

$$\frac{d^{(2)}}{dt} = u^{(2)} \frac{\partial}{\partial x} + v^{(2)} \frac{\partial}{\partial y}$$

$$\left.\begin{aligned} H^{(2)} &= T^{(2)} + (\gamma - 1)M^2\left(u^{(0)}u^{(2)} + v^{(0)}v^{(2)} + \frac{u^{(1)^2} + v^{(1)^2}}{2}\right) \\ n^{(2)} &= u_x^{(2)} + v_y^{(2)} \end{aligned}\right\} \quad (16)$$

In the case of the potential flow, if the velocity potential is expanded as

$$\varphi = x + \epsilon\varphi^{(1)} + \epsilon^2\varphi^{(2)} + \cdots \quad (17)$$

there will occur, similarly, equations for the first- and second-order quantities. These are: For the first order

$$\beta^2\varphi_{xx}^{(1)} - \varphi_{yy}^{(1)} = 0 \quad (18)$$

and for the second order

$$\beta^2\varphi_{xx}^{(2)} - \varphi_{yy}^{(2)} = -2M^2\left[\left(1 + \frac{\gamma - 1}{2}M^2\right)\varphi_x^{(1)}\varphi_{xx}^{(1)} + \varphi_y^{(1)}\varphi_{yy}^{(1)}\right] \quad (19)$$

where $\beta = \sqrt{M^2 - 1}$.

FIRST-ORDER SOLUTION - UPSTREAM, $x < 0$

Let the point of incidence be chosen as the origin of the Cartesian coordinates. Then, negative x will be called upstream, and positive x, downstream, of the point of incidence. The various regions will be numbered by 1, 2, and 3 as shown in figure 1 in which OS indicates shock and OM, the limiting Mach line of region 2.

As it has been assumed that the basic flow is a laminar boundary-layer flow of a Blasius type, such as considered by Von Kármán and Tsien (reference 2) and by Emmons and Brainerd (references 4 and 5), system (11) simply reduces to the well-known Prandtl boundary-layer equations, whose solution has already been found in these references.

Since the basic flow is a boundary-layer flow with constant pressure $p^{(0)}$, system (13) can be simplified. From experiments it has been established that the space variation of the perturbed quantities is much more rapid than that of the unperturbed quantities. By the boundary-layer approximation, the ratio of the partial derivatives $\partial/\partial x : \partial/\partial y$ is $1:R$. For large Reynolds number, the x-derivatives of the basic flow, as well as $v^{(0)}$, which is of the order R^{-1}, can be neglected in comparison with the y-derivatives. That is, $u^{(0)}$ and $\rho^{(0)}$ are functions of y only. This approximation is confirmed by experiments and, as a matter of fact, it is customarily used in the pressure measurements, because the wave is shifted forward and back relative to a fixed pressure orifice to measure the pressure distribution before and behind the wave. In the case of unit Prandtl number, $H^{(0)}$ is a constant. Then, by dropping terms such as $v^{(0)}u_y^{(1)}$ and $u_x^{(0)}u^{(1)}$, system (13) becomes

$$\left.\begin{aligned}
&\rho^{(0)}\left(u^{(0)}u_x^{(1)} + u_y^{(0)}v^{(1)}\right) = -p_x^{(1)} + \frac{1}{R}\left(\Delta u^{(1)} + \frac{1}{3}\,n_x^{(1)}\right)\\
&\rho^{(0)}u^{(0)}v_x^{(1)} = -p_y^{(1)} + \frac{1}{R}\left(\Delta v^{(1)} + \frac{1}{3}\,n_y^{(1)}\right)\\
&\rho^{(0)}n^{(1)} + u^{(0)}\rho_x^{(1)} + v^{(1)}\rho_y^{(0)} = 0\\
&\rho^{(0)}u^{(0)}H_x^{(1)} = \frac{1}{R}\,\Delta H^{(1)} + \frac{(\gamma-1)M^2}{R}\left[\left(u^{(0)}u_x^{(1)} + v^{(1)}u_y^{(0)}\right)_x + \left(u^{(0)}v_x^{(1)}\right)_y - \frac{2}{3}\left(u^{(0)}n^{(1)}\right)_x\right]\\
&p^{(1)} = \left(\gamma M^2\right)^{-1}\left(\rho^{(0)}T^{(1)} + \rho^{(1)}T^{(0)}\right)
\end{aligned}\right\} \qquad (20)$$

Incompressible Layer

It is noted that the coefficients of system (20) depend on the basic velocity profile $u^{(0)}(y)$. Since $u^{(0)}(y)$ cannot be expressed by simple functions, in order to simplify the analytical work further simplifications are necessary.

First of all, in the case of insulated plate, the temperature and, hence, the density in the basic flow will have a vanishing gradient on the plate. This makes the variation of the density in the viscous layer much smaller than that of the velocity. When the flow is subject to an adverse pressure gradient, the flow will be further retarded. When the backflow occurs, the average speed will be very low and, consequently, the representative average Mach number will be small. Under this condition, the change of density is less important than that of the pressure. A layer where this approximation is valid is called an "incompressible layer" and the dominant effects will be pressure and frictional forces.

Of course, it is difficult to define the thickness of this layer beforehand. Generally, it would correspond to the subsonic portion of the viscous layer. In the basic flow, the sonic boundary can be exactly calculated. When the flow is perturbed, it is unknown, but certainly will be thicker, for the flow is subject to an adverse pressure gradient. Owing to this fact and also for mathematical expediency, the thickness will be taken in accordance with the way the velocity profile $u^{(0)}(y)$ is represented. This will become clear below and the thickness defined turns out to be nearly half the original boundary-layer thickness.

Because of the assumption that density is constant and assumes the value $\rho_o^{(0)}$ on the plate, system (20) simplifies to

$$\left.\begin{aligned}
&\rho_o^{(0)}\left(u^{(0)}u_x(1) + u_y(0)v(1)\right) = -p_x(1) + \frac{1}{R}\Delta u(1)\\
&\rho_o^{(0)}u^{(0)}v_x(1) = -p_y(1) + \frac{1}{R}\Delta v(1)\\
&n(1) = 0\\
&\rho_o^{(0)}u^{(0)}H_x(1) = \frac{1}{R}\Delta H(1) + \frac{2(\gamma - 1)M^2}{R}u_y(0)v_x(1)
\end{aligned}\right\} \qquad (21)$$

Thus, the velocities, pressure, and temperature can be dealt with independently. For the velocities, the first three equations yield by elimination of $p^{(1)}$:

$$\left.\begin{aligned} &\rho_o^{(0)}u^{(0)}\left(u_y^{(1)} - v_x^{(1)}\right)_x + \rho_o^{(0)}u_{yy}^{(0)}v^{(1)} = \frac{1}{R}\Delta\left(u_y^{(1)} - v_x^{(1)}\right) \\ &n^{(1)} = 0 \end{aligned}\right\} \quad (22)$$

After the velocities are known, the temperature will be given by the energy equation. In the present problem, however, temperature is not an interesting quantity and will subsequently not be mentioned. To solve equations (22), let a stream function $\psi^{(1)}(x,y)$ be introduced by the relations

$$u^{(1)} = \psi_y^{(1)}$$

$$v^{(1)} = -\psi_x^{(1)}$$

From equations (22) $\psi^{(1)}$ then satisfies the equation

$$\rho_o^{(0)}u^{(0)}\Delta\psi_x^{(1)} = \frac{1}{R}\Delta\,\Delta\psi^{(1)} + \rho_o^{(0)}u_{yy}^{(0)}\psi_x^{(1)} \quad (23)$$

By neglecting the compressibility effect in the inner layer, the basic velocity profile $u^{(0)}(y)$ becomes the Blasius profile. The variable coefficients of equation (23), for small values of y, will be power series in y. However, it has been recognized that in the case of Blasius profile the velocity attains the free-stream value fairly rapidly and the initial portion is nearly linear. Consequently, it will not involve serious error to replace the continuous profile by a broken-line one, so that the initial part is proportional to y and the remaining part, constant with the free-stream value unity. If the skin friction agrees with the exact value, the velocity profile can then be defined as

$$\left.\begin{aligned} u^{(0)}(y) &= \alpha y \quad \text{when} \quad 0 \leqq y \leqq y_1 \\ u^{(0)}(y) &= 1 \quad \text{when} \quad y_1 < y \leqq \infty \end{aligned}\right\} \quad (24)$$

If the velocity is continuous at $y = y_1$, then $y_1 = \alpha^{-1}$ which is about half the boundary-layer thickness, namely $y_1 \sim 3$. If the incompressible layer is defined as the interval $0 \leq y \leq y_1$, then equation (23) becomes

$$\tilde{\alpha} y \, \Delta\psi_x^{(1)} = \Delta \, \Delta\psi^{(1)} \tag{25}$$

where $\tilde{\alpha} = \rho_o^{(0)} \alpha R$.

To solve equation (25), it is natural to assume the form

$$\left.\begin{aligned} \psi^{(1)} &= \psi(y) e^{\lambda x} \\ \lambda &> 0 \end{aligned}\right\} \tag{26}$$

for region 1 where $x < 0$. This assumes a special form of compression waves induced in the potential field; that is, the solution of equation (18)

$$\varphi^{(1)} = \frac{A}{\lambda} e^{\lambda(x-\beta y)} \tag{27}$$

where A is a constant to be determined. This is entirely in agreement with the conclusions reached in reference 1. Substituting equations (26) in equation (25) and simultaneously putting

$$\psi'' + \lambda^2 \psi = z(y) \tag{28}$$

there results

$$z'' \mp \left(\lambda \tilde{\alpha} y - \lambda^2\right) z = 0 \tag{29}$$

The general solution of this equation is

$$z = C_1 \eta^{1/2} K_{\frac{1}{3}}\left(\frac{2}{3} \eta^{3/2}\right) + C_2 \eta^{1/2} I_{\frac{1}{3}}\left(\frac{2}{3} \eta^{3/2}\right) \tag{30}$$

where

$$\eta = (\lambda\tilde{\alpha})^{1/3}\left(y - \lambda\tilde{\alpha}^{-1}\right) \tag{31}$$

C_1 and C_2 are constants, and $I_{\frac{1}{3}}\left(\frac{2}{3}\eta^{3/2}\right)$ and $K_{\frac{1}{3}}\left(\frac{2}{3}\eta^{3/2}\right)$ denote the Bessel functions of the first and second kind with imaginary argument. With z known, the solution of equation (28) is

$$\psi = C_3 \cos \tau\eta + C_4 \sin \tau\eta +$$

$$\frac{\sin \tau\eta}{\tau}\int_{\eta_o}^{\eta} (\cos \tau\eta)z(\eta)\, d\eta - \frac{\cos \tau\eta}{\tau}\int_{\eta_o}^{\eta} (\sin \tau\eta)z(\eta)\, d\eta \tag{28a}$$

with $\tau = \lambda(\lambda\tilde{\alpha})^{-1/3}$. On the plate $y = 0$ and $u^{(1)} = v^{(1)} = 0$; hence $\psi(0) = \psi'(0) = 0$. For large Reynolds number and small values of λ, $y = 0$ corresponds approximately to $\eta = 0$. The boundary conditions thus require $C_3 = C_4 = 0$. Moreover, at $y = y_1$, η will be large, and since $\tau\eta_1 = \lambda y_1 < 1$, the integrals $\int_0^{\eta} \eta^{1/2} \begin{Bmatrix}\cos \\ \sin\end{Bmatrix} \tau\eta\, I_{\frac{1}{3}}\left(\frac{2}{3}\eta^{3/2}\right) d\eta$ will diverge like $\int_0^{\eta} e^{\frac{2}{3}\eta^{3/2}}\, d\eta$ as η approaches infinity. Therefore, $C_2 = 0$. The solution in the incompressible layer can then be read as follows

$$\psi^{(1)} = \frac{C_1}{\tau}\left[(\sin \tau\eta)\int_0^{\eta} \eta^{1/2}(\cos \tau\eta)K_{\frac{1}{3}}\left(\frac{2}{3}\eta^{3/2}\right) d\eta - \right.$$

$$\left. \cos \tau\eta \int_0^{\eta} \eta^{1/2}(\sin \tau\eta)K_{\frac{1}{3}}\left(\frac{2}{3}\eta^{3/2}\right) d\eta\right] e^{\lambda x} \tag{32}$$

Thereby the velocity components are

$$\left.\begin{aligned} u^{(1)} = C_1(\tilde{\alpha}\lambda)^{1/3}\Bigg[&(\cos\tau\eta)\int_0^\eta \eta^{1/2}(\cos\tau\eta)K_{\frac{1}{3}}\left(\tfrac{2}{3}\eta^{3/2}\right)d\eta + \\ &(\sin\tau\eta)\int_0^\eta \eta^{1/2}(\sin\tau\eta)K_{\frac{1}{3}}\left(\tfrac{2}{3}\eta^{3/2}\right)d\eta\Bigg]e^{\lambda x} \\ v^{(1)} = -C_1(\tilde{\alpha}\lambda)^{1/3}\Bigg[&(\sin\tau\eta)\int_0^\eta (\cos\tau\eta)K_{\frac{1}{3}}\left(\tfrac{2}{3}\eta^{3/2}\right)d\eta - \\ &(\cos\tau\eta)\int_0^\eta \eta^{1/2}(\sin\tau\eta)K_{\frac{1}{3}}\left(\tfrac{2}{3}\eta^{3/2}\right)d\eta\Bigg]e^{\lambda x} \end{aligned}\right\} \quad (33)$$

On the other hand, the pressure can be obtained by integration of the first of equations (21) and is, by the form of solution,

$$p^{(1)} = -\rho_o{}^{(0)}u^{(0)}u^{(1)} - \frac{\rho_o{}^{(0)}u_y{}^{(0)}v^{(1)}}{\lambda} + \frac{1}{\lambda R}\left(\psi^{(1)} + \lambda^2\psi'\right)e^{\lambda x}$$

where the constant of integration vanishes by the condition at negative infinity. Substituting $u^{(1)}$ and $v^{(1)}$ from equation (33) and making use of equation (28), a straightforward reduction yields

$$\begin{aligned} p^{(1)} = \frac{\rho_o{}^{(0)}\alpha C_1}{\tau}\Bigg\{&-\tau\eta K_{\frac{2}{3}}\left(\tfrac{2}{3}\eta^{3/2}\right) + (\sin\tau\eta)\int_0^\eta \eta^{1/2}(\cos\tau\eta)K_{\frac{1}{3}}\left(\tfrac{2}{3}\eta^{3/2}\right)d\eta - \\ &(\cos\tau\eta)\int_0^\eta \eta^{1/2}(\sin\tau\eta)K_{\frac{1}{3}}\left(\tfrac{2}{3}\eta^{3/2}\right)d\eta - \\ &\tau\eta\Bigg[(\cos\tau\eta)\int_0^\eta \eta^{1/2}(\cos\tau\eta)K_{\frac{1}{3}}\left(\tfrac{2}{3}\eta^{3/2}\right)d\eta + \\ &(\sin\tau\eta)\int_0^\eta \eta^{1/2}(\sin\tau\eta)K_{\frac{1}{3}}\left(\tfrac{2}{3}\eta^{3/2}\right)d\eta\Bigg]\Bigg\}e^{\lambda x} \end{aligned} \quad (34)$$

On the plate $y = \eta = 0$ this reduces to

$$p^{(1)}(x,0) = -\rho_o{}^{(0)}\alpha C_1\left[\eta K_{\frac{2}{3}}\left(\frac{2}{3}\ \eta^{3/2}\right)\right]_{\eta=0} e^{\lambda x} \tag{34a}$$

Compressible Layer

In the compressible layer, because of the forward momentum of the potential flow outside, the velocity is everywhere positive and differs from the basic flow by a small amount in order to support the pressure rise. As the velocity is high, both compressibility and viscous effects will become important. Under this condition, the problem is considerably simplified by taking a uniform basic flow, namely $u^{(0)} = \rho^{(0)} = 1$, as discussed above. Accordingly, equations (20) reduce to

$$\left.\begin{aligned} u_x{}^{(1)} &= -p_x{}^{(1)} + \frac{1}{R}\left(\Delta u^{(1)} + \frac{1}{3}\ n_x\right) \\ v_x{}^{(1)} &= -p_y{}^{(1)} + \frac{1}{R}\left(\Delta v^{(1)} + \frac{1}{3}\ n_y\right) \\ n^{(1)} &+ \rho_x{}^{(1)} = 0 \\ H_x{}^{(1)} &= \frac{1}{R}\ \Delta H^{(1)} + \frac{(\gamma - 1)M^2}{R}\ n_x{}^{(1)} \\ p^{(1)} &= \left(\gamma M^2\right)^{-1}\left(T^{(1)} + \rho^{(1)}\right) \end{aligned}\right\} \tag{35}$$

where

$$H^{(1)} = T^{(1)} + (\gamma - 1)M^2 u^{(1)}$$

The elimination of $p^{(1)}$ from the first two equations gives

$$\left(u_y{}^{(1)} - v_x{}^{(1)}\right)_x = \frac{1}{R}\ \Delta\left(u_y{}^{(1)} - v_x{}^{(1)}\right) \tag{36}$$

After differentiating the first and the second of equations (35) with respect to x and y, respectively, an addition yields

$$\Delta p^{(1)} = -n_x^{(1)} + \frac{4}{3R}\Delta n^{(1)}$$

moreover, by definition

$$H_x^{(1)} = \gamma M^2 p_x^{(1)} + (\gamma - 1)M^2 u_x^{(1)} + n^{(1)}$$

A substitution of $H_{xx}^{(1)}$ and $\Delta H_x^{(1)}$ in the energy equation leads to

$$n_x^{(1)} - M^2 u_{xx}^{(1)} + \frac{\gamma M^2}{R}\left(\Delta u_x^{(1)} + \frac{1}{3} n_{xx}^{(1)}\right) = \frac{1}{R}\left[\Delta n^{(1)} - \frac{4 - \gamma}{3} M^2 n_{xx}^{(1)} + \frac{4\gamma M^2}{3R}\Delta n_x^{(1)} + (\gamma - 1)M^2\left(u_y^{(1)} - v_x^{(1)}\right)_{xy}\right] \tag{37}$$

Equations (36) and (37) form a system of linear partial differential equations for $u^{(1)}$ and $v^{(1)}$ with constant coefficients. The solutions, if carried out, are expressible in terms of trigonometric and exponential functions. According to the arguments of these functions, they fall into two groups: One varies slowly and is "potential-like"; while the other varies rapidly and, therefore, is "boundary-layer-like." The latter group consists of two exponentials whose arguments differ by a term of $O\left(\frac{1}{R}\right)$. Hence, for large Reynolds number, the latter two exponentials will degenerate into one. It was found that this form of solution can be obtained by solving a much simpler problem, namely, by assuming $H^{(1)} = 0$. This assumption appears to be nothing but a method of approximating the solution of equations (36) and (37) in the case of large Reynolds number.

If $H^{(1)}$ is taken to be zero, then instead of equation (37) there is in its place

$$-n^{(1)} + M^2 u_x^{(1)} = \frac{\gamma M^2}{R}\left(\Delta u^{(1)} + \frac{1}{3} n_x^{(1)}\right) \tag{38}$$

by elimination of $p^{(1)}$ and $T^{(1)}$. To solve the system (36) and (38), two scalar functions $F^{(1)}$ and $G^{(1)}$ are introduced through the relations

$$\left.\begin{aligned} u^{(1)} &= F_x{}^{(1)} + G_y{}^{(1)} \\ v^{(1)} &= F_y{}^{(1)} - G_x{}^{(1)} \end{aligned}\right\} \tag{39}$$

The equivalent system, then, is as follows:

$$\left.\begin{aligned} \Delta G_x{}^{(1)} &= \frac{1}{R}\,\Delta\,\Delta G^{(1)} \\ -\Delta F^{(1)} + M^2 F_{xx}{}^{(1)} &= \frac{4\gamma M^2}{3R}\,\Delta F_x{}^{(1)} - M^2 G_{xy}{}^{(1)} + \frac{\gamma M^2}{R}\,\Delta G_y{}^{(1)} \end{aligned}\right\} \tag{40}$$

According to the form of the potential solution, it will again be assumed that

$$G^{(1)} = g_1(y)e^{\lambda x}$$

$$F^{(1)} = f_1(y)e^{\lambda x}$$

By the condition that $G^{(1)}$ is finite at infinity, the solution is shown to be

$$g_1 = C_3 \cos \lambda y + C_4 \sin \lambda y + \frac{C_2}{\lambda R}\, e^{-\sigma y} \tag{41}$$

where C_2, C_3, and C_4 are constants of integration and

$$\sigma^2 = \lambda R - \lambda^2 \tag{42}$$

By substituting g_1 from equation (41) in the second of equations (40) the solution for f_1 was found to be

$$f_1 = C_3 \sin \lambda y - C_4 \cos \lambda y + C_5 e^{-\beta_1 \lambda y} + C_6 e^{\beta_1 \lambda y} + \frac{(\gamma - 1)M^2}{R^2 + \left(\frac{4\gamma}{3} - 1\right)\lambda M^2 R} \frac{\sigma C_2}{\lambda} e^{-\sigma y} \tag{43}$$

where

$$\beta_1{}^2 = \left(\beta^2 - \frac{4\gamma M^2 \lambda}{3R}\right) \Bigg/ \left(1 + \frac{4\gamma M^2 \lambda}{3R}\right)$$

The velocity components for $y > y_1$, by equation (39), are given by

$$u(1) = \left\{ \lambda C_5 e^{-\beta_1 \lambda (y - y_1)} + \lambda C_6 e^{\beta_1 \lambda (y - y_1)} + \left[\frac{(\gamma - 1)M^2}{R^2 + \left(\frac{4\gamma}{3} - 1\right)\lambda M^2 R} - \frac{1}{\lambda R} \right] \sigma C_2 e^{-\sigma (y - y_1)} \right\} e^{\lambda x} \tag{44}$$

$$v(1) = \left\{ -\beta_1 \lambda C_5 e^{-\beta_1 \lambda (y - y_1)} + \beta_1 \lambda C_6 e^{\beta_1 \lambda (y - y_1)} - \left[\frac{(\gamma - 1)M^2}{\lambda R^2 + \left(\frac{4\gamma}{3} - 1\right)\lambda^2 M^2 R} + \frac{1}{R} \right] C_2 e^{-\sigma (y - y_1)} \right\} e^{\lambda x}$$

by redefining the constants C. It is noticed that the first group of exponentials varies with both x and y with a slope proportional to λ, which, according to experimental evidence for this type of flow, is a small number; that is, the variation with x is relatively slow. On the other hand, the second exponential varies with y with derivative proportional to σ, which is of $O(\sqrt{\lambda R})$. For large Reynolds number, it appears that σ could be thousands of times larger than λ. Therefore, in the case of large Reynolds number where the viscous layer is thin, the first group of terms changes only slightly while the second exponential drops to zero. Applying the boundary-layer concept, the potential-like terms will be taken as constant and equal to the boundary value of the potential solution. Consequently, the solution can be written as

$$\left.\begin{aligned} u^{(1)} &= \left[A + \left(k - \frac{1}{\lambda R}\right)\sigma C_2 e^{-\sigma(y-y_1)}\right]e^{\lambda x} \\ v^{(1)} &= \left[-\beta A - \left(\frac{k\sigma^2}{\lambda} + \frac{1}{R}\right)C_2 e^{-\sigma(y-y_1)}\right]e^{\lambda x} \end{aligned}\right\} \tag{44a}$$

with

$$k = (\gamma - 1)M^2 \Big/ R^2\left[1 + \left(\frac{4\gamma}{3} - 1\right)\frac{\lambda M^2}{R}\right]$$

It is seen that when $\sigma(y - y_1)$ becomes large, this solution joins the potential solution at $y = 0$ and the constants C_5 and C_6 will be considered as eliminated. By means of this approximate solution the pressure $p^{(1)}$ is shown to be

$$p^{(1)} = -\left[\tilde{k}A - \frac{k\sigma}{3} C_2 e^{-\sigma(y-y_1)}\right]e^{\lambda x} \tag{45}$$

where

$$\tilde{k} = \left[1 + \frac{4}{3}(\gamma - 1)\frac{M^2\lambda}{R}\right] \Big/ \left(1 + \frac{4}{3}\,\frac{\gamma M^2 \lambda}{R}\right)$$

Eigenvalues λ

In the last two sections, the velocity and pressure have been calculated by entirely different methods of approximation in two different layers. For the incompressible layer, the nonslip conditions are satisfied on the plate, whereas in the compressible layer, the velocity agrees with the potential flow at infinity. The complete solution is then left with three undetermined constants C_1, C_2, and A and with an arbitrary parameter λ. To determine these constants, it is assumed that the two solutions (33) and (34) and (44) and (45) must join at the interface $y = y_1$. Now, because of the simplification made in connection with equation (44), the conditions at the interface are to be stated as follows for $y = y_1$:

$$\left.\begin{aligned} u_c^{(1)} &= u_i^{(1)} \\ v_c^{(1)} &= v_i^{(1)} \\ p_c^{(1)} &= p_i^{(1)} \end{aligned}\right\} \tag{46}$$

where the subscripts c and i indicate, respectively, solutions of compressible and incompressible layers. The u velocity profile thus will have a discontinuity in slope. This could be improved by dropping the assumption $H^{(1)} = 0$. However, as pressure depends only on the velocity and its second derivatives, an error in shear can produce only minor contributions and can be ignored. By substituting the solutions in equations (46), there results the following system of equations:

$$\left.\begin{aligned} A + \left(k - \frac{1}{\lambda R}\right)\sigma C_2 - U^{(1)}(\eta_1)C_1 &= 0 \\ -\beta A - \left(\frac{k\sigma^2}{\lambda} + \frac{1}{R}\right)C_2 + V^{(1)}(\eta_1)C_1 &= 0 \\ -\tilde{k}A + \frac{k\sigma}{3}C_2 - P^{(1)}(\eta_1)C_1 &= 0 \end{aligned}\right\} \tag{47}$$

where $U^{(1)}$, $V^{(1)}$, and $P^{(1)}$ are defined by

$$U^{(1)} = (\tilde{\alpha}\lambda)^{1/3}\left[(\cos \tau\eta_1)\int_0^{\eta_1} \eta^{1/2}(\cos \tau\eta)K_{\frac{1}{3}}\, d\eta + (\sin \tau\eta_1)\int_0^{\eta_1} \eta^{1/2}(\sin \tau\eta)K_{\frac{1}{3}}\, d\eta\right]$$

$$V^{(1)} = (\tilde{\alpha}\lambda)^{1/3}\left[(\sin \tau\eta_1)\int_0^{\eta_1} \eta^{1/2}(\cos \tau\eta)K_{\frac{1}{3}}\, d\eta - (\cos \tau\eta_1)\int_0^{\eta_1} \eta^{1/2}(\sin \tau\eta)K_{\frac{1}{3}}\, d\eta\right]$$

$$P^{(1)} = \frac{\rho_o(0)_\alpha}{\tau}\left[-\tau\eta_1 K_{\frac{2}{3}}\left(\frac{2}{3}\,\eta_1^{3/2}\right) + (\tilde{\alpha}\lambda)^{-1/3}V(1) - \tau\eta_1(\tilde{\alpha}\lambda)^{-1/3}U(1)\right]$$

In order that linear system (47) will admit a nontrivial solution for C_1, C_2, and A, it is both necessary and sufficient that the determinant

$$\begin{vmatrix} 1 & \left(k - \frac{1}{\lambda R}\right)\sigma & U^{(1)} \\ \beta & \left(\frac{k\sigma^2}{\lambda} + \frac{1}{R}\right) & V^{(1)} \\ -\tilde{k} & \frac{1}{3}\,k\sigma & P^{(1)} \end{vmatrix} = 0 \qquad (48)$$

vanish. This equation serves to determine all proper values of λ. After λ has been determined, the constants C_1 and C_2 corresponding to this λ can be solved for in terms of A, namely

$$\left.\begin{aligned} C_1 &= A\,\frac{\sigma\left(k-\frac{1}{\lambda R}\right)\beta-\left(\frac{k\sigma^2}{\lambda}+\frac{1}{R}\right)}{\sigma\left(k-\frac{1}{\lambda R}\right)V^{(1)}-\left(\frac{k\sigma^2}{\lambda}+\frac{1}{R}\right)U^{(1)}} \\ C_2 &= A\,\frac{\beta U^{(1)}-V^{(1)}}{\sigma\left(k-\frac{1}{R\lambda}\right)V^{(1)}-\left(\frac{k\sigma^2}{\lambda}+\frac{1}{R}\right)U^{(1)}} \end{aligned}\right\} \tag{49}$$

where the constant A remains to be determined.

To solve determinantal equation (48) analytically even for this simplest case does not seem to be possible. The procedure from here on is essentially numerical. For the present purpose, the numerical solution will be carried out, based on the approximation that η_1 will be taken mathematically as infinity and $\tau\eta_1$, small. Accordingly, the integrals in $U^{(1)}$, $V^{(1)}$, and $P^{(1)}$ will have an infinite upper limit and $\cos \tau\eta_1 \approx 1$ and $\sin \tau\eta_1 \approx \lambda y_1$. Furthermore, for large values of η_1 the Bessel function $K_{\frac{1}{3}}\left(\frac{2}{3}\eta_1^{3/2}\right) \approx \eta_1^{-3/4} e^{-\frac{2}{3}\eta_1^{3/2}}$ will be very small and can, therefore, be neglected. Equation (48) is finally expressed explicitly in terms of the parameters R, β, and α. To retain terms up to the order $O\left(R^{-5/6}\right)$, the determinantal equation becomes

$$\beta y_1 \lambda^2 - \tilde{\alpha}^{1/3} r y_1 \lambda^{4/3} + \lambda + \rho_o^{(0)} \alpha\beta = 0 \tag{50}$$

where $r = \Gamma\left(\frac{1}{3}\right)\Big/3^{2/3}$.

For $M = 2$, $R = 774$, and $\alpha = 0.332$, there are two pairs of positive and negative roots. The negative roots would make the perturbation infinite at negative infinity, which is contrary to assumption. Therefore, negative roots are not admitted. For the pair of positive roots, one is roughly 20 times the other which is 0.0467. For large Reynolds number, these would correspond to $\lambda_1 \approx \beta^{-3/2} R^{1/2}$ and $\lambda_2 \approx \beta^{3/4} R^{-1/4}$.

In region 1, x is negative. The disturbance with a logarithmic rate of decay λ_1 will quickly disappear. The observed disturbance must have a decay rate equal to λ_2.

According to this solution, the dependence of the distance influenced by pressure disturbance on the Mach number and Reynolds number can be discussed. By the form of the first-order solution, the pressure decays exponentially from the point of incidence. For a given value of ϵ, when $-\lambda_2 X = d$, d being a constant, the pressure disturbance would have dropped to a certain fraction of its initial value. Thus, $-X = d/\lambda_2$ would serve as a measure of the distance reached by the pressure. Therefore, by varying M and R, the distance X'/L will change according to the law $\beta^{-3/4}R^{-3/4}$. Namely, by increasing both Mach number and Reynolds number, the distance reached by pressure disturbances will decrease. This result is quantitatively different from that arrived at in reference 1, which is $\beta^{-1/2}R^{-1/2}$. By comparison there is an increase of both compressibility and viscous effects in the new result. This shows how gross an error can be made if the boundary-layer approximation is applied. It is surprising also that the upstream pressure propagation depends only on M and R but, to the first order at least, is independent of the shock strength. This seems to be in agreement with experiment (reference 6).

It can be shown from equations (33) and (34) that for arbitrary values of A the pressure $p^{(1)}(x_{sep},0)$ at the point of separation where $u_y = 0$ is proportional to $\beta^{-1/2}R^{-1/2}$.

FIRST-ORDER SOLUTION - DOWNSTREAM $x > 0$

As in the upstream first-order solution, one must start with the potential solution. In order to determine the flow in region 2, the interaction between the incoming wave ${}_1\varphi^{(1)}$ and the shock must be considered.

Potential Solution

In equation (27) the incoming wave is given by

$$ {}_1\varphi^{(1)} = \frac{A}{\lambda} e^{\lambda(x-\beta y)} $$

When this train of waves hits the shock, the shock will be slightly modified according to Rankine-Hugoniot conditions. The velocity potential in region 2 with these conditions satisfied is shown to be (appendixes A and B)

$$ {}_2\varphi^{(1)} = \frac{1}{\beta}(x + \beta y) + \frac{A}{\lambda} e^{\lambda(x-\beta y)} \tag{51} $$

That is, to the first order, the flow in region 2 is simply a superposition of a step wave upon the transmitted wave. Since the conditions are prescribed on the shock OS, they are uniquely defined in region 2, terminated only by the extreme Mach line OM.

To continue this solution into region 3, two possibilities present themselves. It may be either continuous or discontinuous there. If it were continuous on OM, there would be a discontinuity in pressure at the point of incidence. In the case of inviscid flow, this, of course, would be admissible. But, by the condition that the viscous layer will join smoothly with the potential field, this would make the velocity $u^{(1)}(x,y)$ discontinuous at the origin $x = 0$. Hence, the first possibility must be discarded. If the solution is discontinuous at OM, and the pressure as well as the velocity $u^{(1)}$ are continuous at the origin, then the discontinuity must correspond to an expansion. This, of course, is what has been observed.

Assuming that the pressure returns to the value just in front of the shock, a simple calculation shows that the turn of the flow through a Prandtl-Meyer expansion has to be

$$ -\epsilon\beta\left({}_1u^{(1)}(0) - {}_2u^{(1)}(0)\right) $$

where ${}_1u^{(1)}(0)$ and ${}_2u^{(1)}(0)$ are, respectively, the velocity $u^{(1)}$ just before and after the shock. By means of solutions (27) and (51), the turn required is ϵ. Now the direction of the flow before the expansion is $\epsilon(1 - \beta A)$; therefore the total inclination of the velocity vector at OM is

$$ \epsilon(2 - \beta A) $$

A solution in region 3 subject to these conditions is found to be (appendix B):

$$ {}_3\varphi^{(1)} = \frac{1}{\beta}(x + \beta y) - \frac{1}{\beta}(x - \beta y) + \frac{A}{\lambda} e^{\lambda(x-\beta y)} \tag{52} $$

The velocity in region 3 can then be given by

$$ {}_3u^{(1)} = Ae^{\lambda(x-\beta y)} $$

$$ {}_3v^{(1)} = 2 - \beta Ae^{\lambda(x-\beta y)} $$

Were the perturbation velocity to remain finite at infinity, λ would have to be negative in region 3, as $x - \beta y \geqq 0$.

Viscous Solutions

As potential solution (52) in region 3 is a superposition of two different types of waves, namely, step waves and transmitted waves, it is expected that the viscous solution will also be composed of two different parts, each associated with a special wave in the external field. Since the origin and character of the disturbances are different, they can best be discussed separately as the following:

In view of the fact that the step waves are opposite in sign, they do not change the pressure but give rise to a uniform vertical velocity in the potential field. The flow in the viscous layer due to this uniform deflection may vary rapidly in the y-direction but certainly not in the x-direction because of the constancy of pressure. The main effect of the step waves, first of all, then, is to produce a constant deflection along the edge of the viscous layer. If the velocities due to step waves are $u_s^{(1)}$ and $v_s^{(1)}$, the problem should be solved subject to the boundary conditions:

$$ \left.\begin{aligned} & u_s^{(1)} = v_s^{(1)} = 0 && \text{when } y = 0 \\ & u_s^{(1)} = 0, \quad v_s^{(1)} = 2 && \text{at outer edge of viscous layer} \\ & u_s^{(1)} = 0 && \text{when } x = 0, \quad y \geqq 0 \end{aligned}\right\} \qquad (53) $$

It must be borne in mind that generally the flow in region 1 has been separated, with a considerable region of backflow in the neighborhood of the point of incidence; the resultant flow in the incompressible layer must be small. If $u_s^{(1)}$ and $v_s^{(1)}$ are considered as additional

perturbations due to the step waves, the problem can then be simplified by neglecting the inertia forces in the neighborhood of the plate. The perturbation stream function $\psi_s^{(1)}$ then satisfies

$$\Delta\,\Delta\psi_s^{(1)} = 0 \tag{54}$$

in the incompressible layer $0 \leqq y \leqq y_1$.

As the objective here is to demonstrate approximately the effect of the step waves on the viscous layer, only simple solutions will be considered. A simple solution that satisfies both the first and third of conditions (53) is clearly

$$\psi_s^{(1)} = D\left(\frac{y}{y_1}\right)^2\left(1 - \frac{2}{3}\,\frac{y}{y_1}\right)x \tag{55}$$

for y in $0 \leqq y \leqq y_1$, where D is a constant. The velocities are thereby

$$\left.\begin{aligned} u_s^{(1)} &= 2D\,\frac{y}{y_1}\left(1 - \frac{y}{y_1}\right)\frac{x}{y_1} \\ v_s^{(1)} &= -D\left(\frac{y}{y_1}\right)^2\left(1 - \frac{2}{3}\,\frac{y}{y_1}\right) \end{aligned}\right\} \tag{56}$$

Accordingly, the pressure, or the pressure gradients, in the incompressible layer due to the step waves is of the order R^{-1} and for the present approximation will be neglected.

In the compressible layer where the viscous effect is not as important as the compressibility effect, a flow that does not associate with a pressure rise can either be a uniform field or the one with a vertical velocity varying linearly as y. According to equation (37), the following, with the second of equations (53) satisfied, is a solution for $y_1 \leqq y \leqq y_2$, y_2 being defined as the outer edge of the compressible layer:

$$\left.\begin{aligned} u_s^{(1)} &= 0 \\ V_s^{(1)} &= 2\left(\frac{y}{y_1}\right) \end{aligned}\right\} \tag{57}$$

The fact that equation (57) is a solution shows the importance of both the compressibility and the viscosity in this layer, which allow the independent variation of $\rho^{(1)}$ and $T^{(1)}$. The joining condition at the interface gives the constant D a value $-6y_1/y_2$.

Thus, it is seen that the deflection of the flow due to step-waves, though it contributes no pressure, induces a forward velocity in the incompressible layer. Since it increases linearly with x, the back-flow should be expected to be reduced in the downstream direction. Of course, the possibility exists that an additional pressure might also enter if the inertia forces, though small, were not neglected. Nevertheless, it can be safely stated that the pressure is always of the secondary importance in this case and hence the above conclusions will remain valid.

On the other hand, the perturbation velocities $u_t^{(1)}$ and $v_t^{(1)}$ due to the transmitted wave, according to equation (52), are subject to boundary conditions

$$\left.\begin{aligned} u_t^{(1)} &= v_t^{(1)} = 0 && \text{when } y = 0 \\ u_t^{(1)} &= Ae^{\lambda x} \qquad v_t^{(1)} = -\beta Ae^{\lambda x} && \text{when } y = \infty \\ u_t^{(1)} &= u^{(1)} && \text{when } x = 0, \quad y \geqq 0 \end{aligned}\right\} \tag{58}$$

To solve this problem, the viscous layer is again subdivided into incompressible and compressible layers. Since the boundary conditions and the differential equations are the same, $u_t^{(1)}$ and $v_t^{(1)}$ will have the same forms as those given in equations (33) and (44), with eigenvalue λ satisfying equation (48). Now if the perturbation is required to vanish at positive infinity, λ should be negative. But were λ negative, solutions (33) and (44) would be highly oscillatory, as the

arguments of both Bessel and the exponential functions involve a factor $\sqrt{\lambda R}$. That is, the solution of the incompressible layer would involve $J_{\frac{1}{3}}\left(\frac{2}{3}\sqrt{\rho_o{}^{(0)}\alpha\lambda R}\, y^{3/2}\right)$ and that of the compressible layer would have $\cos \sqrt{\lambda R}\, y$ and $\sin \sqrt{\lambda R}\, y$. For large Reynolds number, these types of solutions for a steady laminar flow must be rejected as impossible. By the same reason, complex roots are excluded. The only alternative is to accept the positive λ.

If λ is positive, it follows that the velocity $u_t{}^{(1)}$ and pressure $p_t{}^{(1)}$ will continue to increase until the process of linearization breaks down. This would imply that in the potential field the train of compression waves, immediately following the expansion, will grow exponentially with x. The flow direction as well as the curvature of the streamlines will also increase sharply. For such a flow, it is well-known that the Mach waves will converge and form an envelope. Therefore, in region 3 a shock eventually must be developed. On the other hand, in the viscous field, as $u_t{}^{(1)} + u_s{}^{(1)}$ for any constant y will increase with x, backflow, though slightly reduced by the step waves, will become stronger in the downstream direction. Now, it has been well-established that the laminar velocity profile with a point of inflection is highly unstable. As the pressure continues to grow at a Reynolds number generally above the critical value, transition must occur after a critical pressure gradient is reached. The flow from there on cannot be theoretically studied without considering unsteady flow.

It is therefore concluded that in the case of an incident compression shock, laminar flow is not possible for the whole viscous layer and transition always occurs. This appears to be in complete agreement with the present available experimental observations.

Character of Flow After Transition

Although the flow from a certain point on is unknown, the interesting fact is, however, that the flow up to the point of transition is very insensitive to what happens beyond the point of transition. In the previous sections, the problem has been reduced to depend only on one constant A on which the quantitative behavior, but not the character of the flow, depends. A quite similar conclusion has also been reached in reference 1 and seems to be an experimental fact (reference 7). In one of his experiments, Liepmann introduced an expansion wave immediately after the incident shock, and the observed upstream flow field was practically unchanged. Therefore, in order to account

for the observed pressure distribution, say it is sufficient just to take approximately the effect of the flow downstream of the point of transition.

Assume that the second shock starts at the edge of the viscous layer and, by linear theory, has the same strength ϵ. Inasmuch as the direction of the flow on OM is constant and equal to $\epsilon(2 - \beta A)$, if the flow after the shock TR (fig. 2) is parallel to the plate, the direction in front of the shock at large distance must be ϵ. This condition gives $A = \beta^{-1}$. Moreover, as the velocity vector is turning away from the plate, the pressure continues to rise and will be stopped only by transition. In that event, the sudden increase of shear of the viscous layer will thicken the viscous layer. This thickening will make the flow expand and consequently a drop of pressure will ensue. After this, the streamlines will gradually level off and the reattachment of the partially turbulent layer, if not yet accomplished prior to the transition point, will be certain to follow. If the point of transition is chosen to coincide with the point where $v = 0$ along the boundary streamline, the location is then determined by $\lambda x_1 = \log_e 2$.

For values of x greater than x_1, the flow in the immediate neighborhood of transition would have a greater influence than that far downstream where the flow is more uniform. Since the flow in the transition region is of a boundary-layer type, namely, the backflow ceases to be a factor, it can again be approximately represented by the integrated effects, such as the momentum and pressure. If the flows before and after the point of transition have the same pressure and total momentum, the dynamical equilibrium can then be maintained. According to the solution given in reference 1, the pressure distribution in the transition region is approximately

$$\frac{2}{\beta} + K_1 e^{\lambda_1 x} + K_2 e^{\lambda_2 x}$$

where λ_1 and λ_2 are negative constants, being functions of M and R and K_1 and K_2 are integration constants. By the conditions that at $x = x_1$ the pressure and its derivative are continuous, K_1 and K_2 can then be determined.

It must be emphasized again that the conditions stated in this section are tentative. No obvious reasons beyond the ones outlined at the beginning of the section can be given at this moment.

NUMERICAL EXAMPLES

As a numerical example, the case of $M = 2$ and $R = 774$ is presented. First, the determinantal equation (50) is solved numerically for only one Mach number 2 but at different Reynolds numbers. The results are shown in figure 3. At this Reynolds number, λ is 0.0467. The velocity $u(x,y)$ and the surface pressure $p(x,0)$ for this λ are calculated. It is seen that for the shock strength of $\epsilon = -1^{\circ}$, the boundary layer first separates at $x_{sep} = 1.106$ (fig. 4(a)) and, subsequently, backflow sets in. When the shock strength is increased to $\epsilon = -3^{\circ}$, say, the separation occurs at a much earlier station, namely at $x_{sep} = -22.4$. The region of backflow is proportionally wider (fig. 4(b)). However, if the step waves are taken into account, then in the case of $\epsilon = -1^{\circ}$ there would be no separation (dashed curve in fig. 4(a) for $y_1 = 3$ and $y_2 = 9$); whereas in the case of $\epsilon = -3^{\circ}$ the flow at the same location remains separated but the backflow has been very much reduced (dashed curve in fig. 4(b)). These results show quite the same characteristics as the experimental measurements by Ackeret, Feldman, and Rott (reference 8) of the velocity distribution over a curved plate.

The pressure distributions over the plate for these cases are shown in figure 5. For the weaker shock $\epsilon = -1^{\circ}$, surprisingly good agreement with experiment (reference 6) is obtained. This very fact seems to justify the present assumptions regarding the structure of the viscous layer. In the case of stronger shock, for example, $\epsilon = -3^{\circ}$, there is, however, a distinct difference between theory and experiment. Theoretically, the pressure would still decay exponentially upstream but would begin with a larger amplitude. Experimentally, it was found, strangely enough, that, over a considerable range of the upstream disturbed region, the pressure first decreases very slowly and then decays more or less exponentially. This "pressure bump" seems to be characteristic of the pressure distribution in the case of interaction between stronger shocks and the laminar boundary layer. This bumpy character in the pressure distribution, by all evidences, must be attributed to the nonlinear effect of the flow. This will be exhibited in the following section.

APPRAISAL OF HIGHER-ORDER EFFECTS

It has been shown that, if there is no backflow in region 1, the pressure disturbances will decay exponentially. When the shock strength increases, however, the pressure in the disturbed region becomes much higher and drops much more slowly than that predicted by the theory. This appears to be due to the fact that when backflow develops, there

will be an underestimate of the perturbed velocity and, consequently, a much lower pressure.

To estimate the effect due to higher-order terms, a second-order solution is found and is given in appendix C. According to the second-order solution, the correction terms for wall pressure would be

$$P_1 e^{\lambda x} + P_2 e^{2\lambda x}$$

In view of the fact that there is an overestimation of the first-order pressure by the condition $A = \beta^{-1}$, the correction term is expected to be negative for small values of x and positive far upstream. Then $P_1 > 0$ and $P_2 < 0$. Since $e^{2\lambda x}$ increases faster than x^2 and $e^{\lambda x}$, when x is positive, the correction would be negatively large far downstream. It has been pointed out previously that the iteration process fails for positive values of x; this solution shows further that it diverges oscillatorily. In order that the solution will behave properly, it will have to be carried to an odd order, such as one or three. To third order, the correction for wall pressure would be

$$P_1 e^{\lambda x} + P_2 e^{2\lambda x} + P_3 e^{3\lambda x}$$

If $P_1 = 0.75$, $P_2 = -1.83$, and $P_3 = 1$, the wall-pressure distribution for $\epsilon = -3^\circ$ would resemble the curve as shown in figure 6, which does exhibit the same character as measured by experiments. This, of course, cannot be considered as conclusive evidence, but at least it shows that higher-order terms such as given above do have the possibility of accounting for the observed behavior of the wall-pressure distribution. It is very important that this step be carried out.

DISCUSSION

This study being intended as an exploratory study, the numerical results obtained are not expected to be exact, but only accurate enough to insure the conclusions. As far as the first-order solution is concerned, the entire problem depends on the determination of one parameter λ, which was calculated on the basis of two main approximations:

(a) the contribution of the integral $\int_{\eta_1}^{\infty} \eta^{1/2} K_{\frac{1}{3}}\left(\frac{2}{3}\eta^{3/2}\right) d\eta$ is negligible

and (b) λy_1 is small such that terms of order $(\lambda y_1)^2$ and higher can be neglected. The subsequent solution for λ satisfies this criterion. The question remains, however, whether $\lambda y_1 = n(1)$ is also a solution or not. If $\lambda y_1 = n(1)$, the integrals $\int_0^{\eta_1} \eta^{1/2} \begin{Bmatrix} \cos \\ \sin \end{Bmatrix} \tau\eta \, K_{\frac{1}{3}}\left(\frac{2}{3}\eta^{3/2}\right) d\eta$ would require a more elaborate evaluation. The possibility exists and is worth testing.

As from the outset the boundary-layer approximation is rejected, it is of interest to examine the character of the perturbed flow in the light of boundary-layer theory. According to the boundary-layer approximation, if the velocity $u' = O(U_\infty)$ and $\partial/\partial x' = O(L^{-1})$, then the velocity $v' = O(U_\infty R^{-1})$ and $\partial/\partial y' = O(L^{-1}R)$. Now, from the character of the solution for perturbed flow in the present theory, $\partial/\partial x' = O(L^{-1}R^{3/4})$ and $\partial/\partial y' = O(L^{-1}R^{5/4})$. By comparison, the derivatives for the perturbed flow are much larger than the corresponding derivatives of boundary-layer theory. Moreover, from the equation of continuity the ratio $v^{(1)}/u^{(1)}$ of the perturbed velocities is $O(R^{-1/2})$. As in the vicinity of the wall $u^{(1)} \approx u^{(0)}$, $v^{(1)}$ is much larger than the vertical component in the boundary layer. Since in this case $\partial/\partial x' < \partial/\partial y'$ and $v^{(1)} < u^{(1)}$, a set of equations analogous to those for the boundary-layer flow can be deduced as long as backflow does not take place. Therefore, for expansion and even weak compression incident waves, a much simpler problem would be feasible.

Finally, it might also be noted that, owing to the assumption that the flow far away from the plate is inviscid and irrotational, there is introduced a sharp discontinuity in higher derivatives at the demarcation line between the two flow fields. Because of the presence of shock, however, a first-order discontinuity is also expected, because, by the assumption of frictionless flow at large distance, a smooth transition from small shock thickness at large distance to a larger one at the vicinity of the wall is precluded. The viscous-layer concept then idealizes the situation by taking the shock as a discontinuity in the outer field but continuous in the viscous flow. The effect of this is exhibited in a discontinuity in slope of the streamlines. This picture is entirely in agreement with the observed flow patterns.

According to the numerical example, the step waves tend to weaken the backflow downstream of the point of incidence but are unable to make

the flow reattach if the separation has occurred upstream of the point of incidence. This may very well be due to the poor approximation inherent in the Stokes flow which may underestimate the rate of change in the y-direction. If a more exact solution is given, reattachment of the separated flow might be accomplished in the laminar regime. This point should be considered as open.

CONCLUSIONS

The following conclusions are drawn from an analysis by the differential-equation method of the interaction of an oblique shock wave with a laminar boundary layer along a flat plate:

1. The pressure perturbation decays exponentially forward of the point of incidence and the distance of pressure propagation varies with different Mach and Reynolds numbers as $\beta^{-3/4}R^{-3/4}$ (where β is $\sqrt{M^2 - 1}$, M is Mach number, and R is Reynolds number) and very slowly with the shock strength.

2. If the shock strength is strong enough, separation of the flow always occurs. For given Mach and Reynolds numbers, the separation point depends strongly on the shock strength.

3. The pressure at the point of separation varies with Mach and Reynolds numbers as $\beta^{-1/2}R^{-1/2}$.

4. In the viscous layer, laminar flow is not possible everywhere, no matter whether the incident shock is strong or weak. In the distance of about two or three boundary-layer thicknesses, transition would occur.

5. The curvature of the streamlines after the shock is positive and the Mach waves in the potential field must coalesce to form a shock which approaches asymptotically the regularly reflected shock in the inviscid fluid. As its position depends on the point of transition, the exact location cannot be predicted by the present theory.

6. From the calculated pressure distribution over the wall, it is definitely proved that the observed overcompression of the wall pressure is a consequence of the positive curvature of the streamlines and the expansion is associated with transition.

7. The observed "bump" in the pressure distribution in region 1 for strong shocks is definitely a nonlinear effect and is an indirect consequence of separation.

APPENDIX A

PERTURBATION OF AN OBLIQUE SHOCK

Let ${}_1u_{\parallel}$, ${}_1u_{\perp}$, p_1, and ρ_1 denote, respectively, the parallel and normal velocities with respect to an oblique shock, the pressure and density in front of the shock, and, by replacing 1 by 2, the corresponding quantities behind the shock. These variables are related to each other by the Rankine-Hugoniot conditions:

$$\left.\begin{aligned} &\rho_1\,{}_1u_{\perp} = \rho_2\,{}_2u_{\perp} \\ &{}_1u_{\parallel} = {}_2u_{\parallel} \\ &p_1 + \rho_1\,{}_1u_{\perp}^2 = p_2 + \rho_2\,{}_2u_{\perp}^2 \\ &\frac{\gamma}{\gamma - 1}\frac{p_1}{\rho_1} + \frac{1}{2}\,{}_1u_{\perp}^2 = \frac{\gamma}{\gamma - 1}\frac{p_2}{\rho_2} + \frac{1}{2}\,{}_2u_{\perp}^2 \end{aligned}\right\} \tag{A1}$$

If the flow in front of shock is given, equations (A1) yield the following solutions:

$$\left.\begin{aligned} p_2 &= p_1 + \frac{2}{\gamma + 1}\rho_1\left({}_1u_{\perp}^2 - a_1^2\right) \\ \rho_2 &= \rho_1\frac{\gamma + 1}{\gamma - 1 + 2\left(\dfrac{a_1}{{}_1u_{\perp}}\right)^2} \\ {}_2u_{\perp} &= {}_1u_{\perp}\left(\frac{\gamma - 1}{\gamma + 1} + \frac{2}{\gamma + 1}\frac{a_1^2}{{}_1u_1^2}\right) \end{aligned}\right\} \tag{A2}$$

where a_1 is the speed of sound in front of the shock. If a_∞ and U_∞ are the speed of sound and velocity at infinity, then a_1 can be expressed in terms of velocities by the relation:

$$a_1^2 + \frac{\gamma - 1}{2}\left(u_1^2 + v_1^2\right) = a_\infty^2 + \frac{\gamma - 1}{2} U_\infty^2$$

Furthermore, if ω is the angle between the velocity (u_1, v_1) and the shock, it is easy to show that the Cartesian components before and after the shock are related by

$$\left.\begin{aligned} u_2 &= u_1 + \frac{2}{\gamma + 1}\left(u_1 \sin^2\omega + V_1 \sin\omega \cos\omega\right)\left(\frac{a_1^2}{q_1^2 \sin^2\omega} - 1\right) \\ V_2 &= V_1 - \frac{2}{\gamma + 1}\left(u_1 \cos\omega \sin\omega - V_1 \sin^2\omega\right)\left(\frac{a_1^2}{q_1^2 \sin^2\omega} - 1\right) \end{aligned}\right\} \qquad (A3)$$

with $q_1^2 = u_1^2 + V_1^2$.

In the case of weak shock, the shock angle ω can be expanded in terms of the deflection angle ϵ. Then $\cos\omega$ and $\sin\omega$ are shown to be

$$\left.\begin{aligned} \cos\omega &= \frac{\beta}{M}\left\{1 + \frac{\gamma + 1}{4\beta^3} M^2\epsilon - \right. \\ &\qquad \left. \frac{(\gamma + 1)M^2}{4\beta^4}\left[\frac{(\gamma + 1)M^2}{8\beta^2}\left(2M^2 + 1\right) - 1\right]\epsilon^2 + \cdots\right\} \\ \sin\omega &= \frac{1}{M}\left\{1 - \frac{\gamma + 1}{4\beta} M^2\epsilon + \right. \\ &\qquad \left. \frac{(\gamma + 1)}{4\beta^2} M^2\left[\frac{(\gamma + 1)M^2}{8\beta^2}\left(M^2 + 1\right) - 1\right]\epsilon^2 + \cdots\right\} \end{aligned}\right\} \qquad (A4)$$

Now since the velocity components u_1 and v_1 can be expanded:

$$u_1 = 1 + \epsilon u_1^{(1)} + \epsilon^2 u_1^{(2)} + \cdots$$

$$v_1 = \epsilon v_1^{(1)} + \epsilon^2 v_1^{(2)} + \cdots$$

If ω has the expansion:

$$\omega = \omega^{(0)} + \epsilon\omega^{(1)} + \epsilon^2\omega^{(2)} + \cdots$$

and $\omega^{(0)}$ is defined by equations (A4), then a straightforward reduction gives

$$u_2 = 1 + \epsilon u_2^{(1)} + \epsilon^2 u_2^{(2)} + \cdots$$

$$v_2 = \epsilon v_2^{(1)} + \epsilon^2 v_2^{(2)} + \cdots \tag{A5}$$

where

$$\left.\begin{aligned}
u_2^{(1)} &= \left[1 - \frac{4}{\gamma+1}\left(\frac{\gamma-1}{2} + \frac{1}{M}\right)\right]u_1^{(1)} + \frac{1}{\beta}\left[1 + \frac{4\beta^2\omega^{(1)}}{(\gamma+1)M^2}\right] \\
v_2^{(1)} &= v_1^{(1)} - \frac{4\beta}{\gamma+1}u_1^{(1)}\left(\frac{\gamma-1}{2} + \frac{1}{M^2}\right) + \left[1 + \frac{4\beta^2\omega^{(1)}}{(\gamma+1)M^2}\right] \\
u_2^{(2)} &= \left[1 - \frac{4}{\gamma+1}\left(\frac{\gamma-1}{2} + \frac{1}{M^2}\right)\right]u_1^{(2)} + \frac{1}{\beta}\left[1 + \frac{4\beta^2\omega^{(1)}}{(\gamma+1)M^2}\right]\left(u_1^{(1)} - \frac{v_1^{(1)}}{\beta}\right) + \\
&\quad \frac{2}{\gamma+1}\left(\frac{\gamma-1}{2} + \frac{1}{M^2}\right)\left[\left(u_1^{(1)}\right)^2 - \left(v_1^{(1)}\right)^2\right] + \frac{4\beta}{\gamma+1}\left(\frac{\gamma-1}{2} + \frac{1}{M^2}\right)u_1^{(1)}v_1^{(1)} + \\
&\quad \left[-\frac{1}{\beta^2}\left(\frac{\gamma+1}{4}\frac{M^4}{\beta^2} - 1\right) - \frac{(M^2-2)}{\beta^2}\omega^{(1)} + \frac{4\beta\omega^{(2)}}{(\gamma+1)M^2} - \frac{2(M^2-2)}{(\gamma+1)M^2}\left(\omega^{(1)}\right)^2\right] \\
v_2^{(2)} &= -\frac{4\beta}{\gamma+1}\left(\frac{\gamma-1}{2} + \frac{1}{M^2}\right)u_1^{(2)} + v_1^{(2)} + \frac{2\beta}{\gamma+1}\left(\frac{\gamma-1}{2} + \frac{1}{M^2}\right)\left[\left(u_1^{(1)}\right)^2 - \left(v_1^{(1)}\right)^2\right] - \\
&\quad \frac{1}{\beta}\left(1 + \frac{4\beta^2\omega^{(1)}}{(\gamma+1)M^2}\right)\left(1 + \frac{\gamma-1}{2}M^2\right)u_1^{(1)} + \frac{1}{\beta}\left[1 + \frac{4\beta^2\omega^{(1)}}{(\gamma+1)M^2}\right]v_1^{(1)} - \\
&\quad \frac{4}{\gamma+1}\left(\frac{\gamma-1}{2} + \frac{1}{M^2}\right)u_1^{(1)}v_1^{(1)} + \left[\frac{1}{\beta} + \frac{M^2+2}{\beta}\omega^{(1)} + \frac{4\beta^2\omega^{(2)}}{(\gamma+1)M^2} + \frac{2\beta(1+M^2)}{(\gamma+1)M^2}\left(\omega^{(1)}\right)^2\right]
\end{aligned}\right\} \tag{A6}$$

APPENDIX B

POTENTIAL FLOW IN REGION 2

If the flow in region 2 is irrotational, there exists a potential ${}_2\varphi(x,y)$ and, if the shock conditions are satisfied, it must possess the expansion:

$$ {}_2\varphi = x + \epsilon\, {}_2\varphi^{(1)} + \epsilon^2\, {}_2\varphi^{(2)} + \cdots \tag{B1} $$

For the first-order solution of the shock conditions, namely, on a line $x + \beta y = 0$,

$$ \left.\begin{aligned} {}_2\varphi_x{}^{(1)} &= \left[1 - \frac{4}{\gamma+1}\left(\frac{\gamma-1}{2} + \frac{1}{M^2}\right)\right] u_1{}^{(1)} + \frac{1}{\beta}\left(1 + \frac{4\beta^2\omega^{(1)}}{(\gamma+1)M^2}\right) \\ {}_2\varphi_y{}^{(1)} &= v_1{}^{(1)} - \frac{4\beta}{\gamma+1}\left(\frac{\gamma-1}{2} + \frac{1}{M^2}\right) u_1{}^{(1)} + 1 + \frac{4\beta^2\omega^{(1)}}{(\gamma+1)M^2} \end{aligned}\right\} \tag{B2} $$

Now on the shock

$$ u_1{}^{(1)} = Ae^{2\lambda x} $$

$$ v_1{}^{(1)} = -\beta Ae^{2\lambda x} $$

If the perturbed shock angle is

$$ \omega^{(1)} = se^{\lambda(x-\beta y)} $$

the solution ${}_2\varphi^{(1)}$ must be

$$ {}_2\varphi^{(1)} = \frac{1}{\beta}(x + \beta y) + te^{\lambda(x-\beta y)} \tag{B3} $$

Substituting $\omega^{(1)}$ and ${}_2\varphi^{(1)}$ in equation (B2), the two equations yield uniquely

$$\left.\begin{aligned} s &= \frac{A}{\lambda} \\ t &= \frac{M^2}{\beta}\left(\frac{\gamma - 1}{2} + \frac{1}{M^2}\right)A \end{aligned}\right\} \tag{B4}$$

The solution in region 2 is thus a superposition of the transmitted waves $e^{\lambda(x-\beta y)}$ and a uniform step wave $x + \beta y$ introduced by external agency.

Since this solution will terminate on the Mach line OM, the solution in region 3 will be found by the condition that on $x - \beta y = 0$,

$${}_3u^{(1)} = {}_1u^{(1)} \tag{B5}$$

By this condition, the Prandtl-Meyer flow requires a deflection

$$\delta\vartheta = -\epsilon\beta\ {}_1u^{(1)}(0) - {}_2u^{(1)}(0) \tag{B6}$$

Solution (A3) gives $\delta\vartheta = \epsilon$. Consequently, the initial direction of the flow in region 3, to the first order, is

$${}_2v^{(1)}(0) + \delta\vartheta = (2 - \beta A)\epsilon \tag{B7}$$

APPENDIX C

SECOND-ORDER SOLUTION

Potential Field

If the first-order potential is of the form:

$$\varphi^{(1)} = \frac{A}{\lambda} e^{\lambda(x-\beta y)}$$

it can be shown that the second-order equation (19) admits a solution which reduces, at the edge of viscous layer $y = 0$, to

$$\left.\begin{aligned} u^{(2)} &= Be^{\lambda x} + Ce^{2\lambda x} \\ v^{(2)} &= -\beta Be^{\lambda x} - \beta\left[C + \frac{(\gamma+1)M^4A^2}{4\beta^2}\right]e^{2\lambda x} \end{aligned}\right\} \tag{C1}$$

where B and C are arbitrary constants and the term $-\frac{(\gamma+1)M^4A^2}{4\beta} e^{2\lambda x}$ is derived from the particular integral $-\frac{(\gamma+1)M^2A^2}{4\beta} ye^{2\lambda(x-\beta y)}$. The reason that both $e^{2\lambda x}$ and $e^{\lambda x}$ are included in the complementary part of the solution is that the solution in region 2, according to equation (A6), contains both solutions.

Incompressible Layer

Assuming that, to the second order, the density in the inner layer remains constant, the system of equations (15) simplifies to

$$\Delta\Delta\psi^{(2)} - \tilde{\alpha}y\,\Delta\psi_x^{(2)} = R\left(\psi_y^{(1)}\Delta\psi_x^{(1)} - \psi_x^{(1)}\Delta\psi_y^{(1)}\right) \tag{C2}$$

where the second-order stream function $\psi^{(2)}$ is defined as

$$u^{(2)} = \psi_y{}^{(2)}$$

$$v^{(2)} = -\psi_x{}^{(2)}$$

By substituting $\psi^{(1)}$ into the right-hand side of equation (C2), the particular integral can be found; this is

$$\psi_p{}^{(2)} = \left[\frac{\sin \tilde{\tau}\tilde{\eta}}{\tilde{\tau}(2\tilde{\alpha}\lambda)^{2/3}} \int_0^{\tilde{\eta}} (\cos \tilde{\tau}\tilde{\eta}) Z(\tilde{\eta})\, d\tilde{\eta} - \frac{\cos \tilde{\tau}\tilde{\eta}}{\tilde{\tau}(2\tilde{\alpha}\lambda)^{2/3}} \int_0^{\tilde{\eta}} (\sin \tilde{\tau}\tilde{\eta}) Z(\tilde{\eta})\, d\tilde{\eta} \right] e^{2\lambda x} \tag{C3}$$

where the function $Z(\tilde{\eta})$ stands for

$$Z(\tilde{\eta}) = \frac{2}{3}\, \tilde{\eta}^{1/2} I_{\frac{1}{3}}\left(\frac{2}{3}\, \tilde{\eta}^{3/2}\right) \left[\int_\infty^{\tilde{\eta}} \tilde{\eta}^{1/2} K_{\frac{1}{3}}\left(\frac{2}{3}\, \tilde{\eta}^{3/2}\right) \Lambda(\eta)\, d\tilde{\eta} \right] - \frac{2}{3}\, \tilde{\eta}^{1/2} K_{\frac{1}{3}}\left(\frac{2}{3}\, \tilde{\eta}^{3/2}\right) \left[\int_0^{\tilde{\eta}} \tilde{\eta}^{1/2} I_{\frac{1}{3}}\left(\frac{2}{3}\, \tilde{\eta}^{3/2}\right) \Lambda(\eta)\, d\tilde{\eta} \right] \tag{C4}$$

with

$$\Lambda(\eta) = \frac{1}{4}(2\tilde{\alpha}\lambda)^{4/3}\frac{{C_1}^2}{{\rho_o}^{(0)}{}_\alpha}\left\{\eta^{1/2}K_{\frac{1}{3}}\left(\frac{2}{3}\eta^{3/2}\right)\left[(\cos\tau\eta)\int_0^\eta \eta^{1/2}(\cos\tau\eta)K_{\frac{1}{3}}\,d\eta + (\sin\tau\eta)\int_0^\eta \eta^{1/2}(\sin\tau\eta)K_{\frac{1}{3}}\,d\eta\right] - \frac{1}{\tau}\eta K_{\frac{2}{3}}\left(\frac{2}{3}\eta^{3/2}\right)\left[(\sin\tau\eta)\int_0^\eta \eta^{1/2}(\cos\tau\eta)K_{\frac{1}{3}}\,d\eta - (\cos\tau\eta)\int_0^\eta \eta^{1/2}(\sin\tau\eta)K_{\frac{1}{3}}\,d\eta\right]\right\} \tag{C5}$$

and the variables:

$$\tilde{\eta} = (2\tilde{\alpha}\lambda)^{1/3}\left(y - \frac{2\gamma}{\tilde{\alpha}}\right) \tag{C6}$$

$$\tilde{\tau} = 2\lambda/(2\tilde{\alpha}\lambda)^{1/3} \tag{C7}$$

The general solution, consequently, can be written as

$$\psi^{(2)} = \psi_c{}^{(2)} + \psi_p{}^{(2)} \tag{C8}$$

where the complementary integral $\psi_c{}^{(2)}$, by the first-order solution, will be given by

$$\psi_c{}^{(2)} = C_3\psi^{(1)}{}_{(\eta)}e^{\lambda x} + C_4\psi^{(1)}{}_{(\tilde{\eta})}e^{2\lambda x} \tag{C9}$$

Since the form of $\psi^{(1)}(\eta)$ is known, and, furthermore, $\psi^{(1)}(0) = \psi^{(1)'}(0) = 0$ the solution $\psi^{(2)}$ is determined with two arbitrary constants C_3 and C_4.

With $\psi^{(2)}$ determined, the second-order pressure $p^{(2)}(x,0)$ on the plate can be written, similarly, as

$$p^{(2)}(x,0) = P_1 e^{\lambda x} + P_2 e^{2\lambda x} + P_p e^{2\lambda x} \tag{C10}$$

where

$$P_p = -\frac{(2\tilde{\alpha}\lambda)^{1/3} 3^{2/3}}{3\Gamma\left(\frac{1}{3}\right)(\lambda R)} \int_0^\infty \eta^{1/2} K_{\frac{1}{3}}\left(\frac{2}{3}\eta^{3/2}\right) \Lambda(\eta)\, d\tilde{\eta}$$

and P_1 and P_2 take the same form as the symbol P for the first-order pressure $p^{(1)}$.

Compressible Layer

In the compressible layer, $\rho^{(0)} = u^{(0)} = T^{(0)} = 1$. Again, if $H^{(2)} = 0$, equations (15) become

$$\left.\begin{aligned}
&\left(u_y^{(2)} - v_x^{(2)}\right)_x - \frac{1}{R}\Delta\left(u_y^{(2)} - v_x^{(2)}\right) = \lambda\left(u^{(1)}{}_{\Delta G}{}^{(1)} + v^{(1)}{}_{\Delta F}{}^{(1)}\right) + \\
&\qquad\qquad v^{(1)}{}_{\Delta G_y}{}^{(1)} - u^{(1)}{}_{\Delta F_y}{}^{(1)} \\
&M^2 u_x^{(2)} - n^{(2)} - \frac{\gamma M^2}{R}\left(\Delta u^{(2)} + \frac{1}{3} n_x^{(2)}\right) = -\left(1 + \gamma M^2\right) v^{(1)}{}_{u_y}{}^{(1)} + \\
&\left[2\beta^2 - \left(1 + \gamma M^2\right)\right] u^{(1)}{}_{v_y}{}^{(1)} - 2\lambda\left(1 + \frac{\gamma - 1}{2} M^2\right)\left(u^{(1)}\right)^2 + \\
&\lambda M^2(\gamma - 1)\left(v^{(1)}\right)^2 - \frac{1}{\lambda}\left(v_y^{(1)}\right)^2 - \frac{1}{\lambda} v^{(1)}{}_{v_{yy}}{}^{(1)}
\end{aligned}\right\} \tag{C11}$$

Similarly, by introducing $F^{(2)}$ and $G^{(2)}$ through the relations

$$u^{(2)} = F_x{}^{(2)} + G_y{}^{(2)}$$

$$v^{(2)} = F_y{}^{(2)} - G_x{}^{(2)}$$

there result the following equations:

$$\left.\begin{aligned}
&\Delta G_x{}^{(2)} - \frac{1}{R}\Delta\,\Delta G^{(2)} = \lambda\left(u^{(1)}{}_{\Delta G}{}^{(1)} + v^{(1)}{}_{\Delta F}{}^{(1)}\right) + \\
&\qquad v^{(1)}{}_{\Delta G_y}{}^{(1)} - u^{(1)}{}_{\Delta F_y}{}^{(1)} \\
&M^2\left(F_{xx}{}^{(2)} + G_{xy}{}^{(2)}\right) - \Delta F^{(2)} - \frac{\gamma M^2}{R}\left[\Delta\left(F_x{}^{(2)} + G_y{}^{(2)}\right) + \frac{1}{3}\Delta\,\Delta F^{(2)}\right] = \\
&-\left(1 + \gamma M^2\right)v^{(1)}{}_{u_y}{}^{(1)} + \left[2\beta^2 - \left(1 + \gamma M^2\right)\right]u^{(1)}{}_{v_y}{}^{(1)} - \\
&2\lambda\left(1 + \frac{\gamma - 1}{2}M^2\right)u^{(1)2} + \lambda(\gamma - 1)M^2 v^{(1)2} - \frac{1}{\lambda}v_y{}^{(1)2} - \frac{1}{\lambda}v^{(1)}{}_{v_{yy}}{}^{(1)}
\end{aligned}\right\} \quad (C12)$$

The solutions $F^{(2)}$ and $G^{(2)}$ can be written in an analogous manner. That is:

$$\left.\begin{aligned}
F^{(2)} &= F_C{}^{(2)} + F_p{}^{(2)} \\
G^{(2)} &= G_C{}^{(2)} + G_p{}^{(2)}
\end{aligned}\right\} \quad (C13)$$

Here $F_C{}^{(2)}$ and $G_C{}^{(2)}$ are known from the first-order solution and $F_p{}^{(2)}$ and $G_p{}^{(2)}$ are given as follows:

$$\left.\begin{aligned}
F_p{}^{(2)} &= \left(K_1 + K_2 e^{-\sigma y} + K_3 e^{-2\sigma y}\right)e^{2\lambda x} \\
G_p{}^{(2)} &= K_4 e^{-\sigma y + 2\lambda x}
\end{aligned}\right\} \quad (C14)$$

where the constants K are defined by

$$K_1 = \frac{1 + \left(\beta^2/\beta_1^2\right)}{8\lambda\left(\beta_1^2 - \beta_2^2\right)} \frac{\left[4 + (\gamma - 1)M^2\right]\beta_1^2 + (\gamma - 1)M^2 + 2 + 2\beta_1^4}{1 + \frac{8}{3}\frac{\gamma M^2 \lambda}{R}} A^2 +$$

$$\frac{1 - \left(\beta^2/\beta_1^2\right)}{8\lambda\beta_2^2} \frac{\left[2\beta^2 - (\gamma - 1)M^2\right]\beta_1^2 + 2 + (\gamma - 1)M^2}{1 + \frac{8}{3}\frac{\gamma M^2 \lambda}{R}} A^2$$

$$K_2 = \frac{1 - (\beta/\beta_1)}{2\left(1 + \frac{8}{3}\frac{\gamma M^2 \lambda}{R}\right)}\Bigg[\gamma(\lambda\beta_1 - \sigma)M^2\left[\frac{2}{\gamma} - \frac{4\lambda^2 + (\lambda\beta_1 - \sigma)^2}{\lambda R}\right] \times$$

$$\frac{\left(\lambda^2\beta_1^2 - \sigma^2\right)\left[\frac{K\sigma^2}{\lambda^2} - R^{-1} + \beta_1\sigma(K + R^{-1})\lambda^{-1}\right]}{8\lambda^2(1 - 2\lambda R^{-1}) + (\lambda\beta_1 - \sigma)^2 + 2(1 - 4\lambda R^{-1}) - (\lambda R)^{-1}(\lambda\beta_1 - \sigma)^4} +$$

$$\beta_1(1 + \gamma M^2) - \frac{\sigma K R}{\lambda}\left\{4 + 2(\gamma - 1)M^2 + \beta_1^2\left[2 + (\gamma - 1)M^2 - \beta^2\right]\right\} +$$

$$\left(\frac{\sigma^2 K}{\lambda^2} - R^{-1}\right)\left(\lambda\beta_1\left(\beta_1^2 + \frac{\sigma^2}{\lambda^2} + 2M^2 + 2\right) + \sigma\left\{1 + \gamma M^2 + \beta_1^2\left[(\gamma - 1)M^2 - \beta^2\right]\right\}\right)\Bigg] \times$$

$$\frac{C_2 A}{(\lambda\beta_1 + \sigma)^2 - 4\lambda^2\beta_2^2} +$$

$$\frac{1 + (\beta/\beta_1)}{2\left(1 + \frac{8}{3}\frac{\gamma M^2 \lambda}{R}\right)}\Bigg(\frac{\gamma(\lambda\beta_1 + \sigma)M^2\left\{-\frac{2}{\gamma} + (\lambda R)^{-1}\left[4\lambda^2 + (\lambda\beta_1 - \sigma)^2\right]\right\}\left(\lambda^2\beta_1^2 - \sigma^2\right)\left[K\frac{\sigma^2}{\lambda^2} - \frac{1}{R} - \frac{\beta_1\sigma}{\lambda}(K + R^{-1})\right]}{8\lambda^2\left(1 - \frac{2\lambda}{R}\right) + 2(\lambda\beta_1 + \sigma)^2\left(1 - \frac{4\lambda}{R}\right) - (\lambda R)^{-1}(\lambda\beta_1 + \sigma)^4} -$$

$$\beta_1(1 + \gamma M^2) - \frac{\sigma K R}{\lambda}\left\{\beta_1^2\left[2 + (\gamma - 1)M^2 - \beta^2\right] + 4 + 2(\gamma - 1)M^2\right\} +$$

$$\left(K\frac{\sigma^2}{\lambda^2} - R^{-1}\right)\left\{-\lambda\beta_1\left(\beta_1^2 + \sigma^2 + 2M^2 + 2\right) + \frac{\sigma}{\lambda}\left\{1 + \gamma M^2 + \beta_1^2\lambda\left[(\gamma - 1)M^2 - \beta^2\right]\right\}\right) \times$$

$$\frac{C_2 A}{(\lambda\beta_1 + \sigma)^2 - 4\lambda^2\beta_2^2}$$

$$K_3 = -\left(1 + \frac{8}{3}\frac{\gamma M^2\lambda}{R}\right)^{-1}\left\{(\gamma - 1)M^2R\left(\frac{K\sigma^2}{\lambda^2} - R^{-1}\right) - \left[2 + (\gamma - 1)M^2\right]\frac{\sigma^2K^2R^2}{\lambda^3}\right\}C_2{}^2$$

$$K_4 = \frac{\left(\lambda\beta_1{}^2 - \sigma^2\right)(1 + \beta/\beta_1)\left[K\frac{\sigma^2}{\lambda^2} - R^{-1} - \frac{\beta_1\sigma}{\lambda}\left(K + \frac{1}{R}\right)\right]AC_2}{2\lambda\left[8\lambda^2(1 - 2\lambda R^{-1}) + 2(\lambda\beta_1 + \sigma)^2(1 - 4\lambda R^{-1}) - (\lambda R)^{-1}(\lambda\beta_1 + \sigma)^4\right]} +$$

$$\frac{\left(\lambda^2\beta_1{}^2 - \sigma^2\right)(1 - \beta/\beta_1)\left[K\frac{\sigma^2}{\lambda^2} - R^{-1} + \frac{\beta_1\sigma}{\lambda}\left(K + \frac{1}{R}\right)\right]AC_2}{2\lambda\left[8\lambda^2(1 - 2\lambda R^{-1}) + 2(\lambda\beta_1 - \sigma)^2(1 - 4\lambda R^{-1}) - (\lambda R)^{-1}(\lambda\beta_1 - \sigma)^4\right]}$$

and the constants K and β_2 stand for

$$K = -\frac{(\gamma - 1)\frac{M^2}{R}\lambda}{R + \left(\frac{4}{3}\gamma - 1\right)M^2\lambda}$$

$$\beta_2{}^2 = \frac{\beta^2 - \frac{8}{3}\frac{\gamma M^2\lambda}{R}}{1 + \frac{8}{3}\frac{\gamma M^2\lambda}{R}} \tag{C15}$$

The second-order solution now involves six arbitrary constants and, by the conditions at the interface, all but one can be determined.

REFERENCES

1. Ritter, Alfred, and Kuo, Yung-Huai: Reflection of a Weak Shock Wave From a Boundary Layer Along a Flat Plate. I - Interaction of Weak Shock Waves With Laminar and Turbulent Boundary Layers Analyzed by Momentum-Integral Method. NACA TN 2868, 1953.

2. Von Kármán, Th., and Tsien, H. S.: Boundary Layer in Compressible Fluids. Jour. Aero. Sci., vol. 5, no. 6, April 1938, pp. 227-232.

3. Tsien, Hsue-Shen, and Finston, Morton: Interaction between Parallel Streams of Subsonic and Supersonic Velocities. Jour. Aero. Sci., vol. 16, no. 9, Sept. 1949, pp. 515-528.

4. Emmons, H. W., and Brainerd, J. G.: Temperature Effects in a Laminar Compressible-Fluid Boundary Layer Along a Flat Plate. Jour. Appl. Mech., vol. 8, no. 3, Sept. 1941, pp. A-105 - A-110.

5. Brainerd, J. G., and Emmons, H. W.: Effect of a Variable Viscosity on Boundary Layers, With a Discussion of Drag Measurements. Jour. Appl. Mech., vol. 9, no. 1, March 1942, pp. A-1 - A-6.

6. Barry, F. W., Shapiro, A. H., and Neumann, E. P.: The Interaction of Shock Waves With Boundary Layers on a Flat Surface. Jour. Aero. Sci., vol. 18, no. 4, April 1951, pp. 229-238.

7. Liepmann, H. W., Roshko, A., and Dhawan, S.: On the Reflection of Shock Waves From Boundary Layers. NACA Rep. TN 2334, 1951.

8. Ackeret, J., Feldmann, F., and Rott, N.: Investigations of Compression Shocks and Boundary Layers in Gases Moving at High Speed. NACA TM 1113, 1947.

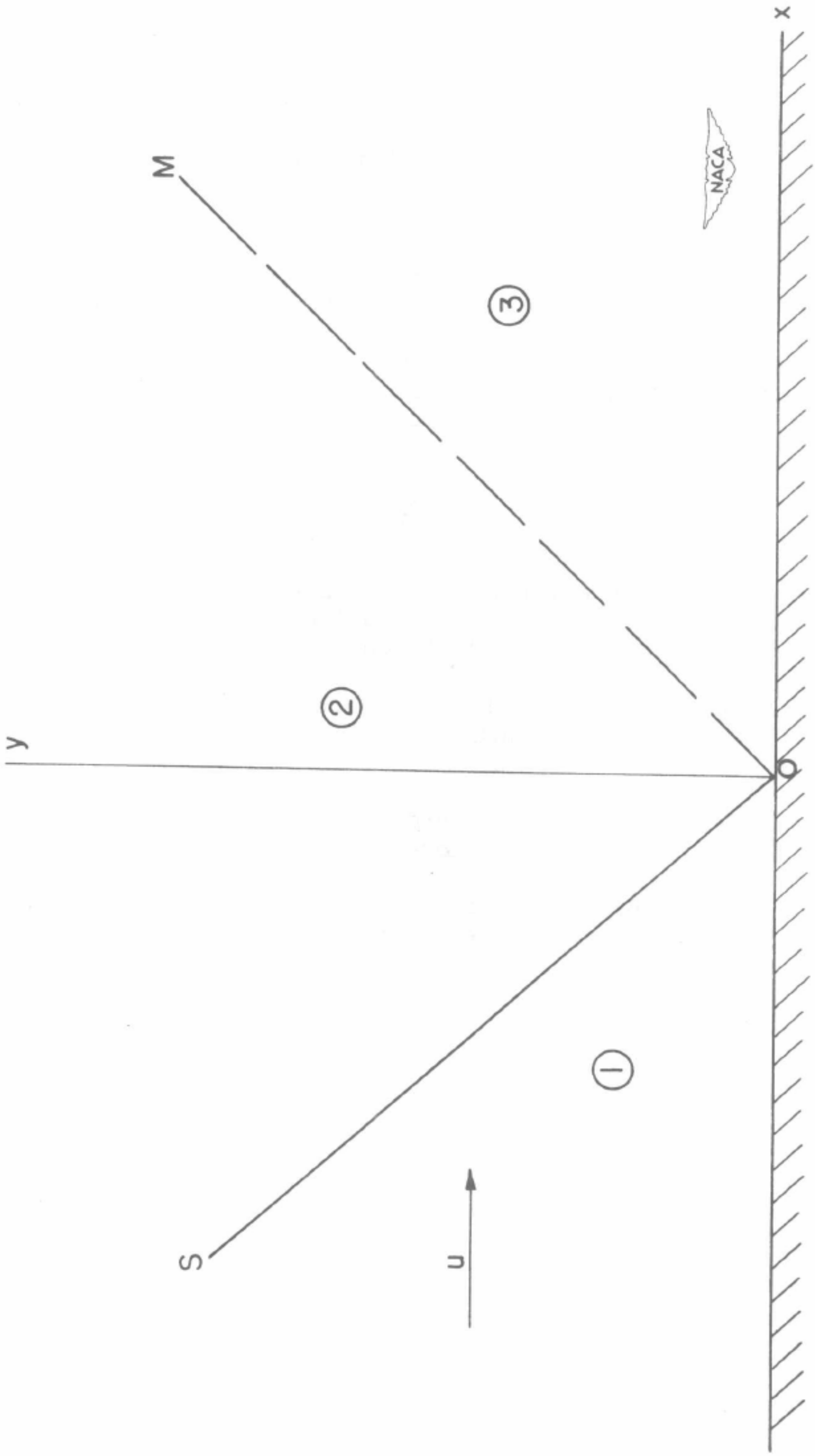

Figure 1.- Diagram of flow field.

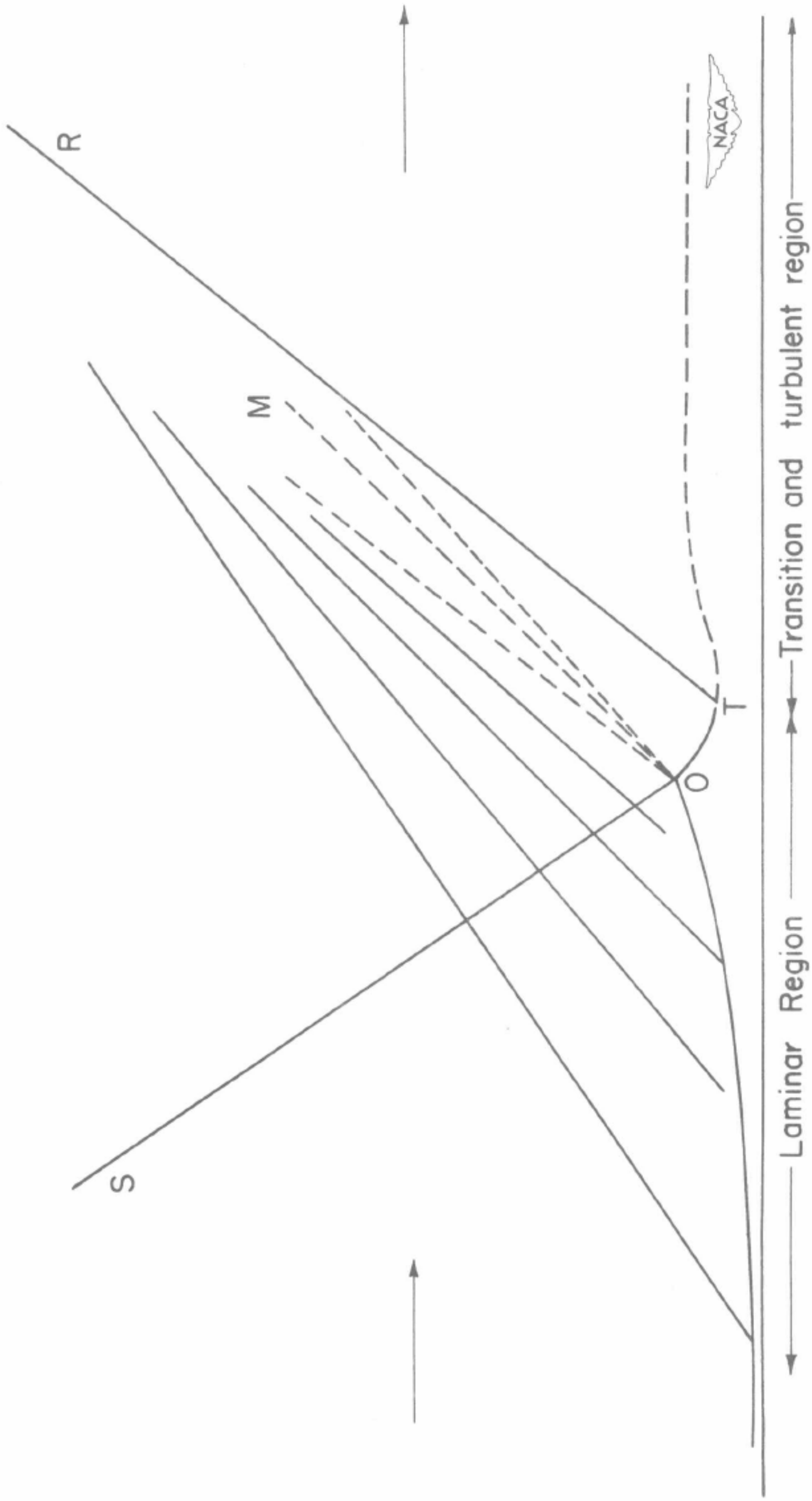

Figure 2.- Sketch of flow field according to first-order theory.

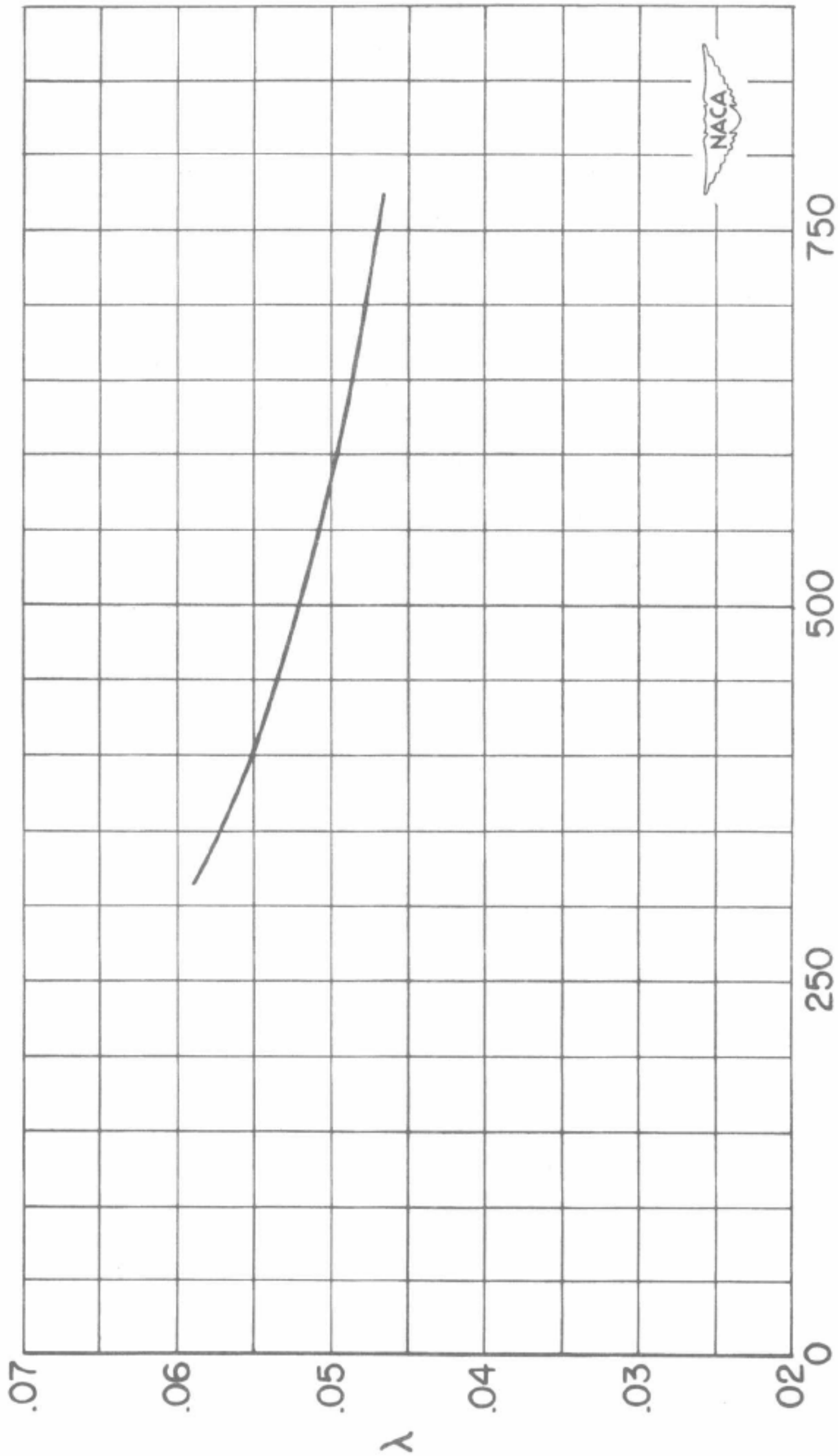

Figure 3.- Curve of λ against R for M = 2.

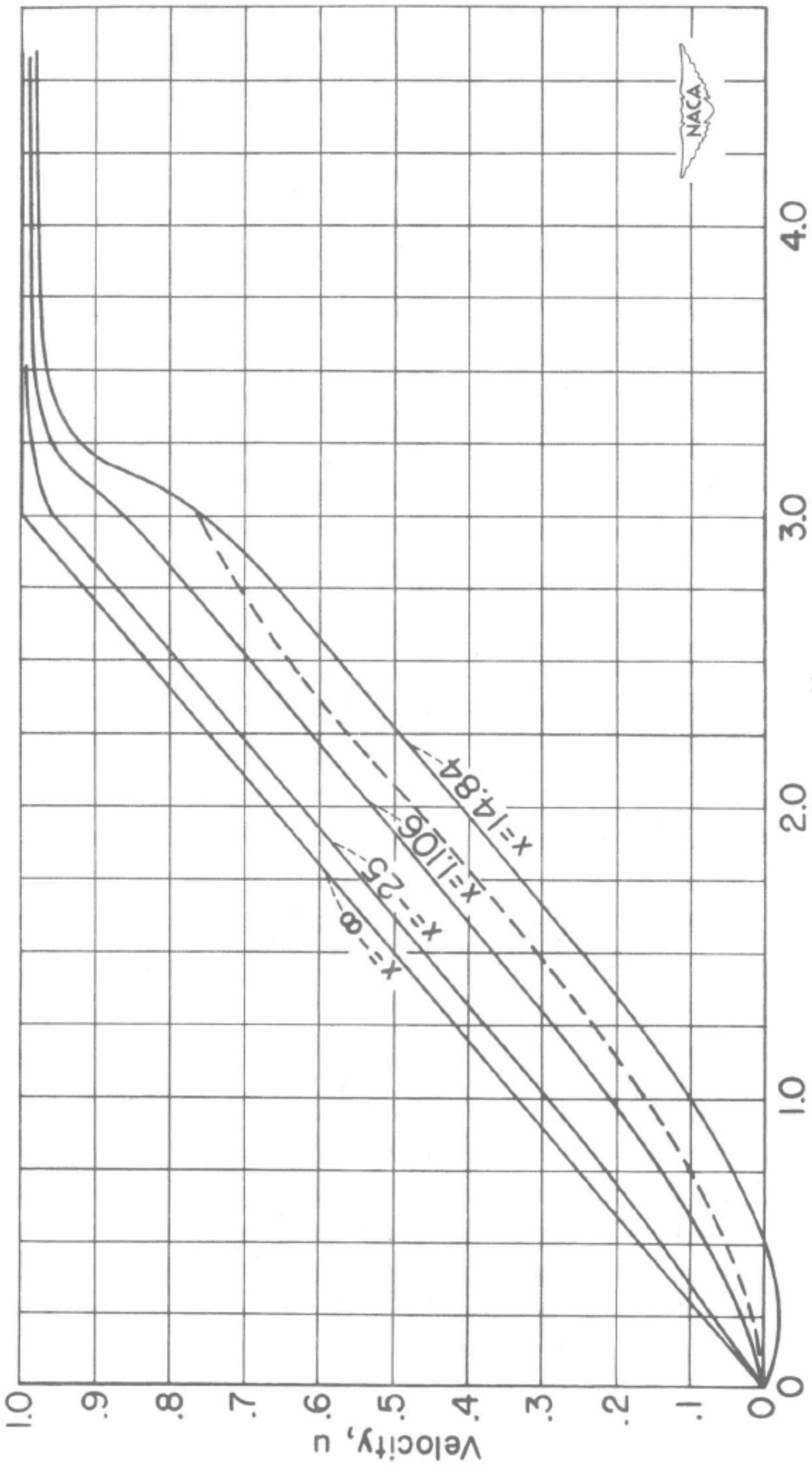

(a) $\epsilon = -1^{o}$; M = 2; R = 774.

Figure 4.- Velocity distribution.

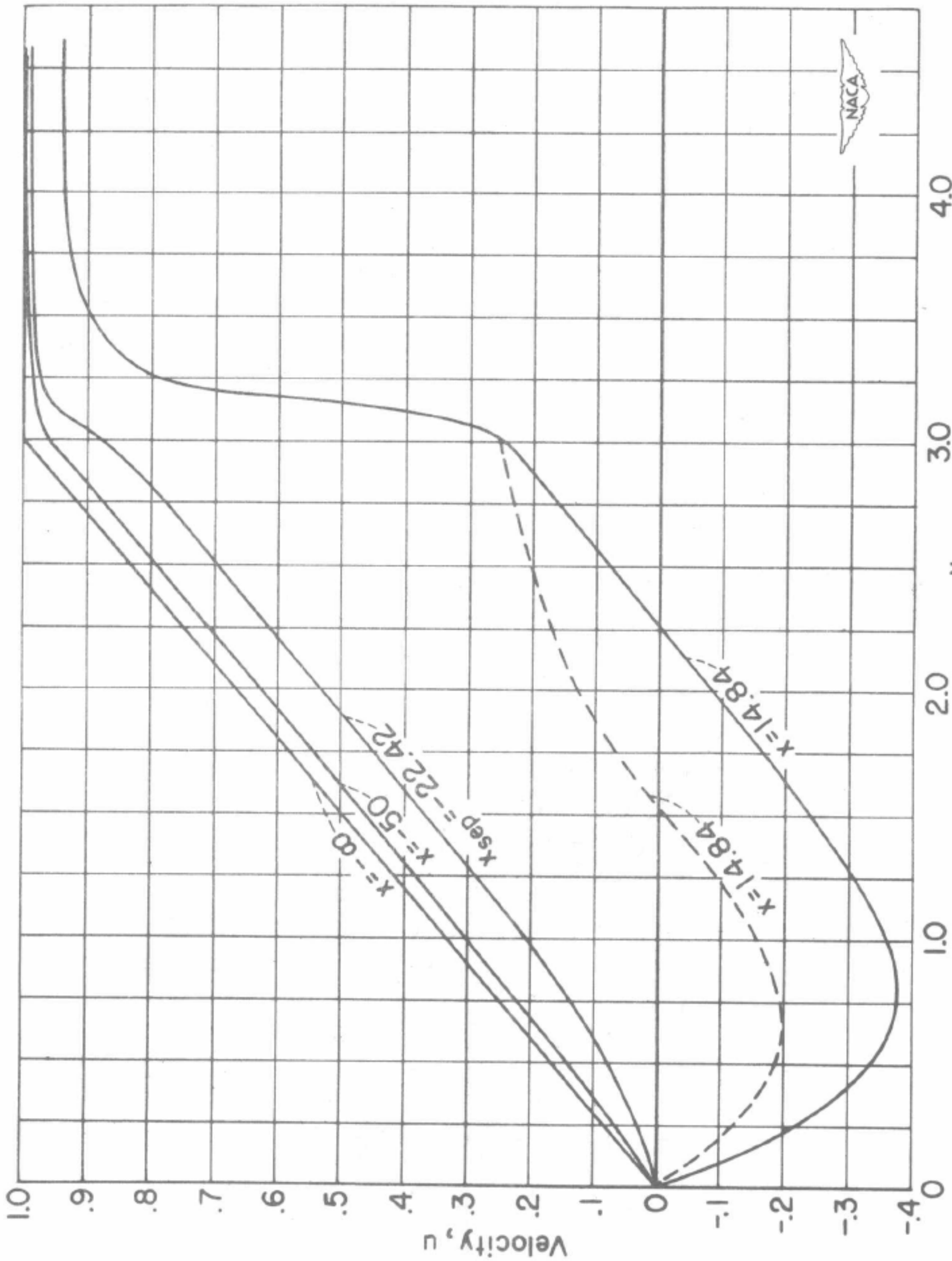

(b) $\epsilon = -3^{\circ}$; M = 2; R = 774.

Figure 4.- Concluded.

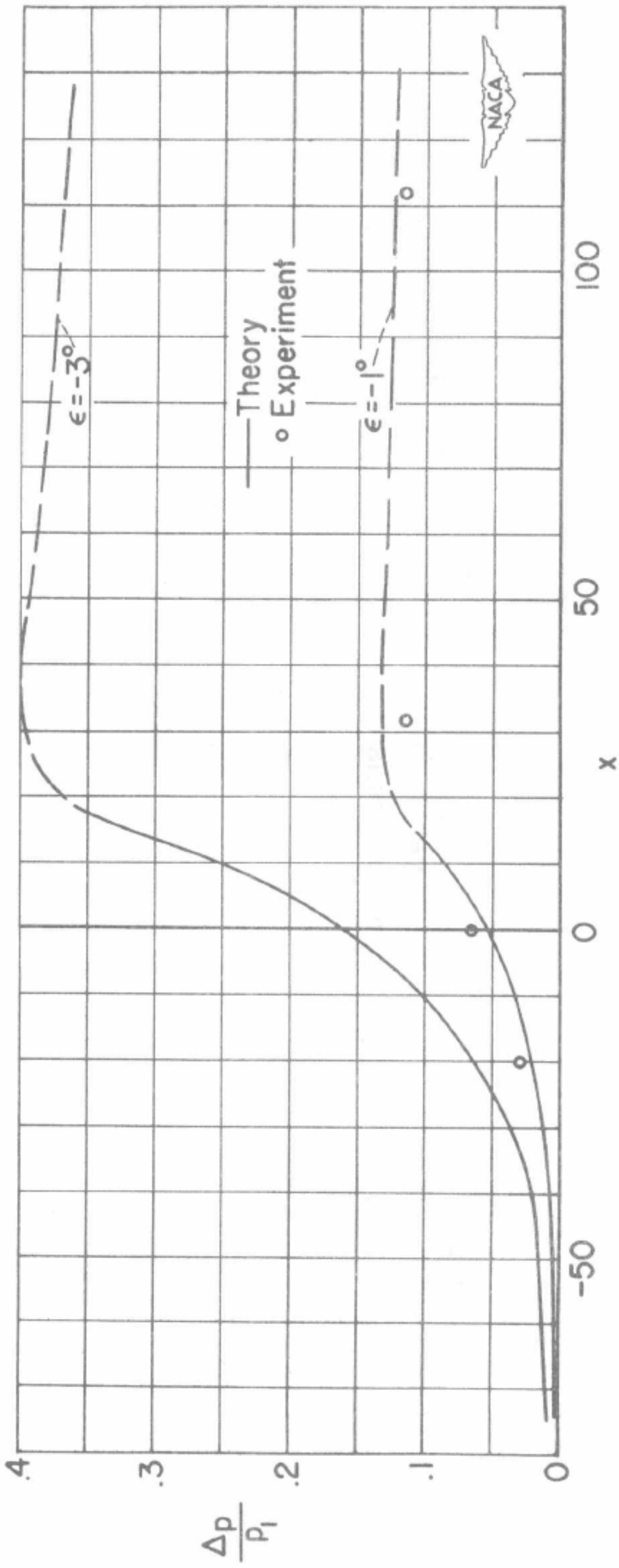
NACA
Theory
o Experiment
ε=-3°
ε=-1°
o
o
o

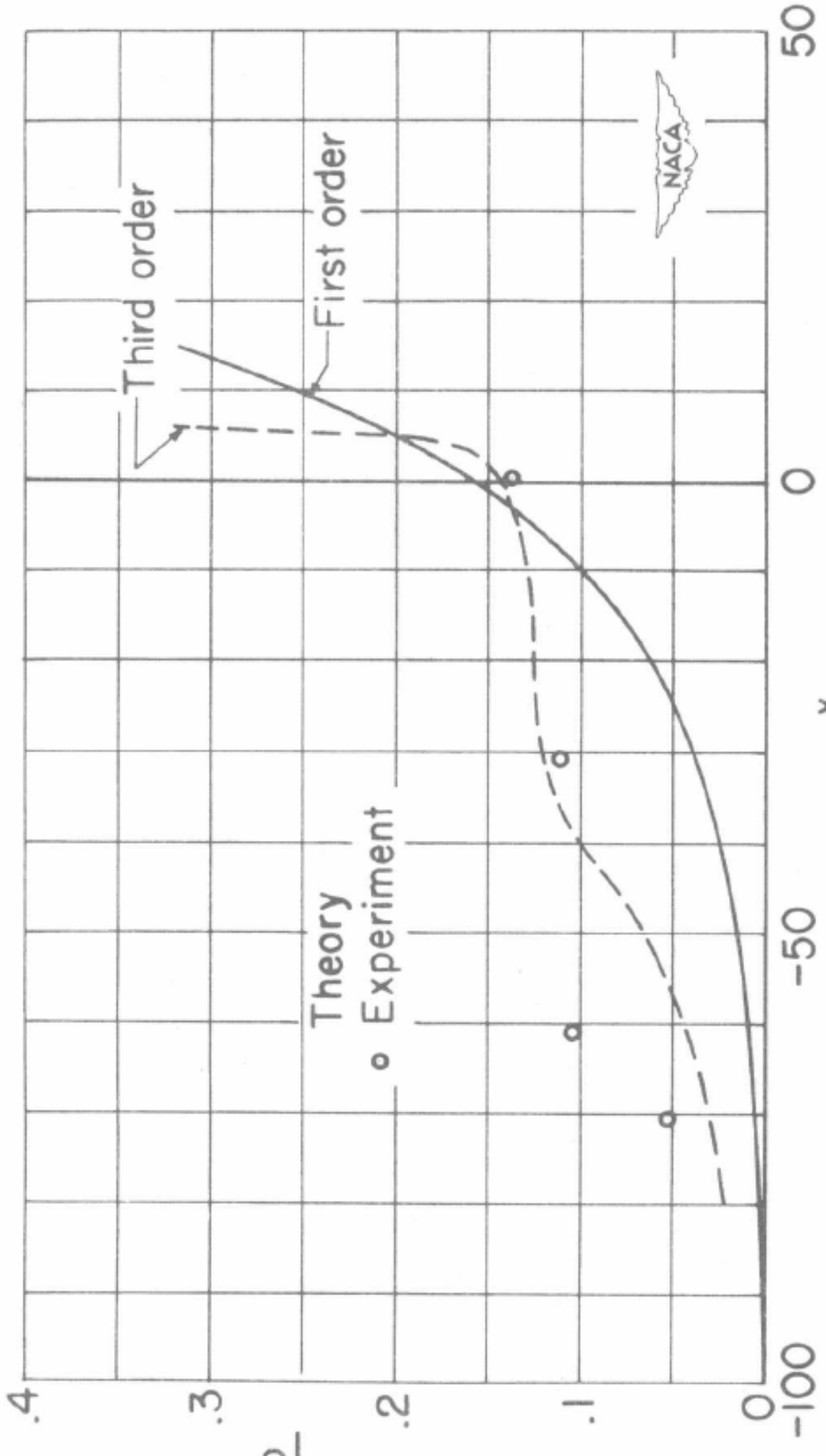

Figure 6.- Pressure distribution on plate for third- and first-order terms for $\epsilon = -3^{\circ}$. M = 2; R = 774.

NACA-Langley - 1-28-53 - 1000

SECTION F

PLANE SUBSONIC AND TRANSONIC POTENTIAL FLOWS [1]

Y. H. KUO
W. R. SEARS

F,1. Introduction. In classical hydrodynamics we take as a model a fluid that is both inviscid and incompressible. If the flow is assumed to be irrotational, as is frequently justified on physical grounds, a mathematical theory of hydrodynamics is built up upon the branch of mathematical physics known as potential theory. Fundamental questions of the existence and uniqueness of solutions can be answered with great generality in this framework. Once the hypothesis of incompressibility is rejected, however, the differential equations of the problem are nonlinear. Thus, high speed aerodynamics has a distinctive character, as has already been pointed out in Sec. A, and is no longer a branch of classical potential theory.

To meet this situation, a number of approximate techniques have been developed, and useful results obtained; these are the methods described in Sec. C, D, and E of this volume. In general, however, these do not suffice to answer questions such as existence and uniqueness of solutions. Moreover, they usually involve approximations of unknown magnitudes, so that their accuracy cannot be assessed, and it is desirable to compare their predictions with exact solutions, if such can be found. In the special case of steady plane flow, these objectives can be realized to some extent by the introduction of the *hodograph* method, i.e. the use of velocity components as independent variables. This is the subject of the present section.

In a broad sense, the hodograph method is not new in fluid mechanics. Prior to its application in high speed aerodynamics, Helmholtz [*58*] solved a number of problems involving plane walls and constant pressure surfaces (free boundaries), using the velocity plane to simplify the boundary-value problems. This method was subsequently perfected and has become a standard technique in dealing with this type of problem in hydrodynamics. The importance of this device as a means to linearize the equation of a certain gas flow was first recognized by Riemann [*1*] in his famous investigation of wave propagation.

1) Published in *General theory of high speed aerodynamics*, section F. 1954, 490~582

F,1 · *INTRODUCTION*

Finally, at the end of the nineteenth century, Molenbroeck [*59*] and Chaplygin [*2*] gave essentially the method used in this section, and thus succeeded in reducing the steady potential flow of a gas to a linear problem in the hodograph plane.

Between the problem of jets considered by Molenbroeck and Chaplygin and the typical aerodynamic problem of flow past a cylindrical obstacle, however, there is an essential difference. The hodograph method is ideally suited to describe the free surface boundary condition that occurs in the jet problems described above. In the problem of flow past a cylinder, however, it linearizes the problem but complicates the boundary conditions, for specified physical conditions in the flow plane correspond to unknown boundaries in the velocity plane. What is even more serious, the boundary is dependent upon a parameter of the flow, such as free stream Mach number. The advantage gained by the transformation is therefore compensated, to a great extent, by the loss of simplicity in the boundary-value problem. Nevertheless, when the exact shape of boundary is not essential, exact solutions for particular boundaries are obtainable, and the salient features of a nonlinear motion can be studied.

In this section, we shall deal with isentropic plane potential flows that are either subsonic everywhere or partly subsonic and partly supersonic; the latter may be called mixed flows or transonic potential flows. Those involving shock waves or computed by methods other than the hodograph transformation will be excluded; these are discussed in Sec. G and H. Inasmuch as purely subsonic flows do not yield the most interesting new phenomena, our main concern will be the mixed subsonic-supersonic flows.

As mentioned above, a solution constructed in the hodograph plane cannot usually be made to satisfy a prescribed boundary condition in the flow plane for flow past a surface. Instead, a guess has to be made, in the hodograph plane, as to the form of solution which, when transformed, will yield a useful flow pattern. There are two such procedures, due, respectively, to Chaplygin and Cherry. In the case of a closed body, Chaplygin's method proceeds by analogy with an incompressible flow, namely, the solution in the limit of vanishing Mach number reduces to a known flow in the flow plane (Art. 5–8). On the other hand, when such an analogy is not possible, a solution has to be selected possessing the desired singular behavior in the whole velocity plane (Art. 9). In principle, Cherry's method is the same as Chaplygin's, as both involve first the determination of the analytic behavior of the solution, but Cherry's approach is indirect, as will be seen in Art. 9 below, and hence more difficult but also more general.

In the closing articles of this section, we discuss the apparent nonappearance of steady, mixed, potential flows in experiment, and some of the proposed explanations of this dilemma.

F · *PLANE POTENTIAL FLOWS*

In the space available in this volume, it has been found impossible to reproduce in complete detail even the most important works using these methods. We are also forced to omit entirely a number of interesting investigations and merely to list them in an appended bibliography. In spite of this, the amount of mathematical analysis included in the section may seem objectionable to some readers (while it will certainly be considered insufficient by others). It has been our intention to point out the main features of the methods without unnecessary mathematical elaboration, but it must be agreed that many of these main features are mathematical in nature, and therefore cannot be discussed without equations and formulas. One compromise has been to collect in an appendix (Art. 16) a number of lemmas and formulas pertaining to the hypergeometric functions which are used occasionally throughout the section.

F,2. The Hodograph Transformation. Let u, v be the velocity components in the directions of the Cartesian coordinates x, y, respectively, and let ρ be the density of the fluid. If the flow is steady, isentropic, and irrotational, there exist both velocity potential $\phi(x, y)$ and stream function $\psi(x, y)$, defined by

$$u = \frac{\partial \phi}{\partial x}, \qquad v = \frac{\partial \phi}{\partial y}$$

and

$$\rho u = \rho^0 \frac{\partial \psi}{\partial y}, \qquad \rho v = -\rho^0 \frac{\partial \psi}{\partial x} \tag{2-1}$$

where ρ^0 is the stagnation density. By the elimination of u and v, we have as one fundamental system for two-dimensional flow,

$$\begin{aligned} \frac{\partial \phi}{\partial x} &= \frac{\rho^0}{\rho} \frac{\partial \psi}{\partial y} \\ \frac{\partial \phi}{\partial y} &= -\frac{\rho^0}{\rho} \frac{\partial \psi}{\partial x} \end{aligned} \tag{2-2}$$

In the case of isentropic potential flow, pressure p and density ρ are related by the equation of state

$$p = k\rho^\gamma \tag{2-3}$$

where k is a constant and γ the ratio of specific heats. In this case the equation of motion for steady flow can be integrated to give ρ in terms of the speed q $(= \sqrt{u^2 + v^2})$:

$$\rho = \rho^0 \left[1 - \frac{\gamma - 1}{2} \frac{q^2}{(a^0)^2} \right]^{\frac{1}{\gamma - 1}} \tag{2-4}$$

where a^0 is the speed of sound $a = \sqrt{\gamma p/\rho}$ at stagnation conditions.

F,2 · *THE HODOGRAPH TRANSFORMATION*

By means of Eq. 2-4, the elimination of the stream function ψ from Eq. 2-2 yields a differential equation for ϕ (cf. III,A,9, Eq. 9-11):

$$(a^2 - \phi_x^2)\phi_{xx} - 2\phi_x\phi_y\phi_{xy} + (a^2 - \phi_y^2)\phi_{yy} = 0 \qquad (2\text{-}5)$$

where the subscripts denote partial differentiation and the speed of sound a is

$$a^2 = (a^0)^2 - \frac{\gamma - 1}{2} q^2 = (a^0)^2 - \frac{\gamma - 1}{2}(\phi_x^2 + \phi_y^2) \qquad (2\text{-}6)$$

Eq. 2-5 is a second order, nonlinear, differential equation with coefficients involving the first derivatives of the unknown function. For flows in which q is everywhere less than the speed of sound a, the differential equation is of *elliptic* type. For flows in which q is everywhere greater than a, the equation is of *hyperbolic* type. Since the coefficients are variable, conditions may occur where both elliptic and hyperbolic domains coexist and the flow therefore changes its character locally. For example, in the flow past an object placed in a subsonic stream of gas, the flow may locally become supersonic and then return again to subsonic. The possibility of the existence of such smooth, mixed, transonic flows is of both mathematical and practical importance.

In the hyperbolic domain, the differential equation (2-5) is associated with two families of real characteristics, described by the ordinary differential equation

$$(a^2 - u^2)dy^2 + 2uvdxdy + (a^2 - v^2)dx^2 = 0$$

or

$$(a^2 - u^2)dy = (-uv \pm a\sqrt{q^2 - a^2})dx \qquad (2\text{-}7)$$

The significance of these characteristic curves in the hyperbolic region is discussed in several parts of the volume (see B, 2). Mathematically, it may be said the analyticity of the solution in a supersonic region may break down along these lines, instead of at isolated points as in the subsonic region. Physically, these lines of discontinuity represent weak disturbances or wave fronts whose orientation with respect to local flow direction was first given by E. Mach. They are the *Mach lines* frequently visible in schlieren photographs. Eq. 2-7 shows that Eq. 2-5 actually changes its type, as described above, along lines where $q = a = a^*$.

This brief discussion shows us that the transonic character of isentropic compressible flow is intimately related to the nonlinearity of the differential equation (2-5). In studying this type of flow, therefore, we cannot avoid this nonlinearity. On the other hand, we have no adequate technique to deal directly with such nonlinear equations. To get around this difficulty, the differential equation may be transformed to a linear form by a method first suggested by Riemann [*1*], in which the roles of dependent and independent variables are interchanged. In the following,

we shall give two well-known methods, namely, the Chaplygin transformation and the Legendre transformation.

Chaplygin transformation. The Chaplygin transformation consists of a straightforward change of independent variables from the coordinates x. y to the hodograph coordinates q, θ, where q is the magnitude of the flow velocity vector and θ its inclination relative to the x axis. The functions ϕ and ψ are retained as dependent variables. The analysis given here is substantially that of Chaplygin's original paper [2]. A different derivation, essentially geometrical, has been given by von Kármán [3] and is reproduced in III,A,13; it is suggested that the reader compare these methods.

To effect this transformation, we start by writing

$$\begin{aligned} d\phi &= udx + vdy \\ \rho^0 d\psi &= -\rho v dx + \rho u dy \end{aligned} \tag{2-8}$$

in accord with Eq. 2-1. If $\rho q \neq 0$, the inverse relations are

$$\begin{aligned} dx &= \frac{1}{q}\left[\cos\theta d\phi - \frac{\rho^0}{\rho}\sin\theta d\psi\right] \\ dy &= \frac{1}{q}\left[\sin\theta d\phi + \frac{\rho^0}{\rho}\cos\theta d\psi\right] \end{aligned} \tag{2-9}$$

where θ is the inclination of the velocity vector defined above. Now, if q and θ are taken as independent variables, and ϕ and ψ are now treated as functions of q and θ, we can write

$$\begin{aligned} d\phi &= \phi_q dq + \phi_\theta d\theta \\ d\psi &= \psi_q dq + \psi_\theta d\theta \end{aligned}$$

Substituting these expressions for $d\phi$ and $d\psi$ into Eq. 2-9 we have

$$\begin{aligned} dx &= \frac{1}{q}\left[\cos\theta\phi_q - \frac{\rho^0}{\rho}\sin\theta\psi_q\right]dq + \frac{1}{q}\left[\cos\theta\phi_\theta - \frac{\rho^0}{\rho}\sin\theta\psi_\theta\right]d\theta \\ dy &= \frac{1}{q}\left[\sin\theta\phi_q + \frac{\rho^0}{\rho}\cos\theta\psi_q\right]dq + \frac{1}{q}\left[\sin\theta\phi_\theta + \frac{\rho^0}{\rho}\cos\theta\psi_\theta\right]d\theta \end{aligned} \tag{2-10}$$

Since both dx and dy are total differentials, the condition of integrability requires that

$$\begin{aligned} \frac{\partial}{\partial\theta}\left[\frac{\cos\theta}{q}\phi_q - \frac{\rho^0}{\rho}\frac{\sin\theta}{q}\psi_q\right] &= \frac{\partial}{\partial q}\left[\frac{\cos\theta}{q}\phi_\theta - \frac{\rho^0}{\rho}\frac{\sin\theta}{q}\psi_\theta\right] \\ \frac{\partial}{\partial\theta}\left[\frac{\sin\theta}{q}\phi_q + \frac{\rho^0}{\rho}\frac{\cos\theta}{q}\psi_q\right] &= \frac{\partial}{\partial q}\left[\frac{\sin\theta}{q}\phi_\theta + \frac{\rho^0}{\rho}\frac{\cos\theta}{q}\psi_\theta\right] \end{aligned}$$

F,2 · *THE HODOGRAPH TRANSFORMATION*

A simple reduction gives

$$\left(\frac{1}{q}\phi_\theta - \frac{\rho^0}{\rho}\psi_q\right)\cos\theta - \left[-\frac{1}{q}\phi_q + \frac{d}{dq}\left(\frac{\rho^0}{\rho q}\right)\psi_\theta\right]\sin\theta = 0$$

$$\left[-\frac{1}{q}\phi_q + \frac{d}{dq}\left(\frac{\rho^0}{\rho q}\right)\psi_\theta\right]\cos\theta + \left(\frac{1}{q}\phi_\theta - \frac{\rho^0}{\rho}\psi_q\right)\sin\theta = 0$$

For any θ, the vanishing of the determinant leads to

$$\begin{aligned}\phi_q &= -\frac{\rho^0}{\rho q}(1 - M^2)\psi_\theta \\ \frac{1}{q}\phi_\theta &= \frac{\rho^0}{\rho}\psi_q\end{aligned} \tag{2-11}$$

where we have made use of the relations

$$\frac{d}{dq}\left(\frac{\rho^0}{\rho q}\right) = -\frac{\rho^0}{\rho q^2}(1 - M^2) \tag{2-11a}$$

and $M = q/a$. The fundamental system Eq. 2-11 in the q, θ plane, i.e. the *hodograph plane*, is equivalent to the system Eq. 2-2 in the x, y plane. The essential difference is, however, that the transformed system Eq. 2-11 is linear. The linearization is valid as long as the Jacobian of the transformation, $J \equiv \partial(x, y)/\partial(q, \theta)$, is finite and nonvanishing.

Thus, we see that in the hodograph variable the equations are linear, and thus the principle of superposition of solutions is allowed. In other words, if particular solutions are obtained, linear combinations of such solutions are also solutions. By this principle, general solutions can be constructed. However, the fact that most of the physically interesting solutions are many-valued in the hodograph plane makes the actual construction of such solutions very difficult in practice.

Legendre transformation. To effect this transformation, the velocity components u, v are introduced as independent variables and a new function $\chi(u, v)$, related to the stream function, is introduced according to the following definition:

$$\chi = xu + yv - \phi, \qquad x = \chi_u, \qquad y = \chi_v \tag{2-12}$$

The differential equation corresponding to Eq. 2-5 is [*62*]

$$(a^2 - u^2)\chi_{vv} + 2uv\chi_{uv} + (a^2 - v^2)\chi_{uu} = 0 \tag{2-13}$$

The relation between χ and the stream function follows from Eq. 2-1 and 2-12; it is

$$\begin{aligned}\frac{\rho^0}{\rho}\psi_u &= v\chi_{vu} - u\chi_{uv} \\ \frac{\rho^0}{\rho}\psi_v &= v\chi_{uv} - u\chi_{vv}\end{aligned} \tag{2-14}$$

F · *PLANE POTENTIAL FLOWS*

Eq. 2-13 and 2-14 form a complete system equivalent to the system Eq. 2-11. This transformation is also subject to the same condition as stated above for system Eq. 2-11.

Coordinate functions. When the stream function $\psi(q, \theta)$ is given in the hodograph plane, the streamlines in the flow plane, corresponding to constant values of ψ, can be calculated by integrating Eq. 2-10. One way to accomplish this purpose is to perform the partial integration of the equations as they stand, viz.

$$\begin{aligned} x &= \frac{1}{q}\int\left[\cos\theta\phi_\theta - \frac{\rho^0}{\rho}\sin\theta\psi_\theta\right]d\theta + \mathfrak{x}(q) \\ y &= \frac{1}{q}\int\left[\sin\theta\phi_\theta + \frac{\rho^0}{\rho}\cos\psi_\theta\right]d\theta + \mathfrak{y}(q) \end{aligned} \tag{2-15}$$

The arbitrary functions $\mathfrak{x}(q)$ and $\mathfrak{y}(q)$ introduced as a result of the integration can be determined from

$$\begin{aligned} x_q &= \frac{1}{q}\left[\cos\theta\phi_q - \frac{\rho^0}{\rho}\sin\theta\psi_q\right] \\ y_q &= \frac{1}{q}\left[\sin\theta\phi_q + \frac{\rho^0}{\rho}\cos\theta\psi_q\right] \end{aligned} \tag{2-16}$$

It will be clear later that, when ψ and hence also ϕ are expressed in the form of certain infinite series, the integration in Eq. 2-15 can easily be carried out.

In the case of the Legendre transformation, once χ is specified the coordinate functions can be obtained by differentiation. However, we have to integrate Eq. 2-14 to get ψ in order to define a relation between the velocity components, hence there is no obvious advantage to the Legendre transformation in our problem. If not otherwise stated, we shall follow the Chaplygin procedure.

F,3. The Particular Solutions of the Chaplygin Equation. In this article we shall obtain some particular solutions of the transformed linear equations (2-11), which are useful in the construction of practical flow patterns. Except for the simple solutions given in Eq. 3-8 and 3-10, below, these will involve the special functions known in mathematical literature as the *hypergeometric functions.*

By eliminating ϕ from the system (2-11), there results a differential equation satisfied by $\psi(q, \theta)$:

$$q^2\psi_{qq} + (1 + M^2)q\psi_q + (1 - M^2)\psi_{\theta\theta} = 0 \tag{3-1}$$

Since M depends only on q, this equation is linear and its solutions can be built up by adding together particular solutions. As particular solu-

tions we can choose

$$\psi = q^{\nu}F_{\nu}(\tau)e^{i\nu\vartheta}, \qquad \tau = \frac{\gamma - 1}{2}\frac{q^2}{a^{02}}$$

where ν is a real number and the function $F_{\nu}(\tau)$ is a solution of the equation

$$\tau(1-\tau)F''_{\nu} + [\nu + 1 - (a_{\nu} + b_{\nu} + 1)\tau]F'_{\nu} - a_{\nu}b_{\nu}F_{\nu} = 0 \qquad (3\text{-}2)$$

where the parameters a_{ν} and b_{ν} are defined by

$$a_{\nu} + b_{\nu} = \nu - \beta, \qquad a_{\nu}b_{\nu} = -\frac{\beta\nu(\nu+1)}{2} \qquad (3\text{-}3)$$

and

$$\beta = \frac{1}{\gamma - 1}$$

This is a special hypergeometric equation involving two arbitrary parameters, ν and γ. The two independent solutions are denoted by

$$F(a_{\nu}, b_{\nu}; \nu + 1; \tau), \qquad \tau^{-\nu}F(a_{\nu} - \nu, b_{\nu} - \nu; 1 - \nu; \tau) \qquad (3\text{-}4)$$

$F(a_{\nu}, b_{\nu}; \nu + 1; \tau)$ is known as the *hypergeometric function* [4, p. 281] and is defined by the power series

$$F(a_{\nu}, b_{\nu}; \nu + 1; \tau) = \frac{\Gamma(\nu+1)}{\Gamma(a_{\nu})\Gamma(b_{\nu})}\sum_{0}^{\infty}\frac{\Gamma(a_{\nu}+m)\Gamma(b_{\nu}+m)}{\Gamma(\nu+1+m)}\frac{\tau^m}{m!} \qquad (3\text{-}5)$$

which is uniformly convergent in a domain $|\tau| < |$.

The reader should note at this point the significance of the several parameters involved in each of these hypergeometric functions. The independent variable, for our work, is the variable τ, which, for a specified gas, is uniquely related to the local Mach number $\sqrt{2\beta\tau/(1-\tau)}$. There are two parameters: the adiabatic exponent γ, which characterizes the gas, and the index ν, which will be given various values in order to construct solutions to satisfy given boundary conditions.

Now, as q increases from zero to the maximum possible value $q_{\max} = \sqrt{2/(\gamma-1)}a^0$, τ varies from zero to unity. The condition $q = a^*$, or $M = 1$, is given by $\tau^* = (\gamma - 1)/(\gamma + 1)$. Therefore, the integral as defined by the series (3-5) holds for the whole range of possible flow speeds.

The case $\tau = 0$ may be taken to represent either very low speed flow or the flow of an incompressible fluid. For this value of τ, $F_{\nu}(0) = 1$ for all $\nu > 0$; thus the particular solutions considered here reduce to the familiar particular solutions of the incompressible case. Thus, each of the particular solutions of Chaplygin's equation may be thought of as the analogue of a certain incompressible solution. This analogy was used by

Chaplygin and will be mentioned again in the detailed work of this section.

When the parameter ν is a positive integer, the second solution cannot be represented by a single power series. In this situation another independent solution is needed to replace the second of Eq. 3-4; it is given by [*4*, p. 201; *25*]

$$\tau^{-n}[-h_n\tau^n \ln \tau\, F(a_n, b_n; n+1; \tau) + \Psi_1(n)\tau^n F(a_n, b_n; n+1; \tau) + \tau^n G_n(\tau) + H_n(\tau)] \quad (3\text{-}6)$$

where the functions $G_n(\tau)$ and $H_n(\tau)$ are defined by

$$G_n(\tau) = \frac{\Gamma(n+1-b_n)}{\Gamma(a_n-n)\Gamma(n)} \sum_0^\infty \Psi_2(n, m) \frac{\Gamma(a_n+m)(-1)^m}{\Gamma(1-b_n-m)\Gamma(n+m+1)} \frac{\tau^m}{m!} \qquad |\tau| < 1$$

$$H_n(\tau) = \frac{\Gamma(n+1-b_n)}{\Gamma(a_n-n)\Gamma(n)} \sum_0^{n-1} \frac{\Gamma(a_n-n+m)\Gamma(n-m)}{\Gamma(n+1-b_n-m)} \frac{\tau^m}{m!}$$

$$\Psi_1(n) = h_n\left[\psi(n+1) + \psi(1) - \psi(a_n) - \psi(1-b_n) + \frac{d}{dn}\ln h_n\right]$$

$$\Psi_2(n, m) = \psi(1-b_n) - \psi(1-b_n-m) + \psi(a_n) - \psi(a_n+m) + \psi(m+1) - \psi(1) + \psi(n+m+1) - \psi(n+1)$$

$$h_n = \frac{\Gamma(a_n)\Gamma(n+1-b_n)}{\Gamma(a_n-n)\Gamma(1-b_n)\Gamma(n)\Gamma(n+1)}$$

$$\psi(z) = \frac{d}{dz}\ln \Gamma(z)$$

Here the constants a_n and b_n are chosen to be positive and negative, respectively, for $n > 1$.[1] Having the forms of the second solution defined as in Eq. 3-4 and 3-6, according to ν being nonintegral and integral, respectively, we can write the particular solutions of Eq. 3-1 as

$$q^\nu F_\nu(\tau)e^{-i\nu\theta}, \qquad q^{-\nu}F_{-\nu}(\tau)e^{i\nu\theta} \quad (3\text{-}7)$$

where

$$F_\nu(\tau) = F(a_\nu, b_\nu; \nu+1; \tau)$$

and $F_{-\nu}(\tau)$ denotes either $F(a_\nu - \nu, b_\nu - \nu; 1-\nu; \tau)$ (for nonintegral ν) or the expression within the brackets in Eq. 3-6 (for $\nu = n$, an integer).

Distinct from this class of solutions we have also for $\nu = 0$

$$\theta \quad \text{and} \quad \int^\tau (1-\tau)^\beta \frac{d\tau}{\tau} \quad (3\text{-}8)$$

The latter, in the limit of incompressible flow, reduces to $2 \ln q$.

[1] For $n = 1$, $F(1, -\beta; 2; \tau) = \frac{1}{(\beta+1)\tau}[1 - (1-\tau)^{\beta+1}]$ and $F_{-1}(\tau) = 1 + \frac{\beta}{2}\tau F_1(\tau)$.

F,4 · *SOLUTIONS FROM THE LEGENDRE TRANSFORMATION*

These are our particular solutions for the stream function $\psi(q, \theta)$. We need now to find the corresponding particular velocity potentials $\phi(q, \theta)$. This can be done with the aid of the fundamental relations (2-11). We have

$$d\phi = -\frac{\rho^0}{\rho}(1 - M^2)\frac{1}{q}\psi_\theta dq + \frac{\rho^0}{\rho} q\psi_q d\theta$$

If $\psi(q, \theta)$ is given by the first of Eq. 3-7, then[2]

$$d\phi = i\frac{\rho^0}{\rho}(1 - M^2)\nu q^{\nu-1}F_\nu(\tau)e^{-i\nu\theta}dq + \frac{\rho^0}{\rho} q \frac{d}{dq} q^\nu F_\nu(\tau)e^{-i\nu\theta}d\theta$$

This can be integrated without difficulty with the aid of the differential equation (3-1), an alternative form of which is

$$\frac{\partial}{\partial q}\left(\frac{\rho^0}{\rho} q\psi_q\right) + \frac{\rho^0}{\rho q}(1 - M^2)\psi_{\theta\theta} = 0$$

or, in terms of the particular solution now under consideration,

$$\frac{\rho^0}{\rho}(1 - M^2)\nu q^{\nu-1}F_\nu(\tau) = \frac{1}{\nu}\frac{d}{dq}\left[\frac{\rho^0}{\rho} q \frac{d}{dq} q^\nu F_\nu(\tau)\right] = \frac{d}{dq}\left[\frac{\rho^0}{\rho} q^\nu F_\nu(\tau)\xi_\nu(\tau)\right]$$

where $\xi_\nu(\tau)$ denotes $2\left(\frac{\tau}{\nu}\right)\frac{d}{d\tau}\ln \tau^{\nu/2}F_\nu(\tau)$. The integral is

$$\phi = i\frac{\rho^0}{\rho} q^\nu F_\nu(\tau)\xi_\nu(\tau)e^{-i\nu\theta} + \text{const}$$

Therefore, the corresponding particular solutions for ϕ, corresponding to Eq. 3-7, are for $\nu \neq 0$

$$i\frac{\rho^0}{\rho} q^\nu F_\nu(\tau)\xi_\nu(\tau)e^{-i\nu\theta} \quad \text{and} \quad i\frac{\rho^0}{\rho} q^{-\nu}F_{-\nu}(\tau)\xi_{-\nu}(\tau)e^{i\nu\theta} \tag{3-9}$$

and, corresponding to Eq. 3-8, for $\nu = 0$

$$(1 - \tau)^{-\beta} - \frac{1}{2}\int^\tau (1 - \tau)^{-\beta}\frac{d\tau}{\tau} \quad \text{and} \quad \theta \tag{3-10}$$

F,4. Particular Solutions of the Equations Resulting from the Legendre Transformation. In analogous fashion, let us determine some particular solutions of the linear equation (2-13) which we obtained by the Legendre transformation. In the first place, from the relations (2-14) in polar coordinates, we have

$$\psi_\theta = -\frac{\rho^0}{\rho}(q\chi_q + \chi_{\theta\theta}) \tag{4-1}$$

[2] If $\psi(q, \theta)$ is given by the second of Eq. 3-7, we need only change ν to $-\nu$ in the subsequent formulas.

where $\chi(q, \theta)$ satisfies

$$q^2\chi_{qq} + (1 - M^2)q\chi_q + (1 - M^2)\chi_{\theta\theta} = 0 \qquad (4\text{-}2)$$

If we assume again

$$\chi = q^\nu F(\tilde{a}_\nu, \tilde{b}_\nu; \nu + 1; \tau)e^{-i\nu\theta} \qquad (4\text{-}3)$$

Eq. 4-2 reduces to

$$\tau(1 - \tau)\bar{F}''_\nu + [\nu + 1 - (\tilde{a}_\nu + \tilde{b}_\nu + 1)\tau]\bar{F}'_\nu - \tilde{a}_\nu\tilde{b}_\nu\bar{F}_\nu = 0 \qquad (4\text{-}4)$$

where

$$\tilde{a}_\nu + \tilde{b}_\nu = \nu + \beta, \qquad \tilde{a}_\nu\tilde{b}_\nu = -\frac{\beta\nu(\nu - 1)}{2} \qquad (4\text{-}5)$$

and

$$\bar{F}_\nu(\tau) = F(\tilde{a}_\nu, \tilde{b}_\nu; \nu + 1; \tau)$$

Eq. 4-4 is again the hypergeometric equation (cf. Eq. 3-2), the only difference being that the parameters have been defined differently in terms of ν and γ. Thus, the particular functions $\chi(q, \theta)$ involve the same hypergeometric functions as we used in Art. 3, but with slightly different meanings of the parameters.

Let us now determine the forms of the particular stream functions $\psi(q, \theta)$ corresponding to these particular $\chi(q, \theta)$'s. Substituting $\chi(q, \theta)$ from Eq. 4-3 into Eq. 4-1, we have

$$\psi_\theta = -\frac{\rho^0}{\rho}[2\tau\bar{F}'_\nu - \nu(\nu - 1)\bar{F}_\nu]q^\nu e^{-i\nu\theta}$$

and by Eq. 4-4

$$\psi_\theta = -2(\gamma - 1)(1 - \tau)^{1+\beta}[\tau\bar{F}''_\nu + (\nu + 1)\bar{F}'_\nu]q^\nu e^{-i\nu\theta} \qquad (4\text{-}6)$$

Following T. M. Cherry [5], we notice the identity

$$\tau\bar{F}''_\nu + \nu\bar{F}'_\nu = \nu F(\tilde{a}_\nu, \tilde{b}_\nu; \nu; \tau)$$

By differentiation,

$$\tau\bar{F}''_\nu + (\nu + 1)\bar{F}'_\nu = \tilde{a}_\nu\tilde{b}_\nu F(\tilde{a}_\nu + 1, \tilde{b}_\nu + 1; \nu + 1; \tau) \qquad (4\text{-}7)$$

It is easily verified that the hypergeometric equation satisfied by $F(\tilde{a}_\nu + 1, \tilde{b}_\nu + 1; \nu + 1; \tau)$ can be transformed into Eq. 3-2 by the substitution

$$F(\tilde{a}_\nu + 1, \tilde{b}_\nu + 1; \nu + 1; \tau) = (1 - \tau)^{-1-\beta}F_\nu(\tau) \qquad (4\text{-}8)$$

By means of Eq. 4-8 and 4-7, partial integration of Eq. 4-6 gives us

$$\psi(q, \theta) = i(\nu - 1)q^\nu F_\nu(\tau)e^{-i\nu\theta} \qquad (4\text{-}9)$$

where the arbitrary function of q can only be the second of Eq. 3-8 and therefore has been omitted.

F,5 · *CHAPLYGIN-KÁRMÁN-TSIEN APPROXIMATION*

Corresponding to this particular solution (4-3), the coordinate functions are

$$\begin{aligned} x &= q^{\nu-1}[2\tau\bar{F}'_\nu(\tau)\cos\theta e^{-i\nu\theta} + \nu\bar{F}_\nu(\tau)e^{-i(\nu-1)\theta}] + \text{const} \\ y &= q^{\nu-1}[2\tau\bar{F}'_\nu(\tau)\sin\theta e^{-i\nu\theta} - i\nu\bar{F}_\nu(\tau)e^{-i(\nu-1)\theta}] + \text{const} \end{aligned} \tag{4-10}$$

where the prime denotes differentiation with respect to τ. These functions $\bar{F}_\nu(\tau)$ and $\bar{F}'_\nu(\tau)$ can be expressed in terms of $F_\nu(\tau)$ and $F'_\nu(\tau)$ as follows [*24,63*]:

$$\begin{aligned} (1-\tau)^\beta\bar{F}_\nu(\tau) &= (\nu+1)F_\nu(\tau) + \frac{2\tau}{\nu}F'_\nu(\tau) \\ \frac{2\tau}{\nu}(1-\tau)^\beta\bar{F}'_\nu(\tau) &= (\nu-1)\left[\nu F_\nu(\tau) + \frac{2\tau}{\nu}F'_\nu(\tau)\right] \end{aligned} \tag{4-11}$$

In like manner, if $\chi = q^{-\nu}\bar{F}_{-\nu}(\tau)e^{+i\nu\theta}$, we find

$$\chi = +i(\nu+1)q^{-\nu}F_{-\nu}(\tau)e^{i\nu\theta} \tag{4-12}$$

Thus, it turns out that the particular stream functions corresponding to our elementary $\chi(q, \theta)$'s differ only in multiplicative factors from those selected in Art. 3 as elementary solutions of Chaplygin's equation. This identification is due to Cherry [*5*].

F,5. The Chaplygin-Kármán-Tsien Approximation. Before we proceed to treat the problem more exactly, let us deal first with an approximate method which has had considerable application in practice. It was first noted by Chaplygin [*2*] that, if we put $\gamma = -1$, the system (2-11) can be greatly simplified and its solutions are none other than those of the familiar Laplace equation. This can easily be established by the fact that, for $\gamma = -1$, the solutions of the hypergeometric equation (3-2) become[3]

$$\begin{aligned} F_\nu(\tau) &= \left\{\frac{2}{1+[1+q^2/(a^0)^2]^{\frac{1}{2}}}\right\}^\nu, \\ q^{-2\nu}F_{-\nu}(\tau) &= \left\{\frac{2q^2}{1+[1+q^2/(a^0)^2]^{\frac{1}{2}}}\right\}^{-\nu} \end{aligned} \tag{5-1}$$

Thus, if we introduce as a new variable

$$q_1 = \frac{2q}{1+[1+q^2/(a^0)^2]^{\frac{1}{2}}} \tag{5-2}$$

[3] This follows from the identity

$$F\left(\frac{\nu}{2}, \frac{\nu}{2}+\frac{1}{2}; \nu+1; -\frac{q^2}{(a^0)^2}\right) = 2^\nu\left[1+\sqrt{1+\frac{q^2}{(a^0)^2}}\right]^{-\nu}$$

(Forsyth, A. R. *A Treatise on Differential Equations*. 1885, p. 207.)

the particular integrals of Eq. 3-1 are

$$q_1^{\nu} e^{-i\nu\theta} \quad \text{and} \quad q_1^{-\nu} e^{i\nu\theta} \tag{5-3}$$

Consequently, the boundary-value problem of a compressible flow having a value of γ equal to -1 becomes, in a q_1, θ plane, identically that of an incompressible flow.

The question remains, however, whether this simplification has any meaning physically. We can look at this problem from two aspects. Following Chaplygin we can write the system (2-11) in the form

$$\begin{aligned} \phi_{q_1} &= K(\tau)\psi_\theta \\ \phi_\theta &= -\psi_{q_1} \end{aligned} \tag{5-4}$$

where

$$q_1 = -\frac{1}{2}\int^{\tau} (1-\tau)^{\beta} \frac{d\tau}{\tau}$$

(which agrees with Eq. 5-2 in the case $\gamma = -1$) and $K(\tau) = (1 - \alpha^2\tau)/(1-\tau)^{\alpha}$, with $\alpha^2 = (\gamma+1)/(\gamma-1)$. The coefficient $K(\tau)$ varies very slowly with τ and is practically constant and close to unity if τ is small, i.e. for small Mach number. Therefore, the case $\gamma = -1$, for which $K = 1$, can be regarded as an approximation, to the order τ^2, for a purely subsonic flow.

On the other hand, it is seen that, for an isentropic flow, the pressure and density will be related by $p \sim \rho^{-1}$ when $\gamma = -1$. This can be interpreted as an approximation by a line tangent to the adiabatic curve in the pressure-volume diagram (Fig. F,5a). In a flow field, if pressure and density do not vary through a wide range, this linear law of state can give a fairly close approximation to the true situation governed by the adiabatic law. If the point of tangency is chosen to correspond to the free stream condition, the approximate equation of state given by von Kármán and Tsien [*3,6*] is obtained:

$$p - p_\infty = -\rho_\infty^2 a_\infty^2 \left(\frac{1}{\rho} - \frac{1}{\rho_\infty}\right) \tag{5-5}$$

Here the subscript ∞ indicates the free stream condition. It is easy to verify that, at free stream conditions, this equation gives the exact slope, $(dp/d\rho)_\infty = a_\infty^2$.

With this linear equation of state, the integrated equation of motion, Eq. 2-6, becomes

$$a^2 - q^2 = (a^0)^2 \tag{5-6}$$

which, in conjunction with Eq. 5-5, gives

$$\frac{\rho^0}{\rho} = \left[1 + \frac{q^2}{(a^0)^2}\right]^{\frac{1}{\gamma}} \tag{5-7}$$

Thus, we see from Eq. 5-6 that in this approximation the sonic speed can never be attained in the flow field.

In his original treatment [*2*], Chaplygin employed a different equation of state, since he chose the stagnation condition p^0, ρ^0 as the point of tangency to the adiabatic curve, rather than p_∞, ρ_∞. The Kármán-Tsien approximation seems better suited to most aeronautical applications.

It might be mentioned here that the Kármán-Tsien approximation can be adapted, at least formally, to the study of purely supersonic plane

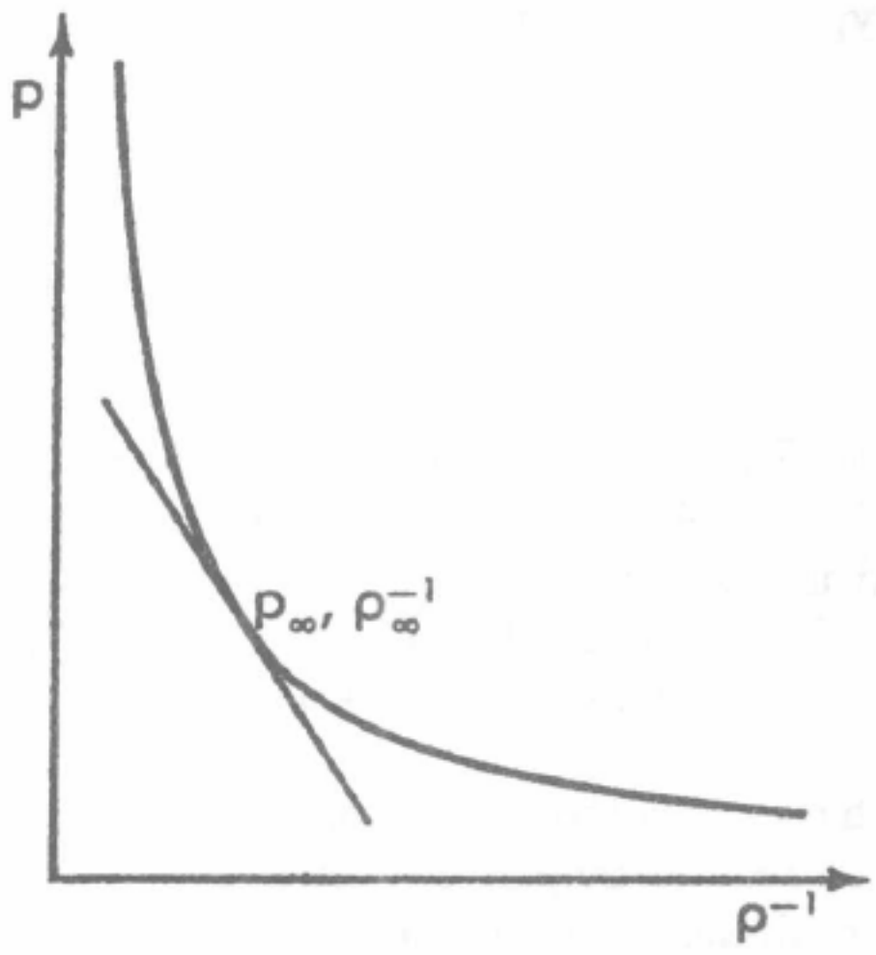

Fig. F,5a. Approximation to true isentropic pressure-volume curve.

flows [*64*]. The hodograph equation (5-4) assumes a simple hyperbolic form. The value of this procedure is difficult to assess, especially in comparison with other available techniques such as the numerical method of characteristics (Sec. G).

Transformation of incompressible to compressible flows. As a result of this simplification, we are able to show that, given an incompressible flow, a "similar" compressible flow, subsonic everywhere, can be constructed. Let $U_i W_i = \phi_i + i\psi_i$ be the given complex potential of an incompressible flow and U_i its undisturbed stream velocity. We have already seen, in connection with Eq. 5-3, that the functions

$$\phi = \phi_i(q_i, \theta), \qquad \psi = \psi_i(q_i, \theta) \tag{5-8}$$

represent the velocity potential and stream function of a compressible flow in terms of the quantity q_i defined in Eq. 5-2. Once ϕ and ψ are known, the coordinate functions (2-9) can be expressed as

$$dz = \frac{e^{i\theta}}{q}\left[d\phi_i + i\frac{\rho^0}{\rho}d\psi_i\right] \tag{5-9}$$

where $dz = dx + idy$. To eliminate q, we have, by Eq. 5-2,

$$q = \frac{q_1}{1 - q_1^2/4(a^0)^2}$$

whence

$$\frac{\rho^0}{\rho} = \frac{1 + q_1^2/4(a^0)^2}{1 - q_1^2/4(a^0)^2}$$

Substitution of q and ρ^0/ρ in Eq. 5-9 yields an expression for dz in terms of quantities of the q_1, θ plane only:

$$dz = \frac{1}{q_1 e^{-i\theta}} \left\{ \left[1 - \frac{q_1^2}{4(a^0)^2} \right] d\phi_1 + i \left[1 + \frac{q_1^2}{4(a^0)^2} \right] d\psi_1 \right\} \qquad (5\text{-}10)$$

Furthermore, define

$$w_1 = q_1 e^{-i\theta}, \qquad dz_1 = \frac{U_1 dW}{w_1}$$

so that dz_1 is the increment of the position vector z_1 in the original incompressible flow corresponding to increments $d\phi_1$, $d\psi_1$ of the velocity potential and stream function. We can now relate this increment dz_1 to the analogous incremental vector dz of the compressible flow, which corresponds to the same increments $d\phi_1$, $d\psi_1$ of its velocity potential and stream function. We have, namely,

$$dz = dz_1 - \lambda^2 \left(\frac{d\bar{W}_1}{d\bar{z}_1} \right)^2 d\bar{z}_1 \qquad (5\text{-}11)$$

where $\bar{W}_1$ and $\bar{z}_1$ are the complex conjugates of W_1 and z_1, respectively, and λ stands for $M_\infty/(1 + \sqrt{1 - M_\infty^2})$, M_∞ being the free stream Mach number. Integration of Eq. 5-11 gives

$$z = z_1 - \lambda^2 \int \left(\frac{d\bar{W}_1}{d\bar{z}_1} \right)^2 d\bar{z}_1 \qquad (5\text{-}12)$$

The constant of integration can be determined by proper choice of the origins of the two coordinate systems z and z_1. Eq. 5-12 can now be considered as a mapping function which transforms a given incompressible flow pattern into a compressible flow around a "similar" but different contour. Given the incompressible flow pattern, the second term of Eq. 5-12 is a correction to the complex coordinate of the compressible flow at which any given values ϕ, ψ are found. The similarity of the two patterns is closer as the Mach number M_∞ diminishes, until an identity occurs when $M_\infty = 0$.

A difficulty however is that, if the incompressible flow involves circulation, then the correction term in Eq. 5-12 is no longer single-valued. A closed boundary in the z_1 plane will be mapped into an unclosed one in the z plane. Hence, Eq. 5-12 in the present form fails to deal with circula-

tory flow. This problem was attacked by several authors [*7–11*]. We shall briefly present Lin's method, which appears to be most simple and general.

Lin's suggestion is to interpret w_1 more generally than was done by Tsien, as reproduced above; namely, we can choose

$$w_1 = k(z_1)q_1e^{-i\theta} \tag{5-13}$$

and $dz_1 = U_1dW_1/w_1$ as before, where $k(z_1)$ is another analytic function. Instead of Eq. 5-11, we then have, from Eq. 5-10,

$$dz = k(z_1)dz_1 - \lambda^2\left(\frac{d\overline{W}_1}{dz_1}\right)^2\frac{\overline{dz_1}}{k(z_1)} \tag{5-14}$$

and, instead of Eq. 5-12,

$$z = \int k(z_1)dz_1 - \lambda^2\int\left(\frac{d\overline{W}_1}{dz_1}\right)^2\frac{\overline{dz_1}}{k(z_1)} \tag{5-15}$$

We now impose two conditions on the function $k(z_1)$. The first is that Eq. 5-13 be analytic; this leads [*7*] to

$$|\tfrac{1}{2}W_1'(\zeta)| < |k(z_1)| < \infty \tag{5-16}$$

Secondly, to insure that a closed contour in the z_1 plane will be mapped on a closed contour in the z plane, we have, from Eq. 5-15

$$\oint k(z_1)dz_1 - \lambda^2\oint\left(\frac{d\overline{W}_1}{dz_1}\right)^2\frac{\overline{dz_1}}{k(z_1)} = 0 \tag{5-17}$$

Thus, given a function W_1 which represents an incompressible flow with circulation, we can always construct a related compressible flow with circulation by choosing properly the auxiliary function $k(z_1)$, subject to Eq. 5-16 and 5-17. In Lin's paper, the problem is formulated in such a way as to place it within the scope of familiar incompressible fluid airfoil theory.

Pressure correction. When the flow about a certain body is determined, the pressure distribution over the surface can be calculated, although the numerical work may be somewhat tedious. The main interest in subsonic flow appears to be the effect of the compressibility of the fluid on the pressure distribution, under given geometrical conditions. Within the approximation permitted by the assumptions of the present theory, this has been achieved by von Kármán and Tsien.

Let C_p be the pressure coefficient at a point in the flow field, defined by

$$C_p = \frac{p - p_\infty}{\frac{1}{2}\rho_\infty U^2}$$

where p is the local pressure and p_∞, ρ_∞, and U denote, respectively, the free stream pressure, density, and velocity. By making use of Eq. 5-5

and 5-7, we find

$$C_p = \frac{2}{M_\infty^2}\left[1 - \sqrt{1 - M_\infty^2}\,\frac{1 + q_i^2/4(a^0)^2}{1 - q_i^2/4(a^0)^2}\right] \tag{5-18}$$

Now q_i is associated with a contour in z_i plane, while C_p is the pressure coefficient on a contour in the z plane. According to Eq. 5-12, these two contours are different. Consequently, the determination of C_p for a given contour involves the calculation of the incompressible flow about a different contour, which must be determined by use of the mapping function. Tsien has carried out this process for the case of compressible flow about an elliptical cylinder [*6*].

For practical engineering work, however, Tsien has suggested using a further approximation to avoid this lengthy procedure, namely, to neglect the difference between the two contours involved. If we ignore this difference, we can regard Eq. 5-18 as a formula relating the pressure coefficient C_p to the pressure coefficient on the same body in incompressible flow. The pressure coefficient in the incompressible flow would be

$$C_{p_{\text{inc}}} = 1 - \left(\frac{q_i}{U_i}\right)^2 \tag{5-19}$$

Eliminating q_i and after simple reduction, we obtain

$$C_p = C_{p_{\text{inc}}}\left[\sqrt{1 - M_\infty^2} + \frac{M_\infty^2}{1 + \sqrt{1 - M_\infty^2}}\,\frac{C_{p_{\text{inc}}}}{2}\right]^{-1} \tag{5-20}$$

This is the famous Kármán-Tsien pressure correction formula. It has frequently been used in engineering practice. Having the form $C_p = C_p(C_{p_{\text{inc}}}, M_\infty)$, it replaces the Prandtl-Glauert rule for plane flow (C,6)

It is clear that formula (5-20) becomes identical to the Prandtl-Glauert rule if the second term in the denominator is neglected, i.e. $C_{p_{\text{P.G.}}} = C_{p_{\text{inc}}}(1 - M_\infty^2)^{-\frac{1}{2}}$. Furthermore, the nature of the improvement afforded by Eq. 5-20 over the simpler first order result can easily be seen, viz.

$$C_p < C_{p_{\text{P.G.}}}$$

Thus, the Kármán-Tsien rule predicts pressure coefficients that are numerically greater in regions where $C_{p_{\text{inc}}}$ is negative and smaller where $C_{p_{\text{inc}}}$ is positive. Reference to the data of C,8 will confirm that this tendency is, qualitatively, in the right direction.

It seems clear that the validity of this result rests on the assumption that the distortion of the boundary due to compressibility is negligible. We can study this by taking $|d\overline{W}_i/d\bar{z}_i|$ in Eq. 5-12 to be $O(1)$, the integral $\int(d\overline{W}_i/d\bar{z}_i)^2 d\bar{z}_i$ must then be of the order of the body dimension. If τ and τ_i are the thickness ratios of the bodies in the z and z_i planes, respectively, a rough estimate shows that $\tau/\tau_i = 1 + O(M_\infty^2\tau_i)$. But we have shown

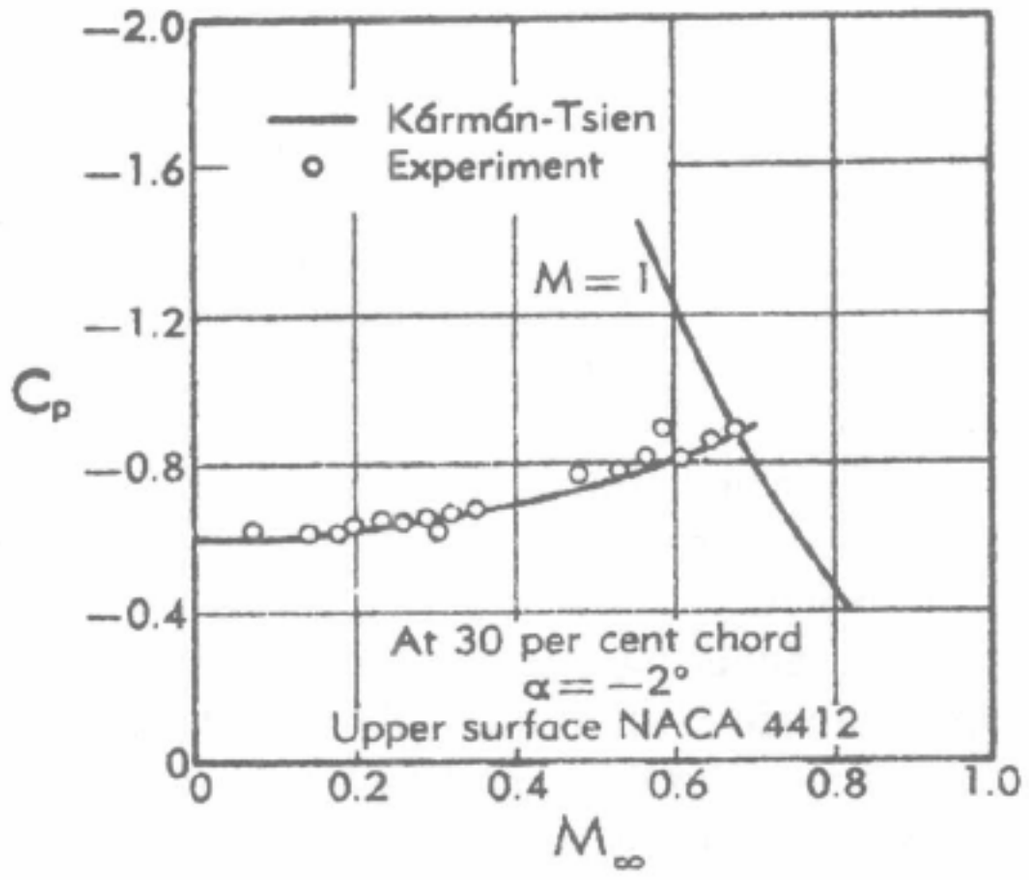

Fig. F,5b. Comparison of pressure correction formula with experiments [*70*] at different free stream Mach numbers M_∞, for NACA 4412. At 30 per cent chord, upper surface, $\alpha = -2°$.

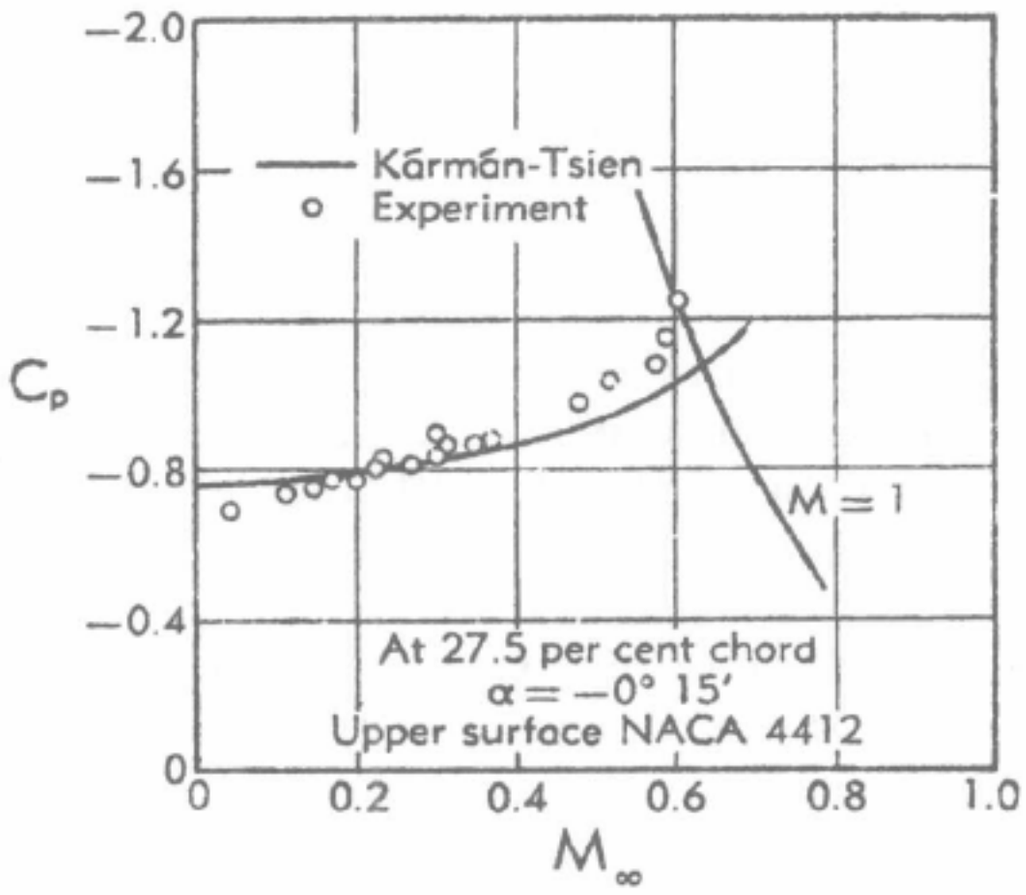

Fig. F,5c. Comparison of pressure-correction formula with experiments [*70*] at different free stream Mach numbers M_∞, for NACA 4412. At 27.5 per cent chord, upper surface, $\alpha = -0°15'$.

that Chaplygin's approximation holds only for small Mach numbers, and the idea of replacing the adiabatic curve by its tangent further precludes cases of large disturbance or thick bodies. Therefore, when both M_∞ and τ are restricted to be small, the distortion, being of $O(M_\infty^2\tau_1)$, can, of course, be neglected.

The merit of Kármán-Tsien formula, however, is not that it has a theoretically sound basis but rather that it is justified by its practical

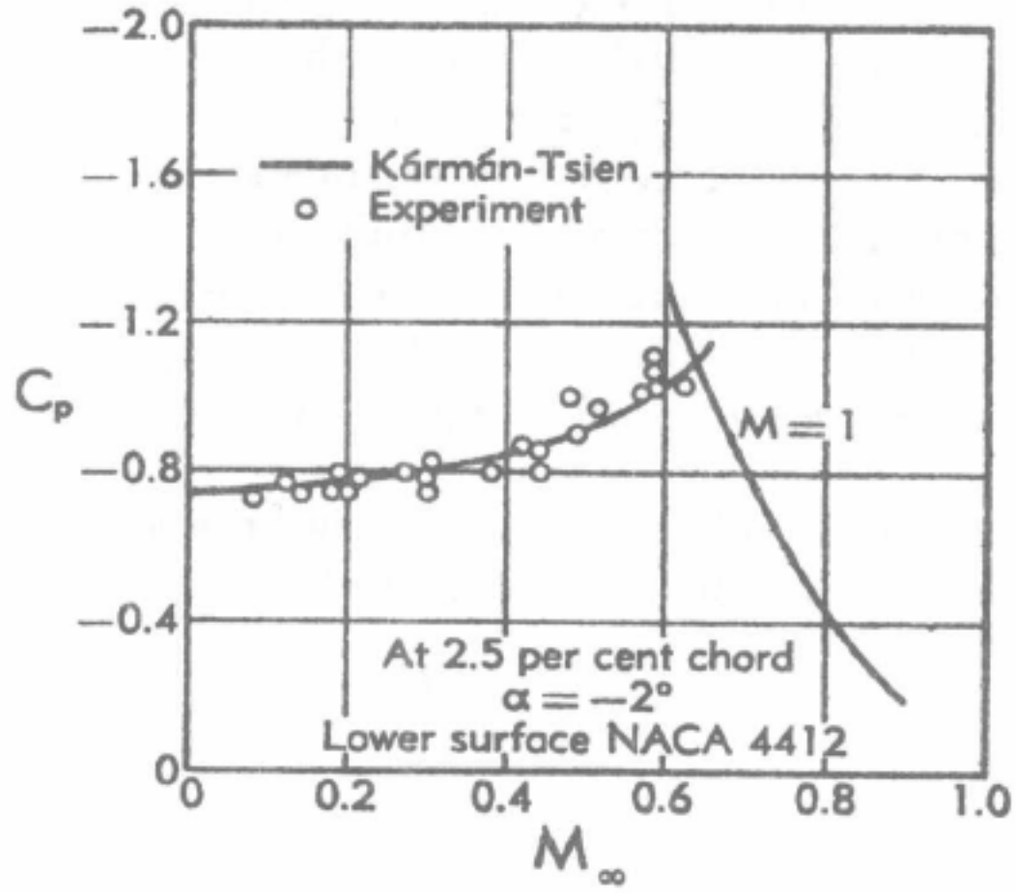

Fig. F,5d. Comparison of pressure-correction formula with experiments [*70*] at different free stream Mach numbers M_∞ for NACA 4412. At 25 per cent chord, lower surface, $\alpha = -2°$.

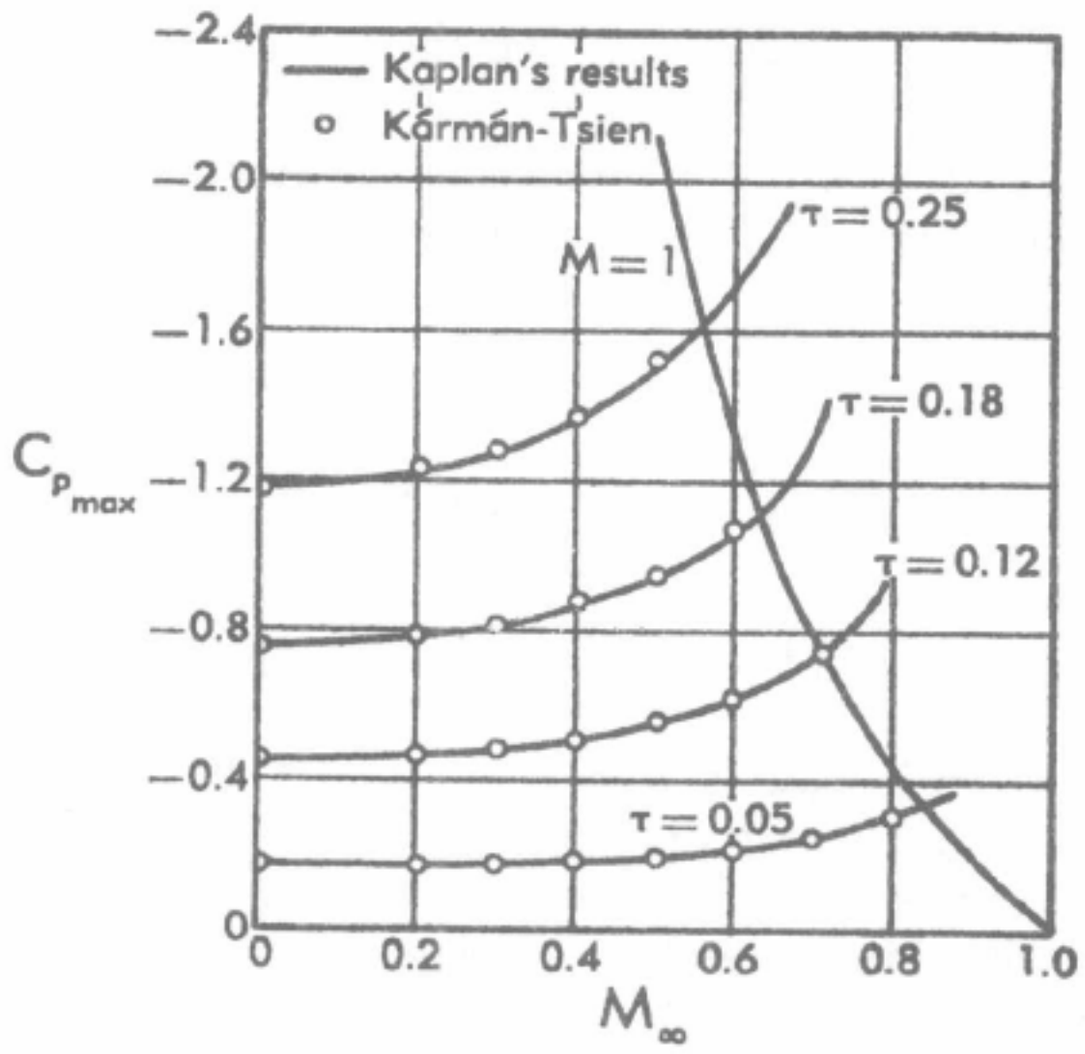

Fig. F,5e. Comparison of theoretical maximum pressure coefficient on a bump with pressure-correction formula at different free stream Mach numbers M_∞ and thickness ratios τ. (From [*55*].)

utility. In practice, we find close agreement between experimental results and theoretical predictions, even when the formula is applied at rather large subsonic Mach numbers. Examples are presented in Fig. F,5b to F,5e.

Tsien's tentative explanation [*12*] of this phenomenon can be sum-

marized as follows. By examining Fig. F,5a, we notice that the linear equation of state generally *underestimates* the pressure. On the other hand, transformation of a body in the incompressible flow to that in compressible flow, as will be shown later, *increases* the thickness ratio of the body. Ignoring this increase is equivalent to *overestimating* the pressure in regions of reduced pressure. As the two effects work in opposite directions, they may counteract each other. A rigorous mathematical proof has not yet been offered. This subject is discussed in some detail in E,2.

Application to elliptic cylinder. As an example let us take W_1 to be the complex potential for flow about an elliptic cylinder.

$$W_1 = \zeta + \frac{b^2}{\zeta} \tag{5-21}$$

and

$$z_1 = \zeta + \frac{1}{\zeta}$$

Substitution of this W_1 into Eq. 5-12 gives us, after integration,

$$z = \zeta + \frac{1}{\zeta} - \lambda^2\left[\bar{\zeta} + \frac{b^4}{\bar{\zeta}} + \frac{(b^2-1)^2}{2}\ln\frac{\bar{\zeta}-1}{\bar{\zeta}+1}\right]$$

Now, the body contour in the z_1 plane is given by $\zeta = be^{i\theta}$ in the ζ plane; the parametric equations for the contour in the z plane are therefore

$$x = \left(b + \frac{1}{b}\right)\cos\theta - \lambda^2\left[b(b^2+1)\cos\theta + \frac{(b^2-1)^2}{4}\ln\frac{b^2-2b\cos\theta+1}{b^2+2b\cos\theta+1}\right] \tag{5-22}$$

$$y = \left(b - \frac{1}{b}\right)\sin\theta - \lambda^2\left[b(b^2-1)\sin\theta - \frac{(b^2-1)^2}{2}\tan^{-1}\frac{2b\sin\theta}{b^2-1}\right]$$

The derived contour is again symmetrical (Fig. F,5f) but is not an ellipse except when M_∞ (and therefore λ) is zero. The deviation from an ellipse, due to the presence of the ln (. . .) and $\tan^{-1}$ (. . .) terms in Eq. 5-22, grows rapidly with Mach number; in fact, it is proportional to M_∞^2. As a measure of the change of the incompressible flow contour in going over to compressible flow, let us define a thickness parameter τ as the ratio of the minor to the major axis, namely

$$\tau = \tau_1 \frac{1 - \lambda^2\left[b^2 - \frac{1}{2}b(b^2-1)\tan^{-1}\frac{2b}{b^2-1}\right]}{1 - \lambda^2\left[b^2 + \frac{b(b^2-1)^2}{2(b^2+1)}\ln\frac{b-1}{b+1}\right]} \tag{5-23}$$

where $\tau_1 = (b^2-1)/(b^2+1)$.

F · *PLANE POTENTIAL FLOWS*

As the parameter b ranges from 0 to ∞, the elliptical cylinder in the z_i plane ranges from a flat plate to a circular cylinder. Throughout this range of b, the ratio τ/τ_i is always greater than unity. A calculation, based on Eq. 5-23, for ellipses of small thickness ratio τ_i leads to the approximate relation

$$\tau = \tau_i \left[1 + \frac{\pi}{2} \frac{\lambda^2}{1 - \lambda^2} \tau_i + O(\tau_i^2) \right] \tag{5-24}$$

This confirms our earlier estimate, which was $\tau/\tau_i = 1 + O(M_\infty^2 \tau_i)$.

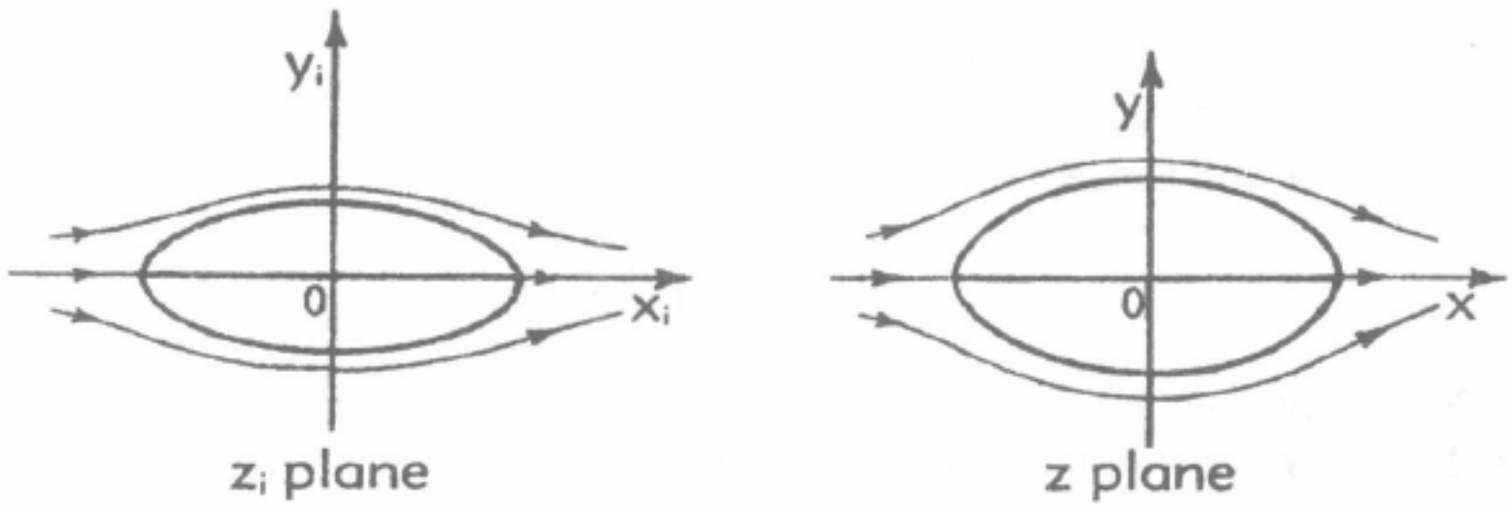

Fig. F,5f. Relationship between bodies in z_i and z planes.

F,6. Examples of Simple Flows. As was shown in the preceding section, the approximation $\gamma = -1$ makes it possible to transform the problem of subsonic compressible flow to one of incompressible flow. Clearly, if the problem is to be solved exactly, no such simplification generally exists. A quite different method has to be employed. To begin with, let us consider some simple flows such as sink, vortex, doublet, and so on, for which the solutions require no superposition.

Source or sink. Let the fluid be at rest at infinity and flow radially from or toward a center. When the steady state is established, the stream function must be a function of θ alone, that is

$$\psi = C\theta \tag{6-1}$$

where the constant C is arbitrary. Then, from the system (2-11)

$$\phi = -C \int \frac{\rho^0}{\rho q} (1 - M^2) dq + \text{const} \tag{6-2}$$

With this form of ψ, the coordinate functions can easily be obtained from Eq. 2-15:

$$x = C \frac{\rho^0}{\rho q} \cos\theta + \hat{x}(q)$$

$$y = C \frac{\rho^0}{\rho q} \sin\theta + \hat{y}(q)$$

since $\phi_\theta = 0$. Moreover, $\hat{x}(q)$ and $\hat{y}(q)$ must be constants, as a consequence of Eq. 2-16 and 2-11a. Let us choose the coordinate system such

that $\hat{x}(q) = \hat{y}(q) = 0$; we have, then

$$x = C\frac{\rho^0}{\rho q}\cos\theta, \qquad y = C\frac{\rho^0}{\rho q}\sin\theta \tag{6-3}$$

As the streamlines are given by $\theta = \text{const}$, it is clear that these lines are radial. By elimination of θ, the equation of the lines of constant q, which are the equipotentials in this case, is found:

$$x^2 + y^2 = \frac{\rho^{02}C^2}{\rho^2 q^2} \tag{6-4}$$

These lines are concentric circles. If the constant C is so chosen that $\rho^{02}C^2 = (\rho^*)^2(a^*)^2$, asterisk indicating the value at $q = a = a^*$, then the equation of these circles can be written

$$x^2 + y^2 = \left(\frac{\rho^* a^*}{\rho q}\right)^2 \tag{6-5}$$

Now, the mass flow ρq is a function of q, which has a maximum value at $M = 1$, as is clear from Eq. 2-11a. The fact introduces an interesting phenomenon in the present problem, namely, the radius of the equipotentials (6-5) has a minimum value; our flow pattern is confined to the region outside of a certain circle at which sonic speed occurs.

If we differentiate Eq. 6-5 with respect to q along a streamline, viz.

$$\frac{d}{dq}(x^2 + y^2) = -2\left(\frac{\rho^* a^*}{\rho q}\right)^2 \frac{1 - M^2}{q}$$

we see that the radius of the circle decreases as q increases. But when the minimum circle is reached, at which $M = 1$, further increase of q increases the radius again, because $d(x^2 + y^2)/dq > 0$. Thus, we obtain another possible flow of the source or sink type, which has sonic speed at the minimum radius and increasing supersonic speeds at all greater radii, reaching maximum speed at infinity. (Naturally, for physical reasons we cut off this solution at some speed less than $q_{\max}$, the speed corresponding to zero density, or, perhaps make an abrupt transition from supersonic flow through a shock.) The fact that these two different flows appear to be plotted on top of each other in the x, y plane here is of no significance. Given the boundary condition $M = 1$ at $x^2 + y^2 = 1$, we will have either one or the other of these flows, depending on the conditions specified at larger radii.

To be sure, the fact that these compressible source and sink flows possess a minimum radius where $dq/d\sqrt{x^2 + y^2}$ becomes infinite is, in this example, simply a manifestation of the familiar phenomenon of choking in a nozzle throat: The flow cannot progress inside of the minimum radius because the stream tube area does not increase there. Nevertheless, we shall find below that this is but a special example of a more general and profound phenomenon of plane isentropic compressible flow.

F · *PLANE POTENTIAL FLOWS*

Vortex. For a vortex, we have, on the other hand,

$$\phi = C\theta \tag{6-6}$$

Then, system (2-11) gives

$$\psi = C \int \frac{\rho}{\rho^0} \frac{dq}{q} \tag{6-7}$$

Thus, in this case constant q lines are streamlines.

The coordinate functions, accordingly, are

$$x = C \frac{\sin \theta}{q} + \hat{x}(q)$$

$$y = -C \frac{\cos \theta}{q} + \hat{y}(q)$$

where $\hat{x}(q)$ and $\hat{y}(q)$ are again constant and can be taken equal to zero. The streamlines, by elimination of θ, are circles:

$$x^2 + y^2 = \frac{C^2}{q^2} \tag{6-8}$$

Thus, in contrast to the case of source flow, the speed varies monotonically with the radius, being subsonic at large radii and changing smoothly to supersonic at a specific radius. At a sufficiently small radius, q reaches q_{max}, a vacuum is theoretically created and, of course, no flow is possible. Therefore, in this case a core again exists, though the physical nature is entirely different from the previous case.

Doublet: flow around an edge. We know that the incompressible flow whose complex potential W_i has the form of a doublet in the hodograph plane, viz.

$$W_i = \frac{C}{w}$$

corresponds to flow about an edge in the z_i plane. The complex velocity for this flow in the z_i plane is given by the formula

$$w = \sqrt{\frac{C}{2z_i}}$$

where C is real and positive. The streamlines of this flow in both the flow plane and the hodograph plane are sketched in Fig. F,6a. If the fluid is compressible, the analogous flow pattern, in the analogy suggested by Chaplygin (Art. 3), would be described by the stream function

$$\psi = Cq^{-1}F_{-1}(\tau)e^{i\theta}$$

For the particular value $\nu = -1$, it can easily be verified that the hypergeometric equation (3-2) has the following solutions (cf. note 1):

$$F_{-1}(\tau) = \text{const} \quad \text{and} \quad F_{-1}(\tau) = \text{const}\ (1 - \tau)^{1+\beta}$$

F,6 · *EXAMPLES OF SIMPLE FLOWS*

The first of these corresponds to the second solution mentioned in Eq. 3-5. Let us follow Ringleb [*13*] and study the case $F_{-1} = \text{const}$,[4] i.e. we take for the stream function the simple form

$$\psi = C\frac{\cos\theta}{q} \tag{6-9}$$

where the constant C is again real. The streamlines in the hodograph plane are therefore the system of circles passing through the origin.

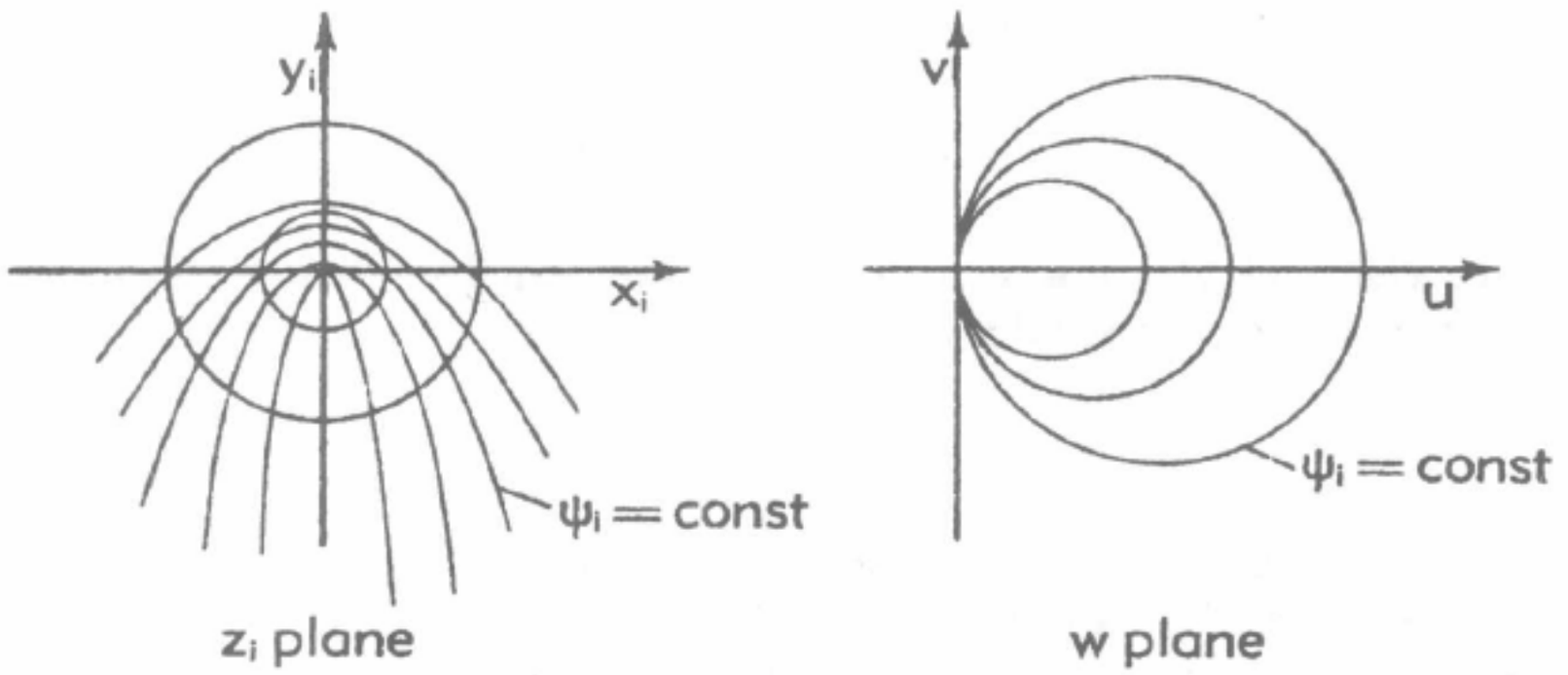

Fig. F,6a. Incompressible flow patterns around an edge in z_i and w planes.

Furthermore, by integration of Eq. 2-11,

$$\phi = -\frac{C\rho^0}{\rho q}\sin\theta \tag{6-10}$$

With these forms of ϕ and ψ, partial integration of Eq. 2-15, gives us

$$x = -\frac{C}{2q^2}(1-\tau)^{-\beta}\sin 2\theta + \hat{x}(q)$$

$$y = \frac{C}{2q^2}(1-\tau)^{-\beta}\cos 2\theta + \hat{y}(q)$$

where the arbitrary functions $\hat{x}(q)$ and $\hat{y}(q)$, by Eq. 2-16, satisfy

$$\hat{x}'(q) = 0, \qquad \hat{y}'(q) = -C\beta(1-\tau)^{-1-\beta}\frac{\tau}{q^3}$$

Integrating,

$$\hat{x}(q) = C_1 \quad \text{and} \quad \hat{y}(q) = -\frac{C}{4(a^0)^2}\int^{\tau}(1-\tau)^{-1-\beta}\frac{d\tau}{\tau} + C_2$$

where C_1 and C_2 are constants which can be taken to be zero. Finally, we

[4] The other solution has been studied by Temple and Yarwood [*14*]

have our coordinate functions

$$\frac{x}{l} = -\frac{1}{4\beta}\frac{\sin 2\theta}{\tau(1-\tau)^{\beta}}$$
$$\frac{y}{l} = \frac{1}{4\beta}\frac{\cos 2\theta}{\tau(1-\tau)^{\beta}} - \frac{1}{4}\int^{\tau} \tau^{-1}(1-\tau)^{-1-\beta}d\tau \qquad (6\text{-}11)$$

if $C = l(a^0)^2$.

We note that, after elimination of θ, the constant q or constant τ lines are again circles:

$$\left(\frac{x}{l}\right)^2 + \left(\frac{y}{l} - y_0\right)^2 = R^2$$

where

$$y_0 = -\frac{1}{4}\int^{\tau} \tau^{-1}(1-\tau)^{-1-\beta}d\tau \quad \text{and} \quad R = \frac{1}{4\beta}\tau^{-1}(1-\tau)^{-\beta}$$

As the streamline hodographs are circles, namely

$$\tau^{\frac{1}{2}} = k^{\frac{1}{2}}\cos\theta \qquad (6\text{-}12)$$

where k is a constant depending only on ψ, we can eliminate θ between Eq. 6-11 and Eq. 6-12. The resulting parametric equations for the stream-

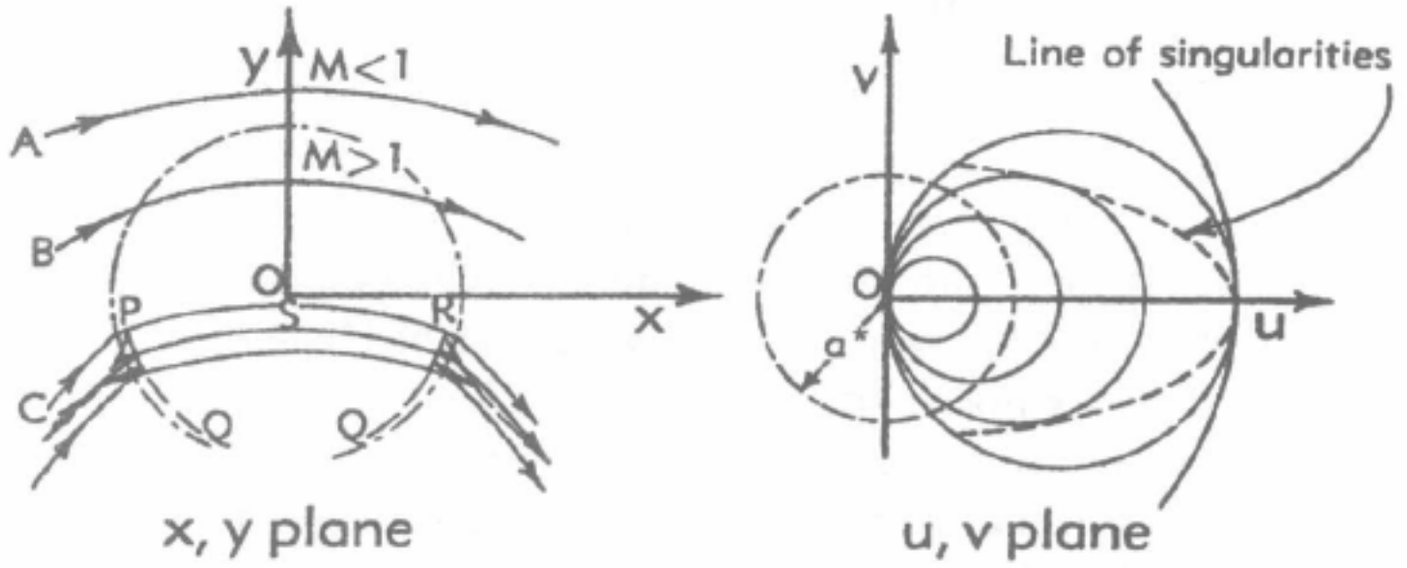

Fig. F,6b. The derived compressible flow patterns in x, y and u, v planes.

lines in the physical plane are

$$\frac{x}{l} = -\frac{1}{2\beta}k^{-\frac{1}{2}}(1-\tau)^{-\beta}\left(\frac{1}{\tau} - \frac{1}{k}\right)^{\frac{1}{2}}$$
$$\frac{y}{l} = -\frac{1}{2}\beta^{-1}(1-\tau)^{-\beta}\left(\frac{1}{2\tau} - \frac{1}{k}\right) - \frac{1}{4}\int^{\tau} \tau^{-1}(1-\tau)^{-1-\beta}d\tau \qquad (6\text{-}13)$$

For various values of k, the streamlines are shown in Fig. F,6b.

Examining the flow pattern, we notice that the flow field is divided into subsonic and supersonic regions by the sonic circle $q = a^*$. In the subsonic region, which lies outside the circle, there is a striking resemblance between this flow and that of the incompressible flow around the edge (Fig. F,6a). However, in the supersonic region this similarity

gradually disappears, and as the speed increases an entirely new phenomenon appears. First of all, the streamlines in the central region tend to bend more rapidly and hence become flatter than those of the incompressible case. This flattening produces two "throats" in each stream tube, at the two sonic lines, and between them the familiar expansion that is characteristic of supersonic ducts. As we move toward the origin, there occurs a first streamline (curve C in the figure) on which an infinite pressure gradient occurs. From there on, every streamline, instead of proceeding smoothly to the other side, makes four abrupt turns in the form of cusps. No streamlines enter the region $PSRQ$; consequently, we have again encountered an area in which no solution is possible.

Upon closer examination of the equations of the streamlines, it is easy to see the mathematical reasons why this happens. For if we differentiate these equations (6-13), the elements dx, dy, and $d\tau$ are related by

$$\frac{dx}{l} = \frac{1}{4\beta}\tau^{-2}(1-\tau)^{-1-\beta}\left(\frac{k}{\tau}-1\right)^{-\frac{1}{2}}\left[1-\alpha^2\tau+2\beta\frac{\tau^2}{k}\right]d\tau$$

$$\frac{dy}{l} = \frac{1}{4\beta}\tau^{-2}(1-\tau)^{-1-\beta}\left[1-\alpha^2\tau+2\beta\frac{\tau^2}{k}\right]d\tau$$

Thus, when a critical value of τ is reached whereby

$$1-\alpha^2\tau+2\beta\frac{\tau^2}{k}=0$$

dx and dy momentarily vanish for given $d\tau$, i.e. they become differentials of higher order. As a result all space derivatives such as $\partial/\partial x$ and $\partial/\partial y$ become locally indeterminate. The implication of this singular line PQR (Fig. F,6b) will be explored further in Art. 12.

From a different point of view, the example is not without practical interest. If two streamlines such as A and B are taken as channel walls, we find that the flow through this channel is partly subsonic and partly supersonic. It starts from rest at one end, accelerates to a supersonic speed, and then decelerates continuously, without shocks, back to subsonic speed again. Thus Ringleb's results emphasized the fact that sonic speed is not a theoretical barrier to smooth, isentropic, accelerating-decelerating flow, contrary to earlier beliefs (e.g. Taylor [*15*]). By suitable choice of wall shape according to these results, a supersonic Mach number as high as 2.5 can be reached, with subsequent deceleration, without occurrence of any abnormal effect. The fact that a mixed smooth transonic flow can be established theoretically is of considerable importance. This is one of the significant results of the hodograph method of attacking the nonlinear equations of gas flow. Its practical meaning, in terms of the design of ducts or airfoils, has not yet been completely established; flows of this type have apparently never been observed experimentally.

F · *PLANE POTENTIAL FLOWS*

F,7. Two-dimensional Gas Jets. The first step toward the solution of the general problem was made by Chaplygin [*2*] in his study of the efflux of gas from a slit. The technique used to overcome, to a certain extent, the difficulty of boundary conditions is to imitate the analogous incompressible flow. For this purpose, we shall begin with an investigation of the incompressible problem.

The incompressible jet. Suppose the half-plane $x_1 \leqq 0$ to be filled with incompressible fluid at a given pressure. If the plane $x_1 = 0$ has an opening AA' symmetrical with respect to the x_i axis, the gas, when it

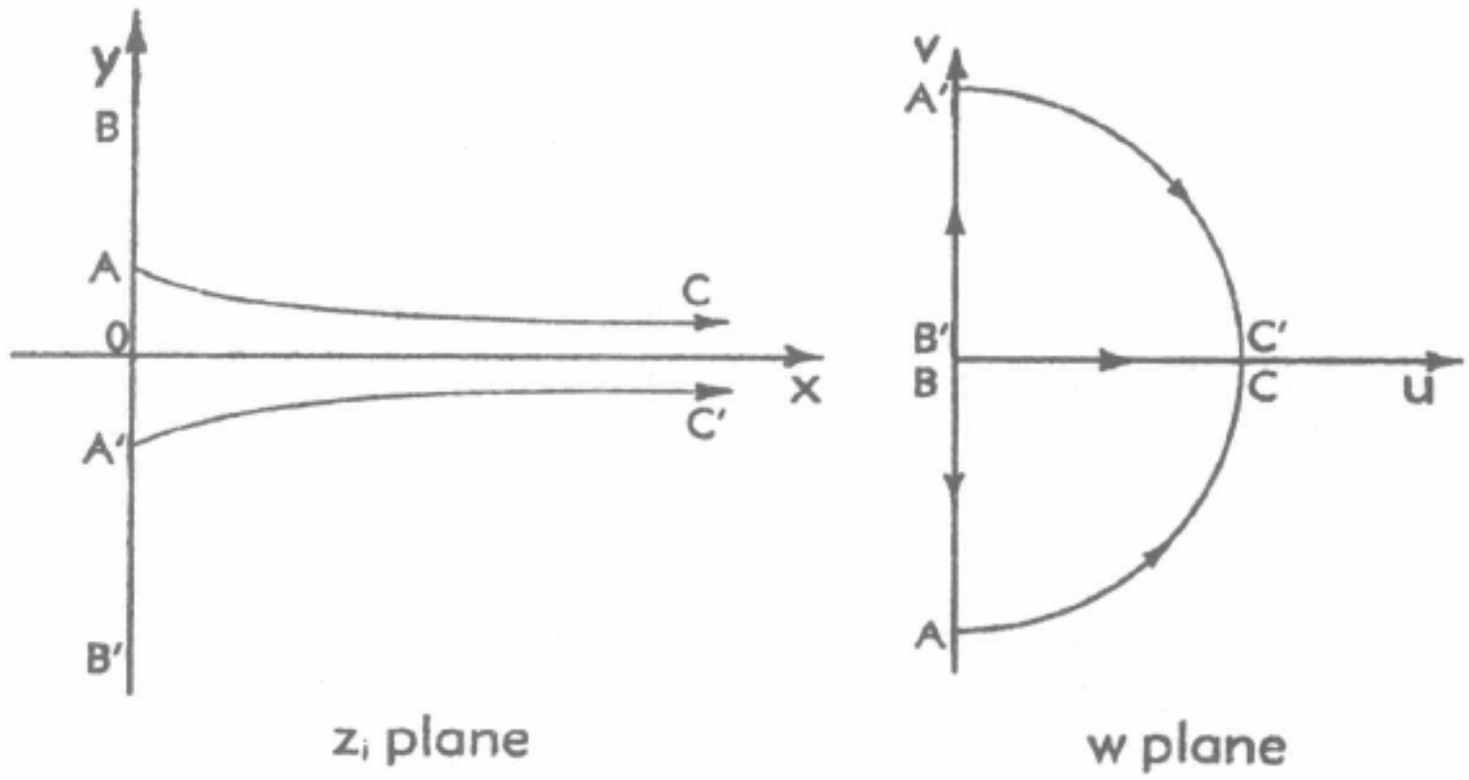

Fig. F,7a. Flow patterns in z_1 and w planes.

rushes out through this slit, produces a jet bounded by two free boundaries AC and $A'C'$ on which pressure is constant (Fig. F,7a). The flow starts with zero velocity at infinity and converges to a parallel jet at positive infinity. The problem is to determine the shape of the free boundary and the velocity distribution inside the jet.

The first solution of this incompressible flow problem was given by Helmholtz by the hodograph method. To map conformally the flow on the w plane, we proceed as follows: Since the pressure of the free boundaries is constant, they correspond to a semicircle $ACC'A'$ in the w plane (Fig. F,7a), while the walls AB and $A'B'$ appear as segments of the v axis inside the circle. The whole flow field is therefore mapped into a region inside the semicircle. This region can be further mapped into half-plane R.P.$\{\zeta\} \geqq 0$ (Fig. F,7b) by the so-called Joukowski transformation

$$2\zeta = -w + \frac{U^2}{w} \tag{7-1}$$

and

$$w = qe^{-i\theta} = u - iv$$

where U is the velocity on the free boundary AC or $A'C'$.

To establish a relation between ζ and W_1, we note that on the wall

and the free boundary the stream function ψ_1 is constant. If the quantity of flow through the slit is Q, it is clear that $\psi_1 = \frac{1}{2}Q$ on BAC and $\psi_1 = -\frac{1}{2}Q$ on $B'A'C'$. The flow field in the W_1 plane therefore lies in a

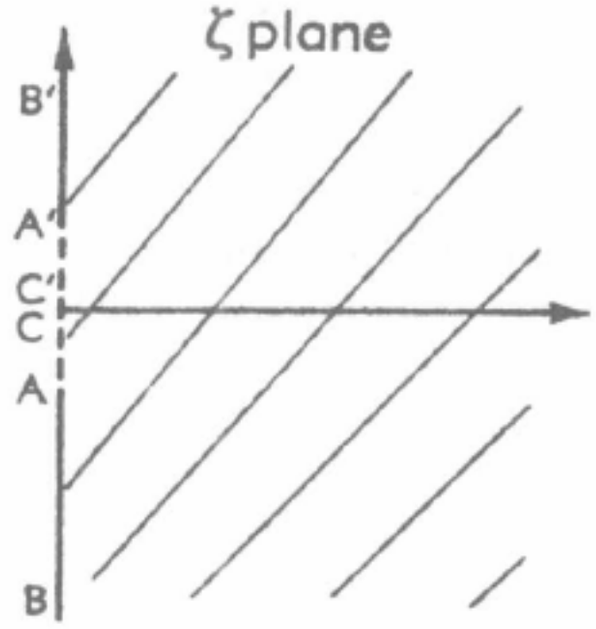

Fig. F,7b. Flow field in ζ plane.

strip (Fig. F,7c). The transformation of the half-plane into this strip can be effected by

$$W_1 = -\frac{Q}{\pi} \ln \frac{\zeta}{U} \tag{7-2}$$

By substituting ζ from Eq. 7-1 in 7-2, we finally arrive at the expression for the complex potential W_1 in the hodograph plane:

$$W_1 = -\frac{Q}{\pi} \ln \left(\frac{U}{w} - \frac{w}{U} \right) \tag{7-3}$$

Study of this expression shows that the flow pattern in the w plane (considered, for the moment, as a flow plane itself, rather than the

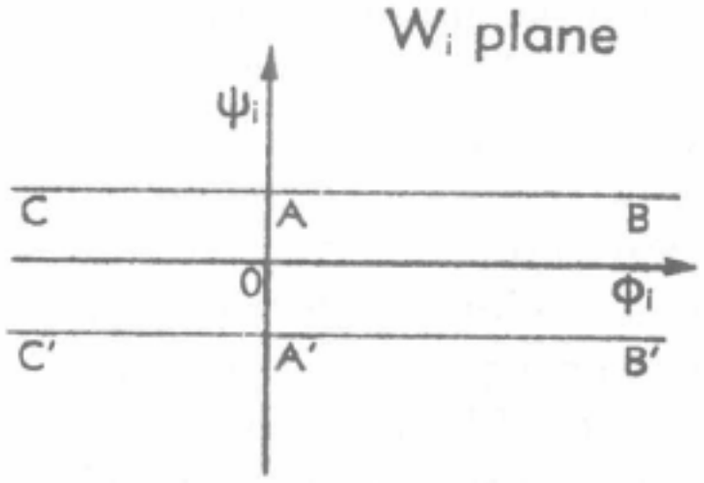

Fig. F,7c. Flow field in W_1 plane.

hodograph of another flow pattern) consists of the superposition of a source at the origin and two sinks at $w = \pm U$. The function W_1 is single-valued in the cut plane $-\pi < \theta < \pi$ and for $|w| < U$ possesses an expansion

$$W_1 = \frac{Q}{\pi} \ln \frac{2w}{U} + \frac{Q}{\pi} \sum_1^\infty \frac{1}{n} \left(\frac{w}{U} \right)^{2n}, \qquad |w| < U \tag{7-3a}$$

Separating this into real and imaginary parts, we have

$$\phi_i = \frac{Q}{\pi} \ln \frac{2q}{U} + \frac{Q}{\pi} \sum_1^\infty \frac{1}{n} \left(\frac{q}{U}\right)^{2n} \cos 2n\theta$$

$$q < U \quad (7\text{-}4)$$

$$\psi_i = -\frac{Q}{\pi}\theta - \frac{Q}{\pi} \sum_1^\infty \frac{1}{n} \left(\frac{q}{U}\right)^{2n} \sin 2n\theta$$

The compressible jet. On the basis of Eq. 7-4, Chaplygin chose the form of solution for the compressible jet to be

$$\psi = -\frac{Q}{\pi}\theta - \frac{Q}{\pi} \sum_1^\infty \frac{1}{n} \left(\frac{q}{U}\right)^{2n} \frac{F_{2n}(\tau)}{F_{2n}(\tau_1)} \sin 2n\theta \qquad (7\text{-}5)$$

in $-\pi < \theta < \pi$ and $q < U$ where τ_1 is the value of τ at $q = U$. It is seen that when a^0 is infinite ($\tau = \tau_1 = 0$) the solution reduces identically to the incompressible flow. In any case, on the free boundary $q = U$, $\psi = \psi_1(U, \theta) = \pm Q/2$ and the same value occurs on the walls $\theta = \pm\pi/2$, thus, formally Eq. 7-5 is a solution satisfying the boundary condition. To establish its convergence, we need only demonstrate the inequality: as $n \to \infty$

$$\left| \frac{1}{n} \left(\frac{q}{U}\right)^{2n} \frac{F_{2n}(\tau)}{F_{2n}(\tau_1)} \right| < \frac{C}{n} \left[\frac{T(\tau)q}{T_1 U} \right]^{2n}$$

where T is the function defined in the appendix to this section, and T_1 denotes the value $T(\tau_1)$. This can easily be done, making use of the asymptotic properties of $F_n(\tau)$ discussed in the appendix (Eq. 16-3), provided that the flow is everywhere subsonic. Moreover, since $d(Tq)/dq > 0$, $Tq < T_1 U$. Therefore, the dominant series converges absolutely if $Tq < T_1 U$, and it follows that series (7-5) converges uniformly in any closed domain $Tq \leqq T_1 U - \delta$, $\delta > 0$.

From Eq. 7-5 together with Eq. 3-9 and 3-10, the velocity potential ϕ is

$$\phi = \frac{Q}{\pi} \left[(1-\tau)^{-\beta} - \frac{1}{2} \int^\tau \tau^{-1}(1-\tau)^{-\beta} d\tau \right]$$

$$+ \frac{Q}{\pi} (1-\tau)^{-\beta} \sum_1^\infty \frac{1}{n} \left(\frac{q}{U}\right)^{2n} \frac{F_{2n}(\tau)}{F_{2n}(\tau_1)} \xi_{2n}(\tau) \cos 2n\theta, \qquad q < U \quad (7\text{-}6)$$

This series converges in the same domain as Eq. 7-5, since $|\xi_{2n}(\tau)| = O(1)$ as $n \to \infty$ by Eq. 16-7, for subsonic flow.

At this point both ϕ and ψ are determined up to an arbitrary multiplier Q, proportional to the mass flow. The coordinate functions now can

be integrated in the following manner: Upon substitution of Eq. 7-5 and 7-6 in Eq. 2-15, partial integration yields

$$x = \frac{Q}{\pi}\frac{(1-\tau)^{-\beta}}{q}\left\{\sum_1^\infty \left(\frac{q}{U}\right)^{2n}\frac{F_{2n}(\tau)}{F_{2n}(\tau_1)}\,\xi_{2n}(\tau)\left[\frac{\cos(2n+1)\theta}{2n+1}+\frac{\cos(2n-1)\theta}{2n-1}\right]\right.$$
$$\left.-\sum_1^\infty \left(\frac{q}{U}\right)^{2n}\frac{F_{2n}(\tau)}{F_{2n}(\tau_1)}\left[\frac{\cos(2n+1)\theta}{2n+1}-\frac{\cos(2n-1)\theta}{2n-1}\right]-\cos\theta\right\}+\hat{x}(q)$$

(7-7)

$$y = \frac{Q}{\pi}\frac{(1-\tau)^{-\beta}}{q}\left\{\sum_1^\infty \left(\frac{q}{U}\right)^{2n}\frac{F_{2n}(\tau)}{F_{2n}(\tau_1)}\,\xi_{2n}(\tau)\left[\frac{\sin(2n+1)\theta}{2n+1}-\frac{\sin(2n-1)\theta}{2n-1}\right]\right.$$
$$\left.-\sum_1^\infty \left(\frac{q}{U}\right)^{2n}\frac{F_{2n}(\tau)}{F_{2n}(\tau_1)}\left[\frac{\sin(2n+1)\theta}{2n+1}+\frac{\sin(2n-1)\theta}{2n-1}\right]-\sin\theta\right\}+\hat{y}(q)$$

Now $x = 0$ and $y = 0$ when $\theta = \pi/2$ and 0 respectively, hence, we must have

$$\hat{x} = \hat{y} = 0$$

Thus, the coordinate functions have the forms

$$x = \frac{Q}{\pi}\frac{(1-\tau)^{-\beta}}{q}\left\{\sum_1^\infty \left(\frac{q}{U}\right)^{2n}\frac{F_{2n}(\tau)}{F_{2n}(\tau_1)}\left[\xi_{2n}(\tau)C_{2n}^{(1)}(\theta)-C_{2n}^{(2)}(\theta)\right]-\cos\theta\right\}$$

(7-8)

$$y = \frac{Q}{\pi}\frac{(1-\tau)^{-\beta}}{q}\left\{\sum_1^\infty \left(\frac{q}{U}\right)^{2n}\frac{F_{2n}(\tau)}{F_{2n}(\tau_1)}\left[\xi_{2n}(\tau)S_{2n}^{(2)}(\theta)-S_{2n}^{(1)}(\theta)\right]-\sin\theta\right\}$$

where the coefficients $C_{2n}^{(1)}$, $C_{2n}^{(2)}$, $S_{2n}^{(1)}$, and $S_{2n}^{(2)}$ denote the four trigonometric functions of θ that appear in square brackets in Eq. 7-7, i.e.

$$C_{2n}^{(1)}(\theta) = \frac{\cos(2n+1)\theta}{2n+1}+\frac{\cos(2n-1)\theta}{2n-1}$$

$$C_{2n}^{(2)}(\theta) = \frac{\cos(2n+1)\theta}{2n+1}-\frac{\cos(2n-1)\theta}{2n-1}$$

$$S_{2n}^{(1)}(\theta) = \frac{\sin(2n+1)\theta}{2n+1}+\frac{\sin(2n-1)\theta}{2n-1}$$

$$S_{2n}^{(2)}(\theta) = \frac{\sin(2n+1)\theta}{2n+1}-\frac{\sin(2n-1)\theta}{2n-1}$$

On the jet boundary, $q = U$ and $\tau = \tau_1$, the parametric equations for

the curve are

$$x = \frac{Q}{\pi}\frac{(1-\tau_1)^{-\beta}}{U}\left\{\sum_1^\infty [\xi_{2n}(\tau_1)C_{2n}^{(1)}(\theta) - C_{2n}^{(2)}(\theta)] - \cos\theta\right\}$$

$$y = \frac{Q}{\pi}\frac{(1-\tau_1)^{-\beta}}{U}\left\{\sum_1^\infty [\xi_{2n}(\tau_1)S_{2n}^{(2)}(\theta) - S_{2n}^{(1)}(\theta)] - \sin\theta\right\}$$

or

$$x = \frac{Q}{\pi}\frac{(1-\tau_1)^{-\beta}}{U}\sum_1^\infty \xi_{2n}(\tau_1)C_{2n}^{(1)}(\theta)$$

$$y = \frac{Q}{\pi}\frac{(1-\tau_1)^{-\beta}}{U}\left[\sum_1^\infty \xi_{2n}(\tau_1)S_{2n}^{(2)}(\theta) - \frac{\pi}{2}\right]$$

as, for $0 < \theta < \pi$, it is known that

$$\sum_1^\infty \frac{\sin(2n-1)\theta}{2n-1} = \frac{\pi}{4}$$

and

$$\sum_1^\infty C_{2n}^{(2)}(\theta) = -\cos\theta$$

Let $2b$ be the width of the jet at infinity, and let Q be defined as

$$Q = 2bU(1-\tau_1)^\beta.$$

We have

$$\frac{y}{b} = -\frac{2}{\pi}\left[\frac{\pi}{2} - \sum_1^\infty \xi_{2n}(\tau_1)S_{2n}^{(2)}(\theta)\right]$$

If the aperture of the slit in the wall is $2a$, then, for $\theta = \pi/2$, $y = -a$. The contraction ratio is therefore

$$\frac{\bar{b}}{a} = \left[1 + \frac{8}{\pi}\sum_1^\infty (-1)^{n-1}\frac{n\xi_{2n}(\tau_1)}{4n^2-1}\right]^{-1} \tag{7-9}$$

This ratio was calculated by Chaplygin for a series of Mach numbers. He found that the ratio increases with the Mach number from the lowest value of 0.611 at zero Mach number to 0.74 when the maximum Mach number, i.e. the Mach number at infinity and along the free boundary, is close to 1 (Fig. F,7d).

F,8 · *FLOW AROUND A CLOSED BODY*

When the pressure in the receiver is lower than the critical value corresponding to unit Mach number, the jet boundary is mapped on a circular arc in the hodograph plane with radius greater than sonic speed. The flow in the jet is then partly subsonic and partly supersonic, with the transition taking place along sonic curves projecting into the flow from points A and A'. At these two points the speed jumps from subsonic to supersonic in a discontinuous way. Consequently, the boundary hodograph curve is not closed, and the method used here to solve the problem

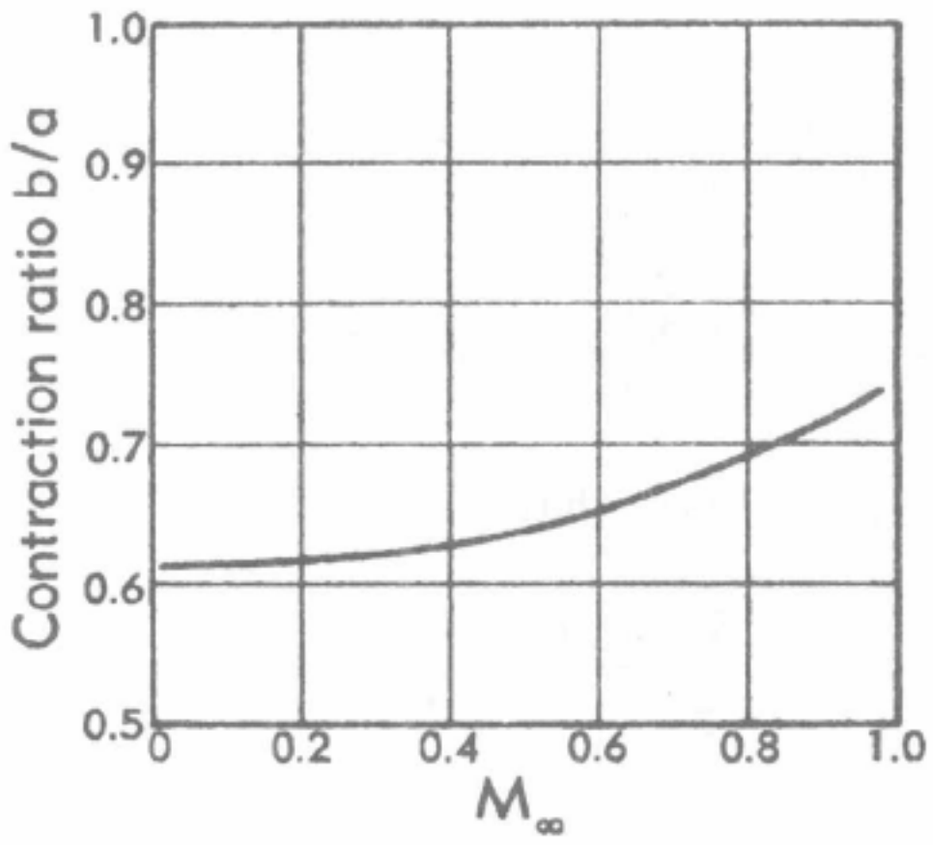

Fig. F,7d. Increase of contraction ratio with Mach number at infinity of the jet.

fails. For further development along this line, reference should be made to the work of Frankl [*16*] and Guderley [*17*] (cf. H,9).

F,8. Flow Around a Closed Body. As a generalization of Chaplygin's method, let us consider now the typical aeronautical problem of flow around a closed body. In the absence of circulation, the problem is to be solved subject to the following conditions: (1) the solution for the compressible flow should have the same analytic behavior as does the solution for a given incompressible flow; and (2) in the limiting case of vanishing Mach number, it must reduce to the incompressible solution. It appears that once more we must study the incompressible flow as our first step.

Conformal mapping of incompressible flow. For a simple example, we consider the flow about a circular cylinder. If the flow at infinity is represented by $w = 1$, then on the cylinder the well-known result is $|w| = 2\cos\theta$. In going over from the z_i to the w plane, we observe, in the first place, that the infinity of the z_i plane corresponds to a point $w = 1$ in the w plane; the parts of the real axis outside the cylinder are mapped on the segment $v = 0, 0 \leqq u \leqq 1$; and the imaginary axis for $1 \leqq y_i < \infty$,

on which v is again zero, is mapped on $1 \leqq u \leqq 2$ (see Fig. F,8a). Furthermore, the streamline $S_-P_+S_+$ in the z_i plane, according to the result just mentioned above, corresponds to the circle $S_-P_+S_+$ in the hodograph plane. Thus, the streamline $R_-P_+R_+$ appears as this circle together with the segment $v = 0$, $0 \leqq u \leqq 1$, on which both R_-S_- and S_+R_+ overlap. Since the highest velocity of the flow field is attained on the boundary, according to a general theorem for flows of this type, the whole upper half of the flow field must be mapped into the interior of the circle with

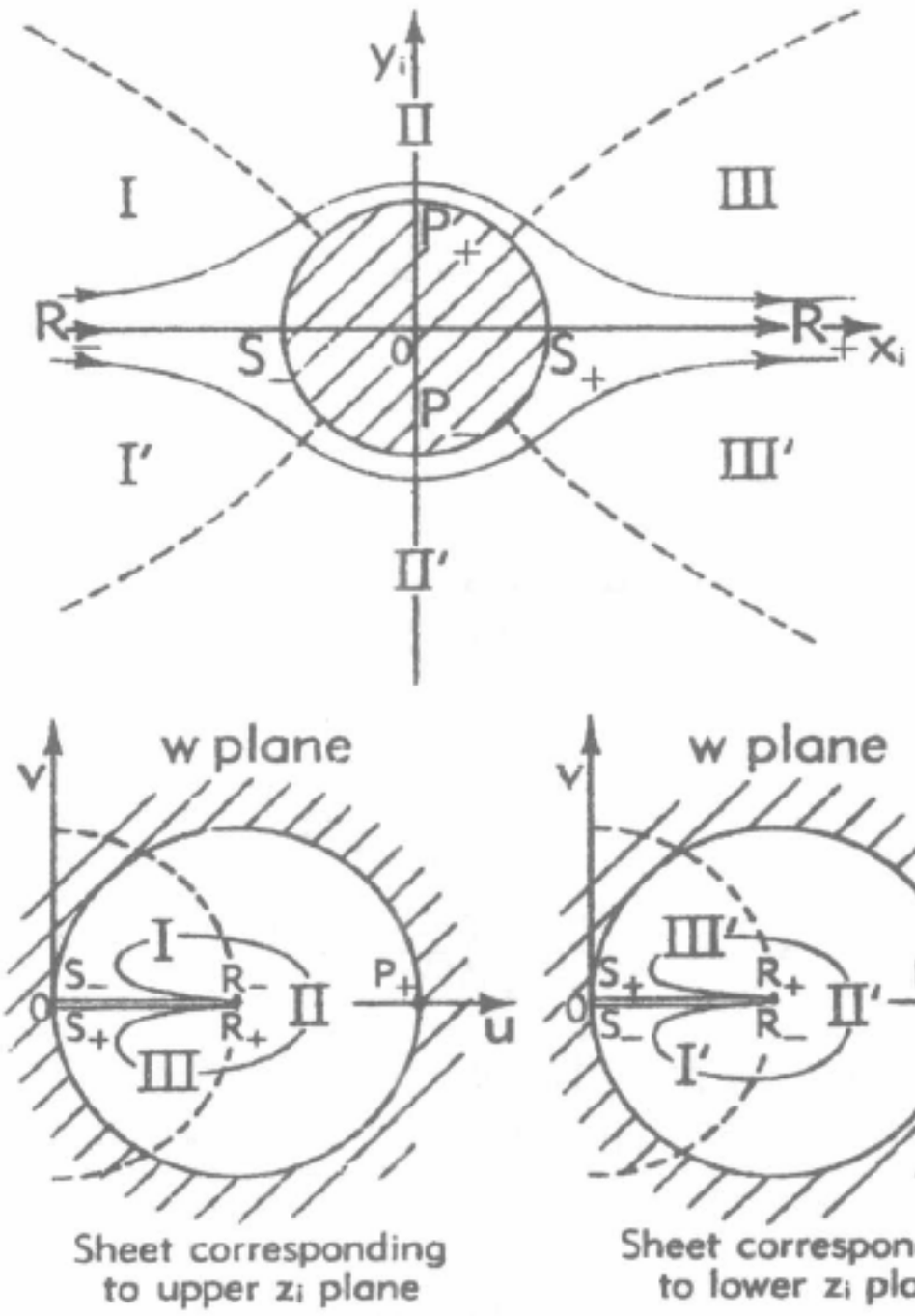

Fig. F,8a. Conformal mapping of incompressible flow from z_i into w plane.

center at $w = 1$. Proceeding to the lower half of the z_i plane, we have, by symmetry, the same mapping, as is also shown in Fig. F,8a.

Consequently, we see that the z_i plane, when transformed into the w plane, will be two-sheeted, i.e. will cover two w planes.

In Fig. F,8a six regions of the flow field, designated I, II, III, I′, II′, and III′ are indicated, their boundaries being the x_i axis and the lines along which $|w| = 1$. The locations of these regions in the two hodograph sheets are also shown; here, of course, their boundaries are the real axis and the unit circle.

The mapping can be considered one-valued if a cut is put in from $w = 0$ to $w = 1$, i.e. along R_-S_- and S_+R_+. This cut prevents our passing

from the upper to the lower half of the flow field; thus, the w plane represents one or the other, but not both We shall consider the upper half first, and obtain the flow in the lower by symmetry.

Even in the cut plane, it is not possible to write down a single expansion for W_i, in the form needed to carry out Chaplygin's method, which is valid throughout the region of interest. This is due to the presence of a singularity at the point $w = 1$, where all streamlines converge. Instead, it is necessary to use the following expansions in the various regions of the w plane:

$$
\begin{aligned}
{}_1W_i &= \sum_0^\infty A_n w^n, && |w| < 1 \\
{}_2W_i &= i\sum_0^\infty B_n w^{-\nu}, \qquad \nu = n - \tfrac{1}{2} && |w| > 1 \qquad (8\text{-}1) \\
{}_3W_i &= -\sum_0^\infty A_n w^n, && |w| < 1
\end{aligned}
$$

where ${}_1W_i$, ${}_2W_i$, and ${}_3W_i$ are the proper expansions for W_i in the regions I, II, and III of Fig. F,8a, respectively. In the case of a circular cylinder, the constants A_n and B_n are

$$
A_n = -\frac{(n-1)\Gamma(n-\frac{1}{2})}{\Gamma(\frac{1}{2})\Gamma(n+1)}
$$

$$
B_n = -\frac{(n+\frac{1}{2})\Gamma(n-\frac{1}{2})}{\Gamma(\frac{1}{2})\Gamma(n+1)}
$$

By symmetry, the complex potential in the other sheet (lower half of the flow field) is related to these expansions by the relations

$$
{}_3W_i' = {}_3W_i, \qquad {}_2W_i' = -{}_2W_i, \qquad {}_1W_i' = {}_1W_i \qquad (8\text{-}2)
$$

Thus, when W_i is determined, W_i' is known.

A trial solution of compressible flow: region I. Following the principle of the preceding article, we can at once construct a solution for compressible flow about a distorted circular cylinder by applying Chaplygin's analogy to the expansions (8-1), if the flow is subsonic at infinity.

With considerable generality, we can select for our solution in region I the expansion

$$
W_1 = \sum_0^\infty A_n f_n(\tau_1) F_n(\tau) w^n, \qquad |w| < 1
$$

where W_1 has ψ_1 as its imaginary part, $F_n(\tau)$ is the hypergeometric function and $f_n(\tau_1)$ is a function of n and τ_1, τ_1 being the value of τ corresponding to the free stream condition.

F · *PLANE POTENTIAL FLOWS*

To satisfy the conditions (1) and (2) stated at the beginning of this article, $f_n(\tau_1)$ must be chosen so that $f_n(0) = 1$ (since $F_n(0) = 1$); and for large n, since $F_n(\tau)$ is asymptotic to a multiple of T^n for $\alpha^2\tau < 1$ by Eq. 16-3, $f_n(\tau_1)$ must be asymptotic to a multiple of T_1^{-n} if W_1 and ${}_1W_1$ are to have the same analytic behavior at $\tau = \tau_1$. Clearly, to meet these requirements, $f_n(\tau_1)$ may either be $F_n(\tau_1)^{-1}$ (as in the example of our preceding article) or T_1^{-n}. Both of these forms have been used, but the latter, as pointed out by both Lighthill [*18*] and Cherry [*5*], is a more suitable choice if the boundary involved is closed. Accordingly, we take as our trial solution in region I the expansion

$$W_1 = \sum_0^\infty A_n \mathfrak{F}_n(\tau) w^n, \qquad |w| < 1 \tag{8-3}$$

where $\mathfrak{F}_n(\tau) = F_n(\tau)/T_1^n$.

Formally, we now have a solution satisfying both conditions (1) and (2). In order that it actually be a solution valid in the region indicated, we have to show that it converges. In the first place, we have the inequality

$$\left|\sum_0^\infty A_n \mathfrak{F}_n(\tau) w^n\right| \leqq \sum_0^\infty |A_n \mathfrak{F}_n w^n|$$

But from Eq. 16-3, $\mathfrak{F}_n(\tau) < C(T/T_1)^n$ if $\alpha^2\tau < 1$ and n is large. It follows, therefore, that

$$|A_n \mathfrak{F}_n(\tau) w^n| < C|A_n| \left(\frac{Tq}{T_1}\right)^n$$

the dominant series is then convergent absolutely if $Tq < T_1$. Consequently, series (8-3) converges uniformly and absolutely for any closed domain $Tq \leqq T_1 - \delta$, $\delta > 0$. Furthermore, as Tq is zero when $q = 0$, is T_1 when $q = 1$, and is monotonic in between, the series has exactly the same radius of convergence as Eq. 8-1, i.e. $|w| < 1$.

Continuation into region II. The solution, however, is still incomplete. In order to have a complete solution for all the regions, the question of analytic continuation arises. We obviously cannot write down an expansion for region II, for example, without making sure that it is the correct continuation of Eq. 8-3. This problem has been attacked by several authors [*5,18–22*] by different techniques—not all of which are correct. The method of Lighthill [*18*] and Cherry [*5*] is presented here.

The flow within region I is purely subsonic; it was discovered by Lighthill and Cherry that in this case $\mathfrak{F}_n(\tau)$ possesses the following representation (cf. Eq. 16-6):

$$\mathfrak{F}_n(\tau) = \left(\frac{T}{T_1}\right)^n \left[f(\tau) - \sum_1^\infty \frac{h_m \tau^m T^m F_m(\tau)}{n+m}\right] \tag{8-4}$$

F,8 · *FLOW AROUND A CLOSED BODY*

By virtue of Eq. 8-4, expansion (8-3) can be rewritten[5] as

$$W_1 = f(\tau)_1 W_i \left(\frac{T}{T_1} w\right) - \sum_0^\infty A_n \left(\frac{T}{T_1} w\right)^n \sum_2^\infty \frac{h_m \tau^m T^m F_m(\tau)}{n+m}$$

Since both series in this solution are absolutely convergent in region I, we may interchange the order of summation:

$$W_1 = f(\tau)_1 W_i \left(\frac{T}{T_1} w\right) - \sum_2^\infty h_m \tau^m T^m F_m(\tau) \left(\frac{T}{T_1} w\right)^{-m} \sum_0^\infty \frac{A_n \left(\frac{T}{T_1} w\right)^{n+m}}{n+m}$$

But, in view of Eq. 8-1, it is easily verified that

$$\sum_0^\infty \frac{A \left(\frac{T}{T_1} w\right)^{n+m}}{n+m} = \int_0^\zeta \zeta^{m-1}{}_1 W_i d\zeta$$

with $\zeta = Tw/T_1$. It follows that

$$W_1 = f(\tau)_1 W_i(\zeta) - \sum_2^\infty h_m (\tau_I \tau)^{\frac{m}{2}} F_m(\tau) e^{im\theta} \int_0^\zeta \zeta^{m-1}{}_1 W_i d\zeta \qquad (8\text{-}5)$$

Now, although we have restricted ourselves to region I ($|w| < 1$, i.e. $|\zeta| < 1$), Eq. 8-5 is actually in a form that constitutes a continuation into a larger region. For in region I, ${}_1W_i$ converges to W_i, which is an analytic function throughout a larger region, while the infinite series in Eq. 8-5 can also be shown to possess a larger radius of convergence. To prove this, we need only note that the integral appearing there (when we read once more W_i for ${}_1W_i(\zeta)$) is bounded for all ζ, provided that the path of integration avoids the singular point $\zeta = w = 1$, where W_i itself is infinite, i.e.

$$\left| \int_0^\zeta \zeta^{m-1}{}_1 W_i d\zeta \right| \leqq \frac{C}{m} |\zeta|^m$$

Therefore the series in Eq. 8-5 is dominated by $\sum h_m \tau^m T^m F_m(\tau)/m$ which converges for all $\alpha^2 \tau < 1$; hence, it is uniformly and absolutely convergent in any closed region where the flow is subsonic. Thus Lighthill and Cherry have succeeded in Eq. 8-5 in continuing W beyond region I into all subsonic and supersonic regions of the flow excepting, of course, the point $w = 1$.

[5] It is interesting to note that, in the special case $\gamma = -1$ considered in an earlier article, this solution becomes the one used by von Kármán and Tsien. For in that case $f(\tau) = 1$ and all the h_n's vanish (see Art. 16); thus $W_1 = W_i(q_i e^{-i\theta})$.

F · *PLANE POTENTIAL FLOWS*

For simplicity, in going from region I to region II, let us perform the integration in Eq. 8-5 along the following path:

$$\int_0^{\zeta} = \int_0^{1-} + \curvearrowright + \int_{1+}^{\zeta}$$

where the second contribution along the semicircle about the branch point vanishes, and ζ is restricted to values corresponding to $\tau(\zeta)$ in $\tau_1 < \tau(\zeta) < 1$. Now in region II, according to Eq. 8-1

$$\int_{1+}^{\zeta} \zeta^{m-1}{}_2W_i d\zeta = i \sum_0^{\infty} \frac{B_n}{-\nu + m} \zeta^{-\nu+m} - i \sum_0^{\infty} \frac{B_n}{-\nu + m}$$

Substituting in Eq. 8-5 and again interchanging the order of summation, we finally arrive at a solution in region II, $|w| > 1$ and $\tau_1 < \tau < 1$:

$$W_2 = i \sum_0^{\infty} B_n \mathfrak{F}_{-\nu}(\tau) w^{-\nu} - \sum_2^{\infty} h_m g_m (\sqrt{\tau_1}\, T_1)^m \psi_m(\tau) e^{im\theta} \qquad (8\text{-}6)$$

where

$$g_m = \int_0^1 \zeta^{m-1}{}_1W_i d\zeta - i \sum_0^{\infty} \frac{B_n}{-\nu + m} \text{ and } \psi_m(\tau) = \tau^{\frac{m}{2}} F_m(\tau)$$

In the present example

$${}_1W_i = -(1-\zeta)^{\frac{1}{2}} - (1-\zeta)^{-\frac{1}{2}}$$

whence

$$\int_0^1 \zeta^{m-1}{}_1W_1 d\zeta = -\frac{(m+1)\Gamma(m)\Gamma(\frac{1}{2})}{\Gamma(m+\frac{3}{2})}$$

and

$$\sum_0^{\infty} \frac{B_n}{-\nu + m} = \frac{1}{m+\frac{1}{2}} \frac{\Gamma(-m+\frac{1}{2})\Gamma(\frac{3}{2})}{\Gamma(-m+1)} + \frac{1}{m-\frac{1}{2}} \frac{\Gamma(-m+\frac{3}{2})\Gamma(\frac{1}{2})}{\Gamma(-m+1)}$$

As m is a positive integer, $1/\Gamma(-m+1) \equiv 0$; therefore, g_m is real and equal to

$$g_m = -\frac{(m+1)\Gamma(m)\Gamma(\frac{1}{2})}{\Gamma(m+\frac{3}{2})} \qquad (8\text{-}7)$$

It is interesting to note that the continued solution (8-6), which we have derived by continuation of Eq. 8-3, differs in form from its "parent solution," i.e. ${}_2W_i$ in Eq. 8-1, by the presence of an additional series. This series vanishes with vanishing τ, as it must, but destroys the symmetry of the required solution.

Modified solution and continuation. As the contour in the limit of incompressible flow is a circular cylinder, the solution of the compressible flow must at least possess fore-and-aft symmetry, which our trial solution

fails to exhibit. We need, therefore, to revise our solution to permit supersonic local conditions.

Again we follow Lighthill [*18*] and Cherry [*5*] to accomplish this. Their method is to replace Eq. 8-3 by a different form of solution for region I; in fact, they add to Eq. 8-3 a series of exactly the form that gives trouble in region II, i.e.

$$W_1 = \sum_0^\infty A_n \mathcal{F}_n(\tau) w^n + \sum_2^\infty h_n g_n (\sqrt{\tau_1}\, T_1)^n \psi_n(\tau) e^{in\theta} \tag{8-8}$$

Since the second series converges in $\tau_1 , < \tau < 1$ only the first series has to be continued. By repeating the above process, we find the solution in region II:

$$W_2 = i \sum_0^\infty B_n \mathcal{F}_{-\nu}(\tau) w^{-\nu}, \qquad |w| > 1 \tag{8-9}$$

In the subsonic range, by Eq. 16-3 the series (8-9) is dominated by

$$\sum_0^\infty \left| B_n \left(\frac{Tw}{T_1} \right)^{-\nu} \right|$$

which, according to Eq. 8-1, converges if $Tq > T_1$, which we have seen to be true. Again, in the supersonic range, the dominant is

$$\sum_0^\infty \left| B_n \left(\frac{r}{\sqrt{\tau_1}\, T_1} \right)^{-\nu} \right|$$

which converges if $\sqrt{\tau_1}\, T_1 < r$ (see Eq. 16-4). This inequality is found to be true in connection with the proof of Eq. 16-6. Consequently, the continued series (8-9) converges uniformly and absolutely in any closed domain in $1 < |w| < q_{\max}$.

To complete our solution, we have only to extend it into region III. If the path of integration for the integral in Eq. 8-5 is taken from $\zeta = 0$, around $w = 1$, back to $\zeta = 0$, and thence to an arbitrary point in III, we have

$$\begin{aligned} \int_0^\zeta \zeta^{m-1} W_i d\zeta &= \int_0^{1-} \zeta^{m-1}{}_1 W_i d\zeta + \int_{1-}^0 \zeta^{m-1}{}_2 W_i d\zeta + \int_0^\zeta \zeta^{m-1}{}_3 W_i d\zeta \\ &= -2g_m + \int_0^\zeta \zeta^{m-1}{}_3 W_i d\zeta \end{aligned} \tag{8-10}$$

by virtue of Eq. 8-1, where again the contribution from the circle about $\zeta = 1$ is zero. Substituting Eq. 8-10 in the continued solution, corresponding to Eq. 8-5, the solution valid in region III is

$$W_3 = -\sum_0^\infty A_n \mathcal{F}_n(\tau) w^n - \sum_2^\infty h_n g_n (\sqrt{\tau_1}\, T_1)^n \psi_n(\tau) e^{in\theta} \tag{8-11}$$

F · *PLANE POTENTIAL FLOWS*

The three expressions (8-8), (8-9), and (8-11) taken together make up the solution in the first complete Riemann sheet and, moreover, satisfy the conditions (1) and (2) at the beginning of this article. This final solution has another important advantage over our "trial solution" discussed above, namely, that it represents a flow symmetric about the y axis, while the solution based on Eq. 8-3, upon continuation into region III, is found to be asymmetric. Thus, even for purely subsonic flow patterns, the "trial solution" was inappropriate for the present problem.

By symmetry, the solution in the second Riemann sheet, representing the lower half of the flow plane, can also be given as in Eq. 8-2, namely

$$W_3' = W_3, \qquad W_2' = -W_2, \qquad W_1' = W_1 \tag{8-12}$$

Thus, it can be stated that, given an incompressible flow without circulation around a body, the Lighthill-Cherry method with proper conditions, such as symmetry, closed body, etc., leads to a unique solution for compressible flow [*18*]. The extension to the case of a body with an isolated infinite curvature, e.g. the trailing edge of an airfoil, can easily be carried out if the formula (16-6) is modified to include negative integers; this has been done by Kuo [*23*].

Coordinate functions. To complete our solution, we must calculate the coordinate functions relating x and y to the hodograph variables. The stream function is found by taking the imaginary parts of Eq. 8-8, 8-9, and 8-10 for the three regions of the plane. The methods of Art. 3 then lead, without difficulty, to the following expressions for the velocity potential:

$$\begin{aligned}
\phi_1 &= (1-\tau)^{-\beta} \sum_0^\infty \tilde{A}_n q^n \mathcal{F}_n(\tau)\xi_n(\tau) \cos n\theta, \qquad 1 > q \\
\phi_2 &= (1-\tau)^{-\beta} \sum_0^\infty B_n q^{-\nu} \mathcal{F}_{-\nu}(\tau)\xi_{-\nu}(\tau) \sin \nu\theta, \qquad 1 < q < q_{\max} \\
\phi_3 &= -(1-\tau)^{-\beta} \sum_0^\infty \tilde{A}_n q^n \mathcal{F}_n(\tau)\xi_n(\tau) \cos n\theta, \qquad 1 > q
\end{aligned} \tag{8-13}$$

where $\tilde{A}_n = A_n - h_n g_n (\sqrt{\tau_1}\, T_1)^{2n}$.

Both ψ and ϕ being known, the integration of Eq. 2-15 and 2-16 can be performed. The results are as follows: if the stagnation point is taken to be $x_1 = +x_0$ and $y = 0$, we have, for $q < 1$, $\theta > 0$,

$$\begin{aligned}
x_1 &= +x_0 + \frac{(1-\tau)^{-\beta}}{2q} \sum_2^\infty n\tilde{A}_n q^n \mathcal{F}_n(\tau)[\xi_n(\tau) C_n^{(1)}(\theta) - C_n^{(2)}(\theta)] \\
y_1 &= \frac{(1-\tau)^{-\beta}}{2q} \sum_2^\infty n\tilde{A}_n q^n \mathcal{F}_n(\tau)[\xi_n(\tau) S_n^{(2)}(\theta) - S_n^{(1)}(\theta)]
\end{aligned} \tag{8-14}$$

where the coefficients $C_n^{(1)}$, $C_n^{(2)}$, $S_n^{(1)}$, and $S_n^{(2)}$ are the trigonometric functions defined in connection with Eq. 7-8. Similarly, in $1 < q < q_{max}$ and $-\pi/2 < \theta < \pi/2$

$$x_2 = \frac{(1-\tau)^{-\beta}}{2q} \sum_0^\infty \nu B_n q^{-\nu} \mathfrak{F}_{-\nu}(\tau)[\xi_{-\nu}(\tau) S_\nu^{(1)}(\theta) - S_\nu^{(2)}(\theta)]$$

$$y_2 = y_0 - \frac{(1-\tau)^{-\beta}}{2q} \sum_0^\infty \nu B_n q^{-\nu} \mathfrak{F}_{-\nu}(\tau)[\xi_{-\nu}(\tau) C_\nu^{(2)}(\theta) - C_\nu^{(1)}(\theta)] \tag{8-15}$$

and in $q < 1$, $\theta < 0$

$$\begin{aligned} x_3 &= -x_1 \\ y_3 &= -y_1 \end{aligned} \tag{8-16}$$

The constant in x_2 has been determined so that $x_2 = 0$ when $\theta = 0$; the constants x_0 and y_0 will be determined by the condition that, on $q = 1$ and $\theta = \theta_0$ on the body, i.e. $\psi(1, \theta_0) = 0$, we have

$$x_1 = x_2, \qquad y_1 = y_2 \tag{8-17}$$

By symmetry, the coordinate functions of the second branch (lower part of the flow field) are given by

$$\begin{aligned} x_3' &= x_3, & y_3' &= y_3 \\ x_2' &= -x_2, & y_2' &= -y_2 \\ x_1' &= x_1, & y_1' &= y_1 \end{aligned} \tag{8-18}$$

Results. The theory outlined in this article has been applied by Cherry [*24*] to the flow about a blunt symmetric cylinder. The case studied by Cherry is the one that reduces to a circular cylinder when the Mach number is zero. His results are reproduced in Fig. F,8b, where several streamlines are plotted for flow at a stream Mach number of 0.5098. The cylinder is very nearly circular at this Mach number. The values of τ noted in the figure indicate various values of the speed, sonic speed corresponding to $\tau = 0.1684$. A local supersonic region appears with a maximum value of τ that indicates a local Mach number of about 1.39. In the same paper, Cherry has extended the theory to handle a cylinder that is symmetric fore and aft but has camber, and has again calculated and plotted the streamlines and local speeds.

Method of Tsien and Kuo. There is another method [*19,20*] that is mathematically simple and shcuild be briefly mentioned. We return to a discussion of the form to be assumed for the stream function in region I and its continuation into the other regions. If, as in Eq. 8-3, the solution inside the unit circle is

$$\psi^{(1)} = -\sum_1^\infty \tilde{A}_n \mathfrak{F}_n(\tau) q^n \sin n\theta, \qquad 0 < \theta < 2\pi, \tag{8-19}$$

F · *PLANE POTENTIAL FLOWS*

the solution for $q > 1$ and $0 < \theta < 2\pi$ can be assumed to be

$$\psi^{(0)} = \sum_0^\infty B_n q^{-\nu} \mathfrak{F}_{-\nu}(\tau) \cos \nu\theta + \sum_1^\infty \tilde{C}_n q^{-n} \mathfrak{F}_{-n}(\tau) \sin n\theta \qquad (8\text{-}20)$$

In order that $\psi^{(0)}$ be the analytic continuation of $\psi^{(i)}$, they must coincide on $q = 1, 0 < \theta < 2\pi$, i.e.

$$\begin{aligned} \psi^{(i)}(1, \theta) &= \psi^{(0)}(1, \theta) \\ \psi_q^{(i)}(1, \theta) &= \psi_q^{(0)}(1, \theta) \end{aligned} \qquad (8\text{-}21)$$

If the B_n are supposed to be given by Eq. 8-1, then the constants $\tilde{A}_n$ and $\tilde{C}_n$ are determined from Eq. 8-21 by Fourier's theorem. Multiplying

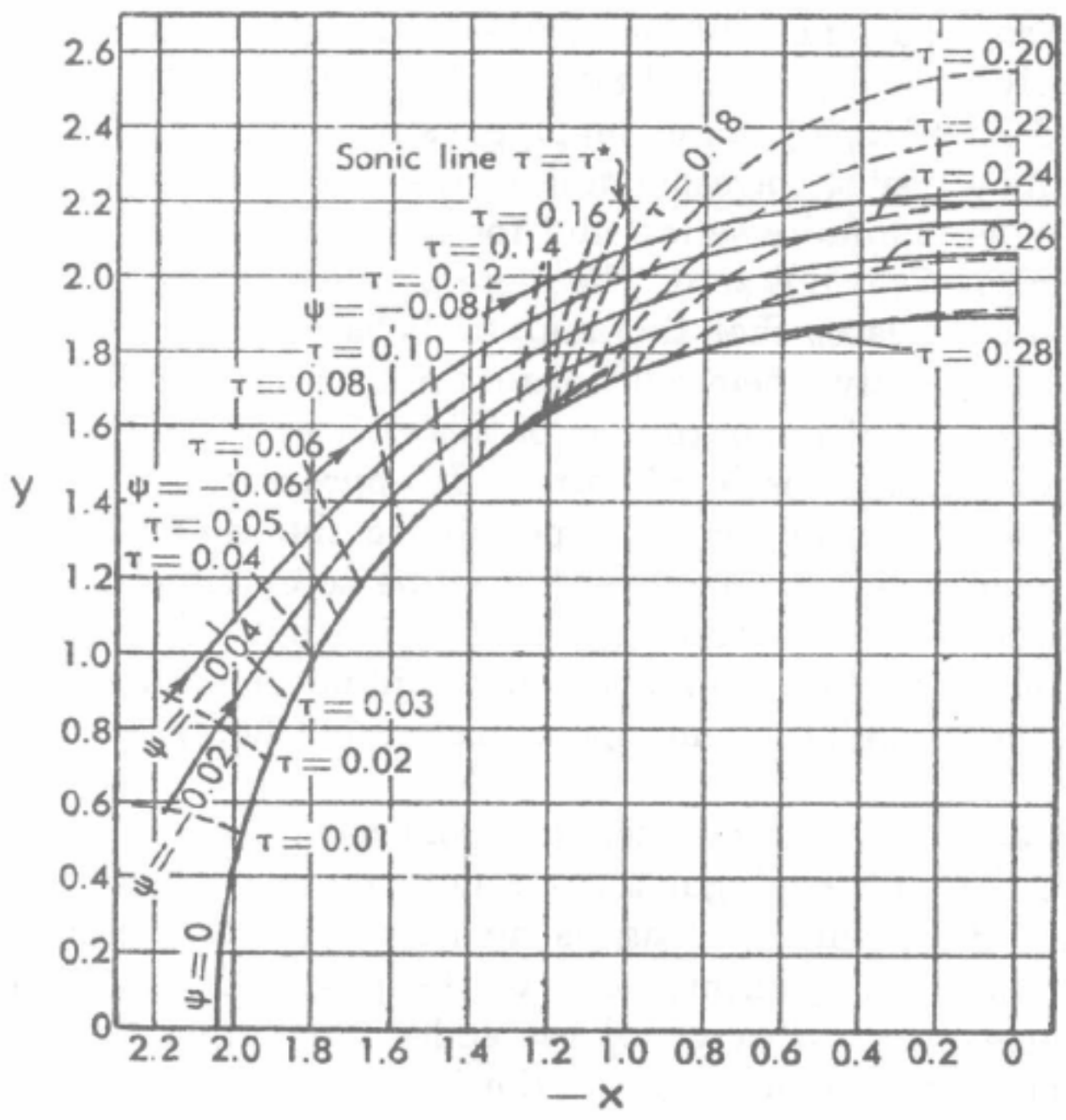

Fig. F,8b. Streamlines and constant-speed lines for flow at $M_\infty = 0.5098$ past a symmetrical cylinder, derived from incompressible flow around a circular cylinder [24]. $\gamma = 1.405$.

both sides by $\sin n\theta$ and integrating from $\theta = 0$ to $\theta = 2\pi$, we obtain

$$\begin{aligned} \tilde{A}_n \mathfrak{F}_n(\tau_1) - \tilde{C}_n \mathfrak{F}_{-n}(\tau_1) &= \frac{1}{\pi} \sum_0^\infty B_m \mathfrak{F}_{-\mu}(\tau_1) I_{n\mu} \\ n\tilde{A}_n \mathfrak{F}_n(\tau_1) \xi_n(\tau_1) - n\tilde{C}_n \mathfrak{F}_{-n}(\tau_1) \xi_{-n}(\tau_1) &= \frac{1}{\pi} \sum_0^\infty B_m \mathfrak{F}_{-\mu}(\tau_1) \xi_{-\mu}(\tau_1) I_{n\mu} \end{aligned} \qquad (8\text{-}22)$$

where $I_{n\mu} = (n + \mu)^{-1} + (n - \mu)^{-1}$ and $\mu = m + \frac{1}{2}$. Now, by means of Eq. 16-6 together with Eq. 8-1, the first sum of Eq. 8-22 is shown to be

$$A_n \mathfrak{F}_n(\tau_1) - h_n g_n (\tau_1 T_1)^n F_n(\tau_1) \tag{8-23}$$

and the second, by similar process, is

$$nA_n \mathfrak{F}_n(\tau_1)\xi_n(\tau_1) - nh_n g_n (\tau_1 T_1^2)^n \mathfrak{F}_n(\tau_1)\xi_n(\tau_1) \tag{8-24}$$

When these are substituted back in Eq. 8-22, the algebraic equations yield the solution

$$\begin{aligned} \tilde{A}_n &= A_n - h_n g_n (\tau_1 T_1^2)^n \\ \tilde{C}_n &= 0 \end{aligned} \tag{8-25}$$

It is seen that the solution represented by Eq. 8-19 and 8-20 agree respectively with Eq. 8-8 and 8-9. In their original treatment, however, Tsien and Kuo [*19,20*] chose Chaplygin's form, viz. $F_n(\tau)/F_n(\tau_1)$ instead of $\mathfrak{F}_n(\tau)$. As a result, corresponding to the second terms in Eq. 8-23 and 8-24, they have infinite series, and for any nonvanishing Mach number the coefficient C_n is not zero. The mere presence of this additional series in Eq. 8-20 indicates that the analytic behavior of ψ and ψ_1 is not the same. Consequently, their solutions do not have the character required by conditions (1) at the beginning of this article. Tsien and Kuo's results cannot, in fact, be considered correct. It appears, nevertheless, that the error is not numerically great, especially in the most interesting (transonic) regions, and that their results can be accepted as approximations. This is true of the interesting velocity distribution over a symmetric cylinder, calculated by Kuo [*20*], which exhibits smooth acceleration and deceleration through the sonic speed, just as do Cherry's results described above.

Conclusion. To summarize, the problem of constructing a solution along the line of Chaplygin for the flow about a closed body can be adequately dealt with so long as no circulation is present. However, when circulation is present, none of the proposed techniques is completely satisfactory. Cherry [*25*] has added circulation to the case mentioned above, where the body in the incompressible fluid is a circular cylinder; the results seem to be so involved as to be impractical for numerical application. More general problems involving circulation and obtained by modification of incompressible solutions have been treated by Lighthill [*18*]. Again the results are too complicated for utility.

Finally, we should call the reader's attention to Bergman's method [*26,27*] of constructing a solution for compressible flow by "integral-operator" methods. Due to the form of the solution, it does not appear suitable for practical computations (except perhaps by machine methods, as suggested by Bergman). Cherry [*28*] has shown that Bergman's solutions can be converted to Chaplygin's form; hence, the details of his technique will not be reproduced here.

F · *PLANE POTENTIAL FLOWS*

F,9. Two-dimensional Laval Nozzle. The flow through a convergent-divergent symmetric channel can be either symmetric or asymmetric. The symmetric flow starts from rest at negative infinity, accelerates smoothly to a maximum speed in the throat, and then decelerates gradually in the divergent section to rest at positive infinity. For a given channel, the flow may either be entirely subsonic or may have local supersonic regions attached to the walls at the throat. This type of flow was first studied approximately by Taylor [*29*]. It can be treated exactly by the methods dealt with in the previous articles.

Distinct from this is the asymmetric flow, which, in the same channel, is subsonic in the convergent section but supersonic in the divergent one. Physically, it occurs when the pressure ratio is sufficiently increased beyond that of a subsonic symmetric flow. First, a shock wave appears downstream of the throat and then, as the pressure ratio is increased further, the shock moves downstream leaving the flow behind it as described here. From the mathematical standpoint, it is a new type of problem, and, furthermore, it is characteristically different from the one involving flow about a closed body. First of all, we note that, when the flow is mapped onto the hodograph plane, the streamlines cross one another in the supersonic region and, therefore, the hydrodynamic functions must be many-valued. Secondly, in a hyperbolic region, singularities, if they occur, cannot be isolated points but must be curves in the region. Consequently, the problem of analytic continuation must be expected to be very tricky.

Before we discuss the actual task of constructing a solution, let us determine the nature of the singularities involved in this type of flow. This can be accomplished by investigating the solution in the neighborhood of the sonic region. We know that, although the functions $\phi(q, \theta)$ and $\psi(q, \theta)$ are many-valued, the inverse functions $q(\phi, \psi)$ and $\theta(\phi, \psi)$ are, nevertheless, single-valued. Thus, in the neighborhood of the sonic region in the center of the throat, we can assume the expansions

$$\begin{aligned} \theta &= f_1\psi + \tfrac{1}{6}f_3\psi^3 + \cdots \\ \bar{q} &= f_0 + \tfrac{1}{2}f_2\psi^2 + \cdots \end{aligned} \tag{9-1}$$

where $f_0, f_1, f_2, f_3, \ldots$ are functions of ϕ, and $\bar{q}$ denotes $q - 1$ normalized with respect to sonic speed. For this form of solution, we have to invert the system (2-11). By approximating the coefficients in the sonic region by linear functions of $\bar{q}$, we find

$$\begin{aligned} \theta_\phi &= a\bar{q}_\psi \\ \theta_\psi &= 2b\bar{q}\bar{q}_\phi \end{aligned} \tag{9-2}$$

where $a = \left(\frac{2}{\gamma+1}\right)^\beta$ and $b = \left(\frac{\gamma+1}{2}\right)^{1+\beta}$ Upon substitution of Eq. 9-1

in Eq. 9-2, there result

$$f_1 = 2bf_0f_0'$$
$$f_2 = a^{-1}f_1'$$
$$f_3 = 2b(f_0f_2' + f_0'f_2)$$
$$\cdots\cdots\cdots\cdots$$

or

$$f_1 = 2bf_0f_0'$$
$$f_2 = 2ba^{-1}(f_0f_0'' + f_0'^2) \tag{9-3}$$
$$f_3 = 4b^2a^{-1}(f_0'^3 + 4f_0f_0'f_0'' + f_0^2f_0''')$$
$$\cdots\cdots\cdots\cdots\cdots\cdots\cdots\cdots$$

Thus, the problem is uniquely determined if the axial velocity distribution $f_0(\phi)$ is specified. In the neighborhood of the origin, let us assume that f_0' is constant and equal to $k > 0$; θ can then be expressed as

$$\theta = 2bk\psi[\bar{q} - \tfrac{2}{3}k^2\psi^2 + \cdots] \tag{9-4}$$

Consider the region near the origin, wherein the approximation represented by the first two terms of Eq. 9-4 is valid. In the subsonic region $\bar{q} < 0$, according to this approximation, constant θ corresponds to only one real value of ψ. However, when $\bar{q} > 0$, i.e. in the supersonic region, constant θ corresponds to three real values of ψ. For $\theta = 0$, we have, for example, $\psi = 0$ and $\psi = \pm k^{-1}(3\bar{q}/2)^{\frac{1}{2}}$. This leads us to conclude that, in the supersonic region, $\psi(q, \theta)$ will be given by a Riemann surface of three sheets, joined at the branch lines

$$\theta_\psi = 0$$

Therefore, the branch lines, or envelopes of streamlines in the hodograph plane, are found to be

$$\theta = \pm \frac{2^{\frac{1}{2}}}{3}\left(\frac{\gamma+1}{2}\right)^{\frac{1}{2}} q^{\frac{3}{2}} \tag{9-5}$$

These results were first discovered by Lighthill [*65*].

It is interesting to note that this singular curve in the hodograph plane is independent of the velocity distribution $f_0(\phi)$ and, therefore, independent of the wall shape. As a result, the branch lines are fixed universal curves in the hodograph plane; they exist under all boundary conditions. It can, furthermore, be shown that each will belong to one family of characteristics of Eq. 3-1 (cf. Art. 12). Since the three surfaces overlap and are joined across two branch lines in two different planes, there must be four characteristics at the origin O; Fig. F,9a is a sketch showing the three surfaces and the branch lines.

F · *PLANE POTENTIAL FLOWS*

Cherry's method of solution. From the previous discussions, we notice that in the case of asymmetric channel flows Chaplygin's analogy between incompressible and compressible solutions breaks down. We have shown, however, that the singular behavior of the solution for this type of flow is independent of the conditions at the boundary. Therefore, any possible solution must possess the following properties:

1. It is single-valued in the subsonic region and triple-valued in the supersonic region.
2. It has two branch lines Ω^+ and Ω^-.
3. It is finite and has finite partial derivatives.

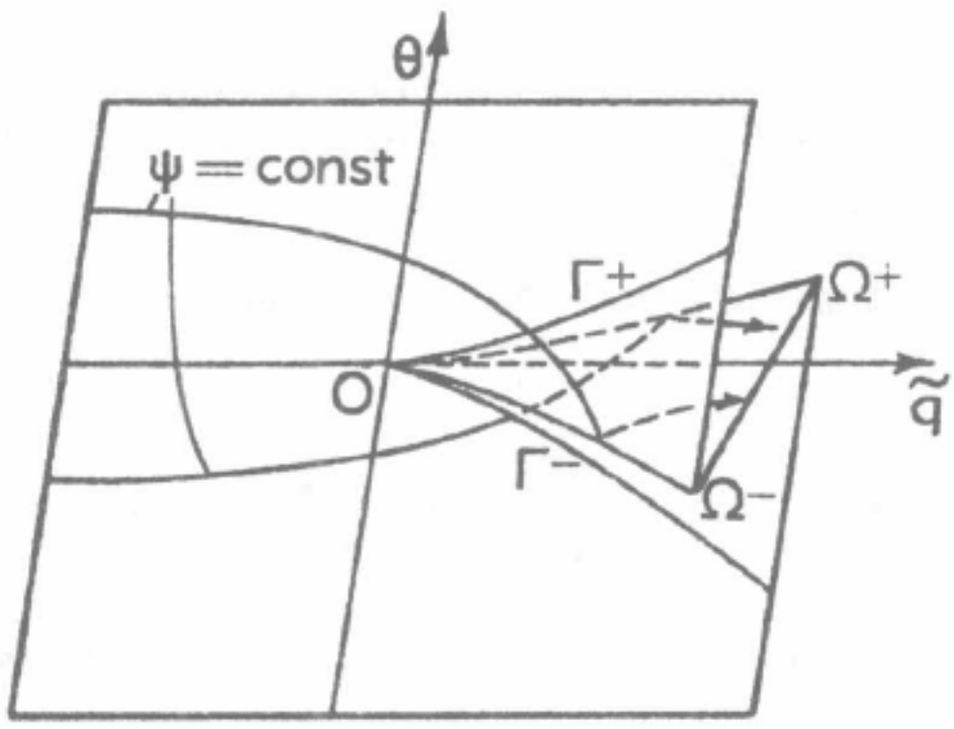

Fig. F,9a. Riemann surface of ψ in q, θ plane.

To construct such a solution for the Legendre potential, it is observed by Cherry [*30*] that the hypergeometric and Bessel functions have similar properties, as shown in Art. 16. If the solution is

$$\sum_0^\infty C_n q^n \tilde{F}_n(\tau) e^{in\theta}$$

it can be transformed into a new series involving Bessel functions by means of Eq. 16-9 and 16-11. By a suitable choice of the C_n, part of the resulting series will be found to be summable.

We begin by considering a solution

$$\sum_0^\infty \frac{(n/e)^n \chi_n(\tau) e^{-in\theta}}{r^n \Gamma(n+1)} + \sum_1^\infty \frac{\tilde{h}_n r^n \Gamma(n) \chi_n(\tau) e^{in\theta}}{(n/e)^n} \tag{9-6}$$

where $\chi_n(\tau)$ denotes $\tau^{n/2}\tilde{F}_n(\tau)$ and r, $\tilde{h}_n$ are defined respectively in Eq. 16-4 and 16-10. These series, according to Eq. 16-9 and Eq. 16-11, can be transformed into

$$Q(\tau)\left[1+2\sum_{1}^{\infty}J_n(nt)\cos n\theta\right]$$

$$-\sum_{\mu}f_\mu\left[\frac{1}{\mu}+\sum_{1}^{\infty}J_n(nt)\left(\frac{e^{-in\theta}}{\mu-n}+\frac{e^{in\theta}}{\mu+n}\right)\right] \quad (9\text{-}7)$$

where the summation $\sum_\mu$ is taken over the roots of $J_\mu(\mu t)=0$ and $f_\mu(\tau)$ is defined in Eq. 16-11, provided rearrangement of the double series is allowed. The rearrangement can be shown to be permissible for $\alpha^2\tau<1$ or $t<1$. (The variable t is defined in terms of τ in Art. 16; see Eq. 16-4a and 16-11.)

The solution then is a superposition of Kapteyn series and, on account of the Bessel functions, considerable simplification results. Call

$$K(t,\theta)=1+2\sum_{1}^{\infty}J_n(nt)\cos n\theta \quad (9\text{-}8)$$

$$L_\mu(t,\theta)=\frac{1}{\mu}+\sum_{1}^{\infty}J_n(nt)\left(\frac{e^{-in\theta}}{\mu-n}+\frac{e^{in\theta}}{\mu+n}\right) \quad (9\text{-}9)$$

We can then write Eq. 9-8 and 9-9, when $0<t<1$, as

$$QK+\sum_{\mu}f_\mu L_\mu \quad (9\text{-}10)$$

The series $K(t,\theta)$ is a well-known Kapteyn series and has the sum

$$K(t,\theta)=1+2\sum_{1}^{\infty}J_n(nt)\cos n\theta=\frac{1}{1-t\cos\xi} \quad (9\text{-}11)$$

where ξ is the root of

$$\xi-t\sin\xi=\theta \quad (9\text{-}12)$$

This is the celebrated Kepler equation. These relations (9-11) and (9-12) make it remarkably simple to verify that our solution has the correct behavior. In the first place, the Kapteyn series (9-11) provides a means of analytic continuation beyond $t=1$, i.e. into the supersonic region, and the Kepler equation serves to determine the character of the solution. For $t\leqq 1$, the solution $\xi(t,\theta)$ is single-valued, but for $t>1$ is triple-valued as in the neighborhood of $\xi=0$ and $t=1$,

$$\theta=\xi-t(\xi-\tfrac{1}{6}\xi^3)+\cdots$$

which is the same as Eq. 9-4 if ξ is replaced by ψ. Furthermore, the branch lines are

$$\theta_\xi=1-t\cos\xi=0$$

i.e. $t = \sec \xi$. With this value of ξ, we have from Eq. 9-12 the equation of the branch lines

$$\theta = \pm(\tan^{-1}\sqrt{t^2-1} - \sqrt{t^2-1}) \tag{9-13}$$

But according to Eq. 16-10, the right-hand side of Eq. 9-13 is just $\pm\omega$, where ω is the quantity defined in Eq. 16-4a; i.e., the curves $\theta = \pm\omega$ are characteristic curves (epicycloids) passing through the sonic point on the axis in the hodograph plane. This verifies that K has the required singular behavior, except that it becomes infinite on the branch lines, in violation of (3) above. Consequently, Eq. 9-7 is a possible solution for the present problem. To establish its validity, we need, however, to

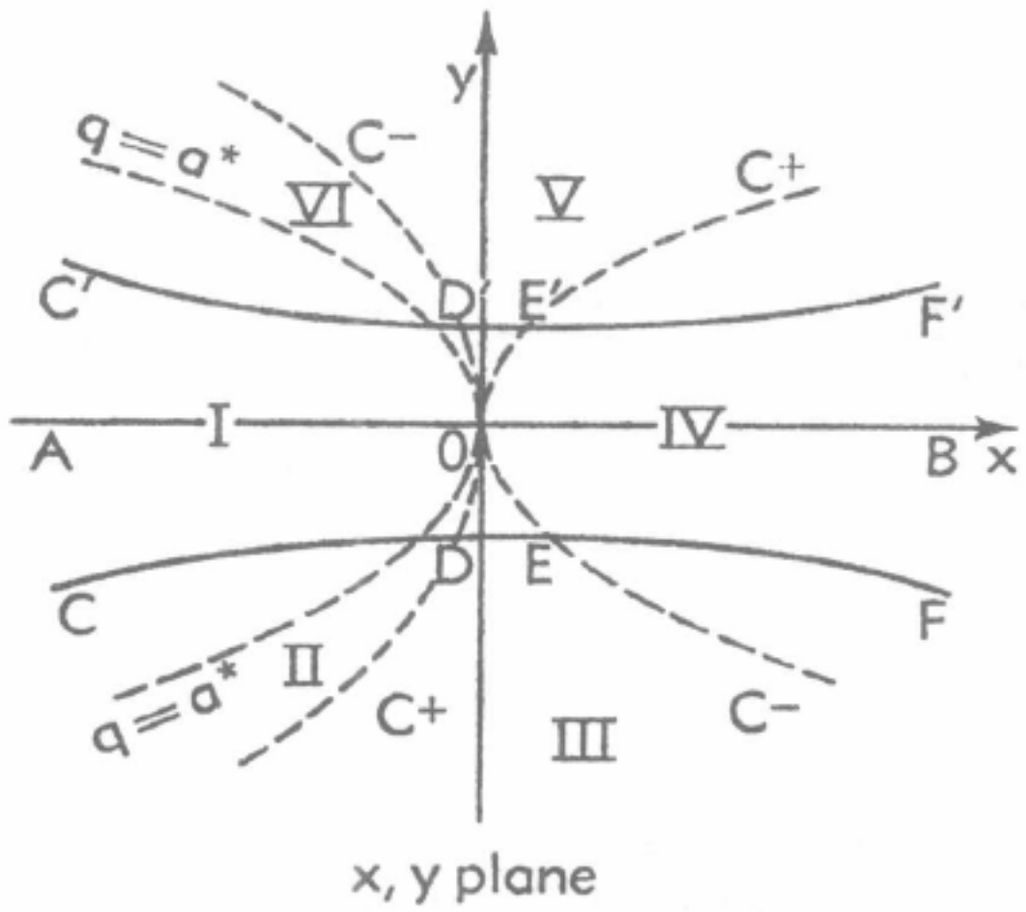

Fig. F,9b. Flow in a nozzle in x, y plane.

continue it into the supersonic region, verify the singular behavior of L_μ, and remove the infinities on the branch lines.

Analytic continuation of K and L_μ. Corresponding regions in the physical and hodograph planes are numbered as shown in Fig. F,9b and F,9c. The functions valid in the respective regions will be numbered accordingly, such as χ_{I}, χ_{II}, etc. In order ultimately to obtain the complete, continued solution in the form of a definite integral, we return to the series form for K in Eq. 9-11. Thus, both K and L_μ must be continued. To illustrate the principle employed, only K will be briefly considered here.

Since the Kapteyn series is convergent in $0 < t < 1$ and $-\pi \leqq \theta \leqq \pi$, then in region I we have, by definition,

$$K = 1 + 2\sum_{1}^{\infty} J_n(nt)\cos n\theta = K_{\text{I}} \tag{9-14}$$

To continue K we consider in the half-plane R.P.$\{\nu\} > 0$ the integral

F,9 · *TWO-DIMENSIONAL LAVAL NOZZLE*

$$\oint \frac{e^{i\nu(\pi-\theta)}}{\sin \nu\pi} J_\nu(\nu t)d\nu$$

along a closed path. By choosing the path to be an appropriate semi-circle in the half-plane R.P.$\{\nu\} > 0$, it can be shown by Cauchy's theorem that

$$\sum_1^\infty J_n(nt)e^{-in\theta} = \frac{1}{2i}\int_{\delta-\infty i}^{\delta+\infty i} \frac{e^{i\nu(\pi-\theta)}}{\sin \nu\pi} J_\nu(\nu t)d\nu \qquad (9\text{-}15)$$

where the series represents the contributions from the simple poles $\nu = 1, 2, \ldots$ and the path of integration crosses the real axis between

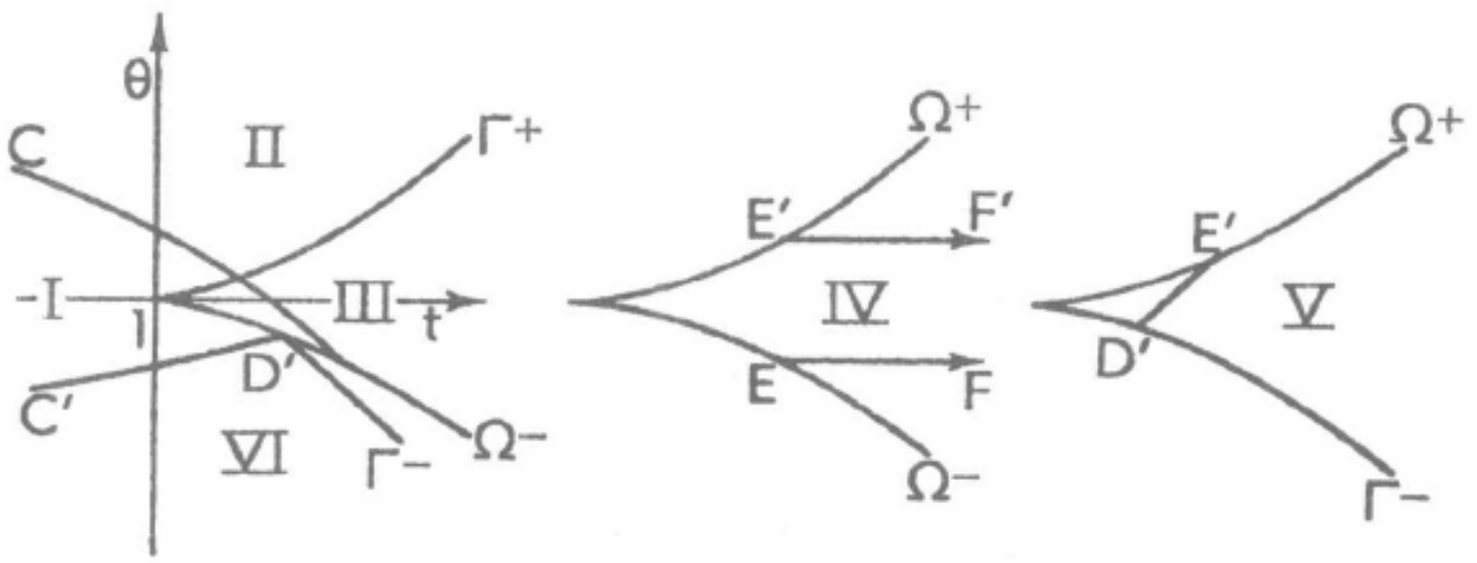

t, θ plane

Fig. F,9c. Riemann surface in t, θ plane.

0 and 1, i.e. $0 < \delta < 1$. But, by the properties of $J_\nu(\nu t)$ near $t = 1$, we can verify that this integral actually converges uniformly in a small region G, surrounding $t = 1$, of a complex t plane, provided θ is also suitably restricted in a complex θ plane. Specifically, it converges uniformly for $|t - 1| < r$ and $\eta(r) <$ R.P.$\{\theta\} < 2\pi - \eta(r)$ where $\eta \to 0$ as $r \to 0$.

Thus, in Eq. 9-15 we have a form that constitutes a continuation of the series from I into a small region G around $t = 1$. The next step is to identify this, along a part of the real axis in G, with a form that permits continuation throughout II. This is done, for $t \geqq 1$, by distorting the path of integration of Eq. 9-15 to lie along the rays arg $\nu = \pm\pi$, avoiding the points $\nu = 0, -1, -2, \ldots$ by indentations. We obtain

$$\sum_1^\infty J_n(nt)e^{-in\theta} = \int_0^\infty J_{-\nu}(\nu t)e^{-i\nu(\pi-\theta)}d\nu - 1 - \sum_1^\infty J_n(nt)e^{in\theta}$$

or

$$1 + 2\sum_1^\infty J_n(nt)\cos n\theta = \int_0^\infty J_{-\nu}(\nu t)e^{-i\nu(\pi-\theta)}d\nu \qquad (9\text{-}16)$$

The integral in Eq. 9-16 converges in $t \geqq 1$ and $\omega < \theta < 2\pi - \omega$, where $\theta = \pm\omega$ again defines two characteristics. In consequence, we have

succeeded in continuing K through G into region II. The continued form is given by Eq. 9-16, i.e.

$$K_{II} = \int_0^\infty J_{-\nu}(\nu t)e^{-i\nu(\pi-\theta)}d\nu \tag{9-17}$$

For the continuation into III, it is most convenient to consider fixed $t > 1$ and K_{II} an analytic function of θ. From the relations between the Bessel and Hankel functions, it can be shown that the integral is regular in the half-plane I.P.$\{\theta\} > 0$, is singular at $\theta = -\omega$ and $\theta = 2\pi + \omega$, and can be continued between these points into the half plane I.P.$\{\theta\} < 0$. In particular, Eq. 9-17 is valid in region III, where $t \geqq 1$, $-\omega < \theta < \omega$.

Now, the singularity of the integral (9-17) at $\theta = -\omega$ in the θ plane can be shown to be a simple branch point. In order to obtain a function K_{IV} different from K_{III}, as required by condition (1) above, it is necessary to choose the other branch in passing over from $\theta > -\omega$ to $\theta < -\omega$, viz. [*30*, p. 560]

$$K_{IV} = -\int_0^\infty J_\nu(\nu t)e^{i\nu\theta}d\nu \tag{9-18}$$

This branch diverges at $\theta = \pm\omega$ and is symmetric in θ; thus $\theta = \omega$ is again a simple branch point, and by a process similar to the above it is found that

$$K_V = \int_0^\infty J_{-\nu}(\nu t)e^{-i\nu(\pi+\theta)}d\nu \tag{9-19}$$

By comparison of Eq. 9-17 and 9-19, the symmetry of the solution is verified.

In the case of L_μ, the key formula analogous to Eq. 9-15 is

$$\sum_1^\infty \frac{J_n(nt)e^{-in\theta}}{n-\mu} + \frac{\pi J_\mu(\mu t)e^{i\mu(\pi-\theta)}}{\sin \mu\pi} = \int_{\infty e^{\pi i}}^{(0-)} \frac{J_\nu(\nu t)e^{i\nu(\pi-\theta)}}{(\nu-\mu)\sin \nu\pi}\,d\nu \tag{9-20}$$

Here we assume, for the moment, that μ is complex and I.P.$\{\mu\} > 0$. After the continuation, however, it will be put equal to a zero of $J_\mu(\mu t)$, as in our definition of L_μ. By carrying out the similar steps, we can deduce that L_μ has the same character as K and has, in the various regions, the following continuations:

$$\begin{aligned}
(L_\mu)_I &= \sum_0^\infty \frac{J_n(nt)e^{in\theta}}{n+\mu} + \sum_1^\infty \frac{J_n(nt)e^{-in\theta}}{-n+\mu} = (L_\mu)_{II} \\
(L_\mu)_{II} &= \int_0^\infty \frac{J_{-\nu}(\nu t)e^{-i\nu(\pi-\theta)}}{\nu+\mu}\,d\nu = (L_\mu)_{III} \\
(L_\mu)_{IV} &= \int_0^\infty \frac{J_\nu(\nu t)e^{-i\nu\theta}}{\nu-\mu}\,d\nu \\
(L_\mu)_V &= \int_0^\infty \frac{J_{-\nu}(\nu t)e^{i\nu(\pi+\theta)}}{\nu+\mu}\,d\nu
\end{aligned} \tag{9-21}$$

F,9 *TWO-DIMENSIONAL LAVAL NOZZLE*

Analytic continuation of χ. We have shown that both K and L_μ satisfy the conditions (1) and (2) and, therefore, Eq. 9-10 can be accepted as a possible solution. Let this solution be denoted by χ. Then in region I, i.e. $0 < t < 1$ and θ real, we have by definition

$$\chi_{\mathrm{I}} = QK - \sum_{\mu} f_\mu (L_\mu)_{\mathrm{I}}$$

Since in region I rearrangement of the double series is allowed, by applying Eq. 16-9 and 16-11, the series can be reconverted into Eq. 9-6, namely

$$\chi_{\mathrm{I}} = \sum_{0}^{\infty} \frac{(n/e)^n \chi_n(\tau) e^{-in\theta}}{r^n \Gamma(n+1)} + \sum_{1}^{\infty} \frac{f_n r^n \Gamma(n) \chi_n(\tau) e^{in\theta}}{(n/e)^n} \tag{9-22}$$

The continuation of χ_{I} to region II, according to Eq. 9-16 and 9-21, can be expressed in the same form as Eq. 9-22, namely

$$\chi_{\mathrm{II}} = \chi_{\mathrm{I}} \tag{9-23}$$

provided $t \geqq 1$ and $\omega < \theta < 2\pi - \omega$.

In region III, taking the proper forms of K and L_μ, we have, on the other hand

$$\chi_{\mathrm{III}} = Q \int_0^\infty J_{-\nu}(\nu t) e^{-i\nu(\pi-\theta)} d\nu - \sum_{\mu} f_\mu \int_0^\infty \frac{J_{-\nu}(\nu t) e^{-i\nu(\pi-\theta)}}{\nu + \mu} d\nu$$

By an interchange of the summation and integral signs, it follows that

$$\chi_{\mathrm{III}} = \int_0^\infty J_{-\nu}(\nu t) e^{-i\nu(\pi-\theta)} \left(Q - \sum_{\mu} \frac{f_\mu}{\mu + \nu} \right) d\nu$$

From Eq. 16-9 we have finally

$$\chi_{\mathrm{III}} = \int_0^\infty \frac{\Gamma(\nu) r^\nu \sin \nu\pi \chi_{-\nu}(\tau) e^{-i\nu(\pi-\theta)}}{\pi (\nu/e)^\nu} d\nu \tag{9-24}$$

Similarly, in regions IV and V the continuations are respectively

$$\chi_{\mathrm{IV}} = -\int_0^\infty \frac{(\nu/e)^\nu \chi_\nu(\tau) e^{-i\nu\theta}}{r^\nu \Gamma(\nu+1)} d\nu \tag{9-25}$$

and

$$\chi_{\mathrm{V}} = \int_0^\infty \frac{\Gamma(\nu) r^\nu \sin \nu\pi \chi_{-\nu}(\tau) e^{i\nu(\pi+\theta)}}{\pi (\nu/e)^\nu} d\nu \tag{9-26}$$

Having verified that the solution made up by Eq. 9-22 to 9-26 satisfies the conditions (1) and (2), we notice, however, that according to Eq. 9-11 it is infinite on the branch lines Ω^- and Ω^+ and hence violates condition

(3). In order to remove this infinity, we can integrate the solution twice with respect to θ, because partial integration of a solution with respect to θ also yields a solution. The arbitrary functions introduced by integration must vanish if the branch character is to be preserved. Once this is done, the condition (3) will clearly be satisfied. As this final step involves no new principle, its details are omitted here.

For details of Cherry's analysis, the reader must refer to his original paper [*30*]. To date, no numerical examples of the flows obtained by this theory are available.

F,10. Approximate Solutions for Transonic Flows: Channel Flows. In the case of flow past boundaries with small curvature, the flow field may be expected to be nearly sonic everywhere, except possibly near stagnation points, if it is near sonic at infinity. For this type of flow, the problem can be considerably simplified.

We begin by making approximations to the fundamental system of Eq. 2-11. In this article it is most convenient to redefine the stream function, replacing ρ^0 by ρ^*, i.e. $\rho u = \rho^* \psi_y$ and $\rho v = -\rho^* \psi_x$; then the fundamental relations are

$$\begin{aligned} \phi_q &= -\frac{\rho^*}{\rho q}(1 - M^2)\psi_\theta \\ \frac{1}{q}\phi_\theta &= \frac{\rho^*}{\rho}\psi_q \end{aligned} \tag{10-1}$$

where, as usual, the asterisk denotes sonic conditions. Let us define a new variable

$$\bar{q} = \int_{a^*}^{q} \frac{\rho}{\rho^*}\frac{dq}{q}$$

Now we are assuming $q = a^* + q'$, where q' is much smaller than a^*; under this assumption, we obtain the approximate relations

$$1 - M^2 \cong (\gamma + 1)\frac{q'}{a^*}$$

$$\bar{q} \cong \frac{q'}{a^*}$$

whereupon Eq. 10-1 become, approximately,

$$\begin{aligned} \phi_{\bar{q}} &= (\gamma + 1)\bar{q}\psi_\theta \\ \phi_\theta &= \psi_{\bar{q}} \end{aligned} \tag{10-2}$$

The approximate differential equation for the stream function then becomes

$$\psi_{\bar{q}\bar{q}} - (\gamma + 1)\bar{q}\psi_{\theta\theta} = 0 \tag{10-3}$$

It is seen that this equation is elliptic if $\bar{q} < 0$, i.e. in the subsonic region, and hyperbolic if $\bar{q} > 0$, i.e. in the supersonic region. This is known as Tricomi's equation [*31*]; it is simple, and yet it possesses all the important features of the exact equation in the transonic region. It is, in fact, the equation obtained by applying the hodograph transformation to the Kármán-Guderley transonic equation discussed in A,7, D,32, and D,33.

A number of interesting solutions has been obtained from the Tricomi equation, both for smooth flow past special boundaries and for supersonic flows involving shock waves. In the former category are the investigation of von Kármán and Fabri of flow past a corrugated wall [*32*] and the studies by Tomotika and Tamada [*33*] regarding transonic flow about certain cylinders. In the second category, involving weak shock waves, are the calculations of Guderley and Yoshihara [*34*,*35*], Cole [*36*], and Vincenti [*37*]. Flows of this type are discussed in some detail in H, 6–H,13.

In the present article, we shall present an application of this approximation to flow through convergent-divergent channels. This is also based on the work of Tomotika and Tamada [*38*].

Tomotika-Tamada solution for channel flows. We begin by interchanging the roles of the dependent and independent variables; we transform Eq. 10-2 into

$$\begin{aligned} \theta_\phi &= \bar{q}_\psi \\ \theta_\psi &= (\gamma + 1)\bar{q}\bar{q}_\phi \end{aligned} \tag{10-4}$$

(cf. Eq. 9-2). Elimination of θ yields

$$\frac{\partial^2 \bar{q}}{\partial \psi^2} - \frac{\gamma + 1}{2} \frac{\partial^2 (\bar{q}^2)}{\partial \phi^2} = 0 \tag{10-5}$$

This equation is nonlinear and hence cannot generally be solved in any simple manner. However, as Tomotika and Tamada [*38*] have shown, a special group of solutions can easily be discovered. In the following, we shall outline their derivation of the one that gives convergent-divergent channel flow. Let the form of solution be

$$\frac{\gamma + 1}{2} \bar{q} = Z(\zeta) + 2\psi^2 \tag{10-6}$$

where

$$\zeta = \phi + \psi^2$$

With $\bar{q}$ written in the form of Eq. 10-6 together with Eq. 10-8, the second of Eq. 10-4 gives, upon integration,

$$(\gamma + 1)\theta = 4\psi[Z(\zeta) + 2\phi + \tfrac{2}{3}\psi^2] \tag{10-7}$$

by noticing that

$$\frac{\partial}{\partial \psi}(\psi Z) = Z + 2\psi^2 \frac{dZ}{d\zeta}$$

where the arbitrary function of ϕ is chosen to be zero. In view of the striking similarity between this form and Eq. 9-4, it is expected that the flow represented by Eq. 10-7 in the x, y plane must be of the Laval nozzle type. The function $Z(\zeta)$ serves to describe the axial velocity distribution.

If $\bar{q}$ in this form is substituted in Eq. 10-5, there results the following ordinary differential equation for Z:

$$\frac{d}{d\zeta}\left(Z\frac{dZ}{d\zeta}\right) - \frac{dZ}{d\zeta} - 2 = 0$$

or

$$Z\frac{dZ}{d\zeta} - Z = 2\zeta \tag{10-8}$$

where the constant of integration has been absorbed in ζ, as both ϕ and ψ are arbitrary in this regard. To integrate Eq. 10-8 let us introduce a new variable η defined by

$$\frac{d\zeta}{d\eta} = Z \tag{10-9}$$

Then

$$\frac{d^2\zeta}{d\eta^2} = \frac{dZ}{d\zeta}\frac{d\zeta}{d\eta} = Z\frac{dZ}{d\zeta}$$

As a result, instead of Eq. 10-8 we have the linear equation

$$\frac{d^2\zeta}{d\eta^2} - \frac{d\zeta}{d\eta} - 2\zeta = 0$$

of which the solution is

$$\zeta = c_1 e^{2\eta} + c_2 e^{-\eta} \tag{10-10}$$

Thus, according to Eq. 10-9, the function Z in terms of the variable η is

$$Z = 2c_1 e^{2\eta} - c_2 e^{-\eta} \tag{10-11}$$

Elimination of η between Eq. 10-10 and 10-11 leads to an integral

$$(Z + \zeta)(Z - 2\zeta)^2 = 2c^3 \tag{10-12}$$

where c is a constant.

To understand the nature of the flow, we shall discuss only the behavior of $Z(\zeta)$, leaving out the numerical details, which can be found in the work of Tomotika and Tamada. First, we note that for $c = 0$, $Z(\zeta)$ reduces to two straight lines through the origin, viz. $Z = -\zeta$ and $Z = 2\zeta$. Secondly, if c^3 is considered as a function of the two variables Z and ζ, it evidently changes sign when Z and ζ both change sign, and hence is antisymmetric in this sense. The integral curves $Z(\zeta)$ will lie in two distinct groups according as $c < 0$ and $c > 0$. These curves are

shown in Fig. F,10a for the values $c = 0, \pm 0.05$ and ± 0.10. There are four branches A, B, A', and B' with $Z = -\zeta$ and $Z = 2\zeta$ as asymptotes.

By Eq. 10-6, when $Z(\zeta)$ is positive, q is positive and the flow is supersonic. Branch A' (see Fig. F,10a) therefore corresponds to purely supersonic flow and is of very little practical interest. B and B', on

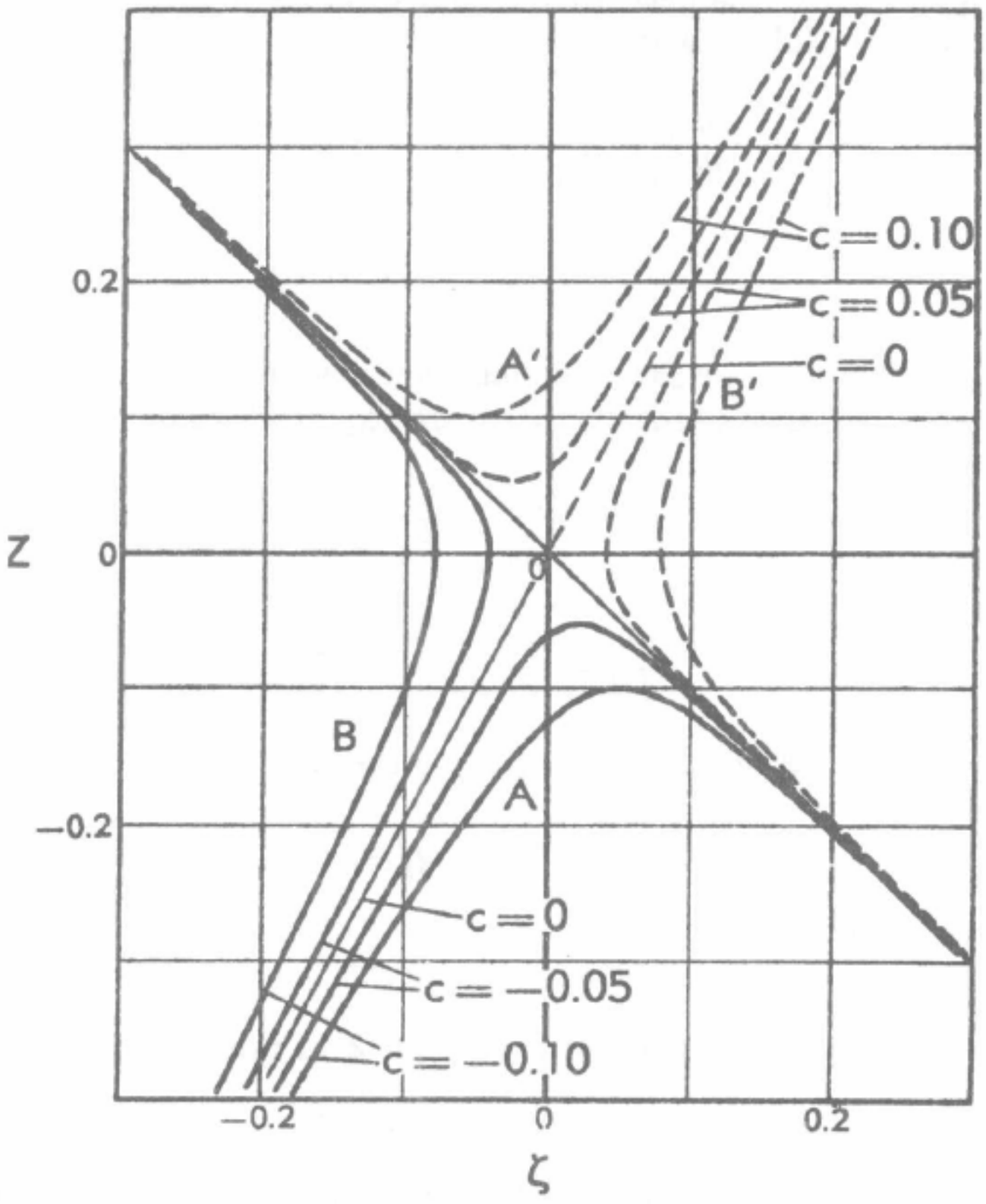

Fig. F,10a. Families of integral curves $Z(\zeta)$ [38].

the other hand, have singularities $dZ/d\zeta = \infty$ on $Z = 0$. However, $q_\psi = [4/(\gamma + 1)][Z'(\zeta) + 2]\psi$ and $q_\phi = [2/(\gamma + 1)]\, Z'(\zeta)$. Infinite q_ψ and q_ϕ imply that the Jacobian $J \equiv \partial(x, y)/\partial(q, \theta)$ is zero; for

$$J^{-1} = \frac{\partial(q, \theta)}{\partial(\phi, \psi)} \frac{\partial(\phi, \psi)}{\partial(x, y)} \cong (a^*)^2 [(\gamma + 1) q q_\phi^2 - q_\psi^2]$$

in the present approximation. A solution with this type of singularity is physically impossible (cf. Art. 12) and hence must also be rejected.

On branch A, we have $Z(\zeta)$ everywhere negative and the axial

velocity therefore subsonic. If the stream function is increased in either the positive or negative direction, $\bar{q}$ increases from its axial value and attains the largest value on the wall, i.e. at $\psi = \pm\psi_0$, say. Where $-Z(\zeta)$ is small, the value attained by $\bar{q}$ at the wall may be positive; i.e., the flow may be supersonic near the wall. We note that this occurs only near $\zeta = 0$, which means that supersonic flow can appear only in the neighborhood of the throat. This type of flow is shown in Fig. F,10b, for the particular case $c = -0.10$. This will be designated Taylor's type of flow [*29*]; it is the sort of flow called "symmetric" in Art. 9.

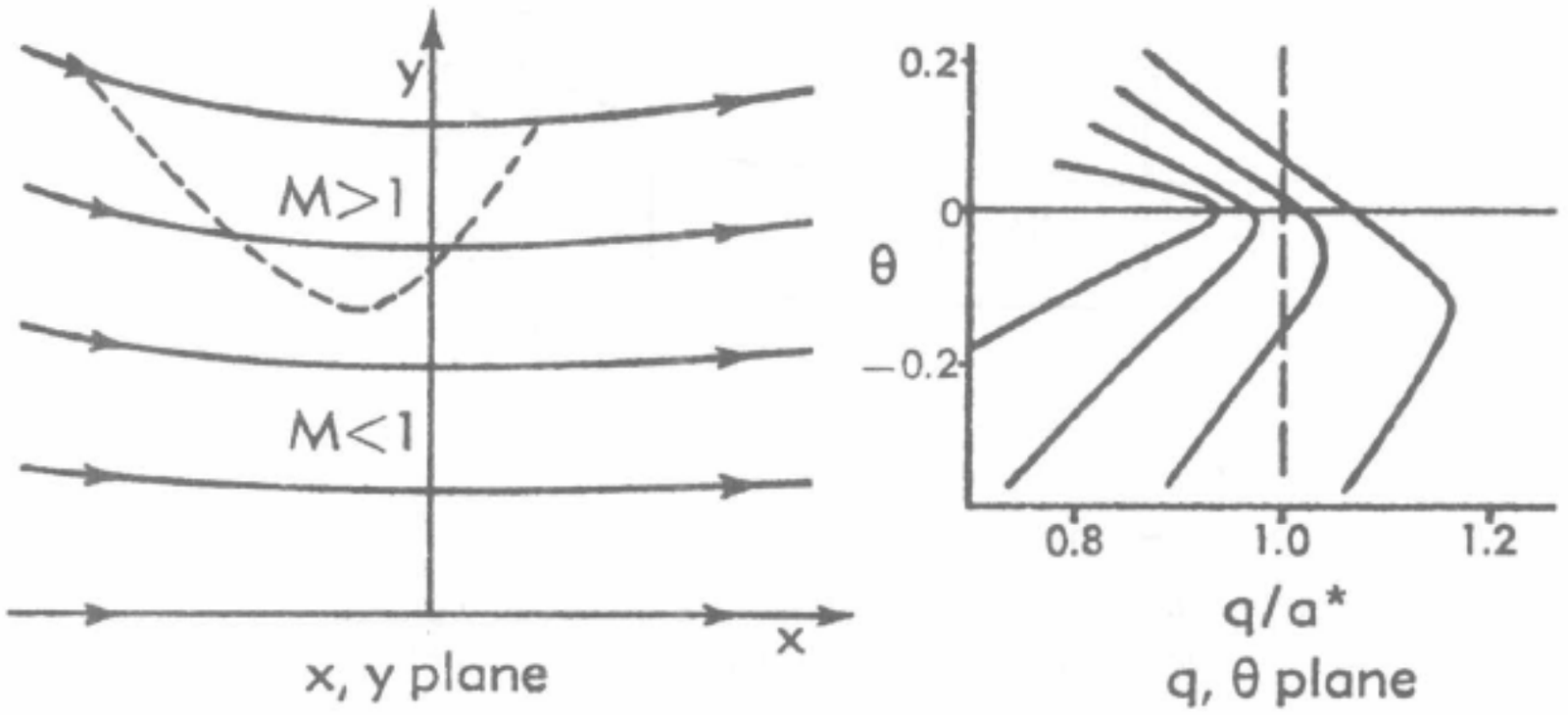

Fig. F,10b. Flow patterns in x, y and q, θ planes for $c = 0.10$, Taylor's type [*38*].

The limiting case of this family of solutions is the case $c = 0$, i.e.

$$Z = -\zeta, \qquad \zeta > 0$$

$$= 2\zeta, \qquad \zeta < 0$$

The supersonic region then extends all the way to the axis at one point, viz. $\phi = 0, \psi = 0$. This solution has a discontinuity in $Z'(\zeta)$ at $\zeta = Z = 0$, i.e. along the curve $\phi + \psi^2 = 0$ in the flow plane. Since this singular curve lies in the supersonic region ($\bar{q} > 0$) and is a characteristic of Eq. 10-5, it must correspond to a Mach wave in the physical plane (cf. Art. 12).

On this singular line the velocity is continuous, but the curvature of the streamlines is discontinuous. This curvature is $qd\theta/d\phi = 4q\psi[Z'(\zeta) + 2]$; thus a discontinuity in $Z'(\zeta)$ causes a jump in its value in crossing the singular line from $\zeta > 0$ to $\zeta < 0$. If a slight discontinuity of wall curvature is allowed, this limiting solution may still represent a feasible flow (Fig. F,10c).

On the other hand, if the whole branch $Z = -\zeta$ for both positive and negative ζ is considered, the axial velocity is purely subsonic on one side, $\zeta > 0$, and supersonic on the other, $\zeta < 0$. This evidently corresponds to Meyer's type of flow, i.e. Laval nozzle flow (Fig. F,10d). In this case

again there is a singularity on a characteristic. But the discontinuity in $(dy/dx)_{\hat{q}}$ and $d\theta/d\phi$ does not occur, and the flow is a physically possible flow, of a type for which an exact solution has already been given in the preceding article.

These solutions, although approximate, are interesting in several aspects. In the first place, from the practical point of view the calculation

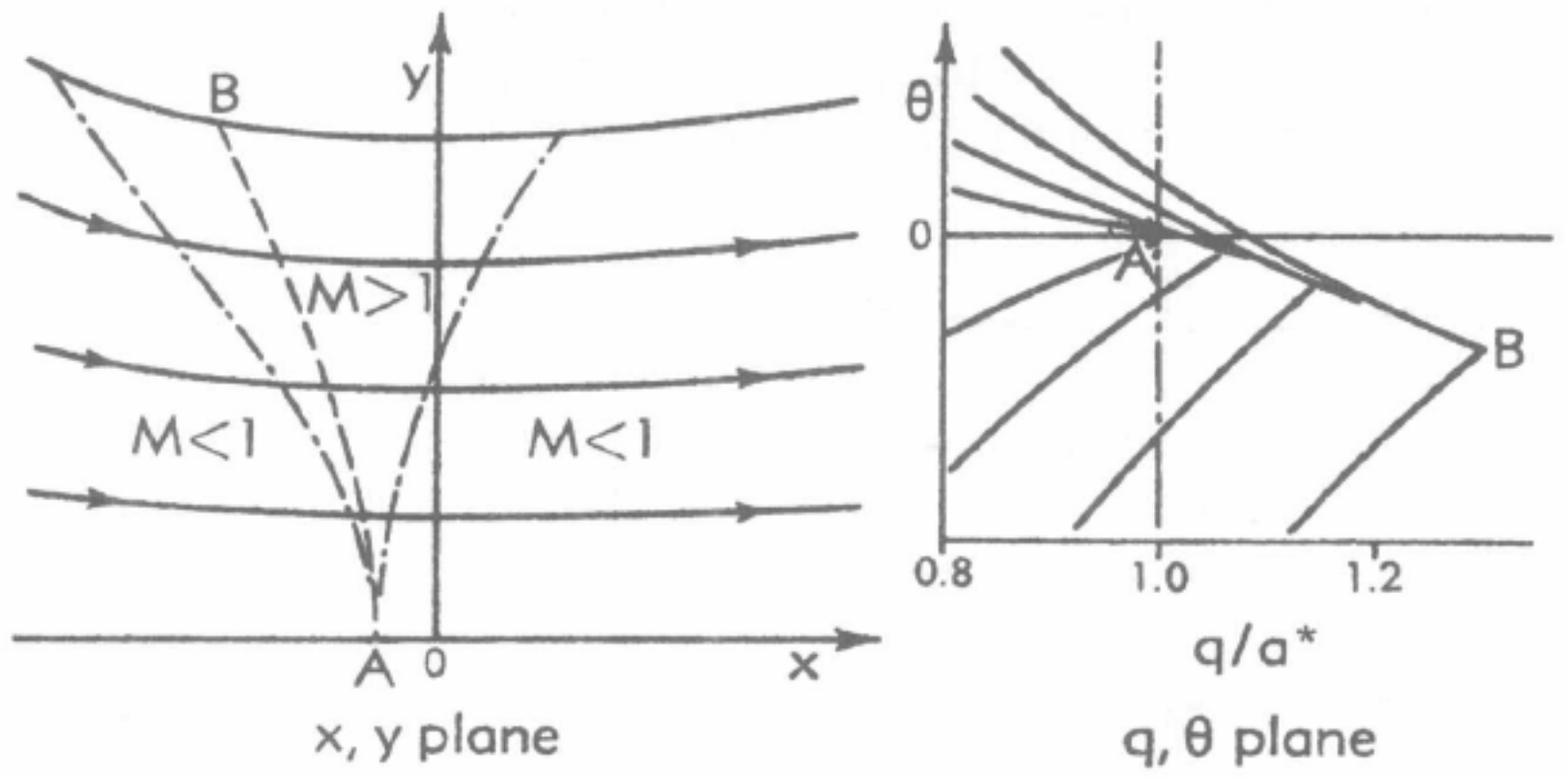

Fig. F,10c. Flow patterns in x, y and q, θ planes for $c = 0$, the last of the family $c < 0$ [*38*].

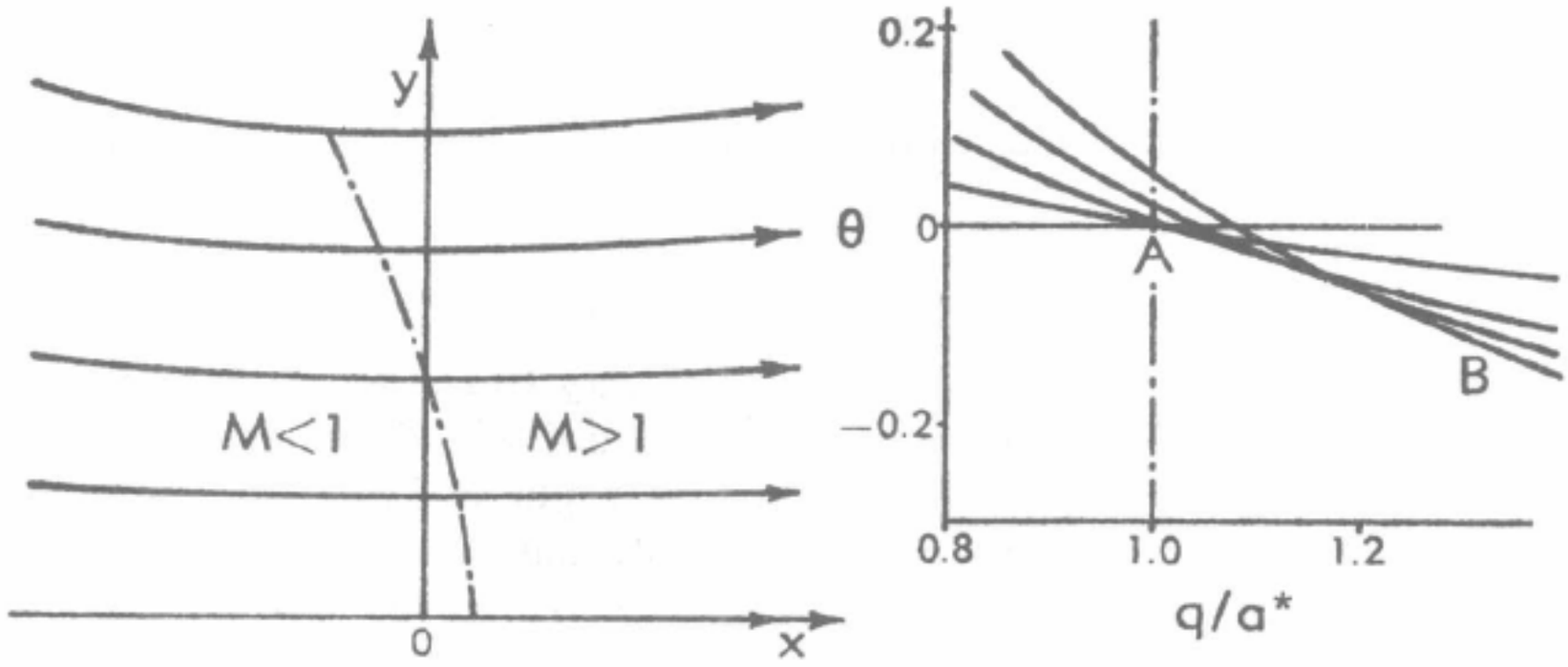

Fig. F,10d. Flow patterns in x, y and q, θ planes for $c = 0$, Meyer's type [*38*].

is simple and applies with sufficient accuracy in the important throat region. Secondly, they unify this type of channel flow in one family of solutions and clearly show why power series fail to deal with the limiting case of Taylor's type of flow (Fig. F,10c), namely, because of the appearance of discontinuities in the derivatives of velocities. The simplification afforded by this method has its origin in the fact that the solution is single-valued in the ϕ, ψ plane, although it may become many-valued in

the q, θ plane. This many-valuedness, it will be recalled, is essentially the reason why the solution given in Art. 9 has such a complex nature.

F,11. Approximate Solution for Transonic Flow Past an Airfoil. Since the approximation made in the previous case consists in a simplification of the coefficients of the fundamental system (2-11), the region of validity of the solutions is, of course, restricted. To extend the region

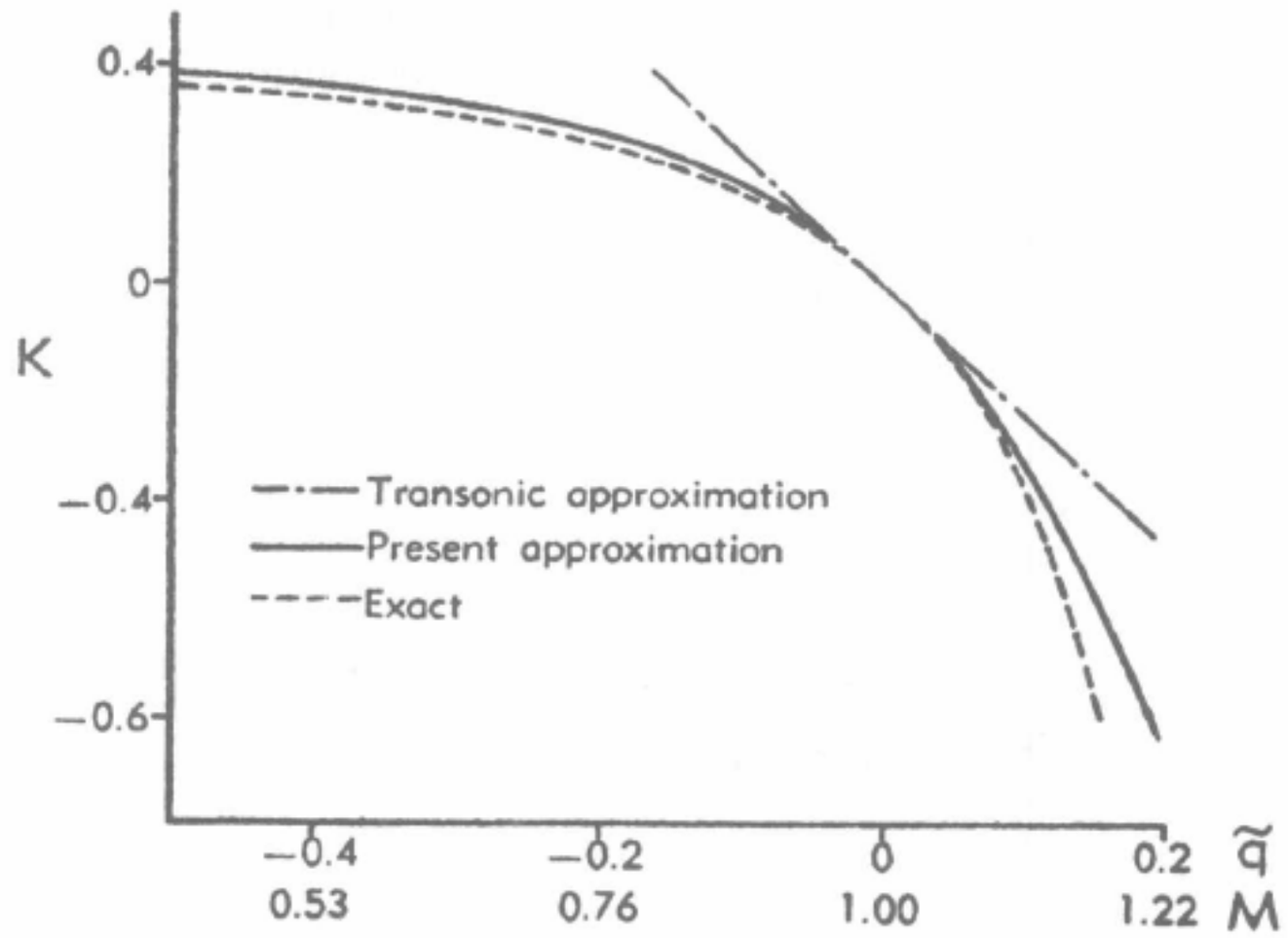

Fig. F,11a. Approximations to the exact function $K(\tilde{q})$.

of validity, but without complication of the mathematical problem, an alternative approximation was proposed by Tomotika and Tamada [*39*].

Let us again introduce the variable

$$\tilde{q} = \int_{a^*}^{q} (\rho/\rho^*) dq/q$$

The system (10-1), without approximation, becomes

$$\begin{aligned} \phi_{\tilde{q}} &= -K(q)\psi_\theta \\ \phi_\theta &= \psi_{\tilde{q}} \end{aligned} \tag{11-1}$$

where $K(q)$ is defined by

$$K(q) = \left(\frac{\rho^*}{\rho}\right)^2 (1 - M^2)$$

The new approximation proposed by Tomotika and Tamada is

$$K(q) = \left(\frac{2}{\gamma + 1}\right)^{2\beta} (1 - e^{2k\tilde{q}}) \tag{11-2}$$

with

$$k = \left(\frac{\gamma+1}{2}\right)^{\alpha^2}, \quad \alpha^2 = \frac{\gamma+1}{\gamma-1}$$

The differential equation for the stream function ψ then becomes

$$\psi_{\bar{q}\bar{q}} + \left(\frac{2}{\gamma+1}\right)^{2\beta}(1 - e^{2k\bar{q}})\psi_{\theta\theta} = 0 \qquad (11\text{-}3)$$

Before we proceed further, let us examine this approximation. Since both the exact $K(\bar{q})$ and the approximate one defined by Eq. 11-2 are

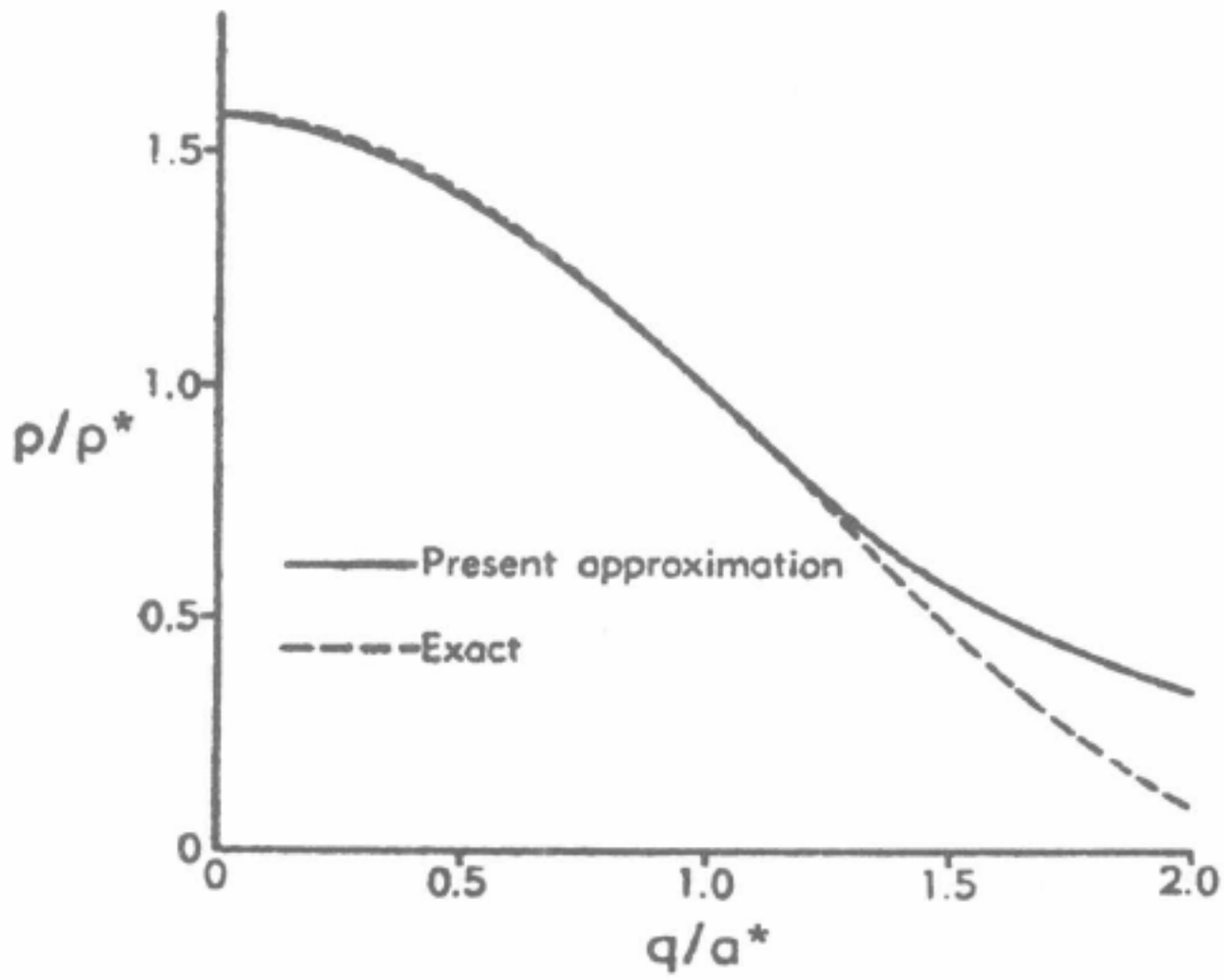

Fig. F,11b. Approximation to the exact density $\rho(\bar{q})$.

functions of $\bar{q}$, they can be plotted on one graph, as in Fig. F,11a. (The linear approximation to K represented by our previous approximation, Eq. 10-4, is also plotted for comparison.) As the present approximation to K is chosen to have the same value and tangent at both the stagnation point $\bar{q} = -\infty$ and the sonic point $\bar{q} = 0$, relatively good agreement is secured in the whole subsonic range. Thus, for any transonic flow with moderate local supersonic speeds, the approximation can be expected to be useful.

Accepting Eq. 11-2 to be valid, we can now determine the corresponding density law $\rho(\bar{q})$ implied by the relations

$$K = \left(\frac{\rho^*}{\rho}\right)^2(1 - M^2) = \left(\frac{2}{\gamma+1}\right)^{2\beta}(1 - e^{2k\bar{q}})$$

Making use of the definition of $\bar{q}$, we find a differential equation for ρq which has been integrated numerically by Tomotika and Tamada. Their result is shown in Fig. F,11b. By comparison, in the range $0 < q < 1.2a^*$,

the difference between the exact and approximate laws is indeed negligible.

Method of constructing solutions. We now introduce new variables

$$\sigma = e^{k\tilde{q}}, \qquad \tilde{\theta} = \left(\frac{\gamma+1}{2}\right)^{1+3\beta}\theta \tag{11-4}$$

by which the differential equation (11-3) becomes

$$\sigma^2\psi_{\sigma\sigma} + \sigma\psi_\sigma + (1-\sigma^2)\psi_{\tilde{\theta}\tilde{\theta}} = 0 \tag{11-5}$$

By definition, $\sigma = 0$ corresponds to $\tilde{q} = -\infty$ (stagnation) and $\sigma = 1$ to $\tilde{q} = 0$. Thus, in subsonic flow σ lies between 0 and 1, and in supersonic flow $\sigma > 1$; consequently, σ can be interpreted as some kind of Mach number.

The particular integrals of Eq. 11-5 are well known, and can be expressed as

$$J_\nu(\nu\sigma)e^{-i\nu\theta} \qquad \text{and} \qquad J_{-\nu}(\nu\sigma)e^{i\nu\tilde{\theta}} \tag{11-6}$$

It is of interest to compare this approximate solution with the exact one given by Cherry and reproduced in Art. 9. The similarity of these two solutions demonstrates again the degree of accuracy of the new approximation.

A general symmetric solution valid in the neighborhood of the stagnation point has the form

$$W = \sum_0^\infty A_n J_n(n\sigma)e^{-in\tilde{\theta}}, \qquad \sigma < 1 \tag{11-7}$$

Since $\tilde{\theta}$ is a constant nonintegral multiple of θ according to Eq. 11-4, the expansion (11-7) involves a very complicated singularity at the origin of the $\tilde{q}$, θ plane. Nevertheless, in a cut plane the change of variable from θ to $\tilde{\theta}$ is merely a distortion of the hodograph plane, and, if discontinuity of tangents is admitted at the stagnation point, such as a sharp leading or trailing edge, uscful solutions can be found.

Now for Bessel's function $J_\nu(\nu\sigma)$, there is an integral representation [*40*, p. 20]

$$J_n(n\sigma) = \frac{1}{2\pi i}\int^{(0+)}\left[z^{-1}e^{\frac{\sigma}{2}(z-z^{-1})}\right]^n\frac{dz}{z}$$

where the path is taken around the origin in a positive sense. Substituting it in Eq. 11-7 and rearranging, we have

$$W = \frac{1}{2\pi i}\int^{(0+)}\sum_0^\infty A_n\left[z^{-1}e^{\frac{\sigma}{2}(z-z^{-1})-i\tilde{\theta}}\right]^n\frac{dz}{z} \tag{11-8}$$

provided the interchange of the order of integration and summation is

justified. This is justified if the series is absolutely convergent, as can easily be shown for $\sigma > 1$.

Special solution. A case of special interest is $A_n = \lambda^{-n}$ where λ is a positive constant, as yet undetermined. It will develop, in what follows, that flows of interesting nature can be derived by proper selection of λ. For this form of A_n, the solution (11-8) becomes

$$W = \frac{1}{2\pi i} \int^{(0+)} \frac{1}{1 - e^z} \frac{dz}{z}$$

with (11-9)

$$Z(z) = \frac{\sigma}{2}(z - z^{-1}) - \ln z - i\tilde{\theta} - \ln \lambda$$

This integral can be evaluated by calculating the residues at the roots of $Z(z) = 0$ inside the contour, since the contribution at the origin is zero. Let us fix our attention on the solution obtained by including only one root in the contour, say $z = z_0$. If this is a root, $Z(z)$ can be written in the form

$$Z(z) = \left[\frac{\sigma}{2}\left(1 + \frac{1}{z_0 z}\right) - \frac{\ln z - \ln z_0}{z - z_0}\right](z - z_0)$$

The residue of $z^{-1}(1 - e^z)^{-1}$ is therefore

$$\left[-\frac{\sigma}{2}(z_0 + z_0^{-1}) + 1\right]^{-1}$$

Writing $z_0 = e^{-i\Theta}$ where Θ is complex, the integral (11-9) yields

$$W = \frac{1}{1 - \sigma \cos \Theta}$$

and from the second of Eq. 11-9 (11-10)

$$\tilde{\theta} - i \ln \lambda = \Theta - \sigma \sin \Theta$$

Eq. 11–10 are formally the same as we obtained in Eq. 9-11 and 9-12, except that complex values are involved here. The elimination of Θ gives W as a function of σ and $\tilde{\theta}$. From our analysis of Eq. 9-11 and 9-12, we deduce immediately that the function $\Theta(\sigma, \tilde{\theta})$ has branch lines given by

$$\theta_\Theta = 1 - \sigma \cos \Theta = 0$$

or, in terms of $\tilde{\theta}$,

$$\tilde{\theta} = \pm \cos^{-1}\frac{1}{\sigma} \mp \sqrt{\sigma^2 - 1} + i \ln \lambda \qquad (11\text{-}11)$$

There are two possibilities of finding interesting flow patterns here: namely, the branch lines may occur in the supersonic ($\sigma > 1$) or subsonic ($\sigma < 1$) regions. Consider first the supersonic case; here Eq. 11-11 leads to

$$\ln \lambda = 0$$

and

$$\bar{\theta} = \pm \cos^{-1}\frac{1}{\sigma} \mp \sqrt{\sigma^2 - 1} = \pm\omega(\sigma) \tag{11-12}$$

The last equation is the equation of two characteristics of an approximate differential equation (11-5). Thus, by choosing $\lambda = 1$ in this solution, one obtains a flow of the type (Laval nozzle flow) discussed in Art. 9.

The other possibility is of more interest to us in this article. For $\sigma < 1$, Eq. 11-11 should be rewritten as

$$\bar{\theta} = i \cosh^{-1}\frac{1}{\sigma} - i\sqrt{1 - \sigma^2} + i \ln \lambda$$

whence

$$\bar{\theta} = 0 \tag{11-13}$$
$$\ln \lambda = \pm \sqrt{1 - \sigma^2} \mp \cosh^{-1}\frac{1}{\sigma}$$

We see that the branch line in this case has degenerated into a single point. On the basis of our experience in Art. 8 with mixed flow past closed bodies, we immediately identify this branch point with flow conditions at infinity; i.e. we write

$$\bar{\theta}_\infty = 0 \quad \text{and} \quad \ln \lambda = \pm \sqrt{1 - \sigma_\infty^2} \mp \cosh^{-1}\frac{1}{\sigma_\infty}$$

This means that, by proper selection of the constant λ for any given subsonic stream Mach number, we obtain here a flow, parallel and horizontal at infinity, of the same character as the exact solutions treated in Art. 8.

The integral of this solution of Eq. 11-10 with respect to $\bar{\theta}$ is also a solution of the differential equation (11-5); Tomotika and Tamada find that it is desirable to include it in order to set up an airfoil type flow. The inclusion of the integral does not affect the singular behavior at infinity, which was determined above. The integral is

$$\int \frac{d\bar{\theta}}{1 - \sigma\cos\Theta} = \int \frac{1}{1 - \sigma\cos\Theta}\frac{d\Theta}{d\bar{\theta}/d\Theta} = \Theta + \text{const} \tag{11-14}$$
$$= \bar{\theta} + \sigma \sin\Theta + \text{const}$$

according to Eq. 11-10. But $\bar{\theta}$ is clearly a particular solution of the differential equation (11-5), so it can be omitted from Eq. 11-14. We therefore take as our complete solution

$$\psi = \text{I.P.}\left\{\frac{1}{1 - \sigma\cos\Theta} + iK\sigma \sin\Theta\right\} \tag{11-15}$$

with $\bar{\theta} - i \ln \lambda = \Theta - \sigma \sin\Theta$ where K is arbitrary.

Flow past a symmetric airfoil. To produce the transonic potential flow about a certain symmetric airfoil profile, we begin by choosing K

to make the leading edge a stagnation point; i.e. we choose K so as to place the point $\sigma = 0 = \psi$ on the real axis in the finite region. An appropriate choice turns out to be $K = (1 - \lambda^2)/(1 + \lambda^2)$.

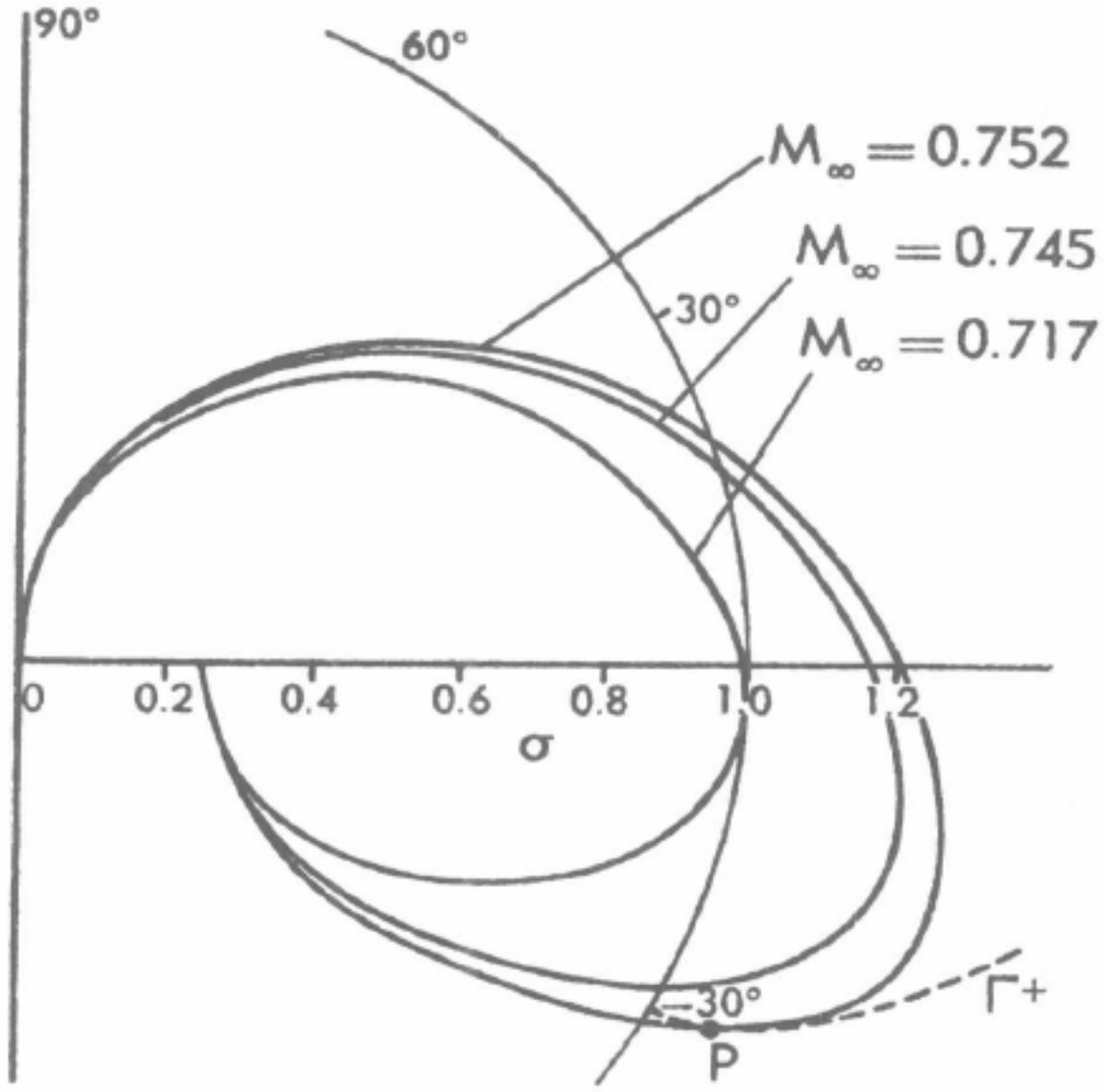

Fig. F,11c. Zero streamlines in the hodograph plane for free stream Mach numbers 0.717, 0.745, and 0.752 [*39*].

In terms of the variables σ and $\tilde{\theta}$, our fundamental set (11-1) reads

$$\phi_\sigma = \left(\frac{2}{\gamma+1}\right)^\beta \left(\sigma - \frac{1}{\sigma}\right)\psi_{\tilde{\theta}}$$
$$\phi_{\tilde{\theta}} = \left(\frac{2}{\gamma+1}\right)^\beta \sigma\psi_\sigma \tag{11-16}$$

Upon integration of these, the velocity potential corresponding to Eq. 11-15 is found to be

$$\phi = \left(\frac{2}{\gamma+1}\right)^\beta \sigma \,\text{I.P.}\left\{\frac{\sin\Theta}{1-\sigma\cos\Theta} - iK\left(\frac{\sigma}{2} + \cos\Theta\right)\right\} \tag{11-17}$$

Finally, the transformation from the $(\sigma, \tilde{\theta})$ to the (x, y) plane has been carried out by Tomotika and Tamada for three different Mach numbers M_∞. The relation between M_∞ and σ_∞ is

$$M_\infty = \left[1 + \left(\frac{\rho_\infty}{\rho^*}\right)^2 \left(\frac{2}{\gamma+1}\right)^{2\beta} (\sigma_\infty^2 - 1)\right] \tag{11-18}$$

The resulting streamlines $\psi = 0$, together with velocity distributions, are shown in Fig. F,11c and F,11d. The calculated airfoil sections are

quite similar to a 10 per cent thick symmetric Joukowski section, except that the leading edge is not rounded—as was already predicted in connection with our discussion of the approximation earlier in this article.

It is an interesting fact that the airfoil profiles for the three Mach numbers of Fig. F,11d are almost identical; the differences cannot be

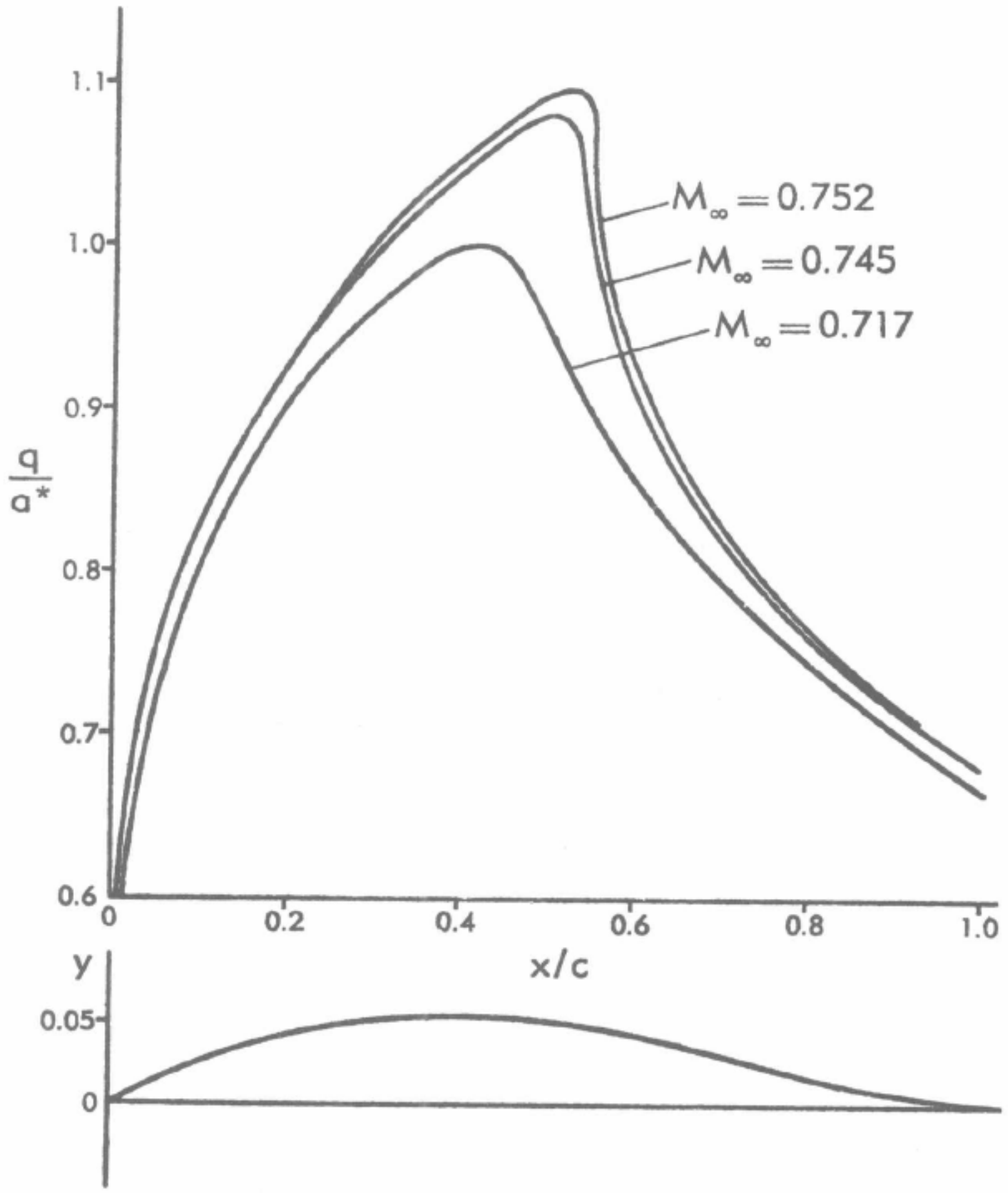

Fig. F,11d. Airfoil sections and surface q distribution at Mach numbers 0.717, 0.745, and 0.752 [*39*].

plotted in the figure. Thus, from the Tomotika-Tamada results, we obtain a close approximation to the flow at three Mach numbers about a fixed profile. The lowest of these Mach numbers produces entirely subsonic flow; the second, mixed flow with a considerable supersonic region and a maximum local speed of about $1.10a^*$. The highest Mach

number produces still greater local speeds and exhibits the phenomenon of the singularity $J = 0$ at one point of the upper surface contour, and, of course, at a symmetrically located point of the lower surface. The significance of this type of singularity is discussed in the next article.

F,12. Singularities of the Hodograph Transformation. Let u and v be the velocity components of a flow in the x, y plane. Consider (dx, dy), an element in the x, y plane, and (du, dv) an element in the u, v plane. If they correspond to each other, they must be related by

$$du = u_x dx + u_y dy$$

$$dv = v_x dx + v_y dy$$

These equations define du and dv uniquely if the functions $u(x, y)$ and $v(x, y)$ are known and are differentiable, and dx and dy are given. From a different point of view, we can consider the system as a transformation. If the transformation is locally one-to-one, the transformation Jacobian $J\ (= \partial(x, y)/\partial(u, v))$ does not vanish nor become infinite. When these conditions are violated, the hodograph transformation fails and singularities occur. If this Jacobian vanishes identically throughout any region, u and v are no longer independent of each other. The flow in this case is particularly simple and is known as Prandtl-Meyer flow or simple wave flow (see E,3 and G,5). In the following, we will confine our attention to two distinct types of singularities, which are of special interest in connection with the mixed subsonic-supersonic potential flows. These are called, respectively, "limiting lines" [*42*] and "branch lines" [*65*].

Limiting lines: $J = 0$. When J becomes zero, viz.

$$J = \frac{\partial(x, y)}{\partial(q, \theta)} \equiv -\left(\frac{\rho^0}{\rho}\right)^2 \frac{1}{q}\left[\psi_q^2 - \left(\frac{1}{a^2} - \frac{1}{q^2}\right)\psi_\theta^2\right] = 0 \qquad (12\text{-}1)$$

we must have, since $\rho^2 q$ cannot become infinite,

$$q^2\psi_q^2 - (M^2 - 1)\psi_\theta^2 = 0 \qquad (12\text{-}2)$$

For subsonic flow, this requires

$$q\psi_q = \psi_\theta = 0$$

This means that in a subsonic field, the singularities are isolated. The singularity may be either a stagnation point or a point where the streamline has infinite curvature. To show this, we note first of all, from the system Eq. 2-11,

$$q\phi_q = \phi_\theta = 0$$

Now the first partial derivatives of x and y are given in terms of the partial derivatives of ϕ and ψ by Eq. 2-15 and 2-16. It follows, then, that at the singular point, if the partial derivatives of x and y are finite, q must

be zero. If q does not vanish, then the partial derivatives must be zero and in the flow plane the velocity gradient or the acceleration of the fluid particle must be infinite. As the acceleration is proportional to the curvature of the streamline, we see that $J = 0$ occurs at such points as the sharp trailing edge of an airfoil, as well as at stagnation points. This possibility was first noticed by Kuo [*23*] and later confirmed by Cherry. [*71*]

When $M > 1$, ψ_q and ψ_θ may either vanish identically in a region or satisfy the differential relation (12-2) along certain lines. Since $\psi = \text{const}$ is a trivial solution, we must consider the second alternative; we have the solutions

$$\begin{aligned} &\text{on } \Lambda^+ && q\psi_q - \sqrt{M^2-1}\,\psi_\theta = 0 \\ &\text{on } \Lambda^- && q\psi_q + \sqrt{M^2-1}\,\psi_\theta = 0 \end{aligned} \tag{12-3}$$

It can be shown that on each line J has a simple root, because on Λ^+

$$J_\theta = -\left(\frac{\rho^0}{\rho}\right)^2 \frac{1}{q^3}(q\psi_q + \sqrt{M^2-1}\,\psi_\theta)(q\psi_{q\theta} - \sqrt{M^2-1}\,\psi_{\theta\theta}) \neq 0$$

In the vicinity of these lines, a small neighborhood in the x, y plane corresponds to two different regions in the q, θ plane. This is seen clearly from the transformation (2-10), which on a streamline reduces to

$$dx = -\frac{\rho^0 \cos\theta}{\rho q^2 \psi_\theta}[(q\psi_q + \sqrt{M^2-1}\,\psi_\theta)(q\psi_q - \sqrt{M^2-1}\,\psi_\theta)]dq$$

$$dy = -\frac{\rho^0 \sin\theta}{\rho q^2 \psi_\theta}[(q\psi_q + \sqrt{M^2-1}\,\psi_\theta)(q\psi_q - \sqrt{M^2-1}\,\psi_\theta)]dq$$

Since J has simple zero, dx and dy both change their signs upon proceeding from one side of Λ^+ to the other, but without affecting the slope of the streamline. Thus, the streamline must have a cusp there, and as a result the stream function becomes many-valued, as shown in Fig. F,12a, the branches coming together along the singular line or "limiting line" L^+, which is the image in the flow plane of Λ^+. The immediate consequence of this singular line is that all space derivatives, such as pressure gradient, curvature of the streamline, and so on, are infinite there. Hence, once this singularity occurs, the solution will no longer be physically possible and must be rejected.

Now, let us investigate the geometric relationship between the Mach waves in the x, y plane and the characteristic hodographs in the q, θ plane. We know, from Eq. 3-1, that the characteristic hodographs are the curves that satisfy

$$q^2 d\theta^2 - (M^2-1)dq^2 = 0$$

or,

$$\begin{aligned} &\text{on } \Gamma^+ && qd\theta - \sqrt{M^2-1}\,dq = 0 \\ &\text{on } \Gamma^- && qd\theta + \sqrt{M^2-1}\,dq = 0 \end{aligned} \tag{12-4}$$

These equations can be integrated to give two families of fixed curves Γ^+ and Γ^- in the q, θ plane:

Γ^+ $\qquad \theta - \omega = \text{const}$

Γ^- $\qquad \theta + \omega = \text{const}$

where ω is defined in Eq. 16-4. It is easy to verify (G,3) that these curves are epicycloids, all radiating from the sonic circle and converging

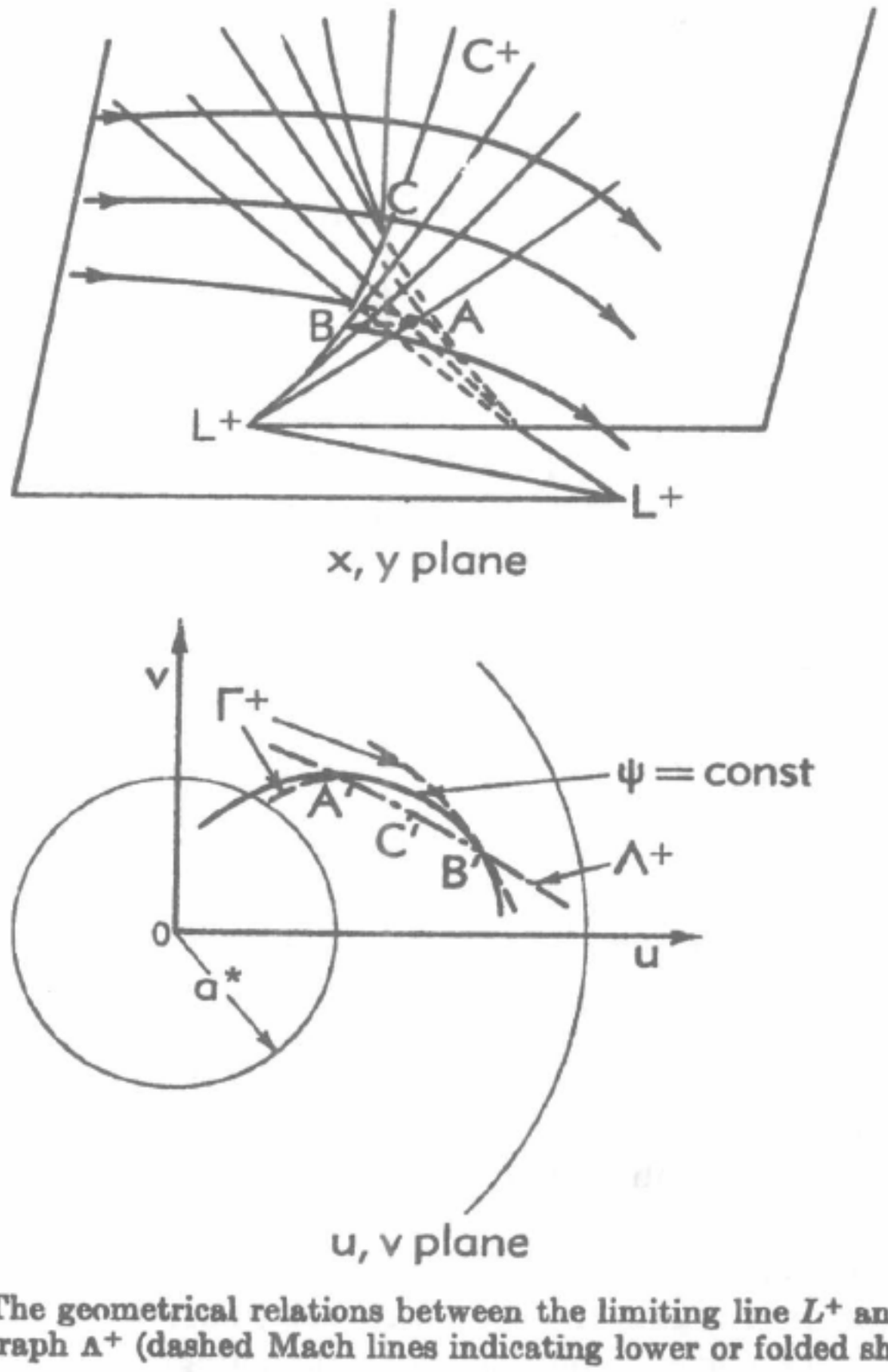

Fig. F,12a. The geometrical relations between the limiting line L^+ and the limiting hodograph Λ^+ (dashed Mach lines indicating lower or folded sheets).

asymptotically to the limit circle, $q = q_{max}$ or $M = \infty$. The corresponding lines in the physical plane are characteristics of Eq. 2-7, namely,

$$\text{on } C^+ \qquad \frac{dy}{dx} = \tan(\theta + \mu)$$

$$\text{on } C^- \qquad \frac{dy}{dx} = \tan(\theta - \mu) \tag{12-5}$$

with

$$\mu = \sin^{-1}\frac{1}{M}$$

Theodore von Kármán [3] first noticed that the singular line Λ^+ or Λ^- is the locus of the points of tangency of the streamline hodographs with one family of characteristic hodographs Γ^- or Γ^+. For along every streamline

$$\left(\frac{d\theta}{dq}\right)_\psi = -\frac{\psi_q}{\psi_\theta}$$

On the line Λ^+

$$q\psi_q - \sqrt{M^2-1}\,\psi_\theta = 0$$

Thus, whenever a streamline intersects the line Λ^+, this derivative must have the value

$$\left(\frac{d\theta}{dq}\right)_\psi = -\frac{\sqrt{M^2-1}}{q} = \left(\frac{d\theta}{dq}\right)_{\Gamma^-} \tag{12-6}$$

according to Eq. 12-4. Similarly, on Λ^-

$$\left(\frac{d\theta}{dq}\right)_\psi = \frac{\sqrt{M^2-1}}{q} = \left(\frac{d\theta}{dq}\right)_{\Gamma^+} \tag{12-7}$$

Each streamline generally exhibits two such points of tangency, i.e. intersects the line Λ^+, for example, in two points, such as A' and B' in Fig. F,12a. At the image points A and B in the flow plane, the streamline forms cusps. When the streamline just touches Λ^+ in the hodograph plane, such as at C', the streamline in the flow plane has no cusp but the limiting line L^+ does.

Next let us transform the Mach waves C^+ and C^- into the q, θ plane by means of Eq. 2-7 and 2-10; there result, respectively,

$$\begin{aligned} &\text{on } C^+ \qquad (\sqrt{M^2-1}\,dq - qd\theta)(q\psi_q - \sqrt{M^2-1}\,\psi_\theta) = 0 \\ &\text{on } C^- \qquad (\sqrt{M^2-1}\,dq + qd\theta)(q\psi_q + \sqrt{M^2-1}\,\psi_\theta) = 0 \end{aligned} \tag{12-8}$$

The Mach waves C^+ and C^- thus have as images the characteristics Γ^+ and Γ^- for $J \neq 0$. As $J = 0$ defines two lines Λ^+ and Λ^- that nowhere coincide with Γ^+ and Γ^-, Mach wave C^+ can touch the limiting line L^+ only at one point.

To see this, the behavior of one family of Mach waves is studied in the neighborhood of Λ^+. By eliminating $qd\theta = -\sqrt{M^2-1}\,dq$ from Eq. 2-10, we can define a small element of C^- by

$$\begin{aligned} dx &= -\frac{\rho^0}{\rho q^2}(q\psi_q - \sqrt{M^2-1}\,\psi_\theta)(\sqrt{M^2-1}\cos\theta + \sin\theta)dq \\ dy &= -\frac{\rho^0}{\rho q^2}(q\psi_q - \sqrt{M^2-1}\,\psi_\theta)(\sqrt{M^2-1}\sin\theta - \cos\theta)dq \end{aligned} \tag{12-9}$$

In the neighborhood of Λ^+, dx and dy vanish and, consequently, along

any member of C^- the space derivatives of physical quantities, such as q or θ, will be infinite. This means that the characteristic curves of the other family C^+ are densely piled up on one another at such a point; i.e., they form an envelope L^+ that corresponds to Λ^+ in the hodograph plane.

Thus, we arrive at the conclusion that the singular lines Λ^+ and Λ^- correspond respectively to the limiting lines L^+ and L^-, and that on one of these limiting lines, L^+ say, the Mach waves C^+ form an envelope, while the streamlines and the Mach lines C^- have cusps (Fig. F,12a). Similarly, on the line L^- the Mach waves C^- form an envelope while the streamlines and the waves C^+ have cusps.

We have seen several examples of the appearance of limiting lines in the present section. The first example was the behavior of our source-or-sink flow (Art. 6) at the sonic circle. To be sure, this singularity was recognized as the familiar "choking" phenomenon of a nozzle. Nevertheless, it is easy to verify that $J = 0$ at $M = 1$ in this case, for $\phi_q = 0$ and ψ_θ is a constant, so that J is proportional to $M^2 - 1$. This is confirmed by the behavior of the streamlines, which reverse their directions at the sonic circle. Consequently, in this simple flow pattern, the sonic circle is a limiting line, and the anomalous behavior there can immediately be attributed to our specification of the streamline pattern. In more general cases, as we shall see, the explanation for the appearance of a limiting line in the calculated flow pattern is not so obvious.

Our second encounter with limiting lines was in the flow around an edge (Ringleb's case) in Art. 6. Again, it is easy to verify from the equations of that article that the Jacobian J vanishes along PQR (Fig. F,6b). The appearance of cusps in the streamlines and the folding of the flow plane have already been noted; this relatively simple case might be taken, in fact, as typical of the phenomenon discussed here (cf. Fig. F,6b and F,12a).

Again, in the Tomotika-Tamada results (Fig. F,11c and F,11d), the phenomenon of vanishing J was noted at a single point, where the hodograph of the streamline $\psi = 0$ became tangent to a characteristic. Fig. F,11d confirms that the pressure gradient becomes infinite at such a point. The same phenomenon appears in a flow calculated by Cherry [*24*] and mentioned above in Art. 8, namely, the flow about a slightly cambered cylinder. This flow pattern is reproduced in Fig. F,12b.

Branch lines. $J = \infty$. Let us consider the possibility of the occurrence of a different sort of singularity, namely, $J = \infty$. In subsonic flow, as we see in Eq. 12-1, this might occur at a stagnation point or at a point where

$$q^2\psi_q^2 + (1 - M^2)\psi_\theta^2 = \infty$$

It is easier to understand this condition if we compute the reciprocal of J, viz.,

F · *PLANE POTENTIAL FLOWS*

$$J^{-1} = \frac{\partial(q, \theta)}{\partial(\phi, \psi)} \frac{\partial(\phi, \psi)}{\partial(x, y)} = -\left(\frac{\rho}{\rho^0}\right)^2 q \left[q_\psi^2 + \left(\frac{\rho^0}{\rho}\right)^2 (1 - M^2) q_\phi^2\right]$$

For this to vanish, except at a stagnation point, implies $q_\phi = q_\psi = 0$ and therefore $\theta_\phi = \theta_\psi = 0$. These relations can define only an isolated singularity [*41*] or a trivial flow.

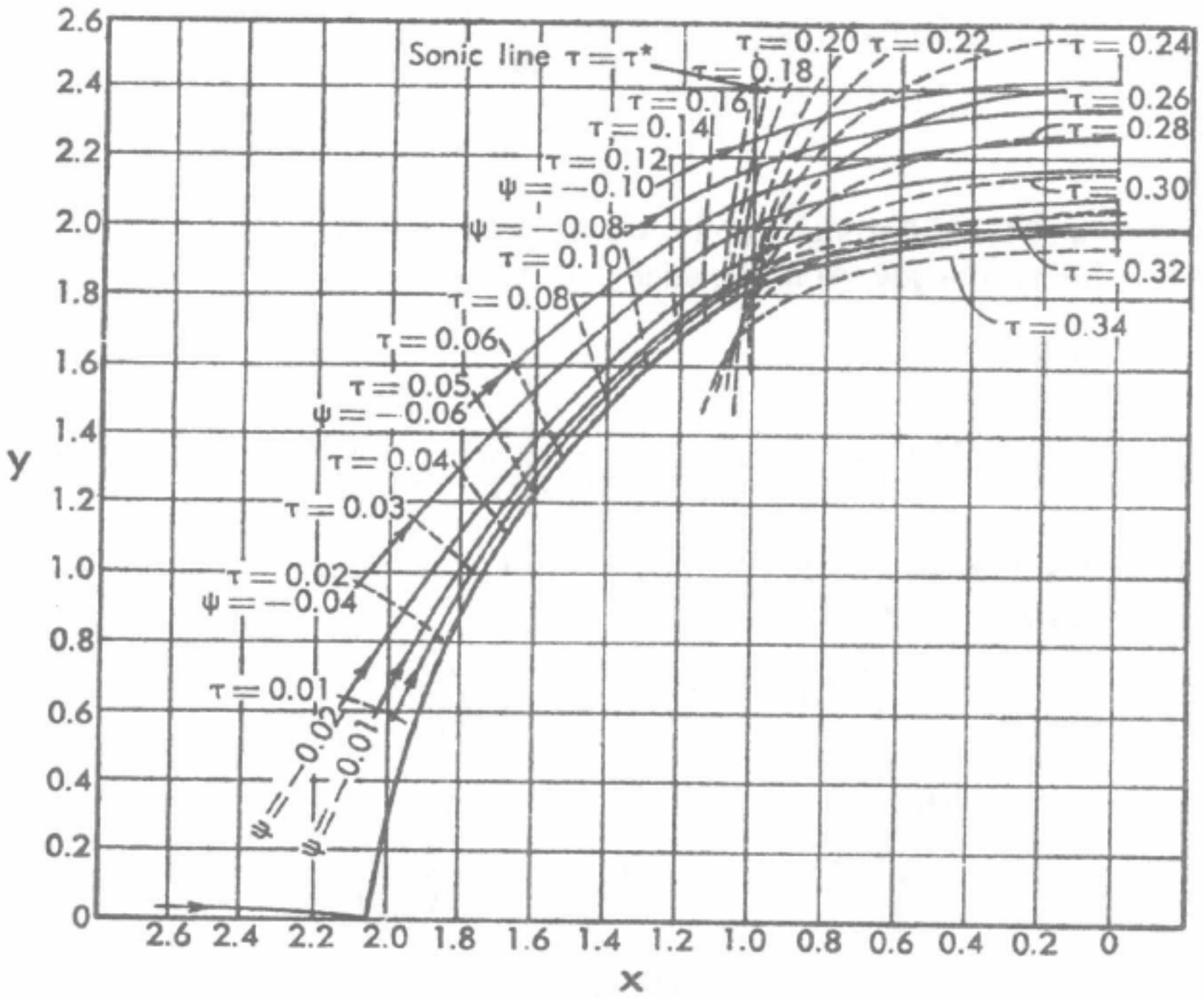

Fig. F,12b. Streamlines and constant-speed lines for flow at $M_\infty = 0.5098$ past a slightly cambered cylinder [*24*]. Note first appearance of limiting line at the boundary (near $x = 1.0$). $\gamma = 1.405$.

On the other hand, when $M > 1$, we have the possibility of singular curves in the flow; namely, we have the following solutions:

$$\begin{aligned} &\text{on } \Omega^+ && q\psi_q - \sqrt{M^2 - 1}\,\psi_\theta = \infty \\ & && q\psi_q + \sqrt{M^2 - 1}\,\psi_\theta \quad \text{is finite} \\ &\text{on } \Omega^- && q\psi_q + \sqrt{M^2 - 1}\,\psi_\theta = \infty \\ & && q\psi_q - \sqrt{M^2 - 1}\,\psi_\theta \quad \text{is finite} \end{aligned} \tag{12-10}$$

provided $\rho \neq 0$. In either case, both ψ_q and ψ_θ must be infinite but the ratio ψ_q/ψ_θ is finite.

To show that the singular lines Ω^+ and Ω^- are, in fact, characteristics

Γ^+ and Γ^- respectively, we consider a line

$$q\psi_q - \sqrt{M^2-1}\,\psi_\theta = \text{const}$$

By taking the total derivative along this line, we obtain

$$\left[q\psi_{qq} + \psi_q - \sqrt{M^2-1}\,\psi_{\theta q} - \frac{M^2\left(1+\frac{\gamma-1}{2}M^2\right)}{q\sqrt{M^2-1}}\right] + [q\psi_{q\theta} - \sqrt{M^2-1}\,\psi_{\theta\theta}]\frac{d\theta}{dq} = 0$$

By means of the differential (3-1), we simplify this expression and obtain for the derivative $qd\theta/dq$ along such a line

$$q\frac{d\theta}{dq} = \sqrt{M^2-1}\left\{1 - \frac{M^2[2\sqrt{M^2-1}\,(q\psi_q - \sqrt{M^2-1}\,\psi_\theta) + (\gamma+1)M^2\psi_\theta]}{2(M^2-1)(\sqrt{M^2-1}\,\psi_{\theta\theta} - q\psi_{q\theta})}\right\}$$

But on the line Ω^+, both ψ_q/ψ_θ and $\psi_{\theta\theta}/\psi_{q\theta}$ are finite, while $\psi_\theta/\psi_{q\theta}$ is zero; we have, therefore

$$\left(\frac{d\theta}{dq}\right)_{\Omega^+} = \frac{\sqrt{M^2-1}}{q} = \left(\frac{d\theta}{dq}\right)_{\Gamma^+} \tag{12-11}$$

Similarly, we have

$$\left(\frac{d\theta}{dq}\right)_{\Omega^-} = -\frac{\sqrt{M^2-1}}{q} = \left(\frac{d\theta}{dq}\right)_{\Gamma^-} \tag{12-12}$$

Moreover, the streamline hodographs become tangent to these singular characteristic curves. This is clear from the fact that $q\psi_q + \sqrt{M^2-1}\,\psi_\theta$ remains finite along Ω^+, for example, while both ψ_q and ψ_θ become infinite. This can only mean that the ratio ψ_q/ψ_θ has the limiting value $-\sqrt{M^2-1}/q$; but this is just to say that

$$\left(\frac{d\theta}{dq}\right)_{\psi} = -\frac{\psi_q}{\psi_\theta} = \left(\frac{d\theta}{dq}\right)_{\Omega^+}$$

and similarly for Ω^-. The streamlines do not coincide with characteristics except in Prandtl-Meyer flow; thus, the singular characteristics Ω^+ and Ω^- must be envelopes of streamlines. This situation is sketched, for example, in Fig. F,10d.

Now consider the nature of these singular characteristics in the flow plane. According to Eq. 12-9 and 12-10, the elements dx, dy remain finite even when the characteristic C^- (for example) is the singular member of the family. Thus, infinite curvature of streamlines and infinite pressure

gradient do not occur at singular curves of this type, and solutions possessing this kind of singularity are physically acceptable. Flows through convergent-divergent nozzles, such as we described in Art. 9 and 10, are typical examples. The significance of such singular curves is mathematical, since they imply the multivaluedness of $\psi(q, \theta)$ that makes the boundary-value problems difficult, as in Art. 9.

A much fuller discussion of these singularities, and others, has been given in a paper by Craggs [*41*], to which the interested reader is referred.

Significance of the limiting line. We have already seen examples of flow patterns calculated by the hodograph technique that exhibit the phenomenon of the limiting line. This situation appears to be quite general, so that whenever a family of flows is controlled by a parameter such as a stream Mach number, M_∞, there is the danger that sufficiently large values of the parameter will cause these singular curves to appear. As has already been pointed out above, the behavior of the streamlines in such a case is physically inacceptable and the flow pattern must be rejected. Tollmien [*42*] has proved that, if a limiting line appears, it is impossible to continue the smooth isentropic flow pattern across it.

When limiting lines were first encountered, for example in the paper by Ringleb [*13*], the phenomenon stimulated considerable interest in the scientific world. It was interpreted as a sign that irrotational, isentropic, plane flow had become impossible, and that other effects in the flow, such as viscosity and heat conduction, had become predominant. The name "shock wave" was even applied to the limiting line. Following this line of reasoning, the appearance of limiting lines was held directly responsible for the breakdown of potential flow, and the stream Mach number M_∞ at which the phenomenon first appeared was called the "upper critical Mach number."

But we must remember that, when we calculate a family of related flows about closed bodies using the present hodograph methods, the streamlines alter in shape as M_∞ varies, and this is also true of the boundary streamline. In Ringleb's problem, the effect is observed if any two streamlines are considered as channel walls; as the boundary streamlines are selected closer to the high speed regions of flow (Fig. F,6b), their shape is changed. The fundamental question therefore remains: Is there a critical Mach number at which the limiting line first appears, for flow about a given smooth boundary? In the earlier interpretation, this possibility was implied.

A qualified answer to this question has been given by Friedrichs [*43*], who showed that, assuming the existence of a family of analytic[6] coordinate functions $x(u, v)$ and $y(u, v)$ dependent on a parameter M_∞ and satisfying smooth boundary conditions (which may vary with M_∞), the

[6] More recently, Morawetz and Kolodner [*66*] have proved Friedrichs' theorem assuming only that $x(u, v)$ and $y(u, v)$ have continuous derivatives.

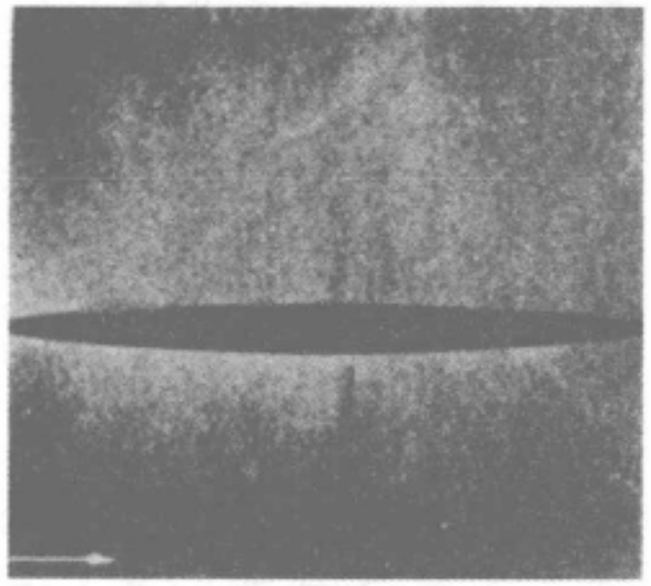

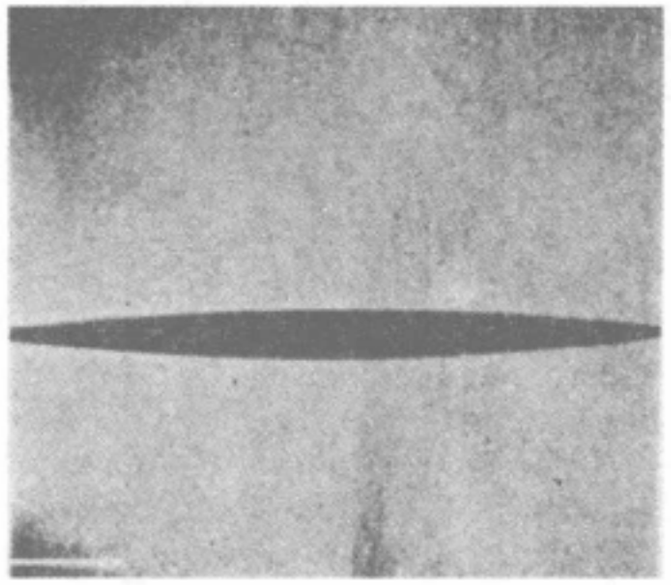

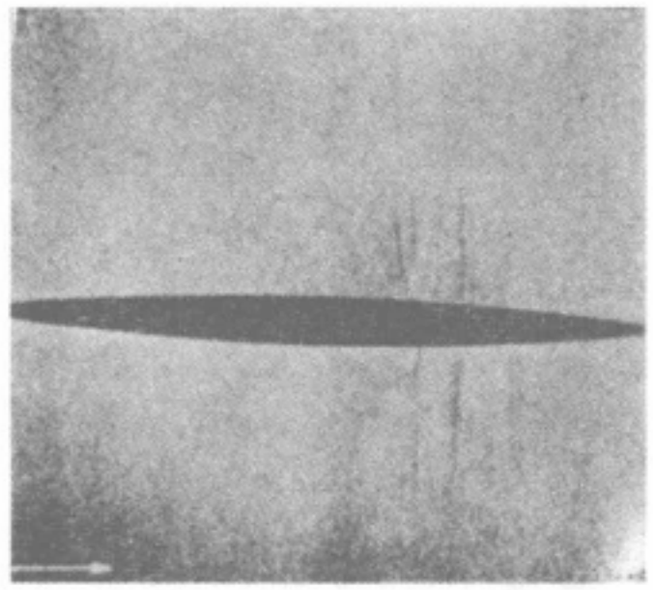

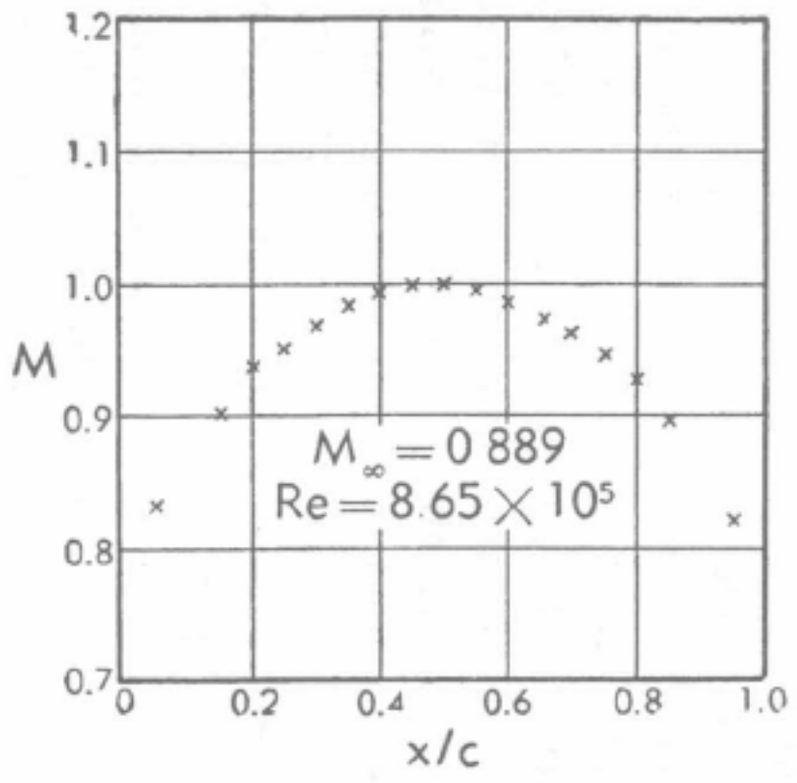

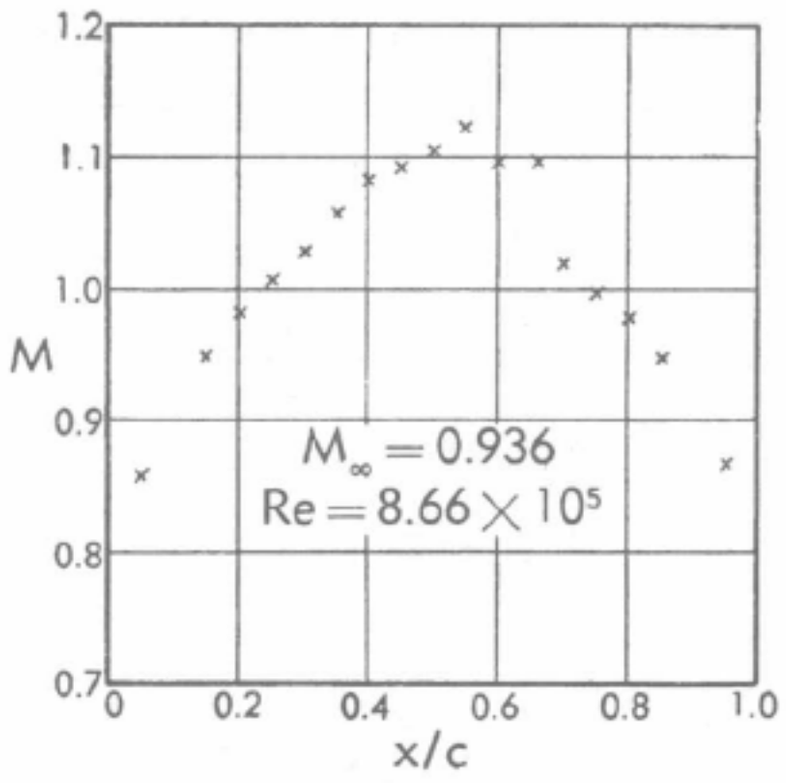

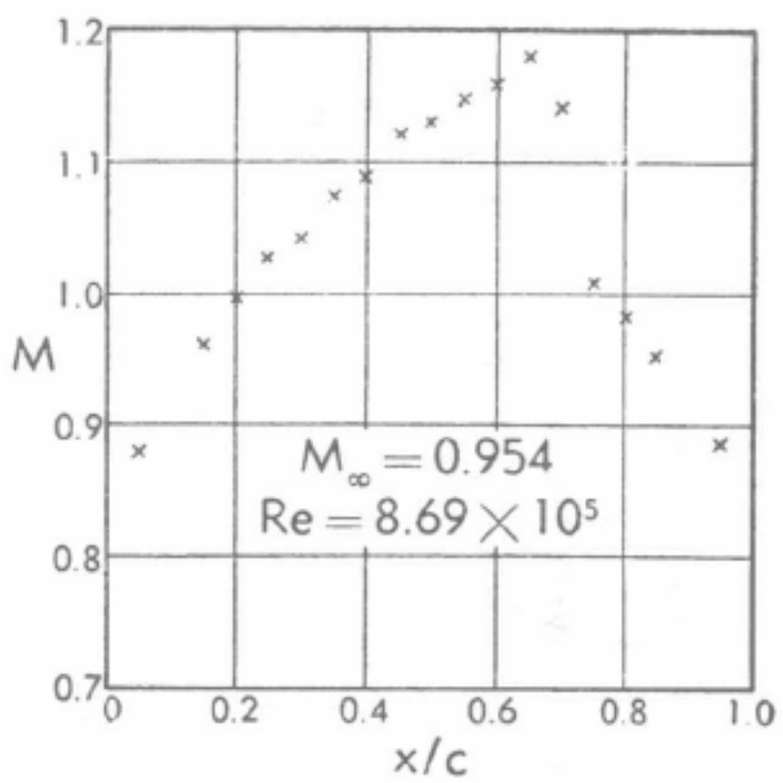

Plate F.13a, b, and c. Measured Mach number distributions over a biconvex circular arc airfoil at three free stream Mach numbers M_∞ and Reynolds numbers Re [47].

limiting line cannot occur. His argument runs substantially as follows: Assume $-J > 0$ everywhere for sufficiently small M_∞. (Note that $-J$ is always positive in subsonic flow.) Then, if the limiting line is to appear in the flow at some values of M_∞, say M_c, it follows from continuity of J that $J = 0$ somewhere at $M_\infty = M_c$. He proves this to be impossible. The proof has been extended by Manwell [*44*], who concludes that at $M_\infty = M_c$, J cannot vanish in any region nor along any line. Similar conclusions were previously reached by Nikolsky and Taganoff [*45*] by a different approach.

This does not completely answer the question posed above, because the existence of the analytic functions $x(u, v)$, $y(u, v)$ has not been proved. To be sure, their existence may be assumed to be quite independent of the vanishing of J, but there is no conclusive evidence of the existence or nonexistence of such functions, dependent upon a parameter M_∞, for flows past a prescribed boundary streamline.

It does not seem possible to proceed further along this line, since the use of the hodograph equations, to date, appears to eliminate the possibility of satisfying prescribed physical boundary conditions. It must be concluded that the identification of the limiting line as the cause of breakdown of potential flow should be viewed with suspicion, at least.

F,13. Conflicts between Theory and Experiment. Both the exact and the approximate solutions of this section have established beyond doubt the theoretical existence of continuous, steady, mixed transonic flows past solid boundaries. Other approximate methods of calculation, such as those discussed in Sec. E and in [*46*], have also predicted flows of this type. Theoretically, then, the fluid particle in such a flow should be able to decelerate isentropically to a subsonic speed after it has been accelerated isentropically to a supersonic state. Were this proved possible in practice, an aircraft might fly in the transonic regime without any greater drag than that caused by skin friction. In the case of the 10 per cent thick symmetric airfoil calculated by Tomotika and Tamada (Fig. F,11d), a free stream Mach number as high as 0.75 might be attained with substantial supersonic local speeds, the flow remaining smooth and free of shock waves.

Wind tunnel experiments, however, contradict these theoretical predictions, for when the sonic speed is exceeded anywhere on a solid boundary, the flow either becomes unsteady or involves shock waves, or both. Typically, the deceleration from supersonic speed takes place in shock waves rather than by isentropic compression. Apparently, the sequence of events as the Mach number is gradually increased is as follows: Immediately after the occurrence of local sonic speed at the surface, highly unsteady disturbances begin to appear in the flow field near the surface, downstream of the minimum pressure point. As the

Mach number is gradually raised, the traveling disturbances become proportionately stronger, although the pressure distribution over the surface may still show no peculiarities, except that far downstream there is some distortion due to the thickening of the boundary layer. But when the Mach number is high enough, the disturbances suddenly coalesce to form a stationary shock. The shock, involving as it does an irreversible thermodynamic process, causes drag; moreover, it changes the pressure distribution appreciably, and may produce boundary layer separation and all of the attendant effects.

H. W. Liepmann and his associates [*47*] have studied this type of flow over a six per cent, biconvex, circular arc airfoil in a 2 × 20 in. transonic wind tunnel. For each free stream Mach number, the local Mach number distribution over the surface was measured. Local supersonic speeds were reached when the free stream Mach number was slightly below 0.889. At $M_\infty = 0.889$, the highest local Mach number appeared to be 1.01. The Mach number distribution still maintained its low speed character, as can be seen in Plate F,13a. Yet the disturbances are already visible in the accompanying schlieren photograph. When the free stream Mach number was raised to 0.936, the disturbances were more clearly seen in the schlieren picture and the Mach number distribution also showed some irregularities at about 60 per cent chord, possibly due to boundary layer transition (Plate F,13b). A stationary shock was definitely formed at a slightly higher Mach number, viz. 0.954, as shown by the Mach number distribution curve (Plate F,13c).

In this series of experiments, steady laminar boundary layer was maintained over most of the airfoil, and transition most likely occurred in each case near the trailing edge.

In any region of boundary layer transition and turbulence, unsteady disturbances are excited, and these propagate into the fluid in all directions. All except those traveling against the main flow quickly disappear, due to their relatively high speed of propagation. Those traveling against the stream have a tendency to accumulate, particularly in the transonic region. If there is no mechanism to dissipate the energy of these waves, they have sufficient time to grow and eventually to destroy the smooth flow. There is strong experimental evidence that smooth, plane, transonic flows involving local supersonic regions are not stable to small disturbances, and that the flow pattern becomes stable only when stationary shocks are formed. It seems certain that phenomena similar to those described here do occur in channel flow that is substantially one-dimensional, but it is not completely clear how far this description applies to more general classes of flows. This problem is discussed further in the next article.

As an alternative to the instability theory to explain the conflict between experiment and potential flow theory, it has been proposed that

F,13 · *CONFLICTS BETWEEN THEORY AND EXPERIMENT*

the error lies in the neglect of viscosity in our theory. For example, the difference between theory and experiment might be due to the presence of the boundary layer. In support of this idea, it has been pointed out that the smooth deceleration can be thought of as the result of effects carried rearward by the family of Mach waves originating farther forward, as sketched in Fig. F,13a, and that a distortion to the contour, as might be caused by a boundary layer, would suffice to cause an envelope

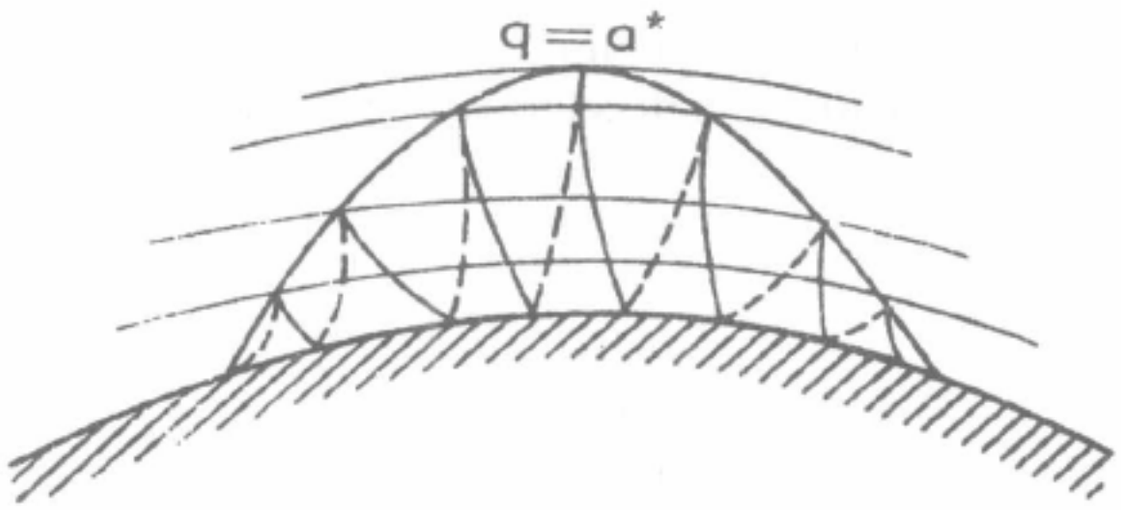

Fig. F,13a. Structure of local supersonic region.

of waves, as in Fig. F,13b. Such a discontinuity, of course, marks the breakdown of potential flow, and the pattern must be replaced by one involving a shock. But this would imply that a slightly different body, producing the Mach waves of Plate F,13a outside of its boundary layer, would permit smooth potential flow. This proposal hardly seems adequate to explain the complete absence of flows of this type in experiments.

Moreover, if this explanation is correct, it should be possible to achieve shockless mixed flows experimentally with the aid of boundary

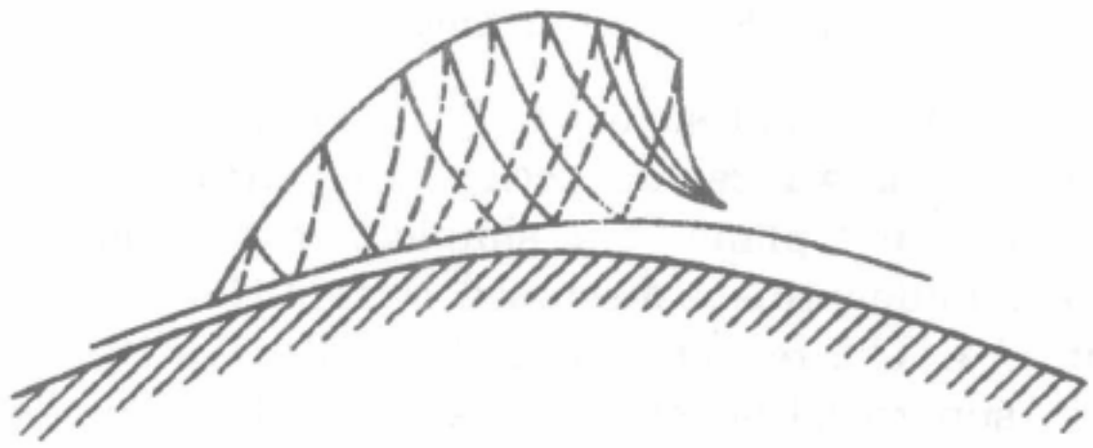

Fig. F,13b. The distortion of transonic flow by a boundary layer.

layer removal. It seems important to decide whether or not the inviscid potential flow itself has any peculiarities that would make it impossible.

A third proposal has been advanced to explain the discrepancy; namely, the smooth potential flows exist, even theoretically, only for certain special boundary shapes. If these are, in fact, special flows without neighboring solutions for slightly different boundaries, their nonappearance in nature would be explained, for real boundaries are always slightly different from ideal ones. The boundary layer would also consti-

tute a deviation from the ideal special shape; hence, this proposal is not completely unrelated to the preceding one.

This suggestion, like the instability theory, has a parallel in channel theory, where it can easily be shown that, due to multiple reflections from channel walls, any small geometrical deviation from an ideal transonic diffuser shape must lead to large alterations of the flow pattern. The theory of nonexistence of neighboring solutions is discussed briefly in Art. 15.

We have already pointed out that there would be practical advantages to achieving smooth transonic deceleration in practice. Furthermore, it is

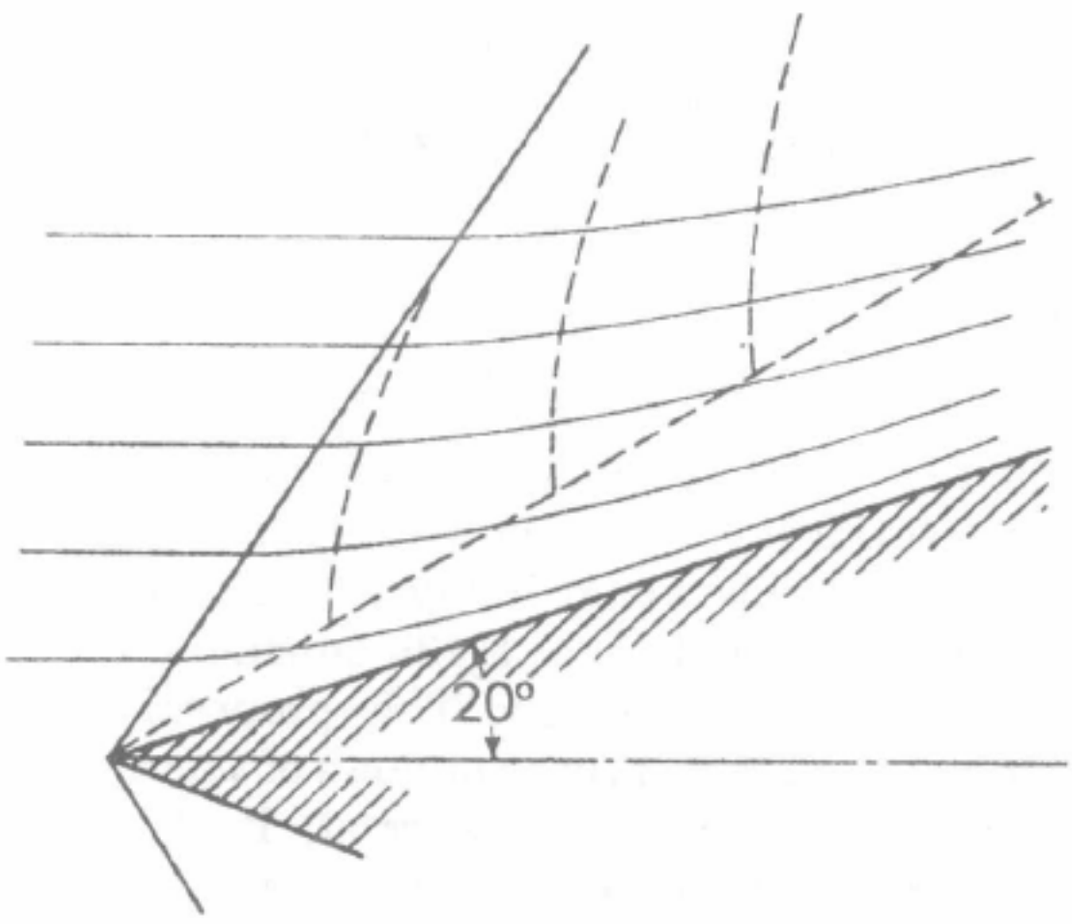

Fig. F,13c. Smooth transonic flow over a cone.

important to remember that such steady decelerations through the sonic speed, without shock waves, do occur in experiment in several cases wherein the flow is not plane. The simplest case is that of flow past a yawed infinite cylinder; this is discussed, within the limitations of linearized theory in C,4. The reader can easily verify that the same principle of solution by superposition of plane and axial flows is valid without linearization, and that extensive supersonic regions are possible without appearance of any shocks. This is confirmed by experiment.

Another famous example of isentropic compression from supersonic to subsonic speeds is afforded by the right circular cone solutions discussed in H,17–H,19; in certain ranges of Mach number and cone angle, there is supersonic flow behind the conical shock wave that is subsequently decelerated isentropically to subsonic speeds (Fig. F,13c). The existence of this flow has been well confirmed by experiment. To be sure, the exactly conical flow postulated in H,17–H,19 cannot be achieved in experiment because of the finite dimensions of the models tested. Never-

theless, the results [*68,69*] clearly show that for a given cone angle there is a range of Mach numbers for which there is no appreciable deviation from conical conditions near the tip of the cone, and the shock-free deceleration discussed here is observed. Consequently, this case of cone flow stands as evidence that isentropic irrotational deceleration through the sonic speed is not always impossible or unstable.

F,14. Theory of Stability of Transonic Flows. An approximate theory of the propagation of one-dimensional unsteady disturbances in a transonic decelerating channel flow has been given by Kantrowitz [*48*] and is discussed in III,C,7. In briefest outline, Kantrowitz's method is as follows: The histories of expansion and compression disturbances (pulses) originating downstream of a linearly decelerating sonic region are traced by means of the equations for one-dimensional unsteady isentropic flow. It is found that such disturbances are deformed as they propagate upstream, and that the disturbances tend to collect in the sonic region. Actually, the deformation of the pulse shape causes weak shock waves to form, either at head front or rear of the pulse. Expansion pulses, which terminate in shock waves at their rear, are subsequently "consumed" by their own shock waves, while compression pulses, which have shock fronts, grow in strength as their shock fronts progress into the supersonic region. Ultimately, in a real channel, they would destroy the supersonic flow, converting it into subsonic flow.

Although this is an approximate theory, since the isentropic process of deformation and propagation and nonisentropic shock processes are treated separately, it probably provides a correct explanation of the instability of channel flows. A more elaborate treatment of similar questions has been given by Meyer [*49*], who arrives at substantially the same conclusions.

It is desirable to carry out analogous studies relating to two-dimensional flows involving isentropic acceleration and deceleration. There is an obvious difference between such flows and the quasi-one-dimensional channel flows treated by Kantrowitz; viz., the propagation of disturbances in the curved nonuniform flow field must be essentially more complex than that of his one-dimensional pulses in a channel. It is surely possible that the lateral propagation in such nonuniform field might provide just the dissipative mechanism required to stabilize the flow under some circumstances.

Such a study has been made by Kuo [*50*] for thin cylinders. Let the velocity potential of the flow be

$$\phi(x, y, t) = \Phi(x, y) + \varphi(x, y, t) \tag{14-1}$$

where $\varphi(x, y, t)$ denotes the potential of the small transient disturbance superimposed on the steady transonic flow $\Phi(x, y)$. Now, substitution of

F · *PLANE POTENTIAL FLOWS*

Eq. 14-1 into the differential equation in III,A, Eq. 9-8 for isentropic, irrotational, unsteady flow, even neglecting second order terms in $\varphi(x, y, t)$, results in a linear partial differential equation with variable coefficients whose solution cannot readily be expressed in a form convenient for the present investigation. Moreover, this linearization is questionable, since the processes under study may be expected to exhibit typically nonlinear behavior in the neighborhood of the sonic speed.

To avoid these difficulties, we restrict ourselves to such cases that the steady flow itself, represented by $\Phi(x, y)$, differs only slightly from a parallel stream, and therefore a perturbation potential $\Phi'(x, y)$ satisfies the Kármán-Guderley nonlinear approximation (A,9 and D,32,33), at least in the region close to the sonic lines. This assumption determines the relative orders of magnitude of the derivatives of $\Phi'(x, y)$ in the differential equation, in terms of the body thickness parameter τ. Kuo also draws analogous conclusions regarding the derivatives of $\varphi(x, y, t)$, and extends them to the time derivatives. Since the sonic region is most critical, and since the interesting disturbances travel slowly in this region, he assumes that the disturbances take on the character typical of sonic flow; i.e. their space derivatives have the same relative orders of magnitude as those of $\Phi'(x, y)$. This leads to a conclusion about the time derivatives; it turns out that there is only one possibility here that gives a reasonable result for the nonstationary flow. The differential equation can now be simplified greatly by neglecting higher order terms, and the result is

$$(\gamma + 1)(\Phi'_x + \varphi_x)\varphi_{xx} + 2\varphi_{xt} + (\gamma + 1)\Phi'_{xx}\varphi_x = \varphi_{yy} - (\gamma + 1)\Phi'_{xx}\varphi_t - \varphi_{tt} \quad (14\text{-}2)$$

where now Φ' and φ and also the coordinates x, y, and t have been made dimensionless in terms of a^* and a characteristic length l.

It is likely that the disturbances present in such a flow have their origin in a boundary layer or wake farther downstream. Since the flow is nearly parallel and close to sonic, such disturbances will be approximately plane waves propagating upstream when they arrive in the critical area. Furthermore, the process of steepening, in Riemann's sense, described just above, will long since have converted the disturbances to the characteristic triangular pulses considered by Kantrowitz. This is the type of disturbance considered by Kuo, i.e. a triangular pulse propagating from the rear, with a shock at its head (compression pulse) or tail (expansion pulse), and with velocity dropping off linearly to zero behind or before the shock. The boundary condition at the solid wall requires that the perturbation velocity always be parallel to the wall contour, which is approximated as parabolic in the sonic region.

The simplifications made are sufficient to permit a solution $\varphi(x, y, t)$ for the sonic region, provided Φ'_x is approximated as varying linearly with

F,15 · *NONEXISTENCE OF SMOOTH TRANSONIC FLOWS*

both x and y. The solution satisfies Eq. 14-2 and the wall boundary condition, and has the form required for a triangular pulse. It contains two arbitrary constants, which can be replaced in terms of the initial form and strength of the pulse. The pulse strength drops off linearly with distance normal to the surface. The solution permits the history of a pulse to be followed as it propagates into the sonic region. It is found that expansion pulses always decay to sound waves, whereas compression pulses decay as they propagate in accelerating sonic flow but grow in decelerating sonic flow.

As a consequence, Kuo concludes that smooth transonic plane flow is dynamically unstable to upstream-moving compression pulses.

Since this result is the same as Kantrowitz's, mentioned above, the question arises whether Kuo has succeeded in introducing the typically two-dimensional character of the flow, or whether his approximations have actually been equivalent to reducing the problem essentially to the one-dimensional one. The latter possibility seems to exist, both in the thin-body approximations, which emphasize the streamwise derivatives, and in the very special kind of pulse shape treated. Surely, the theory is a rough one and involves a combination of mathematical and physical approximations whose impact on the final conclusions is difficult to assess. It is our suggestion that this investigation be considered as an initial step only, and that the question of stability of highly curved transonic potential flows be recognized as still open to question.

F,15. Theory of Nonexistence of Smooth Transonic Flows. The suggestion has already been made above that the smooth transonic flows calculated by the hodograph technique may be exceptional cases pertaining to particular ideal boundary shapes, and that they have no neighboring solutions for slightly different boundaries as would necessarily exist in nature.[7] In favor of this theory it is argued that the effect on the flow pattern of a small alteration of the boundary is very much different in supersonic than in subsonic flow.

Consider, for example, the case sketched in Fig. F,15a, which is taken from a paper by Busemann [*51*]. It is supposed that there exists a smooth transonic flow over the original smooth boundary, and the flow past a slightly altered boundary, having a symmetric depression at the center, is to be studied. Since the local flow is supersonic, the effects of this alteration, in the new steady flow pattern, will be confined to an "alley" leading to the sonic curve, from which point it is reflected back to the body, and so forth, as sketched. But according to this process it finally

[7] This "theory of nonexistence' may even be an alternative explanation of a situation that is unstable in the sense of the preceding article; that is, the two phenomena may go hand in hand, as they do in the case of the decelerating transonic nozzle (see below).

affects the nearly sonic flow toward the rear, and we know that the pressure, density, and speed increments will be magnified in such a region. Thus a small change of the boundary shape must produce a large change in the flow pattern: i.e. there is no neighboring solution. Substantially the same argument has been put forth by Frankl [*52*].

All this is quite analogous to the case of decelerating channel flow. It is easy to draw up a channel for smooth deceleration of supersonic flow,

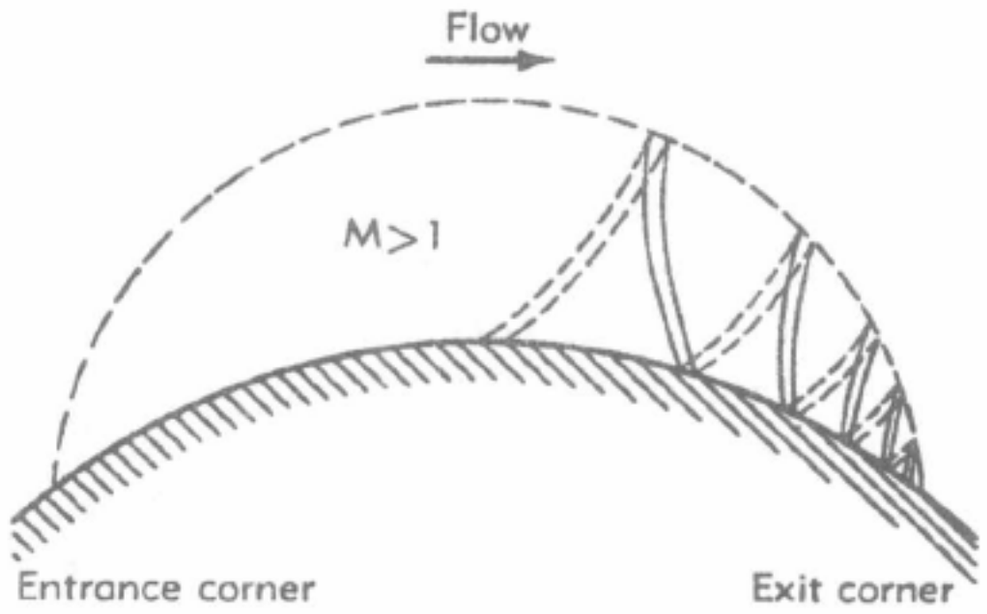

Fig. F,15a. Sketch showing the unsymmetric disturbance pattern.

through sonic, to subsonic; in fact, the channel is simply a Laval nozzle in reverse (Fig. F,15b). But the flow is unreal because there is no neighboring solution. A slight change of the contour at A produces violent effects at B. The real flow is the one involving a shock wave.

Another parallel is afforded by a familiar argument in statistical thermodynamics. An ordinary motion of the molecules of a gas, with increasing entropy, would produce decreasing entropy if followed in

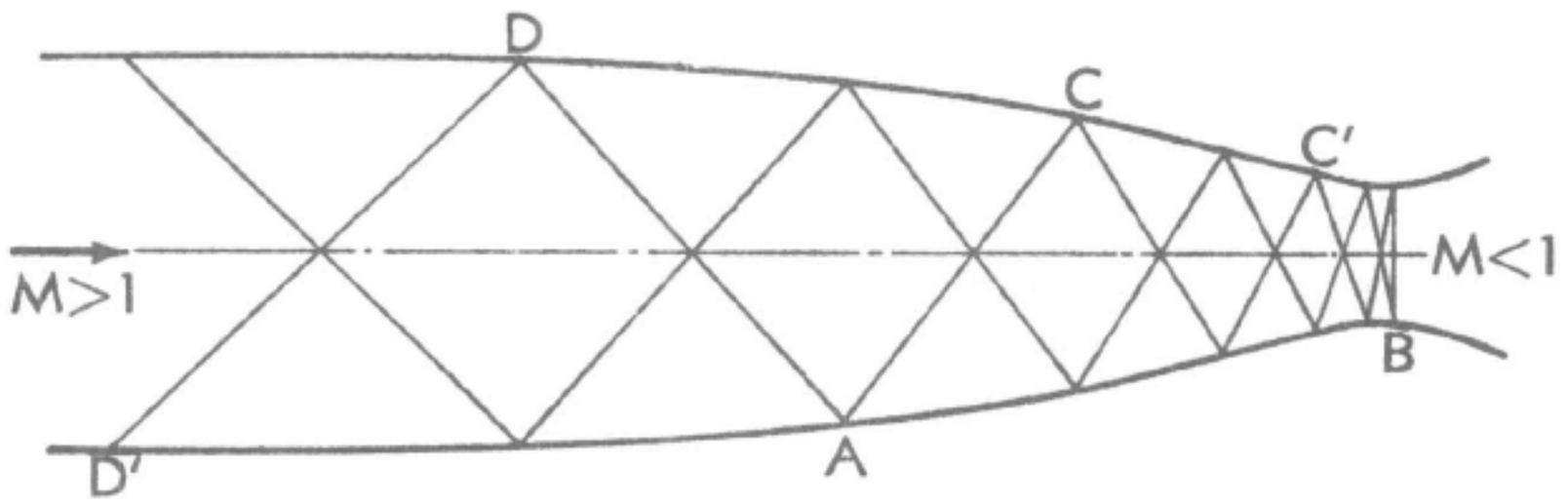

Fig. F,15b. Sketch showing reversed Laval nozzle for deceleration of supersonic flow to subsonic.

reverse; but again, the reversed motion is unreal because there is no neighboring solution.

Thus, Busemann's explanation is certainly very plausible. It would be indisputable if the perturbation at the sonic curve did not actually affect the whole flow pattern through the subsonic flow, but of course it does. To carry along the channel analogy, the trouble at B (Fig. F,15b)

can be avoided by a small alteration at C or C', or by an alteration upstream, as at D or D', which would cancel the effect at A. It is possible that the integrated effects of the disturbances produced in the subsonic flow where the "alleys" reach the sonic curve are just sufficient to modify the upstream part of the flow and to cancel the large effect of the boundary change.

Thus the correctness of Busemann's and Frankl's conjectures can only be ascertained by more detailed calculation. An attempt in this direction has been provided by Busemann and Guderley [*53*]. They consider a

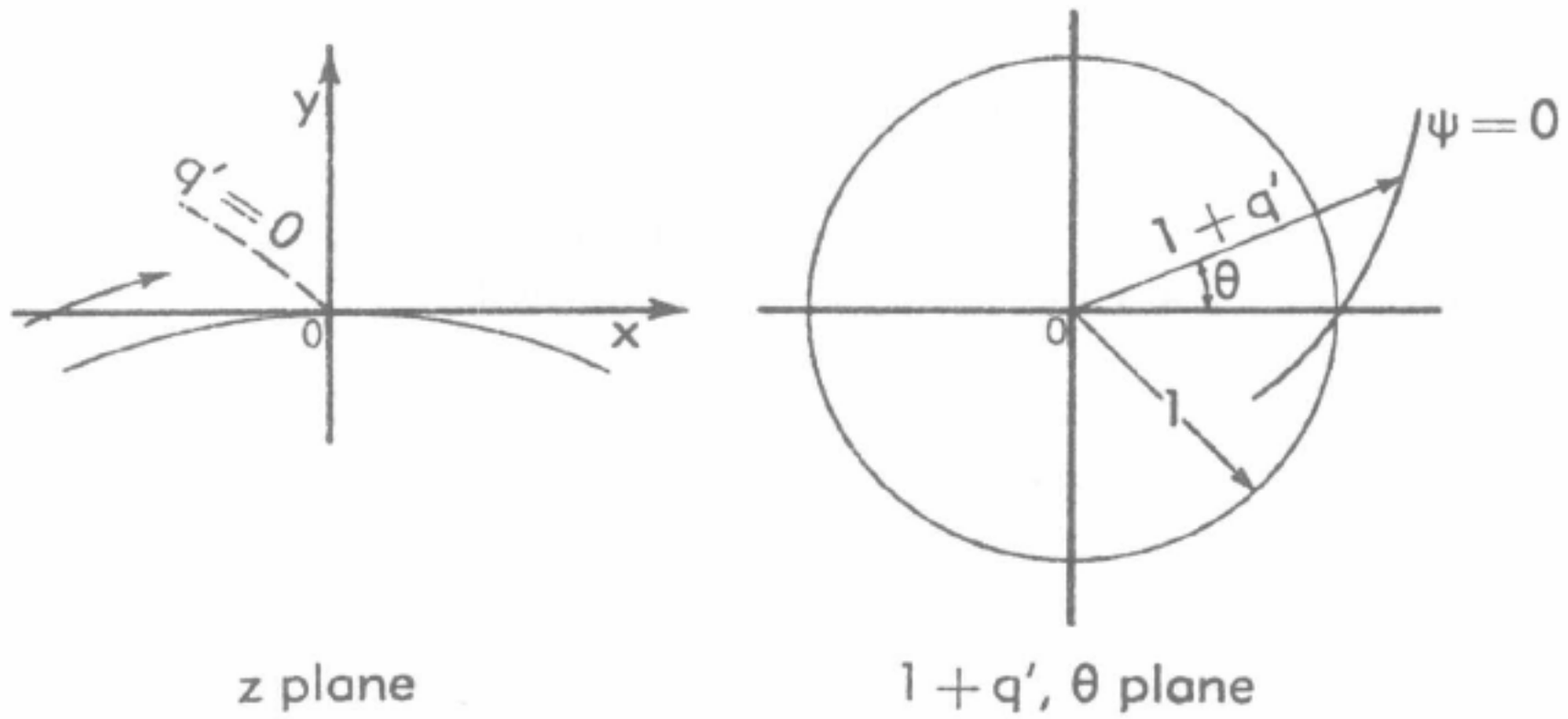

Fig. F,15c. Diagram showing the relationship between the x, y and q', θ planes.

known plane smooth transonic flow, described in the hodograph plane by a transformed potential function $\chi^{(1)}(q, \theta)$. Assuming that the flow speed is everywhere near sonic, it is convenient to use the coordinates q', θ where q' denotes $q/a^* - 1$. The approximate form assumed by Eq. 4-2 is then

$$\chi_{q'q'} - (\gamma + 1)q'\chi_{q'} - (\gamma + 1)q'\chi_{\theta\theta} = 0 \qquad (15\text{-}1)$$

It is assumed that $\chi^{(1)}(q', \theta)$ satisfies this equation.

Let the coordinates be orientated so that $q' = 0$ and $\theta = 0$ correspond to $x = 0$ and $y = 0$ on the surface of the body (Fig. F,15c). If the basic flow is perturbed by an infinitesimal amount $\chi^{(2)}(q', \theta)$, the velocity at any point in the field will be altered by an amount $(\Delta q', \Delta\theta)$. The corresponding displacement of any point in the physical plane originally specified by q' and θ is calculated by means of the coordinate functions (2-12)

$$\Delta x = \chi^{(1)}_{q'q'}\Delta q' + (\chi^{(1)i}_{q'\theta} - \chi^{(1)}_{\theta\theta})\Delta\theta + \chi^{(2)}_{q'}$$
$$\Delta y = (\chi^{(1)}_{q'\theta} - \chi^{(1)}_{\theta})\Delta q' + (\chi^{(1)}_{q'} + \chi^{(1)}_{\theta\theta})\Delta\theta + \chi^{(2)}_{\theta}$$

where both q' and θ can be assumed small. But, as we are fixing our attentions on a fixed point in the physical plane, the displacement must be

zero, and the disturbance velocity at the corresponding point can be determined in terms of $\chi^{(1)}$ and $\chi^{(2)}$, namely

$$\Delta q' = D^{-1}[-(\chi^{(1)}_{\theta\theta} + \chi^{(1)}_{q'})\chi^{(2)}_{q'} + (\chi^{(1)}_{q'\theta} - \chi^{(1)}_{\theta})\chi^{(2)}_{\theta}]$$
$$\Delta\theta = D^{-1}[(\chi^{(1)}_{q'\theta} - \chi^{(1)}_{\theta})\chi^{(2)}_{q'} - \chi^{(1)}_{q'q'}\chi^{(2)}_{\theta}] \tag{15-2}$$

where

$$D = \chi^{(1)}_{q'q'}(\chi^{(1)}_{\theta\theta} + \chi^{(1)}_{q'}) - (\chi^{(1)}_{q\theta} - \chi^{(1)}_{\theta})^2$$

In a small neighborhood of the origin, the potential $\chi^{(1)}$ is assumed to be of the form

$$\chi^{(1)} = -Rq'\theta + R\epsilon\theta^2 + \frac{\gamma+1}{6} R\epsilon q'^3 + \cdots \tag{15-3}$$

where K is the arbitrary radius of curvature at the sonic point and ϵ is a constant. Upon substitution of this form in Eq. 15-2, there result, approximately

$$R\Delta q' = \epsilon\chi^{(2)}_{q'} + \chi^{(2)}_{\theta}$$
$$R\Delta\theta = \chi^{(2)}_{q'} + (\gamma+1)\epsilon q'\chi^{(2)}_{\theta} \tag{15-4}$$

with

$$D \cong -R^2$$

Furthermore, from Eq. 15-3 and the coordinate functions, we obtain as boundary condition an approximate relation between q' and θ for points on the surface near the sonic point (origin)

$$q' \cong \epsilon\theta, \qquad |q'| \ll 1 \tag{15-5}$$

Having thus established a relationship between the change of velocity and the perturbation potential Eq. 15-4, Busemann and Guderley formulate, besides more general ones, two simple boundary-value problems in conjunction with Eq. 15-5. First, if the boundary in the neighborhood of the sonic line is rigid, then when $q' = \xi_0\epsilon\theta$

(a) $$\Delta\theta = 0 \tag{15-6}$$

where ξ_0 is a constant.

Secondly, if the boundary is soft, like a boundary layer, then when $q' = \xi_0\epsilon\theta$

(b) $$\Delta q' = 0 \tag{15-7}$$

The problem remaining is to find a solution $\chi^{(2)}(q', \theta)$ satisfying Eq. 15-1 and condition 15-6, and corresponding to some small alteration of the boundary shape in the supersonic region. Busemann and Guderley claim that it is impossible to find any such $\chi^{(2)}(q', \theta)$ that is finite at the origin, in any case where a disturbance persists downstream of the last boundary alteration (i.e. excluding the "cancellation" possibility mentioned in connection with Fig. F,15b above). To demonstrate this,

they assume their asymptotic solution in the form

$$\chi^{(2)} = \theta^n f(\xi) \sin\bar{\theta} + \frac{\gamma+1}{3}\theta^{n-\frac{1}{2}}\epsilon^{-\frac{1}{2}}q'^3 f(\xi)\cos\bar{\theta} + \frac{4n+1}{6}\theta^{n-\frac{1}{2}}\epsilon^{\frac{1}{2}}q' f'(\xi)\cos\bar{\theta} \quad (15\text{-}8a)$$

where $f(\xi)$ is a solution of the equation

$$f''(\xi) + (\gamma+1)\xi f(\xi) = 0 \quad (15\text{-}8b)$$

with $f(-\infty) = 0$, $\xi = q'/\epsilon\theta$, and $\bar{\theta} = 2/\epsilon^{\frac{1}{2}}\theta^{\frac{1}{2}}$; thus the boundary corresponds to $\xi = \xi_0$. The constant n is to be determined by boundary condition (a) or (b). To satisfy these conditions they select $n = -\frac{1}{4}$ in both cases and specify for the values of $f(\xi)$ at the boundary either (a) $f'(\xi_0) = 0$ or (b) $f(\xi_0) = 0$. In either case, the disturbance velocity $\Delta q'$ becomes infinite at the origin, and it is concluded that any small change of flow pattern in the supersonic region must involve a strong singularity where the sonic line meets the body surface.

Subsequently, Guderley [*54*] continued the analysis, using a series solution in place of Eq. 15-8a, attempting to provide a solution valid over a greater range of speed. The analysis is much more complex, but the same asymptotic singularity appears at the sonic point and his conclusions are therefore unchanged.

In criticism of Busemann's and Guderley's theory, it may be argued that they have not proved beyond doubt that nonsingular solutions of the boundary-value problem of the perturbed flow do not exist. The asymptotic form of Eq. 15-8a, as well as Guderley's asymptotic series, seems very special. There are indications that families of finite solutions that satisfy Busemann's and Guderley's problem, at least locally, can be found. It is also disturbing that their solution $\chi^{(2)}(q', \theta)$ is singular at both accelerating and decelerating sonic points. Since we do not expect any large disturbances at the upstream accelerating sonic point, nor observe any such disturbances in schlieren photographs, it seems possible that the whole solution of Eq. 15-8a should be rejected as physically inadmissible, removing the trouble at the downstream point as well. Busemann appeals to viscous effects to resolve this difficulty.

From a broader viewpoint, it is difficult to reconcile any theory of nonexistence of solutions with the fact that numerous continuous transonic solutions have been calculated for quite arbitrary boundary shapes by approximate methods. There are, for example, the results of Taylor [*29*] and Görtler [*67*] for the hyperbolic nozzle, Kaplan's results [*55*] for flow over a bump (see also E,2), and Emmons' numerical work by the relaxation method [*56*]. All of these show smooth transonic flows with acceleration and subsequent deceleration through the speed of sound, and in all three cases the boundary shapes were predetermined for all

Mach numbers. Although these are only approximate methods, it seems very likely that nonexistence of exact solutions would cause extreme difficulties in the calculations.

Another attack on the question of nonexistence of solutions for arbitrary boundaries is being made by Kaplan [*57*], who works directly with the nonlinear equation in the physical plane and seeks solutions in series form. His aim, it appears, is not to provide additional approximate flow patterns but to determine the convergence of the solutions in the transonic regime, and thus to answer the questions of this article.

The conclusion to be drawn at this writing appears to be the following: The argument presented by Busemann (Fig. F,15a) is surely plausible from the physical viewpoint. Nevertheless, his conjecture has not been convincingly proved in a mathematical way, possibly because the formulation of the problem has been inadequate.

F,16. Properties of the Hypergeometric Functions. For use in the present section, certain analytic properties of $F_\nu(\tau)$ and $\bar{F}_\nu(\tau)$ are required. For easy reference they are presented as a series of lemmas, each followed by a demonstration, which may be skipped over by readers who are not concerned with mathematical detail.

(i) *If* $\nu > 0$ and $0 \leqq \tau < \tau^*$, $F_\nu(\tau) > 0$ [*2,60*].

Let $\psi_\nu(\tau) = \tau^{\nu/2}F_\nu(\tau)$ and $d\eta = \tau^{-1}(1-\tau)^\beta d\tau$; from Eq. 3-1,

$$\frac{d^2\psi_\nu}{d\eta^2} = \nu^2 \frac{1-\alpha^2\tau}{4(1-\tau)^{\alpha^2}}\psi_\nu$$

If $\tau < \tau^*$, $d^2\psi_\nu/d\eta^2$ and ψ_ν are of the same sign. But in the neighborhood of $\tau = 0$, $\psi_\nu > 0$ and $\psi_\nu(0) = 0$ as $\nu > 0$; hence $d^2\psi_\nu/d\eta^2 > 0$. Therefore, for small τ the slope $d\psi_\nu/d\eta$ or $d\psi_\nu/d\tau$ will continue to increase until $\tau = \tau^*$ is reached. Since $\tau^{\nu/2} > 0$, it follows that $F_\nu(\tau) > 0$.

(ii) *In* $|\tau| < 1$, $F_\nu(\tau)$ *is an analytic function of* ν, *with simple poles at* $\nu = -n$, n *being a positive integer greater than 1* [*5,60*].

From Eq. 3-5, $F_\nu(\tau)$ is an analytic function of τ and ν if $|\tau| < 1$ and $\nu \neq -n$. When $\nu = -n$ and $n > 1$, $F_\nu(\tau)$ can be written as

$$F_\nu(\tau) = F_\nu^{(1)}(\tau) + \frac{1}{\nu+n}F_\nu^{(2)}(\tau)$$

where

$$F_\nu^{(1)}(\tau) = 1 + \frac{a_\nu b_\nu}{\nu+1}\tau + \cdots + \frac{a_\nu(a_\nu+1)\cdots(a_\nu+n-2)b_\nu(b_\nu+1)\cdots(b_\nu+n-2)}{(\nu+1)(\nu+2)\cdots(\nu+n-1)}\frac{\tau^{n-1}}{(n-1)!}$$

$$F_\nu^{(2)}(\tau) = \frac{a_\nu(a_\nu+1)\cdots(a_\nu+n-1)b_\nu(b_\nu+1)\cdots(b_\nu+n-1)}{(\nu+1)(\nu+2)\cdots(\nu+n-1)n!}\tau^n \left[1 + \frac{(a_\nu+n)(b_\nu+n)}{(\nu+n+1)(n+1)}\tau + \cdots\right]$$

This shows that at $\nu = -n$, both $F_\nu^{(1)}$ and $F_\nu^{(2)}$ remain regular. Therefore, the points $\nu = -n$ are simple poles of $F_\nu(\tau)$. The residue is evidently

$$\lim_{\nu \to -n} (\nu + n) F_\nu(\tau) = F_n^{(2)}(\tau)$$

where

$$F_n^{(2)}(\tau)$$

$$= \frac{a_{-n}(a_{-n}+1)\cdots(a_{-n}+n-1)b_{-n}(b_{-n}+1)\cdots(b_{-n}+n-1)}{(-1)^n(n-1)!n!}$$

$$\tau^n F(a_{-n}+n, b_{-n}+n; n+1; \tau)$$

Since

$$(a_{-n}+n)+(b_{-n}+n) = a_n + b_n$$

and

$$(a_{-n}+n)(b_{-n}+n) = a_n b_n$$

we can take

$$a_{-n}+n = a_n, \qquad b_{-n}+n = b_n$$

As a result, we have

$$F_n^{(2)}(\tau) = -h_n \tau^n F_n(\tau) \tag{16-1}$$

where, since $b_n < 0$,

$$h_n = \frac{\Gamma(a_n)\Gamma(n+1-b_n)}{\Gamma(a_n-n)\Gamma(1-b_n)(n-1)!n!} > 0 \tag{16-2}$$

It is noted that when $n = 1$, $a_1 = 1$, $h_1(\gamma) \equiv 0$. Furthermore, when $\gamma = -1$ (a case discussed in Art. 5), $a_n = (n+1)/2$ and $b_n = -n/2$; then h_n will involve factors $\sin[\pi(n+1)/2] \sin(\pi n/2)$. Hence $h_n \equiv 0$ in this special case.

(iii) *If the negative integers in the ν plane are excluded, then as $|\nu| \to \infty$ [19,60,63]*

$$F_\nu(\tau) = f(\tau)[T(\tau)]^\nu \left[1 + O\left(\frac{1}{\nu}\right)\right],$$

$$F_{-\nu}(\tau) = f(\tau)[T(\tau)]^{-\nu} \left[1 + O\left(\frac{1}{\nu}\right)\right], \qquad \tau < \tau^* \tag{16-3}$$

where $q^{-2\nu}F_{-\nu}(\tau)$ denotes the second solution and

$$f(\tau) = (1-\tau)^{\alpha^2/4}(1-\alpha^2\tau)^{-\frac{1}{4}}$$

$$T(\tau) = \frac{2[\alpha(1-\tau)^{\frac{1}{2}} + (1-\alpha^2\tau)^{\frac{1}{2}}]^\alpha}{(1+\alpha)^\alpha[(1-\tau)^{\frac{1}{2}} + (1-\alpha^2\tau)^{\frac{1}{2}}]}$$

$$\alpha^2 = \frac{\gamma+1}{\gamma-1}$$

Also, $\tau^* < \tau < 1$

$$F_\nu(\tau) = f(\tau)[T(\tau)]^\nu \cos\left(\nu\omega - \frac{\pi}{4}\right)\left[1 + O\left(\frac{1}{\nu}\right)\right]$$

$$F_{-\nu}(\tau) = \frac{1}{2} f(\tau)[T(\tau)]^{-\nu}\left[\cos\left(\nu\omega + \frac{\pi}{4}\right) + \cot \nu\pi \sin\left(\nu\omega + \frac{\pi}{4}\right)\right] \qquad (16\text{-}4)$$

$$\left[1 + O\left(\frac{1}{\nu}\right)\right]$$

where

$$f(\tau) = 2(1-\tau)^{\alpha^2/4}(\alpha^2\tau - 1)^{-\frac{1}{4}}$$

$$T(\tau) = r\tau^{-\frac{1}{2}}$$

$$r = 2(\alpha-1)^{\frac{\alpha-1}{2}}(\alpha+1)^{-\frac{\alpha+1}{2}} \qquad (16\text{-}4a)$$

$$\omega(\tau) = \alpha \tan^{-1}\frac{1}{\alpha}\sqrt{\frac{\alpha^2\tau - 1}{1-\tau}} - \tan^{-1}\sqrt{\frac{\alpha^2\tau - 1}{1-\tau}}$$

Let $F_\nu(\tau) = \tau^{-\frac{\nu+1}{2}}(1-\tau)^{\frac{1}{2(\gamma+1)}} g_\nu(\tau)$; then Eq. 3-2 reduces to

$$g_\nu'' - \left[\nu^2\sigma(\tau) - \sigma + \frac{2\gamma - 1}{4(\gamma-1)(1-\tau)^2}\right] g_\nu = 0 \qquad (16\text{-}5)$$

where

$$\sigma(\tau) = \frac{1 - \alpha^2\tau}{4\tau^2(1-\tau)}$$

When $|\nu|$ is large, by excluding the negative real axis, we deduce from Eq. 16-5 that

$$g_\nu = \sigma^{-\frac{1}{4}} e^{\nu\zeta(\tau)}\left[1 + \frac{g_1}{\nu} + \cdots\right], \qquad \alpha^2\tau < 1$$

where $\zeta = \int^\tau \sigma^{\frac{1}{2}} d\tau$. Evaluating the integral ζ and assuming, for the dominating terms, $g_\nu(0) = 1$ we obtain Eq. 16-3.

When $\tau^* < \tau < 1$, ζ becomes a purely imaginary quantity and the form of representation (16-3) fails. In that case, the asymptotic solutions for both regions $\tau < \tau^*$ and $\tau^* < \tau < 1$ are discontinuous at $\tau = \tau^*$. The method of continuation of the solution from $\tau < \tau^*$ to $\tau > \tau^*$ is generally quite elaborate. In the present problem, $\sigma(\tau)$ has a simple zero at $\tau = \tau^*$, and a technique originally due to Jeffreys proves to be convenient. According to this, Eq. 16-5, for large ν, is solved exactly at $\tau = \tau^*$ and hence reduces to the well-known Stokes equation with solution involving Bessel functions of one-third order. By carrying out this procedure, we find a phase constant of $-\pi/4$ and also a multiplicative factor of 2 in going over from $\tau < \tau^*$ to $\tau > \tau^*$. For details the reader is referred to the Jeffreys' book [*61*, p. 488].

(iv) *If* $0 < \tau < \tau^*$ *and* $\nu \neq -n$, *n being integer* [*5,60*]

$$[T(\tau)]^{-\nu}F_\nu(\tau) = f(\tau) - \sum_2^\infty \frac{h_m \tau^m T^m F_m(\tau)}{\nu + m} \qquad (16\text{-}6)$$

From Lemma (ii), $F_\nu(\tau)$ has simple poles at $\nu = -n$, and from Lemma (iii), $|T^{-\nu}F_\nu(\tau)|$ is bounded on $|\nu| = n + \frac{1}{2}$ as $n \to \infty$. Then, by applying Mittag-Leffler's theorem,

$$T^{-\nu}F_\nu(\tau) = F_0(\tau) + \sum_1^\infty R_m \left(\frac{1}{\nu + m} - \frac{1}{m}\right)$$

where R_m is the residue of $T^{-\nu}F_\nu(\tau)$ at $\nu = -m$ and, since $|T^{-\nu}F_\nu(\tau)| \to f(\tau)$, we have

$$f(\tau) = F_0(\tau) - \sum_1^\infty \frac{R_m}{m}$$

Eliminating $F_0(\tau)$ and R_m by Eq. 16-1, we have Eq. 16-6.

To show that the series in Eq. 16-6 converges, we deduce from Eq. 16-2, for large m, that

$$|h_m| < M \left[\frac{(1+\alpha)^{\frac{\alpha+1}{2}}}{2(\alpha-1)^{\frac{\alpha-1}{2}}}\right]^{2m}$$

by means of the properties of $\Gamma(z)$ at large z, where M is a constant. The series is therefore dominated by

$$\sum_1^\infty \left[\frac{(\alpha+1)^{\frac{\alpha+1}{2}}}{2(\alpha-1)^{\frac{\alpha-1}{2}}} \tau^{\frac{1}{2}} T(\tau)\right]^{2m}$$

and therefore converges if $\tau^{-1}\tau^{\frac{1}{2}}T < 1$. It can be verified that the radius of convergence is the speed of sound $\tau = \tau^*$, for $\tau T^2 = \tau^2$ when $\tau = \tau^*$ (cf. Eq. 16-4).

(v) *If* $0 < \tau < \tau^*$ *and* $\nu > 0$ *and large* [*20*]

$$\xi_\nu(\tau) = \sqrt{\frac{1 - \alpha^2\tau}{1 - \tau}} + O\left(\frac{1}{\nu}\right) \qquad (16\text{-}7)$$

This follows directly from Eq. 16-3.

(vi) *When* $0 < \tau < \tau^*$, *the values of* $\nu(\tau)$ *for which* $F_\nu(\tau) = 0$ *can be written* $\nu_1, \nu_2, \nu_3, \ldots$, *where* $-(n+1) < \nu_n < -n$ [*60*].

For $0 < \tau < \tau^*$, $F_\nu(\tau) > 0$ from Lemma (i). Furthermore, by Lemma (ii), $F_{-1}(\tau) = 1 + \tau F_1\ (1, -\beta;\ 2;\ \tau)$, which is positive. But, we have, when $\nu + 2 > 0$,

$$F_\nu(\tau) \to -\infty \text{ as } \nu + 2 \to 0$$

according to Eq. 16-1. Hence $F_{\nu_2}(\tau) = 0$ and $-2 < \nu_2 < -1$. As soon as ν passes over to the other side of the pole $\nu = -2$, $F_{-2+\delta}(\tau) > 0$, $\delta > 0$, and $F_{-3+\delta}(\tau) < 0$; therefore $-3 < V_3 < -2$ and so on. From Eq. 16-6, when $|\nu_n| \to \infty$, we have, approximately

$$0 = T^{-\nu_n} F_\nu(\tau) \cong f(\tau) - \frac{h_n \tau^n T^n F_n(\tau)}{\nu_n + n} - \cdots$$

Therefore as $|\nu_n| \to \infty$

$$\nu_n \to -n + O(\epsilon^n) \tag{16-8}$$

where

$$\epsilon = r^{-2}\tau T^2 < 1$$

(vii) *For* $0 \leqq \tau < 1$ *and* $|\arg \nu| \leqq \pi$ *[30]*

$$\frac{(\nu/e)^\nu \chi_\nu(\tau)}{r^\nu \Gamma(\nu+1)} = J_\nu(\nu t)\left[Q(\tau) + \sum_\mu \frac{f_\mu(\tau)}{\nu - \mu}\right] \tag{16-9}$$

where $\chi_\nu(\tau) = \tau^{\frac{\nu}{2}} \tilde{F}_\nu(\tau)$ and $Q(\tau) = (1-\tau)^{\frac{1}{2} - \frac{\alpha^2}{4}} \left(\frac{t^2-1}{\alpha^2\tau - 1}\right)^{\frac{1}{4}}$. Here t is a continuous function of τ defined by

$$\omega' \equiv \sqrt{t^2-1} - \tan^{-1}\sqrt{t^2-1} = \omega(\tau) \tag{16-10}$$

and

$$f_\mu(\tau) = \frac{(\mu/e)^\mu \chi_\mu(\tau)}{r^n}\left[\frac{\partial}{\partial \nu}\Gamma(\nu+1)J_\nu(\nu t)\right]^{-1}_{\nu=\mu}$$

The summation in Eq. 16-9 is over the zeros of $J_\mu(\mu t)$.

In the first place, from Eq. 3-16 and 3-17 we can conclude that $\tilde{F}_\nu(\tau)$ behaves exactly the same as $F_\nu(\tau)$. Moreover, for $\tau > 1$ and large $|\nu|$ with $|\arg \nu| \leqq \pi$, $J_\nu(\nu t)$ possesses the representation *[40]*

$$J_\nu(\nu t) = \left(\frac{2}{\nu\pi\sqrt{t^2-1}}\right)^{\frac{1}{2}}\left[\cos\left(\nu\omega' - \frac{\pi}{4}\right) + O\left(\frac{1}{\nu}\right)\right]$$

and, similar to Eq. 16-4, we have, for $\alpha^2\tau > 1$

$$\chi_\nu(\tau) = \frac{2(1-\tau)^{\frac{1}{2}-\frac{\alpha^2}{4}}}{(\alpha^2\tau - 1)^{\frac{1}{4}}} r^\nu \cos\left(\nu\omega - \frac{\pi}{4}\right)\left[1 + O\left(\frac{1}{\nu}\right)\right]$$

These expressions together with the asymptotic expansions of $\Gamma(\nu+1)$ and Eq. 16-10 leads to

$$\frac{(\nu/e)^\nu \chi_\nu(\tau)}{r^\nu \Gamma(\nu+1) J_\nu(\nu t)} = Q(\tau) + O\left(\frac{1}{\nu}\right)$$

which can be easily verified from the asymptotic properties of $J_\nu(\nu t)$, $\Gamma(\nu+1)$, and $\chi_\nu(\tau)$. Now both $\chi_\nu(\tau)$ and $\Gamma(\nu+1)J_\nu(\nu t)$ have simple poles

F,17 · *CITED REFERENCES AND BIBLIOGRAPHY*

at $\nu = -n$, the poles of $(\nu/e)^{\nu}\chi_{\nu}(\tau)/r^{\nu}\Gamma(\nu+1)J_{\nu}(\nu t)$ are therefore the zeros of $\Gamma(\nu+1)J_{\nu}(\nu t)$. Consequently, the residue is

$$(\nu/e)^{\mu}\chi_{\mu}(\tau)r^{-\mu}\left[\frac{\partial}{\partial\nu}\Gamma(\nu+1)J_{\nu}(\nu t)\right]^{-1}_{\nu=\mu}$$

Then, from Mittag-Leffler's theorem, we immediately obtain Eq. 16-9.

Once this is established for $t > 1$ and $\alpha^2\tau > 1$, it is obvious that it is equally true for $t < 1$ or $\alpha^2\tau < 1$. In that case, the only change lies in the fact that the asymptotic representations of $\chi_{\nu}(\tau)$ and $J_{\nu}(\nu t)$ are exponential and ω', ω become purely imaginary.

(*viii*) *For* $0 \leqq \tau < 1$ *and* $\nu \to -n$, n *being a positive integer* [*30*],

$$\frac{\bar{h}_n r^n \Gamma(n)\chi_n(\tau)}{(n/e)^n} = J_n(nt)\left(Q - \sum_{\mu}\frac{f_{\mu}}{\mu+n}\right) \tag{16-11}$$

where

$$\bar{h}_n = \frac{n+1}{n-1}h_n$$

Replacing ν by $\nu e^{\pi i}$, and by virtue of $J_{-\nu}(ze^{\pi i}) = e^{-\nu\pi i}J_{-\nu}(z)$ we have

$$\frac{\Gamma(\nu)\sin\nu\pi\chi_{-\nu}(\tau)}{\pi r^{-\nu}(\nu/e)^{\nu}} = J_{-\nu}(\nu t)\left(Q - \sum_{\mu}\frac{f_{\mu}}{\mu+\nu}\right) \tag{16-12}$$

Now $\chi_{-\nu}(\tau)$ has simple poles at $\nu = n$ at which its residues are $\bar{h}_n\chi_n(\tau)$ and $J_{-n}(z) = (-1)^n J_n(z)$. Therefore, as $\nu \to n$, Eq. 16-12 reduces to Eq. 16-11.

F,17. Cited References and Bibliography.

Cited References

1. Riemann, B. Über die Fortpflanzung ebener Luftwellen von endlicher Schwingungsweite. *Abhandlungen d. Gesellschaft d. Wissenschaften zu Göttingen, Math.-Phys. Klasse 8*, 43–65 (1858–1859).
2. Chaplygin, S. A. On gas jets. *Sci. Annals Imp. Univ. of Moscow, Phys.-Math. Div. 21*, Moscow (1904). Also *NACA Technical Memorandum 1063*. 1944.
3. von Kármán, Th. Compressibility effects in aerodynamics. *J. Aero. Sci. 8*, 337–356 (1941).
4. Whittaker, E. T., and Watson, G. N. *A Course of Modern Analysis*. Cambridge Univ. Press, 1940.
5. Cherry, T. M. Flow of a compressible fluid about a cylinder. *Proc. Roy. Soc. A192*, 45–79 (1947).
6. Tsien, H. S. Two-dimensional subsonic flow of compressible fluids. *J. Aero. Sci. 6*, 399–407 (1939).
7. Lin, C. C. On an extension of the von Kármán-Tsien method to two-dimensional subsonic flows with circulation around closed profiles. *Quart. Appl. Math. 4*, 291–297 (1946–1947).
8. Bers, L. On a method of constructing two-dimensional subsonic compressible flows around closed profiles. *NACA Technical Note 969*. 1945.
9. Gelbart, A. On subsonic compressible flows by a method of correspondence. *NACA Technical Note 1170*. 1947.

F · *PLANE POTENTIAL FLOWS*

10. Christianovich, S. A., and Yuriev, I. M. Subsonic gas flow past a wing profile. *Prikladnaya Matematika i Mekhanika 11* (1947). Also *NACA Technical Memorandum 1250*. 1950.
11. Germain, P. Fluides compressibles. Étude directe du cas simplifié de Chaplygin. *C.R. Acad. Sci. Paris 223*, 532–534 (1946).
12. Tsien, H. S. Notes on Aerodynamics of Compressible Fluids. Mass. Inst. of Tech., Cambridge, 1948.
13. Ringleb, F. Exakte Lösungen der Differentialgleichungen einer adiabatischen Gasströmung, *ZAMM 20*, 185–189 (1940).
14. Temple, G., and Yarwood, J. Compressible flow in a convergent-divergent nozzle. *ARC Reports and Memoranda 2077*. 1947.
15. Taylor, G. I., and Sherman, C. F. A mechanical method for solving problems of flow in compressible fluids. *Proc. Roy. Soc. A121*, 194–217 (1928).
16. Frankl, F. On the problems of Chaplygin for mixed subsonic and supersonic flows *Bull. Acad. Sci. URSS 9*, 121–143 (1945). Also *NACA Technical Memorandum 1155*. 1947.
17. Guderley, G. Considerations of the structure of mixed subsonic-supersonic flow pattern. *Wright Field Report F-TR-2168-ND*. 1947.
18. Lighthill, M. J. Hodograph transformation in transonic flow. III. Flow round a body. *Proc. Roy. Soc. A191*, 352–369 (1947).
19. Tsien, H. S., and Kuo, Y. H. Two-dimensional mixed subsonic and supersonic flow of a compressible fluid and the upper critical Mach number. *NACA Technical Note 995*. 1946.
20. Kuo, Y. H. Two-dimensional irrotational transonic flows. *NACA Technical Note 1445*. 1948.
21. Guderley, G. On the compressible potential flow over a closed body. *Wright Field Report F-TR-2176-ND*. 1947.
22. Bergman, S. On two-dimensional flows of compressible fluids. *NACA Technical Note 972*. 1945.
23. Kuo, Y. H. Two-dimensional transonic flow past airfoils. *NACA Technical Note 2356*. 1951.
24. Cherry, T. M. Numerical solutions for compressible flow past a cylinder. *Council for Sci. and Ind. Res. Report A48*. Melbourne, 1948. Or *Proc. Roy. Soc. A196*, 32–36 (1949).
25 Cherry, T. M. Flow of a compressible fluid about a cylinder. *Proc. Roy. Soc. A196*. 1–31 (1949).
26. Bergman, S. Methods for determination and computation of flow patterns of a compressible fluid. *NACA Technical Note 1018*. 1946.
27. Bergman, S., and Greenstone, L. Numerical determination by use of special computational devices of an integral operator in the theory of compressible fluids, *J. Math. and Phys. 26*, 1–9 (1947).
28. Cherry, T. M. Relation between Bergman's and Chaplygin's methods of solving the hodograph equations. *Quart. Appl. Math. 9*, 91–94 (1951).
29. Taylor, G. I. The flow of air at high speeds past curved surfaces. *ARC Reports and Memoranda 1381*. 1930.
30. Cherry, T. M. Exact solutions for flow of a perfect gas in a two-dimensional Laval nozzle. *Proc. Roy. Soc. A203*, 551–571 (1950).
31. Tricomi, F. Sulle equazioni lineari derivate parziali del secondo ordine, di tipo misto, parts 1–7. *Memorie Reale Accad. Nazl. Lincei, classe sci. fis. mat. e nat. (ser. 5) 14*, 133–247 (1923). Also *Brown Univ. Transl. A9-T-26*.
32. von Kármán, Th. and Fabri, J. Écoulement transsonique à deux dimensions le long d'une paroi ondulée. *C.R. Acad. Sci. Paris 231*, 1271–1274 (1950).
33. Tomotika, S. and Tamada, K Studies on two-dimensional transonic flows of a compressible fluid. II. *Quart. Appl. Math. 8*, 127–136 (1950).
34. Guderley, G. and Yoshihara, H. The flow over a wedge profile at Mach number 1. *J. Aero. Sci. 17*, 723–735 (1950).
35. Guderley, G. Two-dimensional flow patterns with a free-stream Mach number close to one. *Wright Field Report F-TR-6343*. 1951.

F,17 · *CITED REFERENCES AND BIBLIOGRAPHY*

36. Cole, J. D. Drag of a finite wedge at high subsonic speeds. *J. Math. and Phys. 30*, 79–93 (1951).
37. Vincenti, W. G., and Wagoner, C. B. Transonic flow past a wedge profile with detached bow wave—details of analysis. *NACA Technical Note 2588*. 1951.
38. Tomotika, S., and Tamada, K. Studies on two-dimensional transonic flows of compressible fluid. I. *Quart. Appl. Math. 7*, 381–397 (1950).
39. Tomotika, S., and Tamada, K. Studies on two-dimensional transonic flows of compressible fluids. III. *Quart. Appl. Math. 9*, 129–147 (1951).
40. Watson, G. N. *A Treatise on the Theory of Bessel Functions*. Cambridge Univ. Press, 1945.
41. Craggs, J. W. The breakdown of the hodograph transformation for irrotational compressible fluid flow in two dimensions. *Proc. Camb. Phil. Soc. 44*, 360–379 (1948).
42. Tollmien, W. Grenzlinien adiabatischen Potentialströmungen. *ZAMM 21*, 140–152 (1941).
43. Friedrichs, K. O. On the non-occurrence of a limiting line in transonic flow. *Comm. on Pure and Appl. Math. 1*, 287–299 (1948).
44. Manwell, A. R. Note on hodograph transformation. *Quart. Appl. Math. 10*, 177–184 (1952).
45. Nikolsky, A. A., and Taganoff, G. I. Flow of a gas in a local supersonic zone and some conditions for the breakdown of potential flow. *Prikladnaya Matematika i Mekhanika 10*, 481–502 (1946). Also *Brown Univ. Trans. A9-T-17*. 1948.
46. Sears, W. R. Transonic potential flow of a compressible fluid. *J. Appl. Phys. 21*, 771–778 (1950).
47. Liepmann, H. W., Ashkenas, H., and Cole, J. D. Experiments in transonic flow. *Wright Field Technical Report 5667*. 1950.
48. Kantrowitz, A. The formation and stability of normal shock waves in channel flows. *NACA Technical Note 1225*. 1947.
49. Meyer, R. E. Waves of finite amplitude in ducts. *Quart J. Mech. Appl. Math. 5*, 257–291 (1952).
50. Kuo, Y. H. On the stability of two-dimensional smooth transonic flows. *J. Aero. Sci. 18*, 1–6 (1951).
51. Busemann, A. The drag problem at high subsonic speeds. *J. Aero. Sci. 16*, 337–344 (1949).
52. Frankl, F. I. On the formation of shock waves in subsonic flows with local supersonic velocities. *Prikladnaya Matematika i Mekhanika 11*, 199–202 (1947). Also *Brown Univ. Trans. F-TS-1223-IA*. 1949.
53. Busemann, A., and Guderley, G. The problem of drag at high subsonic speeds. *MOS Reports and Translations 184*. 1947.
54. Guderley, G. On the transition from a transonic potential flow to a flow with shocks. *Wright Field Report F-TR-2160-ND*. 1947.
55. Kaplan, C. The flow of a compressible fluid past a curved surface. *NACA Report 768*. 1943.
56. Emmons, H. W. The theoretical flow of a frictionless, adiabatic, perfect gas inside of a two-dimensional hyperbolic nozzle. *NACA Technical Note 1003* (1946).
57. Kaplan, C. On a solution of the nonlinear differential equation for transonic flow past a wave-shaped wall. *NACA Technical Note 2383*. 1951.
58. von Helmholtz, H. On discontinuous movements of fluids. *Phil. Mag. 36*, 337–346 (1868). Also *Monatsber. preussischen Akad. Wiss. Berlin*, 125 (1868).
59. Molenbroeck, P. Über einige Bewegungen eines Gases bei Annahme eines Geschwindigkeitspotentials. *Archiv. Math. und Phys., Grunert Hoppe, 9*, 157–195 (1890).
60. Lighthill, M. J. The hodograph transformation in transonic flow. II. *Proc. Roy. Soc. A191*, 341–351 (1947).
61. Jeffreys, H., and Jeffreys, B. S. *Methods of Mathematical Physics*. Cambridge Univ. Press, 1946.
62. Bateman, H. Notes on a differential equation which occurs in the two-dimensional motion of a compressible fluid and the associated variational problem. *Proc. Roy. Soc. A125*, 598–618 (1929).

F · *PLANE POTENTIAL FLOWS*

63. Cherry, T. M. Asymptotic expansions for the hypergeometric functions occurring in gas-flow theory. *Proc. Roy. Soc. A202*, 507–522 (1950).
64. Coburn, N. The Kármán-Tsien pressure-volume relation in the two-dimensional supersonic flow of compressible fluids. *Quart. Appl. Math. 3*, 106–116 (1945).
65. Lighthill, M. J. The hodograph transformation in transonic flow. I. Symmetric channels. *Proc. Roy. Soc. A191*, 323–341 (1947).
66. Morawetz, C. S., and Kolodner, I. On the non-occurrence of the limiting lines in transonic flow. *Comm. on Pure and Appl. Math. 6* (1953).
67. Görtler, H. Zum Übergang von Unterschall zu Überschallgeschwindigkeiten in Düsen. *ZAMM 19*, 325–337 (1939).
68. Taylor, G. I. and Maccoll, J. W. The air pressure on a cone moving at high speeds. II. *Proc. Roy. Soc. A139*, 298–311 (1933).
69. Solomon, G. E. Transonic flow past cone-cylinders. *Guggenheim Aeronautical Laboratory, California Institute of Technology*. 1953. Also *NACA Technical Note 3213*. 1954.
70. Stack, J., Lindsey, W. F., and Littell, R. E. The compressibility burble and the effect of compressibility on pressure and force acting on an airfoil. *NACA Report 646*. 1939.
71. Cherry, T. M. A transformation of the hodograph equation and the determination of certain fluid motions. *Trans. Roy. Soc. 245*, 583–624 (1953).

Supplementary Bibliography

Mathematical papers.

Bers, L., and Gelbart, A. On a class of differential equations in mechanics of continua. *Quart. Appl. Math. 1*, 168–188 (1943).
Bers, L. On the continuation of a potential gas flow across the sonic line. *NACA Technical Note 2058*. 1950.
Frankl, F. I. On the Cauchy problem for equations of mixed elliptic-hyperbolic type with initial data on the parabolic line. *Bull. Acad. Sci. URSS 18*, 195–245 (1945).
Frankl, F. I. Asymptotic resolution of Chaplygin's functions. *Trans. Acad. Sci. URSS 58*. 1947. Also *Wright Field Technical Report F-TS-1212-IA*. 1949.
Bergman, S. Two-dimensional subsonic flows of a compressible fluid and their singularities. *Trans. Amer. Math. Soc. 62*, 452–498 (1947).
Weinstein, A. Discontinuous integrals and generalized potential theory. *Trans. Amer. Math. Soc. 63*, 342–354 (1948).
Cherry, T. M. Uniform asymptotic formulae for functions with transition points. *Trans. Amer. Math. Soc. 68*, 224–257 (1950).
Carrier, G. F., and Ehlers, F. E. On some singular solutions of the Tricomi equation. *Quart. Appl. Math. 6*, 331–334 (1948).
Goldstein, S., and Lighthill, M. J. A note on the hodograph transformation for the two-dimensional vortex flow of an incompressible fluid. *Quart. J. Mech. and Appl. Math. 3*, 297–302 (1950).
Loewner, C. A transformation theory of the partial differential equations of gas dynamics. *NACA Technical Note 2065*. 1950.

General theory.

Tollmien, W. The direct hodograph method in the theory of the flow of compressible fluids. *H. Reissner Anniv. Vol., Contributions to Appl. Mech.* Edwards Bros., 1949.
Bergman, S. A formula for the stream function of a certain flow. *Proc. Nat. Acad. Washington 29*, 276–281 (1943).
Bergman, S. On two-dimensional flows of compressible fluids. *NACA Technical Note 972*. 1945.
Goldstein, S., Lighthill, M. J., and Craggs, J. W. On the hodograph transformation for high-speed flow. I. A flow without circulation. *Quart. J. Mech. and Appl. Math. 1*, 344–357 (1948).
Lighthill, M. J. On the hodograph transformation for high-speed flow. II. A flow with circulation. *Quart. J. Mech. and Appl. Math. 1*, 442–450 (1948).

F,17 · *CITED REFERENCES AND BIBLIOGRAPHY*

Levey, H. C. High-speed flow of a gas past an approximately elliptic cylinder. *Proc. Camb. Phil. Soc. 46*, 479–491 (1950).

Chang, C. C. General consideration of problems in compressible flow using the hodograph method. *NACA Technical Note 2582*. 1952.

Mackie, A. G., and Pack, D. C. Transonic flow past finite wedges. *Proc. Camb. Phil. Soc. 48*, 178–187 (1951).

Ovsiannikov, L. V. Gas flow with straight transition line. *Prikladnaya Matematika i Mekhanika 13* (1949). Also *NACA Technical Memorandum 1295*. 1951.

Approximate subsonic solutions.

Riabouchinsky, D. Mouvement d'un fluide compressible autour d'un obstacle. *C.R. Acad. Sci. Paris 194*, 1215 (1932).

Demtchenko, B. Sur les mouvements lents des fluides compressibles. *C.R. Acad. Sci. Paris 194*, 1218–1222 (1932).

Busemann, A. Die Expansionsberichtigung der Kontraktionsziffer von Blenden. *Forschungsbericht 4*, 186–187 (1933).

Busemann, A. Hodographenmethode der Gasdynamik. *ZAMM 12*, 73–79 (1937).

Tamada, K. Application of the hodograph method to the flow of a compressible fluid past a circular cylinder. *Proc. Phys. Math. Soc. Japan 22*, 207–219 (1940).

Suzuki, H. On the subsonic flow of a compressible fluid past a circular cylinder. *Proc. Phys. Math. Soc. Japan 23*, 337 (1941).

Tomotika, S., and Tamada, K. Application of the hodograph method to the flow of a compressible fluid past an elliptic cylinder. *Proc. Phys. Math. Soc. Japan 23*, 958 (1941).

Bers, L. On the circulatory subsonic flow of a compressible fluid past a circular cylinder. *NACA Technical Note 970*. 1945.

Bers, L. Velocity distribution on wing sections of arbitrary shape in compressible potential flow. I. Symmetric flows obeying simplified density-speed relation. *NACA Report 1006*. 1946.

Bers, L. Velocity distribution on wing sections of arbitrary shape in compressible potential flow. III. Circulatory flows obeying the simplified density-speed relation. *NACA Technical Note 2056*. 1950.

Bartnoff, S., and Gelbart, A. On subsonic compressible flows by a method of correspondence. II. Application of methods to studies of flow with circulation about a circular cylinder. *NACA Technical Note 1171*. 1947.

Gelbart, A., and Resch, A. A method of computing subsonic flows around given airfoils. *NACA Technical Note 2057*. 1950.

Leray, J. Fluides compressibles. Application a l'aile portante d'envergure infinie de la méthode approchée de Tchapliguine. *J. Math. Pures Appl. 28*, 181–191 (1949).

Bugaenko, G. A. On the problem of gas flow over an infinite cascade using Chaplygin's approximation. *Prikladnaya Matematik i Mekhanika 13* (1949). Also *NACA Technical Memorandum 1298*. 1951.

Clauser, F. H. Two-dimensional compressible flows having arbitrary specified pressure distributions for gases with gamma equal to minus one. *Symposium on Theoretical Compressible Flow, 28 June 1949*. Nav. Ord. Lab. Report 1132, 1–33 (1950).

Bers, L. Velocity distribution on wing sections of arbitrary shape in compressible potential flow. II. Subsonic symmetric adiabatic flows. *NACA Technical Note 1012*. 1946.

Garrick, I. E., and Kaplan, C. On the flow of a compressible fluid by hodograph method. I. Unification and extension of present-day results. *NACA Technical Report 789*. 1944.

Temple, G., and Yarwood, J. The approximate solution of the hodograph equations for compressible flow. *Armament Research Establishment Report S.M.E. 3201*. 1942.

Imai, I. Application of the W.K.B. method to the flow of a compressible fluid, I. *J. Math. and Phys. 28*, 173–182 (1949).

Imai, I., and Hasimoto, H. Application of the W.K.B. method to the flow of a compressible fluid. II. *J. Math. and Phys. 28*, 205–214 (1950).

F · *PLANE POTENTIAL FLOWS*

Craggs, J. W. The application of the hodograph method to problems of subsonic flow in two dimensions. *ARC Reports and Memoranda 2273 (9801)*. 1949.

Transonic approximations.

Falkovich, S. V. On the theory of Laval nozzle. *Prikladnaya Matematika i Mekhanika 10* (1946). Also *NACA Technical Memorandum 1212*. 1949.

Falkovich, S. V. On a class of Laval nozzles. *Prikladnaya Matematika i Mekhanika 11* (1947). Also *Wright Field Technical Report F-TS-1223-IA*. 1949.

Germain, P. Application de l'approximation homographique a l'étude des écoulements transsoniques. *C.R. Acad. Sci. Paris 232*, 1811–1813 (1951).

Frankl, F. I. On a family of particular solutions of the equation of Darboux-Tricomi and their application to the approximate calculation of the critical velocity in a given plane-parallel Laval nozzle. *Doklady Akad. Nauk SSSR 56*, 683–686 (1947).

Ehlers, F. E. Methods of linearization in compressible flow. II. Hodograph method (Supplement 1, The transonic flow through a deLaval nozzle). *Wright Field Technical Report 102-AC49/5-100*. 1949.

Kiebel, I. A. Some stydies of the flow of a gas in the region of transition through velocity of sound. *Izvestia Akad. Nauk SSSR 3*, 253–259 (1947). Also *NACA Technical Memorandum 1252*. 1950.

Special solutions.

Daymond, S. D. Some solutions of the hodograph equations governing the two-dimensional flow of a compressible fluid. *Quart. J. Math. 16*, 78–85 (1945).

Williams, J. The two-dimensional irrotational flow of a compressible fluid in the acute region made by two rectilinear walls. *Quart. J. Math. 20*, 129–134 (1949).

Kraft, H., and Dibble, C. G. Some two-dimensional, adiabatic compressible flow patterns. *J. Aero. Sci. 11*, 283–298 (1944).

Saito, O. On some exact solutions of the two-dimensional steady flow of compressible fluid. *J. Phys. Math. Soc. Japan 6*, 248–254 (1951).

Craggs, J. W. The compressible flow corresponding to a line doublet. *Quart. Appl. Math. 10*, 88–93 (1952).

Tables of the hypergeometric functions.

Ferguson, D. F., and Lighthill, M. J. The hodograph transformation in transonic flow. IV. Tables. *Proc. Roy. Soc. A192*, 135–142 (1947).

Huckel, V. Tables of hypergeometric functions for use in compressible flow theory. *NACA Technical Note 1716*. 1948.

Chang, C. C., and O'Brien, V. Some exact solutions of two-dimensional flow of compressible fluid with hodograph method. *NACA Technical Note 2885*. 1953.

Munk, M. M., and Rawling, G. Tables of Chaplygin functions. *Nav. Ord. Lab. Memorandum 10816*. 1950.

Cherry, T. M. Tables and approximate formulae for hypergeometric functions, of high order, occurring in gas-flow theory. *Proc. Roy. Soc. A217*, 222–234 (1935).

504 JOURNAL OF THE AERONAUTICAL SCIENCES—JULY, 1955

A Similarity Rule for the Interaction Between a Conical Field and a Plane Shock* [1)]

Y. H. Kuo
Graduate School of Aeronautical Engineering, Cornell University, Ithaca, N.Y.

January 14, 1955

IN THREE-DIMENSIONAL SUPERSONIC steady flow past an obstacle, it frequently happens that a conical field touches, and thereby interacts with, a plane shock, resulting in a phenomenon known as a "triple point." In the limit of infinitesimal shock strength, problems of this kind have been treated by linear theory, in which the "triple point" is disguised as a logarithmic singularity superposed on an algebraic one at the Mach cone. In reality, of course, the shock cannot change discontinuously but decays to zero strength under the action of the conical field through a definite region whose dimensions depend on the strength of the shock. Consequently, a correct description of this phenomenon necessitates a re-examination of the approximation assumed in the linear theory.

In the case of a weak shock, the flow behind it may still be considered as isentropic and irrotational. Let the velocity potential be φ in the cylindrical coordinate system (ρ, θ, z) in which z is in the free-stream direction. If the flow is conical, $\varphi = Uz[1 + f(r, \theta)]$ where $r = \beta\rho/z$ and $\beta = \sqrt{M_\infty^2 - 1}$; U and M_∞ are, respectively, the free-stream velocity and Mach Number. The differential equation satisfied by the function $f(r, \theta)$, according to Lighthill,[1] is

$$\{1 - r^2 - (\gamma + 1)M_\infty^2\beta^{-2}r^2[f - rf_r + (1/2)(f - rf_r)^2] - (\gamma - 1)M_\infty^2[f - rf_r + (1/2)(f - rf_r)^2 + (1/2)(r^2 + \beta^2)(f_r^2 + r^{-2}f_\theta^2)] + 2M_\infty^2 rf_r(1 + f - rf_r) - M_\infty^2\beta^2 f_r^2\}f_{rr} + [1 - (\gamma - 1)M_\infty^2(f - rf_r)] \times (r^{-1}f_r + r^{-2}f_{\theta\theta}) - 2M_\infty^2(r^{-2}f_\theta - r^{-1}f_{r\theta})f_\theta + C = 0 \quad (1)$$

Here C and γ stand for, respectively, the cubic terms of the exact equation, not containing f_{rr}, and the ratio of the specific heats. Subscripts denote partial differentiation. When the disturbances are small and no terms other than linear ones are kept, the coefficient of f_{rr} is approximated by $1 - r^2$ and the equation becomes linear. For such cases, $r = 1$ defines the singular Mach cone. It is no surprise that linear theory breaks down in the neighborhood of $r = 1$, inasmuch as the terms neglected are of the same order as $1 - r$. To remove the ambiguities inherent in the linear solution in that neighborhood, nonlinear terms are indispensable.

If the small parameter of the flow is α, such as the angle of attack of a wing, the shock strength, and so the velocity disturbances, will be of the order α. In the region of interaction let it be assumed that

$$\left.\begin{aligned} f &= (1/\beta)\alpha^l k^m F(\xi,\eta) \\ 1 - r &= (\alpha k)^m \xi \\ \theta - \theta_0 &= (\alpha k)^n \eta \end{aligned}\right\} \quad (2)$$

where θ_0 is a constant giving the location of the interaction zone and k is another constant to be determined. It is now assumed, on the basis of the fact that the interaction takes place far from the solid boundary, that the character of interaction—namely, the exponents l, m, and n—depends solely on the local conditions and the differential equation. Since the shock strength and the velocity disturbance $\varphi_z - U = U(f - rf_r)$ are both of order α, $l - m = 1$. If, in the coefficient of f_{rr}, $1 - r^2$ is of the same order as $f - rf_r$, then m must be unity. These two conditions uniquely define l to be 2. The first term of Eq. (1) is therefore $0(\alpha)$. Now if $f_{\theta\theta}$ is also of the first order, n must be 1/2. Therefore, by retaining only the first-order terms, Eq. (1) simplifies to

$$(2\xi - F_\xi)F_{\xi\xi} - F_\xi + F_{\eta\eta} = 0 \quad (3)$$

with

$$k = (\gamma + 1)M_\infty^4\beta^{-3}$$

This shows that the effect of the interaction would confine itself to a region that extends in the radial direction a distance of $0(\alpha)$ and subtends an angle of $0(\sqrt{\alpha})$ and that two flow fields described by $f_1(r, \theta)$ and $f_2(r, \theta)$ are similar if the product $k\alpha$ is the same for both cases. It is of interest to point out that, by a different interpretation of the variables, this similarity rule holds equally true for unsteady two-dimensional flow, such as the diffraction of a plane shock by a corner.

One of the boundary conditions that the solution to Eq. (3) must satisfy is the shock condition—namely, across the shock[1] (a) f is continuous, and, (b)

$$\Delta f_r = [2/(\gamma + 1)]\,[(\gamma - 1)(f - f_r) + 2M_\infty^{-2}f - 2f_r + 2M_\infty^{-4}\beta^2(r - 1) - M_\infty^{-4}\beta^2(dr/d\theta)^2] + \ldots \quad (4)$$

where Δf_r signifies the jump in f_r. From the similarity transformation, f is $0(\alpha^2)$ and therefore the shock condition reduces to

$$F_\xi = 4\xi + 2(d\xi/d\eta)^2 \quad (5)$$

if the disturbances in front of shock are zero.

If there is no disturbance outside the Mach cone and if both $(f_- - rf_r)$ and $1 - r$ near the Mach cone are of the order α^2, the same argument leads to the following similarity transformation

$$\left.\begin{aligned} f &= (1/\beta)k^3\alpha^4 F(\xi, \eta) \\ 1 - r &= (k\alpha)^2\xi \\ \vartheta - \vartheta_0 &= k\alpha\eta \end{aligned}\right\} \quad (6)$$

without affecting the validity of both Eq. (3) and Eq. (5).

The similarity considerations above show that in the (r, ϑ)-plane a three-dimensional purely supersonic conical flow in the neighborhood of both the "triple point" and the Mach cone $r = 1$ is governed by not a linear but a nonlinear differential equation of the mixed type, with the transitional line $F_\xi = 2\xi$ separating the elliptic and hyperbolic regions. These similarity rules lead us to conclude, without solving the differential Eq. (3), that the perturbed shock strength of a first-order plane shock can be expressed in the form

$$\Delta p/p_\infty = -[(\gamma M_\infty^2\alpha)/\beta]F_\xi(\xi, \eta) \quad (7)$$

with a shock curve of the form

$$1 - r = k\alpha\xi(\eta) \quad (7.1)$$

and that the shock strength of the Mach cone without disturbances in front of it has the form

$$\Delta p/p_\infty = -[(\gamma M_\infty^2 k\alpha^2)/\beta]F_\xi(\xi, \eta) \quad (8)$$

with a shock curve

$$1 - r = (k\alpha)^2\xi(\eta) \quad (8.1)$$

Two special solutions of Eq. (3) have been studied. They will be briefly discussed in the following:

(A) Suppose:

$$F = H(\mu) - 2\mu[\xi_0 + \sigma(1 - 2\sigma)(\eta + \eta_0)^2] + g(\eta) \quad (9)$$

and

$$\mu = \xi + \xi_0 + \sigma(\eta + \eta_0)^2$$

where $g(\eta)$ is a polynomial of degree 4 and ξ_0, η_0, and σ are constants. The differential equation for $H(\mu)$ is, from Eq. (3),

$$(2\mu - H')H'' - (1 - 2\sigma)H' - 4\sigma(1 - 2\sigma)\mu = 0 \quad (10)$$

where $H' = dH/d\mu$. This equation can be explicitly integrated with the result: for $6\sigma \neq 1$

$$(H' - 4\sigma\mu)\,[H' - (1 - 2\sigma)\mu]^{-(1 + 2\sigma)/[2(1 - 2\sigma)]} = \text{const.} \quad (11)$$

* This study was sponsored by the Mechanics Branch of the Office of Naval Research.

1) Published in *Journal of the Aeronautical Sciences*, 1955, 22(7): 504~505

When $6\sigma = 1$, the solution can similarly be found and contains a logarithmic term.

If the constant σ lies in $-1/2 < \sigma < 1/2$, the integral curve (H', μ) will have a modal point at $\mu = 0$. For small μ, one branch is positive and the other is negative and intersects the singular line $H' = 2\mu$ at $\mu < 0$ with infinite slope. In the special case where there is no disturbance outside the Mach cone, $\sigma = 0$, then $F_\xi = H'(\mu)$. Thus, on the expansion side where $H' \geq 0$, the flow across the Mach cone is continuous. On the other hand, on the compression side where $H' < 0$, the flow across the Mach cone must be discontinuous with a shock strength from Eq. (8) proportional to $-k\alpha^2\beta^{-1}H'(\mu_0)$ and shock cone $1 - \tau = 4^{-1}(k\alpha)^2H'(\mu_0)$ according to Eq. (5). These results seem to confirm Lighthill's earlier conclusions regarding the character of the shock in the case of a triangular wing with angle of attack, lying inside the Mach cone.

(B) By the similarity rule, assume

$$F = (\eta + \eta_0)^4 G(\zeta) \tag{12}$$

where

$$\zeta = \xi/(\eta + \eta_0)^2$$

With this form of solution, it is evident from the shock condition [Eq. (5)] that an admissible shock curve is $\zeta = \text{const.} = \zeta_0$. In the case of a conical field interacting with a shock, such as the tip Mach cone from a rectangular wing at angle of attack, the velocity disturbance F_ξ and the coordinates (ξ, η) of the "triple point" are, respectively, -1 and $(-1/2, 1/\sqrt{2})$ from the shock condition. With these values, it is easy to deduce $G'(\zeta_0) = 2\zeta_0$. The shock condition [Eq. (5)] then determines $\zeta_0 = -(1/4)$, from which it follows that $\eta_0 = 1/(\sqrt{2})$. One can conclude finally that the perturbed shock curve is $\xi = -(1/4)\,(\eta + 1/\sqrt{2})^2$ on which the shock strength decays according to $(\eta + 1/\sqrt{2})^2$.

The numerical integration of the resulting equation for G

$$(2\zeta + 4\zeta^2 - G')G'' - (1 + 10\zeta)G' + 12G = 0 \tag{13}$$

with the initial values $\xi = -(1/4)$, $G = (1/24)$, and $G' = -(1/2)$ shows, however, that the integral curve (G', ζ) forms a cusp after hitting the singular line $G' = 2\zeta + 4\zeta^2$ at $\zeta = 0$. The solution in this neighborhood is of the form $\sum_3^\infty C_m|\zeta|^{m/2}$. There is, at the moment, no evidence to support the existence of this singularity in the interaction zone, even though other properties of the solution are acceptable. Further exploration along this line is certainly desirable.

It might be mentioned, in passing, that in trying to solve the same problem, Legras[2] chose a similar shock curve as the initial line to construct a solution in power series. Unfortunately, his process has not been pursued far enough to determine whether this form of solution is actually possible. In the light of the new results, it seems to be a matter of fundamental importance that Legras' solution be reexamined.

References

[1] Lighthill, M. J., *The Shock Strength in Supersonic "Conical Fields,"* Phil. Mag., No. 11, pp. 1202–1223, 1949.

[2] Legras, J., *Nouvelles Applications de la méthode de Lighthill à l'etude des ondes de choc*, O.N.E.R.A., No. 66, 1953.

Viscous Flow Along a Flat Plate Moving at High Supersonic Speeds*[1)]

Y. H. KUO†
Cornell University

SUMMARY

By the distortion of coordinates, it is shown that, in the case of supersonic viscous flow past a flat plate, the boundary-layer and simple wave theories can be combined to give a complete representation of the velocity and pressure fields. Consistent first-order solutions are considered. An expression for the induced pressure on the plate, correct to the second order, is obtained. At high Mach Numbers the important parameter satisfies the hypersonic similarity law; and for arbitrary Mach and Reynolds Numbers and for different gases, the theoretical curve correlates closely the experimental data. Asymptotic shock curve and skin-friction coefficient are also deduced, but the experimental verifications are yet to be made.

SYMBOLS

$Re = \rho_\infty UL/\mu_\infty$
$\beta = \sqrt{M^2 - 1}$
Physical variables defined in Eqs. (2.1) and (3.1)
T_w, ω defined in Eq. (2.7)
v_e defined in Eq. (3.3)
ϵ, v_0 defined in Eq. (3.4)
J defined in Eq. (3.5)
f_1, g_1 defined in Eq. (4.1)
$p^{(2)}$ defined in Eq. (4.10)
C_2 defined in Eq. (8.3)
θ defined in Eq. (9.1)
K, χ defined in Eq. (10.4)
Superscripts indicate order of approximation
Subscripts indicate partial differentiation
Primes indicate total differentiation

(1) INTRODUCTION

WHEN A SEMI-INFINITE FLAT PLATE moves edgewise through a gas of infinite extent with a constant flight speed, the gas close to the plate will be brought into motion by the action of viscosity of the gas. If the gas is incompressible, the flow is mainly a diffusion phenomenon and, consequently, can be conveniently described by a variable following the law of molecular diffusion, as has been done by Blasius.

As the flight speed increases, the simple hypothesis of incompressibility of gases is no longer valid and the effect of compressibility has to be considered. Because of the motion of the plate, the forward propagating family of waves generated by the viscous displacement of the flow tends to collect and form a shock with strength varying with flight Mach Number as well as with the distance from the leading edge of the plate. After a shock is formed, the pressure waves, which would have disappeared into infinity, are caught by the shock; and being a poor reflector, the shock will deflect more and more of the flow, which will, in turn, generate stronger waves. This interplay of two dominant effects, viscosity and compressibility, eventually reaches a permanent state, for a given Mach Number, as observed in high-speed flight or in the wind tunnel.

Distinct from the incompressible case, the induced quantities, such as the viscous deflection of streamlines and the pressure, are not small. At flight Mach Number 6, say, the shock strength near the plate becomes as high as 5 atmospheres. Furthermore, their order of magnitude changes as the distance from the leading edge varies. This, in essence, is the reason why simple mathematical descriptions, such as in the Blasius problem, are not possible. Of course, one might attempt to find a solution by iteration with boundary-layer theory at one's disposal. But the difficulty one will face is that if the Blasius solution is chosen as the basic approximation, it will lead to a second-order deflection infinitely large at infinity and a strong singularity near the leading-edge shock. The process of iteration thus diverges. If, on the other hand, the flow is assumed to follow the law of similarity, as Lees has proposed,[1] simple solutions can be found but, from experimental evidence, their range of application is very limited.

In the light of these difficulties, it is believed that in dealing with problems of this nature only solutions that bear a resemblance to exact ones can be useful. This requires that the analytic behavior of the solution should closely follow the character of the exact solution, if not every detail. In other words, near the plate, where the boundary-layer approximation is valid, the solution should agree with the predictions of boundary-layer theory. When the distance from the plate is large—namely, at the edge of the boundary layer—it should merge smoothly with the inviscid field. Thus, at any section of the plate, the solution gradually shifts from the character of the boundary-layer solution to that of the inviscid field, which is what the exact solution does. If such a solution were available, it would, at least, give the most outstanding features of the high-speed viscous flow. In what follows, in the hope of attaining this goal, an attempt, based on an extension of the idea of Lighthill,[2] has been made. The results are not entirely without interest even though there are still points that have not yet been clarified. It will

Received December 10, 1954. Revised and received July 23, 1955.

* This work was carried out at the Daniel and Florence Guggenheim Jet Propulsion Center, California Institute of Technology, while the author was on leave of absence from Cornell University. The continued interests of, and the frequent discussions with, Prof. H. S. Tsien were invaluable for a clearer understanding of the problem.

† Professor, Graduate School of Aeronautical Engineering.

1) Published in *Journal of the Aeronautical Sciences*, 1956, 23(2): 125~136

serve a useful purpose if further interests are stimulated.

As a trial, the first-order problem will be treated first. To this order—i.e., to the order of viscous displacement of streamlines—the solution is made uniformly valid at the edge of the boundary layer and is singular only at the leading edge. In this sense, the solution obtained below is asymptotic and can be regarded as the counterpart of the Blasius solution for low-speed flow.

The most fundamental hypothesis in this paper is that the fluid dealt with is a continuum. This means that the Navier-Stokes equations as well as the nonslip condition at the surface of the plate are assumed to be valid. There is no question that on the whole this is acceptable. It is debatable, however, whether it would give a true physical picture near the leading edge in the range of Mach Number considered, aside from objections on purely pedagogical grounds. Nevertheless, from all indications, classical hydrodynamics does provide a correct order of magnitude for all the practically interesting quantities and, at this stage, should be of great value to engineers.

In the following, the problem will be subdivided into four sections. Sections (I) and (II) are devoted, as a preparation, to methods of solution for the viscous and inviscid fields. Section (III) deals with the main problem of interaction between these two fields of flow, which constitute the foundation of the entire problem. The remarkable result in Section (III) is that the two distinct fields of flow are made to overlap, which is conceptually much broader than the usual notion of "smooth joining." Finally, Section (IV) contains the results deduced from solutions in Section (III). One of the conclusions is that, due to the interaction of the leading-edge shock with the boundary layer, the shear stress on the plate first increases, reaches a maximum, and then asymptotically follows the classical law of friction, with increasing distance from the leading edge of the plate. Thus, the question whether this phenomenon is primarily caused by slip-flow or by the presence of shock can easily be settled by experiments.

(I) Viscous Field

(2) Boundary-Layer Equations

Suppose a uniform stream of viscous gas flows at high supersonic speeds past a semi-infinite flat plate at no angle of attack. The motion around the plate is considered to be two-dimensional and steady. Near the surface of the plate, the flow problem can be dealt with by boundary-layer theory according to Shen[3] and Lees[1] under suitable restrictions of Reynolds and Mach Numbers. However, if the whole flow field is to be considered, the boundary-layer equations have to be modified.

In a Cartesian system, let the velocity components $\bar{u}$ and $\bar{v}$ be parallel respectively to $\bar{x}$ and $\bar{y}$-axes, and let the plate be defined by $\bar{y} = 0$ and $0 \leq \bar{x}$. If the density $\bar{\rho}$, temperature $\bar{T}$, pressure $\bar{p}$, and viscosity $\bar{\mu}$ are respectively ρ_∞, T_∞, p_∞, and μ_∞ at infinity, the following nondimensional variables are introduced:

$$\left.\begin{aligned} u &= \bar{u}/U \\ V &= (Re/C)^{1/2}\bar{v}/U = (Re/C)^{1/2}v \\ p &= \bar{p}/p_\infty \\ x &= \bar{x}/L \\ Y &= (Re/C)^{1/2}\bar{y}/L = (Re/C)^{1/2}y \\ \rho &= \bar{\rho}/\rho_\infty \\ T &= \bar{T}/T_\infty \\ \mu &= \bar{\mu}/\mu_\infty \end{aligned}\right\} \tag{2.1}$$

where Re denotes the Reynolds Number $\rho_\infty UL/\mu_\infty$, U and L are the flight speed and a measure of the length of plate, respectively; and C is a constant to be defined below. Since L is not a characteristic length of the problem, it will drop out from the final results.

In terms of these variables and using the subscript notation for partial differentiation, the modified boundary-layer equations can be written as

$$\left.\begin{aligned} &\Psi_Y\left(\frac{1}{\rho}\Psi_Y\right)_x - \Psi_x\left(\frac{1}{\rho}\Psi_Y\right)_Y = \\ &\qquad -\frac{1}{\gamma M^2}p_x + \left[\frac{\mu}{C}\left(\frac{1}{\rho}\Psi_Y\right)_Y\right]_Y \\ &-\frac{1}{\gamma M^2}p_Y + \frac{C}{Re}\left\{\Psi_Y\left(\frac{1}{\rho}\Psi_x\right)_x - \Psi_x\left(\frac{1}{\rho}\Psi_x\right)_Y - \right. \\ &\qquad \frac{4}{3}\left[\frac{\mu}{C}\left(\frac{1}{\rho}\Psi_x\right)_Y\right]_Y - \frac{2}{3}\left[\frac{\mu}{C}\left(\frac{1}{\rho}\Psi_Y\right)_x\right]_Y + \\ &\qquad \left.\left[\frac{\mu}{C}\left(\frac{1}{\rho}\Psi_Y\right)_Y\right]_x\right\} = 0 \end{aligned}\right\} \tag{2.2}$$

and for a perfect gas the equation of state:

$$p = \rho T \tag{2.3}$$

Here $\Psi(x, Y)$ denotes the stream function defined by

$$\rho u = \Psi_Y, \quad \rho V = -\Psi_x \tag{2.4}$$

γ is the ratio of the specific heats, and M is the free-stream Mach Number $U/(\gamma p_\infty/\rho_\infty)^{1/2}$. In the case where the plate is thermally insulated and the Prandtl Number is unity, the energy equation admits a relation between temperature and velocity:

$$T = 1 + [(\gamma - 1)/2]M^2(1 - u^2) \tag{2.5}$$

It was noticed by Howarth[4] that if μ varies linearly with temperature, the differential equations [Eqs. (2.2)] can be considerably simplified by a transformation of Y. This approximation, however, was found to underestimate the compressibility effects at high Mach Numbers. To improve its accuracy, a form due to Chapman and Rubesin[5] has been adopted—namely,

$$\mu = CT \tag{2.6}$$

where the constant C will be so chosen as to give the

best fit in the important temperature range with the measured viscosity coefficient. As the high temperature region usually occurs in the neighborhood of the wall, it is customary to make the fit at the wall. If the viscosity obeys the power law T^{ω} where ω is 0.76 for air and 0.75 for helium, it follows from Eqs. (2.5) and (2.6) that

$$C = T_w^{\omega-1} = \{1 + [(\gamma - 1)/2]M^2\}^{\omega-1} \quad (2.7)$$

where T_w denotes the temperature at the plate. This relation will be consistently used in the subsequent deductions.

(3) Method of Solution

From Eqs. (2.2), it is seen that the determination of the function Ψ, within the limitations of the boundary-layer approximation, is possible when the pressure in the main stream is prescribed. In the present problem, however, the pressure, which is a result of the mutual interaction of the viscous and compressible effects of the gas in the presence of a solid boundary, is at first unknown. In what follows, a process of iteration will be developed by which ultimately both the velocity and pressure fields can be calculated.

In view of the fact that the pressure in the case of a flat plate moving at high supersonic speeds is a first-order quantity, it seems possible to begin the iteration by taking the pressure to be constant. The zero-order solution is then the classical case treated by von Kármán and Tsien[6] and, by means of Howarth's transformation, reduces to that of Blasius. Due to the boundary-layer approximation, which neglects the curvature effect of the streamlines, this perturbation, if carried out, would lead, however, to a second-order velocity which diverges at infinity, besides the singularity at the leading edge. This difficulty can be avoided by modifying the method of perturbation according to a concept of Lighthill.[2] Namely, by writing

$$\left.\begin{aligned} \Psi &= \sqrt{p}\,\psi \\ \psi &= \psi^{(0)}(\xi, \eta) + \epsilon\psi^{(1)}(\xi, \eta) + \dots \\ p &= 1 + \epsilon p^{(1)}(\xi, \eta) + \epsilon^2 p^{(2)}(\xi, \eta) + \dots \\ T &= T^{(0)}(\xi, \eta) + \epsilon\, T^{(1)}(\xi, \eta) + \dots \\ x &= \xi + \epsilon\, x^{(1)}(\xi, \eta) + \dots \end{aligned}\right\} \quad (3.1)$$

and, as a measure of simplification, Howarth's transformation is also incorporated:

$$Y = \frac{1}{\sqrt{p}} \int_0^{\eta} T dz \quad (3.2)$$

Here ξ, η may be considered as new parameters related to the old variables x and Y by Eqs. (3.1) and (3.2). The perturbation parameter ϵ can be interpreted as the lateral displacement of a streamline because, to the first order, the pressure, as will be shown in Section (II) is proportional to the velocity v_e at the edge of the boundary layer, which according to Howarth's approximation is

$$V_e = \sqrt{C/Re}[0.860 + 0.596(\gamma - 1)M^2]\,(1/\sqrt{x}) \quad (3.3)$$

Without loss of generality, let the parameter ϵ and the constant v_0 be defined by

$$\left.\begin{aligned} \epsilon &= \sqrt{C/Re} \\ v_0 &= 0.860 + 0.596\,(\gamma - 1)M^2 \end{aligned}\right\} \quad (3.4)$$

Following the transformation [Eqs. (3.1) and (3.2)], the derivatives $\partial/\partial x$ and $\partial/\partial Y$ in Eqs. (2.2) are replaced by, respectively,

$$\left.\begin{aligned} \frac{\partial}{\partial x} &= \frac{\partial}{\partial \xi} - \frac{\sqrt{p}}{T} Y_{\xi} \frac{\partial}{\partial \eta} + \epsilon\,(J x_{\eta}^{(1)} - x_{\xi}^{(1)}) \times \\ &\qquad \left(\frac{\partial}{\partial \xi} - J\,\frac{\partial}{\partial \eta}\right) + \dots \\ \frac{\partial}{\partial Y} &= \frac{\sqrt{p}}{T}\left[\frac{\partial}{\partial \eta} + \epsilon\, x_{\eta}^{(1)}\left(J\,\frac{\partial}{\partial \eta} - \frac{\partial}{\partial \xi}\right) + \dots\right] \end{aligned}\right\} \quad (3.5)$$

where J is defined by $(1/T^{(0)}) \int_0^{\eta} T_{\xi}^{(0)} dz$. Eqs. (3.2) and (3.5), although not strictly expansions in powers of ϵ, are preferable because of the fact that the simplification brought by Howarth's transformation will be preserved. After the transformation is completed, the expansion can then be carried out. If Ψ, p, and T are now substituted from Eqs. (3.1) in the transformed equations, the zero-order equations resulting from the vanishing of the coefficient of ϵ^0 of both equations lead to the conclusions that $\psi^{(0)}$ has the same form as the famous Blasius solution for the case of incompressible fluid and that $p^{(1)}$ can be a function of ξ alone. Furthermore, the vanishing of the coefficient of ϵ of the first equation and that of ϵ^2 of the second equation yields the system:

$$\begin{aligned} L(\psi_{\eta}^{(1)}) &= \psi_{\eta\eta\eta}^{(0)} x_{\xi}^{(1)} + [L(\psi_{\xi}^{(0)}) - 2\psi_{\xi\eta\eta}^{(0)} + \\ &J\psi_{\eta\eta\eta}^{(0)} - J_{\xi}\,\psi_{\eta}^{(0)^2} + J_{\eta}(\psi_{\xi}^{(0)}\psi_{\eta}^{(0)} + 3\psi_{\eta\eta}^{(0)}) + \\ &J_{\eta\eta}\psi_{\eta}^{(0)}]\, x_{\eta}^{(1)} + (\psi_{\xi}^{(0)} - J\psi_{\eta}^{(0)})\psi_{\eta}^{(0)} x_{\xi\eta}^{(1)} - \\ &[3\psi_{\xi\eta}^{(0)} + \psi_{\xi}^{(0)^2} - 2J_{\eta}\,\psi_{\eta}^{(0)} - J(\psi_{\xi}^{(0)}\psi_{\eta}^{(0)} + \\ &3\psi_{\eta\eta}^{(0)})]x_{\eta\eta}^{(1)} - (\psi_{\xi}^{(0)} - J\psi_{\eta}^{(0)})\, x_{\eta\eta\eta}^{(1)} + \\ &\frac{1}{2} p_{\xi}^{(1)}\left[\psi^{(0)}\psi_{\eta\eta}^{(0)} - \frac{\gamma - 1}{\gamma}(1 - \psi_{\eta}^{(0)^2}) - \frac{2}{\gamma M^2}\right] \end{aligned} \quad (3.6)$$

$$\begin{aligned} &- \frac{1}{\gamma M^2}\,(p_{\eta}^{(2)} - x_{\eta}^{(1)}\, p_{\xi}^{(1)}) = - T^{(0)} L(\psi_{\xi}^{(0)}) - T_{\xi}^{(0)} \times \\ &\left(2\psi_{\xi}^{(0)}\psi_{\eta}^{(0)} + \frac{10}{3}\,\psi_{\eta\eta}^{(0)}\right) + T_{\eta}^{(0)}\left(\psi_{\xi}^{(0)^2} + \frac{10}{3}\,\psi_{\xi\eta}^{(0)}\right) + \\ &\frac{4}{3}\,(T_{\eta\eta}^{(0)}\,\psi_{\xi}^{(0)} - T_{\xi\eta}^{(0)}\,\psi_{\eta}^{(0)}) + \psi_{\eta}^{(0)^2} Y_{\xi\xi}^{(0)} \end{aligned} \quad (3.7)$$

where $L(\psi_{\eta}^{(1)})$ and $L(\psi_{\xi}^{(0)})$ are defined by

$$\left.\begin{aligned} L(x_{\eta}^{(1)}) &\equiv \psi_{\eta}^{(0)}\psi_{\xi\eta}^{(1)} + \psi_{\xi\eta}^{(0)}\psi_{\eta}^{(1)} - \\ &\qquad \psi_{\xi}^{(0)}\psi_{\eta\eta}^{(1)} - \psi_{\eta\eta}^{(0)}\psi_{\xi}^{(1)} - \psi_{\eta\eta\eta}^{(1)} \\ L(\psi_{\xi}^{(0)}) &\equiv \psi_{\eta}^{(0)}\psi_{\xi\xi}^{(0)} - \psi_{\xi}^{(0)}\psi_{\xi\eta}^{(0)} - \psi_{\eta\eta\xi}^{(0)} \end{aligned}\right\} \quad (3.8)$$

As concluded above, $\psi^{(0)} = \sqrt{\xi}\, f_0(\zeta)$ and $\zeta = \eta/\sqrt{\xi}$ according to Blasius. The properties of the function $f_0(\zeta)$ which satisfies a total differential equation are well known. With $\psi^{(0)}$ so chosen, the velocities, to the first approximation, can be calculated by the rules of transformation (3.5); and from $u^{(0)}$, $T^{(0)}$ is known by Eq. (2.5). It can be verified that the velocities $u^{(0)}$ and $\epsilon v^{(1)}$ vanish on the wall and approach, respectively, the asymptotic values 1 and v_2 in Eq. (3.3) when ζ becomes infinite. Because of this asymptotic value of v_2, there induces in the external field a pressure $p^{(1)}$ equal to $\gamma M^2 v_0/\beta\sqrt{\xi}$, β being $\sqrt{M^2 - 1}$, as will be shown in Section (II). Consequently, in Eqs. (3.6) and (3.7) there are left three functions $\psi^{(1)}$, $x^{(1)}$, and $p^{(2)}$ to be determined.

(4) Coordinate Distortion in the Viscous Field

The forms of $\psi^{(0)}$ and $p^{(1)}$ together with the differential equation [Eq. (3.6)] demands that

$$\psi^{(1)} = (v_0/\beta) f_1(\zeta), \quad x^{(1)} = (v_0/\beta)\sqrt{\xi}\, g_1(\zeta) \tag{4.1}$$

From Eqs. (2.4), (2.5), and (3.5) it follows that the velocities and temperature in the boundary layer are, respectively,

$$u = f_0' + \frac{v_0\epsilon}{\beta\sqrt{\xi}}\left(f_1' + \frac{v_1}{T^{(0)}}\, g_1'\right) + \ldots \tag{4.2}$$

$$v = \frac{\epsilon v_1}{\sqrt{\xi}} + \frac{v_0\epsilon^2}{2\beta\xi}\left\{\left(f_1' + \frac{v_1}{T^{(0)}}\, g_1'\right) \times \left[(\gamma - 1)M^2 f_0 f_0' + \int_0^\zeta T^{(0)} d\zeta\right] + \frac{\gamma M^2}{2}\,(2f_0 T^{(0)} - v_1 g_1)\right\} + \ldots \tag{4.3}$$

$$T = T^{(0)} - \frac{(\gamma - 1)M^2 v_0\epsilon}{\beta\sqrt{\xi}}\, f_0'\left(f_1' + \frac{v_1}{T^{(0)}}\, g_1'\right) + \ldots \tag{4.4}$$

where the prime denotes total differentiation with respect to ζ and v_1 and $T^{(0)}$ are defined by

$$\left.\begin{aligned} v_1 &= \frac{1}{2}\,(\zeta f_0' - f_0)T^{(0)} - \frac{1}{2} f_0' \int_0^\zeta \zeta\, \frac{dT^{(0)}}{d\zeta}\, d\zeta \\ T^{(0)} &= 1 + [(\gamma - 1)/2]M^2(1 - f_0'^2) \end{aligned}\right\} \tag{4.5}$$

It will be shown in Section (II) that with the first-order v and p in the external field defined above there will associate a first-order u equal to $-v_0/\beta\sqrt{\xi}$. In order that the velocity joins smoothly at the edge of the boundary layer, the following condition must be satisfied

$$f_1' + (v_1/T^{(0)})g_1' = -1, \quad \zeta = \infty \tag{4.6}$$

Moreover, the condition of no-slip together with the fact that $\Psi = 0$ on the wall lead to

$$f_1 = f_1' + (v_1/T^{(0)})g_1' = 0, \quad \zeta = 0 \tag{4.7}$$

By substituting $\psi^{(1)}$ and $x^{(1)}$ from Eqs. (4.1) in Eq. (3.6) and eliminating simultaneously $\psi^{(0)}$ and $p^{(1)}$, there results a total differential equation of the third order for f_1 and g_1. This equation can be twice integrated, and by using the second of the conditions (4.7), the result can be written as

$$f_1' + \frac{v_1}{T^{(0)}}\, g_1' = -\frac{1}{2}\,\zeta f_0'' g_1 + \frac{f_0''}{2}\int_0^\zeta \frac{g_1'}{T^{(0)}} \times \left(\int_0^\zeta \zeta \frac{dT^{(0)}}{d\zeta}\, d\zeta\right) d\zeta - \frac{\gamma M^2}{2}\left(\zeta f_0'' - \frac{\gamma - 1}{\gamma} f_0' + \frac{T_w}{\gamma M^2} f_0'' \int_0^\zeta \frac{\zeta d\zeta}{f_0''}\right) + C_1 f_0'' \int_0^\zeta \frac{d\zeta}{f_0''} \tag{4.8}$$

where C_1 is a constant of integration. From the properties of f_0, it can be shown that the product $f_0'' \int_0^\zeta d\zeta/f_0''$ tends to zero when ζ is infinite. It appears that C_1 might be indeterminate. It is noted, however, that for large ζ this product is of the order $(1/\zeta)$. This would make the solution [Eq. (4.8)] approach the boundary value [Eq. (4.6)] very much slower than does f_0', which is contrary to the character of the boundary-layer solutions. In order that both f_1'' and g_1'' tend to zero exponentially at infinity, it is necessary to cancel the slowly varying terms by choosing C_1:

$$C_1 = 0.860\, T_w \tag{4.9}$$

Now, since $f_0'' \int_0^\zeta (\zeta - 1.720)d\zeta/f_0''$ approaches the asymptotic value 2 at infinity, the condition (4.6) is, as a consequence, fulfilled.

The solution [Eq. (4.8)] now contains two functions, f_1 and g_1. In an attempt to eliminate this indeterminacy, the asymptotic behavior of the second-order velocity $v^{(2)}$ and pressure $p^{(2)}$ are examined. In Eq. (3.7) if $\psi^{(0)}$, $x^{(1)}$, $p^{(1)}$ are substituted by their similarity solutions and if $p^{(2)}$ is replaced by

$$p^{(2)} = [(\gamma M^2 v_0^2)/(\beta^2\xi)]p_2(\zeta) \tag{4.10}$$

the resulting total differential equation can again be integrated to give the solution:

$$g_1 + 2p_2 = \frac{\beta^2}{v_0^2}\left\{\frac{f_0}{2}\,(\zeta f_0' - f_0) + \zeta f_0'' + \frac{\gamma - 1}{4}\, M^2 \times \left[f_0(\zeta f_0' - f_0) + 0.664(f_0 f_0' + 2f_0'') + 2\zeta f_0'' - 4f_0''^2 + \frac{4}{3} f_0 f_0' f_0''\right]\right\} + C_2 \tag{4.11}$$

where C_2 is an integration constant. At the edge of the boundary layer $\zeta \to \infty$, the asymptotic properties of f_0 lead to the result

$$g_1 + 2p_2 \sim [(\beta^2/v_0)\zeta] + \text{constant} + 0(e^{-\zeta^2}) \tag{4.12}$$

Eq. (4.12) shows that if the coordinate-distortion function g_1 were absent, then the second-order pressure would be infinite at infinity. It might be argued that at the physical edge of the boundary layer ζ is

really not infinite. Nevertheless, if ζ were eliminated in terms of x and y according to Eqs. (2.1) and (3.2), $\epsilon^2 p^{(2)}$ would give a first-order term $\gamma M^2 v_0 \epsilon y / 2x^{3/2}$ which would make the overlap of pressure fields for arbitrarily large y impossible. A more reasonable solution would be to require the second-order pressure to remain finite across the boundary layer. Then at the edge of the boundary layer, $\zeta \to \infty$

$$g_1 \sim [(\beta^2/v_0)\zeta] + \text{constant} + 0(e^{-\zeta^2}) \quad (4.13)$$

Thus, by causing the second-order pressure $p^{(2)}$ to behave satisfactorily at the edge of the boundary layer, the coordinate-distortion function is fixed in that region.

With the asymptotic form of g_1 specified by (4.13), the second-order velocity $v^{(2)}$ as calculated from Eq. (4.3) is finite for $\zeta \to \infty$. This very satisfactory result is radically different from the previous classical perturbation analysis without coordinate distortion carried out by Maslen.[7] Maslen's $v^{(2)}$ is infinite for infinite ζ. Although Maslen did not compute $p^{(2)}$, it is certain that had he computed it, $p^{(2)}$ would also be found infinite as $\zeta \to \infty$. Such anomalies of the classical perturbation calculation are objectionable not only from the point of view of physical reality but also on the ground of leading to divergent successive iterations. By introducing the coordinate-distortion function g_1 as specified by (4.13), these difficulties are resolved and the boundary-layer solution is rendered uniformly valid for all ζ. However, as yet g_1 is not determined for the complete range of from $\zeta = 0$ to infinity. To do this, the question of joining the solutions with those of the inviscid field has to be considered.

(II) Inviscid Field

(5) Differential Equations of Steady Isoenergetic Flow

Outside the boundary-layer region where the viscous shear stresses become unimportant, the motion is governed by the system:

$$\left.\begin{aligned} \rho u u_x + \rho v u_y &= -[1/(\gamma M^2)]p_x \\ \rho u v_x + \rho v v_y &= -[1/(\gamma M^2)]p_y \\ (\rho u)_x + (\rho v)_y &= 0 \end{aligned}\right\} \quad (5.1)$$

and for perfect gas

$$p = \rho T$$

By virtue of the conservation of energy, the temperature can be expressed in terms of velocity:

$$T = 1 + [(\gamma - 1)/2]M^2(1 - u^2 - v^2) \quad (5.2)$$

Since the flow in the external field is produced mainly by the viscous deflection of the streamlines, the velocity component v at large ζ as given by Eq. (3.3) can be considered as the boundary value of the inviscid field. In view of the fact that the Reynolds Number is large, v will stay small even though the Mach Number may be in the hypersonic range. For this reason, a fact that is not enjoyed by the flow around a solid body with a nonzero thickness, the present problem can be linearized by expanding:

$$\left.\begin{aligned} u &= 1 + \epsilon u^{(1)} + \epsilon^2 u^{(2)} + \ldots \\ v &= \epsilon v^{(1)} + \epsilon^2 v^{(2)} + \ldots \\ p &= 1 + \epsilon p^{(1)} + \epsilon^2 p^{(2)} + \ldots \\ \rho &= 1 + \epsilon \rho^{(1)} + \epsilon^2 \rho^{(2)} + \ldots \\ T &= 1 + \epsilon T^{(1)} + \epsilon^2 T^{(2)} + \ldots \end{aligned}\right\} \quad (5.3)$$

provided $u^{(n)}$, $v^{(n)}$, $M^{-2}p^{(n)}$, $M^{-2}\rho^{(n)}$ are not large where ϵ is the same parameter as defined by Eq. (3.4). Because of the boundary value of $v^{(1)}$ as described by Eq. (3.3), the first-order quantities must vanish at infinity. Consequently, the zero-order shock must be a Mach wave.

It must be recalled, however, that as $v^{(1)}$ satisfies a boundary value [Eq. (3.3)] which is singular at the leading edge, in a supersonic field this singularity must be propagated along the whole Mach line through the leading edge. As a result, all first-order quantities are singular there. Moreover, if the perturbation is pushed to high orders, the singularity of all high-order solutions will progressively become stronger, and the approximation, consequently, is poor as the leading edge is approached. In order to prevent the unnecessarily high-order singularity of the second- or higher-order quantities from appearing, the coordinate x will be expanded once again:

$$\left.\begin{aligned} x &= \xi + \epsilon x^{(1)}(\xi, \eta) + \ldots \\ y &= \eta \end{aligned}\right\} \quad (5.4)$$

Taking into account the transformation (5.4), the substitution of u, v, p, ρ, T, from Eqs. (5.4) in Eqs. (5.1) yields, for order ϵ, the system:

$$\left.\begin{aligned} u_\xi^{(1)} &= -[1/(\gamma M^2)]p_\xi^{(1)} \\ v_\xi^{(1)} &= -1/\gamma M^2\, p_\eta^{(1)} \\ (u^{(1)} + \rho^{(1)})_\xi + v_\eta^{(1)} &= 0 \\ p^{(1)} &= \rho^{(1)} - (\gamma - 1)M^2 u^{(1)} \end{aligned}\right\} \quad (5.5)$$

and, by making use of Eq. (5.2),

$$T^{(1)} = -(\gamma - 1)M^2 u^{(1)} \quad (5.6)$$

For order ϵ^2, one has

$$\left.\begin{aligned} u_\xi^{(2)} + [1/(\gamma M^2)]p_\xi^{(2)} &= \\ &\quad -(u^{(1)} + \rho^{(1)})u_\xi^{(1)} - v^{(1)}u_\eta^{(1)} \\ v_\xi^{(2)} + [1/(\gamma M^2)]p_\eta^{(2)} &= -(u^{(1)} + \rho^{(1)})v_\xi^{(1)} - \\ &\quad v^{(1)}v_\eta^{(1)} + v_\xi^{(1)}x_\xi^{(1)} + [1/(\gamma M^2)]p_\xi^{(1)}x_\eta^{(1)} \\ (u^{(2)} + \rho^{(2)})_\xi + v_\eta^{(2)} &= -(\rho^{(1)}u^{(1)})_\xi - \\ &\quad (\rho^{(1)}v^{(1)})_\eta + (u^{(1)} + \rho^{(1)})_\xi x_\xi^{(1)} + v_\xi^{(1)}x_\eta^{(1)} \\ p^{(2)} &= \rho^{(2)} - (\gamma - 1)M^2 u^{(2)} - \\ &\quad (\gamma - 1)M^2[\rho^{(1)}u^{(1)} + (1/2)\,(u^{(1)^2} + v^{(1)^2})] \end{aligned}\right\} \quad (5.7)$$

and from the energy equation

$$T^{(2)} = -(\gamma - 1)M^2[u^{(2)} + (1/2)\,(u^{(1)^2} + v^{(1)^2})] \quad (5.8)$$

(6) First-Order Solution

The elimination of $\zeta^{(1)}$ between the last two of Eqs. (5.5) gives a relation connecting the derivatives of $u^{(1)}$, $p^{(1)}$, and $v^{(1)}$ which, on combining with the first of Eqs. (5.5), can express $v_\eta{}^{(1)}$ in terms of $p_\xi{}^{(1)}$. Thus, for the first-order problem the fundamental system can be expressed as:

$$\left.\begin{aligned} v_\xi{}^{(1)} &= -[1/(\gamma M^2)]p_\eta{}^{(1)} \\ v_\eta{}^{(1)} &= -[\beta^2/(\gamma M^2)]p_\xi{}^{(1)} \end{aligned}\right\} \quad (6.1)$$

The advantage of this system is that even if the flow is rotational the potential character of the mathematical problem is preserved.

For a given problem, after $v^{(1)}$ and $p^{(1)}$ are determined by solving Eqs. (6.1) subject to a prescribed boundary condition, such as being described by Eq. (3.3) for $\eta = 0$, $u^{(1)}$ can be obtained by partial integration of the first of Eqs. (5.5). If the flow is rotational, the arbitrary function of η will serve to determine the vorticity from the shock conditions. In case the leading-edge shock, to the zero order, is a Mach wave $\xi - \beta\eta = 0$, the vorticity will be of high order and, consequently, the reflected waves are absent. If $F(\xi - \beta\eta)$ represents a simple wave, the complete solutions of the first-order problem are given below:

$$\left.\begin{aligned} &v^{(1)} = F(\xi - \beta\eta), \quad u^{(1)} = -(1/\beta)F(\xi - \beta\eta) \\ &p^{(1)} = \\ &(\gamma M^2/\beta)F(\xi - \beta\eta), \quad \rho^{(1)} = (M^2/\beta)F(\xi - \beta\eta) \end{aligned}\right\} \quad (6.2)$$

which are the well-known Ackeret's formulas.

This shows that for a given problem if any one quantity such as $v^{(1)}$ is described, the rest are all defined. For instance, if $v^{(1)}$ takes on the value given by Eq. (3.3) on $\eta = 0$, it follows immediately from Eqs. (6.2) that

$$F = v_0/\sqrt{\xi - \beta\eta} \quad (6.3)$$

The singularity of the first-order solution at the leading-edge Mach line is, consequently, $(\xi - \beta\eta)^{-1/2}$. This implies that there must be a rapid change of flow properties in the neighborhood of this limiting Mach line, and the order of magnitude as defined by Eqs. (5.3) may very likely alter. This problem will be investigated in detail in Section (III).

(7) Determination of the Coordinate Distortion Function

After the elimination of $u^{(2)}$ from the first of Eqs. (5.7), the fundamental system of the second-order problem will read:

$$\left.\begin{aligned} v_\xi{}^{(2)} + [1/(\gamma M^2)]p_\eta{}^{(2)} &= q_1 \\ v_\eta{}^{(2)} + [\beta^2/(\gamma M^2)]p_\xi{}^{(2)} &= q_2 \end{aligned}\right\} \quad (7.1)$$

where q_1 and q_2 are known functions of the first-order quantities such as $u^{(1)}$, $v^{(1)}$, $x^{(1)}$, . . . , etc. If the first-order solutions are simple waves as given by Eqs. (6.2), q_1 and q_2 are simplified to

$$\left.\begin{aligned} q_1 &= (\beta^{-1}x_\eta{}^{(1)} + x_\xi{}^{(1)})F' \\ q_2 &= (\gamma + 1)\,(M^4/\beta^2)FF' + (\beta x_\xi{}^{(1)} + x_\eta{}^{(1)})F' \end{aligned}\right\} \quad (7.2)$$

If the integration of the system [Eqs. (7.1)] were carried out, because of its inhomogeneity, the second-order solution would contain a singular term such as $(\xi + \beta\eta)\,(\xi - \beta\eta)^{-2}$. It is clear that due to this strong singularity, the second-order solution would not give better accuracy than the first-order solution, particularly in the neighborhood of $\xi - \beta\eta = 0$. The process of perturbation then actually diverges. This singular term disappears only if $x^{(1)}$ satisfies

$$F'(\beta^2 x_{\xi\xi}{}^{(1)} - x_{\eta\eta}{}^{(1)}) + 2\beta F''(\beta x_\xi{}^{(1)} + x_\eta{}^{(1)}) + (\gamma + 1)\,(M^4/\beta)\,(F'^2 + FF'') = 0 \quad (7.3)$$

whereupon $v^{(2)}$ will satisfy a homogeneous equation

$$\beta^2 v_{\xi\xi}{}^{(2)} - v_{\eta\eta}{}^{(2)} = 0 \quad (7.4)$$

For a given problem, if $v^{(2)}$ is obtained by solving Eq. (7.4) satisfying prescribed conditions, then the integration of Eqs. (7.1) leads to

$$p^{(2)} = \frac{\gamma M^2}{\beta}\left(v^{(2)} + \frac{\gamma + 1}{4}\,\frac{M^4}{\beta^3}\,\frac{v_0{}^2}{\xi - \beta\eta}\right) \quad (7.5)$$

Let the characteristic parameters be introduced:

$$s = \xi - \beta\eta, \quad t = \xi + \beta\eta$$

Eq. (7.3) can then be integrated with the result:

$$x^{(1)} = -\frac{(\gamma + 1)}{4}\,\frac{M^4}{\beta^3}\,\frac{v_0 t}{\sqrt{s}} + A(s) + s^{3/2}B(t) \quad (7.6)$$

where A and B are, respectively, functions of s and t. $x^{(1)}$, in this general form, ensures only the analytic behavior of the solutions near the leading-edge shock. The determination of A and B again cannot be done until the mutual relationship between the two fields of flow is considered.

(III) Interaction Between Viscous and Inviscid Fields

(8) Determination of the Transformation

As shown in Section (4), the choice of g_1 [Eq. (4.13)] at large ζ guarantees the rapid approach to constant values of second-order normal velocity $v^{(2)}$ and pressure $p^{(2)}$ at the edge of boundary layer. These constant values of velocity and pressure are otherwise unspecified. A moment's reflection on the method of solution adopted here shows that the iteration procedure starts with $v^{(1)}$. From $v^{(1)}$, $p^{(1)}$ is determined. From $p^{(1)}$, $v^{(2)}$ is computed. Then $p^{(2)}$ is computed. This process can be carried on and on; with each additional step there is an improvement of the accuracy. However, with emphasis on the pressure along the plate, it is important to have an exact expression for this quantity even if other quantities have to be computed by iteration. This can be accomplished by choosing the

coordinate such that $p^{(2)} \equiv 0$ throughout the field. Then the pressure is *exactly* $1 + \epsilon p^{(1)}$. Now within the boundary layer, since $p^{(1)}$ is only a function of ξ, the exact pressure is also a function of ξ only. This then gives a physical meaning to the independent variable ξ: Lines of constant ξ are lines of constant pressure within the boundary layer. The meaning of the independent variable η is obtained through $\zeta = \eta/\sqrt{\xi}$: ζ is the similarity parameter of the solution.

The fact that the pressure is constant for constant values of ξ does not imply that pressure is constant for constant x. Actually, along constant x in the boundary layer, the pressure changes are of the $0(\epsilon^2)$. This is the correct order of magnitude.

With $p^{(2)} \equiv 0$, Eq. (4.11) gives the coordinate distortion function g_1 in the boundary layer,

$$g_1 = \frac{\beta^2}{v_0^2}\left\{\frac{1}{2} f_0(\zeta f_0' - f_0) + \zeta f_0'' + \frac{\gamma - 1}{4} M^2\left[f_0(\zeta f_0' - f_0) + 0.664\,(f_0 f_0' + 2f_0'') + 2\zeta f_0'' - 4f_0''^2 + \frac{4}{3} f_0 f_0' f_0''\right]\right\} + C_2 \quad (8.1)$$

With g_1 fixed, f_1 can be determined by using Eqs. (4.8) and (4.9).

In the inviscid field, the vanishing of $p^{(2)}$ leads to $u^{(2)} = 0$ and determines $v^{(2)}$ according to Eq. (7.5). Thus

$$v^{(2)} = -[(\gamma + 1)/4]\,(M^4/\beta^3)\,(v_0^2/s) \quad (8.2)$$

This form of second-order normal velocity in the inviscid region must now join smoothly to the asymptotic value of $v^{(2)}$ in Eq. (4.3) at the edge of the boundary layer. At the edge of the boundary layer, $s \simeq \xi$. Then the continuity of $v^{(2)}$ at $\zeta \to \infty$ determines the constant

$$C_2 = [(\gamma + 1)/2]\,(M^4/\beta^2) - 2 \quad (8.3)$$

The solution within the boundary layer is now completely determined. It is interesting to note that the second-order normal velocity $v^{(2)}$ at the edge of the boundary layer is negative. This actually is accompanied by a decrease of temperature and density.

It remains to determine the functions $A(s)$ and $B(t)$ in the coordinate-distortion function [Eq. (7.6)] of the inviscid field. To do this, consider again the junction of functions at the edge of the boundary layer. From Eqs. (2.1) and (3.2), together with Eqs. (4.5) and (4.8), y in the boundary layer can be calculated as a function of ξ and ζ. Thus

$$y = \epsilon\sqrt{\frac{\xi}{p}}\int_0^\zeta T d\zeta = \epsilon\sqrt{\frac{\xi}{p}}\left[y_1(\zeta) + \frac{\epsilon}{\sqrt{\xi}} y_2(\zeta) + \ldots\right] \quad (8.5)$$

where

$$y_1 = T_w\zeta - [(\gamma - 1)/2]M^2(f_0 f_0' + 2f_0'' - 0.664)$$
$$y_2 = \left\{[(\gamma - 1)M^2 v_0]/\beta\right\}\,[\zeta + I(\zeta)] \quad (8.6)$$

The function $I(\zeta)$ has the properties that $I = 0(\zeta)$ if ζ is small and tends asymptotically to a constant at infinity. Thus, when ζ is large, y as a function of ξ and ζ reduces to

$$y = \epsilon\sqrt{\frac{\xi}{p}}\left[1 + \frac{(\gamma - 1)M^2 v_0 \epsilon}{\beta\sqrt{\xi}}\right]\zeta + 1.19(\gamma - 1)M^2\,\epsilon\sqrt{\frac{\xi}{p}} + 0(\epsilon^2) \quad (8.7)$$

On the other hand, the coordinate x, according to Eqs. (3.1), and (8.1), for large ζ is

$$x = \xi + \frac{v_0\epsilon}{\beta}\left(\frac{\beta^2}{v_0}\zeta + C_2 - 1.72\frac{\beta^2}{v_0}\right)\sqrt{\xi} + \ldots \quad (8.8)$$

The elimination of $\zeta\sqrt{\xi}$ between Eqs. (8.7) and (8.8) leads to a relation expressing ξ as a function of x and y—viz.,

$$\xi^{3/2} + \frac{v_0\epsilon}{\beta}M^2\left(\frac{\gamma + 1}{2}\frac{M^2}{\beta^2} - 2\right)\xi - (x - \beta y)\xi^{1/2} + \frac{(2 - \gamma)M^2 v_0 \epsilon\, y}{2} = 0 \quad (8.9)$$

It is interesting to note that ξ, and so the velocity at large ζ, is constant on straight lines in x, y-plane. It will be shown later that these straight lines are the outgoing Mach waves. This point will be further amplified below.

By comparing Eq. (8.9) with Eqs. (5.4) and (7.6), the arbitrary function $B(t)$ must be zero, and $A(s)$ is equal to $v_0 c_3\sqrt{s}/\beta$. The transformation equation for the inviscid field can then be written as

$$s^{3/2} + \frac{v_0\epsilon}{\beta}\left(c_3 - \frac{\gamma + 1}{4}\frac{M^4}{\beta^2}\right)s - (x - \beta y)s^{1/2} - \frac{(\gamma + 1)M^4 v_0 \epsilon y}{2\beta^2} = 0 \quad (8.10)$$

As the velocities in the viscous field at $\zeta \to \infty$ are functions of ξ and those of the inviscid field are functions of s by Eqs. (4.6) and (6.2), the velocity field will agree at a point (x, y) only when their arguments agree. To the first approximation, this condition is fulfilled if

$$c_3 = -[(5 - 3\gamma)M^2 - 8]M^2/4\beta^2$$

as in the region of overlapping y is of the order ϵ. In order to make the joining accurate to $0(\epsilon^2)$, the second-order term $\epsilon^2\psi^{(2)}$ in Eq. (3.1) will have to be considered.

This completes the problem of continuation of the viscous solution into the external inviscid field. What has been done here is essentially the restoration of the correct analytic behavior at the edge of the boundary layer to the first-order velocities and the suppression of the second-order pressure in the whole field. Moreover, by means of coordinate distortion the viscous and inviscid solutions are made to overlap in a region rather than along a line, and consequently a smooth transition from viscous to inviscid field has been achieved.

(9) Properties of the Transformation

The analytic behavior of the transformation determined in the preceding section can now be investigated. From Eq. (8.10) it is clear that the inverse transformation of Eq. (5.4) will be three-sheeted. The branch-point is given by

$$x_s = 0$$

which corresponds also to the vanishing of the Jacobian of the transformation. As the flow behind the shock is regular, the Jacobian is expected to be finite and non-vanishing.

It can be proved very simply from Eq. (8.10) that the branch $\sqrt{s} > 0$ covers the whole right half (x, y) plane singly but folds three times in the left half plane. The envelope begins to form at negative infinity $(\sqrt{s} = \infty, x = y = -\infty)$ and moves forward to a point $x = -0(\epsilon^2)$, $y = 0(\epsilon^2)$, $[\sqrt{s} = 0(\epsilon)]$ where it has cusp and turns abruptly toward the origin $(\sqrt{s} = 0)$ with a horizontal tangent. Therefore, in the physical domain $x \geq 0$ and $y \geq 0$ and $0\ (\epsilon) < \sqrt{s}$, the transformation is regular.

The relationship between the parameter s and (x, y) as expressed by Eq. (8.10) has a very simple geometrical interpretation. s = constant are parallel straight lines in the ξ, η-plane, which belong to the out-going family of Mach waves by the linearized theory. Now, if s is held constant in Eq. (8.10), there results a linear relation betwcen x and y. The equation of this straight line can be written as

$$\left[1 - \frac{(\gamma + 1)\ M^4}{2 \quad \beta^3}\,\theta(s)\right] y = \frac{x}{\beta} - \frac{s}{\beta}\left\{1 - \frac{[(3 - \gamma)M^2 - 4]M^2}{2\,\beta^3}\,\theta(s)\right\} \quad (9.1)$$

whcre $\theta(s) = \epsilon v_0/\sqrt{s}$. It can be readily verified that this equation, to the first order, represents just the out-going family of Mach waves in the x, y-plane if θ is interpreted as the local deflection of the flow. Thus, the original parallel straight Mach wavcs in the ξ, η-plane become a family of straight waves in the x, y-plane, whose slope increases toward the leading edge.

These conclusions, in part, cover also the transformations (3.1) and (3.2), for as ζ is large they tend to merge and, consequently, must share the same property. When ζ is not large, a separate study has to be made. The Jacobian of the transformations (3.1) and (3.2), to the first order, is proportional to

$$1 + [(\epsilon v_0)/(2\beta\sqrt{\xi})]\ [C_2 + 0(\zeta^3)] > 0$$

when ζ is small and $g_1 \simeq C_2 + 0(\zeta)$. Therefore, the transformations (3.1) and (3.2) can be singular only at the origin $\xi = 0$ for small ζ. By increasing ζ, the factor in the bracket will first change sign and then gradually tends to the asymptotic value of the inviscid case. Since both g_1 and $T^{(0)}$ are regular functions of ζ, the above argument is sufficient to establish the regularity of the transformations (3.1) and (3.2).

The relationship between the pair of variables (ξ, η) and (x, y) can be ascertained by study, to the first order, of the equations:

$$\left.\begin{aligned} x &= \xi + [(v_0\epsilon)/\beta]\ g_1\sqrt{\xi} + 0(\epsilon^2) \\ y &= \epsilon\sqrt{\xi/p}\ y_1 + 0(\epsilon^2) \end{aligned}\right\} \quad (9.2)$$

where g_1 and y_1 are defined respectively in Eqs. (8.1) and (8.6). If this transformation is considered exact, it would follow that $\xi = 0$ is transformed to the origin of the x, y-plane. To any ξ = const. $\neq 0$ there corresponds a curve that begins at the wall with a positive slope and approaches asymptotically a straight line at infinity. On the other hand, ζ = const. lines, which are parabolas with vertices at the origin, correspond to lines in the x, y-plane

$$y = \frac{\epsilon}{\sqrt{p}}\,y_1\left(-\frac{1}{2}\tilde{g} + \sqrt{x + \frac{1}{4}\tilde{g}^2}\right), \qquad \sqrt{\xi} > 0 \quad (9.3)$$

where $\tilde{g} = v_0\epsilon g_1/\beta$. Since $y_1 \geq 0$ for $\zeta \geq 0$, $y = 0$ when $x = 0$; and $y \equiv 0$ when $\zeta = 0$. It follows that all curves pass through the origin.

This shows that without considering high-order effects, the viscous region remains in the region $x \geq 0$ and $y \geq 0$, as in the Blasius problem. The boundary-layer thickness, however, grows as $x^{3/2}$ near the leading edge, instead of as $\sqrt{x}$, according to the Blasius solution. The constant of proportionality is approximately $1/(\epsilon v_0 M^2)$ at high Mach Number (a factor depending on γ has been left out). When x is large, according to Eq. (9.3), the boundary-layer thickness asymptotically tends to $\epsilon y_1[\sqrt{x} - (1/2)\tilde{g}]$.

It might be of interest to point out that previously Schaaf,[8] by a simple consideration that takes into account slip effect but neglects pressure, had reached the conclusion that the boundary layer initially grows linearly with x, which can also be deduced from Eq. (9.3) by putting $p = 1$. From this it follows also that the initial slope of the boundary-layer thickness is $2/(\gamma + 1)M$, being independent of Reynolds Number. The difference betwcen these two results is large and should serve as a crucial test for the two different assumptions. The implications of the new result will be further discussed in connection with the shock pattern near the leading edge.

(IV) Results and Conclusions

(10) Pressure on the Plate

According to the method adopted in Sections (6) and (7), the induced pressurc is determined, by the knowledge of the maximum viscous displacement of a streamline, in terms of a characteristic parameter—namely, the out-going Mach waves. By continuation of the velocity and pressure fields as established in Section (8), it is shown that the pressure in the boundary layer reads

$$p = 1 + [(\gamma M^2 v_0\epsilon)/(\beta\sqrt{\xi})] + 0(\epsilon^3) \quad (10.1)$$

As ξ is a function of both x and y, the pressure in the

boundary layer, consequently, varies in both directions x and y.

On the plate where y vanishes, g_1 reduces to C_2, and the equation governing ξ and x becomes

$$\xi + [(v_0 C_2 \epsilon)/\beta] \sqrt{\xi} - x = 0 \qquad (10.2)$$

or

$$\sqrt{\xi} = -\frac{v_0\epsilon}{2\beta}\left(\frac{\gamma+1}{2}\frac{M^4}{\beta^2} - 2\right) + \sqrt{x + \frac{v_0^2\epsilon^2}{4\beta^2}\left(\frac{\gamma+1}{2}\frac{M^4}{\beta^2} - 2\right)^2}$$

The elimination of ξ between Eqs. (10.2) and (10.1) leads to the expression:

$$p = 1 + \frac{\gamma M^2 v_0\epsilon}{\beta\sqrt{x}}\left[\frac{v_0\epsilon}{2\beta\sqrt{x}}\left(\frac{\gamma+1}{2}\frac{M^4}{\beta^2} - 2\right) + \sqrt{1 + \frac{v_0^2\epsilon^2}{4\beta^2 x}\left(\frac{\gamma+1}{2}\frac{M^4}{\beta^2} - 2\right)^2}\right] \qquad (10.3)$$

By defining two parameters K and χ:

$$K = \gamma M^2 \Big/ \left(\frac{\gamma+1}{2}\frac{M^4}{\beta^2} - 2\right),$$

$$\chi = \frac{v_0\epsilon}{\beta\sqrt{x}}\left(\frac{\gamma+1}{2}\frac{M^4}{\beta^2} - 2\right) \qquad (10.4)$$

the pressure given in Eq. (10.3) can be expressed as

$$\frac{p-1}{K} = \chi\left(\frac{1}{2}\chi + \sqrt{1 + \frac{1}{4}\chi^2}\right) \qquad (10.5)$$

It is interesting to remark that as for large x, $v_0\epsilon/\sqrt{x}$ is approximately the deflection θ of the flow at the edge of the boundary layer, the parameter χ at hypersonic Mach Numbers reduces to $(\gamma+1)M\theta/2$ and the pressure given in Eq. (10.5) becomes identical to the pressure on a wedge airfoil, deduced first by Linnell.[9] In the present case, however, as the surface deflection is not uniform, it implies that Linnell's formula, although derived for the case of uniform flow, can be applied to calculate the pressure on a curved surface. This has been also independently verified by Probstein* at Princeton, and good agreement with the characteristics method has been obtained. It is also of interest to note that, using the shock-expansion theory Lighthill[10] has shown that for small θ the pressure given by Eq. (10.3) is accurate to $0(\theta^3)$.

The universal form for the pressure on the plate in Eq. (10.5) is plotted in Fig. 1. In view of the fact discussed above, the available experimental data† at different Reynolds and Mach Numbers and for different gases have been converted on the same graph by Eq. (10.5). As χ is directly proportional to $M^{2+\omega}$ and inversely to $\sqrt{Rex}$, the increase of χ may either mean

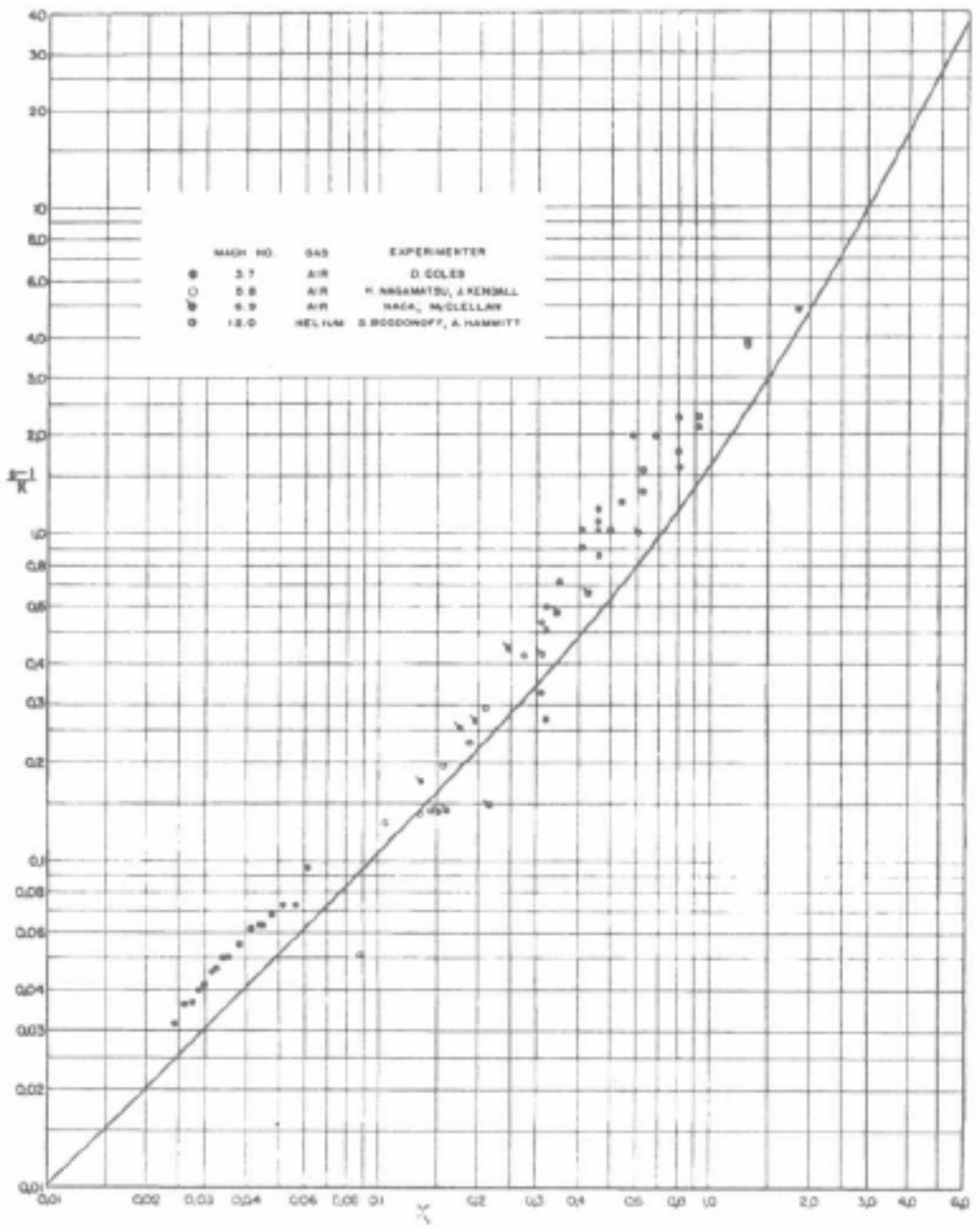

FIG. 1. Pressure distribution along the plate. The solid curve represents Eq. (10.5). Points denote experimental data by Coles,[13] Nagamatsu and Kendall,[14] Bertram,[15] and Bogdonoff and Hammitt.[16] *Correction:* "McClellan" appearing within the drawing should read "Bertram."

increase of Mach Number or decrease of x. Thus, in the weak interaction zone, the curve is nearly linear. It tends to be quadratic in the strong interaction zone. At present stage, the experimental accuracy is still difficult to assess, but within the range of experimental scattering the theoretical curve does seem to give a consistent correlation. In order to establish this formula firmly, more experimental data are, of course, urgently needed.

(11) Velocity Field

The formulas for the velocities in the boundary layer are already given by Eqs. (4.2) and (4.3). These formulas together with the function g_1 in Eq. (8.1) describe the velocity distribution in the boundary layer. In this preliminary study, however, detailed numerical calculations will not be made. A simple qualitative discussion will be given below.

First, for small ζ, the pair of transformation equations can be approximated by

$$\left.\begin{aligned} x &= \xi + \frac{v_0\epsilon}{\beta}\left(C_2 + \frac{0.32\beta^2 T_w}{v_0}\zeta\right)\sqrt{\xi} + 0(\zeta^3) \\ y &= (\epsilon T_w/\sqrt{p})\zeta\sqrt{\xi} + 0(\zeta^3) \end{aligned}\right\} \qquad (11.1)$$

where p is the pressure on the plate given by Eq. (10.3). To the same approximation, the velocities u and v are

$$\left.\begin{aligned} u &= 0.332\,\zeta + \ldots \\ v &= [(0.332\,T_w\epsilon)/(4\sqrt{p})]\,(\zeta^2/\sqrt{\xi}) + \ldots \end{aligned}\right\} \qquad (11.2)$$

* Unpublished.

† The author is indebted to Prof. Lester Lees of the California Institute of Technology for supplying him with the assembled experimental data.

Since p is singular at the leading edge and by Eq. (10.3) $\sqrt{p} \sim v_0 M\epsilon/\sqrt{x}$ for $\sqrt{x} << \epsilon v_0 c_2/2\beta$, the transformation equations yield

$$\sqrt{\xi} \sim [\beta/(\epsilon v_0 c_2)]x[1 - \alpha M^2\epsilon(y/x^{3/2})]$$

where $\alpha = 0.332\sqrt{\gamma(\gamma+1)/2}$. Within the boundary layer and for small ζ, the quantity in the second set of brackets is never zero. Therefore, in a small neighborhood at the leading edge, $u = \tilde{u}(y/x^{3/2})$ and $v = x^{-1/2}\tilde{v}(y/x^{3/2})$. The existence of the parameter $y/x^{3/2}$ is in agreement with the behavior of the boundary-layer thickness near the leading edge The fact that the velocity field exhibits such a singularity at $x = 0$ indicates that the solutions will not be valid for $x < 0(M^6\epsilon^2)$.

When $x = 0(M^6\epsilon^2)$ but $\chi < 1$, it follows that p is proportional to $1/\sqrt{x}$, $u = \tilde{u}(y/x^{3/4})$, and $v = \bar{x}^{-1/4}\tilde{v}(y/x^{3/4})$ approximately. These are essentially the forms deduced by the similarity hypothesis. In view of the fact that in this range of x the parameter χ is almost unity, the approximation of the pressure Eq. (10.3) by the leading term $K\chi$, as in the case of the similarity solutions, is clearly difficult to justify. This might be the reason why the validity of the similarity solutions is restricted.

If x is large, the effect of the coordinate distortion will be small. x then will be approximately ξ, and p is almost unity. In other words, in the weak interaction zone the flow in the boundary layer will have much the same characteristics as that under constant pressure.

On the other hand, for arbitrary x as ζ is large, the velocities Eqs. (4.2) and (4.3) reduce to

$$\left.\begin{aligned} u &= 1 - [(\epsilon v_0)/(\beta\sqrt{\xi})] + 0(\epsilon^3) \\ v &= [(\epsilon v_0)/\sqrt{\xi}] - \{[\epsilon^2 v_0^2(\gamma+1)M^4]/(4\beta^3\xi)\} + 0(\epsilon^3) \end{aligned}\right\} \tag{11.3}$$

From Eqs. (8.9) and (8.10) ξ approaches asymptotically s as ζ becomes infinite, u and v then merge smoothly with the external field described by Eqs. (5.3) and (6.2). As pointed out previously—s = constant lines are out-going Mach lines in the x, y-plane—the velocity field in the boundary layer then approaches the values described by the simple wave theory.

(12) Determination of Shock Strength

Let the shock curve be represented by $y_s = y_s(x)$. Then, the shock strength $p - 1$, according to the Rankine-Hugoniot relations, is given by

$$p - 1 = [(2\gamma)/(\gamma+1)]\{[(M^2 y_s'^2)/(1 + y_s'^2)] - 1\} \tag{12.1}$$

where the prime denotes differentiation with respect to x. From Eqs. (5.3) and (6.2), y_s' can be solved in terms of $\theta(s)$:

$$y_s'^2 = \frac{1}{\beta^2}\left\{\left[1 + \frac{\gamma+1}{2}\frac{M^2}{\beta}\theta(s)\right] \div \left[1 - \frac{\gamma+1}{2}\frac{M^2}{\beta^3}\theta(s)\right]\right\} \tag{12.2}$$

where s as function of x and y is given by Eq. (8.10).

Since the deflection of the flow $\theta(s)$ increases with decreasing s, the denominator of Eq. (12.2) will diminish toward the leading edge. Accordingly, the slope of the shock curve will increase as one proceeds along the shock from infinity and becomes infinite when the denominator vanishes. This critical point at large Mach Number is found to be $\sqrt{s} = 0(M\epsilon)$. However, the smallest value that $\sqrt{s}$ is allowed to reach is, from Section (9), $0(M^3\epsilon)$, where the Mach line will be parallel to the y-axis. Therefore, infinite slope cannot occur in a physically realizable region, and, as a consequence, the shock can be assumed to begin at the leading edge where $\sqrt{s} = \sqrt{s_0} = [(\gamma+1)/(2\beta^3)]M\epsilon v_0$, by Eq. (9.1).

Since the largest value of $(\gamma+1)M^2\theta(s)/2\beta^3$ in the denominator of Eq. (12.2) is $0(1/M^2)$, Eq. (12.2) can be simplified by writing:

$$\dot{y}_s = (1/\beta)\{1 + [(\gamma+1)/2](M^4/\beta^3)\theta(s)\}^{1/2}\dot{x} \tag{12.3}$$

where $(\dot{})$ denotes differentiation with respect to s. From Eq. (8.10), on the other hand, y can be expressed in terms of both x and s—namely,

$$\beta y_s = [1 - (2\epsilon\sigma/\sqrt{s})]^{-1}(x - s + 2\epsilon\sigma m\sqrt{s}) \tag{12.4}$$

where $\sigma = (\gamma+1)M^4 v_0/4\beta^3$ and $m = [(3-\gamma)M^2 - 4]/(\gamma+1)M^2$. By differentiating Eq. (12.4) with respect to s along the shock, there will result a new relationship between $\dot{x}$ and $\dot{y}_s$. This relation, together with Eq. (12.3), then yields

$$\dot{x} - P(s)x = Q(s) \tag{12.5}$$

where

$$P(s) = \epsilon\sigma s^{-3/2}\left(1 - \frac{2\epsilon\sigma}{\sqrt{s}}\right)^{-1} \times \left[1 - \left(1 - \frac{2\epsilon\sigma}{\sqrt{s}}\right)\left(1 + \frac{2\epsilon\sigma}{\sqrt{s}}\right)^{1/2}\right]^{-1}$$

$$Q(s) = \left[1 - \left(1 - \frac{2\epsilon\sigma}{\sqrt{s}}\right)\left(1 + \frac{2\epsilon\sigma}{\sqrt{s}}\right)^{1/2}\right]^{-1} \times \left(1 - \frac{\epsilon\sigma m}{\sqrt{s}} - \left\{\left[\epsilon\sigma\left(1 - \frac{2\epsilon\sigma m}{\sqrt{s}}\right)\right] \div \left[\sqrt{s}\left(1 - \frac{2\epsilon\sigma}{\sqrt{s}}\right)\right]\right\}\right)$$

From the initial condition that when $s = s_0$, $x(s_0) = 0$, there follows the solution:

$$x = e^{\int_{s_0}^{s} P ds}\int_{s_0}^{s} Q\, e^{-\int_{s_0} P ds}\, ds \tag{12.6}$$

which together with Eq. (12.4) gives a parametric representation of the shock curve.

When s is large, $P \sim 1/s$ and $Q \sim \sqrt{s}/\epsilon\sigma$. Eq. (12.6) then gives

$$x \sim [2/(\epsilon\sigma)]s^{3/2} + 0(s)$$

From Eq. (12.4), the shock curve asymptotically tends to

$$\beta y_s \sim x + (3/2^{2/3})\,(\epsilon\sigma x)^{2/3},\ x >> 1 \qquad (12.7)$$

When x is small, $s \sim s_0$. From Eqs. (11.9) and (12.3)

$$y_s \sim \sqrt{2}\,(x/M) \qquad (12.8)$$

The shock curve according to Eqs. (12.7) and (12.8), together with the Mach waves Eq. (11.8), is illustrated in Fig. 2. It shows that the shock begins at the leading edge and increases linearly with x with a slope twice as large as that of the boundary-layer thickness in that region. The fact that the character of the shock near the leading edge does not depend on the viscous effect may indicate either the breakdown of the no-slip hypothesis for $\sqrt{x} < \epsilon\sigma$ or that the flow near the leading edge is dominated mainly by compressibility effects. Neither case, however, supports the view that near the leading edge the shock and the boundary-layer thickness coincide.

With the asymptotic shock curve Eq. (12.7), it can be deduced that the shock strength decays asymptotically according to

$$p - 1 \sim [\gamma/(\gamma + 1)]\,(\sqrt{2}\,\sigma\epsilon)^{2/3}x^{-1/3}, x \gg 1 \qquad (12.9)$$

That is, the shock strength falls off with a rate much slower than the decay of pressure along the plate. This is consistent with the fact that for large x the shock is nearly parallel to the Mach waves, along which the flow properties are constant.

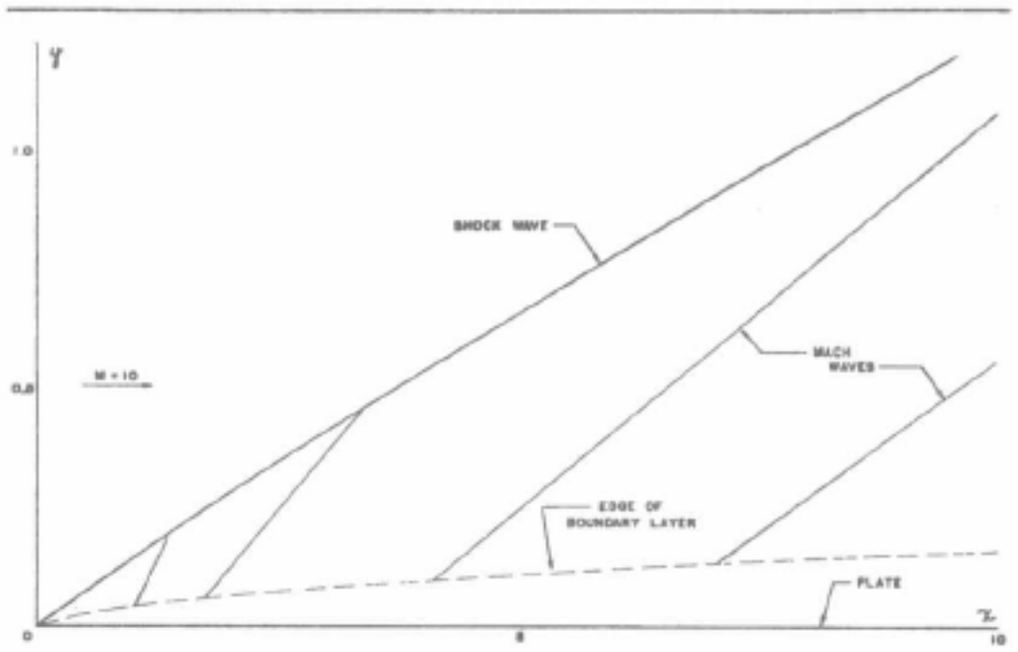

FIG. 2. Wave system in the inviscid field outside the boundary layer for $\gamma = 1.40$, $\epsilon = 10^{-3}$, and $M = 10$. In the figure the scale of the ordinate has been magnified by a factor of ten.

(13) Skin Friction

Following the definitions of Eqs. (2.1), (2.4), and (3.1), the shear stress on the wall can be calculated by

$$\bar{\mu}_w(\partial\bar{u}/\partial\bar{y})_w = (U\mu_\infty/L)C\epsilon^{-1}p^{1/2}(\psi_{YY})_w$$

where p is the pressure given by Eq. (10.3). If the skin-friction coefficient c_f is introduced, then

$$c_f = \bar{\mu}_w(\partial\bar{u}/\partial\bar{y})_w/(1/2)\rho_\infty U^2 = 2\epsilon p^{1/2}(\psi_{YY})_w \qquad (13.1)$$

From the transformation (3.5)

$$(\psi_{YY})_w = (0.322/\sqrt{\xi}) - [(\epsilon v_0\alpha_1)/(\beta\xi)] + \ldots$$

The substitution in Eq. (13.1) gives

$$c_f = 2\epsilon p^{1/2}\{(0.332/\sqrt{\xi}) - [(\epsilon v_0\alpha_1)/(\beta\xi)] + \ldots\} \qquad (13.2)$$

where $\alpha_1 = (0.332/2)\,(C_2 + M^2) - 0.860T_w$ and $\sqrt{\xi}$ is defined in Eq. (10.2).

Thus, the skin friction on the plate is determined by two opposing effects: the second term in the braces, which represents the contribution by the shock, tends to diminish the friction, while the induced pressure tends to increase it. Shock decreases the velocity outside of the boundary layer, and hence the slope of the velocity profile is reduced, resulting in smaller skin friction. Pressure increases the density of the fluid and contracts the boundary layer; it thus tends to increase the slope of the velocity profile and the skin friction. In the weak interaction zone, the effect of the coordinate contraction is strong, and the shear is in excess of the value deduced by the von Kármán and Tsien theory. In the strong interaction zone, however, the effect of the shock is dominant; the shear increases at a slower rate than according to the classical law and falls off after a maximum has been reached (Fig. 3). A simple calculation shows that the shear vanishes at $\sqrt{\xi} = \epsilon v_0\alpha_1/0.332\beta$. In the case of air at $M = 10$, $\epsilon = 10^{-3}$ this corresponds to x approximately 0.01 cm.

This shows that the combined effects of interaction produce near the leading edge a phenomenon that is similar to ordinary boundary-layer flow under favorable pressure gradient, for which the shear continually increases in the direction of the flow. In the case of high-speed flow, this has customarily been attributed to the slip effect, but this conjecture has not been borne out by the present investigation. It is believed that with proper accuracy the Navier-Stokes equations can still give a correct physical picture without the necessity of introducing new hypotheses.

(14) Conclusions and Discussions

To summarize, it can be concluded that at high supersonic speeds, the flow past a flat plate can still be subdivided into viscous and nonviscous fields. In the outer, inviscid field, the flow is irrotational and can be described, to at least second order, by Friedrichs' simple waves,[11] which are shown by Lighthill[12] to be correct to this order. In the inner, viscous field, the flow is of the boundary-layer type, but the problem has to be dealt with by a combination of the boundary-layer theory and Lighthill's method of straining the coordinates. Concrete results concerning the flow are as follows:

(1) The leading-edge shock is attached, with an initial shock strength $2\gamma/(\gamma + 1)$ for $M \gg 1$ and an initial slope $\sqrt{2}/M$. Far away from the leading edge it approaches the Mach wave with a rate proportional to $(\epsilon\sigma)^{2/3}x^{-1/3}$, according to which its strength decays.

(2) The pressure along the plate can be expressed in a form in which the parameter can be interpreted as the

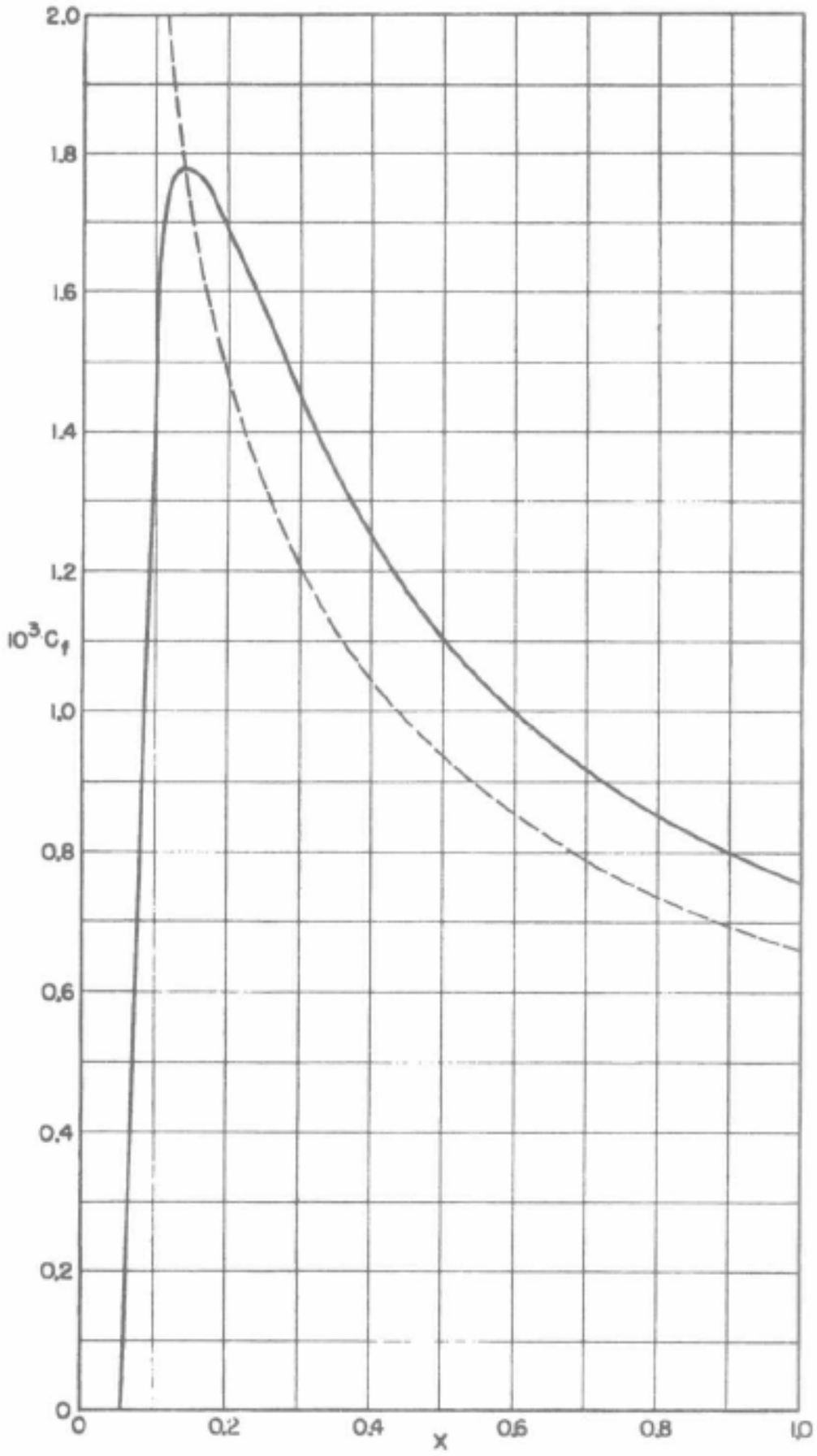

FIG. 3. Local skin friction along the plate for $\gamma = 1.40$, $\epsilon = 10^{-3}$, and $M = 10$. The dashed curve shows the skin friction when the shock wave is absent.

local deflection of a streamline. In the hypersonic range the pressure formula reduces to the same form as that on a wedge airfoil. In fact, for both the viscous and the inviscid fields, the solutions depend on a parameter that corresponds to Tsien's hypersonic parameter—i.e., $Mv_e \sim M^{2+\omega}/\sqrt{Rex}$. This is in full agreement with Lees' hypothesis.[1]

(3) The second-order vertical velocity component is directed inward, and, consequently, there results a reduction of boundary-layer thickness, as compared with the case of a shock-free flow.

(4) The boundary-layer thickness grows like $x^{3/2}$ near the leading edge due to the singularity of the pressure. If the pressure were regular at the leading edge, the boundary layer would grow linearly with x. When x is large, it assumes the behavior of the ordinary boundary layer.

(5) The skin friction on the plate is larger than for the case in which the pressure is constant, when x is large. As x decreases toward the leading edge, the skin friction increases gradually and falls off after it reaches a maximum. If the singularity were shifted toward the other side of the flow field, the skin friction would be finite at the leading edge.

In view of the fact that the shock is initially independent of the viscous effects, it must be concluded that the initial behavior of the boundary-layer thickness cannot be proportional to $x^{3/2}$. For this would imply that the flow would follow concave streamlines and would be compressive but continuous; then the viscous effects would have a strong influence on the shock and Mach waves. This seems to indicate that the solution cannot be valid when x is less than $0(m^6\epsilon^2)$.

The deficiency of the first-order theory can be seen also from Eqs. (8.9) and (8.10) in connection with the continuation of the solutions from one to the other field. If in the transformation (3.1) a term $\epsilon^2 x^{(2)}$ were added, then it would be possible to make Eqs. (8.9) and (8.10) agree to the order ϵ^2. In that event, when $\sqrt{\xi}$ is $0(M^3\epsilon)$, the transformation equation [Eq. (3.1)] would likely cease to converge, and a different approach near the leading edge would have to be contemplated.

REFERENCES

[1] Lees, L., *On Boundary-Layer Equations in Hypersonic Flow and Their Approximate Solutions*, Journal of the Aeronautical Sciences, Vol. 20, pp. 143–145, 1953.

[2] Lighthill, M. J., *A Technique for Rendering Approximate Solutions to Physical Problems Uniformly Valid*, Phil. Mag., Vol. 40, pp. 1179–1201, 1949.

[3] Shen, S. F., *An Estimate of Viscosity Effect on the Hypersonic Flow over an Insulated Wedge*, J. of Mathematics and Physics, Vol. 31, pp. 192–205, 1952.

[4] Howarth, L., *Concerning the Effect of Compressibility on Laminar Boundary Layers and Their Separation*, Proc. Roy. Soc., A 194, pp. 16–42, 1948.

[5] Chapman, D. R., and Rubesin, M. W., *Temperature and Velocity Profiles in Compressible Laminar Boundary Layer with Arbitrary Distribution of Surface Temperature*, Journal of the Aeronautical Sciences, Vol. 16, pp. 547–565, 1949.

[6] von Kármán, Th., and Tsien, H. S., *Boundary Layer in Compressible Fluids*, Journal of the Aeronautical Sciences, Vol. 5, pp. 227–232, 1938.

[7] Maslen, S. H., *Second Approximation to Laminar Compressible Boundary Layer on Flat Plate in Slip Flow*, NACA TX 2818, 1952.

[8] Schaaf, S. A., *A Note on the Flat Plate Drag Coefficient*, Univ. of California, Engineering Research Report No. HE-150-66, February, 1950.

[9] Linnell, R. D., *Two-dimensional Airfoil in Hypersonic Flows*, Journal of the Aeronautical Sciences, Vol. 16, pp. 22–30, 1949.

[10] Lighthill, M. J., *High-speed Aerodynamics and Jet Propulsion*, Vol. VI, Sec. E, Princeton University Press, p. 387, 1954.

[11] Friedrichs, K. O., *Formation and Decay of Shock Waves*, Communications on Pure and Applied Math., Vol. 1, pp. 211–245, 1948.

[12] Lighthill, M. J., *The Energy Distribution Behind Decaying Shocks*, Phil. Mag., Vol. 41, No. 7, pp. 1101–1128, 1950.

[13] Coles, D., *Measurements in the Boundary Layer on a Smooth Flat Plate in Supersonic Flow*, Ph.D. thesis, California Institute of Technology, 1953.

[14] Nagamatsu, H., and Kendall, J., Guggenheim Aeronautical Laboratory, California Institute of Technology, Preliminary data, Unpublished.

[15] Bertram, M. H., *An Approximate Method for Determining the Displacement Effects and Viscous Drag of Laminar Boundary Layers in Two-Dimensional Hypersonic Flow*, NACA TN 2773, September, 1952.

[16] Bogdonoff, S. M., and Hammitt, A. G., Department of Aeronautical Engineering, Princeton University, Preliminary data, unpublished, 1954.

Viscous Flow Along a Flat Plate Moving at High Supersonic Speeds* 1)

Y. H. Kuo
Graduate School of Aeronautical Engineering, Cornell University, Ithaca, New York
June 7, 1956

At the Annual Meeting of the Institute of the Aeronautical Sciences, January, 1956, James M. Kendall, Jr., presented a set of highly interesting data on the characteristics of the flow over a flat plate at Mach Number 5.8, obtained from the GALCIT 5- by 5-in. hypersonic wind tunnel.[1] By measuring the impact-pressure profiles and the static pressure along the plate, as previously reported by H. T. Nagamatsu,[2] he was able to deduce the detailed structural features of the flow field. These results reveal definitely that the flow field between the shock and the plate has two distinct regions—the one which is close to the plate is of the boundary-layer type, and the other which is far from the plate is nearly inviscid and of the simple-wave type. This picture is in complete accord with the model that has been used in a theoretical calculation.[3] To substantiate this point of view, it is proposed to make further quantitative comparisons.

Of the results reported by Kendall, the surface pressure was measured with the greatest degree of certainty. As the leading edge of the plate was thin (0.0002 in.), the thickness effects must have been very much reduced, if not entirely eliminated. The surface pressure affords, for this reason, the best chance of a check of the theoretical result. This comparison is made in Fig. 1. The experimental points for three different Reynolds numbers fall very close to the theoretical curve for the parameter $\bar{\chi}$ less than 2 and lie below it beyond that value of $\bar{\chi}$, i.e., very close to the leading edge.

Previously, D. Coles has made a similar measurement at Mach 3.7, which, when compared with theoretical values, was found consistently high.[3] The good agreement now achieved by Kendall's results shows definitely that the leading-edge geometry of Cole's plate caused an additional deflection of the flow, as in the case of a wedge and, therefore, gave rise to a slightly higher pressure.

The divergence of the measurements and calculations beyond $\bar{\chi}$ equal to 2 may well be attributed to the inaccuracies of either the pressures measured or those calculated in the neighborhood of the leading edge (less than 0.08 in. from the leading edge, say). Without further careful measurements nothing definite can be said at this moment.

Based on the impact-pressure profiles, Kendall deduces approximately the flow properties behind the shock, such as velocity, mass flow, static pressure, etc. Of these quantities, the static-pressure profile is the most interesting. It shows not only the behavior of the pressure inside the boundary layer and in the inviscid field but also the outer edge of the flow field—namely, the shock curve. The comparison with the estimated values at $x = 0.64$ in. is given in Fig. 2. That the measured surface pressure at $x = 0.64$ in. is too high—an anomaly pointed out by Kendall—seems to be borne out by the calculations. On the whole, the agreement in this case is qualitative only.

From the impact-pressure profiles, Kendall also defines the shock curve and the edge of the boundary layer. These are compared with the corresponding calculated ones in Fig. 3. The shock curve has been calculated not by means of the accurate formula but by its asymptotic form and is fitted to the measured value at $x = 0.25$ in. As a result, the agreement for large x is not

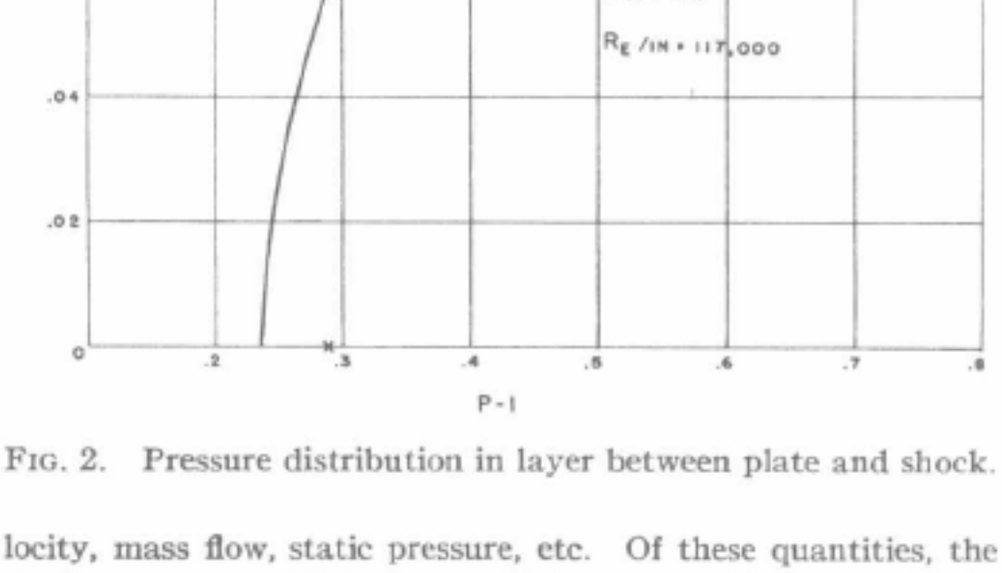

Fig. 2. Pressure distribution in layer between plate and shock.

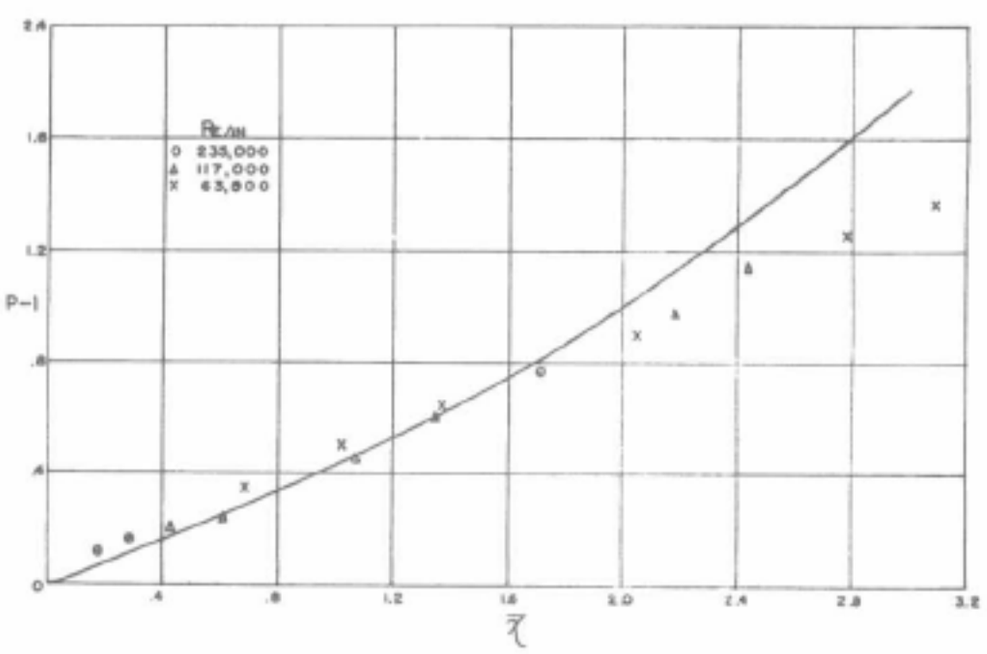

Fig. 1. Pressure distribution along the plate at $M = 5.8$

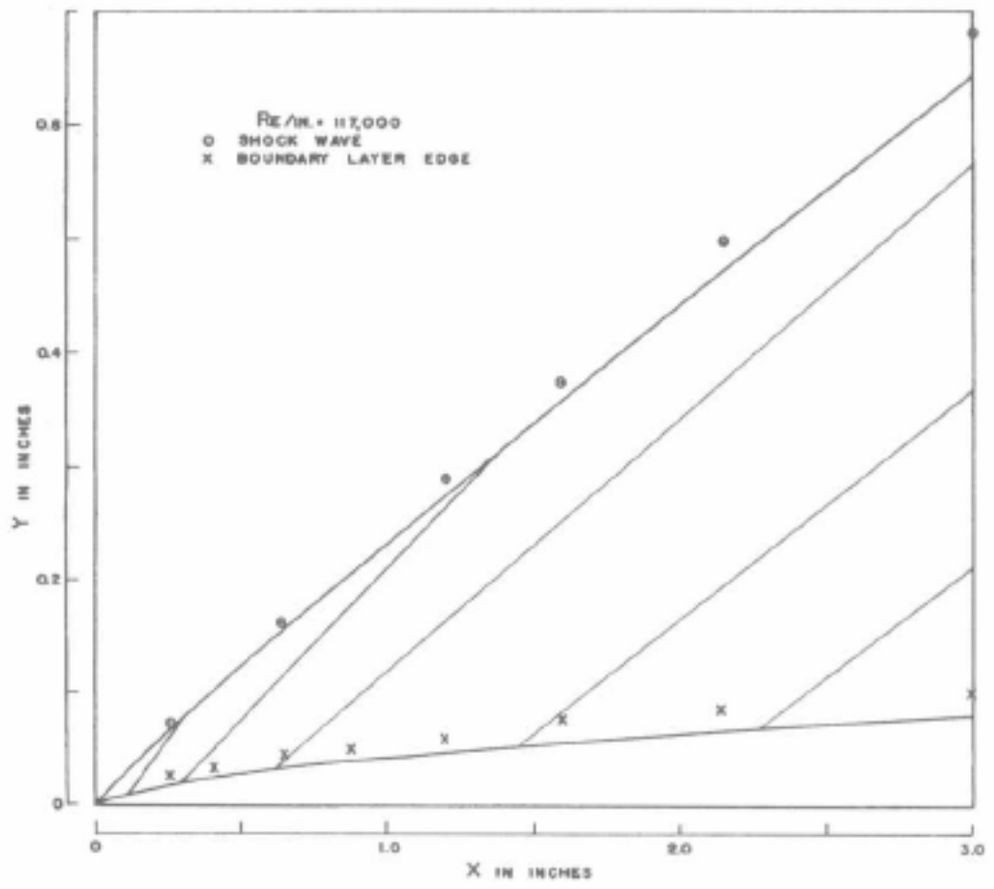

Fig. 3. Shock curve and edge of boundary layer at $M = 5.8$.

* This study was carried out at the suggestion of Dr. W. R. Sears, Director of the Graduate School of Aeronautical Engineering, with the financial support of the Mechanics Branch, Office of Naval Research. Reproduction in whole or in part is permitted for any purpose of the United States Government.

1) Published in *Journal of the Aeronautical Sciences*, 1956, 23(10): 977~978

so good as expected. On the other hand, the calculated boundary-layer edge lies consistently below the estimated curve. This discrepancy can possibly be explained by the fact that the calculation was based on the choice of the similarity parameter to be 7 instead of 8. In any case, the agreement in the boundary-layer curve is quite close.

References

[1] Kendall, Jr., James M., *Experimental investigation of leading edge shock wave-boundary layer interaction at hypersonic speeds*, Hypersonic Project Mem. No. 30, January, 1956.

[2] Nagamatsu, Henry T., *Summary of Recent GALCIT Hypersonic Experimental Investigations*, Journal of the Aeronautical Sciences, Vol. 22, No. 3, pp. 165–172, March, 1955.

[3] Kuo, Y. H., *Viscous Flow Along a Flat Plate Moving at High Supersonic Speeds*, Journal of the Aeronautical Sciences, Vol. 23, No. 2, pp. 125–136, February, 1956.

1058 JOURNAL OF THE AERONAUTICAL SCIENCES—NOVEMBER, 1956

The Effects of Prandtl Number on High-Speed Viscous Flows over a Flat Plate* [1)]

Y. H. Kuo
Professor, Graduate School of Engineering, Cornell University, Ithaca, N.Y.

July 16, 1956

THE FLOW of a viscous perfect gas over a semi-infinite flat plate at high flight Mach Number M was considered in a previous article[1] under the assumptions that (1) the plate is thermally insulated, (2) the Prandtl Number Pr is equal to unity, and (3) the viscosity μ varies linearly with temperature T. With the choice of a special coordinate system, the problem was treated by a method of perturbation, with the case of uniform pressure as the zeroth approximation. To the first order, the method yields a velocity field and pressure which approach at large distance from the plate the simple wave solution. Being of the simple wave type in the inviscid field, these solutions are actually correct to second order there.

The results of this analysis reveal an important parameter v_0 (defined further below), besides the Reynolds Number Re ($= U_\infty L/\nu_\infty$, U_∞, ν_∞ and L being, respectively, the velocity and viscosity of the gas at infinity). Together they appear in all flow quantities. Unlike the Reynolds Number, which characterizes the viscous effects, v_0 depends primarily on the temperature distribution and, therefore, is a function of Mach Number and represents the compressibility effects of the gases. It is the purpose of this note to investigate the functional dependence of v_0 on both Mach and Prandtl Numbers for both the case of an insulated plate and that of heat transfer—i.e., cold wall.

As shown in reference 1, the boundary layer deflects the main flow at a given point to the first approximation, by an amount which is proportional to v_0.

$$v_0 = 0.860 - \int_0^\infty \zeta T_0' \, d\zeta \tag{1}$$

where T_0 is the temperature ratio corresponding to constant pressure in the main stream and ζ, the similarity variable. The prime under the integral sign denotes total differentiation with respect to ζ. In the case of constant Prandtl Number and constant wall temperature, the temperature T_0 was found to be

$$T_0 = 1 + [(\gamma - 1)/2] M^2 \theta_{10}(\zeta, Pr) \tag{2}$$

for the insulated plate and

$$T_0 = 1 + [(\gamma - 1)/2] M^2 \theta_{10}(\zeta, Pr) + \left\{1 + [(\gamma - 1)/2] M^2 \sqrt{Pr} - T_w\right\} \theta_{20}(\zeta, Pr) \tag{3}$$

for heat transfer. Here T_w and γ are, respectively, the wall temperature ratio and the ratio of specific heats. The functions θ_{10} and θ_{20} are defined in terms of the Blasius function $f_0(\zeta)$.[2] For both cases, v_0 as an explicit function of γ, M, T_w, and Pr can be found by evaluating two integrals.

$$I_1 = \int_0^\infty \zeta (f_0'')^{Pr} \left[\int_0^\zeta (f_0'')^{2-Pr} \, d\zeta\right] d\zeta \tag{4}$$

and

$$I_2 = \int_0^\infty \zeta \left(\frac{f_0''}{\alpha_0}\right)^{Pr} d\zeta \tag{5}$$

where α_0 denotes the initial value of f_0''.

Numerical integration shows that I_1 is 1.54 and 2.04 for Pr equal to 0.72 and 0.50, respectively. From this, together with the value at $Pr = 1$, it is proposed to approximate I_1 by the formula

$$I_1 = 1.192 \, (Pr)^{-0.773} \tag{6}$$

This agrees with the exact values at $Pr = 1$ and 0.72 and gives a value of 2.00 at $Pr = 0.5$, with an error of only 2 per cent. In the case of I_2, the usual method of approximation, namely to replace f_0''/α_0 in the integrand by $\exp[-\alpha_0\zeta^3/12]$, leads to

$$I_2 = \left(\frac{2}{3}\right)^{1/3} \frac{3\Gamma[1 + (2/3)]}{(\alpha_0 Pr)^{2/3}} = \frac{4.93}{(Pr)^{2/3}} \tag{7}$$

On the other hand, at $Pr = 0.72$, numerical integration yields an answer of 6.55, while the approximate Eq. (7) gives 6.14. To improve this approximation, Eq. (7) is modified to read

$$I_2 = 5.182/(Pr)^{2/3} \tag{8}$$

This formula again agrees with the exact value at $Pr = 1$ but gives a value 6.45 at $Pr = 0.72$, which is in error by about 1.6 per cent.

If the approximate Eqs. (6) and (8) are accepted, at very high Mach Number v_0 can be approximated by

$$v_0 \doteq 0.596 \, (\gamma - 1) Pr^{0.227} M^2 \tag{9}$$

for the insulated wall; and

$$v_0 \doteq [0.596 Pr^{0.227} - 0.430 Pr^{1/6}] \, (\gamma - 1) M^2 \tag{10}$$

for the case of cooling with low wall temperature. From these it can be concluded that for Pr different from unity the hypersonic parameter $\bar{\chi}$ (see reference 3) has to be modified in the following manner: it is

$$Pr^{0.227} M^3 Re^{-(1/2)} \tag{11}$$

for the insulated plate; and

$$[Pr^{0.227} - 0.721 \, Pr^{1/6}] M^3 \, Re^{-(1/2)} \tag{12}$$

for heat transfer. It is further noted that, in the case of cooling at high Mach Number, the compressibility effects will be greatly reduced, in fact, the induced pressure at the same Reynolds Number is almost 70 per cent less than that if the plate were insulated. In the case of the insulated plate, the effect of reduced Pr is a slight reduction of the deflection of the streamlines and, hence, an attendant reduction of the induced pressure.

In the problem of high-speed flight, it is of importance to know, in addition to the local friction, the rate of local heat transfer at a specified constant wall temperature. For arbitrary Prandtl Number, a calculation similar to that in reference 1 can be carried out. This gives a local skin-friction coefficient c_f and a local heat-transfer number Nu, as follows:

$$c_f = 2\sqrt{c/Re}\sqrt{p/\xi} \, [\alpha_0 - \sqrt{c/Re} \, (v_0\alpha_1/\beta\sqrt{\xi}) + \ldots] \tag{13}$$

$$Nu = Pr^{1/3}\sqrt{cRe}\sqrt{p/\xi} \, [\alpha_0 - \sqrt{c/Re} \, (v_0\tilde{\alpha}_1/\beta\sqrt{\xi}) + \ldots] \tag{14}$$

where p and ξ are, respectively, the local pressure ratio and a parameter, both being functions of the distance x from the leading edge;[1] α_1, $\tilde{\alpha}_1$, and β are defined by

$$\alpha_1 = (\alpha_0/2) \left\{\gamma M^2 + [(\gamma + 1)/2] \, (M^4/\beta^2) - 2 - (v_0/\alpha_0)\right\}$$

$$\tilde{\alpha}_1 = \alpha_0 \left[\frac{(3\gamma + 1)M^4 - 2\gamma M^2}{4\beta^2} - 1\right]$$

$$\beta = \sqrt{M^2 - 1} \tag{15}$$

and, finally, the Chapman-Rubesin constant C, in the present case, is chosen as

$$C = [0.45 + 0.55 T_w + 0.09(\gamma - 1) M^2 \sqrt{Pr}]^{\omega - 1} \tag{16}$$

by assuming that the viscosity-temperature law at the point where it coincides with the linear relation is proportional to T^ω. In the case of large M, α_1 and $\tilde{\alpha}_1$ can be approximated by

$$\left.\begin{aligned} \alpha_1 &= \left\{[\alpha_0(3\gamma + 1)/4(\gamma - 1)] - 0.596 Pr^{0.227} + 0.430 Pr^{1/6}\right\} (\gamma - 1) M^2 \\ \alpha_1 &= \alpha_0 [(3\gamma + 1)/4] M^2 \end{aligned}\right\} \tag{17}$$

It is interesting to note that both constants α_1 and v_0 are greatly affected by cooling but the product $\alpha_1 v_0$ remains practically unchanged by heat transfer. Thus, insofar as cooling can decrease the skin friction, it is effected mainly through the reduction of pressure.

* This work was carried out as part of a research program at the Graduate School of Aeronautical Engineering and was supported by the Office of Naval Research. Reproduction in whole or in part is permitted for any purpose of the United States Government.

1) Published in *Journal of the Aeronautical Sciences*, 1956, 23(11): 1058~1059

REFERENCES

[1] Kuo, Y. H., *Viscous Flow Along a Flat Plate Moving at High Supersonic Speeds*, Journal of the Aeronautical Sciences, Vol. 23, No. 2, pp. 125–136, February, 1956.

[2] Schlichting, H., *Boundary Layer Theory*, pp. 265–267, McGraw-Hill Book Company, Inc., New York, 1955.

[3] Lees, L., *On Boundary-Layer Equations in Hypersonic Flow and Their Approximate Solutions*, Journal of the Aeronautical Sciences, Readers' Forum, Vol. 20, No. 2, pp. 143–145, February, 1953.

COMPRESSIBLE VISCOUS FLOW PAST A WEDGE MOVING AT HYPERSONIC SPEEDS* [1)]

By L. J. Pan and Y. H. Kuo

1. Introduction. When a thin sharp-nosed body flies at hypersonic speeds, the flow around the body is characterized by its high temperature and low density near the surface, due largely to the loss of kinetic energy of the fluid by the action of viscosity. The consequence of expansion of the gas in the boundary layer is an enormous increase of the viscous deflection of the outer flow, which in turn causes a strong shock at the leading edge. Previous investigations (Refs. 1, 2, 3) have laid special emphasis on the increase of the effective thickness of the body due to viscous deflection of the stream-lines but have neglected the entropy or vorticity generated by the shock.

In view of the fact that at hypersonic Mach numbers the change across the shock, even in the case of thin bodies, can be large, an increase of entropy could be accompanied by an appreciable increase of temperature of the flow. This heating may lead to further expansion of the gas, resulting in additional changes of pressure and skin friction. If, however, these effects were taken into account, the flow behind the shock would involve the interaction of both families of Mach waves and, therefore, would present formidable difficulties for theoretical solution. On the other hand, if the basis for the simple-wave theory can be established, the solution of the problem can be greatly simplified as has been demonstrated in the case of the flat plate (Ref. 4). It is, for this reason, important to clarify to what extent entropy will be of significance.

With a motivation to answer this question, it is proposed to consider a special case of an infinite wedge with large wedge angle, for which a strong shock exists even at infinity. Inasmuch as, at high Mach numbers the characteristics of the flow over thin sharp-nosed bodies depend very little on the shape of the body, the results obtained for one case may well cast light on the other. Merely for the purpose of estimating these effects, the investigations can be restricted to the weak interaction zone for which an asymptotic solution can be easily found. It is shown that at hypersonic Mach numbers the contributions due to entropy rise are small even for large wedge angles. It can therefore be concluded that, as in the case of inviscid rotational flows (Ref. 5), the waves reflected by the shock play only a minor role in influencing the flow and can be neglected at hypersonic Mach numbers.

2. Equations of motion. In the Cartesian system $(\bar{x}, \bar{y})$, let the surface of the wedge be defined by $0 \leqq \bar{x}$, and $\bar{y} = 0$. The flow field in question is supersonic and is bounded by the leading-edge shock $0S$ (Fig. 1) and the surface

* This work, being part of a thesis by L. J. Pan, was carried out at the Graduate School of Aeronautical Engineering under the sponsorship of the Mechanics Branch, Office of Naval Research. Reproduction in whole or in part is permitted for any purpose of the United States Government.

1) Published in *Journal of Mathematics and Physics*, 1956, 35(2): 179~193

of the wedge. Let $\bar{u}$, $\bar{v}$ be the velocities in the $\bar{x}$, $\bar{y}$ directions respectively and let $\bar{p}$, $\bar{\rho}$, $\bar{T}$ and $\bar{\mu}$ be, respectively, the pressure, density, temperature and viscosity coefficient. If the velocity U_∞, the thermal variables p_∞, ρ_∞, T_∞ and the viscosity μ_∞ far downstream are taken as references, the variables can be normalized as follows:

$$\left.\begin{aligned} x &= \bar{x}/L, & Y &= (Re/C)^{\frac{1}{2}}\bar{y}/L = (Re/C)^{\frac{1}{2}}y \\ u &= \bar{u}/U_\infty, & V &= (Re/C)^{\frac{1}{2}}\bar{v}/U_\infty = (Re/C)^{\frac{1}{2}}v, \quad p = \bar{p}/p_\infty \\ \rho &= \bar{\rho}/\rho_\infty, & T &= \bar{T}/T_\infty, \qquad \mu = \bar{\mu}/\mu_\infty \end{aligned}\right\} \tag{2.1}$$

where $Re = \rho_\infty U_\infty L/\mu_\infty$. Here L is an arbitrary length and C is a constant to be defined later. It is remarked, however, that the scale L is introduced only as a convenience in formulation and will drop out in the final solutions.

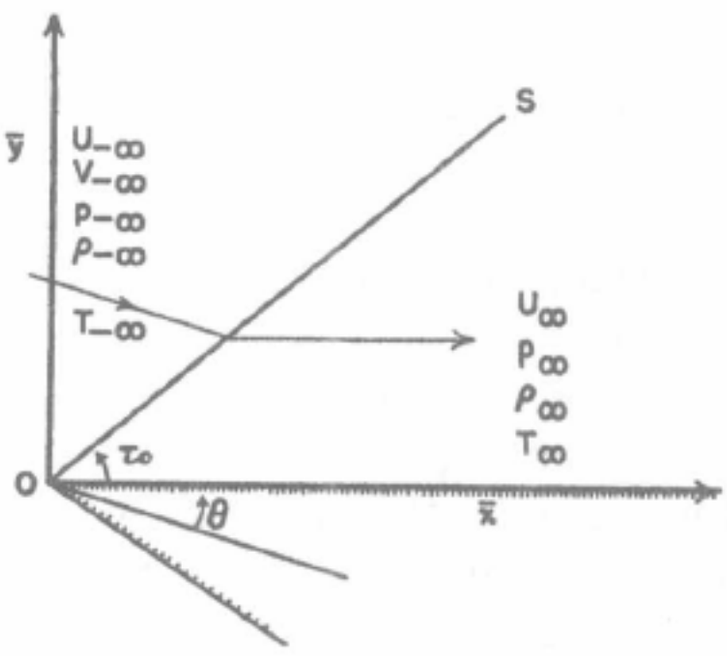

FIG. 1. Diagram showing the unperturbed supersonic flow over infinite wedge

In terms of these variables, the Navier-Stokes equations for a compressible viscous fluid can be expressed as:

$$\left.\begin{aligned} \rho\frac{Du}{Dt} &= -\left[\frac{p}{\gamma M^2} + \frac{2}{3Re}\mu\Theta\right]_x + \frac{1}{Re}\{2(\mu u_x)_x + [\mu(u_y + v_x)]_y\} \\ \rho\frac{Dv}{Dt} &= -\left[\frac{p}{\gamma M^2} + \frac{2}{3Re}\mu\Theta\right]_y + \frac{1}{Re}\{[\mu(u_y + v_x)]_x + 2(\mu v_y)_y\} \\ (\rho u)_x &+ (\rho v)_y = 0 \end{aligned}\right\} \tag{2.2}$$

with

$$\frac{D}{Dt} = u\frac{\partial}{\partial x} + v\frac{\partial}{\partial y} \qquad \text{and} \qquad \Theta = u_x + v_y$$

where γ is the ratio of the specific heats, $M = U_\infty/a_\infty$, a_∞ being the speed of sound at positive infinity, and the subscripts denote partial differentiation with respect to the variables indicated.

In the case of gases, the above equations involving both ρ and T by the dependency on temperature of the viscosity, cannot form a complete system with-

out consideration of the energy balance and the equation of state. For Prandtl number unity, these are, respectively,

$$\rho \frac{DT}{Dt} = \frac{\gamma - 1}{\gamma} \frac{Dp}{Dt} + \frac{(\gamma - 1)M^2}{Re} [-\tfrac{2}{3}\mu\Theta^2 + 2\mu(u_x^2 + v_y^2) + \mu(u_y + v_x)^2] + \frac{1}{Re} [(\mu T_x)_x + (\mu T_y)_y] \tag{2.3}$$

and, for perfect gases,

$$p = \rho T \tag{2.4}$$

In the following, it is proposed to attack this problem approximately by two different methods according to the distance from the surface. At large y, the deviation of the flow properties from those of the uniform state at infinity is small and the solution can be obtained by perturbation, taking the uniform flow as the zero approximation. This region will be subsequently called *external field*. Near the surface, where the viscous effect is important, boundary-layer approximations will be employed. This region will be called the *boundary layer*.

3. First-order solution of the external field. As the non-uniformity of the flow behind the shock is caused primarily by the viscous displacement of the streamlines, the velocity in the external field must join, to the first approximation, with the velocity produced by the boundary layer along a flat plate, which is

$$\sqrt{\frac{C}{Re}} \frac{0.860 + 0.596(\gamma - 1)M^2}{\sqrt{x}}$$

Thus, at $y = 0$, the external field must satisfy:

$$v = \epsilon v_1 / \sqrt{x} \tag{3.1}$$

where

$$\epsilon = \sqrt{C/Re} \quad \text{and} \quad v_1 = 0.860 + 0.596(\gamma - 1)M^2$$

The parameter ϵ so defined can serve as a measure of the first-order viscous effect.

With this definition of ϵ, the following expansions can be attempted: for $\epsilon \ll 1$

$$\left.\begin{aligned} u &= 1 + \epsilon u^{(1)} + \epsilon^{\frac{3}{2}} u^{(\frac{3}{2})} + \cdots \\ v &= \quad \epsilon v^{(1)} + \epsilon^{\frac{3}{2}} v^{(\frac{3}{2})} + \cdots \\ p &= 1 + \epsilon p^{(1)} + \epsilon^{\frac{3}{2}} p^{(\frac{3}{2})} + \cdots \\ \rho &= 1 + \epsilon \rho^{(1)} + \epsilon^{\frac{3}{2}} \rho^{(\frac{3}{2})} + \cdots \\ T &= 1 + \epsilon T^{(1)} + \epsilon^{\frac{3}{2}} T^{(\frac{3}{2})} + \cdots \end{aligned}\right\} \tag{3.2}$$

By substituting the expansions (3.2) in Eqs. (2.2), (2.3) and (2.4), it can be readily seen that the first-order solutions satisfy a differential system which

is identically the same as the first-order inviscid differential system. Solutions of such a system have been already obtained by Chu (Ref. 6); these are as follows:

$$\left.\begin{aligned} v^{(1)} &= v_1[F_1(x-\beta y)+G_1(x+\beta y)] \\ p^{(1)} &= (\gamma M^2 v_1/\beta)[F_1(x-\beta y)-G_1(x+\beta y)] \\ u^{(1)} &= -(v_1/\beta)[F_1(x-\beta y)-G_1(x+\beta y)]-S_1(y) \\ \rho^{(1)} &= (M^2 v_1/\beta)[F_1(x-\beta y)-G_1(x+\beta y)]-(\gamma-1)M^2 S_1(y) \\ T^{(1)} &= [(\gamma-1)M^2 v_1/\beta]\,[F_1(x-\beta y)-G_1(x+\beta y)]+(\gamma-1)M^2 S_1(y) \end{aligned}\right\} \tag{3.3}$$

where $\beta = \sqrt{M^2-1}$; F_1, G_1 and S_1 are arbitrary functions.

This shows that the first-order solutions consist of both the outgoing and the reflected families of plane waves and, in addition, a "vorticity wake." From the definition of entropy, viz. $\ln p\rho^{-\gamma}$, $S_1(y)$ is simply proportional to the first-order entropy which is, therefore, constant on $y =$ constant lines. It is interesting to note that the effect of the entropy generated by the shock, to the first order, is to decrease the velocity and density but to increase the temperature, as compared with an irrotational flow.

The flow field described above can now be determined jointly with the shape of the shock by satisfying the Rankine-Hugoniot shock relations and the condition (3.1). As the thickness of the shock is much smaller than the thickness of the boundary layer, the shock, to the first approximation, can be described by a curve:

$$dy/dx = \tan\tau \tag{3.4}$$

where τ is the local shock angle. The expansion of the shock conditions according to (3.2), together with

$$\tau = \tau_0 + \epsilon\tau_1 + \cdots \tag{3.5}$$

where τ_0 is the shock angle at infinity and is determined by the half wedge angle θ and the Mach number $M_{-\infty}$ in front of the shock, leads to a set of first-order relations (Ref. 6) on the shock $y = x\tan\tau_0$. From these it follows, by elimination that

$$p^{(1)} = \gamma M^2 v^{(1)} \tan\lambda \tag{3.6}$$

$$\tau^{(1)} = \tfrac{1}{2}(\gamma+1)\csc 2\tau_0\, p^{(1)}/\gamma M^2 \tag{3.7}$$

$$S_1 = \tfrac{1}{2}\frac{(1-M^2\sin^2\tau_0)^2}{\sin^2\tau_0[1+\tfrac{1}{2}(\gamma-1)\,M^2\sin^2\tau_0]}\frac{p^{(1)}}{\gamma M^4} \tag{3.8}$$

where

$$\tan\lambda = \frac{M^2[1+\tfrac{1}{2}(\gamma-1)M^2\sin^2\tau_0]\sin 2\tau_0}{\beta^2[1+\tfrac{1}{2}(\gamma-1)M^2\sin^2\tau_0]+M^2[\gamma M^2\sin^2\tau_0-\tfrac{1}{2}(\gamma-1)]\cos^2\tau_0} \tag{3.9}$$

These relations will be valid as long as the flow is supersonic and the shock belongs to the weak family.

To satisfy the conditions (3.1) and (3.6), the functions F_1 and G_1 may have the forms:

$$F_1 = \frac{1 - A_1}{\sqrt{x - \beta y}}, \qquad G_1 = \frac{A_1}{\sqrt{x + \beta y}} \tag{3.10}$$

The constant A_1, by (3.6), is determined to be

$$A_1 = \frac{(1 - \beta \tan \lambda)}{(1 - \beta \tan \lambda) + \sqrt{(1 - \beta \tan \tau_0)/(1 + \beta \tan \tau_0)}\,(1 + \beta \tan \lambda)} \tag{3.11}$$

As soon as the pressure $p^{(1)}$ is known, it follows from (3.7) and (3.8) that

$$\tau^{(1)} = \frac{\gamma + 1}{2} \frac{v_1}{\beta \sin 2\tau_0} \left[\frac{1 - A_1}{\sqrt{1 - \beta \tan \tau_0}} - \frac{A_1}{\sqrt{1 + \beta \tan \tau_0}} \right] \frac{1}{\sqrt{x}} \tag{3.12}$$

and

$$S_1 = \frac{B_1}{\sqrt{y}} \tag{3.13}$$

where

$$B_1 = \tfrac{1}{2} \frac{(1 - M^2 \sin^2 \tau_0)^2}{\beta M^2 \sin^2 \tau_0 [1 + \tfrac{1}{2}(\gamma - 1) M^2 \sin^2 \tau_0]} \cdot \left[\frac{1 - A_1}{\sqrt{\cot \tau_0 - \beta}} - \frac{A_1}{\sqrt{\cot \tau_0 + \beta}} \right] \tag{3.14}$$

On account of (3.12), to the first order, the shock curve is:

$$y = x \tan \tau_0 + \frac{(\gamma + 1) \epsilon v_1}{\beta^2 \cos^2 \tau_0 \sin 2\tau_0} \cdot \left[\frac{1 - A_1}{\sqrt{1 - \beta \tan \tau_0}} - \frac{A_1}{\sqrt{1 + \beta \tan \tau_0}} \right] \sqrt{x} + \cdots \tag{3.15}$$

It is observed that the first-order solutions given above are singular at $y = 0$ due to the presence in the flow of non-uniform entropy. This implies that in the neighborhood of the edge of the boundary layer the velocity gradient will not be small, as is the case of an irrotational external flow, and consequently, a "sharp boundary" between the boundary layer and the external field ceases to exist. As a result of this gradual transition from the viscous boundary layer to the inviscid external field, the familiar concept of matching the boundary-layer solution to that of the external field must be radically modified. This new problem will be solved in Section 6.

4. Singular solution of the order $\epsilon^{\frac{1}{2}}$. In view of the singular term S_1, it is inevitable that singular terms of the type $y^{-l}x^m$ will appear in the high-order solutions at small y, where the exponents l and m are positive and l increases with the order of approximation. For instance, by substituting

$$u = 1 - \epsilon S_1 - \epsilon^2 S_2 - \cdots - \epsilon^n S_n - \cdots \tag{4.1}$$
$$v = \epsilon v_1 / \sqrt{x}$$

in the first of Eqs. (2.2), leaving out the regular terms, one finds that the highest singular term in S_2 is $B_1v_1y^{-\frac{1}{2}}x^{\frac{1}{2}}$; and the highest singular term in S_3 is $(\frac{3}{4})B_1(1 + 2v_1^2)y^{-\frac{1}{2}}x$, etc. To continue the process, it can be shown that for the nth highest singular term S_{1n} in S_n there is an equation:

$$S_{1(n+2)x} + (v_1/\sqrt{x})S_{1(n+1)y} = S_{1nyy}, \quad n = 1, 2, 3, \cdots \tag{4.2}$$

From the first three solutions, it can be generalized that Eq. (4.2) admits a solution:

$$S_{1n} = B_1C_ny^{-n+\frac{1}{2}}x^{(n-1)/2}, \qquad S_{11} = S_1 \tag{4.3}$$

A substitution of (4.3) in Eq. (4.2) yields the recurrence formula: for $n = 1, 2, 3, \cdots$

$$C_{n+2} = [2/(n + 1)]\,[v_1(n + \tfrac{1}{2})C_{n+1} + (n^2 - \tfrac{1}{4})C_n] \tag{4.4}$$

with

$$C_1 = 1, \qquad C_2 = v_1$$

This particular sequence on summation gives a solution in the form of (4.1):

$$u = 1 - B_1\sum_1^\infty \epsilon^n C_n y^{-n+\frac{1}{2}}x^{(n-1)/2} + \cdots$$

This series has the property that when $y = 0(\epsilon)$, all terms become the same order, $\epsilon^{\frac{1}{2}}$, and the series converges if $\epsilon\sqrt{x} < y$. For this reason, when $y = 0(\epsilon)$, the complete solution for u is:

$$u = 1 - \sqrt{\epsilon}u^{(\frac{1}{2})} + \epsilon\tilde{u}^{(1)} + \cdots$$

where

$$u^{(\frac{1}{2})} = B_1\sum_1^\infty \epsilon^{n-\frac{1}{2}}C_n y^{-n+\frac{1}{2}}x^{(n-1)/2} \tag{4.5}$$

and $\tilde{u}^{(1)}$, being the regular part of $u^{(1)}$ defined in (3.3), is a linear combination of F_1 and G_1.

As one proceeds to still higher approximations, singular terms like (4.3), which are of the order ϵ, $\epsilon^{\frac{3}{2}}$, etc., have to be considered. For the present study, which stops at the first order, this problem will not be pursued further.

5. Boundary-layer equations. Consider now the solution in the inner, viscous layer. In the case of large Reynolds number, the viscous layer will be thin and the boundary-layer theory a legitimate approximation. Accordingly, the equations (2.2) can be satisfied to:

$$\left.\begin{aligned} \rho[uu_x + Vu_Y] &= -(1/\gamma M^2)p_x + 1/C[\mu u_Y]_Y \\ 0 &= (1/\gamma M^2)p_Y \\ (\rho u)_x + (\rho V)_Y &= 0 \end{aligned}\right\} \tag{5.1}$$

by neglecting terms of the order ϵ^2. If the surface is thermally insulated, the energy equation admits a solution:

$$T = 1 + \tfrac{1}{2}(\gamma - 1)M^2(1 - u^2) \tag{5.2}$$

Furthermore, it is assumed that the viscosity-temperature relation is linear. Following Chapman and Rubesin (Ref. 7),

$$\mu = CT \tag{5.3}$$

Here the constant C is chosen such that μ at the surface agrees with the power law T^ω, ω being a constant for individual gases. This determines

$$C = T_w^{\omega-1} = [1 + \tfrac{1}{2}(\gamma - 1)M^2]^{\omega-1} \tag{5.4}$$

where T_w is the temperature of the surface.

On account of (5.3), Eqs. (5.1) can be further reduced by introducing Howarth's transformation (Ref. 8)

$$\Psi = \sqrt{p}\varphi(\xi, \eta), \qquad x = \xi, \qquad Y = \frac{1}{\sqrt{p}}\int_0^\eta T\, dz \tag{5.5}$$

where Ψ is the non-dimensional stream function defined by:

$$\rho u = \Psi_Y, \qquad \rho V = -\Psi_x \tag{5.6}$$

According to the transformation (5.5), the velocities u and V can be expressed in terms of φ, T, and p:

$$\begin{aligned} u &= \varphi_\eta \\ V &= -\frac{1}{\sqrt{p}}\left[T\varphi_\xi - \varphi_\eta \int_0^\eta T_\xi\, dz\right] + \frac{p'}{2p}\left(T\varphi + \varphi_\eta \int_0^\eta T\, dz\right) \end{aligned} \tag{5.7}$$

A substitution of u and V in (5.1), by making use of the equation of state, leads to an equation:

$$\varphi_\eta\varphi_{\xi\eta} - \varphi_\xi\varphi_{\eta\eta} = \frac{p'}{p}\left[\tfrac{1}{2}\varphi\varphi_{\eta\eta} - \frac{\gamma - 1}{2\gamma}(1 - \varphi_\eta^2) - \frac{1}{\gamma M^2}\right] + \varphi_{\eta\eta\eta} \tag{5.8}$$

where the pressure p is a function of ξ alone. The solution of (5.8) must satisfy the conditions:

$$\begin{aligned} \varphi = \varphi_\eta &= 0, \qquad \eta = 0 \\ \varphi_\eta &= U(\xi, \eta), \qquad \eta \to \infty \end{aligned} \tag{5.9}$$

where $U(\xi, \eta)$ will be specified later.

6. Solutions for the viscous layer. From (4.5), the velocity u near the edge of the boundary layer is, instead of (3.2),

$$u = 1 + \sqrt{\epsilon}\, u^{(\frac{1}{2})} + \epsilon\tilde{u}^{(1)} + \cdots$$

for $y = 0(\epsilon)$. Accordingly, the solutions in the viscous layer take the form:

$$\left.\begin{aligned} \varphi &= \varphi^{(0)} + \sqrt{\epsilon}\varphi^{(\frac{1}{2})} + \epsilon\varphi^{(1)} + \cdots \\ p &= 1 + \epsilon p^{(1)} + \epsilon^{\frac{3}{2}} p^{(\frac{3}{2})} + \cdots \end{aligned}\right\} \tag{6.1}$$

These expansions lead, from (5.7) and (5.2), to the expressions

$$\left.\begin{aligned} u &= \varphi_\eta^{(0)} + \sqrt{\epsilon}\varphi_\eta^{(\frac{1}{2})} + \cdots \\ V &= v^{(1)} + \sqrt{\epsilon} v^{(\frac{3}{2})} + \cdots \\ T &= T^{(0)} + \sqrt{\epsilon} T^{(\frac{1}{2})} + \cdots \end{aligned}\right\} \tag{6.2}$$

where $v^{(1)}$, $v^{(\frac{3}{2})}$, $T^{(0)}$ and $T^{(\frac{1}{2})}$ are defined by:

$$\left.\begin{aligned} v^{(1)} &= -T^{(0)}\varphi_\xi^{(0)} + \varphi_\eta^{(0)} \int_0^\eta T_\xi^{(0)}\, dz \\ v^{(\frac{3}{2})} &= -T^{(0)}\varphi_\xi^{(\frac{1}{2})} - T^{(\frac{1}{2})}\varphi_\xi^{(0)} + \varphi_\eta^{(0)} \int_0^\eta T_\xi^{(\frac{1}{2})}\, dz + \varphi_\eta^{(\frac{1}{2})} \int_0^\eta T_\xi^{(0)}\, dz \\ T^{(0)} &= 1 + \frac{\gamma - 1}{2} M^2(1 - \varphi_\eta^{2(0)}), \qquad T^{(\frac{1}{2})} = -(\gamma - 1)M^2 \varphi_\eta^{(0)} \varphi_\eta^{(\frac{1}{2})} \end{aligned}\right\} \tag{6.3}$$

By expanding (5.8) and equating to zero the coefficients of ϵ^0 and $\epsilon^{\frac{1}{2}}$, there result

$$\varphi_\eta^{(0)}\varphi_{\xi\eta}^{(0)} - \varphi_\xi^{(0)}\varphi_{\eta\eta}^{(0)} - \varphi_{\eta\eta\eta}^{(0)} = 0 \tag{6.4}$$

and

$$\varphi_\eta^{(0)}\varphi_{\xi\eta}^{(\frac{1}{2})} + \varphi_{\xi\eta}^{(0)}\varphi_\eta^{(\frac{1}{2})} - \varphi_\xi^{(0)}\varphi_{\eta\eta}^{(\frac{1}{2})} - \varphi_{\eta\eta}^{(0)}\varphi_\xi^{(\frac{1}{2})} - \varphi_{\eta\eta\eta}^{(\frac{1}{2})} = 0 \tag{6.5}$$

The boundary conditions for $\varphi^{(0)}$ and $\varphi^{(\frac{1}{2})}$ are:

$$\left.\begin{aligned} \varphi^{(0)} = \varphi_\eta^{(0)} = \varphi^{(\frac{1}{2})} = \varphi_\eta^{(\frac{1}{2})} = 0, \qquad \eta = 0 \\ \varphi_\eta^{(0)} = 1, \qquad \varphi_\eta^{(\frac{1}{2})} = u^{(\frac{1}{2})}(\xi, \eta), \qquad \eta \to \infty \end{aligned}\right\} \tag{6.6}$$

where $u^{(\frac{1}{2})}(\xi, \eta)$ is required to equal the series defined by (4.5).

Thus, the zero-order solution, as expected, is simply the boundary-layer solution for a flat plate under uniform pressure. The solution of Eq. (6.4) according to Blasius is

$$\varphi^{(0)} = \sqrt{\xi} f_0(\zeta) \tag{6.7}$$

with $\zeta = \eta/2\sqrt{\xi}$. Eq. (6.4) then reduces to

$$f_0''' + f_0 f_0'' = 0 \tag{6.8}$$

with the boundary conditions:

$$\left.\begin{aligned} f_0 = f_0' = 0, \qquad \zeta = 0 \\ f_0' = 2, \qquad \zeta = \infty \end{aligned}\right\} \tag{6.9}$$

The solution is well-known. For ζ near the origin, the solution can be expanded in a power series

$$f_0 = \frac{\alpha_0 \zeta^2}{2!} - \frac{\alpha_0^2 \zeta^5}{5!} + \frac{11\alpha_0^3 \zeta^8}{8!} - \frac{375\alpha_0^4 \zeta^{11}}{11!} + \cdots \tag{6.10}$$

where $\alpha_0 = 1.328$. On the other hand, when ζ is large, the solution is asymptotically

$$f_0 \sim 2\zeta - \beta_0 + 0(e^{-\zeta^2}) \tag{6.11}$$

where $\beta_0 = 1.720$.

Given f_0 above, both $u^{(0)}$ and $v^{(1)}$ in (6.2) can be expressed in terms of f_0 and its derivatives. From the asymptotic behavior of f_0, it can easily be shown that $v^{(1)}(\xi, \eta)$ approaches the value (3.1) as ζ becomes infinite.

With f_0 so calculated, it follows that the solution $\varphi^{(\frac{1}{2})}$ must be

$$\varphi^{(\frac{1}{2})} = -B_1 \xi^{\frac{1}{2}} f_{\frac{1}{2}}(\zeta) \tag{6.12}$$

where the constant B_1 is defined in (3.14). Eq. (6.5) is, consequently, reduced to

$$2f_{\frac{1}{2}}''' + 2f_0 f_{\frac{1}{2}}'' + f_0' f_{\frac{1}{2}}' + f_0'' f_{\frac{1}{2}} = 0 \tag{6.13}$$

with the boundary conditions

$$\left.\begin{aligned} f_{\frac{1}{2}} = f_{\frac{1}{2}}' = 0, \qquad & \zeta = 0 \\ f_{\frac{1}{2}}' = 2\textstyle\sum_1^\infty C_n(2\zeta - \beta_0 + 2v_1)^{-n+\frac{1}{2}}, \qquad & \zeta \to \infty \end{aligned}\right\} \tag{6.14}$$

where C_n is defined by (4.4).

It should be pointed out that, as already mentioned in Section 3, owing to the strong entropy gradient near the surface of the wedge, the two velocity fields, if they are truly matched, should be matched for all their derivatives in a region of large ζ; $\zeta = 5$, say. This is actually what is prescribed by the second of (6.14). Finally, the problem will be completed after it is verified that the required asymptotic behavior is exactly the value of the external velocity given by (4.5).

First, by satisfying the conditions at $\zeta = 0$ the power-series development yields

$$f_{\frac{1}{2}} = \alpha_{\frac{1}{2}} \left[\frac{\zeta^2}{2!} - 3\alpha_0 \frac{\zeta^5}{5!} + 54\alpha_0^2 \frac{\zeta^8}{8!} - 2586\alpha_0^3 \frac{\zeta''}{11!} + \cdots \right] \tag{6.15}$$

where $\alpha_{\frac{1}{2}}$ determined by numerical integration, is 1.83150. Secondly, when ζ is large, by approximating f_0 according to (6.11), Eq. (6.13) is simplified to

$$f_{\frac{1}{2}}''' + (2\zeta - \beta_0) f_{\frac{1}{2}}'' + f_{\frac{1}{2}}' = 0 \tag{6.16}$$

Upon introduction of a new variable, $\sigma = 2\zeta - \beta_0$, the resulting equation can be integrated in terms of Bessel functions of imaginary argument. Namely,

$$\frac{df_{\frac{1}{2}}}{d\sigma} = \sqrt{\sigma} e^{-\sigma^2/2} \left[D_1 I_{\frac{1}{4}}\left(\frac{\sigma^2}{2}\right) + D_2 K_{\frac{1}{4}}\left(\frac{\sigma^2}{2}\right) \right] \tag{6.17}$$

Now as $\sigma \to \infty$, asymptotically

$$I_{\frac{1}{4}}\left(\frac{\sigma^2}{2}\right) \sim \frac{e^{\sigma^2/2}}{\sqrt{\pi}} \sum_0^\infty \frac{(-1)^m \Gamma(\frac{3}{4} + m)}{m!\Gamma(\frac{3}{4} - m)} \sigma^{-2m-1} + 0(e^{-\sigma^2/2})$$

$$K_{\frac{1}{4}}\left(\frac{\sigma^2}{2}\right) \sim 0(e^{-\sigma^2/2})$$

It follows that as $\zeta \to \infty$ asymptotically

$$\frac{df_{\frac{1}{2}}}{d\zeta} \sim \frac{2D_1}{\sqrt{\pi}} \sum_0^\infty \frac{(-1)^m \Gamma(\frac{3}{4}+m)}{m!\Gamma(\frac{3}{4}-m)} \sigma^{-2m-1} + 0(e^{-\zeta^2/2}) \tag{6.18}$$

From the transformation (5.5), when ζ is large the relation between x, y and ζ, to the first approximation, is

$$\frac{y}{\epsilon\sqrt{x}} = 2\zeta - \beta_0 + 2v_1 \tag{6.19}$$

By writing $\sigma = (2\zeta - \beta_0 + 2v_1) - 2v_1$ and replacing in (6.18)

$$\left(1 - \frac{2v_1}{\sigma + 2v_1}\right)^{-2m-1} \quad \text{by} \quad \sum_0^\infty \frac{\Gamma(2m+1+l)}{l!\Gamma(2m+1)} (\sigma + 2v_1)^{-l}(2v_1)^l$$

there will result a double series which, in the domain of validity, can be converted into a single series by Cauchy's method of multiplication:

$$f'_{\frac{1}{2}} = \frac{2D_1}{\sqrt{\pi}} \sum_1^\infty C_n(2\zeta - \beta_0 + 2v_1)^{-n+\frac{1}{2}} + 0(e^{-\zeta^2}) \tag{6.20}$$

The coefficients C_n satisfy exactly the same recurrence formula (4.4) if $C_1 = 1$. Therefore, if $D_1 = \sqrt{\pi}$, the solution $f'_{\frac{1}{2}}$ will satisfy the imposed condition (6.14) at infinity, which by (6.19) is just $\xi^{\frac{1}{2}}u^{(\frac{1}{2})}$ defined by (4.5).

It is interesting to observe that, although the boundary-layer solution does approach the prescribed inviscid field exponentially, the displacement boundary-layer thickness, nevertheless, cannot be defined due to the singular behavior of the inviscid solution at $y = 0$. Under such circumstances, it seems that the concept of the displacement thickness has to be dropped in favor of the well-defined quantity v. It must be pointed out also that in spite of the fact that the boundary-layer thickness, according to (5.5), is increased due to the presence of the entropy field, the displacement boundary-layer thickness, if defined, will be decreased, since the flow deflection is decreased, as will be shown later.

7. $v^{(\frac{1}{2})}$ and $p^{(\frac{1}{2})}$ of the external field. In the preceding sections, it was shown that the first-order entropy field produced by a curved shock will induce, inside the boundary layer, velocity (u), density and temperature increments of the order $\epsilon^{\frac{1}{2}}$ but a velocity (v) increment of the order $\epsilon^{\frac{3}{2}}$. This modification of the flow deflection will in turn generate new trains of waves in the external field. To calculate these quantities, the process of Section 3 can be repeated. According to (6.3), the velocity $v^{(\frac{1}{2})}$ expressed in terms of f_0, $f_{\frac{1}{2}}$ is

$$\begin{aligned} v^{(\frac{1}{2})} = \frac{B_1\xi^{-\frac{1}{2}}}{8}\Bigg\{ & 2(f_{\frac{1}{2}} - 2\zeta f'_{\frac{1}{2}}) + \frac{(\gamma-1)M^2}{2}\Bigg[2\left(1 - \frac{f'^2_0}{4}\right)(f_{\frac{1}{2}} - 2\zeta f'_{\frac{1}{2}}) \\ & + f'_0(f''_{\frac{1}{2}} - \zeta f'_0 f'_{\frac{1}{2}} + \tfrac{1}{2}f'_0 f_{\frac{1}{2}} - \alpha_{\frac{1}{2}}) + f'_{\frac{1}{2}}(f''_0 - \alpha_0)\Bigg]\Bigg\} \end{aligned} \tag{7.1}$$

when ζ is large, the asymptotic expansions of f_0 and $f_{\frac{1}{2}}$ lead to:

$$v^{(\frac{1}{2})} \sim -\frac{B_1 \xi^{-\frac{1}{2}}}{8}\left[(\gamma - 1)\, M^2(\alpha_{\frac{1}{2}} + \beta_{\frac{1}{2}}) + 2\beta_{\frac{1}{2}} + 0\left(\frac{1}{\zeta}\right)\right] \tag{7.2}$$

where $\beta_{\frac{1}{2}} = 0.1977$, being the constant defined as $f_{\frac{1}{2}} \sim -\beta_{\frac{1}{2}} + 0(\sqrt{\zeta})$ as ζ becomes large.

This negative value of $v^{(\frac{1}{2})}$ at infinity shows that the entropy field, contrary to the viscous effect, turns the flow toward the wall and, therefore, reduces the viscous displacement of the stream lines. There is an attendant reduction of pressure.

Following Section 3, if the asymptotic value in (7.2) is considered as the boundary value of the external field, the solutions must satisfy:

$$v^{(\frac{1}{2})} = -v_{\frac{1}{2}}/x^{\frac{1}{2}}, \qquad y = 0 \tag{7.3}$$

where

$$v_{\frac{1}{2}} = \tfrac{1}{8}B_1[2\beta_{\frac{1}{2}} + (\gamma - 1)M^2(\alpha_{\frac{1}{2}} + \beta_{\frac{1}{2}})]$$

Inasmuch as the shock relations to this order remain the same as those from (3.6) to (3.8), it follows therefore that $v^{(\frac{1}{2})}$ and $p^{(\frac{1}{2})}$ are,

$$\left.\begin{aligned} v^{(\frac{1}{2})} &= -v_{\frac{1}{2}}\left[\frac{1 - A_{\frac{1}{2}}}{(x - \beta y)^{\frac{1}{2}}} + \frac{A_{\frac{1}{2}}}{(x + \beta y)^{\frac{1}{2}}}\right] \\ p^{(\frac{1}{2})} &= -\frac{\gamma M^2 v_{\frac{1}{2}}}{\beta}\left[\frac{1 - A_{\frac{1}{2}}}{(x - \beta y)^{\frac{1}{2}}} - \frac{A_{\frac{1}{2}}}{(x + \beta y)^{\frac{1}{2}}}\right] \end{aligned}\right\} \tag{7.4}$$

where the constant $A_{\frac{1}{2}}$ is defined by

$$A_{\frac{1}{2}} = \frac{1 - \beta \tan \lambda}{(1 - \beta \tan \lambda) + \left[\dfrac{1 - \beta \tan \tau_0}{1 + \beta \tan \tau_0}\right]^{\frac{1}{2}} (1 + \beta \tan \lambda)} \tag{7.5}$$

Similarly, the quantities $\tau_{\frac{1}{2}}$, $S_{\frac{1}{2}}$, etc. can be deduced.

8. Discussion of the results. The solutions given in (3.3) and (3.10) show that the first-order solutions such as pressure, velocity, etc. due to reflected and incident waves bear a common ratio $A_1\sqrt{x - \beta y}/(1 - A_1)\sqrt{x + \beta y}$. As $x - \beta y$ is less than $x + \beta y$ in the inviscid field, this ratio will be everywhere less than the value $A_1/(1 - A_1)$ at the surface $y = 0$. According to Fig. 2, this value can be at most 0.14 for $\theta = 15°$ at a flight Mach number of 12. Therefore, for θ less than 10°, the effects due to reflected waves are generally of no consequence and may be neglected.

It is interesting to point out that although the deflection associated with the reflected waves is positive, the pressure and temperature they induce are both negative. In this respect, they act in the opposite sense to that of the entropy wake, as shown below. Hence, in speaking of the effects of vorticity, these distinctions have to be made.

As to the entropy effects, it is noted, first of all, that, following the solutions

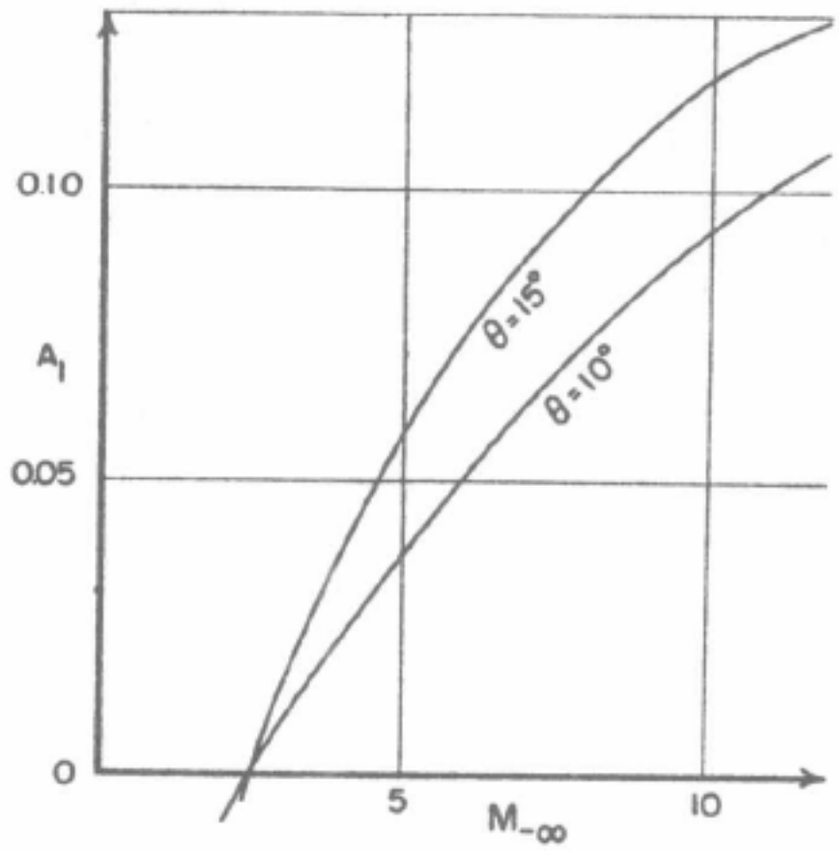

FIG. 2. Variation of A_1 with $M_{-\infty}$ for $\theta = 10°, 15°$ and $\gamma = 1.40$

of the preceding section, the pressure due to the entropy is of the order $\epsilon^{\frac{3}{2}}$. With this correction, the total pressure, for $M \gg 1$, is

$$p - 1 = 0.596\gamma(\gamma - 1)(1 - 2A_1)\chi\left[1 - \frac{\alpha_{\frac{1}{2}} B_1(1 - 2A_{\frac{1}{2}})}{4.77(1 - 2A_1)} \sqrt[4]{\frac{C}{Re_x}} + \cdots\right]$$

with

$$\chi = M^3\sqrt{C/Re_x} \tag{8.1}$$

This shows in the first place that the pressure correction due to the first-order entropy generated by the perturbed shock is negative, and, moreover, by numerical calculation it is found to be small. From Figs. 3 and 4, at flight Mach 10 and $\theta = 15°$, the correction amounts to only 6 per cent. This is in direct contradiction to the prediction of Professor Lees (Ref. 9) that shock heating due to the generation of entropy induces a non-trivial positive pressure.

Furthermore, the velocity reduction by entropy is also small, from (6.1) and (6:12) it can be verified that

$$u = \tfrac{1}{2}f_0' - \frac{B_1}{2} f_{\frac{1}{2}}' \sqrt[4]{\frac{C}{Re_x}} + \cdots \tag{8.2}$$

From Fig. 3, B_1 is less than unity and, for $C/Re_x < 1$, the correction should be everywhere small and in fact, by Fig. 5, can be at most 10 per cent. The local skin friction is shown to be

$$C_f = \frac{p^{\frac{1}{2}}}{2}\sqrt{\frac{C}{Re_x}}\left[\alpha_0 - B_1\alpha_{\frac{1}{2}}\sqrt[4]{\frac{C}{Re_x}} + \cdots\right] \tag{8.3}$$

and the correction in this case is also small as long as $C/Re_x < 1$.

While it is true that the effect of entropy on pressure and velocity (u) is negligible, it contributes a considerable portion to the temperature near the

edge of the boundary layer. Under the conditions specified in Fig. 6, at places the correction could be 100 per cent at the edge of the boundary layer. It can therefore be concluded that the shock heating of the gas in the cool layer is absorbed largely by expansion of the flow under practically the pressure $\epsilon p^{(1)}$ due to viscous deflection alone.

From the velocity and temperature distributions shown in Figs. 5 and 6, it is observed that as the leading edge is approached, the boundary layer deviates gradually from the unperturbed one and becomes less and less distinct from the inviscid field. This probably is generally the case whenever the external flow is rotational and has a large velocity gradient. Under this circumstance, as already

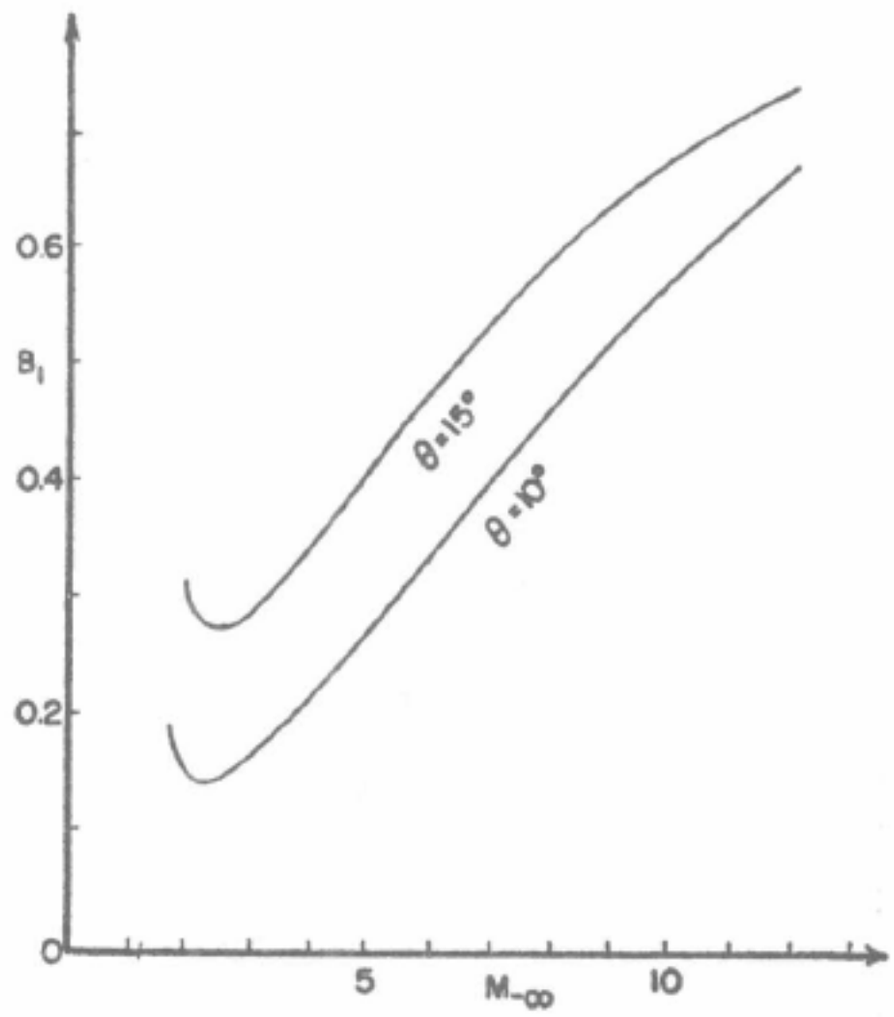

FIG. 3. Variation of B_1 with $M_{-\infty}$ for $\theta = 10°$, 15° and $\gamma = 1.4$

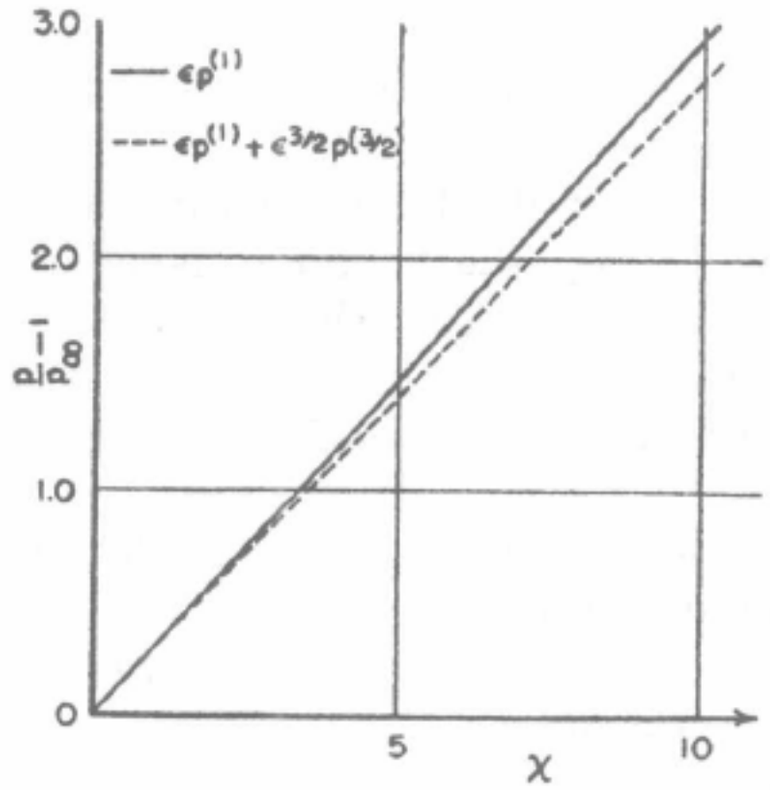

FIG. 4. Surface pressure for $\theta = 15°$, $M_\infty = 5.3$ and $\gamma = 1.40$

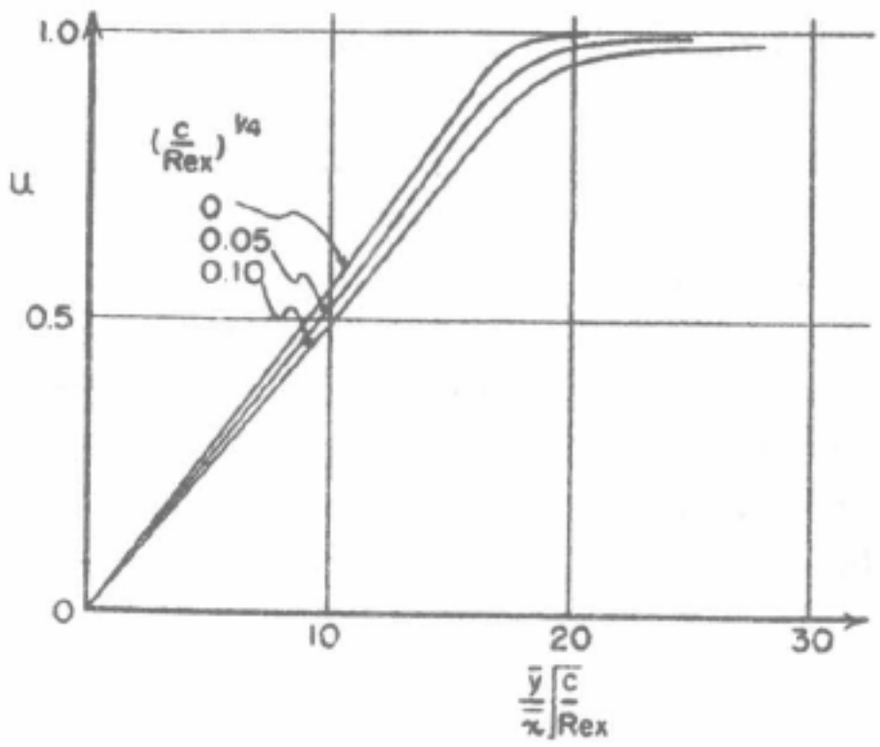

FIG. 5. Velocity distribution at three locations for $\theta = 15°$, $M_\infty = 5.3$ and $\gamma = 1.4$

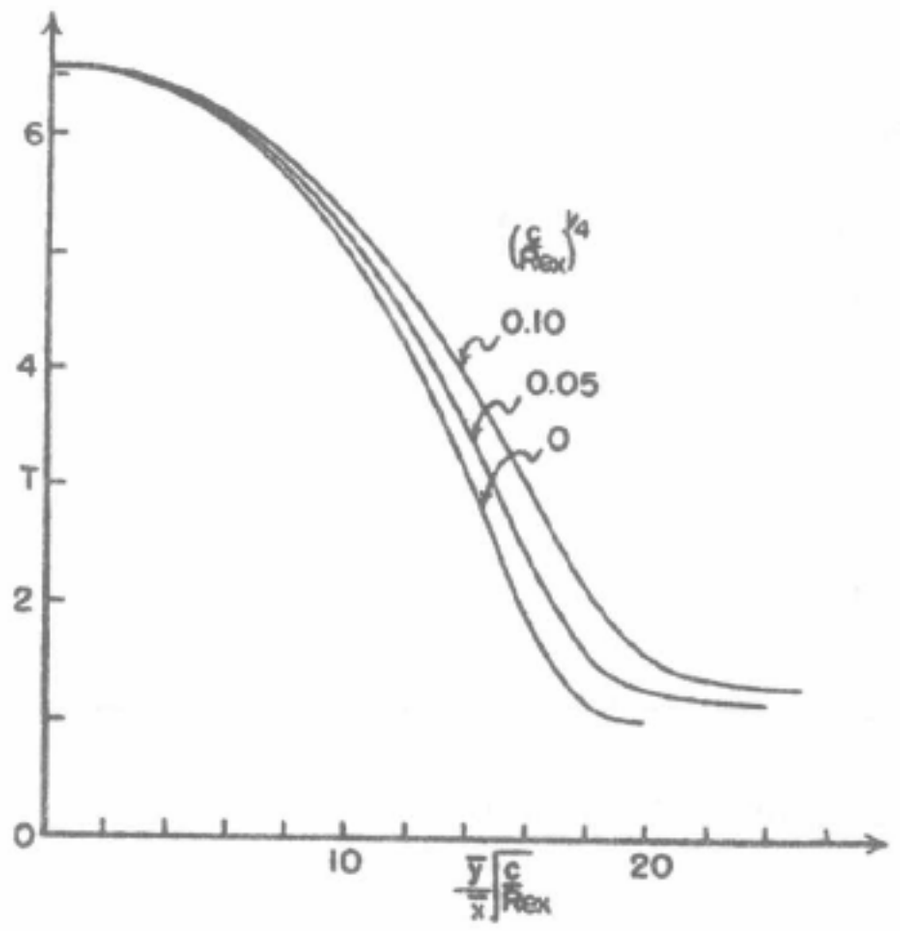

FIG. 6. Temperature distribution at three locations for $\theta = 15°$, $M_\infty = 5.3$ and $\gamma = 1.40$

pointed out, the definition of the displacement thickness is ambiguous, and it would be meaningless to identify the boundary-layer thickness with the displacement thickness. The present result shows that, at least in the case of wedge, this identification would be wrong.

From these results, there arrive the conclusions that, at hypersonic speeds and half wedge angle $\theta \leqq 10°$,

(i) The effects due to the reflected waves at the leading-edge shock and the entropy generated therein are small.

(ii) Entropy raises considerably the temperature in the cool layer but generates a small negative pressure.

(iii) As far as pressure and skin friction are concerned, the application of the simple-wave theory to such problems can be justified.

It is remarked, finally, that, owing to the presence of the singular term S_1, there appear in high-order approximations sequences of singular solutions of which the leading one is given in Section 4. Similarly, the corresponding term $S_{\frac{1}{2}}$ in the $(\frac{3}{2})^{th}$-order solution leads to other sequences of singular solutions of which the leading one is of the order $\epsilon^{\frac{1}{2}}$, and so on. Generally, it is clear that between two consecutive integral powers of ϵ, such as (0, 1), (2, 3) etc., in the expansion of φ there will be a series $\sum_1^\infty \epsilon^{\lambda_n}\varphi^{(\lambda_n)}$, λ_n being a function of the integer n. For example, between $\varphi^{(0)}$ and $\varphi^{(1)}$, the function λ_n is $(2^n - 1)/2^n$. Therefore, if a consistent first-order solution is required, this series has to be calculated. This shows that the method of perturbation as expressed in (6.1) is actually impossible. As long as the vorticity in the external field is singular at $y = 0$, the boundary-layer solution has to be expanded in a sum of two series $\sum_0^\infty \epsilon^n\varphi^{(n)}$ and $\sum_m \sum_n \epsilon^{\lambda_{mn}}\varphi^{(\lambda_{mn})}$. In this sense, the problem cannot be considered as solved—but this in no way affects the conclusions drawn above, which are consistent up to the order $\epsilon^{\frac{1}{2}}$.

REFERENCES

1. Shen, S. F. *An estimate of viscosity effect on hypersonic flow over an insulated wedge*, Jour. of Math. and Phys. **31** (1952) 192–205.
2. Lees, Lester and Probstein, Ronald F., *Hypersonic viscious flow over flat plate*, Aeronautical Engineering Laboratory, Princeton, Report no. 195 (1952).
3. Li, Ting-Yi, and Nagamatsu, H., *Shock wave effects on the laminar skin friction of an insulated flat plate at hypersonic speeds*, Jour. Aero. Sci. **20** (1953) 345–355.
4. Kuo, Y. H., *Viscous flow along a flat plate moving at high supersonic speeds*, Jour. Aero. Sci. **23** (1956) 125–136.
5. Eggers, A. J. and Syvertson, C. A., *Inviscid flow about airfoils at high supersonic speeds*, NACA T.N. 2646 (1952).
6. Chu, Boa-Teh, *On weak interaction of strong shock and Mach waves generated downstream of the shock*, Jour. Aero. Sci. **19** (1952) 433–445.
7. Chapman, D. R. and Rubesin, M. W., *Temperature and velocity profiles in compressible laminar boundary layer with arbitrary distribution of surface temperature*. Jour. Aero. Sci. **16** (1949) 547–565.
8. Howarth, L., *Concerning the effect of compressibility on laminar boundary layers and their separation*, Proc. Roy. Soc., A194 (1948) 16–42.
9. Lees, Lester, *Influence of the leading-edge shock wave on the laminar boundary layer at hypersonic speeds*, Technical Report no. 1, GALCIT (1954).

Cornell University

(Received July 26, 1955)

Dissociation Effects in Hypersonic Viscous Flows† [1)]

Y. H. KUO*
Cornell University

SUMMARY

The problem of boundary-layer flow is formulated for a gaseous mixture, resulting from the dissociation of a single perfect diatomic gas. Under the assumption that the mixture is in dissociative equilibrium, the flow quantities, such as surface temperature and skin-friction and heat-transfer coefficients, are evaluated, and the importance of the transport coefficients—namely, the viscosity, conductivity, and diffusion coefficient—are examined. It is shown that under the condition of equilibrium dissociation the effects of dissociation on the transfer coefficients are not large at very high speed.

(1) INTRODUCTION

IN RECENT YEARS the growing interest in high-speed flight has led to the study of the flow phenomena prevailing at Mach Numbers in the hypersonic range. One of these problems concerns the flow of air past a body with either sharp or blunt nose in the limit of very large Mach Numbers. The problem has usually been formulated under the assumptions that air is a slightly viscous, heat-conducting, continuous medium but obeys the laws of a perfect gas. In the low Mach Number range the theory is well founded and has yielded results fully in accord with experiments. In the hypersonic range, however, the temperature of the gas may reach a point that makes the simple hypothesis of perfect gas untenable because under the existing temperature conditions some molecules are split up under the strong bombardment of the fast-moving particles. When this process affects a considerable proportion of the gas molecules, the gas is said to be *dissociated*.

After dissociation has taken place, part of the kinetic energy of the molecules, which would have been stored in the gas as heat energy, is lost in decomposing the molecules. As a result, the temperature of the gas drops. This difference of temperature between the real dissociated and ideal undissociated gases grows rapidly as the process of dissociation proceeds at higher and higher temperatures. In the problem of hypersonic flow over a body, the calculations have been made on the basis of the information obtained previously without including the effect of dissociation. Since the effects generated by the viscous thickening of the boundary layer depend greatly on the temperature field, an error made in temperature will ultimately be manifested in every other calculated quantity.

In view of the increasing importance of high-speed flow, it is imperative that the basis of the classical theory be further broadened to adapt it to the new situation in which polyatomic gases would dissociate, in order to lend reality to the theoretical conclusions. This paper, as a first attempt, proposes to formulate the boundary-layer problem at high temperature under the suppositions that (1) the fluid in the main stream is a simple diatomic gas, and (2), when dissociated, the resulting mixture is in dissociative equilibrium. The justification for these assumptions lies in the fact that the main objective in such preliminary investigation is first to be able to express the dissociation effects in terms of convenient physical parameters and estimate them effectively for the case of a single gas. As air is almost 80 per cent nitrogen, its thermodynamic properties will certainly be overwhelmingly dominated by nitrogen. Hence, any information gained for nitrogen can be helpful toward the understanding of the phenomena observed in air.

(2) THERMODYNAMIC FUNCTIONS OF A GASEOUS MIXTURE

It is assumed that the gaseous mixture to be considered below results from the dissociation of some molecules A_2 in an originally pure diatomic gas and that the constituents A_2 and A of the mixture are in chemical equilibrium and react reversibly according to

$$A_2 \rightleftarrows 2A \tag{2.1}$$

under given temperature and pressure. For this mixture, the relative amount of the constituents A_2 and A can be conveniently characterized by the *degree of dissociation*, defined as the fraction of the original gas A_2 transformed in the reaction. Let the total number of molecules A_2 before dissociation takes place be N_0. The number of molecules A_2 and atoms A in the mixture is then, respectively, $N_0(1 - \epsilon)$ and $2N_0\epsilon$. It can be verified that in the present case the mass fraction of A becomes identically the same as the degree of dissociation.

In the mixture, let the partial pressures of the gases A_2 and A be, respectively, p_{A_2} and p_A. In the case of perfect gases, they are related to the density ρ and temperature T of the mixture by

Received June 18, 1956.

† This work was carried out at the Graduate School of Aeronautical Engineering under the sponsorship of the Mechanics Branch, Office of Naval Research. Reproduction in whole or in part is permitted for any purpose of the United States Government. The author has enjoyed and greatly profited by the frequent discussions with Dr. Frank E. Marble during his stay at Cornell University.

* Professor, Graduate School of Engineering.

1) Published in *Journal of the Aeronautical Sciences*, 1957, 24(5): 345~350

$$\left.\begin{aligned} p_A &= 2\epsilon R\rho T \\ p_{A_2} &= (1-\epsilon)R\rho T \end{aligned}\right\} \tag{2.2}$$

where R is the gas constant referred to unit mass of the original gas. The total pressure of the mixture, according to Dalton's law, will be the sum of p_A and p_{A_2}—namely,

$$p = \{1+\epsilon\}R\rho T \tag{2.3}$$

Similarly, let the specific heat content of the pure gases A and A_2 be, respectively, H_A and H_{A_2}. In the temperature range considered, the translational and rotational motions of the particles are fully excited but the vibrational and electronic states are partially excited. To the first approximation, if the molecule A_2 rotates like a rigid rotator and, independently, vibrates like a harmonic oscillator with frequency ν with the lowest energy zero, the statistical-mechanical calculations give

$$\left.\begin{aligned} II_A &= c(A)2\epsilon RT \\ II_{A_2} &= c(A_2)(1-\epsilon)RT \end{aligned}\right\} \tag{2.4}$$

where $c(A)$ and $c(A_2)$ are defined by

$$\begin{aligned} c(A) &= (5/2) + \left[\sum_n g_n \mathcal{E}_n(A) e^{-\mathcal{E}_n(A)} / \sum_n g_n e^{-\mathcal{E}_n(A)}\right] \\ c(A_2) &= (7/2) + [(h\nu/kT)/(e^{h\nu/kT}-1)] + \\ &\quad \left[\sum_n g_n \mathcal{E}_n(A_2) e^{-\mathcal{E}_n(A_2)} / \sum_n g_n e^{-\mathcal{E}_n(A_2)}\right] \end{aligned} \tag{2.5}$$

with

$$\mathcal{E}_n(A) = E_n(A)/kT \qquad \text{and} \qquad \mathcal{E}_n(A_2) = E_n(A_2)/kT$$

In the above expressions, 5/2 and 7/2 are easily recognized as the classical values for specific heat at constant pressure; the term $(h\nu/kT)/(e^{h\nu/kT}-1)$ is the vibrational energy of a diatomic molecule A_2 and, finally, the last term in both cases represents the contributions from the electronic excitations. The constants g_n, h, and k are, respectively, the number of electronic states of energy E_n of which the ground state is chosen to be zero, Planck's constant, and Boltzmann's constant. For a given particle, the values of g_n and E_n can be calculated either theoretically or by spectroscopic analysis.

With the temperature held much below that of complete dissociation, the above approximation is adequate and the sums in each case can be replaced by the first few terms. If the temperature goes beyond the range 10,000°K., say, then high-order effects such as anharmonicity of the oscillations, the coupling between oscillation and rotation, etc., should be considered. A calculation of this type has been made by H. A. Bethe.[1]

If the energy of dissociation per molecule is D, the total heat content per unit mass of the mixture is

$$II = [c(A_2)(1-\epsilon) + c(A)2\epsilon + (D/kT)\epsilon]RT \tag{2.6}$$

Here the first two terms inside the square bracket can be called the thermodynamic heat content and the last term which arises from the heat absorbed by the reaction (2.1) can be called chemical heat content. It will be noted that, in an aerodynamic problem of this nature, the total heat content, instead of the partial heat content, will appear as the convenient thermodynamic variable.

(3) Chemical Equilibrium

It is seen from the preceding section that for a two-component mixture, the thermodynamic functions contain not only thermal variables T and p but also the concentration of one of the constituents. In a mixture in which there is chemical reaction, the determination of this quantity requires knowledge of the law that governs the rate of chemical reaction, like the case of a combustion process. In cases where the reaction, under given temperature and pressure, cannot proceed indefinitely, an equilibrium state will ultimately be established. If this condition is satisfied, the partial pressures p_A and p_{A_2} will be such that

$$K_p = p_A^2/p_{A_2} \tag{3.1}$$

where K_p is constant for given temperature and is known as the equilibrium constant.

From the definition of partial pressures of Eq. (2.2), it follows that

$$K_p = [4\epsilon^2/(1-\epsilon^2)]p \tag{3.2}$$

In thermodynamics, the condition of equilibrium such as defined above can be expressed by the fact that, holding the temperature and pressure constant, the thermodynamic potential of the system cannot be changed by any variation of the partial pressures. With this principle, statistical mechanics[2] gives the result

$$K_p = \Lambda[Z^2(A)/Z(A_2)]T^{3/2}e^{-D/kT} \tag{3.3}$$

where $Z(A)$ and $Z(A_2)$, known as the sum-over-states, or partition function, denote

$$\left.\begin{aligned} Z(A) &= \sum_n g_n e^{-\mathcal{E}_n(A)} \\ Z(A_2) &= (1-e^{-h\nu/kT})^{-1} \sum_n g_n e^{-\mathcal{E}_n(A_2)} \end{aligned}\right\} \tag{3.4}$$

and the constant Λ is

$$\Lambda = [2(2\pi k)^{3/2}/h^3](m_A/2)^{3/2}(h^2/8\pi^2 I) \tag{3.5}$$

Here m_A is the mass of the particle A, and I is the moment of inertia of the molecule A_2.

Knowing K_p as a function of temperature, the equilibrium degree of dissociation can then be calculated from Eq. (3.2)—namely,

$$\epsilon = [K_p/(4p + K_p)]^{1/2} \tag{3.6}$$

This relation can finally express the enthalpy H in terms of the thermodynamic variables T and p.

(4) Boundary-Layer Equations

Consider a two-dimensional steady flow of a diatomic gas past a fixed semi-infinite flat plate. In a Cartesian

system (x, y), let $y = 0$ and $0 \leq x$ be the plate and let u and v be, respectively, the x- and y-components of the velocity of the fluid. By the boundary-layer theory, the equations of motion reduce to

$$\rho u(\partial u/\partial x) + \rho v(\partial u/\partial y) = -(dp/dx) + (\partial/\partial y)[\mu(\partial u/\partial y)] \quad (4.1)$$

$$(\partial/\partial x)(\rho u) + (\partial/\partial y)(\rho v) = 0 \quad (4.2)$$

where μ is the viscosity coefficient of the gaseous mixture.

For a binary mixture, the energy equation, by the same approximation, assumes the form:

$$\rho u(\partial H/\partial x) + \rho v(\partial H/\partial y) = u(dp/dx) + (\partial/\partial y) \times [\lambda(\partial T/\partial y) + (H_A - H_{A_2})\rho\mathfrak{D}(\partial\epsilon/\partial y)] + \mu(\partial u/\partial y)^2 \quad (4.3)$$

where H denotes the total specific heat content of the mixture defined by (2.6); λ and $\mathfrak{D}$ are, respectively, the thermal conductivity and binary diffusion coefficients. The second term in the square bracket represents the heat flux transported by diffusion. The effects of thermal diffusion are generally small and, therefore, are neglected. Since the composition of the mixture varies in the flow field, the mass fraction of the individual species is required to satisfy

$$\rho u(\partial\epsilon/\partial x) + \rho v(\partial\epsilon/\partial y) = (\partial/\partial y)[\rho\mathfrak{D}(\partial\epsilon/\partial y)] + \Phi \quad (4.4)$$

where Φ is the amount of A_2 dissociated per unit volume per unit time. These equations, together with the equation of state (2.3), constitute the complete mathematical problem of the flow of a binary gaseous mixture in the boundary layer.

For the present, it will be assumed that the mixture in the flow is always in dissociative equilibrium. This is equivalent to saying that the rate of the reaction is fast in comparison with the process of diffusion. Under this condition, the degree of dissociation as a function of temperature and pressure is completely determined as shown in Section (3); and the equation of diffusion is made simply to be a relation defining the reaction rate Φ and, consequently, requires no further consideration.

To simplify the energy equation in the case of equilibrium, let the heat capacity at constant pressure be defined by[3]

$$c_p = (\partial H/\partial T)_p \quad (4.5)$$

In accordance with the assumptions of dissociative equilibrium and boundary-layer approximations, the energy equation can be written as

$$\rho u(\partial H/\partial x) + \rho v(\partial H/\partial y) = u(dp/dx) + (\partial/\partial y) \times \left((\mu/Pr)\{1 + [(H_A - H_{A_2})/c_p]Le(d\epsilon/dT)\}(\partial H/\partial y)\right) + \mu(\partial u/\partial y)^2 \quad (4.6)$$

where Pr $(= c_p\mu/\lambda)$ and $Le(= \rho\mathfrak{D}c_p/\lambda)$ are, respectively, the Prandtl and Lewis Numbers.

(5) An Approximate Method of Solution

Let the stream function Ψ, the heat content H and the pressure p be nondimensionalized as follows:

$$\left.\begin{aligned} \Psi &= \rho_\infty U_\infty L\sqrt{C/Re}\,\psi(\xi, \eta) \\ H &= c_p^{(0)} T_\infty \chi(\xi, \eta) \\ p &= \rho_\infty U_\infty^2 P(\xi) \end{aligned}\right\} \quad (5.1)$$

where U_∞, ρ_∞, and T_∞ are, respectively, the velocity, density, and temperature of the free stream; $c_p^{(0)}$ denotes the specific heat at constant pressure of the undissociated gas A_2; L an arbitrary length; Re the Reynolds Number, defined by $\rho_\infty U_\infty L/\mu_\infty$; and C a constant defined in Eq. (5.5). The nondimensional variables ξ and η are related to the physical variables x and y by the transformation

$$\left.\begin{aligned} x &= L\xi \\ y &= L\sqrt{C/Re}\int_0^\eta [dz/(\rho/\rho_\infty)] \end{aligned}\right\} \quad (5.2)$$

From the transformations (5.1) and (5.2), it follows that

$$\left.\begin{aligned} u &= U_\infty \psi_\eta \\ \rho v &= -U_\infty \rho_\infty \sqrt{C/Re}[\psi_\xi + L\eta_x \psi_\eta] \end{aligned}\right\} \quad (5.3)$$

The elimination of the velocities according to Eq. (5.3) from Eqs. (4.1) and (4.6) leads to

$$\left.\begin{aligned} \frac{\partial\psi}{\partial\eta}\frac{\partial^2\psi}{\partial\xi\partial\eta} - \frac{\partial\psi}{\partial\xi}\frac{\partial^2\psi}{\partial\eta^2} &= -\frac{\rho_\infty}{\rho}\frac{dP}{d\xi} + \frac{\partial}{\partial\eta}\left[\frac{\mu\rho}{C\mu_\infty\rho_\infty}\frac{\partial^2\psi}{\partial\eta^2}\right] \\ \frac{\partial\psi}{\partial\eta}\frac{\partial\chi}{\partial\xi} - \frac{\partial\psi}{\partial\xi}\frac{\partial\chi}{\partial\eta} &= (\gamma - 1)M^2 \times \left[\frac{\rho_\infty}{\rho}\frac{\partial\psi}{\partial\eta}\frac{dP}{d\xi} + \frac{\mu\rho}{C\mu_\infty\rho_\infty}\left(\frac{\partial^2\psi}{\partial\eta^2}\right)^2\right] + \\ &\quad \frac{\partial}{\partial\eta}\frac{\mu\rho}{C\mu_\infty\rho_\infty}\frac{1}{Pr}\left[1 + \frac{H_A - H_{A_2}}{c_p}Le\frac{d\epsilon}{dT}\right]\frac{\partial\chi}{\partial\eta} \end{aligned}\right\} \quad (5.4)$$

where γ is the ratio of the specific heats of the undissociated gas A_2, and M the Mach Number defined by $U_\infty/\sqrt{\gamma p_\infty/\rho_\infty}$.

In these variables, it is seen that the problem is further simplified by the appearance in both equations of a quantity $\mu\rho$. In view of the fact that ρ and μ vary with temperature in opposite directions, the rate of variation of the product $\mu\rho$ with temperature will be greatly reduced. This was found true in the case of a pure gas or nonreacting gaseous mixture when the temperature is moderately high. In the case of a reacting mixture, the heat of reaction involved may alter the transport properties to an extent that $\mu\rho$ may change appreciably with temperature. However, if the mixture is in dissociative equilibrium, the effect of the heat release on the mean-free path will be small and the viscosity coefficient for such a mixture

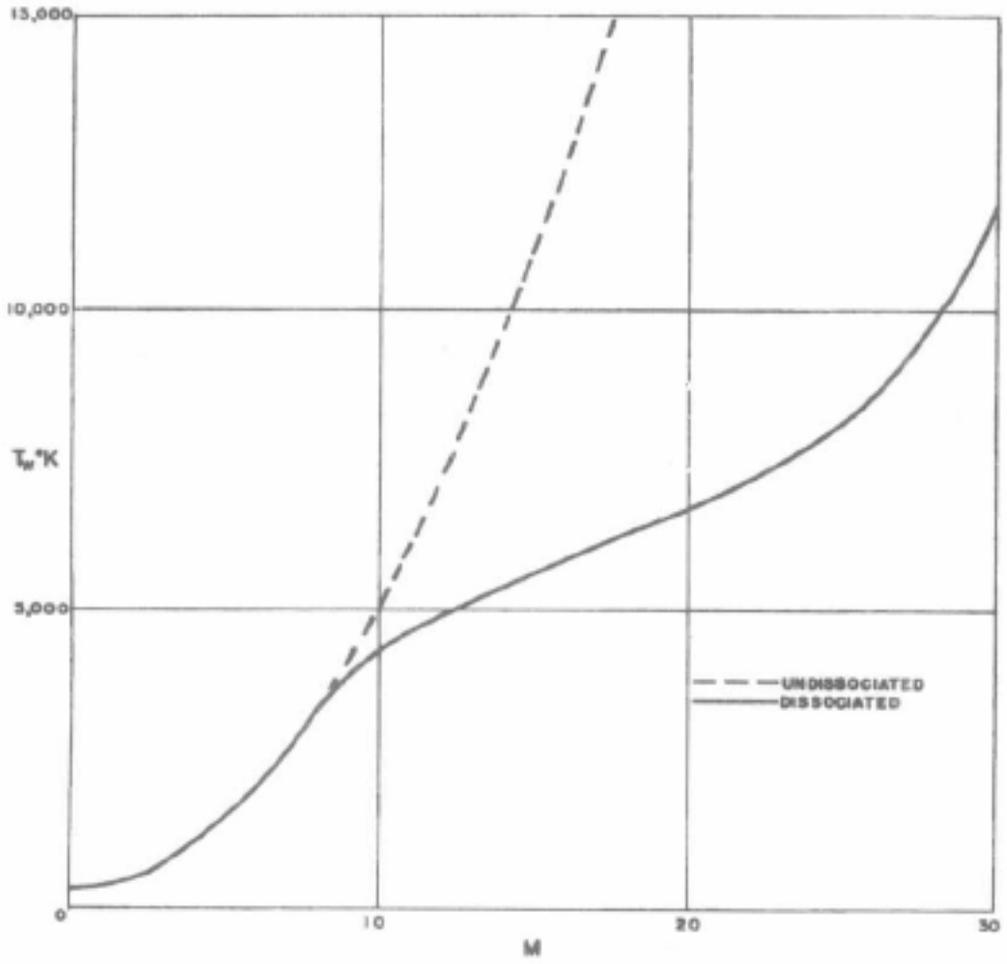

FIG. 1. Adiabatic wall temperature vs. flight Mach Number for dissociated and undissociated nitrogen at $p_\infty = 1$ atm., $T_\infty = 300°$K., and $Pr = 0.72\sigma$.

can be considered, to the first approximation, to be the same as that of a nonreacting mixture.

For a binary mixture of nonreacting gases, according to the kinetic theory, the viscosity coefficient can be expressed, to a first approximation, in terms of the viscosities of the constituent gases, the ratios of concentrations and constants, depending on the character of interaction between particles. If the force between particles varies inversely as some power of the distance between them, the viscosity then varies, like that of a single gas, with temperature according to a power law T^ω, ω being a constant varying slightly with concentration of the mixture.[4] Also, at constant temperature, the variation of viscosity with concentration is, on the whole, very small. It can, therefore, be concluded that, as in the single gas, the product $\mu\rho$ must also vary slowly with temperature. By the same argument, the Lewis Number must vary with temperature in a similar manner as in a nonreacting mixture.

On the other hand, one observes that the Prandtl Number depends on the ratio of heat capacity c_p to the thermal conductivity λ both of which are strongly dependent on the heat of reaction. In the case of a mixture in dissociative equilibrium, the heat capacity c_p can be calculated from Eqs. (2.6) and (3.6) in terms of the degree of dissociation ϵ and heat of dissociation D. As for the thermal conductivity coefficient λ, it can be shown approximately that it varies very nearly as $c_v\mu$, c_v being the heat capacity at constant volume.[5] It is, therefore, not difficult to verify that the Prandtl Number is also insensitive to change of temperature. By a slightly different argument, C. F. Hansen has arrived at the same conclusion.[6]

Moreover, it can be shown that the ratio of the heat flux transported by diffusion to that by conduction in the case of dissociative equilibrium is approximately

$$Le\,\frac{[(D/2kT) - 2]\epsilon(1 - \epsilon^2)(D/kT)}{\epsilon + 9 + [(1/2) + (D/kT)]\epsilon(1 - \epsilon^2)(D/kT)}$$

when the vibrational states are fully excited. The most important factor in this expression is evidently D/kT for nonvanishing ϵ. When the first term in the denominator becomes unimportant, the ratio reduces to the value 0.5. It is clear that, over a wide range of temperature, the ratio must vary slowly with temperature. In the case of nitrogen, it has the values of 0.26 at 5,000°K., 0.29 at 6,000°K. and 0.23 at 8,000°K.

Following the accepted practice in the compressible boundary-layer theory for a nonreacting gas, the following approximations are proposed:

$$\left.\begin{aligned} \mu\rho &= C\mu_\infty\rho_\infty \\ Pr &= \text{constant} \\ Le &= \text{constant} \\ \sigma &= 1 + Le \times \\ &\quad \frac{[(D/2RT) - 2]\epsilon(1 - \epsilon^2)(D/kT)}{\epsilon + 9 + [(1/2) + (D/kT)]\epsilon(1 - \epsilon^2)(D/kT)} \\ &= \text{constant} \end{aligned}\right\} \tag{5.5}$$

On account of Eqs. (5.5), Eqs. (5.4) reduce to

$$\left.\begin{aligned} \frac{\partial\psi}{\partial\eta}\frac{\partial^2\psi}{\partial\xi\partial\eta} - \frac{\partial\psi}{\partial\xi}\frac{\partial^2\psi}{\partial\eta^2} &= -\frac{\rho_\infty}{\rho}\frac{dP}{d\xi} + \frac{\partial^3\psi}{\partial\eta^3} \\ \frac{\partial\psi}{\partial\eta}\frac{\partial\chi}{\partial\xi} - \frac{\partial\psi}{\partial\xi}\frac{\partial\chi}{\partial\eta} &= (\gamma - 1)M^2 \times \\ &\quad \left[\frac{\rho_\infty}{\rho}\frac{\partial\psi}{\partial\eta}\frac{dP}{d\xi} + \left(\frac{\partial^2\psi}{\partial\eta^2}\right)^2\right] + \frac{\sigma}{Pr}\frac{\partial^2\chi}{\partial\eta^2} \end{aligned}\right\} \tag{5.6}$$

The problem thus is reduced to that of incompressible boundary layer with an equivalent Prandtl Number σ/Pr and pressure gradient $(\rho_\infty/\rho)dP/d\xi$. The aerodynamic effects of dissociation can thereby be investigated without integrating the differential system (5.4).

(a) *Insulated Flat Plate*

In the case of insulated plate $dP/d\xi = 0$, with the Blasius solution $f(\zeta)$ given, ζ being the similarity parameter $\eta/\sqrt{\xi}$, the energy equation can be readily integrated in terms of f, first shown by Pohlhausen. On the plate $\zeta = 0$, χ reduces to

$$\chi(T_w/T_\infty) = 1 + [(\gamma - 1)/2]M^2\sqrt{Pr/\sigma} \tag{5.7}$$

where T_w denotes the temperature of the plate. For an undissociated gas, $\chi(T_w/T_\infty)$ is identically T_w/T_∞. Now, on account of Eqs. (2.6) and (3.6), it is a rather complex function of both T and p. At standard temperature and pressure, the temperature of the plate for nitrogen N_2 is plotted against M and is shown in Fig. 1. For comparison, the plate temperature for undissociated N_2 is also given. It is seen that at one atmospheric pressure and $T_\infty = 300°$K., dissociation starts at about 3,500°K., corresponding to a Mach

Number of about 8, and nearly completes at about 10,000°K. with Mach Number of around 28. In this temperature range, the difference in temperature for dissociated and undissociated gases is large; for instance, when dissociation is half completed at 6,000°K., the temperature for the undissociated gas would have been 14,000°K. This clearly demonstrates how far in error the predictions can be if this effect is ignored at high temperature.

On account of the fact that the surface temperature has been considerably reduced by dissociation of the gas, there will be less expansion of the streamlines in the normal direction than that of the undissociated gas at the same Mach Number and, hence, a corresponding decrease of the boundary-layer thickness and the velocity v. For, as $\zeta = \infty$, its asymptotic value is

$$v = U_\infty \sqrt{C/Re_x} \left\{ 0.860 + (1/2) \int_0^\infty \times [(1 + \epsilon)(T/T_\infty) - 1]\, d\zeta \right\} \quad (5.8)$$

It is known that at high Mach Number the second term inside the brace predominates and, from Fig. 1, the value of the integral will be much smaller if dissociation of the gases is allowed.

To investigate the effect of dissociation on the skin friction, let the constant C be chosen by the same convention as that adopted in the case of undissociated gas. Namely, the assumed viscosity-temperature law agrees with true value of $\rho\mu$ at the surface where the temperature is the highest. That is, at $\zeta = 0$,

$$C = (\mu\rho/\mu_\infty\rho_\infty)_w \quad (5.9)$$

From this value of C, it follows that the ratio of the skin-friction coefficient c_f to that $c_f^{(0)}$ of the undissociated gas is

$$c_f/c_f^{(0)} = \sqrt{(\rho\mu/\rho^{(0)}\mu^{(0)})_w} \quad (5.10)$$

This result shows that if the quantity $\rho\mu$ in both cases is held constant but has the correct value at the highest point of the temperature field, then the change of the skin friction by dissociation, at the same Reynolds and Mach Numbers, can be expressed in terms of the change of $\rho\mu$ by dissociation. In the case of undissociated gas, the quantity $\rho^{(0)}\mu^{(0)}$ can be calculated with reasonable accuracy at high temperature from the knowledge of the viscosity at normal temperature. When dissociation takes place, the situation will be entirely different. Although the quantity $\rho\mu$ behaves much like that of a neutral mixture (as argued in the previous discussion), quantitatively it is quite another matter. It is known from the kinetic theory that the viscosity of a nonreacting mixture depends upon the viscosities of all the constituents. In the present problem, one of the species is a monatomic gas which exists only at high temperature, and the calculation of its viscosity will be very different from that of nonreacting particles at normal temperature. Under these circumstances, the very question of the nature of interaction between particles, namely whether the interaction is attraction or repulsion, depends on the state of excitation of the colliding particles. As far as is known, this type of calculation has not yet been made.

There is evidence that these effects do exist. For instance, when atomic hydrogen diffuses into molecular nitrogen, the calculated diffusion coefficient by the kinetic theory agrees with the value measured by experiments. However, when hydrogen atoms diffuse into molecular hydrogen, the measured diffusion coefficient is about 4 times as large as has been calculated.[7] If this abnormal increase in diffusion coefficient is observed in the case of hydrogen atoms diffusing through hydrogen molecules, there must be a similar increase in other transport coefficients. For this reason, the numerical verification of Eq. (5.10) cannot be given.

(b) *Cooled Flat Plate*

From the above results, it is observed that if the plate is thermally insulated, the surface temperature will generally be high enough to melt (even to vaporize) steel, for a flight Mach Number greater than 6 at sea level. It is clear that if high-speed flight is to be possible, the heat generated by friction must be removed by means of cooling. Let the surface temperature be T_w and the ambient temperature T_∞. The solution satisfying these conditions is

$$\chi = 1 + [(\gamma - 1)/2]M^2\theta_1(\zeta) + \{\chi_w - 1 - [(\gamma - 1)/2]M^2\sqrt{Pr/\sigma}\}\theta_2(\zeta) \quad (5.11)$$

where θ_1 and θ_2 are functions of the similarity parameter ζ. These functions, like the Blasius function $f(\zeta)$, are tabulated for different values of Pr/σ (see reference 8).

For nitrogen at $M = 20$, $Pr = 0.72\sigma$, $Le = 0.72$, $T_\infty = 300$°K., and $p_\infty = 1$ atmosphere, the temperature distribution is presented in Fig. 2 for a wall temperature of 1,200°K. Under these conditions, the temperature reaches a maximum of about 4,200°K. in the neighborhood of the plate. Since nitrogen begins to dissociate at 3,500°K. at one atmosphere, there is a sizable portion of the high temperature zone

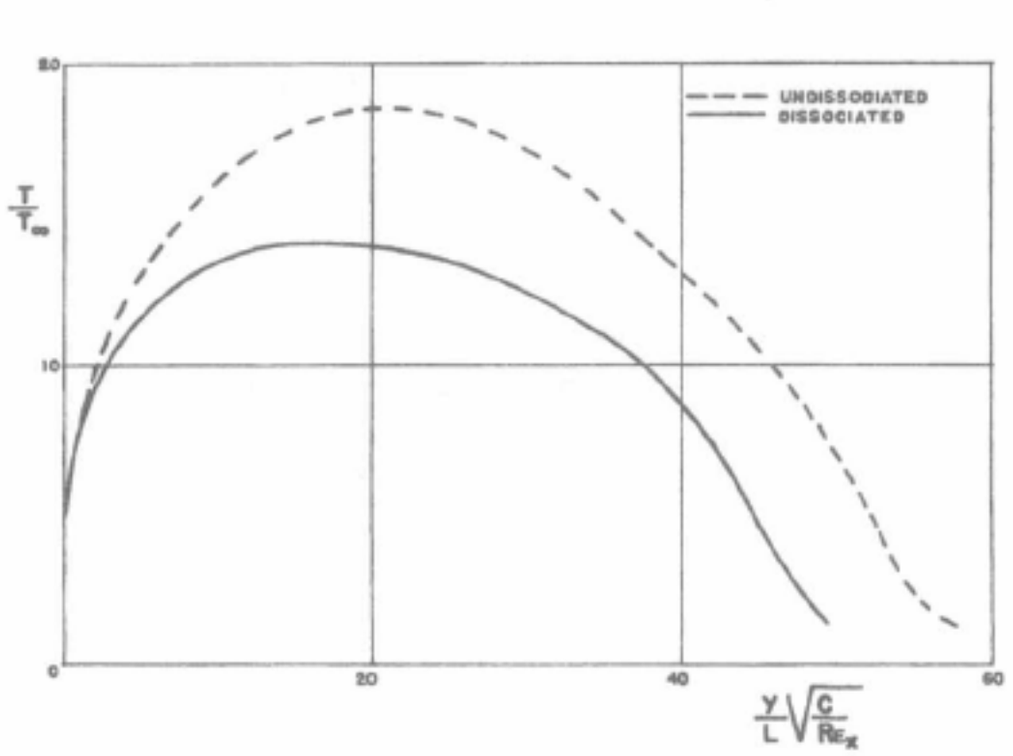

FIG. 2. Temperature distribution in the boundary layer for dissociated and undissociated nitrogen at $p_\infty = 1$ atm., $T_\infty = 300$°K., $M = 20$, and $Pr = 0.72$.

in which the gas is partially dissociated. For comparison, the temperature field with no dissociation taken place, is also plotted for the same constant C. It is noted that one of the effects of dissociation is to reduce the boundary-layer thickness.

In the present case where the surface is cooled, it is learned from the calculations of compressible boundary layer that if the constant C is chosen to correspond to the true value of $\rho\mu/\rho_\infty\mu_\infty$ at the neighborhood of the maximum temperature instead of at the surface as in the previous case, the skin friction and the heat transferred to the surface can be similarly calculated. In the case where the gas is in dissociative equilibrium, the heat flux across the surface is given by

$$q = -[\lambda(\partial T/\partial y) + \rho\mathfrak{D}(H_A - H_{A_2})(d\epsilon/dT)(\partial T/\partial y)]_w \quad (5.12)$$

On account of Eqs. (5.1), (5.2), (5.5), and (5.11), the heat flux q can be written as

$$q = q^{(0)} \left(\frac{\sigma Pr^{(0)}}{Pr}\right)^{2/3} \sqrt{\frac{C}{C^{(0)}}} \times \frac{1 + [(\gamma - 1)/2]M^2\sqrt{Pr/\sigma} - \chi_w}{1 + [(\gamma - 1)/2]M^2\sqrt{Pr^{(0)}} - T_w} \quad (5.13)$$

where $q^{(0)}$ denotes the heat flux in the case of the undissociated gas and $Pr^{(0)}$ and $C^{(0)}$, the corresponding constants as defined in Eqs. (5.5). When the Mach Number is very large and the wall temperature is low, the ratio of the heat fluxes is approximately

$$q/q^{(0)} = (\sigma Pr^{(0)}/Pr)^{1/6}\sqrt{C/C^{(0)}} \quad (5.14)$$

It can be concluded from this result that, unless the change of Prandtl Number is large due to dissociation, the effect of dissociation on the heat flux due to change of Prandtl Number is small; and, like the skin-friction coefficient, the ratio of the heat fluxes is sensibly proportional to $(\mu\rho/\mu^{(0)}\rho^{(0)})^{1/2}$. As in the case of cooling, the difference of temperature between dissociated and undissociated gases is greatly reduced, the ratio $(\mu\rho/\mu^{(0)}\rho^{(0)})^{1/2}$ cannot be much different from unity. Generally, it seems that if the surface temperature is low, the effect of dissociation cannot be large, even if the Mach Number is high.

Of course, it must be emphasized that these conclusions have been reached on the assumptions that the mixture is in dissociative equilibrium. When this restriction is dropped by including such phenomena as relaxation and recombination, the results may well be considerably modified.

References

[1] Bethe, H. A., *The Specific Heat of Air up to 25,000°K.*, Department of Commerce, Report PB-27307, 1942.

[2] Tolman, Richard C., *The Principles of Statistical Mechanics*, p. 610; Oxford University Press, 1938.

[3] Epstein, Paul S., *Textbook of Thermodynamics*, p 316; John Wiley & Sons, Inc., New York, 1937.

[4] Chapman, Sydney, and Cowling, T. G., *The Mathematical Theory of Non-uniform Gases*, p. 232; Cambridge University Press, 1939.

[5] Rossini, Frederick D., (Ed.), *High Speed Aerodynamics and Jet Propulsion*, Vol. I, "Thermodynamics and Physics of Matter," p 411; Princeton University Press, 1955.

[6] Hansen, C. Frederick, *Note on the Prandtl Number for Dissociated Air*, Journal of Aeronautical Sciences, Vol. 20, No. 11, p. 789, November, 1953.

[7] Langmuir, Irving, *Phenomena, Atoms and Molecules*, pp. 189, 200–201, Philosophical Library, 1950.

[8] Low, George M., *The Compressible Laminar Boundary Layer with Heat Transfer and Small Pressure Gradients*, NACA TN 3028, 1953.

現代空气动力学的問題[1)]

郭 永 怀

（中国科学院力学研究所）

航空工業从开始以来，一个很重要的目标，就是不断地提高飞行器的速度。因为速度的增加，气流里所产生的現象，就逐漸复杂起来。

二十几年前，飞行速度平均在每小时三四百公里左右，建立在空气是不可压縮沒有粘性的假設上的流体力学，对于飞机的設計，就有了很大的貢献。后来为了战爭的要求，飞行的速度提到六七百公里，在飞行和制造上，就第一次發生了困难，就是所謂“空气可压縮的困难”。因此空气动力学就不得不抛去它本来的假設，而換为空气是一个可压縮的理想气体。它的研究的对象，就由純粹計算流場的几何圖形，轉到考虑因为流动所引起的热力学的变态，这就發現冲击波一类的新現象。空气动力学就达到流体力学与热力学的結合。

現在各国又从事技术和軍事的竞賽，洲际导彈和人造衛星不久即將成为事实，于是我們就又面临第三个新时代的开始。如果远距离航行实現，飞速总須在20倍声速以上，在这样高的速度下，气流里的温度，至少是在6000°C以上。空气的温度这样高，它就不能保持本来的状态，而發生分离和电离的現象。要了解这一类的問題，于是空气动力学就不得不进一步和物理化学匯合了。

空气动力学的范圍，既是如是之广，一个全面的叙述是不可能的。我現在专就飞行器外表的气流，順着速度的次序，很簡单地介紹一下近十几年来空气动力学在这方面存在的一些問題，并且可能的話，指出这些問題今后發展的方向。

跨声速气流

假設我們作这样一个实驗：把一个二元的机翼模型架在風洞里，讓空气吹过去。風速漸漸增加，翼截面上的气流就会慢慢地快起来，等到速度最高的一点达到那点的声速以后，我們就开始看到一些新現象。最显著的是流場里忽然發生了一些不稳定的扰动，用密度观察仪，我們就能看到許許多多的弱小的波动，跳来跳去(圖1)。繼續增加速度，这些小波动便次第变强，最后便堆垒一起而形成一个所謂λ冲击波（圖2）。

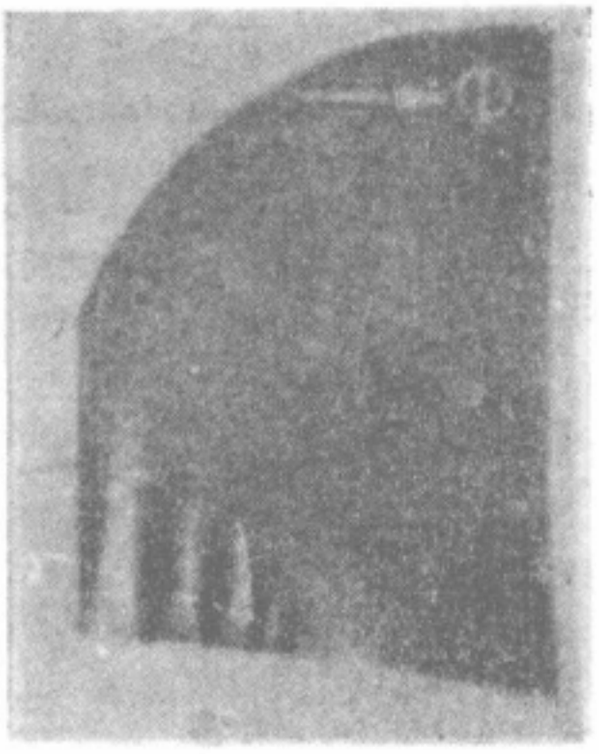

圖 1

如果我們在这样一个实驗里，从事測量飞机模型所受的举力和阻力，我們就發現以下的結果。若是飞行的馬赫数（即飞速和大气里的声速的比数）繼續增加，飞机所受的举力，开始的时候因为表面上气流膨脹的关系，它就慢慢地升高，达到相当的程度，在λ波形成之后，翼表面上的压力就不随飞速很快地变化；相反地，腹面上的压力就很快地随速度的增加而降低，結果举力到了最高点便又下跌(圖3)。当微波开始出現以后，無旋流場就不存在。不断地增加馬赫数，弱小的击波就逐漸地变强；因为击波的产生，在流場里就有了压力增加的不連續面，这就減低了流場一部份的动能，結果便出現了波阻力；冲击波愈强阻力就愈大。所以在举力下降的时候，阻力是很大的，这就产生所謂“空气可压縮的困难”(圖4)。在实际飞行时，最危險的是在举力下降时，力距由正轉負，發生因机头重而引起的在飞行时的控制的問題(圖5)。

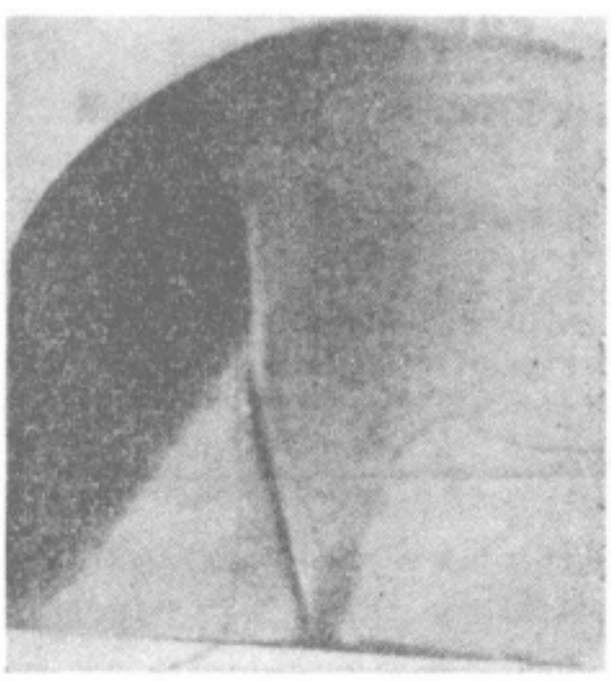

圖 2

从理論方面看，这又是怎么一个問題呢？我們知道，要是沒有冲击波出現，在飞速到达一个特殊数目后（即全流場仅仅翼截面上最高流速等于那点的声速），再提高飞速，貼着翼截面外边就有一或两个小区域是超声速流場，飞速增高，它們的面积也随着扩大。

1) 发表在《科学通报》, 1957, (10): 289~295

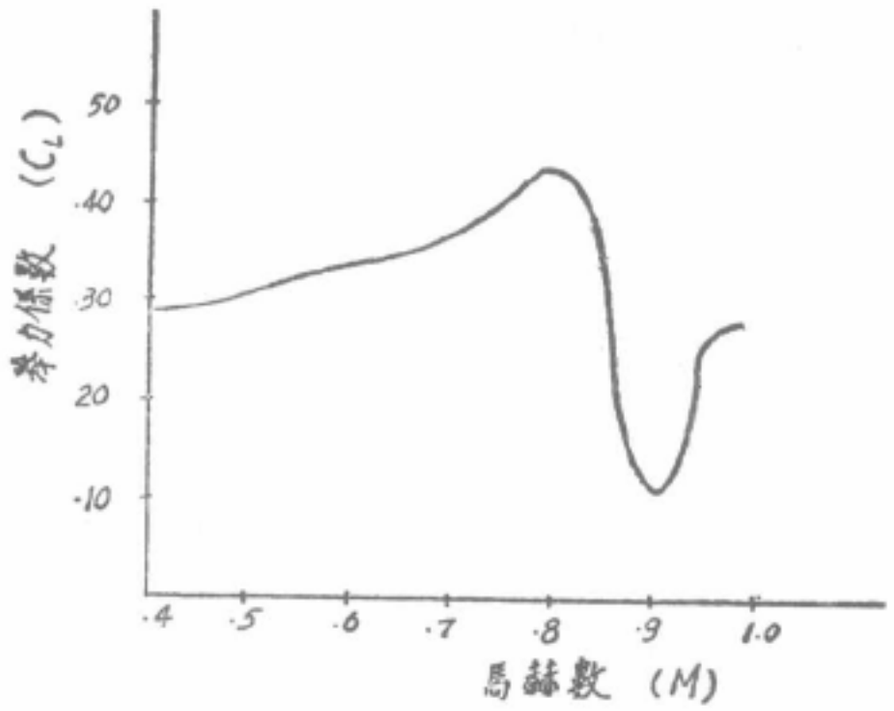

圖 3　举力系数与馬赫数之关系，仰角 3°

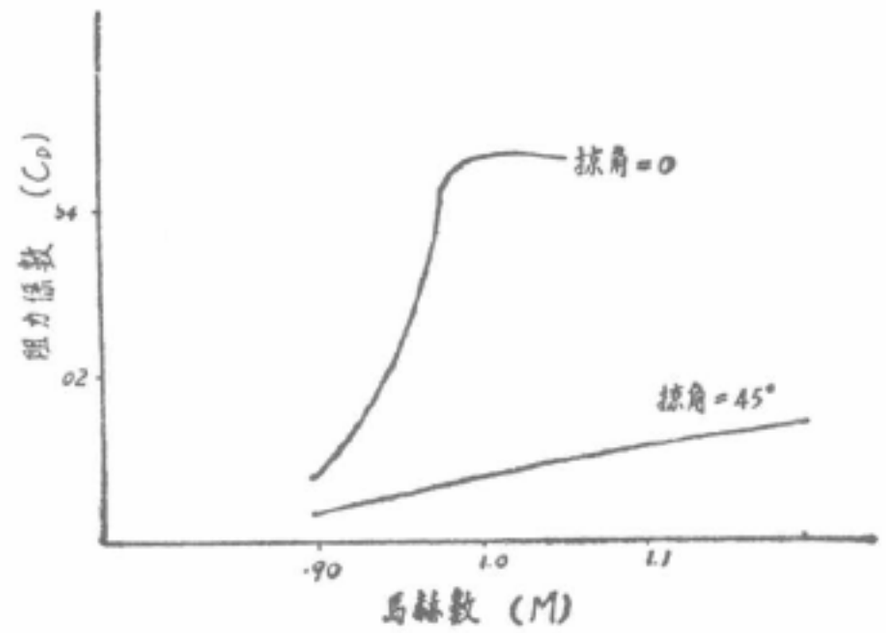

圖 4　阻力系数与馬赫数在掠角为 0° 和 45° 时的关系

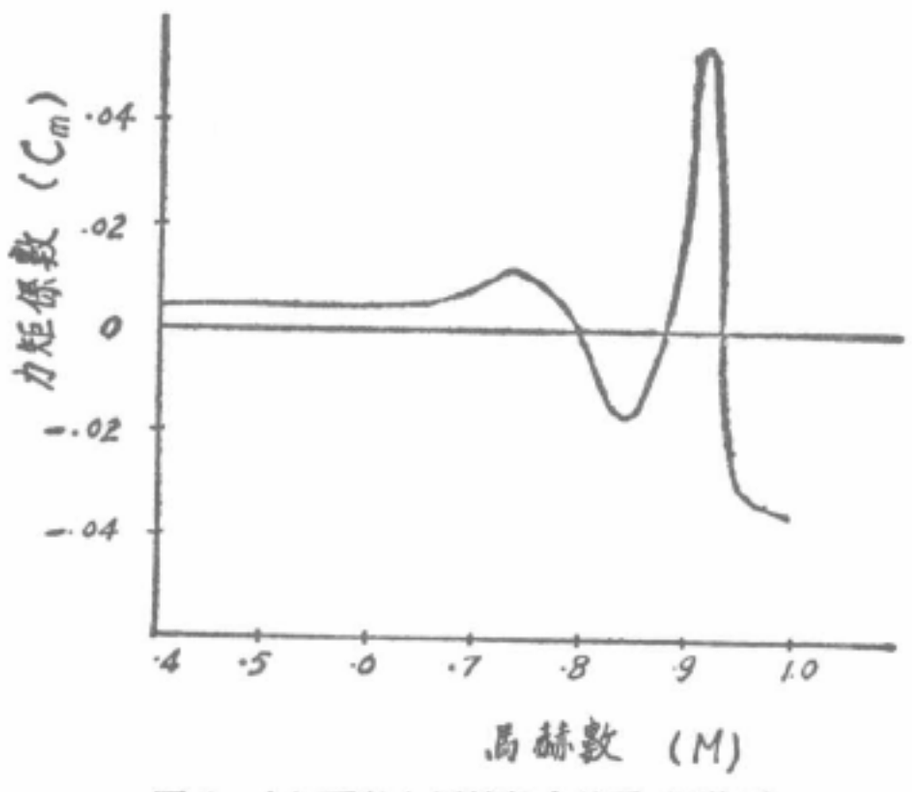

圖 5　力矩系数与馬赫数之关系，仰角 3°

这样一个超亚声速混合的流場，要是能够使它实現，前面所看到的那些不利的現象就可以避免，跨声速飞行的問題就可以簡单，推动机的能量也不需加大。

要解答这样的流場存在不存在的問題，我們首先要从理論方面看看，流場所适合的方程式的解存在不存在？因为流場有超亚声速并肩存在的特性，描写它的二次偏微分方程也就有不同的性格：在亚声速区域里是橢圓类型，在超声速区域里是双曲綫类型。一个二次二元偏微分方程是屬于哪一类型，完全看它的三个主要系数所符合的一个数学的关系。从一区到另外一区，它的类型不同，这个数学关系就必須变号。因为系数包括速势位的导数，所以描写跨声速流場的方程式，就必須是非綫型的。在把一个翼截面的形状（直綫的如菱形除外）确定之后，找这样一个微分方程的解，并且还要适合边界条件，是一个非常困难的問題。这可以說是空气动力学里沒有解决的問題之一。

这样一个問題要是解决了，究竟有什么好处？我們知道在古典流体力学里有一个很有力的定理，就是固体在流体里以等速运动，如果流場是無旋并且是連續的，固体所受的力就是等于零。所以，要是我們能够找到一个解并且还能証明它的存在，我們就有了高效能的跨声速飞行的理論的根据。我們就可以期望提高飞机的速度，而不过分影响推进机的能量。

理論方面既得不到解决，同时在实驗里我們又看到翼截面上最高流速达到声速以后，冲击波就开始形成，于是就有了两种揣測：一个是說在翼截面决定之后，無旋連續流場只有在某一些飞行馬赫数才存在，也就是說，方程式的解对于飞行馬赫数不是連續的，正同繩索振动的頻率一样。因此，在实际飞行时，馬赫数如果不符合理論的要求，冲击波就会产生出来。另外一个說法是方程式的解对于馬赫数是連續的，但是并不稳定。这就是說，一有扰动，这种扰动就不会消灭，而漸漸滋长，至形成冲击波为止。这两种說法的結論是不冲突的，但是对导致这种現象的原因的看法，就根本不同。最后的解决，还要从方程式出發，所以哪种观点正确是很不容易証明的。

从正面既然不能克服跨声速飞行的困难，气体动力学家便提出一个延緩这个困难的發生的办法：就是采用有后掠角的机翼（圖 6）。它的理論是，在二元的机翼外的流場，加一等速的横流（即垂直飞行方向），如果流場是無粘性的，它便不会增加或减少飞机本来所受的举力和阻力，其結果便把阻力增加和举力减少的現象移到更高的飞行馬赫数了。在后掠角等于 45° 的时候，飞行的馬赫数就能提高到 40% 左右。

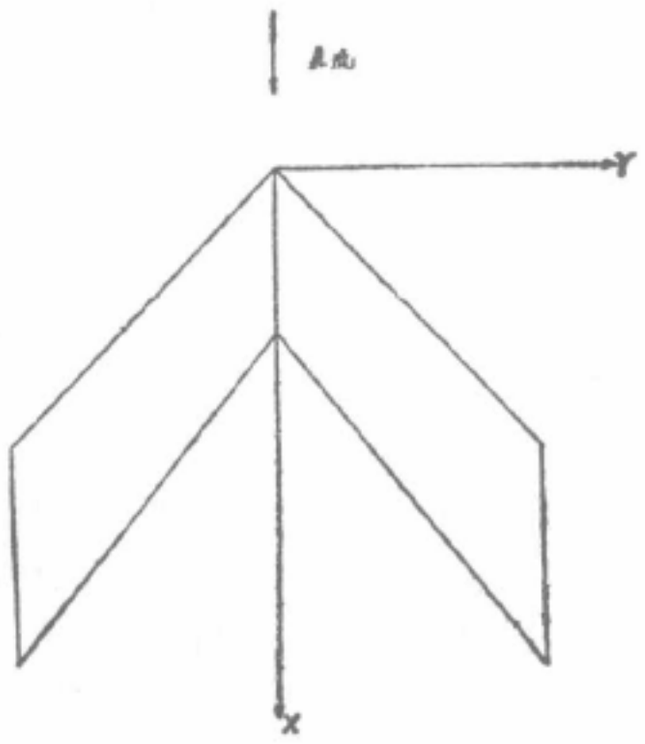

圖 6　机翼平面圖形

实际上事情当然不是这样简单，因为机身机翼两端的存在，飞机外面流場就不是二元的，結果就减低了飞机的理想效能。此外翼面上的附面層，因为机翼的后掠，就發生不平均的分离現象，改变举力的分布，降低飞机的性能。虽然如此，采用后掠角的办法，依然削减了阻力，实現了跨声速飞行(圖4)。

超声速气流

超声速气流和跨声速气流不同，它的特点是稳定，并且所存在的冲击波，一般的極其微弱。因此就沒有跨声速气流里的困难，飞行的問題就比較簡单。

超声速流場和亚声速流場的另一区别，是超声速流場里要是有了扰动，它就不能向四处多方傳播。譬如一个压力点源，在空气里移动，如果它移动的速度比声速小，那么它的压力的影响，虽有上下游的不同，但仍能向各方傳送。它在不同时間所达到的地方，就像圖 7a 里那些圓所标示的一样。如果它的速度比声速高，不同时間所發出的信号，就能彼此相切而形成一个圓錐面(圖 7b)，压力的影响就只限于圓錐里面，它外边就得不到信号。这就把流場分为两个区域：一个是靜止区，一个是扰动区。划分这两个区域的圓錐面，便叫做馬赫圓錐。因为这个关系，超声速流場的計算和亚声速流場是很不同的。

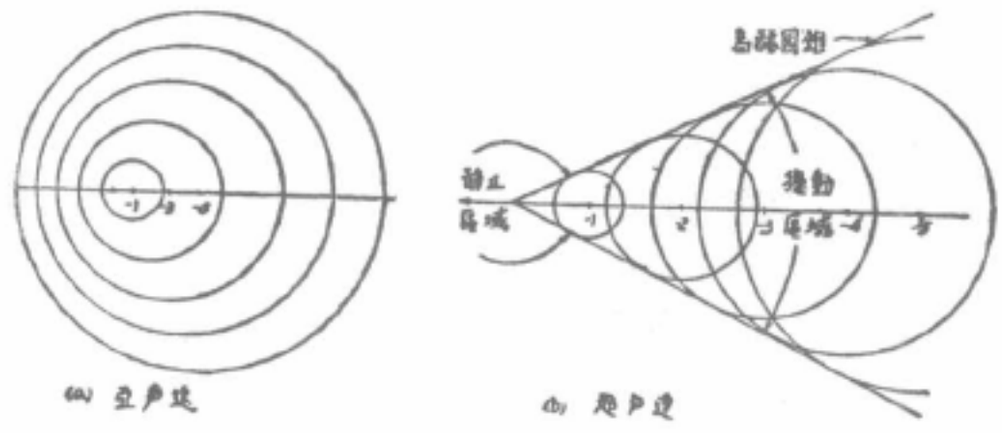

圖 7　点源在可压縮气体內移动

假如机翼的厚度小，飞行馬赫数又不过高，飞机产生的扰动就比飞速小，这时描写流場的方程式，就能根据逐次逼近的方法化为綫性的。在机翼薄的假定下，气流在翼面垂直方向的詳細情况可以忽略，翼形就可以用它的投影替代(圖 6)，来簡化边界条件。超声速机翼的理論，就是这样建立的。一般說来，因为題目的性質不同，我們可以分用以下三种方法。

重叠法　因为算学的問題是綫性的，所以在边界条件确定之后，就可以用重叠法把方程式的基本解(即源) 积分起来 (即源的分布)，便得到一个解。这个方法的应用很广泛，它可以用到超声速或亚声速前椽的情形(就是与前椽垂直的流速高于或低于声速)，也可以用到超亚声速混合的前椽的情形。計算的問題，在一般情形下，都可以化为求一对阿伯尔 (Abel) 的积分方程的解。这个方法是 J. C. 依法尔 (Evvard) 和 E. A. 克拉舍持柯娃 (Красильщикова) 大約同时發現的。

此外还要注意后椽的問題。在超声速机翼理論里，后椽也有超声和亚声的区别。在亚声速时，与后椽垂直的流速低于声速，那里的流場就有亚声速流場的特性，它要适合庫塔-儒柯夫斯基 (Kutta-Joukowsky)的条件。在超声速后椽的时候，那里的流場就有超声速流場的特性，翼面上下的压力在那里就可以不連續，而底上两面的流速的方向，就必須一样。

同样，因为有超亚声速前椽的分别，在那条綫上流場的性質就也不同，这在阻力的計算上是很重要的。在超声速前椽的情况，問題比較簡单。可是在亚声速前椽的时候，那条綫上的流速便是無穷大，这对于阻力就有了貢献，这个貢献是"吸力"还是"推力"，就要看前椽的几何形状。所以在超声速机翼理論中，考虑前椽的阻力和它的几何形的关系，是很重要的。

圓錐形流　由于超声速流場的特性，在很多情况下流場变量会在通过一点的直綫上不变，而仅随經緯两个方面改移。結果流場方程式就由三元化为二元，并且压力的分布，在綫性的假設下，又能进一步从拉普拉斯方程式导得，計算的困难就大大减低(圖 8)。

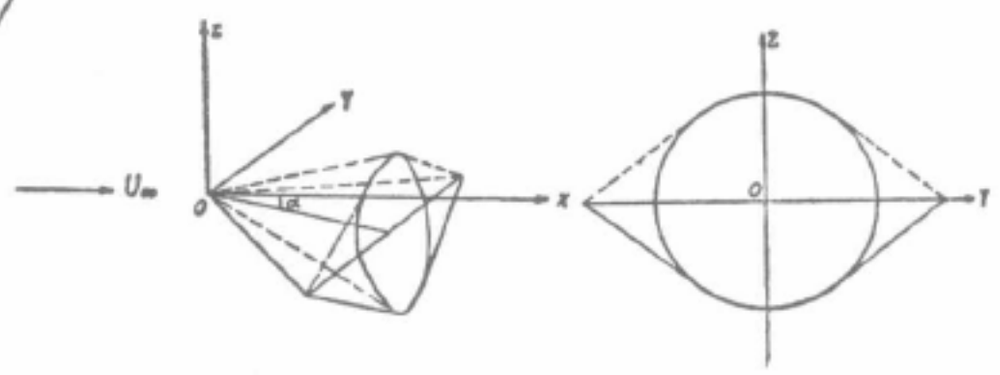

圖 8　圓錐形流

圓錐形流的重要性是，适合于这个条件的非綫性的三元流場也可以計算。在一般情形下，三元机翼理論的建立是很困难的，准确的解几乎是不可能。可是有了圓錐的特性，算学的問題就可以变为一个二元的，数字的計算就可以进行，所得的結果用来了解气流的問題和校勘近似解的准确度，都是很有用的。圖 8 里的三角机翼，在仰角 4° 和馬赫数 3 的时候，近似解与准确解的比較，不論是冲击波，馬赫圓錐和压力分布，两种計算的差别是很大的(圖 9)。

細长机翼　当机翼細长的时候，例如縱横比小而掠角大的机翼，或者是一个飞彈，气流在飞行的方向变移較慢，势位的方程式中的一項，包含在飞行方向的导数，就可略去不計。这就是說，要是流場在任何截面确定之后，在其它的截面上的問題就是一个二元的(圖 10)。这个省略的方法，用到超声速机翼的問題上，是 R. T. 郑司 (Jones) 首先倡导的，它同亚声速里的有名的 M. M. 茫克 (Munk) 方法是一样的。在

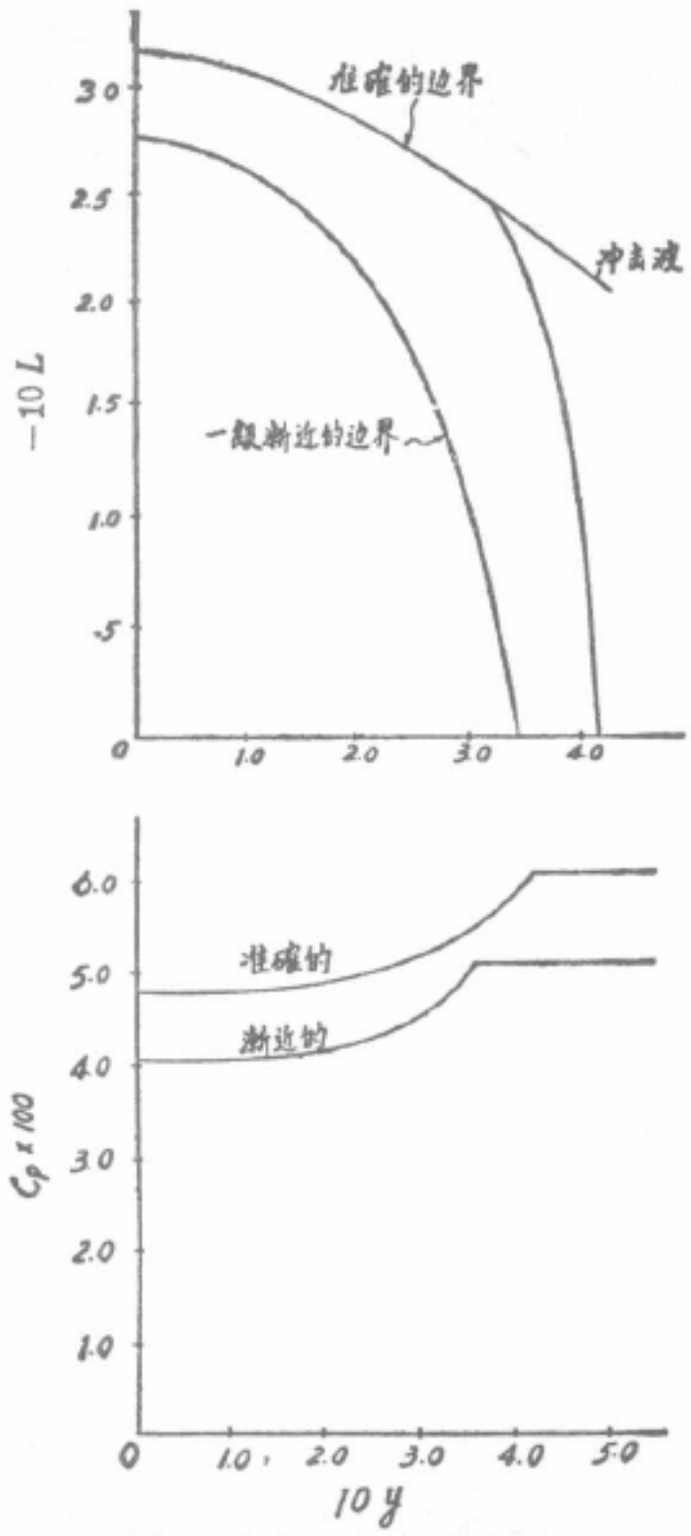

圖 9　准确与近似解的比較
$\alpha=4°$，$\gamma=45°$，$M=3.0$

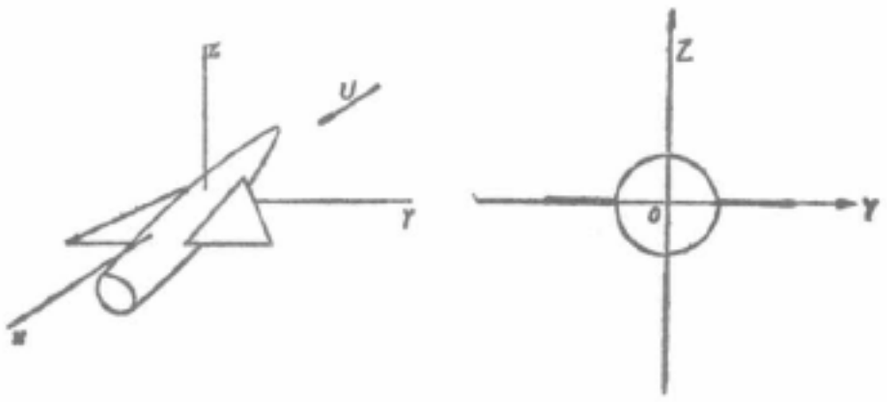

圖 10　縱横比小的飞机

縱横比小的情况，机身和机翼的干扰就产生較大的影响，有了郑司的方法，这問題便得到了解决。

近年来在实驗上發現，細长飞机的阻力，在接近声速时，和它的軸向截面积分布有直接关系。要是一个飞机的軸向截面积分布和一个軸向对称的物体的截面分布一样，它們的阻力就是相似。例如三个机形：A 是一个軸向对称体，B 是一个軸向对称体和一对后掠 45° 的翼，C 是把B的机身修削过，使它的截面积分布和A一样。它們的阻力如圖 11 所示。当馬赫數低于 1.4，飞机 C 的阻力就比 B 的阻力少很多。

从理論上說，这是一个最小阻力的問題。就是当机身和机翼規定后，机身应如何变形，才能得到最小

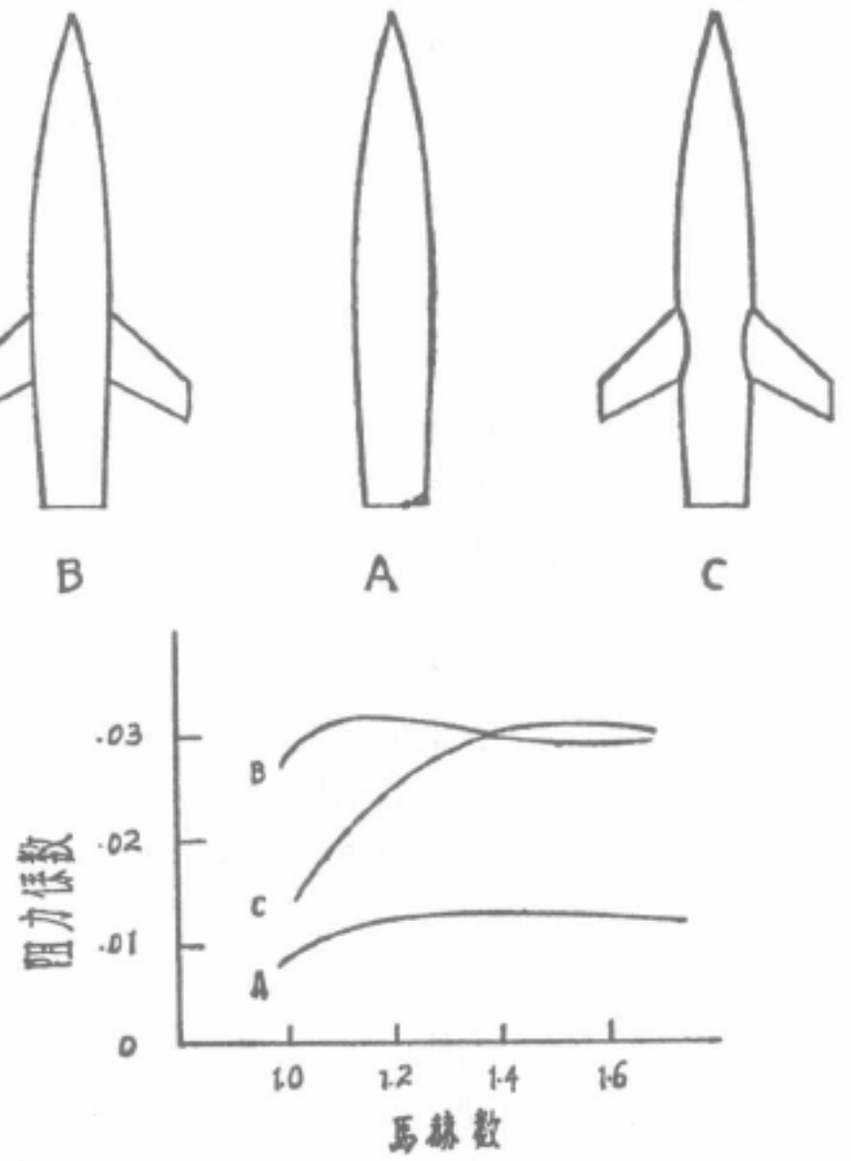

圖 11　机身修削对于阻力的影响

阻力。这一类問題，也因有了郑司的方法而解决。

以上所說的这些方法，由于方程式的綫性化，就有这样一个后果：就是在流場里所發生的扰动，它不能用当地的声速傳播，而是按照远处空气里的声速傳播，不随流量的变移而不同，結果所算出的冲击波形状就不够准确(圖 9)。要是在一个問題里存在着复杂的冲击波的結构，因为波形的計算不准确，所算出的压力在翼面上的分布就不会可靠。最簡单的一个例子，就是一个三角形翼所产生的斜击波与馬赫圓錐的干扰。因为有冲击波的存在，一級近似解和准确計算的結果，相差就很大(圖 9)。这是一个極普通的情形，在重要的問題里，这是必須注意的。

高超声速流

从实际数字的計算我們發現，馬赫数增大，一級

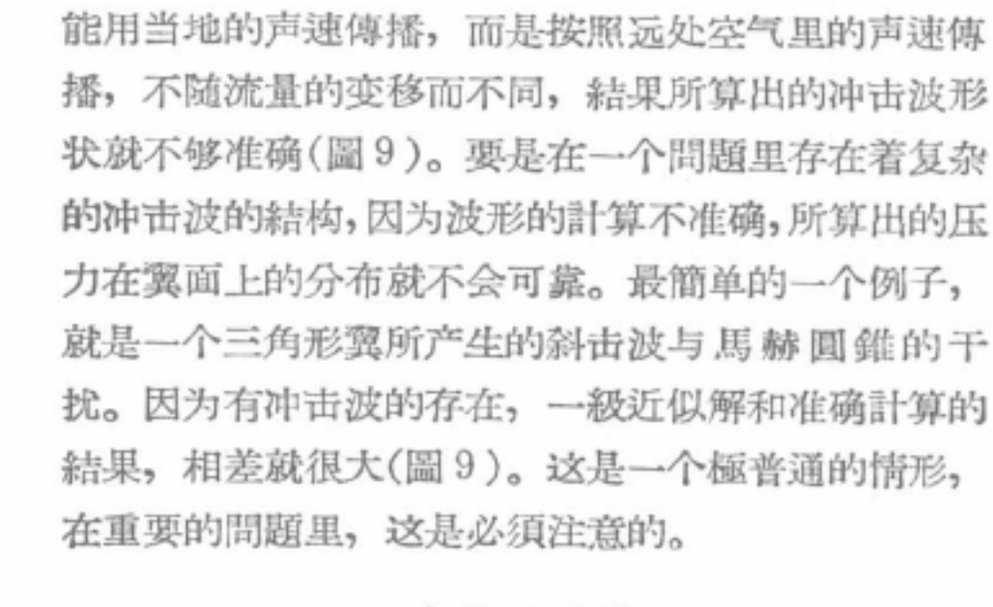

圖 12　近似解的准确度在低速与高速时的比較

近似解的准确度就漸漸減低。例如計算在圓錐子午面里的薄板上的压力，高速和低速两种情况之下，准确和近似的結果，相差就很大(圖 12)。这就証明，在厚度小的假設下，馬赫数大的时候，一級近似法所忽略的項目就会很重要。

当飞速超过声速很大，即所謂高超声速，机翼的厚度虽小，而产生的扰动倒不一定小。在这种情况之下，流場里的馬赫角就很小，斜冲击波的角也很小。假如馬赫角和机翼的厚度同样小，它們的比就是一个重要的数目。根据这个假設，我們就可以重新估計描写流場的方程式的各个項目，并且还可进一步把这个簡化了的非綫型的方程式，轉換为一个同机翼厚度和馬赫数無关的方程式。也就是說，两个翼面相似而厚度不同，如果厚度和飞行的馬赫数的乘积一样，这两个流場便也相似。这个相似律是錢学森先生首先發現的。

这定律的应用很广泛。它可以应用到二元和三元流場，也不受無旋或有旋的限制。它在实际問題中的重要性，是在寻找不到三元的高超声速流場的解的时候，这个定律便能預先告訴我們举力和阻力与机翼的厚度和馬赫数的关系，这对整理实驗的数据是很有用处的 (圖 13)。

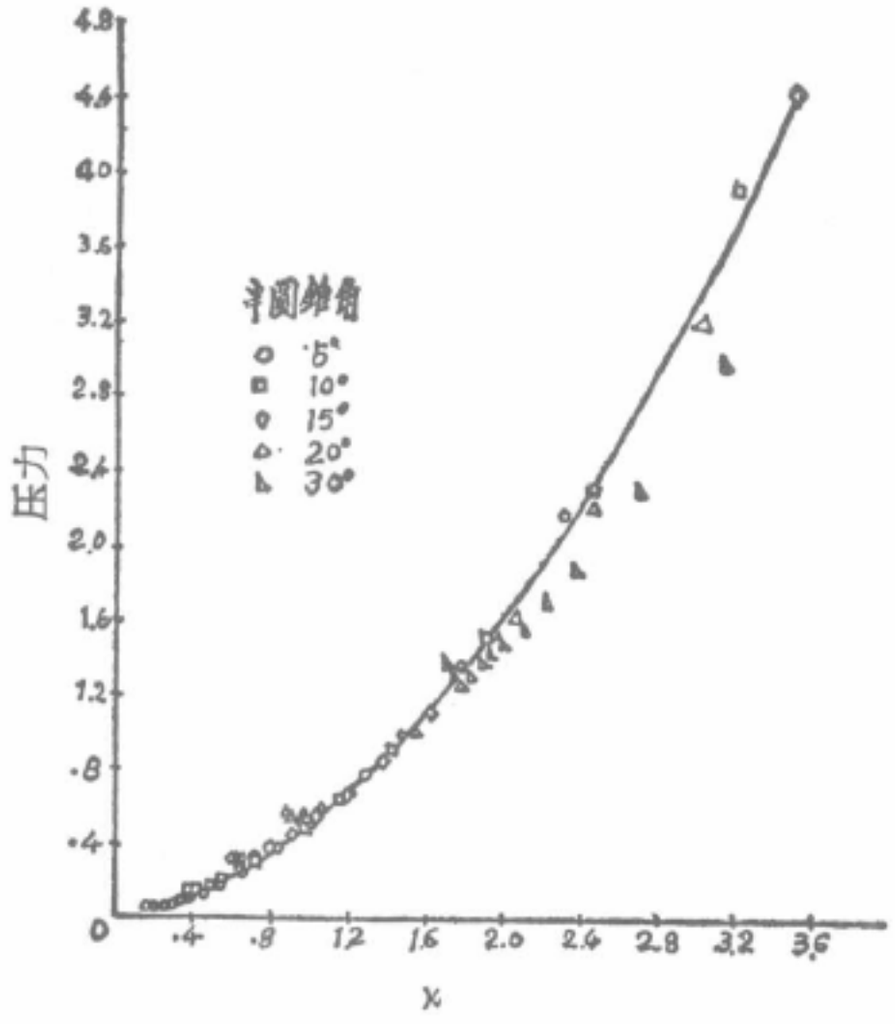

圖 13　表面压力与相似数之关系

高超声度的另一問題，是飞体的頂端不尖，如圓形或方形。这样飞体前面的冲击波，就不能与飞体接触而保持一定距离。因此冲击波后面的流場就不能是純超声速而是跨声速，計算上不論是二元还是三元的流場都是極其困难的。这是于实际有关的一个問題，很有研究的价值(圖 14)。

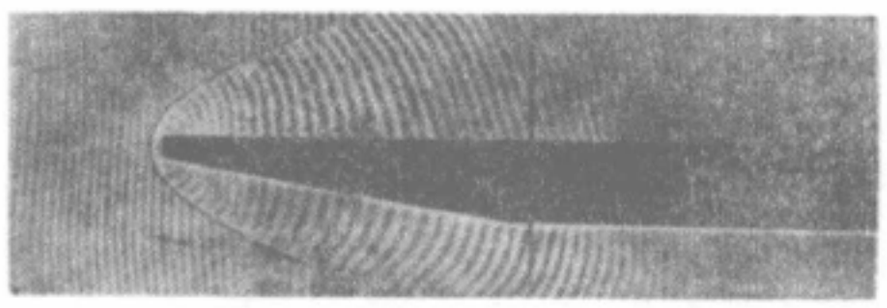

圖 14

高超声速流——粘性的影响

当空气吹过一个平薄板时，因为粘性的关系，板的表面一層气流就被滞緩下来。在風速低的时候，这个粘性層是很小的。可是在風速高的时候，因为动能的消耗大而产生很高的温度，于是附面層里的气体就膨脹，附面層就会很厚。根据附面層的理論，我們知道附面層的厚度是和馬赫数的平方成正比，和雷諾数的平方根成反比。所以在馬赫数大（即速度高）的时候，附面層是可以很厚的。

在高超声速的情况下，因为有这样厚的一層气流被滞慢下来，为了保持物質連續条件，薄板附近的流綫的旁轉角就要增大，如同繞过一个有厚度的固体一样。結果純粹由于粘性，就产生一个强烈的冲击波和高温度。从这个观点出發，这个問題是可以同一个無粘性气流吹过有厚度的固体一样处理的(圖 15)。

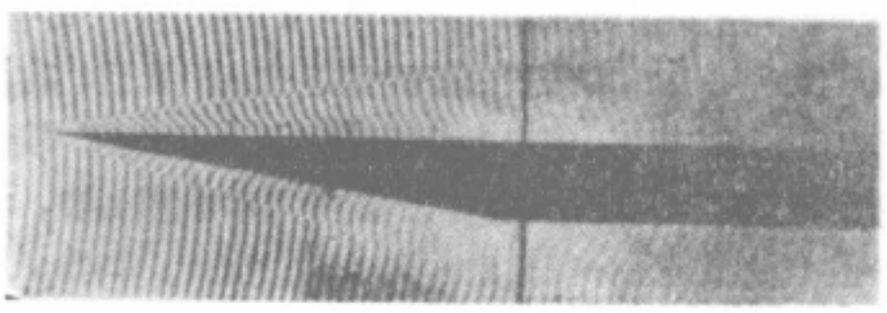

圖 15

这里一个極有趣的問題，就是如何計算薄板極尖端的流場。在那里的流場，很显然的，不会是屬于附面層类型的。要解决这个問題，就牽涉到納費尔-斯篤克斯 (Navier—Stokes) 方程式的解在那点的特性。这是一个基本的問題，它的解决，新的观点是必要的。

高超声速流——分离电离的影响

一个飞彈在空气中飞行，因为頂端与空气挤压，那里就产生最高的温度，(即所謂駐点温度)。如果空气是个理想气体，这点的温度与外界之差，就等于飞行的馬赫数的平方乘外界温度的五分之一。

第二次世界大战，德国 V—2 飞彈的馬赫数大約是 5。根据这个算法，它頂头上的温度，在将近地面时，就在 1500°C 左右，这就很近于鉄的熔点了。在不同的馬赫数和一定的高度，我們可以画一条曲綫。从这曲綫可以看出，当飞行的馬赫数是 10，在四公里上空，飞彈的最高絕对温度就达到五千多度 (圖 16)。換句話說，飞彈速度在十倍于声速的时候，它的頂端

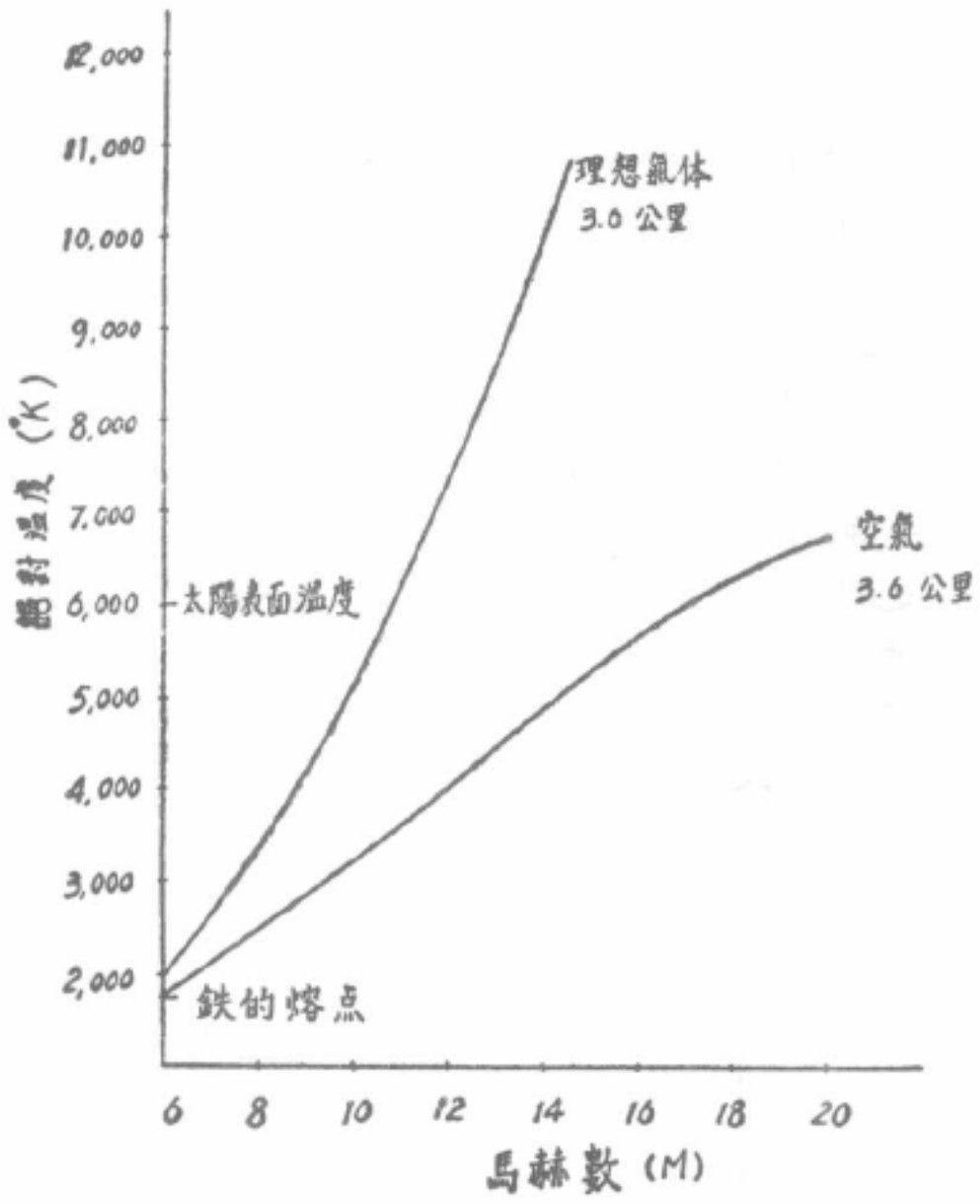

圖 16　駐点温度与馬赫数之关系

上的温度，就几乎同太陽表面的温度一样了。

事实上我們知道，这是不够准确的。因为当馬赫数超过 5 以上，空气的分子的热运动就很强烈，在分子剧烈地碰撞时，便發生分离現象。飞得越快，温度愈高，分离現象就愈强。从击波管实驗我們知道，在 50 公里的高度，分离現象在两千絕对温度、相当于馬赫数 6 左右，就开始發生，到了四千多度，氧的分子

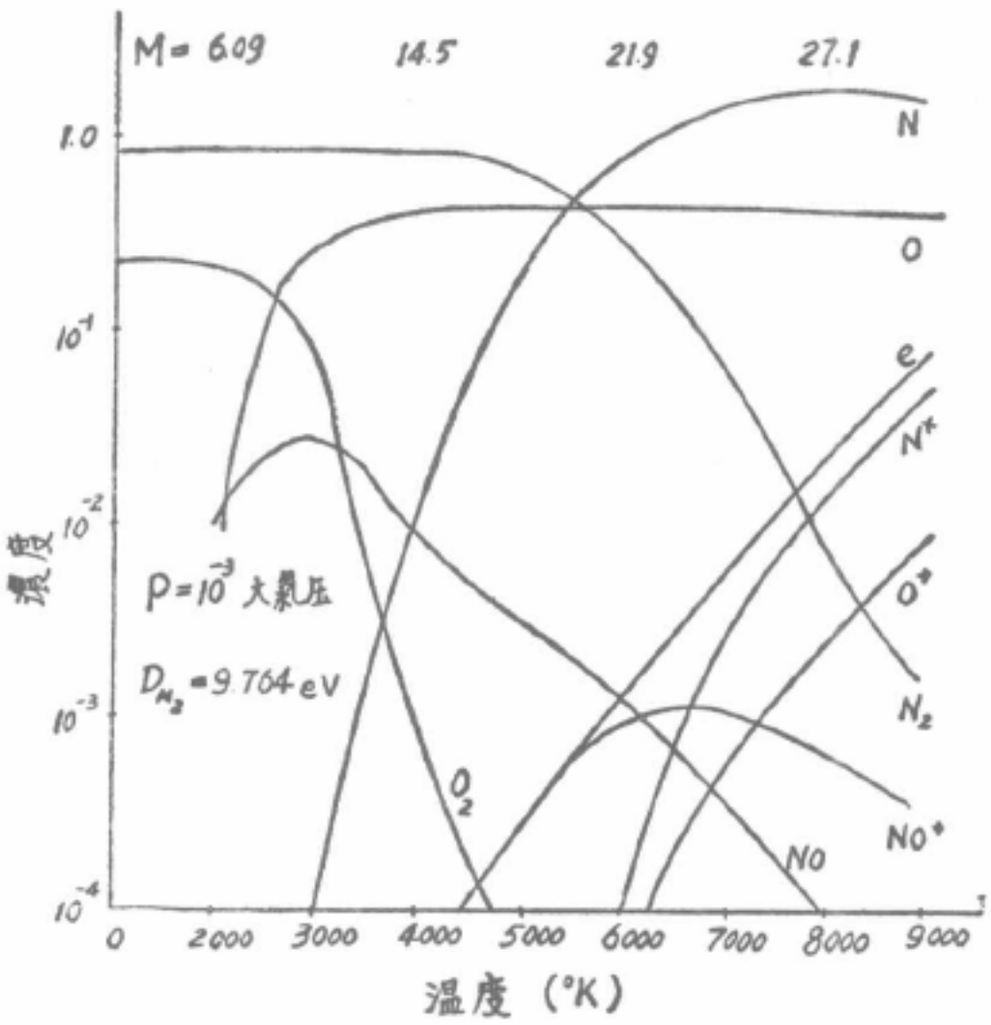

圖 17　空气的分离与电离

就完全分离，电离現象接着就开始了(圖 17)。

在这样情况下，显然我們不能再把空气看作簡单的理想气体，而应当看作相当复杂的混合气体。在討論气体流动所产生的現象时，分离电离以及因分离而引起的化学鏈式反应的影响，就不能不管。例如在估計駐点温度时，要是把这些現象算在里边，但是假設它們都在平衡状态，我們就可以得到一个結果(圖16)，它同原来根据理想气体的假設所算出的結果相差很大。在馬赫数 12，实际上能达到的温度，几乎是理想气体中的温度的一半。对于駐点温度的影响是这样大，对于流場其它的变量也是一样。这类現象对于未来航空工業的重要，是不难想見的。

因为有分离电离的發生，在空气动力学里就产生以下的一些問題：

(1) 空气的組成　在普通温度和高度下，除了微量稀有气体，空气含有 78% 的氮和 21% 的氧。当飞速增加而發生分子分离后，从实驗上知道，不仅有氮和氧的原子出現，还有一氧化氮存在。根据这个事实，在平衡状态下就可以算出不同温度和压力下各种气体的濃度(圖 17)。在考虑空气分离發生后的不平衡現象时，一氧化氮的所以产生就是一个很重要的問題。

(2) 弛豫时間　在分离、电离等現象發生以后，实际問題里所要知道的，便是决定从这个現象的开始到达热力学的平衡状态的过渡时間。知道了这个时間，我們方能决定，在一个問題里，哪里的气体已达到平衡，哪里的气体是在非平衡状态。在各种情形下，决定这个时間，便是一个很基本的研究。

举氮气的分离来說。如果分离的發生是由于两个原子的自由振动被激动过猛而破裂的結果，那么所算出的弛豫时間，在 2000°C左右，大約是千分之一秒。如果温度高，分子相碰的动能强，分离的發生就可以不必等待自由振动的激动。这样的話，在 9000°C 时，弛豫时間便是 10^{-7} 秒。实驗証明这是正确的。

有了这两个不同的結果，我們便可以看出它在实际問題里的影响。假設气流的速度是每秒 6000 米，須要达到平衡的长度，根据头一个弛豫时間，就要 6 米，根据第二个便是 0.06 厘米了。这就是說，弛豫时間如果是千分之一秒，6 米长的机身，在飞速是每秒 6000 米的时候，机身外的气流，便都不在平衡状态，这对于飞机設計上所需要的数据的計算是很困难的。

此外，我們还要知道：(1) 空气的热力学函数，(2)傳送系数(即热傳导，扩散，粘性等系数)，(3)碰击截面，(4)化学反应速率，等等。这一系列問題的研究，是要从理論和实驗双方进行的，它們的解决，对于将来航空工業的新技术的發展，是有莫大的貢献的。

电磁流体力学

根据实驗的結果，在20公里高度，飞速在15倍声速左右，空气便是很好的电导体(圖18)。因此最高速的气流便能用电場和磁場来控制，这个技术的应用产生了一門新科学：电磁流体力学。

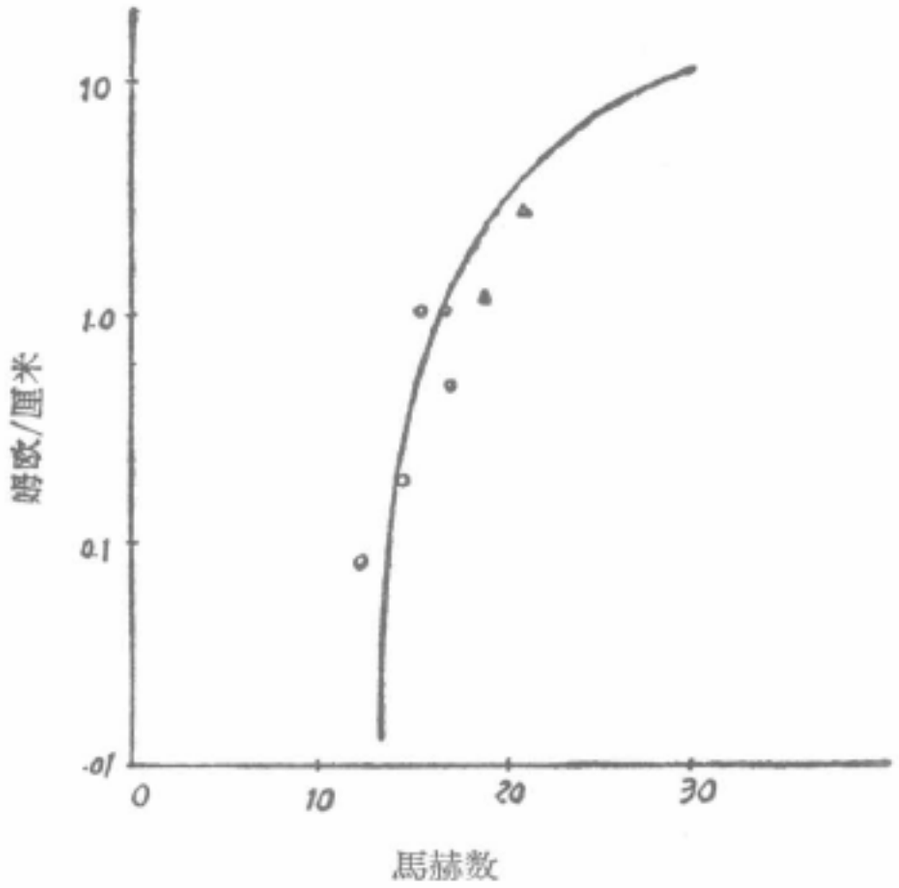

圖18 空气电导与馬赫数之关系

Δ P_1=1毫米水銀柱；○ P_1=1厘米水銀柱

$P_1=\frac{1}{10}$大气压

举个例来說，一个电导流体(如流体金屬)装在直圓管里，在管的垂直方向再加一均匀磁場(圖19)。因为流場和磁場的相互感应，便产生电流場，在管的横

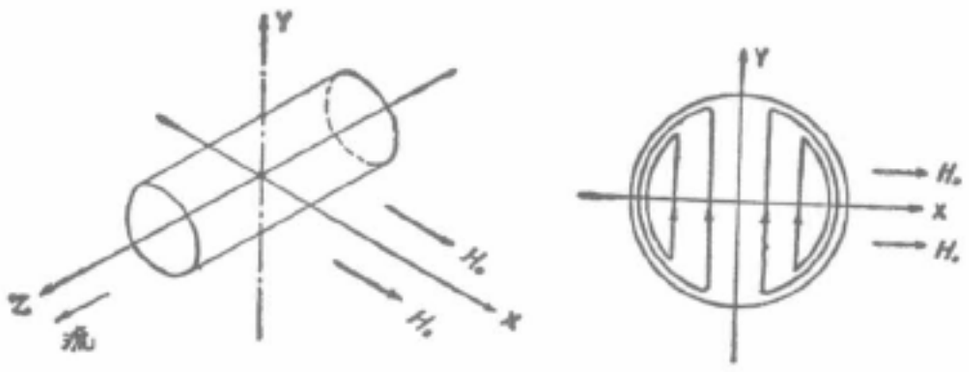

圖19 电磁流量計和感应电流的分布

截面上下就有电位差；在管的两端就建立了压力差，这就保持电导体的流动。这种办法已經用于循环原子反应堆里有放射性的冷却剂。同样的，在气体变成电导体时，气流里的动能和电能的交換，也是可能的。

高溫下的冷却問題

高速飞行的最重要的一个障碍，就是高速度带来的高温度。为了解决高速飞行，如何冷却机身，便是一个最基本的实际問題。我們知道，当飞速逐漸增加，从热附面層傳到机身的热，不論是在層流或湍流的时候，是和馬赫数的平方成正比的。因此在高速飞行时，这个热量是很大的。

如果附面層是層流，这个热量是可以計算的。可是在湍流的时候，这个問題就很困难。速度要是低，这問題的处理，是一面靠实驗，一面用动量与热量交換相似的观念，得到些估計。但这些办法，用到高速的問題上就完全不对。馮卡芒(von Kármán)在1936年曾为阻力作了一个估計。近几年来，有不少人(例如范錐斯特 van Driest) 想改进他的計算，可是結果与实驗比較，一点也不符合(圖20)。阻力(即动量)既無法估計，进一步的热的交換問題就不能討論。

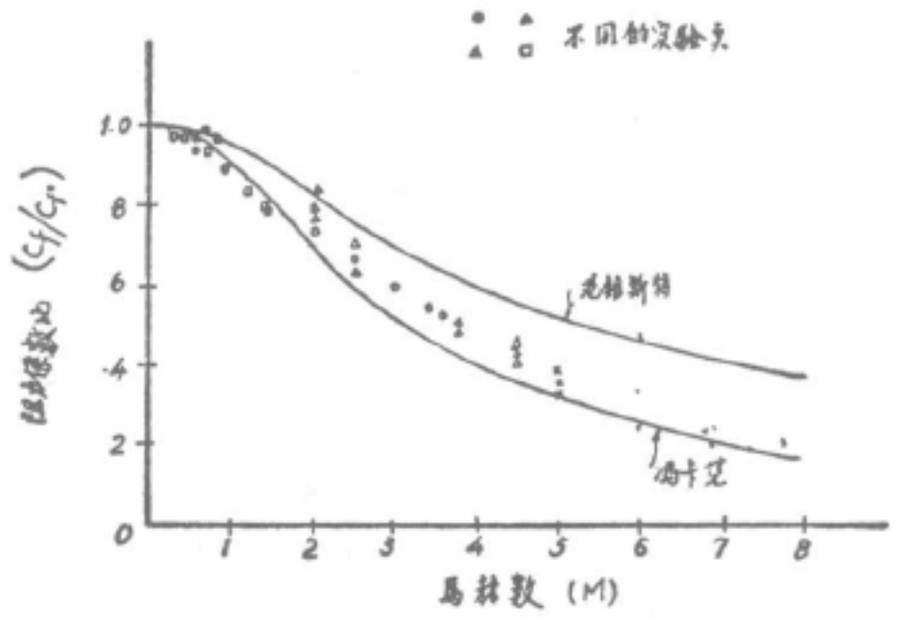

圖 20

温度再行上升，到分离和电离發生以后，在固体表面上就有再結合的現象，放出大量的热，热的傳导問題就更加复杂。这类問題的研究，也是剛剛开始，还沒有具体成就。

从这个簡略的介紹可以看出，空气动力学还是一門比較年輕的科学。它的生活力还很强，将来的發展是無限的。在这个紧要关头，希望我們的空气动力学工作者，能够抓着时机，尽量地充实自己，好在空气动力学發展史上的第三个年代里，作些貢献。本文承錢学森先生讀过，提出不少宝貴意見，特此志謝。

在关于苏联发射成功第一颗人造卫星座谈会上的发言记录

（中国科学院、中华全国自然科学专门学会联合会、中华全国科学技术普及协会在1957年10月13日召开了一次关于苏联发射成功世界上第一个人造卫星的座谈会。到会的有天文学、物理学、力学、空气动力学、化学、无线电学、电子学、地球物理学、通讯学等方面的科学家38人。会议由竺可祯副院长主持。）

郭永怀的发言：

10月4日苏联发射人造卫星的意义，各位都已讲了，我现在想补充两点。我觉得这件事是在进入原子能时代以后的第二件大事，对整个人类都有影响。人类一向是在二度空间活动的动物，现在有了人造卫星的成就，就如爬高有了梯子一样，以后去宇宙活动，已经不是梦想，可以实现了。另外一点，就是这件事发生在我们社会主义国家里，这样对和平事业的影响一定很大。我认为人造卫星对和平事业起的作用是正的，不是负的。

人造卫星关系到许多技术部门，我愿意在许多技术中提两点来谈一谈。第一点是发射人造卫星的工具，也就是火箭问题。火箭的发明是很早的了，中国早已制造过火箭。在近代推进器中，火箭有两个特点：一个特点是在很短时间放出很大的能量，另一个特点是他用自己的力量推进，因此火箭的活动不受外界影响，不用外界空气作推动力，所以离开空气层在真空中也能前进。那末过去为什么对星际旅行的意见会有不一致呢？这并不是因为对火箭作推进器有疑问，而是由于燃料的问题。用普通的化学品燃料，可以简单地算出，推出地球几乎是不可能的。由于这样，因此用了多节火箭，苏联这次用的就是三节火箭。

现在说说苏联的成就。苏联卫星是83公斤，高程900公里，要把这样的卫星发射出去，可用已经算好的资料为例：如100公斤三级火箭，用的燃料是化学燃料，这当然与苏联现用的燃料不同，化学燃料是用液体氧与肼（肼有自燃的特性）。火箭可以有各种设计，一种设计大约是这样的数据：第一节总重量（火箭与载重、燃料）是91吨；第二节的总重量是15吨；第三节总重量是1.7吨，其中有100公斤是载重。三节的总重量是109吨。这么大的重量是很难想像的。

现在看一看输送力，因为最后一节也达到高空，苏联现在的最后一节也是在高空上，因此把最后一节也算作被输送的，那末总的输送能力，是总重量的1/64。输送能力大约是总重量的1/64，现在英美设计的火箭也是这样的数目字。把火箭送上去所用总的推力，第一节是181吨，第二节的推力是31吨的样子。假使我们要用的火箭发动机是5个，这个推力是太大了，每个发动机的推力是36吨，普通的发动机远远在这数字的下面。美国准备发射的卫星的重量比苏联的差八倍，每个推进器的推力只不过3—4吨。

另外，从人造卫星的发射到进入轨道，需要很精确的分析。第一节达到的高度与最后的速度问题，以及第二节开始的速度，到什么时候停火，第三节怎样达到轨道，这要很精确的计算。在轨道确定以后，要作各种规划，这完全是自动控制的问题。由此也可见到苏联

在自动控制、电子学等各方面，都有很高水平。

最后要强调一下，赵先生已经说过，苏联从十月革命到现在不过四十年，苏联在这四十年中除了文化和经济建设的发展以外，科学方面的进展，尤其是最近二十年来在航空、原子能、高温物理等方面的进展，简直不可想像。苏联的科学为什么会发展得这样快，我想在座诸位也都知道，要发展科学，只有在社会主义国家，有共产党领导才能够。

超高速鈍体湍流

傳热問題

指　　导：郭永怀

参加工作者：呼和敖德

牛家玉

中国科学院力学研究所

1963年10月

目　　录

一、引　　言

二、处理問題方法

基本方程式的轉換

表面摩擦阻力

动量积分方程积分

三、摩擦阻力係数

四、热交換率

五、計算結果

六、結　　論

七、附录：可压縮湍流边界层轉換

八、主要参考文献

九、附　　图：

图1：高冷却湍流边界层内流体性質的分布

图2：半球錐体压力分布（实驗值）

图3：热交換率計算值与 C_{RESCi} 实驗比較

图4：热交換率計算值与 NACATN4125 实驗点比較

$M=2.0$, $Re=3.43\times10^6$

图5：根据 C_{RESCi} 模型計算的 $g^{1/3}(\tilde{s})$ 因子随 $\tilde{s}$ 分布曲綫

一、引　　言

在超高速飞行的条件下，沿飞行器表面絶大部分的边界层是处於湍流状态，这就将使飞行器表面上的傳热率比在层流时增加数倍。因此，在設計工作中，准确的估計在順压梯度的情况下，湍流的热交換率是很重要的。

当前发表的文献中，已有許多人对此类問題进行了研究，例如，在超声速领域里就有 Spence[1]，Rashotko 和 Tucker[2]等。Rashotko 和 Tucker 通过解联立动量和动量矩积分方程，对型参数的变化对結果的影响进行了比較細緻的研究；并引入 Eckert[3]参考焓对气体的性质作了修正。这一方法虽然比較合理，但計算量太大。在超高速领域里，Vaglio-Laurin[4]，Libby和 Cresci[5][15]，Rose，probstein 和 adams[6]等，对沿鈍体的边界层作了研究。在这些理論中，中心問題是选取一組合理的假設，例如摩擦阻力与局部动量边界层厚度雷諾数的关係，並选取駐点或边界层外緣的条件作为气体性质的修正，型参数取为常数等。此外，另有一种局部平板参考焓的近似方法[5]，它的理論基础是在高冷却的条件下，压力梯度对湍流边界层的影响是可以忽略的。

对文献〔4〕—〔6〕和〔15〕各种方法进行分析的結果，发現这些方法所得結果反不如簡单的局部平板参考焓方法。这个現象的出現是由於某些因素处理得不十分合理，第一：动量积分方程中可压縮边界层型参数取为常数。如果是不可压縮順压力梯度的问題，我們把型参数看作某一

个适当的常数是一个比較好的近似，但对可压縮的問題却不然了。例如，平板可压縮边界层的可压縮型参数与不可压縮型参数 J_i 之間可近似表示为 $\delta^*/\theta = \frac{T_w}{T_e} J_i + \frac{T_r}{T_e} - 1$ （ T_w 、 T_e 、 T_r 分别为表面溫度、边界层外緣温度和恢复温度）。由此可见，即使不可压縮順压梯度的型参数 J_i 近似等於常数，但是由於壁溫比和局部 M 数的变化将使型参数不能保持常数。因此我們认为为了使計算准确应該考虑型参数的变化。第二：选用駐点或边界层外緣作为修正气体性质的参考条件。可以指出，駐点的条件只适用於鈍头体头部 $M<1$ 的区域，但在大部湍流区域中 M 数已可以从0・3 到3 了，因此边界层内温度的变化是很大的。在这情况下选駐点的条件就不再适用了。同样选边界层外緣作为参考条件也不十分适合，因为在高速的条件下，边界层边緣和表面温度差往往悬殊很大，外緣上的温度自然不能作为边界层温度的代表。

在超高速飞行时，由於强冲激波的出现，飞行器头部边界层处緣 M 数比較小，經过强膨胀后，在下游的 M 数也不过 3 、 4 。这种边界层的特点是被順压梯度所控制，而且表面与边界层外緣的温差較大。根据实驗結果〔13〕和〔14〕，在超高速高冷却条件下，边界层的平均速度分布和低速边界层的一样（ 見图1 ），也可用冪次形式表示。这説明了在高冷却、高速湍流中的脈动混合机理是不改变的。根据低速的情况，順压梯度对边界层的　度分布的作用是不大的。在高速的情况下，通过 Howarth — Бородинцын 的轉換，从运动方程我們可以清楚看到压力梯度的确是可以忽略的。这是由於压力梯度一項的因子〔$\rho_e/\rho - (u/u_e)^2$〕，

在高冷却条件下，确实是很小的（图一）。

从这一观点出发，我们採用了 Mager-Смелянов-Mangler 联合轉換式，把边界层方程轉換为二維不可压縮边界层問題，然后再按建立在大量实驗基础上的經典方法求解，从而避开了象上述文献中的一些不合理的假設。为了提高精确度，我们採用了 Eckert 凭經驗提出的，后来由 Burggraf [7] 等从理論上給予驗証的局部参考焓，修正在轉換中引进的近似。Burggraf 等指出，Eckert 的参考焓是相应於湍流边界层的层流次层和湍流层交界面上的焓值。根据交界面特性，选此处温度作为边界层温度代表是能較好的反映实际情况。

为了簡化計算，在求得阻力后，对傳热問題我們採用了修正雷諾比拟式。当然，我們也可以直接对能量方程求解，但是，根据 Rubesin [12] 和 Sibulkin [13] 一些人的工作，这种做法並不提高精度，反而增加了計算的复杂性。最后，所得結果和发表的一些实驗数据 [15], [16] 比較是很一致的，和其他方法比我们的结果也更接近於实驗，而且計算量也並不太大。这証明了，在可压縮湍流边界层中採用单参数方法並用 Eckert 参考焓作为气体性质的修正是很合适的，同时也証明了人們认为没有理論根据的局部平板参考法是一个比較好的近似方法。

二、处理問題的方法

下面採用三步来求解动量积分方程。首先把边界层轉化为不可压縮問題，然后引入单参数表示的摩擦阻力係数和型参数，最后借助於綫性化的近似关係对动量积分方程进行积分。

基本方程式的轉換：轴对称可压縮湍流边界层方程：

$$\left.\begin{aligned}&\frac{\partial \rho u r}{\partial x}+\frac{\partial \rho v r}{\partial y}=0\\&\rho u\frac{\partial u}{\partial x}+(\rho v+\overline{\rho' v'})\frac{\partial u}{\partial y}=-\frac{\partial p}{\partial x}+\frac{\partial}{\partial y}\left(\mu\frac{\partial u}{\partial y}-\overline{\rho v'u'}\right)\end{aligned}\right\}\quad -(1)$$

根据 Mager[8]—Cменанов-Hangler 联合转换式

$$\left.\begin{aligned}&X=\int_0^x (r/R_0)^2 F G\,dx\\&Y=(r/R_0)F\int_0^y (\rho/\rho_0)\,dy\end{aligned}\right\}\quad -(2)$$

其中 $F=\rho_e/\rho_0$ ， $G=(\rho\mu)^*/(\rho\mu)_0$ ， R_0 是头部半徑，是从对称軸到外表面的徑向距离，脚註“ 0 ”、“ e ”和“ * ”分别代表駐点、边界层外緣和参考条件。为了得到簡单的动量积分文程，我們引进以下近似假設第一：首先採用 $(-\overline{\rho v'u'})=\varepsilon\frac{\partial u}{\partial y}$ ， ε 是湍流交換係数，并假設交換係数在轉換过程中保持不变，这是和 Mager 的假設一致的。第二：假設 $\rho\mu=(\rho\mu)_*$ ，而 $(\rho\mu)_*$ 仅仅是座 X 的函数。这一假設是有一定近似性，对於超高速边界层 $(\rho\mu)$ 变化是比較大的，因此，参考量 $(\rho\mu)_*$ 必須是随 X 而变化的。由此轉換的結果（詳見附录）

$$\left.\begin{aligned}&\frac{\partial u^*}{\partial X}+\frac{\partial v^*}{\partial Y}=0\\&u^*\frac{\partial u^*}{\partial X}+v^*\frac{\partial u^*}{\partial Y}=u_e^*\frac{\partial u_e^*}{\partial X}\frac{H}{H_e}+\frac{\partial}{\partial Y}\left[(\mu+\varepsilon)/\mu\cdot\nu_0\frac{\partial u^*}{\partial Y}\right]\end{aligned}\right\}\quad -(3)$$

上标“ * ”表示轉換后的量，H 为总焓。

我們注意到轉換后的动量方程的压力梯度增加了一个焓比的因子：H/H_e 。根据定义，焓比在边界层内从表面上的 h_w/H_e 增长到边界

层外缘的1，如果 $R_{w/He}<1$，那么在边界层内焓比 H/He 是小於1的。从实驗的結果看，温度和速度一般在很小的范圍内就从表面上的数值上升到最大值，而且越是表面温度低这种上升的速度就越高。所以定性地我們可以説，焓比对速度分布的影响是不大的。在平板的情况下当 $P_r=1$，焓 h 和速度 u 的关係是已知的；根据 Spence[9]

$$h=h_w+(h_r-h_w)\frac{u}{u_e}-(h_r-h_e)\left(\frac{u}{u_e}\right)^2$$

通过上述近似，动量积分方程具有以下形式：

$$\frac{d\theta^*}{dx}+\frac{\theta^*}{u_e^*}\frac{du_e^*}{dx}\left[2+\left(\frac{h_w}{H_e}-1\right)J_{isp}+J_i\right]=\frac{\tau_w^*}{\rho_0 u_e^{*2}} \qquad (4)$$

其中 $\vartheta^*=\int_0^\delta \frac{u}{u_e}\left(1-\frac{u}{u_e}\right)dy$ 轉換后的动量厚度。

$J_i=\int_0^\delta\left(1-\frac{u}{u_e}\right)dy\Big/\int_0^\delta\frac{u}{u_e}\left(1-\frac{u}{u_e}\right)dy$，轉換后型参数。脚註“ W ”和“ r ”分别代表壁面和恢复条件。$J_{isp}=1+2n$，是平板型参数，n 为幂次速度律的指数。一般取为1／7。

表面摩擦阻力：方程(4)已成为二維不可压縮的形式，因此，对方程中的阻力可以採用經典的阻力律。在很早由 Buri[10]，后来又由 Лойцянский[11]等，引入单参数

$$\Gamma=\frac{\theta^*}{u_e^*}\frac{du_e^*}{dx}\left(\frac{\theta^* u_e^*}{\nu_0}\right)^{\frac{1}{N}} \qquad (5)$$

給出了以单参数表示的阻力

$$\frac{\tau_w^*}{\rho_0 u_e^{*2}}=f_1(\Gamma)\left(\theta^* u_e^*/\nu_0\right)^{-\frac{1}{N}} \qquad (6)$$

其中 N 是指数阻力律的指数，$f_1(\Gamma)$ 是单参数函数，对平板边界层 $f_1(\Gamma)$是常数，对順压力梯度边界层 $f_1(\Gamma)$的变化也比較小；而对逆压梯度具有很大的变化。这些結果在低速实驗中已被証实，因此在我們分析

中也採用上述阻力公式。

动量积分方程积分：在积分方程(4)的时候需要借助經典理論同处理阻力一样，把型参数 J_c 做为单参数，表示为

$$J_c = f_2(\Gamma) \qquad (7)$$

对逆压梯度 $f_2(\Gamma)$ 随压力梯度增加而增加。对順压力梯度则相反，並且变化也比較小。对平板可取为常数1·3。

把(6)和(7)式代入方程(4)，並在两边乘上因子($\theta^* u_e^*/\nu_0$)，並加以整理得到

$$\frac{d}{d\bar{x}}\left[\theta^*(\theta^* u_e^*/\nu_0)^{\frac{1}{N}}\right] = \frac{N+1}{N} f_1(\Gamma) - \left(2+\frac{1}{N}+\frac{1+N}{N} f_2(\Gamma)+D\right)\Gamma \qquad (8)$$

其中 $D=\left(\frac{N+1}{N}\right)\left(\frac{h_w}{H_e}-1\right)J_{1/2}$，为了使方程可积，假設方程右边仅仅是单参数$\Gamma$ 的綫性函数。

$$\frac{1+N}{N} f_1(\Gamma) - \left[2+\frac{1}{N}+\frac{N+1}{N} f_2(\Gamma)+D\right]\Gamma = a - d\Gamma \qquad (9)$$

把(9)式代入(8)式，根据 $\tilde{S}=0$ 时 $Re\theta^*=0$ 条件，积分得到轉換后动量厚度：

$$\theta^{*\,-\frac{1}{N}} = (u_e^*/\nu_0)^{\frac{1}{N(N+1)}} u_e^{*\frac{d}{N+1}} \left[a\int_0^{\bar{x}} u_e^{*d}\, d\bar{x}\right]^{-\frac{1}{N+1}}$$

或

$$\theta^{*\,-\frac{1}{N}} = F^{\frac{1}{N}}(x,G)^{-\frac{1}{N+1}}(r/R_0)^{-\frac{2}{N+1}}(u_e/\nu_0)^{\frac{1}{N(N+1)}}\left[\frac{F^{1-d}G(r/R_0)u_e^d x}{a\int_0^x F^{1-d}G(r/R_0)^2 u_e^d\, dx}\right]^{\frac{1}{N+1}} \qquad (10)$$

根据轉換前后动量厚度关係

$$\theta^* = F(\rho/\rho_0)(r/R_0)\theta$$

得到动量厚度

$$\theta^{-\frac{1}{N}}=(\nu/R_0)^{\frac{N-1}{N(N+1)}}(u_e/\nu_0)^{\frac{1}{N(N+1)}}(x\cdot G)^{-\frac{1}{N+1}}\left[\frac{F^{1-d}G(r/R_0)^2u_e^d x}{a\int_0^x F^{1-d}G(r/R_0)^2u_e^d dx}\right]^{\frac{1}{N+1}} \quad (11)$$

其中 $\tilde{S}=x/R_0$，$Re\theta^*=\theta^*u_e^*/\nu_0$ 。下面对公式(9)綫性假設作一説明。Burri[10]和 Лойцянский[17] 等对不可压縮問題研究結果證明存在一个近似的綫性关係。这綫性函数的係数是两个固定常数。现在对轉換成不可压縮形式的方程也假設存在这样一个綫性关係，不同的是多了一个焓比因子。我们通过为数不多的实驗确定了綫性函数的两个係数，其中 a = 0 • 0 1 6 ，这和不可压縮情况下的选擇一样，$d=3.5+2.5(\frac{h_w}{H_e}-1)$ 当 $h_w/H_e=1$ 时 d 的值也和不可压相近。但当焓比有变化时，係数 d 是焓比的函数。

三、摩擦阻力係数

根据前述，顺压力梯度对磨擦阻力係数的影响是很小的，因此下面求阻力的时候我們採用以动量厚度雷諾数指数形式表示的，阻力律：

$$C_f^*/2=B(Re_G^*)^{-\frac{1}{N}} \quad (12)$$

其中 B = 0 • 0 1 3 ，N = 4 。把公式(10)代入(12)得到

$$C_f^*/2=A\,Re_x^{-\frac{1}{N+1}}(\nu_e/\nu_0)^{\frac{1}{N+1}}G^{-\frac{1}{N+1}}(r/R_0)^{-\frac{2}{N+1}}(g(\tilde{S}))^{\frac{1}{N+1}} \quad (13)$$

其中

$$g(\tilde{S})=(F^{1-d}G(\tfrac{r}{R_0})^2\tilde{u}_e^d\tilde{S})\Big/\int_0^{\tilde{S}}F^{1-d}G(\tfrac{r}{R_0})^2\tilde{u}_e^d d\tilde{S} \quad (14)$$

$\tilde{u}_e=u_e/\sqrt{H_e}$ ，根据轉換关係(2)和前述假設 $\rho\mu=(\rho\mu)_*$ ，得到轉換前后摩擦阻力关係

$$\tau_w=(\mu\frac{\partial u}{\partial y})_w=(F^2Gr/R_0)\tau_w^*$$

所以

$$C_f = (\rho_x/\rho_e)(\mu_x/\mu_0)(r/R_0)C_f^* \qquad \text{—— (15)}$$

把(13)代入(15)，局部摩擦阻力係数具有如下形式

$$C_f = (\rho_*/\rho_e)^{\frac{N}{N+1}}(\mu_*/\mu_e)^{\frac{1}{N+1}}(\mu_*/\mu_0)^{\frac{N-1}{N+1}}(r/R_0)^{\frac{N-1}{N+1}}(g(\tilde{s}))^{\frac{1}{N+1}}C_{f0}$$

其中 $C_{f0} = A\,Rex^{-\frac{1}{N+1}}$，$Rex = u_{ex}/\nu_e$，$A = 0.0296$. —— (16)

公式(16)中，$(\rho_x/\rho_e)^{\frac{N}{N+1}}(\mu_*/\mu_e)^{\frac{1}{N+1}}(\mu_x/\mu_0)^{\frac{N-1}{N+1}}$因子是对气体性质所作的修正。至於压力梯度影响主要包括在 $g(\tilde{s})$ 因子当中，对平板問題 $g(\tilde{s})=1$ 阻力公式中参考量的选擇，不論从邏輯推理或从实驗考驗，Eckert 参考焓作参考量是比較适合的。

公式(16)中粘性係数根据 Sutherlant 粘性温度关係确定

$$\mu/\mu_* = (T/T_*)^{3/2}\frac{T_* + 122}{T + 122} \qquad \text{—— (17)}$$

对参考温度选 Eckert

$$h_* = 0.5(h_w + h_e) + 0.22(h_r - h_e) \qquad \text{—— (18)}$$

四、热交換率

最后为了求出热交換率，用雷諾比拟关係代替能量方程。这种代替是一个很好的近似。目前对此問題已有許多人作过研究。在平板的情况下，当 $P_r=1$ 时，动量和热交換之間存在一个严格的比拟关係 $S_t = C_f/2$

S_t 数是热交換率係数。当 $P_r \neq 1$，而且 $dP/dx \neq 0$ 的情况下，这种比拟关係是不严格的。Rubesin[12] 指出，P_r 数的影响是比較大的，因此他提出一个修正雷諾比拟式 $S_t = C_f/2S$，其中修正因子 $S = P_r^{2/3}$。至於压力梯度的影响至今不十分清楚，但在順压梯度情况下 Sibulkin[13]

研究的結果表明这种影响只有百分之几。此外，可压縮性和壁焓比对雷諾比拟关係的影响也有人已研究过，如Rubesin[12]和Lobb[14]根据实驗結果証实了这两种影响也是很小的。因此我们採用修正雷諾比拟式

$$St = \frac{1}{2}\frac{C_f}{2} \qquad \text{——(19)}$$

根据 St 数定义

$$St = -q_w / \rho_e u_e (h_r - h_w)$$

利用(19)式热流表示为

$$q_w = Pr^{-2/3}(h_r - h_w)\rho_e u_e C_f/2 \qquad \text{——(20)}$$

热交換率係数Nu 数的定义

$$Nu = q_w (C_p)_0 R_0 / k_0 (H_e - h_w) \qquad \text{——(21)}$$

其中 C_p 为定压比热，k 为热傳导係数。把(20)代入(21)式得到用Nu 数表示的热交換率公式

$$\frac{Nu}{\widetilde{Re}_0^{4/5}} = Pr^{1/3} K \widetilde{\rho}_e \widetilde{u}_e Re_0^{1/5} \varphi_0^{-3/5} C_f/2 \qquad \text{——(22)}$$

其中 $Pr = 0.71$，$\widetilde{\rho}_e = \rho_e/\rho_0$，$Re_0 = R_0\sqrt{H_e}/\nu_0$，$\varphi_0 = P_0/P_{0He} = \frac{\gamma-1}{\gamma}$，$\gamma$ 为比热比，$\widetilde{Re}_0 = Re_0 \varphi_0^{1/2}$，$K = (h_r - h_w)/(H_e - h_w)$ 把(17)代入(22)式得到热交換率最后表达式

$$\frac{Nu}{\widetilde{Re}_0^{4/5}} = \frac{0.0296 Pr^{2/3} K}{\varphi_0^{2/5}} \left(\frac{\widetilde{u}_e \widetilde{S}}{\widetilde{\nu}_e}\right)^{4/5} \frac{(r/R_0)^{3/5}}{\widetilde{S}} \left(\frac{\rho_*}{\rho_e}\right)^{4/5} \left(\frac{\mu_e}{\rho\mu_*}\right)^{4/5} \left(\frac{\mu_*}{\mu_0}\right)^{8/5} g^{(S)} \qquad \text{——(23)}$$

其中 $\widetilde{\nu}_e = \nu_e/\nu_0$ 是动粘性係数之比。公式(23)是利用指数阻力律得到的，因此它适用於較大 Re数情况。

五、計算結果：

为了驗証公式(23)，利用两組实驗作了比較，一组實驗是利用复盖技术在风洞中进行的[15]，模型駐点最大温度和压力分别是900°K和12·2大气压，而焓比約为2。模型是由半球錐体构成，半錐角 $\alpha=30^\circ$（見右图）；模型从对称軸到表面的距离表示为

$$r(\bar{s})=\begin{cases} R_0\sin\beta, & \beta\le\alpha \\ R_0\left[(\bar{s}-\pi\alpha/180)\cos\alpha+\sin\alpha\right], & \beta\ge\alpha \end{cases}$$

β 是对称軸与徑綫之間夹角。

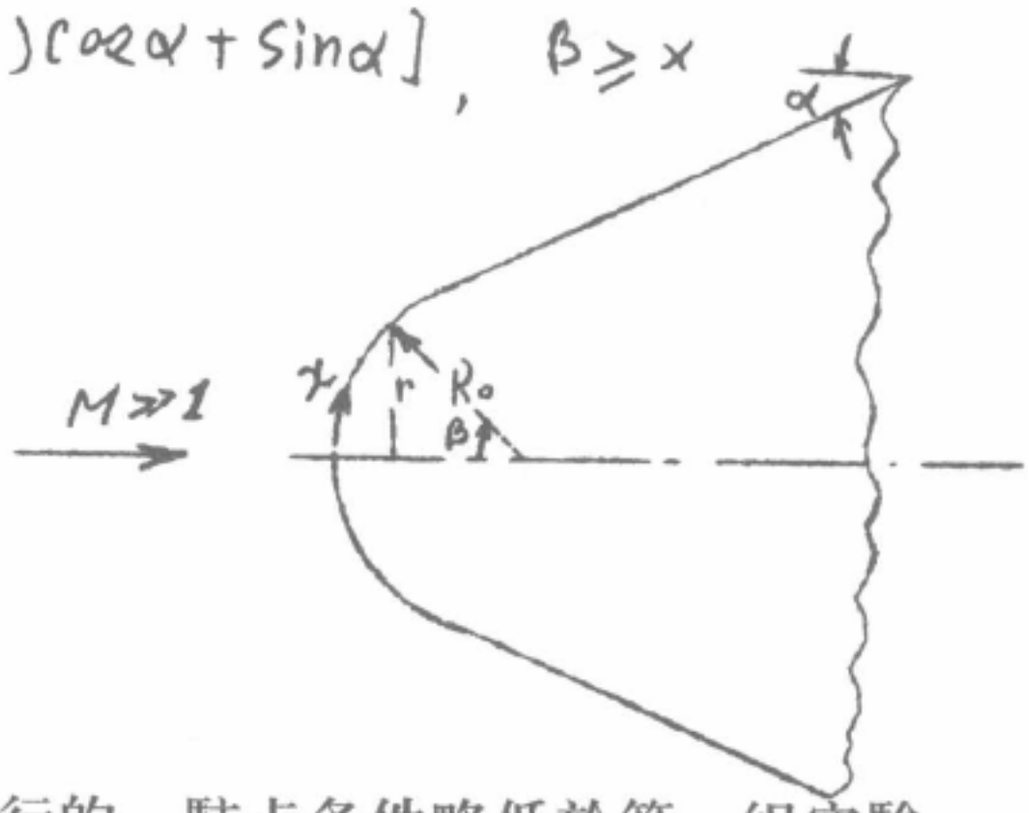

在图2上給出了模型上測量的压力分布。根据上述条件用公式(23)計算結果表示在图3上。

第二組实驗是在球型模型上进行的，駐点条件略低於第一组实驗，以来流参数和直徑定义的 Re 数約为 $3\cdot4\times10^6$，用公式(23)計算結果表示在图4上。为了便於和局部平板参数焓方法比較，公式(23)中包括压力梯度和空間效应的因子 $g(\bar{s})^{1/5}$ 表示在图5上。

上述計算和实驗比較的結果表明，在完全被湍流所控制的錐部上，理論計算和实驗很符合。在过渡区域，用湍流公式計算的結果必然偏高於实驗数据。同时，在图3和4上给出了其他理論計算曲綫。取可压缩边界层型参数为負1，並用边界层外緣条件作参考的 $Cresci'$ 方法所得結果在錐部低於实驗約20%，但是局部平板参考焓法却很符合实驗。

六、結　　論

上述分析説明了以下几点事实：

(1)本文的方法适合於計算中等M数，較大Re数的超高速鈍体湍流热交換率。

(2)当用动量积分方法求解超高速鈍体湍流傳热率时，应該考虑由於M数，焓比和压力梯度对型参数的影响。取型参数为常数一般是不合理的。

(3)上面事实证明，用 Eckert 参考 修正在轉換中所引入的近似比其他参考条件要合理，而且也符合实驗。

(4)根据图5，計算结果表明，反映压力梯度和空間效应的$g(\tilde{s})^{1/5}$因子在半球錐体的錐部上趋於1。这説明在錐部上压力梯度和空間效应都变得很小，因此，証明了局部平板参考焓法的确可以用来計算鈍体后部的湍流傳热問题。图3和4上計算結果已經说明了这点。

七、附录：可压縮湍流边界层轉換

Mager－Смещанов－Mangler 联合轉換式：为了使可压縮軸对称边界层方程轉为不可压縮平面問題，所以採用了Mager[8] 的由可压縮边界层轉化为不可压縮边界层的轉換式和 Смещанов－Mangler 的由軸对称边界层轉为平面問題的轉換式的联合形式

$$\left.\begin{aligned} X &= \int_0^x FG(r/R_0)^2\,dx \\ Y &= F(r/R_0)\int_0^y \rho/\rho_0\,dy \end{aligned}\right\} \qquad \text{——(A-1)}$$

其中 $F=a_e/a_0$，$G=(\rho\mu)_x/(\rho\mu)_0$，$F$，$G$ 仅仅为X函数。 a是声速、

ρ为密度，μ为粘性系数。引入流函数ψ，则

$$\left.\begin{aligned} \rho u r &= \rho_0 R_0 \frac{\partial \psi}{\partial y} \\ (\rho_0 + \overline{\rho' v'})\, r &= -\rho_0 R_0 \frac{\partial \psi}{\partial x} \end{aligned}\right\} \qquad \text{—— (A-2)}$$

为了保証轉換前后两个边界层真正一致相应，量度在边界层内包含的质量流的函数应该在轉換过程中保持不变，$\psi = \psi^*$，由此得到

$$u^* = \partial \psi^* / \partial y \quad , \quad v^* = -\partial \psi^* / \partial x \qquad \text{—— (A-3)}$$

利用（A—2）和（A—3）得到轉換前后边界层速度关係

$$\left.\begin{aligned} u &= F u^* \\ (\rho v + \overline{\rho' v'})\, r &= \rho_0 R_0 \left[(r/R_0)^2 F G v^* - \gamma_x u^* \right] \end{aligned}\right\} \qquad \text{—— (A-4)}$$

基本方程的轉換：軸对称可压縮湍流边界层方程：

$$\left.\begin{aligned} &\frac{\partial \rho u r}{\partial x} + \frac{\partial (\rho v + \overline{\rho v'})}{\partial y} = 0 \\ &\rho u \frac{\partial u}{\partial x} + (\rho v + \overline{\rho' v'}) \frac{\partial u}{\partial y} = -\frac{\partial p}{\partial x} + \frac{\partial}{\partial y}\left[\left(\mu \frac{\partial u}{\partial y} \right) - \rho \overline{v' u'} \right] \end{aligned}\right\} \qquad \text{—— (A-5)}$$

轉換前引入两个近似假設(1)湍流应力表示为 $(-\rho \overline{v'u'}) = \varepsilon \partial u / \partial y$，其中假設湍流粘性係数$\varepsilon$在轉換过程中保持不变。(2)假設 $\rho\mu = (\rho\mu)_*$，利用上述近似关係轉換运动方程为如下形式

$$\frac{\partial u^*}{\partial x} + \frac{\partial v^*}{\partial y} = 0$$

$$u^* \frac{\partial u^*}{\partial x} + v^* \frac{\partial u^*}{\partial y} = u_e^* \frac{\partial u_e^*}{\partial x} \left[\frac{\frac{1}{\rho} + \frac{1}{F}\frac{dF}{d\rho} u^2}{\frac{1}{\rho_e} + \frac{1}{F}\frac{dF}{d\rho} u_e^2} \right] + \frac{\partial}{\partial y} \left[\frac{(\mu + \varepsilon)}{\mu} \nu_0 \frac{\partial u^*}{\partial y} \right] \qquad \text{—— (A-6)}$$

取 $dF/F = \frac{\gamma - 1}{2\gamma} d\rho/\rho$，上式变为

$$\left.\begin{aligned} &\frac{\partial u^*}{\partial x} + \frac{\partial v^*}{\partial y} = 0 \\ &u^* \frac{\partial u^*}{\partial x} + v^* \frac{\partial u^*}{\partial y} = u_e^* \frac{\partial u_e^*}{\partial x} \frac{H}{H_e} + \frac{\partial}{\partial y}\left[\frac{\mu + \varepsilon}{\mu} \nu_0 \frac{\partial u^*}{\partial y} \right] \end{aligned}\right\} \qquad \text{—— (A-7)}$$

其中H为边界层内总　，P为压力。

动量积分方程式的推导：把方程（A—7）对Y座标从零到Δ积分，得到

$$\frac{d\theta^*}{dX}+\frac{\theta^*}{u_e^*}\frac{du_e^*}{dX}\left[2+J_i+\int_0^{\Delta}\left(\frac{H}{H_e}-1\right)dY/\theta^*\right]=\frac{\tau_w^*}{\rho_0 u_e^{*2}} \qquad \text{—— (A-8)}$$

其中Δ为轉換后边界层厚度

$J_i=\delta_i^*/\theta^*$，是型参数。

$\delta_i^*=\int_0^{\Delta}(1-\frac{u}{u_e})dY$，是轉換后边界层位移厚度。

$\theta^*=\int_0^{\Delta}\frac{u}{u_e}(1-\frac{u}{u_e})dY$，是轉換后边界层动量厚度

$\tau_w^*=\mu_0\partial u^*/\partial Y$，是轉換后表面摩擦阻力。

利用平板的焓和速度关係

$$h=h_w+(h_r-h_w)\frac{u}{u_e}-(h_r-h_p)(\frac{u}{u_e})^2$$

或用总焓表示

$$\frac{H}{H_e}=\frac{h_w}{H_e}+\frac{u}{u_e}(h_r-h_w)/H_e-(\frac{u}{u_e})^2(h_r-H_0)/H_e \qquad \text{—— (A-9)}$$

并用冪次速度律　$u/u_e=(Y/\Delta)^n$，得到

$$\int_0^{\Delta}(\frac{H}{H_e}-1)dY/\theta^*=(h_w/H_t-1)(2n+1) \qquad \text{—— (A-10)}$$

其中 h_n 为壁面焓，h_r 为恢复焓。当引入 $J_{ifp}=1+2n$　，方程（A—8）变为以下形式

$$\frac{d\theta^*}{dx}+\frac{\theta^*}{u_e^*}\frac{du_e^*}{dx}\left[2+J_i+(\frac{h_w}{H_e}-1)J_{ifp}\right]=\tau_w^*/\rho_0 u_e^{*2}$$

—— (A-11)

八、主要参考文献

[1]: Spence, D.A., ARC RM-3191.A59.

[2]: Roshotko, E 和 Tucker, Maurice., NACA TN-4154 1957年.

[3]: Eckert, E.R.G., Journal of the Aeronautical Sciences P585 1955年.

[4]: Vaglio-Laurin, Roberto., Journal of the Aero Space Sciences. Vol.27 No.1 1960年.

[5]: Libby, P.A. 和 Cresci, R.J., WADC TN -57-72 1957年.

[6]: Rose, P.H., Probstein, R.F. 和 Adams, M.C., Heat transfer and fluid Mechanics institute 1958年.

[7]: Burggraf, C.R., Journal of the Aero Space Sciences Vol.29 No.4 1962年.

[8]: Mager, Artur., Journal of the Aeronautical Sciences. Vol.25 No.5 1958年.

[9]: Spence, D.A., Journal of fluid Mechanics Vol.8 part 3. 1960年.

[10]: Schlichting: "Boundary Layer theory" Mcgraw-Hill Book Company, Inc. 1960年

[11]: 陆述江编: 附面层理論. 北京科学教育出版社1961年.

[12]: Rubesin, M. W., NACA TN-2917 1953年.

[13]: Mezwin, Sibulkin., Journal of the Aeronautical Sciences. Vol. 23. No.2 1956年.

[14]: Lobb, R. K., Winkler, E, M. and Persh, J., Journal of the Aeronautical Sciences. Vol. 22 No.1 1955年

[15]: Cresci, R. J., Mackenzie, D. A and Libby, P. A., Journal of the Aero Space Sciencee Vol. 27 No. 6 1960年.

[16]: Beckwith, Ivan. E. and Gallagher, James. J., NACA TN-4125 1957年.

宇宙飞船的回地问题*

郭 永 怀

一、引 言

当飞船在外层空间完成各种飞行任务后，如绕地球飞行，或探测月球等，再返回地球时，它都将处在高速运动状态．象“东方号”卫星式飞船在到达空气层外缘时，它的速度就是每秒 7.8 公里． 对于星际航行来说，这虽然是起码的速度，但是就目前人类掌握的飞行技术来说，这仍然是相当高的；它比最快的超声速飞机的速度要高 10 几倍．从能量的大小来看，那也是很可观的．如果飞船的重量是 5 吨，它的动能就要比一列 5000 吨，每小时行驶 40 公里的火车的能量还大 500 倍．能量既然是这样大，怎样能把飞船“刹住”，使它顺利通过大气层，并保证最后安全降落，便成为星际航行在现阶段的一个关键问题．

从原则上讲，解决这个问题，我们可以采用反推火箭，也就是说，火箭喷气方向与飞行方向一致，来产生一个与飞行方向相反的力，逐渐将飞船“刹住”．这种减速的方式虽然简单，但是却不现实；一个粗略的估计便会告诉我们，火箭的重量几乎是有效载荷和结构的 13 倍．

另一个方案是利用空气阻力减速．从减轻重量方面考虑，这是前一方案所不能比较的，但是它也带来一些危险．由于阻力不能自由控制，飞船会不会象流星一样遭受 100g（g——重力加速度）以上的超重？同时，在剧烈的减速过程中，由动能转化来的大量的热会不会把它象流星一样气化为灰烬？因此，这一方案能不能实现，就在于我们能不能做到：(i) 加速度不大于 10g；(ii) 能处理导入飞船壳体的热量．

我现在将针对“东方号”宇宙飞船的回地飞行来分析以上两方面的问题．根据发表的资料，有关“东方号”的轨道参数是：速度 7.8 公里/秒，近地点高度 180 公里，远地点高度 327 公里，飞船重 4,700 公斤． 飞船在越过远地点以后（在非洲上空）(图 1) 开始发动制动装置，将飞船从卫星轨道上改入下降轨道，飞行 10 分钟进入大气层．又 20 分钟飞船才通过大气层降落到预定地点．这一段飞行的距离是 8000 公里，历时 30 分钟．

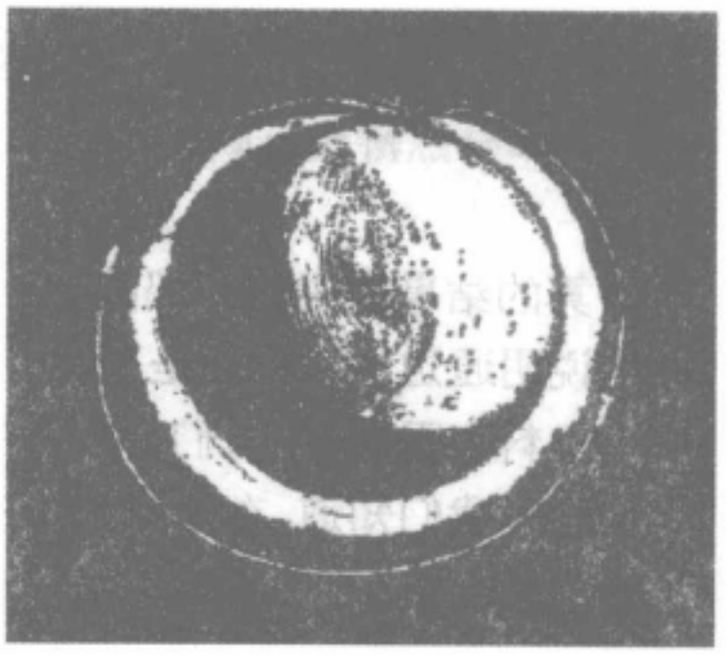

图 1 “东方号”宇宙飞船飞行路线示意图

以下的讨论的一个基本假设是：“东方号”飞

---

* 第四次星际航行座谈会的中心发言．原载“星际航行科技资料汇编”(第一集)，中国科学院新技术局，科学出版社，1965．

船是不带举力面的，因此它在稠密大气层内飞行将完全依靠气动力阻力减速，而且外形是不变的．为了估计的便利，在计算时飞船头部的半径将取为 50 厘米，而船体半径为 100 厘米。

二、空气阻力减速问题

飞船进入空气层以后，它是同时在气动阻力和地心引力作用之下飞行的．如果飞船的外形是不变的，阻力系数在超高速飞行的情况下几乎与速度无关．阻力便与空气密度 ρ，飞行速度 V 的平方成正比．在 100 公里高度范围内，这个变化可以用指数函数来描述．在这些条件下，如果进入大气层的速度和方向（与水平所成的角度 θ）给定，运动方程便可进行数值积分．

假定进入角度 θ_c 是 2°，初速是 7.6 公里/秒，速度与高度的关系示于图 2．从 150 公里到 70 公里，速度的变化是慢的．但是到了 60 几公里的高度，速度骤然减低；在 15 公里范围内，速度从每秒 7 公里减到每秒 2 公里．如果我们把减速度随高度的变化也表示出来，在速度变化剧烈的高度内便出现一个最大值；在计算的条件下，这个高度是 40 公里左右（图 3）．

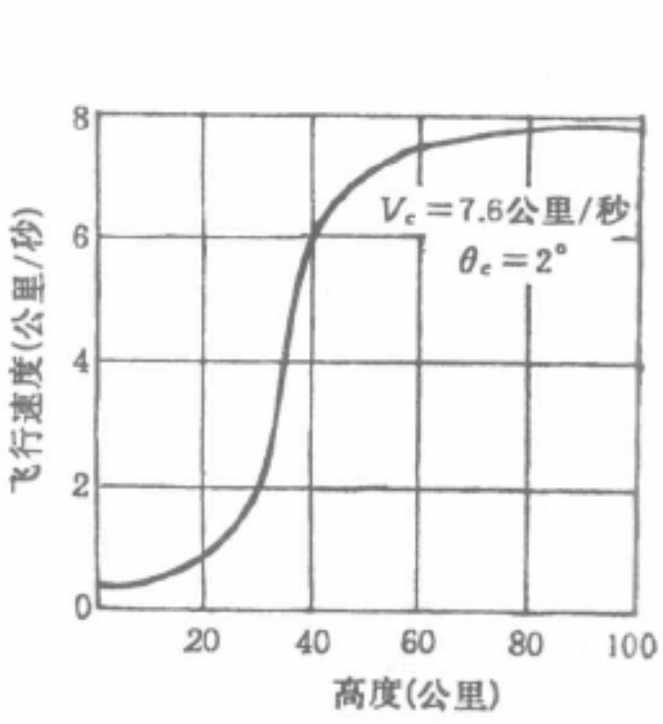

图 2　速度随高度的变化

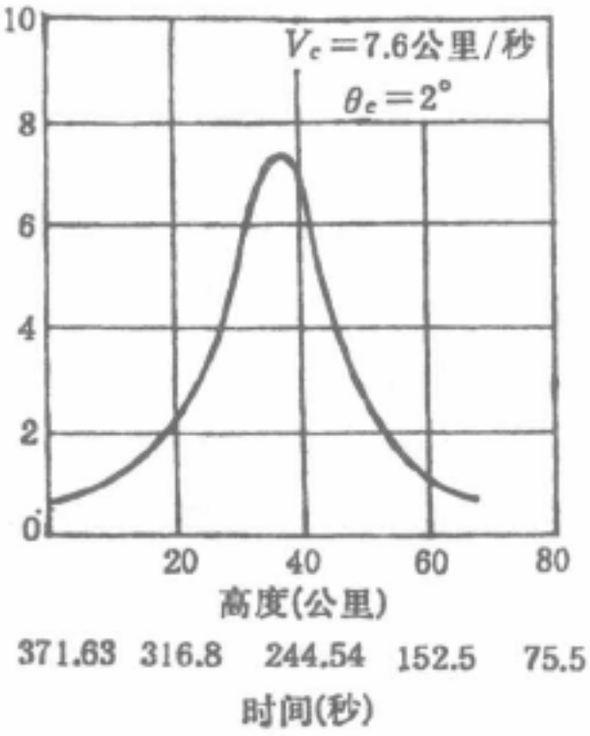

图 3　减速度随高度的变化

计算的结果表明，飞船的速度在 3 公里的高度已经减到声速以下，即低于每秒 300 米．这说明通过空气阻力是可以减速的，而且 6g—8g 的超重所存在的时间不超过 30 秒从实验资料来看，这是人们可以忍受的．

从图 3 我们知道，在减速最快的范围内，阻力远比重力重要（θ 很小的缘故）．因此，为了探讨飞船的重量、几何形状、飞行等参数与最大减速度和出现最大减速度的高度的关系，我们可以近似地把重力略去不计，并且近似地将密度随高度的变化表示为

$$\frac{\rho}{\rho_0} = 0.715e^{-\frac{y}{7.55}} = \alpha e^{-\beta y}$$

这里，ρ_0 是海平面的密度（克/厘米^3），y 是高度（公里）．通过简单计算给出的最大减速度是

$$-\frac{1}{g}\left(\frac{dV}{dt}\right)_{\max} = \frac{\beta\theta_e}{5.44g}V_e^2$$

与这个数值对应的高度是

$$Y_1 = \frac{1}{\beta}\ln\frac{C_D A}{W}\cdot\frac{1}{\theta_e}\cdot\frac{\alpha\rho_0 g}{\beta}$$

这里 V_e, θ_e, C_D, A, W 分别是初速、进入角、阻力系数、截面积、重量. 这个结果告诉我们，对于每一种回地问题，在 V_e 已经给定的情况下，要减轻超重的严重性，只有降低进入角度 θ_e，而与其它参数无关. 另一方面，出现最大减速度的高度是随参数 W/C_DA 及 θ_e 的减小而增加. 由于是对数函数关系，这些参数的选择对相应于最大减速度的高度的影响是比较小的.

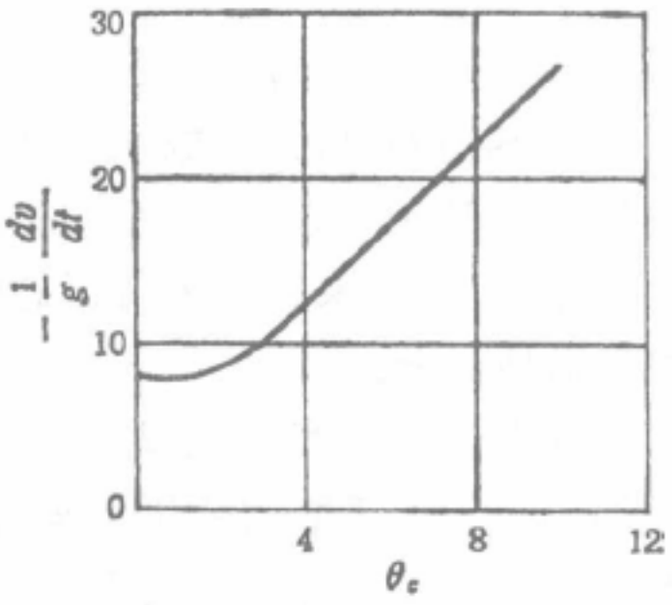

图 4 减速度与进入角的关系

准确的计算表明，在进入角 θ_e 小于 4°，最大减速度基本上不随进入角 θ_e 变化，即当 V_e 为每秒 7.6 公里时，最大减速度与 θ_e 的关系曲线开始时几乎保 持不变（8g 左右）. 但是当 θ_e 大于 4° 时，最大减速度就将随着 θ_e 的增加而增大（图4）

三、气动力加热问题

从前面的计算看来，利用空气阻力减速是现实的，但是由于减速度的变化大，在一段飞行过程中，动能转化来的热的危险性可能是严重的. 为了对采取有效措施提供依据，传热量必须加以分析.

如飞船的初速为 7.6 公里/秒，那么，对应于 1 公斤质量的动能就等于 28×10^6 焦耳，如果将这个能量全部化为热，它足够把 30 公斤的钢（熔点 1500℃）加热到 2000℃. 在这种情况下，要想使飞船不被烧毁，唯一办法是把大量的热与飞船隔离，即削减导热量.

对于没有举力面的“东方号”来说，解决这个问题的途径是选择有利的几何形状，特别是受热最大的头部的几何形状. 我们知道飞船在飞行的时候，尤其是在减速度很高的飞行阶段，它周围的气体是炽热的，因而使大量的热流向飞船的壳体. 根据热与动量相似的原则，飞船每秒所吸收的热量可以近似地表达为

$$Q = \frac{1}{4}C_f S\rho V^3$$

另一方面，飞船在阻力作用下，每秒所损失的动能是

$$E = \frac{1}{2}\rho V^2 C_D A V$$

因此，传入飞船体内的热流与总热量有以下关系：

$$Q = E\left(\frac{1}{2}\frac{C_f S}{C_D A}\right)$$

这里，C_f 是粘性阻力系数，S 是飞船的表面积. 从这个关系式我们清楚地看到：要减少传热流 Q，就要尽量选择 C_fS/C_DA 小. 对于飞船来说，表面积大致是截面积的两、三

倍．因此，要想使 C_fS/C_DA 小，我们只有设计外形使 C_f/C_D 小．这就是说，选择飞船外形的原则必须与高速飞机相反，不是要船体细而长而是粗而短，特别是头部必须有一定的半径，即钝体．对于这样的物体，粘性系数就将占总阻力系数很小的一部分（譬如说，百分之一）．

这样，物体在超高声速飞行时，它将不断地、猛烈地压缩它前面的空气，结果在空气中便产生一个强冲激波，并将空气加热到 6000—8000℃．空气分子与飞船表面反复撞击的结果，使它们的速度（热运动）很快地提高．在它们从固体返回去的时候，它们当中有很多便又与前面新冲来的分子碰撞，使它们不与固体面接触而是把它们散射到气流中去．这样就把大量的热排卸在冲激波与飞船之间的空间里（图 5）．这部分的热量是很大的，几乎占总热量的 98％，仅有 1—2％ 的热量才通过热传导和扩散传入飞船的壳体．

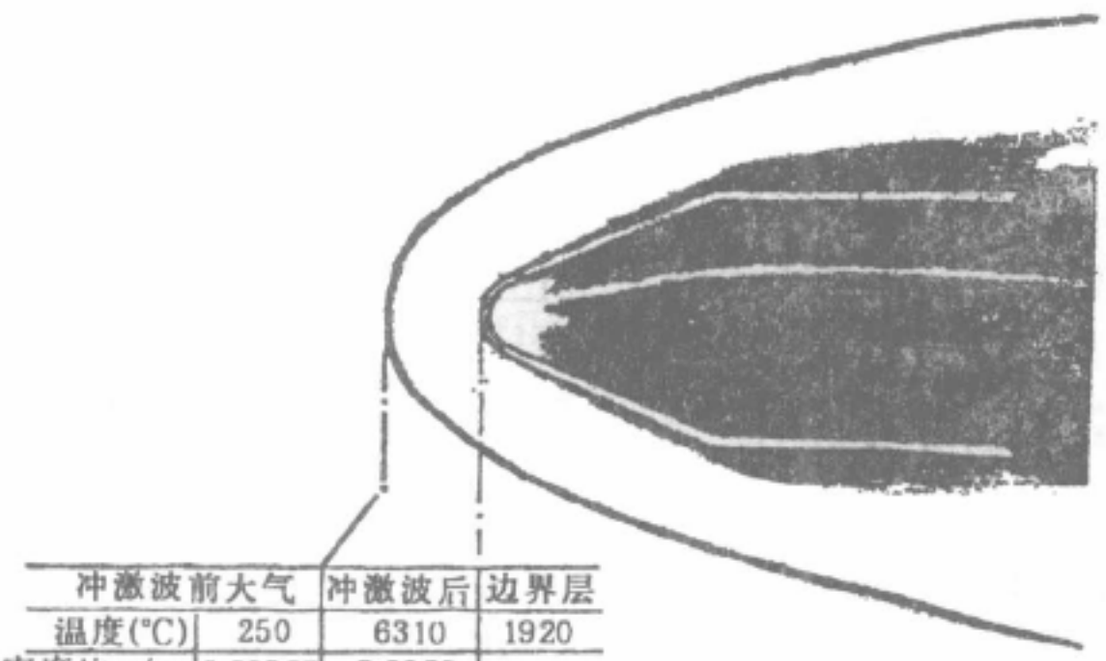

冲激波前大气		冲激波后	边界层
温度(℃)	250	6310	1920
密度比 ρ/ρ_0	0.00025	0.0036	
主要成分	O_2 N_2 A	N_2 O	N O^+ A	N^+ NO e

图 5　冲击波层内的主要参数

当飞船的速度在每秒 6—7 公里范围内，冲激波与飞船之间的空气是处在高温（6000—8000 °K）状态，大部分氮、氧分子在强烈的热运动的作用下已经分离，小部分甚至电离．这时冲激波与飞船之间的流场就存在两个性质不同的区域：贴近飞船表面的粘性层和这一层以外一直到冲激波的流场（图 5）．在粘性层以外的区域里，温度、压力的变化是小的，因此分离了的气体几乎处于平衡状态．粘性层（边界层）则不同．如固体表面通过冷却维持在 1000°K 左右，在这个厚度很小（毫米数量级）的粘性层里就造成很大的温度和气体浓度梯度．这样在边界层内就引起很强流向固体壁的热流，同时由于原子浓度内外不一样，处在高温的原子便向冷的区域扩散，结果也由于重新结合而释放一部分热来．

为了得一数量上的概念，我们可以对驻点的热流 q 进行估计．如果边界层是处在层流状态，这个问题是解决了的．计算的结果通过简化是（采用功的单位）

$$q = 6.66\sqrt{\frac{\rho}{R}}\,V^3(\text{千瓦/厘米}^2)$$

这里 ρ 是冲波前的空气密度（克/厘米^3），R（厘米）是头部半径，V（公里/秒）是飞行速度．

从以上这个关系式我们可以看出，如果 V 给定，要降低导热率就要选取最大可能的头部半径 R．同时我们也注意到，热流与密度的关系，虽然与减速度和密度、速度的关系不一样，但是，在飞船下降的过程中，q 也将出现一极大值．根据前一节的近似，这个最大值 q_{max} 及它出现的高度 Y_2 分别是：

$$q_{max} = 6.66\sqrt{\frac{W}{C_DA}\cdot\frac{\beta\theta_e}{8.13gR}}V_e^3$$

$$Y_2 = \frac{1}{\beta}\ln\left[\frac{1}{\frac{W}{C_D A}} \cdot \frac{3\rho_0 \alpha g}{\beta\theta_e}\right]$$

导热率的最大值却与最大减速度不同，它是同飞行器的特性，如外形和重量有密切关系的．如果飞行器的阻力参数 W/C_DA 愈大，热流将愈大，而发生的高度也愈低．对防热问题来说，这种情况是不利的．对于宇宙飞行来说，在 W/C_DA 确定之后，降低热流的途径，同减轻超重一样，是要尽量选择最小可能的进入角度 θ_e．根据“东方号”的参数，在 θ_e 为 2° 时声速点的热流随时间的变化示于图 6．这里最大热流是 310 瓦/厘米²，发生的高度是 38 公里左右．

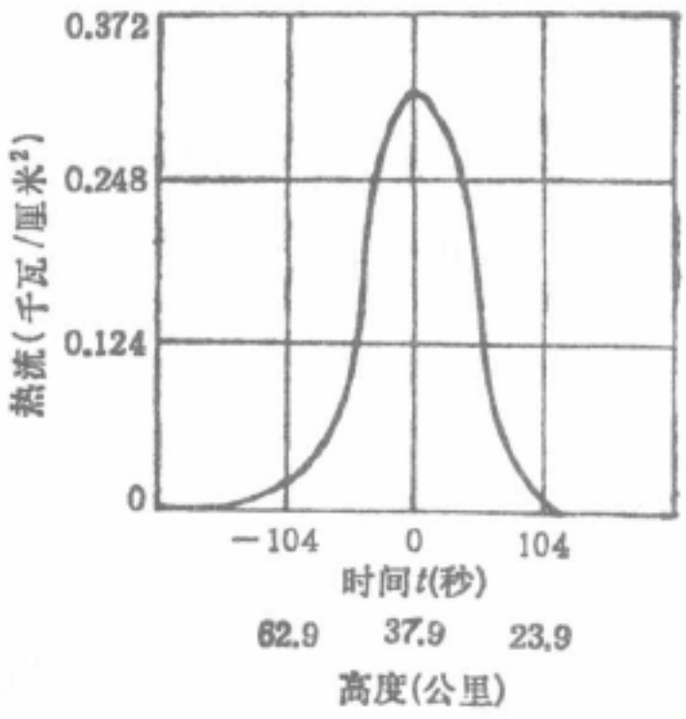

图 6　声速点热流随时间的变化

我们应当注意：θ_e 小固然降低了传热率，但是却增加了总传热量，因为总传热量是与 $\sqrt{\theta_e}$ 成反比．如果进入角不是太小的话，这个影响还是不严重的．

四、回地轨道

“东方号”飞船回地轨道有三个阶段：制动飞行段，无反推力飞行段和大气层内的飞行段（图 7）．

为了使飞船在预定地点降落，飞船必须按给定的轨道飞行，而轨道选择的原则必须是避免过大的减速度和传热量．现在就设计这样轨道进行以下分析．

(i) 制动飞行（图 7 中 AB 段）

为了简化计算，设飞船绕地球运行轨道为圆形的．根据“东方号”的资料，制动火箭开动不在远地点而且在越过那点以后（非洲上空）．我们可以设想：这时它的高度（即圆形轨道的高度）是 250 公里．在空气层以外的一段飞行，下降 100 公里左右，而航程则已经是 3000—4000 公里．因此，飞行的轨道与原来的圆形轨道是接近的．这样，在制动火箭开动后的轨道的改变便可以按一级微量计算了．

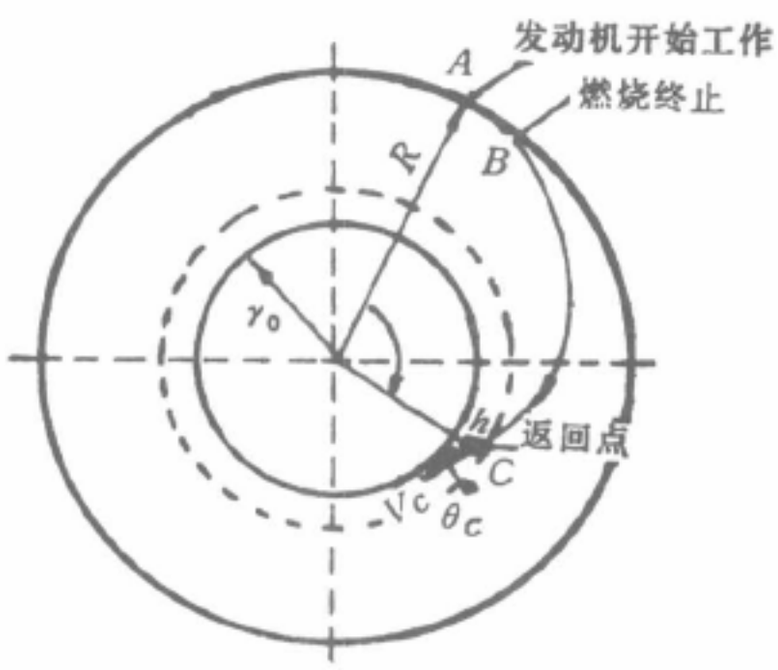

图 7　宇宙飞船回地的路线

计算的结果表明，制动火箭可以采用推力大、小两种．推力小，燃烧时间就长；相反，推力大，燃烧时间就短．对比起来，前一种方式推力虽小而燃烧时间长，从推进剂耗量来考虑是不合适的．现在我就后一种方式进行估计．

根据这种方式计算，如果反推力 T 与重量 W 的比例是 0.63，飞行距离 $\overset{\frown}{BA}$ 为 396 公里，燃烧时间为 50 秒．设飞船重量为 5000 公斤，那么推力 T 将为 3150 公斤．取推进剂的比冲量为 250 秒，每秒燃烧量为 12 公斤，结果推进剂总重为 600 公

斤．这样火箭的重量就占总重的 12％ 或 13％．

假设火箭的推力再大一些，如 6400 公斤，燃烧时间就会缩短一半以上（23 秒），但是推进剂的重量则仅减轻了 20 公斤，这样看来，燃烧时间尽管缩短，火箭的重量则变化不大，这个数值应不低于总重的 11％．

(ii) 无反推力飞行段

在火箭停火以后，飞船将在重力作用下按椭圆轨道飞行．在下降 100 公里时，它已飞行 3780 公里．这时轨道与空气层外缘所成的进入角度为 2.7°（从水平线量起），飞行时间为 9 分钟，飞行速度为 7.6 公里/秒．如果再下降 30 公里，这时轨道与水平所成的角度将为 3° 左右．

根据二、三两节的结果，飞船进入大气层的速度和进入角度分别为 7.6 公里/秒和 2°—3°，证明以上两阶段轨道的选择是合适的，而且利用固体推剂火箭也是不难实现的．

(iii) 大气层内飞行段

飞船进入大气层内的运动在第二节内已经论述，通过准确计算证明，飞船的速度在 3 公里高度处，已经下降到声速附近，即每秒 300 米．这时降落伞就可以打开，然后逐渐下降．在 3 公里高度以上的飞行时间约为 6 分钟，航程 4360 公里．

如果降落伞飘下时间为 10—15 分钟，那么，根据以上的估计，全程共历时 25—30 分钟，航程 8540 公里（地面距离要小些）．这些结果同发表资料大致是符合的．

五、防 热 问 题

根据层流边界层的理论，在一个半球-圆柱的组合体上，热流由驻点的最大值逐渐沿轴线降低，到了球与柱体衔接处，热流仅有驻点热流的百分之四到五（速度足够高）．对于球-圆锥-圆柱的组合体（图 5）．热流的分布也大致类似．因此，从受热的严重性来看，飞船的头部是最需要防护的．

假定头部平均受热量是 200 瓦/厘米^2（偏高的估计），受热时间是 100 秒．如果头部的面积是 $2\pi R^2$（偏高），那么，总受热量将是

$$200\text{ 瓦/厘米}^2\times 100\text{ 秒}\times 2\pi(100)^2\text{ 厘米}^2=12\times 10^8\text{ 焦耳},$$

这大致就是总热量的百分之一，对于一般钝体说来，这个估计是差不多的．

为了保证飞船的安全，这样一个数量级的热量必须在它发生的瞬间内完全加以控制或隔离，使它不能导致飞船壳体的破坏．解决瞬时大热流的防热问题，在卫星或飞船回地问题上，目前有两类可能的冷却方案：发汗和烧蚀．兹分别叙述如下：

(i) 发汗

飞船头部的外壳的制造可以采用松散、多孔的材料，并且在这层壳下面储藏冷却剂．当外表面温度升高，冷却剂就将由液态或固态转变为气态．由于容积的增加，气体在发生以后，就沿孔道向外蒸发，这样就将大量的热吸收，从而在固体表面形成一层低温保护层．

从目前的情况看，固体冷却剂的资料还很不全，一般说来，升华点低的材料吸热量也

比较低．另一个可能性是采用液体，例如液态氮．当一公斤液态氮蒸发时就将吸收 10⁷ 焦耳的热．如果我们用液态氮作为冷却剂，将全部热量吸收，20 几公斤的氮就够了．

这个方案的优点是，在飞行过程中飞船的头部外形保持不变，这对保证飞行性能是很重要的．但缺点是，由于液体的储存和输送系统较为复杂，而且给飞船添了不少重量．另一方面，多孔材料的制备在工艺上的要求也很高，例如孔道的分布要均匀，否则将由于堵塞而导致局部破坏．因此，这个方案目前实现还有困难．

(ii) 烧蚀

当固态物质一旦投入高温（低于一万度）的环境内，它一般将由固态逐步过渡到液态以至气态．在物理状态和化学改变过程中，它将吸收一定热量．过去几年的研究，发现一些材料，它们一方面在改变状态时吸收大量的热；同时它们在固态时又具有很高的绝缘性能．这样当它在高温的气流作用下，既能通过材料的损失，如蒸发等将传过来的热送回气流，又能将高温区与船的内壳隔离（绝缘）．这一种现象（广义地说）就叫做烧蚀．

根据国外的资料，比较有前途的材料是玻璃丝或硅丝加强的塑料（树脂）．这种材料每一公斤在烧蚀时能够吸收 12×10^6 焦耳的热，而且制备的工艺比较简单，作为“东方号”这样飞船的保护层所需的量大约 100 公斤．看来这个方案不仅可以满足要求，也是完全可以实现的．

当然，这里有一个外表变形的问题．估计在加热强烈的一分钟内，由于表面质量的消耗，头部的表面将以不同速度后退，最大可能达到一个厘米．由于烧蚀而破坏了飞船的对称性，从而造成飞行轨道的误差，这是不可避免的；但这在“东方号”飞船的降落上，至少在目前阶段，这种误差是允许的．

六、结　束　语

从轨道设计的结果与公布资料符合的情况来判断，对反推火箭和进入角度所确定的范围大体是正确的．沿着这种轨道进入空气层所引起的超重、防热以及导航、操纵等技术问题，在当前科学技术水平的条件下，是完全可以解决的．进一步的问题是利用举力面，一方面降低卫星式飞船的超重，另一方面试图解决速度更高的月球飞船的回地问题．

激 波 的 介 绍

郭 永 怀

无论是爆竹的爆炸或是大炮的发射，在我们听到“啪”或“轰”的一声的时候，假如空气密度的疏密是眼睛看得见的话，我们就会看见一个密度很大的空气层从我后身上掠过去。这时如果把空气里的压强分布用曲面表示出来，在那个密度大的气层里，这个面就像个小山峰一样。要是用照像的方法把它照下来，像片上就呈现为一条黑线，图 1 所表示的便是大炮发射最初一瞬的情形。这里最外面的圆形黑线，便是上面所说压强高峰的侧影，这就是我们所要介绍的激波。

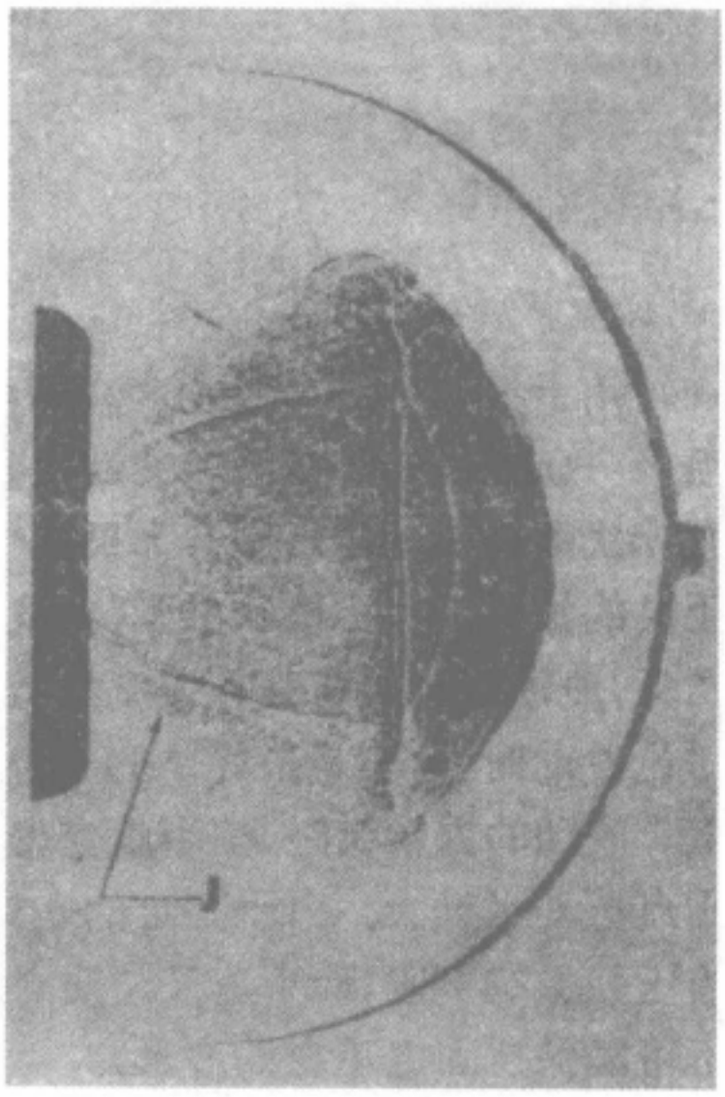

图 1

一般地说来，产生激波有两种方法：一种方法是利用火药的爆炸，放炮便是一个例子；另外一种方法是利用物体的高速运动，例如发射出去的炮弹和超声速飞行的飞机。图 2 所表示的情况便是属于后面这一类。这里从炮弹尖端所发出的两条黑斜线就是激波，由于压强在激波上突然地增加，当炮弹或高速飞机飞过我们时，我们便能听到“啪”的一声响。从这两个例子我们也可以看出，激波的形状并不都是一样大。大体说来激波共有以下几类：球面、柱面、平面（又分正面和斜面两种）。它们的共同之点是，在和波面垂直的方向，压强、温度、密度的变化是突然的。在普通情况下这种变化可以利用跃变来表示（图 3）。这个不连续的跃变差（通常用压强差 ΔP 来表示）便叫做激波的强度。激波愈强，跃变差就愈大。

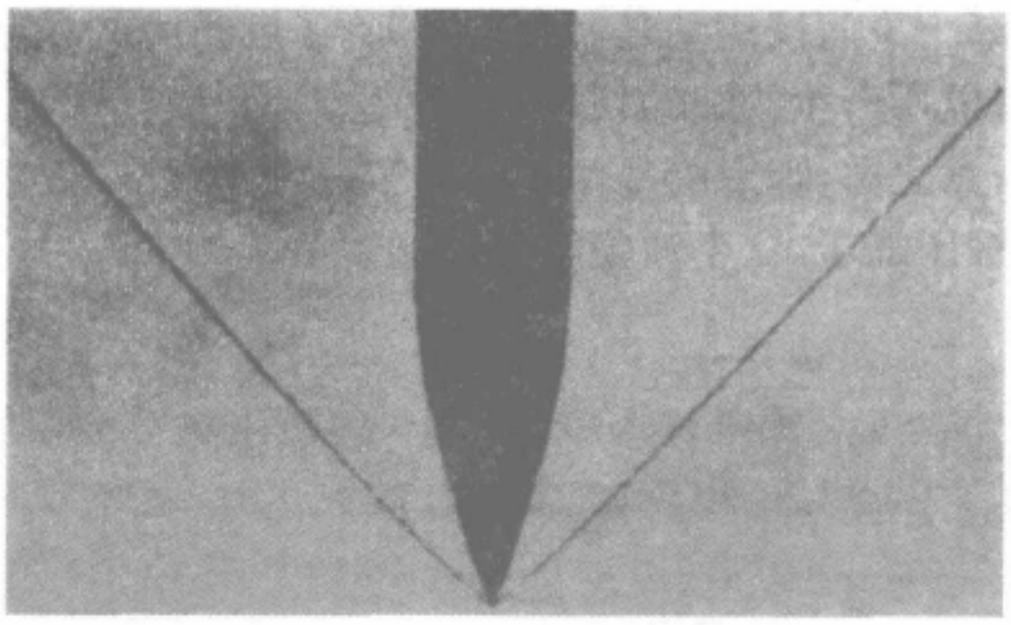

图 2

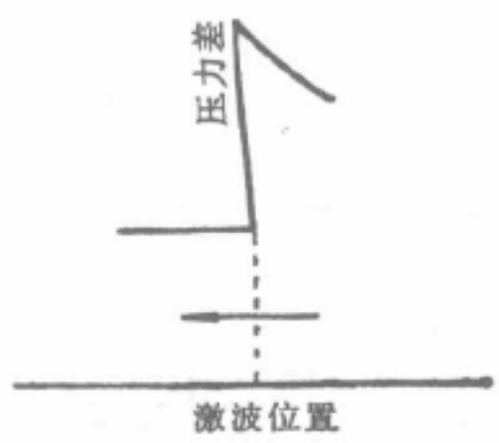

图 3 球面波径向压强分布

类似这种不连续的传播现象，在自然界里是常常出现的，在有坡度的河流里出现“水

跃”便是个例子．甚至在城市中的人群里也会发生．譬如说，一群赛跑的人，如最前面的一个忽然被交通挡住，而同时来不及警告后面的人，结果大家都来不及准备，便一个跟着一个地碰在一起，这个密度大的人堆，即激波，便从很高的速度对着跑的人传播过来（参看图 4）．

图 4

激波的形成

如果空气里忽然发生压强变化，这种变化便向各方传播，这就产生大家所熟知的所谓“波动”——像投一块石头到水里时，在水面上所出现的现象一样．如果波动区域里压强的起伏小，便叫做小振幅波．平常的声波便是属于这一类的．如果波动区域里压强起伏很大，便叫做大振幅波．

由于振幅小的关系，声波的传播对于气体的压强和密度影响非常小，结果声波就像沿着一条细长线而传播的波动一样，完全和这时介质的运动情况无关，而是只取决于空气在未扰动情况下的状态．如果大气是均匀的，声波相对于介质的传播速度便是个与波长无关的恒量．在标准状态下，如我们所熟知的，这个数值是每秒 331 米．传播速度既然是恒量，波动区域里压强和速度的微弱变化，即“波形”，便能保持固定不变地向前传播．在讨论波动时，这便是最简单的一种类型．

波动的振幅大时，情形就变得很复杂．波动所产生的压强变化大，在气体里所引起的质点运动也就大．对于固定的坐标说，大振幅的传播速度便是质点速度与声速之和．因为压强影响声速，而声速又与质点的速度有直接关系，结果大振幅的波动在传播过程中便不可能保持固定不变的波形．

在很简单的情况下，我们可以假设空气是个没有粘性的理想气体，并且波形是连续的（即圆滑、没有突变的）．在这样的运动中，气态的变化是可逆的，也就是说，熵这个量在传播过程中是不变的．为了便于讨论，我们进一步假设运动是一维的，即除了随时间的变化外，运动仅在传播方向有变化，在一根直管里所产生的波动便是这样．这种波动可分为两类：膨胀波和压缩波．如果一个波经过一点之后，那点的气体是膨胀了，这个波就叫做膨胀波（图 5）．相反地，如果波通过后气体被压缩了，这个波便叫做压缩波（图 6）．

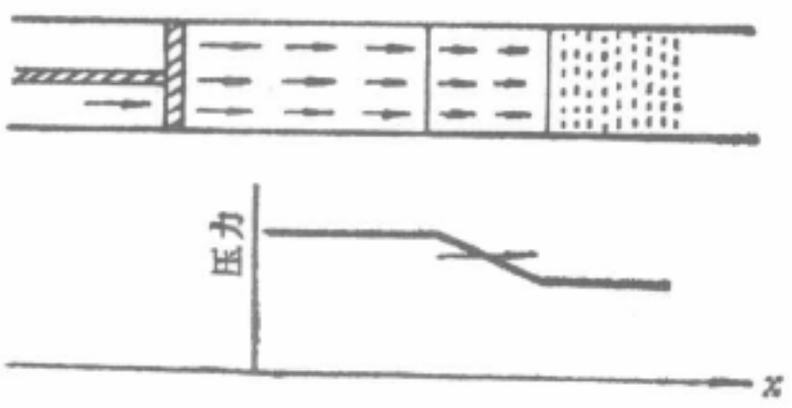

图 5　膨胀波的波形

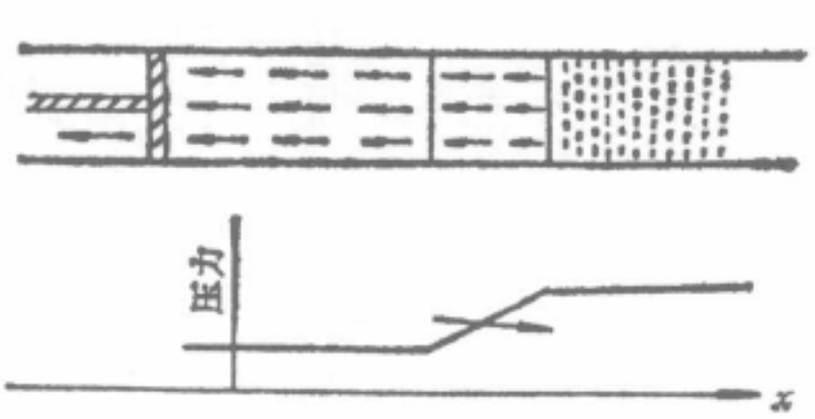

图 6　压缩波的波形

设想在某一瞬间空气里产生了一个向右传播的膨胀波．从前面的讨论我们知道，压强高的地方，质点速度和声速都大；由于在膨胀波中波头的压强高而波尾的压强低，波头的传播速度总比波尾大，因此，这样一个膨胀波发生后不久就会逐渐消失（图 7）．相反地，如果在空气里产生了一个向右传播的压缩波，那么尾部的传播速度要比头部为大，结果原来一个连续变化的压缩波，变化的坡度在传播过程中将不断增加，以致在一定的时间内便演变成为一个不连续的波（图 8）．

图 7　膨胀波形的演变

图 8　压缩波形的演变

这便是瑞曼（1859）的激波形成的理论．在这个理论中，他发现像图 6 所示的单值波形，在一定的时间以后，便能演变为三值的图形．这就是说，在某一点的坡度达到无穷值以后，原来的假设就不再适用．于是他推测，当坡度无穷大的时候，实际上就可能出现不连续的现象，如激波．他的这个推测已经完全为实验所证实了．

激 波 的 传 播

我们可以设想做这样一个简单的实验：在一个很长的直管里装置一个活塞（图 9），使活塞前后运动，在管内静止的气体里就能发生波动．当活塞急速往后退使它附近气体膨胀时，所发出向前传播的波便是一个膨胀波，因为显然波头的压强高而波尾的压强低．如果活塞向前急速地推进，使附近气体压缩，则在气体里产生一个向前传播的压缩波．根

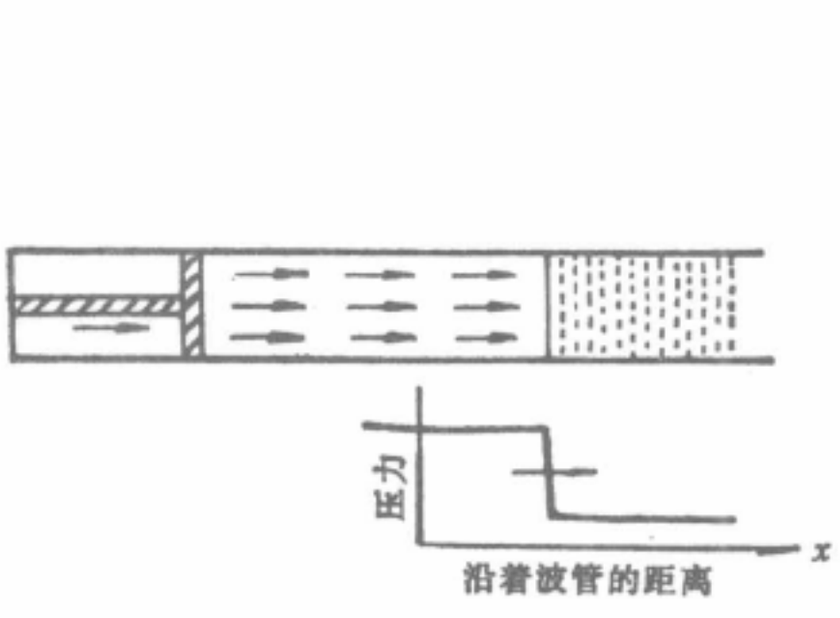

图 9　激波的传播

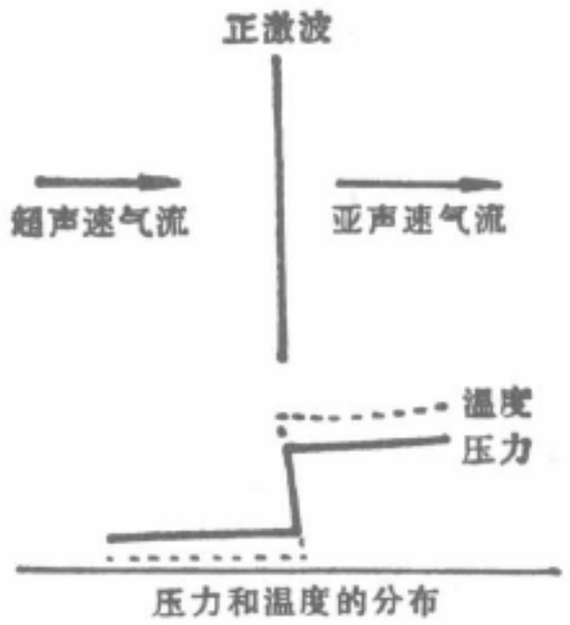

图 10　压强和温度在激波前后的情形

据前面的理论，这个连续的压缩波会很快地演变成为一个不连续的波，即激波．当激波形成以后，它就向前传播．如果活塞的速度不变，激波的传播速度也就不变，对于随着激波一起运动的坐标来说，这个运动便是一个定常运动（图 10）．由于传播方向与波面垂直，这个激波也叫做正激波．

在一般的情况下，这个运动所牵涉到的参数有激波前后气体的压强、密度、温度以及

激波和活塞的速度．在实际的问题里，波前气体的状态总是事先就可以肯定的，至于与活塞运动相应的速度或激波传播的速度，则一般不能预知而是需要给定或测量的．决定这样的问题首先就要解决激波的传播问题．在定常的情况下（参看图 10），激波面上各处的流量（单位时间内流过单位面积的质量）、动量（单位面积上的压强和由于流量所产生的作用）和能量（单位质量的动能和焓）在通过激波时是不变的（当然还须假设气体通过激波后并不发生化学变化）．

这三个条件中的前两个通常叫“力学条件”，激波满足这两个条件是毫无疑问的．只有在能量守恒这个问题上，就不是那么明显．因为从理论上讲，气体是没有粘性的，如果没有粘性，能量守恒就意味着热力学里的熵也不变，这也就是说，不连续运动是不可能发生的．因此，通过激波的变化就必须是绝热、不可逆的．这就引进一个重要的辅助条件：通过激波时熵是向正的方向跃变的．

这些关系在气体动力学里就叫做激波条件．它们可以适用于激波，也同样适用于比较复杂的柱面波和球面波．根据这三个条件，我们可以把波后和波前的压强、温度、密度比表作波前的压强、密度、气体的特性和激波速度的函数．在这些关系中所出现的最重要的一个参数便是激波速度和波前的声速的比值．从熵增加这一条件我们可以断定，这个比值，称为马赫数，永远大于 1．这就是说，激波的速度永远大于声速．由于激波的压缩而产生的压强、温度、密度增加的倍数是和马赫数的平方成正比的．当激波趋近于声波（弱激波）时，马赫数便趋近于 1，波前后的状态也便趋近均等．相反地，随激波的强度的增加，波后的压强和温度便很迅速地上升．另一方面，密度虽然也有增加，但是增加很慢，在激波极端强烈时，密度比便趋近一个恒量．对于空气来说，这个恒量几乎等于 6，这也就是说，利用激波来压缩空气，密度最大不能超过 6 倍（图 11）．

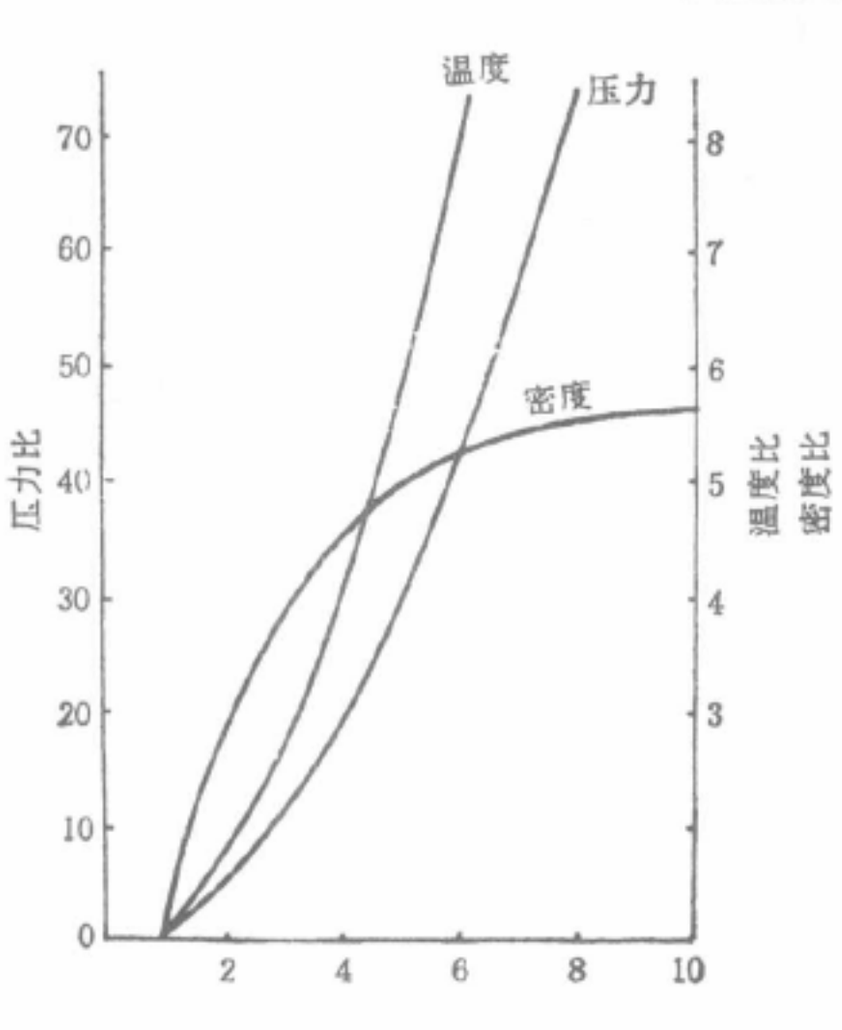

图 11　压强、温度、密度与马赫数的关系

压强和温度的情况就不一样．激波的速度提高，即马赫数提高，压强和温度比就与马赫数的平方成正比地提高（图 11）．温度和压强的这种变化是由于气体冲过激波之后（图 11），立刻受到压缩的过程中大量的动能转变为热能．速度愈大，压缩愈强，温度也愈高．由于动能转变为热，通过激波以后气体的动能大大减低．对于激波说，波前的气流是超声速的，而波后的气流则是亚声速的．

简单说来，这便是激波前后的情况．只要激波不是过于强时，这些理论上的推测是符合事实的．但是假使激波的强度很大，譬如说马赫数大于 10，这个理论对于实际的气体说，就不够准确．原因是这样：在激波不强时，为了使空气（譬如说）的热运动状态能从波前的平衡状态过渡到波后的平衡状态，所需要的分子碰击次数不到 10．这就是说，从激波一边到另一边的厚度，不到 10 个分子碰撞自由程．在一般的情况下，即马赫数为 1 或 2，这个厚度的确是很小的，大约是 10^{-4} 厘米左右．前面所说的不可逆过程就是在这

极狭小的区域里发生的．因此，理论上的不连续的假说，实际上是一个很准确的近似．

但是在激波很强的时候，由于激波后面的温度高，分子的剧烈碰击可能发生分离甚至电离现象．分子如果破裂，气体的分子数目就要增加，结果气体的热容量就要增加，温度就要降低．在这样情况下，通过激波的气体仍旧保持单纯的理想气体的假设已不能适用．我们必须进一步考虑气体分离或电离的影响以及这些物理现象发生的过程．这些研究对于今后新技术的发展将是很重要的．

激波对实际问题的重要性

激波是一个很普通的现象：它发生在高速气流里；强烈的燃烧里，即爆震波；也出现在星的爆炸和太阳表面气体的冲射．在技术方面，为了提高航空和火药爆炸的新技术，研究激波对于气流和激波对于导致火药爆炸的影响和作用都是很重要的．近年来天文物理学家还引用激波的特点来理解星际间的现象．在这里我们特别讨论一下下面的问题．

1. 高速飞行

从图 2 里我们可以看出来，一个物体要以高于声速的速度飞行，它的前端便发生激波．激波的产生对于物体所产生的气流有什么影响呢？它的主要的影响是产生阻力（阻力大体上说可分为两种：一种来自粘性，一种就是来自激波），我们现在先谈激波阻力．

前面已经说过，激波的产生是通过一个不可逆的过程，一个运动中如果有激波发生，熵便不可能保持不变．这是因为当气体冲进激波从而被压缩以后，它同时便接受了由于耗损所生的热，结果熵便有增加．由于内耗的关系，动能便有损失．这个量的关系在热力学里是一个很著名的规律．在物体飞行的问题，这种损耗就表现成为对物体的阻力．

在炮弹和超声速飞行的研究中，如何选择飞体的几何形状以便减少动能的损失，是一个中心问题．从前面的讨论我们知道，激波的强弱决定熵增加的多少；同时熵的增加又决定了阻力．所以要达到减阻的目标，就要避免强激波出现．避免强激波最直接的办法是降低飞行速度，但是在高速飞行的先决条件下，这自然是不许可的．另外的一个方法则是

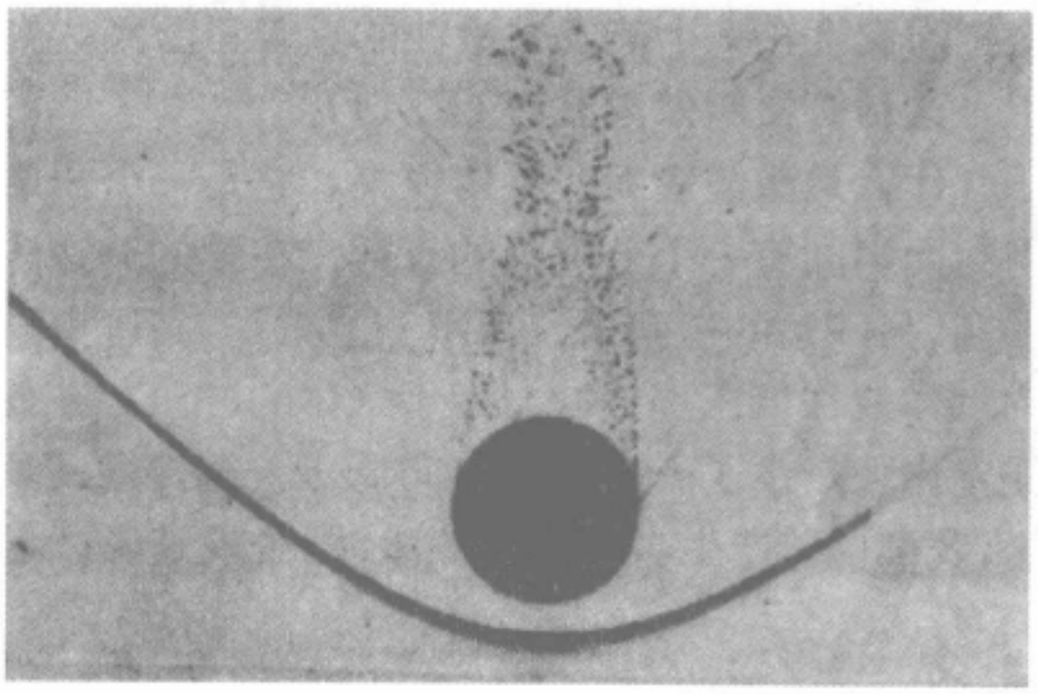

图 12

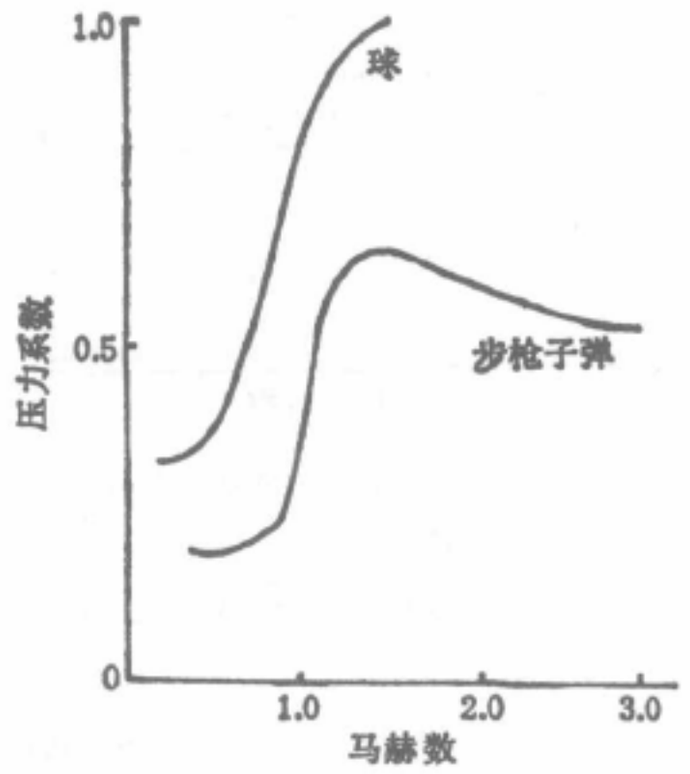

图 13　几何形状对阻力的影响

以下面的事实为依据的.

在飞速指定后,我们可以比较两种情形: 一个是正激波;一个是斜激波,即激波与飞行方向成一锐角 (参看图 2). 我们知道,通过激波的跃变只限于与波面垂直方向的速度和动量,结果同样的飞速斜激波所导致的跃进显然就要小些,因此所引起的阻力也就小些. 所以,在飞体的设计上,我们总是选择产生类似斜激波的几何形状. 根据经验我们知道,钝头而厚的飞体,如球 (图 12),比尖头、细而扁的形状 (图 2) 产生更强的激波. 在不同的速度这两种物体阻力的比较,请参看图 13.

阻力大究竟有什么不好呢? 我们知道,物体的飞行是依靠推力或爆炸所产生的动能. 有了动能的损失,在炮弹的情形,同样的炮和炮弹,当然就发射不远;在飞行的情形,同样的飞速,阻力如果大,就需要强大的发动机,这就要增加发动机的重量和耗油量. 所以,在实际问题里,激波与飞体或管道 (推进器的) 的几何形状间的相互关系,是具有重要意义的研究题目.

2. 实验的工具

上面所讲的是激波有害的一面,现在我们再谈谈它的有利的一面.

从激波的特性看来,正激波是一个很有效的压缩和产生温度的工具. 譬如说,激波的马赫数等于 4 或 5,激波后面的压强就有 20 到 30 个大气压而温度就能达到 1800°K. 在实验室里产生这样强度的激波是很容易的.有了这样的工具,我们便能利用它来研究化学反应的问题. 因为激波的温度是可以预先拟定的,我们便能在各种情形下进行这类的研究. 这对于探索化学连锁反应问题是极有用的.

另一方面,近几年来由于远距离导弹的成功,高速飞行已有实现的可能. 飞行的速度很高,譬如说马赫数等于 10,物体前端的激波就很强,它足以使气体里的分子发生化学变化. 从空气的实验里我们知道,在温度近一万度绝对温度时,气体的组成便变为很复杂. 由于空气分子在这样的高温下的分离、化合和电离,空气的特性就有很大的变化,它对于飞体外表的气流的影响也是巨大的. 因此,为了设计效率高的飞行器,高温下气体性质的研究是很重要的.

研究高温下的气体的特性,激波也是一个有利的工具. 为了要在实验室里进行这种研究,首先就需要产生近一万度绝对温度的温度,这样的温度在一个能发生激波的直管里已经达到了. 这种管便叫做激波管 (图 14).

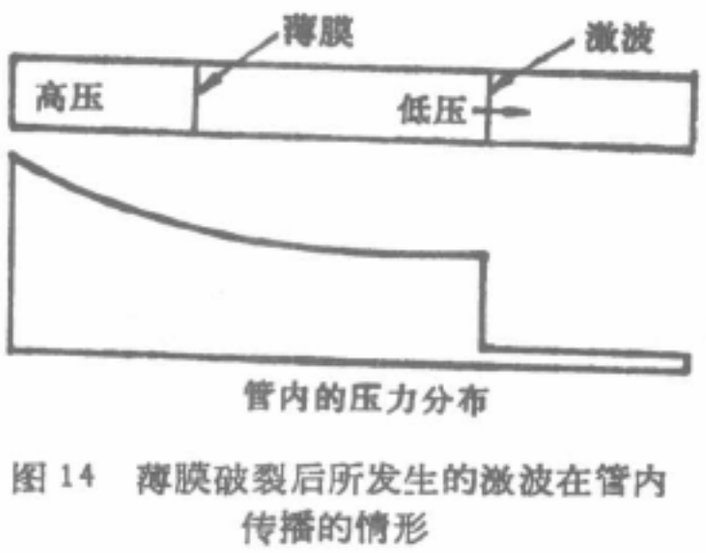

图 14 薄膜破裂后所发生的激波在管内传播的情形

什么是激波管呢? 具体说来,它是一个两端密封而中间有一个分隔膜的直管. 在膜的一边压强高,另一边的压强低. 薄膜一旦破裂,高压室内的气体就往低压那边冲. 由于气体的冲激,在低压室内便产生了一个激波,向低压一端传播. 利用不同的薄膜以及高压和低压室的压强比,我们便能产生各种不同的激波,也就是说,各种压强下的不同温度.

这一方面的技术目前还正在迅速发展,前途是无限的.

郭永怀生平

- 1909 年 4 月　　出生于山东省荣成县西滩郭家村
- 1929 年 9 月　　考入南开大学预科理工班
- 1933 年 9 月　　进入北京大学物理系学习光学
- 1935 年 7 月　　北京大学毕业，留任助教
- 1937 年 9 月　　回山东威海中学任教
- 1938 年 4 月　　西南联大学习流体力学
- 1940 年 9 月　　在加拿大多伦多大学应用数学系学习
- 1941 年 5 月　　获硕士学位，赴美国加州理工学院航空工程系学习
- 1945 年　　获博士学位，次年发表“可压缩流体二维亚声速和超声速混合型流动和上临界马赫数”的论文（跨声速流动研究代表作）
- 1946 年 10 月　　赴康乃尔大学参与创办航空研究院
- 1953 年　　发表“中等雷诺数下不可压缩黏性流体绕平板的流动”（PLK 方法的代表作）
- 1956 年 11 月　　回到祖国
- 1957 年 5 月　　当选为数理化学部学部委员
- 1958 年 1 月　　任《力学学报》主编
- 1958 年 4 月　　任力学研究所常务副所长
- 1958 年 9 月　　任中国科技大学化学物理系主任
- 1960 年 5 月　　任二机部第九研究院副院长
- 1961 年 10 月　　参加中国科学院举办的星际航行座谈会，并做“宇宙飞船的回地问题”的中心发言
- 1964 年 3 月　　领导再入物理现象的研究工作
- 1965 年 1 月　　参与领导人造卫星设计院的工作，任中国航空学会副理事长
- 1965 年 6 月　　任 541 地空导弹项目总设计师
- 1966 年 5 月　　科学出版社出版郭永怀译作《流体力学概论》（普朗特著）
- 1967 年 7 月　　任国防科委空气动力研究院筹备组副组长
- 1968 年 12 月 5 日　　从基地回返北京，因飞机失事不幸牺牲，享年 59 岁
- 1968 年 12 月 25 日　　中华人民共和国内务部授予郭永怀烈士称号
- 1999 年　　中华人民共和国授予“两弹一星”元勋称号

郭永怀传*

郭永怀是我国卓越的力学家、应用数学家，他在跨声速流和奇异摄动理论领域取得杰出的学术成就。郭永怀是我国近代力学事业的组织者和奠基者之一，也是我国核武器研制单位的主要技术负责人之一。他为发展我国的国防科研事业，在倡导高速空气动力学、电磁流体力学、爆炸力学等新兴的力学学科方面，在培养青年力学科技人才方面都做出了杰出贡献。1968 年 12 月 5 日，郭永怀从西北核试验基地返京时，因飞机失事不幸牺牲。郭永怀虽然只活了 59 岁，但其为国际所公认的科学成就，严肃认真的治学态度，正直朴实的思想品德，刻苦勤奋的工作作风，受到了人们的普遍爱戴和尊重。我们在此谨以怀念和崇敬的心情，来记述郭永怀先生光辉的一生。

一、学生时代

1909 年 4 月 4 日，郭永怀出生在山东荣成西滩郭家村。小学就读石岛镇明德小学，1926 年，郭永怀考取青岛大学附属中学的公费生。1929 年 9 月毕业后，郭永怀又考入南开大学预科理工班，学制两年。由于课程大都由教授担任，所选用的教材也多是英文原版书，因而预科班学生的实际水平高于普通高中。在此期间，对郭永怀影响较大的是申又枨教授，他是中国数学界老前辈姜立夫先生的高足，许多杰出的数学家如江泽涵、陈省身、吴大任等都出自姜先生的门下。申又枨教授担任预科的数学教学，讲课很有特色，给人以外松内紧的感觉。虽然他上课风趣，轻松，但对学生要求却十分严格，经常布置大量的习题。这样既加深了学生们的数学功底，也培养了学生对数学的兴趣。著名数学家胡世华教授就是在他的引导下走上专门从事数学研究道路的。郭永怀对申先生布置的难题总是埋头研究，独立完成，还经常帮助同伴。预科的两年使郭永怀打下了坚实的数学基础，为他以后专门从事力学理论研究创造了条件。郭永怀很得申先生赏识，师生间结下了深厚的感情。郭永怀留学回国后还常常去看望申先生。

郭永怀在预科期间，饶毓泰是理学院院长，物理系主任。他是中国物理学界的老前辈，他于 1913 年留美，1922 年回国在南开大学创办了物理系，培养了大批优秀的物理学家。1929 年，饶先生前往德国研究碱金属原子的斯塔克效应。这样，郭永怀所在班的物理课程由美国麻省理工学院回国的卢祖诒任教，助教是吴大猷。吴先生除批改学生的作业外，还负责物理实验。

南开大学所收学费标准比一般大学要高，能进入这所大学的，有不少是有钱人家，特别是天津当地的纨绔子弟。郭永怀来自农村，他不屑同这些人来往，只知道专心学习。他的宿舍中一共有四个人，都是家境贫寒的。这几个志同道合的年轻人发起成立了一个读书会“微社”。“微社”的成员只有六人，郭永怀是其中主要成员。他们每周举行一次讨论会，轮流介绍心得，交流经验。讨论的内容很宽，例如，后来成为数理逻辑学家的胡世华曾做过“四度空间”的小型学术报告。这个小小的读书会培养了年轻人好学上进的精神，对他们后来的学术生涯影响很大。著名经济学家陈振汉、胡世华回忆起微社仍

---

* 根据李家春、李成智《郭永怀》一文节选，原文刊于《两弹一星元勋传》，宋健主编，北京：清华大学出版社，2001。

很留恋，胡先生还说："正是'微社'培养了我们作学术研究的兴趣。"

这期间，郭永怀还迷恋起摄影了。一天，他买来一架照相机玩了起来。同学们都很惊奇，一方面因为大家没想到他还喜欢摄影，另一方面因为这架相机竟是德国名牌 Leica。追问之下，才知道他买相机是为了实现研究光学的理想。他一面学摄影，一面细致研究相机的结构，了解透镜成像原理，学习胶片感光方面的知识。

1931 年 7 月，郭永怀预科毕业。按南开大学的惯例，预科毕业生进入本科还要经过严格的考试。学生向校方提议免去考试，陈振汉在《南大周刊》上写了一篇小文章"为预科学生请命"，向校方呼吁。校方采纳了学生的意见。这样，郭永怀等都顺利地进入本科学习，郭永怀以他数学上的专长和对光学的浓厚兴趣，决定选择物理专业。当时学理科没有多少出路，而学采矿科和工商科，毕业后谋事容易。因此同伴都劝阻他不要选择物理学。这不仅是因为物理学难学，而且日后"饭碗"都难找。但郭永怀不为所动，同学们的劝告他只是报以微笑。

郭永怀转入本科时，吴大猷赴美留学，物理教师更缺。后来他听说电机系有一位顾静薇教授是搞物理的，便投入她的门下，成了她唯一的一位物理专业学生。郭永怀良好的数学基础和孜孜不倦的求学精神深得顾静薇赏识。她为他单独开课，使他在学业上有很大长进。1932 年 8 月，饶毓泰回国并应北京大学之邀担任北京大学物理系主任，顾先生认为，郭永怀应当到光学专家饶毓泰那里去深造。当时适逢南开大学办学经费紧张，拟缩小学生规模，鼓励学生转学。郭永怀便参加了北京大学入学考试。北大请清华大学教授周培源对郭永怀进行口试，内容是理论力学。经过一小时的问答后，周培源先生发现郭永怀对这门课程掌握得很好，并且懂得运用力学规律来解算实际问题，周先生十分满意，给了他很高的分数。其他考试课程郭永怀也都答得很好。这样，1933 年 9 月，郭永怀如愿以偿进入北京大学物理系，插班在三年级学习。

北京大学物理系曾有几度兴衰。饶先生来后，先后请来一批有名的教授，包括周同庆、孙宗鑫、朱物华、郑华炽以及刚刚留学回来的吴大猷，使物理系各方面都出现了崭新局面。郭永怀在本科的两年中所学的主要物理学课程有：朱物华开设的"应用电学和无线电学"；郑华炽教授开设的"热学和热力学"；孙宗鑫教授开设的"几何光学"；饶毓泰教授开设的"电磁学"；吴大猷教授开设的"古典力学"、"量子力学"和"理论物理学"等。其中"量子力学"系国内首次开设，听的人很少，只有高年级学生选修。郭永怀对所有课程都认真听讲，仔细钻研，成绩优异，获得任课教师的好评。

在北大期间，郭永怀曾选修了一门饶毓泰开设的"大气物理学"。这些课程对他日后专门从事高速空气动力学研究奠定了坚实基础。在北大求学期间，郭永怀从不放弃任何学习新知识的机会。优良的学习环境加上郭永怀的勤奋好学精神，使他扎扎实实地掌握了各门课程。1935 年郭永怀毕业时，在全班 30 位学生中，郭永怀的总成绩名列前茅。吴大猷在《回忆》一书中，还谈到他当年教过的，日后取得重大成就的郭永怀、马仕俊等，对他们有很深的印象。

郭永怀本科毕业后，饶毓泰留他做自己的助教和研究生。饶先生认为，郭永怀应当出国深造，为此他尽量不给他安排更多的事，以便给他提供足够的时间准备留学考试。

所以，他这段时间的主要精力都放在充实和巩固自己的知识上，也进行了一些物理学的研究工作。当时吴大猷、郑华炽等教授和几位助教正在利用简陋的设备从事拉曼效应的实验研究工作。拉曼效应是印度物理学家拉曼（C.V. Raman）于 1928 年发现，并获 1930 年度诺贝尔物理学奖。拉曼效应表明，入射光线照射到介质表面后，散射光线不仅包含原来的辐射，还有与入射光线波长不同的辐射，这一发现为研究物质化学结构提供有力工具。利用拉曼效应研究分子物理学具有设备简单、研究范围广、效果好等特点。他们以此研究了碳同位素，获得了当时世界领先的成果。1937 年 5 月丹麦物理学家玻尔(N. Bohr)来华访问，对他们的工作十分赞扬。玻尔在清华大学发表讲演时，郭永怀也前去听讲，还当场多次提问，深受同学们的钦佩。鉴于拉曼效应研究的重要性，饶先生建议郭永怀也进行一些这一方面的研究。但由于芦沟桥事变爆发了，郭永怀只能回到山东威海中学执教，但这段时间的工作使他得到如何从事科学研究的锻炼。

北大、清华、南开三校迁到长沙后组建新校，定名长沙临时大学。1937 年底，战火迫近长沙，教育部又令长沙临时大学西迁昆明。1938 年 4 月师生抵达昆明，奉教育部令改校名为西南联合大学后正式复课。正在家乡中学任教的郭永怀得知这一消息后，决定前往昆明。5 月底前后，郭永怀辗转来到西南联合大学，开始了两年的半工半读生活。西南联大教师队伍集中了三校精英，物理系教授阵容更是强大。正像抗战时期知识界的情况一样，联大的大多数有民族正义感的教师和学生看到日寇在中国领土上横行霸道，烧杀抢掠，他们在心中早就激起了一股强烈的科学救国愿望，所以当时联大内教书、学习都朝气蓬勃。1938 年至 1940 年冬，由于校园生活充实，学习氛围良好，同学们在这一时期进步最快。

国难当头，更增强了青年郭永怀科学救国的信念。他觉得要使国家强盛起来，首先要发展军事科学技术，发展航空事业。为此，他放弃了专修光学的宿愿，立志改学航空工程。抗战期间，同样有许多教师也放弃或暂停原来的专业，学习或研究与国防有关的学科，希望能对抗日战争做些事情。当时与航空密切有关的力学学科正蓬勃发展，物理系的周培源教授由原来的广义相对论转向弹道学和流体力学研究，并在联大开设《流体力学》课程。郭永怀从学习这门课开始，正式步入空气动力学学习和研究的科学道路。周培源教授很早就开始从事湍流理论研究。抗战期间，他继续带领年轻人探究这项世界性难题，郭永怀、林家翘、胡宁等人也都自愿跟随周先生工作。1942 年，周先生领导的湍流理论的研究取得了重要进展，并获得教育部第二届学术会议自然科学类一等奖。这段时间的工作对郭永怀等几位年轻人以后选择科学生涯起到了引导作用。郭永怀、林家翘都是从这里起步的，他们日后都为该学科的发展作出了重大贡献。

郭永怀在西南联大期间，借住在昆华中学高中部。一个小小的四合院可谓人才济济，其中就有钱伟长、林家翘、傅承义、段学复、汪德熙等人。1938 年夏，中英庚款留学生委员会拟举办第七届留学生招生考试。消息传来后，小院里多数人跃跃欲试，郭永怀也决心从中争得一席之地。出国留学对年轻人来说是难得的深造机会，虽然招生人数只有 20 名，但报考者却多达三千。小院里 11 个人报名，结果竟有 7 人榜上有名。郭永怀报考的力学专业只有 1 个名额，但有 50 余人报名。结果他与钱伟长、林家翘总分竟一模一样，

五门课超过了 350 分。经清华大学的叶企荪教授、北京大学的饶毓泰教授在重庆考选委员会上竭力争取，破格将三人一同录取。于是原定招生 20 人，而实际录取了 22 人。

然而好事多磨，正当留学生一行 22 人聚集香港准备从海路前往英国时，欧战爆发了，英国对德宣战而无法接纳中国留学生。他们只好返回各自的学校，等待新的安排。1940 年 1 月，经中国英庚款委员会与英方协商，英国政府同意这批学生转到英联邦成员国学习。中英庚款委员会通知留学生到上海集合，准备前往加拿大。但在上船后，留学生们才拿到护照，打开一看，上面竟有日本领事的签证，允许他们在横滨停船三天上岸游览。留学生怒不可遏，他们向英代办提出强烈抗议："这不行，中日已经断交，我们不能接受这个签证。"这使英代办大为恼火，甚至以取消留学资格相要挟。但留学生不为所动，他们一个个毅然走下即将启航的轮船。几经交涉之后，直到当年 8 月他们第三次接到通知在上海集合，再度出发，终于成行。就这样，郭永怀开始了长达 16 年的留学生涯。

二、留学生涯

1940 年 9 月，郭永怀等一行五人来到加拿大东部的多伦多大学。他和钱伟长、林家翘三人进入应用数学系，段学复和曹飞进入数学系。那时候中国人在国外地位低下，应用数学系主任辛格(Synge)教授以怀疑的态度接待了三位来自中国的年轻人。他看了他们的成绩单，在一起进行了面试，发现他们基础扎实，在国内已经做了许多高深的研究工作，这才令辛格教授刮目相看。因此，决定把他们都留在身边，亲自指导。

辛格教授的第一堂课给他们三位留下深刻印象，也为他们今后的研究工作提供了终身受益的指导，下决心以应用数学为目标，掌握精深的数学分析方法，为解决力学或其他领域的实际问题服务。如果现有数学方法不够，可以发展对解决具体问题有用的新方法，这样便极大地拓展了研究范围。这一重要的治学思想在他们三人后来的科学生涯中都得到了很好的体现。多伦多大学对硕士生的要求侧重于学习基础课，而论文则放在次要地位，主要为将来攻读博士学位打下基础并积累研究的经验，因此郭永怀他们在多伦多大学修课和从事论文研究都比较轻松。郭永怀、钱伟长、林家翘三人在多伦多大学应用数学系都只用了半年多的时间就完成了硕士学位论文。他们的优异成绩和取得的出色成果使辛格教授大为赞叹："想不到中国竟有这样出色的人才，他们是我一生中很少遇到的优秀青年学者。"郭永怀所做的硕士论文题目是《可压缩黏性流体在直管中的流动》，并以这篇论文获得硕士学位。

郭永怀接着向辛格教授要求做一个更难的题目：跨声速流动的不连续性问题。由于辛格教授的专业是固体力学，对气体动力学问题不甚熟悉，郭永怀便决心求教于当代航空大师冯·卡门。郭永怀和林家翘准备前往美国，这使辛格教授感到很失望，因为那时的研究生并不多，而且像他们这样优秀的人才更少。但为了他们的前途，辛格教授仍然很支持他们投奔名师，成就学业。钱伟长仍留在多伦多大学，他和导师辛格教授合作进行板壳内禀统一理论的研究，直到 1942 年获得博士学位后才去了美国。

1941 年 5 月，郭永怀来到美国西部加州帕萨迪那，进入加州理工学院(CIT)。早在 20 年代初，该校校长密立根就认为加州理工学院应大力发展航空工程学。1926 年他亲自

出马，说服古根汉姆基金会同意资助兴建一个航空实验室，即后来的国际著名的古根汉姆航空实验室（GALCIT）。1929 年实验室建成，他又请来冯·卡门(von Kármán)担任实验室主任，使古根汉姆航空实验室成为世界空气动力学研究中心。经过 10 年的努力，冯·卡门集中了一批流体力学精英于此，使 GALCIT 成为空气动力学研究的国际中心。郭永怀正值这个时候来到 GALCIT，无疑是如鱼得水，为他在空气动力学领域一试身手创造了有利条件。

20 世纪 30 年代，航空技术已有了长足进步。当时，活塞式飞机已达到了相当完善的程度，飞机所创造的各项飞行纪录，已近乎达到活塞式飞机的极限，在俯冲阶段的飞行速度已接近声速。加州理工学院同道格拉斯飞机公司合作发展了 DC 系列飞机，飞机速度达到了每小时 700 公里。1935 年沃尔塔会议后，开始研究更高速的飞机。德·哈维兰父子就开始采用早期古别林喷气发动机研制高速喷气飞机。德国首先在 1941 年将 Me-262 型后掠翼喷气式战斗机投入实战，美国也在加紧研制高速飞机。洛克希德公司的双引擎 P-38 型战斗机(闪电式战斗机的前身)虽然在时速 900 公里左右时性能良好，但在越过声速时出了故障。当飞机的飞行速度接近声速时，此时会发生剧烈的抖振，变得不稳定，有时甚至失去操纵或解体，许多飞行员因此而丧命，英国著名飞机设计师杰弗里·德·哈维兰的儿子小杰弗里就是其中之一。该公司设计的 DH-108 飞机于 1946 年 4 月创造了时速 937 公里的世界纪录。1946 年 11 月 19 日，小杰弗里准备驾机实现超声速飞行并一举创造新的速度纪录。然而，就在飞机接近声速时，发生空中解体事故，小杰弗里献出了年轻的生命，成为探索突破声障的第一个牺牲者。

当飞行速度接近声速时，人们遇到了极大的技术困难。一些飞行员在进行跨声速飞行试验时，突然感到阻力剧增、升力骤降、航陀失灵，甚至导致机翼、机身强烈振动。多少飞行员试图逾越声障，结果是机毁人亡。于是，声障就像一堵高墙，阻碍着航空事业的发展。许多人曾错误地认为声障是不可逾越的，突破声障成了当时工程界和科学界共同奋斗的目标。力学家在研究这一奇特的现象时，进行了实验研究，发现在翼面上产生激波是气动特性恶化的主要原因。从空气动力学的原理来分析，激波出现以后，等熵条件破坏，流体的一部分机械能转变为热能，增加了波阻，上表面后部压力增加，产生分离和旋涡，于是升力减小，产生负的俯仰力矩，从而使飞机失速，失稳，失控。激波的无规运动使机翼产生强烈震动。因此，研究翼型绕流出现激波的现象成了当时跨声速领域研究的关键科学问题。

郭永怀的博士论文《跨声速流动的不连续解》就是研究这个最具有挑战性的课题，并且最终要回答在翼型上什么时候理论上的连续解是不可能的；什么时候会在实际流场中产生激波；激波对翼型气动性能的影响；控制与克服声障的措施等重要问题。这个工作无论在理论上还是在工程实际中都有难以估量的重要意义。但要在理论上解决这一课题决不是一件轻而易举的事。因为这时支配流体运动规律的数学方程兼有椭圆型、双曲线型特性的非线性混合型方程。而且由于速度的增大，空气不可压缩的近似假设已不再能精确反映出真实气体的特征。非线性、混合型、可压缩与不连续这些难点交织在一起，更使问题变得异常复杂，根本没有现成的方法可供运用。当时 GALCIT 正处于鼎盛时期，

人才济济，但很少有人敢沾这个难题的边。郭永怀恰恰选定了这个难题。正如钱学森所说的："永怀同志因问题对技术发展有重要意义，故知难而进，下决心攻关。"当郭永怀向冯·卡门教授提出自己的想法时，这位热情的航空大师非常高兴，十分钦佩这个年轻人的胆略和勇气。他尽力为他创造良好的研究条件，使他能集中精力工作。他逢人便说："郭正在作一个最难的课题，我们不要用零碎事情打扰他。"

冯·卡门是郭永怀的导师，由于他工作异常繁忙，因此他推荐已经博士毕业，并晋升为副教授的钱学森协助他指导郭永怀的论文研究。从此，郭永怀全力以赴投入工作。他深知借鉴他人成果和经验教训的重要性，他广泛查阅各种文献资料，密切注意国际最新研究动态和研究进展，同挚友钱学森共同切磋商讨。空气动力学理论研究几乎全是和高深的数学理论打交道，特别是那些超越几何函数、复变函数、线性和非线性微分方程，异常复杂，没有良好的数学造诣和高度的耐心与毅力是难以胜任的。郭永怀毫不退缩。当时在加州理工学院还有不少中国学者如钱伟长、林家翘、傅承义等。1943 年周培源教授也来到这里，在美国战时科学研究与发展局、海军军工试验站做战时科学研究。郭永怀除了和同胞们一道进行学术讨论和假日共同聚会外，几乎断绝了一切娱乐活动。加州理工学院离美国影城好莱坞不远，但据说他在这里的四年半时间只看过半场电影，这正是他辛勤工作的写照。功夫不负有心人。1945 年，郭永怀终于以顽强的毅力，凭借他在数学、物理学和空气动力学领域的扎实功底，完成了有关跨声速流动不连续解的出色论文，并获得博士学位。

郭永怀的论文从理论上证明了，当来流马赫数足够高时，物体的二维定常位势绕流可以是局部超声速的，该超声速区总是贴近在物体的表面，其范围将随着马赫数的增大而扩大。进一步研究发现：从亚声速到超声速或者从超声速到亚声速的过度是连续的，这种光滑流动发生在一定的马赫数范围内。只有当马赫数达到某一值后，速度图变换存在奇异性使极限线出现时，理论上的连续解才是不可能的，这一马赫数被称为临界马赫数。在来流马赫数达到某一值时，在翼面上会首先出现超声速区，随后才可能出现极限线。所以，称前者为下临界马赫数，称后者为上临界马赫数。由于出现激波是影响机翼绕流特性的主要因素，所以，真正有意义的是钱学森和郭永怀共同提出的上临界马赫数；然而，风洞实验表明，应该在理论上出现光滑的连续解时，往往这种解被带有激波的流动所取代，显然，解释理论与实际的矛盾对于避免或推迟激波发生是十分必要的。郭永怀的研究证明了，对于薄翼，在流动的加速区，这种光滑的连续流动是稳定的；在减速区，这种光滑的连续流动不稳定，于是便可在低于上临界马赫数时出现激波(一般都介于上下临界马赫数之间)。而且，厚度效应主要以物面的斜率体现出来。所以，只要超声速区在物体的平直部分，理论依然成立。这一项研究不仅解决了理论同实验的矛盾，而且是高效气动外型设计的先驱性工作。钱学森对此作了恰如其分的评价："郭做博士论文找了一个谁也不想沾边的题目，但他孜孜不倦地干，得到的结果出人意料。"

郭永怀取得博士学位后，即留在 GALCIT 做研究工作，继续从事跨声速空气动力学研究。这期间他又完成并发表了几篇学术论文。

三、科学研究的黄金时期

1946 年，冯·卡门的优秀学生西尔斯（W. R. Sears）在康乃尔大学创建航空研究院。由于郭永怀的才能和出色的成就，他特地聘请郭永怀前去任教，并共同主持该研究院。1946 年 10 月，郭永怀来到康乃尔大学任副教授。

在康乃尔大学，郭永怀一方面继续从事跨声速理论研究，另一方面把主要精力放在黏性流体力学、高超声速空气动力学研究上，这是因为要真正了解激波是如何影响飞机气动性能的机理，必须研究激波与边界层的相互作用。同时由于飞行器速度的提高，郭永怀敏锐地意识到，在突破声障以后，热障问题必将会提到议事日程上来。事实上，无论是在理论上还是在应用方面，黏性流动是现代流体力学中最困难的部分。在研究激波边界层相互作用时，郭永怀感到霍华斯(L. Howarth)等人虽然提出了改进的物面附近的速度型模型，但由于没有真正考虑黏性效应，所以至多只能给出定性的结果。郭永怀从两种不同途径研究了弱激波从平板边界层的反射，并真正地考虑了黏性作用。研究结果得到了在入射点压力向上游衰减，沿下游过度压缩再恢复到正规反射的正常值，激波的几何结构和流线曲率等规律；指出层流边界层与湍流边界层影响上游范围的差异；尤其是压力梯度可能导致分离的后果。这些理论预测为李普曼(H.W. Liepmann)的实验所证实。这是边界层与激波相互作用理论的重大进展。关于高超声速流动，郭永怀研究了沿平板和楔的高超声速黏性绕流，普朗特数对平板高超声速黏性绕流的影响，超声速黏性流动中的离解效应等问题，其中许多都是开创性的工作。

值得一提的是，这一时期郭永怀在应用数学上取得了突出成就。钱学森回忆起这段有意义的经历时说："1949 年，我再次搬家，又到美国加州理工学院任教，所以再一次开车西去，中途到康乃尔。这次我们都结了婚，是家人相聚了，蒋英也再次见到了我经常称道的郭永怀和李佩同志。这次聚会还有西尔斯夫妇，都是我们在加州理工学院的熟朋友。我们都是老师冯·卡门的学生，学术见解很一致，谈起来逸趣横生。这时，郭永怀同志已对跨声速空气动力学提出了一个新课题：既然超出上临界马赫数后不可能有连续解，在流场的超声速区就要出现激波，而激波的形状和位置是受附面层影响的，因此必须研究激波与附面层的相互作用。这个问题比上临界马赫数问题更难，连数学方法都得另辟新途径。这就是 PLK 方法中 Kuo(郭)的来源，现在我们称奇异摄动法。这项工作是郭永怀的又一重大贡献。"莱特希尔的推广被广泛应用于气体动力学，如：轴对称体的定常超声速绕流的激波位置，星系中球面激波的传播以及声爆问题等。现在，郭永怀将莱特希尔的思想推广应用于边界层，而且零阶近似本身是非线性的问题。除了激波边界层相互作用外，郭永怀还将该方法应用于高超声速流动。1953 年，郭永怀乘休假到加州理工学院讲学，并与莱特希尔、钱学森进行学术讨论，最后，将这项优秀成果总结在《中等雷诺数下绕平板的不可压缩黏性流动》的论文中，于 1953 年发表在数学物理杂志上。钱学森专门在应用力学进展上撰文评述这一成果，并将它命名为 PLK 方法。在 PLK 方法提出以后，得到了广泛应用。著名力学家莱特希尔、谷一郎教授专门来信请郭永怀前去讲学。

康乃尔大学的十年，是郭永怀成果丰硕的十年。正在他的科学研究处于黄金时期，

他作出了出乎人们意料的回国决定。

四、返回祖国

郭永怀早就抱着科学救国的思想出国留学。尽管在国外十余年，条件变化了，但他报效祖国的理想矢志不移。其实，在他受聘于康乃尔大学时，一进校园就向校方表示："我来贵校是暂时的，将来在适当的时候就要离开。"因此，他在是否申请接触机密资料的表格栏中填了个"不"字。对于让他申请加入美国籍的来信，一概置之不理。新中国成立前夕，他参加了"留美中国科学工作者协会"康乃尔分会，经常把活跃分子请到家中，热烈地讨论祖国的命运和未来。郭永怀以往很少参加社交活动，但这个分会的活动他却很积极。1949 年 10 月 1 日中华人民共和国诞生了。回祖国探亲的李佩给他带来了祖国发生沧桑巨变的消息，使他万分激动。身居海外的知识分子终于有了报效祖国的时机。但当时中美关系被蒙上一层阴影，他回国的愿望一直未能实现。

50 年代初，美国政府不允许钱学森回国，并限制他的人身自由。钱学森满腔怒火，每次有机会和郭永怀见面时都倾诉回国的迫切心情。其实郭永怀的心情也是一样的，但他克制地规劝好友说："不能着急，也许要等到 1960 年美国总统选举后，形势才能转化，我们才能回国。"他们握手相约，一有机会就立即回国。形势的发展比预期的快。1955 年在日内瓦的外交会议上，周恩来总理代表中华人民共和国赢得了外交上的胜利。1955 年 10 月钱学森回国了，郭永怀更是归心似箭。尽管郭永怀当年在康乃尔大学刚刚晋升为正教授(终身教授)，这对一个外国人来说是相当不容易的，但郭永怀初衷不改。

1956 年初夏，康乃尔大学航空研究院师生为送别郭永怀夫妇而举行野餐晚会。这天晚会余兴的高潮却是大家没有想到的。郭永怀在与同事和学生们讨论一项大家感兴趣的学术问题的同时，把自己教书十余年积累的厚厚书稿一页页投入烤肉的篝火里，烧成灰烬。这一举动使大家惊呆了，在一旁的李佩也感到惋惜。事后才知道那装在他脑子里的科学知识是属于他自己的，烧不掉的。美国同事和学生们都深情地挽留："郭先生，我们希望您改变计划留下来!"中国和亚洲的同学非常钦佩地表示："老师，您给我们指明了道路，我们应当回到我们所属的地方去。"欧洲同学表示理解："先生，以您的学术成就，走到哪里都会做出对人类有益的贡献。"

1956 年 9 月，郭永怀、李佩踏上归程。谈镐生赶到芝加哥来送行。因谈镐生当时正在创建热工研究所，暂时不能成行。但他们相约，一定要为祖国推进科学事业的发展。他们彻夜长谈，依依惜别。后又来到 CIT 与同事、好友告别。10 月下旬，郭永怀和李佩终于乘上了开往祖国的"克里弗兰总统"号轮船。1956 年 11 月初，郭永怀和夫人李佩终于回到了阔别多年的祖国。前去迎接同船的张文裕夫妇的何祚庥把钱学森的信转交给郭永怀。钱学森在信中热情洋溢地邀请郭永怀加入刚刚成立的中国科学院力学研究所工作。回到阔别 16 年的祖国，郭永怀激动不已。建国七年来，到处洋溢着勃勃生机。当他在北京见到多年的知己钱学森时，素来沉静的郭永怀再也按捺不住内心的喜悦之情。他兴奋地说："想不到建国七年就发生了这么大的变化，是我们干一番事业的时候了。"不久，领导上正式决定让郭永怀同钱学森一道领导成立不久的力学研究所。开始他担任了所里

的学术秘书职务，随后他被任命为副所长。从此，他把全部热情和精力都倾注到我国力学科学和尖端技术的研究事业上了。

五、奠基近代力学事业

1956 年我国开始制定 12 年科学技术发展远景规划，郭永怀回国后即投身到这一工作，担任了科技规划力学专业组副组长。他和周培源、钱学森、钱伟长、沈元等一道，规划了我国高等院校力学专业设置。他和同仁们运筹帷幄，认真研究了近代力学的发展动向，开拓了一些有重要意义的新领域，制定了力学学科的近期发展规划和远期奋斗目标，使我国的力学学科的面貌大为改观。特别是近代力学科学技术一起步就有很高的起点，并在某些方面开始朝着世界先进水平的目标奋斗。

中国科学院力学研究所正式成立于 1956 年 1 月 5 日。所长由钱学森担任，建所初期钱伟长兼任副所长。力学所的初创时期还是一个规模较小的研究机构。郭永怀来到所里后，同钱学森、钱伟长一道，为建设和发展力学研究所付出了极大的努力，使力学所很快发展起来。郭永怀首先关注研究所的学科设置、研究领域和方向任务。1958 年，我国经济建设和科学发展的步伐加快。春夏的一天，力学所所长钱学森、副所长郭永怀和党委书记杨刚毅，忙里偷闲，泛舟昆明湖，谈笑间，决定了力学所的大政方针：着手研制人造卫星，发展高速空气动力学、水动力学、火钻技术，开辟若干为国民经济服务的研究领域，并简单地将这一方针概括为“上天、入地、下海、工农业生产中的重大问题”四大方面。这个过程后来传出去，被外界描述得不仅充满诗意，而且蒙上浪漫色彩。这一方针的制定固然受到当时社会背景的影响，但以钱学森和郭永怀的阅历和水平，他们制定的长远目标仍然是经过深思熟虑，持有科学态度的。同时，也说明了力学所学术领导人的博大胸怀。在该所发展的几十年历程中，就主流而言，力学所在不断开拓新的学科领域的同时，始终把主要力量放在解决国民经济和国家安全有关的中长期重大的综合性力学问题上。

力学所开展的工作始终是为工程实际服务的。“大跃进”年代，国家重大项目的关、停、并、转十分频繁。1958 年 11 月，力学所和上海市联合组建了上海机电设计院，研究探索人造卫星，力学所的气动研究直接为其服务。不久由于调整，上海机电设计院改为研制探空火箭，这样气动部分失去了服务目标。为此郭永怀和钱学森提议力学所的气动研究部分与现在的北京空气动力学研究所建立协作关系，确定力学所的研究方向是：为中程导弹的空气动力学和气动热力学提供实验数据和工程计算方法，并开展探索性研究，重点是烧蚀防热问题。为了适应新的需要，力学所组建空气动力学研究室，并大量补充了研究人员。郭永怀和其他领导及高级研究人员，详细讨论了气动研究的方向和目标，设置了七个专门的研究组。这些研究组的研究方向重点各异，有中、长期的，也有短期的，包括基础、理论性探索，也包括实验性研究和工程服务性研究。这个总体研究布局充分体现了他们的雄心和胆略。郭永怀还直接指导激波管和激波风洞实验研究组、湍流边界层研究组。

为了开展高超声速空气动力学实验研究，郭永怀始终如一地大抓高超声速实验设备

的研制工作。为了在条件极为艰难的情况下开展实验研究，他提出了符合我国国情的建议。他认为：搞实验研究要符合我国的国情，决不能贪大求洋。他说："就像高能物理研究那样，我们不能搞昂贵的大型高能加速器，但可以用小型设备来观测宇宙线。我们搞气动研究的，不能一上来就搞大型风洞，而搞激波管、激波风洞却是力所能及的捷径。"他曾多次强调说："要少花钱，用简单设备作高水平的研究。"他还说："看来我们也将研制航天飞行器，为此高超声速流实验是必不可少的。我国资金电力不足，不可能走美国靠常规加热高超声速风洞的道路。即便有了这种大型风洞，由于受材料性能的限制，所能达到的气体加热温度极限仍不能满足回地环境模拟的要求。我们应及早探索新途径，利用激波加热可能是一种有前途的办法。如果能在十年内获得成功，对我国的航天事业将是非常有用的。"中国科学院力学研究所几十年来，利用激波管、激波风洞设备为解决两弹一星中的气动热、气动力关键问题做出了重要贡献。事实证明，郭永怀的这一思想是很有预见性的。

郭永怀回国后积极倡导开展新兴力学学科的研究，开拓了几个有重要发展前景的新领域。其中，取得突出成绩的有高超声速空气动力学、电磁流体力学和爆炸力学。

早在 1957 年 2 月，郭永怀在第一次全国力学学术报告会上作了关于"现代空气动力学的问题"的报告。这篇报告后来发表在《科学通报》上。郭永怀以他丰富的学识，指出了现代空气动力学发展的前沿领域和尚待解决的重大课题。他还特别就当时对正在蓬勃发展的高超声速空气动力学发表了许多精深的见解。他说："现在各国又从事技术和军事的竞赛，洲际导弹和人造卫星不久将成为事实，于是我们面临着（空气动力学）第三个新时代的开始。"为国内空气动力学的研究发展指明了方向。

高超声速是钱学森早年研究高超声速相似律时提出的概念。一般认为，来流速度大于 5 倍声速的流动称为高超声速流。为了使人们更加注意飞行器周围空气经强烈压缩后的高温环境中的物理、化学现象，郭永怀把分子振动、离解和化学反应对流场有重大影响的流动称为超高声速流，并认为必须着重研究这种流动。日后的发展证实了这种认识的正确性。他所提出的超高声速气体动力学的名词和概念，已被国内广泛采用。并且为了包括工业应用，现称高温气体动力学。

为了在国内尽快将这一重要领域的研究工作铺开，1961 年他把在北京地区的许多老、中、青空气动力学工作者组织起来，成立了高超声速讨论班。讨论内容瞄准了理论发展与工程实际的最前沿。正如钱学森在讨论班的第一次会议上所说的那样："这不是一般的讨论班，而是在最新发展的高层次上进行探讨。"可以说这个讨论班研究的问题已与当时的国际最高水平接轨。讨论班每周一次的例会，郭永怀总是风雨无阻，亲临指导。他与大家一起报告学术动向、研究进展，讨论不成熟的见解。讨论班学术气氛活跃、民主，只服从真理，颇有点像加州理工学院古根汉姆实验室的风格。

在这个讨论班上，郭永怀提出了许多有重要意义的精辟见解。1963 年郭永怀指出，由于高超声速钝体绕流会在后身的表面附近形成熵层，在一定情况下，后身流场中可能产生"悬挂"激波。在他的指导下，他的研究生用熵层分析方法进行了理论分析，获得了压力和其他物理量的合理分布，解释了压力过度膨胀和回升现象，并给出了二次激波

的条件。郭永怀在钝体高超声速绕流的最大熵值线问题、真实气体效应问题及钝体绕流的激波形状研究工作上都做出了成绩。郭永怀十分注意抓研究中的新苗头。早在 1964 年，他就注意到带灰尘粒子的高超声速流动，比国外早几年提出开展“云粒子侵蚀”效应研究的设想。当时他解释说：“我总觉得弹头穿过核爆区，灰尘粒子会有影响。”随后，他的学生开始研究含灰尘气体穿过激波的运动。郭永怀倡导并组织的高超声速讨论班，进行了很多探索性研究工作，取得了前沿领域的研究成果。这些成果不断地推广运用到工程实践部门，为发展我国的导弹、航天事业做出了贡献。正是由于郭永怀等人的出色组织才能，使这个讨论班达到了当时的世界先进水平。在高超声速领域，由于飞行器周围空气的强烈压缩和摩擦，造成几千度高温，普通材料制成的飞行器必然烧毁，这就是所谓热障。它同声障一样是必须加以克服和解决的。郭永怀早在星际航行座谈会上就专门探讨过烧蚀防热和烧蚀材料等问题。他在倡导国内开展烧蚀机理研究的同时，还指出必须大力开展烧蚀的实验研究。在国际上技术极端保密的情况下，国内必须因陋就简进行探索。60 年代初，他支持用电弧风洞进行了上百次试验。在以后的动乱年代，力学所和有关单位仍按照郭永怀的设想，继续进行实验和理论研究，在极其困难的条件下，摸索出了有效的防热措施。我国返回式卫星和洲际导弹的试验成功，标志着我国在突破热障方面取得了成功，在这里面凝聚着郭永怀的一份心血和贡献。

电磁流体力学是 40 年代以来出现的一门新兴学科，主要研究导电流体在磁场中的运动规律。当时它只是天体物理和气体放电方面的研究领域。50 年代后，由于能源危机迫在眉睫，也由于超高声速气动力学中电离现象的出现，这一新兴学科才引起了重视。郭永怀抓住这个苗头，在力学所亲自筹划建立了电磁流体力学研究组(后发展成研究室)。1961 年该研究组即开始工作。他将几个学不同专业的人召集到一起，谈了他的想法。他说：“为什么要搞电磁流体力学呢，主要有三个方面原因：第一，人类将来势必要从受控核聚变反应中取得大量能源，而研究高温等离子体、磁流体理论乃是研究受控热核反应的基础；第二，航天器再入返回大气层时，也会碰到气体电离、磁流体力学问题；第三，可以通过磁流体发电方式，直接获取能源。”

关于受控热核反应研究，郭永怀最关心的是加热和等离子体不稳定问题。他认为可以通过在磁压作用下柱形激波的收缩，达到中心反射后获得最高的温度，并力图将气体动力学的戈德莱相似解的研究成果推广到磁流体力学中来。尽管当时物理学家是从寻找合适的磁场位形的角度来研究不稳定问题，郭永怀建议研究瑞利-泰勒界面不稳定问题。他的目标很明确：我们是从力学角度为聚变出力，为核科学技术出力。磁流体直接发电是一项解决未来能源问题的重要课题。由于用导电流体代替机械转子，减少了中间环节，因而可使发电效率大为提高。当时国外搞得比较多的是直流发电试验装置。郭永怀向这个组的负责同志提议：我们不仅在搞直流发电装置，而且要探索交流的。力学所磁流体力学组开始了以液态金属为工质的三相交流发电器的研究，用两年时间建立了国内第一个液态金属回路，与当时国外的实验几乎同步。郭永怀还提出磁流体发电原理应当和原子能技术结合起来，这是很富有创造性的设想。郭永怀提出利用电磁离心方法分离同位素的新颖想法。由于机械式离心机转速最高为 500~600 m/s，而电磁力加速电离气体可以

达到很高的旋转速度，从而改善分离性能。这个设想当时在国际上也是先进的。以往铀同位素的分离一般采用气体扩散法和电磁分离法，这两种方法都需要庞大的工厂和昂贵的设备(美国曼哈顿工程中为分离铀同位素使用了 14700 吨纯银制造电磁铁)。如果电磁离心分离同位素的设想能够付诸实施，就可用一台小型设备代替庞大的气体扩散工厂，将为原子能事业提供强有力的后盾。

在他的大力支持和具体指导下，这个室取得了一批成果，发表了一些专著和论文。这支研究队伍成为我国电磁流体力学和等离子体物理研究领域的中坚力量。在我国等离子体物理学会中，这个室有三位同志被推选为理事。从该室调出的一位同志担任了专门研究所的副所长。他原先留学苏联学原子能，由于以后在电磁流体力学组积累了高温等离子体物理和聚变的知识，三十年后成为聚变-裂变混合堆的实现者，该所也成为国际上算得相当规模的研究基地。他不无感慨地说："郭永怀先生不愧是电磁流体力学的奠基者，力学、物理学领域的一代宗师。"力学研究所在随后的年代里继续了这一领域的研究，在材料制备和加工的应用方面作出了突出成绩，可以说郭永怀辛勤耕耘的这块"自留地"已开花结果了。以后的实践也证实了郭永怀的许多预见是正确的。

爆炸力学这门新兴学科也是在郭永怀等的倡导下，在国内开展起来的。50 年代末期，他就亲自过问，在力学所组织了一支研究队伍。60 年代初，他负责爆炸力学研究室。为使大家深刻理解爆炸力学在我国国民经济建设的重要性，他打开中国地图，对从事这项工作的年轻同志解释说："你们看，我国的高原和丘陵地带占有多大的比例！要建设就要用炸药，如果我们能使炸药的爆炸效力提高百分之几，就能为国家节省多少人力物力啊。"在他的记事本中，爆炸力学的各项任务课题始终占着重要地位。他时刻挂记着长江三峡水电站、成昆铁路以及大型国防工程的建设。

郭永怀除了对爆炸成型、水坝安全、铁路建设等课题给予关心和指导外，还提出了爆炸力学的军事应用课题。文革前后，他向聂荣臻同志汇报了用定向爆破方法修筑工事的设想，并抽调几个人进行这方面的研究。在他的支持和当时的室主任郑哲敏的带领下，爆炸力学研究室迅速成长起来。多年来，他们进行了成百上千次大型实验和现场施工，完成了爆炸成型、定向爆破、穿甲爆破等多方面重大任务，取得了优异的成绩。特别是在爆炸成型的理论和实践上有较突出的成果，为我国的经济建设和国防建设作出了积极贡献，多次获得国家重大科技成果奖。

郭永怀不仅是一位优秀的科学家，也是一位出色的科研组织者。他在科研组织上有许多深刻的思想和独特的做法。

郭永怀始终认为科研部门应当有相对独立的科研计划，包括近、中、远期各个阶段的计划，做到近期有安排，中期有准备，远期有目标。要保证科研计划持续、循序渐进地进行，使研究工作有继承性。同时，他还十分强调制定科研规划应有明确的服务方向，科研成果要不断地反馈到生产实践中去。从这个意义上讲，他的一切工作都是面向实际的。他参与制定的力学所大计方针就体现了这一思想。

郭永怀对选择科研课题的重要指导思想是：一、要瞄准当时科技发展的前沿；二、要与国民经济的发展结合起来；三、要重视基础性研究；四、要强调为国防建设服务。

他不主张做小题目，写小文章，更反对在“文章缝里”找课题做。他指定的研究方向，都是重大的探索性课题，大都会有重要的应用价值。

郭永怀极为重视并大力提倡开展基础研究，因为“基础研究是科学研究的基础，没有基础研究，科学技术的现代化就要落空。”他总是鼓励年轻人要热爱基础研究。他多次在各种场合谈到：“一旦生产上提出需要，基础研究就会变成巨大的生产力。”他还用半导体、火箭和喷气技术的发展历史来说明这个问题。大跃进时期，社会上出现了片面强调科研必须为生产服务，从而忽视基础研究的倾向。针对这一情况，郭永怀在 1959 年春为力学所作年度计划时，写下了《研究工作与工程技术工作如何衔接》的短文。他指出：“理论研究与工程技术工作有区别，也应有交叉。一个研究机构不能是设计院，然而在一定范围内又要执行设计院的任务；它离不开设计院，但不能包括设计院。如果这样做，研究机构势必十分庞大；那样既没有必要，也不可能。”他对流行的两种说法进行了分析。一种是认为理论研究与设计可以分开，独立、分段地进行；一种是认为研究是为生产服务的，因此研究的目的在于实现某一具体任务。他指出，第一种说法势必脱离实际。第二种说法只在某些特殊场合是对的，一般说来是不对的。他的观点实际上为是力学所的发展方向作了规划，即：作为一个研究单位，力学所应以理论研究为主，同时强调为工程实际服务，但决不能成为一个设计部门。

在郭永怀的科学研究生涯中，他主要从事理论分析研究。但他仍然十分重视和强调实验研究，并有自己的见地。他认为科学研究有两种手段，即理论研究和实验研究。理论研究是就工程实验中所遇到的问题进行理论上的分析探讨，以寻求解决的途径和方法，得出有规律性的东西。实验研究一方面用于检验一种新的理论、新的思想；另一方面还在于通过实验来发现新的现象，揭示新规律，探索新方法。这两种研究手段是相互联系、相互依赖、相互补充、相互验证的。因此，理论研究和实验研究具有同等重要的地位，不能偏向任何一方，也不能把实验简单地看作是试验或验证。

郭永怀曾是中国力学学会的常务理事，《力学学报》的主编，力学所的常务副所长，对力学所全局的建设和发展，乃至我国的近代力学事业作出了卓越贡献。曾任力学所所长的钱学森先生说：“郭永怀同志归国后，奋力工作，是中国科学院力学所的主要学术领导人。他做的要比我多得多。”在力学所发展的第一个重要时期(1956~1966 年)，该所承担或参与了许多重大科研项目，规划了总体研究方向和任务，筹建了实验基地和许多实验设备，设立了多种新兴力学学科，培养了一大批科研人才。该所的研究队伍逐步形成，涌现了一批有价值的成果。这一时期，郭永怀及力学所的同志进行了艰苦的创业工作，为该所后来的发展打下了良好的基础。这一时期力学所人数最多时达 1300 多人，其中相当一部分人员有效地支援了其他部门的建设。力学所的发展壮大与郭永怀的不懈努力是分不开的。郭永怀逝世后 30 年来，人们经常重复的一句话是：“他要是还活着就好了。”这句朴实的话语，寄托着人们对郭永怀的深切怀念之情。

六、献身“两弹一星”

(一) 提倡发展我国航天事业

郭永怀对我国发展航天技术和研制人造卫星的贡献主要包括四个方面：第一，积极提倡发展我国的航天事业；第二，参与发展航天事业的规划；第三，亲自参加重大课题的研究工作；第四，参与组织、领导中国科学院的人造卫星本体设计。

1957 年 10 月 4 日，原苏联发射成功世界第一颗人造卫星，震动了全世界，在我国科技界也引起强烈反响。10 月 13 日，中国科学院、中华全国自然科学专门学会联合会、中华全国科学技术普及学会组织召开了“关于苏联发射成功第一颗人造卫星的座谈会”，到会的有许多是在京的各个专业领域的著名科学家。郭永怀也参加了这次大会，并发言：“我觉得这件事是在进入原子能时代以后的第二件大事，对整个人类都有影响。人类一向是在二度空间活动的动物，现在有了人造卫星的成就，就如爬高有了梯子一样，以后去宇宙活动已经不是梦想，可以实现了。”然后，他以从国外获得的资料，就发射人造卫星的运载工具及其推力、火箭发动机的推进剂、卫星进入轨道的姿态控制、苏联同西方国家火箭技术的比较等具体技术问题作了分析介绍，并发表了自己的观点。

1958 年，郭永怀参与制定力学所的科研规划时，就和所里其他领导共同提出研制人造卫星的倡议。1958 年 5 月 17 日，毛泽东主席在八届二次会议上指出：“我们也要搞人造卫星。”于是趁着大跃进的热情，研制人造卫星的任务很快落实到中国科学院。中科院把研制人造卫星列为 1958 年的第一号重点任务，称“581 工程”。随后组建了三个设计院，其中第一设计院以力学所为主建立的，承担人造卫星本体及其运载火箭的研制工作。受大跃进影响，当时提出了不切实际的目标：1959 年发射第一颗人造卫星。但在实际工作中，困难重重，不符合当时的国力。1959 年 1 月，国家决定 581 工程随即暂缓进行。

1961 年 4 月 12 日，前苏联宇航员尤里·加加林首次进入太空，对我国又是一次极大的促进。为了使我国的航天事业循序渐进，以科学的态度逐步发展上去，在一些著名科学家的提议下，中国科学院举办了星际航行座谈会。此后的三年时间里，共召开了 12 次专门会议。郭永怀除在第四次座谈会上作中心报告外，其他历次会议他都参加了讨论。他以他在空气动力学、气体热力学以及数学、物理学方面的专长，提出过许多重要见解和主张。1961 年 10 月，在星际航行座谈会第四次会议上，郭永怀做了《宇宙飞船的回地问题》的报告。郭永怀重点讨论了宇宙飞船在返回地面过程中，怎样才能安全再入大气层，并保证顺利降落回收。他从理论上定量分析计算了飞船再入段的空气阻力减速、气动加热、回地轨道的设计和烧蚀防热等重要课题，得出了符合当时已掌握的实际资料的结果。他还指出，现有飞船是没有举力面的，所以无法利用空气产生必要的升力。他认为，未来的宇宙飞船可以设计成有翼的形式，一方面可以降低卫星式飞船的超重；另一方面可以部分解决回地速度更高的月球飞船的再入与回收问题。他还主张研究优化转移变轨的方案，为十多年后的工作作了准备。星际航行座谈会历时三年，为我国逐步进入航天大国行列进行探索，郭永怀就是做了许多有益工作的航天事业开拓者之一。

1965 年，随着我国战略导弹事业的顺利进行，研制和发射人造地球卫星的任务再次

提到议事日程上来。581 项目演化为 651 项目。中国科学院在钱学森和郭永怀的参与下，成立了以党委书记杨刚毅为首的人造卫星设计院，承担人造卫星本体设计任务。设计院另设一组，负责回地式卫星(即返回式卫星)方案及气动设计。回地式卫星设计组自 1965 年到 1967 年，提出了卫星回收方案，包括下降轨道设计、制动火箭控制方案、卫星气动外形、结构布局等，并对再入段气动加热及烧蚀特性作了较详细的计算。此外，他们还对以后的研究工作提出了具体建议。后来，由于工作重点的调整，这些成果均转到第七机械工业部和空间技术研究院，为我国研制人造卫星和发展航天事业发挥了重要作用，并打下良好的基础。

(二) 规划筹建气动研究基地

1964 年初，国防科委为了促进我国空气动力学研究工作的发展，满足型号研制对空气动力学的要求，决定成立国防科委空气动力学专业组，即第 16 专业组。专业组由钱学森、郭永怀、沈元等国内 15 位著名空气动力学家组成，其主要任务是：协调风洞实验任务，提出并讨论全国空气动力学实验的规划，提出有关空气动力学发展的重大技术措施的建议和组织空气动力学的学术交流。这个专业组颇有些类似于专家咨询委员会，相当于国防科委发展空气动力学的高级智囊团和参谋部。16 专业组成立后，郭永怀和其他成员一道组织了全国风洞群建设规划的论证，并提出了风洞建设建议，进行了重点型号气动分析会诊工作，讨论了我国空气动力学研究队伍建设中的有关问题。同时开展了技术交流，并就一些新的领域进行了讨论。他们还向国家提出尽快成立我国空气动力研究院的建议，它应独立于型号研究院之外，为型号研制和自身发展服务。1965 年，国防部第五、第六研究院分别划归第七、第三机械工业部建制。16 专业组的活动基本停止。

文化大革命开始后，为了减少动乱所造成的损失，推动国防科研事业的发展，1967 年 9 月，聂荣臻在《关于国防科研体制调整改组方案的报告》中，建议成立 18 个研究院，得到中共中央的批准。空气动力学名列第 17，所以被称为第 17 研究院。为组建 17 研究院，国防科委成立了筹备组。钱学森任组长，郭永怀、严文祥任副组长，郭永怀负责技术工作。郭永怀以他丰富的学识和深邃的思想，通过考察我国气动力研究的现状，同时结合国外先进经验，同钱学森等科学家一道，提出了许多重要建议和主张：

第一、空气动力学的主要服务对象仍然是航空和航天事业，这样才会有立足点，并使其自身得到发展。在我国航空和航天事业刚刚起步之时，迫切需要空气动力学理论指导的特点尤为突出。

第二、空气动力学研究要形成国家层次的中心。在我国空气动力学发展中，曾有一个时期，各个部门分头建设风洞等实验设备，这种局面必然造成耗资多，周期长，配套能力差，技术力量分散。因此，建立一个国家级中心，集中有限的人力、物力和财力，统一规划、统一组织实施，乃是一个快、好、省的办法。这个中心可以同时为教学、科研、设计和生产服务。

第三、空气动力研究院应具有鲜明的特色，一是速度、尺寸、品种和功能配套互补；二是符合我国的国情；三是近、中、远期相结合；四是研究手段应实现理论研究、实验研究和模型自由飞相结合。

第四、郭永怀还详细地分析探讨了一些具体的技术途径，其中许多设想是同我国国情紧密结合的。为了发展我国的航天事业，在风洞建设上，除了要求达到低、高、超高速配套外，郭永怀认为应该重点搞高速、超高速实验风洞，瞄准第一和第二宇宙速度。

基于上述思想，钱学森和郭永怀为 17 研究院的建制规划了一幅宏伟蓝图，包括各个专业研究所的设置、辅助设施、人员配备，以及具体的技术途径和各种实验设备，使研究院具有空气动力学研究的“全天候”能力。郭永怀强调指出，17 院应独立于型号研究院之外，对先进的飞行器如飞机、火箭的气动布局有重大的发言权。通过空气动力学研究，及时提出新概念、新建议，为具体的型号总体设计作出贡献。这无疑是很有见地的。

即使在轻视理论，强调应用的风气下，对于在研究院各专业研究所的设置上，郭永怀还坚持要建立搞基础研究的理论研究所。在 1968 年 6 月的一次会议上，他明确指出：“目前重点安排一、二、五所的建设是可以的，六所虽可暂缓一下，但不能不建。”(一、二、五所分别是低速、高速、超高速所，六所是理论所)。郭永怀十分关心我国计算流体力学的发展，很早就给予了充分的肯定和支持。在郭永怀等科学家的倡导下，我国的计算空气动力学起步较早，虽然在实际发展过程中受到计算机条件的限制，但仍取得了一批丰硕成果。其中有的先进计算格式如 NND 得到国际学术界的关注。

郭永怀迫切希望空气动力学研究院能早日建成，以便为型号研制服务。在 1968 年 2 月的一次会议上，他重点谈了领导班子问题。他说：“已经进入 1968 年了，但 17 院仍只是一个筹备组，所以应报请国防科委解决领导班子问题。所级干部这么多，应当分批解决。”更令人不能忘怀的是，1968 年 10 月，在他要离开北京赴西北草原筹划导弹核武器试验的前一天，他还来到 17 院筹备组，要求一位同志起草一份关于高空模拟试车台和 17 院进行统一规划的报告，等他参试回来后再一起讨论。同时还告诉大家，他要出差了，询问有什么事情要他做的。没想到这次会面竟成了永诀。事隔 30 多年后，当年在 17 院与郭永怀一道工作的同志仍然深深地铭记着这件平常而又极不平常的事。每每想起它，都激起他们对郭永怀无限敬佩与怀念之情。

1976 年，国务院、中央军委决定在风洞指挥部(17 院是该机构的前身)的基础上，调整组建空气动力学研究与发展中心。经过多年的建设，气动中心现已成为试验设备齐全，研究手段完备，技术力量雄厚，测试数据可信的实验研究基地，已成为航空航天飞行器及风工程研制与发展的重要技术支柱，在国际上也享有盛誉。一些国际同行参观了气动中心后，交口称赞“了不起”。1998 年 8 月，郭永怀在美国期间指导的博士生，后担任 CALSPAN 高技术中心主任的瑞特(A. Ritter)，访问气动中心后说：贵中心风洞设备的规划建设显然包含了郭永怀教授的思想。作为一个开拓者和奠基人，郭永怀在这项伟大的建设工作中，具有不可磨灭的功绩。

(三) 为实现核弹武器化献身

1959 年 6 月，二机部遵照中央确定的方针，决心要独立自主地完成原子弹研制任务。1960 年初，九院即开始了原子弹技术的研究与探索。为了适应自力更生研制原子弹的需要，中央决定从全国抽调技术力量加强九院。许多著名科学家包括王淦昌、彭桓武、程开甲等都先后被调到九院工作。由于这项任务里面有许多工程力学问题，二机部副部长

钱三强约见钱学森，让他推荐从事这方面工作的技术负责人人选。钱学森说："我看郭永怀完全可以胜任！他学术上造诣很深，而且作风正派，工作扎实，现在又担任力学所副所长"。钱三强在向上级汇报后，亲自找到郭永怀。郭永怀表示："这个工作我虽没搞过，但经过努力，我想还是可以的。"他沉思了一会儿说："不过，我的力学所副所长工作如何安排？"钱三强说："可由二机部和中国科学院协商解决。"这样，郭永怀于 1960 年 5 月来到九院，后来还担任了副院长。在原子弹研制初期，王淦昌负责物理实验，彭桓武负责理论设计，郭永怀负责力学方面的技术领导工作。这些著名科学家以及大量技术骨干调到九院后，大大加强了九院的力量。许多中央领导同志曾来到九院看望他们，陈毅还说："有你们科学家撑腰，我这个外交部长也好当了。"

1．第一颗原子弹

原子弹的引爆方式大致有两种，一种是所谓"枪法"，另一种是内爆法。前一种采用两块亚临界核材料，利用常规炸药爆炸时的冲击力把子弹射到靶子上，两块核材料达到超临界状态，实现核爆炸。内爆法的原理则是：在亚临界状态的核材料周围布置常规炸药，如果控制爆轰波形状使之聚焦，就能引爆原子弹。因此，内爆法就是使球对称的常规炸药的爆轰波聚集成内向的球形冲击波，挤压核材料使之达到超临界状态，实现核爆炸。"枪法"固然简单，但浪费核材料太多，而且对核材料的纯度要求较高，对以钚为核材料的原子弹则根本不能使用。内爆法没有上述问题，但要实现精确的球对称内压力，技术上的困难很大。实际上，美国曼哈顿工程在解决这个问题时也遇到重重困难。美国科学家内德迈尔提出内爆设想，并得到洛斯·阿拉莫斯实验室负责人奥本海默的支持，但解决内爆方案中种种困难也花了几年时间。就在"内爆法"和"枪法"争论很大，难以取舍之时，郭永怀通过比较两种方式的优越性，结合我国的实际，提出了"争取高的，准备低的"的方针，以较高级的内爆法作为主攻方向，同时为稳妥起见也探索较低级的"枪法"。

内爆过程的理论计算是困难的，属于非定常气体动力学问题，且涉及多学科领域，十分复杂，而且是当时还不知道应采用什么方法最合适。郭永怀同大家一道讨论，向大家提出了几种可供选择的计算方法。郭永怀不仅在理论上给予指导，还亲自参与计算工作，使大家对压紧过程的流体力学机理有了更深入的理解。

爆轰学是实现内爆法的理论基础。为了使大家了解爆轰学，郭永怀以他渊博的学识给大家讲授爆炸物理学。这是一门涉及气体动力学、高温物理学和反应动力学的边缘学科。他讲得深入浅出，引人入胜，不仅使中青年科技人员得到很大教益，连老科学家也都觉得获益良多。同时，他还找到当时仅能见到的一本书：苏联的鲍姆等编的《爆轰学》，组织大家分头翻译，最后由他进行了认真的校阅。这本书出版时翻译者署名为"众智"，这份宝贵的资料确实体现了九院科技人员的集体智慧。

爆轰物理试验是突破原子弹技术的重要一环。为取得第一手资料，他鼓励设计人员参加爆轰试验，他自己也经常与王淦昌等老科学家深入现场，了解情况，分析数据，指导工作，并协助开展试验，有时还钻进帐篷里，和技术人员一道搅拌炸药。在两种可供试验用的设计方案中，他提出了"两路并进，最后择优"的办法，确定最佳方案。这一

方案不仅为第一颗原子弹采用，整个第一代武器研制过程中都一直沿用。负责爆轰物理试验的青年科学家陈能宽，以他坚实的理论基础并参照国外有关资料，提出了爆轰试验的新方案。这个方案能够加快原子弹的研制，但困难和风险大。郭永怀从力学角度进行了理论估算，大胆地支持了这一方案。经过科学家的详细论证，这个方案终于得到采纳并付诸实施。为了配合爆轰试验，郭永怀和龙文光指导设计部科技人员进行了不同试验装置的结构设计，使得整个爆轰试验得以顺利进行。随着研制工作的顺利进行，大型爆轰试验在西北草原开始了：1963 年 12 月 24 日一比二模型爆轰试验取得成功；1964 年 6 月 6 日，全尺寸爆轰试验也达到了预期的目的，这是一次唯独不装核材料的完整试验。这次试验成功的取得，预示着原子弹成功在握。从 1962 年 9 月到 1964 年四季度，经过 21 个月的艰苦工作，原子弹理论、试验、设计和生产工作都按计划全部完成。

1964 年 10 月 16 日 15 时(技术上称零时)，我国第一颗原子弹装置爆炸试验取得圆满成功。当闪光火球和蘑菇状烟云冉冉升起时，全体参试人员完全忘却了紧张和疲劳，为胜利而欢呼。当时郭永怀就在试验现场，亲眼目睹了这一极为壮观的场景，内心的喜悦和激动是可想而知的。这项对我国具有深远政治、军事、科技发展意义的巨大成就，有他的一份功劳。

2. 核航弹

为了实现武器化，郭永怀早就安排了许多与核航弹有关的预研性课题，包括核航弹的结构设计、外形设计、飞行弹道、物理引信、环境试验等，任务艰巨，他在方方面面起了主导作用。

为了加强结构设计的力量，郭永怀亲自聘请我国著名固体力学专家、北京航空学院王德荣教授作技术顾问，给大家讲授结构力学的理论，并指导弹体结构设计。核航弹外形结构最初采用钢板卷压焊接的方法，这种设计的弊端是强度指标分配不合理，且十分笨重。为此，郭永怀提出参照飞机外形的桁架蒙皮结构进行设计，从而实现了减轻航弹结构重量的要求。由于文革的影响，他的设想直到 70 年代末才得以实现。核航弹的气动外形有独特的技术要求。为了保证飞机在投放过程中保持稳定，并能及时安全脱离危险区，核航弹还必须要有很好的增阻特性。对这些难题，郭永怀不仅给予悉心的指导，还亲自参与外形和飞行弹道的理论计算工作。

无论核航弹还是核导弹，在飞行过程中总要经受各种常规和非常规的动态考验，因此，各种环境试验是武器化阶段很重要的一环。郭永怀从技术人员的配备、课题的安排、试验项目的确定以及试验设备的研制等多方面周密安排，保证环境模拟试验顺利进行。正是在郭永怀的直接领导下，当时只有为数不多的科研人员的环境试验组，逐渐发展成为一个具有相当规模的研究所，培养了一批批专门的技术骨干，配备了一整套大型、精密的，测试范围较广的核武器试验设备，包括冲击、噪声、振动、过载、温度、湿度、霉菌、盐雾的组合试验设备。比如，在他的关心下研制了可测试数百 g 的大型离心机等。他的指导思想是：我们的设备应该更先进，所用人员应该更少。核航弹的结构振动试验设备小，只有 500kg 的试验能力，有人主张用小部件试验。向郭永怀汇报后，他说，小部件试验可以取得一些有用结果，但不能代替整机试验。于是，在他的支持下，论证、

设计、加工并调试了一个放大支架，并按时完成核航弹的整机振动试验。

为了确保核试验的安全，郭永怀还提出了“安全论证”的课题。核弹引信的可靠性和有效性对安全异常重要，所以在每次听取炸弹引信汇报时，他都要参加，利用他渊博的空气动力学知识，对弹上静压孔布局、管路汇流系统和引信误差计算都一一提出他的具体意见，对计算数据都一一核对。同时，安全也对核航弹外形设计提出了新的要求：气压引信要求在飞行过程中，某特定部位感受的压力接近当时当地的大气压，能正确反映航弹当时所处的真实高度；为了保证无线引信的天线发送接收装置正常工作，要求弹轴摆动角度越小越好，这需要增大航弹的阻力系数和阻尼力矩；为了保证核航弹能命中目标，又要求航弹尽可能减少阻力系数和增加升力系数，并提高其运动的稳定性等等。这就要求在众多复杂的，甚至相互矛盾的要求中寻找最合理的方案。在他的直接关心和指导下，航弹外形设计与安全论证工作进行得很细致，因此，每一次试验的飞机都安全返航。

1965 年 5 月 14 日，一架经过改装的图-16 轰炸机携带我国第一枚核航弹起飞了。飞机在预定高度把核航弹准确投向预定靶标，接着，核航弹在预定高度实现核爆炸。这次试验的成功使我国有了初步可用于实战的核武器。

3. 热核武器与核导弹

九院的工作有许多是齐头并进的。早在 1963 年秋，第一颗原子弹理论设计完成后，九院就组织人力进行热核武器的理论探索。郭永怀则针对氢弹的结构设计、气动外形、环境试验等方面，组织有关人员开展工作。

我国第一颗氢弹采用空投方式，困难和危险都是很大的。美国第一颗氢弹是在一辆破旧的火车上试验的，法国第一颗氢弹是在一条破船上试验的。空投方式给空气动力学带来新的课题。由于氢弹的爆炸当量远远超过了原子弹，因而安全问题更加突出。郭永怀抽调几个人组成调研组，就国内外能见到的资料进行分析。由于氢弹的增阻特性要求高，采用普通的减速板达不到要求，因而提出减速伞方案。通过对软伞、金属伞、气球等途径比较，决定采用软伞。但这种减速伞与普通的航空救生伞相比有更高的要求，如：增阻大、开伞冲击小、摆动小、稳定性好等。国内航空部门尚未开展这方面的工作，因而在提供调研资料、提出指标要求、委托加工制作等过程中，也推动了兄弟单位的发展。弹体加伞后，还有一个伞—弹弹道的计算问题。这也是在郭永怀直接指导下进行的。当有人估计采用软伞产生的漂移可能很大时，郭永怀说：“这不可能，弹体这么重，随便让它飘也飘不出多远。”

在核航弹的结构设计中，由于指导方针是力求稳妥可靠，所以弹体结构搞得很笨重，体积和重量较大。郭永怀认为这不符合实战要求。他是学航空出身，深深懂得“航空产品要为节省每一克重量而奋斗”这句话的真正含义。他多次向负责结构设计的人员指出：“作为原理试验弹采用金属铸件结构是可以的，但要达到实用化，必须搞轻型的薄壳结构。”他还说：“航弹和导弹都是飞的，既然是飞的，就应该采用航空结构，把造船的本领一丝不苟地运用到航空上去怎么行呢。”由于郭永怀的正确主张并付诸实施，使结构重量降低了 20%以上。自第一颗氢弹后，我国历次核试验大都采用这种轻型结构。有趣的

一件事是，1966 年 1 月 17 日，美国的一架装载核武器的 B-52 轰炸机在西班牙上空和一架加油机在加油时相撞，机上携带的四枚氢弹(没有引爆装置)坠落。这件事在国际上引起轩然大波。郭永怀搞到一张这些氢弹的照片，他马上拿来同大家一道研究，从氢弹的外形分析其增阻、增稳以及边界层性能，并进行了一些风洞试验，收获很大。照片上氢弹弹体上有一处明显的坠落时留下的凹痕，从而判断美国的氢弹也采用了薄壳结构。这就从另一侧面证明了郭永怀主张的正确性。

我国第一颗氢弹各方面工作进展很快。郭永怀负责的总体设计、环境模拟试验以及安全论证等工作也都按时顺利完成。为了保证试验成功，1966 年 12 月 28 日，首先进行了氢弹原理试验。测量数据表明，这次试验预示着氢弹原理已经突破。1967 年 4 月，在空军某地进行了弹道特性试验，达到了预期目的。1967 年 6 月 17 日，我国第一颗氢弹爆炸试验成功。从第一颗原子弹到第一颗氢弹，美国人用了七年，苏联人用了四年，而我国只用了二年零八个月，且赶在法国前面。这一历史性壮举震惊了世界。

继核航弹、氢弹的试验成功，导弹核武器研制迅速纳入正轨。核导弹与航弹相比，体积和重量要大幅度减小，对环境条件的要求也更加苛刻。郭永怀早在 1964 年就提出了要开展随机振动和噪声动态试验研究。当时他说："噪声试验是核弹武器化，特别是洲际导弹再入时必过的一关。声致疲劳试验也很重要，这方面工作国外已经搞了，而我们还没有开展，应该特别抓一抓，把这项试验搞起来，为以后的发展做准备。"郭永怀对试验设备、试验参数十分关心。当他听说压力气源有困难时，他以商量的口气说："你们没有见过风洞试验用的气源吗？国内有，你们去看看，会有启发的。"在他的关心和指导下，得到中国科学院的专家帮助，我国的噪声试验设备终于有了着落。由于当时国内只能模拟正弦振动环境，为真实地模拟核武器所处的随机振动环境，经过调研，有人提出只能进口。当请示郭永怀时，他肯定地说："这是技术引进，应该的。"随即在设备单上签字。后来，有关设备从英国进口，解决了核弹头的随机振动试验问题。

如果说核航弹是初步可用于实战的核武器，核导弹则是真正具有实战价值的核武器。1966 年 10 月 27 日，我国成功地进行了东风二号甲导弹核武器试验。

总之，郭永怀对我国核武器研制的贡献是多方面的。他凭借在爆炸力学、气体动力学、空气动力学、飞行力学等诸多学科领域的渊博知识，对内爆过程、结构设计、气动外形、环境试验等许多关键技术问题进行指导，为我国的原子弹、氢弹及其武器化、系列化呕心沥血，无私奉献。1968 年 10 月，郭永怀赴西北草原进行我国第一颗热核弹头发射试验前的准备工作。准备工作结束后，12 月 5 日郭永怀从兰州乘飞机回京。当飞机在北京机场降落时，发生一等事故，郭永怀不幸以身殉职，终年 59 岁。

周恩来总理得知郭永怀乘飞机失事牺牲的消息后，立即下令彻查这一事故，并责成人民日报发布这一不幸消息。12 月 13 日《人民日报》在第四版报道："新华社十一日讯，中国共产党党员，全国人民代表大会代表郭永怀同志，因不幸事故牺牲，终年五十九岁。郭永怀同志在从事的科学技术工作中，做出了贡献。" 12 月 25 日，他被追认为烈士。

郭永怀对我国国防科技事业，特别是"两弹一星"研制做出了卓越贡献，得到了党和人民的充分肯定。1999 年 9 月 18 日，在共和国庆祝建国 50 周年之际，中共中央、国

务院、中央军委作出决定，表彰为研制“两弹一星”做出突出贡献的科技专家，并授与他们“两弹一星功勋奖章”，郭永怀就是其中之一。中央的决定指出：“这 23 位科技专家是人民共和国的功臣，是老一辈科技工作者的杰出代表，是新一代科技工作者的光辉榜样。”